# NATIONAL URANIUM TAILINGS PROGRAM

Energy, Mines and Resources Canada
Énergie, Mines et Ressources Canada

Canada

# PROBABILISTIC MODEL DEVELOPMENT FOR THE ASSESSMENT OF THE LONG-TERM EFFECTS OF URANIUM MILL TAILINGS IN CANADA - PHASE III

## VOLUME 1 - SUMMARY REPORT

A Research Report Prepared under:
Contract #0SQ85-00182

for

The National Uranium Tailings Program
Canada Centre for Mineral and Energy Technology
Energy, Mines and Resources Canada
555 Booth Street
Ottawa, Ontario
K1A 0G1

by

SENES Consultants Limited
499 McNicoll Avenue
Willowdale, Ontario
M2H 2C9

July 1986

103 pp

MICROMEDIA

## ABSTRACT

This study represents part of the ongoing efforts of the National Uranium Tailings Program (NUTP) to develop the capability to predict the long-term effects of Canadian uranium mill tailings. The study was conducted to further refine the probabilistic assessment tool developed during two previous phases of work. In particular, the work involved expanding the system model to include: additional radionuclides, additional pathways of exposure and the ability to perform calculations over much greater distances. The primary product of this study is a revised, more comprehensive Uranium Tailings Assessment Program (UTAP).

The project report has been prepared in 4 volumes, of which this is Volume 1. This volume provides an overview of the project activities and results. The concepts of probabilistic analysis are reviewed and the approach taken to modelling uranium mill tailings is discussed. Results for two different disposal scenarios are presented for a generic, reference tailings site.

---

## NOTICE

This report was prepared by SENES Consultants Limited (SENES) under contract to the National Uranium Tailings Program (NUTP). Neither the NUTP nor SENES makes any warranty, expressed or implied, or assumes any liability with respect to any damage or loss incurred as a result of the use made of the information contained in this publication.

# TABLE OF CONTENTS
## Phase III Volume I

Page

Abstract i
Notice i

1.0 INTRODUCTION 1-1
- 1.1 Background 1-1
- 1.2 Scope of Phase III Studies 1-2
- 1.3 Report Structure 1-3

2.0 PROBABILISTIC ANALYSIS CONCEPTS 2-1
- 2.1 The Concept of Probabilistic Analysis 2-2
- 2.2 Presentation of Probabilistic Results 2-4
- 2.3 Interpretation of Probabilistic Results 2-5
- 2.4 Confidence in Probabilistic Results 2-7
- 2.5 Some Aspects of Time Dependency 2-10
- 2.6 Model Aggregation 2-12
- 2.7 Parameter Importance Analysis 2-13
- 2.8 Identifying and Incorporating Parameter Correlation 2-14

3.0 APPROACH TO MODELLING 3-1
- 3.1 The Reference Site 3-1
- 3.2 Environmental Pathways 3-3
- 3.3 Environmental Models 3-3
  - 3.3.1 The Tailings Source Term 3-4
  - 3.3.2 Environmental Dispersion 3-8
  - 3.3.3 Environmental Transfer Models 3-10
  - 3.3.4 Dose Models 3-11
  - 3.3.5 Disposal Options 3-12

4.0 STRUCTURE AND FEATURES OF THE URANIUM TAILINGS ASSESSMENT PROGRAM (UTAP) 4-1
- 4.1 UTAP Structure 4-1
- 4.2 UTAP Features 4-3

5.0 PHASE III PROBABILISTIC ASSESSMENT RESULTS 5-1
- 5.1 Introduction 5-1
- 5.2 Scenario 1: The Base Case 5-2
  - 5.2.1 Dose by Pathway 5-3
  - 5.2.2 The Water Pathways 5-4
  - 5.2.3 Importance Analysis 5-8
- 5.3 Spatial Characteristics 5-9
- 5.4 Scenario 2: Pyrite Reduction and Lime Addition 5-9

6.0 SUMMARY AND RECOMMENDATIONS 6-1
- 6.1 Summary 6-1
- 6.2 Recommendations 6-3

7.0 References 7-1

# LIST OF TABLES

Follows Page

3.1 Characteristics of Reference Watershed 3-2

5.1 Parameter Sensitivity Index Values for the Base Case (Scenario 1) 5-8

5.2 Selected Parameter Definitions 5-8

# LIST OF FIGURES

| | | Follows Page |
|---|---|---|
| 2.1 | Concept of Probabilistic Analysis | 2-3 |
| 2.2 | Displaying Probabilistic Results | 2-4 |
| 2.3 | Confidence Bands | 2-9 |
| 2.4 | Time Dependent Output | 2-11 |
| 3.1 | Reference Site: Tailings Area | 3-1 |
| 3.2 | Reference Site: Overview | 3-2 |
| 3.3 | Exposure Pathways Analysed | 3-3 |
| 3.4 | Concept Adopted for Modelling The Tailings Source Term | 3-4 |
| 4.1 | The System Model | 4-1 |
| 4.2 | UTAP Control Module Structure | 4-2 |
| 4.3 | UTAP Component Module Structure | 4-2 |
| 4.4 | UTAP Overview of Spatial Features | 4-6 |
| 5.1 | Exposure Pathways Analysed in Phase III | 5-1 |
| 5.2 | Dose vs. Time by Pathway (Scenario 1) | 5-3 |
| 5.3 | Total Dose Histogram (Scenario 1) | 5-4 |
| 5.4 | 95% Confidence Band onTotal Dose at t=500 Years (Scenario 1) | 5-4 |
| 5.5 | Drinking Water Dose vs. Time by Radionuclide (Scenario 1) | 5-4 |
| 5.6 | Tailings Source Inputs of Radium-226 Activity (Scenario 1) | 5-6 |
| 5.7 | Radionuclide Activity vs. Time (Scenario 1) | 5-7 |
| 5.8 | Drinking Water Dose vs. Time for Three Receptors (Scenario 1) | 5-9 |
| 5.9 | pH vs. Time for Three Watershed Locations (Scenario 1) | 5-9 |
| 5.10 | Radon Dose vs. Time for Three Receptors (Scenario 1) | 5-9 |

List of Figures (Cont'd.)

| | Follows Page |
|---|---|
| 5.11 pH vs. Time at Three Watershed Locations (Scenario 2) | 5-10 |
| 5.12 Dose vs. Time by Pathway (Scenario 2) | 5-11 |
| 5.13 Total Dose Histogram (Scenario 2) | 5-12 |
| 5.14 Drinking Water Dose vs. Time by Radionuclide (Scenario 2) | 5-12 |
| 5.15 Comparison of Total Dose Distributions for Scenarios 1 and 2 | 5-13 |
| 5.16 Comparison of Scenario 1 95% Confidence Bands with Scenario 2 | 5-13 |

# 1.0 INTRODUCTION

## 1.1 Background

In 1982 Energy, Mines and Resources Canada established the National Uranium Tailings Program (NUTP) to pull together previous work on Canadian uranium mill tailings, to fund additional work where significant information gaps were found and to develop the capability to predict the long-term effects of tailings with a known degree of confidence while incorporating variability and uncertainty in the input data. Such evaluations require the use of mathematical models to simulate the behaviour of the real system.

An earlier study (Phase I) funded by the NUTP demonstrated how probabilistic techniques could be used to take account of the variability and uncertainty in model input parameters in such a simulation analysis (SENES 1984). In Phase I quasi-steady-state models of a simplified, hypothetical, reference tailings site were used to demonstrate the feasibility and appropriateness of probabilistic analysis. Environmental pathways models were used to estimate human exposure from the release of radium-226 to the air and water and radon-222 to the air. A number of related technical and philosophical matters were addressed in a series of review papers.

Subsequently, the NUTP sponsored a followup study (Phase II) to extend and refine the probabilistic tools developed in the Phase I study and to investigate various issues of technical interest involved in carrying out and interpreting a probabilistic analysis (SENES, 1985). The Phase II work built upon Phase I results in order to demonstrate broader application of the probabilistic technique. In particular, the environmental component models and overall systems framework were modified and expanded to explicitly incorporate the time-varying behaviour of the natural system. As well, an additional radionuclide (thorium), several inorganic chemical species (calcium, sulphate and iron) and pH were modelled.

Sensitivity/uncertainty analysis techniques were investigated in detail in Phase II and were applied to probabilistic results, indicating pathways and parameters of importance to the hypothetical reference site. Order of magnitude estimates of the long-term effects (and associated uncertainties) of a number of different tailings management "scenarios" were also obtained.

As well, a number of special topics were investigated in Phase II including:

- interpretation of probabilistic results
- methods for estimating confidence regions on output distributions
- techniques for handling correlated parameters
- model response to time-variant input parameters
- implications of model aggregation for use in assessment models.

## 1.2 Scope of Phase III Studies

The underlying objective of the Phase III studies, which are described in this report, was to extend the capabilities of the Phase II system model and then to apply the Phase III system model to an expanded hypothetical reference site. Among the tasks addressed in Phase III were:

- expand the simulation models to include additional major radionuclides and water erosion of tailings cover materials
- expand the simulation models to include additional selected pathways of exposure
- modify the system model to permit air dispersion calculations to be carried out to greater distances in all directions
- modify the system model to permit water dispersion calculations to be performed on an entire watershed
- streamline the system code, update the documentation and prepare a user's manual

As well, a number of special activities related to the development, use, or interpretation of probabilistic assessment codes were carried out, including:

- an extensive program of software quality assurance including: testing of the random number generator; an intercomparison study with two other probabilistic assessment codes; testing of the system's control modules; and testing of the Phase III component modules, both on a stand alone basis and integrated within the system model
- further investigation of the use of aggregate models in environmental assessment
- implementation of a technique for placing confidence bands on the output of probabilistic (i.e. Monte Carlo) calculations

## 1.3 Report Structure

Because the Phase III studies covered a variety of aspects of substantially different form and content and because of the sheer volume of material, the Phase III report has been prepared in the following four volumes:

Volume 1: Probabilistic Model Development for the Assessment of Uranium Mill Tailings in Canada - Phase III, Volume 1: Summary Report.

Volume 2: Probabilistic Model Development for the Assessment of Uranium Mill Tailings in Canada - Phase III, Volume 2: System Description and Control Module Documentation.

Volume 3: Probabilistic Model Development for the Assessment of Uranium Mill Tailings in Canada - Phase III, Volume 3: Component Model Documentation.

Volume 4: Probabilistic Model Development for the Assessment of Uranium Mill Tailings in Canada - Phase III, Volume 4: Uranium Tailings Assessment Program (UTAP) User's Manual.

## 2.0 PROBABILISTIC ANALYSIS CONCEPTS

The focus of the NUTP modelling work, of which this study is part, is to provide a tool which can be used to quantitatively assess the long-term effects of uranium mill tailings. It is important to recognize that real systems, such as uranium tailings facilities are quite complex and will vary from site to site. Moreover, the physical and chemical features of existing uranium tailings sites will undoubtedly change with time.

In this, and the previous two studies, the uranium mill tailings system is represented by a network of interconnected component models. At the Phase III level of development the mathematical models are a mix of quite complex component models (e.g. the tailings source term) and simpler aggregate models (e.g. transfer of radionuclides from water to fish flesh). This approach provides a flexible structure which can easily accommodate changes in component models and model input parameters. The models, to date, have been developed for a hypothetical, "reference" tailings facility. The computer implementation of these models (along with the probabilistic infrastructure) is known as the Uranium Tailings Assessment Program (UTAP).

Traditionally, the models have been evaluated in a deterministic fashion. Specifically, this means that a single value is selected for each input parameter of the simulation model(s) resulting in a single estimate of some environmental consequence, such as dose to an individual in the critical group, or pH in a downstream lake. However, by their very nature, models are at best imperfect reflections of real systems. Moreover, many of the parameters used as inputs to the models are either imperfectly known or inherently variable. Over the past decade or so considerable effort has been directed at developing techniques for explicitly incorporating such uncertainty (and variability) directly into the model prediction. In general terms we refer to this as probabilistic analysis.

Two fundamental types of uncertainty need to be considered in the evaluation of uranium mill tailings. First, there is uncertainty about how well the mathematical, assessment models describe the essential physical and chemical processes associated with the uranium tailings system and surroundings. Second, there is uncertainty introduced by imperfectly known or variable parameters. The first type of uncertainty is related to model validation; that is, demonstration that the mathematical representation and the associated computer code adequately describe the real system. Clearly, the effects of this type of uncertainty are difficult to quantify during model development. In this report we adopt the position that our mathematical descriptions of the real system are appropriate for assessment purposes. Furthermore, we attempt to ensure that the mathematical abstractions are correctly implemented in computer code through an extensive quality assurance program (see Volume 2, Appendix A).

The focus of this report, as was the case in the Phase I and Phase II studies (SENES, 1984; SENES, 1985), is, therefore,the development of a probabilistic assessment tool which takes into account the uncertainty (or lack of knowledge), and the inherent variability in model input parameters. The remainder of this chapter reviews some concepts relevant to performing such a probabilistic analysis and interpreting the output results. Some general comments on the use of aggregate component models are also provided. Throughout this overview discussion, reference is made to appropriate sections of the Phase I, II and III studies where more detail may be found.

Later sections of this report describe the way in which the reference tailings site was modelled, the UTAP code itself and some results from an assessment of the hypothetical reference site.

## 2.1 The Concept of Probabilistic Analysis

As with any predictive assessment, probabilistic analysis involves a mathematical expression (model) of some physical system, in this case a uranium mill tailings site. The model is a mathematical expression to which information is supplied in the form of numerical values for one or more input variables and it produces the corresponding numerical values of one or more output variables.

Most of the input variables required by such a model are not known with certainty. The uncertainty arises because of normal experimental error in their measurement or because (sometimes) actual measurements are impossible and judgement must be used. Also, some input variables such as mean annual wind speed or mean annual precipitation necessarily vary from year to year. Consequently, it is impossible for most input variables to be adequately characterized by any single number. Fortunately, our full state of knowledge about any input variable can be described in the form of a (subjective) probability distribution.

Having specified the input distributions it is necessary to determine the corresponding values of the output variables. Because many of the input parameters are specified as distributions, rather than as single numbers, distributions, rather than single numbers will be obtained for the calculated variables. The distribution of calculated results is obtained by using a statistical sampling or Monte Carlo procedure which involves drawing many samples from each input parameter distribution. The procedure, illustrated in Figure 2.1, is a repetitive one. At each repetition a single value is drawn for each input variable from its probability distribution. These values of the input variables are substituted into the mathematical model (the component models) to obtain a single value for each output variable. This process, which is referred to as a trial, is then repeated as often as desired. For further details, the interested reader is referred to Appendix B of the Phase I study (SENES, 1984) and Volume 2 of this report.

The output variable(s) from such an analysis can be considered as a sample(s) on an objective random variable(s) corresponding to that output variable(s). From the sample, the mean, variance, probability density function (pdf) or cumulative distribution function (cdf) may be estimated as desired. This information may be interpreted as describing the output variable in terms of subjective probability; telling us quantitatively what we are entitled to believe about the output variable.

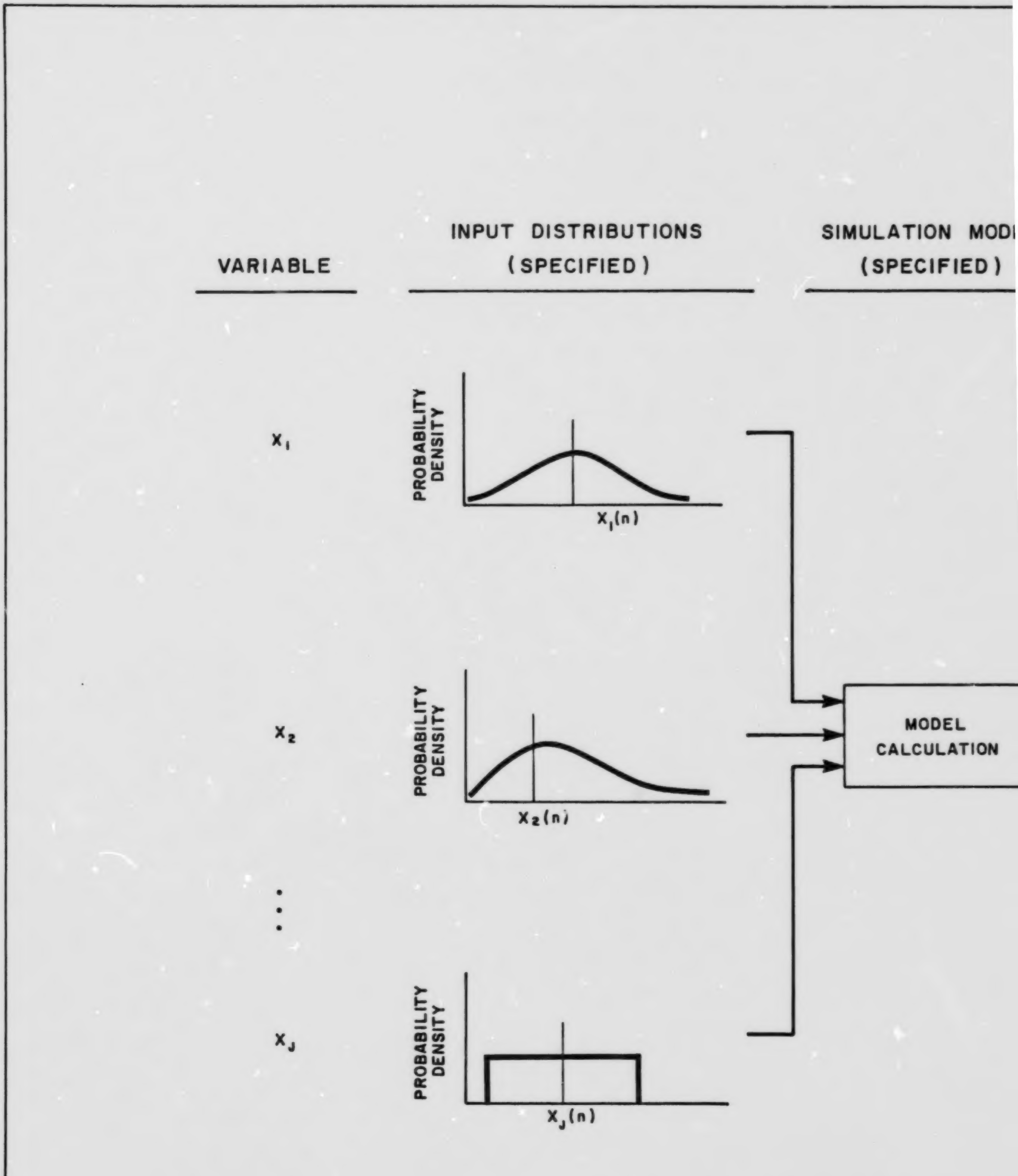
VARIABLE
INPUT DISTRIBUTIONS (SPECIFIED)
SIMULATION MOD
(SPECIFIED)
$X_1$
PROBABILITY DENSITY
$X_1(n)$
$X_2$
PROBABILITY DENSITY
$X_2(n)$
$X_J$
PROBABILITY DENSITY
$X_J(n)$
MODEL CALCULATION
REPEATED EACH TRIAL

FIGURE 2.1

CONCEPT OF PROBABILISTIC ANALYSIS

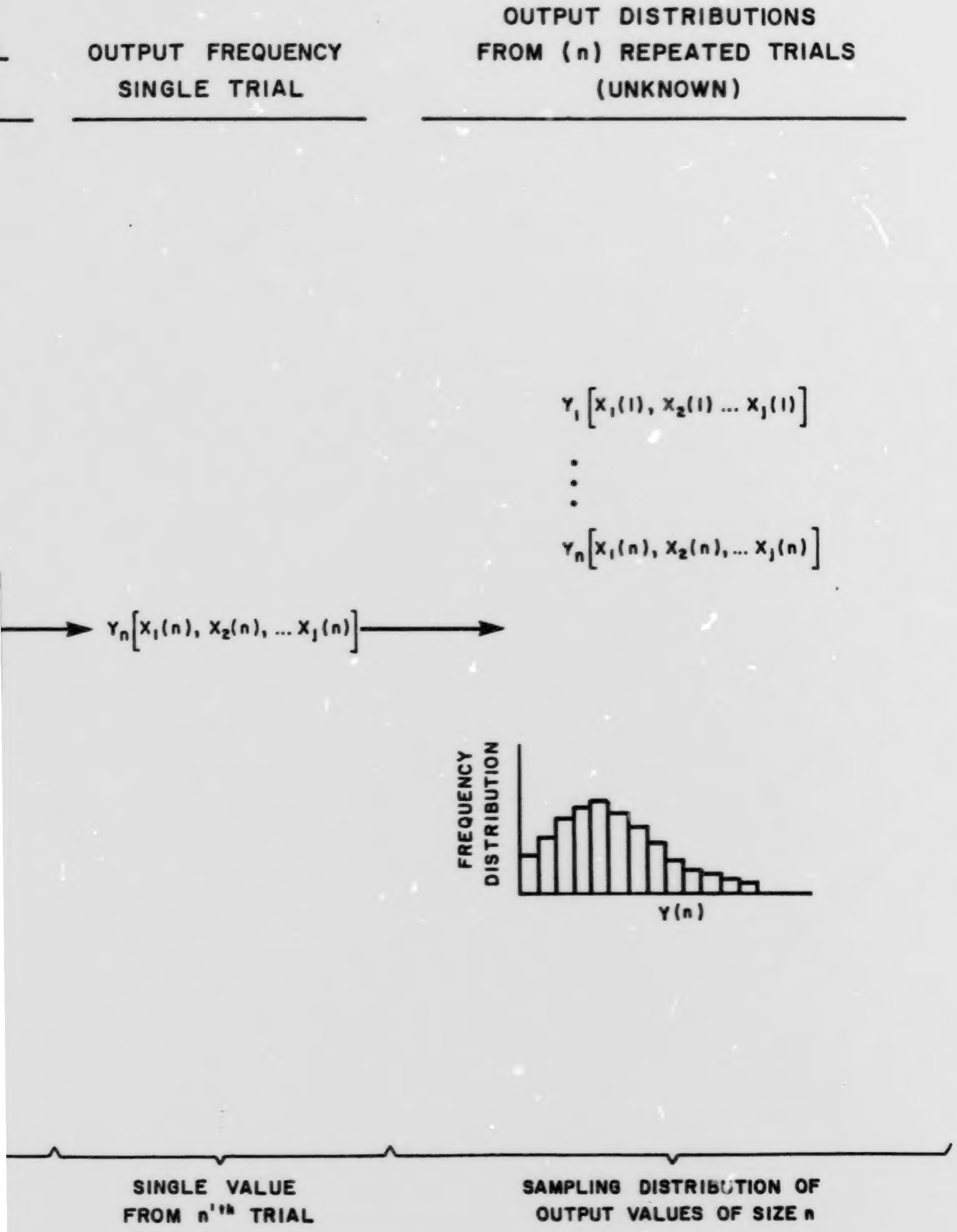
OUTPUT FREQUENCY
SINGLE TRIAL
OUTPUT DISTRIBUTIONS
FROM (n) REPEATED TRIALS
(UNKNOWN)
$Y_1\left[X_1(1), X_2(1) \dots X_j(1)\right]$
$Y_n\left[X_1(n), X_2(n), \dots X_j(n)\right]$
$Y_n\left[X_1(n), X_2(n), \dots X_j(n)\right]$
FREQUENCY DISTRIBUTION
Y(n)
SINGLE VALUE
FROM n'th TRIAL
SAMPLING DISTRIBUTION OF
OUTPUT VALUES OF SIZE n

## 2.2 Presentation of Probabilistic Results

The most important output from a Monte Carlo calculation is often the probability density function (pdf). However, the cumulative distribution function (cdf) is also useful in displaying certain kinds of information about the output variable. A representative pdf and cdf are shown on Figure 2.2. As indicated above, sample statistics such as mean or geometric mean can be calculated for the variable(s) output from a probabilistic assessment. Some statistics which we have found useful in evaluating the output of a probabilistic assessment are shown in Figure 2.2a. A review of some useful statistical concepts is provided in Appendix A of the Phase I report (SENES, 1984).

Figures 2.2a and 2.2b are actually a sample frequency diagram (histogram) and cumulative frequency diagram respectively. These staircase-like histograms are not identical to the probability density function (pdf) and cumulative distribution function (cdf) which are shown as smooth curves on Figures 2.2a and 2.2b respectively. However, as the number of samples (i.e. trials), and the number of discrete "bins" increase, the sample frequency curves generated by the analysis would be expected to resemble the (true) population probability curves more and more closely. In the following discussion we do not distinguish between "sample frequency curves" and "probability or cumulative probability curves" since we always use the sample frequency curves as our estimates of the true probability functions.

While both representations of the output variable contain the same information (the cdf is simply the integral of the pdf) the two representations are most useful for illustrating different characteristics of the output variables. In general terms the pdf is superior for communicating the qualitative features of the output distributions:

- the relative probability of specific values
- the most likely value (i.e. the mode)
- a crude estimate of the mean
- the shape of the distribution, skewness, kurtosis, etc

FIGURE 2.2

DISPLAYING PROBABILISTIC RESULTS

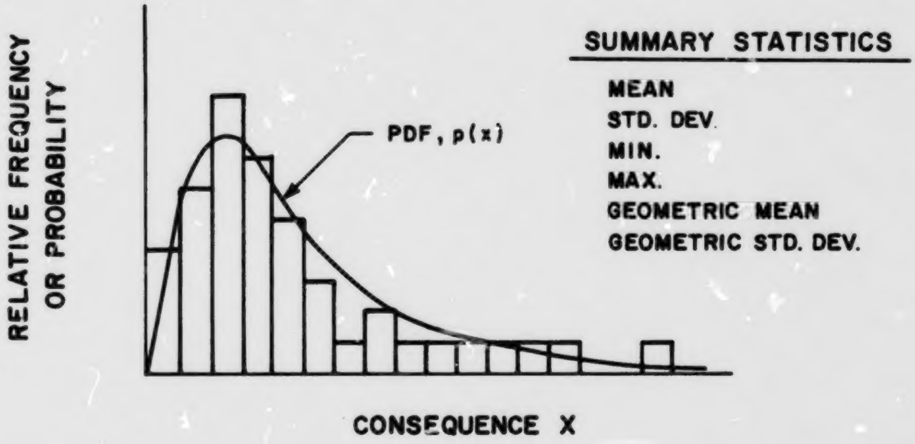

A) RELATIVE FREQUENCY HISTOGRAM AND CORRESPONDING PROBABILITY DENSITY FUNCTION (PDF)

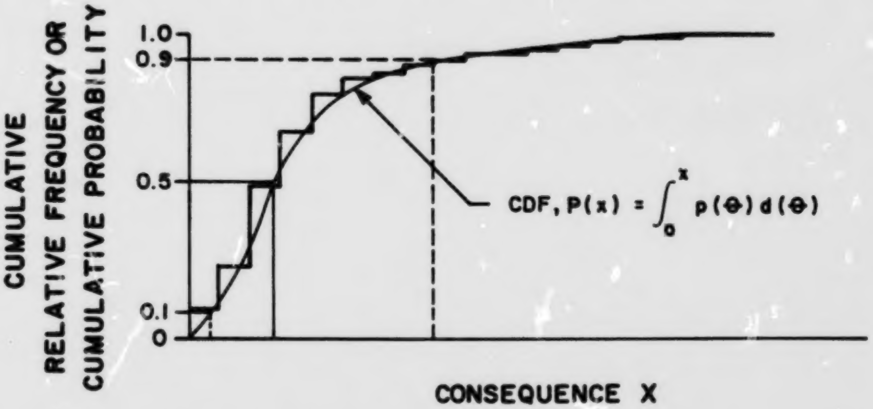

B) CUMULATIVE RELATIVE FREQUENCY AND CORRESPONDING CUMULATIVE DISTRIBUTION FUNCTION (CDF)

- small changes in probability density

In contrast, the cdf is best for communicating the numeric characteristics of the output distribution:

- fractiles, including the median
- the probability of intervals, including confidence intervals
- tail areas

Thus, since the cdf and pdf are better at communicating different features of the same distribution it is sometimes desirable to publish both together.

## 2.3 Interpretation of Probabilistic Results

In previous sections we have noted that the output distribution(s) from a probabilistic analysis describe, in terms of subjective probability, what we are entitled to believe about the output variable(s). In this study and in the previous Phase I and Phase II studies, we have developed a tool (UTAP) for analyzing the uncertainty about a particular disposal scenario. In doing so, we assume that the component models we are using provide a true (or at least reasonably true) representation of how a particular (hypothetical, reference) tailings site will evolve over time. In performing such an analysis it is necessary to select distributions for many input parameters, some of which may not only be uncertain due to lack of observational data or measurement error but also may be inherently variable either in space or time. In either case the input distributions involve some element of subjective probability in that they have been selected, by a modeller, in the belief that they best represent the data. Where the observational data base is large, the modeller may feel very confident in a data set and use it directly with the assessment; in other cases, where the modeller believes less strongly that the data base is appropriate, he may, perhaps in consultation with other experts, choose to modify the distribution before using it his model. In any event the modeller must be careful to avoid broadening the distribution so much that it loses meaning in the context of the scenario he is trying to analyse.

For example, in a model of the transfer of a radionuclide from water to fish flesh, a simple "transfer factor" might express the relationship between the radionuclide concentration in water and in fish flesh. Considerable data might be available for transfer factors determined throughout the world, for many species of fish. Such data might represent the global uncertainty about the value of the transfer factor, but would not be particularly appropriate for an analysis of a particular site. A modeller must select that subset of the global data which is applicable to the site or scenarios being modelled. Thus data for waters with certain characteristics (e.g. low alkalinity) and for certain fish species (e.g. game fish) might be selected. In summary, if the distributions are too wide, because of the inclusion of inappropriate data, the situation being modelled becomes very poorly defined, and the results may not be interpretable.

The interpretation of Figure 2.2 is dependent on the interpretation given to the distributions used to represent the uncertainties in the model input parameters. Assume for the moment that every input parameter is a constant in the real world and the input distributions represent our estimates of the degree of uncertainty about the true value of each input, i.e. each parameter has a "true" value but we are uncertain about what that true value is. The consequence is then also a fixed single value and the output of the probabilistic assessment represents our degree of uncertainty about that true value. Our "best guess" of the true value is the expected value or mean (or perhaps geometric mean) of the output distribution. The width of the output distribution represents uncertainty about the true constant value.

Alternatively, consider a second case in which all the input parameters are truly random variables such as mean annual wind speed. The input distributions then represent the annual variability in each parameter (along with any uncertainty we may have due to limited observational data). The output distribution of the probabilistic assessment then represents the year-to-year variability in the consequence. The consequence varies from year to year because the inputs vary from year to year.

In the first case noted above, the uncertainty in the predicted consequence arises from our lack of knowledge of the constant values, in the other, from our inability to predict a variable. The uncertainty is there in both cases and is characterized by the output distributions. In all cases, the output distributions can be interpreted as a subjective probability telling us quantitatively what we are entitled to believe about the output variable.

## 2.4 Confidence in Probabilistic Results

It is important to distinguish between inherent uncertainty in the value of the output variable which stems from uncertainty in the input variables, and uncertainty in the information about the output variables which is the result of sampling error caused by the Monte Carlo process. Suppose we are using UTAP to determine the probability density function of a particular output variable. If we perform only 100 trials, the frequency diagram, which is an estimate of the probability density function, is likely to be very ragged and thus it will be very difficult to estimate from it the probability density function. If many trials, say 10,000 or 100,000 are used, the frequency diagram will be smooth(er) and will represent the probability density function more closely. However, the actual value of the output variable which will be attained in the real world is still uncertain and the uncertainty is communicated quantitatively by the probability density function. This is the inherent uncertainty in the value of the variable. When only 100 trials were used there was an additional uncertainty in the determination of the (true) probability density function.

The number of Monte Carlo trials required for a particular problem depends on what information is desired about the characteristics of the output variables. If only the mean or geometric mean is desired, 50-100 repetitions are often more than ample. On the other hand if a precise estimate of the probability density function is required (i.e. a relatively smooth sample frequency diagram) it will be necessary to perform many more trials. Considerations as to how confident we can feel about the results of a probabilistic analyses are reviewed briefly below; details are provided in Appendix C of Volume 2 of the

Phase II report (SENES, 1985) and Appendices E and F of Volume 2 of this report.

## Point and Interval Estimates

Sample statistics (such as the mean and variance) calculated from the output of a probabilistic analysis provide estimates of the corresponding parameters of the underlying population. The assumption that samples are randomly drawn from the underlying population is important to ensure that the samples are representative of the underlying population and that, in turn, sample statistics are fair estimates of the population parameters. However, sample statistics such as sample mean and variance, while providing estimates of the corresponding population parameters are not, in general, exactly correct because of sampling variation. Thus, it is important to infer from the properties of the sample the range within which the (population) parameter is likely to lie.

Confidence intervals form one type of interval estimation. They define an interval within which the value of the estimated parameter is believed to be, with a stated percent confidence. The confidence level is usually high, at least 90%. The word "confidence" in this context is a very carefully defined technical term, the meaning of which is discussed below.

A confidence interval describes the unknown but constant value of a parameter in terms of an interval which is calculated from the observations of a sample. On repeatedly taking the same sized sample under the same conditions, and calculating confidence limits each time, the confidence limits will change from sample to sample while the true value of the parameter will remain constant. However, if the number of samples is indefinitely large, the fraction of confidence limits which enclose the true value approaches the stated level of confidence. The actual stated confidence interval is always calculated from a single sample set, but its explanation is in terms of the imagined scheme of indefinitely repeated sampling.

The range of values and various percentile estimates are other common measures of the dispersion in sample data. The range is simply the difference between the largest and smallest values in a sample. Percentile estimates such as the median (50th percentile), can be obtained directly from the cumulative relative frequency histograms (or cumulative distribution functions). As another example the difference between the 10th and the 90th percentile might be called the 80% probability limit and includes inherent uncertainty in the output variable (as well as residual sampling error). This is different from the confidence interval on the mean discussed previously since the uncertainty described by the confidence interval on the mean results only from sampling error. It bears no relation to the inherent uncertainty in the variable which would be conveyed by its probability density function. For example, the confidence interval for the mean would be very narrow if a very large number of Monte Carlo trials had been used, even if the distribution of the random variable were broad.

## Confidence Bands

We have already noted that the sample frequency curves (histograms) are not identical to the true underlying population probability curves, but that they would resemble the population curves more and more closely as the sample size (number of trials) increases. In the Phase I and Phase II studies (SENES, 1984 and SENES, 1985) a distribution-free technique based on an extension of the Kolmogorov-Smirnov goodness-of-fit test (as described in Kendall and Stuart (1961) or Crow et al., (1960)) was used to develop confidence bands for the cumulative distribution function. This technique illustrated in Figure 2.3(a) allows a staircase-like figure to be drawn above and below the cumulative frequency plot which establishes a confidence region for the cumulative probability function with basically the same meaning as the confidence intervals already described. That is, if the sampling were to be repeated indefinitely under the same conditions, the region between the confidence bands, which varies from sample to sample (the width of the confidence bands decreasing with increasing sample size), would completely enclose the true cumulative probability function, which remains stationary,

FIGURE 2.3
CONFIDENCE BANDS

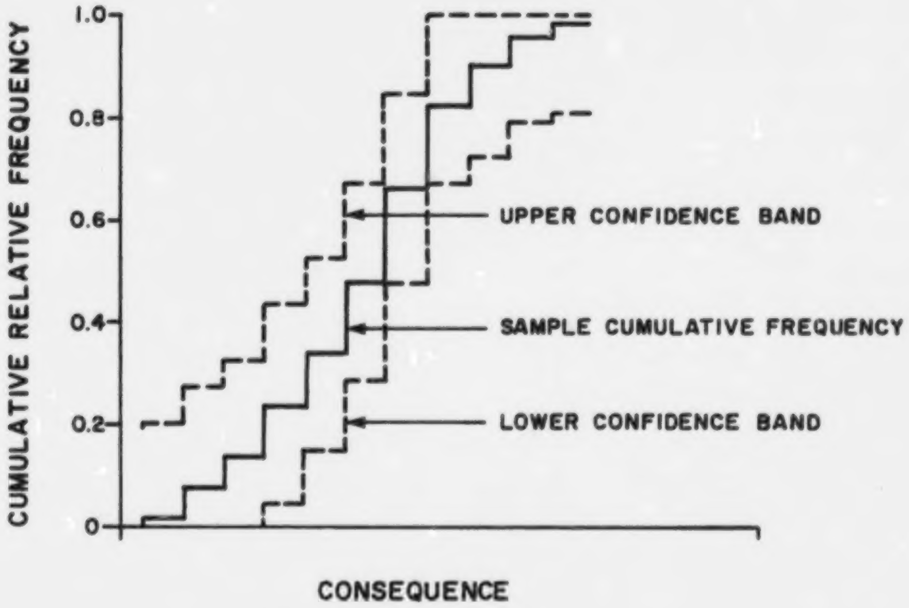

A) KOLMOGOROV-SMIRNOV TECHNIQUE

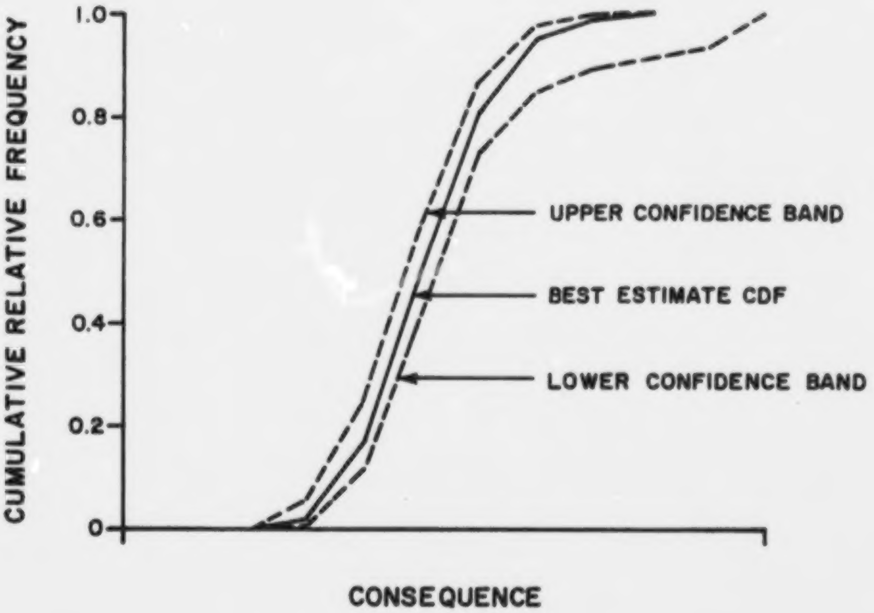

B) CHENG AND ILES TECHNIQUE

for a fraction of the samples which is numerically equal to the confidence level. The technique produces confidence bands of constant (vertical) width.

The technique, while attractive because it is simple to use, has the disadvantage of being too conservative, especially in the tails where ordinate values of less than zero for the left tail and greater than one for the right tail are produced. This weakness led to the investigation of alternative techniques for establishing confidence bands on the output of Monte Carlo trial. (see for example, the paper by Reilly and Duever and the paper by Kaplan in Volume 2) As described in Volume 2 of this report (especially Chapter 4 and Appendix F) Reilly and Duever have developed a method of estimating confidence bands from the output of a Monte Carlo simulation, based on a technique developed by Chang and Iles, (1983) within which the true probability density function (pdf) or cumulative density function (cdf) can be expected to lie with a given level of confidence. This technique has been implemented in computer code (see Appendix G of Volume 2) during Phase III and is available as a post processing option to UTAP. It provides more realistic confidence bands than the Kolmogorov-Smirnov technique, as illustrated on Figure 2.3(b). The reader interested in the technical aspects of this technique is referred to the relevant sections of Volume 2.

## 2.5 Some Aspects of Time Dependence

In the deterministic evaluation of a time-dependent simulation model, input parameters are entered into the mathematical model and values of the time-dependent output variable(s) are calculated as the system evolves in time from a specified initial state. This approach also holds in a probabilistic evaluation of the model. In this case, however, the input parameter values are not uniquely specified, but rather for each trial (i.e. each individual simulation) a set of parameter values are selected by randomly sampling from a probability distribution of possible values for each parameter. The system is then allowed to evolve through time with the parameter values fixed at the initially-selected values. In the next trial, new parameter values are selected by randomly sampling again from the specified input parameter distributions, and the system is allowed to evolve once more in time. The process is repeated until the desired number of trials have been carried out. This process is illustrated in Figure 2.4a.

In essence this procedure produces a family of (time) curves, one curve for each trial. Each curve represents the behaviour of the time-dependent variable with respect to the particular set of randomly-selected input parameters. Consider now a specific consequence (for example, total dose). Each trial will produce a different curve of consequence versus time. At any specific time the actual values calculated for the total dose may differ widely from one trial to the next. Values at a particular time from all of the trials can be used to construct a relative frequency diagram and to estimate sample statistics such as the mean and variance. The "sample" in this instance is the ensemble of individual values of total dose obtained for the same time for each trial as suggested in Figure 2.4b.

However, some input parameters, such as the quantity "mean annual precipitation" may vary from year to year. The value of this parameter in any past year is known (in the sense that it can be estimated from observational data) and is a single constant value (except for observational uncertainty). However, the mean annual precipitation varies from year to year and hence, even if there were no observational uncertainty, the amount of precipitation in any future year would be inherently uncertain, in the sense that it would vary from year to year. Variability from year to year in input parameters also gives rise to uncertainty in the output variable. In general terms, such time-varying parameters can be treated in UTAP, in one of three ways:

1) where a time increment of one year is used in the simulation each time-variant parameter is sampled directly from the distribution of annual values at each time increment;

FIGURE 2.4

TIME DEPENDENT OUTPUT

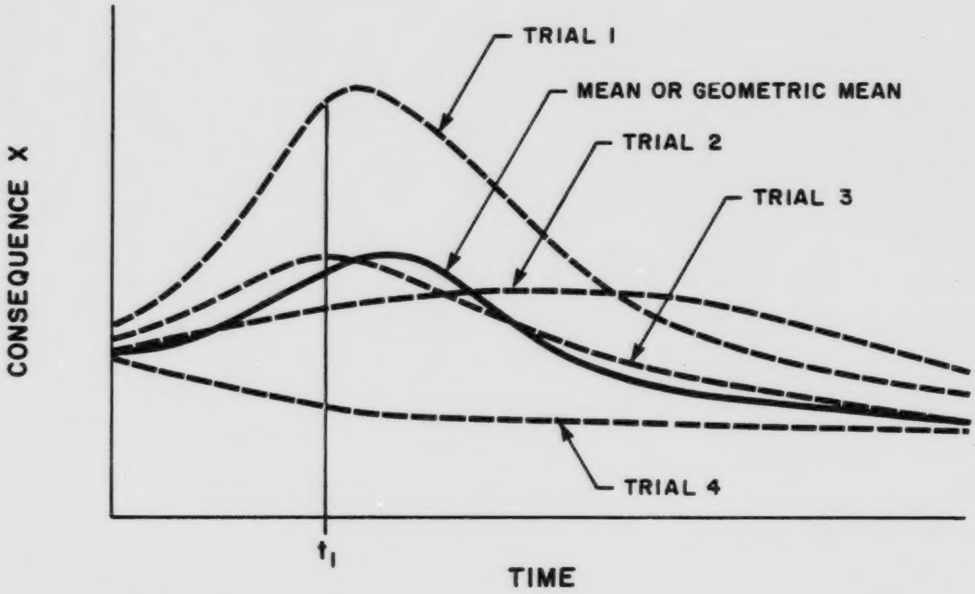

A) CONSEQUENCE, X vs. TIME

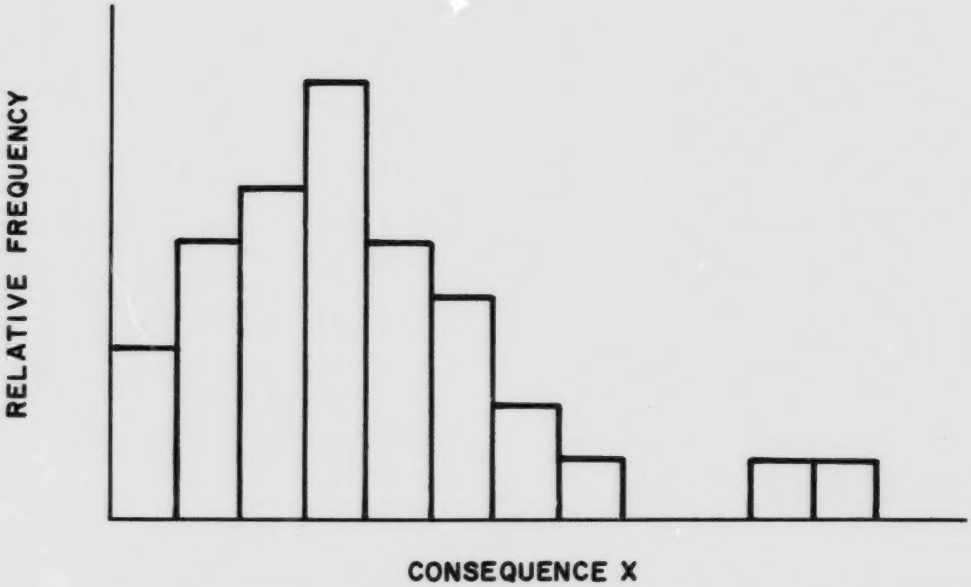

B) RELATIVE FREQUENCY HISTOGRAM AT $t_1$

2) where a larger time increment is used in the simulation, the distribution of mean annual parameter values requires adjustment. (Specifically, the mean of the distribution is preserved, while the standard deviation is reduced by $1/\sqrt{n}$, where n = the size of the time step.)

3) time varying parameters such as precipitation can be treated as constants set at their long-term mean value

As noted in Section 4 of this volume and in Volume 2, two time-steps, namely 1 year and 10 years were implemented within UTAP and can be used without any programming changes. For most purposes a time step of 10 years is recommended.

To summarize, uncertainty in model predictions(s) may arise from a lack of knowledge of the constant input parameters or from a lack of ability to predict the time-variant parameters. Uncertainty of both sorts is propagated through the mathematical models and is inherent in the output distribution(s) (SENES, 1985). The effect of accounting for the uncertainty in time-variant parameters was examined in depth in Appendix D of Volume 2 of Phase II. In any case the output distribution(s), which can be interpreted in terms of subjective probability, describes how strongly one is entitled to believe in a particular consequence in a particular year.

## 2.6 Model Aggregation

In modelling complex systems such as uranium mill tailings and their environs, there is a natural tendency to develop detailed mathematical models to simulate the complex, multi-variate processes which affect contaminant release and movement. Indeed, complex models are desirable for studying and understanding system dynamics. However, for assessment purposes, where the objective is to predict effects many years (or perhaps even hundreds of years) into the future, a much simpler model can often be used to make reliable predictions. The term model aggregation as used herein refers to the mathematical "lumping" of complex multi-variate processes into simpler expressions.

The UTAP code contains component models with varying levels of complexity. In general, the source term component models are relatively complex, since what happens in the tailings strongly influences the environmental and dose consequences. The air and water dispersion models are moderately complex while the environmental transfer and dose models are relatively simple.

The use of simple, aggregate models of radium-226 transfer to fish flesh from water and to vegetation from air was investigated in Phase II (see Appendices G and J respectively of Volume 2; SENES, 1985). This work was supported by a followup investigation on uranium transfer to fish flesh from water in this study (see Appendix B of Volume 3). The results of these investigations support the use of the aggregate models for predicting contaminant levels in environmental media in long-term simulations such as provided by the UTAP code. The more complex models were found to be most appropriate for predicting dynamic response to short-term changes.

## 2.7 Parameter Importance Analysis

In probabilistic modelling, the terms sensitivity and uncertainty analysis refer to techniques which seek to define the relationship(s) between model inputs and model predictions. The term "sensitivity analysis" refers to establishing the sensitivity of the magnitude of the model output to changes in the magnitudes of the input parameters. The term "uncertainty analysis" refers to establishing how much the uncertainty (or spread) associated with each parameter contributes to the total uncertainty (or spread) of the model predictions. Parameters to which model predictions are sensitive and/or parameters which contribute an appreciable fraction of the uncertainty to the model predictions are called "important" parameters in this report. The use of sensitivity and uncertainty analysis techniques to isolate and/or rank the most "important" parameters, i.e. those which have the greatest influence on the model predictions, is referred to as "importance" analysis. The techniques are equally useful in identifying those parameters and pathways which are important, and also those which are unimportant and thus can be de-emphasized in planning future research investigations.

Two sensitivity and uncertainty analysis techniques, namely the sensitivity index and step-wise regression were selected for use in the Phase II studies and applied to the results of the Phase II assessment. No further examination of the techniques of importance analysis were carried out in Phase III and thus importance analysis techniques are not discussed further in the Phase III documentation.

The reader interested in the various techniques of sensitivity and uncertainty analysis is referred to the Phase II report (SENES, 1985) and the extensive literature on the subject including, for example, recent articles such as those by Iman and Helton (1985), Downing et al., (1985), Gardner (1985), Hoffman and Gardner (1983), Hendrickson (1984), INTERA (1983), and Rose and Swartzman (1981). For a fuller discussion of regression analysis the reader should refer to Draper and Smith (1981) and Edwards (1979).

## 2.8 Identifying and Incorporating Parameter Correlation

During the Phase II studies, Andres and Goodwin (SENES, 1985; Volume 2) examined various techniques to generate correlated parameter values for use in probabilistic assessment. In part as an outcome of these investigations, a two-pronged approach to incorporating parameter correlation was adopted in Phase III.

First, where the form of a relationship between parameters was known or suspected, a functional relationship was considered to be the easiest way to express the dependence. A functional relationship is a formula that expresses one parameter as an explicit function of other, more basic, parameters. One of the benefits of developing functional relationships among parameters is the opportunity provided to put components of the model to experimental test. It is much easier to generate evidence to reject a faulty relationship than it is to reject a correlation coefficient.

Second, for situations where correlation was believed to exist but where it was not possible to establish functional relations (the preferred approach) a technique developed by Kleijnen (1974) for enforcing pair-wise correlation was selected for use.

The technique of Kleijnen achieves uniqueness in generating a sample from a pair of correlated variables by preserving the entire distribution of one variable, the mean and variance of the second variable, and the correlation coefficient between the two. (The algorithm is presented in the paper by Andres and Goodwin in Appendix E of Volume 2, Phase II (SENES, 1985)). This technique has been implemented and forms part of the UTAP code as noted in Chapter 4 of this volume and in Volume 2.

Early in the Phase III studies it became clear that it is often not easy to identify where correlations exist and how strong they are. According to Andres (Volume 2, Appendix H of this report) observing correlations in experimental data is the preferred approach. However, research programs to obtain the experimental data for such an analysis may not be possible for cost or other reasons. For example, in the case of uranium mill tailings we are often interested in looking tens to hundreds of years into the future. Experiments over such a time frame are simply not possible. Thus, in many situations of practical interest, it is necessary to rely on the opinions of knowledgeable persons to identify where parameter correlations may exist and, if they are believed to exist, how strong they are.

In his paper, Andres proposes a systematic approach toward the identification of parameter correlation using expert opinion (see Appendix H of Volume 2). The Phase III radon flux model was used in Appendix I of Volume 2 as the basis for the trial application of Andres' technique. Subsequently Kleijnen's technique was used to investigate the effect of introducing correlated parameters into the Phase III radon flux model. As noted in Appendix I of Volume 2 one of the principle benefits of attempting to identify parameter correlation is the considerable insight the exercise provides into the nature of the actual physical processes and their mathematical representation.

## 3.0 APPROACH TO MODELLING

The development of mathematical models describing the physical and chemical characteristics of the tailings and surrounding environment formed a major part of this study. To facilitate model development, review and modification, the models were developed in a modular fashion. Thus, each "component model", as they are termed, reflects one aspect of the environment being modelled. At the present level of development, the mathematical models used to simulate the tailings system are a mix of quite complex component models (e.g. the tailings source term) and simpler aggregate models (e.g. transfer of radionuclides from water to fish flesh).

This chapter provides an overview of the modelling approach employed in this study. The reference tailings site, the human receptors, and environmental pathways modelled are all described. As well, the concepts underlying many of the component models are outlined briefly.

### 3.1 The Reference Site

The basic characteristics of the hypothetical, reference, tailings site used in previous NUTP modelling studies (SENES, 1984; SENES, 1985) have been preserved in this study. As shown on Figure 3.1, the tailings disposal site occupies a natural depression, formed within the upper reach of a valley. The tailings are contained behind a conventional, slightly pervious dam constructed across the low point. Surface and groundwater flows from the site are assumed to follow the valley surface features with ultimate discharge to a major river which flows into a lake.

The reference tailings site is defined to have a surface area of 50 ha and an average tailings depth of 10 m for a total volume of $5 \times 10^6$ $m^3$. The reference tailings have characteristics representative of those resulting from the acid leaching of low-grade pyritic uranium ore containing approximately 0.1% uranium. Most of the uranium is assumed to be recovered during milling, while all of the other radionuclides are assumed to remain with the tailings.

FIGURE 3.1

## REFERENCE SITE: TAILINGS AREA

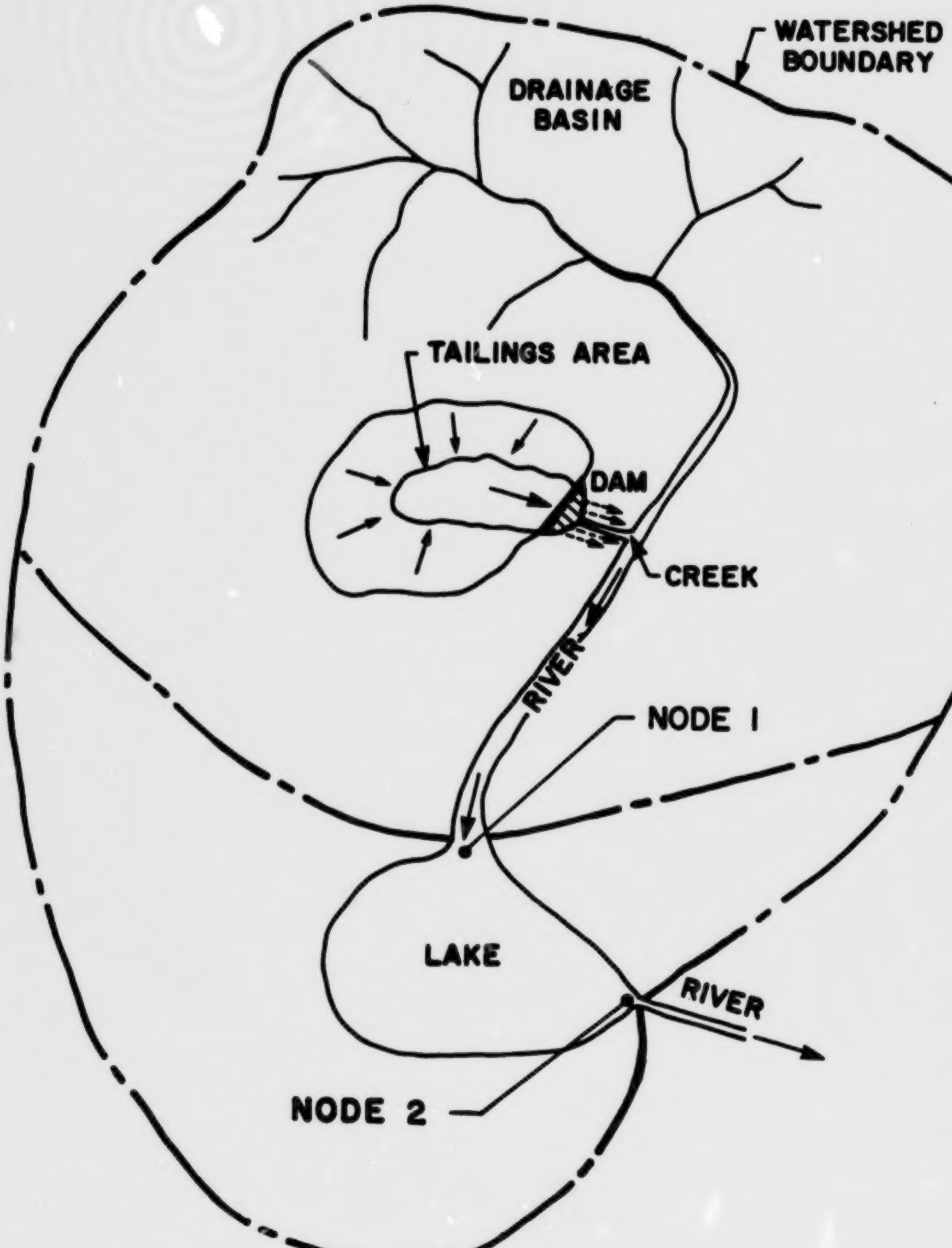

WATERSHED BOUNDARY
DRAINAGE BASIN
TAILINGS AREA
DAM
CREEK
RIVER
NODE 1
LAKE
RIVER
NODE 2

The tailings are neutralized in the mill by lime addition prior to discharge to the tailings areas.

In this study, the effects of the tailings on a much larger environment than in previous studies are modelled. The Uranium Tailings Assessment Program (UTAP) is designed to make predictions in all directions, for up to a 50 km radius from the tailings. The program also models an entire watershed, receiving surface and groundwater flows from the tailings area. An overview of the reference tailings area, in the context of its larger setting is presented in Figure 3.2.

As indicated on the figure, the entire reference site now includes an area of 50 km radius, centered on the tailings. The reference watershed is composed of a series of river and lake segments, which are specified in the program as "nodes". Thus, (as indicated on Figures 3.1 and 3.2) node 1 represents the river which receives runoff and groundwater seepage from the tailings area. Node 2 represents the first lake in the watershed, and so on. The first river and lake in the system have the same characteristics as the receiving river and lake in previous phases. The physical characteristics of the reference watershed modelled in this study are summarized in Table 3.1.

UTAP allows the calculation of the consequences (i.e. dose) to receptors living in any or all of the 80 locations indicated on Figure 3.2. Most of the results presented in this study (see Chapter 5) involve the dose to a "critical" type receptor living 2 km due east of the tailings (i.e. in ring 1, sector 5 on Figure 3.2), who obtains his drinking water from node 2 of the watershed (i.e. the first lake). In keeping with previous studies, this receptor was chosen to be on adult male (i.e. Reference Man as defined in ICRP 23 (1975)) who primarily lives off the land. He derives much of his diet from local sources, including vegetables, meat and fish. His drinking water and fish are taken from the first lake downstream of the tailings area. In addition to the specific critical receptor examined in most of the analyses, "average"-type receptors can also be modelled. The average receptors are assumed to have more conventional lifestyles; deriving very little of their

FIGURE 3.2
REFERENCE SITE: OVERVIEW

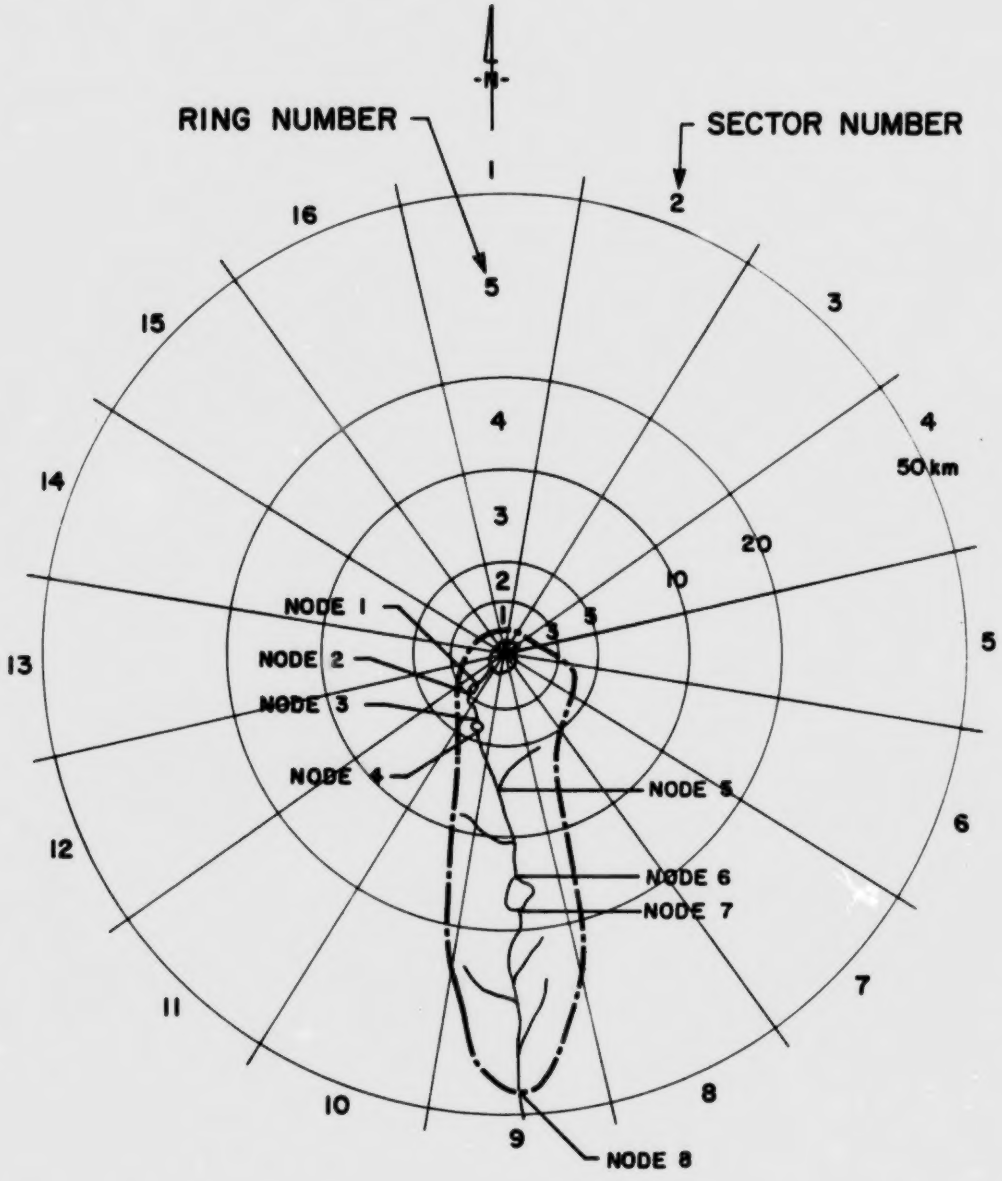
N
RING NUMBER
SECTOR NUMBER
1
2
3
4
5
6
7
8
9
10
11
12
13
14
15
16
5
4
3
2
1
3
5
10
20
50 km
NODE 1
NODE 2
NODE 3
NODE 4
NODE 5
NODE 6
NODE 7
NODE 8

Table 3.1

## CHARACTERISTICS OF REFERENCE WATERSHED

| | Segment Details | | | | Watershed Area | | | |
|---|---|---|---|---|---|---|---|---|
| End Node No. | Segment Type | River Reach Length (m) | Lake Mean Depth (m) | Lake Surface Area (m**2) | Sub-basin Area (km**2) | Cumulative Area (km**2) | End Node Windrose Location Sector | Ring |
| 1 | River | 3.0E3 | | -- | 15 | 15 | 11 | 1 |
| 2 | Lake | -- | 10 | 5.0E5 | 5 | 20 | 11 | 1 |
| 3 | River | 3.5E3 | | -- | 12 | 32 | 10 | 2 |
| 4 | Lake | -- | 4 | 2.5E5 | 6 | 38 | 10 | 2 |
| 5 | River | 7.0E3 | | -- | 32 | 70 | 9 | 3 |
| 6 | River | 1.3E4 | | -- | 50 | 120 | 9 | 4 |
| 7 | Lake | -- | 5 | 4.0E6 | 20 | 140 | 9 | 4 |
| 8 | River | 3.0E4 | | -- | 260 | 400 | 9 | 5 |

food from local sources. These receptors were modelled in a number of different locations.

## 3.2 Environmental Pathways

Assessment of the radiation dose to the receptor(s) from radionuclides released from the reference tailings site was undertaken by pathways analysis. A simplified diagram showing the pathways selected for investigation in Phase III is presented in Figure 3.3. The exposure pathways include:

- radon inhalation
- dust inhalation
- external exposure (groundshine)
- ingestion of vegetables
- ingestion of meat (caribou and moose)
- ingestion of water
- ingestion of fish

A number of pathways (or parts of pathways) not considered in Phase II were included in this study. The first additional model was the subsurface water transport model; which was considered only peripherally in Phase II. It provides a source of additional radionuclide loading to the surface water pathways. Aquatic plants were also modelled in this study. They represent a path of radionuclide transfer from water to moose. The entire moose pathway is also new. Another new element in the analysis is the soil compartment. Radionuclide accumulation in the soil contributes to the uptake of radionuclides by plants and also acts as a source of external exposure (groundshine).

## 3.3 Environmental Models

To fulfill the Phase III objectives, many modifications and additions were required to the mathematical models developed in Phase II. The following section provides a brief description of the essential elements of the Phase

FIGURE 3.3

EXPOSURE PATHWAYS ANALYZED

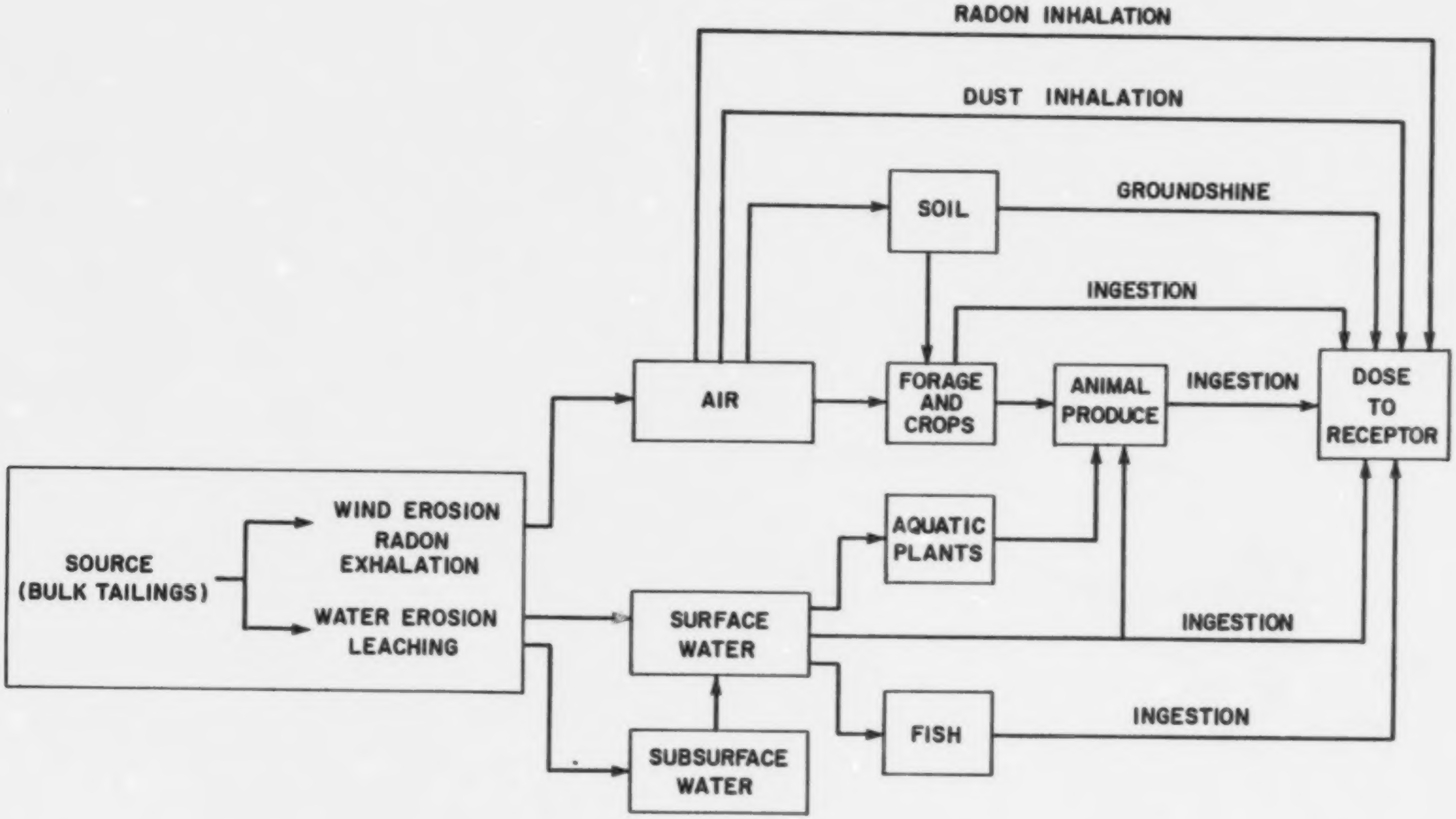
RADON INHALATION
DUST INHALATION
SOIL
GROUNDSHINE
INGESTION
AIR
FORAGE AND CROPS
ANIMAL PRODUCE
INGESTION
DOSE TO RECEPTOR
SOURCE (BULK TAILINGS)
WIND EROSION
RADON EXHALATION
WATER EROSION
LEACHING
AQUATIC PLANTS
SURFACE WATER
INGESTION
FISH
INGESTION
SUBSURFACE WATER

III component models. The reader interested in the details of the mathematical formulations as well as a description of the model parameters, is referred to the model descriptions in Volume 3 of this report.

### 3.3.1 The Tailings Source Term

Radioactive and non-radioactive constituents from the tailings are released to air and water and are subsequently transferred to, and accumulate in, the various environmental compartments. The rate of release of constituents to the environment changes with time. Consequently, the physical and chemical processes, which describe the behaviour of radionuclides within the tailings mass, determine to a large extent the overall time-dependent behaviour of the system. The water and air components of the tailings source term are discussed below.

#### The Water Source Term

In Phase III, the tailings are modelled as a layered system, much as in Phase II. The layered structure is illustrated in Figure 3.4 and explained in more detail in Chapter 3 of Volume 3. As indicated on the figure, the tailings consist of an upper, unsaturated (oxidizing) zone and a much thicker, saturated (reducing) zone. The tailings contain significant quantities of gypsum ($CaSO_4$) and other sulphate complexes. Over time, these sulphate compounds dissolve, and are gradually depleted. The depletion is hypothesized to proceed as a series of fronts moving downward through the tailings. Since the different sulphate compounds have different solubilities, the fronts may move at different rates. The tailings above each front are thus depleted of the sulphate complex, while the layer below the front is enriched in the same compound.

The upper 1 m of the saturated zone has been specified for modelling purposes as a 'mixing layer' in which adsorption of several species may occur. This feature is necessary to account for the natural retardation processes which occur in large tailings areas.

FIGURE 3.4

CONCEPT ADOPTED FOR MODELLING THE TAILINGS SOURCE TERM

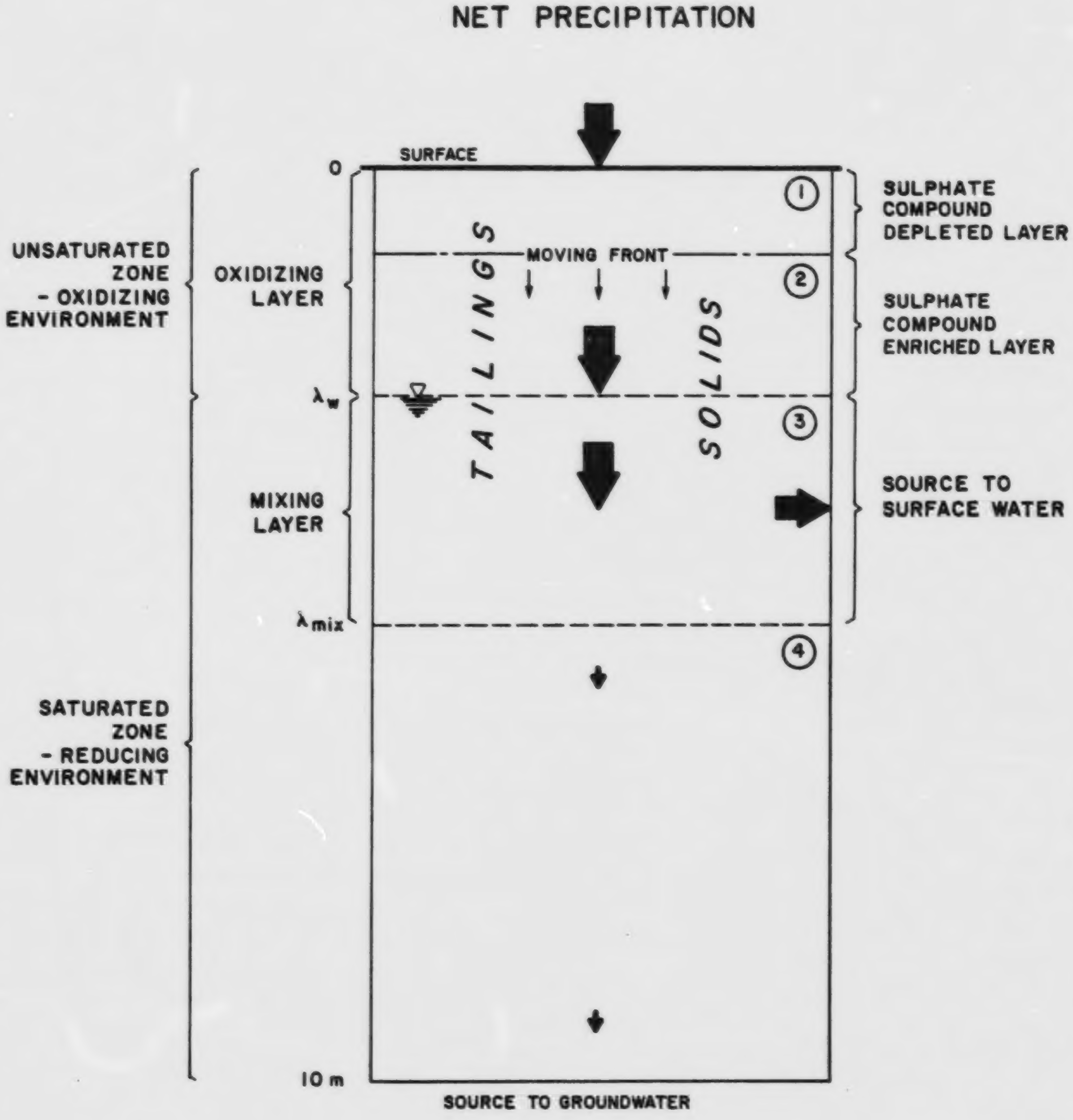
NET PRECIPITATION
SURFACE
0
UNSATURATED ZONE - OXIDIZING ENVIRONMENT
OXIDIZING LAYER
①
SULPHATE COMPOUND DEPLETED LAYER
MOVING FRONT
②
SULPHATE COMPOUND ENRICHED LAYER
TAILINGS
SOLIDS
$\lambda_w$
③
MIXING LAYER
SOURCE TO SURFACE WATER
$\lambda_{mix}$
④
SATURATED ZONE - REDUCING ENVIRONMENT
10 m
SOURCE TO GROUNDWATER

The species modelled within the water source term include sulphate, calcium, iron, natural uranium (U-nat), total thorium (Th-230 + Th-232), radium-226 and lead-210. The pH of the tailings porewater is also calculated, based on ionic equilibrium considerations. To model the liquid phase concentrations of the aforementioned species, solid phase concentrations of a number of compounds are also determined.

Much of the chemical behaviour of the tailings is directly or indirectly dependent on the oxidation of pyrite ($FeS_2$), which results in the production of sulphate ions ($SO_4^{2-}$). Sulphate ions are also produced via the dissolution of gypsum and other sulphate compounds. Because of pyrite oxidation, the sulphate concentration increases with depth in the unsaturated tailings zone. Hence, sulphate compounds which dissolve near the tailings surface may reprecipitate lower in the unsaturated zone, as the sulphate concentration increases. As mentioned previously, this results in upper layers depleted of sulphate compounds and lower layers enriched in the same sulphate compounds. The fronts separating the layers move at different rates depending on the compound's solubility. Three such sulphate compounds are modelled in Phase III; calcium sulphate ($CaSO_4$), barium sulphate ($BaSO_4$) and lead sulphate ($PbSO_4$).

The pH in the tailings is largely determined by the concentrations of sulphate, calcium and iron ions in the various tailings layers. Since gypsum dissolution acts as the only source of calcium (unless limestone has been added to the tailings as a disposal option), and since it also affects the sulphate concentration, it has a major bearing on the calculation of pH.

Soluble uranium is assumed to be associated with pyrite. Hence, as pyrite oxidizes, the associated uranium dissolves. This results in a decrease in dissolved uranium concentration with time as the pyrite inventory is depleted.

The dissolution of thorium is modelled as a function of porewater pH. Available information indicates that as the pH rises above 4.0 to 4.5, the solubility of thorium decreases rapidly. Thus, dissolved thorium concentrations decrease with time as the porewater pH increases.

All of the soluble radium-226 is assumed to exist as a co-precipitate with barium sulphate. Thus as the $BaSO_4$ dissolves, the associated radium-226 also dissolves: as $BaSO_4$ reprecipitates, so does radium-226. Because barium radium sulphate forms a non-ideal solid solution, the fraction of radium-226 in the reprecipitated solid phase is greater than that in the surrounding porewater. Hence radium-226 tends to concentrate in the $BaSO_4$ enriched zone; resulting in ever increasing solid and liquid phase radium concentrations as the thickness of the enriched zone decreases to zero.

The lead-210 is modelled in a manner analagous to radium-226. Soluble lead-210 is assumed to exist as a solid co-precipitate with other lead isotopes as lead sulphate ($PbSO_4$). Lead-210 undergoes dissolution and reprecipitation as just described. However, because it forms an ideal solid solution, it does not tend to concentrate in the $PbSO_4$ enriched layer. That is, the fraction of lead-210 in $PbSO_4$ does not change with time or depth in the tailings.

All of the radionuclides are assumed to be affected by adsorption in the saturated zone. This reflects the natural retardation processes which occur in large tailings areas. Adsorption on organic and inorganic solids and chemical precipitates has been found to retard significantly the movement of radionuclides. In most cases the absorption of radionuclides is modelled as a function of $K_d$; the liquid-to-solid phase distribution coefficient. Seepage entering the surface water flow regime, is assumed to have the characteristics of porewater in the (homogeneous) mixing layer. Similarly, the mixing layer is the source of recharge to the deep saturated tailings zone which feeds the subsurface flow regime beneath the tailings pile.

### Tailings Revegetation and Erosion

Sheet erosion of the tailings surface by water action was modelled using the Universal Soil Loss Equation (USLE). Erosion results in a solids and radionuclide loading to the surface water regime. The tailings are expected to revegetate slowly over time, resulting in decreased erosion by wind and water action. The rate of tailings revegetation depends on whether any human actions are taken to aid the process. Revegetation is assumed not to occur as long as the pH of the tailings surface is below 4.0.

## Air Source Terms

As in Phase II, an empirical model, based on experimental work at mining operations in the United States, was used to simulate the dust source term (CDOH, 1984). The key input parameters to the dust source model are: the silt content of tailings (actually the fraction of tailings of erodible size), the percentage of time that the wind speed exceeds a threshold velocity for wind erosion (5.4 $m.s^{-1}$) and the number of days on which there is measureable precipitation (>0.25 mm). A conservative approach was used to estimate the meteorological conditions for the dust source model. The two meteorological parameters (wind speed and precipitation) were derived from observations of a representative northern Ontario monitoring station, taken during the six summer months. These conditions were assumed to prevail for the entire year. In actuality the dust suspension during the winter months is likely to be minimal, hence the model may overestimate this quantity by as much as a factor of two.

The airborne radionuclide release rate decreases with time as the radioactive constituents are leached from the tailings surface layer and the tailings surface is revegetated (see previous discussions).

The approach used in Phase III to model the release of radon-222 assumes that the tailings consist of an unsaturated layer (the source of radon), and a saturated layer. The saturated layer does not act as a source of radon-222 because the water effectively inhibits its diffusion.

The unsaturated layer is divided into the two zones described in the water source model: an upper $BaSO_4$-depleted zone (i.e. a zone of reduced radium content) and a lower $BaSO_4$-enriched (i.e. radium-enriched) zone. The depth of the interface between the two zones increases with time until the entire unsaturated layer is depleted of $BaSO_4$. The behaviour of the interface is determined by the water source term and depends, in a complex manner, on the chemistry of the system.

In terms of radon-222 release to the atmosphere, the two zones are considered to be homogeneous, with each zone characterized by an average radium-226 concentration, moisture content, porosity, etc. This model for radon-222 release is equivalent to a covered tailings model in which the tailings are of finite thickness and the cover also contains radium-226, i.e. the "cover" is the upper zone and the "tailings" are the lower zone. The theoretical development of such a model was carried out by Rogers et al. (1980).

More details on the air source models can be found in Chapter 4 of Volume 3.

### 3.3.2 Environmental Dispersion

#### Dispersion in Surface Water

The surface water dispersion model was developed to model an entire watershed rather than the single river and lake modelled in previous studies. In addition, the model is structured so that the watershed characteristics are easily varied. A typical watershed involves a series of lakes linked by rivers. Such a watershed is specified in this study as comprising a series of nodes; with each node representing the outflow from a watershed sub-basin. The distances between the nodes are known as "segments". Two types of watershed segments have been defined; rivers and lakes.

Selected physical and chemical characteristics for each segment are specified as model inputs, for example, drainage area size, river reach length, lake depth and lake area. The behaviour of various ionic species, radionuclides and pH is modelled for each segment. Dilution is the only mechanism accounted for by the river model. The lake model, on the other hand, accounts for transfer to and from lake sediment as well as dilution. Radioactive ingrowth and decay is taken into account for the short-lived radionuclides. Surface water pH is calculated assuming ionic equilibrium. Species considered in the pH calculations include iron, aluminum, calcium, sodium, potassium, magnesium, sulphate and carbonate.

The pH levels calculated for each watershed segment are used in the model to determine the viability of fish populations. This factor is taken into account subsequently in estimating the amount of fish that can be consumed by any specified receptor.

Further details regarding dispersion in the surface water environment and uptake by the aquatic biota are provided in Chapters 10 and 11 of Volume 3, respectively.

### Dispersion Via Subsurface Transport

In the subsurface transport model the movement of radionuclides carried with tailings porewater emerging from the bottom of the tailings pile is traced along a single groundwater flowpath (i.e. a subsurface flow system). The model takes into consideration radionuclide retardation in calculating the concentration as a function of time at any selected point(s) along the flowpath. In this study, concentrations were calculated at the point where the groundwater flowpath discharges from the aquifer and becomes surface runoff.

The model is essentially a mass balance which includes several hydrogeological and geochemical processes (i.e., advection, retardation and dispersion). In the mass balance calculations one-dimensional, steady-state flow conditions are assumed. The groundwater flowpath for the reference tailings site is through a glaciofluvial sandy aquifer underlying the main dam structure at an outlet valley. The calculated radionuclide concentrations at the point of discharge are converted into contaminant fluxes and are subsequently utilized by the watershed (river/lake system) model. The details of this model are provided in Chapter 9 of Volume 3.

### Dispersion in Air

The air dispersion model used in the Phase I and II studies was modified to allow dispersion calculations to be performed for many directions and distances from the tailings. The Phase III model assumes that the wind data are resolved into 16 sectors, each of angular width 22 1/2°. In addition, the user can specify up to 5 radial distances (or rings, as shown in Figure 3.2) ranging from a minimum distance of 1 km to a maximum of 50 km from the centre of the tailings area. Thus, up to 80 air concentrations are calculated by the air dispersion model.

The fundamental air dispersion equation is still the same sector-averaged Gaussian plume model used in the Phase I and II studies. However, considerably more data is required to perform the calculations required in Phase III. Specifically, the model requires the fraction of time the wind blows in each of the 16 sectors for each of 6 stability classes, the mean wind velocity in each sector for each stability class and the fraction of time the wind velocity exceeds 5.4 $m.s^{-1}$. The model also requires a vertical dispersion coefficient which is determined as a function of direction and stability class. A virtual source correction is made to account for an area source as opposed to a point source. More details regarding this model are provided in Chapter 5 of Volume 3.

### 3.3.3 Environmental Transfer Models

Once the radionuclides from the tailings area have been dispersed in air and water, their movement in the environment is modelled by several environmental transfer models. Most of the environmental transfer models are simple, aggregate models, which employ a "transfer factor" approach. A transfer factor is a multiplicative factor by which the concentration of a substance in some environmental compartment is calculated, given its concentration in an adjacent or surrounding compartment. For example the concentration of radium-

226 in fish is calculated as:

$$[Ra]_{fish} = TF\ [Ra]_{water}$$

where:

$[Ra]_{fish}$ = concentration of radium-226 in fish ($Bq.kg^{-1}$)
$[Ra]_{water}$ = concentration of radium-226 in water ($Bq.m^{-3}$)
TF = Transfer factor ($m^3.kg^{-1}$)

Models of this type include the transfer of radionuclides from:

- air to vegetation
- soil to vegetation
- vegetation to animal produce (flesh)
- surface water to animal produce
- surface water to fish
- surface water to aquatic plants
- aquatic plants to animal produce

The transfer of radionuclides from air to soil is modelled in a more detailed manner. The model predicts the concentration of radionuclides in several soil layers, resulting from the deposition of airborne particulates. Processes considered in the model include:

- incoming airborne radioactivity
- radioactivity leaving the soil compartment in solution in the soil water via leaching
- radioactivity leaving the surface soil compartment in solution via runoff and
- radioactive decay

### 3.3.4 Dose Models

As indicated previously (Figure 3.3) seven pathways of human exposure to radioactivity are modelled in this study. Four of these pathways involve ingestion of radionuclides, two involve inhalation and one involves external exposure to radiation. These exposure pathways contribute to an annual average effective whole body radiation dose equivalent committment, referred to in this report as annual average dose or, even more simply, dose.

The external exposure (groundshine) dose model differs considerably from the other six dose models. The groundshine model calculates the gamma radiation flux from the soil surface, resulting from the presence of radionuclides in the various soil layers. This gamma radiation flux results in an external radiation dose to any human receptor(s) in the area. The groundshine model accounts for self-shielding by overlying soil layers and the loss of gamma ray flux via radon emanation and subsequent exhalation to the atmosphere. The model also accounts for the attenuation of gamma rays as a function of gamma energy.

The inhalation and ingestion models all involve two main aspects; calculation of the receptor's intake and multiplication of that intake by a dose conversion factor (DCF). The intake masses or volumes (of air, water vegetables, etc.) are derived from a variety of sources, and often differ between the average and critical receptors. The critical receptor consumes much more locally grown produce and locally caught meat and fish than does the average receptor. Dose conversion factors used are for an adult male with average physical characteristics (a "reference man"). The use of DCF's for radium-226 and lead-210 is relatively straightforward since they are modelled as individual, specific radionuclides. However, natural uranium and total thorium, which are being modelled in this study, are a mixture of radionuclides and their resultant DCF's are based on the proper combination of the DCF's of the individual uranium and thorium isotopes.

### 3.3.5 Disposal Options

In keeping with the project objectives, the models were developed to permit the analysis of two primary disposal options. The base case disposal option involves no additional treatment of the tailings following shutdown of the mill. The second scenario involves the reduction of the pyrite content of the upper tailings layer. Physically, depyritization would involve the placement of a cover of pyrite-reduced tailings on the surface of a tailings area. This second option also involves the incorporation of limestone ($CaCO_3$) into the upper (unsaturated) tailings layer. No model modifications were required to accommodate the effect of pyrite reduction. However, several aspects of the water source term model were modified to analyze the effect of limestone addition. The calculations involving calcium concentration, gypsum dissolution and porewater pH are performed differently depending on whether limestone is specified as being present or absent. The effects of incorporating limestone are to significantly decrease the rate of pyrite oxidation and increase the porewater pH.

## 4.0 STRUCTURE AND FEATURES OF THE URANIUM TAILINGS ASSESSMENT PROGRAM (UTAP)

The Uranium Tailings Assessment Program (UTAP) was designed to satisfy the general objectives outlined in Chapter 1. The underlying objective was to allow the probabilistic analysis of the behaviour and environmental effects of uranium mill tailings, following closeout of milling operations. More specifically, the program was designed to allow predictions to be made for distances up to 50 kilometres in all directions from the tailings area, and for time periods of up to 1000 years. In addition, the program provides many other features. These include the ability to incorporate different receptors and site characteristics and to deal with input parameters which vary with time. In this chapter, the program structure, and its features, are discussed in more detail.

### 4.1 UTAP Structure

Given the many objectives and the potential complexity of UTAP, a modular approach was taken to its development. Thus, the program functions are accomplished by way of a number of modules. These may be classified as either component or control modules depending on their function. Component modules are the computer sub-programs directly concerned with the simulation of a uranium tailings physical system. That is, they represent the computer implementation of the mathematical models of the uranium tailings and surrounding environment. Control modules provide the infrastructure for probabilistic analysis of the component modules. These functions include probabilistic sampling of input parameters, and many input, output and bookkeeping functions. The integrated control and component modules are referred to as the system model, system program, or UTAP. The relationship between control and component modules and the basic functions of these modules is illustrated in Figure 4.1.

The flow of information between the various control and component modules is achieved via a computer feature known as the "labelled common block." Once a variable is referenced in a common block, its current value is available in

FIGURE 4.1

THE SYSTEM MODEL

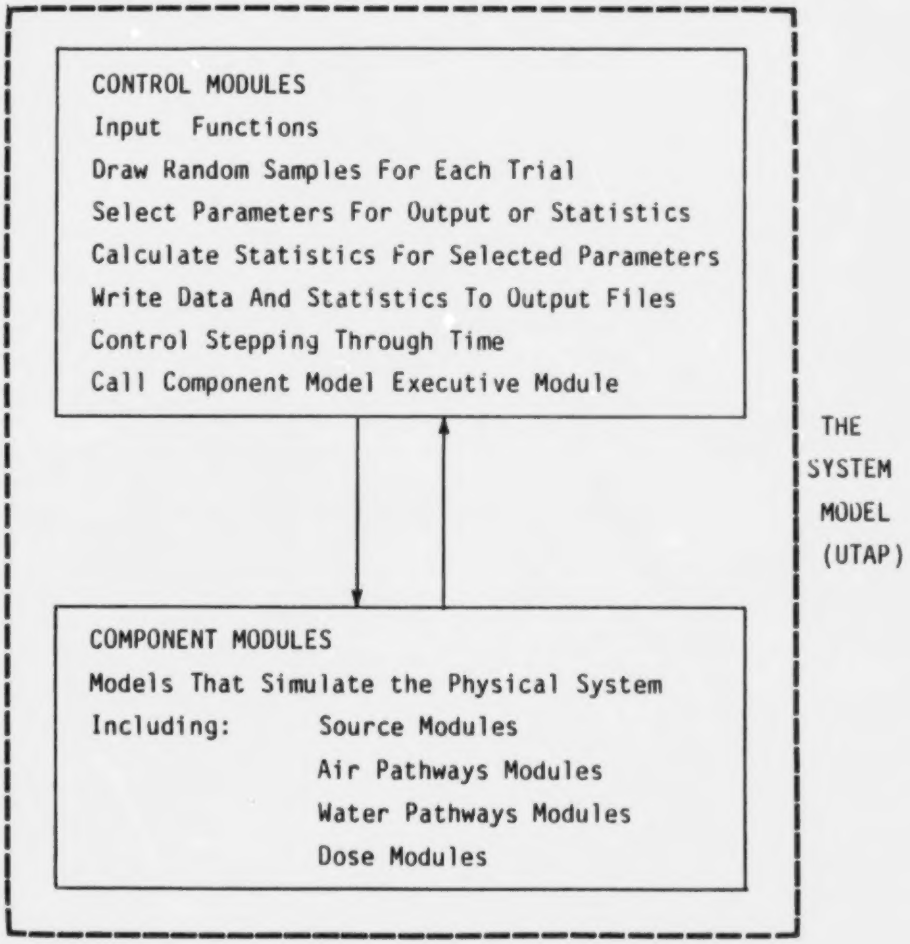
CONTROL MODULES
Input Functions
Draw Random Samples For Each Trial
Select Parameters For Output or Statistics
Calculate Statistics For Selected Parameters
Write Data And Statistics To Output Files
Control Stepping Through Time
Call Component Model Executive Module
THE SYSTEM MODEL (UTAP)
COMPONENT MODULES
Models That Simulate the Physical System
Including:
Source Modules
Air Pathways Modules
Water Pathways Modules
Dose Modules

every module in which that common block appears. If a variable's value is changed via some calculation, the value stored in the common block also changes. The new value will then be used in all subsequent calculations. This approach eliminates many concerns regarding information storage, transfer and management.

The control modules are executed in a logical sequence by the primary control module (EXEC). As illustrated on Figure 4.2, the control module functions can be grouped in several categories, namely: sampling, selecting parameters for output, calculating summary statistics, and generating output. Many of the control modules, particularly those involved with drawing samples and calculating statistics, were extracted from the RANSIM program, which provided much of the control module structure for the Phase II analysis (SENES, 1985). These control modules have undergone extensive testing over several phases of the project and are believed to be technically very sound. The control modules are completely documented in Volume 2 of this report.

The component module interactions are illustrated in more detail in Figure 4.3. The figure indicates the modular approach taken to component model development. In fact, the program is even more modular than is shown, since several of the modules shown are actually implemented as 2, 3 or 4 modules.

Although Figure 4.3 may be difficult to follow initially, it is interesting to compare it with the pathways diagram presented earlier (Figure 3.3). One can then identify a number of modules which comprise the source model, others which represent air and water dispersion, others which perform environmental transfer calculations and finally modules which calculate individual receptor and population dose. The component modules are documented completely in Volume 3 of this report.

The modular approach taken in this study facilitated model development, review and coding. The structure will also make it easier for future users to modify aspects of UTAP which they feel are inappropriate for a given application. For instance, aspects of the source model could be easily modified, or the

FIGURE 4.2

UTAP CONTROL MODULE STRUCTURE

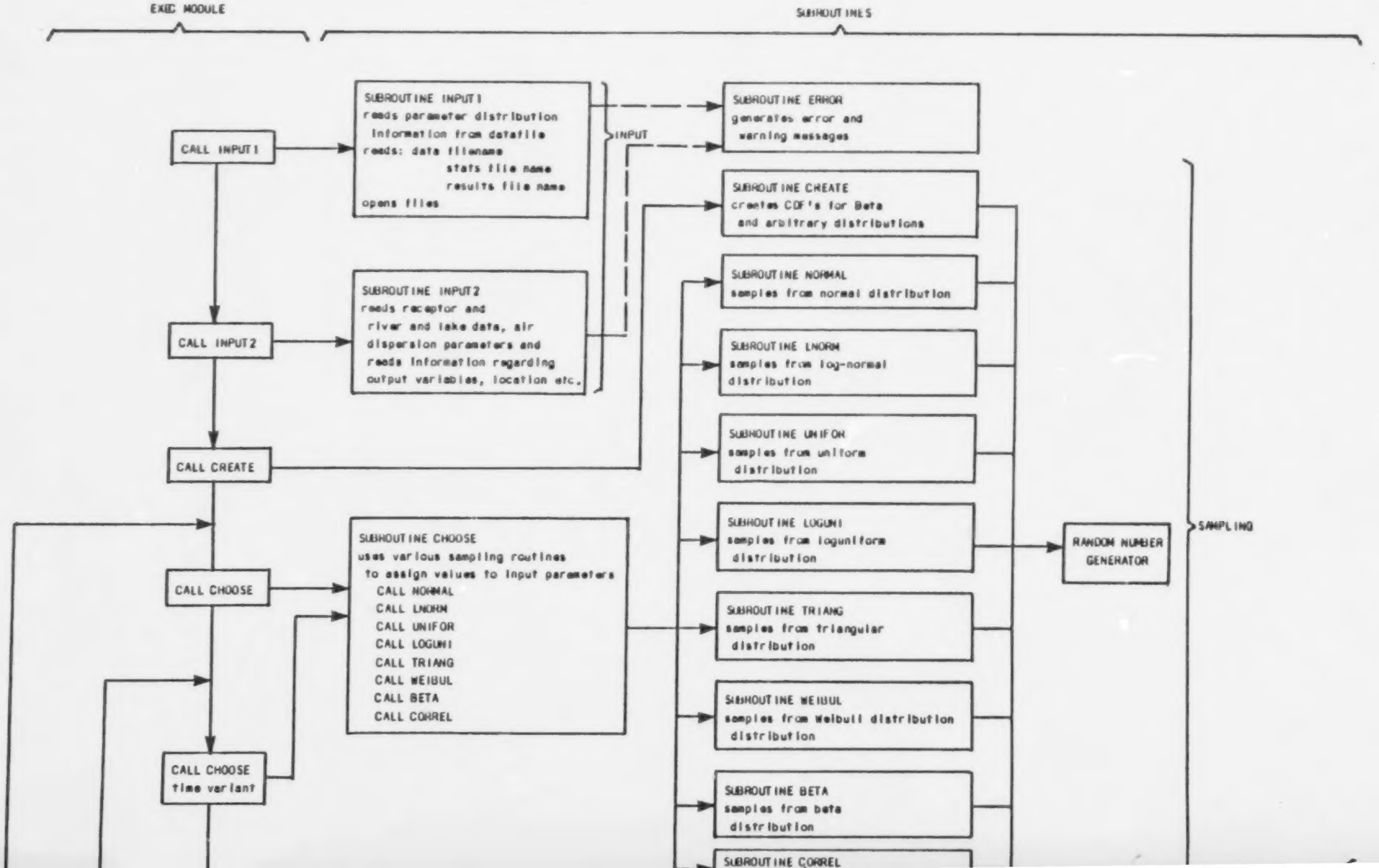
EXEC MODULE
SUBROUTINES
CALL INPUT1
CALL INPUT2
CALL CREATE
CALL CHOOSE
CALL CHOOSE time variant
SUBROUTINE INPUT1 reads parameter distribution information from datafile reads: data filename stats file name results file name opens files
SUBROUTINE INPUT2 reads receptor and river and lake data, air dispersion parameters and reads information regarding output variables, location etc.
INPUT
SUBROUTINE CHOOSE uses various sampling routines to assign values to input parameters CALL NORMAL CALL LNORM CALL UNIFOR CALL LOGUNI CALL TRIANG CALL WEIBUL CALL BETA CALL CORREL
SUBROUTINE ERROR generates error and warning messages
SUBROUTINE CREATE creates CDF's for Beta and arbitrary distributions
SUBROUTINE NORMAL samples from normal distribution
SUBROUTINE LNORM samples from log-normal distribution
SUBROUTINE UNIFOR samples from uniform distribution
SUBROUTINE LOGUNI samples from loguniform distribution
SUBROUTINE TRIANG samples from triangular distribution
SUBROUTINE WEIBUL samples from Weibull distribution distribution
SUBROUTINE BETA samples from beta distribution
SUBROUTINE CORREL
RANDOM NUMBER GENERATOR
SAMPLING

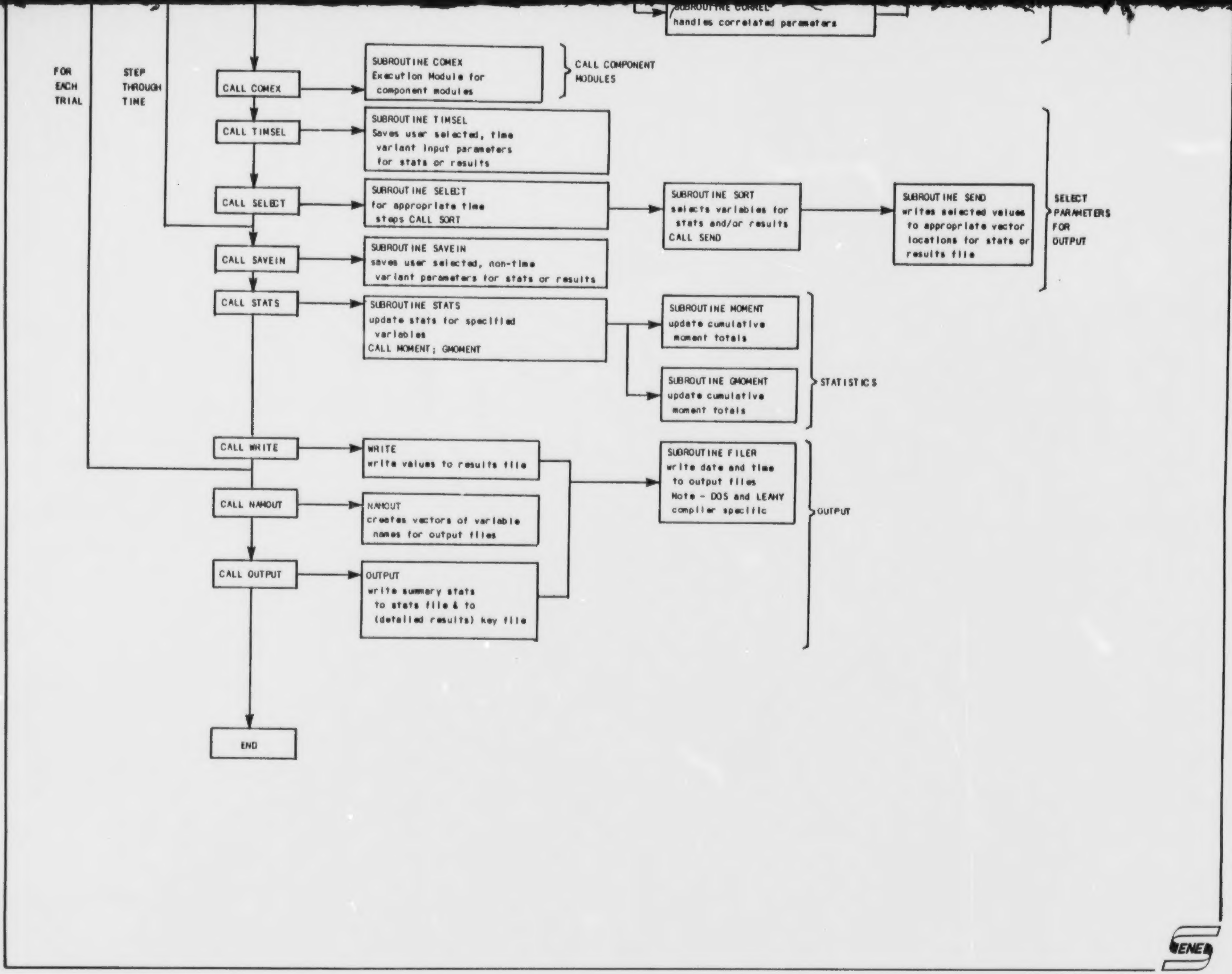
SUBROUTINE CORREL
handles correlated parameters
FOR EACH TRIAL
STEP THROUGH TIME
CALL COMEX
SUBROUTINE COMEX
Execution Module for component modules
CALL COMPONENT MODULES
CALL TIMSEL
SUBROUTINE TIMSEL
Saves user selected, time variant input parameters for stats or results
CALL SELECT
SUBROUTINE SELECT
for appropriate time steps CALL SORT
SUBROUTINE SORT
selects variables for stats and/or results
CALL SEND
SUBROUTINE SEND
writes selected values to appropriate vector locations for stats or results file
SELECT PARAMETERS FOR OUTPUT
CALL SAVEIN
SUBROUTINE SAVEIN
saves user selected, non-time variant parameters for stats or results
CALL STATS
SUBROUTINE STATS
update stats for specified variables
CALL MOMENT; GMOMENT
SUBROUTINE MOMENT
update cumulative moment totals
SUBROUTINE GMOMENT
update cumulative moment totals
STATISTICS
CALL WRITE
WRITE
write values to results file
CALL NAMOUT
NAMOUT
creates vectors of variable names for output files
CALL OUTPUT
OUTPUT
write summary stats to stats file & to (detailed results) key file
SUBROUTINE FILER
write date and time to output files
Note - DOS and LEAHY compiler specific
OUTPUT
END

FIGURE 4.3

UTAP COMPONENT MODULE STRUCTURE

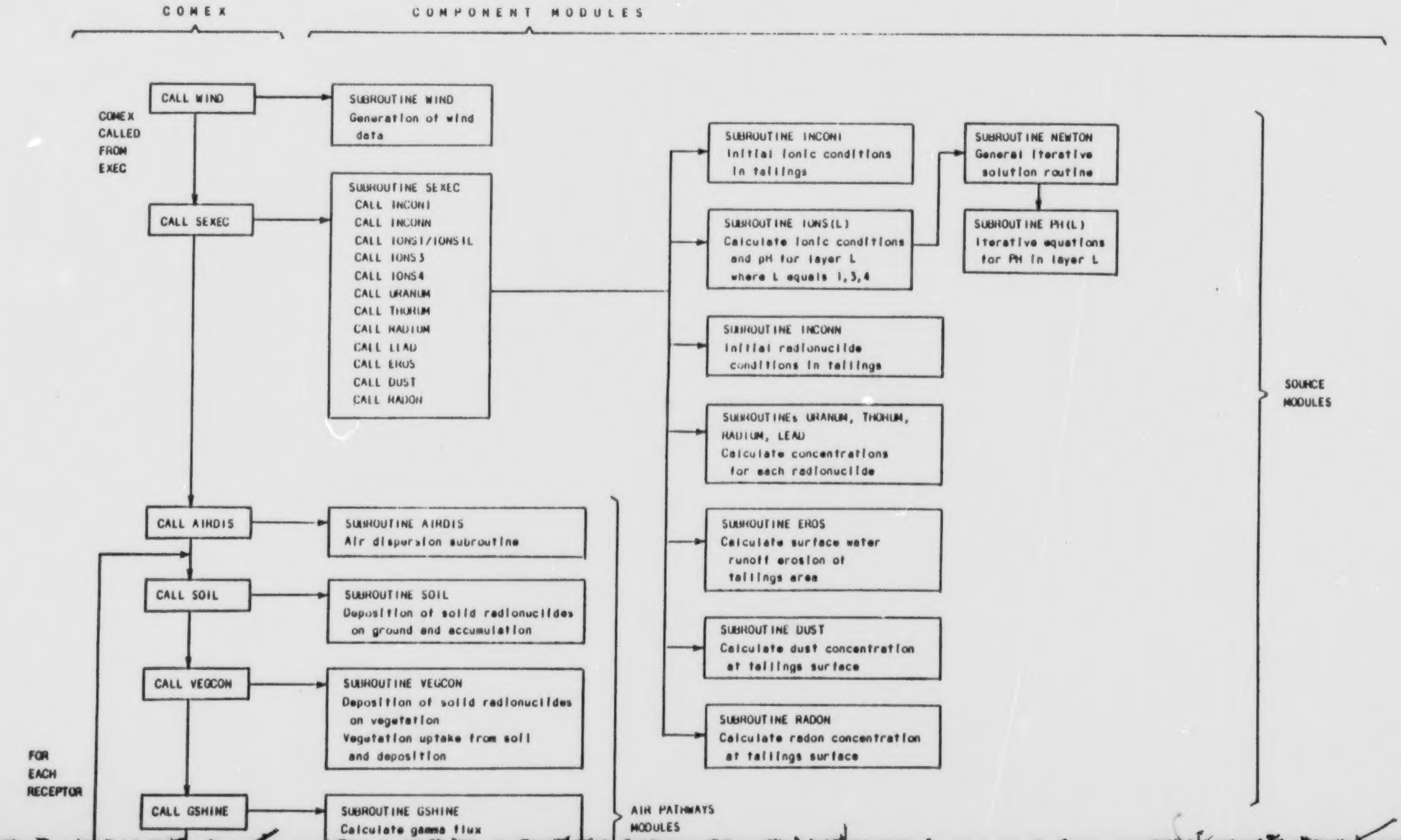
COMEX
COMPONENT MODULES
CALL WIND
COMEX CALLED FROM EXEC
SUBROUTINE WIND
Generation of wind data
CALL SEXEC
SUBROUTINE SEXEC
CALL INCONI
CALL INCONN
CALL IONS1/IONS1L
CALL IONS3
CALL IONS4
CALL URANUM
CALL THORUM
CALL RADIUM
CALL LEAD
CALL EROS
CALL DUST
CALL RADON
SUBROUTINE INCONI
Initial ionic conditions in tailings
SUBROUTINE IONS(L)
Calculate ionic conditions and pH for layer L where L equals 1,3,4
SUBROUTINE NEWTON
General iterative solution routine
SUBROUTINE PH(L)
Iterative equations for PH in layer L
SUBROUTINE INCONN
Initial radionuclide conditions in tailings
SUBROUTINEs URANUM, THORUM, RADIUM, LEAD
Calculate concentrations for each radionuclide
SUBROUTINE EROS
Calculate surface water runoff erosion of tailings area
SUBROUTINE DUST
Calculate dust concentration at tailings surface
SUBROUTINE RADON
Calculate radon concentration at tailings surface
SOURCE MODULES
CALL AIRDIS
SUBROUTINE AIRDIS
Air dispersion subroutine
CALL SOIL
SUBROUTINE SOIL
Deposition of solid radionuclides on ground and accumulation
CALL VEGCON
SUBROUTINE VEGCON
Deposition of solid radionuclides on vegetation
Vegetation uptake from soil and deposition
FOR EACH RECEPTOR
CALL GSHINE
SUBROUTINE GSHINE
Calculate gamma flux
AIR PATHWAYS MODULES

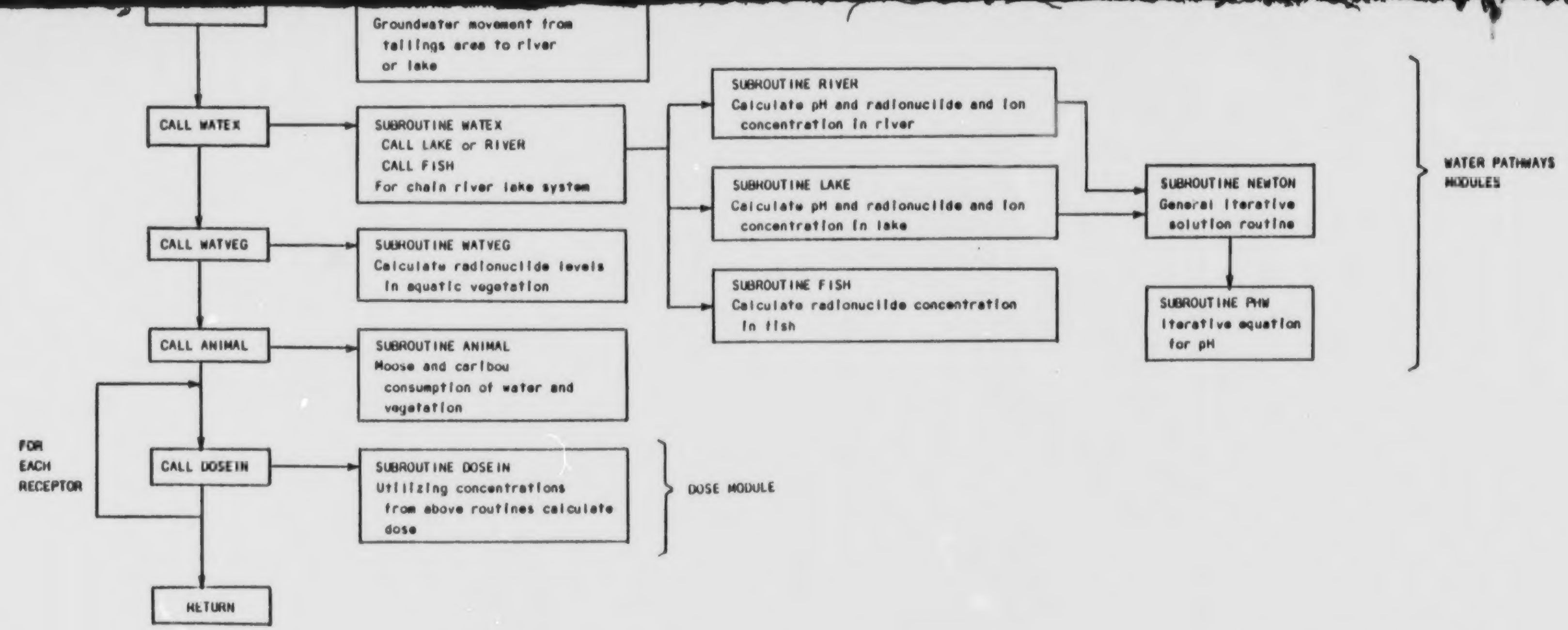
Groundwater movement from tailings area to river or lake
CALL WATEX
SUBROUTINE WATEX
CALL LAKE or RIVER
CALL FISH
For chain river lake system
SUBROUTINE RIVER
Calculate pH and radionuclide and ion concentration in river
SUBROUTINE LAKE
Calculate pH and radionuclide and ion concentration in lake
SUBROUTINE FISH
Calculate radionuclide concentration in fish
SUBROUTINE NEWTON
General iterative solution routine
SUBROUTINE PHW
Iterative equation for pH
WATER PATHWAYS MODULES
CALL WATVEG
SUBROUTINE WATVEG
Calculate radionuclide levels in aquatic vegetation
CALL ANIMAL
SUBROUTINE ANIMAL
Moose and caribou consumption of water and vegetation
FOR EACH RECEPTOR
CALL DOSEIN
SUBROUTINE DOSEIN
Utilizing concentrations from above routines calculate dose
DOSE MODULE
RETURN

entire source model could be replaced, new pathways could be added or deleted. In summary, the modular structure has produced a high quality product which can be easily modified for future application.

## 4.2 UTAP Features

UTAP was designed to provide considerable flexibility in the analysis of uranium mill tailings. The program allows a variety of physical situations and scenarios to be modelled and also allows the user to easily access a large amount of information generated during the simulation. The flexibility arises from the fact that much of the information required by the program is supplied by the user, rather than being "built in" to the program. This is in contrast to computer codes which require very little input from the user, and consequently have very limited, specific applications. These features are discussed below.

### Probabilistic Input Parameters

Many "input parameters" are required by the mathematical models developed to simulate the tailings and their effects on the environment. Since there is uncertainty regarding the "true value" of many of these parameters, they are specified as probability distributions, rather than as single numbers, in the analysis. At present, 216 input parameters are specified in an input data file. The value, or range of values of any parameter named in the input data file may be modified simply by changing a few numbers in the input file. Thus it is a trivial task to perform "what if" type analysis; modifying the input value or range of one parameter and examining its effect on some selected result. A number of parameters appear in the data file with constant values rather than as distributions. Simply having the parameter present as an input, rather than "built in" to the code provides flexibility should the user wish to change its value to another constant value or to a probability distribution.

At present, the input parameters can be described by any of 10 different probability distributions:

constant (a trivial case)
normal
lognormal
uniform
loguniform
triangular
weibull
beta
arbitrary
correlated.

Each distribution is specified somewhat differently. For instance a normal distribution would be characterized by its mean, standard deviation, a minimum and a maximum value; a uniform distribution is fully specified by its minimum and maximum values.

The input parameters in this first input file are all explicitly required by the component (simulation) modules. Other information, specified in a second input file, serves primarily to describe the dimensions/characteristics of the physical system being modelled and specify the calculations which are to be performed and saved.

## Air Dispersion Data

The air dispersion model implemented in UTAP requires a considerable amount of input information. The information is primarily in the form of meteorological "star data," giving annual joint frequencies of occurrence of wind speeds, wind directions and stability classes. These annual values change from year to year, hence 20 years of such data (obtained from the Atmospheric Environment Service (AES)) are currently supplied in a data file. Should UTAP be applied to a site with very different air dispersion characteristics, an appropriate star-data set should be substituted for the current data.

From the 20 year set of annual values, two further data sets were constructed. The first consists of 20 sets of 10-year average values, and the second consists of a set of long-term average values. Further discussion of the two additional data sets is provided in Chapter 5.2 of Volume 3. The use of these data sets is discussed below along with other "temporal considerations."

## Spatial Characteristics

As mentioned previously, UTAP has the capability to make predictions within a 50 km radius from the tailings. The program is constructed so that, starting at 1 km, the user may divide any or all of the 50 km radius into a series of concentric circles. Specifically, up to 5 radial divisions, located at any distances from 1 to 50 km may be specified, dividing the system into 5 concentric circles (or rings). Calculations are then performed at the midpoint of each ring. Thus, to provide an overview of the entire area, one might specify radial divisions at 1, 3, 10, 20 and 50 km. To focus in more detail on one location (e.g. a townsite located 10 km from the tailings), one might specify divisions at 8, 9, 10, 11 and 12 km.

In addition to the radial divisions, the program automatically makes predictions in all directions from the tailings source. The 360° of the circle has been divided into 16 equal-width sectors (22.5°) for this analysis. This is in keeping with a traditional wind-rose structure. The UTAP approach to spatial considerations is summarized in Figure 4.4. As can be seen from the figure, the 16 directions and 5 rings make up a co-ordinate system which includes 80 different locations (or segments).

## Watershed Characteristics

The program is designed to allow the user to specify the configuration and characteristics of a watershed, to correspond to the physical system being modelled. Thus, while the watershed characteristics will remain fixed for a given analysis, they may be easily modified when performing subsequent analyses.

The watershed must be specified as a series of lake and river linkages. Up to 10 such segments, each representing a river, a part of a river or a lake may be specified. In addition to specifying the linkages between the segments, certain characteristics of each segment (e.g. area, depth, etc.) must also be specified. Calculations are performed for the end of each segment (referred to as a node). Finally, the user must specify the location of the various watershed elements in the spatial coordinate system defined previously (Figure 4.4).

## Receptor Locations and Characteristics

In addition to the previous features, UTAP allows the user to specify the location and some characteristics of the receptors to be modelled. The models and probabilistic inputs define two receptor types; a critical receptor and an average receptor. The critical receptor is an adult male, characteristic of a northern hunter/trapper. He spends much of his time outdoors and derives much of his diet from local sources. The average receptor, on the other hand, is assumed to have a much less rugged lifestyle, and to eat far less food from local sources.

UTAP is designed to allow up to 80 receptors to be placed in any segment of the coordinate system described earlier (Figure 4.4). For each receptor, the coordinate location and the source of drinking water must be specified. Drinking water may be derived from any node on the watershed or from some other source, unaffected by the tailings. By definition, a critical receptor is generally placed close to the tailings area, and assumed to derive his drinking water from the tailings watershed.

Average receptors may be located as desired, depending on the physical system being modelled and/or on the information desired from the simulation. For instance, if one were interested in how receptor dose decreased with distance, one might model 5 receptors; 1 in each of 5 rings moving away from the tailings in a straight line.

FIGURE 4.4

UTAP OVERVIEW
OF SPATIAL FEATURES

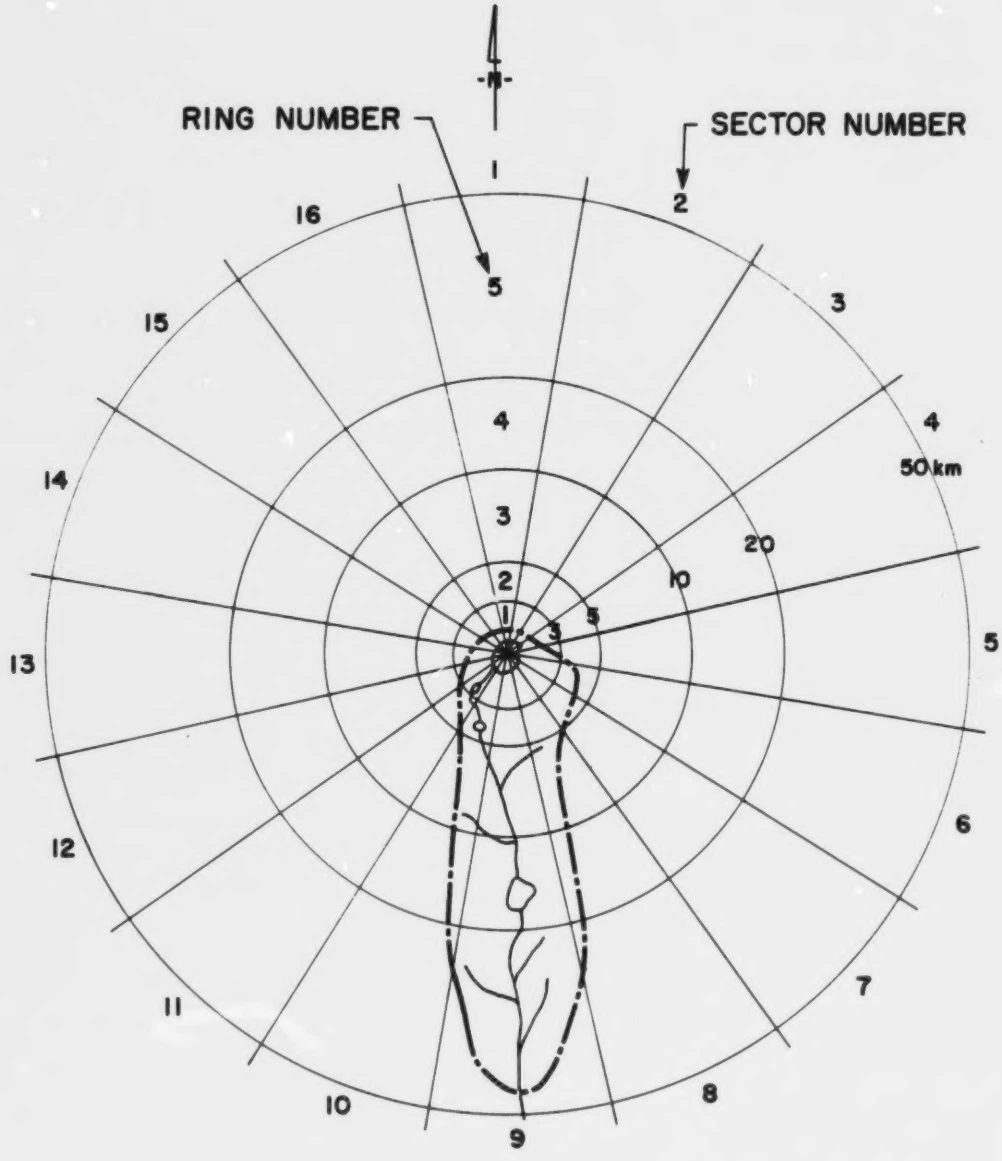
N
RING NUMBER
SECTOR NUMBER
1
2
3
4
5
6
7
8
9
10
11
12
13
14
15
16
5
4
3
2
1
50 km
20
10
5
3

### Temporal Considerations

The program was designed to allow simulations to be performed for time periods of up to 1000 years, in one or ten year time-steps. Thus, for any simulation, the user must select the length of time to be simulated and the time-step to be used. Most of the results presented in this report were generated using a 10-year time-step.

Several of the model input parameters are expected to vary from year to year. These "time-variant" parameters are primarily meteorological variables such as mean annual precipitation and wind speed, direction and stability arrays "star-data." The program samples such parameters once each time-step rather than only once each trial as for most of the parameters. The wind data is sampled from either the file of 1 year or 10 year average values or set constant to long-term mean values. The distributions of the remaining time-varying parameters must be adjusted to correspond to the time-step used.

### Disposal Options

Although a variety of situations can be modelled simply by modifying the values of the input parameters, UTAP is constructed to analyse two distinct management scenarios or disposal options. The first option represents a situation in which no extraordinary measures are taken while closing out the tailings area. In particular, no limestone is incorporated into the tailings. Conversely, the second option simulates a situation in which limestone is incorporated into the upper layer of depyritized tailings.

The distinction between these two options is stressed, because they are simulated by different modules within the UTAP code. Other options can certainly be simulated, simply by changing input parameter distributions. Still further options could be modelled by modifying various component modules (particularly the source term) as required.

## Selecting Results

The discussion to this point has focussed on those UTAP features which allow a user to specify the physical situation to be modelled, using input data and requiring no programming changes. A number of UTAP features also allow the user to access much of the information generated during the simulation, again with no programming changes. Once again, this flexibility is provided by specifying information as input, rather than building it into the code.

First of all, the user may select from a "menu" of information which is available for output. The menu currently consists of 32 computer storage arrays, several with at least 2 dimensions. In general, the information which is available includes the concentrations of radionuclides at any point in the pathways shown earlier (Figure 3.3). The radionuclide concentrations in the various environmental compartments, at any receptor or in any watershed segment can be accessed. Considerable information is also available regarding conditions within the tailings source term, water quality indicators (e.g. pH) in the watershed, and, of course, dose to any or all the receptors, for all pathways.

Since most (if not all) of the aforementioned results vary with time over the simulation period, UTAP also allows the user to select the times at which results are to be saved. In particular, the user may select up to 11 different times for which results are to be saved. These may be equally spaced over the simulation period or focus more closely on time periods of greater interest.

## Output Capabilities

The results of interest, selected as outlined above, may be saved and/or displayed in several different ways; again at the user's request. First of all, UTAP permits summary statistics on all selected variables to be calculated and saved to a disk file. These statistics include:

mean
standard deviation
geometric mean
geometric standard deviation
minimum value
maximum value.

These are all calculated using recursive ("on-the-fly") methods and thus can be determined without saving all results from all trials. They provide a useful summary of a simulation, and may be most beneficial when storing the detailed results of a large simulation might result in disk storage problems.

An alternative to the summary statistics is to save the results of each trial for each parameter of interest. These detailed results are written to a disk file, along with some additional information. The additional information takes the form of a "key file" providing a key to, and summary statistics for, the parameters in the detailed results file. Such detailed results are necessary if one wishes to construct frequency histograms for any parameters or to perform regression analysis to determine important parameters. One may opt for summary statistics on a number of selected parameters and yet select detailed results for others. Alternatively, both summary statistics and detailed results can be saved for the same parameters.

The construction of output frequency histograms, regression analysis, graphical routines and the like are not provided by UTAP. The detailed results from UTAP may be processed using one of the many commercially available data management and analysis systems. However, two post processing programs are supplied with UTAP. These permit the calculation of 95% confidence bands for either the relative frequency histogram (pdf) or the cumulative distribution (cdf) for user-selected variables.

## Limitations of UTAP

Although UTAP posesses may useful features, like any computer program, it has its limitations.

These arise partly because of assumptions used in component model development, and partly because of decisions made during computer implementation of the models. The most significant component model limitations include:

- single tailings source
- discharge to a single watershed
- single subsurface flow path
- shallow subsurface flow through clay or till (not fractured rock)
- selected group of pathways (not exhaustive)
- selected group of radionuclides (not exhaustive)
- predictions for distances between 1 and 50 km
- time steps of 1 or 10 years (limited by wind data)
- tailings considered to be homogeneous over the entire area
- water table at same depth throughout tailings area

To avoid these limitations, changes to the component modules would be required. Given the modular structure of UTAP, changes to individual components should be fairly straightforward, and may (in some instances) be done with little effect on other modules. Other changes, such as adding further radionuclides, would require changes to a number of modules.

Some further limitations imposed on UTAP by the control modules include:

- number and type of input parameter distributions
- limits on available output
  - number of time-steps
  - number of total variables
  - variables easily accessed

These primarily involve arbitrary limits on the sizes of computer storage arrays. They may be easily modified by changing array sizes in the computer program.

## 5.0 PHASE III PROBABILISTIC ASSESSMENT RESULTS

### 5.1 Introduction

The approach to modelling the hypothetical reference tailings site is described in Chapter 3 and the structure of the Phase III Uranium Tailings Assessment Program (UTAP) is described in Chapter 4. In this chapter, a number of results are presented from the probabilistic assessment of the hypothetical, reference tailings site for two disposal scenarios; namely, a walk away, do-nothing-further scenario (referred to as the Base Case or Scenario 1) and a scenario in which limestone is added to the uppermost unsaturated layer of tailings from which much of the pyrite has been removed (Scenario 2).

The exposure pathways considered in the Phase III assessment are shown on Figure 5.1. Except for the source term, shown inside the dashed box on the figure, the basic structure of the component models and their interelations do not change from Scenario 1 to Scenario 2.

The component models which simulate the behaviour of the tailings and of the environment over time can be used to predict the behaviour of various radioactive species in the environment and the resulting dose to man (see Chapter 3 of this volume and Volume 3). The release and behaviour of non-radioactive species is also simulated with the Phase III models. These non-radioactive species are used in the calculation of pH which is examined in the present assessment of the tailings and receiving waters.

The Phase III system model is capable of producing an enormous amount of information about the effects of the reference tailings site on the surrounding environment. Thus, in a practical sense, with the Phase III system model, one is limited not by what predictions one can make, but rather by what information one is capable of processing and analyzing. Hence, in the following discussion, an approach to assessment is outlined that allows the important factors in the reference tailings - environment system to be

FIGURE 5.1

EXPOSURE PATHWAYS ANALYZED IN PHASE III

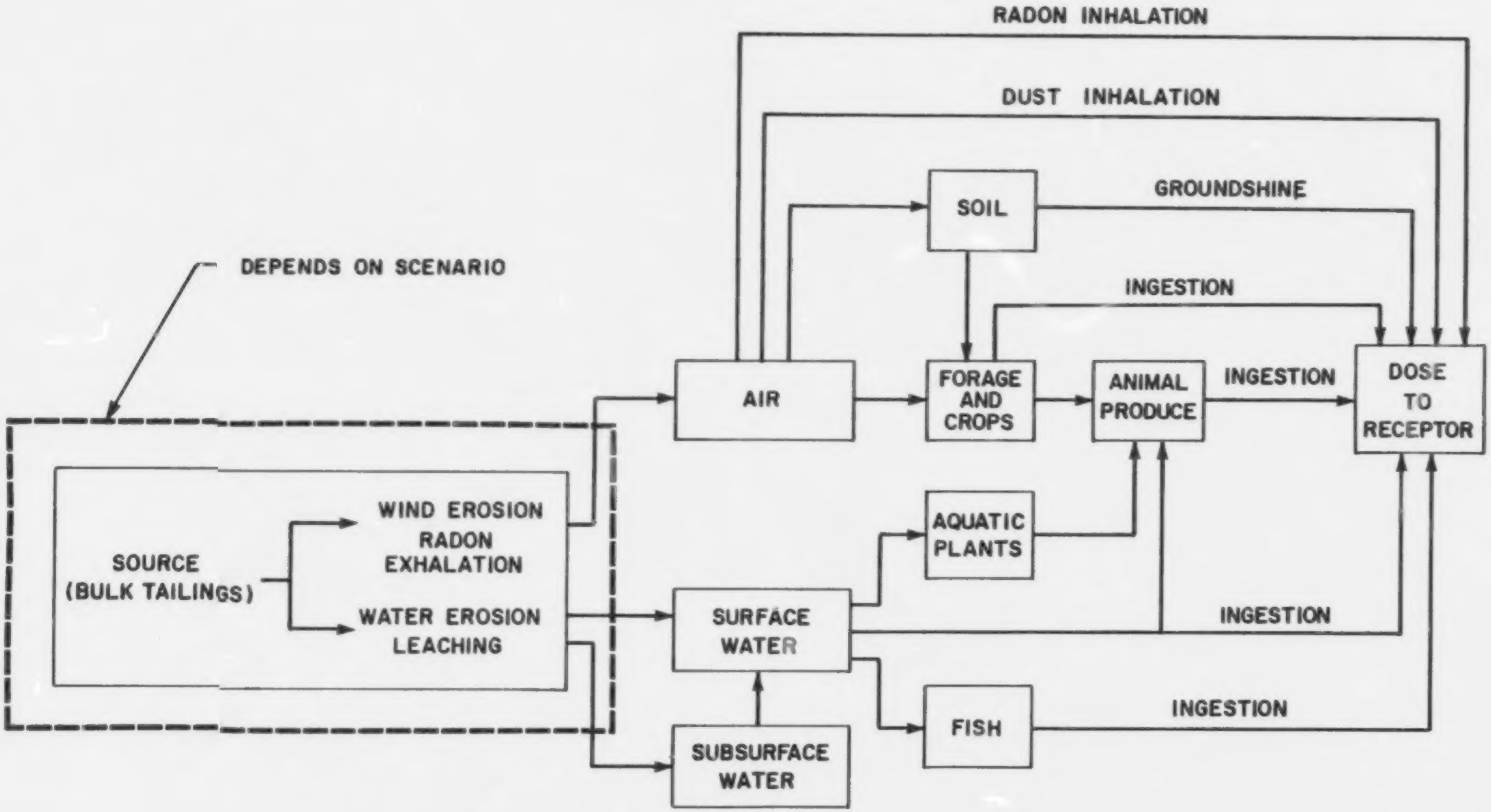
DEPENDS ON SCENARIO
SOURCE (BULK TAILINGS)
WIND EROSION
RADON EXHALATION
WATER EROSION
LEACHING
AIR
SURFACE WATER
SUBSURFACE WATER
SOIL
FORAGE AND CROPS
AQUATIC PLANTS
FISH
ANIMAL PRODUCE
DOSE TO RECEPTOR
RADON INHALATION
DUST INHALATION
GROUNDSHINE
INGESTION
INGESTION
INGESTION
INGESTION

isolated. This allows us to focus our analytical effort on the important areas, as well as producing an assessment with a minimum of extraneous information.

The suggested approach first entails identification of important pathways by examining the relative contributions of the different pathways to total dose over the simulation period. Once the important pathway(s) are identified we move down that pathway(s) and investigate the mechanisms and parameters that most significantly influence those pathways. Both graphical and importance analysis techniques are used to achieve this end.

Some of the refinements developed in Phase III are also illustrated in this chapter; specifically, the estimation of confidence bands, demonstration of the watershed model and demonstration of the windrose spatial grid that allows multiple receptor locations. Also a second tailings management scenario involving tailings depyritization and the addition of limestone is examined.

The number of trials required for a particular simulation depends on the information desired regarding the calculated variable(s). If only an estimate of the mean and its associated standard deviation are needed, a relatively small number of trials (say 50) is often sufficient. If estimation of the frequency distribution is desired many more trials are necessary. Except where stated otherwise, the basic statistics and histograms for the analyses described in this section were generated from 200 trials.

## 5.2 Scenario 1: The Base Case

The basic features of the reference tailings site and environment are described in Chapter 3. Full details are provided in Volume 3 of this report. In short, the Base Case scenario examines the effects of walking away from the tailings site at the cessation of the mill operating life (i.e. doing nothing further to mitigate any environmental effects).

### 5.2.1 Dose By Pathway

Figure 5.2 is a plot of geometric mean dose versus time for all of the pathways except groundshine. Dose from the groundshine pathway is several orders of magnitude lower than dose from the vegetation pathway and for the sake of clarity, was not shown in Figure 5.2. Total dose from all pathways (including groundshine), is also shown on the graph. The distributions of dose were found to tend toward lognormality, hence the geometric mean was used as an indicator of the central tendency of these data.

Figure 5.2 indicates that dose due to drinking water consumption is the dominant pathway throughout the entire simulation period, with most of total dose accounted for in this one pathway. Dose due to fish consumption, another water-related pathway, is the second most important contributor to total dose.

The total dose curve shown on Figure 5.2 declines rapidly from year t = 0 to about year t = 150 and thereafter declines much more slowly. The behaviour of this curve is influenced by several factors. First, the air-related pathways (radon dose, dust inhalation dose and vegetation dose) decrease monotonically with time. This occurs as leaching of radionuclides from the unsaturated tailings layer progressively reduces the inventory of radionuclides in the portion of the tailings mass that affects the air source terms, namely radon flux and wind erosion of tailings. Between 200 and 500 years the dose from air pathways related to windborne dust declines by an order of magnitude to a new quasi-steady level. This is due to establishment of a vegetative cover on the tailings as soon as the pH at the tailings surface permits growth (i.e. pH greater than about 4.0).

Second, the geometric mean dose from the drinking water pathway also declines monotonically over time. This is explained further in the next section. The mean dose from the meat pathways closely parallels the water pathway indicating that radionuclide transfer to moose and caribou from water is more important than transfer via terrestrial vegetation. The geometric mean dose

FIGURE 5.2

DOSE vs. TIME BY PATHWAY
(SCENARIO I)

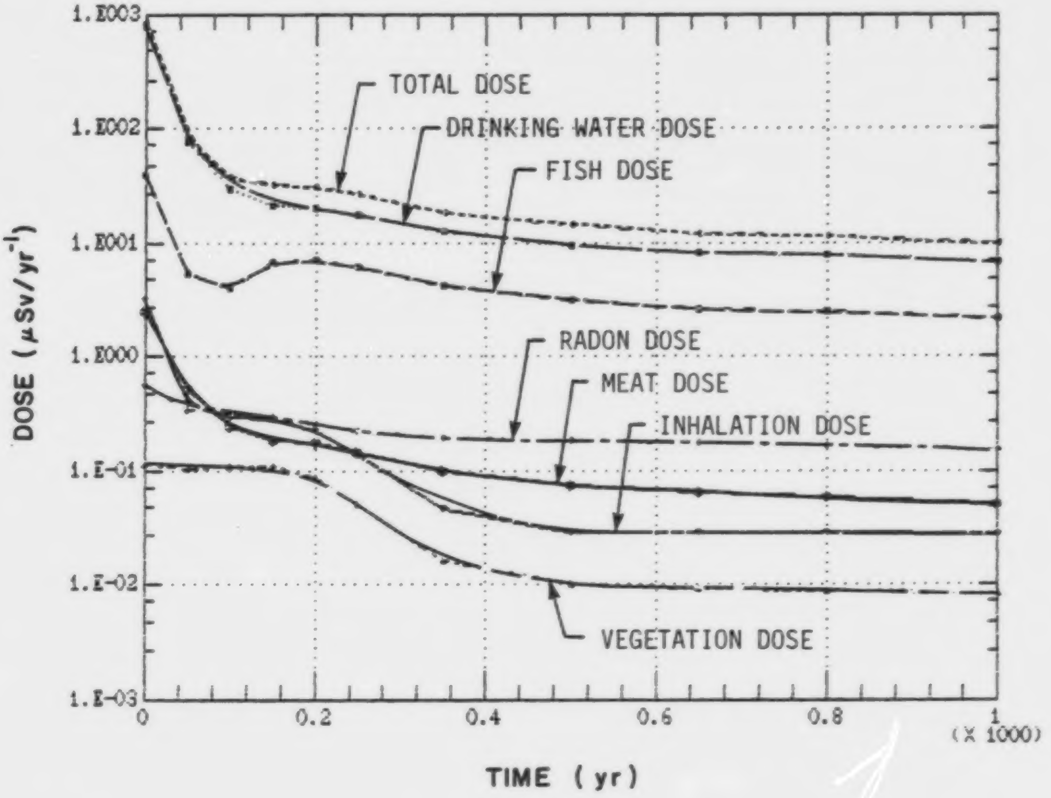

NOTE:

GEOMETRIC MEAN VALUES OF 200 TRIALS

via the fish pathway on the other hand declines for the first 100 or so years, then increases, peaking locally at about year 200, from which time it too exhibits an essentially monotonic decrease with time. The reasons for this behaviour are discussed in the next section in which we focus on the water pathway and investigate the major factors and important mechanisms and parameters which contribute to this pathway.

Figures 5.3a and 5.3b are histograms of total dose at t = 0 and t = 250 years. Figure 5.4 shows the confidence bands calculated for the total dose at t = 500 years using the confidence bands program provided with UTAP. The histograms show a substantial reduction in the mean and maximum doses with time from t = 0 to t = 250 years.

The histograms in Figure 5.3 show the skewed shape characteristic of the lognormal distribution. Because Figure 5.4 is a plot of logarithmic values, the curve is nearly normal. The confidence bands are quite narrow on both Figure 5.4(a) and (b) even though they were calculated from only 200 trials.

### 5.2.2 The Water Pathways

The drinking water pathway was isolated as the dominant pathway in the previous discussion. Several questions concerning this pathway have already been noted. Another question which arises is, which radionuclides contribute most to dose? Figure 5.5 illustrates the contribution of the four radionuclides to total drinking water dose.

The contribution of the four radionuclides to total drinking water dose can be explained as follows. At early times, thorium and lead are the primary contributors. The dissolution of thorium is controlled by pH; thorium solubility decreasing rapidly as the pH rises above pH 4.0 to 4.5. The pH of the tailings porewater is controlled largely by the oxidation of pyrite, which occurs relatively rapidly in the early years of the simulation. As the pyrite content decreases, acid generation is reduced, and the pH gradually rises, and thorium solubility decreases. Hence, with time, less thorium is carried in

FIGURE 5.3

TOTAL DOSE HISTOGRAM
(SCENARIO I)

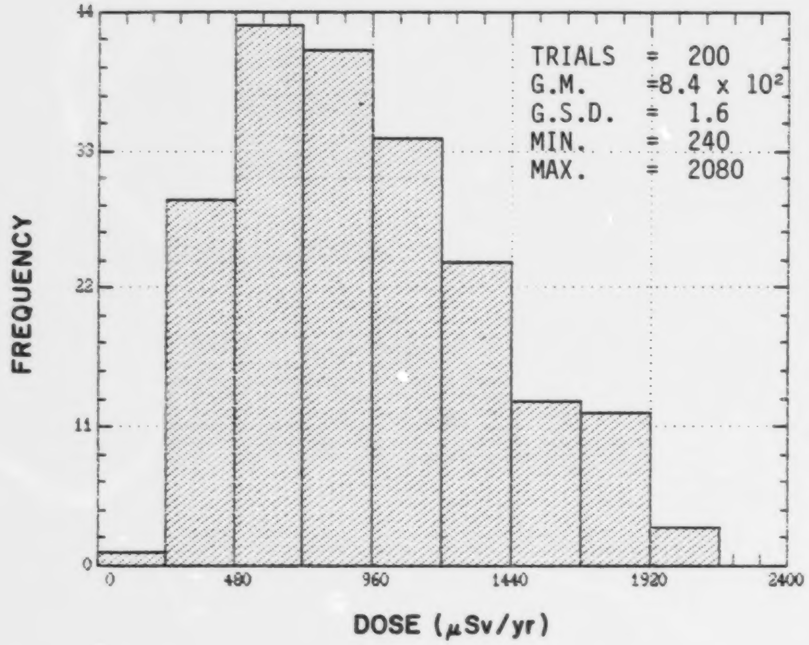

A) t = 0 YEARS

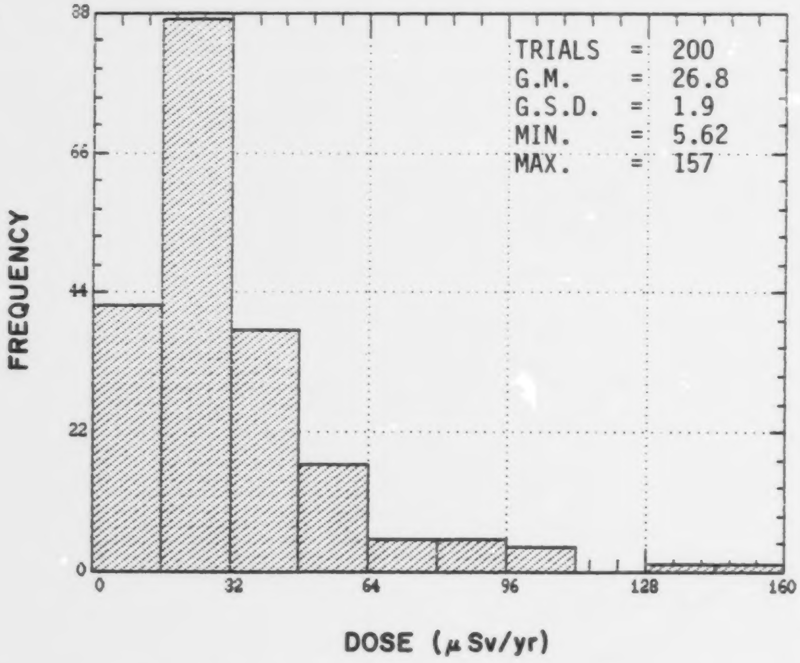

B) t = 250 YEARS

FIGURE 5.4

95% CONFIDENCE BANDS
ON TOTAL DOSE AT t = 500 YEARS
( SCENARIO I )

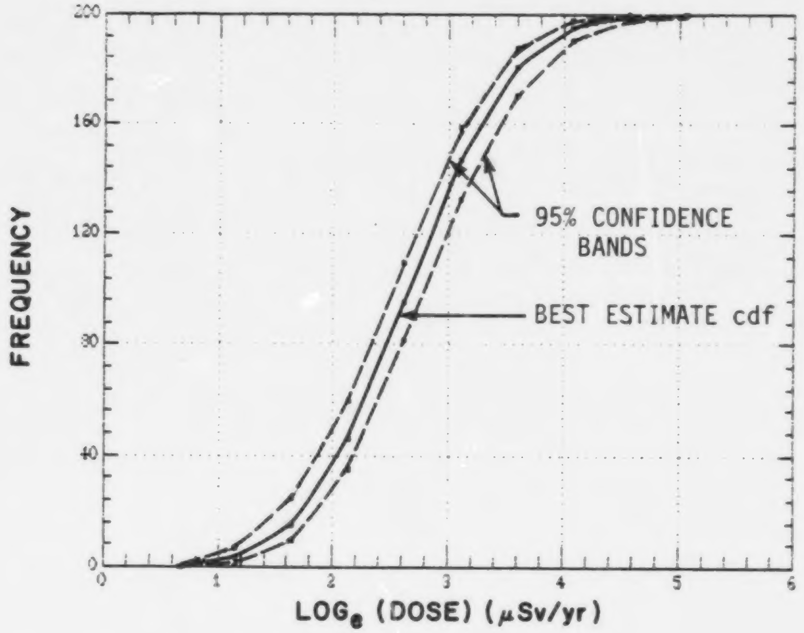

A) CUMULATIVE DISTRIBUTION FUNCTION

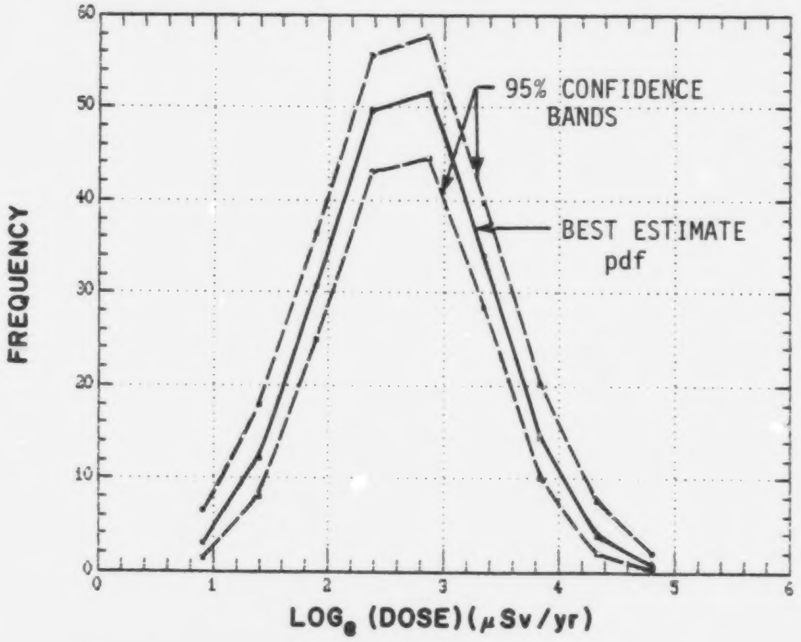

B) PROBABILITY DENSITY FUNCTION

## FIGURE 5.5

## DRINKING WATER DOSE vs. TIME BY RADIONUCLIDE (SCENARIO I)

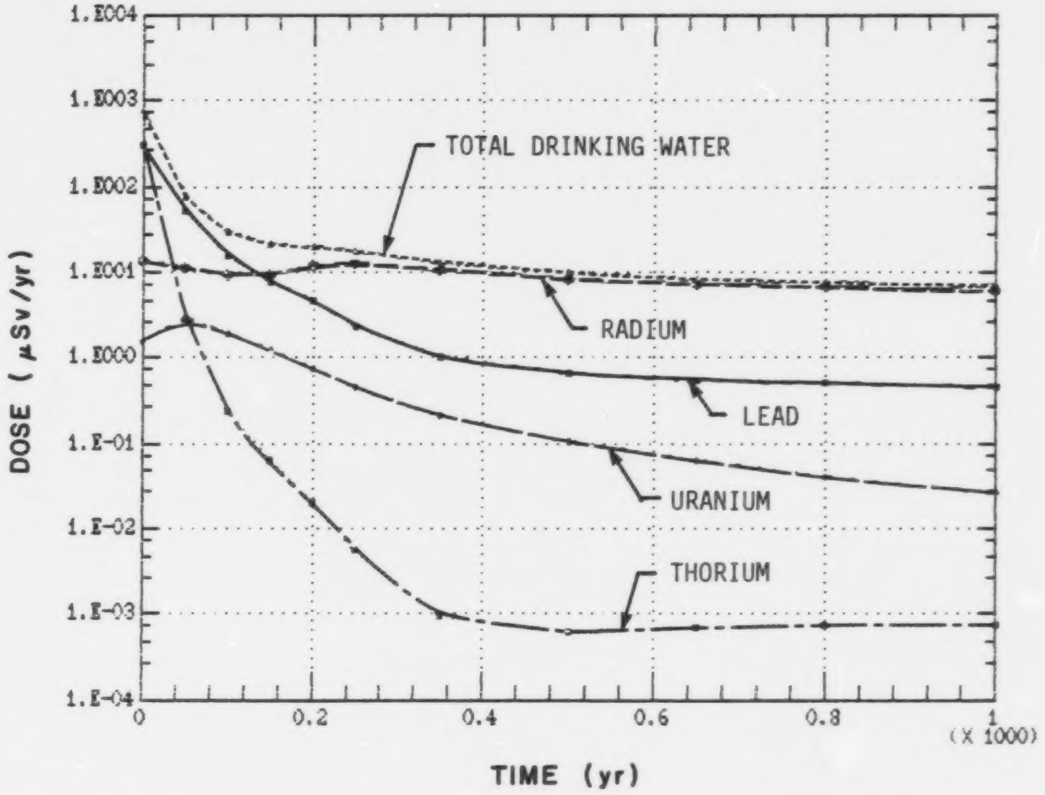

**NOTE:**

GEOMETRIC MEAN VALUES OF 200 TRIALS

the tailings porewater which enters the nearby surface waters.

Most of the lead-210 present in the tailings is assumed to exist in soluble form as a co-precipitate with lead sulphate ($PbSO_4$). This inventory of relatively soluble lead-210 results in the large initial contribution of lead-210 to total dose. However, lead-210 has a relatively short radioactive half-life (22 years), which significantly reduces its contribution to total drinking water dose with time. Lead-210 also ingrows from its radioactive parent, radium-226. This provides a long-term source of lead-210 and causes the dose via lead-210 to mirror that of radium-226 in the long-term. Lead-210 does not track radium-226 in the short term because the inventory of potentially soluble radium is much less than that of lead-210. Hence there is insufficient radium-226 to counter the radioactive decay of lead-210.

After several decades the contributions of thorium and lead decrease and the dissolution and leaching of radium-226 from the tailings system into the environment begins to dominate the water pathway.

The time pattern of radium-226 behaviour is explained by the gradual dissolution of barite (barium-radium sulphate) in the unsaturated tailings layer. Precipitation passing through the tailings dissolves the barium-radium sulphate in the uppermost tailings layer. However, concurrent pyrite oxidation in the uppermost layer produces an abundance of sulphate ions causing the reprecipitation of some of the dissolved radium-226 as a barium-radium sulphate coprecipitate in lower layers. As pyrite is depleted from the unsaturated layer the solid phase coprecipitate gradually dissolves and releases radium-226 to the porewater. Because radium forms a non-ideal solid solution with barium sulphate, the reprecipitated barium-radium sulphate contains a higher concentration of radium than the original coprecipitate. This results in increased dose between 100 and 300 years, as the reprecipitated barium radium sulphate dissolves. Once the unsaturated layer has been depleted of barite and of the reconcentrated radium-226 (i.e. the solid phase coprecipitate) the lower tailings layers act as the only source of radium-226, resulting in a slowly declining dose from radium-226 with time.

Uranium is the least important contributor to dose from the drinking water pathway. Its behaviour can be explained by noting that we assume uranium is released to porewater as pyrite oxidizes and dissolves. Thus uranium in porewater tracks the behaviour of pyrite.

The geometric mean dose from the drinking water pathway exhibits a monotonically decreasing behaviour over time. This is explained by the rapid decrease in the contributions from thorium and lead-210, and the continually declining radium-226 and uranium concentrations in tailings porewater as explained above.

As noted in the previous section, dose via the fish pathway does not track the pattern of dose via drinking water between 50 and 300 years. As with the drinking water dose, the fish dose for the first 50 years is likely due to high initial thorium and lead concentrations, which decrease rapidly. The increase in fish dose after about 100 years is due not to an increase in radionuclide concentration in water or fish flesh, but rather results from a feature of the phase III models which correlate fish productivity (and hence availability) with lake pH. At the low pH's encountered initially, fish productivity is low. As the pH in the receiving water increases (as discussed in a later section), the fish population is restored and there is an increased chance of catching fish, which in turn leads to an increased dose via this pathway. Once the pH in the receiving waters reaches a certain level, dose from the fish pathway tracks the dose from the drinking water pathway as would be anticipated.

Another question we can ask about the water pathways is, which of the three contributing sources (surface runoff, groundwater (subsurface) flow or tailings erosion) makes the greatest contribution to activity in the watershed. As an example, we consider the relative contribution of each source to the radium-226 activity in the first lake downstream of the tailings site, as illustrated in Figure 5.6. In Figure 5.6, the contribution of seepage discharge from the 3rd layer of the tailings to the surface flow from

## FIGURE 5.6
## TAILINGS SOURCE INPUTS OF RADIUM - 226 ACTIVITY (SCENARIO I)

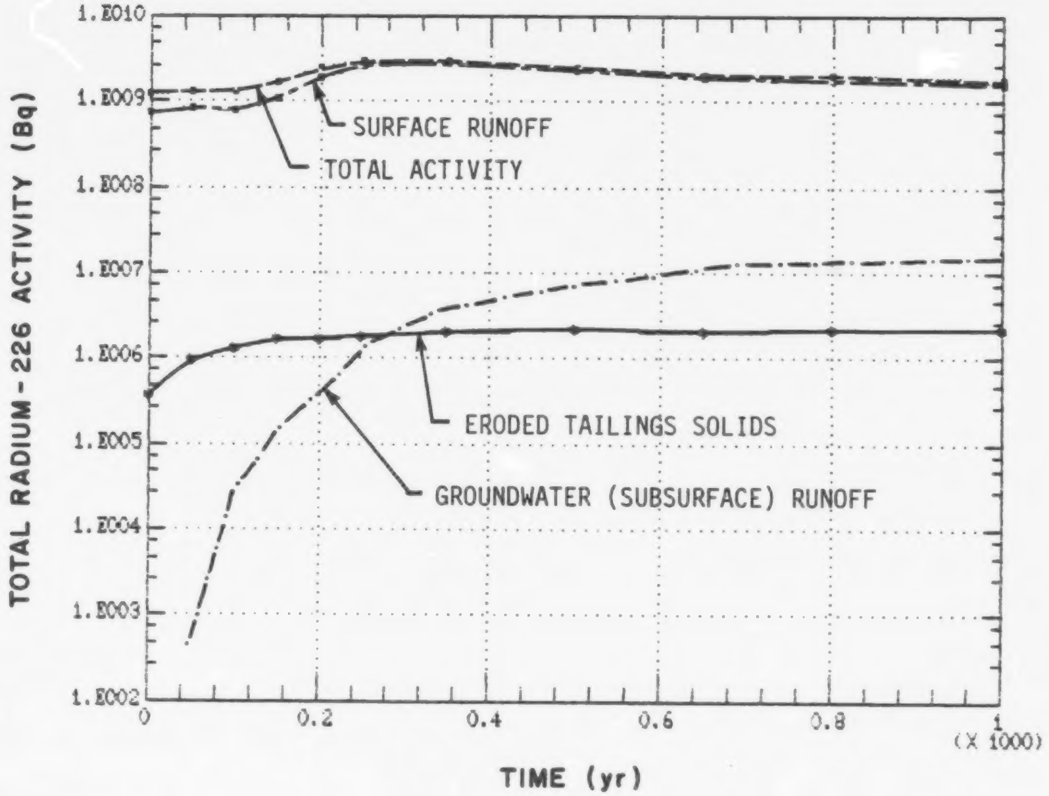

NOTE:

GEOMETRIC MEAN VALUES OF 30 TRIALS

GROUNDWATER ACTIVITY AT t = 0 YEARS IS ZERO, WHICH CANNOT BE SHOWN ON A LOG PLOT the site (i.e. the curve designated surface runoff) is the dominant contributor of radium-226 activity in the lake at all times. Tailings erosion and groundwater flow are generally two to three orders of magnitude lower within the 1000 year simulation period.

Figure 5.7 focuses more closely on the relationship between radionuclide concentrations in the tailings porewater (the mixing layer which is the source of surface runoff from the tailings site) and concentration in the receiving water at node 2 in the watershed (the first lake downstream of the tailings site). Figure 5.7(a) is a plot of concentration versus time for the four radionuclides in the lake and Figure 5.7(b) is a plot of concentration versus time of the four radionuclides in the mixing zone. In general terms the patterns track each other as would be anticipated. For example, the radium-226 curves on the two figures are very similar. The lead-210, thorium and uranium curves are also similar although the patterns indicate a longer response time in the watershed. This observation is due primarily to feed back from the bottom sediments to the water column. A substantial inventory of the radionuclides is removed with sedimenting solids. As the solids decay a portion of the radionuclide content is released back to the water phase. This phenomena explains why the curves on Figure 5.7(a) change more slowly than the corresponding curves on Figure 5.7(b). The thorium concentration curves most clearly demonstrate the influence of feedback from the lake sediments. Whereas the thorium curve for tailings porewater (Figure 5.7(b)) levels off at a low residual concentration in less than 200 years, the comparable curve for the lake (Figure 5.7(a)) does not reach a steady concentration until nearly year 400. This arises because the thorium concentration in tailings porewater is a strong function of pH, at low pH's, but reaches a relatively constant level as porewater pH rises above approximately 5.0.

Another factor which influences the shape of the concentration profile of the short-lived radionuclides is ingrowth from the parent nuclide. This influence is most evident for the lead-210 profile which is seen to parallel the radium-226 curves in the long-term (beyond about 400 to 500 years) in both parts of

FIGURE 5.7

RADIONUCLIDE ACTIVITY vs. TIME
( SCENARIO I )

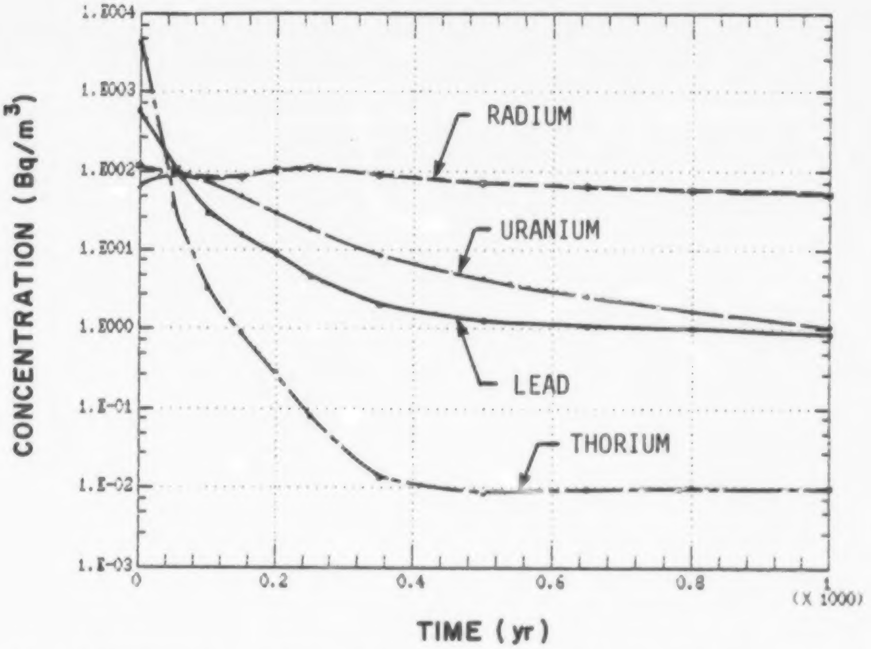

A) RECEIVING WATER ACTIVITY AT OUTLET OF FIRST LAKE (NODE 2)

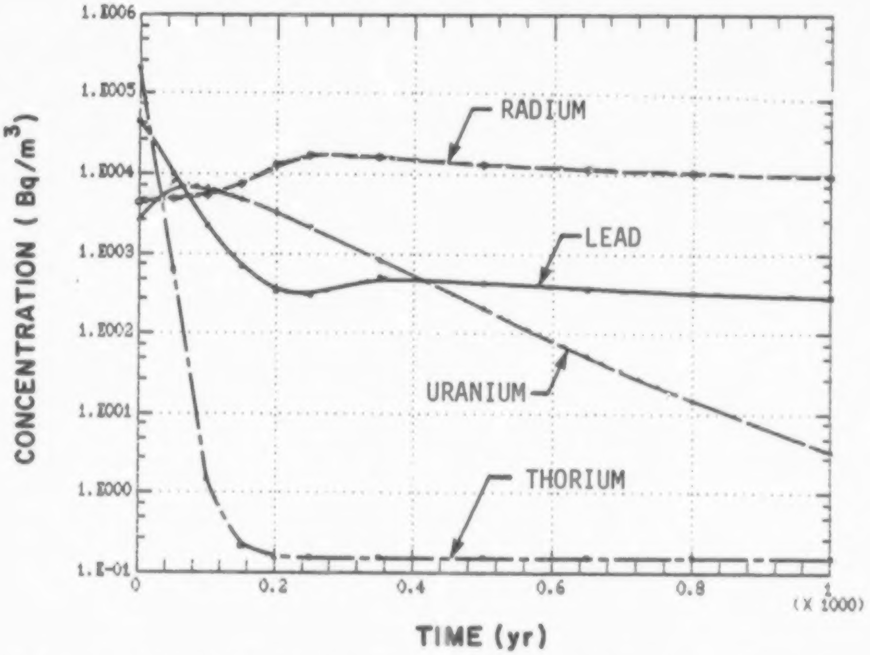

B) TAILINGS POREWATER ACTIVITY IN MIXING ZONE (LAYER 3)

Figure 5.7.

### 5.2.3 Importance Analysis

The Phase II studies (SENES, 1985), examined many tools for parameter importance analysis. At that time the sensitivity index was found to be a simple but effective tool for isolating important variables and has been selected for use in this Phase III demonstration. The sensitivity index for a particular input parameter is calculated by holding all other parameters constant at their nominal values and calculating the desired output at the minimum and maximum values of the input parameter being studied. The sensitivity index (SI) is calculated as:

$$SI = 1 - \frac{\text{Low Result}}{\text{High Result}}$$

Parameters with SI values near 1 are considered to be important whereas parameters with SI values near 0 have little influence on the model calculations. A detailed discussion of the sensitivity index can be found in Volume 2 of Phase II (SENES, 1985).

The parameters with the largest sensitivity indices are shown for total dose and drinking water dose in Table 5.1 for 0 and 250 years. Not surprisingly, there is a great deal of similarity between the important parameters for total dose and drinking water dose, since it has already been shown that drinking water is the main contribution to total dose. All parameters listed in Table 5.1 are defined further in Table 5.2. A review of the parameters listed in Table 5.1 indicates that nearly all of the parameters are associated with the tailings source term component model. The only exceptions are the parameters relating the transfer of radium-226 and lead-210 from water to fish flesh (BIOACR and BIOACP), the transfer of lead-210 from water to sedimenting solids (WKDPB) and the fraction of the annual water consumption that is derived from a local source by the receptor (WFLOCI). These parameters are all related to the water pathways.

Table 5.1

## PARAMETER SENSITIVITY INDEX[a] (SI) VALUES
## FOR THE BASE CASE (SCENARIO 1)

| Sensitivity of Total Dose | | | | | Sensitivity of Drinking Water Dose | | | | |
|---|---|---|---|---|---|---|---|---|---|
| Time | SI | List[b] | Sign[c] | Parameter[d] | Time | SI | List[b] | Sign[c] | Parameter[d] |
| 0 | 0.680 | 1 | + | SULPRD | 0 | 0.682 | 1 | + | SULPRD |
| | 0.672 | 2 | + | O2DIFF | | 0.673 | 2 | + | O2DIFF |
| | 0.609 | 3 | - | FRACTH | | 0.610 | 3 | - | FRACTH |
| | 0.544 | 4 | + | RHOTAL | | 0.545 | 4 | + | RHOTAL |
| | 0.434 | 5 | + | FACTCO | | 0.435 | 5 | + | FACTCO |
| | 0.413 | 6 | - | CLEADI | | 0.412 | 6 | - | CLEADI |
| | 0.413 | 7 | - | WKDPB | | 0.412 | 7 | - | WKDPB |
| | 0.387 | 8 | - | KPRIME | | 0.389 | 8 | - | NPRCP |
| | 0.385 | 9 | - | NPRCP | | 0.388 | 9 | - | KPRIME |
| | 0.247 | 10 | - | FNPRCP | | 0.247 | 10 | - | FNPRCP |
| 250 | 0.722 | 1 | + | BIOACR | 250 | 0.548 | 1 | + | NPRCP |
| | 0.582 | 2 | + | BIOACP | | 0.509 | 2 | - | KDRAD |
| | 0.542 | 3 | + | NPRCP | | 0.411 | 3 | + | SILT |
| | 0.508 | 4 | - | KDRAD | | 0.357 | 4 | + | PYRITI |
| | 0.416 | 5 | + | SILT | | 0.346 | 5 | - | RHOTAL |
| | 0.360 | 6 | + | PYRITI | | 0.304 | 6 | + | DUNSAT |
| | 0.350 | 7 | - | RHOTAL | | 0.296 | 7 | - | SULPRD |
| | 0.308 | 8 | + | DUNSAT | | 0.287 | 8 | - | WKDPB |
| | 0.301 | 9 | - | SULPRD | | 0.243 | 9 | - | DMIX |
| | 0.292 | 10 | - | WKDPB | | 0.200 | 10 | + | WFLOC1 |

Note

a $SI = 1 - \frac{\text{low result}}{\text{high result}}$

b ranking of parameters on basis of sensitivity index

c indicates whether the parameter has a positive or negative influence on the dose calculation

d parameter name used in computer code (see Table 5.2 for definitions)

Table 5.2

## SELECTED PARAMETER DEFINITIONS

| Computer Symbol | Definition |
|---|---|
| SULPRD | Sulphate production rate from pyrite oxidation. |
| O2DIFF | Oxygen diffusivity through tailings. |
| FRACTH | Fraction of thorium hydroxide which is crystalline (i.e. less soluble). |
| RHOTAL | Tailings bulk density. |
| FACTCO | Activity coefficient for divalent ions. |
| CLEADI | Initial concentration of lead sulphate ($PbSO_4$) in the tailings. |
| WKDPB | Lead-210 distribution coefficient between lake sediment and water. |
| KPRIME | Ratio of $O_2$ half saturation constant to $O_2$ concentration. |
| NPRCP | Net annual precipitation. |
| FNPRCP | Fraction of precipitation entering lower tailings layer. |
| BIOACR | Radium-226 bioaccumulation factor in fish flesh. |

Table 5.2, Continued

| | |
|---|---|
| BIOACP | Lead-210 bioaccumulation factor in fish flesh. |
| KDRAD | Radium-226 solid-to-liquid distribution coefficient. |
| SILT | Silt content of the tailings (% of particles < 75 ™m). |
| PYRITI | Initial concentration of pyrite in the tailings. |
| DUNSAT | Thickness of the tailings unsaturated zone. |
| DMIX | Thickness of the tailings mixing zone. |
| WFLOCI | Fraction of annual water consumption that is local. |

## 5.3 Spatial Characteristics

The Phase III models were developed to include up to 10 river or lake segments and up to 80 receptors located on the windrose grid. Figure 5.8 illustrates the decline in geometric mean drinking water dose to receptors who obtain their water from three lakes moving outward from the tailings pile. Dilution and adsorption of radionuclides on lake sediments are responsible for the reduction in radionuclide concentrations from lake 1 to lake 3. The downward trend on all the curves is due to gradual depletion of the tailings source term inventory as previously discussed.

Figure 5.9 is a plot of pH values for the same three nodes on the watershed (i.e. at the outlets of the three lakes). As would be expected, the pH is highest at the farthest downstream node (lake 3) due to dilution and buffering with fresh water flow. The pH profiles in the lakes increase gradually with time from initial values of between 4.0 to 4.5 to slightly above pH = 7.2 in 150 years (lake 3) to 250 years (lake 1). The recovery parallels the depletion of oxidizable pyrite in tailings pile.

Figure 5.10 illustrates the decline in the geometric mean radon dose when the receptor is located at increasing distances from the tailings pile. The effects of dispersion are evident from a comparison of the curves. Due to gradual leaching of radium-226 from the tailings, the radon dose decreases monotonically with time as expected. Although the results are not shown here, the dust inhalation pathway behaves in a similar manner.

## 5.4 Scenario 2: Pyrite Reduction and Lime Addition

This scenario assumes the pyrite content of the unsaturated tailings zone has been reduced from about 6.5% to about 0.6% and that limestone ($CaCO_3$) has been added to the depyritized tailings in the amount of 1% by weight.

Pyrite removal reduces the acid generating potential of the tailings. The limestone addition maintains a near neutral pH in the porewater thus reducing

FIGURE 5.8

# DRINKING WATER DOSE vs. TIME FOR THREE RECEPTORS (SCENARIO I)

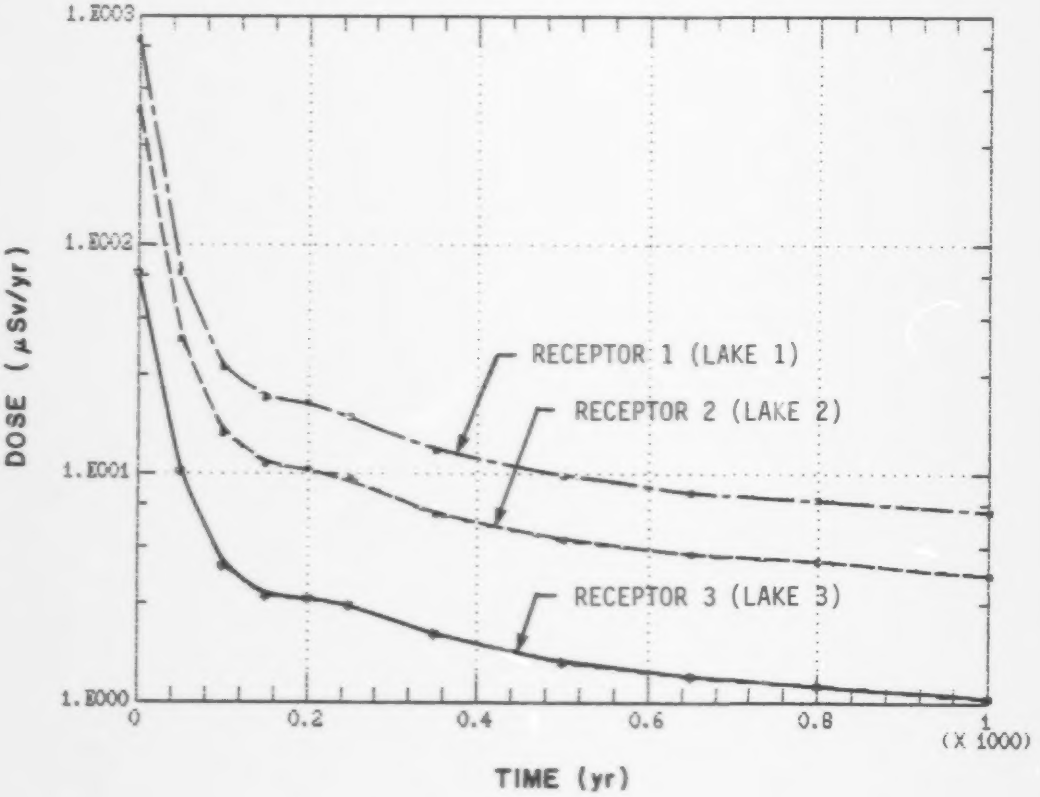

**NOTE:**

GEOMETRIC MEAN VALUES OF 200 TRIALS

FIGURE 5.9

**pH vs. TIME**
**FOR THREE WATERSHED LOCATIONS**
**( SCENARIO I )**

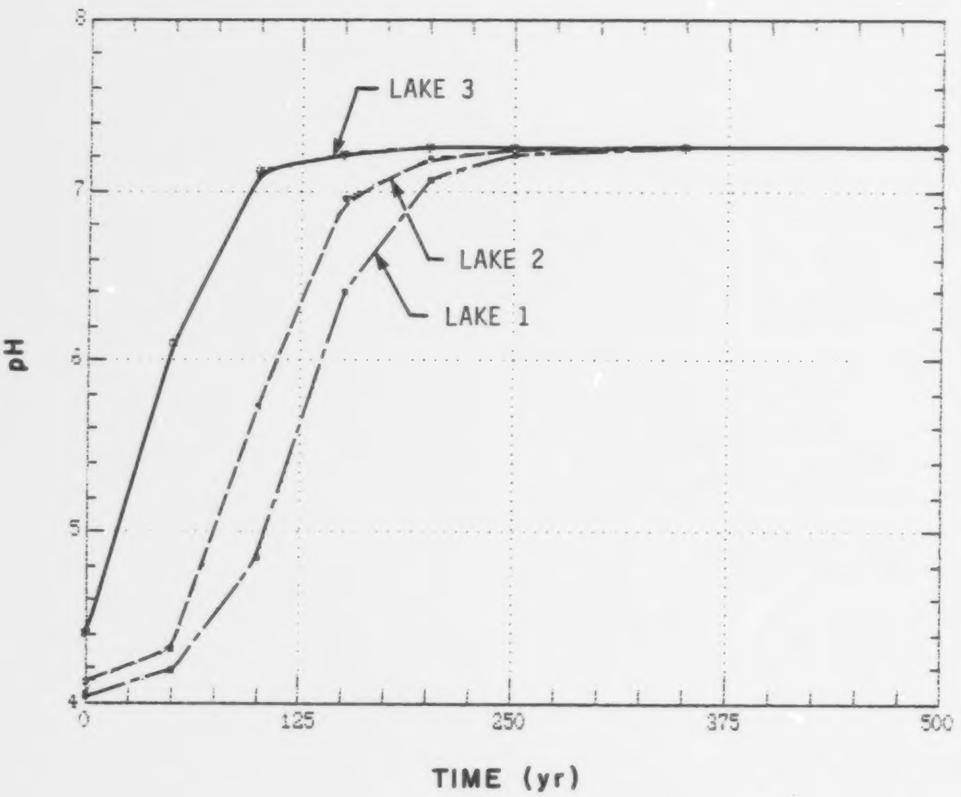

**NOTE :**

GEOMETRIC MEAN VALUES OF 200 TRIALS

FIGURE 5.10

# RADON DOSE vs. TIME TO THREE RECEPTORS ( SCENARIO I )

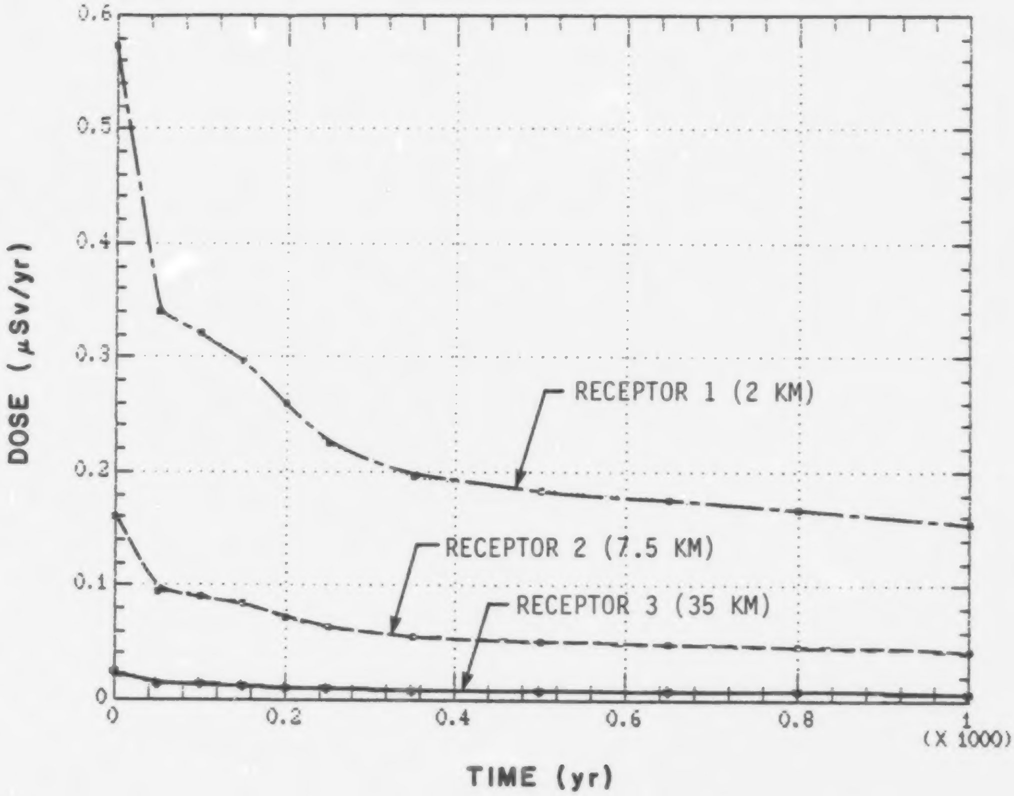

NOTE:

GEOMETRIC MEAN VALUES OF 200 TRIALS

the rate of bacteria-assisted pyrite oxidation. It serves also to neutralize any acid produced from residual pyrite oxidation. Thus, as noted previously, the source term models used to evaluate Scenario 1 had to be modified for use in evaluating Scenario 2. This modification is discussed in Chapter 3 of Volume 3.

Figure 5.11 is a plot of the pH values at the outlets of the three lakes in the watershed (i.e. at nodes 2, 4 and 7). The results are quite different from those for Scenario 1 shown on Figure 5.9. Most significantly the pH levels in the watershed lakes are considerably higher than predicted in Scenario 1. This observation is due to two key factors; the reduced pyrite inventory which necessarily limits the acid production in Scenario 2 and the presence of limestone which limits the rate of pyrite oxidation and neutralizes acidity produced from residual pyrite oxidation. The rise, fall and rise again of pH at the three watershed locations during the first 100 years is attributable to a number of factors. Firstly, the rise from year 0 to year 50 reflects a slow but gradual decrease in the rate of acid production in the tailings which is mirrored by a decrease in the acidity reaching the watershed and thus a gradual increase in pH. This is most evident in Lake 1 which shows a rise from about pH = 6.0 to 6.9 in the first fifty years. The change in pH in Lakes 2 and 3 is less significant due to increased dilution with fresh water inflows at downstream locations.

Secondly, the decline in pH in the lakes between years 50 and 100 coincides with exhaustion of the limestone content in the tailings. Once the limestone is exhausted, the rate of pyrite oxidation increases and the acid generated is no longer neutralized by the buffering capacity of the limestone. These two factors result in an increase in the acid load discharged from the tailings pile to the receiving water system and a downward shift in pH as noted on Figure 5.11.

Finally, the extent of the downward pH shift is limited by the fact that the residual pyrite content on the upper tailings layer is rapidly oxidized. Subsequently the pH in the watershed recovers to neutrality as indicated by

FIGURE 5.11

## pH vs TIME
## AT THREE WATERSHED LOCATIONS
## (SCENARIO 2)

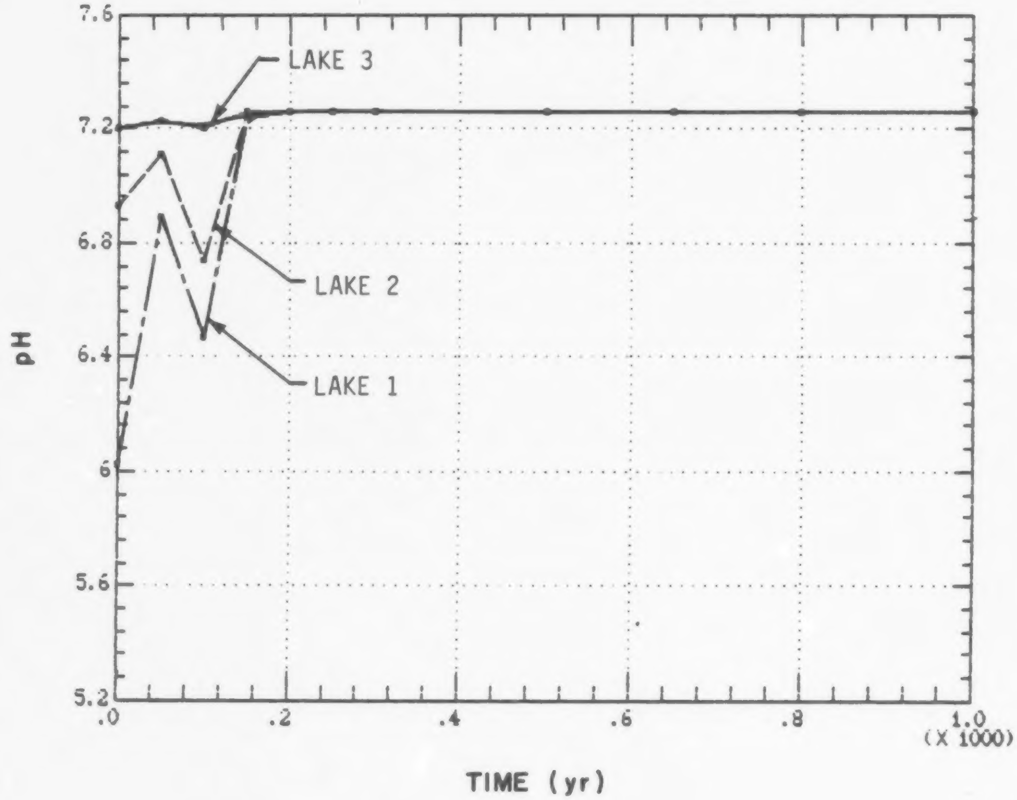

**NOTE:**

GEOMETRIC MEAN VALUES OF 200 TRIALS

the recovery in pH between years 100 and 150 at all three locations. In the long-term, once the pyrite content and readily leachable chemical precipitate (e.g. gypsum) inventories have been essentially exhausted, the pH on the watershed stabilizes at about pH = 7.2 to 7.3 as shown on Figure 5.10.

Figure 5.12 is a plot of geometric mean dose versus time for all pathways except groundshine. The general pattern of total dose is similar to that shown for the Base Case in Figure 5.2, although the magnitude of the geometric mean dose is larger. Drinking water and fish dose are the two largest dose contributors, as in the Base Case. Unlike the Base Case however, the fish dose in Scenario 2 tracks the water dose at all times. This occurs because the pH in the receiving waters is never sufficiently depressed to substantially affect the fish dynamics.

The air pathways for Scenario 2 are also somewhat different than those of the Scenario 1. The airborne dust pathways (inhalation and vegetation) show an early decline in geometric mean dose followed by an increase in dose from about year 50 to year 100 in turn followed by another decline. The initial decline is attributable to gradual leaching of radionuclides from the tailings combined with tailings revegetation. Around year 50 or so, the buffering capacity of the limestone has been depleted and the uppermost unsaturated layer of tailings becomes acidic reducing the vegetative cover. The result is an increase in wind borne dust and consequently dose via the air pathways. Once the pyrite content of the upper tailings layer is exhausted around year 100, the tailings surface revegetates, resulting in reduced wind erosion and dose via the air pathways.

Two pathways, the radon pathway and the vegetation dose pathway actually exhibit a small gradual increase from about year 200 to the end of the simulation. This is explained by the fact that in Scenario 2 thorium is not leached as rapidly from the upper tailings layer as it is in Scenario 1. Hence radium-226 will attempt to grow towards equilibrium with its parent thorium-230. This in turn leads to higher radon flux (and dose) and a higher radium content in the tailings solids than in Scenario 1. The increase in

## FIGURE 5.12

## DOSE vs. TIME
## BY PATHWAY
## ( SCENARIO 2 )

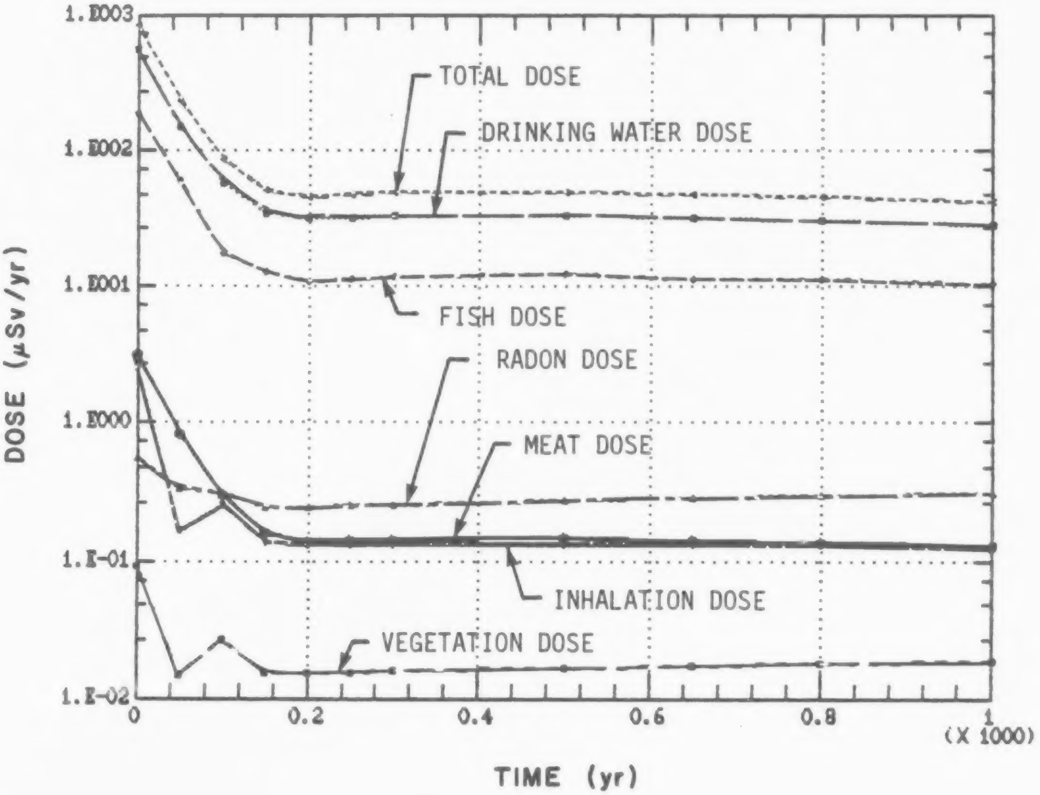

**NOTE:**

GEOMETRIC MEAN VALUES OF 200 TRIALS

dose via the vegetation pathway is thus due to the increase in radium-226 (and lead-210) content in the erodible tailings solids.

As noted previously the total dose at all times (beyond the first timestep) from Scenario 2 is somewhat larger than the total dose from Scenario 1. This is primarily due to the reduction in pyrite oxidation which leads to lower porewater concentration of dissolved sulphate ions and hence higher levels of dissolved radium-226 and lead-210 over the length of the simulation period. These radionuclides contribute mainly to the doses from drinking water and fish which, as before, are the significant contributors to the total dose.

Figure 5.13 shows relative frequency histograms for Scenario 2 at t = 0 (Figure 5.13a) and at t = 250 (Figure 5.13b). These figures can be compared to Figure 5.3a and 5.3b respectively. As in Scenario 1 these histograms have long tails extending to the right which suggests that the geometric mean may be an appropriate descriptor of central tendency.

Figure 5.14 is a plot of geometric mean dose versus time for the drinking water pathway by radionuclide. At early times the water dose is dominated by lead-210 and beyond about year 100 by radium-226. The time pattern of the radionuclide contributions to dose is explained by the dependence of thorium solubility on pH, the assumption that soluble uranium tracks pyrite oxidation and that radium-226 and lead-210 solubility are controlled by the sulphate ion level. Because the pH of the tailings porewater does not reach the low levels seen in Scenario 1, the initial thorium concentration in the source discharge and hence in the watershed is much lower in Scenario 2. The uranium dose via the water pathways is very similar in the two scenarios. This arises because the radionuclide inventory was held constant even though the pyrite inventory was reduced in scenario 2. Hence, although there is less pyrite to oxidize in scenario 2, the mass fraction of uranium in pyrite is greater, and the two effects essentially cancel each other. On the other hand, because the sulphate level from pyrite oxidation is much lower in Scenario 2, much more barite and lead sulphate are dissolved in the source discharge, thus, substantially increasing the radium-226 and lead-210 doses via the water

FIGURE 5.13

TOTAL DOSE HISTORAM
( SCENARIO 2 )

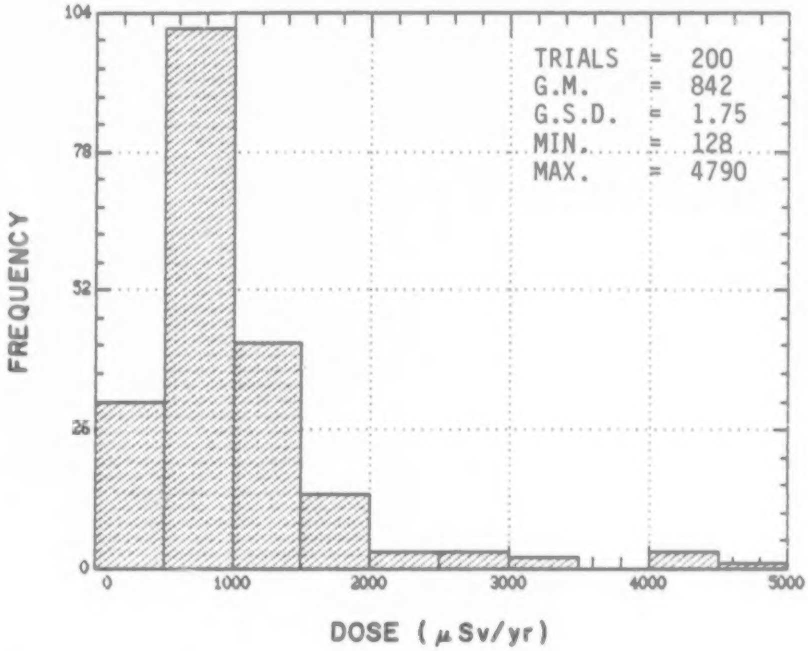

A) t = 0 YEARS

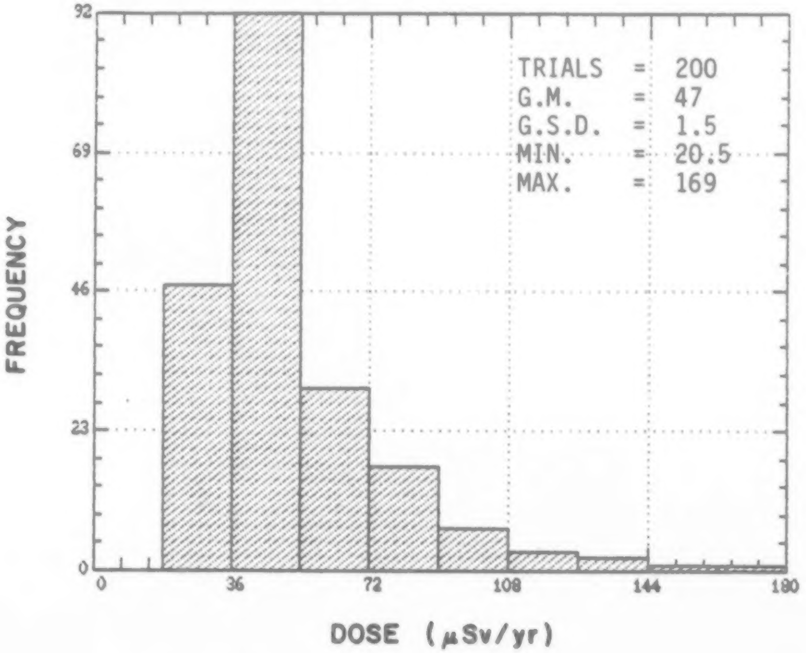

B) t = 250 YEARS

## FIGURE 5.14

## DRINKING WATER DOSE vs TIME BY RADIONUCLIDE ( SCENARIO 2 )

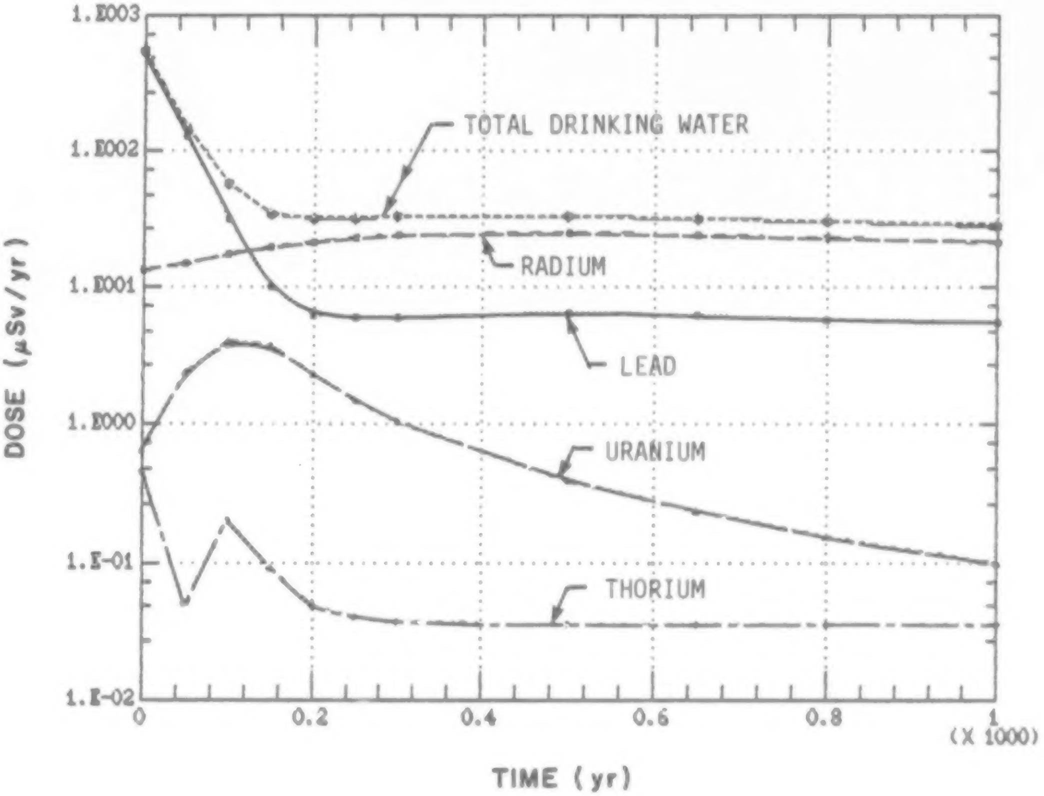

**NOTE:**

GEOMETRIC MEAN VALUES OF 200 TRIALS

pathways.

In Figure 5.15 we compare the cumulative relative frequencies for total dose for Scenario 1 and Scenario 2 at t = 0 years (Figure 5.15a) and t = 250 years (Figure 5.15b). At t = 0 years the cumulative curves are quite similar except that Scenario 2 has a higher percentage of dose values in the upper tail (e.g the upper 5% say). At t = 250 years the situation is quite different. The dose for Scenario 2 is much higher than for Scenario 1.

The comparison of dose at t = 250 years is illustrated further in Figure 5.16 where we superimpose on the same scale the cumulative relative frequency and 95% confidence band for Scenario 1 and the cumulative relative frequency for Scenario 2. The fact that the curve for Scenario 2 falls outside the confidence bands on Scenario 1 clearly demonstrates that the distributions of dose are different.

FIGURE 5.15

COMPARISON OF TOTAL DOSE DISTRIBUTIONS
FOR SCENARIOS 1 AND 2

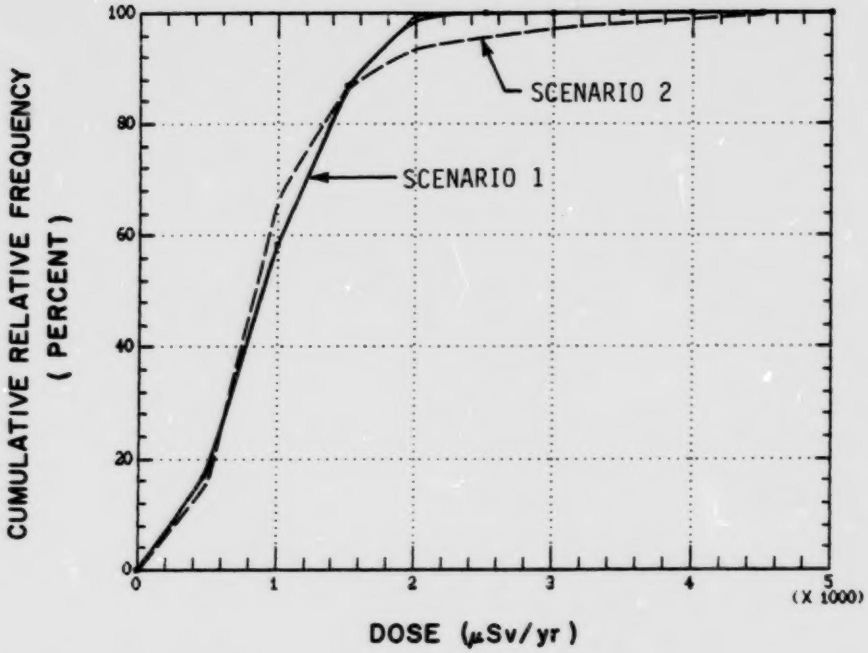

A) t = 0 YEARS

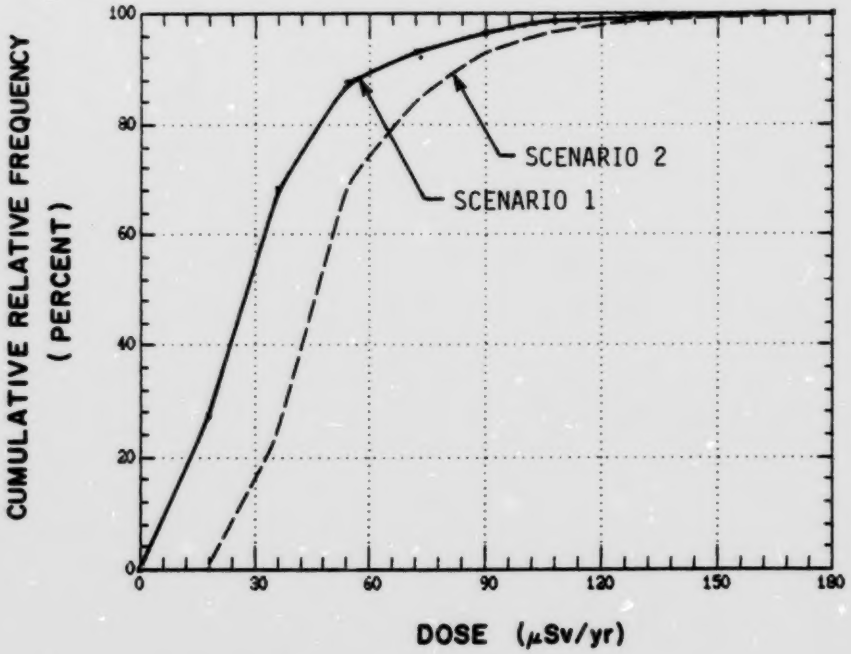

B) t = 250 YEARS

FIGURE 5.16

COMPARISON OF SCENARIO I 95% CONFIDENCE BANDS
WITH SCENARIO 2
( TOTAL DOSE AT t = 250 YEARS )

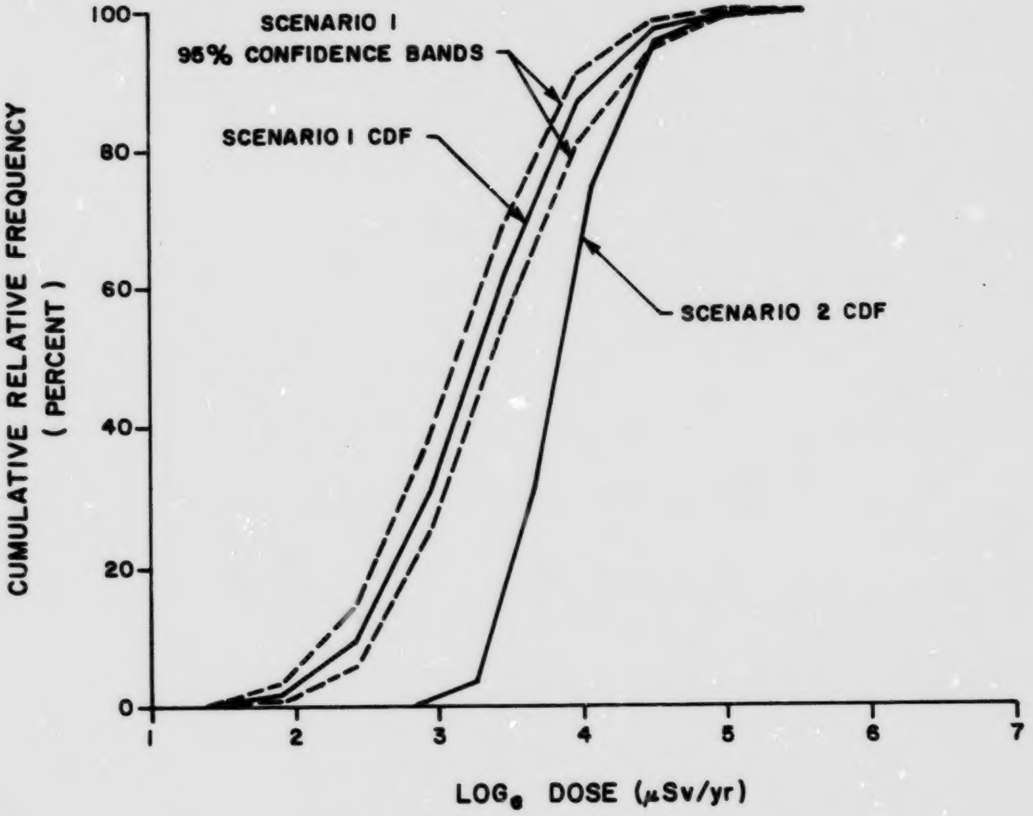

## 6.0 SUMMARY AND RECOMMENDATIONS

### 6.1 Summary

This study, which built upon two previous phases of work has greatly enhanced the capabilities of the Uranium Tailings Assessment Program (UTAP). The current version of UTAP provides great flexibility in analyzing the long-term effects of Canadian uranium mill tailings. It has been used to simulate the behaviour and environmental impacts of a hypothetical, reference tailings facility, containing low-grade, pyritic tailings, typical of those found in northern Ontario.

UTAP was developed in a modular fashion, and consists of a number of "control" and "component" modules. Component modules are the computer implementation of the mathematical models used to describe the tailings and surrounding environment. Control modules provide the infrastructure required for probabilistic analysis. The modular approach facilitated program development and quality assurance and will allow UTAP to be easily modified in the future for application to specific sites.

The current version of UTAP models the behaviour of four radionuclides (natural uranium, total thorium, radium-226 and lead-210) and a number of inorganic chemical species as well as pH. Seven different exposure pathways are modelled, including:

- radon inhalation
- dust inhalation
- external exposure (groundshine)
- ingestion of vegetables
- ingestion of meat (caribou and moose)
- ingestion of water
- ingestion of fish

UTAP requires considerable information as user-specified input to the program.

This provides much greater flexibility than having the same information "built-in" to the computer program. Some noteworthy UTAP features include the capabilities to:

- perform calculations in all directions, for up to 50 km from the tailings site
- incorporate an entire watershed, with user-specified characteristics
- model receptors of two types, at up to 80 different locations
- perform calculations for up to 1000 years, in time steps of 1 or 10 years
- model two distinctly different tailings disposal scenarios
- simulate further disposal scenarios by modifying input parameter distributions and/or component modules.

These capabilities allow one to generate and access a large amount of information. The assimilation, analysis and interpretation of this quantity of information can become a very complex task. It is substantively simplified in UTAP by the computation of recursive ("on the fly") summary statistics. However, access to commercially available data management software is required to enhance data manipulation and reduction.

The results generated by UTAP for the hypothetical, reference tailings facility indicate that water-related pathways contribute the greatest dose to those receptors on the affected watershed. These primary exposure pathways involve direct consumption of water and fish.

For the base case (or walk-away) scenario, the total dose to the critical receptor decreases continuously over the 1000 years modelling period. Thorium and lead initially contribute most to the total dose, while radium dominates over the long-term. The second scenario involves a reduction of the pyrite content of the upper tailings layer and the addition of limestone as a buffering agent. An immediate benefit is an increase in the tailings porewater and receiving water pH, which lasts as long as limestone is present. The dose via radium and lead are significantly higher with this scenario, while the doses via uranium and thorium are much reduced from the first scenario. Overall, the critical receptor receives a higher total dose over most of the simulation period.

In addition to developing the improved version of UTAP, this project examined several other technical issues relevant to probabilistic analysis. In particular, a post-processing program was developed which generates "confidence bands" on selected parameter distributions calculated by UTAP. A second study involved a further examination of model aggregation. It concluded that an aggregate (transfer factor) model was as appropriate as more complex models for modelling the transfer of radionuclides (specifically uranium) from water to fish. A third study examined the issue of identifying correlations between model parameters. The preferred approach would be to determine such correlations from experimental data, but in practice the opinions of experts may have to suffice.

## 6.2 Recommendations

While this Phase III study has produced a powerful, flexible tool for the analysis of uranium mill tailings, there are several areas which could profit from further work. Our primary recommendation is that UTAP be adapted for, and applied to the analysis of an actual tailings facility. Work to this point has been directed at analyzing a hypothetical, reference facility. While this has resulted in the development of a fairly general tool, the ultimate use of UTAP must be in the analysis of existing facilities. Application to a specific site would also indicate the level of effort required to use UTAP in this way. It is envisioned that certain aspects of UTAP would require some modifications to be applicable to any specific site. These might include, for instance, the tailings source term model and input parameter distributions.

A second recommendation is that the component models be validated to whatever extent is possible. As mentioned previously, models are never exact representations of reality, but comparison with actual observations can help to improve the quality of the models used. We recognize that, because of the nature of this modelling exercise, model validation may only be possible on a relatively small scale. It is possible that model validation and the application of UTAP to a specific site could be done concurrently.

Third, consideration should be given to embedding UTAP within a more "user-friendly" computing environment. The current version of UTAP is quite powerful, and can generate large quantities of information. The real task at this point is to organize this information in a meaningful way, so that it can be easily understood, manipulated and communicated to a variety of audiences. Experience at SENES indicates that a fourth generation computing language or sophisticated data-base management package provides considerable power in this area. If UTAP is to be used to its fullest potential, it should be made available along with an interface to a selected, commercially available post-processing facility.

Finally, efforts should continue to examine the interpretation and communication of probabilistic analysis results. Probabilistic analysis is finding increasing use and acceptance in a variety of applications throughout the world. Since many technical issues in this area remain unresolved, the NUTP should continue to exchange technical information with other practitioners in the field. To ultimately be most useful, probabilistic analysis techniques and results will have to be accepted by, and explained to a variety of groups and individuals (e.g. mining companies, regulatory agencies, etc.). Efforts should continue to improve the communication of the concepts and results of probabilistic analysis.

## 7.0 REFERENCES

Colorado Department of Health (CDOH), 1984. "Fugitive Particulate Emissions." Interoffice Memo from T. Tistinic, Dated July 2.

Cheng, R.C.H. and Iles, T.C., 1983. "Confidence Bands for Cumulative Distribution Functions of Continuous Random Variables." Technometrics, Vol. 25, No. 1, pp. 77-86.

Crow, E.L., Davis, F.A., and Maxfield, M.W., 1960. Statistics Manual, Dover, N.Y.

Downing, D.J., Gardner, R.H., and Hoffman, F.O., 1985. "An Examination of Response-Surface Methodologies for Uncertainty Analysis in Assessment Models." Technometrics, Vol. 27, No. 2, pp. 151-163, May.

Draper, V. and Smith, H., 1981. "Applied Regression Analysis." Second Edition, John Wiley & Sons Inc., New York.

Edwards, A.L., 1979. "Multiple Regression and the Analysis of Variance and Covariance." W.H. Freeman & Co.

Gardner, R.A., 1985. (in press). "Error Analysis and Sensitivity Analysis." Encyclopedia of Systems and Control, M. Singh (ed.), Pergamon Press, London.

Hendrickson, R.G., 1984. "A Survey of Sensitivity Analysis Methodology." U.S. Department of Commerce, National Bureau of Standards, Report NBSIR 84-2814, Washington, DC.

Hoffman, F.O. and Gardner, R.H., 1983. "Evaluation of Uncertainties in Environmental Radiological Assessment Models." In: Radiological Assessment: A Textbook on Environmental Dose Assessment, J.E. Till and H.R. Meyer (eds.), NUREG/CR-3332, ORNL-5968. U.S. Nuclear Regulatory Commission, Washington, D.C.

Iman, R.L. and Helton, J.C., 1985. "A Comparison of Uncertainty and Sensitivity Analysis Techniques for Computer Models." NUREG/CR-3904; SAND84-1461 Sandia National Laboratories, Albuquerque, New Mexico.

INTERA Environmental Consultants Inc., 1983. "A Proposed Approach to Uncertainty Analysis." Prepared for Office of Nuclear Waste Isolation (ONWI), Battelle Memorial Institute, Columbus, Ohio, ONWI-488.

International Commission on Radiological Protection (ICRP), Publication 23, 1975. "Report of the Task Group on Reference Man." Published by Pergamon Press.

Kendall, M., and Stuart, A., 1961. "The Advanced Theory of Statistics, Vol. 2: Inference and Relationship." 1st Edition, Hafner Publishing Co.

Kleijnen, J.P.C., 1974. "Statistical Techniques in Simulation - Part 1." Marcel Dekker, Inc., New York.

Rogers, V.C., Overmeyer, R.F., Putzig, K.M., Jensen, C.M., Nielson, K.K., and Sermon, B.W., 1980. "Characterization of Uranium Tailings Cover Materials for Radon Flux Reduction." Prepared by Ford, Bacon and Davis Utah, Inc., for U.S. Nuclear Regulatory Commission, Report NUREG/CR-1081., FBDU-218-2.

Rose, K.A., and Swartzman, G.L., 1981. "A Review of Parameter Sensitivity Methods Applicable to Ecosystem Models." NUREG/CR-2016, U.S. Nuclear Regulatory Commission, Washington, DC.

SENES Consultants Limited, 1984. "A Study to Develop and Demonstrate Techniques for the Probabilistic Assessment of the Long-Term Effects of Uranium Mill Tailings in Canada - Phase I." Research Report prepared for the National Uranium Tailings Program, CANMET, EMR, under Supply and Services Canada Contract No. 0SQ83-00236.

SENES Consultants Limited, 1985. "A Study to Develop and Demonstrate Techniques for the Probabilistic Assessment of the Long-Term Effects of Uranium Mill Tailings in Canada - Phase II." Research Report prepared for the National Uranium Tailings Program, CANMET, EMR, under Supply and Services Canada Contract No. 0SQ84-00207.

# Volume

# 2

# NATIONAL
# URANIUM
# TAILINGS
# PROGRAM

Energy, Mines and Resources Canada
Énergie, Mines et Ressources Canada

Canada

# PROBABILISTIC MODEL DEVELOPMENT FOR THE ASSESSMENT OF THE LONG-TERM EFFECTS OF URANIUM MILL TAILINGS IN CANADA - PHASE III

## VOLUME 2 - URANIUM TAILINGS ASSESSMENT PROGRAM (UTAP): SYSTEM DESCRIPTION AND CONTROL MODULE DOCUMENTATION

A Research Report prepared under:
Contract #0SQ85-00182

for

The National Uranium Tailings Program
Canada Centre for Mineral and Energy Technology
Energy, Mines and Resources Canada
555 Booth Street
Ottawa, Ontario
K1A 0G1

by

SENES Consultants Limited
499 McNicoll Avenue
Willowdale, Ontario
M2H 2C9

July 1986

389 pp

MICROMEDIA

## ABSTRACT

This study represents part of the ongoing efforts of the National Uranium Tailings Program (NUTP) to develop the capability to predict the long-term effects of Canadian uranium mill tailings. The study was conducted to further refine the probabilistic assessment tool developed during two previous phases of work. In particular, the work involved expanding the system model to include: additional radionuclides, additional pathways of exposure and the ability to perform calculations over much greater distances. The primary product of this study is a revised, more comprehensive Uranium Tailings Assessment Program (UTAP).

The project report has been prepared in four volumes, of which this is Volume 2. This volume provides an overview of the system model structure and documentation for the "control module" aspects of UTAP. The "control modules" provide the infrastructure for probabilistic analyses; including sampling input parameters and many input, output and bookkeeping functions. This volume also contains a number of technical appendices on topics ranging from software development and quality assurance to statements of confidence in probabilistic results.

---

## NOTICE

This report was prepared by SENES Consultants Limited (SENES) under contract to the National Uranium Tailings Program (NUTP). Neither the NUTP nor SENES makes any warranty, expressed or implied, or assumes any liability with respect to any damage or loss incurred as a result of the use made of the information contained in this publication.

## TABLE OF CONTENTS

Page

Abstract i

Notice i

1.0 INTRODUCTION 1-1
- 1.1 Background 1-1
- 1.2 System Model Overview 1-2
- 1.3 The Software Development Process 1-3

2.0 CONTROL MODULE OBJECTIVES AND CONCEPTUAL SPECIFICATIONS 2-1
- 2.1 Control Module Features 2-1
- 2.2 Input Modules 2-2
- 2.3 Random Sampling Modules 2-2
- 2.4 Output Selection Modules 2-3
  - 2.4.1 Compute Summary Statistics 2-3
  - 2.4.2 Write Detailed Results to Output File 2-3
- 2.5 Stepping Through Time 2-4
- 2.6 Confidence Bands 2-4

3.0 CONTROL MODULE DESCRIPTIONS 3-1
- 3.1 Main Program (EXEC) 3-1
- 3.2 Input Modules 3-2
  - 3.2.1 First Input Routine (SUBROUTINE INPUT1) 3-2
  - 3.2.2 Second Input Routine (SUBROUTINE INPUT2) 3-4
  - 3.2.3 Generation of Error and Warning Messages (SUBROUTINE ERROR) 3-6
- 3.3 Sampling Routines 3-7
  - 3.3.1 Objective 3-7
  - 3.3.2 General Concepts 3-7
  - 3.3.3 The Random Number Generator (FUNCTION SUBROUTINE RANDOM) 3-9

Table of Contents (continued)

Page

3.3.4 Creation of a Cumulative Distribution Function (SUBROUTINE CREATE) 3-13

3.3.5 Choice of Sampling Routine (SUBROUTINE CHOOSE) 3-15

3.3.6 Normal Distribution (SUBROUTINE NORMAL) 3-16

3.3.7 Lognormal Distribution (SUBROUTINE LNORM) 3-17

3.3.8 Uniform Distribution (SUBROUTINE UNIFOR) 3-17

3.3.9 Loguniform Distribution (SUBROUTINE LOGUNI) 3-18

3.3.10 Triangular Distribution (SUBROUTINE TRIANG) 3-19

3.3.11 Weibull Distribution (SUBROUTINE WEIBUL) 3-20

3.3.12 Arbitrary and Beta Distributions (SUBROUTINE BETA) 3-21

3.3.13 Correlated Parameters (SUBROUTINE CORREL) 3-22

3.4 Output Selection Routines 3-24

3.4.1 Saving Time-Variant Sampled Parameters (SUBROUTINE TIMSEL) 3-24

3.4.2 Selection of Output Time Steps (SUBROUTINE SELECT) 3-26

3.4.3 Sorting of Output Variables (SUBROUTINE SORT) 3-26

3.4.4 Saving Output Variables (SUBROUTINE SEND) 3-27

3.4.5 Saving Non-Time-Variant Sampled Parameters (SUBROUTINE SAVEIN) 3-27

Table of Contents (continued)

Page

3.5 Statistics Routines 3-28
3.5.1 Computing Summary Statistics (SUBROUTINE STATS) 3-28
3.5.2 Computing Moment Values (SUBROUTINES MOMENT and GMOMEN) 3-31
3.6 Output Routines 3-32
3.6.1 Output of Detailed Results (SUBROUTINE WRITE) 3-32
3.6.2 Creation of Output Labels (SUBROUTINE NAMOUT) 3-32
3.6.3 Output of Summary Statistics (SUBROUTINE OUTPUT) 3-33

4.0 CONFIDENCE BANDS PROGRAM DESCRIPTION 4-1
4.1 Introduction and Background 4-1
4.2 The General Nature of the Confidence Bands Programs 4-2
4.2.1 The Binning Program (BIN) 4-2
4.2.2 The Confidence Band Program (OPAN) 4-3
4.3 Examples 4-5

**REFERENCES**
**APPENDIX A** The Software Development and Quality Assurance Program
**APPENDIX B** Control Modules Code Listing and Variable Dictionary
**APPENDIX C** Testing of Random Number Generator UNIRAN
**APPENDIX D** Comparison of Selected Probabilistic Assessement Tools
**APPENDIX E** A Bayesian Approach to Assessing Confidence in Monte Carlo Output Distributions
**APPENDIX F** Development and Implementation of a Procedure for Establishing Confidence Regions for Output from Monte Carlo Calculations

Table of Contents (continued)

**APPENDIX G** Confidence Bands Programs Code Listing and Variable Dictionary

**APPENDIX H** Identification of Parameter Correlations and Functional Relationships Using Expert Opinion

**APPENDIX I** An Examination of Parameter Correlation in the Radon Source Term Model

## LIST OF FIGURES

| | | Follows Page |
|---|---|---|
| 1.1 | The System Model | 1-3 |
| 1.2 | Control Module Structure | 1-3 |
| 1.3 | Subroutine COMEX and the Component Modules | 1-3 |
| 3.1 | Function of First Input Module | 3-3 |
| 3.2 | Function of Second Input Module | 3-5 |
| 3.3 | Sampling from Cumulative Probability Function | 3-9 |
| 3.4 | An Arbitrary Probability Density Function | 3-14 |
| 3.5 | Forms of the Beta Distribution Probability Density Function | 3-14 |
| 3.6 | Plot of Frequency Histogram (500 Samples) and Probability Distribution for Normal Distribution | 3-16 |
| 3.7 | Plot of Frequency Histogram (500 Samples) and Probability Distribution for Lognormal Distribution | 3-17 |
| 3.8 | Plot of Frequency Histogram (500 Samples) and Probability Distribution for Uniform Distribution | 3-17 |
| 3.9 | Plot of Frequency Histogram (500 Samples) and Probability Distribution for Log-Uniform Distribution | 3-18 |
| 3.10 | A Triangular Probability Density Function | 3-19 |
| 3.11 | Plot of Frequency Histogram (500 Samples) and Probability Distribution for Triangular Distribution | 3-19 |
| 3.12 | Plot of Frequency Histogram (500 Samples) and Probability Distribution for Weibull Distribution | 3-20 |
| 3.13 | Cumulative Probability Function for Beta or Arbitrary Distributions | 3-21 |
| 3.14 | Plot of Frequency Histogram (500 Samples) for Arbitrary Distribution | 3-21 |
| 3.15 | Plot of Frequency Histogram (500 Samples) and Probability Distribution for Beta Distribution | 3-21 |

List of Figures (continued)

Follows Page

3.16 Parameter Correlated to Normal Distribution (500 samples) 3-23
3.17 Structure of Vector for Output Parameters 3-25
3.18 Saving of Labels for Output 3-32
4.1 Relation of Confidence Band Programs to UTAP 4-2
4.2 Binning Program (BIN) Structure 4-2
4.3 Confidence Bands Program (OPAN) Structure 4-3
4.4 Plots of 95% Confidence Bands for a Normal Distribution (500 Trials) 4-5
4.5 Plots of 95% Confidence Bands for a Log-Transformed Lognormal Distribution (500 Trials) 4-5
4.6 Plots of 95% Confidence Bands for the Logarithm of Radium in Fish at 100 Years (200 Trials) 4-5

## LIST OF TABLES

Follows Page

2.1 Summary of Control Module Objectives 2-1
3.1 Code Listing of Main Program, EXEC 3-1
3.2 Sample of First Input File 3-3
3.3 Code Listing of SUBROUTINE INPUT1 3-3
3.4 Distribution Descriptors 3-3
3.5 Code Listing of SUBROUTINE INPUT2 3-5
3.6 Sample of Second Input File 3-5
3.7 Output Parameters 3-5
3.8 Code Listing of SUBROUTINE ERROR 3-6
3.9 Code Listing of FUNCTION RANDOM 3-12
3.10 Code Listing of SUBROUTINE CREATE 3-14
3.11 Code Listing of SUBROUTINE CHOOSE 3-15
3.12 Code Listing of SUBROUTINE NORMAL 3-16
3.13 Code Listing of SUBROUTINE LNORM 3-17
3.14 Code Listing of SUBROUTINE UNIFOR 3-17
3.15 Code Listing of SUBROUTINE LOGUNI 3-18
3.16 Code Listing of SUBROUTINE TRIANG 3-19
3.17 Code Listing of SUBROUTINE WEIBUL 3-20
3.18 Code Listing of SUBROUTINE BETA 3-21
3.19 Code Listing of SUBROUTINE CORREL 3-23
3.20 Code Listing of SUBROUTINE TIMSEL 3-25
3.21 Code Listing of SUBROUTINE SELECT 3-26
3.22 Code Listing of SUBROUTINE SORT 3-26
3.23 Code Listing of SUBROUTINE SEND 3-27
3.24 Code Listing of SUBROUTINE SAVEIN 3-27
3.25 Code Listing of SUBROUTINE STATS 3-30
3.26 Code Listing of SUBROUTINE MOMENT 3-31
3.27 Code Listing of SUBROUTINE GMOMEN 3-31
3.28 Code Listing of SUBROUTINE WRITE 3-32
3.29 Code Listing of SUBROUTINE NAMOUT 3-32
3.30 Code Listing of SUBROUTINE OUTPUT 3-33

# 1.0 INTRODUCTION

## 1.1 Background

In 1982 Energy, Mines and Resources Canada established the National Uranium Tailings Program (NUTP) to pull together previous work on Canadian uranium mill tailings, to fund additional work where significant information on gaps were found and to develop the capability to predict the long-term effects of tailings with a known degree of confidence while incorporating variability and uncertainty in the input data. Such evaluations require the use of mathematical models to simulate the behaviour of the real system.

An earlier study (Phase I) funded by the NUTP demonstrated how probabilistic techniques could be used to take account of the variability and uncertainty in model input parameters in such a simulation analysis (SENES, 1984). Subsequently, the NUTP sponsored a followup study (Phase II, SENES, 1985) to extend and refine the probabilistic tools developed in the Phase I study and to investigate various issues of technical interest involved in carrying out and interpreting a probabilistic analysis.

The objectives of the current Phase III study were to extend the capabilities of the Phase II system model and then apply the upgraded (Phase III) system model to a hypothetical reference site. More specifically, Phase III was designed to:

- expand the simulation models to include additional major radionuclides
- expand the simulation models to include additional selected pathways of exposure
- modify the sytem model to permit calculations over greater distances
- develop a model for simulating the water erosion of tailings or cover material
- streamline the system code, update the documentation and prepare a user's manual

A number of related issues were also investigated.

The Phase III work involved extensive modifications and additions to the computer programs developed during the previous studies. The products of the current phase of work is a revised Uranium Tailings Assessment Program (UTAP). Because the Phase III studies covered a variety of aspects of substantially different form and content and because of the sheer volume of material, the Phase III report has been prepared in four volumes, of which this is Volume 2. Volume 1 is a summary of the project activities and major results. This volume documents several aspects of the computer code and contains a number of technical appendices. Volume 3 documents the simulation models used in the analysis and Volume 4 is a UTAP user's manual.

## 1.2 System Model Overview

The principal objective of the Uranium Tailings Assessment Program (UTAP) is to perform a probabilistic analysis of the behaviour and environmental effects of uranium mill tailings, following closeout of milling operations. The models in this Phase III study are primarily assessment level models, rather than detailed research models. They have been designed to allow predictions to be made for distances up to 50 kilometres in all directions from the tailings area, and for time periods of up to 1000 years. In addition, the models provide many other features. These include the ability to incorporate different receptors and site characteristics and to deal with input parameters which vary with time. A more complete discussion of the program objectives and features is presented in Volume 1 of this report.

To achieve its objectives, UTAP is composed of a number of modules. These may be classified as either component or control modules. Component modules (or models) are the computer sub-programs directly concerned with the simulation of a uranium tailings physical system; i.e. the computer implementation of the mathematical models representing the uranium tailings pile and surrounding environment. Control modules provide the infrastructure for probabilistic analysis of the component modules. These functions include probabilistic sampling of input parameters, and many input, output and bookkeeping functions. The integrated control and component modules are referred to as the system model, system program, or UTAP. The relationship between control and component modules and the basic functions of these modules is illustrated in Figure 1.1. This volume (Volume 2) provides a detailed description of the control modules, while the component modules are documented in Volume 3.

The control modules are called in a logical sequence by a primary control module (EXEC). The program EXEC and the other control modules and their functions are illustrated in flowchart form in Figure 1.2. These modules are discussed in this volume. The component module executive subroutine, COMEX, is called by EXEC for each trial and time step. This subroutine and the component modules it calls are illustrated in Figure 1.3. Since SUBROUTINE COMEX is primarily concerned with the execution of the component modules, it is presented in detail in Volume 3, rather than in this volume.

This volume, and Volume 3 of this report, provide documentation for the control and component modules respectively, for Phase III of the National Uranium Tailings Program (NUTP) modelling studies. These two volumes, then, describe UTAP, which is the end result of a top down, evolutionary approach toward software development. The software development process is outlined briefly below and is described in detail in Appendix A of this volume.

## 1.3 The Software Development Process

The first step in the development process involved defining the general objectives and conceptual specifications for the overall program. The program was then broken into a series of smaller units, or modules. Objectives and specifications were subsequently developed for each module. All objectives and specifications were subjected to intensive review and re-evaluation. The modules were then developed, documented, reviewed and modified as appropriate. Following successful development, documentation and review, the modules were coded. The code for each module was tested to ensure that it performed according to its objectives and specifications. The modules were then

FIGURE 1.1

THE SYSTEM MODEL

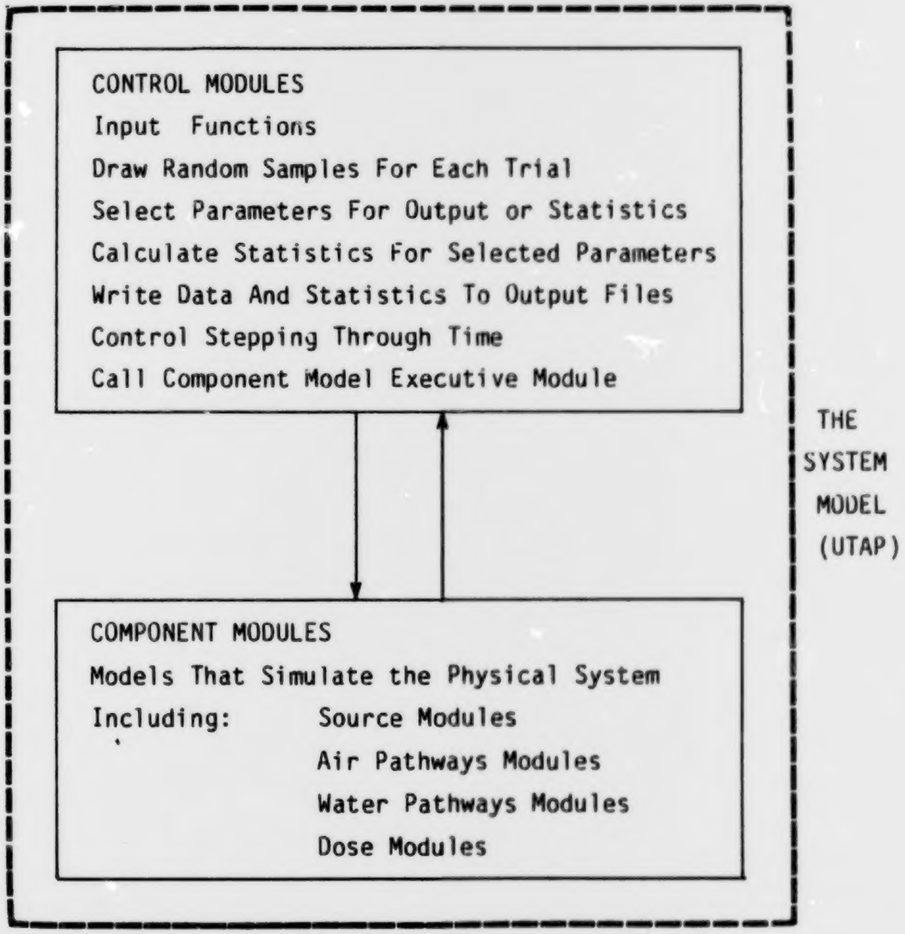
CONTROL MODULES
Input Functions
Draw Random Samples For Each Trial
Select Parameters For Output or Statistics
Calculate Statistics For Selected Parameters
Write Data And Statistics To Output Files
Control Stepping Through Time
Call Component Model Executive Module
THE SYSTEM MODEL (UTAP)
COMPONENT MODULES
Models That Simulate the Physical System
Including:
Source Modules
Air Pathways Modules
Water Pathways Modules
Dose Modules

FIGURE 1.2

THE CONTROL MODULE STRUCTURE

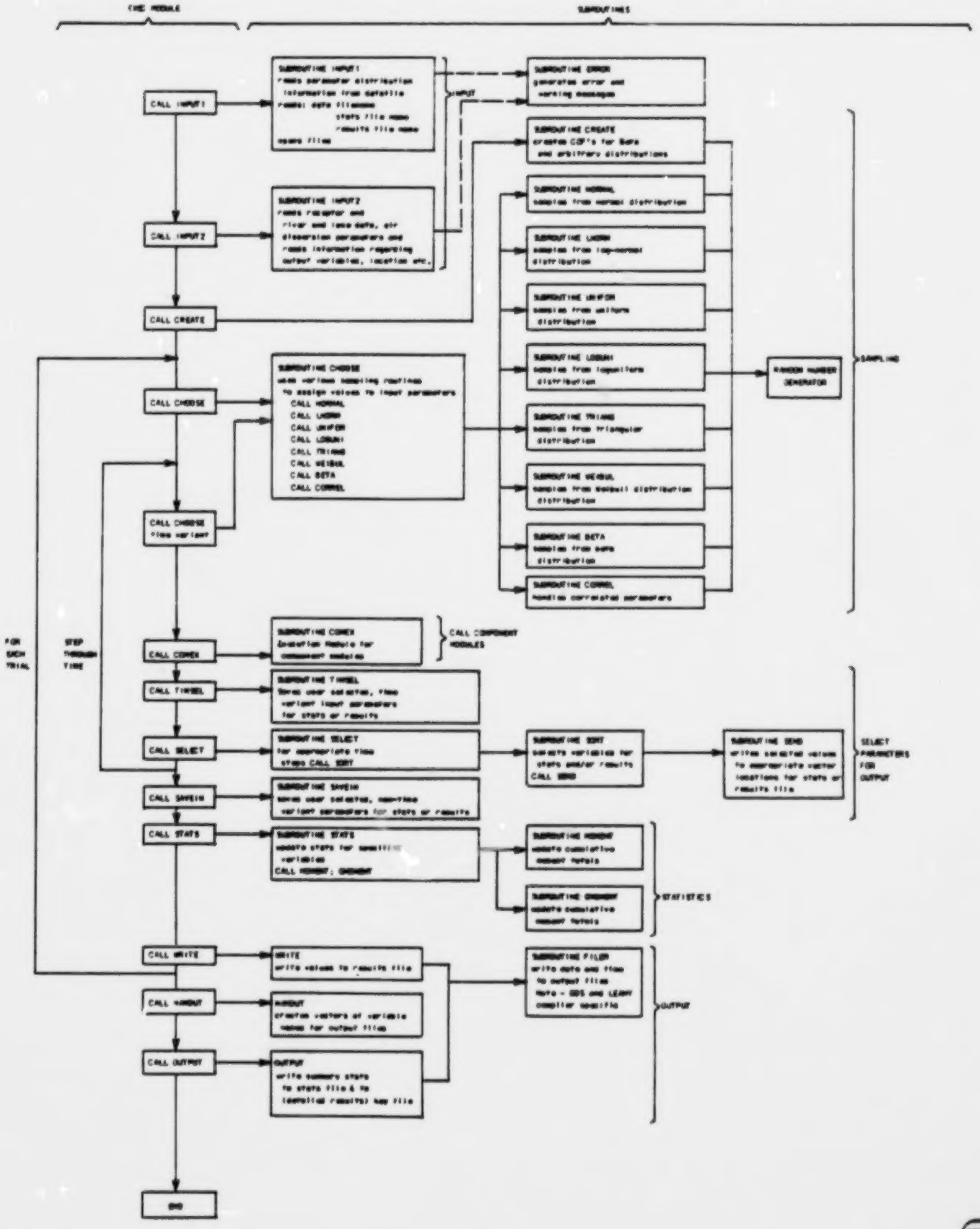
THE MODULE
SUBROUTINES
CALL INPUT1
CALL INPUT2
CALL CREATE
CALL CHOOSE
CALL CHOOSE time variant
CALL COMEX
CALL TIMSEL
CALL SELECT
CALL SAVEIN
CALL STATS
CALL WRITE
CALL VARDUT
CALL OUTPUT
END
FOR EACH TRIAL
STEP THROUGH TIME
SUBROUTINE INPUT1 reads parameter distribution information from datafile reads: data filename stats file name results file name opens files
SUBROUTINE INPUT2 reads receptor and river and lake data, air dispersion parameters and reads information regarding output variables, location etc.
INPUT
SUBROUTINE ERROR generates error and warning messages
SUBROUTINE CREATE creates CDF's for Beta and arbitrary distributions
SUBROUTINE NORMAL samples from normal distribution
SUBROUTINE LNORM samples from log-normal distribution
SUBROUTINE UNIFOR samples from uniform distribution
SUBROUTINE LOGUNI samples from loguniform distribution
SUBROUTINE TRIANG samples from triangular distribution
SUBROUTINE WEIBUL samples from Weibull distribution distribution
SUBROUTINE BETA samples from beta distribution
SUBROUTINE CORREL handles correlated parameters
SUBROUTINE CHOOSE uses various sampling routines to assign values to input parameters CALL NORMAL CALL LNORM CALL UNIFOR CALL LOGUNI CALL TRIANG CALL WEIBUL CALL BETA CALL CORREL
RANDOM NUMBER GENERATOR
SAMPLING
SUBROUTINE COMEX Execution Module for component modules
CALL COMPONENT MODULES
SUBROUTINE TIMSEL Saves user selected, time variant input parameters for stats or results
SUBROUTINE SELECT for appropriate time steps CALL SORT
SUBROUTINE SORT selects variables for stats and/or results CALL SEND
SUBROUTINE SEND writes selected values to appropriate vector locations for stats or results file
SELECT PARAMETERS FOR OUTPUT
SUBROUTINE SAVEIN saves user selected, non-time variant parameters for stats or results
SUBROUTINE STATS update stats for specified variables CALL MOMENT; GMOMENT
SUBROUTINE MOMENT update cumulative moment totals
SUBROUTINE GMOMENT update cumulative moment totals
STATISTICS
WRITE write values to results file
VARDUT creates vectors of variable names for output files
OUTPUT write summary stats to stats file & to (detailed results) key file
SUBROUTINE FILER write data and time to output files Note - CDS and LEAHY compiler specific
OUTPUT

# FIGURE 1.3
# THE SUBROUTINE COMEX AND COMPONENT MODULES

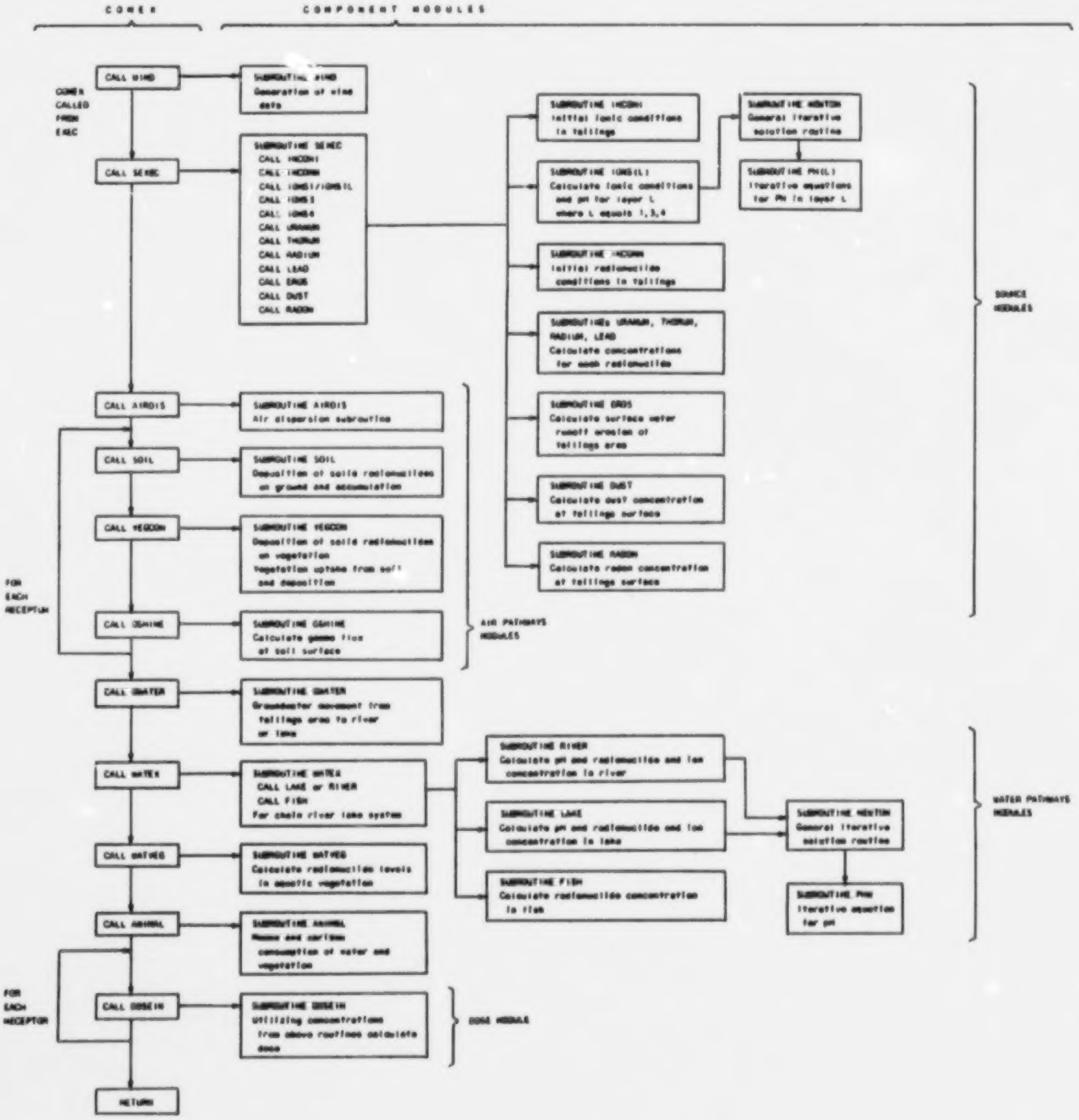
COMEX
COMPONENT MODULES
COMEX CALLED FROM EXEC
CALL WIND
SUBROUTINE WIND
Generation of wind data
CALL SEXEC
SUBROUTINE SEXEC
CALL INCONI
CALL INCONR
CALL IONS1/IONS1L
CALL IONS3
CALL IONS4
CALL URANUM
CALL THORUM
CALL RADIUM
CALL LEAD
CALL EROS
CALL DUST
CALL RADON
SUBROUTINE INCONI
Initial ionic conditions in tailings
SUBROUTINE IONS(L)
Calculate ionic conditions and pH for layer L where L equals 1,3,4
SUBROUTINE NEWTON
General iterative solution routine
SUBROUTINE PH(L)
Iterative equations for PH in layer L
SUBROUTINE INCONR
Initial radionuclide conditions in tailings
SUBROUTINEs URANUM, THORUM, RADIUM, LEAD
Calculate concentrations for each radionuclide
SUBROUTINE EROS
Calculate surface water runoff erosion of tailings area
SUBROUTINE DUST
Calculate dust concentration at tailings surface
SUBROUTINE RADON
Calculate radon concentration at tailings surface
SOURCE MODULES
CALL AIRDIS
SUBROUTINE AIRDIS
Air dispersion subroutine
CALL SOIL
SUBROUTINE SOIL
Deposition of solid radionuclides on ground and accumulation
CALL VEGCON
SUBROUTINE VEGCON
Deposition of solid radionuclides on vegetation
Vegetation uptake from soil and deposition
FOR EACH RECEPTOR
CALL GAMINE
SUBROUTINE GAMINE
Calculate gamma flux at soil surface
AIR PATHWAYS MODULES
CALL GWATER
SUBROUTINE GWATER
Groundwater movement from tailings area to river or lake
CALL WATEX
SUBROUTINE WATEX
CALL LAKE or RIVER
CALL FISH
For chain river lake system
SUBROUTINE RIVER
Calculate pH and radionuclide and ion concentration in river
SUBROUTINE LAKE
Calculate pH and radionuclide and ion concentration in lake
SUBROUTINE FISH
Calculate radionuclide concentration in fish
SUBROUTINE NEWTON
General iterative solution routine
SUBROUTINE PHW
Iterative equation for pH
WATER PATHWAYS MODULES
CALL WATVEG
SUBROUTINE WATVEG
Calculate radionuclide levels in aquatic vegetation
CALL ANIMAL
SUBROUTINE ANIMAL
Moose and caribou consumption of water and vegetation
FOR EACH RECEPTOR
CALL DOSEIN
SUBROUTINE DOSEIN
Utilizing concentrations from above routines calculate dose
DOSE MODULES
RETURN

integrated into UTAP and again tested.

Quality assurance is inherent in this type of software development process; a quality model being defined as one that performs the functions for which it was designed. The objectives and specifications set out in this study served as the quality assurance criteria against which the performance of the model was evaluated. In other words, the question was repeated at all levels of development, "Is the program (product) performing as intended?"

Volumes 2 and 3 document many aspects of the software development process and hence serve not only as model documentation, but also as quality assurance documents. The reader will be able to trace the development of general objectives, the division of the program into modules and the generation of secondary objectives for the modules. Where appropriate, the mathematical models used are described by algorithms that bridge the gap between model conception and its coded implementation. Finally, representative test cases and illustrative example results are provided for many of the modules.

## 2.0 CONTROL MODULE OBJECTIVES AND CONCEPTUAL SPECIFICATIONS

### 2.1 Control Module Features

The control modules are required to provide the infrastructure for performing probabilistic analyses. In addition to the most basic control module functions such as randomly sampling from input parameter distributions, the Phase III control modules contain a number of features which facilitate the probabilistic analysis of uranium mill tailings. The input and output features allow a variety of real systems to be simulated and considerable information about them to be accessed, with no computer programming changes required. The objectives for the control modules are summarized in Table 2.1. Some of the notable control module features are mentioned below. All are discussed in more detail in the subsequent sections.

Many features of the tailings area being modelled can be specified in the form of input information (i.e. without altering the program code). First and most obviously, this includes any model input parameter distributions. These may be altered simply by changing the specifications of the input distributions. Secondly, the characteristics of the watershed receiving aqueous discharge from the tailings are specified. The watershed is specified as a defined linkage of river and lake segments each with certain characteristics. The local air dispersion characteristics of the site are also specified. Finally, the location and certain characteristics of the receptor(s) being modelled are specified as input information. Receptors may be specified in up to 80 different locations; two types of receptor (average and critical) are available.

Much of the information generated during a simulation can be accessed, again with no programming changes. The information made available to the user includes most of the calculated quantities which are passed between environmental compartments. This information is stored in a series of computer arrays. Users may access the available information for any specific time(s) during the simulation period. Finally, the detailed results

Table 2.1

## SUMMARY OF CONTROL MODULE OBJECTIVES

| INPUT DISTRIBUTIONS | SITE SPECIFICATION | AVAILABLE OUTPUT INFORMATION | OUTPUT FORMAT |
|---|---|---|---|
| Constant | Receptor Locations and Characteristics (up to 80 locations) (two receptor types) | May select information contained in many specified arrays | May save detailed results |
| Normal | | | |
| Log-normal | | | May request summary statistics on desired variables:<br>. maximum<br>. minimum<br>. mean<br>. standard deviation<br>. geometric mean<br>. geometric standard deviation |
| Uniform | | May select information at any simulation time step (up to 11 steps) | |
| Log-uniform | Watershed Characteristics | | |
| Triangular | Air Dispersion Characteristics | | |
| Weibull | | | |
| Beta | | | |
| Arbitrary | | | |
| Correlated | | | |

themselves may be saved for subsequent analysis, or alternatively, summary statistics on the variables of interest may be saved. All of these features are described in more detail in the subsequent sections.

## 2.2 Input Modules

The input control modules open, access and read all of the input files required for the probabilistic assessment of uranium tailings. There are three input files required.

The first contains information regarding files to be opened and accessed as well as specifications for all probabilistic input parameter distributions. The second contains further, non-probabilistic information regarding the site being modelled. This includes the location and types of receptors and the physical characteristics of the watershed (e.g. river/lake sizes, linkages etc.). This second file also allows the user to select desired output results. The third file contains information related to the air dispersion characteristics of the site being modelled.

## 2.3 Random Sampling Modules

The sampling routines draw random samples from the following user specified probability distributions:

1) constant (a trivial case)
2) normal
3) lognormal
4) uniform
5) loguniform
6) triangular
7) weibull
8) beta
9) arbitrary
10) correlated

The values selected by random sampling are then made available to the appropriate component modules via "named common blocks".

## 2.4 Output Selection Modules

These modules allow the user to select from a variety of information available for output at desired time intervals without having to alter the programs. This data, primarily calculated concentrations and receptor doses, resides in a series of arrays in the program. Parameter selection for output is achieved by specifying the time intervals desired and the positions (i.e. substance and location) in the concentration and dose arrays required for output. This is done via the second input file. Two output options are available: 1) summary statistics and 2) saving detailed results to a disk file. These two options are discussed below.

### 2.4.1 Compute Summary Statistics

The following summary statistics are computed for user-selected parameters: mean, standard deviation, geometric mean, geometric standard deviation, minimum and maximum. These statistics are written to a disk file named by the user. The parameter names, the location and substance codes, and the time intervals sampled are also output. With this option, the parameter values for each trial are not saved.

### 2.4.2 Write Detailed Results to Output File

All values of the user-selected parameters are written to a disk file on each trial. The following summary statistics for these parameters are also calculated and written to a user-specified disk file; mean, standard deviation, skewness, kurtosis, geometric mean, geometric standard deviation, minimum and maximum. The parameter names, location and substance codes, and time intervals saved are also included in this file. The column order of the variables in the detailed results file corresponds to the row order of the statistics file. Hence the statistics file serves as a "key" file to the data file and aids the user in locating variables. These two files serve additionally as input to the confidence bands program.

## 2.5 Stepping Through Time

Since time-variant parameters may be sampled at every time step and because output may be saved at user-selected time steps, stepping through time is handled by the control modules. For a number of reasons relating to the structure of the component models, only two time steps may be used; namely, 1 and 10 years. The component models were developed to simulate a 1000 year period. While the models are likely valid for longer periods, we recommend that the maximum simulation period be 1000 years.

## 2.6 Confidence Bands

The confidence bands program is a post-processing program that calculates confidence band estimates on user selected parameters. The program processes the detailed results file and the key (statistics) file described in Section 2.4.2 to obtain confidence band estimates. Although this program is not a control module, it is included in this volume, since its function is independent of the simulation of specific component modules.

## 3.0 CONTROL MODULE DESCRIPTIONS

This chapter contains detailed descriptions of all of the control modules. Where appropriate the derivations, and implementation of the modules are described. Code listings are provided, as are several test cases and illustrative examples. A variable dictionary for the control modules is provided in Appendix B, along with a full listing of the program code for all of the control modules.

### 3.1 Main Program (EXEC)

The main program calls the control modules and the component module executive subroutine, COMEX, as illustrated in Figure 1.2. It also controls the looping through time and trials. The current time step and trial number are printed to the screen so that the progress of the program can be easily checked. A code listing of the main program is shown on Table 3.1.

The control modules, called by the main program, fall into five categories. These include input, distribution sampling, output selection, statistics, and output. The modules within each of these categories are described in detail in the following sections.

Table 3.1

### MAIN PROGRAM (EXEC)

```
C
C     EXECUTIVE MODULE CALLS CONTROL MODULES AND COMPONENT
C     MODULES' CONTROL MODULE, STEPPING THROUGH TIME FOR EACH
C     TRIAL
C
      INCLUDE 'IO.INC'
      INCLUDE 'CONC.INC'
      INCLUDE 'RECEP.INC'
      INCLUDE 'STATS.INC'
      INCLUDE 'COUNTS.INC'
      INCLUDE 'INFO.INC'
      INCLUDE 'OUT.INC'
      INCLUDE 'INPT.INC'
      INCLUDE 'UPDATE.INC'
      INCLUDE 'PARAM.INC'
      INCLUDE 'INTERM.INC'
      INCLUDE 'WIND.INC'
C
C     CALL INPUT MODULES
C
      CALL INPUT1
      CALL INPUT2
C
C     CALL SAMPLING MODULES
C
      CALL CREATE
      WRITE(SCRUNT,300)
      DO 10 NUMTRL=1,NTRIAL
C
C        SAMPLE NON-TIME-VARIANT INPUT DISTRIBUTIONS
C
         DO 20 I=1,VARN
            CALL CHOOSE(VARNOT(I))
20       CONTINUE
         NTIME=NYEARS/NDT+1
         DO 30 IYR = 1,NTIME
C
C           SAMPLE TIME-VARIANT DISTRIBUTIONS
C
            IF(VARY.GE.1)THEN
               DO 40 I=1,VARY
                  CALL CHOOSE(VARIED(I))
40             CONTINUE
            ENDIF
            NT=(IYR-1)*NDT
            T=FLOAT(NT)
            WRITE(SCRUNT,100)NUMTRL,NT
C
C           CALL COMPONENT MODULES
C
            CALL COMEX
```

Table 3.1 (continued)

```
C
C           CALL OUTPUT SELECTION ROUTINES
C
            CALL TIMSEL
            CALL SELECT
30       CONTINUE
         CALL SAVEIN
C
C        CALL STATISTICS MODULES
C
         CALL STATS
C
C        CALL OUTPUT MODULES
C
         CALL WRITE
10    CONTINUE
      CALL NAMOUT
      CALL OUTPUT
      WRITE(SCRUNT,300)
      WRITE(SCRUNT,200)
      STOP
100   FORMAT(' TRIAL NUMBER : ',I4,4X,'TIME : ',I5)
200   FORMAT(' RUN COMPLETED')
300   FORMAT(///)
      END
```

## 3.2 Input Modules

The program (UTAP) is designed so that many characteristics of the environment being modelled are specified via input information, rather than being built into the program code. The input information is read from three files by two separate subroutines. The first subroutine reads a file containing the probabilistic parameter descriptions; the second subroutine reads two files containing: 1)the site specific and output selection information, and 2) the air dispersion data. The input data are checked and, if necessary, error messages are generated. More information about data input for UTAP is contained in Volume 4 of this report (the User's Manual).

### 3.2.1. First Input Routine (SUBROUTINE INPUT1)

This subroutine reads the first input data file, which primarily contains the probabilistic parameter descriptions. An example of this data file is provided in Table 3.2. A number of descriptive comments, not actually present in the data file, are included, for illustrative purposes, on Table 3.2. A conceptual flowchart of this input module's functions is presented as Figure 3.1 and a listing of the program code is provided in Table 3.3.

As indicated on Table 3.2, the first item of information specified is a descriptive title, which is subsequently echoed to the output results files. Next, the desired output files are selected and named.

The total number of input parameter distributions as well as the number of arbitrary and correlated distributions are then specified. The number of cells to be computed for any beta distributions are also indicated. The specifics of the run are set up by specifying the random number seed, the number of trials, the simulation time, and the time increment.

All input parameter distributions are then specified. Each type of distribution is specified somewhat differently as outlined on Table 3.4.

Further information is specified for each input parameter by the use of 2 "flags". The "output flag" allows the user to have the values of the input parameter saved to the summary statistics file (S), the detailed results file (F), both (B) or neither (N). The default is no output (i.e. 'N'). The "time-variant flag" allows the user to specify a distribution as time-variant (V). Such distributions are sampled on every time step of every probabilistic trial. Non-time-variant parameters (N) are sampled only once per probabilistic trial and held constant over time.

FIGURE 3.1

FUNCTION OF FIRST INPUT MODULE

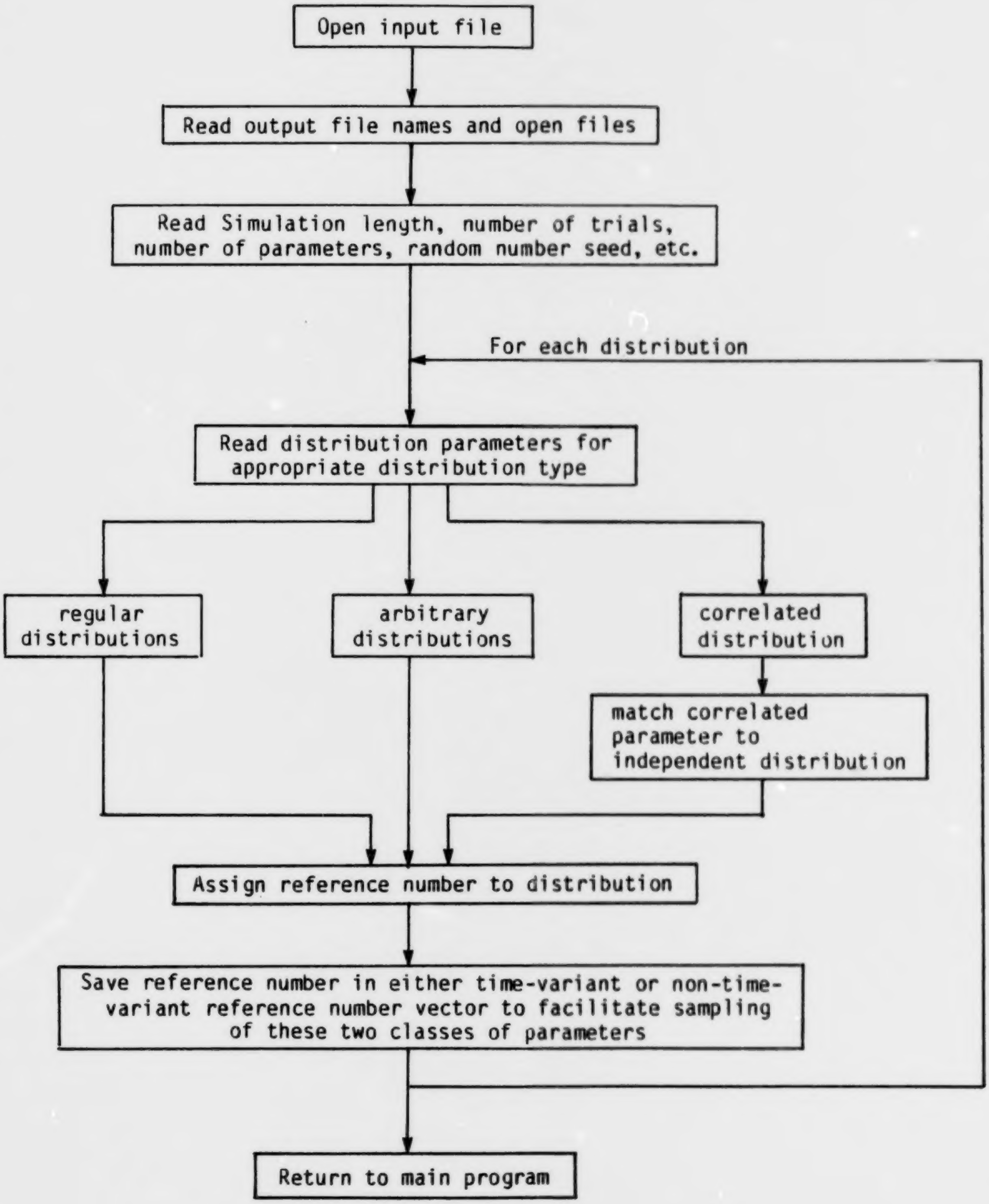
Open input file
Read output file names and open files
Read Simulation length, number of trials, number of parameters, random number seed, etc.
For each distribution
Read distribution parameters for appropriate distribution type
regular distributions
arbitrary distributions
correlated distribution
match correlated parameter to independent distribution
Assign reference number to distribution
Save reference number in either time-variant or non-time-variant reference number vector to facilitate sampling of these two classes of parameters
Return to main program

## Table 3.2

## SAMPLE OF FIRST INPUT FILE

```
     Title
PROBABILISTIC ANALYSIS: TEST CASE
     Statistics file indicator
Y
     Statistics file name
STAT.OUT
     Detailed Results files indicator
Y
     Detailed Results file name
RES.OUT
     Key file name
KEY.OUT
   ┌─Number of input distributions
   │   ┌──Number of arbitrary distributions
   │   │   ┌───Number of correlated parameters
   │   │   │  ┌───Number of cells to be used in computing beta distributions
  10   1   1 25
   ┌─Random number seed
   │         ┌──Number of iterations
0913566091  10
   ┌─Years in simulation
   │   ┌─Time increment in years
 100  10
     Regular distributions:
   ┌──────Parameter name
   │   ┌──────Output flag
   │   │  ┌──────Distribution type number
   │   │  │ ┌──────Time-variant flag
   │   │  │ │                 Distribution descriptors
CONST  N  1 N      2.0
NORMAL N  2 V     10.0         2.0        0.0        20.0
LNORM  N  3 V   1.0E02         1.5        1.0       1.0E3
UNI    S  4 N      1.0         2.0        0.0         0.0
LOGUNI N  5 N     0.01         0.5        0.0         0.0
TRIANG N  6 N     0.01        0.03        0.1         0.0
WEIBUL F  7 V      0.0         1.5        0.9
BETA   N  8 N     10.0       100.0        2.0         2.0
     Arbitrary distributions:
 ┌────────Parameter name
 │     ┌────Output flag
 │     │  ┌─────Distribution type number
 │     │  │ ┌──────Time-variant flag
 │     │  │ │  ┌──────────Number of cells in distribution
 │     │  │ │  │              Distribution descriptors
ARB    N  9 N 10     1.0    11.0  2.0  2.0  2.0  8.0  8.0  8.0 12.0 12.0  4.0  4.0

     Correlated distributions:
   ┌──────Parameter name
   │   ┌──────Output flag
   │   │  ┌──────Distribution type number
   │   │  │ ┌──────Time-variant flag
   │   │  │ │   ┌──────────Name of independent distribution
   │   │  │ │   │              Distribution descriptors
CORREL N 10 N NORMAL      50.0       10.0       0.7       10.0       2.0
```

Table 3.3

```
C
      SUBROUTINE INPUT1
C
C      THE FOLLOWING SUBROUTINE INPUTS THE FILE CONTAINING THE
C      PROBABILISTIC PARAMATER DESCRIPTIONS AND ALLOWS THE USER
C      TO SAVE STATISTICS AND OUTPUT FILES
C
      INCLUDE 'IO.INC'
      INCLUDE 'COUNTS.INC'
      INCLUDE 'PARAM.INC'
      CHARACTER*12 FNAME
      CHARACTER*6 CORNAM
      CHARACTER*1 TVARY(250)
      INTEGER*2 REG,ARB,NCORR
      SCRUNT=0
      FUNIT1=1
      FUNIT2=2
      FUNIT3=3
      FUNIT=4
C
C     OPEN FIRST INPUT FILE
C
      WRITE (SCRUNT,1250)
      READ (SCRUNT,1400) FNAME
      WRITE (SCRUNT,1350) FNAME
      OPEN (FUNIT,FILE=FNAME,STATUS='OLD',IOSTAT=IERR)
      IF (IERR.NE.0) CALL ERROR (29)
      READ (FUNIT,1400,END=998) TITLE
C
C     OPEN OUTPUT FILE(S)
C
      READ (FUNIT,1400,END=998) SSAVE
      READ (FUNIT,1400,END=998) FNAME
      IF (SSAVE.EQ.'Y') THEN
         WRITE (SCRUNT,1350) FNAME
         OPEN (FUNIT3,FILE=FNAME,STATUS='NEW',IOSTAT=IERR)
         IF (IERR.NE.0) THEN
            CALL ERROR (102)
            OPEN (FUNIT3,FILE=FNAME)
         ENDIF
      ENDIF
      READ (FUNIT,1400,END=998) FSAVE
      READ (FUNIT,1400,END=998) FNAME
      IF (FSAVE.EQ.'Y') THEN
         WRITE (SCRUNT,1350) FNAME
         OPEN (FUNIT1,FILE=FNAME,STATUS='NEW',IOSTAT=IERR)
         IF (IERR.NE.0) THEN
            CALL ERROR (102)
            OPEN (FUNIT1,FILE=FNAME)
         ENDIF
      ENDIF
      READ (FUNIT,1400,END=998) FNAME
```

Table 3.3 (continued)

```
      IF (FSAVE.EQ.'Y') THEN
         WRITE (SCRUNT,1350) FNAME
         OPEN (FUNIT2,FILE=FNAME,STATUS='NEW',IOSTAT=IERR)
         IF (IERR.NE.0) THEN
            CALL ERROR (102)
            OPEN (FUNIT2,FILE=FNAME)
         ENDIF
      ENDIF
C
C     READ COUNTERS AND CHECK TIME
C
      NBETA=0
      READ (FUNIT,1450,END=998) NPARM,NARB,NCORR,NCELLS
      READ (FUNIT,1550,END=998) NSTART,NTRIAL
      READ (FUNIT,1450,END=998) NYEARS,NDT
      IF (NDT.NE.1.AND.NDT.NE.10.AND.NDT.NE.20) CALL ERROR (32)
      RYEARS=FLOAT(NYEARS)
      DT=FLOAT(NDT)
      IF (MOD(RYEARS,DT).NE.0) CALL ERROR (19)
      NSTAT=0
      NFILE=0
      VARY=0
      VARN=0
      VARYS=0
      VARYF=0
      REG=NPARM-(NCORR+NARB)
      ARB=NPARM-NCORR
      DO 1050 I=1,NPARM
         IF (I.LE.REG) THEN
C
C           READ REGULAR DISTRIBUTIONS
C
            READ (FUNIT,1500,END=999) VARTIT(I),EFLAG(I),NTYPE(I),
     &         TVARY(I),P1(I),P2(I),P3(I),P4(I)
            IF (NTYPE(I).EQ.9.OR.NTYPE(I).EQ.10) CALL ERROR (6)
            IF (NTYPE(I).EQ.8) NBETA=NBETA+1
         ELSEIF (I.LE.ARB) THEN
C
C           READ ARBITRARY DISTRIBUTIONS
C
            READ (FUNIT,1610,END=999) VARTIT(I),EFLAG(I),NTYPE(I),
     &         TVARY(I),NACELL(I),P1(I),P2(I),(V(I,I2),I2=1,NACELL(I))
            IF (NTYPE(I).NE.9) CALL ERROR (8)
         ELSE
C
C           READ CORRELATED DISTRIBUTIONS
C
            READ (FUNIT,1600,END=999) VARTIT(I),EFLAG(I),NTYPE(I),
     &         TVARY(I),CORNAM,P1(I),P2(I),P3(I),P4(I),P5(I)
            IF (NTYPE(I).NE.10) CALL ERROR (7)
            K=1
10          IF (VARTIT(K).EQ.CORNAM) THEN
               IF (TVARY(K).NE.'V'.OR.(TVARY(K).EQ.'V'.AND.TVARY(I).EQ.
```

Table 3.3 (continued)

```
     &            'V')) THEN
                  CORNUM(I)=K
               ELSE
                  CALL ERROR (18)
               ENDIF
            ELSEIF (K.LT.I) THEN
               K=K+1
               GOTO 10
            ELSE
               CALL ERROR (4)
            ENDIF
         ENDIF
         IF (EFLAG(I).EQ.'B'.OR.EFLAG(I).EQ.'S'.OR.EFLAG(I).EQ.'F') THEN
            IF ((EFLAG(I).EQ.'S'.OR.EFLAG(I).EQ.'B').AND.SSAVE.NE.'Y')
     &         CALL ERROR (12)
            IF ((EFLAG(I).EQ.'F'.OR.EFLAG(I).EQ.'B').AND.FSAVE.NE.'Y')
     &         CALL ERROR (13)
         ENDIF
         IF (TVARY(I).EQ.'V') THEN
            VARY=VARY+1
            VARIED(VARY)=I
            IF (EFLAG(I).EQ.'S'.OR.EFLAG(I).EQ.'B') VARYS=VARYS+1
            IF (EFLAG(I).EQ.'F'.OR.EFLAG(I).EQ.'B') VARYF=VARYF+1
         ELSE
            VARN=VARN+1
            VARNOT(VARN)=I
            IF (EFLAG(I).EQ.'S'.OR.EFLAG(I).EQ.'B') NSTAT=NSTAT+1
            IF (EFLAG(I).EQ.'F'.OR.EFLAG(I).EQ.'B') NFILE=NFILE+1
         ENDIF
1050  CONTINUE
      CLOSE (FUNIT)
      RETURN
998   CALL ERROR (5)
999   CALL ERROR (9)
1250  FORMAT (' FIRST INPUT FILE NAME? ')
1350  FORMAT (' Opening File : ',A12)
1400  FORMAT (A)
1450  FORMAT (4I4)
1500  FORMAT (A6,1X,A1,1X,I2,1X,A1,4E11.6)
1550  FORMAT (I10,I4)
1600  FORMAT (A6,1X,A1,1X,I2,1X,A1,1X,A6,5E11.6)
1610  FORMAT (A6,1X,A1,1X,I2,1X,A1,I3,2E11.6,25(F6.2))
      END
```

Table 3.4

## DISTRIBUTION DESCRIPTORS

| Distribution | Distribution Number | Distribution Descriptors |
|---|---|---|
| Constant | 1 | Constant |
| Normal | 2 | Mean<br>Standard Deviation<br>Minimum<br>Maximum |
| Lognormal | 3 | Geometric Mean<br>Geometric Standard Deviation<br>Minimum<br>Maximum |
| Uniform | 4 | Minimum<br>Maximum |
| Log-uniform | 5 | Minimum<br>Maximum |
| Triangular | 6 | Minimum<br>Mode<br>Maximum |
| Weibull | 7 | Location Parameter<br>Scale Parameter<br>Shape Parameter |
| Beta | 8 | Minimum<br>Maximum<br>a<br>b |
| Arbitrary | 9 | Number of cells (max. 25)<br>Minimum<br>Maximum<br>Ordinate Values |
| Correlated | 10 | Mean of dependent variable<br>Standard Deviation of Dependent Variable<br>Correlation Coefficient<br>Mean of Independent Variable<br>Standard Deviation of Independent Variable |

### 3.2.2. Second Input Routine (SUBROUTINE INPUT2)

This subroutine reads two files. The first contains the receptor information, the watershed information, and the output selection information. The second file contains the air dispersion data. A flowchart of the module's functions is shown in Figure 3.2. The code for INPUT2 is shown on Table 3.5.

An example of the site specification and output selection information file is shown on Table 3.6. The file begins with a flag to indicate if air dispersion is to be time variant and the name of the appropriate air dispersion file to read. Air dispersion information may be selected as time-variant, with time steps of 1 or 10 years. Alternatively, long term mean values (i.e. non-time-variant) may be used for these parameters. This is followed by the receptor information. A system of spatial coordinates is defined by the traditional wind rose structure. There are sixteen direction sectors and up to five rings defining up to 80 wind rose locations. The spacings of the rings are user specified. The number of receptor locations and the details of each are specified. Each receptor location is assigned a watersource segment, a population, and a receptor type (critical (C), average (A))

The watershed model handles up to ten user-specified segments. Each river or lake segment is assigned a reference number and windrose location. The segment type (river or lake), the depth, and cumulative watershed area are defined. The surface areas of lakes and the lengths of rivers are also specified. The program checks that segments are correctly specified; with watershed areas increasing from the upstream end.

The first step in the selection of output information involves specifying the simulation times for which information is to be accessed. Information from up to 11 different times may be sent to either the summary statistics or detailed results files. After specifying the number of years (i.e. time-steps) for which information is to be accessed, the user must specify the times of interest, i.e. the simulation years for which information is to be accessed. Information from different simulation years may be sent to the summary statistics file and to the detailed results file.

The output selections from each array are then specified. The arrays available are indicated on Table 3.7. Substances available generally include all radionuclides modelled as well as selected cations and anions. Locations available include different layers within the tailings, different watershed segments and all receptor locations. The user selects the desired substances and locations, if any, from each of the available arrays, and specifies the destination of each (i.e. summary or detailed results). These output selection features provide easy access to a very large volume of information. Again, further details are provided in Volume 4 (the User's Manual).

The second file read by INPUT2 contains the air dispersion (star) data. Depending on the flag read from the first file, this may be time variant. If so, twenty sets of one or ten year average data are read, depending on the chosen time increment. If the data is not to be varied with time, one set of data, namely the long term (20 year) average values, is read.

FIGURE 3.2

FUNCTION OF SECOND INPUT MODULE

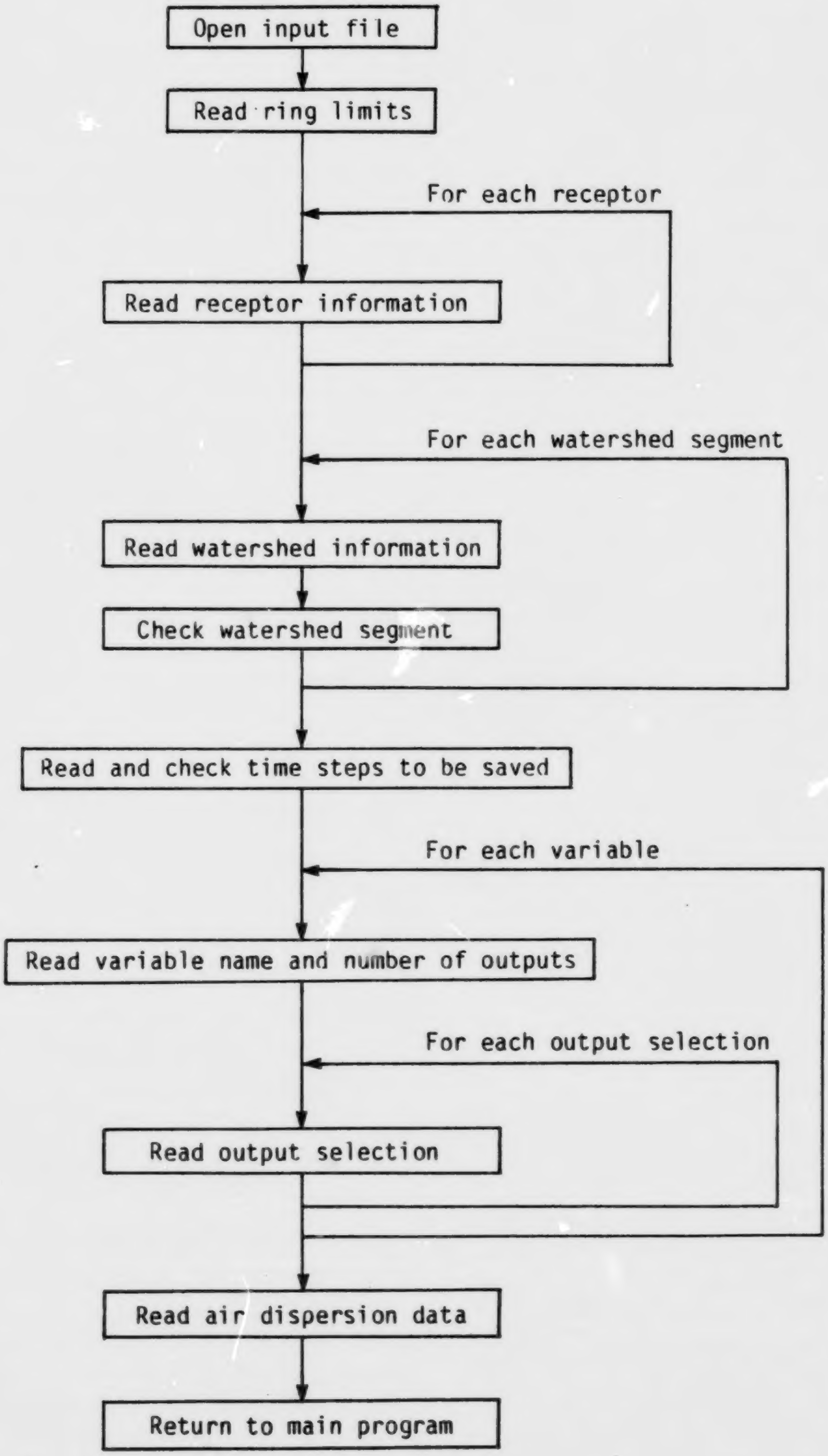
Open input file
Read ring limits
For each receptor
Read receptor information
For each watershed segment
Read watershed information
Check watershed segment
Read and check time steps to be saved
For each variable
Read variable name and number of outputs
For each output selection
Read output selection
Read air dispersion data
Return to main program

Table 3.5

```
C
      SUBROUTINE INPUT2
C
C     SUBROUTINE PROMPTS FOR INPUT FILE AND READS INPUT INFORMATION
C     SPECIFIC TO UTAP INCLUDING:
C        - NAME OF AIR DISPERSION DATA FILE
C        - RECEPTOR DATA
C        - WATERSHED DATA
C        - OUTPUT DATA CONTAINING INFO ON OUTPUT VARIABLES,
C          RECEPTOR NUMBERS, TIMES, ETC. OF VARIABLES TO BE SENT TO
C          DETAILED RESULTS AND STATISTICS FILES
C     AIR DISPERSION FILE IS OPENNED AND DATA READ
C
      INCLUDE 'IO.INC'
      INCLUDE 'RECEP.INC'
      INCLUDE 'COUNTS.INC'
      INCLUDE 'INFO.INC'
      INCLUDE 'WIND.INC'
      INTEGER*2 OLDDIR,OLDRNG,MAXSEG,RCPNUM
      INTEGER*4 R(6)
      CHARACTER*1 TEST
      CHARACTER*12 FNAME
      REAL*4 PI
      DATA PI /3.1415927/
C
C     OPEN SECOND INPUT FILE
C
      WRITE (SCRUNT,700)
      READ (SCRUNT,810) FNAME
      WRITE (SCRUNT,820) FNAME
      OPEN (FUNIT,FILE=FNAME,STATUS='OLD',IOSTAT=IERR)
      IF (IERR.NE.0) CALL ERROR(29)
C
C     READ FLAG FOR TIME VARIANCE OF STAR DATA AND FILE NAME
C
      READ (FUNIT,960,END=999) WINDFG
      READ (FUNIT,810,END=999) FNAME
C
C     READ RECEPTOR INFORMATION
C
      READ (FUNIT,730,END=999) NRECEP
      IF (NRECEP.GT.80) CALL ERROR (20)
      NDREC=NREC+2
      READ (FUNIT,730,END=999) NRING
      IF (NRING.GT.5) CALL ERROR (21)
      I=NRING+1
      READ (FUNIT,710,END=999) (R(J),J=1,I)
      DO 35 J=1,I
         R(J)=1000*R(J)
35    CONTINUE
      TAREA=0.
      DO 30 J=1,NRING
```

Table 3.5 (continued)

```
         IF (R(J).GE.R(J+1)) CALL ERROR (22)
         RNGMID(J)=FLOAT(R(J)+R(J+1))/2.0
         RAREA(J)=PI*(R(J+1)**2-R(J)**2)/16.
         TAREA=TAREA+RAREA(J)
30    CONTINUE
      TAREA=TAREA*16.
      MAXSEG=0
      DO 40 I=1,NRECEP
         READ (FUNIT,720,END=999) RCPNUM,RDIR(I),RRING(I),RWSSEG(I),
     &      RTYPE(I),RPOP(I)
         IF (RCPNUM.NE.I) CALL ERROR (10)
         IF (RRING(I).GT.NRING) CALL ERROR (23)
         IF (RWSSEG(I).GT.MAXSEG) MAXSEG=RWSSEG(I)
         IF (RTYPE(I).NE.'C') RTYPE(I)='A'
40    CONTINUE
C
C     READ & CHECK WATERSHED INFORMATION
C
      OLDDIR=0
      OLDRNG=0
      PSNUM=0
      AREA=0.
      PSAREA=0.
      TEST='R'
      READ (FUNIT,720,END=999) NSEG,GSEG
      IF (MAXSEG.GT.NSEG) CALL ERROR (24)
      DO 50 I=1,NSEG
         READ (FUNIT,730,END=999) NODE,STYPE(I),NODDIR(I),
     &      NODRNG(I),SDEPTH(I),SHEDAR(I),LAREA(I)
         IF (STYPE(I).EQ.'L') LAKVOL(I)=SDEPTH(I)*LAREA(I)
         IF (NODE.NE.I) CALL ERROR (1)
         IF (AREA.GT.SHEDAR(I)) CALL ERROR(2)
         AREA=SHEDAR(I)
         IF (TEST.EQ.'L'.AND.STYPE(I).EQ.'L') CALL ERROR (3)
         TEST=STYPE(I)
         IF (OLDDIR.NE.NODDIR(I).OR.OLDRNG.NE.NODRNG(I)) THEN
            PSNUM=PSNUM+1
            PSDIR(PSNUM)=NODDIR(I)
            PSRING(PSNUM)=NODRNG(I)
            PSAREA=PSAREA+RAREA(NODRNG(I))
         ENDIF
         IF (I.GT.1) THEN
            IF (ABS(OLDRNG-NODRNG(I)).GT.1) CALL ERROR (17)
            IF ((ABS(OLDDIR-NODDIR(I)).GT.1).AND.(OLDDIR.NE.16.OR.
     &         NODDIR(I).NE.1).AND.(OLDDIR.NE.1.OR.NODDIR(I).NE.16))
     &         CALL ERROR (17)
         ENDIF
         OLDDIR=NODDIR(I)
         OLDRNG=NODRNG(I)
50    CONTINUE
      IF (STYPE(1).EQ.'L') CALL ERROR (24)
      IF (STYPE(GSEG).EQ.'L')CALL ERROR(25)
C
```

Table 3.5 (continued)

```
C     READ OUTPUT PARAMETER SPECIFICATIONS
C
      NVARYS=0
      NVARYF=0
C
C     READ TIME STEPS TO BE SAVED
C
      READ (FUNIT,900,END=999) NSTEPS,NSTEPF
53    IF (NSTEPS.GT.0) THEN
         IF (SSAVE.NE.'Y') THEN
            CALL ERROR (105)
            NSTEPS=0
            GOTO 53
         ENDIF
         READ (FUNIT,920,END=999) (TSTAT(I),I=1,NSTEPS)
         NTEST=-1
         DO 51 I=1,NSTEPS
            IF (MOD(TSTAT(I),NDT).NE.0) CALL ERROR (15)
            IF (NTEST.GE.TSTAT(I)) CALL ERROR (11)
            NTEST=TSTAT(I)
51       CONTINUE
         IF (NTEST.GT.NYEARS) CALL ERROR (16)
      ELSE
         READ (FUNIT,810,END=999)
      ENDIF
      TSTAT(NSTEPS+1)=-1
54    IF (NSTEPF.GT.0) THEN
         IF (FSAVE.NE.'Y') THEN
            CALL ERROR (106)
            NSTEPF=0
            GOTO 54
         ENDIF
         READ (FUNIT,920,END=999) (TFILE(I),I=1,NSTEPF)
         NTEST=-1
         DO 52 I=1,NSTEPF
            IF (MOD(TFILE(I),NDT).NE.0) CALL ERROR (15)
            IF (NTEST.GE.TFILE(I)) CALL ERROR (11)
            NTEST=TFILE(I)
52       CONTINUE
         IF (NTEST.GT.NYEARS) CALL ERROR (16)
      ELSE
         READ (FUNIT,810,END=999)
      ENDIF
      TFILE(NSTEPF+1)=-1
C
C     READ OUTPUT PARAMETERS
C
      READ (FUNIT,730) NARRAY
      NSAV=1
      J=1
      DO 10 I=1,NARRAY
         READ (FUNIT,940,END=999) VARNAM(I),NVAR(I)
         IF (NVAR(I).GT.0) THEN
```

Table 3.5 (continued)

```
            NSAV=I
            KK=NVAR(I)
            DO 20 K=1,KK
               READ (FUNIT,950,END=999) NSUB(J),LOC(J),FLAG(J)
               IF (FLAG(J).NE.'F'.AND.FLAG(J).NE.'S') THEN
                  IF (SSAVE.EQ.'Y') THEN
                     FLAG(J)='S'
                  ELSEIF (FSAVE.EQ.'Y') THEN
                     FLAG(J)='F'
                  ELSE
                     CALL ERROR (14)
                  ENDIF
               ENDIF
               IF (FLAG(J).EQ.'F') THEN
                  NVARYF=NVARYF+1
                  IF (FSAVE.NE.'Y') CALL ERROR (13)
               ELSEIF(FLAG(J).EQ.'S')THEN
                  NVARYS=NVARYS+1
                  IF (SSAVE.NE.'Y') CALL ERROR (12)
               ENDIF
               J=J+1
20          CONTINUE
         ENDIF
10    CONTINUE
      NARRAY=NSAV
      ISTAT=(NVARYS+VARYS)*NSTEPS+NSTAT
      IFILE=(NVARYF+VARYF)*NSTEPF+NFILE
      IF (ISTAT.GT.300) CALL ERROR (27)
      IF (IFILE.GT.300) CALL ERROR (28)
C
C     READ AIR DISPERSION DATA
C
      IF (WINDFG.EQ.'Y') THEN
         IF (NDT.NE.1.AND.NDT.NE.10) CALL ERROR (25)
         NYEAR=20
      ELSE
         WINDFG='N'
         NYEAR=1
      ENDIF
      WRITE (SCRUNT,820) FNAME
      OPEN (FUNIT,FILE=FNAME,STATUS='OLD',IOSTAT=IERR)
      IF (IERR.NE.0) CALL ERROR (29)
      DO 60 IY=1,NYEAR
         READ (FUNIT,400,END=999)
         DO 70 J=1,6
            DO 80 I=1,16
               L=I+8
               IF (L.GT.16) L=L-16
               READ (FUNIT,500,END=999) (FWIND(L,J,K,IY),K=1,6)
80          CONTINUE
70       CONTINUE
60    CONTINUE
      CLOSE (FUNIT)
```

Table 3.5 (continued)

```
      RETURN
999   CALL ERROR (5)
400   FORMAT (1X)
500   FORMAT (7X,6(F7.5))
600   FORMAT (6E11.5)
700   FORMAT (' SECOND INPUT FILE NAME? ')
710   FORMAT (6I5)
720   FORMAT (4I3,1X,A1,I5)
730   FORMAT (I3,1X,A1,2I3,3E9.3)
810   FORMAT (A)
820   FORMAT (' Opening File : ',A12)
900   FORMAT (I3,1X,I3)
920   FORMAT (11(I5))
940   FORMAT (A6,I3)
950   FORMAT (2(I3,1X),A1)
960   FORMAT (2X,A1)
      END
```

## Table 3.6

## SAMPLE OF SECOND INPUT FILE (INPUT2.DAT)

```
    Flag to indicate if variable wind data is desired
 N
    File containing appropriate wind data
STARAV.DAT
    Number of receptor locations
 5
    Number of rings
 5
    Ring limits
   1    3    5   10   20   50
    Receptor information:
              Receptor number
                        Sector number
                                  Ring number
                                            Drinking water source segment number
                                                      Receptor type
                                                                Population
 1 16  1  1 C    2
 2 16  3  2 A    5
 3 14  3  2 A    6
 4  1  1  1 C    1
 5  7  3  2 A    3
  Number of watershed segments
         End node number of watershed segment groundwater flows into.
 8  1
   Watershed information:
             End node or segment number
                    Segment type
                              Sector number of end node
                                       Ring number of end node
                                                 Segment depth
                                                         Watershed area
                                                                 Lake area/River length
 1 R 11  1   2.5E-1   1.5E07   3.0E3
 2 L 11  1   1.0E01   2.0E07   5.0E05
 3 R 10  2   0.5      3.2E07   3.5E3
 4 L 10  2   4.0      3.8E07   2.5E05
 5 R  9  3   7.5E-1   7.0E07   7.0E3
 6 R  9  4   1.0      1.2E08   1.3E4
 7 L  9  4   5.0      1.4E08   4.0E06
 8 R  9  5   6.5      4.0E08   3.0E4
        Number of time steps for statistics
            Number of time steps for detailed results files
 4   3
   Time steps for statistics
  0   10   20   30
   Time steps for detailed results
  0   50   90
```

Table 3.6 cont'd

```
       Number of arrays to be checked for output
  36
   ┌── Array name
   │       ┌─Array size
 WCONC   0
 CONC    0
 PH      0
 WATC    2
    ┌──Substance code
    │   ┌────Location code
    │   │  ┌──────Output indicator
   2  3  S
   3  5  S
 WATAVG  3
   1  1  S
   3  1  S
   4  1  F
 WATPH   3
   1  7  S
   1  4  S
   1  2  F
 GWATC   0
 EMRATE  0
 EROTOT  0
 DTAIL   0
 AIRC    0
 SOILC   0
 AVEGC   0
 BVEGC   0
 SUFOC   0
 BRWSC   0
 LICHC   0
 AQVEGC  0
 FISHC   0
 AMOC    0
 WMOC    0
 ACARC   0
 WCARC   0
 WATD    0
 SHINED  0
 INHD    0
 RADD    0
 VEGD    0
 FISHD   0
 MEATD   0
 DOSE    0
 POPDT   0
 BLANK1  0
 BLANK2  0
```

Table 3.7

## OUTPUT PARAMETERS

| Variable | Definition |
|---|---|
| WCONC | Tailings liquid phase concentration |
| CONC | Tailings solid phase concentration |
| PH | Tailings pH |
| WATC | Water concentration |
| WATAVG | Average watershed concentration |
| WATPH | pH in lakes and rivers |
| GWATC | Ground water concentration |
| EMRATE | Emission Rate from tailings |
| EROTOT | Erosion of tailings pile overtime step |
| DTAIL | Cumulative Erosion of tailings pile |
| AIRC | Air concentration |
| SOILC | Soil concentration |
| AVEGC | Above ground vegetation concentration |
| BVEGC | Below ground vegetation concentration |
| SUFOC | Summer folliage concentration |
| BRWSC | Browsing vegetation concentration |
| LICHC | Lichen concentration |
| AQVEGC | Aquatic vegetation concentration |
| FISHC | Fish concentration |
| AMOC | Moose concentration from vegetation |
| WMOC | Moose concentration from water consumption |
| ACARC | Caribou concentration from vegetation |
| WCARC | Caribou concentration from water consumption |
| WATD | Drinking water dose |
| SHINED | Groundshine dose |
| INHD | Inhalation dose |
| RADD | Radon dose |
| VEGD | Vegetable consumption dose |
| FISHD | Fish consumption dose |
| MEATD | Meat consumption dose |
| DOSE | Total Individual Dose |
| POPDT | Total Dose for Entire Study Population |

### 3.2.3 Generation of Error and Warning Messages (SUBROUTINE ERROR (I))

The purpose of this subroutine is to prevent the program from "crashing" and to alert the user to errors in the two input files. This module may be called from various points throughout INPUT1 and INPUT2 where checks of the input data are made and from the sampling routines where limits are checked. If no errors are encountered, this subroutine is not called.

The subroutine argument, I, is the error number. Two types of messages can be generated, depending on the value of I. The first type of message is an error message. If an error occurs, the program is terminated immediately. The second type of message is a warning. If the error encountered is not fatal, the user is alerted to the problem and asked if execution of the program should be continued or stopped.

For all error and warning messages generated, an error number and brief explanation of the nature of the problem are written to the screen. A more detailed discussion of all of these messages can be found in the Users Manual, Appendix A.

A listing of the subroutine code is shown on Table 3.8.

Table 3.8

```
C
      SUBROUTINE ERROR (I)
C
C     SUBROUTINE GENERATES ERROR AND WARNING MESSAGES.  ALL ERRORS
C     TERMINATE THE PROGRAM.  WARNINGS ASK IF EXECUTION IS TO BE STOPPED
C     OR CONTINUED.
C
      INCLUDE 'IO.INC'
      CHARACTER*1 Q
      WRITE (SCRUNT,300)
      IF (I.LE.100) THEN
C
C        GENERATE ERROR MESSAGES
C
         WRITE (SCRUNT,300) ' ***************  ERROR  ***************'
         IF (I.EQ.1) THEN
            WRITE (SCRUNT,300) ' (001) WATER SOURCE SEGMENTS NOT IN ORDE
     &R'
         ELSEIF (I.EQ.2) THEN
            WRITE (SCRUNT,300) ' (002) WATERSHED AREAS MUST INCREASE'
         ELSEIF (I.EQ.3) THEN
            WRITE (SCRUNT,300) ' (003) WATER SOURCE NOs. MUST INCREASE'
         ELSEIF (I.EQ.4) THEN
            WRITE (SCRUNT,300) ' (004) CORRELATED NAME NOT FOUND'
         ELSEIF (I.EQ.5) THEN
            WRITE (SCRUNT,300) ' (005) UNEXPECTED END OF DATA'
         ELSEIF (I.EQ.6) THEN
            WRITE (SCRUNT,300) ' (006) TYPE ERROR IN REGULAR DIST''ns'
         ELSEIF (I.EQ.7) THEN
            WRITE (SCRUNT,300) ' (007) TYPE ERROR IN CORRELATED DIST''ns
     &'
         ELSEIF (I.EQ.8) THEN
            WRITE (SCRUNT,300) ' (008) TYPE ERROR IN ARBITRARY DIST''ns'
         ELSEIF (I.EQ.9) THEN
            WRITE (SCRUNT,300) ' (009) NUMBER OF PARAMETERS INCORRECT'
         ELSEIF (I.EQ.10) THEN
            WRITE (SCRUNT,300) ' (010) RECEPTORS NOT LISTED IN ORDER'
         ELSEIF (I.EQ.11) THEN
            WRITE (SCRUNT,300) ' (011) TIME STEPS MUST INCREASE'
         ELSEIF (I.EQ.12) THEN
            WRITE (SCRUNT,300) ' (012) STATS REQUESTED MUST SPECIFY FILE
     &'
         ELSEIF (I.EQ.13) THEN
            WRITE (SCRUNT,300) ' (013) RESULTS REQUESTED MUST SPECIFY FI
     &LE'
         ELSEIF (I.EQ.14) THEN
            WRITE (SCRUNT,300) ' (014) CAN''T SAVE RESULTS - NO OPEN FIL
     &E'
         ELSEIF (I.EQ.15) THEN
            WRITE (SCRUNT,300) ' (015) CAN''T SAVE TIME STEPS SPECIFIED'
         ELSEIF (I.EQ.16) THEN
            WRITE (SCRUNT,300) ' (016) TIME FOR OUTPUT TOO BIG'
```

Table 3.8 (continued)

```
         ELSEIF (I.EQ.17) THEN
            WRITE (SCRUNT,300) ' (017) WATERSHED DIRECTIONS OR RINGS NOT
     & CONTINUOUS'
         ELSEIF (I.EQ.18) THEN
            WRITE (SCRUNT,300) ' (018) CANNOT CORRELATE PARAMETERS'
         ELSEIF (I.EQ.19) THEN
            WRITE (SCRUNT,300) ' (019) TIME STEPS DON''T MATCH SIMULATIO
     &N TIME'
         ELSEIF (I.EQ.20) THEN
            WRITE (SCRUNT,300) ' (020) MAXIMUM OF 80 RECEPTORS ALLOWED'
         ELSEIF (I.EQ.21) THEN
            WRITE (SCRUNT,300) ' (021) MAXIMUM OF 5 RINGS ALLOWED'
         ELSEIF (I.EQ.22) THEN
            WRITE (SCRUNT,300) ' (022) RING LIMITS MUST INCREASE'
         ELSEIF (I.EQ.23) THEN
            WRITE (SCRUNT,300) ' (023) RECEPTOR RING NUMBER TOO BIG'
         ELSEIF (I.EQ.24) THEN
            WRITE (SCRUNT,300) ' (024) FIRST WATERSHED SEG. MUST BE RIVE
     &R'
         ELSEIF (I.EQ.25) THEN
            WRITE (SCRUNT,300) ' (025) GROUNDWATER MUST FLOW INTO RIVER'
         ELSEIF (I.EQ.27) THEN
            WRITE (SCRUNT,300) ' (027) TOO MANY OUTPUTS TO STATS FILE'
         ELSEIF (I.EQ.28) THEN
            WRITE (SCRUNT,300) ' (028) TOO MANY OUTPUTS TO RESULTS FILE'
         ELSEIF (I.EQ.29) THEN
            WRITE (SCRUNT,300) ' (029) FILE NOT FOUND'
         ELSEIF (I.EQ.30) THEN
            WRITE (SCRUNT,300) ' (030) ERROR IN LOGNORMAL SPECIFIERS'
         ELSEIF (I.EQ.31) THEN
            WRITE (SCRUNT,300) ' (031) ERROR IN NORMAL SPECIFIERS'
         ELSEIF (I.EQ.32) THEN
            WRITE (SCRUNT,300) ' (032) TIME STEP MUST BE 1 OR 10 YEARS'
         ELSEIF (I.EQ.33) THEN
            WRITE (SCRUNT,300) ' (033) ERROR IN TRIANGULAR SPECIFIERS'
         ENDIF
      ELSE
C
C        GENERATE WARNING MESSAGES
C
         WRITE (SCRUNT,300) ' ***************  WARNING  ***************'
         IF (I.EQ.101) THEN
            WRITE (SCRUNT,300) ' (101) TWO CONSECUTIVE LAKES'
         ELSEIF (I.EQ.102) THEN
            WRITE (SCRUNT,300) ' (102) ABOUT TO OVER WRITE EXISTING FILE
     &'
         ELSEIF (I.EQ.105) THEN
            WRITE (SCRUNT,300) ' (105) NOT SAVING TIME STEPS TO STATS'
         ELSEIF (I.EQ.106) THEN
            WRITE (SCRUNT,300) ' (106) NOT SAVING TIME STEPS TO RESULTS'
         ENDIF
         WRITE (SCRUNT,300) '  - OK TO CONTINUE (Y/N)? '
         READ (SCRUNT,300) Q
```

Table 3.8 (continued)

```
         IF (Q.EQ.'Y'.OR.Q.EQ.'y') THEN
C
C           RESUME EXECTION
C
            WRITE (SCRUNT,300) ' RESUMING EXECUTION'
            RETURN
         ENDIF
      ENDIF
C
C     STOP PROGRAM
C
      WRITE (SCRUNT,300) ' PROGRAM TERMINATED'
      WRITE (SCRUNT,300) ' SEE USERS MANUAL APPENDIX A'
      STOP
300   FORMAT (A)
      END
```

## 3.3 Sampling Routines

### 3.3.1. Objective

The objective of the sampling routines is to draw random samples from the following probability distributions:

1) constant
2) normal
3) lognormal
4) uniform
5) loguniform
6) triangular
7) weibull
8) beta
9) arbitrary
10) correlated

Two important concepts used in the sampling routines, namely, computer generated random numbers and the probability integral transformation, are discussed below.

### 3.3.2 General Concepts

Random Numbers

Computers, as traditionally used, carry out programmed calculations such that, given a set of stated inputs, the result is always predictable, subject only to "internal errors" which are highly improbable. It is then interesting to explore how random numbers can be generated by such a device.

In one sense, none of the numbers generated and used by modern computers are random. That is, they generate sequences of numbers which, given the same starting values, can be repeated exactly. However, we may define "random" to describe any sequences of numbers which pass statistical tests which are logically required to be passed by numbers generated by flipping true coins, rolling true dice, etc. Under this definition the numbers generated by computers may have properties at least as good as do those generated by coins or dice. In other words, our knowledge of the detailed mechanism by which numbers are produced does not in itself preclude their use as random numbers. Numbers produced by a computer which pass the required tests for randomness are sometimes called pseudorandom numbers.

The basic strategy used in the following sampling routines is to generate random numbers which are uniformly distributed on the interval 0 to 1 and then to transform them to produce a random number distributed according to the desired distribution. The generation of the uniformly distributed random numbers between 0 and 1 is accomplished through the use of a procedure developed by Marse and Roberts (1983). This random number generator (UNIRAN) has been thoroughly tested, as is described in Appendix C.

### The Probability Integral Transformation

The probability integral transformation, which makes use of the cumulative probability function F(x), is used to generate random variables from the arbitrary, beta, triangular and Weibull distributions. The concept is described in the following paragraphs. Random variables from the remaining distributions are generated using more specific techniques, as described in subsequent sections.

Let X be a random variable with cumulative probability function F(x). By definition the probability that $X \leq x$, that is Pr $(X \leq x)$, is the value of the cumulative distribution function at x, where x is an arbitarily chosen value for X. Necessarily, F(x) is a monotonically increasing function of x with a range of 0 to 1. The probability integral transformation is a technique which permits the generation of independent random observations on X, given the ability to generate independent random observations on U, a random variable uniformly distributed over the interval 0 to 1.

Consider Figure 3.3. First, a random observation U is drawn from U (0, 1) and applied to the ordinate as shown. Next, a projection is made horizontally from U over to the graph of F(x) versus X and then downward to the abscissa. This is in effect an illustration of the inverse mapping $X = F^{-1}(U)$. Since F is monotonically increasing over (0, 1) the inverse mapping produces a single unique value of X for each U so selected. Alternatively, consider x to be an arbitrarily chosen possible value of X. The corresponding value of F(x) is shown on Figure 3.3. Then

$$\Pr(X \leq x) = \Pr[U \leq F(x)] = F(x) \qquad (3.1)$$

Hence, by definition, X so generated has the required probability distribution.

### 3.3.3 The Random Number Generator (FUNCTION SUBROUTINE RANDOM)

The purpose of the random number generator is to produce a stream of random numbers between 0 and 1. The random number generator used was taken from Marse and Roberts (1983) for two key reasons. First, it had been extensively tested to demonstrate its random properties. Secondly, it was reported to be easily transported from one computer system to another. The following description was adapted from Marse and Roberts (1983).

Table 3.9 contains the FORTRAN implementation of the Uniform (0,1) generator routine called RANDOM. RANDOM has been successfully transported to several computer systems using various FORTRAN compilers. For the software to be portable, the random number generator must not only compile on different machines, but also must produce identical random number sequences if simulation results are to be machine independent. This has been found to be true.

The RANDOM routine accepts an integer seed in the range $[1, 2^{31} - 2]$ and produces a new seed using a Prime Modulus Multiplicative Congruential

FIGURE 3.3

## SAMPLING FROM CUMULATIVE PROBABILITY FUNCTION

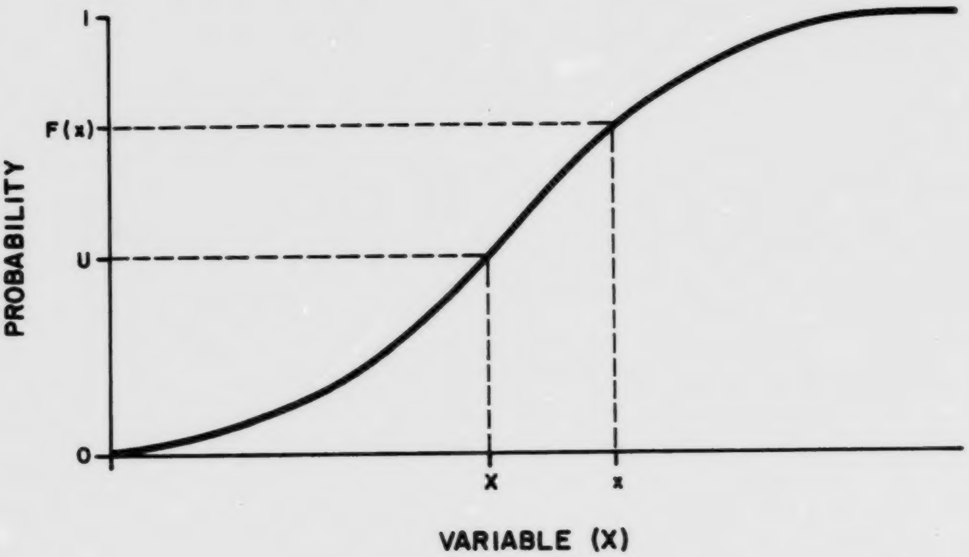
1
F(x)
U
0
PROBABILITY
X
x
VARIABLE (X)

Generator returning this as the function parameter. It converts this integer to a (0,1) single precision random number which is returned as the value of the function. The formal definition of the generator used is:

$$Z_n = (aZ_{n-1})\bmod m \tag{3.2}$$

where the (prime) modulus, m, is $2^{31} - 1$,$Z_0$ is the starting seed, a is the multiplier 630360016, and the Uniform (0,1) value returned is $Z_n/m$. This generator is targeted for any machine having a word size of at least 32 bits, since this nominal size includes the vast majority of large main frame, mini, and microcomputer systems.

The technique of simulating the multiplication and modulus operations by shifting partial products is taken from Schrage (1979) whose generator routine uses 16807 as a multiplier. The fact that the multiplier 630360016 cannot be represented in 15 bits (and could thereby create an intermediate product greater than 32 bits) requires the successive use of Schrage's procedure on the two factors which are less than $2^{15}$. The problems associated with the conversion of the new seed to a Uniform (0,1) value are discussed in Fishman (1978) and the procedure shown in the final statement of the routine was suggested in Fishman and Moore (1980).

The desirability of a Uniform (0,1) generator routine for use on a particular computer system is certainly dependent on the statistical properties of the generator itself, but usually more important are the characteristics of the method used to implement it. RANDOM's strongest feature is that it can be easily implemented in FORTRAN while preserving the stated characteristics of the generator. This ease of implementation includes not only the initial transfer of the routine but the subsequent portability of any software which uses the generator. Its weakest point is that other implementations which take advantage of hardware characteristics of particular computers run faster.

This weakness is muted by two considerations. The first is that, for many applications, the execution speed of the algorithm is not nearly as important as a clear understanding of the properties of the generator and the reliability of the specific implementation. A prime example is the common (but difficult to detect) effect on simulation results that a machine dependent generator causes when it is transported via a general purpose simulation system to various machines. The second consideration is related to the decreasing cost of software development. For an installation which makes infrequent but critical use of a generator, it may be cost-effective to sacrifice execution speed in order to save the man-hours necessary to code and test an efficient machine-dependent algorithm.

The claim of portability for an implementation implies that it executes successfully and produces identical output on different computer systems. Since the algorithm is written in standard FORTRAN, it must be assumed that it will execute successfully on any computer system with a FORTRAN compiler which is compatible with the standard. The algorithm produces two outputs and the portability of each must be considered separately. The argument that the new integer seed produced from a given seed's value is identical on any computer system whose word size is at least 32 bits can be taken directly from Schrage (1979). Since the intermediate products in the routine never exceed $(2^{31} - 1)$, any computer which can represent FORTRAN integer values in the range $[1, (2^{31} - 1)]$ will yield the same output.

The argument that a given seed value produces the same single precision value in the (0,1) interval on different machines is more involved. Many Uniform (0,1) generators merely convert the seed value to a floating point representation and divide by the modulus. The exact value obtained by this procedure is highly machine-dependent as it is a function of not only the word size but the method of representing floating point values. Some of the factors involved in this representation include how the mantissa and exponent are represented, how many bits are allocated to the mantissa, how overflow is handled, and whether excess digits are truncated or rounded during normalization. A more extensive discussion of these considerations can be found in Marse and Roberts (1983). A thorough investigation of the statistical properties of random numbers generated using this procedure can be found in Appendix C.

Finally, the performance of the random number generator is dependent on the seed number. The following numbers were thoroughly tested by Marse and Roberts (1983) and are recommended as seeds:

824064364
913566091
2096730329
281629770

Table 3.9

```
C
      FUNCTION RANDOM (NSTART)
C
C     THIS PORTABLE FORTRAN RANDOM NUMBER GENERATOR WAS
C     ADAPTED FROM THAT DESCRIBED BY K. MARSE AND S.D. ROBERTS
C     ('SIMULATION', OCTOBER, 1983; PP 135-139)
C
      INTEGER*4 B2E15,B2E16,H115,H131,LOW15,LOWPRD,MODLUS,
     &          MULT1,MULT2,OVFLOW
      MULT1=24112
      MULT2=26143
      B2E15=32768
      B2E16=65536
      MODLUS=2147483647
      H115=NSTART/B2E16
      LOWPRD=(NSTART-H115*B2E16)*MULT1
      LOW15=LOWPRD/B2E16
      H131=H115*MULT1+LOW15
      OVFLOW=H131/B2E15
      NSTART=(((LOWPRD-LOW15*B2E16)-MODLUS)+
     &    (H131-OVFLOW*B2E15)*B2E16)+OVFLOW
      IF (NSTART.LT.0) NSTART=NSTART+MODLUS
      H115=NSTART/B2E16
      LOWPRD=(NSTART-H115*B2E16)*MULT2
      LOW15=LOWPRD/B2E16
      H131=H115*MULT2+LOW15
      OVFLOW=H131/B2E15
      NSTART=(((LOWPRD-LOW15*B2E16)-MODLUS)+(H131-OVFLOW*B2E15)*B2E16)
     &    +OVFLOW
      IF (NSTART.LT.0) NSTART=NSTART+MODLUS
      RANDOM=(2*(NSTART/256)+1)/16777216.0
      RETURN
      END
```

### 3.3.4 Creation of a Cumulative Distribution Function (SUBROUTINE CREATE)

Cumulative probability functions are created for both arbitrary and beta distributions in the manner described below.

The Arbitrary Distributions

Random numbers distributed according to a probability distribution of arbitrary shape are generated by direct use of the probability integral transformation. An optional number of ordinates, usually 10, are defined at equal intervals as shown in Figure 3.4.

The ordinates $v_j$ are read off an arbitrary vertical scale and then accumulated and standardized to give the cumulative probability function:

$$F(x_i) = \frac{\sum_{j=1}^{i} v_j}{\sum_{j=1}^{10} v_j} \tag{3.3}$$

The vertical scale usually corresponds to counts of occurences in the bins defined by the x axis.

The function $F(x_i)$ is then sampled using the same procedure as in subroutine BETA.

The Beta Distribution

If the random variable X is distributed as B (a, b), the Beta distribution with shape parameters a and b, it has the probability density function:

$$f(x) = K\ x^{a-1}\ (1 - x)^{b-1} \qquad 0 \leq x < 1 \quad a, b > 0 \tag{3.4}$$

where $k = \dfrac{\Gamma(a + b)}{\Gamma(a)\ \Gamma(b)}$

This distribution can take on almost any shape depending on how the shape parameters a and b are specified (see Figure 3.5).

Beta distributions are treated as arbitrary distributions. The ordinates $v_j$ are calculated as:

$$v_j = x_j^{a - 1}\ (1 - x_j)^{b - 1} \tag{3.5}$$

The term K is constant when a and b are specified as constants. The cumulative distribution function can then be calculated as:

$$F(x_i) = \frac{\sum_{j=1}^{i} v_j}{\sum_{j=1}^{n} v_j} \tag{3.6}$$

where n is the total number of cells (maximum 25). A printout of the source code for SUBROUTINE CREATE is contained in Table 3.10.

FIGURE 3·4

AN ARBITRARY
PROBABILITY DENSITY FUNCTION

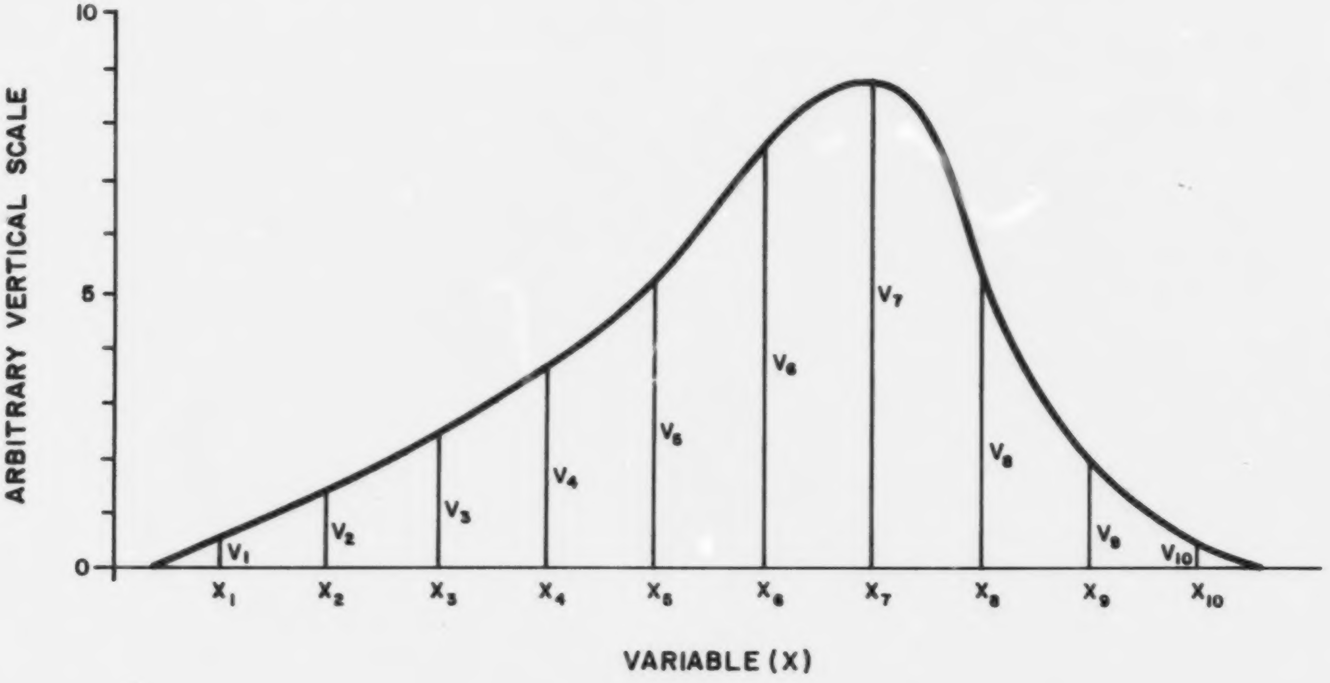

FIGURE 3.5

FORMS OF THE BETA DISTRIBUTION PROBABILITY DENSITY FUNCTION

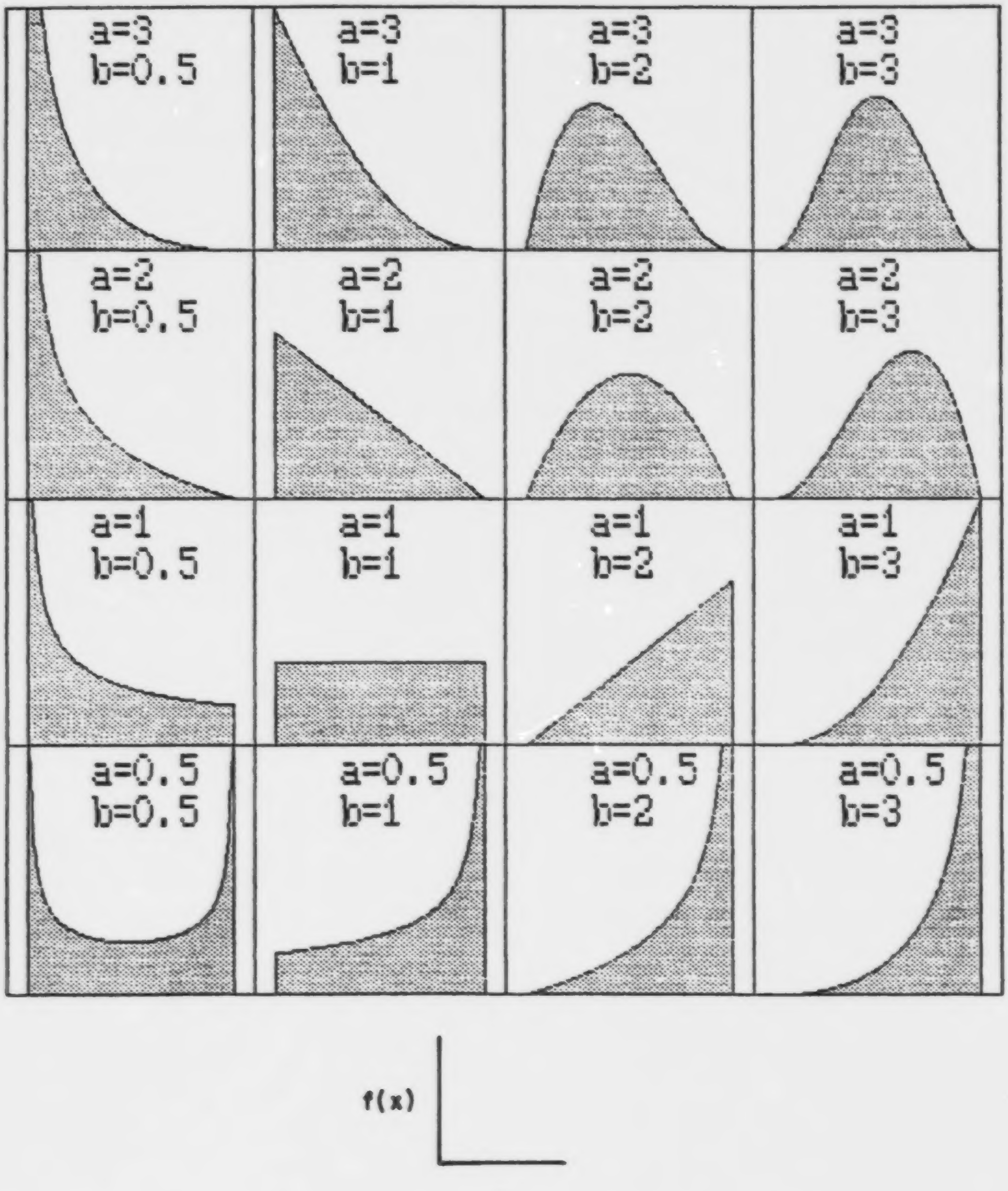

## Table 3.10

```
C
      SUBROUTINE CREATE
C
C     THIS ROUTINE GENERATES COMPLEMENTARY CUMULATIVE PROB-
C     ABILITY FUNCTIONS (CPF) FOR INPUT BETA AND ARBITRARY
C     DISTRIBUTIONS.
C
      INCLUDE 'PARAM.INC'
      INCLUDE 'COUNTS.INC'
      REAL*4 A,B,MAX,MIN,SUM,X
C
C     CHECK IF THERE ARE ANY BETA OR ARBITRARY DISTRIBUTIONS
C
      IF (NBETA.NE.0.OR.NARB.NE.0) THEN
         DO 10 I=1, NPARM
            IF (NTYPE(I).EQ.8.OR.NTYPE(I).EQ.9) THEN
               MIN=P1(I)
               MAX=P2(I)
               IF (NTYPE(I).EQ.8) THEN
C
C              INITIALIZE BETA DISTRIBUTIONS
C
                  NACELL(I)=NCELLS
                  UNIT(I)=(MAX-MIN)/FLOAT(NCELLS)
                  ORIGIN(I)=MIN-(0.5*UNIT(I))
                  A=P3(I)-1.0
                  B=P4(I)-1.0
                  DO 1500 J=1,NCELLS
                     X=(J-0.5)/FLOAT(NCELLS)
                     V(I,J)=(X**A)*((1.0-X)**B)
1500              CONTINUE
               ELSE
C
C                 INITIALIZE ARBITRARY DISTRIBUTIONS
C
                  UNIT(I)=(MAX-MIN)/(FLOAT(NACELL(I))-1.)
                  ORIGIN(I)=MIN-UNIT(I)
               ENDIF
C
C              CALCULATE CUMULATIVE PROBABILITY FUNCTIONS
C
               SUM=0.0
               DO 1800 J=1,NACELL(I)
                  SUM=SUM+V(I,J)
                  CPF(I,J)=SUM
1800           CONTINUE
               DO 1900 J=1,NACELL(I)
                  CPF(I,J)=CPF(I,J)/SUM
1900           CONTINUE
            ENDIF
 10      CONTINUE
      ENDIF
      RETURN
      END
```

### 3.3.5 Choice of Sampling Routine (SUBROUTINE CHOOSE)

The appropriate sampling routine specified by the "distribution type" numbers listed in Section 3.4.1, is called by this subroutine for each parameter. For constants, a subroutine is not called; the constant parameter value is returned. The subroutine BETA is called for both arbitrary and beta distributions. A printout of the source code for SUBROUTINE CHOOSE is contained in Table 3.11.

Table 3.11

```
C
      SUBROUTINE CHOOSE (I)
C
C     THIS ROUTINE WILL RETURN A VALUE FOR EACH PARAMETER.
C     IT CALLS THE APPROPRIATE SUBROUTINE DEPENDING ON THE
C     TYPE OF DISTRIBUTION SPECIFIED:
C                                       1 = CONSTANT
C                                       2 = NORMAL
C                                       3 = LOG NORMAL
C                                       4 = UNIFORM
C                                       5 = LOG UNIFORM
C                                       6 = TRIANGULAR
C                                       7 = WEIBULL
C                                       8 = BETA
C                                       9 = ARBITRARY
C                                      10 = CORRELATED
C
      INCLUDE 'INPT.INC'
      INCLUDE 'PARAM.INC'
      INCLUDE 'COUNTS.INC'
      IF (NTYPE(I).EQ.1) THEN
         XIN(I) = P1(I)
      ELSEIF (NTYPE(I).EQ.2) THEN
         CALL NORMAL (NSTART,P1(I),P2(I),P3(I),P4(I),XIN(I))
      ELSEIF (NTYPE(I).EQ.3) THEN
         CALL LNORM (NSTART,P1(I),P2(I),P3(I),P4(I),XIN(I))
      ELSEIF (NTYPE(I).EQ.4) THEN
         CALL UNIFOR (NSTART,P1(I),P2(I),XIN(I))
      ELSEIF (NTYPE(I).EQ.5) THEN
         CALL LOGUNI (NSTART,P1(I),P2(I),XIN(I))
      ELSEIF (NTYPE(I).EQ.6) THEN
         CALL TRIANG (NSTART,P1(I),P2(I),P3(I),XIN(I))
      ELSEIF (NTYPE(I).EQ.7) THEN
         CALL WEIBUL (NSTART,P1(I),P2(I),P3(I),XIN(I))
      ELSEIF (NTYPE(I).EQ.8.OR.NTYPE(I).EQ.9) THEN
         CALL BETA (NSTART,I,XIN(I))
      ELSEIF (NTYPE(I).EQ.10) THEN
         CALL CORREL (NSTART,P1(I),P2(I),P3(I),P4(I),P5(I),CORNUM(I),
     &       XIN(I))
      ENDIF
      RETURN
      END
```

### 3.3.6. Normal Distribution (SUBROUTINE NORMAL)

The method currently used to generate normally distributed random variables does not use the probability integral transformation. Instead, it uses the central limit theorem which states that if v is a random variable with finite variance, the distribution of the sum of n independent observations on v approaches normal as n becomes indefinitely large. In fact, if the distribution of v is "well-behaved", the approach to normal is quite rapid.

The uniform distribution is one of those which is "well-behaved" and for n=12, the distribution of the sum is very close indeed to normal. It is easily shown that if:

$$X'=-6+\sum_{i=1}^{12} U_i \qquad (3.7)$$

where $U_i$ is the ith of 12 independent observations on a random variable uniformly distributed on the interval 0 to 1, then the expectation of X' is 0 and its variance is 1. Using the approximation to the central limit theorem, the distribution of X' is N(0, 1), called the standard normal.

If a random number X is desired with distribution $N(\mu,\sigma)$ it is found by transforming $X'$ with

$$X = \mu + \sigma X' \qquad (3.8)$$

A printout of the source code for SUBROUTINE NORMAL is contained in Table 3.12 A typical normally distributed random variable sampled by SUBROUTINE NORMAL is shown in Figure 3.6.

Summary sample statistics are presented on the bottom of Figure 3.6 and include the specified mean and standard deviation as well as the mean and standard deviation calculated from the sampled data. The chi-square goodness of fit statistic, a generally accepted test of correspondence between observed

FIGURE 3.6

## PLOT OF FREQUENCY HISTOGRAM (500 SAMPLES) AND PROBABILITY DISTRIBUTION (SMOOTH CURVE) FOR NORMAL DISTRIBUTION

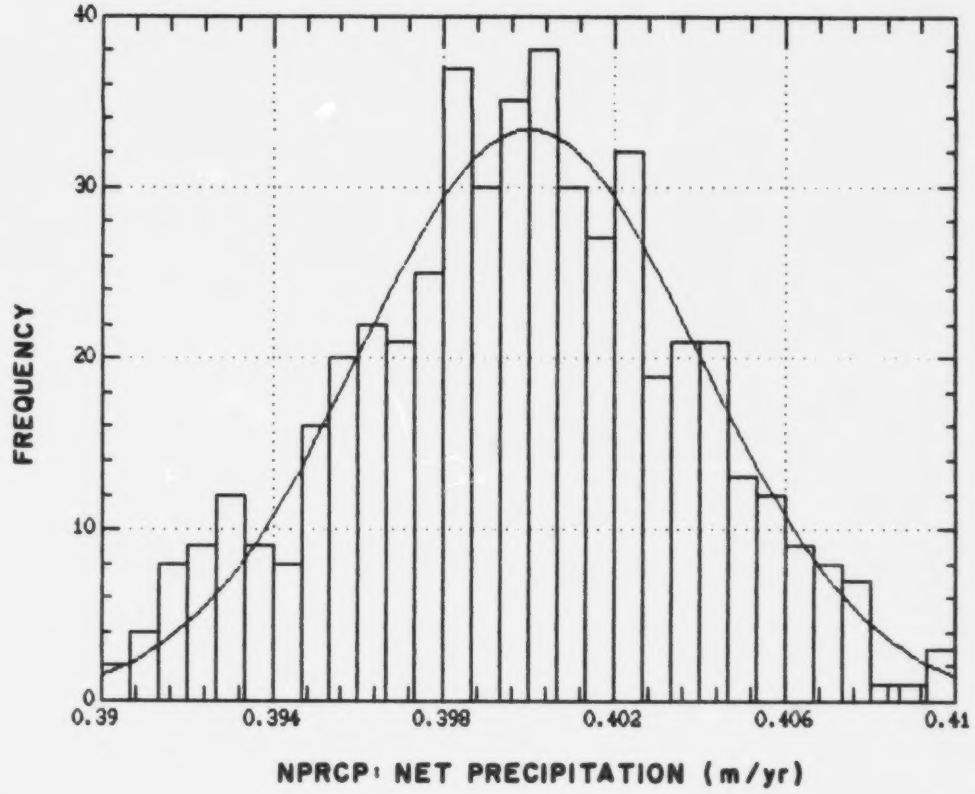

SUMMARY STATISTICS:

| | SPECIFIED INPUT VALUES | CALCULATED SAMPLE VALUES |
|---|---|---|
| MEAN | 0·400 | 0·400 |
| STANDARD DEVIATION | $4 \times 10^{-3}$ | $3.9 \times 10^{-3}$ |

$CHI^2$ GOODNESS-OF-FIT = 19·962 WITH 25 DEGREES OF FREEDOM

Table 3.12

```
C
      SUBROUTINE NORMAL (NSTART,EXPECT,STDEV,MIN,MAX,XIN)
C
C      THIS ROUTINE GENERATES NORMALLY DISTRIBUTED VARIATES
C
      INTEGER*2 I
      REAL*4 XIN,MIN,MAX,EXPECT,STDEV,R,TEMP
      IF (.NOT.MAX.GT.MIN) CALL ERROR (31)
1000  CONTINUE
         TEMP=-6.0
         DO 1100 I=1,12
            R=RANDOM(NSTART)
            TEMP=TEMP+R
1100    CONTINUE
         XIN=TEMP*STDEV+EXPECT
      IF (XIN.LT.MIN.OR.XIN.GT.MAX) GO TO 1000
      RETURN
      END
```

and expected frequencies, is also shown.

### 3.3.7 Lognormal Distribution (SUBROUTINE LNORM)

A random variable is lognormally distributed if its logarithm is normally distributed. Ordinarily the parameters of the lognormally distributed random variable are given as M and S, the geometric mean and geometric standard deviation, respectively. If M and S are given, then $\mu$ = logM, M>0, and $\sigma$ = logS, S>1, are the mean and standard deviation of the logarithm of the lognormally distributed random variable. Hence a lognormally distributed random variable with parameters M and S may be generated by first generating a normally distributed variable N[logM, (logS)] and then finding its antilogarithm. This is the procedure used here.

A printout of SUBROUTINE LNORM is contained in Table 3.13. A typical lognormally distributed random variable sampled by SUBROUTINE LNORM is shown (on a logarithmic axis) in Figure 3.7. Summary statistics and the chi-square goodness of fit statistic are provided on the bottom of Figure 3.7.

### 3.3.8 Uniform Distribution (SUBROUTINE UNIFOR)

A random variable is uniformly distributed if samples are evenly distributed over an interval such as is generated by RANDOM over the interval (0, 1). If the minimum and maximum values are specified as $U_{min}$ and $U_{max}$, respectively, then the uniform distribution is simply the random number, X', transformed from the interval (0, 1) to the interval ($U_{min}$, $U_{max}$). Thus the uniform random number, X, is generated by:

$$X = U_{min} + X' (U_{max} - U_{min}) \tag{3.9}$$

A printout of SUBROUTINE UNIFOR is contained in Table 3.14. A typical uniformly distributed random variable sampled by SUBROUTINE UNIFOR is shown in Figure 3.8. Summary statistics and the chi-square goodness of fit statistic are provided on the bottom of Figure 3.8.

FIGURE 3.7

## PLOT OF FREQUENCY HISTOGRAM (500 SAMPLES) AND PROBABILITY DISTRIBUTION (SMOOTH CURVE) FOR LOGNORMAL DISTRIBUTION

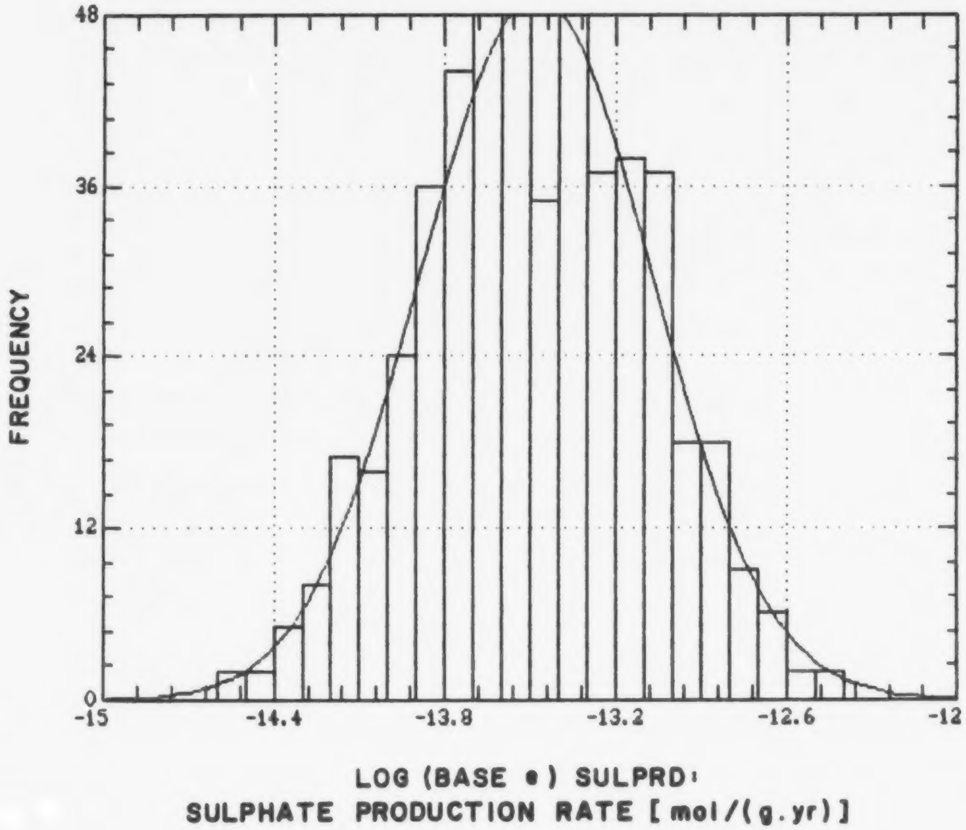

**SUMMARY STATISTICS:**

| | SPECIFIED INPUT VALUES | CALCULATED SAMPLE VALUES |
|---|---|---|
| GEOMETRIC MEAN | $1{\cdot}4 \times 10^{-6}$ | $1{\cdot}4 \times 10^{-6}$ |
| GEOMETRIC STANDARD DEVIATION | 1·5 | 1·5 |

$\text{CHI}^2$ GOODNESS - OF - FIT = 13·991 WITH 18 DEGREES OF FREEDOM

FIGURE 3.8

## PLOT OF FREQUENCY HISTOGRAM (500 SAMPLES) AND PROBABILITY DISTRIBUTION (SMOOTH CURVE) FOR UNIFORM DISTRIBUTION

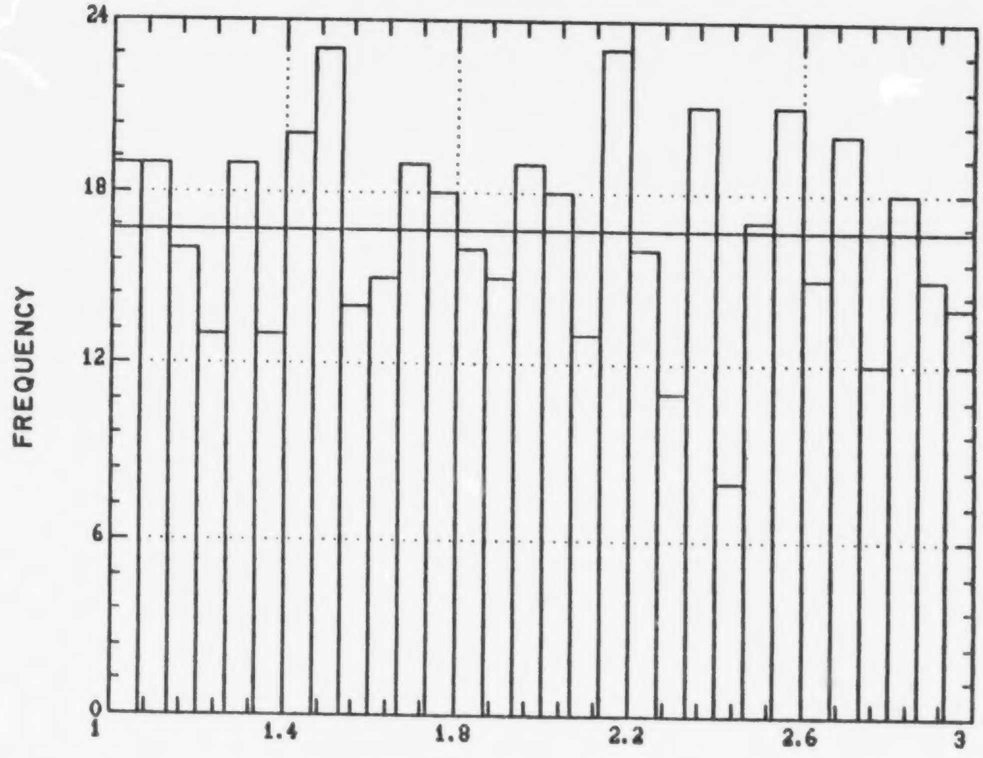

DISTCO: RADIUM SOLID TO LIQUID DISTRIBUTION COEFFICIENT
(UNSATURATED ZONE)

SUMMARY STATISTICS:

| | SPECIFIED INPUT VALUES | CALCULATED SAMPLE VALUES |
|---|---|---|
| MINIMUM | 1 | 1·01 |
| MAXIMUM | 3 | 2·99 |

CHI$^2$ GOODNESS-OF-FIT = 22·12 WITH 29 DEGREES OF FREEDOM

Table 3.13

```
C
      SUBROUTINE LNORM (NSTART,GM,GSD,MIN,MAX,XIN)
C
C     THIS ROUTINE GENERATES LOG-NORMALLY DISTRIBUTED VARIATES
C
      REAL*4 GM, GSD, LGM, LGSD, TMIN, TMAX, TEMP, MIN, MAX, XIN
      LGM=ALOG10(GM)
      LGSD=ALOG10(GSD)
      IF (.NOT.MAX.GT.MIN) CALL ERROR (30)
      IF (MIN.LE.0.0) THEN
         TMIN=-1.0E37
      ELSE
         TMIN=ALOG10(MIN)
      ENDIF
      TMAX=ALOG10(MAX)
      IF (TMIN.GT.TMAX) THEN
         TEMP=TMIN
         TMIN=TMAX
         TMAX=TEMP
      ENDIF
      CALL NORMAL (NSTART,LGM,LGSD,TMIN,TMAX,TEMP)
      XIN=10.**TEMP
      RETURN
      END
```

## Table 3.14

```
C
      SUBROUTINE UNIFOR (NSTART,UMIN,UMAX,XIN)
C
C    THIS ROUTINE GENERATES UNIFORMLY DISTRIBUTED RANDOM NUMBERS
C    BETWEEN UMIN AND UMAX
C
      REAL*4 RANDOM,R,XIN,UMIN,UMAX
1000  R=RANDOM(NSTART)
      IF (UMIN.LE.UMAX) THEN
         XIN=UMIN+R*(UMAX-UMIN)
      ELSE
         XIN=UMAX+R*(UMIN-UMAX)
      ENDIF
      RETURN
      END
```

### 3.3.9 Loguniform Distribution (SUBROUTINE LOGUNI)

A loguniform distribution of a random variable over the interval ($U_{min}$, $U_{max}$) is a distribution for which the log of the variable is uniformly distributed over the interval (log $U_{min}$, log $U_{max}$). Hence, the loguniformally distributed random variable is the antilogarithm of the random variable, X', translated over this interval. This routine uses the equation:

$$\log X = \log U_{min} + X' (\log U_{max} - \log U_{min}) \qquad (3.10)$$

A printout of SUBROUTINE LOGUNI is contained on Table 3.15. A typical loguniformly distributed random variable sampled by SUBROUTINE LOGUNI is shown in Figure 3.9. Summary statistics and the chi-square goodness of fit statistic are provided on the bottom of Figure 3.9.

FIGURE 3.9

## PLOT OF FREQUENCY HISTOGRAM (500 SAMPLES) AND PROBABILITY DISTRIBUTION (SMOOTH CURVE) FOR LOG-UNIFORM DISTRIBUTION

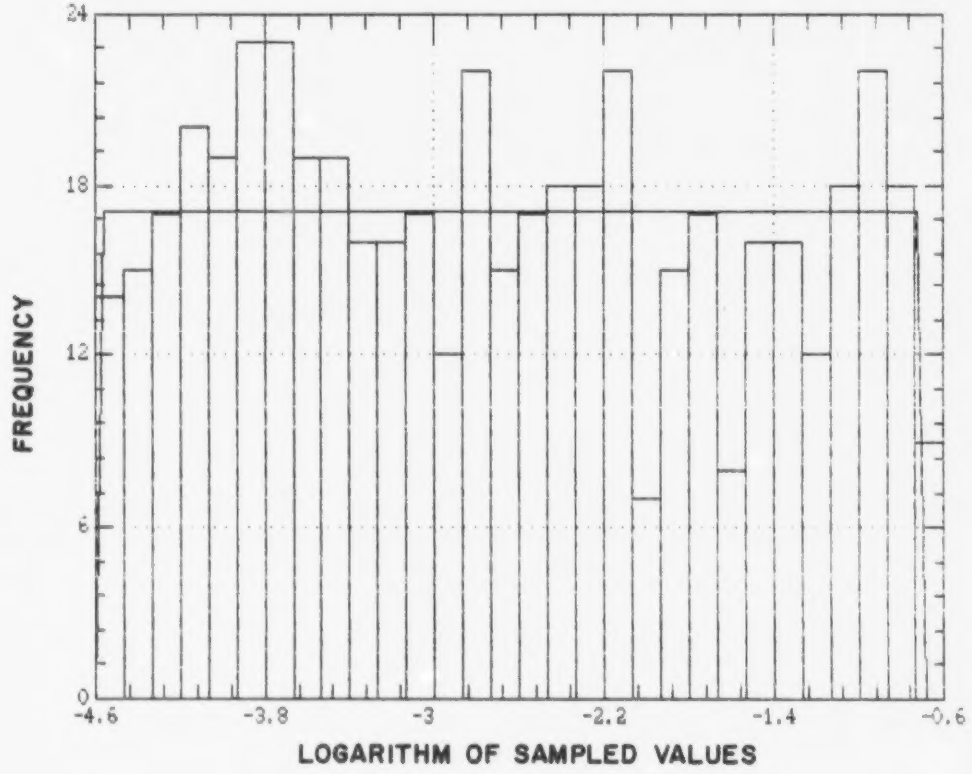

SUMMARY STATISTICS:

| | SPECIFIED INPUT VALUES | CALCULATED SAMPLE VALUES |
|---|---|---|
| MINIMUM | $1.00 \times 10^{-2}$ | $1.01 \times 10^{-2}$ |
| MAXIMUM | 0.500 | 0.499 |

$CHI^2$ GOODNESS-OF-FIT = 25.983 WITH 26 DEGREES OF FREEDOM

Table 3.15

```
C
      SUBROUTINE LOGUNI (NSTART,LMIN,LMAX,XIN)
C
C    THIS ROUTINE GENERATES LOG-UNIFORMLY DISTRIBUTED RANDOM NUMBERS
C    BETWEEN LMIN AND LMAX
C
      REAL*4 RANDOM,R,XIN,LMIN,TEMP,LMAX
1000  R=RANDOM(NSTART)
      TEMP=ALOG10(LMIN)+R*(ALOG10(LMAX)-ALOG10(LMIN))
      XIN=10**TEMP
      RETURN
      END
```

### 3.3.10 Triangular Distribution (SUBROUTINE TRIANG)

A triangular distribution for a random variable X is fully specified by stating its minimum a, its maximum b, and its mode m as shown on Figure 3.10.

As the area under the probability density function must be 1, the probability density at the mode can be shown to be 2/(b - a). Then the cumulative probability function is the area under the probability density function to the left of an abscissa at x.

$$
\begin{aligned}
F(x) &= 0 && x < a \\
F(x) &= \frac{(x-a)^2}{(b-a)\,(m-a)} && a \le x \le m \\
F(x) &= 1 - \left\{\frac{(b-x)^2}{(b-a)\,(b-m)}\right\} && m \le x \le b \\
F(x) &= 1 && x > b
\end{aligned}
\qquad (3.11)
$$

Let U be uniformly distributed on the range 0 to 1. Then by the probability integral transformation, X is found by equating U to F(x) in Equation (3.11) with the result:

$$
\begin{aligned}
X &= a + \Big[U(b-a)\,(m-a)\Big]^{1/2} && U \le \frac{(m-a)}{(b-a)} \\
X &= b - \Big[(1-U)\,(b-a)\,(b-m)\Big]^{1/2} && U > \frac{(m-a)}{(b-a)}
\end{aligned}
\qquad (3.12)
$$

Note that these formulae are applicable if m = a or m = b. A printout of SUBROUTINE TRIANG is contained in Table 3.16. A typical triangularly distributed random variable sampled by SUBROUTINE TRIANG is shown in Figure 3.11. Summary statistics and the chi-square goodness of fit statistics are

FIGURE 3.10

## A TRIANGULAR PROBABILITY DENSITY FUNCTION

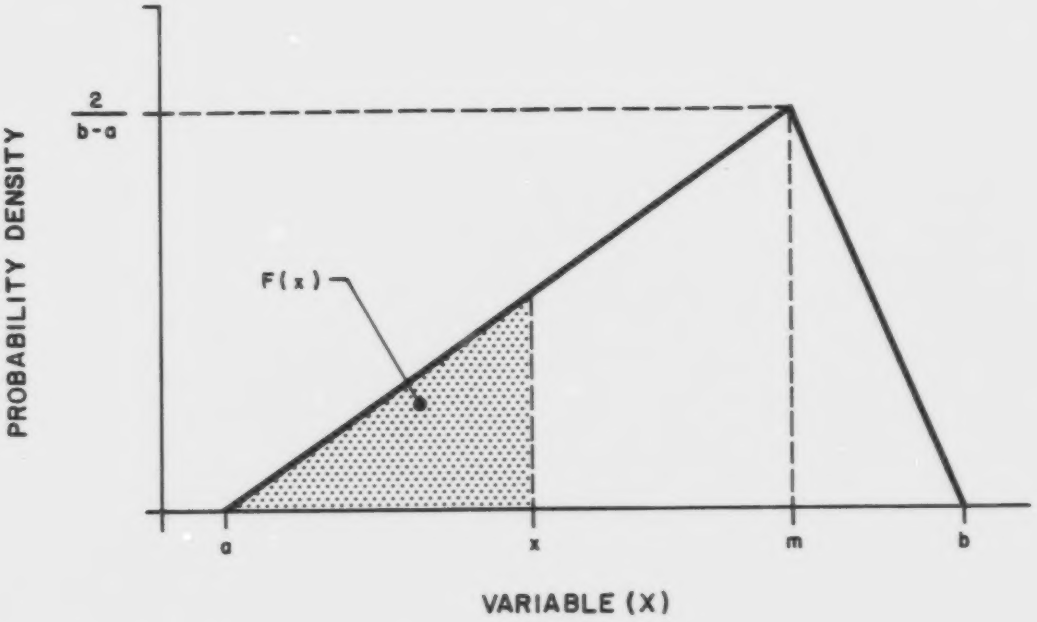

FIGURE 3.11

## PLOT OF FREQUENCY HISTOGRAM (500 SAMPLES) AND PROBABILITY DISTRIBUTION (SMOOTH CURVE) FOR TRIANGULAR DISTRIBUTION

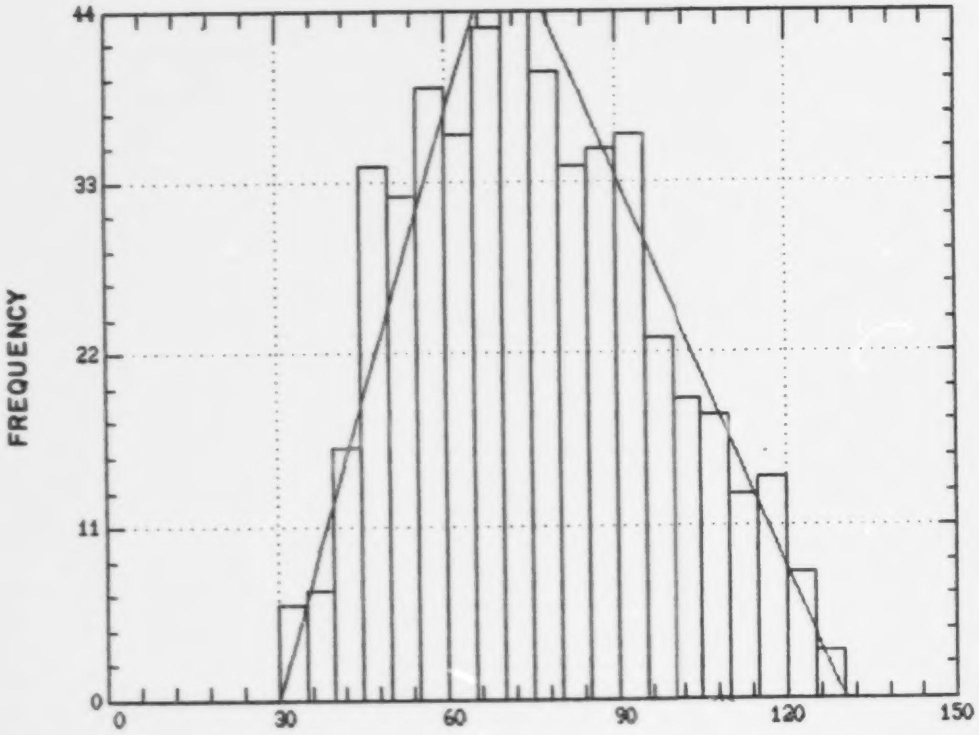

O2DIFF: OXYGEN DIFFUSIVITY THROUGH TAILINGS ($m^2$/yr)

**SUMMARY STATISTICS:**

| | SPECIFIED INPUT VALUES | CALCULATED SAMPLE VALUES |
|---|---|---|
| MINIMUM | 30 | 31·5 |
| MODE | 70 | – |
| MAXIMUM | 130 | 129 |

$CHI^2$ GOODNESS-OF-FIT = 14·482 WITH 17 DEGREES OF FREEDOM

Table 3.16

```
C
      SUBROUTINE TRIANG (NSTART,VMIN,VMODE,VMAX,XIN)
C
C      THIS ROUTINE GENERATES TRIANGULARLY DISTRIBUTED VARIATES
C
      REAL*4  XIN,R,VMAX,VMIN,VMODE,Z1,Z2
1000  R=RANDOM(NSTART)
      Z1=VMAX-VMIN
      Z2=VMODE-VMIN
      IF (Z1.LE.0.0) CALL ERROR (33)
      IF (R.LE.Z2/Z1) THEN
         XIN=VMIN+SQRT(R*Z1*Z2)
      ELSE
         XIN=VMAX-SQRT((1.-R)*(VMAX-VMODE)*Z1)
      ENDIF
      RETURN
      END
```

shown on the bottom of Figure 3.11.

### 3.3.11 Weibull Distribution (SUBROUTINE WEIBUL)

The cumulative probability function for a Weibull-distributed random variable X is given by:

$$F(x) = 1 - \exp\left\{-\left(\frac{x - a}{b}\right)^{c}\right\} \qquad \begin{array}{l} x > a \\ b,\ c > 0 \end{array} \qquad (3.13)$$

where a is a location parameter, b a scale parameter, and c a shape parameter.

For given a, b and c, a random number with the desired Weibull distribution is obtained by equating F(X) in Equation (3.13) to U, an observation on a uniformly distributed random variable with the range 0 to 1. The result is:

$$X = a + b\,[-\ln U]^{1/c} \qquad (3.14)$$

A listing of subroutine WEIBUL is shown on Table 3.17 and a typical sampled distribution is illustrated in Figure 3.12. Summary statistics and the chi-square goodness of fit statistics are shown on the bottom of Figure 3.12.

FIGURE 3.12

# PLOT OF FREQUENCY HISTOGRAM (500 SAMPLES) AND PROBABILITY DISTRIBUTION (SMOOTH CURVE) FOR WEIBULL DISTRIBUTION

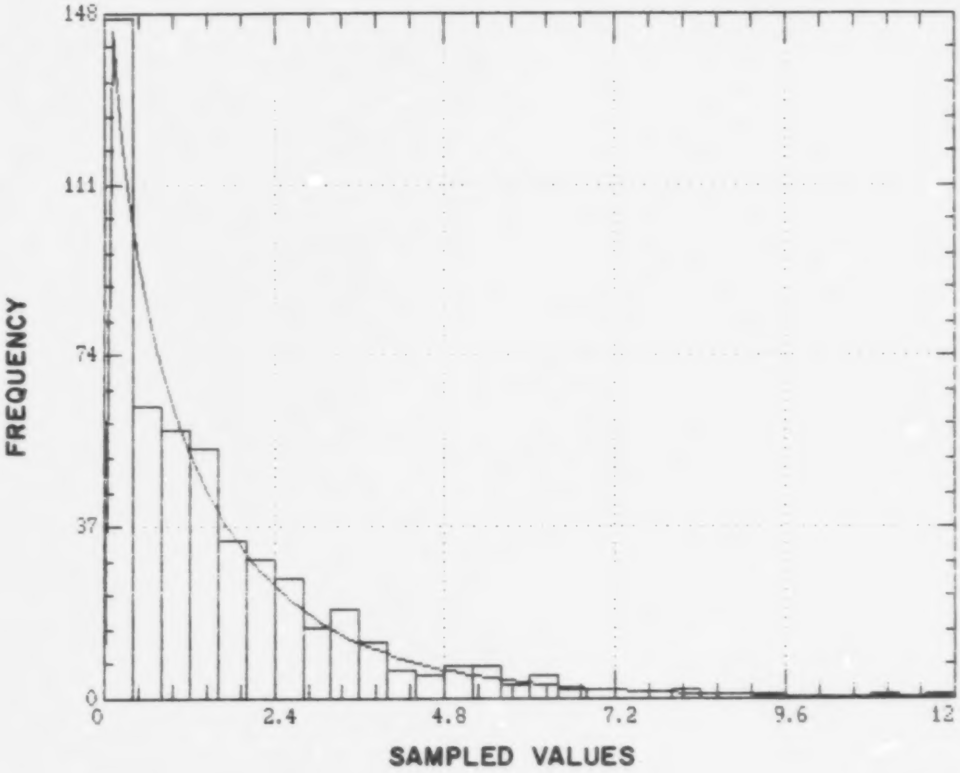

SUMMARY STATISTICS:

| | SPECIFIED INPUT VALUES | CALCULATED SAMPLE VALUES |
|---|---|---|
| SCALE PARAMETER | 1.5 | 1.481 |
| SHAPE PARAMETER | 0.9 | 0.878 |

CHI$^2$ GOODNESS-OF-FIT = 15.457 WITH 13 DEGREES OF FREEDOM

Table 3.17

```
C
      SUBROUTINE WEIBUL (NSTART,A,B,C,XIN)
C
C     THIS SUBROUTINE GENERATES RANDOM SAMPLES FROM WEIBULL
C     DISTRIBUTIONS BY TRANSFORMING UNIFORMLY DISTRIBUTED SAMPLES
C     TO A SPECIFIED WEIBULL DISTRIBUTION
C
      REAL*4 A,B,C,XIN,R
      INTEGER*4 NSTART
1000  R=RANDOM(NSTART)
      XIN=A+B*((-ALOG(R))**(1.0/C))
      RETURN
      END
```

### 3.3.12 Arbitrary and Beta Distributions (SUBROUTINE BETA)

The cumulative probability functions, $F(x_i)$, for the beta and arbitrary distributions are set up in subroutine CREATE using an optional number of cells as discussed previously in Section 3.3.4. Within subroutine BETA, the probability integral transformation is applied to $F(x_i)$ as illustrated in Figure 3.13 where U is a uniformly distributed random number on the interval (0, 1). The number U corresponds to a cell i of the cumulative probability function for a total of n cells. The number $X' = i/n$ is beta (or arbitrary) distributed with the same shape parameters a and b as X, the desired distribution, but its range is 0 to 1. This random number is then transformed to the desired value of X on the interval (MIN, MAX) by:

$$X = MIN + X' (MAX - MIN) \qquad (3.15)$$

A printout of subroutine BETA is shown on Table 3.18. Figure 3.14 shows a typical arbitrary distribution sampled by subroutine BETA and Figure 3.15 illustrates a sampled beta distribution. Summary statistics and the chi-square goodness of fit statistics are also given on Figure 3.15.

FIGURE 3.13

## CUMULATIVE PROBABILITY FUNCTION FOR BETA OR ARBITRARY DISTRIBUTIONS

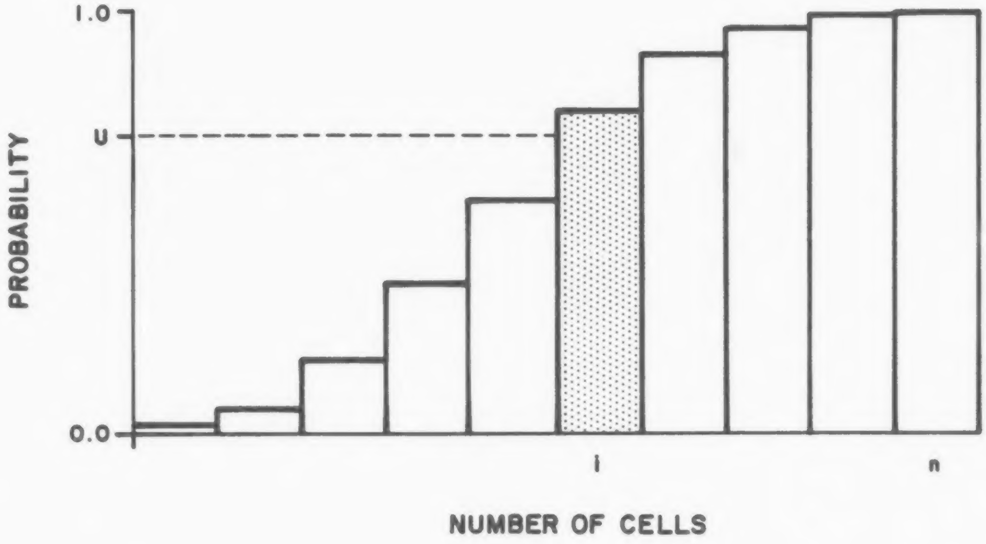

Table 3.18

```
C
      SUBROUTINE BETA (NSTART,I,XIN)
C
C      THIS ROUTINE SAMPLES VALUES OF BETA OR ARBITRARY VARIATES.
C
      INCLUDE 'PARAM.INC'
      INTEGER*2 ICELL,I
      REAL*4 XIN,R
      R=RANDOM(NSTART)
      DO 1100 ICELL=1,NACELL(I)
         IF (CPF(I,ICELL).GE.R) GOTO 1000
1100  CONTINUE
      ICELL=NACELL(I)
1000  XIN=ORIGIN(I)+ICELL*UNIT(I)
      RETURN
      END
```

FIGURE 3.14

PLOT OF FREQUENCY HISTOGRAM (500 SAMPLES)
FOR ARBITRARY DISTRIBUTION

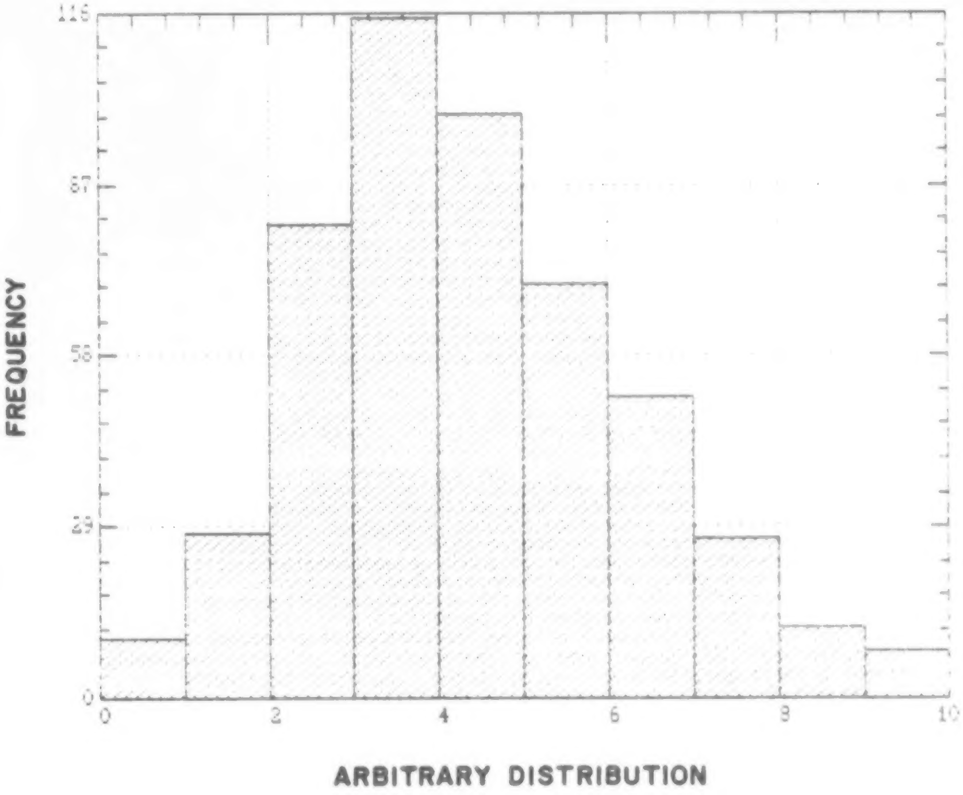

SUMMARY:

| CELL | SPECIFIED INPUT VALUES | CALCULATED SAMPLE VALUES |
|---|---|---|
| 1 | 10 | 10 |
| 2 | 20 | 28 |
| 3 | 80 | 80 |
| 4 | 110 | 115 |
| 5 | 105 | 99 |
| 6 | 75 | 70 |
| 7 | 50 | 51 |
| 8 | 30 | 27 |
| 9 | 15 | 12 |
| 10 | 5 | 8 |

FIGURE 3.15

PLOT OF FREQUENCY HISTOGRAM (500 SAMPLES) AND PROBABILITY DISTRIBUTION (SMOOTH CURVE) FOR BETA DISTRIBUTION

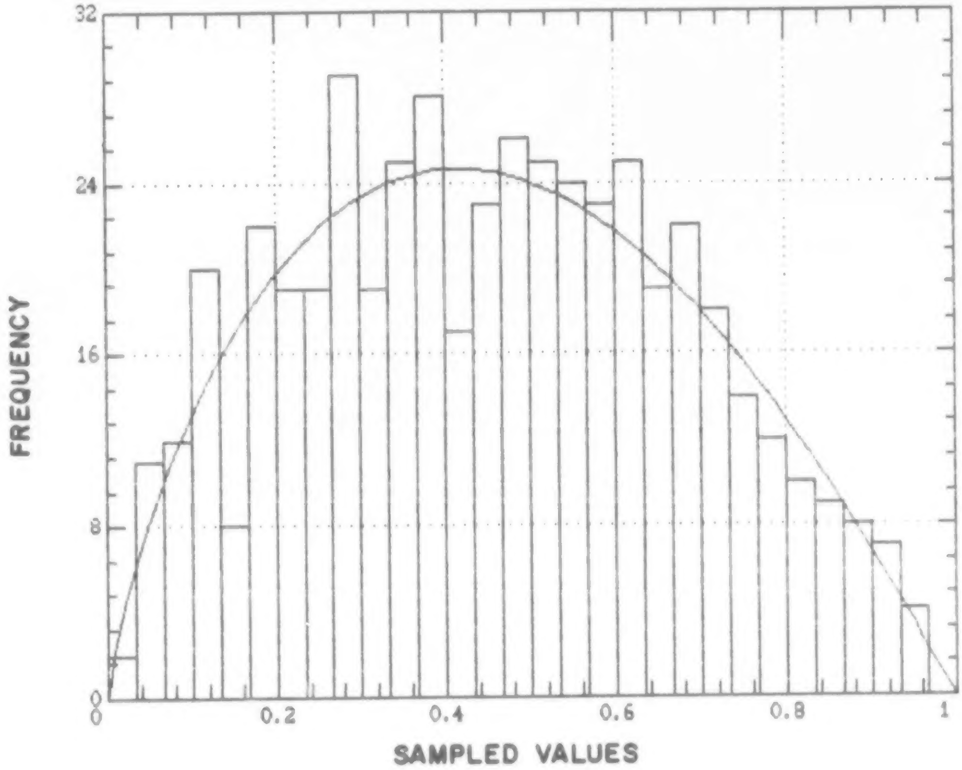

SUMMARY STATISTICS:

| | SPECIFIED INPUT VALUES | CALCULATED SAMPLE VALUES |
|---|---|---|
| a | 1.90 | 1.76 |
| b | 2.10 | 2.07 |

CHI$^2$ GOODNESS-OF-FIT = 15.93 WITH 24 DEGREES OF FREEDOM

### 3.3.13 Correlated Parameters (SUBROUTINE CORREL)

The following discussion was excerpted from Andres and Goodwin (1985). The technique implemented in this study and described here was developed by Kleijnen (1974) for generating pairwise correlated variates. Assume X and Y have means $\mu_X$ and $\mu_Y$ and standard deviations $\sigma_X$ and $\sigma_Y$ respectively and are correlated with correlation coefficient C(X,Y). Let Z be a normal variate with mean 0 and standard deviation 1. Then to sample, both X and Y in a way that preserves the distribution of X, the mean and variance of Y, and the correlation coefficient C(X,Y) use the following algorithm:

1. Sample X and Z from their distributions.
2. Evaluate $Y = aX + b + u$
   where $a = C(X,Y)\ \sigma_Y / \sigma_X$ (3.16)

   $b = \mu_Y - C(X,Y)\ \mu_X \sigma_Y / \sigma_X$

   $u = \sigma_Y\ Z(1-C(X,Y)^2)^{1/2}$

For example, suppose X and Y are both normally distributed, X having mean 5 and standard deviation 1, Y having mean 100 and standard deviation 20. Suppose the correlation coefficient C(X,Y) = 0.80. Then:

$a = 16$
$b = 20$
and $u = 12*Z$

Suppose X is sampled at 3.5 and the intermediate variable Z (normal with mean 0 and variance 1) takes the sampled value 0.5. Then on substitution into Equation (3.16):

$$Y = 16*X + 20 + 12*Z = 82$$

As expected, since X has a low value, Y also has a low value.

This algorithm preserves the distribution of Y as well as the distribution of X if both X and Y are normally-distributed. Otherwise, only the first two moments (mean and variance) of Y's distribution are correct, and its shape may vary from the given distribution.

Figure 3.16 illustrates the results of a correlation with a normally distributed variable. The correlated parameter takes on the normal distribution of the independent parameter. A listing of the subroutine is shown on Table 3.19. Summary statistics and the chi-square goodness of fit test are also given in Figure 3.16.

FIGURE 3.16

PARAMETER CORRELATED TO NORMAL DISTRIBUTION
(500 SAMPLES)

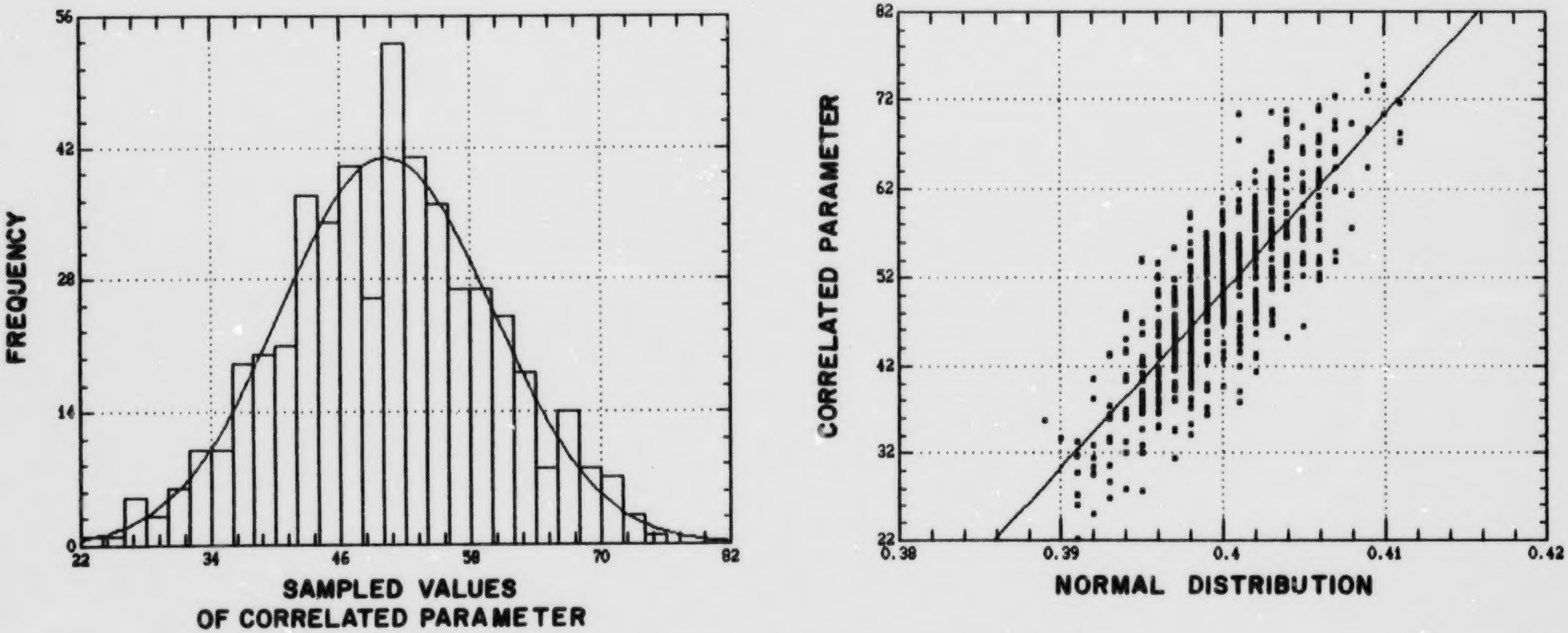

SUMMARY STATISTICS:

| | SPECIFIED INPUT VALUES | CALCULATED SAMPLE VALUES |
|---|---|---|
| MEAN | 50.0 | 50.3 |
| STANDARD DEVIATION | 10.00 | 9.75 |
| CORRELATION COEFFICIENT | 0.800 | 0.818 |

CHI$^2$ GOODNESS-OF-FIT = 18.174 WITH 19 DEGRESS OF FREEDOM

Table 3.19

```
C
      SUBROUTINE CORREL(NSTART,MEANY,SDEVY,CCOEFF,MEANX,SDEVX,CORNUM,XIN
     &)
C
C     THIS SUBROUTINE CALCULATES THE VALUE OF AN INPUT PARAMETER WHICH
C     IS CORRELATED WITH SOME PREVIOUS INPUT PARAMETER.  IT EMPLOYS
C     KLEIJNEN'S CORRELATED GENERATION TECHNIQUE (KLEIJNEN, J.P.C.
C     (1974) STATISTICAL TECHNIQUES IN SIMULATION - PART 1, MARCEL
C     DEKKER,N.Y.) AS PRESENTED BY ANDRES AND GOODWIN (1984).
C
      INCLUDE 'INPT2.INC'
      INTEGER*2 CORNUM
      REAL*4 MEANY,SDEVY,CCOEFF,MEANX,SDEVX,XIN,A,B,U,Z,X,Y
      A=CCOEFF*SDEVY/SDEVX
      B=MEANY-CCOEFF*MEANX*SDEVY/SDEVX
      CALL NORMAL (NSTART,0.0,1.0,-1.0E37,1.0E37,Z)
      U=SDEVY*Z*SQRT(1.0-CCOEFF**2)
      X=XVALUE(CORNUM)
      Y=A*X+B+U
      XIN=Y
      RETURN
      END
```

## 3.4 Output Selection Routines

These routines select, sort, and save all of the parameters for which output is desired at specified time intervals. The values are saved in two vectors, one for the statistics file and one for the detailed result file and key file. These vectors are filled once for each trial. The structure of the vectors is illustrated in Figure 3.17.

The first part of each of the two vectors contains the sampled values of the non-time-variant input distributions saved by subroutine SAVEIN. Next are the sampled values of the time-variant input distributions saved by subroutine TIMSEL. The last set of entries is the calculated output parameters sorted and saved by the subroutines SELECT, SORT, and SEND. These subroutines are called as illustrated previously in Figure 1.2.

At the end of each trial, when the two vectors have been filled, they are used by the statistics routines for updating calculations. Also, on each trial, the contents of the detailed results vector are written to the detailed results file. Finally, when all trials have been completed, summary statistics are written to the appropriate files, as described later in Section 3.6.

### 3.4.1 Saving Time-Variant Sampled Parameters (SUBROUTINE TIMSEL)

This subroutine is called by the executive module, once for each time step and each trial. An initial check is performed at the beginning of this subroutine to determine whether output for any time-variant parameters is desired. If not, the remainder of the subroutine is bypassed.

Should the initial condition be satisfied, a second check is performed to determine whether the current time step is to be saved. If not, the remainder of the subroutine is again bypassed. The time steps for which input parameters will be saved are the same as those selected for the output concentrations and doses as specified in the second input file.

The output flag for each time-variant parameter is then checked to determine whether output of that variable is desired. If it is, the sampled parameter value is sent to one or both of the two vectors of output parameters (i.e. statistics or detailed results or both), as indicated by the output flag.

These values are all sorted to conform to the file structure indicated in Figure 3.17. The time-variant parameters are written to the output vectors, leaving space at the beginning of the vectors for the non-time variant parameters. The time-variant values are sorted so that all of the time steps for each parameter will appear together, in chronological order. To accomplish this, the vectors are not filled sequentially, but rather spaces are left for all the time steps yet to be saved and these are filled when those time steps are reached. The code for subroutine TIMSEL is shown in Table 3.20.

FIGURE 3.17

STRUCTURE OF VECTOR FOR OUTPUT PARAMETERS

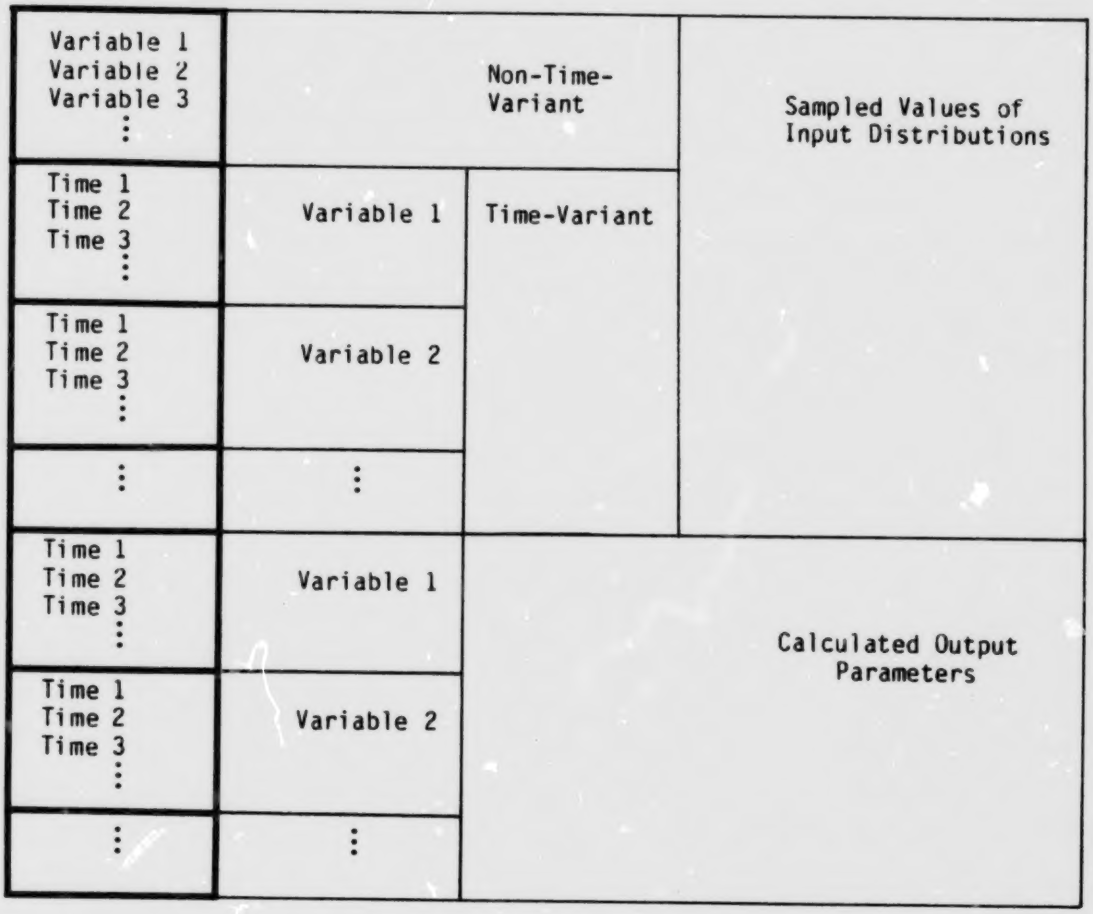
Variable 1
Variable 2
Variable 3
Non-Time-Variant
Sampled Values of Input Distributions
Time 1
Time 2
Time 3
Variable 1
Time-Variant
Time 1
Time 2
Time 3
Variable 2
Time 1
Time 2
Time 3
Variable 1
Calculated Output Parameters
Time 1
Time 2
Time 3
Variable 2

Table 3.20

```
C
      SUBROUTINE TIMSEL
C
C     THIS SUBROUTINE SAVES TIME-VARIANT INPUT VARIABLES
C     FLAGGED FOR OUTPUT TO STATS AND FILE
C
      INCLUDE 'COUNTS.INC'
      INCLUDE 'INPT.INC'
      INCLUDE 'OUT.INC'
      CHARACTER*1 C
      NUMS=1
      NUMF=1
C
C     CHECK IF ANY DISTRIBUTIONS ARE TIME-VARIANT
C
      IF (VARYS.NE.0.OR.VARYF.NE.0) THEN
C
C        INITIALIZE OR INCREMENT TIME COUNTERS
C
         IF (NT.EQ.0) THEN
            TNUMBS=1
            TNUMBF=1
         ENDIF
C
C        CHECK IF THIS TIME TO BE SAVED
C
         IF (TFILE(TNUMBF).EQ.NT.OR.TSTAT(TNUMBS).EQ.NT) THEN
            DO 40 I=1,VARY
               J=VARIED(I)
               C=EFLAG(J)
C
C              CHECK IF VALUE TO BE OUTPUT
C
               IF (C.EQ.'S'.OR.C.EQ.'F'.OR.C.EQ.'B') THEN
                  IF (NSTEPS.GE.TNUMBS) THEN
                     IF (TSTAT(TNUMBS).EQ.NT.AND.(C.EQ.'S'.OR.C.EQ.'B'))
     &                  THEN
C
C                       SORT VALUES AND SAVE FOR STATS
C
                        JS=NSTEPS*(NUMS-1)+NSTAT+TNUMBS
                        NUMS=NUMS+1
                        XOUTS(JS)=XIN(J)
                     ENDIF
                  ENDIF
                  IF (NSTEPF.GE.TNUMBF) THEN
                     IF (TFILE(TNUMBF).EQ.NT.AND.(C.EQ.'F'.OR.C.EQ.'B'))
     &                  THEN
C
C                       SORT VALUES AND SAVE FOR DETAILED RESULTS FILE
C
                        JF=NSTEPF*(NUMF-1)+NFILE+TNUMBF
```

Table 3.20 (continued)

```
                        NUMF=NUMF+1
                        XOUTF(JF)=XIN(J)
                     ENDIF
                  ENDIF
               ENDIF
40          CONTINUE
            IF (TFILE(TNUMBF).EQ.NT) TNUMBF=TNUMBF+1
            IF (TSTAT(TNUMBS).EQ.NT) TNUMBS=TNUMBS+1
         ENDIF
      ENDIF
      RETURN
      END
```

### 3.4.2 Selection of Output Time Steps (SUBROUTINE SELECT)

This subroutine is called by the main program for each time step and each trial. A check is performed to determine whether calculated parameters from this time step are to be routed to the statistics file. The time steps for which data are to be saved are indicated in the second input file (see Section 3.2.2). If data from the current time step are to be saved, subroutine SORT is called. This check is repeated for the detailed results output option and SORT is again called if the values for the current time step are to be saved to the detailed results file. The code for subroutine SELECT is shown on Table 3.21.

### 3.4.3 Sorting of Output Variables (SUBROUTINE SORT (VECTOR))

This module is called by Subroutine SELECT for each time step for which data are to be saved to either or both of the output files and for each trial. The subroutine argument, VECTOR, is a flag that indicates whether the variables are to be saved to the statistics file vector or to the detailed results file vector. Each output parameter is checked to see if it is to be saved to the file indicated by the flag, VECTOR. For each one that is to be saved, SEND is called. The code for subroutine SORT is shown in Table 3.22.

## Table 3.21

```
C
      SUBROUTINE SELECT
C
C     THIS SUBROUTINE CHECKS WHETHER PARAMETER VALUES ARE TO
C     BE SAVED AT EACH TIME, T. IT INDICATES WHETHER VALUES ARE
C     TO BE WRITTEN TO STATISTICS FILE OR DETAILED RESULTS FILE
C     VECTORS
C
      INCLUDE 'COUNTS.INC'
      CHARACTER*1 VECTOR
      NUMS=1
      NUMF=1
      IF (NT.EQ.0) THEN
         TNUMS=1
         TNUMF=1
      ENDIF
C
C     CHECK IF THIS TIME STEP IS TO BE SAVED TO STATS AND/OR DETAILED
C     RESULTS FILE
C
         IF (TSTAT(TNUMS).EQ.NT) THEN
            VECTOR='S'
            CALL SORT (VECTOR)
            TNUMS=TNUMS+1
         ENDIF
         IF (TFILE(TNUMF).EQ.NT) THEN
            VECTOR='F'
            CALL SORT (VECTOR)
            TNUMF=TNUMF+1
         ENDIF
      RETURN
      END
```

Table 3.22

```
C
      SUBROUTINE SORT (VECTOR)
C
C     THIS SUBROUTINE CHECKS ALL OUTPUT ARRAYS.  FOR ANY ARRAYS
C     CONTAINING PARAMETERS TO BE SAVED, THE CURRENT PARAMETER
C     VALUE IS WRITTEN TO A DUMMY VARIABLE FOR TRANSFER TO
C     SUBROUTINE 'SEND'.
C
      INCLUDE 'COUNTS.INC'
      INCLUDE 'INFO.INC'
      INCLUDE 'CONC.INC'
      CHARACTER*1 VECTOR
      REAL*4 XDUM
      K=1
      DO 1000 I=1,NARRAY
         IF (NVAR(I).NE.0) THEN
            DO 2000 J=1,NVAR(I)
               IF (VECTOR.EQ.FLAG(K)) THEN
C
C                 REROUTE TOTALS FOR DOSE TO LAST ARRAY LOCATION
C
                  IF (NUMTRL.EQ.1.AND.NSUB(K).EQ.11) NSUB(K)=5
C
C                 FIND CORRECT OUTPUT VALUE
C
                  IF (I.EQ.1) THEN
                     XDUM=WCONC(NSUB(K),LOC(K),3)
                  ELSEIF (I.EQ.2) THEN
                     XDUM=CONC(NSUB(K),LOC(K),3)
                  ELSEIF (I.EQ.3) THEN
                     XDUM=PH(LOC(K))
                  ELSEIF (I.EQ.4) THEN
                     XDUM=WATC(NSUB(K),LOC(K))
                  ELSEIF (I.EQ.5) THEN
                     XDUM=WATAVG(NSUB(K))
                  ELSEIF (I.EQ.6) THEN
                     XDUM=WATPH(LOC(K))
                  ELSEIF (I.EQ.7) THEN
                     XDUM=GWATC(NSUB(K))
                  ELSEIF (I.EQ.8) THEN
                     XDUM=EMRATE(NSUB(K))
                  ELSEIF (I.EQ.9) THEN
                     XDUM=EROTOT
                  ELSEIF (I.EQ.10) THEN
                     XDUM=DTAIL
                  ELSEIF (I.EQ.11) THEN
                     XDUM=AIRC(NSUB(K),LOC(K))
                  ELSEIF (I.EQ.12) THEN
                     XDUM=SOILC(NSUB(K),LOC(K))
                  ELSEIF (I.EQ.13) THEN
                     XDUM=AVEGC(NSUB(K),LOC(K))
                  ELSEIF (I.EQ.14) THEN
                     XDUM=BVEGC(NSUB(K),LOC(K))
```

Table 3.22 (continued)

```
                  ELSEIF (I.EQ.15) THEN
                     XDUM=SUFOC(NSUB(K))
                  ELSEIF (I.EQ.16) THEN
                     XDUM=BRWSC(NSUB(K))
                  ELSEIF (I.EQ.17) THEN
                     XDUM=LICHC(NSUB(K))
                  ELSEIF (I.EQ.18) THEN
                     XDUM=AQVEGC(NSUB(K))
                  ELSEIF (I.EQ.19) THEN
                     XDUM=FISHC(NSUB(K),LOC(K))
                  ELSEIF (I.EQ.20) THEN
                     XDUM=AMOC(NSUB(K))
                  ELSEIF (I.EQ.21) THEN
                     XDUM=WMOC(NSUB(K))
                  ELSEIF (I.EQ.22) THEN
                     XDUM=ACARC(NSUB(K))
                  ELSEIF (I.EQ.23) THEN
                     XDUM=WCARC(NSUB(K))
                  ELSEIF (I.EQ.24) THEN
                     XDUM=WATD(NSUB(K),LOC(K))
                  ELSEIF (I.EQ.25) THEN
                     XDUM=SHINED(NSUB(K),LOC(K))
                  ELSEIF (I.EQ.26) THEN
                     XDUM=INHD(NSUB(K),LOC(K))
                  ELSEIF (I.EQ.27) THEN
                     XDUM=RADD(LOC(K))
                  ELSEIF (I.EQ.28) THEN
                     XDUM=VEGD(NSUB(K),LOC(K))
                  ELSEIF (I.EQ.29) THEN
                     XDUM=FISHD(NSUB(K),LOC(K))
                  ELSEIF (I.EQ.30) THEN
                     XDUM=MEATD(NSUB(K),LOC(K))
                  ELSEIF (I.EQ.31) THEN
                     XDUM=DOSE(NSUB(K),LOC(K))
                  ELSEIF (I.EQ.32) THEN
                     XDUM=POPDT
                  ELSEIF (I.EQ.33) THEN
                     XDUM=BLANK1(NSUB(K),LOC(K))
                  ELSEIF (I.EQ.34) THEN
                     XDUM=BLANK2(NSUB(K),LOC(K))
                  ENDIF
                  CALL SEND (XDUM,VECTOR)
               ENDIF
               K=K+1
 2000       CONTINUE
         ENDIF
 1000 CONTINUE
      RETURN
      END
```

### 3.4.4 Saving Output Variables (SUBROUTINE SEND (XDUM, VECTOR))

SEND is called by Subroutine SORT for each output variable to be saved, for each time step, and for each trial. The subroutine argument XDUM contains the value to be saved and the argument VECTOR indicates the vector to which the value is to be saved.

The variable, XDUM, is saved to the appropriate vector of output values in its proper position (see Figure 3.17). Values are placed in the vectors of outputs following sampled values of the time-variant distributions. Space is left for these and the non-time-variant parameters as well. Like the time-variant values, the output variables are not entered into the vectors sequentially, but rather space is left for the time steps yet to be saved and these are filled in when those time steps are reached. The code for subroutine SEND is shown on Table 3.23.

### 3.4.5 Saving Non-Time-Variant Sampled Parameters (SUBROUTINE SAVEIN)

Subroutine SAVEIN is called by the main program once for each trial. An initial check is performed to determine whether any of the non-time-variant input parameters are to be saved. If not, the rest of this subroutine is bypassed.

Each non-time-variant parameter is checked to determine whether its sampled value is to be saved for either or both of the statistics or detailed results files. The variables that are to be saved are written sequentially to the vector of values for the appropriate file. The code for subroutine SAVEIN is shown on Table 3.24.

Table 3.23

```
C
      SUBROUTINE SEND (XDUM,VECTOR)
C
C     SUBROUTINE ACCEPTS THE CURRENT VALUE OF A VARIABLE AND ALLOCATES
C     IF TO AN APPROPRIATE POSITION IN AN OUTPUT VECTOR.
C
      INCLUDE 'COUNTS.INC'
      INCLUDE 'OUT.INC'
      CHARACTER*1 VECTOR
      REAL*4 XDUM
      IF (VECTOR.EQ.'S') THEN
C
C        SORT OUTPUTS AND SEND THE VARIABLES TO STATISTICS VECTOR
C
         JS=(NUMS-1+VARYS)*NSTEPS+TNUMS+NSTAT
         XOUTS(JS)=XDUM
         NUMS=NUMS+1
      ELSEIF (VECTOR.EQ.'F') THEN
C
C        SORT OUTPUTS AND SEND THE VARIABLES TO DETAILED RESULTS VECTOR
C
         JF=(NUMF-1+VARYF)*NSTEPF+TNUMF+NFILE
         XOUTF(JF)=XDUM
         NUMF=NUMF+1
      ENDIF
      RETURN
      END
```

Table 3.24

```
C
      SUBROUTINE SAVEIN
C
C     THIS SUBROUTINE SAVES ALL VALUES OF SELECTED NON-TIME-VARIANT
C     INPUT PARAMETERS TO APPROPRIATE VECTORS (XOUTS, XOUTF).
C
      INCLUDE 'OUT.INC'
      INCLUDE 'INPT.INC'
      INCLUDE 'COUNTS.INC'
C
C     CHECK IF ANY INPUT VALUES TO BE SAVED
C
      IF (NSTAT.NE.0.OR.NFILE.NE.0) THEN
         NSTA=0
         NFIL=0
         DO 10 J=1,VARN
            I=VARNOT(J)
            IF (EFLAG(I).EQ.'S'.OR.EFLAG(I).EQ.'B') THEN
C
C              SAVE VALUE TO STATISTICS VECTOR
C
               NSTA=NSTA+1
               XOUTS(NSTA)=XIN(I)
            ENDIF
            IF (EFLAG(I).EQ.'F'.OR.EFLAG(I).EQ.'B') THEN
C
C              SAVE VALUE TO DETAILED RESULTS VECTOR
C
               NFIL=NFIL+1
               XOUTF(NFIL)=XIN(I)
            ENDIF
10       CONTINUE
      ENDIF
      RETURN
      END
```

## 3.5 Statistics Routines

The statistics routines are designed to generate summary statistics for variables contained in two vectors. The first vector (XOUTS) contains variables for which only summary statistics are desired. The individual values of these variables are not saved on every trial. However, the values of those variables in the second vector (XOUTF) are saved to a detailed results file on every probabilistic trial. Summary statistics for these variables are also calculated, and act as a quick summary of, and reference to the detailed results output file.

Because of the desire to be able to compute summary statistics without saving all variable values for all trials (potentially a large quantity of information), an "updating" method is used (Spicer, 1972). This method, which updates the "moment" statistics each time a new observation is considered is described later in section 3.5.2. This approach is in contrast to traditional methods for calculating statistics in which all of the observations of a desired parameter are considered at once.

### 3.5.1 Computing Summary Statistics (SUBROUTINE STATS)

The statistics routine is called once on every probabilistic trial, receiving the two vectors of values saved for each of the two output options (XOUTS and XOUTF). The subroutine combines these two vectors into one larger vector. All subsequent operations are performed on the elements in this larger vector. The first four moments of each variable ($S_1$, $S_2$, $S_3$, $S_4$) are updated by subroutine MOMENT. The first two geometric (logarithmic) moments ($GS_1$, $GS_2$) are updated by subroutine GMOMENT. Following the final trial, the summary statistics are computed as follows:

$$\text{standard deviation} \quad = \left(\frac{S_2}{n-1}\right)^{1/2}$$

skewness $= \dfrac{(S_3/n)}{\left(\frac{S_2}{n}\right)^{1.5}}$

kurtosis $= \dfrac{(S_4/n)}{\left(\frac{S_2}{n}\right)^{2.0}}$

geometric mean $= \exp\,(GS_1)$

geometric standard deviation $= \exp\left[\left(\frac{GS_2}{n-1}\right)^{1/2}\right]$

where the moments are defined as follows:

$$S_1 = \sum_{i=1}^{n} X_i\,/n = \overline{X}$$

$$S_2 = \sum_{i=1}^{n} (X_i - \overline{X})^2$$

$$S_3 = \sum_{i=1}^{n} (X_i - \overline{X})^3$$

$$S_4 = \sum_{i=1}^{n} (X_i - \overline{X})^4$$

$$GS_1 = \sum_{i=1}^{n} (\ln X_i)/n = \overline{\ln X}$$

$$GS_2 = \sum_{i=1}^{n} (\ln X_i - \overline{\ln X})^2$$

The arithmetic mean is not computed since it is simply $S_1$. The calculations are performed subject to appropriate checks such as divisions by zero and logarithms of non-positive numbers. In any cases where the calculations would produce "undefined" results the program will display a zero result. For instance, for a constant parameter, the value of $S_2$, the second statistical moment, is zero and, rigorously, skewness and kurtosis are undefined. They will, however, be displayed as "0.0" rather than as "undefined".

A listing of the program code for this routine is provided in Table 3.25.

Table 3.25

```
C
      SUBROUTINE STATS
C
C     SUBROUTINE STATS CALCULATES SUMMARY STATISTICS FOR VARIABLES
C     CONTAINED IN THE VECTOR XOUT. THE ANALYSIS INVOLVES UPDATING
C     CALCULATIONS WHICH ARE PERFORMED IN SUBROUTINES MOMENT AND
C     GMOMENT.
C
      INCLUDE 'STATS.INC'
      INCLUDE 'OUT.INC'
      INCLUDE 'COUNTS.INC'
      INCLUDE 'UPDATE.INC'
      REAL*4 XOUT(600)
      DOUBLE PRECISION XN,GSD(600),Z1
C
C     INITIALIZE STATISTICS ON FIRST TRIAL
C
      IF (NUMTRL.EQ.1) THEN
         NOUTS=NSTEPS*(VARYS+NVARYS)+NSTAT
         NOUTF=NSTEPF*(VARYF+NVARYF)+NFILE
         NOUT=NOUTS+NOUTF
         DO 1100 IDIST1=1,NOUT
            XMAX(IDIST1)=-1.0E+37
            XMIN(IDIST1)=+1.0E+37
            GN(IDIST1)=0
            N(IDIST1)=0
1100     CONTINUE
      ENDIF
C
C     TRANSFER OUTPUT VARIABLES TO XOUT
C
      IF (NOUTS.GT.0) THEN
         DO 1110 I=1,NOUTS
            XOUT(I)=XOUTS(I)
1110     CONTINUE
      ENDIF
      IF (NOUTF.GT.0) THEN
         KK=NOUTS+1
         DO 1120 I=KK,NOUT
            J=I-NOUTS
            XOUT(I)=XOUTF(J)
1120     CONTINUE
      ENDIF
C
C     ON EACH TRIAL, MAXIMUM,MINIMUM AND VARIOUS MOMENTS ARE UPDATED
C     FOR EACH PARAMETER.
C
      DO 1360 ID=1,NOUT
         Z1=XOUT(ID)
         IF (Z1.GT.XMAX(ID)) XMAX(ID)=Z1
         IF (Z1.LT.XMIN(ID)) XMIN(ID)=Z1
         CALL MOMENT (Z1,N(ID),S1(ID),S2(ID),S3(ID),S4(ID))
```

Table 3.25 (continued)

```
         CALL GMOMEN (Z1,GN(ID),GS1(ID),GS2(ID))
1360  CONTINUE
C
C     FOLLOWING THE FINAL TRIAL, THE CUMULATIVE MOMENT RESULTS ARE
C     USED TO CALCULATE SUMMARY STATISTICS.
C
      IF (NUMTRL.EQ.NTRIAL) THEN
         DO 1400 I=1,NOUT
            XN=DBLE(N(I))
            IF (N(I).LE.1) THEN
               SDEV(I)=0.0
            ELSE
               SDEV(I)=DSQRT(S2(I)/(XN-1.0))
            ENDIF
            IF (XN.EQ.0.0.OR.S2(I).LE.0.0) THEN
               SKEW(I)=0.0
               KURT(I)=0.0
            ELSE
               SKEW(I)=(S3(I)/XN)/((S2(I)/XN)**1.5)
               KURT(I)=(S4(I)/XN)/((S2(I)/XN)**2.0)
            ENDIF
            IF (GN(I).LE.1) THEN
               GSD(I)=0.0
               GMEAN(I)=0.0
            ELSE
               GSD(I)=DSQRT(GS2(I)/DBLE(GN(I)-1))
               GMEAN(I)=DEXP(GS1(I))
            ENDIF
            GSDEV(I)=DEXP(GSD(I))
1400     CONTINUE
      ENDIF
      RETURN
      END
```

### 3.5.2 Computing Moment Values (Subroutines MOMENT and GMOMEN )

As mentioned previously, selected "moments" of each variable are updated on each probabilistic trial. These "moments" are also known as "power sums of deviations about the mean". The algorithm used in these routines and the following discussion was adapted from that presented by Spicer (1972). In general, if n-1 observations ($x_i$) have been read into the computer and a new observation $x_n$ is added, then the new power sums are given by:

$$\sum_{i=1}^{n} (x_i - \overline{x}_n)^r = \sum_{i=1}^{n-1} (d_i - \delta_x)^r + (n-1)^r ( \delta x)^r$$

where:

$\overline{x}_n$ = mean of n observations
$d_i$ = $(x_i - x_{n-1})$
$\delta x$ = $(\overline{x}_n - \overline{x}_{n-1})/n$
r = degree of moment

These formulae allow the power sums to be computed with little rounding error but, of course, at the cost of some extra calculation.

To calculate the geometric moments, the natural logarithms of the observations (i.e. ($\ln(x_i)$)) are used in the above equations in place of the actual observations, $x_i$. In these calculations, one must ensure that the observed values $x_i$ are greater than zero, to perform the logarithmic transforms. Those values of each parameter less than or equal to zero are excluded from the calculations. The number of observations ($n_i$) always reflects these omissions.

Listings of the code for subroutines MOMENT and GMOMEN are provided in Tables 3.26 and 3.27 respectively.

Table 3.26

```
C
      SUBROUTINE MOMENT (X,N,S1,S2,S3,S4)
C
C     THIS SUBROUTINE CALCULATES THE FIRST FOUR MOMENTS
C     OF A RANDOM VARIABLE USING AN ALGORITHM BY C.C. SPICER
C     (APPLIED STATISTICS 21,226-227 (1972)).
C
      DOUBLE PRECISION X,S1,S2,S3,S4,AN,AN1,DX,DX2
      INTEGER*2 N
      N=N+1
      IF (N.EQ.1) THEN
         S1=X
         S2=0.0
         S3=0.0
         S4=0.0
      ELSE
         AN=N
         AN1=AN-1.0
         DX=(X-S1)/AN
         DX2=DX*DX
         S4=S4-DX*(4.0*S3-DX*(6.0*S2+AN1*(1.0+AN1**3)*DX2))
         S3=S3-DX*(3.0*S2-AN*AN1*(AN-2.0)*DX2)
         S2=S2+AN*AN1*DX2
         S1=S1+DX
      ENDIF
      RETURN
      END
```

Table 3.27

```
C
      SUBROUTINE GMOMEN (X,N,GS1,GS2)
C
C     THIS SUBROUTINE CALCULATES THE GEOMETRIC MEAN AND
C     STANDARD DEVIATION USING THE METHOD OUTLINED IN
C     SUBROUTINE 'MOMENTS'.
C
      DOUBLE PRECISION X,GX,GS1,GS2,DX,DX2,AN,AN1
      INTEGER*2 N
      IF (X.GT.0.0) THEN
         GX=DLOG(X)
         N=N+1
         IF (N.EQ.1) THEN
            GS1=GX
            GS2=0.0
         ENDIF
         AN=FLOAT(N)
         AN1=FLOAT(N)-1.0
         DX=(GX-GS1)/AN
         DX2=DX*DX
         GS2=GS2+AN*AN1*DX2
         GS1=GS1+DX
      ENDIF
      RETURN
      END
```

## 3.6 Output Routines

The output routines format and write the summary statistics and the detailed results to disk files opened by the first input routine.

### 3.6.1 Output of Detailed Results (SUBROUTINE WRITE)

Subroutine WRITE is called at the end of each trial. During each trial, the vector, XOUTF, of output data is filled by subroutine SAVEIN with the values of variables for which detailed results are requested (see Section 3.3.5). Subroutine WRITE simply writes this entire vector to the detailed results disk file. The subroutine code is listed on Table 3.28.

### 3.6.2 Creation of Output Labels (SUBROUTINE NAMOUT)

Subroutine NAMOUT creates and stores the parameter labels to be written to the statistics and key files. These labels consist of variable names, substance and location codes and times if appropriate. The subprogram code is shown on Table 3.29.

The labels are stored in two vectors, one each for the statistics file and for the detailed results key file. Each element of these vectors corresponds to the elements of the two vectors of output parameters saved by Subroutine SAVEIN as illustrated previously in Figure 3.17. The labels in either vector correspond to the three main divisions of the output data, the non-time-variant input parameters, the time-variant input parameters, and the calculated variables. The labels for the non-time-variant input distributions are the variable names read in from the probabilistic data file. The labels for the time-variant input distributions are the variable names plus the time for which each value is saved as specified in the site and output specification file. The labels for the output parameters are the variable names, the substance and location codes, and the time steps, all as specified in the site and output information file discussed in Section 3.2.2. The logic flow for this subroutine is illustrated in Figure 3.18.

## Table 3.28

```
C
      SUBROUTINE WRITE
C
C     WRITES VALUES CONTAINED IN 'XOUTF' (SAMPLED INPUTS AND
C     CALCULATED PARAMETERS) TO SPECIFIED OUTPUT FILE.
C
      INCLUDE 'OUT.INC'
      INCLUDE 'IO.INC'
      INCLUDE 'COUNTS.INC'
      IF (NOUTF.GT.0) THEN
         IF (NUMTRL.EQ.1) CALL FILER (FUNIT1)
         WRITE (FUNIT1,900) (XOUTF(I),I=1,NOUTF)
      ENDIF
      RETURN
900   FORMAT (150(1X,E9.3))
      END
```

Table 3.29

```
C
      SUBROUTINE NAMOUT
C
C     ASSIGNS VARIABLE NAMES AND LOCATION AND SUBSTANCE CODES TO
C     CHARACTER VARIABLES FOR OUTPUT IN STATISTICS AND DETAILED
C     RESULTS FILES
C
      INCLUDE 'IO.INC'
      INCLUDE 'INFO.INC'
      INCLUDE 'COUNTS.INC'
      KS=1
      KF=1
C
C     WRITE SAMPLED INPUT VARIABLE NAMES FOR STATISTICS AND/OR DEATAILED
C     RESULTS FILES FOR NON-TIME-VARIANT DISTRIBUTIONS
C
      DO 10 I=1,VARN
         IF (EFLAG(VARNOT(I)).EQ.'S'.OR.EFLAG(VARNOT(I)).EQ.'B') THEN
            WRITE (NAMES(KS),100) VARTIT(VARNOT(I))
            KS=KS+1
         ENDIF
         IF (EFLAG(VARNOT(I)).EQ.'F'.OR.EFLAG(VARNOT(I)).EQ.'B') THEN
            WRITE (NAMEF(KF),100) VARTIT(VARNOT(I))
            KF=KF+1
         ENDIF
 10   CONTINUE
      JJ=1
C
C     WRITE SAMPLED INPUT VARIABLE NAMES FOR STATISTICS AND/OR DETAILED
C     RESULTS FILES FOR TIME-VARIANT DISTRIBUTIONS
C
      IF (VARY.GE.1) THEN
         DO 60 I=1,VARY
            IF (EFLAG(VARIED(I)).EQ.'S'.OR.EFLAG(VARIED(I)).EQ.'B') THEN
               DO 70 J=1,NSTEPS
                  WRITE (NAMES(KS),150) VARTIT(VARIED(I)),TSTAT(J)
                  KS=KS+1
70             CONTINUE
            ENDIF
            IF (EFLAG(VARIED(I)).EQ.'F'.OR.EFLAG(VARIED(I)).EQ.'B') THEN
               DO 80 J=1,NSTEPF
                  WRITE (NAMEF(KF),150) VARTIT(VARIED(I)),TFILE(J)
                  KF=KF+1
80             CONTINUE
            ENDIF
60       CONTINUE
      ENDIF
C
C     WRITE OUTPUT VARIABLE NAMES FOR STATISTICS OR DETAILED RESULTS.
C     NAMES INCLUDE VARIABLE NAME, SUBSTANCE, LOCATION, AND TIME.
C
      DO 20 I=1,NARRAY
```

Table 3.29 (continued)

```
         IF (NVAR(I).GT.0) THEN
            DO 30 J=1,NVAR(I)
               IF (I.GE.24.AND.NSUB(JJ).EQ.5.AND.I.NE.27)NSUB(JJ)=11
               IF (FLAG(JJ).EQ.'S') THEN
                  DO 40 K=1,NSTEPS
                     WRITE (NAMES(KS),200) VARNAM(I),NSUB(JJ),LOC(JJ),
     &                  TSTAT(K)
                     KS=KS+1
40                CONTINUE
               ELSEIF (FLAG(JJ).EQ.'F') THEN
                  DO 50 K=1,NSTEPF
                     WRITE (NAMEF(KF),200) VARNAM(I),NSUB(JJ),LOC(JJ),
     &                  TFILE(K)
                     KF=KF+1
50                CONTINUE
               ENDIF
               JJ=JJ+1
30          CONTINUE
         ENDIF
20    CONTINUE
100   FORMAT (2X,A6)
150   FORMAT (2X,A6,22X,I6)
200   FORMAT (2X,A6,6X,I2,9X,I2,3X,I6)
      RETURN
      END
```

FIGURE 3.18

SAVING OF LABELS FOR OUTPUT

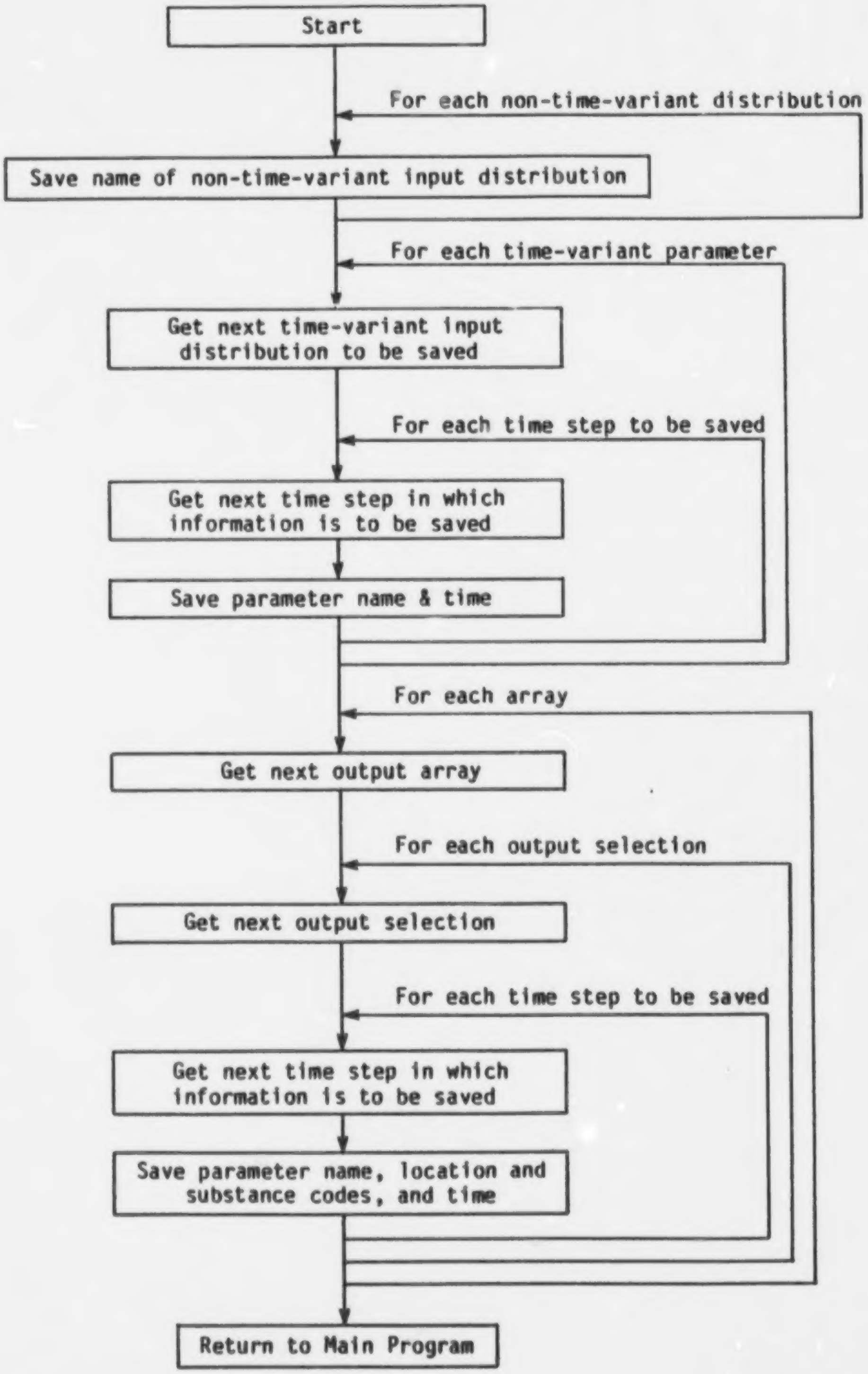
Start
For each non-time-variant distribution
Save name of non-time-variant input distribution
For each time-variant parameter
Get next time-variant input distribution to be saved
For each time step to be saved
Get next time step in which information is to be saved
Save parameter name & time
For each array
Get next output array
For each output selection
Get next output selection
For each time step to be saved
Get next time step in which information is to be saved
Save parameter name, location and substance codes, and time
Return to Main Program

### 3.6.3. Output of Summary Statistics (SUBROUTINE OUTPUT)

Subroutine OUTPUT writes the statistical parameters calculated by subroutine STATS to the statistics file and the detailed results key file. The output to both files includes titles, the number of trials, the variable names, the statistical parameters, and appropriate names and other information for the parameters.

The subroutine code is shown on Table 3.30.

Table 3.30

```
C
      SUBROUTINE OUTPUT
C
C     SUBROUTINE WRITES SUMMARY STATISTISTICS AND VARIABLE NAMES TO
C     STATISTICS FILE AND WRITES STATISTICS AND NAMES OF DETAILED
C     RESULTS PRAMETERS TO A 'KEY' FILE.
C
      INCLUDE 'IO.INC'
      INCLUDE 'STATS.INC'
      INCLUDE 'COUNTS.INC'
C
C     WRITE TO STATISTICS FILE
C
      IF (NOUTS.GT.0) THEN
         CALL FILER (FUNIT3)
         WRITE (FUNIT3,900) TITLE
         WRITE (FUNIT3,930) NTRIAL
         WRITE (FUNIT3,910)
         DO 10 I=1,NOUTS
            WRITE (FUNIT3,920) I,NAMES(I),S1(I),SDEV(I),GMEAN(I),
     &          GSDEV(I),XMIN(I),XMAX(I)
 10      CONTINUE
      ENDIF
C
C     WRITE TO DETAILED RESULTS FILE
C
      IF (NOUTF.GT.0) THEN
        CALL FILER (FUNIT2)
        WRITE (FUNIT2,900) TITLE
        WRITE (FUNIT2,930) NTRIAL
        WRITE (FUNIT2,910) 'SKEWNESS','KURTOSIS'
        KK=NOUTS+1
        DO 20 I=KK,NOUT
           J=I-NOUTS
           WRITE (FUNIT2,920) J,NAMEF(J),S1(I),SDEV(I),GMEAN(I),
     &         GSDEV(I),XMIN(I),XMAX(I),SKEW(I),KURT(I)
 20     CONTINUE
      ENDIF
      CLOSE (FUNIT1)
      CLOSE (FUNIT2)
      CLOSE (FUNIT3)
 900  FORMAT (1X,A40)
 910  FORMAT (5X,'PARAMETER',2X,'SUBSTANCE',2X,'LOCATION',2X,'TIME',5X,
     &   'MEAN',6X,'STD DEV',3X,'GEOM MEAN',3X,'GEOM SD',
     &  4X,'MINIMUM',4X,'MAXIMUM',4X,A8,3X,A8)
 920  FORMAT (I3,2X,A36,1X,8(2X,E9.3))
 930  FORMAT (1X,'NUMBER OF TRIALS: ',I5)
      RETURN
      END
```

# 4.0 CONFIDENCE BANDS PROGRAM DESCRIPTION

## 4.1 Introduction and Background

The most important output from a Monte Carlo calculation is often the probability density function for one or more output variables. Each probability density function is obtained in approximate form as a set of counts in cells which correspond to different values of the variable. The observed relative frequencies in the cells provide an approximation to the probability density function of the variable.

If the number of Monte Carlo trials were extremely large (say $10^9$) and the number of cells moderate (say 20), it would be expected that the graph of the relative frequency values versus the values of the variable corresponding to different cells would be a smooth curve which would agree very closely with the true probability density function. It would also vary little from one Monte Carlo run with the same number of trials to the next.

If, however, only 100 Monte Carlo trials are made with 20 cells, the relative frequency diagram can be expected to be "ragged", and to vary a good deal from one run of 100 trials to the next. Furthermore, the smooth curve drawn through the relative frequency points may not agree closely with the true probability density function.

There are various techniques for estimating the confidence in the output of a finite Monte Carlo calculation. Two were examined in this Phase III study. In Appendix E, Kaplan develops the theoretical basis for a Bayesian approach. In Appendix F, Reilly and Duever provide the theoretical basis for an alternative approach for estimating bounds from the output of a Monte Carlo simulation, within which the true probability density function (pdf) or cumulative density function (cdf) can be expected to lie with a given level of confidence. The Reilly and Duever approach has been implemented as a post-processing option to UTAP. The computer code for the current microcomputer implementation of this confidence band technique is provided in full in

Appendix G of this volume along with variable dictionaries for the confidence band program. This chapter outlines the computer implementation of the confidence band programs.

## 4.2 The General Nature of the Confidence Bands Programs

The confidence bands programs are provided as a post-processing option to UTAP. The general nature of the confidence bands programs and their relation to UTAP are indicated on Figure 4.1.

Prior to executing the confidence bands program, the desired variables must have been saved to the detailed results file generated by UTAP. The first activity within the confidence bands post-processor is then to read the required data from the UTAP output files. The information required by the confidence bands programs consists of the names of the variable(s) to be analysed, the minimum and maximum values, and, of course, the data itself. The user is asked, by the program, for the variable's identification number and whether a log transformation of the data is to be performed.

There are actually two confidence bands programs. The first, BIN, reads the data from UTAP and divides this data into bins or cells. The second program, OPAN, uses the binned data to calculate the confidence bands. BIN and OPAN are described below. The program output is a file containing the cell midpoints, the cell counts, and the counts corresponding to the 95% confidence limits for both the probability density function and the cumulative distribution function.

### 4.2.1. The Binning Program (BIN)

Figure 4.2 shows the flowsheet of the binning program, which bins Monte Carlo realizations of a given variable. The data are read, using subroutine READ, from two output files created by the Monte Carlo sampling program. One file contains the actual Monte Carlo realizations which are read into a vector. The second statistics file supplies the binning program with the variable

FIGURE 4.1

RELATION OF CONFIDENCE BAND PROGRAMS TO UTAP

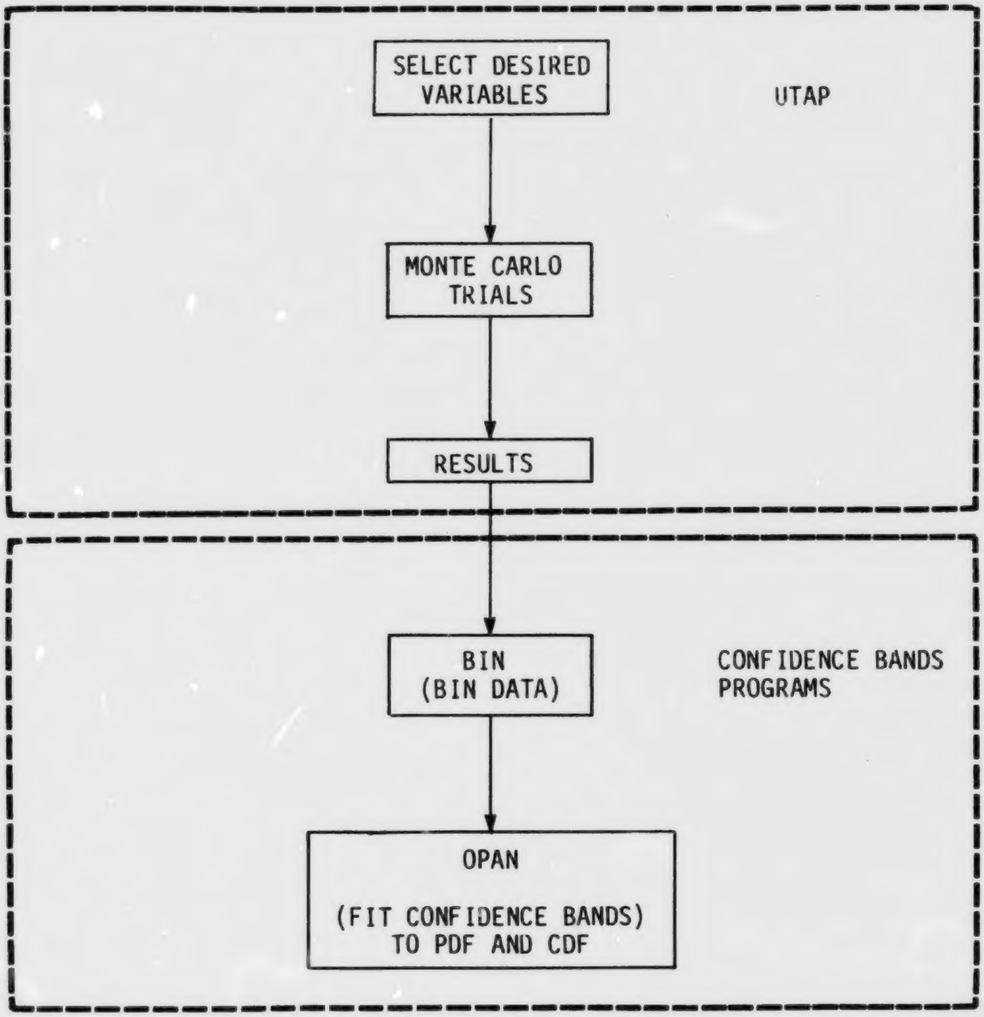
SELECT DESIRED VARIABLES
UTAP
MONTE CARLO TRIALS
RESULTS
BIN (BIN DATA)
CONFIDENCE BANDS PROGRAMS
OPAN
(FIT CONFIDENCE BANDS) TO PDF AND CDF

FIGURE 4.2

BINNING PROGRAM (BIN) STRUCTURE

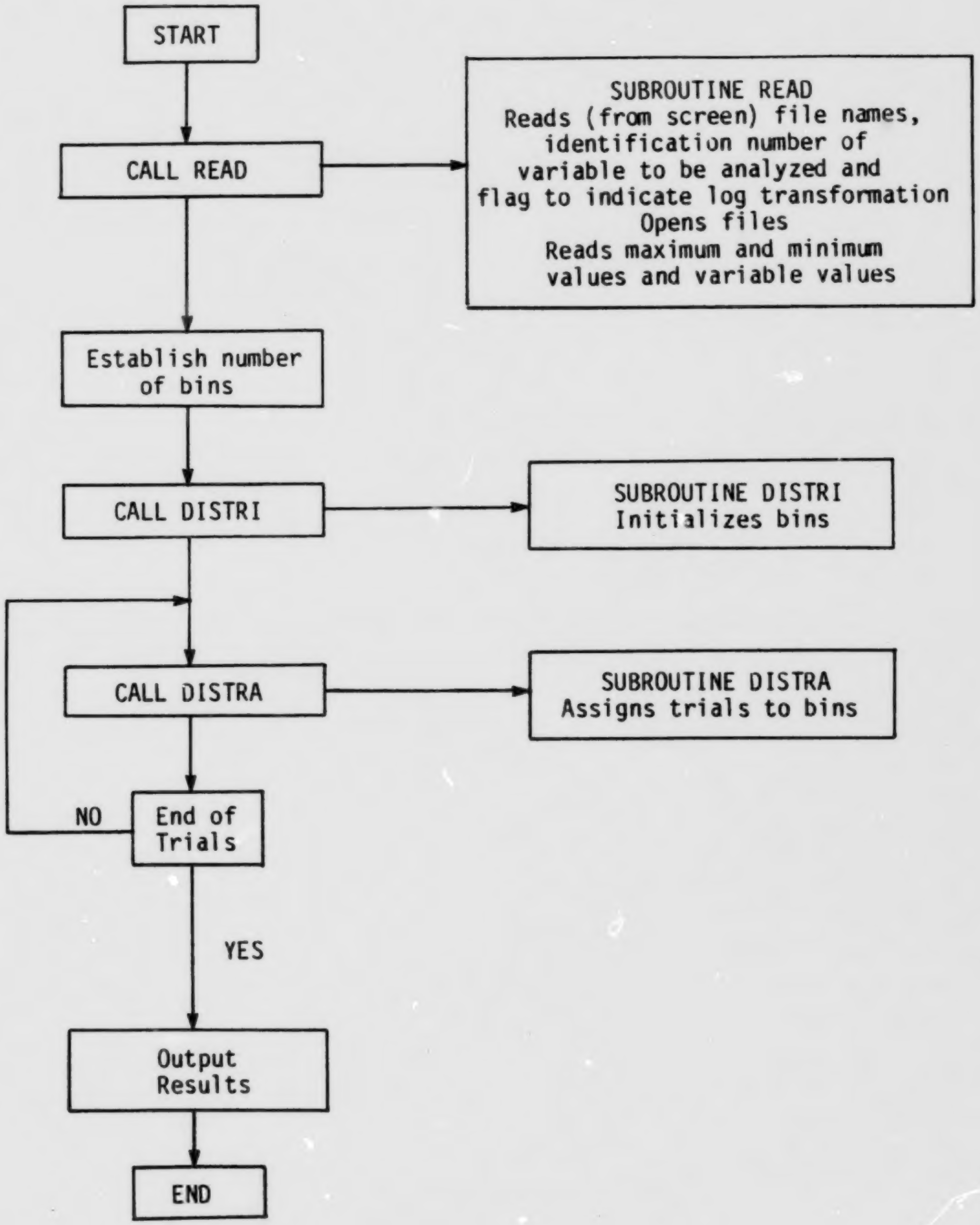
START
CALL READ
SUBROUTINE READ
Reads (from screen) file names, identification number of variable to be analyzed and flag to indicate log transformation
Opens files
Reads maximum and minimum values and variable values
Establish number of bins
CALL DISTRI
SUBROUTINE DISTRI
Initializes bins
CALL DISTRA
SUBROUTINE DISTRA
Assigns trials to bins
NO
End of Trials
YES
Output Results
END

name, and the minimum and maximum values of the variable.

Based on a paper by Sturges (1926) the number of bins used in the program is the nearest integer to the value given by the expression:

$$[\log_{10} (\#\text{of Monte Carlo trials})/\log_{10} (2.0)] + 1.0 \qquad (4.1)$$

The program allows for a logarithmic transformation of the data, which may be required for some highly skewed distributions. The minimum and maximum values for the purpose of binning are chosen to be 20% less than and 20% greater than the actual minimum and maximum values of the variable, respectively.

The binning process is initiated by a call to subroutine DISTRI. The observations are then binned by making a call to subroutine DISTRA for each observation.

Finally, the right hand cell endpoints, the cell counts, and the cell midpoints are stored in a file for use in the confidence bands program, OPAN.

### 4.2.2. The Confidence Band Program (OPAN)

Figure 4.3 is the logic flow sheet for the confidence bands program, OPAN. The program OPAN first reads in the data file generated by the binning program. The information required by OPAN consists of the name of the variable being analysed, the number of cells or bins used, the number of Monte Carlo trials made, a flag indicating whether or not a logarithmic transformation of the data has been made, the right hand cell endpoints, the cell midpoints and the cell counts.

A Newton-Raphson fitting procedure (implemented as subroutine NEWRAP) is used to fit a probability density function to observed cell counts. This subroutine requires two additional subroutines. The first function subroutine calculates the values of the probability density function at any value of x. The second subroutine provides a general solution to the matrix equation:

FIGURE 4.3

CONFIDENCE BANDS PROGRAM (OPAN) STRUCTURE

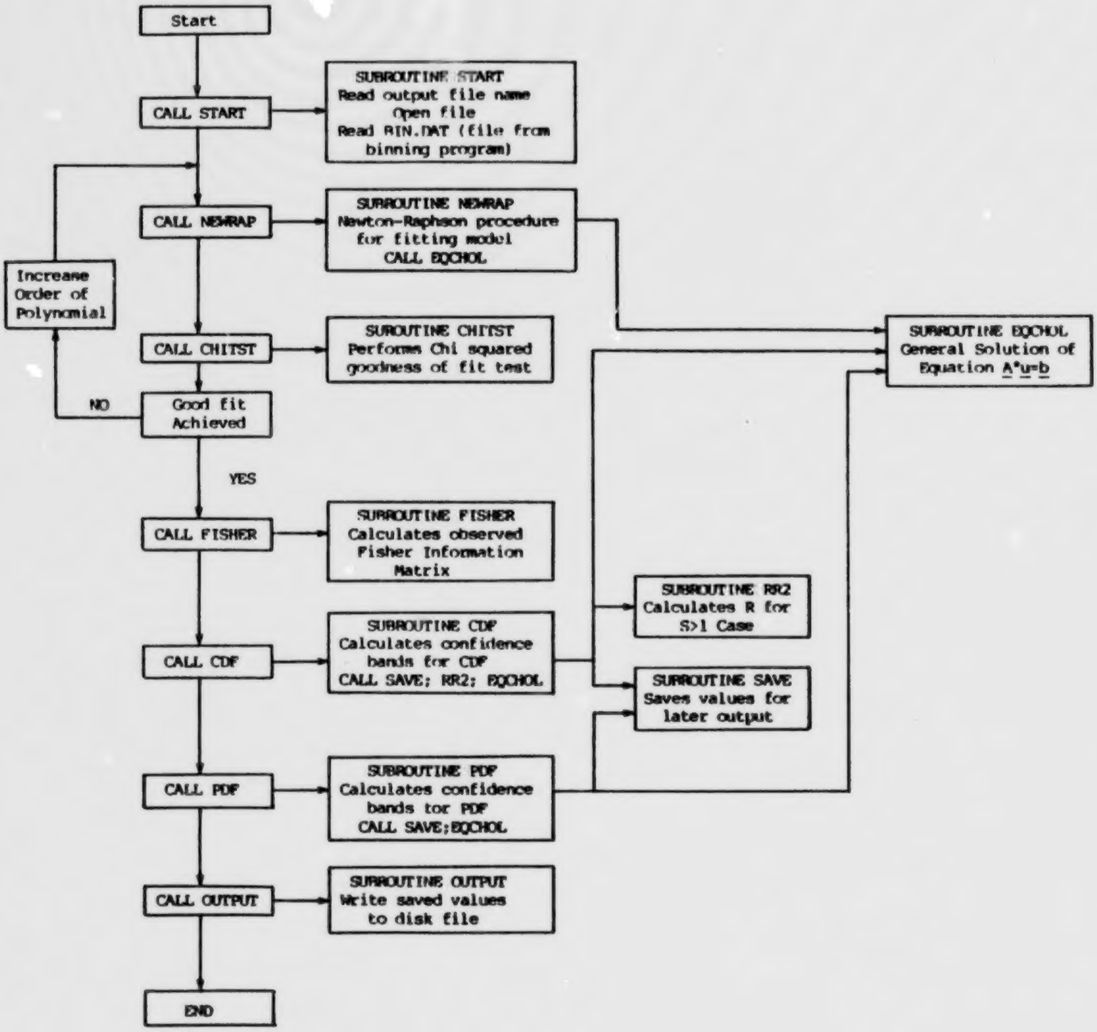
Start
CALL START
SUBROUTINE START
Read output file name
Open file
Read BIN.DAT (file from binning program)
CALL NEWRAP
SUBROUTINE NEWRAP
Newton-Raphson procedure for fitting model
CALL EQCHOL
Increase Order of Polynomial
CALL CHITST
SUROUTINE CHITST
Performs Chi squared goodness of fit test
SUBROUTINE EQCHOL
General Solution of Equation A*u=b
NO
Good fit Achieved
YES
CALL FISHER
SUBROUTINE FISHER
Calculates observed Fisher Information Matrix
SUBROUTINE RR2
Calculates R for S>1 Case
CALL CDF
SUBROUTINE CDF
Calculates confidence bands for CDF
CALL SAVE; RR2; EQCHOL
SUBROUTINE SAVE
Saves values for later output
CALL PDF
SUBROUTINE PDF
Calculates confidence bands for PDF
CALL SAVE;EQCHOL
CALL OUTPUT
SUBROUTINE OUTPUT
Write saved values to disk file
END

$$\underset{n\times n}{\underline{A}}\;\underset{n\times 1}{\underline{u}} = \underset{n\times 1}{\underline{b}} \qquad (4.2)$$

(See Appendix F1) Upon convergence of the fitting procedures a $\chi^2$ goodness of fit test is performed to check whether or not the fitted form of the probability density function adequately describes the binned data. Notice that the degrees of freedom for this test are given by

$$\text{D.F.} = k - s - 1 \qquad (4.3)$$

where

k = no. of cells with fitted numbers of observations greater than 6
s = degree of approximating polynomial

If the fitted number of cell counts for a particular cell are less than 6, then it is collapsed into the next cell. The value of k may therefore be equal to the number of cells but this is not necessarily true. The program iterates, increasing the degree of the polynomial by 1 each iteration until a satisfactory fit is achieved. The goodness of fit is examined using the $\chi^2$ test at the 25% significance level.

Once a model passes the goodness of fit test the program enters the next phase in which confidence bands are evaluated. The first step is to evaluate the observed Fisher information matrix. The 95% confidence bands for the cumulative distribution function are calculated in subroutine CDF and finally the 95% confidence bands for the probability density functions are calculated in subroutine PDF.

Further discussion of the computer implementation of the confidence bands program is provided in Appendix F of this report, as is a discussion of the theoretical basis for the technique. A full listing of the two computer programs used for confidence band estimation (BIN and OPAN) is provided in Appendix G along with variable dictionaries for these two programs.

### 4.3 Examples

Three examples of 95% confidence bands calculated by the programs BIN and OPAN are included in this section.

The first two examples are of known distributions, randomly sampled using 500 trials. Figure 4.4 illustrates confidence bands fitted to the cumulative distribution function and the probability density function of a normal distribution. The confidence bands illustrated in Figure 4.5 are fitted to log transformed random samples drawn from a lognormal distribution.

The third example, shown in Figure 4.6, presents confidence bands fitted to actual output from UTAP. Radium concentration in fish at t=100 years is used in this example. The figure actually represents confidence bands on the log-transformed values obtained from 200 random trials.

## FIGURE 4.4

## PLOTS OF 95% CONFIDENCE BANDS FOR A NORMAL DISTRIBUTION (500 TRIALS)

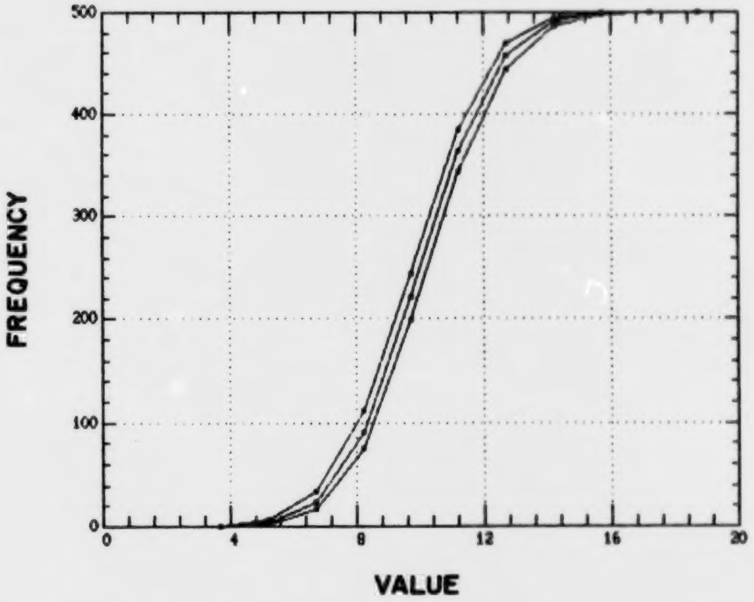

A) CUMULATIVE DISTRIBUTION FUNCTION

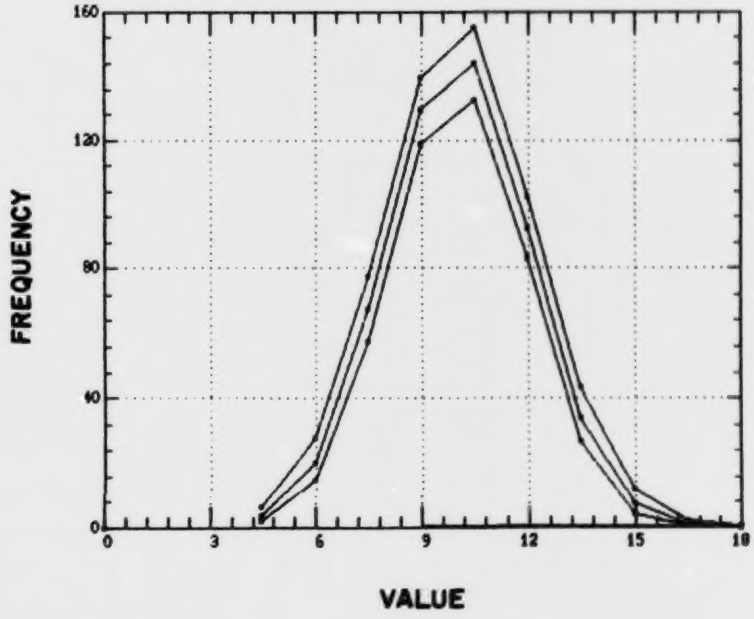

B) PROBABILITY DISTRIBUTION FUNCTION

FIGURE 4.5

PLOTS OF 95% CONFIDENCE BANDS
FOR A LOG-TRANSFORMED LOGNORMAL DISTRIBUTION
(500 TRIALS)

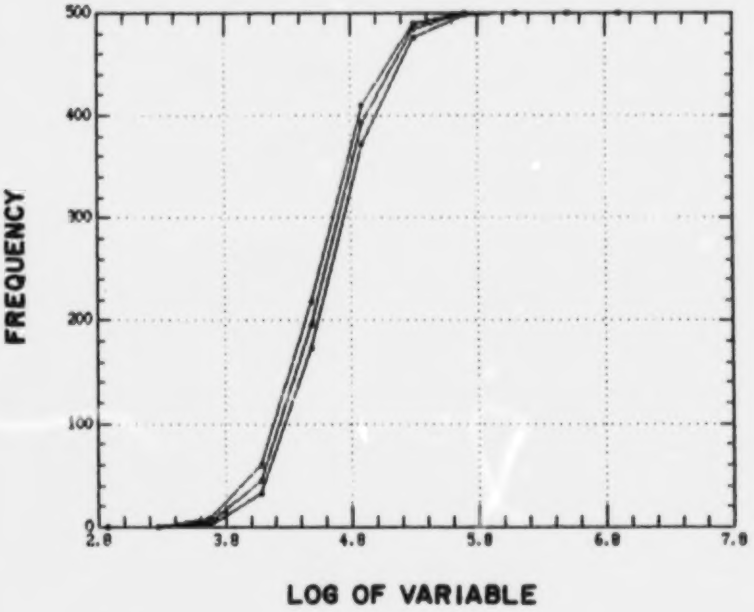

A) CUMULATIVE DISTRIBUTION FUNCTION

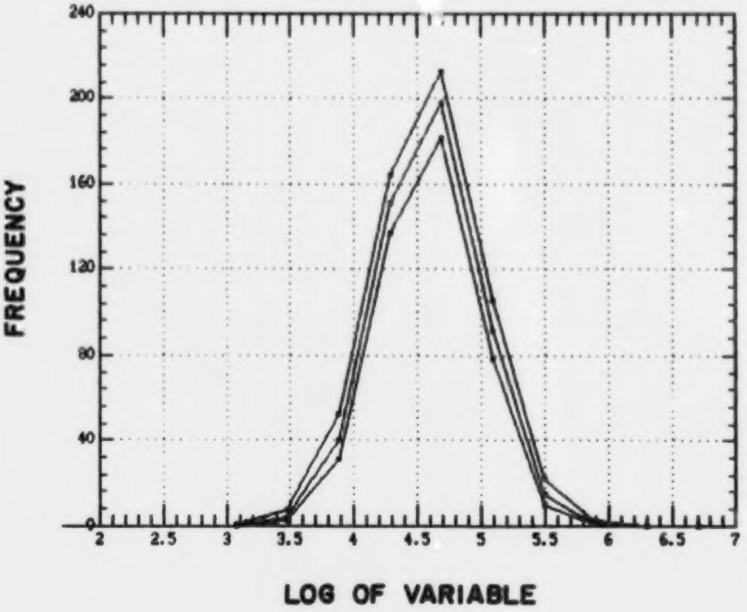

B) PROBABILITY DENSITY FUNCTION

FIGURE 4.6

PLOTS OF 95% CONFIDENCE BANDS
FOR THE LOGARITHM OF RADIUM IN FISH
AT 100 YEARS (200 TRIALS)

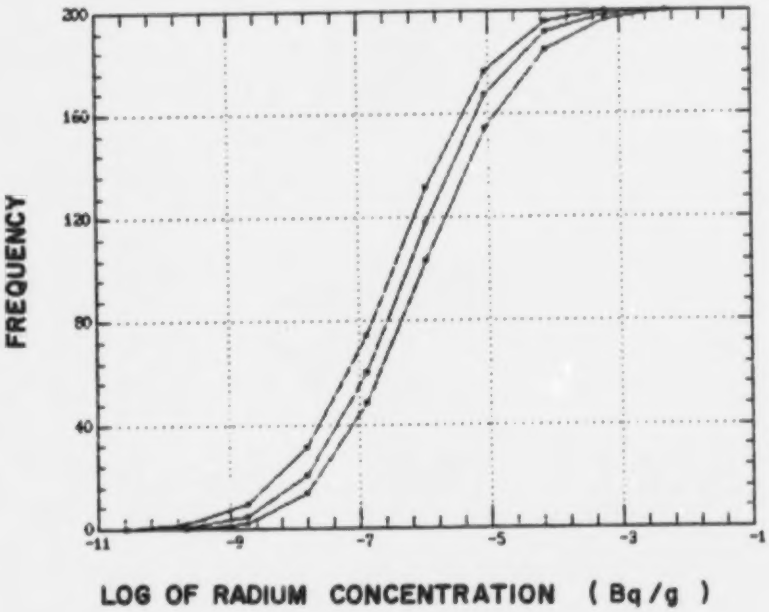

A) CUMULATIVE DISTRIBUTION FUNCTION

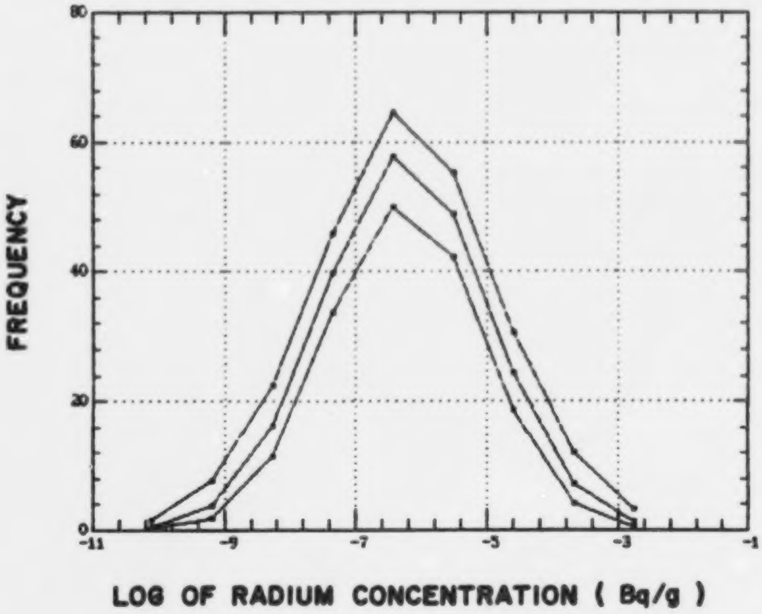

B) PROBABILITY DENSITY FUNCTION

## REFERENCES

Andres, T., and Goodwin, B., 1985. "Techniques for Handling Correlated Parameters."

Fishman, G.S., 1978. "Principles of Discrete Event Simulation, Wiley, N.Y."

Fishman, G.S., and Moore, L.R., 1980. "A Statistical Evaluation of Multiplicative Congruential Generators with Modulus $2^{31}$-1." Technical Report, 78-11, University of North Carolina at Chapel Hill.

Kleijnen, J.P.C., 1974. "Statistical Techniques in Simulation - Part 1." Marcel Dekker Inc., New York.

Marse, K., and Roberts, S.D., 1983 "Implementing a Portable FORTRAN Uniform (0, 1) Generator, Simulation."

Schrage, L., 1979. "A More Portable FORTRAN Random Number Generator ACM Transactions on Mathematical Software 5."

Spicer, C.C., 1972. "Algorithm AS52: Calculation of Power Sums of Deviations about the Mean." Applied Statistics 21, pp. 226-227.

Sturges, H.A., 1926. "The Choice of a Class Interval." Journal of the American Statistical Association. March.

## APPENDIX A

# THE SOFTWARE DEVELOPMENT AND QUALITY ASSURANCE PROGRAM

## ABSTRACT

This appendix outlines the software development and quality assurance (QA) programs employed in this study. Software development and QA both have as their underlying objectives the production of a high quality computer program. Hence, the two are inextricably linked. Several steps in the software development process are described briefly in this appendix. Further attention is given to describing the multi-faceted test program undertaken during software development. The many tests performed on the random simulation tool, the (simulation) component models and the overall system are described.

# The Software Development and Quality Assurance Program

## A.1 INTRODUCTION

Software quality assurance (QA) is inherent in any good software development program. In this appendix, we summarize some relevant concepts regarding both software development and quality assurance. We then go on to indicate the approach to both taken by SENES in this study. Thus, this appendix acts as a summary of all the quality assurance measures taken throughout the development of the Uranium Tailings Assessment Program (UTAP).

As will be described in subsequent sections, software QA has involved a number of different activities. Considerable effort was initially directed at adequately defining objectives and specifications for the overall program. Subsequent efforts focussed on specifying the details of the components which comprise UTAP. A constant QA feedback process was maintained while the components were developed and implemented. The QA efforts then focussed on testing the various components and finally testing the integrated system.

In addition to the mainstream software development/QA activities, several ancillary QA studies were undertaken. One such study involved detailed investigation of the random number generator (UNIRAN). These tests are documented completely in Appendix C. Another study involved comparing the probabilistic results generated by SENES with those generated by two other systems, for a common example. This study is documented in Appendix D. Both of these studies indicated that the probabilistic components of UTAP are fundamentally sound and function as expected.

## A.2 SOME BASIC CONCEPTS AND DEFINITIONS

A conceptual model of the software development/QA process is shown in Figure A.1 (Myers, 1976). This model does not attempt to rigidly define stages that should occur in program development, but merely reflects the common top-down programming structure (i.e. general to specific). The significant features of this model are the various translations that occur (development activities in Figure A.1). These translations represent a communication process between the ultimate user and the software developer. Thus, software errors, representing communication breakdowns, mistakes and/or noise can arise during any one of these activities. A good QA strategy will attempt to avoid and detect faults during all of these processes.

Top-down design is a very important concept, and is further described by Chandler (1986):

> **"Top-down design takes a problem and breaks it into a number of smaller problems. This process is continued until all the design problems are identified. Each design iteration produces a set of software modules based on the breakdown of the modules at the next higher level. During coding, lower level modules are defined to produce a null service but allow the higher level module to be coded and tested at the unit level."**

The fundamental goal of any software development program is the production of a high quality computer program. A quality assurance program possesses this same goal, hence the terms "software development program" and "quality assurance program" are used interchangeably. A high quality computer program is simply defined as one that performs it's intended function. A software development or QA program is defined as a systematic pattern of activities with the goal of producing a product that conforms to established criteria. These "established criteria" are an explicit statement of the product's intended function. The formulation of these criteria is discussed in the next section.

## A.3 REQUIREMENTS, OBJECTIVES AND SPECIFICATIONS

The first step in any software development program is the establishment of quality criteria. All subsequent tasks are designed to produce a model that satisfies these criteria. The generation of quality criteria is a critical phase in the software development process since failure to specify what is

FIGURE A.1

MACRO MODEL
OF SOFTWARE DEVELOPMENT

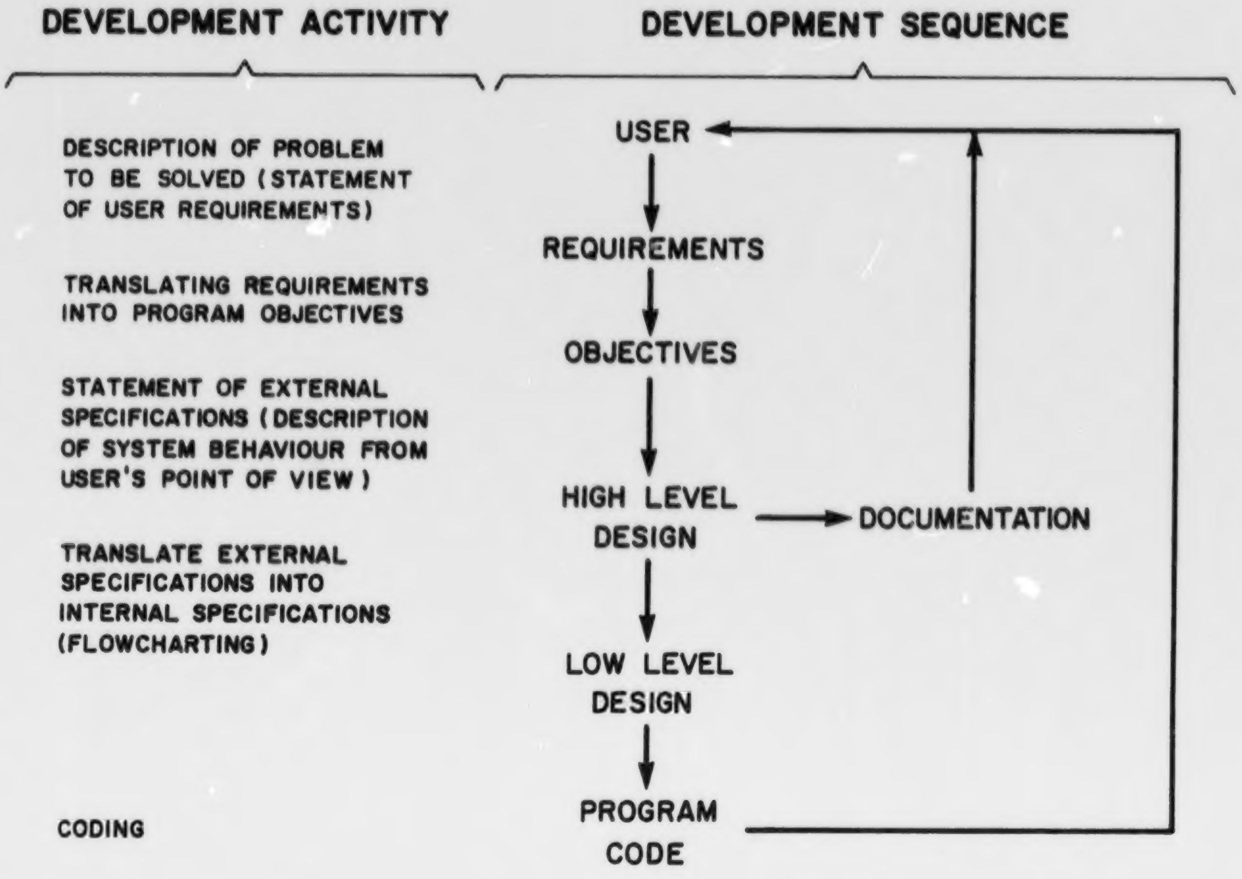
DEVELOPMENT ACTIVITY
DEVELOPMENT SEQUENCE
DESCRIPTION OF PROBLEM TO BE SOLVED (STATEMENT OF USER REQUIREMENTS)
TRANSLATING REQUIREMENTS INTO PROGRAM OBJECTIVES
STATEMENT OF EXTERNAL SPECIFICATIONS (DESCRIPTION OF SYSTEM BEHAVIOUR FROM USER'S POINT OF VIEW)
TRANSLATE EXTERNAL SPECIFICATIONS INTO INTERNAL SPECIFICATIONS (FLOWCHARTING)
CODING
USER
REQUIREMENTS
OBJECTIVES
HIGH LEVEL DESIGN
DOCUMENTATION
LOW LEVEL DESIGN
PROGRAM CODE

SOURCE: AFTER MYERS, 1976

wanted inevitably results in failure to produce what is wanted. The process involves three stages. Firstly, a set of user requirements must be formulated. Secondly, these requirements must be synthesized into a set of program objectives. Finally, these objectives must be translated into a set of specifications referred to as external specifications on Figure A.1.

For the three-step procedure to be effective the user and developer must interact in a feedback review process. The final product of this process is a formalized written document detailing the objectives and specifications for the program. In the Phase III software development process, a formalized set of Objectives and Specifications were submitted to the client for review. Subsequently, with the clients comments incorporated, these objectives and specifications served to direct the software development process. These objectives and specifications are presented in two places in this report. Those relevant to the probabilistic "control modules" are documented in Chapter 2 of this volume while those pertaining primarily to the simulation or "component modes" are presented in Chapter 2 of Volume 3. All of the objectives are summarized in Chapter 1 of Volume 1.

## A.4 INTERNAL DESIGN, REVIEW AND CODING

Once the objectives and specifications have been formalized the process of internal design commences. As an initial step, the internal structure of the model is decomposed into several modules. The logical order of the modules and the interrelationship between the modules is then established. Only after the internal structure of the model has been developed does detailed work commence on the modules.

UTAP is comprised of two basic types of modules. The computer implementation of the mathematical models used to simulate uranium mill tailings are referred to as component modules, while those which provide the probabilistic framework for the simulation are referred to as control modules.

In the case of the component modules, the mathematicl model details, including the species to be modelled, spatial, temporal and other considerations were translated into a series of mathematical formulae and accompanying assumptions. These formulae were often then incorporated into a flowsheet illustrating the algorithm required for implementation.

In the case of control modules, an iterative flowcharting and design process was undertaken until the input/output characteristics indicated in the objectives and specifications were achieved. The control module design, review and coding preceded most of the component model coding. This allowed component models to be coded and tested within the system model context.

## A.5 DOCUMENTATION

Effective documentation is a critical feature of a software development program. Documentation must be done in parallel with model development. This allows assessment of the mathematical models to be used in the simulation, facilitates communication between team members, allows documentation to evolve through a critical review process and provides a record of the software development history. Documentation starts at the requirements/objectives/specifications stage discussed earlier and evolves towards a complete description of the mathematical algorithms, assumptions, techniques and theories used in the program. Use of flowcharts facilitates readability and enhances the iterative review/revision process. The documentation of the component models is presented in Volume III, while the control modules are documented in Chapter 3 of this volume.

## A.6 THE TEST PROGRAM

Once the models are developed and coded, a test program must be instituted. This program must test the models for both computational accuracy and reasonableness. The test program can be divided into three major areas:

1) The Random Simulation Tool
2) The Component Models
3) The System Model

These three test phases are discussed below with references to the Phase III program.

### A.6.1 The Random Simulation Tool

The major objective of the random simulation tool is to randomly sample values from a variety of user-specified probability distributions. The heart of this tool is the random number generator. This module, taken from an extensively tested random number generator (Marse and Roberts, 1983), was subjected to a further battery of tests to check for portability, uniformity, autocorrelation (the lack of), distribution shape and randomness. These tests, detailed in Appendic C, demonstrated that the random number generator conforms to objective statistical criteria.

The ultimate test of the sampling routines is their ability to reproduce the characteristics of the specified distributions. To evaluate this ability, frequency histograms were plotted for all sampling routines and these data were subjected to chi square tests for distribution fit. The histograms and chi square tests are detailed in Section 3.3. The results of these tests demonstrated that the sampling routines are statistically robust.

Many of the sampling and statistics features of the program were taken directly from the RANSIM program developed during the PHASE II study. As a less quantitative, but nevertheless interesting QA exercise, RANSIM was compared with two other probabilistic analysis (i.e. random simulation) tools. The comparison with the SYVAC program, and the DEMOS probabilistic analysis environment is described in detail in Appendix D of this volume. The comparison indicates that RANSIM, and hence many of the sampling and statistics routines used in this study, produce results equivalent to the other two random simulation tools.

### A.6.2 The Component Model Test Program

Since each component module entails different mathemetical formulations, the details of each test program differ. However, component module tests can be divided into three major categories:

1) Hand Calculations
2) Test at Limits
3) Test for Reasonableness

The three types of tests are discussed below.

#### Hand Calculations

A series of hand calculations were done (usually on a detailed printout of the component module output) to check that the model was computing the mathemetical formulae correctly. All component modules were developed with a "detailed printout" option which facilitated these tests. As part of these tests, the code was checked to ensure that it accurately reflected the model algorithm(s).

#### Test at Limits

Most mathematical models have limits at which they can be tested. Often these limits involve time or space. For example in the groundshine model the complex double integration for flux shown in equation 7.1 of Section 7.0 of Volume 3 reduces to the very simple formulation at infinite depth:

$$\phi = \frac{A}{2\mu}$$

where

$\phi$ = gamma flux at receptor (gamma rays.$m^{-2}.s^{-1}$)
A = gamma ray source strength (gamma rays.$m^{-3}.s^{-1}$)
$\mu$ = linear attenuation coefficient ($m^{-1}$)

Infinite depth is effectively about 1m, hence, the groundshine models complex series integration for flux was easily checked.

Another example of a limits test is a steady state test. For example, in the case of the soil model, at steady state the complex solution for soil radionuclide activity in equation (6.7) of Section 6 of Volume 3 reduces to:

$$z(t) = \frac{\beta_0}{\beta_1 + \lambda}$$

where

$z(t)$ = activity (Bq)
$\beta_0$ = input term ($Bq.yr^{-1}$)
$\beta_1$ = soil uptake term ($yr^{-1}$)
$\lambda$ = radioactive decay constant ($yr^{-1}$)

The soil model was checked for approach to and non-exceedence of this limit.

Tests for Reasonableness

Component modules were also examined for "reasonableness". These tests were often qualitative in nature and involved asking the question "Does the model output agree with what I know about the system?" For example, in the case of the erosion model, in a 500 year simulation, the average depletion in depth of the tailings pile was 2 cm. This is a reasonable number, neither too small nor too large.

A more quantitative test for reasonableness is to perform a mass balance. For example, in the case of the soil model, the input of radioactivity to the soil was compared to the soil accumulation, runoff and decay of radioactivity. The input vs. accumulation/output terms matched.

In some instances the predictions of component models were compared to results generated using other models, or to results available from observation of "reasonably" comparable situations. These comparisons were generally qualitative, and served to indicate that the model results were indeed "reasonable."

### A.6.3 The System Model Test Program

The system model test program was designed to test the entire program following integration of the control and component modules. The mathematical stability, accuracy, and reasonableness of the model was tested as well as the input/output capabilities. This is achieved by an extensive series of in-house tests. As well, a "beta test" version of the program was sent to the client to allow the input/output capabilities and the adequacy of the user's manual to be tested.

The first step in the system test program involved examining the detailed results of each component module, generated by the integrated system. The system programmer would provide the detailed results of a test run to the component module developer and other parties involved in the test program. The test run results were reviewed for any erroneous or unexpected results. Any such conditions were noted on the hard copy and pointed out to the system programmer. The cause of each error was subsequently determined and corrected. The procedure was repeated until all parties were satisfied that the component module was performing properly and that all possible errors had been eliminated.

Records of all transactions between the system programmer and the component module developers were retained in organized files for easy reference. The test program involved seven basic tests which were applied in a progressive building block fashion. The tests are described below.

#### Test 1

Detailed output results from one deterministic run using nominal parameter inputs were provided to the model developers for each component module.

Time-variant parameters were set at their nominal values in this test. The source code, input files and a printout of the variable dictionary for the component module were also supplied to the model developers. A simulation length of 100 years with a time step of 10 years was used. The objectives of this test were to perform a detailed check of the computational accuracy of the component modules, verify proper information transfer between modules, evaluate the effects of stepping through time, and check on the reasonableness of nominal results. Changes to the model structure or input parameter values were recorded by the reviewers and reported to the system programmer. The module was then corrected and rerun. The review process was repeated until no further errors or changes were found.

### Test 2

The objective in Test 2 was quite simply to ensure that the code would produce exactly the same output results for two successive trials with the same input parameter values. The test was designed to verify that the code was "resetting" the input values properly for each trial and to confirm the computational accuracy of the modules. The test involved two trials of 100 year duration with a ten year time-step and the same deterministic nominal value data set as in Test 1. The test results were trivial to examine, since identical results, as expected, were generated for each of the two trials.

### Test 3

Test 3 involved two probabilistic trials of 100 year duration with a ten year time-step. The purpose of this test was to verify that the probabilistic trials were performed properly. That is, a detailed parameter printout was checked to ensure that parameters were reset properly on the second trial, that new probabilistic inputs were generated and that the results were reasonable. Time-variant parameters were sampled each time step in this test.

**Test 4**

In this test, ten probabilistic trials were run for a 500 year simulation length using ten year time-steps. The output capabilities of the control modules were used in Test 4 to obtain summary statistics on the time behavior of the pathways and the radionuclide or chemical species. The output results, primarily the mean values of the 10 trials, were again checked for reasonableness. The control module output capabilities were also examined at this stage.

**Test 5**

The time frame of the simulations was extended in test 5 to determine whether or not any of the models become unstable. Ten probabilistic trials were performed for a 1000 year simulation length using ten year time-steps. Again, the output capability of the control modules were used to obtain summary statistics on the time behaviour of pathways and radionuclides or chemical species of interest. The output results were checked for reasonableness as before.

**Test 6**

At this point, the Sensitivity Index Program was run to identify those combinations of input parameter values that produce the highest possible total dose and the lowest possible total dose. The models were then run using these combinations of input values. This test is primarily designed to test the mathematical stability of the models when run at their limits.

**Test 7**

The purpose of Test 7 was to check for model stability in a large number of runs using a new random number seed for each run. The test was repeated numerous times with each run comprising 1000 probabilistic trials of 500 year duration using ten year time-steps. The random number seed for each trial was printed to an output file. If the system model was found to "break down" on a particular run, the "current random number seed" was used to reproduce the run. The cause of the problem was then isolated and corrected.

## Table B.1

## Variable Dictionary for Control Modules

| Variable | Type | Description | Units | Values |
|---|---|---|---|---|
| A | R | LOCATION PARAMETER FOR WEIBULL DISTRIBUTION | | INPUT - WEIBUL |
| ACARC | R (4) | CARIBOU CONCENTRATION FROM VEGETATION CONSUMPTION | BQ/G | CALCULATED - ANIMAL |
| AIRC | R (5,82) | AIR CONCENTRATION | BQ/M**3 | CALCULATED - AIRDIS |
| AMOC | R (4) | MOOSE CONCENTRATION FROM VEGETATION | BQ/G | CALCULATED - ANIMAL |
| AQVEGC | R (4) | CONCENTRATION IN AQUATIC VEGETATION | BQ/G | CALCULATED - WATVEG |
| ARB | I | NUMBER OF REGULAR AND ARBITRARY DISTRIBUTIONS | | CALCULATED - INPUT1 |
| AVEGC | R (4,80) | ABOVE GROUND VEGETABLES CONCENTRATION | BQ/G | CALCULATED - VEGCON |
| B | R | SCALE PARAMETER FOR WEIBULL DISTRIBUTION | | INPUT - WEIBUL |
| BLANK1 | R (4,80) | UNUSED VARIABLE FOR FUTURE OUTPUT | | |
| BLANK2 | R (10,10) | UNUSED VARIABLE FOR FUTURE OUTPUT | | |
| BRWSC | R (4) | AVERAGE WATERSHED BROWSE CONCENTRATION | BQ/G | CALCULATED - VEGCON |
| BVEGC | R (4,80) | BELOW GROUND VEGETABLES CONCENTRATION | BQ/G | CALCULATED - VEGCON |
| C | R | SHAPE PARAMETER FOR WEIBULL DISTRIBUTION | | INPUT - WEIBUL |
| CCOEFF | R | CORRELATION COEFFICIENT FOR CORRELATED DISTRIBUTION | | INPUT - CORREL |
| CONC | R (10,4,3) | TAILINGS SOLID PHASE CONCENTRATION | (BQ OR MOL)/M**3 | CALCULATED - SEXEC |
| CORNAM | C*6 | CORRELATED PARAMETER INDEPENDANT VARIABLE NAME | | INPUT |
| CORNUM | I (200) | CORRELATED PARAMETER INDEPENDENT PARAMETER REFERENCE NUMBER | | CALCULATED - INPUT1 |
| CPF | R (200,25) | BETA AND ARBITRARY CUMULATIVE DISTRIBUTION FUNCTION | | CALCULATED - CREATE |
| DOSE | R (80) | TOTAL INDIVIDUAL DOSE | uSV/YEAR | CALCULATED - DOSEIN |
| DT | R | TIME INCREMENT | YEARS | CALCULATED - INPUT1 |
| DTAIL | R | CUMULATIVE EROSION OF TAILINGS PILE | M | CALCULATED - EROS |
| EFLAG | C*1 (200) | FLAG INDICATING IF SAMPLED VALUES ARE TO BE SAVED | | INPUT - S/F/N =>STATS/FILE/NO |
| EMRATE | R (5) | EMISSION RATE FROM TAILINGS | BQ/S | CALCULATED - DUST, RADON |
| EROTOT | R | EROSION OF TAILINGS PILE OVER TIME STEP | KG | CALCULATED - EROS |
| EXPECT | R | EXPECTED VALUE OF NORMAL DISTRIBUTION | | INPUT - NORMAL |
| FISHC | R (4,10) | CONCENTRATION OF RADIONUCLIDE IN FISH | BQ/G | CALCULATED - FISH |
| FISHD | R (5,80) | DOSE FROM FISH CONSUMPTION | uSV/YEAR | CALCULATED - DOSEIN |
| FLAG | C*1 (300) | OUTPUT PARAMETER FLAG | | INPUT - S/F =>STATS/FILE |
| FNAME | C*12 | FILE NAME | | INPUT |
| FSAVE | C*1 | DETAILED RESULTS FILE INDICATOR | | INPUT - Y/N =>YES/NO |
| FUNIT | I | INPUT FILE UNIT NUMBER | | 4 |
| FUNIT1 | I | DETAILED RESULTS FILE UNIT NUMBER | | 1 |
| FUNIT2 | I | KEY TO RESULTS FILE UNIT NUMBER | | 2 |
| FUNIT3 | I | SUMMARY STATISTICS FILE UNIT NUMBER | | 3 |
| FWIND | R(16,6,6,20) | A.E.S. STAR DATA | KNOTS | INPUT |

Table B.1 (continued)

| Variable | Type | Description | Units | Values |
|---|---|---|---|---|
| GM | R | GEOMETRIC MEAN OF LOGNORMAL DISTRIBUTION | | INPUT - LNORM |
| GMEAN | DP (600) | GEOMETRIC MEAN | | CALCULATED - STATS |
| GN | I (600) | COUNTER USED FOR CALCULATING GEOMETRIC MOMENTS | | CALCULATED - GMOMEN |
| GS1 | DP (600) | VECTOR FOR UPDATING FIRST GEOMETRIC MOMENT | | CALCULATED - GMOMEN |
| GS2 | DP (600) | VECTOR FOR UPDATING SECOND GEOMETRIC MOMENT | | CALCULATED - GMOMEN |
| GSD | DP (600) | NATURAL LOGARITHM OF GEOMETRIC STANDARD DEVIATION | | CALCULATED - STATS |
| GSD | R | GEOMETRIC STANDARD DEVIATION OF LOGNORMAL DISTRIBUTION | | INPUT - LNORM |
| GSDEV | DP (600) | GEOMETRIC STANDARD DEVIATION | | CALCULATED - STATS |
| GSEG | I | WATERSHED SEGMENT NUMBER THAT GROUNDWATER FLOWS INTO | | INPUT |
| GWATC | R (4) | GROUNDWATER CONCENTRATION | BQ/M**3 | CALCULATED - GWATER |
| IERR | I | ERROR CODE FROM OPENING DISK FILES | | CALCULATED - INPUT1, INPUT2 |
| INHD | R (5,80) | DOSE FROM INHALATION | uSV/YEAR | CALCULATED |
| KURT | DP (600) | KURTOSIS | | CALCULATED - STATS |
| LAKVOL | R (10) | LAKE VOLUMES | M**3 | CALCULATED - INPUT2 |
| LAREA | R (10) | LAKE AREAS OR RIVER LENGTHS AS APPROPRIATE | M**2 OR M | INPUT |
| LGM | R | LOGARITHM OF GEOMETRIC MEAN OF LOGNORMAL DISTRIBUTION | | CALCULATED - LNORM |
| LGSD | R | LOG OF GEOMETRIC STANDARD DEVIATION OF LOGNORMAL DIST'N | | CALCULATED - LNORM |
| LICHC | R (4) | AVERAGE LICHEN CONCENTRATION | BQ/G | CALCULATED - VEGCON |
| LMAX | R | MAXIMUM VALUE OF LOGUNIFORM DISTRIBUTION | | INPUT - LOGUNI |
| LMIN | R | MINIMUM VALUE OF LOGUNIFORM DISTRIBUTION | | INPUT - LOGUNI |
| LOC | I (300) | OUTPUT PARAMETER LOCATION CODES | | INPUT |
| MAX | R | MAX. VALUE OF NORMAL, LOGNORMAL, BETA, & ARBITRARY DIST'NS | | INPUT - CREATE,NORMAL,LNORM |
| MAXSEG | I | MAXIMUM RECEPTOR WATER SOURCE SEGMENT NUMBER | | CALCULATED - INPUT2 |
| MEANX | R | MEAN OF INDEPENDENT VARIABLE FOR CORRELATED DISTRIBUTION | | INPUT - CORREL |
| MEANY | R | MEAN OF DEPENDENT VARIABLE FOR CORRELATED DISTRIBUTION | | INPUT - CORREL |
| MEATD | R (5,80) | DOSE FROM MEAT CONSUMPTION | uSV/YEAR | CALCULATED - DOSEIN |
| MIN | R | MIN. VALUE OF NORMAL, LOGNORMAL, BETA, & ARBITRARY DIST'NS | | INPUT - CREATE,NORMAL,LNORM |
| N | I (600) | COUNTER USED FOR CALCULATING STATISTICAL MOMENTS | | CALCULATED - MOMENT |
| NACELL | I (200) | NUMBER OF CELLS IN ARBITRARY DISTRIBUTIONS | | INPUT - MAXIMUM 25 |
| NAMEF | C*36 (300) | LABELS FOR OUTPUTS TO DETAILED RESULTS FILE | | INPUT - NAMOUT |
| NAMES | C*36 (300) | LABELS FOR OUTPUTS TO STATISTICS FILE | | INPUT - NAMOUT |
| NARB | I | NUMBER OF ARBITRARY DISTRIBUTIONS | | INPUT |
| NARRAY | I | NUMBER OF ARRAYS TO BE CHECKED FOR POSSIBLE OUTPUT | | INPUT |
| NBETA | I | NUMBER OF BETA DISTRIBUTIONS | | CALCULATED - INPUT1 |
| NCELLS | I | NUMBER OF CELLS IN BETA DISTRIBUTIONS | | INPUT - MAXIMUM 25 |
| NCORR | I | NUMBER OF CORRELATED PARAMETERS | | INPUT |
| NDT | I | TIME INCREMENT | YEARS | INPUT |
| NFILE | I | NO. OF NON-TIME-VARIANT DISTRIBUTIONS FOR DETAILED RESULTS | | CALCULATED - INPUT1 |

Table B.1 (continued)

| Variable | Type | Description | Units | Values |
|---|---|---|---|---|
| NODDIR | I (10) | WATERSHED SEGMENT END NODE DIRECTIONS | | INPUT |
| NODRNG | I (10) | WATERSHED SEGMENT END NODE RINGS | | INPUT |
| NOUT | I | TOTAL NUMBER OF OUTPUT PARAMETERS | | CALCULATED - STATS |
| NOUTF | I | NUMBER OF PARAMETERS TO BE OUTPUT TO DETAILED RESULTS FILE | | CALCULATED - STATS |
| NOUTS | I | NUMBER OF PARAMETERS TO BE SAVED TO STATISTICS FILE | | CALCULATED - STATS |
| NPARM | I | NUMBER OF INPUT DISTRIBUTIONS | | INPUT - MAXIMUM 200 |
| NRECEP | I | NUMBER OF RECEPTOR LOCATIONS | | INPUT - MAXIMUM 80 |
| NRING | I | NUMBER OF RINGS | | INPUT - MAXIMUM 5 |
| NSEG | I | NUMBER OF WATERSHED SEGMENTS | | INPUT - MAXIMUM 10 |
| NSTART | I | RANDOM NUMBER SEED | | INPUT/CALCULATED - RANDOM |
| NSTAT | I | NUMBER OF NON-TIME-VARIANT DISTRIBUTIONS FOR STATISTICS FILE | | CALCULATED - INPUT1 |
| NSTEPF | I | NUMBER OF TIME STEPS TO BE SAVED TO DETAILED RESULTS FILE | | INPUT - MAXIMUM 11 |
| NSTEPS | I | NUMBER OF TIME STEPS TO BE SAVED TO STATISTICS FILE | | INPUT - MAXIMUM 11 |
| NSUB | I (300) | OUTPUT PARAMETER SUBSTANCE CODES | | INPUT |
| NT | I | CURRENT SIMULATION TIME | YEARS | CALCULATED - EXEC |
| NTRIAL | I | TOTAL NUMBER OF TRIALS TO BE PERFORMED | | INPUT |
| NTYPE | I (200) | DISTRIBUTION TYPE NUMBERS | | INPUT |
| NUMF | I | COUNTER FOR VARIABLES TO BE SAVED TO DETAILED RESULTS FILE | | CALCULATED - TIMSEL α SELECT |
| NUMS | I | COUNTER FOR VARIABLES TO BE SAVED TO STATISTICS FILE | | CALCULATED - TIMSEL α SELECT |
| NUMTRL | I | CURRENT TRIAL COUNT | | CALCULATED - EXEC |
| NVAR | I (200) | NUMBER OF OUTPUTS FOR EACH VARIABLE | | INPUT |
| NVARYF | I | NUMBER OF OUTPUT VARIABLES TO BE SAVED FOR DETAILED RESULTS | | CALCULATED - INPUT2 |
| NVARYS | I | NUMBER OF OUTPUT VARIABLES TO BE SAVED TO STATISTICS FILE | | CALCULATED - INPUT2 |
| NYEARS | I | TOTAL TIME IN SIMULATION | YEARS | INPUT |
| OLDDIR | I | DIRECTION OF LAST WATERSHED SEGMENT READ IN | | CALCULATED - INPUT2 |
| OLDRNG | I | RING NUMBER OF LAST WATERSHED SEGMENT READ IN | | CALCULATED - INPUT2 |
| ORIGIN | R (200) | LOWER END OF FIRST CELL OF BETA AND ARBITRARY DISTRIBUTIONS | | CALCULATED - CREATE |
| P1 | R (200) | INPUT DISTRIBUTION DESCRIPTORS | | INPUT |
| P2 | R (200) | INPUT DISTRIBUTION DESCRIPTORS | | INPUT |
| P3 | R (200) | INPUT DISTRIBUTION DESCRIPTORS | | INPUT |
| P4 | R (200) | INPUT DISTRIBUTION DESCRIPTORS | | INPUT |
| P5 | R (200) | INPUT DISTRIBUTION DESCRIPTORS | | INPUT |
| PH | R (4) | TAILINGS PH | | CALCULATED - SEXEC |
| PI | R | THE VALUE PI | | INPUT |
| POPDT | R | TOTAL DOSE FOR ENTIRE STUDY POPULATION | uSV/YEAR | CALCULATED - DOSEIN |

Table B.1 (continued)

| Variable | Type | Description | Units | Values |
|---|---|---|---|---|
| PSAREA | R | AREA OCCUPIED BY WATERSHED SECTORS | M**2 | CALCULATED - INPUT2 |
| PSDIR | I (10) | DIRECTIONS BY WATERSHED SECTORS | | INPUT |
| PSNUM | I | NUMBER OF SECTORS WATERSHED OCCUPIES | | CALCULATED - INPUT2 |
| PSRING | I (10) | RINGS BY WATERSHED SECTORS | | INPUT |
| R | R (6) | RING LIMITS | M | INPUT |
| R | R | RANDOM NUMBER RETURNED BY FUNCTION SUBROUTINE RANDOM | | CALCULATED |
| RADD | R (80) | DOSE FROM RADON | uSV/YEAR | CALCULATED - DOSEIN |
| RAREA | R (5) | SECTOR AREAS BY RING | M**2 | CALCULATED - INPUT2 |
| RDIR | I (80) | RECEPTOR DIRECTIONS | | INPUT - MAXIMUM 16 |
| REG | I | NUMBER OF REGULAR DISTRIBUTIONS | | CALCULATED - INPUT1 |
| RNGMID | R (5) | RADIAL DISTANCES TO MIDPOINTS OF RINGS | M | CALCULATED - INPUT2 |
| RPOP | I (80) | RECEPTOR POPULATION | | INPUT |
| RRING | I (80) | RECEPTOR RING NUMBERS | | INPUT |
| RTYPE | C*1 (80) | RECEPTOR TYPE | | INPUT - C/A =>CRITICAL/AVERAGE |
| RWSSEG | I (80) | RECEPTOR WATER SOURCE SEGMENT NUMBERS | | INPUT |
| RYEARS | R | TOTAL TIME IN SIMULATION | YEARS | CALCULATED - INPUT1 |
| S1 | DP (600) | MEAN VALUES | | CALCULATED - MOMENT |
| S2 | DP (600) | SECOND MOMENT FOR UPDATING STATISTICS | | CALCULATED - MOMENT |
| S3 | DP (600) | THIRD MOMENT FOR UPDATING STATISTICS | | CALCULATED - MOMENT |
| S4 | DP (600) | FOURTH MOMENT FOR UPDATING STATISTICS | | CALCULATED - MOMENT |
| SCRUNT | I | SCREEN UNIT NUMBER | | |
| SDEPTH | R (10) | WATERSHED SEGMENT DEPTHS | M | INPUT |
| SDEV | DP (600) | STANDARD DEVIATION | | CALCULATED - STATS |
| SDEVX | R | STANDARD DEVIATION OF CORRELATED DIST'N INDEPENDENT VARIABLE | | INPUT - CORREL |
| SDEVY | R | STANDARD DEVIATION OF CORRELATED DIST'N DEPENDENT VARIABLE | | INPUT - CORREL |
| SHEDAR | R (10) | CUMMULATIVE WATERSHED AREAS | M**2 | INPUT |
| SHINED | R (5,80) | DOSE FROM GROUNDSHINE | uSV/YEAR | CALCULATED - DOSEIN |
| SKEW | DP (600) | SKEWNESS | | CALCULATED - STATS |
| SOILC | R (4,82) | SOIL CONCENTRATION | BQ/M**3 | CALCULATED - SOIL |
| SSAVE | C*1 | STATISTICS FILE INDICATOR | | INPUT - Y/N =>YES/NO |
| STDEV | R | STANDARD DEVIATION OF NORMAL DISTRIBUTION | | INPUT - NORMAL |
| STYPE | C*1 (10) | WATERSHED SEGMENT TYPE | | INPUT - R/L =>RIVER/LAKE |
| SUFOC | R (4) | SUMMER FOLLIAGE CONCENTRATION | BQ/G | CALCULATED - VEGCON |
| SUM | R | SUM OF CELL VALUES IN BETA & ARBITRARY DISTRIBUTIONS | | CALCULATED - CREATE |
| T | R | CURRENT SIMULATION TIME | YEARS | CALCULATED - EXEC |
| TAREA | R | TOTAL AREA BETWEEN OUTER AND INNER RING LIMITS | M**2 | CALCULATED - INPUT2 |
| TEST | C*1 | TYPE OF LAST WATERSHED SEGMENT | | CALCULATED - INPUT2 => L/R |
| TFILE | I (12) | VECTOR CONTAINING TIME STEPS TO BE SAVED TO DETAILED RESULTS | | INPUT |
| TITLE | C*40 | RUN TITLE | | INPUT |
| TMAX | R | LOGARITHM OF MAXIMUM VALUE OF LOGNORMAL DISTRIBUTION | | CALCULATED - LNORM |

Table B.1 (continued)

| Variable | Type | Description | Units | Values |
|---|---|---|---|---|
| TMIN | R | LOGARITHM OF MINIMUM VALUE OF LOGNORMAL DISTRIBUTION | | CALCULATED - LNORM |
| TNUMBF | I | COUNT OF TIME STEPS SAVED TO DETAILED RESULTS FILE | | CALCULATED - TIMSEL |
| TNUMBS | I | COUNT OF TIME STEPS SAVED TO STATISTICS FILE | | CALCULATED - TIMSEL |
| TNUMF | I | COUNT OF TIME STEPS SAVED TO DETAILED RESULTS FILE | | CALCULATED - SELECT |
| TNUMS | I | COUNT OF TIME STEPS SAVED TO STATISTICS FILE | | CALCULATED - SELECT |
| TSTAT | I (12) | VECTOR OF TIME STEPS TO BE SAVED TO STATISTICS FILE | | INPUT |
| TVARY | C*1 (200) | TIME-VARIANT FLAG | | INPUT - V/N =>VARIANT/NOT |
| UMAX | R | MAXIMUM VALUE OF UNIFORM DISTRIBUTION | | INPUT - UNIFOR |
| UMIN | R | MINIMUM VALUE OF UNIFORM DISTRIBUTION | | INPUT - UNIFOR |
| UNIT | R (200) | BETA AND ARBITRARY DISTRIBUTION UNIT WIDTH | | CALCULATED - CREATE |
| V | R (200,25) | ARBITRARY AND BETA PROBABILITY DISTRIBUTION FUNCTION | | CALCULATED - CREATE |
| VARIED | I (200) | TIME-VARIANT DISTRIBUTION NUMBERS FOR DIRECT ACCESS | | CALCULATED - INPUT1 |
| VARN | I | NUMBER OF NON-TIME-VARIANT DISTRIBUTIONS | | CALCULATED - INPUT1 |
| VARNAM | C*6 (200) | NAMES OF OUTPUT PARAMETERS | | INPUT |
| VARNOT | I (200) | NON-TIME-VARIANT DISTRIBUTION NUMBERS FOR DIRECT ACCESS | | CALCULATED - INPUT1 |
| VARTIT | C*6 (200) | VECTOR OF NAMES OF INPUT PARAMETERS | | INPUT |
| VARY | I | NUMBER OF TIME-VARIANT DISRIBUTIONS | | CALCULATED - INPUT1 |
| VARYF | I | NUMBER OF TIME-VARIANT DISTRIBUTIONS FOR DETAILED RESULTS | | CALCULATED - INPUT1 |
| VARYS | I | NUMBER OF TIME-VARIANT DISTRIBUTIONS FOR STATISTICS FILE | | CALCULATED - INPUT1 |
| VECTOR | C*1 | INDICATOR OF OUTPUT FILE | | CALCULATED - SELECT |
| VEGD | R (5,80) | DOSE FROM VEGETABLE CONSUMPTION | uSV/YEAR | CALCULATED - DOSEIN |
| VMAX | R | MAXIMUM VALUE OF TRIANGULAR DISTRIBUTION | | INPUT - TRIANG |
| VMIN | R | MINIMUM VALUE OF TRIANGULAR DISTRIBUTION | | INPUT - TRIANG |
| VMODE | R | PEAK VALUE OF TRIANGULAR DISTRIBUTION | | INPUT - TRIANG |
| WATAVG | R (4) | AVERAGE WATER CONCENTRATION BY SUBSTANCE | BQ/M**3 | CALCULATED - RIVER α LAKE |
| WATC | R (8,10) | WATER CONCENTRATION | (BQ OR MOL)/M**3 | CALCULATED - LAKE α RIVER |
| WATD | R (5,80) | DOSE FROM DRINKING WATER CONSUMPTION | uSV/YEAR | CALCULATED - DOSEIN |
| WATPH | R (10) | PH IN LAKES AND RIVERS | | CALCULATED - LAKE |
| WCARC | R (4) | CARIBOU CONCENTRATION FROM WATER CONSUMPTION | BQ/G | CALCULATED - ANIMAL |
| WCONC | R (10,4,3) | TAILINGS LIQUID PHASE CONCENTRATION | (BQ OR MOL)/M**3 | CALCULATED - SEXEC |
| WINDFG | C*1 | FLAG INDICATING IF WIND IS TIME-VARIANT | | INPUT - Y/N =>YES/NO |
| WMOC | R (4) | MOOSE CONCENTRATION FROM WATER PATHWAYS | BQ/G | CALCULATED - ANIMAL |
| XDUM | R | VALUE TO BE SAVED FOR OUTPUT | | CALCULATED - SORT |
| XIN | R (200) | RANDOM VALUES SAMPLED FROM DISTRIBUTIONS | | CALCULATED - CHOOSE |
| XMAX | DP (600) | MAXIMUM VALUES FOR STATISTICS | | CALCULATED - STATS |
| XMIN | DP (600) | MINIMUM VALUES FOR STATISTICS | | CALCULATED - STATS |
| XN | DP | NUMBER OF TRIALS STATISTICS CALCULATED ON | | CALCULATED - STATS |
| XOUT | R (600) | VECTOR OF OUTPUT VALUES | | CALCULATED - STATS |
| XOUTF | R (300) | VECTOR OF VALUES FOR OUTPUT TO DETAILED RESULTS FILE | | CALCULATED |
| XOUTS | R (300) | VECTOR OF VALUES FOR SUMMARY STATISTICS | | CALCULATED |
| XVALUE | R (200) | SAMPLED DISTRIBUTION VALUES (SAME AS XIN) USED IN CORREL | | CALCULATED |

## B.2 Code Listing for Control Modules

### B.2.1 Main Program

```
C FILE 'EXEC.FOR'
C
C     EXECUTIVE MODULE CALLS CONTROL MODULES AND COMPONENT
C     MODULES' CONTROL MODULE, STEPPING THROUGH TIME FOR EACH
C     TRIAL
C
      INCLUDE 'IO.INC'
      INCLUDE 'CONC.INC'
      INCLUDE 'RECEP.INC'
      INCLUDE 'STATS.INC'
      INCLUDE 'COUNTS.INC'
      INCLUDE 'INFO.INC'
      INCLUDE 'OUT.INC'
      INCLUDE 'INPT.INC'
      INCLUDE 'UPDATE.INC'
      INCLUDE 'PARAM.INC'
      INCLUDE 'INTERM.INC'
      INCLUDE 'WIND.INC'
C
C     CALL INPUT MODULES
C
      CALL INPUT1
      CALL INPUT2
C
C     CALL SAMPLING MODULES
C
      CALL CREATE
      WRITE(SCRUNT,300)
      DO 10 NUMTRL=1,NTRIAL
C
C        SAMPLE NON-TIME-VARIANT INPUT DISTRIBUTIONS
C
         DO 20 I=1,VARN
            CALL CHOOSE(VARNOT(I))
20       CONTINUE
         NTIME=NYEARS/NDT+1
         DO 30 IYR = 1,NTIME
C
C           SAMPLE TIME-VARIANT DISTRIBUTIONS
C
            IF(VARY.GE.1)THEN
               DO 40 I=1,VARY
                  CALL CHOOSE(VARIED(I))
40             CONTINUE
            ENDIF
            NT=(IYR-1)*NDT
            T=FLOAT(NT)
            WRITE(SCRUNT,100)NUMTRL,NT
C
C           CALL COMPONENT MODULES
```

```
C
              CALL COMEX
C
C             CALL OUTPUT SELECTION ROUTINES
C
              CALL TIMSEL
              CALL SELECT
30         CONTINUE
           CALL SAVEIN
C
C          CALL STATISTICS MODULES
C
           CALL STATS
C
C          CALL OUTPUT MODULES
C
           CALL WRITE
10      CONTINUE
        CALL NAMOUT
        CALL OUTPUT
        WRITE(SCRUNT,300)
        WRITE(SCRUNT,200)
        STOP
100     FORMAT(' TRIAL NUMBER : ',I4,4X,'TIME : ',I5)
200     FORMAT(' RUN COMPLETED')
300     FORMAT(///)
        END
```

### B.2.2 Input Routines

```
C FILE 'INPUT.FOR'
C
      SUBROUTINE INPUT1
C
C      THE FOLLOWING SUBROUTINE INPUTS THE FILE CONTAINING THE
C      PROBABILISTIC PARAMATER DESCRIPTIONS AND ALLOWS THE USER
C      TO SAVE STATISTICS AND OUTPUT FILES
C
      INCLUDE 'IO.INC'
      INCLUDE 'COUNTS.INC'
      INCLUDE 'PARAM.INC'
      CHARACTER*12 FNAME
      CHARACTER*6 CORNAM
      CHARACTER*1 TVARY(250)
      INTEGER*2 REG,ARB,NCORR
      SCRUNT=0
      FUNIT1=1
      FUNIT2=2
      FUNIT3=3
      FUNIT=4
C
C     OPEN FIRST INPUT FILE
C
      WRITE (SCRUNT,1250)
      READ (SCRUNT,1400) FNAME
      WRITE (SCRUNT,1350) FNAME
      OPEN (FUNIT,FILE=FNAME,STATUS='OLD',IOSTAT=IERR)
      IF (IERR.NE.0) CALL ERROR (29)
      READ (FUNIT,1400,END=998) TITLE
C
C     OPEN OUTPUT FILE(S)
C
      READ (FUNIT,1400,END=998) SSAVE
      READ (FUNIT,1400,END=998) FNAME
      IF (SSAVE.EQ.'Y') THEN
         WRITE (SCRUNT,1350) FNAME
         OPEN (FUNIT3,FILE=FNAME,STATUS='NEW',IOSTAT=IERR)
         IF (IERR.NE.0) THEN
            CALL ERROR (102)
            OPEN (FUNIT3,FILE=FNAME)
         ENDIF
      ENDIF
      READ (FUNIT,1400,END=998) FSAVE
      READ (FUNIT,1400,END=998) FNAME
      IF (FSAVE.EQ.'Y') THEN
         WRITE (SCRUNT,1350) FNAME
         OPEN (FUNIT1,FILE=FNAME,STATUS='NEW',IOSTAT=IERR)
         IF (IERR.NE.0) THEN
            CALL ERROR (102)
            OPEN (FUNIT1,FILE=FNAME)
         ENDIF
      ENDIF
      READ (FUNIT,1400,END=998) FNAME
      IF (FSAVE.EQ.'Y') THEN
         WRITE (SCRUNT,1350) FNAME
         OPEN (FUNIT2,FILE=FNAME,STATUS='NEW',IOSTAT=IERR)
         IF (IERR.NE.0) THEN
            CALL ERROR (102)
            OPEN (FUNIT2,FILE=FNAME)
         ENDIF
      ENDIF
C
C     READ COUNTERS AND CHECK TIME
C
      NBETA=0
      READ (FUNIT,1450,END=998) NPARM,NARB,NCORR,NCELLS
      READ (FUNIT,1550,END=998) NSTART,NTRIAL
      READ (FUNIT,1450,END=998) NYEARS,NDT
      IF (NDT.NE.1.AND.NDT.NE.10.AND.NDT.NE.20) CALL ERROR (32)
      RYEARS=FLOAT(NYEARS)
      DT=FLOAT(NDT)
      IF (MOD(RYEARS,DT).NE.0) CALL ERROR (19)
      NSTAT=0
      NFILE=0
      VARY=0
      VARN=0
      VARYS=0
      VARYF=0
      REG=NPARM-(NCORR+NARB)
      ARB=NPARM-NCORR
      DO 1050 I=1,NPARM
         IF (I.LE.REG) THEN
C
C           READ REGULAR DISTRIBUTIONS
C
            READ (FUNIT,1500,END=999) VARTIT(I),EFLAG(I),NTYPE(I),
     &         TVARY(I),P1(I),P2(I),P3(I),P4(I)
            IF (NTYPE(I).EQ.9.OR.NTYPE(I).EQ.10) CALL ERROR (6)
            IF (NTYPE(I).EQ.8) NBETA=NBETA+1
         ELSEIF (I.LE.ARB) THEN
C
C           READ ARBITRARY DISTRIBUTIONS
C
            READ (FUNIT,1610,END=999) VARTIT(I),EFLAG(I),NTYPE(I),
     &         TVARY(I),NACELL(I),P1(I),P2(I),(V(I,I2),I2=1,NACELL(I))
            IF (NTYPE(I).NE.9) CALL ERROR (8)
         ELSE
C
C           READ CORRELATED DISTRIBUTIONS
C
            READ (FUNIT,1600,END=999) VARTIT(I),EFLAG(I),NTYPE(I),
     &         TVARY(I),CORNAM,P1(I),P2(I),P3(I),P4(I),P5(I)
            IF (NTYPE(I).NE.10) CALL ERROR (7)
            K=1
10          IF (VARTIT(K).EQ.CORNAM) THEN
               IF (TVARY(K).NE.'V'.OR.(TVARY(K).EQ.'V'.AND.TVARY(I).EQ.
     &            'V')) THEN
                  CORNUM(I)=K
               ELSE
                  CALL ERROR (18)
               ENDIF
            ELSEIF (K.LT.I) THEN
               K=K+1
               GOTO 10
            ELSE
               CALL ERROR (4)
            ENDIF
         ENDIF
         IF (EFLAG(I).EQ.'B'.OR.EFLAG(I).EQ.'S'.OR.EFLAG(I).EQ.'F') THEN
            IF ((EFLAG(I).EQ.'S'.OR.EFLAG(I).EQ.'B').AND.SSAVE.NE.'Y')
     &         CALL ERROR (12)
            IF ((EFLAG(I).EQ.'F'.OR.EFLAG(I).EQ.'B').AND.FSAVE.NE.'Y')
     &         CALL ERROR (13)
         ENDIF
         IF (TVARY(I).EQ.'V') THEN
            VARY=VARY+1
            VARIED(VARY)=I
            IF (EFLAG(I).EQ.'S'.OR.EFLAG(I).EQ.'B') VARYS=VARYS+1
            IF (EFLAG(I).EQ.'F'.OR.EFLAG(I).EQ.'B') VARYF=VARYF+1
         ELSE
            VARN=VARN+1
            VARNOT(VARN)=I
            IF (EFLAG(I).EQ.'S'.OR.EFLAG(I).EQ.'B') NSTAT=NSTAT+1
            IF (EFLAG(I).EQ.'F'.OR.EFLAG(I).EQ.'B') NFILE=NFILE+1
         ENDIF
1050  CONTINUE
      CLOSE (FUNIT)
      RETURN
998   CALL ERROR (5)
999   CALL ERROR (9)
1250  FORMAT (' FIRST INPUT FILE NAME? ')
1350  FORMAT (' Opening File : ',A12)
1400  FORMAT (A)
1450  FORMAT (4I4)
1500  FORMAT (A6,1X,A1,1X,I2,1X,A1,4E11.6)
1550  FORMAT (I10,I4)
1600  FORMAT (A6,1X,A1,1X,I2,1X,A1,1X,A6,5E11.6)
1610  FORMAT (A6,1X,A1,1X,I2,1X,A1,I3,2E11.6,25(F6.2))
      END
C
C
C
      SUBROUTINE INPUT2
C
C     SUBROUTINE PROMPTS FOR INPUT FILE AND READS INPUT INFORMATION
C     SPECIFIC TO UTAP INCLUDING:
C        - NAME OF AIR DISPERSION DATA FILE
C        - RECEPTOR DATA
C        - WATERSHED DATA
C        - OUTPUT DATA CONTAINING INFO ON OUTPUT VARIABLES,
C          RECEPTOR NUMBERS, TIMES, ETC. OF VARIABLES TO BE SENT TO
C          DETAILED RESULTS AND STATISTICS FILES
C     AIR DISPERSION FILE IS OPENNED AND DATA READ
```

```
C
      INCLUDE 'IO.INC'
      INCLUDE 'RECEP.INC'
      INCLUDE 'COUNTS.INC'
      INCLUDE 'INFO.INC'
      INCLUDE 'WIND.INC'
      INTEGER*2 OLDDIR,OLDRNG,MAXSEG,RCPNUM
      INTEGER*4 R(6)
      CHARACTER*1 TEST
      CHARACTER*12 FNAME
      REAL*4 PI
      DATA PI /3.1415927/
C
C     OPEN SECOND INPUT FILE
C
      WRITE (SCRUNT,700)
      READ (SCRUNT,810) FNAME
      WRITE (SCRUNT,820) FNAME
      OPEN (FUNIT,FILE=FNAME,STATUS='OLD',IOSTAT=IERR)
      IF (IERR.NE.0) CALL ERROR(29)
C
C     READ FLAG FOR TIME VARIANCE OF STAR DATA AND FILE NAME
C
      READ (FUNIT,960,END=999) WINDFG
      READ (FUNIT,810,END=999) FNAME
C
C     READ RECEPTOR INFORMATION
C
      READ (FUNIT,730,END=999) NRECEP
      IF (NRECEP.GT.80) CALL ERROR (20)
      NDREC=NREC+2
      READ (FUNIT,730,END=999) NRING
      IF (NRING.GT.5) CALL ERROR (21)
      I=NRING+1
      READ (FUNIT,710,END=999) (R(J),J=1,I)
      DO 35 J=1,I
         R(J)=1000*R(J)
35    CONTINUE
      TAREA=0.
      DO 30 J=1,NRING
         IF (R(J).GE.R(J+1)) CALL ERROR (22)
         RNGMID(J)=FLOAT(R(J)+R(J+1))/2.0
         RAREA(J)=PI*(R(J+1)**2-R(J)**2)/16.
         TAREA=TAREA+RAREA(J)
30    CONTINUE
      TAREA=TAREA*16.
      MAXSEG=0
      DO 40 I=1,NRECEP
         READ (FUNIT,720,END=999) RCPNUM,RDIR(I),RRING(I),RWSSEG(I),
     &      RTYPE(I),RPOP(I)
         IF (RCPNUM.NE.I) CALL ERROR (10)
         IF (RRING(I).GT.NRING) CALL ERROR (23)
         IF (RWSSEG(I).GT.MAXSEG) MAXSEG=RWSSEG(I)
         IF (RTYPE(I).NE.'C') RTYPE(I)='A'
40    CONTINUE
```

```
C
C     READ & CHECK WATERSHED INFORMATION
C
      OLDDIR=0
      OLDRNG=0
      PSNUM=0
      AREA=0.
      PSAREA=0.
      TEST='R'
      READ (FUNIT,720,END=999) NSEG,GSEG
      IF (MAXSEG.GT.NSEG) CALL ERROR (24)
      DO 50 I=1,NSEG
         READ (FUNIT,730,END=999) NODE,STYPE(I),NODDIR(I),
     &      NODRNG(I),SDEPTH(I),SHEDAR(I),LAREA(I)
         IF (STYPE(I).EQ.'L') LAKVOL(I)=SDEPTH(I)*LAREA(I)
         IF (NODE.NE.I) CALL ERROR (1)
         IF (AREA.GT.SHEDAR(I)) CALL ERROR(2)
         AREA=SHEDAR(I)
         IF (TEST.EQ.'L'.AND.STYPE(I).EQ.'L') CALL ERROR (3)
         TEST=STYPE(I)
         IF (OLDDIR.NE.NODDIR(I).OR.OLDRNG.NE.NODRNG(I)) THEN
            PSNUM=PSNUM+1
            PSDIR(PSNUM)=NODDIR(I)
            PSRING(PSNUM)=NODRNG(I)
            PSAREA=PSAREA+RAREA(NODRNG(I))
         ENDIF
         IF (I.GT.1) THEN
            IF (ABS(OLDRNG-NODRNG(I)).GT.1) CALL ERROR (17)
            IF ((ABS(OLDDIR-NODDIR(I)).GT.1).AND.(OLDDIR.NE.16.OR.
     &         NODDIR(I).NE.1).AND.(OLDDIR.NE.1.OR.NODDIR(I).NE.16))
     &         CALL ERROR (17)
         ENDIF
         OLDDIR=NODDIR(I)
         OLDRNG=NODRNG(I)
50    CONTINUE
      IF (STYPE(1).EQ.'L') CALL ERROR (24)
      IF (STYPE(GSEG).EQ.'L')CALL ERROR(25)
C
C     READ OUTPUT PARAMETER SPECIFICATIONS
C
      NVARYS=0
      NVARYF=0
C
C     READ TIME STEPS TO BE SAVED
C
      READ (FUNIT,900,END=999) NSTEPS,NSTEPF
53    IF (NSTEPS.GT.0) THEN
         IF (SSAVE.NE.'Y') THEN
            CALL ERROR (105)
            NSTEPS=0
            GOTO 53
         ENDIF
         READ (FU[illegible],920,END=999) (TSTAT(I),I=1,NSTEPS)
         NTEST=-1
         DO 51 I=1,NSTEPS
```

```
                IF (MOD(TSTAT(I),NDT).NE.0) CALL ERROR (15)
                IF (NTEST.GE.TSTAT(I)) CALL ERROR (11)
                NTEST=TSTAT(I)
51             CONTINUE
             IF (NTEST.GT.NYEARS) CALL ERROR (16)
          ELSE
             READ (FUNIT,810,END=999)
          ENDIF
          TSTAT(NSTEPS+1)=-1
54        IF (NSTEPF.GT.0) THEN
             IF (FSAVE.NE.'Y') THEN
                CALL ERROR (106)
                NSTEPF=0
                GOTO 54
             ENDIF
             READ (FUNIT,920,END=999) (TFILE(I),I=1,NSTEPF)
             NTEST=-1
             DO 52 I=1,NSTEPF
                IF (MOD(TFILE(I),NDT).NE.0) CALL ERROR (15)
                IF (NTEST.GE.TFILE(I)) CALL ERROR (11)
                NTEST=TFILE(I)
52           CONTINUE
             IF (NTEST.GT.NYEARS) CALL ERROR (16)
          ELSE
             READ (FUNIT,810,END=999)
          ENDIF
          TFILE(NSTEPF+1)=-1
C
C         READ OUTPUT PARAMETERS
C
          READ (FUNIT,730) NARRAY
          NSAV=1
          J=1
          DO 10 I=1,NARRAY
             READ (FUNIT,940,END=999) VARNAM(I),NVAR(I)
             IF (NVAR(I).GT.0) THEN
                NSAV=I
                KK=NVAR(I)
                DO 20 K=1,KK
                   READ (FUNIT,950,END=999) NSUB(J),LOC(J),FLAG(J)
                   IF (FLAG(J).NE.'F'.AND.FLAG(J).NE.'S') THEN
                      IF (SSAVE.EQ.'Y') THEN
                         FLAG(J)='S'
                      ELSEIF (FSAVE.EQ.'Y') THEN
                         FLAG(J)='F'
                      ELSE
                         CALL ERROR (14)
                      ENDIF
                   ENDIF
                   IF (FLAG(J).EQ.'F') THEN
                      NVARYF=NVARYF+1
                      IF (FSAVE.NE.'Y') CALL ERROR (13)
                   ELSEIF(FLAG(J).EQ.'S')THEN
                      NVARYS=NVARYS+1
                      IF (SSAVE.NE.'Y') CALL ERROR (12)
```

```
               ENDIF
               J=J+1
20          CONTINUE
         ENDIF
10    CONTINUE
      NARRAY=NSAV
      ISTAT=(NVARYS+VARYS)*NSTEPS+NSTAT
      IFILE=(NVARYF+VARYF)*NSTEPF+NFILE
      IF (ISTAT.GT.300) CALL ERROR (27)
      IF (IFILE.GT.300) CALL ERROR (28)
C
C     READ AIR DISPERSION DATA
C
      IF (WINDFG.EQ.'Y') THEN
         IF (NDT.NE.1.AND.NDT.NE.10) CALL ERROR (25)
         NYEAR=20
      ELSE
         WINDFG='N'
         NYEAR=1
      ENDIF
      WRITE (SCRUNT,820) FNAME
      OPEN (FUNIT,FILE=FNAME,STATUS='OLD',IOSTAT=IERR)
      IF (IERR.NE.0) CALL ERROR (29)
      DO 60 IY=1,NYEAR
         READ (FUNIT,400,END=999)
         DO 70 J=1,6
            DO 80 I=1,16
               L=I+8
               IF (L.GT.16) L=L-16
               READ (FUNIT,500,END=999) (FWIND(L,J,K,IY),K=1,6)
80          CONTINUE
70       CONTINUE
60    CONTINUE
      CLOSE (FUNIT)
      RETURN
999   CALL ERROR (5)
400   FORMAT (1X)
500   FORMAT (7X,6(F7.5))
600   FORMAT (6E11.5)
700   FORMAT (' SECOND INPUT FILE NAME? ')
710   FORMAT (6I5)
720   FORMAT (4I3,1X,A1,I5)
730   FORMAT (I3,1X,A1,2I3,3E9.3)
810   FORMAT (A)
820   FORMAT (' Opening File : ',A12)
900   FORMAT (I3,1X,I3)
920   FORMAT (11(I5))
940   FORMAT (A6,I3)
950   FORMAT (2(I3,1X),A1)
960   FORMAT (2X,A1)
      END
C
C
C
      SUBROUTINE ERROR (I)
```

```
C
C     SUBROUTINE GENERATES ERROR AND WARNING MESSAGES.  ALL ERRORS
C     TERMINATE THE PROGRAM.  WARNINGS ASK IF EXECUTION IS TO BE STOPPED
C     OR CONTINUED.
C
      INCLUDE 'IO.INC'
      CHARACTER*1 Q
      WRITE (SCRUNT,300)
      IF (I.LE.100) THEN
C
C        GENERATE ERROR MESSAGES
C
         WRITE (SCRUNT,300) ' ***************  ERROR  ***************'
         IF (I.EQ.1) THEN
            WRITE (SCRUNT,300) ' (001) WATER SOURCE SEGMENTS NOT IN ORDE
     &R'
         ELSEIF (I.EQ.2) THEN
            WRITE (SCRUNT,300) ' (002) WATERSHED AREAS MUST INCREASE'
         ELSEIF (I.EQ.3) THEN
            WRITE (SCRUNT,300) ' (003) WATER SOURCE NOs. MUST INCREASE'
         ELSEIF (I.EQ.4) THEN
            WRITE (SCRUNT,300) ' (004) CORRELATED NAME NOT FOUND'
         ELSEIF (I.EQ.5) THEN
            WRITE (SCRUNT,300) ' (005) UNEXPECTED END OF DATA'
         ELSEIF (I.EQ.6) THEN
            WRITE (SCRUNT,300) ' (006) TYPE ERROR IN REGULAR DIST''ns'
         ELSEIF (I.EQ.7) THEN
            WRITE (SCRUNT,300) ' (007) TYPE ERROR IN CORRELATED DIST''ns
     &'
         ELSEIF (I.EQ.8) THEN
            WRITE (SCRUNT,300) ' (008) TYPE ERROR IN ARBITRARY DIST''ns'
         ELSEIF (I.EQ.9) THEN
            WRITE (SCRUNT,300) ' (009) NUMBER OF PARAMETERS INCORRECT'
         ELSEIF (I.EQ.10) THEN
            WRITE (SCRUNT,300) ' (010) RECEPTORS NOT LISTED IN ORDER'
         ELSEIF (I.EQ.11) THEN
            WRITE (SCRUNT,300) ' (011) TIME STEPS MUST INCREASE'
         ELSEIF (I.EQ.12) THEN
            WRITE (SCRUNT,300) ' (012) STATS REQUESTED MUST SPECIFY FILE
     &'
         ELSEIF (I.EQ.13) THEN
            WRITE (SCRUNT,300) ' (013) RESULTS REQUESTED MUST SPECIFY FI
     &LE'
         ELSEIF (I.EQ.14) THEN
            WRITE (SCRUNT,300) ' (014) CAN''T SAVE RESULTS - NO OPEN FIL
     &E'
         ELSEIF (I.EQ.15) THEN
            WRITE (SCRUNT,300) ' (015) CAN''T SAVE TIME STEPS SPECIFIED'
         ELSEIF (I.EQ.16) THEN
            WRITE (SCRUNT,300) ' (016) TIME FOR OUTPUT TOO BIG'
         ELSEIF (I.EQ.17) THEN
            WRITE (SCRUNT,300) ' (017) WATERSHED DIRECTIONS OR RINGS NOT
     & CONTINUOUS'
         ELSEIF (I.EQ.18) THEN
            WRITE (SCRUNT,300) ' (018) CANNOT CORRELATE PARAMETERS'
         ELSEIF (I.EQ.19) THEN
            WRITE (SCRUNT,300) ' (019) TIME STEPS DON''T MATCH SIMULATIO
     &N TIME'
         ELSEIF (I.EQ.20) THEN
            WRITE (SCRUNT,300) ' (020) MAXIMUM OF 80 RECEPTORS ALLOWED'
         ELSEIF (I.EQ.21) THEN
            WRITE (SCRUNT,300) ' (021) MAXIMUM OF 5 RINGS ALLOWED'
         ELSEIF (I.EQ.22) THEN
            WRITE (SCRUNT,300) ' (022) RING LIMITS MUST INCREASE'
         ELSEIF (I.EQ.23) THEN
            WRITE (SCRUNT,300) ' (023) RECEPTOR RING NUMBER TOO BIG'
         ELSEIF (I.EQ.24) THEN
            WRITE (SCRUNT,300) ' (024) FIRST WATERSHED SEG. MUST BE RIVE
     &R'
         ELSEIF (I.EQ.25) THEN
            WRITE (SCRUNT,300) ' (025) GROUNDWATER MUST FLOW INTO RIVER'
         ELSEIF (I.EQ.27) THEN
            WRITE (SCRUNT,300) ' (027) TOO MANY OUTPUTS TO STATS FILE'
         ELSEIF (I.EQ.28) THEN
            WRITE (SCRUNT,300) ' (028) TOO MANY OUTPUTS TO RESULTS FILE'
         ELSEIF (I.EQ.29) THEN
            WRITE (SCRUNT,300) ' (029) FILE NOT FOUND'
         ELSEIF (I.EQ.30) THEN
            WRITE (SCRUNT,300) ' (030) ERROR IN LOGNORMAL SPECIFIERS'
         ELSEIF (I.EQ.31) THEN
            WRITE (SCRUNT,300) ' (031) ERROR IN NORMAL SPECIFIERS'
         ELSEIF (I.EQ.32) THEN
            WRITE (SCRUNT,300) ' (032) TIME STEP MUST BE 1 OR 10 YEARS'
         ELSEIF (I.EQ.33) THEN
            WRITE (SCRUNT,300) ' (033) ERROR IN TRIANGULAR SPECIFIERS'
         ENDIF
      ELSE
C
C        GENERATE WARNING MESSAGES
C
         WRITE (SCRUNT,300) ' ***************  WARNING  ***************'
         IF (I.EQ.101) THEN
            WRITE (SCRUNT,300) ' (101) TWO CONSECUTIVE LAKES'
         ELSEIF (I.EQ.102) THEN
            WRITE (SCRUNT,300) ' (102) ABOUT TO OVER WRITE EXISTING FILE
     &'
         ELSEIF (I.EQ.105) THEN
            WRITE (SCRUNT,300) ' (105) NOT SAVING TIME STEPS TO STATS'
         ELSEIF (I.EQ.106) THEN
            WRITE (SCRUNT,300) ' (106) NOT SAVING TIME STEPS TO RESULTS'
         ENDIF
         WRITE (SCRUNT,300) '  - OK TO CONTINUE (Y/N)? '
         READ (SCRUNT,300) Q
         IF (Q.EQ.'Y'.OR.Q.EQ.'y') THEN
C
C           RESUME EXECTION
C
            WRITE (SCRUNT,300) ' RESUMING EXECUTION'
            RETURN
         ENDIF
      ENDIF
C
C     STOP PROGRAM
C
      WRITE (SCRUNT,300) ' PROGRAM TERMINATED'
      WRITE (SCRUNT,300) ' SEE USERS MANUAL APPENDIX A'
      STOP
300   FORMAT (A)
      END
```

### B.2.3 Sampling Routines

```
C FILE 'SAMPLE.FOR'
C
      SUBROUTINE CREATE
C
C     THIS ROUTINE GENERATES COMPLEMENTARY CUMULATIVE PROB-
C     ABILITY FUNCTIONS (CPF) FOR INPUT BETA AND ARBITRARY
C     DISTRIBUTIONS.
C
      INCLUDE 'PARAM.INC'
      INCLUDE 'COUNTS.INC'
      REAL*4 A,B,MAX,MIN,SUM,X
C
C     CHECK IF THERE ARE ANY BETA OR ARBITRARY DISTRIBUTIONS
C
      IF (NBETA.NE.0.OR.NARB.NE.0) THEN
         DO 10 I=1, NPARM
            IF (NTYPE(I).EQ.8.OR.NTYPE(I).EQ.9) THEN
               MIN=P1(I)
               MAX=P2(I)
               IF (NTYPE(I).EQ.8) THEN
C
C              INITIALIZE BETA DISTRIBUTIONS
C
                  NACELL(I)=NCELLS
                  UNIT(I)=(MAX-MIN)/FLOAT(NCELLS)
                  ORIGIN(I)=MIN-(0.5*UNIT(I))
                  A=P3(I)-1.0
                  B=P4(I)-1.0
                  DO 1500 J=1,NCELLS
                     X=(J-0.5)/FLOAT(NCELLS)
                     V(I,J)=(X**A)*((1.0-X)**B)
1500              CONTINUE
               ELSE
C
C                 INITIALIZE ARBITRARY DISTRIBUTIONS
C
                  UNIT(I)=(MAX-MIN)/(FLOAT(NACELL(I))-1.)
                  ORIGIN(I)=MIN-UNIT(I)
               ENDIF
C
C              CALCULATE CUMULATIVE PROBABILITY FUNCTIONS
C
               SUM=0.0
               DO 1800 J=1,NACELL(I)
                  SUM=SUM+V(I,J)
                  CPF(I,J)=SUM
1800           CONTINUE
               DO 1900 J=1,NACELL(I)
                  CPF(I,J)=CPF(I,J)/SUM
1900           CONTINUE
            ENDIF
 10      CONTINUE
```

```
      ENDIF
      RETURN
      END
C
C
C
      SUBROUTINE CHOOSE (I)
C
C     THIS ROUTINE WILL RETURN A VALUE FOR EACH PARAMETER.
C     IT CALLS THE APPROPRIATE SUBROUTINE DEPENDING ON THE
C     TYPE OF DISTRIBUTION SPECIFIED:
C                                             1 = CONSTANT
C                                             2 = NORMAL
C                                             3 = LOG NORMAL
C                                             4 = UNIFORM
C                                             5 = LOG UNIFORM
C                                             6 = TRIANGULAR
C                                             7 = WEIBULL
C                                             8 = BETA
C                                             9 = ARBITRARY
C                                            10 = CORRELATED
C
      INCLUDE 'INPT.INC'
      INCLUDE 'PARAM.INC'
      INCLUDE 'COUNTS.INC'
      IF (NTYPE(I).EQ.1) THEN
         XIN(I) = P1(I)
      ELSEIF (NTYPE(I).EQ.2) THEN
         CALL NORMAL (NSTART,P1(I),P2(I),P3(I),P4(I),XIN(I))
      ELSEIF (NTYPE(I).EQ.3) THEN
         CALL LNORM (NSTART,P1(I),P2(I),P3(I),P4(I),XIN(I))
      ELSEIF (NTYPE(I).EQ.4) THEN
         CALL UNIFOR (NSTART,P1(I),P2(I),XIN(I))
      ELSEIF (NTYPE(I).EQ.5) THEN
         CALL LOGUNI (NSTART,P1(I),P2(I),XIN(I))
      ELSEIF (NTYPE(I).EQ.6) THEN
         CALL TRIANG (NSTART,P1(I),P2(I),P3(I),XIN(I))
      ELSEIF (NTYPE(I).EQ.7) THEN
         CALL WEIBUL (NSTART,P1(I),P2(I),P3(I),XIN(I))
      ELSEIF (NTYPE(I).EQ.8.OR.NTYPE(I).EQ.9) THEN
         CALL BETA (NSTART,I,XIN(I))
      ELSEIF (NTYPE(I).EQ.10) THEN
         CALL CORREL (NSTART,P1(I),P2(I),P3(I),P4(I),P5(I),CORNUM(I),
     &       XIN(I))
      ENDIF
      RETURN
      END
C
C
C
      SUBROUTINE NORMAL (NSTART,EXPECT,STDEV,MIN,MAX,XIN)
C
C      THIS ROUTINE GENERATES NORMALLY DISTRIBUTED VARIATES
C
      INTEGER*2 I
      REAL*4 XIN,MIN,MAX,EXPECT,STDEV,R,TEMP
      IF (.NOT.MAX.GT.MIN) CALL ERROR (31)
1000  CONTINUE
         TEMP=-6.0
         DO 1100 I=1,12
            R=RANDOM(NSTART)
            TEMP=TEMP+R
1100    CONTINUE
         XIN=TEMP*STDEV+EXPECT
      IF (XIN.LT.MIN.OR.XIN.GT.MAX) GO TO 1000
      RETURN
      END
C
C
C
      SUBROUTINE LNORM (NSTART,GM,GSD,MIN,MAX,XIN)
C
C     THIS ROUTINE GENERATES LOG-NORMALLY DISTRIBUTED VARIATES
C
      REAL*4 GM, GSD, LGM, LGSD, TMIN, TMAX, TEMP, MIN, MAX, XIN
      LGM=ALOG10(GM)
      LGSD=ALOG10(GSD)
      IF (.NOT.MAX.GT.MIN) CALL ERROR (30)
      IF (MIN.LE.0.0) THEN
         TMIN=-1.0E37
      ELSE
         TMIN=ALOG10(MIN)
      ENDIF
      TMAX=ALOG10(MAX)
      IF (TMIN.GT.TMAX) THEN
         TEMP=TMIN
         TMIN=TMAX
         TMAX=TEMP
      ENDIF
      CALL NORMAL (NSTART,LGM,LGSD,TMIN,TMAX,TEMP)
      XIN=10.**TEMP
      RETURN
      END
C
C
C
      SUBROUTINE UNIFOR (NSTART,UMIN,UMAX,XIN)
C
C    THIS ROUTINE GENERATES UNIFORMLY DISTRIBUTED RANDOM NUMBERS
C    BETWEEN UMIN AND UMAX
C
      REAL*4 RANDOM,R,XIN,UMIN,UMAX
1000  R=RANDOM(NSTART)
      IF (UMIN.LE.UMAX) THEN
         XIN=UMIN+R*(UMAX-UMIN)
      ELSE
         XIN=UMAX+R*(UMIN-UMAX)
      ENDIF
      RETURN
      END
```

```
C
C
C
      SUBROUTINE LOGUNI (NSTART,LMIN,LMAX,XIN)
C
C    THIS ROUTINE GENERATES LOG-UNIFORMLY DISTRIBUTED RANDOM NUMBERS
C    BETWEEN LMIN AND LMAX
C
      REAL*4 RANDOM,R,XIN,LMIN,TEMP,LMAX
1000  R=RANDOM(NSTART)
      TEMP=ALOG10(LMIN)+R*(ALOG10(LMAX)-ALOG10(LMIN))
      XIN=10**TEMP
      RETURN
      END
C
C
C
      SUBROUTINE TRIANG (NSTART,VMIN,VMODE,VMAX,XIN)
C
C      THIS ROUTINE GENERATES TRIANGULARLY DISTRIBUTED VARIATES
C
      REAL*4 XIN,R,VMAX,VMIN,VMODE,Z1,Z2
1000  R=RANDOM(NSTART)
      Z1=VMAX-VMIN
      Z2=VMODE-VMIN
      IF (Z1.LE.0.0) CALL ERROR (33)
      IF (R.LE.Z2/Z1) THEN
         XIN=VMIN+SQRT(R*Z1*Z2)
      ELSE
         XIN=VMAX-SQRT((1.-R)*(VMAX-VMODE)*Z1)
      ENDIF
      RETURN
      END
C
C
C
      SUBROUTINE WEIBUL (NSTART,A,B,C,XIN)
C
C     THIS SUBROUTINE GENERATES RANDOM SAMPLES FROM WEIBULL
C     DISTRIBUTIONS BY TRANSFORMING UNIFORMLY DISTRIBUTED SAMPLES
C     TO A SPECIFIED WEIBULL DISTRIBUTION
C
      REAL*4 A,B,C,XIN,R
      INTEGER*4 NSTART
1000  R=RANDOM(NSTART)
      XIN=A+B*((-ALOG(R))**(1.0/C))
      RETURN
      END
C
C
C
      SUBROUTINE BETA (NSTART,I,XIN)
C
C      THIS ROUTINE SAMPLES VALUES OF BETA OR ARBITRARY VARIATES.
C
```

```
      INCLUDE 'PARAM.INC'
      INTEGER*2 ICELL,I
      REAL*4 XIN,R
      R=RANDOM(NSTART)
      DO 1100 ICELL=1,NACELL(I)
         IF (CPF(I,ICELL).GE.R) GOTO 1000
1100  CONTINUE
      ICELL=NACELL(I)
1000  XIN=ORIGIN(I)+ICELL*UNIT(I)
      RETURN
      END
C
C
C
      SUBROUTINE CORREL(NSTART,MEANY,SDEVY,CCOEFF,MEANX,SDEVX,CORNUM,XIN
     &)
C
C     THIS SUBROUTINE CALCULATES THE VALUE OF AN INPUT PARAMETER WHICH
C     IS CORRELATED WITH SOME PREVIOUS INPUT PARAMETER.  IT EMPLOYS
C     KLEIJNEN'S CORRELATED GENERATION TECHNIQUE (KLEIJNEN, J.P.C.
C     (1974) STATISTICAL TECHNIQUES IN SIMULATION - PART 1, MARCEL
C     DEKKER,N.Y.) AS PRESENTED BY ANDRES AND GOODWIN (1984).
C
      INCLUDE 'INPT2.INC'
      INTEGER*2 CORNUM
      REAL*4 MEANY,SDEVY,CCOEFF,MEANX,SDEVX,XIN,A,B,U,Z,X,Y
      A=CCOEFF*SDEVY/SDEVX
      B=MEANY-CCOEFF*MEANX*SDEVY/SDEVX
      CALL NORMAL (NSTART,0.0,1.0,-1.0E37,1.0E37,Z)
      U=SDEVY*Z*SQRT(1.0-CCOEFF**2)
      X=XVALUE(CORNUM)
      Y=A*X+B+U
      XIN=Y
      RETURN
      END
C
C
C
      FUNCTION RANDOM (NSTART)
C
C     THIS PORTABLE FORTRAN RANDOM NUMBER GENERATOR WAS
C     ADAPTED FROM THAT DESCRIBED BY K. MARSE AND S.D. ROBERTS
C     ('SIMULATION', OCTOBER, 1983; PP 135-139)
C
      INTEGER*4 B2E15,B2E16,H115,H131,LOW15,LOWPRD,MODLUS,
     &          MULT1,MULT2,OVFLOW
      MULT1=24112
      MULT2=26143
      B2E15=32768
      B2E16=65536
      MODLUS=2147483647
      H115=NSTART/B2E16
      LOWPRD=(NSTART-H115*B2E16)*MULT1
      LOW15=LOWPRD/B2E16
      H131=H115*MULT1+LOW15
```

```
 OVFLOW=H131/B2E15
 NSTART=(((LOWPRD-LOW15*B2E16)-MODLUS)+
&   (H131-OVFLOW*B2E15)*B2E16)+OVFLOW
 IF (NSTART.LT.0) NSTART=NSTART+MODLUS
 H115=NSTART/B2E16
 LOWPRD=(NSTART-H115*B2E16)*MULT2
 LOW15=LOWPRD/B2E16
 H131=H115*MULT2+LOW15
 OVFLOW=H131/B2E15
 NSTART=(((LOWPRD-LOW15*B2E16)-MODLUS)+(H131-OVFLOW*B2E15)*B2E16)
&   +OVFLOW
 IF (NSTART.LT.0) NSTART=NSTART+MODLUS
 RANDOM=(2*(NSTART/256)+1)/16777216.0
 RETURN
 END
```

### B.2.4 Results Saving Routines

```
C FILE 'SAVE.FOR'
C
      SUBROUTINE TIMSEL
C
C     THIS SUBROUTINE SAVES TIME-VARIANT INPUT VARIABLES
C     FLAGGED FOR OUTPUT TO STATS AND FILE
C
      INCLUDE 'COUNTS.INC'
      INCLUDE 'INPT.INC'
      INCLUDE 'OUT.INC'
      CHARACTER*1 C
      NUMS=1
      NUMF=1
C
C     CHECK IF ANY DISTRIBUTIONS ARE TIME-VARIANT
C
      IF (VARYS.NE.0.OR.VARYF.NE.0) THEN
C
C        INITIALIZE OR INCREMENT TIME COUNTERS
C
         IF (NT.EQ.0) THEN
            TNUMBS=1
            TNUMBF=1
         ENDIF
C
C        CHECK IF THIS TIME TO BE SAVED
C
         IF (TFILE(TNUMBF).EQ.NT.OR.TSTAT(TNUMBS).EQ.NT) THEN
            DO 40 I=1,VARY
               J=VARIED(I)
               C=EFLAG(J)
C
C              CHECK IF VALUE TO BE OUTPUT
C
               IF (C.EQ.'S'.OR.C.EQ.'F'.OR.C.EQ.'B') THEN
                  IF (NSTEPS.GE.TNUMBS) THEN
                     IF (TSTAT(TNUMBS).EQ.NT.AND.(C.EQ.'S'.OR.C.EQ.'B'))
     &                  THEN
C
C                       SORT VALUES AND SAVE FOR STATS
C
                        JS=NSTEPS*(NUMS-1)+NSTAT+TNUMBS
                        NUMS=NUMS+1
                        XOUTS(JS)=XIN(J)
                     ENDIF
                  ENDIF
                  IF (NSTEPF.GE.TNUMBF) THEN
                     IF (TFILE(TNUMBF).EQ.NT.AND.(C.EQ.'F'.OR.C.EQ.'B'))
     &                  THEN
C
C                       SORT VALUES AND SAVE FOR DETAILED RESULTS FILE
C
                        JF=NSTEPF*(NUMF-1)+NFILE+TNUMBF
```

```
                      NUMF=NUMF+1
                      XOUTF(JF)=XIN(J)
                   ENDIF
                ENDIF
             ENDIF
40        CONTINUE
          IF (TFILE(TNUMBF).EQ.NT) TNUMBF=TNUMBF+1
          IF (TSTAT(TNUMBS).EQ.NT) TNUMBS=TNUMBS+1
        ENDIF
      ENDIF
      RETURN
      END
C
C
C
      SUBROUTINE SELECT
C
C     THIS SUBROUTINE CHECKS WHETHER PARAMETER VALUES ARE TO
C     BE SAVED AT EACH TIME, T. IT INDICATES WHETHER VALUES ARE
C     TO BE WRITTEN TO STATISTICS FILE OR DETAILED RESULTS FILE
C     VECTORS
C
      INCLUDE 'COUNTS.INC'
      CHARACTER*1 VECTOR
      NUMS=1
      NUMF=1
      IF (NT.EQ.0) THEN
         TNUMS=1
         TNUMF=1
      ENDIF
C
C     CHECK IF THIS TIME STEP IS TO BE SAVED TO STATS AND/OR DETAILED
C     RESULTS FILE
C
         IF (TSTAT(TNUMS).EQ.NT) THEN
            VECTOR='S'
            CALL SORT (VECTOR)
            TNUMS=TNUMS+1
         ENDIF
         IF (TFILE(TNUMF).EQ.NT) THEN
            VECTOR='F'
            CALL SORT (VECTOR)
            TNUMF=TNUMF+1
         ENDIF
      RETURN
      END
C
C
C
      SUBROUTINE SORT (VECTOR)
C
C     THIS SUBROUTINE CHECKS ALL OUTPUT ARRAYS.  FOR ANY ARRAYS
C     CONTAINING PARAMETERS TO BE SAVED, THE CURRENT PARAMETER
C     VALUE IS WRITTEN TO A DUMMY VARIABLE FOR TRANSFER TO
C     SUBROUTINE 'SEND'.
```

```
C
      INCLUDE 'COUNTS.INC'
      INCLUDE 'INFO.INC'
      INCLUDE 'CONC.INC'
      CHARACTER*1 VECTOR
      REAL*4 XDUM
      K=1
      DO 1000 I=1,NARRAY
         IF (NVAR(I).NE.0) THEN
            DO 2000 J=1,NVAR(I)
               IF (VECTOR.EQ.FLAG(K)) THEN
C
C                 REROUTE TOTALS FOR DOSE TO LAST ARRAY LOCATION
C
                  IF (NUMTRL.EQ.1.AND.NSUB(K).EQ.11) NSUB(K)=5
C
C                 FIND CORRECT OUTPUT VALUE
C
                  IF (I.EQ.1) THEN
                     XDUM=WCONC(NSUB(K),LOC(K),3)
                  ELSEIF (I.EQ.2) THEN
                     XDUM=CONC(NSUB(K),LOC(K),3)
                  ELSEIF (I.EQ.3) THEN
                     XDUM=PH(LOC(K))
                  ELSEIF (I.EQ.4) THEN
                     XDUM=WATC(NSUB(K),LOC(K))
                  ELSEIF (I.EQ.5) THEN
                     XDUM=WATAVG(NSUB(K))
                  ELSEIF (I.EQ.6) THEN
                     XDUM=WATPH(LOC(K))
                  ELSEIF (I.EQ.7) THEN
                     XDUM=GWATC(NSUB(K))
                  ELSEIF (I.EQ.8) THEN
                     XDUM=EMRATE(NSUB(K))
                  ELSEIF (I.EQ.9) THEN
                     XDUM=EROTOT
                  ELSEIF (I.EQ.10) THEN
                     XDUM=DTAIL
                  ELSEIF (I.EQ.11) THEN
                     XDUM=AIRC(NSUB(K),LOC(K))
                  ELSEIF (I.EQ.12) THEN
                     XDUM=SOILC(NSUB(K),LOC(K))
                  ELSEIF (I.EQ.13) THEN
                     XDUM=AVEGC(NSUB(K),LOC(K))
                  ELSEIF (I.EQ.14) THEN
                     XDUM=BVEGC(NSUB(K),LOC(K))
                  ELSEIF (I.EQ.15) THEN
                     XDUM=SUFOC(NSUB(K))
                  ELSEIF (I.EQ.16) THEN
                     XDUM=BRWSC(NSUB(K))
                  ELSEIF (I.EQ.17) THEN
                     XDUM=LICHC(NSUB(K))
                  ELSEIF (I.EQ.18) THEN
                     XDUM=AQVEGC(NSUB(K))
                  ELSEIF (I.EQ.19) THEN
```

```
                     XDUM=FISHC(NSUB(K),LOC(K))
                  ELSEIF (I.EQ.20) THEN
                     XDUM=AMOC(NSUB(K))
                  ELSEIF (I.EQ.21) THEN
                     XDUM=WMOC(NSUB(K))
                  ELSEIF (I.EQ.22) THEN
                     XDUM=ACARC(NSUB(K))
                  ELSEIF (I.EQ.23) THEN
                     XDUM=WCARC(NSUB(K))
                  ELSEIF (I.EQ.24) THEN
                     XDUM=WATD(NSUB(K),LOC(K))
                  ELSEIF (I.EQ.25) THEN
                     XDUM=SHINED(NSUB(K),LOC(K))
                  ELSEIF (I.EQ.26) THEN
                     XDUM=INHD(NSUB(K),LOC(K))
                  ELSEIF (I.EQ.27) THEN
                     XDUM=RADD(LOC(K))
                  ELSEIF (I.EQ.28) THEN
                     XDUM=VEGD(NSUB(K),LOC(K))
                  ELSEIF (I.EQ.29) THEN
                     XDUM=FISHD(NSUB(K),LOC(K))
                  ELSEIF (I.EQ.30) THEN
                     XDUM=MEATD(NSUB(K),LOC(K))
                  ELSEIF (I.EQ.31) THEN
                     XDUM=DOSE(NSUB(K),LOC(K))
                  ELSEIF (I.EQ.32) THEN
                     XDUM=POPDT
                  ELSEIF (I.EQ.33) THEN
                     XDUM=BLANK1(NSUB(K),LOC(K))
                  ELSEIF (I.EQ.34) THEN
                     XDUM=BLANK2(NSUB(K),LOC(K))
                  ENDIF
                  CALL SEND (XDUM,VECTOR)
               ENDIF
               K=K+1
2000        CONTINUE
         ENDIF
1000  CONTINUE
      RETURN
      END
C
C
C
      SUBROUTINE SEND (XDUM,VECTOR)
C
C     SUBROUTINE ACCEPTS THE CURRENT VALUE OF A VARIABLE AND ALLOCATES
C     IF TO AN APPROPRIATE POSITION IN AN OUTPUT VECTOR.
C
      INCLUDE 'COUNTS.INC'
      INCLUDE 'OUT.INC'
      CHARACTER*1 VECTOR
      REAL*4 XDUM
      IF (VECTOR.EQ.'S') THEN
C
C        SORT OUTPUTS AND SEND THE VARIABLES TO STATISTICS VECTOR
```

```
C
         JS=(NUMS-1+VARYS)*NSTEPS+TNUMS+NSTAT
         XOUTS(JS)=XDUM
         NUMS=NUMS+1
      ELSEIF (VECTOR.EQ.'F') THEN
C
C        SORT OUTPUTS AND SEND THE VARIABLES TO DETAILED RESULTS VECTOR
C
         JF=(NUMF-1+VARYF)*NSTEPF+TNUMF+NFILE
         XOUTF(JF)=XDUM
         NUMF=NUMF+1
      ENDIF
      RETURN
      END
C
C
C
      SUBROUTINE SAVEIN
C
C     THIS SUBROUTINE SAVES ALL VALUES OF SELECTED NON-TIME-VARIANT
C     INPUT PARAMETERS TO APPROPRIATE VECTORS (XOUTS, XOUTF).
C
      INCLUDE 'OUT.INC'
      INCLUDE 'INPT.INC'
      INCLUDE 'COUNTS.INC'
C
C     CHECK IF ANY INPUT VALUES TO BE SAVED
C
      IF (NSTAT.NE.0.OR.NFILE.NE.0) THEN
         NSTA=0
         NFIL=0
         DO 10 J=1,VARN
            I=VARNOT(J)
            IF (EFLAG(I).EQ.'S'.OR.EFLAG(I).EQ.'B') THEN
C
C              SAVE VALUE TO STATISTICS VECTOR
C
               NSTA=NSTA+1
               XOUTS(NSTA)=XIN(I)
            ENDIF
            IF (EFLAG(I).EQ.'F'.OR.EFLAG(I).EQ.'B') THEN
C
C              SAVE VALUE TO DETAILED RESULTS VECTOR
C
               NFIL=NFIL+1
               XOUTF(NFIL)=XIN(I)
            ENDIF
10       CONTINUE
      ENDIF
      RETURN
      END
```

### B.2.5 Statistics Routines

```
C FILE 'STATS.FOR'
C
      SUBROUTINE STATS
C
C     SUBROUTINE STATS CALCULATES SUMMARY STATISTICS FOR VARIABLES
C     CONTAINED IN THE VECTOR XOUT. THE ANALYSIS INVOLVES UPDATING
C     CALCULATIONS WHICH ARE PERFORMED IN SUBROUTINES MOMENT AND
C     GMOMENT.
C
      INCLUDE 'STATS.INC'
      INCLUDE 'OUT.INC'
      INCLUDE 'COUNTS.INC'
      INCLUDE 'UPDATE.INC'
      REAL*4 XOUT(600)
      DOUBLE PRECISION XN,GSD(600),Z1
C
C     INITIALIZE STATISTICS ON FIRST TRIAL
C
      IF (NUMTRL.EQ.1) THEN
         NOUTS=NSTEPS*(VARYS+NVARYS)+NSTAT
         NOUTF=NSTEPF*(VARYF+NVARYF)+NFILE
         NOUT=NOUTS+NOUTF
         DO 1100 IDIST1=1,NOUT
            XMAX(IDIST1)=-1.0E+37
            XMIN(IDIST1)=+1.0E+37
            GN(IDIST1)=0
            N(IDIST1)=0
1100     CONTINUE
      ENDIF
C
C     TRANSFER OUTPUT VARIABLES TO XOUT
C
      IF (NOUTS.GT.0) THEN
         DO 1110 I=1,NOUTS
            XOUT(I)=XOUTS(I)
1110     CONTINUE
      ENDIF
      IF (NOUTF.GT.0) THEN
         KK=NOUTS+1
         DO 1120 I=KK,NOUT
            J=I-NOUTS
            XOUT(I)=XOUTF(J)
1120     CONTINUE
      ENDIF
C
C     ON EACH TRIAL, MAXIMUM,MINIMUM AND VARIOUS MOMENTS ARE UPDATED
C     FOR EACH PARAMETER.
C
      DO 1360 ID=1,NOUT
         Z1=XOUT(ID)
         IF (Z1.GT.XMAX(ID)) XMAX(ID)=Z1
         IF (Z1.LT.XMIN(ID)) XMIN(ID)=Z1
         CALL MOMENT (Z1,N(ID),S1(ID),S2(ID),S3(ID),S4(ID))
         CALL GMOMEN (Z1,GN(ID),GS1(ID),GS2(ID))
 1360 CONTINUE
 C
 C    FOLLOWING THE FINAL TRIAL, THE CUMULATIVE MOMENT RESULTS ARE
 C    USED TO CALCULATE SUMMARY STATISTICS.
 C
      IF (NUMTRL.EQ.NTRIAL) THEN
         DO 1400 I=1,NOUT
            XN=DBLE(N(I))
            IF (N(I).LE.1) THEN
               SDEV(I)=0.0
            ELSE
               SDEV(I)=DSQRT(S2(I)/(XN-1.0))
            ENDIF
            IF (XN.EQ.0.0.OR.S2(I).LE.0.0) THEN
               SKEW(I)=0.0
               KURT(I)=0.0
            ELSE
               SKEW(I)=(S3(I)/XN)/((S2(I)/XN)**1.5)
               KURT(I)=(S4(I)/XN)/((S2(I)/XN)**2.0)
            ENDIF
            IF (GN(I).LE.1) THEN
               GSD(I)=0.0
               GMEAN(I)=0.0
            ELSE
               GSD(I)=DSQRT(GS2(I)/DBLE(GN(I)-1))
               GMEAN(I)=DEXP(GS1(I))
            ENDIF
            GSDEV(I)=DEXP(GSD(I))
 1400    CONTINUE
      ENDIF
      RETURN
      END
 C
 C
 C
      SUBROUTINE MOMENT (X,N,S1,S2,S3,S4)
 C
 C    THIS SUBROUTINE CALCULATES THE FIRST FOUR MOMENTS
 C    OF A RANDOM VARIABLE USING AN ALGORITHM BY C.C. SPICER
 C    (APPLIED STATISTICS 21,226-227 (1972)).
 C
      DOUBLE PRECISION X,S1,S2,S3,S4,AN,AN1,DX,DX2
      INTEGER*2 N
      N=N+1
      IF (N.EQ.1) THEN
         S1=X
         S2=0.0
         S3=0.0
         S4=0.0
      ELSE
         AN=N
         AN1=AN-1.0
         DX=(X-S1)/AN
         DX2=DX*DX
         S4=S4-DX*(4.0*S3-DX*(6.0*S2+AN1*(1.0+AN1**3)*DX2))
         S3=S3-DX*(3.0*S2-AN*AN1*(AN-2.0)*DX2)
         S2=S2+AN*AN1*DX2
         S1=S1+DX
      ENDIF
      RETURN
      END
C
C
C
      SUBROUTINE GMOMEN (X,N,GS1,GS2)
C
C     THIS SUBROUTINE CALCULATES THE GEOMETRIC MEAN AND
C     STANDARD DEVIATION USING THE METHOD OUTLINED IN
C     SUBROUTINE 'MOMENTS'.
C
      DOUBLE PRECISION X,GX,GS1,GS2,DX,DX2,AN,AN1
      INTEGER*2 N
      IF (X.GT.0.0) THEN
         GX=DLOG(X)
         N=N+1
         IF (N.EQ.1) THEN
            GS1=GX
            GS2=0.0
         ENDIF
         AN=FLOAT(N)
         AN1=FLOAT(N)-1.0
         DX=(GX-GS1)/AN
         DX2=DX*DX
         GS2=GS2+AN*AN1*DX2
         GS1=GS1+DX
      ENDIF
      RETURN
      END
```

### B.2.6 Output Routines

```
C FILE 'OUTPUT.FOR'
C
      SUBROUTINE WRITE
C
C     WRITES VALUES CONTAINED IN 'XOUTF' (SAMPLED INPUTS AND
C     CALCULATED PARAMETERS) TO SPECIFIED OUTPUT FILE.
C
      INCLUDE 'OUT.INC'
      INCLUDE 'IO.INC'
      INCLUDE 'COUNTS.INC'
      IF (NOUTF.GT.0) THEN
         IF (NUMTRL.EQ.1) CALL FILER (FUNIT1)
         WRITE (FUNIT1,900) (XOUTF(I),I=1,NOUTF)
      ENDIF
      RETURN
900   FORMAT (150(1X,E9.3))
      END
C
C
C
      SUBROUTINE NAMOUT
C
C     ASSIGNS VARIABLE NAMES AND LOCATION AND SUBSTANCE CODES TO
C     CHARACTER VARIABLES FOR OUTPUT IN STATISTICS AND DETAILED
C     RESULTS FILES
C
      INCLUDE 'IO.INC'
      INCLUDE 'INFO.INC'
      INCLUDE 'COUNTS.INC'
      KS=1
      KF=1
C
C     WRITE SAMPLED INPUT VARIABLE NAMES FOR STATISTICS AND/OR DEATAILED
C     RESULTS FILES FOR NON-TIME-VARIANT DISTRIBUTIONS
C
      DO 10 I=1,VARN
         IF (EFLAG(VARNOT(I)).EQ.'S'.OR.EFLAG(VARNOT(I)).EQ.'B') THEN
            WRITE (NAMES(KS),100) VARTIT(VARNOT(I))
            KS=KS+1
         ENDIF
         IF (EFLAG(VARNOT(I)).EQ.'F'.OR.EFLAG(VARNOT(I)).EQ.'B') THEN
            WRITE (NAMEF(KF),100) VARTIT(VARNOT(I))
            KF=KF+1
         ENDIF
 10   CONTINUE
      JJ=1
C
C     WRITE SAMPLED INPUT VARIABLE NAMES FOR STATISTICS AND/OR DETAILED
C     RESULTS FILES FOR TIME-VARIANT DISTRIBUTIONS
C
      IF (VARY.GE.1) THEN
         DO 60 I=1,VARY
            IF (EFLAG(VARIED(I)).EQ.'S'.OR.EFLAG(VARIED(I)).EQ.'B') THEN
```

```
               DO 70 J=1,NSTEPS
                  WRITE (NAMES(KS),150) VARTIT(VARIED(I)),TSTAT(J)
                  KS=KS+1
70             CONTINUE
            ENDIF
            IF (EFLAG(VARIED(I)).EQ.'F'.OR.EFLAG(VARIED(I)).EQ.'B') THEN
               DO 80 J=1,NSTEPF
                  WRITE (NAMEF(KF),150) VARTIT(VARIED(I)),TFILE(J)
                  KF=KF+1
80             CONTINUE
            ENDIF
60       CONTINUE
      ENDIF
C
C     WRITE OUTPUT VARIABLE NAMES FOR STATISTICS OR DETAILED RESULTS.
C     NAMES INCLUDE VARIABLE NAME, SUBSTANCE, LOCATION, AND TIME.
C
      DO 20 I=1,NARRAY
         IF (NVAR(I).GT.0) THEN
            DO 30 J=1,NVAR(I)
               IF (I.GE.24.AND.NSUB(JJ).EQ.5.AND.I.NE.27)NSUB(JJ)=11
               IF (FLAG(JJ).EQ.'S') THEN
                  DO 40 K=1,NSTEPS
                     WRITE (NAMES(KS),200) VARNAM(I),NSUB(JJ),LOC(JJ),
     &                  TSTAT(K)
                     KS=KS+1
 40               CONTINUE
               ELSEIF (FLAG(JJ).EQ.'F') THEN
                  DO 50 K=1,NSTEPF
                     WRITE (NAMEF(KF),200) VARNAM(I),NSUB(JJ),LOC(JJ),
     &                  TFILE(K)
                     KF=KF+1
 50               CONTINUE
               ENDIF
               JJ=JJ+1
 30         CONTINUE
         ENDIF
 20   CONTINUE
 100  FORMAT (2X,A6)
 150  FORMAT (2X,A6,22X,I6)
 200  FORMAT (2X,A6,6X,I2,9X,I2,3X,I6)
      RETURN
      END
C
C
C
      SUBROUTINE OUTPUT
C
C     SUBROUTINE WRITES SUMMARY STATISTISTICS AND VARIABLE NAMES TO
C     STATISTICS FILE AND WRITES STATISTICS AND NAMES OF DETAILED
C     RESULTS PRAMETERS TO A 'KEY' FILE.
C
      INCLUDE 'IO.INC'
      INCLUDE 'STATS.INC'
      INCLUDE 'COUNTS.INC'
```

```
C
C     WRITE TO STATISTICS FILE
C
      IF (NOUTS.GT.0) THEN
         CALL FILER (FUNIT3)
         WRITE (FUNIT3,900) TITLE
         WRITE (FUNIT3,930) NTRIAL
         WRITE (FUNIT3,910)
         DO 10 I=1,NOUTS
            WRITE (FUNIT3,920) I,NAMES(I),S1(I),SDEV(I),GMEAN(I),
     &          GSDEV(I),XMIN(I),XMAX(I)
 10      CONTINUE
      ENDIF
C
C     WRITE TO DETAILED RESULTS FILE
C
      IF (NOUTF.GT.0) THEN
        CALL FILER (FUNIT2)
        WRITE (FUNIT2,900) TITLE
        WRITE (FUNIT2,930) NTRIAL
        WRITE (FUNIT2,910) 'SKEWNESS','KURTOSIS'
        KK=NOUTS+1
        DO 20 I=KK,NOUT
           J=I-NOUTS
           WRITE (FUNIT2,920) J,NAMEF(J),S1(I),SDEV(I),GMEAN(I),
     &         GSDEV(I),XMIN(I),XMAX(I),SKEW(I),KURT(I)
 20     CONTINUE
      ENDIF
      CLOSE (FUNIT1)
      CLOSE (FUNIT2)
      CLOSE (FUNIT3)
 900  FORMAT (1X,A40)
 910  FORMAT (5X,'PARAMETER',2X,'SUBSTANCE',2X,'LOCATION',2X,'TIME',5X,
     &   'MEAN',6X,'STD DEV',3X,'GEOM MEAN',3X,'GEOM SD',
     &  4X,'MINIMUM',4X,'MAXIMUM',4X,A8,3X,A8)
 920  FORMAT (I3,2X,A36,1X,8(2X,E9.3))
 930  FORMAT (1X,'NUMBER OF TRIALS: ',I5)
      RETURN
      END
C
C
C
      SUBROUTINE FILER(UNIT)
C
C     WRITES DATE AND TIME TO TOP OF OUTPUT FILES
C
      INTEGER*2 UNIT
      CHARACTER*8 DAY, HOUR
      CALL DATE(DAY)
      CALL TIME(HOUR)
      WRITE(UNIT,100)DAY,HOUR
      RETURN
100   FORMAT('FILE CREATED ',A8,' AT ',A8)
      END
```

### B.2.7 Include Files

```
C FILE 'IO.INC'
C
      INTEGER*2 SCRUNT,FUNIT,FUNIT1,FUNIT2,FUNIT3
      COMMON /FILES/ SCRUNT,FUNIT,FUNIT1,FUNIT2,FUNIT3
C
      CHARACTER*40 TITLE
      CHARACTER*6 VARTIT(250), VARNAM(100)
      CHARACTER*1 SSAVE,FSAVE
      CHARACTER*36 NAMES(300), NAMEF(300)
      COMMON /ID/ TITLE, VARTIT, SSAVE, FSAVE, NAMES, NAMEF, VARNAM


C FILE 'CONC.INC'
C
      REAL*4 WCONC(10,4,3),CONC(10,4,3),PH(4),WATC(8,10),WATAVG(4),
     &   WATPH(10),GWATC(4),
     &   EMRATE(5),EROTOT,DTAIL,AIRC(5,82),
     &   SOILC(4,82),AVEGC(4,80),BVEGC(4,80),SUFOC(4),
     &   BRWSC(4),LICHC(4),AQVEGC(4),FISHC(4,10),
     &   AMOC(4),WMOC(4),ACARC(4),WCARC(4),
     &   WATD(5,80),SHINED(5,80),INHD(5,80),RADD(80),
     &   VEGD(5,80),FISHD(5,80),MEATD(5,80),DOSE(5,80),
     &   POPDT,BLANK1(4,80),BLANK2(10,10)
      COMMON /CONCEN/ WCONC,CONC,PH,WATC,WATAVG,WATPH,GWATC,EMRATE,
     &   EROTOT,DTAIL,
     &   AIRC,SOILC,AVEGC,BVEGC,SUFOC,BRWSC,LICHC,AQVEGC,FISHC,
     &   AMOC,WMOC,ACARC,WCARC,WATD,SHINED,INHD,RADD,VEGD,FISHD,
     &   MEATD,DOSE,POPDT,
     &   BLANK1,BLANK2


C FILE 'RECEP.INC'
C
      INTEGER*2 NRECEP,NRING,RDIR(80),RRING(80),RWSSEG(80),
     &   RPOP(80),NREC,NDREC
      REAL*4 RNGMID(5),RAREA(5),TAREA
      CHARACTER*1 RTYPE(80)
      COMMON /RECEPT/ NRECEP,NRING,RDIR,RRING,RWSSEG,RPOP,RNGMID,RTYPE,
     &   RAREA,NREC,TAREA,NDREC
C
      INTEGER*2 NSEG,NODDIR(10),NODRNG(10),PSDIR(10),
     &   PSRING(10),PSNUM,GSEG
      CHARACTER*1 STYPE (10)
      REAL*4 SDEPTH(10), LAREA(10), SHEDAR(10),LAKVOL(10),PSAREA
      COMMON /WATER/ NSEG,NODDIR,NODRNG,STYPE,SDEPTH,LAREA,
     &   SHEDAR,LAKVOL,PSDIR,PSRING,PSNUM,PSAREA,GSEG


C FILE 'STATS.INC'
C
      DOUBLE PRECISION KURT(600), GMEAN(600), GSDEV(600), XMAX(600),
     &                  XMIN(600), SDEV(600), SKEW(600),S1(600)
      COMMON /STATS/ KURT, GMEAN, GSDEV, XMAX, XMIN, SDEV,SKEW,S1
```

```
C FILE 'COUNTS.INC'
C
      INTEGER*2 TFILE(12),TSTAT(12),NSTEPS,NSTEPF,NUMS,NUMF,TNUMS,TNUMF,
     &   TNUMBS,TNUMBF
      COMMON /TSTEP/ TFILE,TSTAT,NSTEPS,NSTEPF,NUMS,NUMF,TNUMS,TNUMF,
     &   TNUMBS,TNUMBF
C
      INTEGER*4 NSTART
      INTEGER*2 NPARM,NCELLS, NBETA,NARB
      COMMON /DISNUM/ NSTART, NPARM, NCELLS, NBETA,NARB
C
      INTEGER*2 NUMTRL, NTRIAL, NYEARS, NDT,NT
      REAL*4 T,RYEARS,DT
      COMMON /TIME/ T, NUMTRL, NTRIAL, NYEARS, NDT,RYEARS,DT,NT
C
      CHARACTER*1 EFLAG(250)
      COMMON /FLAGE/ EFLAG
C
      INTEGER*2 VARY, VARN, VARIED(250), VARNOT(250)
      COMMON /TIMEV/ VARY, VARN, VARIED, VARNOT
C
      INTEGER*2 NSTAT,NFILE,NVARYS,NVARYF,VARYS,VARYF,NOUT,NOUTS,NOUTF
      COMMON /NUMSAV/ NSTAT,NFILE,NVARYS,NVARYF,VARYS,VARYF,NOUT,NOUTS,
     &   NOUTF


C FILE 'INFO.INC'
C
      INTEGER*2 NVAR(100), NSUB(300), LOC(300), NARRAY
      CHARACTER*1 FLAG(300)
      COMMON /INFO/ NVAR, NSUB, LOC, FLAG, NARRAY


C FILE 'OUT.INC'
C
      REAL*4 XOUTF(300),XOUTS(300)
      COMMON /OUT/ XOUTF,XOUTS


C FILE 'INPT.INC'
C
      REAL*4 XIN(250)
      COMMON /INPT/ XIN


C FILE 'INPT2.INC'
C
      REAL*4 XVALUE(250)
      COMMON /INPT/ XVALUE


C FILE 'UPDATE.INC'
C
```

```
      DOUBLE PRECISION S2(600),S3(600),S4(600),GS1(600),GS2(600)
      INTEGER*2 N(600), GN(600)
      COMMON /TEST/ S2,S3,S4,GS1,GS2,N,GN


C FILE 'PARAM.INC'
C
      INTEGER*2 NTYPE(250), NACELL(250), CORNUM(250)
      REAL*4 P1(250), P2(250), P3(250), P4(250), P5(250)
      COMMON /PARAM/ NTYPE, NACELL, P1, P2, P3, P4, P5, CORNUM
C
      REAL*4 UNIT(250), CPF(250,25), ORIGIN(250), V(250,25)
      COMMON /VAL/ UNIT, CPF, ORIGIN, V


C FILE 'INTERM.INC'
C
      REAL*4 DUMMY(4000)
      COMMON /INTERM/ DUMMY
      INTEGER*2 INTS(100)
      COMMON /INTGER/ INTS
      CHARACTER*1 CHR(100)
      COMMON /CHAR/ CHR
      REAL*8 REAL8(1500)
      COMMON /RR8/ REAL8


C FILE 'WIND.INC'
C
      CHARACTER*1 WINDFG
      REAL*4 FWINDT,FWIND1(16),FWIND2(16,6),UWIND(16,6),FWIND(16,6,6,20)
      COMMON /WIND/ FWINDT,FWIND1,UWIND,FWIND2,FWIND,WINDFG
```

## APPENDIX C

# TESTING OF RANDOM NUMBER GENERATOR UNIRAN

by

Park M. Reilly, Ph.D.
Waterloo, Ontario

for

SENES Consultants Limited
Willowdale, Ontario

December 1985

## ABSTRACT

In Phase II of the probabilistic assessment study undertaken by SENES for the NUTP, the random number generator UNIRAN was incorporated into the system code. The program generates uniformly distributed random numbers in the interval 0 to 1 and is claimed by its authors to have excellent global statistical properties and to be highly portable from one computer system to another. This paper describes the results and findings of a set of additional tests which were carried out to verify these claims.

# TESTING OF RANDOM NUMBER GENERATOR UNIRAN

## C.1 INTRODUCTION

SENES Consultants Limited have implemented on their computer system the random number generator UNIRAN which is described by Marse and Roberts (1983). The program generates uniformly distributed random numbers on the interval (0,1) and is said by its authors to have excellent global statistical properties. This report describes a short series of statistical tests which were performed on a set of 5000 numbers generated by the program at SENES and on a second set of 5000 generated at University of Waterloo.

The paper by Marse and Roberts describes the tests of distribution and independence on which they base their favourable claim about statistical properties. The tests which are described in this report include simple tests for distribution and independence which are slightly different from those used by Marse and Roberts and also include tests on the distribution of the extreme values. They therefore may be regarded as complementary to those of Marse and Roberts.

The testing confirms that the set of numbers examined do indeed have excellent statistical properties. With limitations to be pointed out later, presumably all numbers generated by the program share the same properties.

## C.2 THE DATA SETS

A tape containing a file of 5000 random numbers, one to a line, in format E12.6, was provided by SENES. The original intention was to apply several different tests to them by APL but it was found to be cumbersome and expensive to handle the large file in the University of Waterloo APL system.

Instead, a program was written for the WATFIV system which incorporated the REAL FUNCTION UNIRAN in exactly the form quoted by Marse and Roberts. A sequence of 5000 numbers generated by it using the same seed (913566091) as that used by SENES was compared with the SENES file. The numbers which were compared were those of the following ordinal numbers in the set: 1-25, 500, 1000, 1500, 2000...,4500, 5000. In every case they were identical except that the format used by SENES was E12.6 while that on the Waterloo system was F10.7. This comparison justified the decision that all numbers for testing be generated by the WATFIV program. It is also partial confirmation of the claim by Marse and Roberts that the program is portable.

For confirmation of the tests, every one was repeated on a second set of 5000 numbers generated by UNIRAN at the University of Waterloo using the seed 1938444429 which was chosen by a random process. The SENES set is called Set 1 in this report, the Waterloo set is called Set 2.

## C.3 THE MEAN

The arithmetic means of the two sets are 0.5000798 and 0.5034284. They may be considered observations on a normally distributed random variable with mean 0.5 and variance 1/(12x5000). Thus the corresponding standardized values are 0.0195 and 0.8398. The probabilities of a standardized normal variate exceeding these values are 0.4922 and 0.2005, which are very ordinary ones. Hence, we have failed, at any confidence level over 80%, to disprove the null hypothesis. This test, like the others to follow is based on the null hypothesis that the two sets of 5000 consist entirely of independent observations on the uniform (rectangular) distribution covering the interval (0,1). This test gives elementary confirmation that the distribution of the numbers is correct.

## C.4 THE AUTOCORRELATION FUNCTION

The sample autocovariance function is written $C_L$, L=0,1,2,... where

$$C_L = \frac{1}{5000} \sum_{i=1}^{5000-L} (X_i - \bar{x})(X_{i+L} - \bar{x}) \qquad (1)$$

In this equation $X_i$ is the ith random number and x is the average of all of the random numbers in the set. The sample autocovariance function is used to calculate the sample autocorrelation function $r_L$ defined by

$$r_L = \frac{C_L}{C_0} \quad , L = 0,1,2,... \qquad (2)$$

providing L is small relative to 5000. The sample autocorrelation functions for L up to 20 are shown in Table C.1 for the two sets.

Box and Jenkins (1976) describe how, under our null hypothesis, the $r_L$ may be considered approximately normally distributed with mean zero and variance 1/5000.

Consequently, the 95% confidence interval for an individual autocorrelation includes all those possibilities with absolute value less than 1.9600 x $\sqrt{1/5000}$ = 0.0277. Thus, in a set of 20 autocorrelations, all of which are truly zero, there will be a mathematical expectation of one with absolute value greater than 0.0277. Here there happens to be exactly one in each list. It is reasonable to conclude therefore that no autocorrelations are truly different from zero.

Figures C.1 and C.2 show the autocorrelation functions graphically. The fact that there seems to be a slight sinusoidal tendency in both figures is a consequence of the estimation procedure and does not seriously compromise the tests on these functions.

A further property of the autocorrelation function under the null hypothesis is that successive autocorrelations are nearly independent (Jenkins and Watts, 1968). This is supported by the fact that tests on the sequence of signs in the autocorrelation functions of Table C.1 show no evidence of non-randomness. A consequence of this property is that the sum of the squares of the autocorrelations divided by the variance of a single autocorrelation is distributed as $\chi^2$ with, in this case, 20 degrees of freedom. For the two sets these quantities are 17.483 and 14.604; their probabilities of being exceeded by $\chi_{20}^2$ are about 62.5% and 80% respectively. Hence, we have failed, at any confidence level over 40%, to disprove the null hypothesis. The fact that probabilities are ordinary ones indicates that overall the autocorrelations are of a magnitude to be expected from a set of independent random numbers.

The overall conclusion of the work on the autocorrelation function is that both sets of numbers may reasonably be considered to be independent.

## C.5 THE PROBABILITY DISTRIBUTION

The range of the numbers was divided into 100 cells and each of the 5000 members of each set was assigned to its cell according to $0.01(j-1) \leq X_i < 0.01j$, $j = 1,2,\ldots,100$ for the jth cell, where $X_i$ is the ith member of its set.

The most generally accepted test of the overall frequency distribution is the $\chi^2$ test which is discussed in almost all books on statistics. The criterion is:

$$K = \sum_{j=1}^{100} \frac{(n_{oj} - n_{ej})^2}{n_{ej}} \tag{3}$$

where $n_{oj}$ is the observed number of counts in the jth cell and $n_{ej}$ is the expected number of counts in the jth cell. Here $n_{ej} = 50$ for every cell according to our null hypothesis. For the two sets the values of K are 113.48 and 92.52. In cases like this one, the criterion is compared with $\chi^2$ with degrees of freedom equal to the number of cells less 1. The probabilities of $\chi^2_{99}$ exceeding these values of K are 0.152 and 0.664, which give no reason to conclude that the random numbers are not uniformly distributed. In particular, we have failed, at any confidence level over 85%, to disprove the null hypothesis.

Table C.1

## AUTOCORRELATION FUNCTIONS

| L | Set 1 | Set 2 |
|---|---|---|
| 1 | -.0245 | -.0046 |
| 2 | -.0136 | .0156 |
| 3 | -.0154 | -.0120 |
| 4 | .0303 | -.0248 |
| 5 | .0086 | .0135 |
| 6 | -.0135 | .0183 |
| 7 | -.0011 | .0019 |
| 8 | .0006 | .0041 |
| 9 | -.0082 | -.0020 |
| 10 | -.0017 | .0088 |
| 11 | .0039 | .0287 |
| 12 | -.0026 | .0003 |
| 13 | .0156 | -.0020 |
| 14 | .0138 | -.0097 |
| 15 | -.0048 | -.0034 |
| 16 | .0206 | -.0128 |
| 17 | .0173 | .0011 |
| 18 | .0039 | .0087 |
| 19 | .0005 | .0102 |
| 20 | .0032 | -.0003 |

FIGURE C.1

AUTOCORRELATION FUNCTION
FOR SET 1

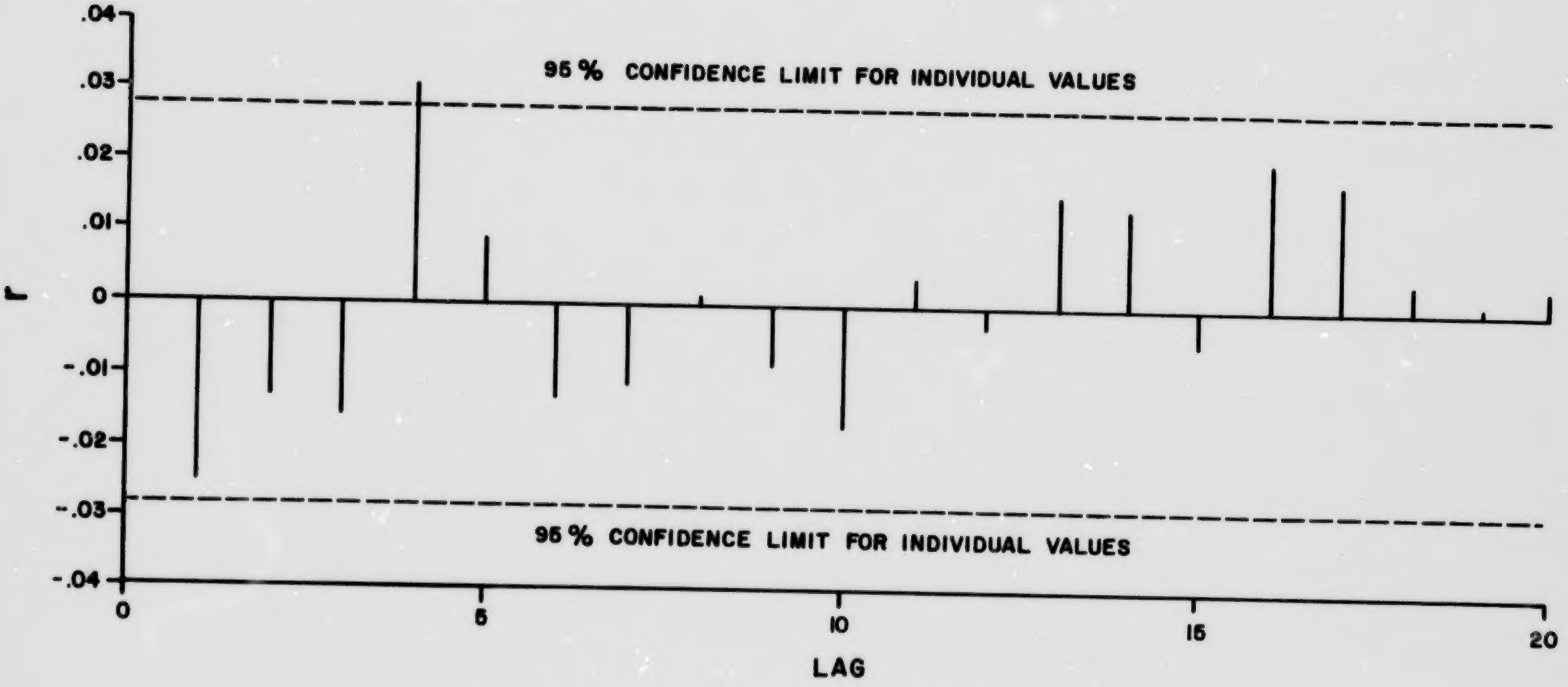

FIGURE C.2

AUTOCORRELATION FUNCTION
FOR SET 2

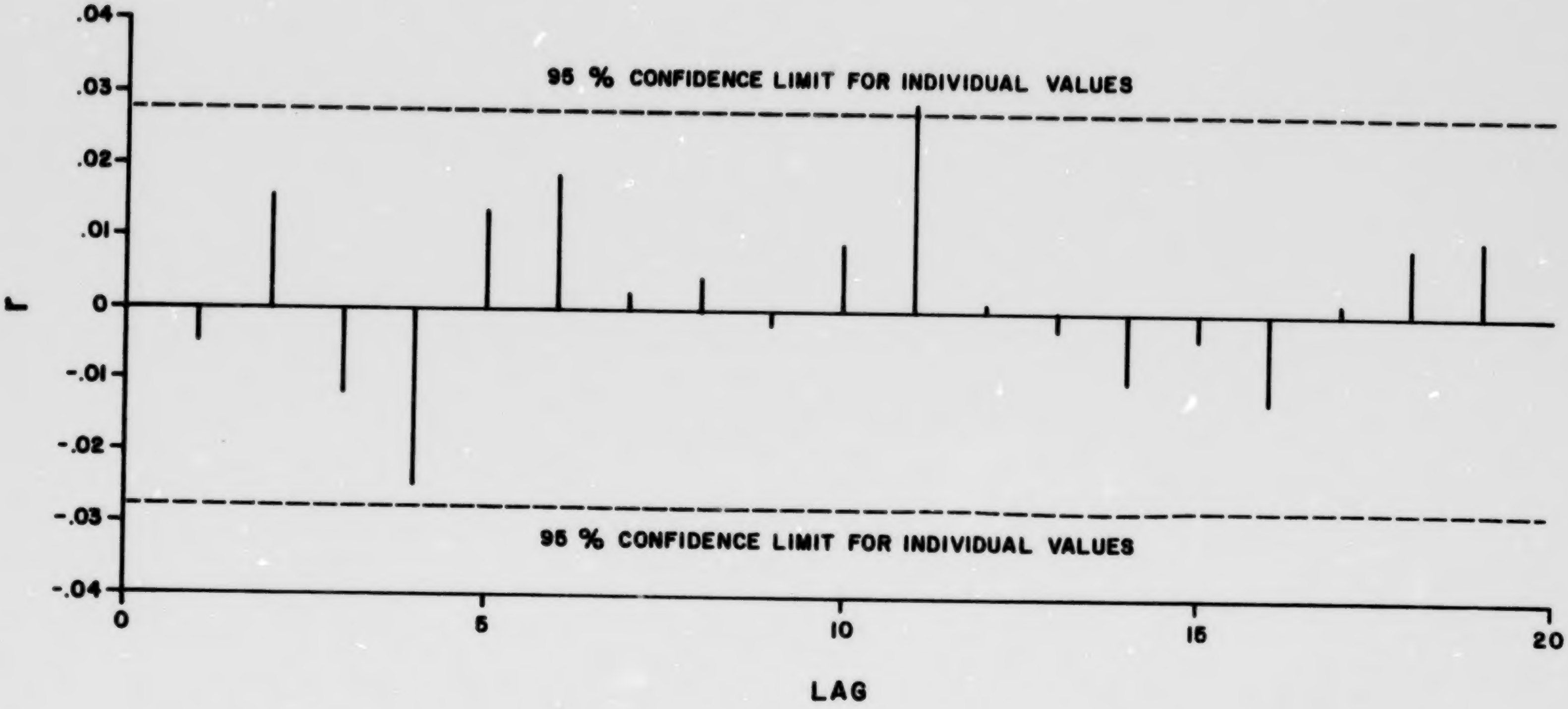

The overall conclusion of the tests on distribution is that there is no evidence that the random numbers are not uniformly distributed on the interval 0 to 1.

## C.6 EXTREME VALUES

Much of the work done by SENES is characterized by special interest in extreme values of the output variables of Monte Carlo calculations, which in turn are often the consequence of extreme values of the random variables which are used. This justifies extra attention to the extreme values in tests of randomness. Columns 2 and 4 of Table C.2 show the 20 largest and the 20 smallest, respectively, numbers in Set 1. Columns 2 and 4 of Table C.3 show the corresponding information for Set 2.

The cumulative probability function for the largest of 5000 observations on a uniformly distributed random variable with the range 0 to 1 is

$$F_1(b_1) = Pr(B_1 \leq b_1) = b_1^{5000} \tag{4}$$

where $B_1$ is the largest of the 5000 random numbers and $b_1$ is a possible value for $B_1$. Note carefully that throughout this section capital letters are used for random variables in the abstract, while lower case letters are used for specific possible values of the random variable. The choice of letter and subscript identify the random variable. Thus equation (4) refers to the probability that the largest of 5000 observations (as yet unrealized) will be equal to or less than a given particular number $b_1$.

Similarly, the cumulative probability function for the smallest $S_1$ is

$$G_1(s_1) = Pr(S_1 \leq s_1) = (1-s_1)^{5000} \tag{5}$$

The ith largest, $B_i$, given that the i-1 largest has the observed value $b_{i-1}$, has cumulative probability function

$$F_i(b_i|b_{i-1}) = Pr[(B_i \leq b_i)\ b_{i-1}] = \left(\frac{b_i}{b_{i-1}}\right)^{5001-i} \qquad (6)$$

where the notation "$b_i|b_{i-1}$" is read, "$b_i$ given $b_{i-1}$".
The ith smallest, $S_i$, given that the i-1 smallest has the observed value $s_{i-1}$, has cumulative probability function

$$G_i(s_i\ s_{i-1}) = Pr[(S_i \leq s_i)\ s_{i-1}] = \left(\frac{1-s_i}{1-s_{i-1}}\right)^{5001-i} \qquad (7)$$

The ith entry in Column 3 of Tables C.2 and C.3 gives $F_i\ (b_i\ b_{i-1})$ as in equations (4) or (6) where $b_i$ and $b_{i-1}$ are the observed values given in Column 2. Accordingly it is the probability that the ith largest of a set of 5000 random numbers would be equal to or less than the observed value $b_i$, given that the i-1 largest has the observed value $b_{i-1}$. In other words, 100 times the ith entry in Column 3 is the percentile to which the observed value $b_i$ belongs in its theoretical distribution, given the observed value $b_{i-1}$.

Similarly, the ith entry in Column 5 of Tables C.2 and C.3 gives, as one interpretation, the probability that the ith smallest of a set of 5000 random numbers would be equal to or less than the observed value $s_i$, given that the i-1 smallest has the observed value $s_{i-1}$.

The transformation of numbers in Columns 2 and 4 of Tables C.2 and C.3 to those in Columns 3 and 5 is a probability integral transformation and hence the entries in Columns 3 and 5 should be independent observations on a uniformly distributed random variable over the interval 0 to 1. That is, random variables drawn from any known distribution are just as likely to be chosen from one percentile as another, and therefore if the entries in Columns 2 and 4 have the distributions given by equations (6) and (7) as our null hypothesis postulates, the entries in Columns 3 and 5 will be independently and uniformly distributed over the range of possible probabilities, i.e. from 0 to 1.

Table C.2

## EXTREME VALUES FOR SET 1

| Col 1<br><br>i | Col 2<br><br>$b_i$, the ith largest number | Col 3<br><br>$F_i(b_i \mid b_{i-1}) = \Pr[(B_i < b_i) \mid b_{i-1}]$ | Col 4<br><br>$s_i$, the ith smallest number | Col 5<br><br>$G_i(s_i \mid s_{i-1}) = \Pr[(S_i < s_i) \mid s_{i-1}]$ |
|---|---|---|---|---|
| 1 | .9999134 | .6485 | .0000224 | .8940 |
| 2 | .9994709 | .1094 | .0002740 | .2842 |
| 3 | .9994344 | .8332 | .0003294 | .7581 |
| 4 | .9983467 | .0043 | .0011582 | .0158 |
| 5 | .9982921 | .7609 | .0012103 | .7706 |
| 6 | .9981729 | .5508 | .0014213 | .3481 |
| 7 | .9976886 | .0886 | .0015388 | .5556 |
| 8 | .9976395 | .7821 | .0015475 | .9574 |
| 9 | .9975800 | .7425 | .0017264 | .4088 |
| 10 | .9974545 | .5337 | .0017309 | .9778 |
| 11 | .9971828 | .2568 | .0020071 | .2514 |
| 12 | .9970935 | .6397 | .0021986 | .3839 |
| 13 | .9968503 | .2962 | .0024448 | .2920 |
| 14 | .9965739 | .2508 | .0029973 | .0631 |
| 15 | .9963459 | .3195 | .0031534 | .4581 |
| 16 | .9961917 | .4623 | .0032626 | .5792 |
| 17 | .9959640 | .3200 | .0034738 | .3478 |
| 18 | .9959487 | .9263 | .0035134 | .8204 |
| 19 | .9958612 | .6455 | .0037289 | .3404 |
| 20 | .9955929 | .2613 | .0039795 | .2856 |

Table C.3

## EXTREME VALUES FOR SET 2

| Col 1 | Col 2 | Col 3 | Col 4 | Col 5 |
|---|---|---|---|---|
| $i$ | $b_i$, the ith largest number | $F_i(b_i \mid b_{i-1}) = \Pr[(B_i < b_i) \mid b_{i-1}]$ | $s_i$, the ith smallest number | $G_i(s_i \mid s_{i-1}) = \Pr[(S_i < s_i) \mid s_{i-1}]$ |
| 1 | .9999124 | .6453 | .0000916 | .6325 |
| 2 | .9996929 | .3337 | .0004264 | .1875 |
| 3 | .9996750 | .9144 | .0012376 | .0173 |
| 4 | .9994931 | .4028 | .0014094 | .4233 |
| 5 | .9993739 | .5511 | .0014835 | .6902 |
| 6 | .9991823 | .3838 | .0020539 | .0576 |
| 7 | .9990094 | .4214 | .0022143 | .4481 |
| 8 | .9988546 | .4613 | .0025452 | .1909 |
| 9 | .9986768 | .4112 | .0025540 | .9569 |
| 10 | .9984720 | .3593 | .0029274 | .1543 |
| 11 | .9982547 | .3375 | .0031530 | .3233 |
| 12 | .9982324 | .8945 | .0034409 | .2367 |
| 13 | .9980888 | .4879 | .0041320 | .0314 |
| 14 | .9978625 | .3228 | .0042314 | .6079 |
| 15 | .9974367 | .1191 | .0042395 | .9603 |
| 16 | .9973877 | .7828 | .0045989 | .1721 |
| 17 | .9973711 | .9204 | .0047571 | .4351 |
| 18 | .9972803 | .6353 | .0049321 | .4163 |
| 19 | .9972534 | .8743 | .0050814 | .4735 |
| 20 | .9962562 | .0069 | .0051499 | .7097 |

Columns 3 and 5 look good in both tables. They can be tested formally by a Kolmogorov-Smirnov test.

Consider the range 0 to 1 of a uniformly distributed random variable U to be divided into 20 sub-intervals,

$$0.05\,(i-1) \leq U < 0.05i,\ i = 1,2,\ldots,20 \qquad (8)$$

Let the null hypothesis be that a sample of size 20 on U, except only for sampling error, will consist of one observation at the midpoint of each of these sub-intervals. This is a reasonable consequence of the uniformity of the distribution of U. Then, if the entries in Columns 3 or 5 from Table C.2 or C.3 are arranged in increasing order, their values should depart only through sampling error from

$$H(i) = 0.025 + 0.05(i-1),\ i = 1,2,\ldots,20 \qquad (9)$$

which is the probability that a random observation on U is equal to or less than the mid-point value of the ith sub-interval described by equation (8). It is easy to test this by the Kolmogorov-Smirnov test.

The Kolmogorov-Smirnov test is based on the maximum difference in probability between the postulated cumulative probability function and the sample cumulative probability function. Figure C.3 shows the graph of these functions for the first few largest observations in Set 1. The step-like graph P(i) is the sample cumulative probability function. Any point on a horizontal section of the graph, except the point at the extreme right end of the section, gives the fraction of the sample ("probability") accumulated by the i, i-1, ...,2,1 smallest probabilities in the sample. The straight line labelled H(i) is the graph of equation (9).

The same information is given in Table C.4. Column 2 gives the numerical values of H(i) from equation (9) for i-1,2,...,20.

Column 3 gives the same quantities as in Column 3 of Table C.2, arranged in increasing order. The heading of Column 3 in Table C.4 is labelled $P(i)^{(1)}$ to indicate that it gives the probability for the top value of each vertical line in the graph of P(i) in Figure C.3. Similarly Column 5 of Table C.4 gives the probability corresponding to the bottom value of each vertical line in Figure C.3. The values $a_i$ and $b_i$, i=1,2,...,20 are the vertical distances between $H_i$ and $P(i)^{(1)}$ for $a_i$, and between $H_i$ and $P(i)^{(2)}$ for $b_i$. The absolute values of $a_i$ and $b_i$ are given in Columns 4 and 6 of Table C.4. The quantity D required by the test is the largest in absolute value of the combined set of all of the $a_i$ and $b_i$. From Table C.4, for the 20 largest members of Set 1 it is 0.1550. Under our null hypothesis the probability of this number being exceeded by chance alone is in the neighbourhood of 40% (see Crow, Davis and Maxfield, 1960; and Kreyszig, 1970) and therefore we fail to prove that the largest 20 numbers in Set 1 do not have the expected distribution.

Table C.5 gives the observed values of D for the 20 largest and 20 smallest of Sets 1 and 2 along with their probability values. They are all seen to be reasonable. Thus we may conclude that the extreme values for both sets have the expected distribution and presumably therefore the UNIRAN generator ordinarily produces extreme values which have the expected distribution in sets of 5000 random numbers.

## C.7 VALUE NEAR ZERO AND UNITY

If the random number seed were exactly zero, all succeeding numbers would also be zero and the generator would collapse. Similar, but not as catastrophic, difficulty could result from the use of too large a seed.

In both sets of numbers used in these tests, the sequence of numbers preceding and following the smallest and largest few were examined by eye and they appeared to be unaffected by their proximity to extreme values.

Table C.4

## CALCULATION OF D FOR KOLMOGOROV-SMIRNOV TEST FOR COLUMN 3 OF TABLE C.2

| Col 1 i | Col 2 H(i) | Col 3 P(i)(1) | Col 4 $\lvert a_i \rvert$ | Col 5 P(i)(2) | Col 6 $\lvert b_i \rvert$ |
|---|---|---|---|---|---|
| 1 | .025 | .0043 | .0207 | 0 | .025 |
| 2 | .075 | .0886 | .0136 | .0043 | .0707 |
| 3 | .125 | .1094 | .0156 | .0886 | .0364 |
| 4 | .175 | .2508 | .0758 | .1094 | .0656 |
| 5 | .225 | .2568 | .0318 | .2508 | .0258 |
| 6 | .275 | .2613 | .0137 | .2568 | .0182 |
| 7 | .325 | .2962 | .0288 | .2613 | .0637 |
| 8 | .375 | .3195 | .0555 | .2962 | .0788 |
| 9 | .425 | .3200 | .1050 | .3195 | .1055 |
| 10 | .475 | .4623 | .0127 | .3200 | .1550* |
| 11 | .525 | .5337 | .0087 | .4623 | .0627 |
| 12 | .575 | .5508 | .0242 | .5337 | .0413 |
| 13 | .625 | .6397 | .0147 | .5508 | .0742 |
| 14 | .675 | .6455 | .0295 | .6397 | .0353 |
| 15 | .725 | .6485 | .0765 | .6455 | .0795 |
| 16 | .775 | .7425 | .0325 | .6485 | .1265 |
| 17 | .825 | .7609 | .0641 | .7425 | .0825 |
| 18 | .875 | .7821 | .0929 | .7609 | .1141 |
| 19 | .925 | .8332 | .0918 | .7821 | .1429 |
| 20 | .975 | .9263 | .0487 | .8332 | .1418 |

* referenced in text

FIGURE C.3

**METHOD OF FINDING 'D'
FOR KOLMOGOROV-SMIRNOV TEST**

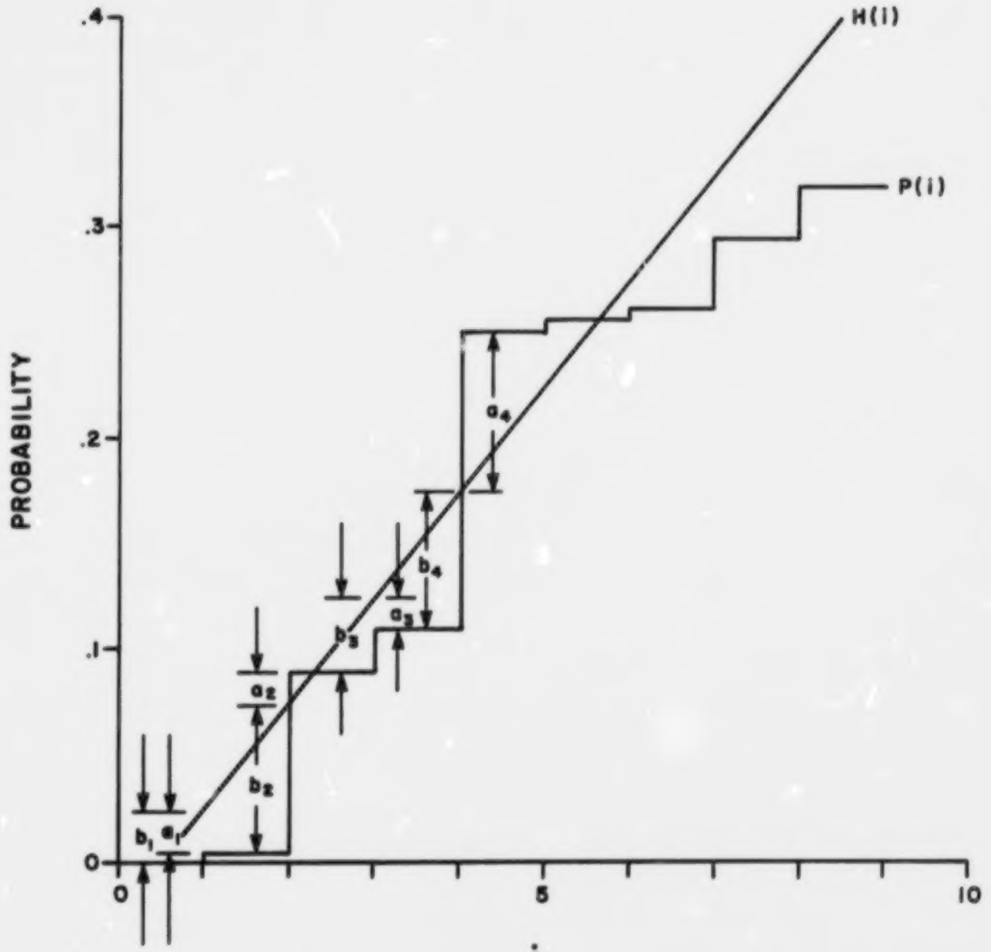

Table C.5

## VALUES OF D FROM KOLMOGOROV-SMIRNOV TESTS

| Set of Extreme Values | D | Approximate Probability of Larger D |
|---|---|---|
| Set 1 - Largest 20 | .1550 | .40 |
| Set 2 - Largest 20 | .1978 | .30 |
| Set 1 - Smallest 20 | .1669 | .35 |
| Set 2 - Smallest 20 | .2514 | .15 |

## C.8 CONCLUSION

The testing reported here was a considerable extension of that done by Marse and Roberts. However, for the two sets of 5000 numbers which were examined, there was no reason found to challenge their conclusion of excellent global statistical properties. As they point out however there may be local sets, i.e. say 5000 numbers generated from some particular seed, which may have undesirable properties. In fact it is a necessary consequence of the property of randomness that some such sets must exist.

## REFERENCES

Box, A.E.P. and Jenkins, G.W., 1976. "Time Series Analysis, Forecasting, and Control". Revised Ed., Holden-Day, p. 32.

Crow, E.L., Davis, F.A. and Maxfield, M.W., 1960. "Statistics Manual." Dover Publications, p. 248

Jenkins, G.M. and Watts, D.G., 1968. "Spectral Analysis and Its Applications". Holden-Day, p. 187.

Kreyszig, E., 1970. "Introductory Mathematical Statistics". Wiley, pp. 254.

Marse, K., and Roberts, S.D., 1983. "Implementing a Portable Fortran Uniform (0,1) Generator". Simulation, October 1983, pp. 135-139.

## APPENDIX D

# COMPARISON OF SELECTED PROBABILISTIC ASSESSMENT TOOLS

by

M.L. Murray, D.B. Chambers, D. I. Beals & B.E. Halbert
SENES Consultants Limited
Willowdale, Ontario

T.H. Andres
Atomic Energy of Canada Limited
Whiteshell Nuclear Research Establishment
Pinawa, Manitoba

M. Henrion
Carnegie-Mellon University
Pittsburgh, Pennsylvania

## ABSTRACT

In this paper, the probabilistic assessment tool RANSIM, developed for application to uranium mill tailings, is compared to two other probabilistic analysis systems. The comparison includes a discussion of the principal features of each system and demonstration of the performance of the systems using a benchmark model. The model selected simulates radon gas release from a uranium tailings area, its atmospheric dispersion and the subsequent exposure of a nearby receptor. The relative importance of the twelve variable input parameters in the model are also assessed in the paper by comparison of the results of a number of different sensitivity/uncertainty analysis techniques.

## COMPARISON OF SELECTED PROBABILISTIC ASSESSMENT TOOLS

### D.1 INTRODUCTION

One of the primary goals of the National Uranium Tailings Program (NUTP) is to develop the capacity to predict the long term effects of uranium mill tailings. Previous studies have demonstrated that a probabilistic approach to modelling can be used to take account of the natural variability and uncertainty in model parameters (SENES, 1984). Using this type of approach, the uncertainty associated with the input parameters is propagated through mathematical models to produce a distribution of calculated results.

In the Phase I study for the NUTP, SENES Consultants Limited identified and implemented a computer program to perform probabilistic analysis. This program, known as OPANAL, was originally developed by Dr. P.M. Reilly for applications in opinion analysis and business decision making (Reilly and Johri, 1969). The program was subsequently modified, renamed and applied in a Phase II study for the NUTP (SENES, 1985). That program, RANSIM, forms the heart of the probabilistic analysis control modules developed in this Phase III project. The previous version (RANSIM) was used for this comparison since it existed in totality at the outset of the Phase III work. All probabilistic functions of RANSIM have been directly incorporated into the current Uranium Tailings Assessment Program (UTAP). Hence, results generated by RANSIM are directly comparable to results generated by UTAP, for the same model(s). Some of the structure of the Phase II system (which RANSIM formed the heart of) has been modified as part of this project.

A number of probabilistic analysis systems have also been developed by other organizations, for various applications. Two such systems, SYVAC and DEMOS, were selected for comparison with RANSIM in this investigation. SYVAC, which stands for SYstems Variability Analysis Code was originally developed for the Canadian Nuclear Fuel Waste Management Program (Dormuth and Sherman, 1981; Wuschke et al., 1981). DEMOS is an interactive probabilistic modelling environment developed by Dr. Max Henrion at Carnegie Mellon University

(Henrion and Morgan, 1985; Henrion and Nair, 1982; Henrion, 1979)

### D.1.1 Objectives

This comparative study was conducted for a number of reasons:

1) As a Quality Assurance (QA) measure. One would expect the results generated by RANSIM (for a given model and set of input parameter distributions) to be very similar to those generated by other probabilistic analysis systems. This is not a rigorous test of the accuracy of any system. It is simply one element in an ongoing QA program applied in the NUTP studies.
2) To examine and compare the techniques used by the various organizations for determining important model parameters. This was to address the ongoing issue of whether the many available techniques for sensitivity and uncertainty analyses produce similar rankings of parameter importance.
3) To qualitatively examine the unique aspects of each system, thus providing information on the current state-of-the-art in probabilistic analysis and indicating areas of potential improvement in our system.

### D.1.2 Outline of the Paper

The paper will, in general, follow the approach used to conduct the comparative study. The benchmark model, including input parameter distributions, is described first. The subsequent sections contain brief descriptions of the three probabilistic analysis systems, a summary of the results generated for the benchmark problem by each, and an outline of the approach to, and results of sensitivity/uncertainty analysis. These results are then compared and discussed. Some further results are presented in the discussion section to clarify specific points.

## D.2 THE BENCHMARK MODEL

Since RANSIM was developed as part of a study to simulate the behaviour of uranium mill tailings, a relevant tailings model was selected for use as a benchmark case. The model simulates radon gas release from a uranium tailings area, its atmospheric dispersion and the subsequent exposure of a nearby receptor.

The mathematical model is outlined in Table D.1, while the input parameters and their assigned distributions are presented in Table D.2. This model was used because of its intermediate level of complexity and easily managed number of variable input parameters. Details regarding its derivation and the physical significance of the parameters and terms are provided elsewhere (SENES, 1984; Lowe et al, 1985). The consequence of interest was taken to be the radiation dose equivalent to the receptor resulting from the inhalation of radon-222 and its daughters. The model was first run deterministically on each of the three systems, to ensure that the model was implemented properly. The model was then evaluated using 250 random trials on each of the systems. The results are outlined in the following sections.

## D.3 RANSIM

### D.3.1 General Description

RANSIM was initially developed as part of the probabilistic analysis system illustrated on Figure D.1. In that application, it was a completely general module which provided the functions necessary for probabilistic analyses. The Parameter Allocation and Control module indicated on the figure acted as an interface between RANSIM and the situation specific simulation models. In the current system (UTAP), RANSIM and PAC have been combined into the "control modules". However, all of the probabilistic functions previously present in RANSIM have been directly transferred to UTAP. Hence the following results and comparisons generated via RANSIM are directly comparable to probabilistic results generated by UTAP. The following discussion considers RANSIM as it existed at the outset of this Phase III study, as illustrated on Figure D.1.

The entire system is coded in IBM FORTRAN and runs on an IBM PC-AT with 512 Kbytes of RAM. The program was also run, with minimal changes, on a Prime minicomputer, to demonstrate its transportability.

The random simulation program (RANSIM) is a variation on the OPANAL program originally developed by Dr. P.M. Reilly (Reilly and Johri, 1969). Its conceptual specifications are outlined in Figure D.2. RANSIM is designed to convert numeric descriptors of many types of distributions into a series of randomly sampled values available for transfer to simulation models. Sampling routines currently available include:

- constant value
- normal
- lognormal
- uniform
- log uniform
- triangular
- beta
- arbitrary
- pairwise correlated.

The beta and arbitrary distribution capabilities allow almost an infinite range of distribution shapes to be specified. Different sampling algorithms are used to sample from each distribution. All depend on a routine to generate random numbers between 0 and 1. The random number generator is based on the UNIRAN algorithm, as outlined by Marse and Roberts (1983).

RANSIM is designed to provide simple rapid feedback from any simulation, as well as to write selected results to disk for further analysis. The immediate feedback is comprised of a variety of summary statistics on either user-specified inputs or calculated parameters. The summary statistics available include: arithmetic mean, arithmetic standard deviation, skewness, kurtosis,

Table D.1

## RADON MODEL

1. Radon Release Rate (Bq.s$^{-1}$)

RNSOUR = ARTLSR*RACNTA*LAMRN*EMANAT*LSUBT*RHOTAL*
((NSUBW*WTSFLX+(12-NSUBW))/12)*exp(-THICK/LSUBC))

LSUBT = (EBKDFC/LAMRN)$^{1/2}$

and

EBKDFC = POROS*.106X10$^{-4}$exp(-0.261*MPCH2O)

2. Atmospheric Dispersion (s.m$^{-3}$)

$P_{0,1}$ = 2.032*FRACT*(WIND*DIST*SIGZED)$^{-1}$*exp(-((HSUBD$^{2}$)*(2*SIGZED$^{2}$)$^{-1}$))

3. Transfer Model: Radon Concentration to Inhalation Dose (Sv.a$^{-1}$.Bq$^{-1}$.m$^{3}$)

$P_{1,10}$ = OCCFAC*DCFIRN

Radon Concentration at Receptor (Bq.m$^{-3}$)

RADCON = RNSOUR*$P_{0,1}$

Dose via Inhalation of Rn-222 (Sv.a$^{-1}$)

DOSRN = RADCON$_{1}$*$P_{1,10}$

Table D.2

## INPUT PARAMETER DISTRIBUTIONS

| Parameter | Definition | Distribution | Descriptors |
|---|---|---|---|
| POROS | porosity of the tailings | constant | 0.4 |
| LAMRN | radon decay constant ($s^{-1}$) | constant | 2.1E-6 |
| ARTLSR | tailings area ($m^2$) | constant | 5.0E5 |
| NSUBW | Number of winter months | constant | 5.0 |
| DIST | effective transport distance (m) | constant | 3.6E3 |
| DCFIRN | radon dose conversion factor ($Sv.a^{-1}.Bq^{-1}.m^3$) | constant | 7.2E-5 |
| MPCH2O | tailings mass water content (%) | triangular | min=5.0; mode=10.0;<br>max=25.0 |
| RACNTA | tailings radium concentration ($Bq.g^{-1}$) | uniform | min=5.0; max=15.0 |
| RHOTAL | tailings density ($g.m^{-3}$) | normal | mean=1.4E6; SD=0.1E6<br>min=1.0E6; max=1.8E6 |
| EMANAT | radon emanation coefficient | triangular | min=0.02; mode=0.2<br>max=0.9 |
| LSUBC | radon diffusion length in cover (m) | uniform | min=0.5; max=1.5 |
| FRACT | fraction of time wind blows to receptor | normal | mean=0.1; SD=0.02<br>min=0.0; max=0.3 |
| WTSFLX | winter/summer radon flux ratio | lognormal | GM*=2.0E-2; GSD**=2.15<br>min=2.0E-3; max=2.0E-1 |
| WIND | wind speed ($m.s^{-1}$) | normal | mean=5.3; SD=0.9<br>min=3.0; max=9.0 |
| SIGZED | vertical dispersion coefficient (m) | lognormal | GM=60.0; GSD=1.73<br>min=10.0; max=300 |
| HSUBD | initial mixing depth (m) | uniform | min=1.0; max.3.0 |
| OCCFAC | occupancy factor | uniform | min=0.3; max=0.9 |
| THICK | tailings cover thickness (m) | triangular | min=0.5; mode=1.0<br>max.2.0 |

* GM refers to Geometric Mean
** GSD refers to Geometric Standard Deviation

## FIGURE D.1

## CONCEPTUAL FLOW DIAGRAM OF SYSTEMS APPROACH

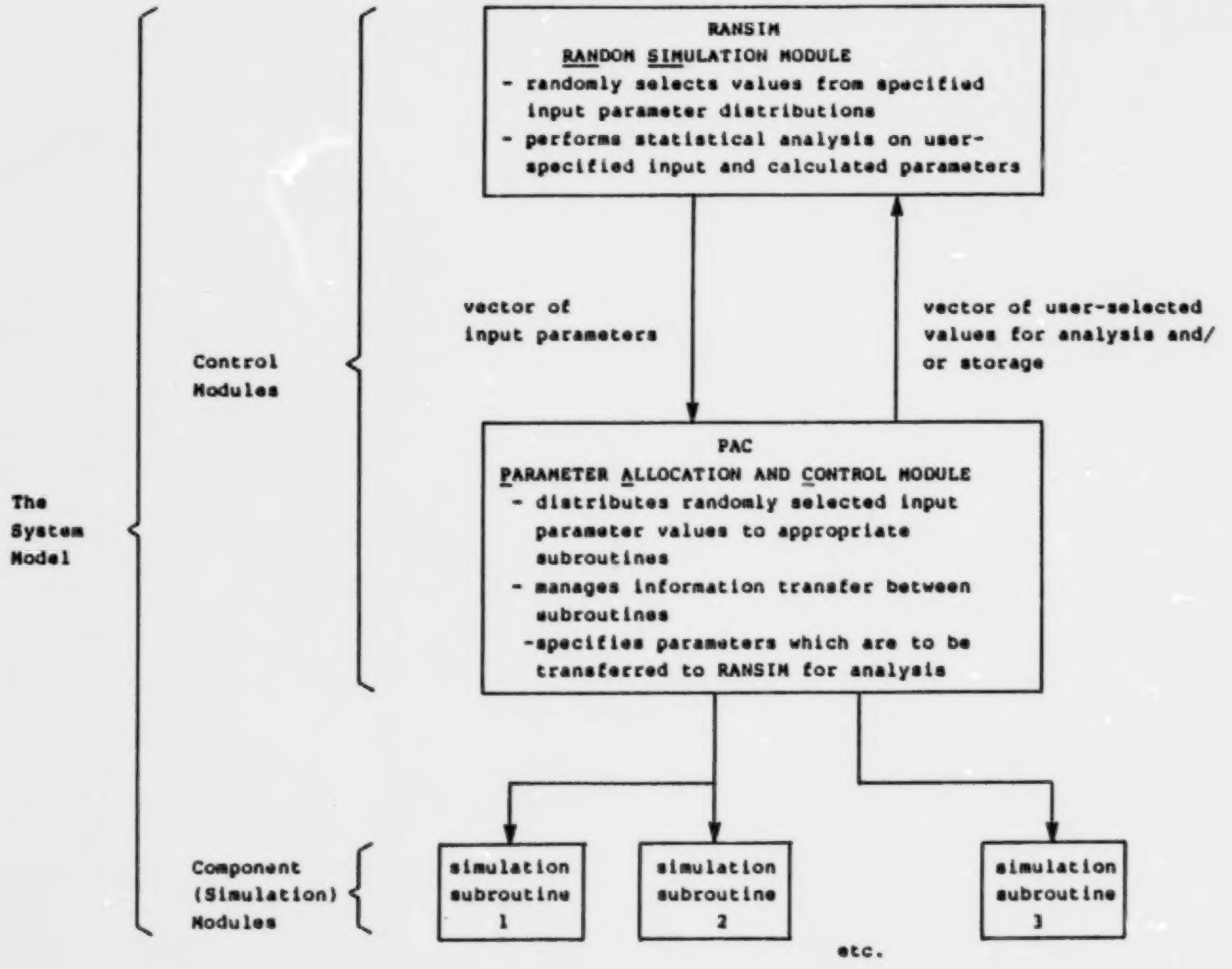
RANSIM
RANDOM SIMULATION MODULE
- randomly selects values from specified input parameter distributions
- performs statistical analysis on user-specified input and calculated parameters
vector of input parameters
vector of user-selected values for analysis and/or storage
PAC
PARAMETER ALLOCATION AND CONTROL MODULE
- distributes randomly selected input parameter values to appropriate subroutines
- manages information transfer between subroutines
-specifies parameters which are to be transferred to RANSIM for analysis
simulation subroutine 1
simulation subroutine 2
simulation subroutine 3
etc.
Control Modules
Component (Simulation) Modules
The System Model

FIGURE D.2

CONCEPTUAL FLOW DIAGRAM OF RANSIM

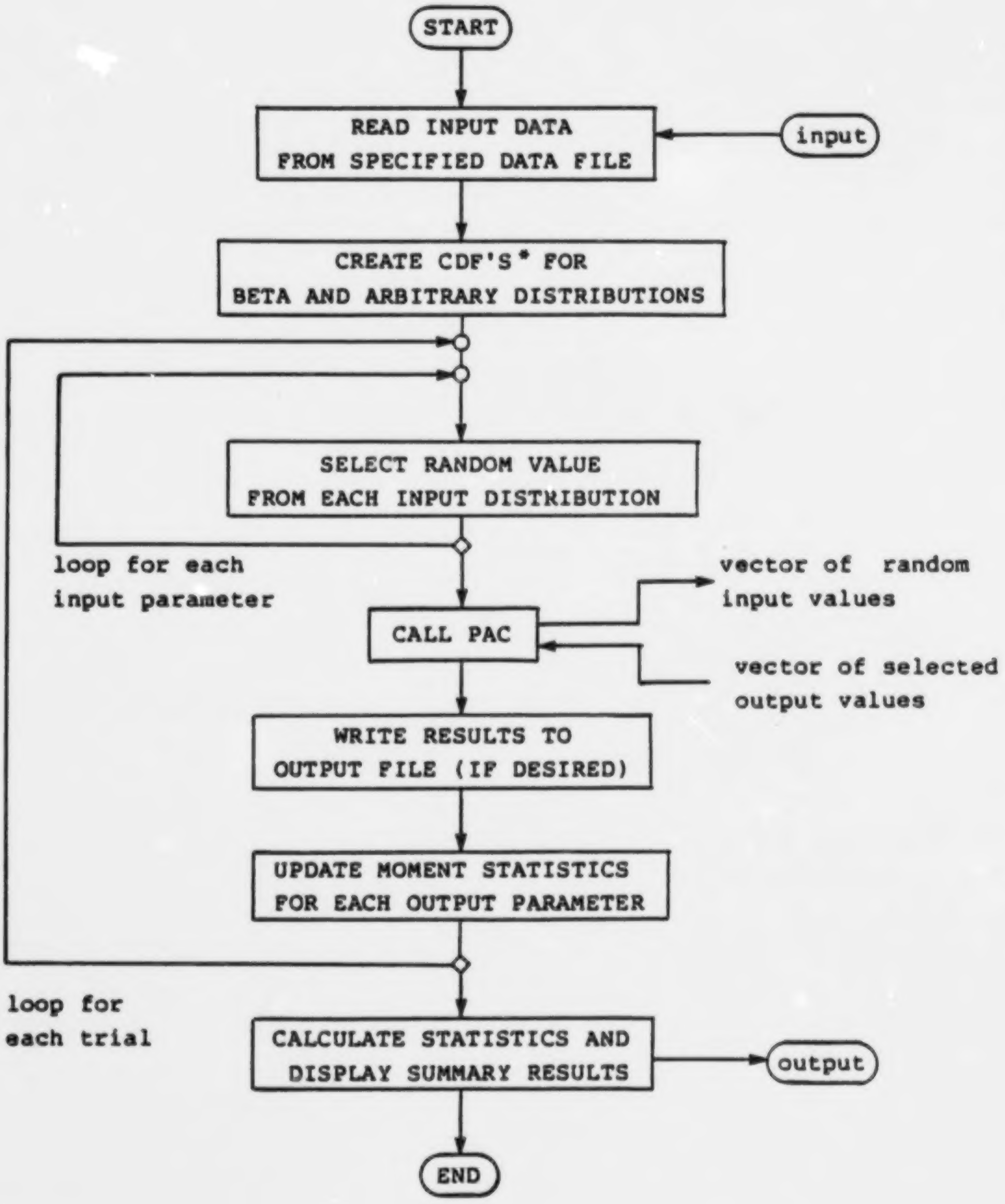
START
READ INPUT DATA FROM SPECIFIED DATA FILE
input
CREATE CDF'S* FOR BETA AND ARBITRARY DISTRIBUTIONS
SELECT RANDOM VALUE FROM EACH INPUT DISTRIBUTION
loop for each input parameter
vector of random input values
CALL PAC
vector of selected output values
WRITE RESULTS TO OUTPUT FILE (IF DESIRED)
UPDATE MOMENT STATISTICS FOR EACH OUTPUT PARAMETER
loop for each trial
CALCULATE STATISTICS AND DISPLAY SUMMARY RESULTS
output
END

* CUMULATIVE DISTRIBUTION FUNCTION

geometric mean, geometric standard deviation, and maximum and minimum values.

These are all calculated using updating ("on-the-fly") methods and thus can be determined regardless of whether one wishes to save all values from all trials or not. They may be most beneficial when the amount of information generated is large and which, if stored, would result in disk storage problems. If one elects to save the results from all trials, they are stored in an output file in a form suitable for subsequent analysis or graphical display by a statistical or graphical package (e.g. SAS, STATGRAPHICS, BMDP, etc).

### D.3.2 RANSIM Results

Summary statistics for all variable input parameters and the consequence of interest (DOSRN) are presented in Table D.3. The summary statistics for the sampled parameters correspond quite well to the parameter specifications (Table D.2). Rigorous statistical tests in previous studies (SENES, 1985) indicated that the distributions as sampled are not significantly different from those specified.

The distribution of the calculated value, DOSRN is displayed as a frequency histogram in Figure D.3(a) and as a cumulative density function (cdf) in Figure D.3(b). These figures, and the graphical presentations of RANSIM results to follow, were generated using STATGRAPHICS, a commercially available statistical/graphical package. Since the distribution of DOSRN is highly skewed, a logarithmic transform was performed. The histogram and CDF for log (DOSRN) are presented in Figure D.4(a) and (b).

### D.3.3 Sensitivity/Uncertainty Analysis: SENES

To avoid many of the disagreements regarding appropriate definitions of sensitivity and uncertainty analysis, we have chosen to refer to them together as "importance analysis". This term is used in the remainder of this section. Two importance analysis techniques were selected for use in this study, namely: stepwise regression and the sensitivity index. Stepwise regression is a relatively complex method of ranking parameters which has considerable statistical support, while the sensitivity index is a simple, more intuitive method. Both are described in more detail below.

The sensitivity index (SI) (Hoffman and Gardner, 1983) provides a simple indication of the response of the model to changes in the input parameters. It is determined by evaluating the model deterministically twice for each input parameter, once with the parameter of interest at its extreme high value and once with the parameter of interest at its extreme low value. All other parameters are held constant at their nominal values. The sensitivity index (for the ith parameter) can then be calculated as:

$$SI_i = 1 - \frac{\text{low calculated result}}{\text{high calculated result}}$$

The closer the SI is to one (i.e. the larger the difference between the high and low calculated results) the more sensitive the model is to the variable.

The sensitivity index must be used with caution since the results will vary depending on the nominal values chosen for the other parameters while examining the effects of one particular parameter. It is also implicitly assumed that the model responds linearly (or nearly so) in a monotically increasing or decreasing fashion over the full range of input parameter values being evaluated. Notwithstanding these limitations, the SI was found to be applicable to all situations and scenarios in which it was used in a previous study (SENES, 1985).

The sensitivity index just described applies, rigorously, only for one set of input parameter values (i.e. at only one point on the "model response surface"). Regression analysis, on the other hand, provides an indication of parameter importance while all parameters are allowed to vary simultaneously over their specified ranges. This type of analysis treats probabilistic results as one would treat the results of many trials of a given experiment. The input parameters represent the independent variables while a calculated

Table D.3

## SUMMARY STATISTICS: RANSIM
(250 Random Simulations)

| Parameter | Mean | Std. Dev. | Geom. Mean | Geom. SD | Minimum | Maximum |
|---|---|---|---|---|---|---|
| RACNTA | 9.625E-00 | 2.871E+00 | 9.186E+00 | 1.365E+00 | 5.032E+00 | 1.494E+01 |
| EMANAT | 4.162E-01 | 1.998E-01 | 3.617E-01 | 1.768E+00 | 4.733E-02 | 8.877E-01 |
| RHOTAL | 1.399E+06 | 9.723E+04 | 1.396E+06 | 1.072E+00 | 1.167E+06 | 1.670E+06 |
| WTSFLX | 2.673E-02 | 2.282E-02 | 1.987E-02 | 2.165E+00 | 2.766E-03 | 1.524E-01 |
| MPCH2O | 1.345E+01 | 4.132E+00 | 1.282E+01 | 1.371E+00 | 5.560E+00 | 2.323E+01 |
| FRACT | 1.012E-01 | 1.943E-02 | 9.923E-02 | 1.225E+00 | 4.379E-02 | 1.559E-01 |
| WIND | 5.234E+00 | 8.771E-01 | 5.160E+00 | 1.186E+00 | 3.140E+00 | 7.502E+00 |
| SIGZED | 6.679E+00 | 3.833E+01 | 5.752E+01 | 1.736E+00 | 1.163E+01 | 2.374E+02 |
| HSUBD | 1.989E+00 | 5.515E-01 | 1.909E+00 | 1.340E+00 | 1.009E+00 | 2.983E+00 |
| LSUBC | 1.027E+00 | 2.939E-01 | 9.823E-01 | 1.362E+00 | 5.016E-01 | 1.500E+00 |
| OCCFAC | 6.208E-01 | 1.687E-01 | 5.962E-01 | 1.340E+00 | 3.012E-01 | 8.996E-01 |
| THICK | 1.165E+00 | 3.024E-01 | 1.125E+01 | 1.309E+00 | 5.189E-01 | 1.938E+00 |
| DOSRN | 3.218E-06 | 4.355E-04 | 1.660E-06 | 3.314E+00 | 9.015E-08 | 2.893E-05 |

## FIGURE D.3a

## RANSIM RESULTS

## FREQUENCY HISTOGRAM: DOSRN

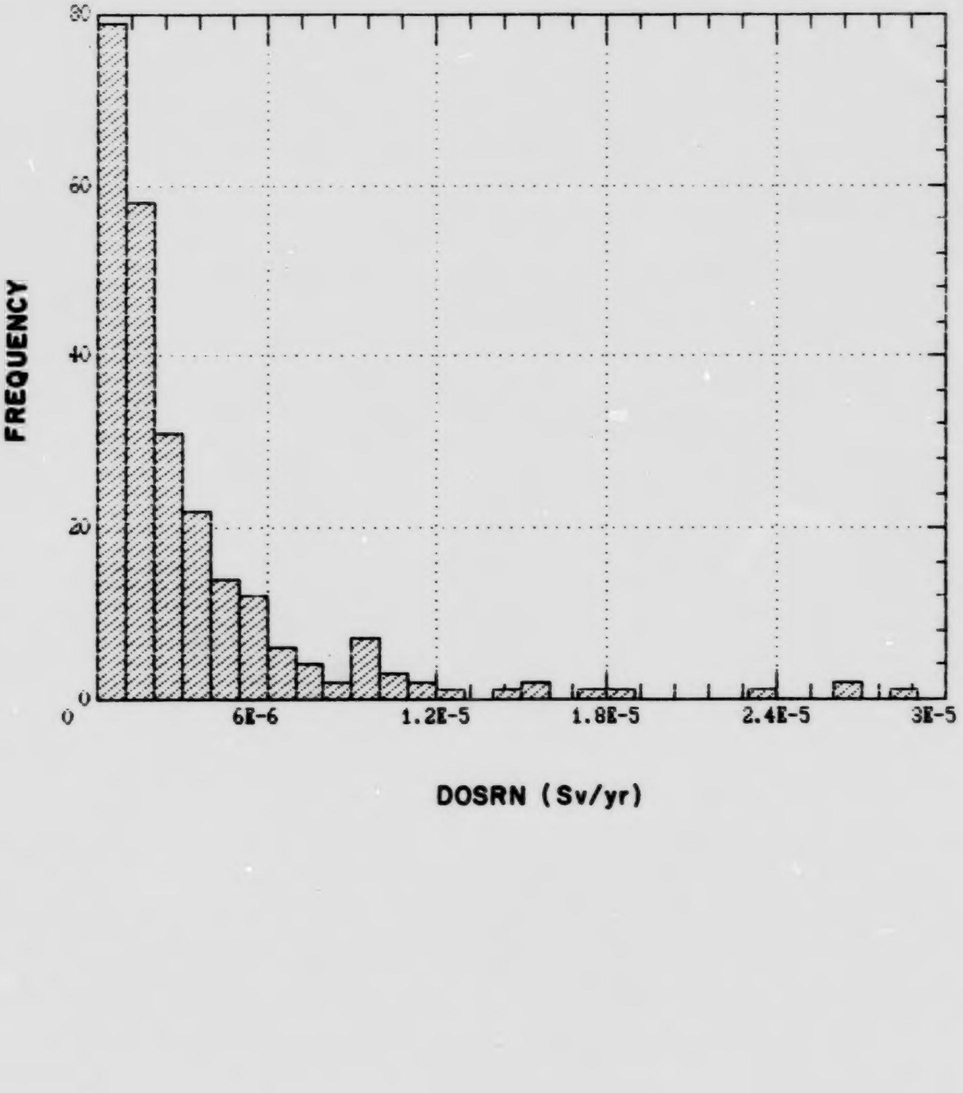

FIGURE D.3b

RANSIM RESULTS
CUMULATIVE RELATIVE FREQUENCY: DOSRN

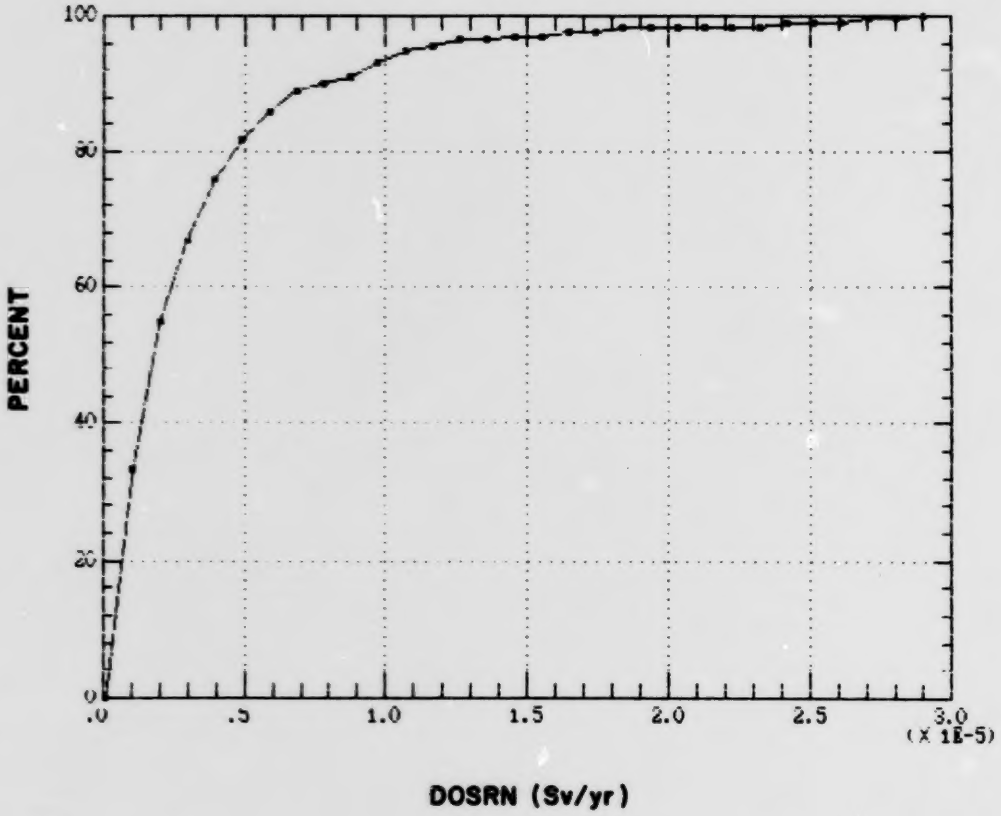

FIGURE D.4a
RANSIM RESULTS
FREQUENCY HISTOGRAM: LOG(DOSRN)

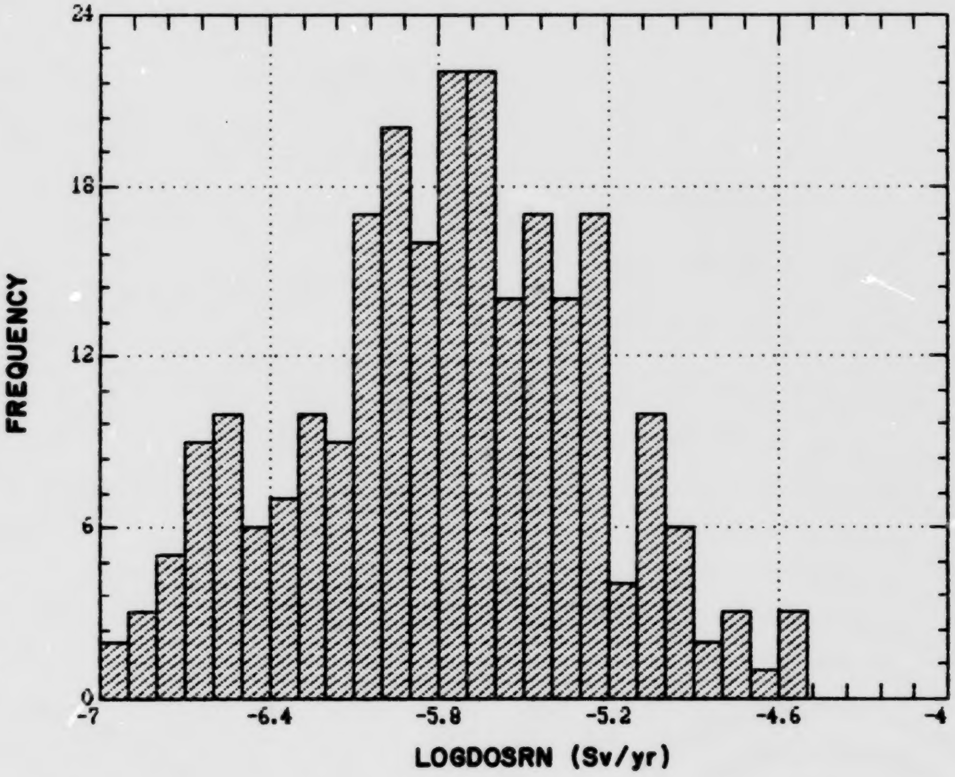

**FIGURE D.4b**

**RANSIM RESULTS**

**CUMULATIVE RELATIVE FREQUENCY: LOG(DOSRN)**

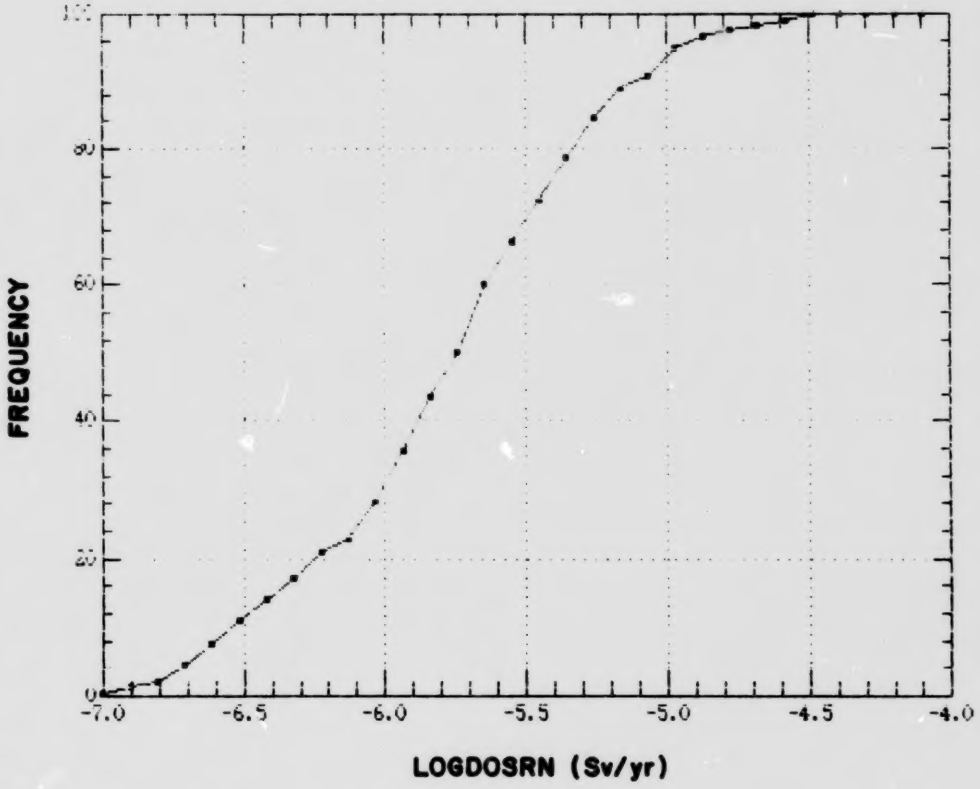

output (eg. DOSRN) is selected as the dependent variable.

Linear regression involves the construction of a linear, predictive equation (using all the independent variables) which accounts for as much of the variation in the dependent variable as possible. The overall correlation coefficient ($R^2$) provides an indication of how much of the variation in the dependent parameter has been accounted for by the given regression equation.

Stepwise linear regression differs somewhat, in that the independent variables are added to the regression equation one-at-a-time, in order of their statistical importance. The order of entry and hence of parameter ranking is based on the relative magnitudes of the "partial correlation coefficients" at each step in the analysis. Thus, a new regression equation, and its associated $R^2$ value are produced at each step in the analysis.

It is easy, in the case of regression analysis to get mired in technical details. However, one must not lose sight of the original objective of the exercise, to identify the important parameters. To emphasize this point, a simplified approach has been taken in presenting the results of stepwise regression.

Table D.4 presents the results of importance analysis, using DOSRN as the dependent variable. The parameters are listed in decreasing order of importance based on the sensitivity index. The magnitude of the sensitivity index is given in the second column, while the ranking based on stepwise regression is given in the third column. Rather than interpreting these results as a strict ranking, we prefer to interpret them as identifying 3 groups of parameters, as indicated. Both methods clearly indicate the three parameters that are the most important. The two methods produce similar parameter groupings with only 2 exceptions (FRACT and HSUBD). We feel that both methods provide useful information regarding parameter importance and should be used to complement each other.

## D.4 SYVAC

The information contained in the following sections was extracted from a discussion paper prepared by T. Andres for SENES Consultants Limited (Andres, 1985).

### D.4.1 General Description

The name SYVAC stands for SYstems Variability Analysis Code. SYVAC is a FORTRAN program originally developed for the Canadian Nuclear Fuel Waste Management Program (Dormuth and Sherman, 1981; Wuschke et al., 1981). The general function of the program is to generate multiple stochastic simulations of a natural system, to determine the environmental impacts of contaminants in the system.

The specific functions of the SYVAC program are shown in Figure D.5. They are:

(1) To run multiple independent simulations. For each simulation,
(2) To sample values of input parameters from probability distributions.
(3) To estimate the total environmental impact by accumulating the effects of multiple independent contaminants (e.g. nuclide decay chains). For each contaminant,
(4) To simulate the behaviour of the entire system by exercising multiple submodels in order.
(5) To assist the modeller by providing a library of routines to manipulate mathematical functions of time, including code to:
    - represent a time function by a time series;
    - add together two time series (e.g. to add together environmental impacts as a function of time);
    - convolute two time series (e.g. to evaluate the output of a model defined by a set of differential equations using an input-response technique).

All simulations in this investigation were carried out using a version of

Table D.4

## SENES IMPORTANCE ANALYSIS RESULTS

| Parameter | Sensitivity Index | Order of Entry In Stepwise Regression | |
|---|---|---|---|
| 1. EMANAT | .98 | 3 | very important |
| 2. MPCH2O | .92 | 2 | |
| 3. SIGZED | .89 | 1 | |
| 4. THICK | .78 | 7 | moderately important |
| 5. LSUBC | .73 | 6 | |
| 6. RACNTA | .67 | 5 | |
| 7. OCCFAC | .67 | 4 | |
| 8. FRACT | .57 | 12 | |
| 9. WIND | .50 | 8 | |
| 10. RHOTAL | .25 | 10 | unimportant |
| 11. WTSFLX | .006 | 11 | |
| 12. HSUBD | .001 | 9 | |

FIGURE D.5

FUNCTIONS OF THE SYVAC PROGRAM

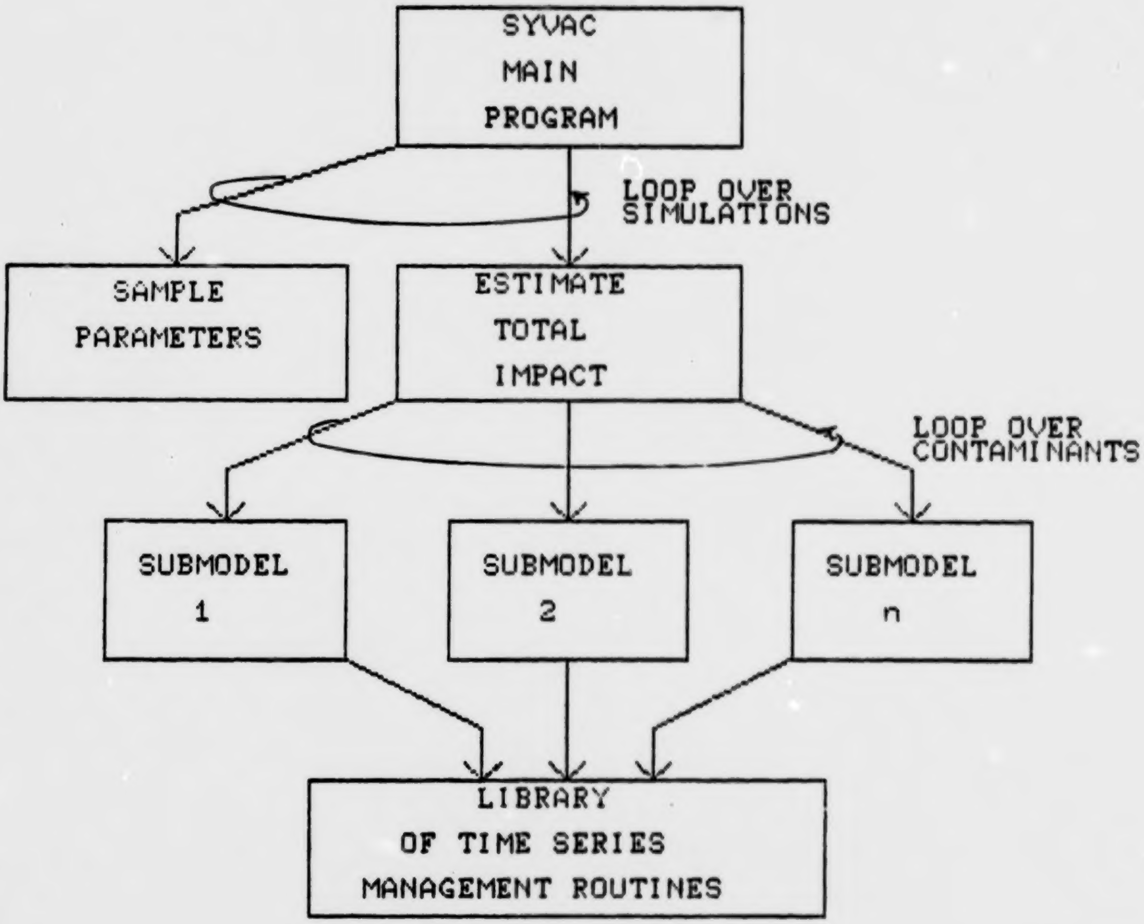
SYVAC
MAIN
PROGRAM
LOOP OVER SIMULATIONS
SAMPLE PARAMETERS
ESTIMATE TOTAL IMPACT
LOOP OVER CONTAMINANTS
SUBMODEL 1
SUBMODEL 2
SUBMODEL n
LIBRARY OF TIME SERIES MANAGEMENT ROUTINES

SYVAC adapted to run on an IBM Personal Computer. This version is known as SYVAC3-T1. The code SYVAC3-T1 is a full implementation of the SYVAC program in Microsoft FORTRAN Version 3.2 on an IBM PC microcomputer. It has all the capabilities listed above (with the qualification that the time series management routines were still being implemented as of this writing). However, not all these capabilities were needed for this project. In particular, only functions (1) and (2) were required to run the radon dose model. SYVAC3-T1 produces an output file containing values of all variables used in each simulation.

A number of routines have been developed to read a SYVAC3-T1 output file and analyze the data. Specifically, routines have been coded to generate sample statistics and descriptive plots (e.g. histograms, cumulative distributions, scatterplots) for variables in the output file. Other routines have been developed to generate fractional factorial designs for input to SYVAC3-T1, and to analyze these simulation results to evaluate sensitivity and uncertainty statistics. All analysis routines used in this project were coded in APL, an interactive programming environment ideal for prototyping applications and quick changes.

SYVAC3-T1 sampling supports the following distribution types for sampling parameters:

- uniform
- log uniform
- piecewise uniform (i.e. a histogram)
- normal
- lognormal
- correlated normal (i.e. a normal variate sampled to be correlated with another sampled normal or lognormal variate)
- correlated lognormal (i.e. a lognormal variate sampled to be correlated with another sampled normal or lognormal variate)
- beta
- triangular

Three types of sampling methods, RANDOM, QUANTILE and ON FILE are available. In one set of simulations, one group of parameters can use one sampling method, and another group can use another sampling method. If two (or more) groups of parameters use RANDOM sampling, then each set will be sampled from a different stream of random numbers.

RANDOM sampling generates random values for the parameters involved using a pseudo-random number generator due to Marsaglia (1968). The generator yields a uniformly distributed value between 0 and 1. This value is then treated as a quantile of the parameter being sampled and it is converted to a value of the parameter using the inverse transform method (Rubinstein, 1981).

QUANTILE sampling also uses the inverse transform method. In this case the quantiles are read from a file. This technique was used in this study for the sensitivity analysis discussed in the folloiwng section.

ON FILE sampling takes the value of each parameter directly from a file. This technique bypasses the probability distributions altogether.

Simulation models can be incorporated into SYVAC3-T1 with minimal modifications to the source code. Parameter distributions are read from input data files. These data files can be internally documented (using comment statements) and hence are readily understandable and easily maintained. SYVAC3-T1 does extensive error checking on the inputs, producing appropriate on-line error messages.

In addition, SYVAC3-T1 has the capability to perform pairwise comparison of simulations. To determine the effect of a single change in a model, or in a parameter's distribution, it is useful to be able to repeat a set of simulations with everything else (e.g. parameter values) staying the same. Then simulations can be compared between the two sets one-by-one or by using a statistical procedure for paired samples. SYVAC3-T1 supports such repetition of simulation sets in two ways. First, changing one (or more) parameter's distribution will not affect values of other parameters since each parameter in RANDOM sampling requires precisely one call to the random number generator, whatever its distribution. Second, multiple streams of random numbers can be defined, so a submodel using one stream can be completely replaced by an alternate submodel without affecting any other submodels using a second stream of random numbers. This feature was not used in this study, but could have been applied in sensitivity and uncertainty analysis.

### D.4.2 Results

Before the benchmark model could be evaluated, several changes to the specifications of the input parameter distributions were required. These changes were required since some of the distribution data (specified on Table D.2) was in a different form from that expected by SYVAC3-T1.

The first transformation involved the normal distribution. The upper and lower bounds on normal distributions were all specified as values, whereas SYVAC3-T1 requires quantile bounds. For example, FRACT was specified as normally-distributed, with mean=0.1; SD=0.02; min=0.0; max=0.3 (where SD=standard deviation). It was necessary to convert the bounds for all normal variates from values to quantiles. The conversion for a normal variate X was:

| Given | Required for SYVAC3-T1 |
|---|---|
| mean | mean |
| SD | SD |
| min | low = Pr ($X \leq min$) |
| max | high = 1-Pr($X > max$) |

The other transformation involved lognormal variates. For example, SIGZED was specified as lognormal with GM=60.0; GSD=1.73; min=10.0; max=300 (where GM=geometric mean, GSD=geometric standard deviation). If X is lognormally-distributed, SYVAC3-T1 takes as parameters the mean and standard deviation of log (base 10). The conversion for a lognormal variate X was:

| Given | Required for SYVAC3-T1 |
|---|---|
| GM | mean of log = log (GM) |
| GSD | SD of log = log (GSD) |
| min | low = Pr (X≤min) |
| max | high = 1-Pr(X>max) |

Table D.5 shows the transformed values for all normal and lognormal distributions specified in Table D.2.

Stochastic simulation results were used to generate summary statistics and plots. All analysis routines were coded in APL (STSC's APL*PLUS/PC for the IBM PC). All calculations were performed in double precision (about 16 significant digits). Summary statistics (from 250 random trials) for all input parameters and the calculated parameter of interest DOSRN, are presented in Table D.6. All statistics for sampled parameters were checked against the parameter distributions. There was general agreement between the specified distributions and the sampling distributions.

The results for DOSRN are presented in histogram form in Figure D.6 (a) and a cumulative distribution function in Figure D.6 (b).

Since DOSRN had a highly skewed distribution, a histogram and CDF were constucted for log DOSRN (Figures D.7 (a) and D.7 (b)).

### D.4.3 Sensitivity/Uncertainty Analysis: Andres

The distinction between sensitivity analysis and uncertainty analysis for this project was made in the Phase I report (SENES, 1984). "Sensitivity analysis refers to the sensitivity of the magnitude of the result to changes in the magnitudes of the input parameters. ...Uncertainty analysis refers to how much the uncertainty (or spread) associated with each parameter contributes to the total uncertainty (or spread) of the result." Both are used to answer the question: "Which parameters/pathways have the greatest effect on model predictions?"

Table D.5

## DISTRIBUTION DATA TRANSFORMED FOR SYVAC3-T1

| Parameter Name | Given Distribution Data | Transformed Distribution Data |
|---|---|---|
| FRACT | mean = 0.1 | mean = 0.1 |
| | SD = 0.02 | SD = 0.02 |
| | min = 0.0 | low = 2.8665158E-7 |
| | max = 0.3 | high = 0.9999999999 |
| RHOTAL | mean = 1.4E6 | mean = 1.4E6 |
| | SD = 0.1E6 | SD = 0.1E6 |
| | min = 1.0E6 | low = 3.1671242E-5 |
| | max = 0.3 | high = 0.9999683287 |
| SIGZED | GM = 60.0 | mean of log = 1.7781513 |
| | GSD = 1.73 | SD of log = 0.23804610 |
| | min = 10.0 | low = 5.3981348E-4 |
| | max = 300. | high = 0.9983391281 |
| WIND | mean = 5.3 | mean = 5.3 |
| | SD = 0.9 | SD = 0.9 |
| | min = 3.0 | low = 5.3009218E-3 |
| | max = 0.3 | high = 0.9999803120 |
| WTSFLX | GM = 2.0E-2 | mean of log = -1.69897000 |
| | GSD = 2.15 | SD of log = 0.33243846 |
| | min = 2.0E-3 | low = 1.3145389E-3 |
| | max = 2.0E-1 | high = 0.9986854611 |

### Table D.6

## SUMMARY STATISTICS: SYVAC3-T1

(250 Random Simulations)

| Parameter | Mean | Std. Dev. | Geo. Mean | Geo. SD | Minimum | Maximum |
|---|---|---|---|---|---|---|
| FRACT | 1.012E-01 | 2.013E-02 | 9.903E-02 | 1.236E+00 | 4.632E-02 | 1.468E-01 |
| HSUBD | 1.968E+00 | 5.606E-01 | 1.885E+00 | 1.353E+00 | 1.003E+00 | 2.996E+00 |
| LSUBC | 1.016E+00 | 2.894E-01 | 9.710E-01 | 1.362E+00 | 5.030E-01 | 1.499E+00 |
| MPCH2O | 1.335E+01 | 4.523E+00 | 1.260E+01 | 1.415E+00 | 5.425E+00 | 2.466E+01 |
| OCCFAC | 6.086E-01 | 1.671E-01 | 5.847E-01 | 1.336E+00 | 3.013E-01 | 8.981E-01 |
| RACNTA | 9.935E+00 | 2.827E+00 | 9.508E+00 | 1.356E+00 | 5.005E+00 | 1.498E+01 |
| RHOTAL | 1.402E+06 | 9.758E+04 | 1.399E+06 | 1.072E+00 | 1.150E-06 | 1.686E+06 |
| SIGZED | 7.375E+01 | 3.893E+01 | 6.456E+01 | 1.698E+00 | 1.204E+01 | 2.272E+02 |
| THICK | 1.160E+00 | 3.220E-01 | 1.115E+00 | 1.332E+00 | 5.115E-01 | 1.990E+00 |
| WIND | 5.320E+00 | 9.284E-01 | 5.238E+00 | 1.196E+00 | 3.317E+00 | 8.407E+00 |
| WTSFLX | 2.804E-02 | 2.156E-02 | 2.134E-02 | 2.162E+00 | 2.356E-03 | 1.296E-01 |
| EMANAT | 3.895E-01 | 1.889E-01 | 3.372E-01 | 1.792E+00 | 4.122E-02 | 8.306E-01 |
| DOSRN | 2.958E-06 | 5.098E-06 | 1.378E-06 | 3.463E+00 | 6.361E-08 | 4.734E-05 |

FIGURE D.6a

SYVAC3-TI RESULTS
RELATIVE FREQUENCY HISTOGRAM: DOSRN

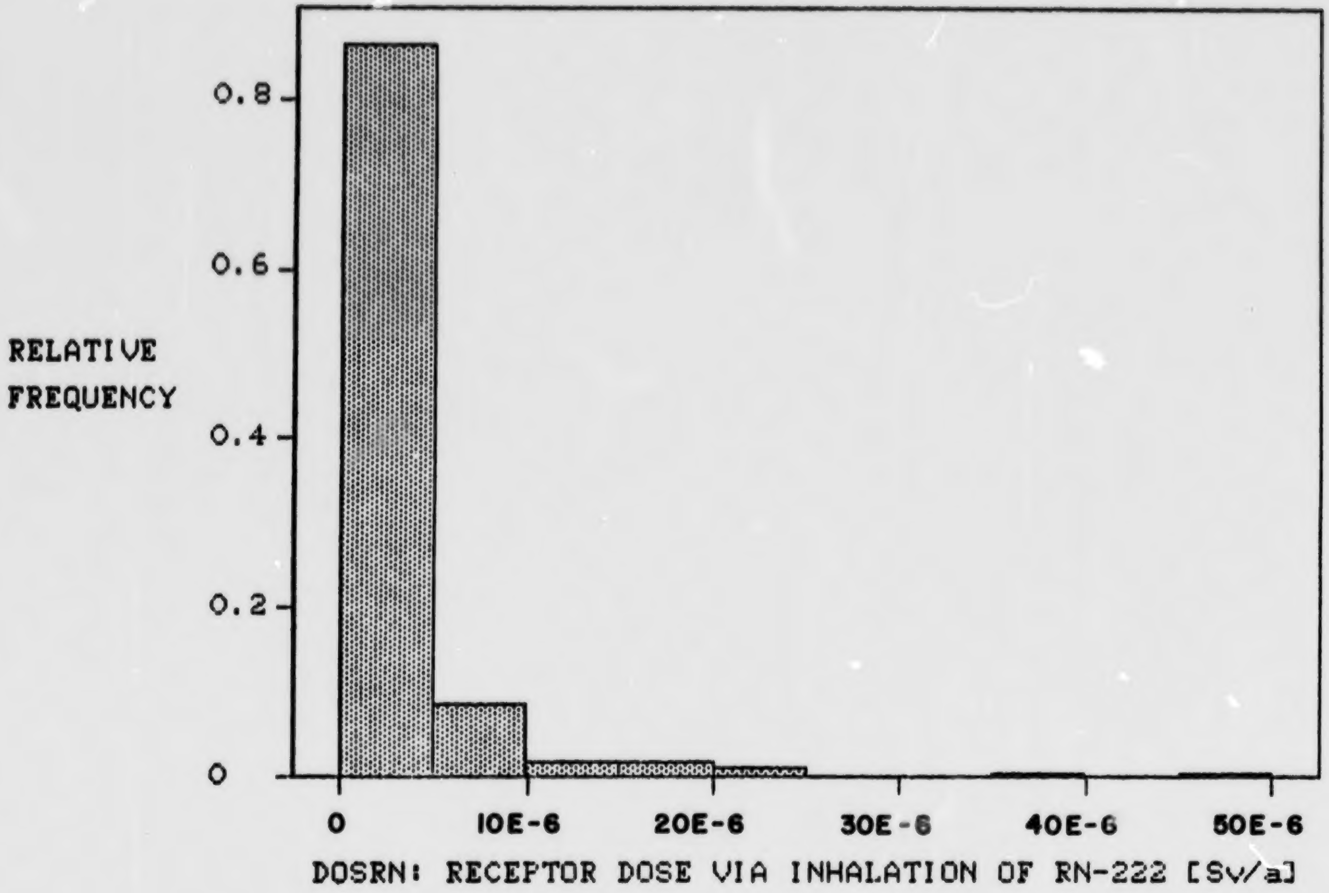

FIGURE D.6b

SYVAC3-TI RESULTS
CUMULATIVE DENSITY FUNCTION: DOSRN

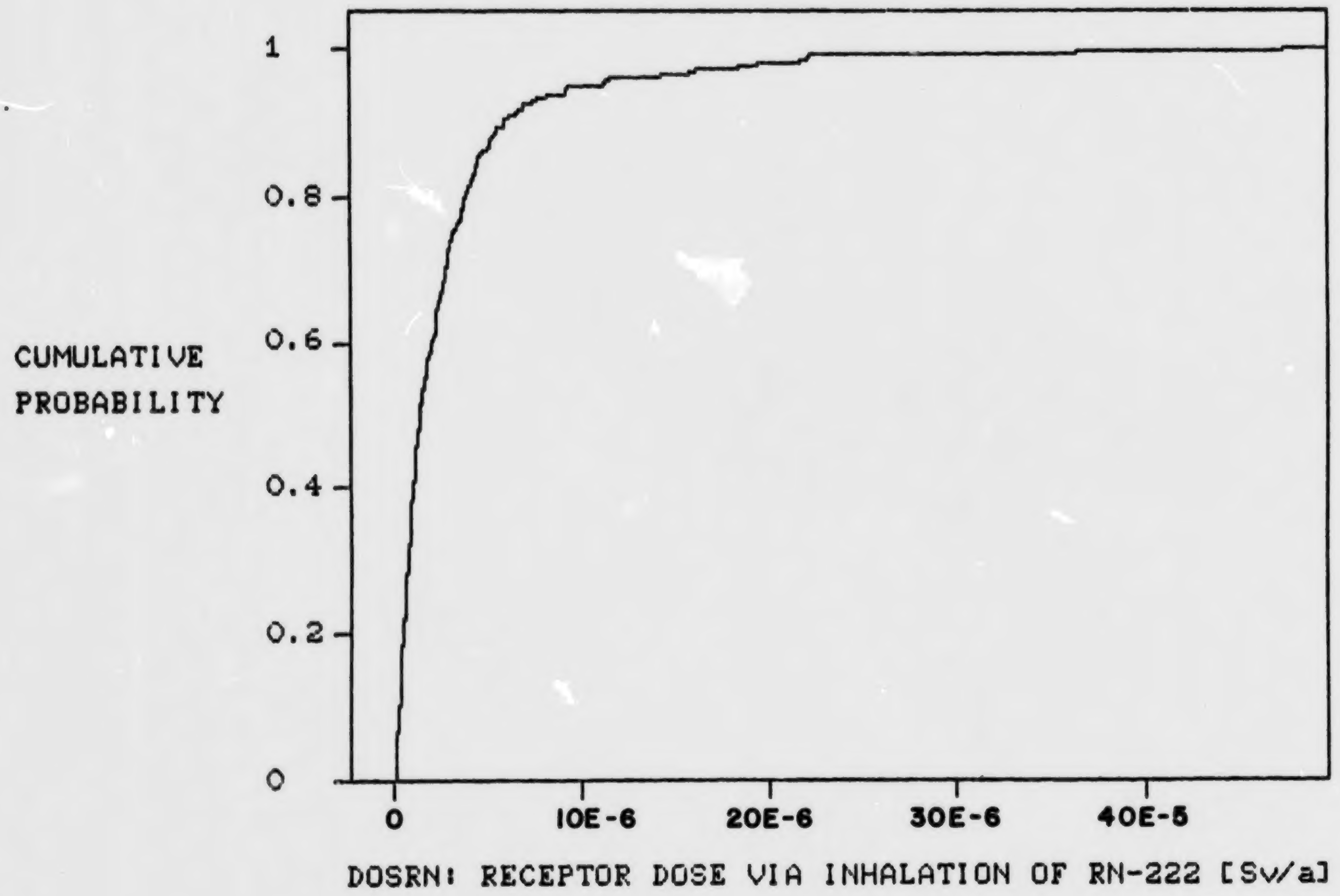

FIGURE D.7a
SYVAC3-TI RESULTS
RELATIVE FREQUENCY HISTOGRAM: LOG (DOSRN)

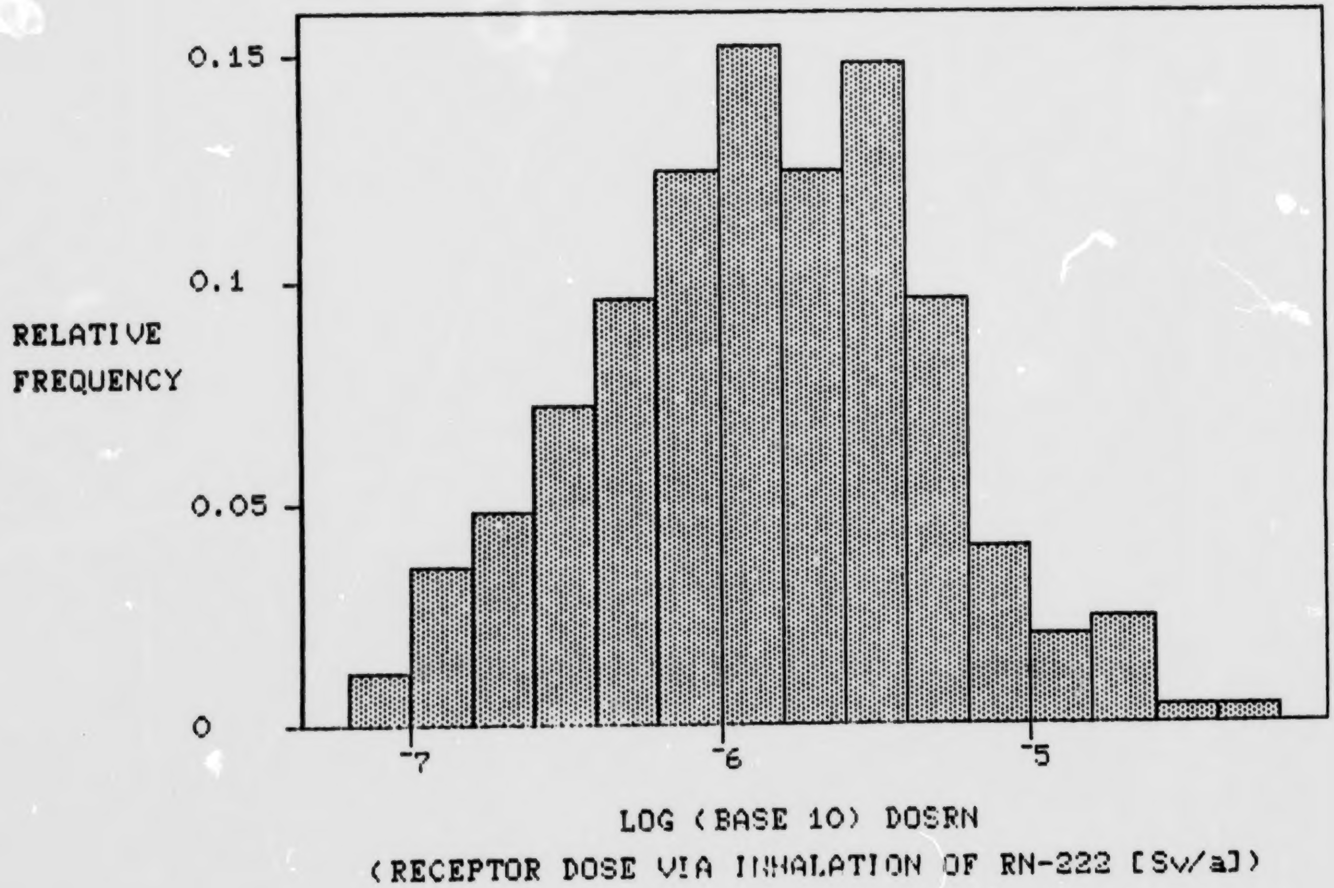

FIGURE D.7b

SYVAC3-TI RESULTS

CUMULATIVE DENSITY FUNCTION: LOG (DOSRN)

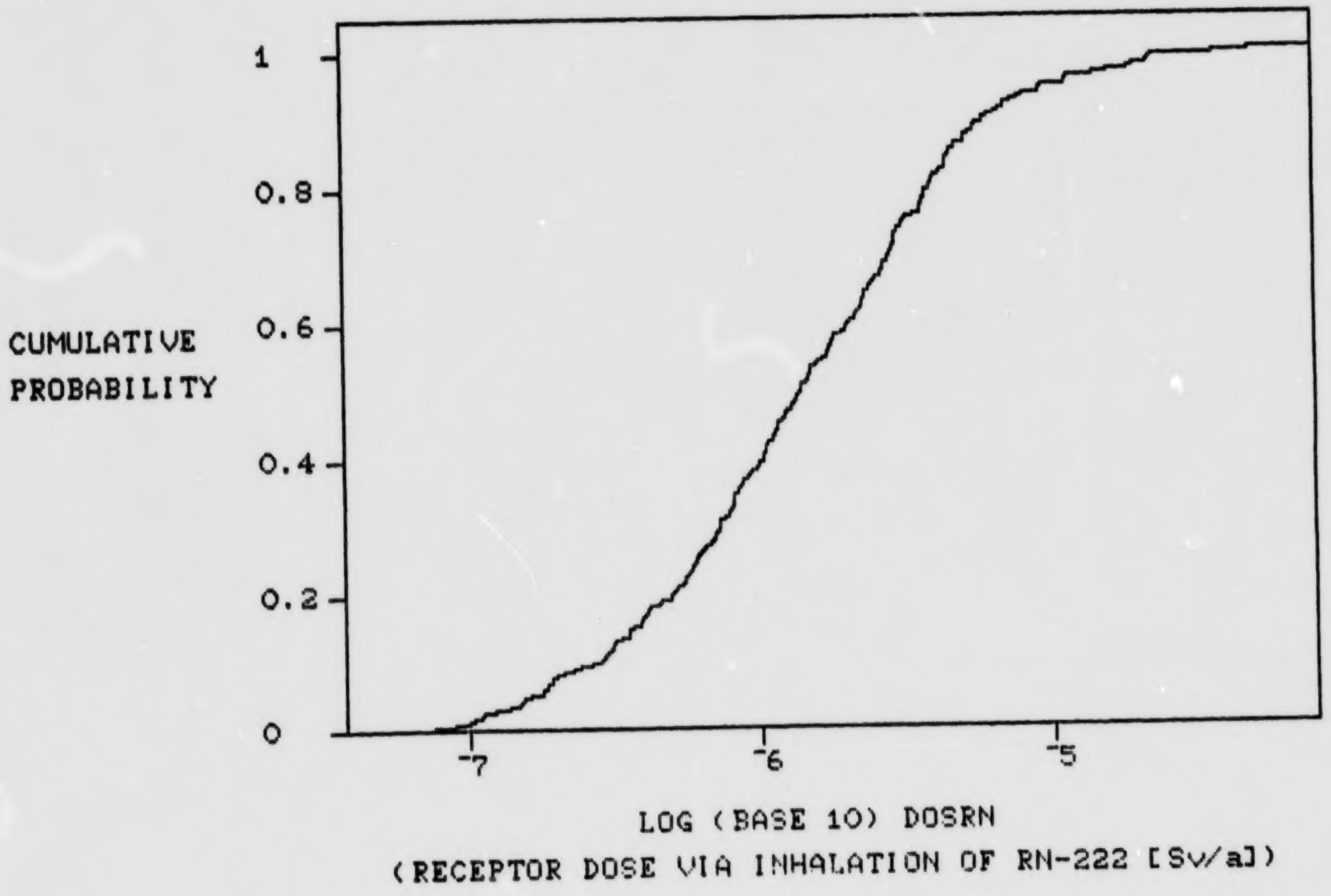

To answer this question for this report, the simulation model was treated like an experimental apparatus and additional experiments (simulations) were conducted. First an experimental design was selected based on the number of parameters and the information to be elicited. Then simulations were conducted with parameter values selected according to the experimental design. The results of these simulations were analyzed to determine the effects of the individual parameters on DOSRN (sensitivity analysis). The experiments were repeated with parameters chosen at different points in their distributions to determine the effects of parameter spreads on DOSRN (uncertainty analysis).

Two-level fractional factorial designs were chosen as being appropriate for this analysis (Box et al., 1978). In these designs, a low value and a high value is chosen for each parameter, and only these two values are used in the set of simulations. The set of simulations is designed to determine the effect of flipping between these two values for each parameter. The average change in radon dose due to a change from low value to high value of a parameter is called the main effect of that parameter.

To conduct the experiment, two values were chosen for each parameter. In fact, to permit uncertainty analysis, several combinations of two values were chosen and analyzed separately. The first combination of two values selected for this experiment consisted of the lower quartile (i.e. the 25th percentile) and the upper quartile (i.e. the 75th percentile) of each parameter's distribution. These values were used in the sensitivity analysis experiment (denoted SV0001 in the following discussion). For uncertainty analysis, the procedure was repeated twice more, once at the 10 and 90 percentile points (SV0002), and once at the 1 and 99 percentile points (SV0003). These additional percentiles were selected because they lie roughly at the start of the distribution tails (10 and 90 percentiles), and far out in the distribution tails (1 and 99 percentiles).

Results from fractional factorial experiments were analyzed to estimate the main effect of each parameter. To permit adequate discrimination among main effects two groups of 64 simulations were used in the experimental design.

### D.4.3.1 Sensitivity Analysis

Analysis based on fractional factorial designs was effective for sensitivity analysis of DOSRN. It was especially precise and effective for analyzing the modified consequence log (DOSRN).

The details of this type of sensitivity analysis are rather technical, and will be covered in a forthcoming paper on the application of fractional factorial designs to sensitivity analysis of probabilitistic simulation models. In this paper the main conclusions can be summarized as follows:

1) All of the parameters of the radon model (and not just the important ones) were ranked exacly in their order of main effect on log (DOSRN) as shown in Table D.7. The table shows that in two different sets of 64 simulations, both the order of the parameters and the values of their main effects were identical. This repeatability is important because it shows that at least in the analysis of log (DOSRN) the ranking of parameters is not subject to the random variation, as a ranking based on random simulations would be.

2) The table shows that the three most important parameters, in dimishing order of main effect, were EMANAT, MPCH2O and SIGZED.

### D.4.3.2 Uncertainty Analysis

Table D.8 shows the main effect estimates for log (DOSRN) ranked in decreasing order for the three sets of simulations SV0001, SV0002, and SV0003. The rankings are similar, indicating that sensitivities are generally consistent across the domains of the parameters. The values are different because log(DOSRN) is more affected by large swings of parameter values than by small swings.

Table D.7

## ESTIMATES OF MAIN EFFECTS ON LOG (DOSRN) IN SV0001

| Variable Number* | Variable Name | Estimate From First 64 Simulations | Estimate From Last 64 Simulations |
|---|---|---|---|
| 19 | EMANAT | 0.36249 | 0.36249 |
| 9 | MPCH2O | -0.35931 | -0.35931 |
| 15 | SIGZED | -0.31988 | -0.31988 |
| 8 | LSUBCC | 0.26876 | 0.26876 |
| 13 | RACNTA | 0.22185 | 0.22185 |
| 11 | OCCFAC | 0.22185 | 0.22185 |
| 16 | THICK | -0.21060 | -0.21060 |
| 5 | FRACT | 0.11789 | 0.11789 |
| 17 | WIND | -0.09916 | -0.09916 |
| 14 | RHOTAL | 0.04188 | 0.04188 |
| 18 | WTSFLX | 0.00656 | 0.00656 |
| 6 | HSUBD | -0.00031 | -0.00031 |
| 2 | ARTLSR** | 0.0 | 0.0 |
| 26 | (not used) | 0.0 | 0.0 |
| 10 | NSUBW** | 0.0 | 0.0 |
| 22 | (not used) | 0.0 | 0.0 |
| 4 | DIST** | 0.0 | 0.0 |
| 12 | POROS** | 0.0 | 0.0 |
| 20 | (not used) | 0.0 | 0.0 |
| 28 | (not used) | 0.0 | 0.0 |
| 7 | LAMRN** | 0.0 | 0.0 |
| 21 | (not used) | 0.0 | 0.0 |
| 31 | (not used) | 0.0 | 0.0 |
| 30 | (not used) | 0.0 | 0.0 |
| 3 | DCFIRN** | 0.0 | 0.0 |
| 23 | (not used) | 0.0 | 0.0 |
| 29 | (not used) | 0.0 | 0.0 |
| 33 | (not used) | 0.0 | 0.0 |
| 24 | (not used) | 0.0 | 0.0 |
| 25 | (not used) | 0.0 | 0.0 |
| 27 | (not used) | 0.0 | 0.0 |
| 32 | (not used) | 0.0 | 0.0 |

* RUN NUMBER is variable number 1, which does not appear in this table.
** Constant parameter

Note
Variable names given as (not used) refer to dummy variables that did not appear in the model, but were included in the analysis as control variables.

Table D.8 shows that one parameter, THICK, behaves anomalously. It rises in importance from position 7 in SV0001, to position 5 in SV0002, to position 4 in SV0003. This behaviour is not due to THICK having a long-tailed distribution, for THICK has a triangular distribution with finite tails. Instead it seems to be caused by the nature of the effect of THICK on DOSRN.

Figure D.8 shows a scatterplot of log (DOSRN) versus THICK. The plot shows a mild trend downward to the right. The trend becomes more evident near the left and right edges, because there are bare spots in the lower left and upper right corners. The scatterplot indicates that the uncertainty (the spread of scatter) in log (DOSRN) is reduced for high values of THICK, and perhaps for low ones as well.

## D.5 DEMOS

The following descriptions of DEMOS are drawn from a number of published sources (Henrion and Morgan, 1985; Henrion and Nair, 1982; and Henrion, 1979) as well as from discussions with its author, Dr. Max Henrion. Dr. Henrion also provided the results referenced later in this section.

### D.5.1 General Description

The name DEMOS stands for DEcision MOdelling System. It is an interactive environment for structuring, analyzing and communicating probabilistic models. It provides general mathematical modelling facilities, but was designed primarily for policy related modelling, using techniques from cost-benefit analysis, engineering economics, risk assessment and decision analysis. The first version of DEMOS was designed by Dr. Henrion, and implemented in the PPL language in 1979-80. The current version is implemented in PASCAL on a Digital Equipment micro-VAX computer.

DEMOS has four particular characteristics which distinguish it from most other general purpose modelling languages:

- Interaction: Model development is usually an iterative process, in which successive versions of a model are constructed, criticized and modified as the modellers identify key issues and deepen their understanding of the problems. To support this, both the parameter values of the model and the structure of the model itself may be defined and edited interactively. Changes may be permanent or exploratory in a "what if " mode. Multiple versions may be stored simultaneously.

- Non-procedural modelling: The user defines variables and their functional relationships in any convenient order, and does not have to program in the conventional sense of specifying control of execution sequences. Conceptually the elements of the model are declared in parallel with each other. The syntax is checked and compiled incrementally as it is defined bit by bit. The system determines when and how to evaluate the model and to store intermediate results according to the dictates of efficiency and consistency, relieving the user from having to worry about these issues.

- Representation of uncertainty: If the value of a quantity is known then it may be specified as a simple number or an array as in many conventional languages. If it is uncertain, the value may be a probability distribution, which can be specified by a standard distribution function or by an arbitrary cumulative distribution function. Standard distributons available include: normal, lognormal, uniform, triangular and beta. Dependent variables are evaluated probabilistically using Monte Carlo simulation. For some quantities, particularly those that represent value judgements (such as the dollar value of saving a life), instead of representing uncertainty by a probability distribution, it is often more useful to specify a vector of alternative values. Any variable that depends on multiple-valued quantities will be evaluated simultaneously for each value of each such quantity, thus producing a multi-dimensional parameteric analysis.

- Integrated documentation: Much of the work in policy modelling and

Table D.8

## COMPARISON OF PARAMETER SENSITIVITIES OVER DIFFERENT PARAMETER DOMAINS

| SV0001 | | SV0002 | | SV0003 | |
|---|---|---|---|---|---|
| Quantiles (0.25, 0.75) | | Quantiles (0.10, 0.90) | | Quantiles (0.01, 0.99) | |
| Variable | Main Effect | Variable | Main Effect | Variable | Main Effect |
| EMANAT | 0.36249 | EMANAT | 0.65019 | EMANAT | 1.13792 |
| MPCH20 | -0.35931 | MPCH20 | -0.64386 | SIGZED | -1.08562 |
| SIGZED | -0.31988 | SIGZED | -0.60669 | MPCH20 | -0.97867 |
| LSUBC | 0.26876 | LSUBC | 0.49356 | THICK | -0.73778 |
| RACNTA | 0.22185 | THICK | -0.43369 | LSUBC | 0.69006 |
| OCCFAC | 0.22185 | OCCFAC | 0.36798 | OCCFAC | 0.46562 |
| THICK | -0.21060 | RACNTA | 0.36798 | RACNTA | 0.46562 |
| FRACT | 0.11789 | FRACT | 0.22770 | FRACT | 0.43778 |
| WIND | -0.09916 | WIND | 0.17348 | WIND | -0.34353 |
| RHOTAL | 0.04188 | RHOTAL | 0.07972 | RHOTAL | 0.14561 |
| WTSFLX | 0.00657 | WTSFLX | 0.01383 | WTSFLX | 0.03308 |
| HSUBD | -0.00031 | HSUBD | -0.00083 | HSUBD | -0.00299 |

FIGURE D.8

SYVAC3-TI RESULTS

SCATTERPLOT: LOG (DOSRN) vs. THICK

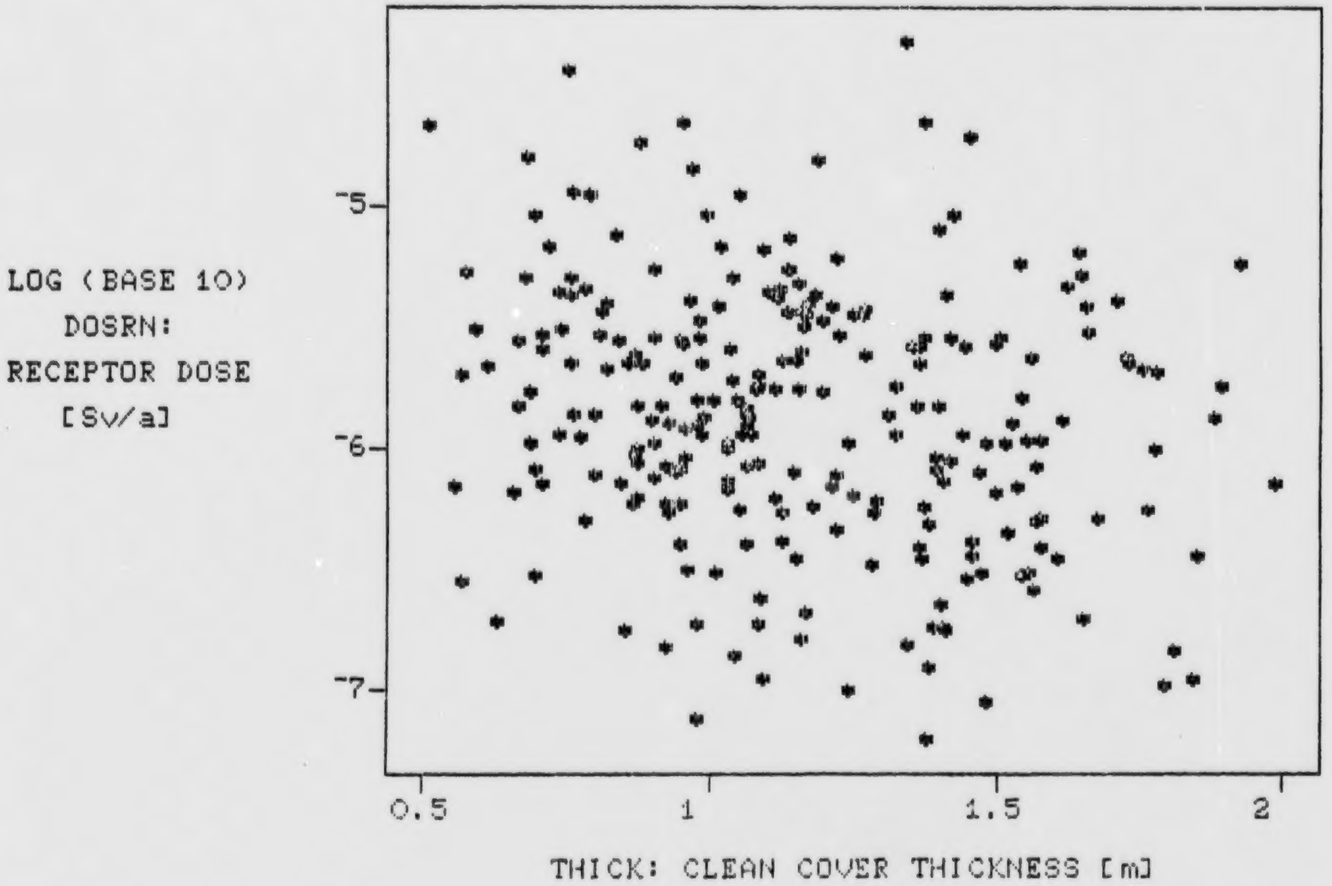

> decision analysis consists of understanding models, their assumptions and implications, and communicating them to reviewers and clients. DEMOS encourages the user to incorporate descriptive and explanatory text within the computer represenation. This can aid understanding of the model by its authors and by reviewers during on-line examination, and it helps in the semi-automatic preparation of comprehensible hardcopy reports. It also helps in maintaining consistency between the model structure and doucumentation.

Several other DEMOS features are particularly noteworthy. DEMOS has the ability to perform operations on variables specified as arrays. Operations on array variables are automatically generalized to all elements in the array. Simple (one word) commands allow preliminary deterministic examination of models by replacing probabilistic input distributions by their median values. Other single word commands ("Pdf", and "Cdf") cause probabilistic distributions of calculated (dependent) variables to be created and displayed on a terminal. Sensitivity analysis is easily performed, again using single word commands. The "What if" command allows exploration of the effect of a change in the definition of one variable on the calculated result, with no permanent effect on any information in the model. The commands "Dy Dx" and "Elasticity" are also useful in performing sensitivity analysis.

Several features have recently been added to DEMOS to improve its use in scientific modelling. Previous versions lacked the branching and looping structures generally required in scientific programming. The addition of dynamic simulation features (eg. specifying $X(t) = f(X(t- t))$) and conditional "IF-THEN-ELSE" statements has considerably enhanced the capacity of DEMOS as a probabilistic tool in complex scientific modelling.

### D.5.2 Results

Summary statistics for the results of 250 random trials are presented in Table D.9. The sampled distributions of input parameters closely reflect the specified input parameter statistics (eg. means, minimums, maximums) given on

Table D.2 previously.

Probability density, and cumulative probability plots of the calculated parameter (DOSRN) are presented in Figure D.9(a) and D.9(b). Unfortunately, plots of the log transformed values of DOSRN were not generated using DEMOS. Moment statistics for DOSRN (Table D.9) show little difference from the benchmark case (SENES) or the SYVAC3-T1 results. The minimum and maximum values of DOSRN are both more extreme than the RANSIM results, but similar to the SYVAC3-T1 results.

### D.5.3 Sensitivity/Uncertainty Analysis: Henrion

Max Henrion, who developed the DEMOS system at Carnegie Mellon University, performed a sensitivity/uncertainty analysis using simple and rank correlation coefficients. The correlation between the 250 sample values of each uncertaint input with the calculated values of DOSRN provides an indication of the "importance" of each input parameter. The simple correlation coefficient is a measure of how much of the uncertainty in the output is contributed by each input; and hence is a measure of the relative importance of each uncertain input. The rank correlation is very similar, but is computed on ranks within each sample rather than the absolute values of the samples. The rank correlation coefficient thus calculated is more robust and less sensitive to extreme values than the simple correlation coefficient. The rank correlation coefficient is often referred to as the Spearman rank correlation coefficient. It has been used in other instances as a measure of parameter sensitivity/uncertainty (Hoffman and Gardner, 1983).

The correlation coefficients between all variable input parameters and DOSRN are presented in Table D.10. These results can be summarized by identifying four groups of parameters, based on the absolute value of the rank correlation coefficients as follows:

Absolute Value: >0.3 ... MPCH2O, SIGZED, EMANAT .... large contribution
>0.2 ... FRACT, LSUBC, OCCFAC... moderate contribution

Table D.9

## SUMMARY STATISTICS: DEMOS
(250 Random Simulations)

| Parameter | Mean | S.D. | Geo. Mean | Geo. SD | Minimum | Maximum |
|---|---|---|---|---|---|---|
| MPCH20 | 1.317E+01 | 4.284E+00 | 1.248E+01 | 1.393E+00 | 5.224E+00 | 2.384E+01 |
| RACNTA | 1.000E+01 | 2.893E+00 | 9.448E+00 | 1.3614+00 | 5.020E+00 | 1.498E+1 |
| RHOTAL | 1.400E+06 | 1.014E+5 | 1.396E+01 | 1.076E+00 | 1.100E+-6 | 1.691E+06 |
| EMANAT | 3.815E-01 | 1.942E-01 | 3.3303E-01 | 1.762E+00 | 5.12E-02 | 8.0687E-01 |
| LSUBC | 1.000E+01 | 2.893E-02 | 9.558E-01 | 1.361E+00 | 5.020E-01 | 1.498E+00 |
| FRAC | 1.000E-01 | 2.030E-02 | 9.780E-02 | 1.241E+00 | 4.190E-02 | 1.581E-01 |
| WTSFLX | 2.720E-02 | 3.51E-02 | 2.000E-02 | 2.125E+00 | 2.226E-03 | 1.885E-01 |
| WIND | 5.300E+01 | 9.122E-01 | 5.219E+00 | 1.965E+00 | 2.685E+00 | 7.915E+00 |
| SIGZED | 7.012E+01 | 4.263E+01 | 5.007E+01 | 1.743E+00 | 1.238E+01 | 2.981E+02 |
| HSUBD | 2.000E+00 | 5.785E-01 | 1.922E+00 | 1.361E+00 | 1.004E+00 | 2.996E+00 |
| OCCFAC | 6.000E-01 | 1.736E-01 | 5.735E-01 | 1.361E+00 | 3.012E-01 | 8.988E-01 |
| THICK | 1.1660E+00 | 3.110E-01 | 1.1244E+00 | 1.319E+00 | 5.224E-01 | 1.900E+00 |
| DOSRN | 2.911E-06 | 4.563E-06 | 1.426E-06 | 3.419E+00 | 5.417E-08 | 4.018E-05 |

FIGURE D.9a

DEMOS RESULTS
PROBABILITY DENSITY: DOSRN

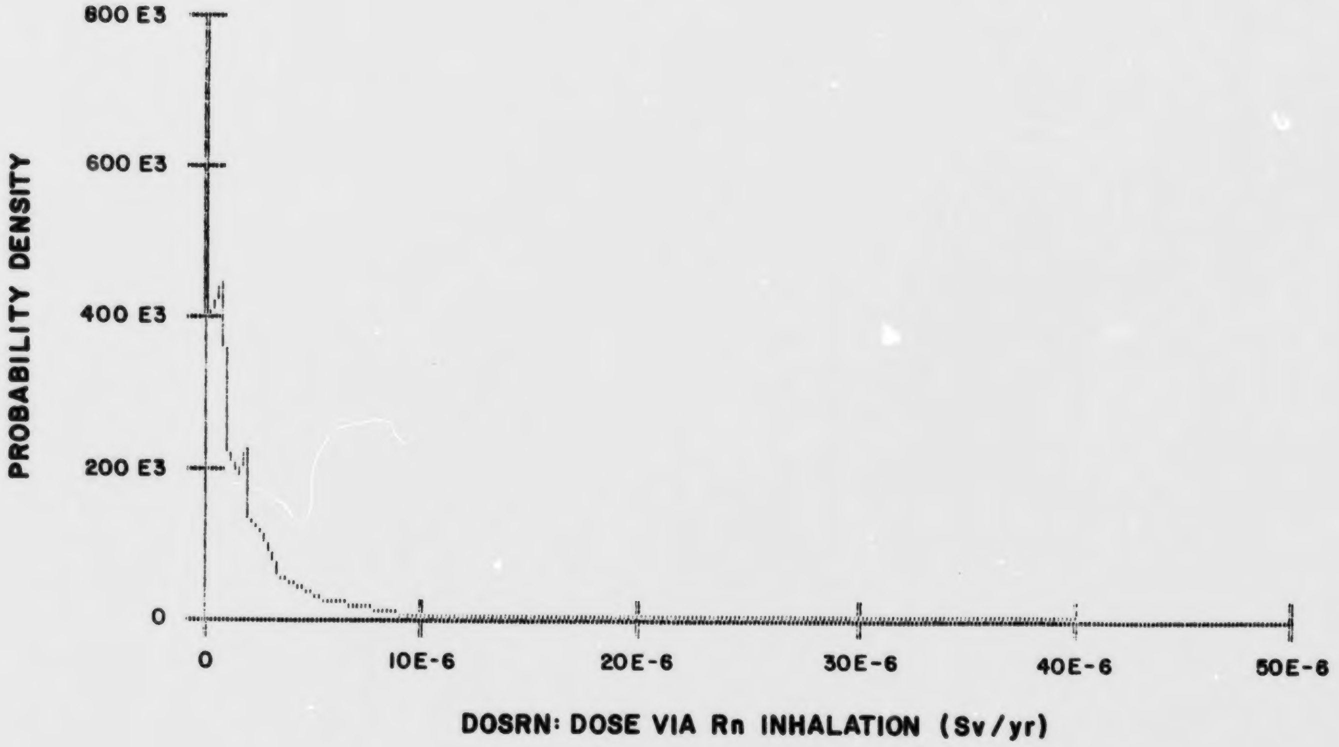

FIGURE D.9b

DEMOS RESULTS
CUMULATIVE PROBABILITY: DOSRN

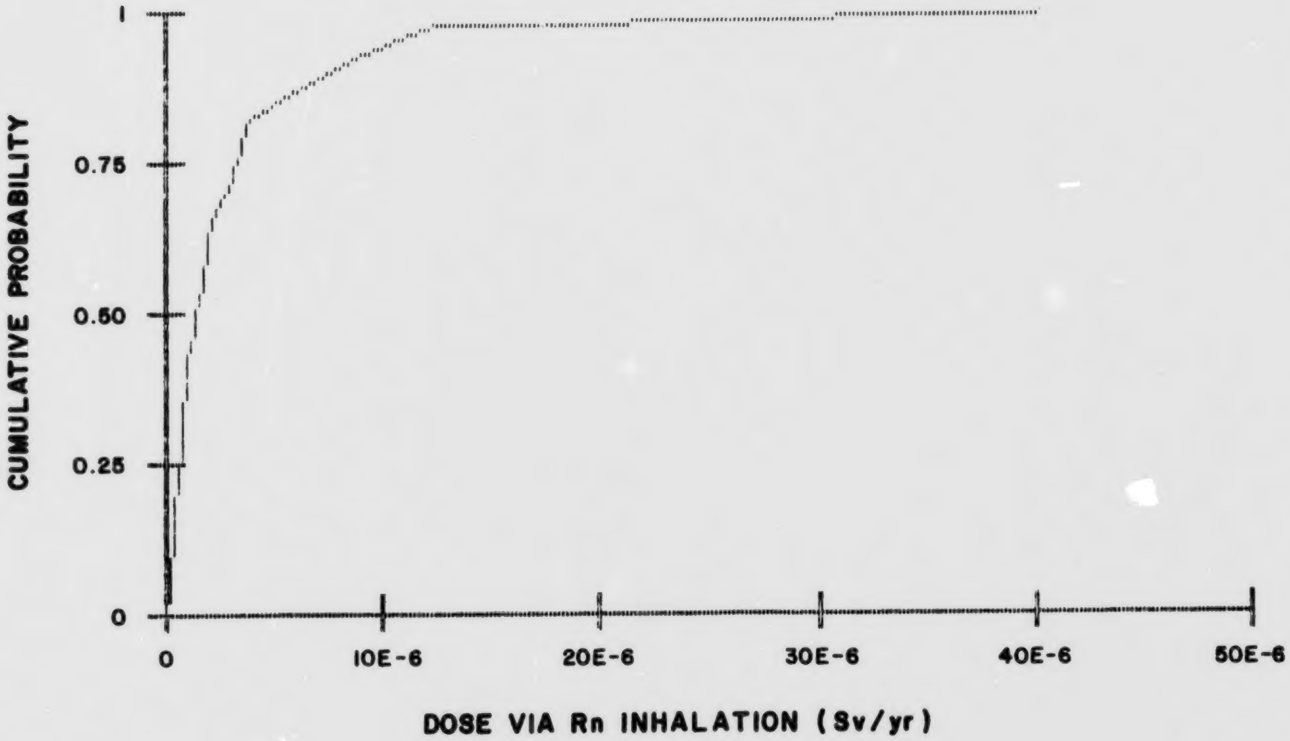

Table D.10

## CORRELATION OF INPUT PARAMETERS WITH DOSRN

| Parameter | Simple Correlation Coefficient | Rank Correlation Coefficient |
|---|---|---|
| MPCH20 | -.37 | -.50 |
| EMANAT | .35 | .46 |
| SIGZED | -.39 | -.45 |
| LSUBC | .17 | .30 |
| FRACT | .10 | .29 |
| OCCFAC | .22 | .22 |
| WIND | -.13 | -.17 |
| THICK | -.12 | -.18 |
| RACNTA | .146 | .11 |
| WTSFLX | .005 | -.09 |
| HSUBD | -.002 | -.07 |
| RHOTAL | .001 | .002 |

>0.1 ... RACNTA, THICK, WIND ... small contribution
<0.1 ... RHOTAL, WTSFLX, HSUBD ... negligible contribution

## D.6 DISCUSSION

### D.6.1 System Features

Before comparing the details or features of the three systems examined in this study, one point must be made. RANSIM and SYVAC3-T1 are computer programs designed to perform probabilistic analysis of any appropriately specified (i.e. coded in FORTRAN) mathematical models. DEMOS, on the other hand, is a probabilistic analysis environment, designed to facilitate the entire modelling process; from model implementation and documentation through the probabilistic analysis itself to the final graphical display of results. Thus, while RANSIM and SYVAC3-T1 are designed to run on personal micro-computers, DEMOS is orders of magnitude larger and more complex.

The three systems all possess the fundamental ability to draw random samples from a variety of input parameter distributions. RANSIM and SYVAC3-T1 currently provide essentially the same set of distributions (normal, lognormal, uniform, log uniform, triangular, beta, arbitrary and correlated) while DEMOS provides a somewhat smaller set.

Both SYVAC3-T1 and RANSIM require that component models be coded in FORTRAN. Input to both systems must be provided via data files. DEMOS, however, is an interactive probabilistic programming environment. Models may be specified in any order, and the user is prompted to provide values or distribution specifications for all independent parameters.

Neither SYVAC3-T1 nor RANSIM possess the on-line output features of DEMOS. DEMOS output is generated by very simple commands such as "pdf (DOSRN)" or "cdf (DOSRN)" to produce probability density functions (pdf's) or cumulative density functions (cdf's). A variety of statistics are also readily available. RANSIM provides summary statistics as on-line, immediate feedback and also provides the option of saving selected results for subsequent detailed analysis and/or graphical display. SYVAC3-T1 has no built in output features relying instead on a set of external analysis routines created using APL. However, SYVAC3-T1 does possess several unique features, including self-documenting input files, and the ability to perform pairwise comparisons of simulations.

In summary, all three systems provide the basic fundamentals of probabilistic analysis. RANSIM is perhaps the most basic, providing a relatively complete set of available parameter distributions and immediate feedback via summary statistics. It is relatively small, simple and portable and may be easily applied to many problems.

SYVAC3-T1 provides the same set of parameter distributions, no built in output features but several interesting additional features. It is also available on a personal computer.

DEMOS represents a level of sophistication beyond either RANSIM or SYVAC3-T1. By providing an interactive probabilistic analysis environment, it eliminates many of the mechanical details required to use either RANSIM or SYVAC3-T1 and facilitates analysis. However, its many features are supported by a very large computer program, limiting its portability and availability.

### D.6.2. Comparison of Results

Results generated by the three systems (Tables D.3, D.6 and D.9) indicate that all systems faithfully reproduce summary statistics for the input parameter distributions. This is an expected result; since the distribution sampling routines form the heart of any probabilistic analysis tool, and hence have been extensively tested.

For comparative purposes, summary statistics on the calculated parameter DOSRN for all three systems are summarized in Table D.11. Also presented on the table are summary statistics from 2 additional computer runs generated using RANSIM with different streams of random numbers (labelled EXTRA1 and EXTRA 2). The results of statistical tests to examine differences between the means and variances of the results are presented on Table D.12. The mean values were compared using the t-test while the variances were compared using the F-test. Since the distributions of DOSRN were highly skewed, and since the standard F-test is very sensitive to deviations of the data from normality, the F-test was performed on the variances of the log transformed data.

As indicated on the table, none of the mean values are significantly different (at the 95% confidence level); while only one of the F ratios indicates a statistically significant difference (between RANSIM and EXTRA1). The difference between the variances (indicated by the F test) may, in fact, be a "false positive" result; indicating a difference where none really exists. The probability of one or more false positive results in 10 signficance tests at the 95% level is approximately 0.4; indicating a 40% chance of at least 1 false positive result in the the tests performed (Reilly, 1986a). In fairness, it should also be noted that there is always a possibility of statistical tests failing to indicate significant differences where such differences actually exist.

It is also interesting that the statistically significant difference was from a comparison of two runs of the same system (RANSIM) and does not indicate any significant differences between the systems. In summary, the statistical tests do not indicate any significant differences between the three systems.

Andres (1985) expressed some concern over the differences in the extreme (minimum and maximum) values generated by RANSIM and SYVAC3-T1. For the runs labelled RANSIM and SYVAC3-T1, it was noted that a smaller minimum and a larger maximum were recorded for the SYVAC3-T1 run. These differences also appear between the RANSIM and DEMOS results. This prompted us to perform two additional computer runs on RANSIM. The two additional runs (labelled EXTRA1 and EXTRA2) were done using different streams of random numbers than the RANSIM benchmark case. The results of these two additional runs indicate that RANSIM is as equally likely as either SYVAC3-T1 or DEMOS to produce the most extreme values in any set of random trials. Of the five sets of results the smallest minimum value was obtained with the run labelled EXTRA1 while the largest minimum value was recorded with the run labelled RANSIM. Similarly, the smallest maximum value was obtained with the run labelled EXTRA1 while the largest maximum value was recorded for the run called EXTRA2.

These results illustrate a fundamental feature of probabilistic analysis. Namely, that different "runs" of the same number of trials, with different streams of random values will produce different distributions of calculated values. For a large number of trials, the central tendency of the calculated parameter will not change significantly, but the number and location of extreme values (i.e. the "tails" of the distributions) will change noticeably.

### B.6.3 Comparison of Sensitivity/Uncertainty Analysis Results

The three groups participating in this study all chose different methods to identify "important" input parameters. Many of the sensitivity/uncertainty analysis techniques applied have been used by other groups in other applications. It is not the intention of this paper to discuss the theoretical merits of any or all of the methods.

The interesting point to note is that all the methods produced similar results. The three most important parameters were consistently identified as EMANAT, MPCH2O and SIGZED; while the three least important were identified consistently as RHOTAL, HSUBD and WTSFLX.

The importance ranking of the remaining six parameters varied somewhat from method to method. This is not particularly surprising and should not be a cause for concern. The goal of sensitivity/uncertainty analysis should always be to identify groups of important and unimportant parameters and not to generate an absolute ranking of the importance of all parameters. There will

## Table D.11

## DOSRN SUMMARY STATISTICS (from 250 Simple Random Simulations)

| | Mean | S.D. | G.M. | GSD | Min. | Max. |
|---|---|---|---|---|---|---|
| RANSIM | 3.22E-06 | 4.36E-06 | 1.66E-06 | 3.31 | 9.01E-05 | 2.89-05 |
| SYVAC3-T1 | 2.96E-06 | 5.10E-06 | 1.38E-06 | 3.46 | 6.36E-05 | 4.73-05 |
| DEMOS | 2.91E-06 | 4.56E-06 | 1.43E-06 | 3.42 | 5.52E-05 | 4.02-05 |
| EXTRA1 | 2.94E-06 | 3.78E-06 | 1.41E-06 | 3.78 | 1.25E-05 | 2.1-05 |
| EXTRA2 | 2.85E-06 | 4.56E-06 | 1.36E-06 | 3.46 | 3.78E-05 | 4.8-05 |

## Table D.12

## STATISTICAL COMPARISONS (of means and variances)

| | RANSIM | SYVAC3-T1 | DEMOS | EXTRA1 | EXTRA2 |
|---|---|---|---|---|---|
| RANSIM | - | | | | |
| SYVAC3-T1 | 0.612(1)<br>1.073(2) | - | | | |
| DEMOS | 0.777<br>1.053 | 0.116<br>1.019 | - | | |
| EXTRA1 | 0.767<br>1.234* | 0.050<br>1.147 | 0.080<br>1.169 | - | |
| EXTRA2 | 0.927<br>1.013 | 0.254<br>1.00 | 0.147<br>1.019 | 0.24<br>1.147 | - |

(1) t-STATISTIC: $t=(X_1-X_2)/\sqrt{2S^2/N}$; $S^2 = \frac{s_1^2 + s_2^2}{2}$

Critical value: $t_{.05}(\infty) = 1.96$

(2) F-statistic: $F = \frac{(\log(GSD_1))^2}{(\log(GSD_2))^2}$

Critical value: $F_{.05}(249,249) = 1.2318$ (Reilly, 1986b)

* significant at 95% level

always be a group of parameters "in the middle", labelled as moderately important or moderately unimportant. Indeed, as has been shown in previous work (SENES, 1985) the relative ranking of the parameters, particularly those that fall in the moderately important group, will change as the conditions of the analysis change (e.g. with time).

## D.7 SUMMARY AND CONCLUSIONS

This comparative study illustrated some interesting features of probabilistic analysis. In particular, different probabilistic systems will produce similar results for a given model and set of input parameter distributions. The differences in results produced by the three systems are the same differences which would be expected from several "runs" (with different streams of random numbers) on any one system. The central tendency (i.e. mean value) of the calculated result will remain relatively constant from run to run (or system to system) but the extreme values will change.

Comparing the features of the three systems, it was obvious that the complete modelling environment provided by DEMOS eliminated many of the mechanical details inherent in using either RANSIM or SYVAC3-T1. Specifically, the DEMOS system is a stand-alone system which facilitates information input, output and model modification. The system however is operable only on a mini-computer. The interactive mode of operation of DEMOS, while encouraging the user to test different hypotheses, may be less desireable than a batch mode of operation for simulations of large, complex systems.

The probabilistic tools, RANSIM and presumably SYVAC3-T1, can be embedded within an advanced computer language to provide some output features comparable to that offered by DEMOS. Current SENES experience with FOCUS (a forth generation computer language) and a statistical post-processor (STATGRAPHICS) supports this view.

The very simple example used in this comparative study was sufficient to demonstrate many of the fundamental features of the three systems. However, its simplicity may not have illustrated all of the features of those probabilistic systems (specifically SYVAC 3-T1) designed for the simulation of large complex systems.

From the results, a number of conclusions can be drawn:

- All three systems are equivalent in that they generated similar results for the given set of input information.
- RANSIM is the most basic program, having been designed to provide only the essential requirements for probabilistic analysis. It is thus also the simplest and most transportable.
- SYVAC3-T1 provides several additional features such as input error checking and pairwise comparison of simulations. It still requires that models be implemented as a traditional computer program (in FORTRAN).
- DEMOS provides a more complete modelling environment. Its capabilities reduce many of the mechanical constraints on probabilistic analysis, at least for the analytical options embedded within it, and allow one to focus more attention on the problem of interest. It is, however, relatively large, complex and not readily transportable.
- All of the sensitivity/uncertainty analysis techniques used provided consistent identification of important and unimportant parameters. However, it is not desirable to rely solely on the results of any one method. Rather, it is preferable to use several of the simplest, most easily understood methods wherever possible.
- In summary, the RANSIM program, developed by SENES for the NUTP, is a viable probabilistic analysis tool; comparable with other tools of similar characteristics.

## REFERENCES

Andres, T.H., 1985. "Demonstration of Probabilistic Assessment Procedures Using a Radon Dose Model." Prepared for SENES Consultants Limited.

Box, G.E.P., Hunter, W.G., and Hunter, J.S., 1978. "Statistics for Experimenters: An Introduction to Design, Data Analysis and Model Building." John Wiley and Sons, Toronto.

Cleveland, W.S., and McGill, R., 1984. "The Many Faces of a Scatterplot." JASA, Vol. 79(338), pp. 807-822.

Dormuth, K.W., and Sherman, G.R., 1981. "SYVAC - A Computer Program for Assessment of Nuclear Fuel Waste Management Systems, Incorporating Parameter Variability." Atomic Energy of Canada Limited, AECL-6814.

Henrion, M., 1979. "Designing a Computer Aid for Decision Analysis." Proceedings of IEEE International Conference on Cybernetics and Society, Symposium on Man-Machine Systems, October.

Henrion, M. and Morgan, M.G., 1985. "A Computer Aid for Risk and Other Policy Analysis." Risk Analysis, Vol. 5, No. 3.

Henrion, M, and Nair, I., 1982. "DEMOS Users Manual, Version Two" Carnegie-Mellon University.

Hoffman, F.O., and Gardner, R.H., 1983. "Evaluation of Uncertainties in Environmental Radiological Assessment Environmental Dose Assessment Models." In: Radiological Assessment: A Textbook on Environmental Dose Assessment, J.E. Till and H.R. Meyer (eds.), NUREG/CR-3332, ORNL-5968. U.S. Nuclear Regulatory Commission, Washington, D.C.

Lowe, L.M., Chambers, D.B., and Murray, M.L., 1985. "Probabilistic Analysis of Radon Released from Uranium Mill Tailings." Presented at the Annual Meeting of the Canadian Radiation Protection Association. Saint John, New Brunswick.

Marsaglia, G., 1968. "Random Numbers Fall Mainly in the Planes." Proceedings of the National Academy of Science, Vol. 61, pp. 25-28.

Marse, K., and Roberts, S.D., 1983. "Implementing a Protable FORTRAN Uniform (0,1) Generator." Simulation.

Reilly, P.M. and Johri, H.P., 1969. "Decision Making Through Opinion Analysis." Chemical Engineering, April 7.

Reilly, P.M., 1986a. Personnal Communication, February.

Reilly, P.M., 1986b. Personal Communication, February. after Kendall, M., and Stuart, A., 1962. "The Advanced Theory of Statistics, Vol. 1." 2nd Edition, Hafner Publishing Co.

Rubinstein, R.Y., 1981. "Simulation and the Monte Carlo Method." John Wiley and Sons, Toronto, p. 39.

SENES Consultants Limited, 1984. "A Study to Develop and Demonstrate Techniques for the Probabilistic Assessment of the Long-term Effects of Uranium Mill Tailings in Canada - Phase I." Research Report Prepared for the National Uranium Tailings Program, CANMET, EMR, Contract No. OSQ83-00236.

SENES Consultants Limited, 1985. "Probabilistic Model Development for the Assessment of the Long-term Effects of Uranium Mill Tailings in Canada - Phase II." Research Report Prepared for the National Uranium Tailings Program, CANMET, EMR, Contract No. OSQ84-00207.

Terrell, G.R., and Scott, D.W., 1985. "Oversmoothed Nonparametric Density Estimates." JASA, Vol. 80(389), pp. 209-214.

Wuschke, D.M., Mehta, K.K., Dormuth, K.W., Andres, T., Sherman, G.R., Rosinger, E.L.J., Goodwin, B.W., Reid, J.A.K., Lyon, R.B., 1981. "Environmental and Safety Assessment Studies for Nuclear Fuel Waste Management - Volume 3: Post-closure Assessment." Atomic Energy of Canada Limited, TR-127-3.

APPENDIX E

# A BAYESIAN APPROACH TO ASSESSING CONFIDENCE IN MONTE CARLO OUTPUT DISTRIBUTIONS

by

S. Kaplan
Kaplan and Associates Inc.

for

SENES Consultants Limited
Willowdale, Ontario

## ABSTRACT

This paper outlines an approach to calculating confidence intervals about an entire output distribution generated by a probabilistic (Monte Carlo) analysis. The method is based on Bayes' Theorem and is essentially another application of the "two stage Bayes'" approach developed by Kaplan. The method proceeds by imagining the "true" output distribution (i.e. the results of an infinite Monte Carlo) as embedded in a suitably chosen approximating function space. On this space a probability distribution is erected using Bayes' Theorem and the evidence of the actual output of the finite Monte Carlo run. From this distribution, best estimates of the true output may be obtained, along with various interesting pictorial ways of visualizing the uncertainty.

# A BAYESIAN APPROACH TO ASSESSING CONFIDENCE IN MONTE CARLO OUTPUT DISTRIBUTIONS

## E.1 INTRODUCTION

A user of the Monte Carlo method for combining input probability distributions must continually be concerned with the general question of the accuracy of his output distribution. More specifically, having run a Monte Carlo calculation with a finite number of trials he wishes to know how close his output distribution is to the distribution he would theoretically get in an infinite number of trials.

Two different approaches to this problem are represented by the work of Andres (1984 a and b), and that of Reilly and Duever (1985). We shall refer to Andres' approach as an "interval" approach, since it seeks to assess the accuracy of the area under the Monte Carlo distribution, over a definite interval on the axis representing the output variable. The interval in question can be varied however and in that way the accuracy of any or all parts of the curve can be assessed.

Nevertheless, the interval approach focuses on one part of the curve at a time. Reilly's approach on the other hand attempts to put confidence bounds on the entire output curve in one fell swoop. It regards the entire curve as a totality. We shall therefore refer to it as a "whole curve" approach.

In a previous discussion paper (Kaplan, 1985) we have described how Bayes' Theorem can be used to develop a version of the interval approach. In the present paper we shall show how one could similarly develop a Bayesian version of the whole curve approach.

We shall begin, in the next section, with a capsule review of the Bayesian interval approach since some ideas from this approach will be used again in the Bayesian whole curve approach. Also, these ideas serve as a good "warm up" for understanding the whole curve approach.

## E.2 THE INTERVAL APPROACH

Let the curve, $\Phi(x)$, of Figure E.1 represent the output of an infinite Monte Carlo calculation. We shall call this a frequency density distribution since

$$\Phi(x)dx$$

is the frequency (in trials per trial) with which the Monte Carlo trials fall in the interval dx about x. The curve $\Psi(x)$ we call the cumulative frequency curve. The ordinate, $\Psi(x)$ corresponding to any x, gives the fraction or frequency of trials falling below that value of x.

These are the "exact" curves. Now let the x axis be divided into two intervals by the value $\hat{x}$ as shown. Let A be the area under the bell curve to the right of $\hat{x}$. Now suppose we have run a finite Monte Carlo calculation of m trials, and found k of them falling to the right of $\hat{x}$. We now ask, from this result, what can we infer about the true value A and with what degree of confidence can we infer it.

As shown in Kaplan (1985) this question may be answered by writing Bayes' Theorem in the form:

$$p_A(a|k:m) = \frac{p_A^o(a)\ p(k:m|a)}{\int_o^1 p_A^o(a)\ p(k:m|a)\ da} \qquad (2-1)$$

where:

$p_A(a|k:m)$ is our "posterior" probability distribution, which expresses our state of confidence about A after we have become aware of the Monte Carlo result that k out of m trials have fallen in the interval $(x,\infty)$

FIGURE E.1

## OUTCOME OF AN INFINITE MONTE CARLO CALCULATION

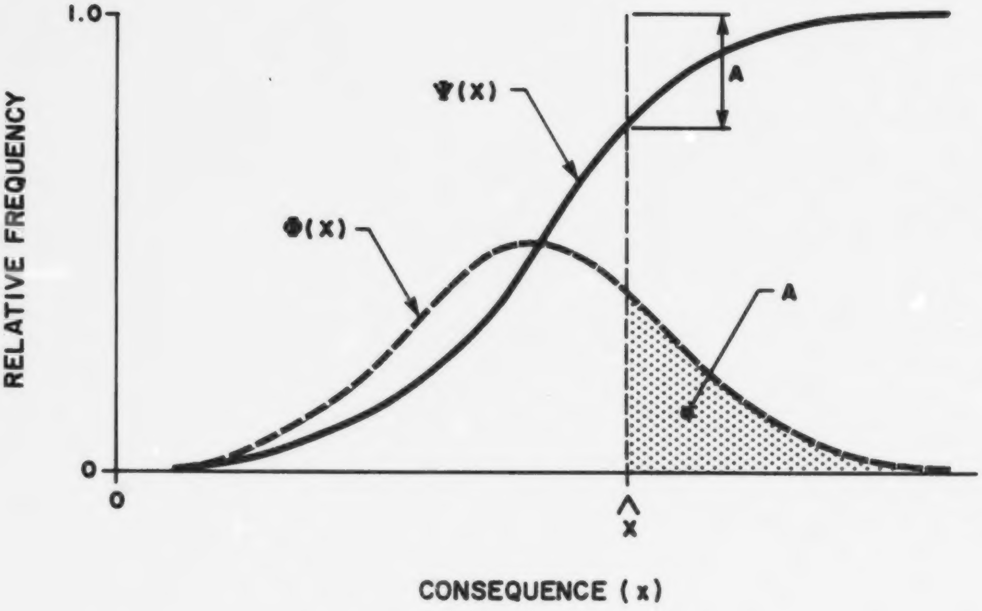

NOTE:

Φ = FREQUENCY DENSITY CURVE ( ——— )

Ψ = CUMULATIVE FREQUENCY CURVE ( ——— )

$\Phi = \frac{d\Psi}{dx}$

$p_A^o(a)$ is our "prior" distribution which expresses our state of knowledge about A before learning the result of the Monte Carlo calculation

and

$p(k{:}m|a)$ is our "likelihood" function, which expresses our degree of confidence, if A were equal to a, that a Monte Carlo run of m trials would yield k outcomes in the interval $(x,\infty)$

More specifically:

$$p_A(a|k{:}m)da \tag{2-2}$$

is our level of confidence, given the evidence of k successes out of m trials, that the true value A lies in the interval da about a. Similarly:

$$p_A^o(a)da \tag{2-3}$$

is our level of confidence, prior to having the evidence of the Monte Carlo run, that A lies in da about a. The likelihood function, as noted in Kaplan (1985) and Andres (1984b), is a binomial function:

$$p(k{:}m|a) = \frac{m!}{k!\ (m-k)!}\ a^k\ (1-a)^{m-k} \tag{2-4}$$

Expressions (2-3) and (2-4) then are all that is needed to calculate the posterior function given by equation (2-2). The result is a probability curve which we can imagine as superimposed on Figure E.1 at $\hat{x}$ as shown in Figure E.2.

Now if we imagine ourselves varying the position of $\hat{x}$ and repeating the process, we obtain a similar bell curve at every point on the x axis. We may then connect equal percentile points, from all these bell curves and obtain a family of curves enveloping $\Psi(x)$ as shown in Figure E.3.

## E.3 THE BAYESIAN WHOLE CURVE APPROACH

This approach is essentially another application of the "two stage Bayes'" approach of Kaplan (1981). The basic line of thought proceeds as follows:

1. We wish to find the exact function, $\Phi(x)$, the result of an infinite Monte Carlo calculation.

2. Since of course we cannot do an infinite Monte Carlo run, we cannot know $\Phi$ exactly. We do have however, the result of a finite Monte Carlo, which we shall think of as a set, $E_1$, of numbers, $x_i$:

   $$E_1 = \{x_i\} \quad , \ i=1\ldots m$$

   Here $x_i$ is the outcome of the ith trial and m is the total number of trials.

3. In addition to the results $E_1$, there are other things we know about $\Phi$ just from our knowledge of the underlying physical problem. Let us denote this other information by $E_0$. Observe that in doing this we have divided our total body of information about $\Phi$ into two parts. One part is $E_1$, the output of the finite Monte Carlo, the other part is "everything else", i.e. $E_0$.

4. Based therefore on this total body of information, $E_0$ and $E_1$, we seek a way to "bound" $\Phi$ in some sense; or, to say it a little better, we seek a way to express our state of knowledge, our state of confidence about exactly what $\Phi$ looks like.

5. Having stated it in this way we recognise it as a perfect problem for Bayes' Theorem. This is a problem of inference; and since Bayes' Theorem is the fundamental law governing logical inference (or even better, the fundamental expression of what we mean by logical inference) it is natural to apply Bayes' Theorem here.

FIGURE E.2

UNCERTAINTY DISTRIBUTION ABOUT 'A'
BASED ON FINITE MONTE CARLO RUN

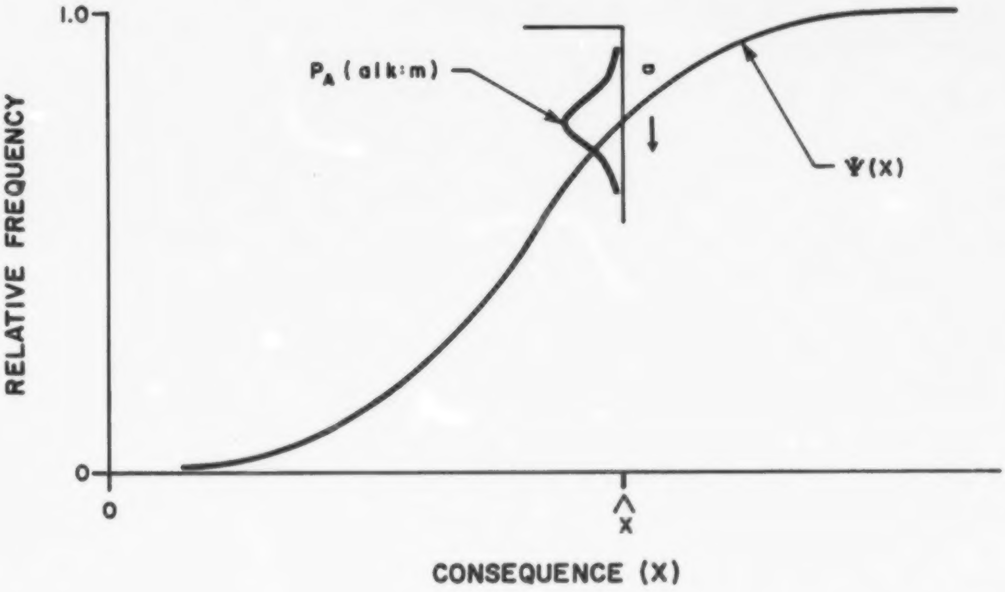

FIGURE E.3

FAMILY OF EQUIPERCENTILE CURVES
COMPUTED FROM FINITE MONTE CARLO RUN

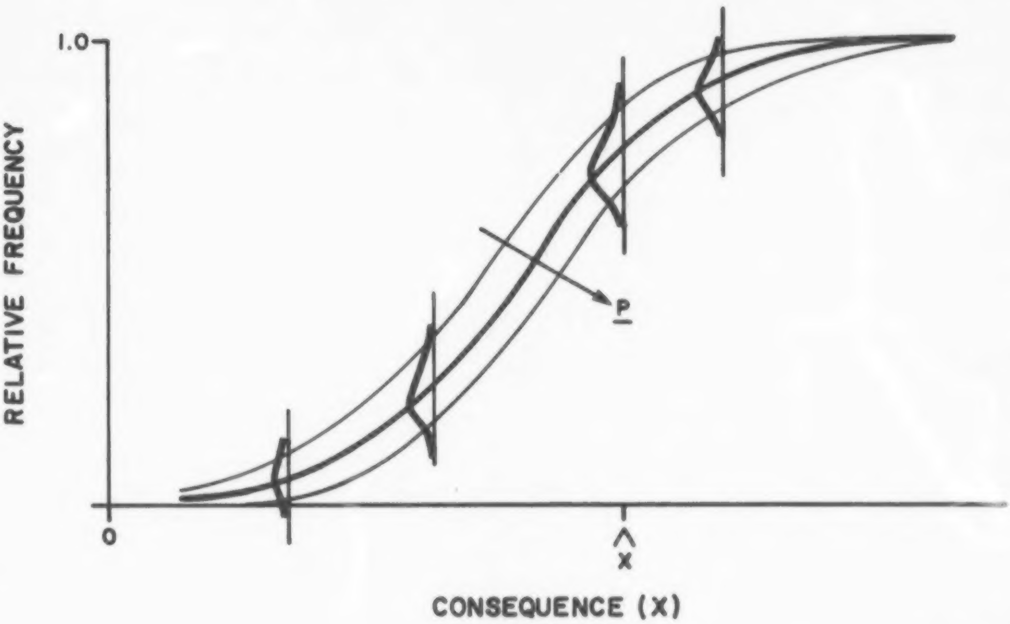

6. For this purpose we write Bayes' Theorem in the form:

$$p_\Phi(\phi|E_1,E_o) = \frac{p_\Phi(\phi|E_o)\ p(E_1|\phi,E_o)}{\int_F p_\Phi(\phi|E_o)p(E_1|\phi,E_o)d\phi} \tag{3-1}$$

where F is the function space of all possible bell curves against x. F therefore contains the exact distribution $\Phi$. The lower case $\phi$, i.e. $\phi(x)$, represents a variable point in F. Thus:

$p_\Phi$ $(\phi|E_1,E_0)$ = our probability, i.e. our degree of confidence based on evidence $E_1$ and $E_0$, that the "true" answer, $\Phi$, is equal to $\phi$.

$p_\Phi$ $(\phi|E_0)$ = the "prior", i.e. our level of confidence that $\Phi = \phi$, before we learned the results of the Monte Carlo run.

$p(E_1|\phi,E_0)$ = our probability, if $\phi$ were the true distribution, that we would have observed the outcome $E_1$ in our finite Monte Carlo.

7. Note the exact parallel between equation (3-1) and our previous equation (2-1). In equation (2-1) we embedded the "unknown number", A, in a space of possible values, i.e. in the interval [0,1]. In equation (3-1) we embed the unknown function, $\Phi(x)$, in a space, F, of possible functions $\phi(x)$. In both cases we then erect over the space, probability distributions expressing our state of knowledge about where within the space the true answer lies.

8. The likelihood function $p(E_1|\phi,E_0)$ in equation (3-1) may be evaluated as follows:

$$p(E_1|\phi,E_o) \propto \prod_{i=1}^{m} \phi(x_i) \tag{3-2}$$

since $\phi(x_i)dx_i$ is in effect the conditional probability, given that $\phi$ is the true distribution, that any particular Monte Carlo trial will yield a result in $dx_i$ about $x_i$.

9. For purposes of numerical evaluation of equation (3-1) it is usually desirable to replace the infinite dimensional space F with a finite approximation. It might be, for example, on the basis of our knowledge $E_0$, that we feel $\Phi$ would be well approximated by a lognormal curve, i.e. a curve of the form

$$\Phi(x) = N(z)\,\frac{dz}{dx} \tag{3-3a}$$

with

$$x = \mu \exp(\sigma z) \tag{3-3b}$$

where z is a standard normal variate, N(z) is the standard normal distribution, $\mu$ is the median and $\sigma$ is the logarithmic standard deviation.

We can now establish on the space of lognormal curves a discrete and finite subset by defining a grid:

$$\mu_1, \mu_2, \ldots \mu_j$$

$$\sigma_1, \sigma_2 \ldots \sigma_k$$

We then replace F by the finite space, $F_1$, of lognormal curves, $\phi_{j,k}$,

$$\phi_{jk}(x) = N(z)\,\frac{dz}{dx} \tag{3-4a}$$

$$x = \mu_j \exp(\sigma_k z) \tag{3-4b}$$

$$\text{i.e.}\quad \phi_{jk}(x) = \frac{1}{x\sigma_k} \quad N\left(\frac{1}{\sigma_k}\ln \frac{x}{\mu_j}\right) \tag{3-4c}$$

10. With this approximation equation (3-1) reduces to:

$$p(\phi_{jk}|E_1,E_o) = \frac{p(\phi_{jk}|E_o)\; p(E_1|\phi_{jk}E_o)}{\sum_{j=1}^{J}\sum_{k=1}^{K} p(\phi_{jk}|E_o)\; p(E_1|\phi_{jk}E_o)} \qquad (3\text{-}5)$$

or simplifying the notation,

$$p_{jk} = \frac{p_{jk}^{o}\; L_{jk}}{\sum_{j,k} p_{jk}^{o} L_{jk}} \qquad (3\text{-}6)$$

where

$$L_{jk} = \prod_{i=1}^{m} \frac{1}{x_i \sigma_k}\; N\left(\frac{1}{\sigma_k} \ln \frac{x_i}{\mu_j}\right) \qquad (3\text{-}7)$$

is the likelihood which evaluates evidence $E_1$ and $p_{jk}^{o}$ is the prior over the $\mu,\sigma$ grid which expresses our knowledge $E_0$. Note that not just the $p^{o}{}_{jk}$, but the selection of the discrete grid itself expresses $E_0$. Thus in numerical work it is often convenient to set $p_{jk}^{o} = 1$ and express $E_0$ in the grid spacing.

11. Equations (3-5) to (3-7) can now be readily evaluated numerically. The resulting posterior distribution, $p_{jk}$, can be conveniently printed out in tabular form, as in Figure E.4.

12. From this figure much interesting information can be derived. First of all we can pick out the maximum likelihood distribution, $\hat{\phi}$, as that $\phi_{jk}$ having the largest $p_{jk}$:

$$\hat{\phi} = \text{maximum likelihood distribution} = \phi_{\hat{j}\,\hat{k}} \qquad (3\text{-}8)$$

where $p_{\hat{j}\,\hat{k}} = \max p_{jk}$

13. Secondly we can obtain the "mean" or "expected" distribution $\bar{\phi}$ as

$$\bar{\phi} = \sum_{jk} p_{j\,k}\, \phi_{j\,k} \qquad (3\text{-}9)$$

This is our "best estimate" distribution.

14. Equations (3-8) and (3-9) are estimates of the true distribution $\Phi$, itself and may be plotted for comparison as in Figure E.5.

15. The comparison is one estimate of uncertainty. Other estimates may be obtained from Figure E.4 in many interesting ways. One way is direct inspection of the figure. Another is to visualize the $p_{jk}$ as effectively a probability surface over the $\mu,\sigma$ axis. We can then imagine contour lines from this surface projected down into the table itself. For example the contour line labelled p = 0.75 in the table would mean that 75 percent of the probability is interior to this line, i.e. we are 75 percent confident that the true distribution lies inside this region of the function space.

16. In particular, rectangular type contour regions are interesting. For example suppose the rectangle in Figure E.6 contained 90% of the probability. We could then plot the four corner distributions along with the mean, obtaining a diagram, looking something like Figure E.7. The four corner curves in effect "bracket" the best estimate. With sufficient number of trials in the Monte Carlo these five curves should come very close together.

17. From the four corner curves we can also obtain confidence bounds on the cumulative distribution $\Psi(x)$. For example let $\bar{\psi}(x)$ be the cumulative form of the best estimate $\bar{\phi}(x)$. We take $\bar{\psi}(x)$ therefore as a best estimate of $\Psi(x)$ and plot it as such in Figure E.8. Now consider the curve $\phi(x)_3$, from the upper right corner. We know that at least 90 percent of the probability distribution in the function space rests on curves having smaller median, $\mu$, and smaller width, $\sigma$, than does curve $\psi_3$. Therefore the upper half of the cumulative curve, $\psi_3$, may be taken as a 90 percentile lower bound to the exact curve. That is to say, we have at least 90 percent confidence that the true curve $\Psi(x)$ lies above this segment of $\psi_3$.

FIGURE E.4

# THE POSTERIOR DISTRIBUTION ($P_{jk}$) OVER THE SPACE OF FUNCTIONS ($\phi_{jk}$)

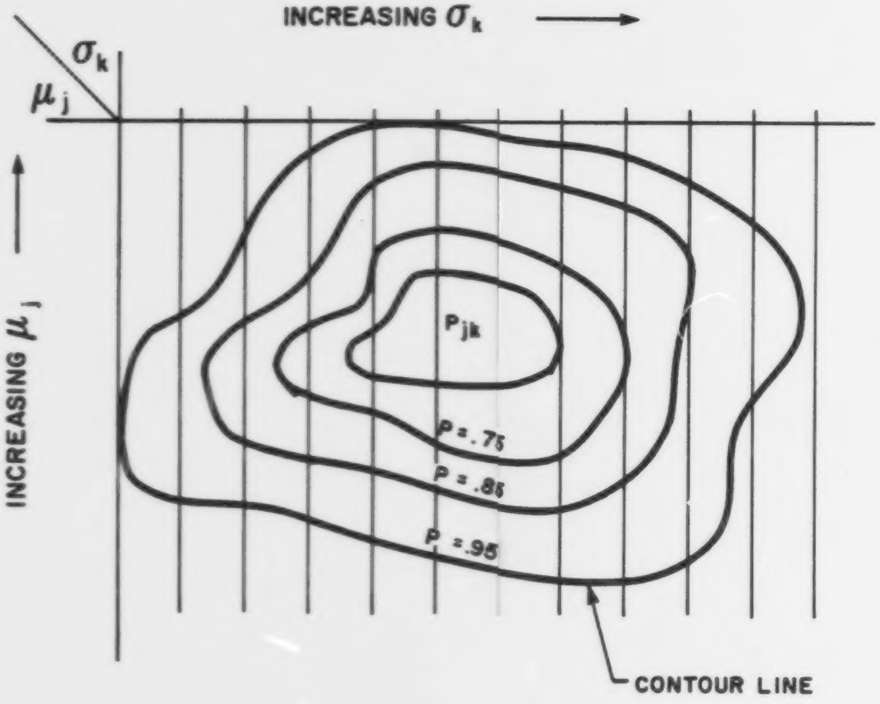
INCREASING $\sigma_k$ ⟶
$\sigma_k$
$\mu_j$
INCREASING $\mu_j$ ⟶
$P_{jk}$
P = .75
P = .85
P = .95
CONTOUR LINE

NOTE:

$P_{jk} = P(\phi_{jk} / E_1, E_0)$

FIGURE E.5

# MAXIMUM LIKELIHOOD AND EXPECTED VALUE ESTIMATES OF THE TRUE DISTRIBUTION $\Phi(X)$

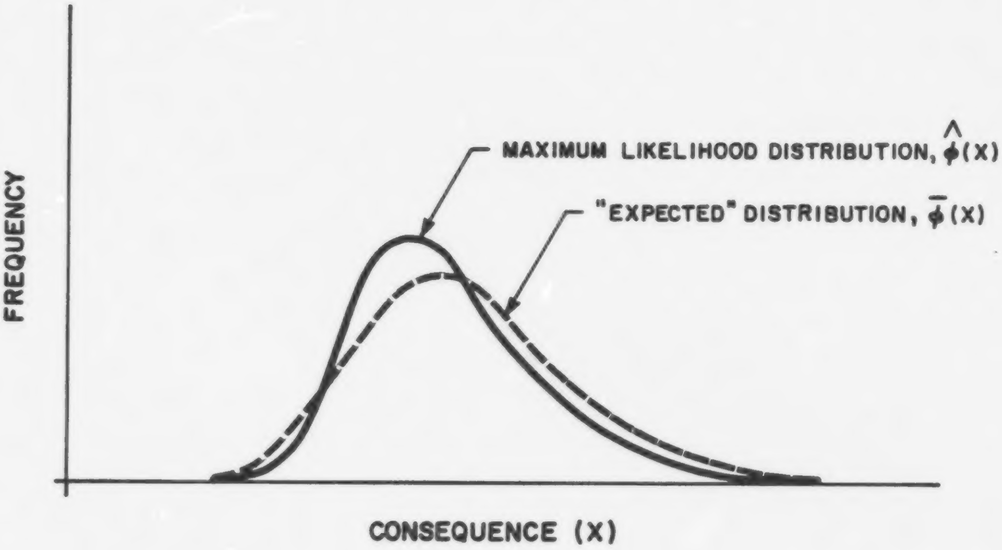

FIGURE E.6

THE POSTERIOR DISTRIBUTION ($P_{jk}$)
SHOWING 90 PERCENTILE
RETANGULAR CONTOUR LINE

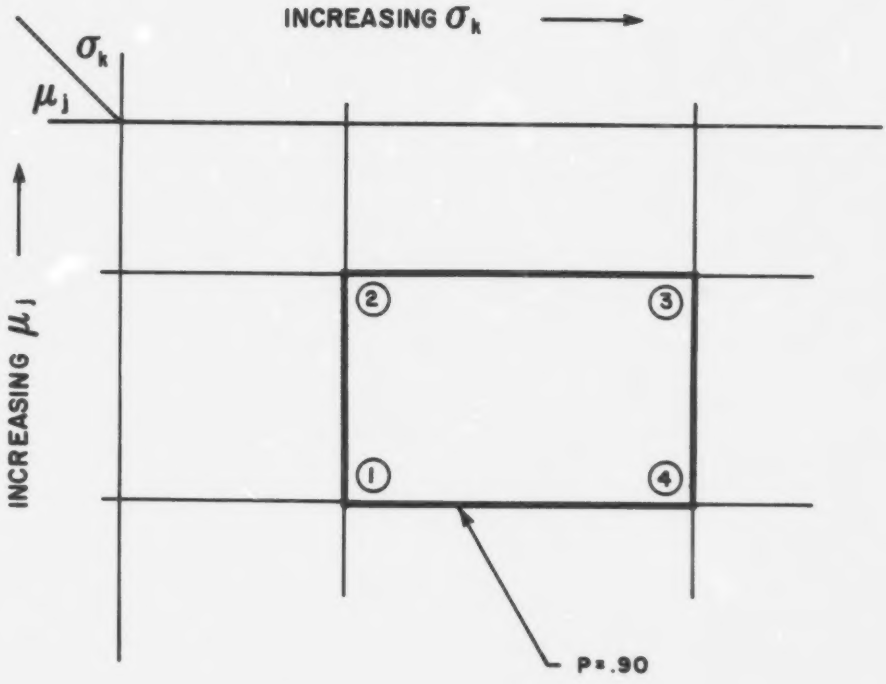
INCREASING $\sigma_k$
$\sigma_k$
$\mu_j$
INCREASING $\mu_j$
②
③
①
④
P=.90

FIGURE E.7

THE BEST ESTIMATE DISTRIBUTION $\bar{\phi}(X)$
SHOWN BRACKETED BY THE CORNER SHAPES
FROM A 90% RECTANGLE

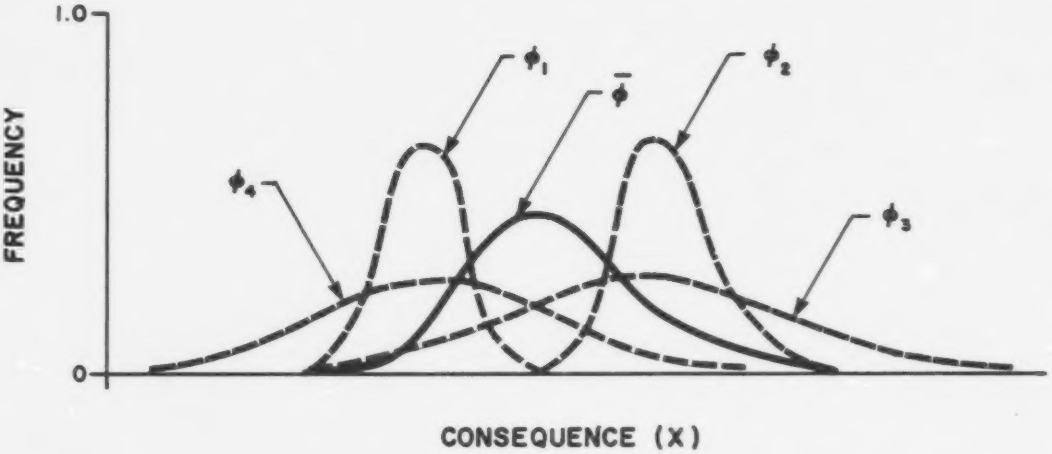

FIGURE E.8

CONFIDENCE BOUNDS
ON THE EXACT DISTRIBUTION
OBTAINED FROM THE FOUR CORNER DISTRIBUTIONS

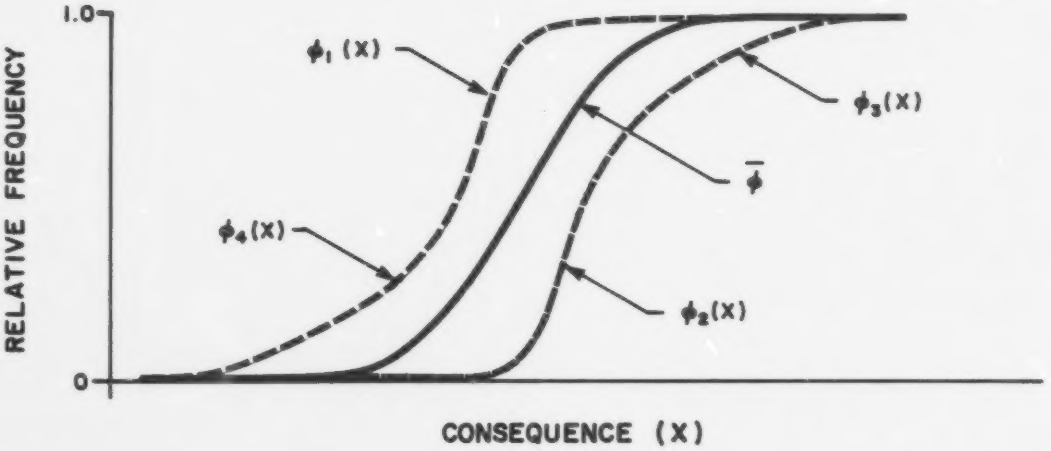

Arguing in the same way we may piece together a 90 percent band on $\Psi$ using segments of the four corner curves as shown in Figure E.8.

## E.4 CONCLUSION

We have presented an easy and interesting method for assessing the accuracy of the output distribution of a finite Monte Carlo calculation. The method proceeds by imagining the "true" output distribution (i.e. the results of an infinite Monte Carlo) as embedded in a suitably chosen approximating function space.

On this space a probability distribution is erected using Bayes' Theorem and the evidence of the actual output of the finite Monte Carlo run. This probability distribution is in itself the measure of accuracy of the finite Monte Carlo output. From this distribution, best estimates of the true output may be obtained, along with various interesting pictorial ways of visualizing the uncertainty.

For our examples we have chosen as a function space a two parameter family of log normal curves. This was illustrative only. Any set of curves, with any number of parameters may be used in any specific application, subject only to the consideration that the space chosen should contain shapes which are good approximations to the true output distribution.

APPENDIX F

# DEVELOPMENT AND IMPLEMENTATION OF A PROCEDURE FOR ESTABLISHING CONFIDENCE REGIONS FOR OUTPUT DISTRIBUTIONS FROM MONTE CARLO CALCULATIONS

by

P. M. Reilly and T. Duever
University of Waterloo

for

SENES Consultants Limited
Willowdale, Ontario

January 1986

## ABSTRACT

This paper describes a method of stating bounds within which the true probability density function or cumulative probability function of the output variable of a Monte Carlo calculation may be expected to lie, at a given confidence level. The method is an extension of work by Cheng and Iles and by Scheffe in which a probability density function of known mathematical form is fitted to observed relative frequency values and, using conventional statistical methods, a joint confidence region for the parameter values is found. The applicability of the method to output results of environmental assessment models is demonstrated. The confidence bands calculated for the cumulative probability function using this method were found to be narrower than the bands derived using a procedure developed by Kolmogorov and Smirnov, which was used in the Phase I study.

## TABLE OF CONTENTS

Page

F.1 INTRODUCTION AND BACKGROUND F-1

F.2 GENERAL FORMS FOR OUTPUT PROBABILITY DENSITY FUNCTIONS F-3

F.3 FITTING THE PROBABILITY DENSITY FUNCTION TO THE DATA F-4

F.4 ESTABLISHING CONFIDENCE BOUNDS FOR THE FITTED PROBABILITY FUNCTION F-7

F.5 ESTABLISHING CONFIDENCE BOUNDS FOR THE CUMULATIVE PROBABILITY FUNCTION F-8

F.6 APPROACH TO COMPUTER IMPLEMENTATION F-9

F.7 ILLUSTRATION OF CONFIDENCE BOUNDS ESTIMATION F-12
- F.7.1 Introduction F-12
- F.7.2 Original Example F-12
- F.7.3 Additional Examples F-14

F.8 CONCLUSIONS F-15

REFERENCES

APPENDIX F1: NEWTON-RAPHSON ITERATIVE SOLUTION

APPENDIX F2: ANALYTICAL SOLUTION FOR $r = 1$

APPENDIX F3: KOLMOGOROV CONFIDENCE BANDS

## LIST OF FIGURES

| | | Follows Page |
|---|---|---|
| Figure F1 | Relation of Confidence Band Programs to UTAP | F-10 |
| Figure F2 | Schematic Flowsheet for Confidence Band Program | F-10 |
| Figure F3 | Fitted Probability Density Functions For s=2, s=4 and s=6 | F-12 |
| Figure F4 | 95% Confidence Limits for Probability Density Function, Classroom Economic Study (s=4) | F-13 |
| Figure F5 | 95% Confidence Limits for Probability Density Function, DOSRN 100 Trials - 2 Parameter Model | F-13 |
| Figure F6 | 95% Confidence Limits for Cumulative Distribution Function, DOSRN 500 Trials - 2 Parameter Model | F-13 |
| Figure F7 | 95% Confidence Limits for Cumulative Distribution Function, DOSRN 100 Trials - 2 Parameter Model | F-13 |
| Figure F8 | 95% Confidence Limits for Probability Density Function, DOSRN 500 Trials - 2 Parameter Model | F-13 |
| Figure F9 | Plots of 95% Confidence Bands for a Normal Distribution (500 Trials) | F-14 |
| Figure F10 | Plots of 95% Confidence Bands for a Log Transformed Lognormal Distribution (500 Trials) | F-14 |
| Figure F11 | Plots of 95% Confidence Bands for Logarithm of Radium in Fish (200 Trials) | F-14 |

## LIST OF TABLES

Follows Page

Table F1 Illustration of Cheng and Iles Technique F-12

Table F2 Variable DOSRN (100 Trials) F-13

Table F3 Variable DOSRN (500 Trials) F-13

# APPENDIX F
# DEVELOPMENT AND IMPLEMENTATION OF A PROCEDURE FOR ESTABLISHING CONFIDENCE REGIONS FOR OUTPUT DISTRIBUTIONS FROM MONTE CARLO CALCULATIONS

## F.1 INTRODUCTION AND BACKGROUND

The most important output from a Monte Carlo calculation is often the probability density function for one or more output variables. Each probability density function is obtained in approximate form as a set of counts in cells which correspond to different interval values of the variable. The observed relative frequencies in the cells provide an approximation to the probability density function of the variable.

If the number of Monte Carlo trials were extremely large (say $10^9$) and the number of cells moderate (say 20), it would be expected that the graph of the relative frequency values versus the values of the variable corresponding to different cells would be a smooth curve which would agree very closely with the true probability density function. It would also vary little from one Monte Carlo run with the same number of trials to the next.

If however only 200 Monte Carlo trials are made with 20 cells, the relative frequency diagram can be expected to be "ragged", to vary a good deal from one run of 200 trials to the next, and the smooth curve drawn through the relative frequency points cannot be expected to agree closely with the true probability density function. It is the object of this exposition to describe a method of stating bounds within which the true probability density function may be expected to lie, at a given confidence level.

In the Phase I SENES study (SENES 1984) a distribution-free technique based on an extension of the Kolmogorov-Smirnov goodness of fit test (Kolmogorov 1941), as described for example in Kendall and Stuart (1961), was used to develop confidence bands for the cumulative distribution function. The test is based on the maximum absolute deviation between the empirical (i.e. observed) cumulative distribution function, and the underlying true cumulative distribution. Unfortunately, while the method is attractive because of its simplicity, it does have the disadvantage of being too conservative, particularly in the tails of the distribution. For example, ordinate values of less than zero for the left tail and greater than one for the right tail are obtained. In practice the confidence bands are truncated at zero or one respectively. This consideration prompted the further investigation of techniques for establishing confidence bands which led to the present paper.

The method discussed in this paper is an extension of the approach of Cheng and Iles (1983) and of Scheffé (1959), in which a probability density function of known mathematical form is fitted to the observed relative frequency values by estimating the values of the parameters in the probability density function. At the same time, by conventional statistical methods, a joint confidence region for the parameter values is found. Then the set of mathematical functions which might, at the confidence level being used, include the true probability density function is the set of mathematical functions obtained by substituting into the known mathematical form of the probability density function all values of the parameters within their joint confidence region. The envelope of this set of functional relations is the confidence region, at the confidence level being used, for the probability density function of the variable.

The theoretical investigations described in this Appendix were carried out originally by Park M. Reilly and T.A. Duever and have been described in a previous report (see the discussion paper on confidence regions by Reilly and Duever in Volume 2 of SENES 1985). Subsequently, Reilly and Duever were asked to develop a procedure to permit computer implementation of their technique for establishing confidence regions for output distributions from Monte Carlo calculations. For completeness and ease of reference it was decided to reproduce the original discussion of Reilly and Duever in this appendix. However, it should be noted that the original discussions by Reilly and Duever (in SENES 1985) have been modified or augmented in several areas. These areas include a discussion of an approach to overcoming ill-conditioned matrices, a revised examples section and a new section outlining the approach to computer implementation.

All theoretical investigations were carried out by Reilly and Duever as was the development of the initial computer routine. SENES in turn adapted the work of Reilly and Duever for inclusion in the Uranium Tailings Assessment Program (UTAP) a post-processing option. The principal SENES contributors in this regard were Donald I. Beals and Cecile E. Hallam. Technical overview and coordination between Reilly and Duever and SENES staff was provided by Douglas B. Chambers of SENES

## F.2 GENERAL FORMS FOR OUTPUT PROBABILITY DENSITY FUNCTIONS

The first requirement in calculating the confidence interval for the probability density function is a method of establishing flexible mathematical forms for the probability density functions to which the observed data may be fitted. Occasionally the output probability density function is of known form because of known forms for the input variables and a simple function relating them to the output variable. In the more interesting cases however, the probability density functions for the output variables are not of simple form.

The following form is proposed for the output probability density function of a random variable represented, possibly in transformed form, by x. The cell mid-points are represented by $x_1, x_2, ..., x_m$.

$$p(x) = \exp(\theta_0 + \theta_1 x + \theta_2 x^2 + .....+ \theta_s x^s) \qquad (F1)$$

$$\sum_{i=1}^{m} p(x_i) = 1$$

where p is the probability density function, s is an integer representing the degree of the approximating polynomial, $\theta_i$ are the constant coefficients of the approximating polynomial, and m is the number of cells.

The variable $\theta_0$ is an auxiliary variable which can be interpreted as a normalizing constant. It can be eliminated if desired by writing (F1) in the following form:

$$p(x) = \frac{\exp(\theta_1 x + \theta_2 x^2 + \ldots .\ \theta_s x^s)}{\sum_{i=1}^{m} [\exp(\theta_1 x + \theta_2 x^2 + \ldots + \theta_s x^s)]} \qquad \text{(F2)}$$

which obviously sum to unity over all $x_i$

In actual practice the data are given as cell counts at a number, usually 10 to 20, of cells (bins), each cell usually representing a small range of values of x. In that case, p(x) in equation (F1) can be interpreted as the probability of a count entering the cell which corresponds to the value of x at the mid-point of the cell. It will be only approximately true that if the p(x), interpreted as cell probabilities, sum to 1, then p(x) interpreted as a probability density as was done above, will integrate to 1. If necessary this deficiency can be corrected by adjusting the value of the normalizing constant.

## F.3 FITTING THE PROBABILITY DENSITY FUNCTION TO THE DATA

Suppose that cell counts have been observed in m cells and the ith cell, the mid-point of which corresponds to the value $x_i$ of the random variable, has recorded $n_i$ counts. It is desired to estimate $\theta_j$, j=0, 1, ..., s so as to fit equation (F1). At this time $p(x_i)$ in equation (F1) will be interpreted as the probability of a count entering the ith cell.

Such a situation is described by the multinomial likelihood function:

$$L(\theta_1,\ldots\theta_s) = \prod_{i=1}^{m} [p_i(x_i)]^{n_i} \qquad \text{(F3)}$$

A very good estimate of $\underline{\theta}$, the maximum likelihood estimate, is obtained by maximizing L, or more conveniently by minimizing its negative logarithm:

$$S(\underline{\theta}) = -\ln L(\underline{\theta}) = -\sum_{i=1}^{m} n_i \ln(p_i) \qquad \text{(F4)}$$

where

$$\ln(p_i) = \theta_0 + \sum_{k=1}^{s} \theta_k x_i^k \qquad \text{(F5)}$$

$$\text{and} \quad \sum_{i=1}^{m} p_i = 1 \qquad \text{(F6)}$$

This system can be solved by first differentiating both sides of equation F6 with respect to $\theta_j$ (F6):

$$\frac{\partial}{\partial\theta_j} \sum_{i=1}^{m} \exp\left\{\theta_0 + \sum_{k=1}^{s} \theta_k x_i^k\right\} = 0 \quad : j = 1,\ 2,\ \ldots S$$

then

$$\sum_{i=1}^{m} p_i \left(\frac{\partial\theta_0}{\partial\theta_j} + x_i^j\right) = 0 \quad : j = 1,\ 2,\ \ldots S$$

Therefore

$$\frac{\partial\theta_0}{\partial\theta_j} = -\frac{\sum_{i=1}^{m} p_i x_i^j}{\sum_{i=1}^{m} p_i} = -\sum_{i=1}^{m} p_i x_i^j; \quad j = 1, \ldots, s \qquad \text{(F7)}$$

To find the minimum of equation (F4) differentiate with respect to $\theta_j$; $j=1,2,\ldots,s$:

$$\frac{\partial S}{\partial \theta_j} = -\sum_{i=1}^{m} n_i \left[\frac{\partial \theta_0}{\partial \theta_j} + x_i^{\,j}\right]$$

$$= -N\,\frac{\partial \theta_0}{\partial \theta_j} - \sum_{i=1}^{m} n_i x_i^{\,j} \qquad \text{(F8)}$$

where

$$N = \sum_{i=1}^{m} n_i$$

Substituting equation (F7) into equation (F8) and setting $\frac{\partial S}{\partial \theta_j}$ in equation (F8) to zero:

$$N \sum_{i=1}^{m} p_i x_i^{\,j} = \sum_{i=1}^{m} n_i x_i^{\,j} \quad : \quad j = 1,2,\ldots,s \qquad \text{(F9)}$$

Note that for $j=0$ equation (F9) reduces to (F6) the constraint from which $\theta_0$ is calculated. While there is a theoretical distinction made between $\theta_0$ and $\underline{\theta}$, the vector of all $\theta$'s except $\theta_0$, they are all found in practice by solving the following nonlinear system of (s+1) equations in (s+1) unknowns.

$$N \sum_{i=1}^{m} p_i x_i^{\,j} = \sum_{i=1}^{m} n_i x_i^{\,j}; \quad j = 0,1,\ldots,s \qquad \text{(F10)}$$

Equation (F10) can be solved by the Newton-Raphson method as described in Appendix F1.

## F.4 ESTABLISHING CONFIDENCE BOUNDS FOR THE FITTED PROBABILITY FUNCTION

The probability function having been fitted to each observed cell frequency, the approach of Cheng and Iles permits confidence bounds on it to be established as outlined previously (SENES, 1985). The first step in this is to establish a joint confidence region for the parameters $\underline{\theta}$. This region is:

$$(\underline{\theta} - \underline{\hat{\theta}})' \underline{M} (\underline{\theta} - \underline{\hat{\theta}}) \leq \gamma \tag{F11}$$

where $\underline{\theta}$ is the sx1 vector of possible parameter values, $\underline{\hat{\theta}}$ is the sx1 vector of parameter estimates and $\underline{M}$ is the sxs Fisher information matrix for the parameters. Also $\gamma$ is a number which has approximately the value of a $\chi^2$-distributed random variable with s degrees of freedom which is exceeded with probability (1-a), where a is the desired confidence level. The (j,k)th element ($m_{jk}$) of the sxs Fisher information matrix is given by:

$$\underline{M} = m_{jk} = \left[ N \sum_{i=1}^{m} p_i x_i^{j+k} - N\left(\sum_{i=1}^{m} p_i x_i^{j}\right)\left(\sum_{i=1}^{m} p_i x_i^{k}\right)\right] \tag{F12}$$

The next step in the Cheng and Iles procedure is to choose values of $\underline{\theta}$, so as to maximize and minimize p(x) in equation (F1) subject to equation (F11). Since exponentiation is a monotone function it will be sufficient to maximize and minimize lnp(x). With $\lambda$ as the Lagrange multiplier the required Lagrangian is:

$$L(\underline{\theta}) = \theta_0 + \sum_{k=1}^{s} \theta_k x^k - \frac{1}{2} \lambda (\underline{\theta} - \underline{\hat{\theta}})' \underline{M} (\underline{\theta} - \underline{\hat{\theta}}) \tag{F13}$$

Solving this leads to the following equation for calculating values of $\underline{\theta}$ which maximize and minimize p:

$$\underline{\theta} = \underline{\hat{\theta}} \pm \sqrt{\frac{\gamma}{(\underline{c}-\underline{b})\ \underline{M}^{-1}(\underline{c}-\underline{b})}}\ \underline{M}^{-1}\ (\underline{c}-\underline{b}) \qquad \text{(F14)}$$

where

$\underline{b} = [\sum_{i=1}^{m} p_i x_i^{\,j}]$ jth element of the sxl vector $\underline{b}$

$\underline{c} = [x^j]$ jth element of the sxl vector $\underline{c}$

Note that equation (F14) requires an iterative solution since $\underline{b}$ is a function of $\underline{\theta}$. A scheme based on simple iteration was found to give rapid convergence.

Having found the limiting values of $\underline{\theta}$, the limits on p are found by substituting these in equation (F1).

## F.5 ESTABLISHING CONFIDENCE BOUNDS FOR THE CUMULATIVE PROBABILITY FUNCTION

If equation (F1) is interpreted as describing the probability density function for X, the cumulative probability function is defined by:

$$F(x) = \Pr(X \leq x) = \int_{-\infty}^{x} p(u)du = \int_{-\infty}^{x} \exp\left\{\theta_0 + \sum_{k=1}^{s} \theta_k\ u^{\,k}\right\} du \qquad \text{(F15)}$$

Confidence limits for F(x) for a fixed x may be found as in the last section by maximizing and minimizing F(x) by varying $\underline{\theta}$ within the limits given by equation (F11). They are found in terms of the vectors $\underline{\theta}$ which produce the maximum and minimum for F(x). The limiting $\underline{\theta}$ are found from the following equation, applied iteratively:

$$\underline{\theta} = \underline{\hat{\theta}} \pm \sqrt{\frac{\gamma}{\underline{r}'\ \underline{M}^{-1}\ \underline{r}}}\ \underline{M}^{-1}\ \underline{r} \qquad \text{(F16)}$$

where $\underline{\theta}$, $\underline{\hat{\theta}}$, $\gamma$ and $\underline{M}$ are as defined previously and $\underline{r}$ is the sxl vector:

$$\underline{r} = \int_{-\infty}^{x} [\underline{d}+\underline{e}] \ \exp\left\{\theta_0 + \sum_{k=1}^{s} \theta_k u^k\right\} du \qquad \text{(F17)}$$

where

$$d_j = \frac{\partial\theta_0}{\partial\underline{\theta}} = -\int_{-\infty}^{-\infty} u^j \exp\left\{\theta_0 + \sum_{k=1}^{s} \theta_k u^k\right\} du$$

is the jth element of the sx1 vector $\underline{d}$

$e_j = [u^j]$ is the jth element of the sx1 vector $\underline{e}$.

Note that $\theta_0$ is now given by:

$$\theta_0 = -\ln\left[\int_{-\infty}^{\infty} \exp\left\{\sum_{k=1}^{s} \theta_k u^k\right\} du\right] \qquad \text{(F18)}$$

For the case where s=1, the required integral can be found analytically as shown in Appendix F2. For s>1, numerical integration will be required. In this paper we have chosen to work with the probability distribution in discrete form. This has the advantage of eliminating the need for numerical integration.

When the limit producing values of $\underline{\theta}$ have been found, the bounds on F(x) are found by substitution into the integral in equation (F15).

## F.6 APPROACH TO COMPUTER IMPLEMENTATION

For their original investigations, Reilly and Duever used various programs available in WATFIV and FORTRAN on the IBM 4341 mainframe computer at the University of Waterloo. The initial set of examples discussed in the next section were developed using the technique on the Waterloo mainframe computer. For the present investigations, Reilly and Duever were asked to develop an integrated micro-computer based approach for their confidence band technique. The way in which the confidence bands programs reside in UTAP is described below.

The general structure of the confidence bands programs and their relation to UTAP is shown on Figure F1. Figure F2 is a general logic flowsheet which outlines the way in which the confidence bands programs have been implemented.

The confidence bands programs are designed as a post-processing option to UTAP. The user identifies variables which are first read and then subdivided into an optimal number of bins or cells in a program named BIN using the expression:

$$[\log_{10} ( \#\text{of Monte Carlo trials})/\log_{10} (2.0)] + 1.0 \qquad \text{(F19)}$$

which is based on a paper by Sturges (1926).

The binned data are then transferred to another program (OPAN) which has been written to perform all of the calculations described in sections F.3, F.4 and F.5. The program OPAN first reads in the data file generated by the binning program. The required information consists of the name of the variable being analysed, the number of cells or bins used, the number of Monte Carlo trials made, a flag indicating whether or not a logarithmic transformation of the data has been made, the right hand cell endpoints and finally the cell midpoints and cell counts.

The Newton-Raphson fitting procedure described in section F.3 is accomplished within subroutine NEWRAP. This subroutine requires two additional subroutines. The first one calculates the values of the probability density function at any value of x. The second subroutine provides a general solution to the matrix equation.

$$\underset{n\times n}{\underline{A}}\ \underset{n\times 1}{\underline{u}} = \underset{n\times 1}{\underline{b}} \qquad \text{(F19)}$$

by Cholesky decomposition (see Appendix F1). Upon convergence of the fitting procedures, a $\chi^2$ goodness of fit test at the 25% significance level is performed to see whether or not the fitted form of the probability density

FIGURE F.1

RELATION OF CONFIDENCE BAND PROGRAMS TO UTAP

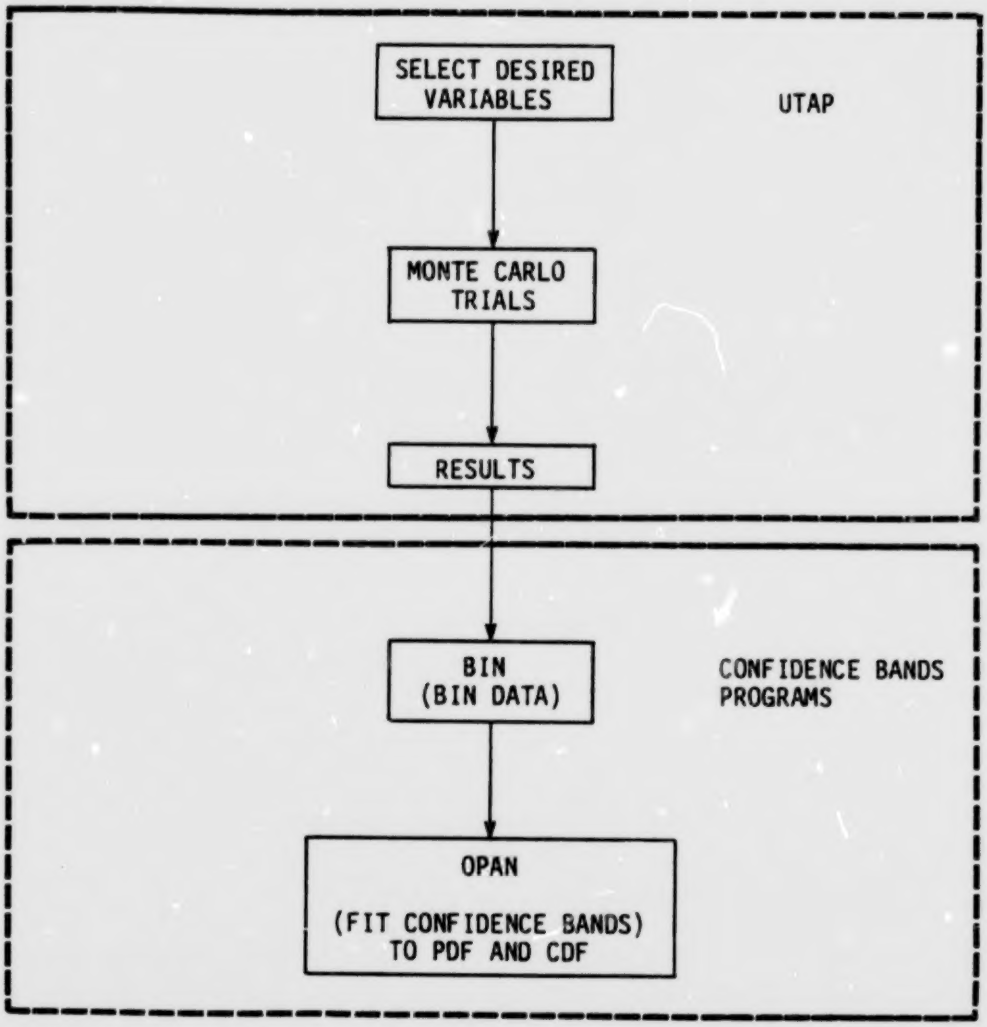
SELECT DESIRED VARIABLES
UTAP
MONTE CARLO TRIALS
RESULTS
BIN (BIN DATA)
CONFIDENCE BANDS PROGRAMS
OPAN
(FIT CONFIDENCE BANDS) TO PDF AND CDF

FIGURE F.2

SCHEMATIC FLOWSHEET
FOR CONFIDENCE BAND PROGRAM

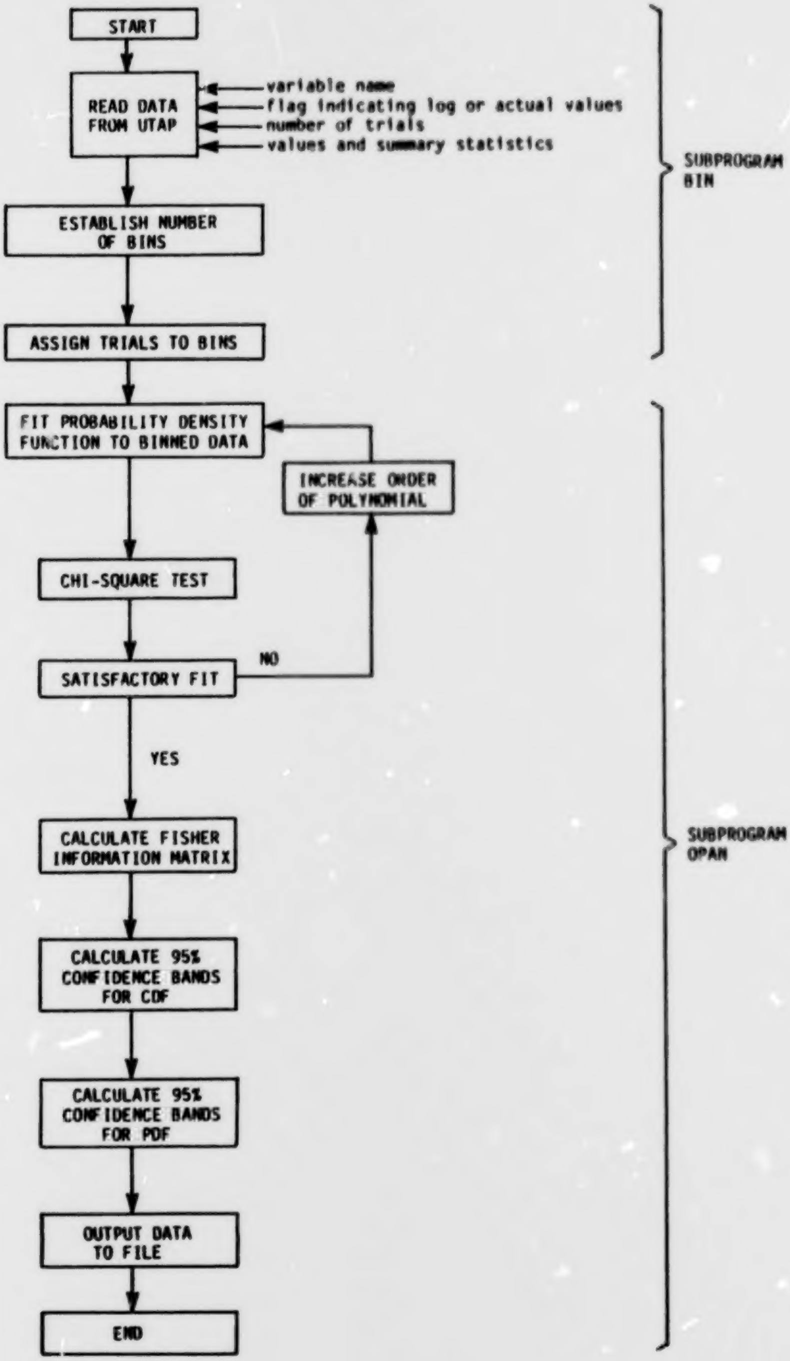
START
READ DATA FROM UTAP
variable name
flag indicating log or actual values
number of trials
values and summary statistics
ESTABLISH NUMBER OF BINS
ASSIGN TRIALS TO BINS
SUBPROGRAM BIN
FIT PROBABILITY DENSITY FUNCTION TO BINNED DATA
INCREASE ORDER OF POLYNOMIAL
CHI-SQUARE TEST
SATISFACTORY FIT
NO
YES
CALCULATE FISHER INFORMATION MATRIX
CALCULATE 95% CONFIDENCE BANDS FOR CDF
CALCULATE 95% CONFIDENCE BANDS FOR PDF
OUTPUT DATA TO FILE
END
SUBPROGRAM OPAN

function adequately describes the binned data. Notice that the degrees of freedom for this test are given by

$$D.F. = k - s - 1$$

where

$k$ = number of cells with fitted numbers of observations greater than 6
$s$ = degree of approximating polynomial

If the fitted number of cell counts for a particular cell are less than 6, then that cell is combined with the next cell. The value of $k$ may therefore be equal to the number of cells but this is not necessarily true. The program iterates, increasing the degree of the polynomial by 1 each iteration until a satisfactory fit is achieved.

Once a model passes the goodness of fit test the program enters the next phase in which confidence bands are evaluated. The first step is to evaluate the observed Fisher information matrix. The 95% confidence bands for the cumulative distribution function are calculated in subroutine CDF and finally the 95% confidence bands for the probability density functions are calculated in subroutine PDF. In both CDF and PDF, when the approximating polynomial is of degree one a very simple closed form solution is available (see Appendix F2).

Further discussion of the computer implementation of the confidence bands program is provided in Chapter 4 of this report. A full listing of the two computer programs used for confidence band estimation (BIN and OPAN) is provided in Appendix G of this report. Variable dictionaries for the two programs are also provided in Appendix G.

## F.7 ILLUSTRATION OF CONFIDENCE BOUNDS ESTIMATION

### F.7.1 Introduction

Two examples of confidence bands estimation were provided by Reilly and Duever in their original paper (see Volume 2 SENES, 1985). These orginal examples are included in this section. In addition, two examples utilizing the current microcomputer based version of the confidence program are also included as further demonstration of the technique.

### F.7.2 Original Example

Table F.1 shows cell counts obtained in N=500 trials in a classroom example which used a random sampling program (OPANAL) in an economic study. The data were fitted using s=2, s=4 and s=6. Using the standard $\chi^2$ test for goodness-of-fit the $\chi^2$ values are respectively 26.54, 7.97 and 2.29 with 9, 7 and 5 degrees of freedom. The null hypothesis in each case is that the corresponding s is correct and that the discrepancies between observed and expected number of counts occur by chance alone. On this basis, the probability of obtaining a set of cell counts which fits the form of the model used more poorly by chance is 0.2% for s=2. Simply put, this indicates that the polynomial of order S=2 provides a very poor fit to the observed cell counts. For s=4 the probability of obtaining a poorer fit by chance is 33.3%, which is considered acceptable. Because of the high probability of a poorer fit for s=6 of 80.8%, it may be considered overfitted; i.e. the use of too many parameters has probably caused the probability density function to be fitted to random fluctuations in the data. The value of s should be chosen to give a probability of a poorer fit roughly in the region of 25% so as to provide a reasonably good fit using as few parameters as possible and at the same time avoiding the fitting of chance fluctuations in the data.

Figure F.3 shows the plotted comparisons between the observed counts and fitted probability density functions for each of the three different degrees of the polynomial. In each case the smooth line is fitted while the heavy

Table F.1

## ILLUSTRATION OF CHENG AND ILES TECHNIQUE

| Cell number | 1 | 2 | 3 | 4 | 5 | 6 | 7 | 8 | 9 | 10 | 11 | 12 |
|---|---|---|---|---|---|---|---|---|---|---|---|---|
| Actual counts ($n_i$) | 1 | 7 | 40 | 68 | 77 | 74 | 62 | 69 | 53 | 26 | 15 | 8 |
| Fitted (s=2) | 8.2 | 17.9 | 33.6 | 53.3 | 72.1 | 82.8 | 80.9 | 67.2 | 47.4 | 28.5 | 14.5 | 6.3 |
| Fitted (s=4) | 1.0 | 10.0 | 35.8 | 65.7 | 79.9 | 78.0 | 69.2 | 59.0 | 47.7 | 33.8 | 18.1 | 5.9 |
| Fitted (s=6) | .8 | 8.5 | 37.6 | 69.9 | 77.0 | 71.4 | 67.7 | 64.7 | 52.3 | 29.8 | 12.9 | 8.5 |
| Upper 95% Confidence Boundary (s=4) | 5.8 | 19.3 | 47.8 | 80.8 | 92.4 | 90.2 | 81.0 | 69.1 | 59.1 | 45.0 | 27.0 | 16.2 |
| Lower 95% Confidence Boundary (s=4) | 0.2 | 4.8 | 25.9 | 52.3 | 67.7 | 65.8 | 57.3 | 48.4 | 36.8 | 24.0 | 11.2 | 1.9 |

FIGURE F.3

**FITTED PROBABILITY DENSITY FUNCTIONS FOR S=2, S=4 AND S=6**

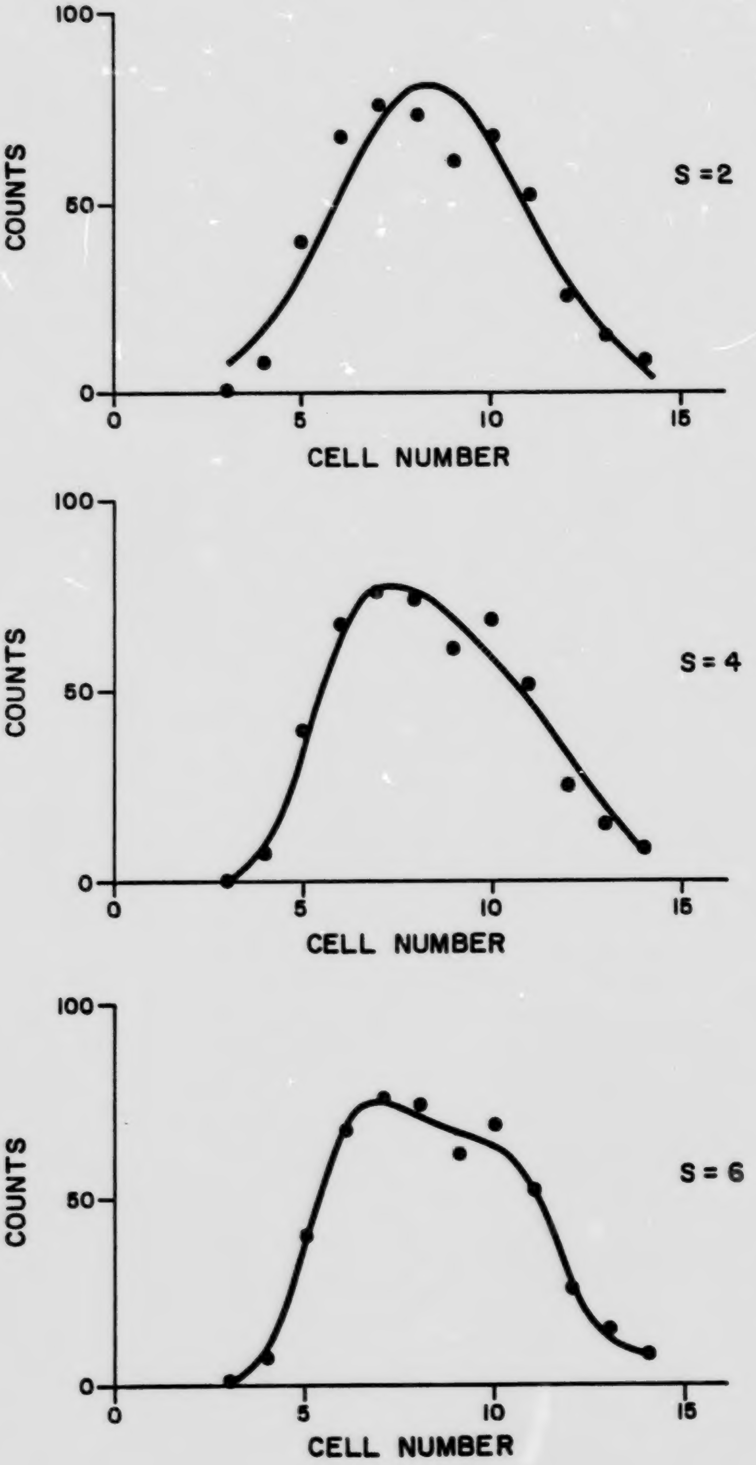

dots are observed values. The appearance of the curve for s=6 is consistent with its being overfitted. The curve for s=2 is the same as the normal probability density function with mean and variance estimated from the data. Figure F.4 shows the original data and the fitted curve for s=4 as in Figure F.2 and also shows 95% confidence limits for the probability density function. Note that fitted values, upper and lower 95% confidence limits were only calculated at those values of x at which observations were available. The smooth curves were obtained by using a smoothing procedure based on cubic spline functions. Smooth curves could have also been obtained by using a higher level of discretization along the axis and then evaluating the fitted function and the limits at a larger number of x-values. Cubic splines were used for numerical convenience only and it is expected that both procedures would produce practically the same curve.

A second example related to uranium mill tailings was also used to illustrate application of the technique. Specifically, two data sets, one of 100 trials and one of 500 trials, of the variable DOSRN were provided by SENES Consultants Limited. The values of the variable DOSRN are estimates of the annual dose to an adult male living year round about 2 km downwind of the reference uranium tailings area described in SENES (1984) and which arises from radon gas released from the tailings area.

Tables F.2 and F.3 show cell counts for the output variable DOSRN for 100 and 500 trials respectively. As shown the $\chi^2$ goodness-of-fit test indicates that in both cases a model with s=2 is suitable. Figures F.5 and F.6 show the observed cell counts, the fitted probability density functions and the 95% confidence limits for these. As expected, the bands obtained at 500 trials are narrower than those at 100 trials.

Figures F.7 and F.8 show the corresponding cumulative distribution functions, including the 95% confidence bounds produced by this method as well as Kolmogorov bands. The procedure for obtaining the Kolmogorov bands is outlined in Appendix F.3.

The solid dots have a different meaning on the probability density function (pdf) plots (Figures F.5 and F.6), than they do on the cumulative distribution function (cdf) plots (Figure F7 and F8). On the pdf plots the dots represent observed data plotted at the cell midpoints. On the cdf plots they represent observed data plotted at the right hand cell endpoint. This arises from the fact that the ordinate is a measure of probability density on the one hand, while it measures cumulative probability on the other hand. In all of Figures F.5 to F.8, the cubic spline smoothing procedure described earlier was used.

### F.7.3 Additional Examples

Two additional examples, calculated using the current microcomputer implementation (the actual computer code is given in Appendix G of this volume) are provided as additional demonstration of the technique.

The first example is a simple application of the technique to two known distributions, one of which uses the raw data and the second the log-transformed data. Figure F.9 illustrates the 95% confidence bands calculated from 500 random samples of a normal distribution. Figure F.10 illustrates the confidence bands calculated from 500 random samples of a lognormal distribution, log transformed by the confidence bands program.

The second example, illustrated in Figure F.11, is confidence bands fitted to actual output from the model UTAP. Two hundred probabilistic trials were used with the confidence bands being fitted to radium concentration in fish, after 100 years, using a log transformation of the data. The broadening of the confidence bands on the last value plotted on the PDF on Figure F.11 simply reflects the uncertainty inherent in a bin with low counts which represents all values greater than some specified value. Similar behaviour is evident in Figure F.5 which shows the PDF for the results of trials of the radon model. The same behaviour persists but is much less evident in Figure F.6 which shows the PDF for the results of 500 trials of the radon model.

FIGURE F.4

95% CONFIDENCE LIMITS
FOR PROBABILITY DENSITY FUNCTION
CLASSROOM ECONOMIC STUDY (S=4)

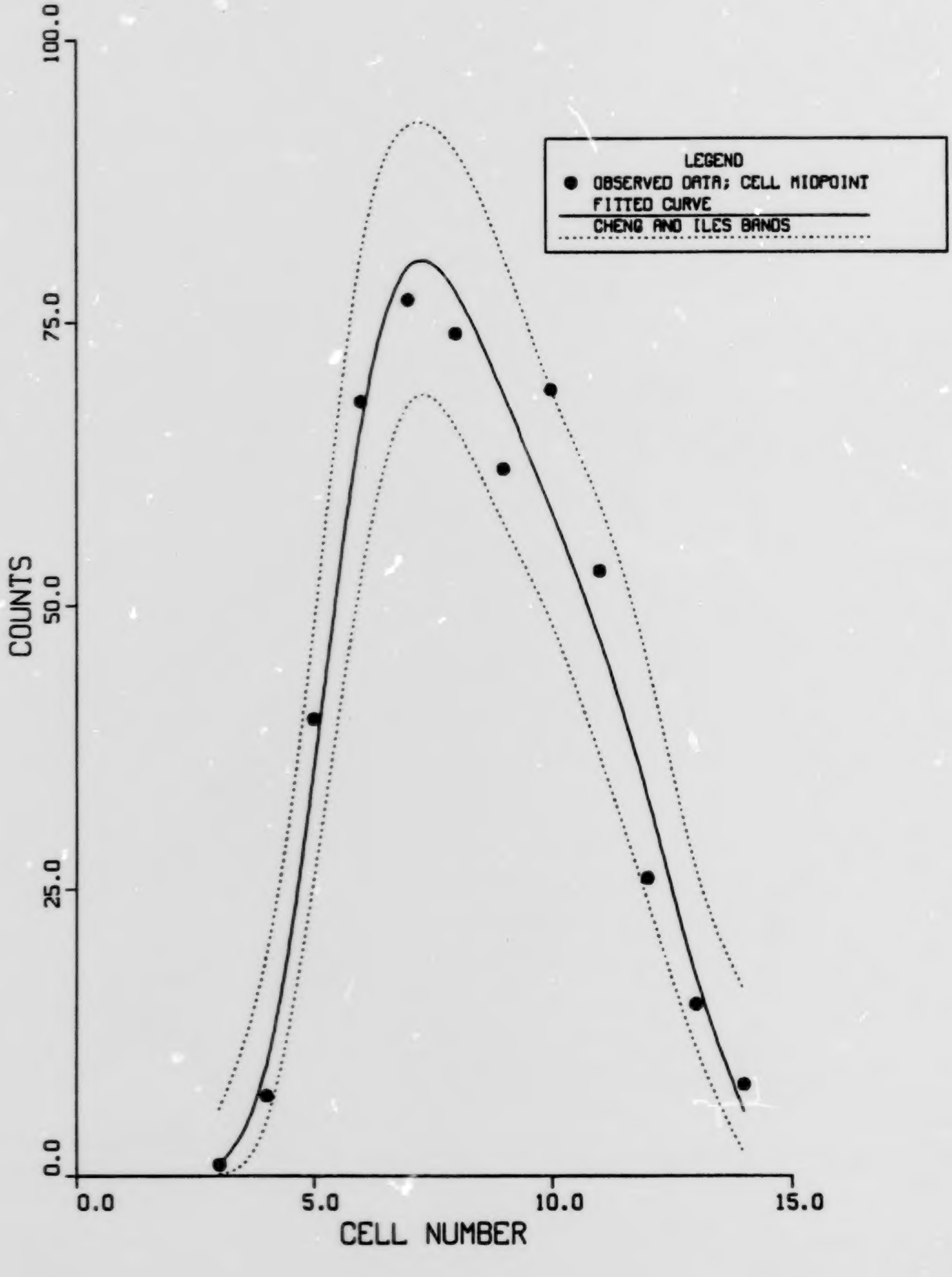

Table F.2

## VARIABLE DOSRN (100 TRIALS)

| Cell Number | Observed Counts | Fitted (s=2) | Upper 95% Conf. Limits | Lower 95% Conf. Limits |
|---|---|---|---|---|
| 1 | 52 | 54.7 | 64.6 | 43.6 |
| 2 | 28 | 23.0 | 25.7 | 19.1 |
| 3 | 9 | 10.4 | 14.1 | 7.2 |
| 4 | 3 | 5.1 | 7.8 | 3.1 |
| 5 | 4 | 2.7 | 4.5 | 1.5 |
| 6 | 2 | 1.5 | 2.8 | 0.8 |
| 7 | 1 | 0.9 | 2.0 | 0.4 |
| 8 | 0 | 0.6 | 1.7 | 0.2 |
| 9 | 0 | 0.4 | 1.9 | 0.1 |
| 10 | 0 | 0.3 | 2.5 | 0.0 |
| 11 | 1 | 0.3 | 4.0 | 0.0 |

Goodness-of-Fit Test

| s | $\chi^2$ | d.f.* | Pr.** |
|---|---|---|---|
| 1 | 3.607 | 3 | 30.7% |
| 2 | 2.47 | 2 | 30.4% |

* d.f. = degrees of freedom
** Pr. = probability of obtaining a poorer fit

Table F.3

## VARIABLE DOSRN (500 TRIALS)

| Cell Number | Observed Counts | Fitted (s=2) | Upper 95% Conf. Limits | Lower 95% Conf. Limits |
|---|---|---|---|---|
| 1 | 290 | 280.9 | 301.7 | 258.4 |
| 2 | 106 | 115.6 | 119.2 | 110.7 |
| 3 | 47 | 50.6 | 56.8 | 44.6 |
| 4 | 25 | 23.6 | 28.5 | 19.3 |
| 5 | 14 | 11.7 | 15.0 | 9.0 |
| 6 | 4 | 6.1 | 8.3 | 4.5 |
| 7 | 4 | 3.4 | 4.9 | 2.4 |
| 8 | 3 | 2.0 | 3.0 | 1.4 |
| 9 | 2 | 1.3 | 2.0 | 0.8 |
| 10 | 1 | 0.9 | 1.4 | 0.5 |
| 11 | 1 | 0.6 | 1.1 | 0.4 |
| 12 | 1 | 0.4 | 0.9 | 0.2 |
| 13 | 1 | 0.4 | 0.8 | 0.2 |
| 14 | 0 | 0.3 | 0.8 | 0.1 |
| 15 | 0 | 0.3 | 0.8 | 0.1 |
| 16 | 0 | 0.3 | 0.9 | 0.1 |
| 17 | 0 | 0.3 | 1.1 | 0.1 |
| 18 | 0 | 0.3 | 1.5 | 0.1 |
| 19 | 0 | 0.4 | 2.2 | 0.1 |
| 20 | 1 | 0.5 | 3.5 | 0.1 |

Goodness of Fit Test

| s | $\chi^2$ | d.f.* | Pr.** |
|---|---|---|---|
| 1 | 20.8 | 5 | 0.1% |
| 2 | 3.24 | 4 | 53.0% |

* d.f. = degrees of freedom
** Pr. = probability of obtaining a poorer fit

FIGURE F.5

## 95% CONFIDENCE LIMITS FOR PROBABILITY DENSITY FUNCTION DOSRN 100 RUNS - 2 PARAMETER MODEL

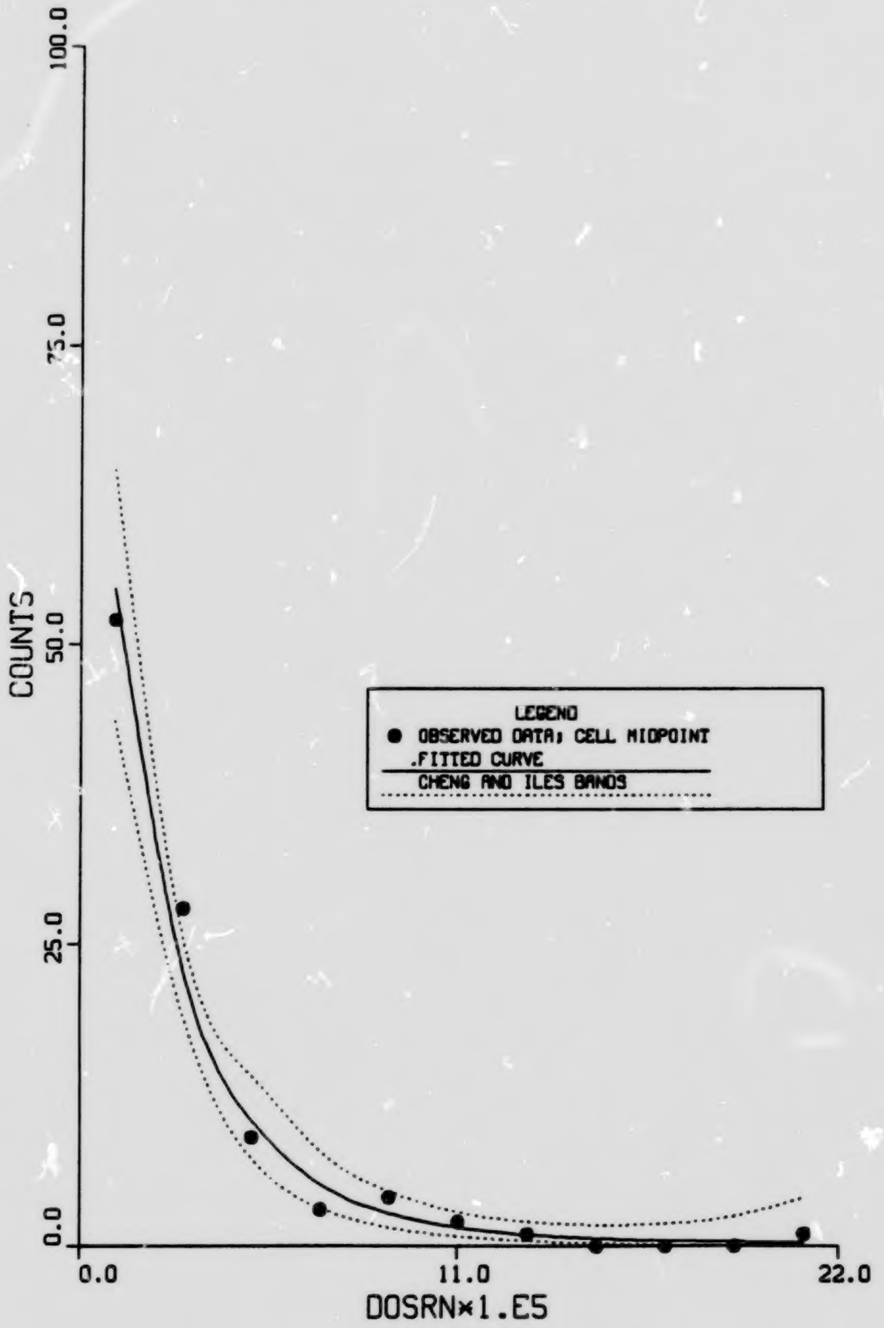

FIGURE F.6

95% CONFIDENCE LIMITS
FOR PROBABILITY DENSITY FUNCTION
DOSRN 500 RUNS - 2 PARAMETER MODEL

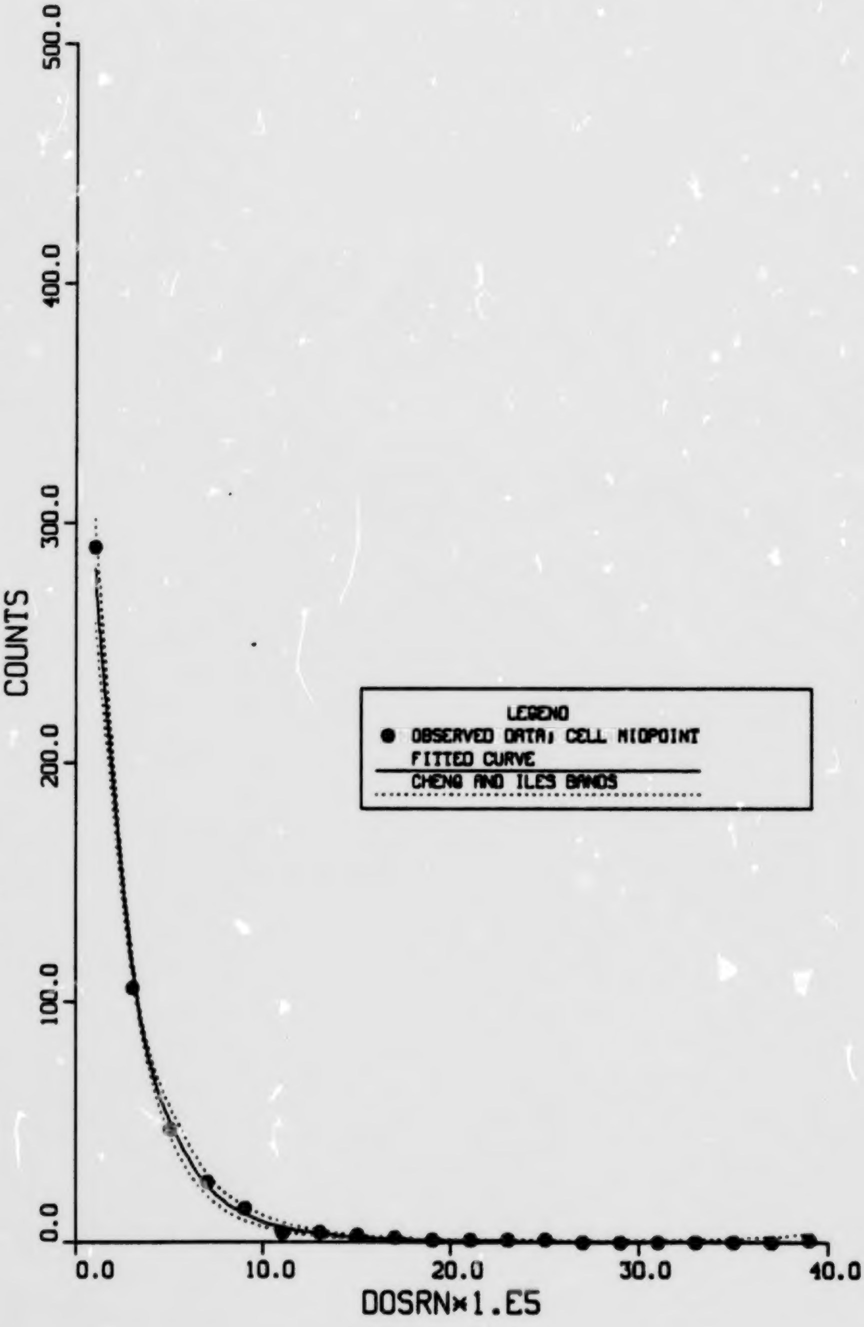

FIGURE F.7

## 95% CONFIDENCE LIMITS FOR CUMULATIVE DISTRIBUTION FUNCTION DOSRN 100 RUNS - 2 PARAMETER MODEL

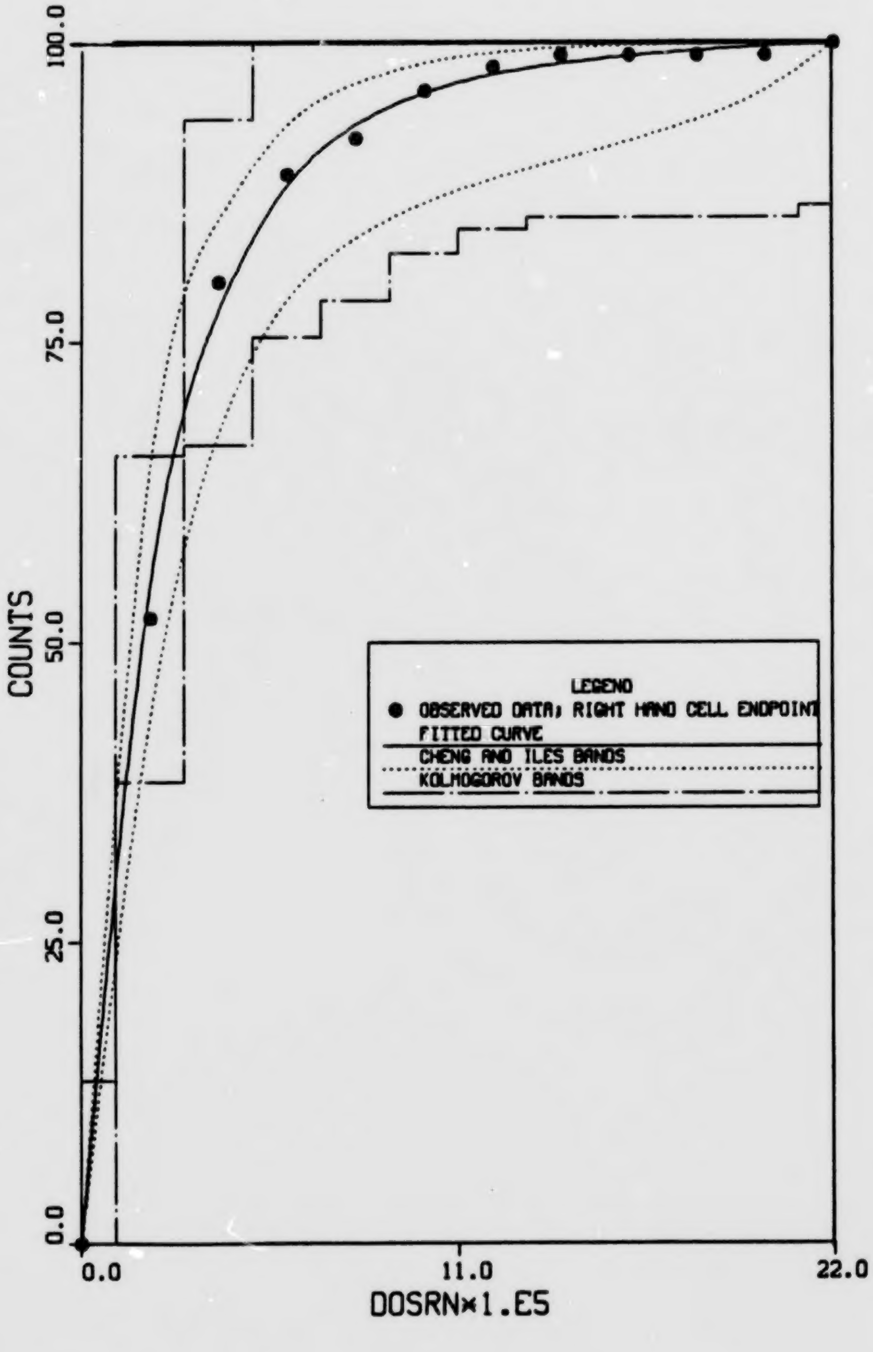

FIGURE F.8

95% CONFIDENCE LIMITS
FOR CUMULATIVE DISTRIBUTION FUNCTION
DOSRN 500 RUNS - 2 PARAMETER MODEL

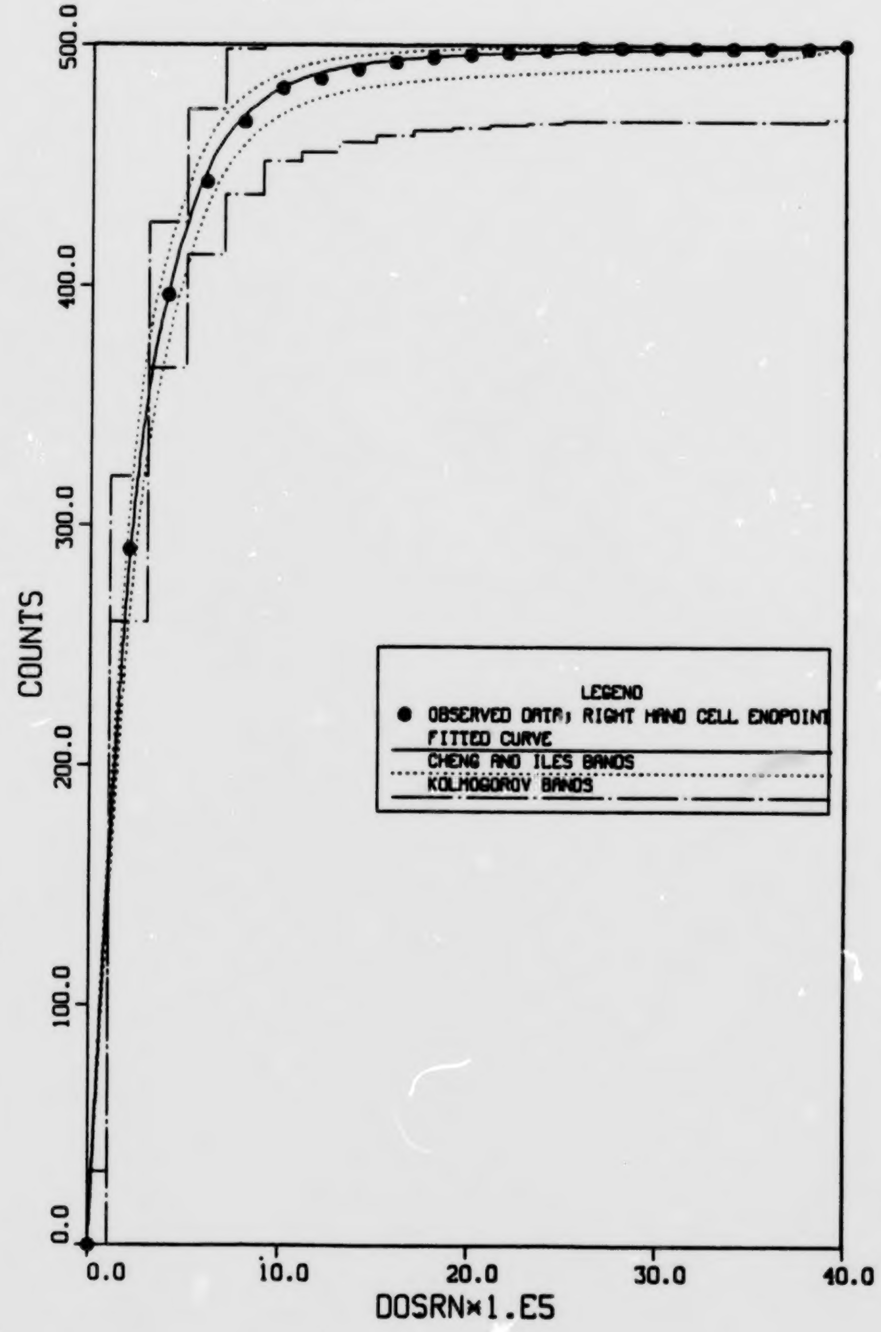

FIGURE F.9

## PLOTS OF 95% CONFIDENCE BANDS FOR A NORMAL DISTRIBUTION (500 TRIALS)

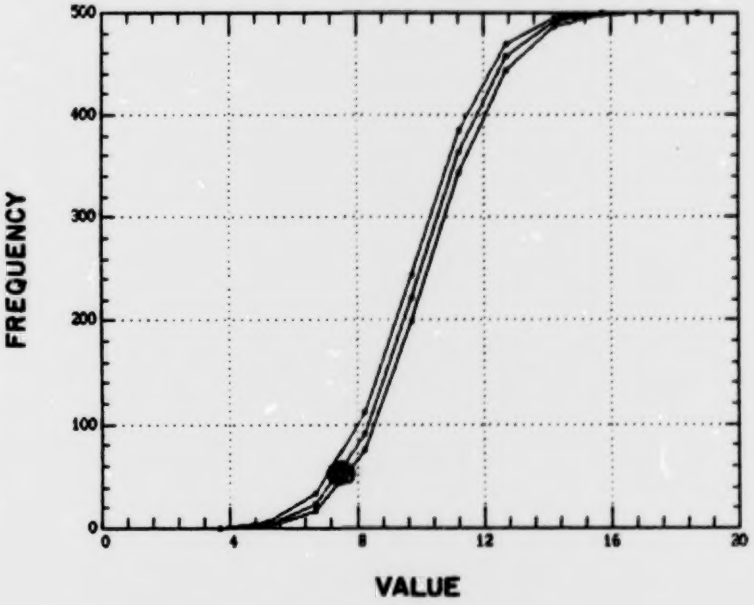

A) CUMULATIVE DISTRIBUTION FUNCTION

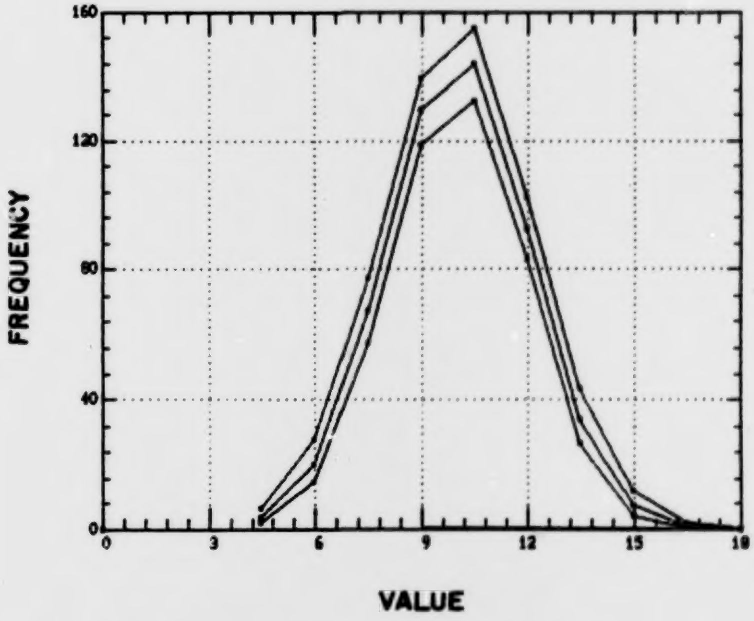

B) PROBABILITY DISTRIBUTION FUNCTION

FIGURE F.10

PLOTS OF 95% CONFIDENCE BANDS
FOR A LOG-TRANSFORMED LOGNORMAL DISTRIBUTION
(500 TRIALS)

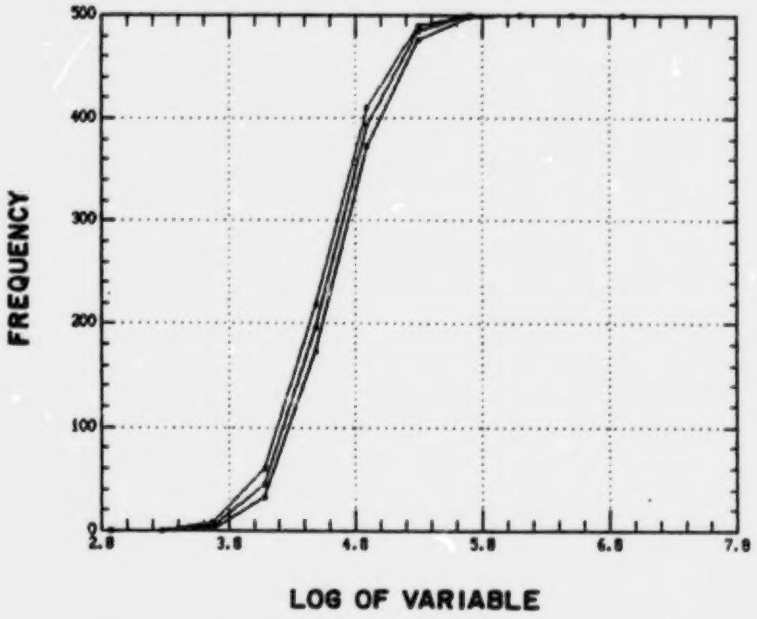

A) CUMULATIVE DISTRIBUTION FUNCTION

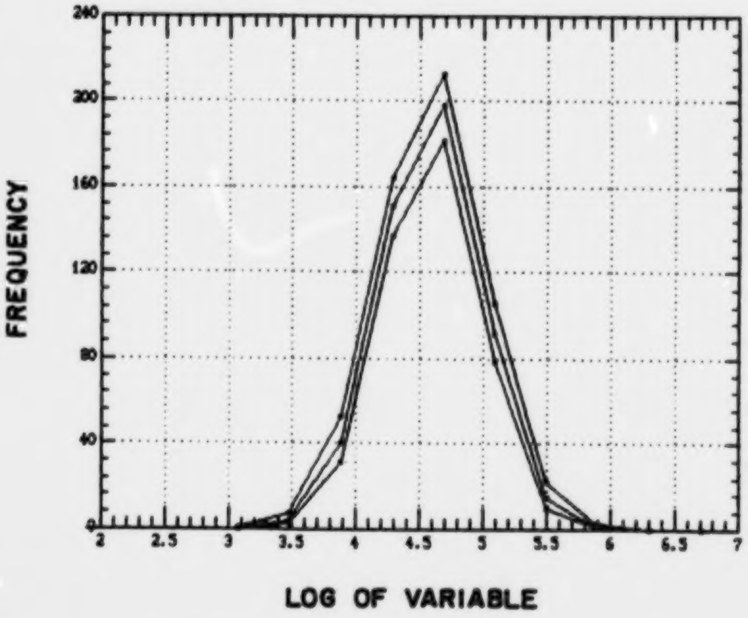

B) PROBABILITY DENSITY FUNCTION

FIGURE F.11

## PLOTS OF 95% CONFIDENCE BANDS FOR THE LOGARITHM OF RADIUM IN FISH AT 100 YEARS (200 TRIALS)

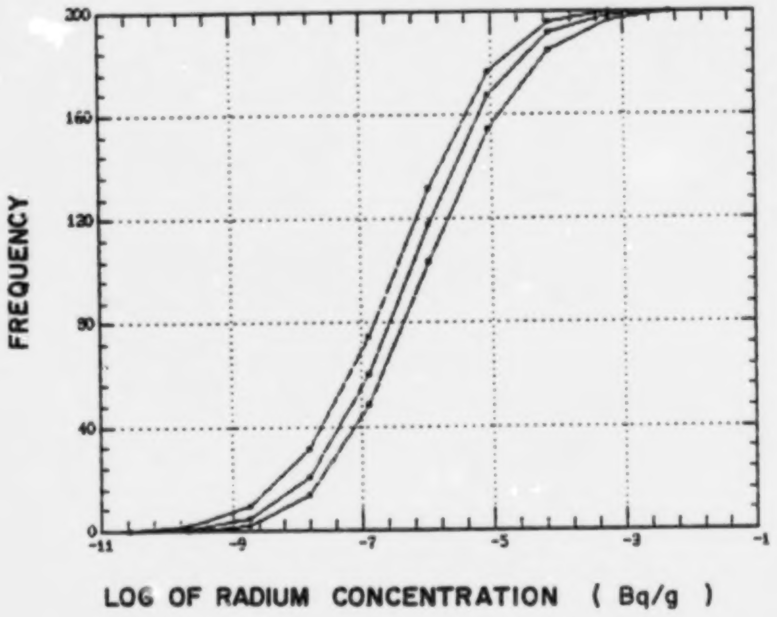

A) CUMULATIVE DISTRIBUTION FUNCTION

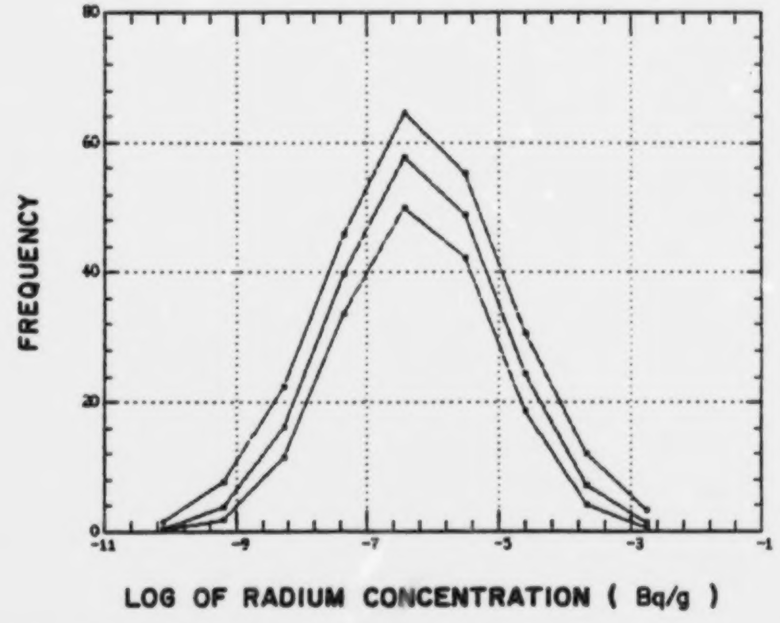

B) PROBABILITY DENSITY FUNCTION

## F.8 CONCLUSIONS

Reilly and Duever have developed a method for fitting a flexible generalized model to the output distribution from Monte Carlo type calculations.

The procedure for calculating confidence bands for probability density functions and cumulative distribution functions of Monte Carlo type output is an extension of the approach formulated by Cheng and Iles and by Scheffe.

The model and confidence band procedure has been successfully applied to environmental assessment model outputs.

The bands for the cdf based on this method compare well with the Kolmogorov bands. They give narrower confidence bands which are however rigorously correct.

## REFERENCES

Bard, Y., 1974. "Nonlinear Parameter Estimation." Academic Press.

Cheng, R.C.H., and Iles, T.C., 1983. "Confidence Bands for Cumulative Distribution Functions of Continuous Random Variables." Technometrics, Vol. 25, pp. 77-86.

Davies, O.L., and Goldsmith, P.L., 1977. "Statistical Methods in Research and Production." Longman Group Ltd., London.

Kendall, M., and Stuart, A., 1961. "The Advanced Theory of Statistics, Vol. 2: Inference and Relationship." 1st Edition, Hafner Publishing Co.

Kolmogorov, A.N., 1941. "Confidence Limits for an Unknown Distribution Function." Ann. Math. Statist., Vol. 12, pp. 461-463.

SENES Consultants Limited, 1984. "A Study to Develop and Demonstrate Techniques for the Probabilistic Assessment of the Long-Term Effects of Uranium Mill Tailings in Canada - Phase I." Prepared for the National Uranium Tailings Program, Energy, Mines and Resources Canada, Ottawa, Ontario.

SENES Consultants Limited, 1985. "A Study to Develop and Demonstrate Techniques for the Probabilistic Assessment of the Long-Term Effects of Uranium Mill Tailings in Canada - Phase II." Prepared for the National Uranium Tailings Program, Energy, Mines and Resources Canada, Ottawa, Ontario.

Scheffe, H., 1959. "The Analysis of Variance." John Wiley and Sons, New York.

Sturges, H.A., 1926. "The Choice of a Class Interval." Journal of the American Statistical Association, March.

## APPENDIX F1: NEWTON-RAPHSON ITERATIVE SOLUTION

An iterative procedure for solving equation (F10) by the Newton-Raphson method is as follows.

Define the (q+1)x1 vector function $\underline{F}(\underline{\theta})$ as:

$$\underline{F}(\underline{\theta}) = \sum_{i=1}^{m} x_i^{u-1} \left[ \frac{n_i}{N} - p_i \right] \quad \text{uth element}$$

where all notation is as used previously and $p_i = p(x_i)$ is defined by equation (F.1). Define the (q+1)x(q+1) Jacobian matrix $\underline{J}(\underline{\theta})$ as:

$$\underline{J}(\underline{\theta}) = \frac{\partial \underline{F}}{\partial \underline{\theta}} = \left[ - \sum_{i=1}^{m} N p_i x_i^{u+v-2} \right] \quad \text{u,v element}$$

Then the iterative scheme consists of choosing a starting vector $\underline{\theta}^{(1)}$ and calculating successive vectors from:

$$\underline{\theta}^{(k+1)} = \underline{\theta}^{(k)} - \underline{\partial}^{(k)}$$

where $\underline{\partial}^{(k)}$ is found by solving the following set of linear equations for $\underline{\partial}^{(k)}$

$$\underline{J}(\underline{\theta}^{(k)})\, \underline{\partial}^{(k)} = \underline{F}(\underline{\theta}^{(k)})$$

If q is large, say greater than 4, steps may be necessary to deal with the fact that $\underline{J}$ will likely be badly conditioned.

The Jacobian, $\underline{J}$, will most likely be ill conditioned, which can lead to numerical problems. To overcome this problem, the following scheme was employed.

let:

$$D_{ii} = \left[ \sum_{j=1}^{m} J_{ij}^2 \right]^{1/2}$$

$D_{ij} = 0, \quad i \neq j$

The $\underline{J} = \underline{D}\ \underline{Q}\ \underline{D}$ where $\underline{Q} = \underline{D}^{-1}\ \underline{J}\ \underline{D}^{-1}$

The equation then becomes, leaving out $\underline{\theta}^{(k)}$

$$\underline{J}\ \underline{\partial} = \underline{F}$$

$$\underline{D}\ \underline{Q}\ \underline{D}\ \underline{\partial} = \underline{F}$$

$$\underline{Q}\ \underline{D}\ \underline{\partial} = \underline{D}^{-1}\ \underline{F}$$

let $\underline{u} = \underline{D}\ \underline{\partial}$

$\underline{Qu} = \underline{D}^{-1}\ \underline{F}$
and $\underline{\partial} = \underline{D}^{-1}\ \underline{u}$

## APPENDIX F2: ANALYTICAL SOLUTION FOR $\underline{r}$ for s=1

Calculation of $\underline{r}$ for s=1:

$$r = \int_{-\infty}^{x} \left[ \int_{-\infty}^{\infty} u \exp \left\{ \theta_0 + \theta_1 u \right\} du + u \right] \exp \left\{ \theta_0 + \theta_1 u \right\} du$$

$$= \int_{-\infty}^{\infty} u \exp \left\{ \theta_0 + \theta_1 u \right\} du \int_{-\infty}^{x} \exp \left\{ \theta_0 + \theta_1 u \right\} du +$$

$$\int_{-\infty}^{x} u \exp \left\{ \theta_0 + \theta_1 u \right\} du$$

$$= \exp (\theta_0) \left[ \int_{-\infty}^{\infty} u \exp(\theta_1 u)\, du \int_{-\infty}^{x} \exp(\theta_1 u)\, du + \int_{-\infty}^{x} u \exp(\theta_1 u)\, du \right]$$

For s=1, problems arise when trying to integrate to $-\infty$. Therefore use the smallest value of x say +a.

$$\exp(\theta_o) = \frac{1}{\int_{+a}^{\infty} \exp(\theta_1 u)\, du} = - \theta_1 \exp(-a\theta_1)$$

$$r = -\frac{1}{\theta} \exp(-a\theta_1) \left[ \left( \frac{\exp(\theta_1 x + a\theta_1) - \exp(2a\theta_1)}{\theta_1} \right) (1 - a\theta_1) \right.$$

$$\left. + \exp(\theta_1 x)(\theta_1 x - 1) + \exp(a\theta_1)(1 - a\theta_1) \right]$$

# APPENDIX F3: KOLMOGOROV CONFIDENCE BANDS

For 95% confidence bands and for a number of trials larger than 50,

$d_{.95} = 1.3581\ n^{-1/2}$; n = number of trials

For DOSRN 100: $d_{.95} = .13581$

For DOSRN 500: $d_{.95} = .06076$

To plot the bands on graphs, multiply d by the sample size.

DOSRN 100: $d_{.95} = 13.6$

DOSRN 500: $d_{.95} = 30.4$

Kolmogorov bands are then obtained by plotting a band $\pm\ d_{.95}$ about the observed cumulative frequency function.

# APPENDIX G

## CONFIDENCE BANDS PROGRAMS

## CODE LISTING

## AND

## VARIABLE DICTIONARY

### G.1.1 Variable Dictionary for BIN

The following list defines the major variables used in BIN.FOR. In some cases, different variables are used for the same purpose in different segments of the program.

| VARIABLE | DEFINITION |
|---|---|
| ABCISA = A | vector of abscissa values for bins; both right hand cell endpoints and cell midpoints. |
| EVNT | particular Monte Carlo outcome of variable being analyzed |
| HALF | one half width of bin interval; needed to calculate abscissa value at cell midpoint |
| HTS = H | vector of cell or bin counts |
| IFLAG | if IFLAG = 0, logarithmic transformation is made. |
| INTVLS | number of bins used given by $[\log_{10}(\mathrm{NTRIAL})/\log_{10}(2.0)] + 1.0$ rounded up to the nearest integer |
| IPL2 | INTVLS + 2 |
| MAX | maximum value of variable from statistics file |

| | |
|---|---|
| MIN | minimum value of variable from statistics file |
| N | integer identifying the variable to be analyzed |
| NAME | character variable specifying the name of the variable under consideration |
| NTRIAL | total number of Monte Carlo trials |
| VAR | vector of Monte Carlo outcomes for variables being considered |
| VARMAX = AMAX | maximum value of variable for purpose of binning |
| VARMIN = AMIN | minimum value of variable for purpose of binning |
| X | $= \lfloor \log_{10}(\mathrm{NTRIAL})/\log_{10}(2.0) \rfloor + 1.0$ |

### G.1.2 Variable Dictionary for OPAN

This list defines the major variables used in OPAN.FOR. Some variables have different meanings depending on the subroutine or function in which they are used. When this is the case, the meaning in each subroutine is given. References made are to sections, equations and appendices of the discussion paper by Reilly and Duever found in Appendix F.

| VARIABLE | | DEFINITION |
|---|---|---|
| A | | "a" used in Appendix F2 |
| ADJUST | | $\sqrt{\frac{\gamma}{M}}$, s=1 equation F14 and F16 |
| CHI25 | | vector containing $\chi^2_{.25}$ quantities with degrees of freedom 1 to 20 |
| CHI05 | | vector of $\chi^2_{.05}$ quantities with degrees of freedom 1 to 20 |
| CHIS2 | | calculated $\chi^2$ value |
| CRIT | | convergence criterion for various interactive procedures |
| CSUM | in CDF | $=\sqrt{\frac{\gamma}{\underline{r}'\underline{M}^{-1}\underline{r}}}$ |
| | in PDF | $=\sqrt{\frac{\gamma}{(\underline{c}-\underline{b})'\underline{M}^{-1}(\underline{c}-\underline{b})}}$ |
| DINV | | $D^{-1}$ in Newton-Raphson procedure |

| | | |
|---|---|---|
| F | | $= \sum_{i=1}^{m} n_i x_i^{j-1} - N \sum_{i=1}^{m} p_i x_i^{j-1}$ where $j=1,2,\ldots,s+1$<br>(see equation F10) |
| FIT | in PDF | fitted cell count for pdf |
| | in CHITST | fitted cell counts for pdf such that $FIT \geq 6$ |
| | in CDF | fitted cumulative cell count |
| FUNPDF | | value of pdf at a given value of x |
| FUN1 | | value of cumulative distribution at a given value of x for $s = 1$ |
| FUN2 | | value of cumulative distribution at a given value of x for $s > 1$ |
| GAMMA | | $= \chi^2_{.05,s}$; s = degree of polynomial |
| G | | $= \frac{r}{M}$ in CDF<br>$= \sum_{i=1}^{n} p_i x_i$ in PDF = b for $s = 1$ |
| ILOG | | flag; if ILOG = 0 then logarithmic transformation has been used |
| IFLAG | | flag; if IFLAG $\neq 1$ then model passes goodness of fit test |
| IDF | | number of counts for which FIT > 6 in CHITST |

| | |
|---|---|
| IDEF | degrees of freedom for $\chi^2$ goodness of fit test |
| LOW | lower confidence band value |
| MAXIT | maximum number of iterations for iterative procedures |
| NAME | name of variable being analyzed |
| NCELLS | number of cells used |
| NI | vector of observed cell counts |
| NRAPH = NR | = s + 1 |
| NTOTAL | total number of Monte Carlo trials |
| OBS | observed cell counts corresponding to FIT in CHITST |
| ONE | = - 1 when k = 1, = + 1 when k = 2 in subroutines CDF and PDF |
| OUT | vector used to save values for output |
| P | vector of fitted probability density values |
| POSDEF | logical variable which has the value .FALSE. if the matrix supplied to EQCHOL is not positive definite |

| | | |
|---|---|---|
| Q | in NEWRAP | - Jacobian matrix of Newton-Raphson procedure; $\underline{Q} = \underline{D}^{-1} \underline{J}\, \underline{D}^{-1}$ refer to Appendix F1.<br>- observed Fisher Information matrix otherwise |
| QEQ | | equal to Q when supplied to EQCHOL. Used to preserve Q since EQCHOL changes the matrix |
| R | in CDF | equal to $\underline{r}$ shown in equation F16 |
| | in PDF | it is the vector $(\underline{c} - \underline{b})$ shown in euqation F14 |
| RMSD | | root-mean-squared difference; used to determine convergence in iterative procedures |
| RPM | in CDF | corresponds to $\underline{M}^{-1}\underline{r}$ |
| | in PDF | corresponds to $\underline{M}^{-1}(\underline{c} - \underline{b})$ |
| RR1 | | the value of r for s=1 case |
| S | | degree of approximating polynomial |
| S2 | | = S x 2 |
| SUMPX | | vector the jth element of which is<br>$\sum_{i=1}^{m} P_i x_i^j \quad j = 1,2,3 \ldots 2s$ |

| | |
|---|---|
| T0 | value of normalizing constant $\theta_0$ |
| T0NEW | maximum likelihood estimate $\hat{\theta}_0$ |
| THETA | vector of upper and lower values of $\underline{\theta}$ given by equations F14 and F16 |
| TNEW | maximum likelihood estimate $\hat{\underline{\theta}}$ |
| TOLD | vector used to store (n-1)th value of $\underline{\theta}$ during nth iteration |
| U | = $\partial$ in Newton-Raphson procedure |
| UPP | upper confidence band limits |
| XCDF | right hand cell end points in actual units of variable; given x - value for CDF |
| XEXP | $= \sum_{i=1}^{m} x^j_i P_i$ for a given value of j |
| XI | vector of indicator variables used in Newton-Raphson procedure. This is used instead of actual x - values for mathematical convenience and since the problem is well conditioned, resulting in easier convergence |
| XPDF | cell midpoints in actual units of variable; given x - values for pdf |

## G.2.1 CODE LISTING OF CONFIDENCE BANDS BINNING PROGRAM - BIN.FOR

```
C     THE PROGRAM, BIN, READS DETAILED RESULTS AND DETAILED RESULTS
C     KEY FILES AS CREATED BY THE PROGRAM, UTAP.  IT ASSIGNS
C     OBSERVATIONS FROM MONTE CARLO TRIALS TO BINS, APPLYING A
C     LOG TRANSFORMATION IF DESIRED.  THE FILE BIN.DAT IS CREATED
C     FOR USE BY THE CONFIDENCE BANDS PROGRAM, OPAN.FOR.
C
      REAL HTS(22)
      DIMENSION ABCISA(22)
      INTEGER*4 SCRUNT,FUNIT1,FUNIT2,FUNIT3,DEBUG
      COMMON /UNITS/ SCRUNT,FUNIT1,FUNIT2,FUNIT3,DEBUG
      REAL*4 VAR(1000),MIN,MAX
      INTEGER*4 NTRIAL,N,IFLAG
      CHARACTER*6 NAME
      COMMON /IN/ VAR,NTRIAL,N,NAME,MIN,MAX,IFLAG
C
      CALL READ
      X=ALOG10(FLOAT(NTRIAL))/ALOG10(2.0)+1.0
      INTVLS = INT(X)
      IF(ABS(X-INTVLS).GT.0.50) INTVLS = INTVLS+1
      IPL2 = INTVLS+2
      IF(IFLAG.EQ.0) THEN
         DO 12 I=1,NTRIAL
            VAR(I) = ALOG(VAR(I))
12       CONTINUE
         IF(MIN.GE.1)THEN
            VARMIN = 0.8*ALOG(MIN)
            VARMAX = 1.2*ALOG(MAX)
         ELSE
            VARMIN=1.2*ALOG(MIN)
            VARMAX=0.8*ALOG(MAX)
         ENDIF
      ELSE
         VARMIN = 0.8*MIN
         VARMAX = 1.2*MAX
      ENDIF
      CALL DISTRI(ABCISA,HTS,INTVLS,VARMIN,VARMAX,IPL2)
      DO 20 I=1,NTRIAL
         CALL DISTRA(ABCISA,HTS,VAR(I),IPL2)
20    CONTINUE
      IF(HTS(2).GT.0)  HTS(3) = HTS(3)+1.0
      HTS(2) = 0.0
      WRITE(FUNIT3,1200) N,NAME,INTVLS,NTRIAL,IFLAG
      DO 30 I=2,IPL2
         WRITE(FUNIT3,1300) ABCISA(I)
30    CONTINUE
      HALF = (ABCISA(4)-ABCISA(3))/2.0
      DO 40 I=3,IPL2
         ABCISA(I) = ABCISA(I)-HALF
         WRITE(FUNIT3,1300) HTS(I),ABCISA(I)
40    CONTINUE
      STOP
1200  FORMAT (1X,I3,1X,A6,5X,I5,2X,E13.6,2X,I5)
```

```
1300  FORMAT (2X,E10.4,2X,E10.4)
      END
C
C ************************************************************************
C
      SUBROUTINE DISTRI (A,H,INTVLS,AMIN,AMAX,IPL2)
C
C     SUBROUTINE INITIALIZES BINS
C
      REAL A(IPL2),H(IPL2)
      INTEGER*4 SCRUNT,FUNIT1,FUNIT2,FUNIT3,DEBUG
      COMMON /UNITS/ SCRUNT,FUNIT1,FUNIT2,FUNIT3,DEBUG
C
      IF(DEBUG.EQ.1)WRITE(SCRUNT,*)' SUBROUTINE DISTRI'
      FINC=ABS((AMAX-AMIN)/INTVLS)
      A(1)=INTVLS+2
      M=A(1)
      A(2)=AMIN
      H(1)=0.0
      H(2)=0.0
      DO 100 I=3,M
         A(I)=A(I-1)+FINC
         H(I)=0.0
100   CONTINUE
      RETURN
      END
C
C ************************************************************************
C
      SUBROUTINE DISTRA (A,H,EVNT,IPL2)
C
C     SUBROUTINE ASSIGNES TRIALS TO BINS
C
      REAL A(IPL2),H(IPL2)
      INTEGER*4 SCRUNT,FUNIT1,FUNIT2,FUNIT3,DEBUG
      COMMON /UNITS/ SCRUNT,FUNIT1,FUNIT2,FUNIT3,DEBUG

      IF(DEBUG.EQ.1)WRITE(SCRUNT,*)' SUBROUTINE DISTRA'
      M=ABS(A(1))
      DO 210 I=2,M
         IF (EVNT.LE.A(I))THEN
            H(I) = H(I)+1.0
            GO TO 225
         ENDIF
  210 CONTINUE
  225 H(1)=H(1)+1.0
      RETURN
      END
C
C ************************************************************************
C
      SUBROUTINE READ
C
C     SUBROUTINE READS INPUT FILES AND OPENS OUTPUT FILE
C
```

```
      INTEGER*4 SCRUNT,FUNIT1,FUNIT2,FUNIT3,DEBUG
      COMMON /UNITS/ SCRUNT,FUNIT1,FUNIT2,FUNIT3,DEBUG
      REAL*4 VAR(1000),MIN,MAX
      INTEGER*4 NTRIAL,N,IFLAG
      CHARACTER*6 NAME
      COMMON /IN/ VAR,NTRIAL,N,NAME,MIN,MAX,IFLAG
      CHARACTER*1 Q
      CHARACTER*12 FNAME
      CHARACTER*18 COLUMN
C
      DEBUG=0
      SCRUNT=0
      IF(DEBUG.EQ.1)WRITE(SCRUNT,*)' SUBROUTINE READ'
      FUNIT1=1
      FUNIT2=2
      FUNIT3=3
      WRITE(SCRUNT,900)' DETAILED RESULTS FILE NAMEπ '
      READ(SCRUNT,900)FNAME
      WRITE(SCRUNT,800)FNAME
      OPEN(FUNIT1,FNAME)
      WRITE(SCRUNT,900)' KEY FILE NAMEπ '
      READ(SCRUNT,900)FNAME
      WRITE(SCRUNT,800)FNAME
      OPEN(FUNIT2,FNAME)
      FNAME='BIN.DAT'
      WRITE(SCRUNT,800)FNAME
      OPEN(FUNIT3,FNAME)
      WRITE(SCRUNT,900) ' ENTER ID. NO. OF VARIABLE TO BE ANALYZED: '
      READ(SCRUNT,901) N
      WRITE(SCRUNT,900) ' DO YOU WANT LOG TRANSFORMATION (Y/N)π '
      READ(SCRUNT,900) Q
      IF(Q.EQ.'Y'.OR.Q.EQ.'y')THEN
         IFLAG=0
      ELSE
         IFLAG=1
      ENDIF
      READ(FUNIT2,100)
      READ(FUNIT2,100)
      READ(FUNIT2,200)NTRIAL
      DO 10 I=1,N
         READ(FUNIT2,100)
10    CONTINUE
      READ(FUNIT2,300)NAME,MIN,MAX
      READ(FUNIT1,100)
      IF(N.GT.1)THEN
         WRITE(COLUMN,102)'(',N-1,'(10X),1X,E9.3)'
         DO 15 I=1,NTRIAL
            READ(FUNIT1,COLUMN)VAR(I)
15       CONTINUE
      ELSE
         DO 20 I=1,NTRIAL
            READ(FUNIT1,400)VAR(I)
20       CONTINUE
      ENDIF
      CLOSE(FUNIT1)
      CLOSE(FUNIT2)
      RETURN
100   FORMAT (1X)
102   FORMAT (A1,I3,A14)
200   FORMAT (19X,I5)
300   FORMAT (7X,A6,73X,2E11.3)
400   FORMAT (E9.3)
800   FORMAT (' Opening file: ',a12)
900   FORMAT (A)
901   FORMAT (I3)
      END
```

## G.2.2 CODE LISTING OF CONFIDENCE BANDS PROGRAM - OPAN.FOR

```
C      PROGRAM, OPAN.FOR, READS THE FILE, BIN.DAT, CREATED BY THE
C      BINNING PROGRAM, BIN.FOR, AND FITS CONFIDENCE BANDS TO THE
C      CUMULATIVE AND PROBABILITY DENSITY FUNCTIONS.
C
       IMPLICIT REAL*8(A-H,O-Z)
       INTEGER*4 FUNIT1,FUNIT2,FUNIT3,SCRUNT,DEBUG
       COMMON /FILES/ FUNIT1,FUNIT2,FUNIT3,SCRUNT,DEBUG
       INTEGER*4 NCELLS,ILOG,S,MAXIT
       CHARACTER*6 NAME
       COMMON /INIT/ NCELLS,ILOG,S,MAXIT,CRIT,NAME
       REAL*8 OUT(20,8)
       COMMON /OUTS/ OUT
       REAL*8 NI,CHI25(20),CHI05(20),NTOTAL,
      α   Q(20,20),QEQ(20,20),DINV(20),F(20),P(20),RPM(20),
      α   SUMPX(20),TNEW(20),TOLD(20),THETA(20),U(20),R(20)
       INTEGER*4 S2
       COMMON/AREA1/XI(20),NI(20),NTOTAL
       COMMON/AREA2/CHI25
       COMMON/AREA3/CHI05
       COMMON/AREA4/XCDF(20),XPDF(20)
C
       CALL START
50     CONTINUE
C
C         START WITH DEGREE OF POLYNOMIAL EQUAL 1 AND INCREASE UNTIL FIT
C         FOUND
C
          S=S+1
          IF(DEBUG.EQ.2)WRITE(FUNIT1,1600) S
          NRAPH = S+1
          TONEW = -1.0
          DO 60 I=1,S
             TNEW(I) = 0.001
60        CONTINUE
          CALL NEWRAP(TONEW,TNEW,NRAPH,DINV,F,P,Q,U,TOLD)
          CALL CHITST(IFLAG,P)
C
C         CHECK IF DEGREE OF POLYNOMIAL EQUALS NUMBER OF BINS
C
          IF (S.GT.NCELLS-1) THEN
70           WRITE(SCRUNT,1700)
             STOP
          ENDIF
       IF(IFLAG.EQ.1) GOTO 50
       IF(DEBUG.EQ.2)THEN
          WRITE(FUNIT1,1800)
          WRITE(FUNIT1,1900)
       ENDIF
       DO 90 I=1,NCELLS
          P(I)=FUNPDF(TONEW,TNEW,XI(I))
          IF(DEBUG.EQ.2)WRITE(FUNIT1,2000) NTOTAL*P(I),NI(I)
90     CONTINUE
```

```
      S2 = 2*S
      CALL FISHER(Q,P,SUMPX,S2)
      CRIT = 1.E-5
      GAMMA = CHI05(S)
      IF(ILOG.NE.1) WRITE(SCRUNT,900) ' LOGARITHM OF VARIABLE IS USED'
      CALL CDF(TONEW,TNEW,Q,GAMMA,QEQ,TOLD,THETA,RPM,R)
      CALL PDF(TONEW,TNEW,Q,GAMMA,QEQ,TOLD,THETA,RPM,R)
      CALL OUTPUT
      STOP
900   FORMAT (A)
1600  FORMAT (/,72('*'),/,5X,'FIT POLYNOMIAL OF DEGREE S = ', I5,//)
1700  FORMAT (/,5X,'PROCEDURE UNSUCCESSFUL, CHECK DATA')
1800  FORMAT (/,5X,'PROBABILITY OF POORER FIT IS GREATER THAN 25%')
1900  FORMAT (/,5X,'FITTED VALUES',5X,'MEASUREMENTS',/)
2000  FORMAT (5X,E13.6,5X,E13.6,/)
2100  FORMAT (1X,A6)
      END
C
C ************************************************************************
C
      SUBROUTINE START
C
C     SUBROUTINE OPENS FILES AND READS INPUT FILE FROM BINNING
C     PROGRAM
C
      IMPLICIT REAL*8(A-H,O-Z)
      INTEGER*4 FUNIT1,FUNIT2,FUNIT3,SCRUNT,DEBUG
      COMMON /FILES/ FUNIT1,FUNIT2,FUNIT3,SCRUNT,DEBUG
      INTEGER*4 NCELLS,ILOG,S,MAXIT
      CHARACTER*6 NAME
      COMMON /INIT/ NCELLS,ILOG,S,MAXIT,CRIT,NAME
      REAL*8 NTOTAL,NI
      COMMON /AREA1 /XI(20), NI(20), NTOTAL
      COMMON /AREA4 /XCDF(20),XPDF(20)
      CHARACTER*12 FNAME
C
      DEBUG=0
      SCRUNT=0
      IF(DEBUG.GE.1)WRITE(SCRUNT,*)' SUBROUTINE START'
      FUNIT1=1
      FUNIT2=2
      FUNIT3=3
      IF(DEBUG.EQ.2)THEN
         FNAME='FIT.OUT'
         WRITE(SCRUNT,800)FNAME
         OPEN(FUNIT1,FNAME)
      ENDIF
      FNAME='BIN.DAT'
      WRITE(SCRUNT,800)FNAME
      OPEN(FUNIT3,FNAME)
      READ(FUNIT3,1000) NAME,NCELLS,NTOTAL,ILOG
      WRITE(SCRUNT,900)
      READ(SCRUNT,700)FNAME
      WRITE(SCRUNT,800)FNAME
      OPEN(FUNIT2,FNAME)
      K = 1+NCELLS
      DO 10 I=1,K
         READ(FUNIT3,1050) XCDF(I)
10    CONTINUE
      S = 0
      MAXIT = 50
      CRIT = 1.E-8
      IF(DEBUG.EQ.2)THEN
         WRITE(FUNIT1,1200) NAME, NTOTAL
         WRITE(FUNIT1,1300) MAXIT,CRIT,NCELLS,S
      ENDIF
      XM = NCELLS
      IF(DMOD(XM,2.0D0).GT.0.0) XM = NCELLS - 1.0
      XM = XM + 1.0
      IF(DEBUG.EQ.2)WRITE(FUNIT1,1400)
      DO 20 I=1,NCELLS
         READ(FUNIT3,1100) NI(I),XPDF(I)
          XI(I)=I-XM/2.
         IF(DEBUG.EQ.2)WRITE(FUNIT1,1500) I,XI(I),I,NI(I)
20    CONTINUE
      RETURN
700   FORMAT(A)
800   FORMAT(' Opening file: ',A12)
900   FORMAT(' ENTER NAME OF OUTPUT FILE: ')
1000  FORMAT(5X,A6,5X,I5,2X,E13.6,2X,I5)
1050  FORMAT(2X,E10.4)
1100  FORMAT(2X,E10.4,2X,E10.4)
1200  FORMAT(/,2X,'VARIABLE: ',A6,/,5X,'NTOTAL = ',E13.6)
1300  FORMAT(/,5X,'MAXIT = ',I5, 2X, 'CRIT = ',E13.6,2X,'NCELLS = ',I5,
     α   2X,'S = ',I5)
1400  FORMAT(/,5X,'RANDOM VARIABLE',12X,'CELL COUNTS')
1500  FORMAT(/,5X,'XI(',I2,') = ',E13.6,5X,'NI(',I2,') = ',E13.6)
      END
C
C***********************************************************************
C
      BLOCK DATA
      REAL*8 CHI25(20)
      REAL*8 CHI05(20)
      COMMON/AREA2/CHI25
      COMMON/AREA3/CHI05
      DATA CHI25/1.32,2.77,4.11,5.39,6.63,7.84,9.04,10.22,11.39,12.55,
     α           13.70,14.85,15.98,17.12,18.25,19.37,20.49,21.60,
     α           22.72,23.83/
      DATA CHI05/3.84,5.99,7.81,9.49,11.07,12.59,14.07,15.51,16.92,
     α          18.31,19.68,21.03,22.36,23.68,25.00,26.30,27.59,
     α          28.87,30.14,31.41/
      END
C
C **********************************************************************
C
      SUBROUTINE NEWRAP(TONEW,TNEW,NR,DINV,F,P,Q,U,TOLD)
C
C     NEWTON-RAPHSON PROCEDURE FOR FITTING MODEL
C
```

```
      IMPLICIT REAL*8(A-H,O-Z)
      INTEGER*4 FUNIT1,FUNIT2,FUNIT3,SCRUNT,DEBUG
      COMMON /FILES/ FUNIT1,FUNIT2,FUNIT3,SCRUNT,DEBUG
      INTEGER*4 NCELLS,ILOG,S,MAXIT
      CHARACTER*6 NAME
      COMMON /INIT/ NCELLS,ILOG,S,MAXIT,CRIT,NAME
      REAL*8 NI, NTOTAL
      LOGICAL POSDEF
      DIMENSION DINV(NR),F(NR),P(NCELLS),Q(NR,NR),U(NR),TOLD(S),TNEW(S)
      COMMON/AREA1/XI(20), NI(20), NTOTAL
C
      IF(DEBUG.GE.1)WRITE(SCRUNT,*)' SUBROUTINE NEWRAP'
      DO 170 I=1,MAXIT
         DO 21 K=1,NR
            DINV(K) = 0.0
            F(K) = 0.0
            DO 20 J = 1,NR
               Q(K,J) = 0.0
20          CONTINUE
21       CONTINUE
         TOOLD = TONEW
         DO 30 I2=1,S
            TOLD(I2) = TNEW(I2)
30       CONTINUE
         DO 80 I1=1,NCELLS
            P(I1)=FUNPDF(TOOLD,TOLD,XI(I1))
            DO 71 I2=1,NR
               X = XI(I1)**(I2-1)
               F(I2) = F(I2) + NI(I1)*X - NTOTAL*P(I1)*X
               DO 70 I3=1,NR
                  K = I2+I3-2
                  IF(K.NE.0)THEN
                     X = XI(I1)**K
                  ELSE
                     X = 1.0
                  ENDIF
                  Q(I2,I3) = Q(I2,I3) + P(I1)*X
70             CONTINUE
71          CONTINUE
80       CONTINUE
         DO 110 K=1,NR
            DO 101 J=1,NR
               Q(K,J) = NTOTAL*Q(K,J)
               DINV(K) = DINV(K) + Q(K,J)**2
101         CONTINUE
            DINV(K) = 1.0/DSQRT(DINV(K))
110      CONTINUE
         DO 130 K=1,NR
            DO 121 L=1,NR
               Q(K,L) = Q(K,L)*DINV(K)*DINV(L)
121         CONTINUE
            U(K) = DINV(K)*F(K)
130      CONTINUE
         CALL EQCHOL(NR,Q,U,POSDEF)
C
```

```
C        CHECK IF EQCHOL SUCCESSFUL
C
         IF(.NOT.POSDEF)THEN
            WRITE(SCRUNT,1500)
            STOP
         ENDIF
         DO 140 K=1,NR
            U(K) = -1.0*DINV(K)*U(K)
140      CONTINUE
         TONEW = TOOLD - U(1)
         DO 150 I1=1,S
            TNEW(I1) = TOLD(I1) - U(I1+1)
150      CONTINUE
         RMSD = 0.0
         DO 160 I1=1,NR
            RMSD = RMSD + DSQRT(U(I1)**2)
160      CONTINUE
         IF(DEBUG.EQ.2)THEN
            WRITE(FUNIT1,1000) I,RMSD
            WRITE(FUNIT1,1100) TONEW, TNEW
         ENDIF
         IF(RMSD.LT.CRIT)GOTO180
170   CONTINUE
180   CONTINUE
      IF(DEBUG.EQ.2)THEN
         WRITE(FUNIT1,1200)
         WRITE(FUNIT1,1300)
         WRITE(FUNIT1,1400) (F(J),J=1,NR)
      ENDIF
      RETURN
1000  FORMAT (/,5X,'*****ITERATION : ',I5,2X,'*****',5X,'RMSD = ',E13.6)
1100  FORMAT (/,5X,'PARAMETER VALUES: ','TO = ',E13.6,/,5X,'THETA:',
     α   2(2X,E13.6))
1200  FORMAT (/,5X,'CONVERGENCE REACHED ±')
1300  FORMAT (/,5X,'FUNCTION AT CONVERGENCE:')
1400  FORMAT (/,5X,E13.6)
1500  FORMAT (/,5X,'POSDEF IS FALSE - CANNOT SOLVE')
      END
C
C***********************************************************************
C
      SUBROUTINE CHITST(IFLAG,P)
C
C     SUBROUTINE PERFORMS CHI SQUARED GOODNESS OF FIT TEST
C
      IMPLICIT REAL*8 (A-H,O-Z)
      INTEGER*4 FUNIT1,FUNIT2,FUNIT3,SCRUNT,DEBUG
      COMMON /FILES/ FUNIT1,FUNIT2,FUNIT3,SCRUNT,DEBUG
      INTEGER*4 NCELLS,ILOG,S,MAXIT
      CHARACTER*6 NAME
      COMMON /INIT/ NCELLS,ILOG,S,MAXIT,CRIT,NAME
      REAL*8 CHI25(20),NI,NTOTAL
      DIMENSION P(NCELLS)
      COMMON/AREA1/XI(20), NI(20), NTOTAL
      COMMON/AREA2/CHI25
```

```
C
      IF(DEBUG.GE.1)WRITE(SCRUNT,*)' SUBROUTINE CHITST'
      IFLAG = 1
      CHISQ = 0.0
      IDF = 0
      I = 1
      IF(I.LT.NCELLS)THEN
10       CONTINUE
            FIT = 0.0
            OBS = 0.0
30          CONTINUE
               FIT = FIT + NTOTAL*P(I)
               OBS = OBS + NI(I)
               I = I+1
            IF(I.LE.NCELLS.AND.FIT.LT.6.0)GOTO 30
            CHISQ = CHISQ + ((OBS-FIT)**2)/FIT
            IDF = IDF + 1
         IF(I.LT.NCELLS)GOTO 10
      ENDIF
      IDEG = IDF - S - 1
C
C     CHECK DEGREES OF FREEDOM
C
      IF(IDEG.GT.20)THEN
         WRITE(SCRUNT,2000)' DEGREES OF FREEDOM GREATER THAN 20'
         STOP
      ENDIF
      IF(IDEG.LE.0)IDEG=1
      IF(DEBUG.EQ.2)WRITE(FUNIT1,1000) CHISQ, IDEG
      IF(CHISQ.LT.CHI25(IDEG)) IFLAG = 0
      RETURN
1000  FORMAT (//,5X,'CHISQ GOODNESS OF FIT TEST RESULT: ',/,5X,'CALCULAT
     αED CHISQ = ',E13.6,'  WITH ',I5,'  DEGREES OF FREEDOM')
2000  FORMAT (A)
      END
C
C***********************************************************************
C
      SUBROUTINE FISHER(Q,P,SUMPX,S2)
C
C     SUBROUTINE CALCULATES OBSERVED FISHER INFORMATION MATRIX
C
      IMPLICIT REAL*8 (A-H,O-Z)
      INTEGER*4 FUNIT1,FUNIT2,FUNIT3,SCRUNT,DEBUG
      COMMON /FILES/ FUNIT1,FUNIT2,FUNIT3,SCRUNT,DEBUG
      INTEGER*4 NCELLS,ILOG,S,MAXIT
      CHARACTER*6 NAME
      COMMON /INIT/ NCELLS,ILOG,S,MAXIT,CRIT,NAME
      REAL*8 NI,NTOTAL
      INTEGER*4 S2
      DIMENSION Q(S,S),SUMPX(S2),P(NCELLS)
      COMMON/AREA1/XI(20), NI(20), NTOTAL
C
      IF(DEBUG.GE.1)WRITE(SCRUNT,*)' SUBROUTINE FISHER'
      K = 2.*S
      DO 10 I=1,K
         SUMPX(I) = 0.0
10    CONTINUE
      DO 20 J=1,K
         DO 21 I=1,NCELLS
            SUMPX(J) = SUMPX(J) + P(I)*XI(I)**J
21       CONTINUE
20    CONTINUE
      DO 30 J=1,S
         DO 31 K=1,S
            Q(J,K) = NTOTAL*(SUMPX(J+K) - SUMPX(J)*SUMPX(K))
31       CONTINUE
30    CONTINUE
      IF(DEBUG.EQ.2)THEN
         WRITE(FUNIT1,1000)
         DO 40 I=1,S
            WRITE(FUNIT1,1200) (Q(I,K), K=1,S,1)
40       CONTINUE
      ENDIF
      RETURN
1000  FORMAT (/,5X,'OBSERVED FISHER INFORMATION MATRIX',/)
1200  FORMAT (/,5X,5(E11.4,1X))
      END
C
C*********************************************************************
C
      SUBROUTINE CDF(TONEW,TNEW,Q,GAMMA,QEQ,TOLD,THETA,RPM,R)
C
C     SUBROUTINE CALCULATES 95% CONFIDENCE BANDS FOR CDF
C
      IMPLICIT REAL*8 (A-H,O-Z)
      INTEGER*4 FUNIT1,FUNIT2,FUNIT3,SCRUNT,DEBUG
      COMMON /FILES/ FUNIT1,FUNIT2,FUNIT3,SCRUNT,DEBUG
      INTEGER*4 NCELLS,ILOG,S,MAXIT
      CHARACTER*6 NAME
      COMMON /INIT/ NCELLS,ILOG,S,MAXIT,CRIT,NAME
      LOGICAL POSDEF
      REAL*8 NI,NTOTAL,FUN1,FUN2,LOW,FIT,UPP,
     α   TOLD(S),THETA(S),TNEW(S),Q(S,S),QEQ(S,S),
     α   RPM(S),R(S)
      COMMON/AREA1/XI(20), NI(20), NTOTAL
      COMMON/AREA4/XCDF(20),XPDF(20)
C
      IF(DEBUG.GE.1)WRITE(SCRUNT,*)' SUBROUTINE CDF'
      IF(S.LE.1)THEN
         ADJUST = DSQRT(GAMMA/Q(1,1))
         DO 10 ICOUNT=1,NCELLS,1
            ONE = -1.0
            G = RR1(TNEW,XI(ICOUNT),XI(1))/Q(1,1)
            IF(G.LT.0.0) ONE = 1.0
            THETA(1) = TNEW(1) + ONE*ADJUST
            LOW = NTOTAL*FUN1(THETA,XI(ICOUNT),XI(1))
            THETA(1)=TNEW(1) - ONE*ADJUST
            UPP = NTOTAL*FUN1(THETA,XI(ICOUNT),XI(1))
            FIT = NTOTAL*FUN1(TNEW,XI(ICOUNT),XI(1))
```

```
                  CALL SAVE(1,ICOUNT,XCDF(ICOUNT),LOW,FIT,UPP)
10             CONTINUE
               K = NCELLS-1
               CALL SAVE(1,K,XCDF(K),NTOTAL,NTOTAL,NTOTAL)
            ELSE
20             LOW = 0.0
               FIT = 0.0
               UPP = 0.0
               CALL SAVE(1,1,XCDF(1),LOW,FIT,UPP)
               DO 150 ICOUNT=1,NCELLS,1
                  ONE = -1.0
                  DO 140 K=1,2,1
                     ONE = ONE**K
                     DO 30 I=1,S,1
                        THETA(I) = TNEW(I)
30                   CONTINUE
                     TO = TONEW
                     IF (ICOUNT.NE.NCELLS)THEN
                        DO 100 L=1,MAXIT,1
                           DO 40 I=1,S,1
                              TOLD(I) = THETA(I)
40                         CONTINUE
                           CALL RR2(TO,THETA,ICOUNT,R)
                           DO 50 I=1,S,1
                              RPM(I) = R(I)
50                         CONTINUE
                           DO 60 I=1,S,1
                              DO 61 J=1,S,1
                                 QEQ(I,J) = Q(I,J)
61                            CONTINUE
60                         CONTINUE
                           CALL EQCHOL(S,QEQ,RPM,POSDEF)
C
C                          CHECK IF EQCHOL SUCCESSFUL
C
                           IF(.NOT.POSDEF)THEN
                              WRITE(SCRUNT,1200)
                              STOP
                           ENDIF
                           CSUM = 0.0
                           DO 70 I=1,S,1
                              CSUM = CSUM + R(I)*RPM(I)
70                         CONTINUE
                           CSUM = DSQRT(GAMMA/CSUM)
                           DO 80 I=1,S,1
                              THETA(I) = TNEW(I) + ONE*CSUM*RPM(I)
80                         CONTINUE
                           TO = THETAO(THETA)
                           RMSD = 0.0
                           DO 90 I=1,S,1
                              RMSD = RMSD + DSQRT((TOLD(I) - THETA(I))**2)
90                         CONTINUE
                           IF(RMSD.LT.CRIT)GOTO 111
100                     CONTINUE
C
```

```
C                 CHECK IF TOLERANCE REACHED
C
                  IF(RMSD.GE.CRIT)THEN
                     WRITE(SCRUNT,1100) ICOUNT,K
                     STOP
                  ENDIF
111            ENDIF
               IF(K.NE.1)THEN
                  UPP = NTOTAL*FUN2(TO,THETA,ICOUNT)
               ELSE
                  LOW = NTOTAL*FUN2(TO,THETA,ICOUNT)
               ENDIF
               FIT = NTOTAL*FUN2(TONEW,TNEW,ICOUNT)
140         CONTINUE
            K = ICOUNT+1
            CALL SAVE(1,K,XCDF(K),LOW,FIT,UPP)
150      CONTINUE
      ENDIF
999   RETURN
1100  FORMAT (/,5X,'CONVERGENCE NOT REACHED FOR ICOUNT =',I5,
     α       2X,'AND K = ',I5)
1200  FORMAT (/,5X,'POSDEF IS FALSE - CANNOT SOLVE')
       END
C
C **********************************************************************
C
      SUBROUTINE PDF(TONEW,TNEW,Q,GAMMA,QEQ,TOLD,
C
C     SUBROUTINE CALCULATES 95% CONFIDENCE BANDS FOR PDF
C
     α   THETA,RPM,R)
      IMPLICIT REAL*8 (A-H,O-Z)
      INTEGER*4 FUNIT1,FUNIT2,FUNIT3,SCRUNT,DEBUG
      COMMON /FILES/ FUNIT1,FUNIT2,FUNIT3,SCRUNT,DEBUG
      INTEGER*4 NCELLS,ILOG,S,MAXIT
      CHARACTER*6 NAME
      COMMON /INIT/ NCELLS,ILOG,S,MAXIT,CRIT,NAME
      LOGICAL POSDEF
      REAL*8 CHI05(20),NI,NTOTAL,FUNPDF,LOW,FIT,UPP
      DIMENSION TOLD(S),THETA(S),TNEW(S),Q(S,S),QEQ(S,S),
     α   RPM(S),R(S)
      COMMON/AREA1/XI(20), NI(20), NTOTAL
      COMMON/AREA3/CHI05
      COMMON/AREA4/XCDF(20),XPDF(20)
C
      IF(DEBUG.GE.1)WRITE(SCRUNT,*)' SUBROUTINE PDF'
      IF(S.LE.1)THEN
         G=0.0
         DO 180 I=1,NCELLS
            G=G+XI(I)*FUNPDF(TONEW,TNEW,XI(I))
180      CONTINUE
         ADJUST = DSQRT(GAMMA/Q(1,1))
         DO 190 ICOUNT = 1,NCELLS
            ONE = -1.0
            IF(G.GT.XI(ICOUNT)) ONE = 1.0
            THETA(1) = TNEW(1) + ONE*ADJUST
            TO=THETAO(THETA)
            LOW = FUNPDF(TO,THETA,XI(ICOUNT))*NTOTAL
            THETA(1) = TNEW(1) - ONE*ADJUST
            TO=THETAO(THETA)
            UPP = FUNPDF(TO,THETA,XI(ICOUNT))*NTOTAL
            FIT = FUNPDF(TONEW,TNEW,XI( ICOUNT))*NTOTAL
            CALL SAVE(2,ICOUNT,XPDF(ICOUNT),LOW,FIT,UPP)
190      CONTINUE
      ELSE
         DO 330 ICOUNT=1,NCELLS
            ONE = -1.0
            DO 320 K=1,2,1
               ONE = ONE**K
               DO 210 I=1,S,1
                  THETA(I) = TNEW(I)
210            CONTINUE
               TO=TONEW
               DO 290 L=1,MAXIT,1
                  DO 220 I=1,S,1
                     TOLD(I) = THETA(I)
220               CONTINUE
                  DO 230 I=1,S,1
                     R(I) = 0.0
                     DO 231 J=1,NCELLS
                        R(I) = R(I) + FUNPDF(TO,THETA,XI(J))*XI(J)**I
231                  CONTINUE
230               CONTINUE
                  DO 240 I=1,S,1
                     R(I) = XI(ICOUNT)**I - R(I)
                     RPM(I) = R(I)
240               CONTINUE
                  DO 250 I=1,S,1
                     DO 251 J=1,S,1
                        QEQ(I,J) = Q(I,J)
251                  CONTINUE
250               CONTINUE
                  CALL EQCHOL(S,QEQ,RPM,POSDEF)
C
C                 CHECK IF EQCHOL SUCCESSFUL
C
                  IF(.NOT.POSDEF)THEN
                     WRITE(SCRUNT,1200)
                     STOP
                  ENDIF
                  CSUM = 0.0
                  DO 260 I=1,S,1
                     CSUM = CSUM + R(I)*RPM(I)
260               CONTINUE
                  CSUM = DSQRT(GAMMA/CSUM)
                  DO 270 I=1,S,1
                     THETA(I) = TNEW(I) + ONE*CSUM*RPM(I)
270               CONTINUE
                  RMSD = 0.0
                  DO 280 I=1,S,1
```

```
                     RMSD = RMSD + DSQRT((TOLD(I) - THETA(I))**2)
280               CONTINUE
                  TO=THETAO(THETA)
C
C                 CHECK IF TOLERANCE REACHED
C
                  IF(RMSD.LT.CRIT)GOTO 300
290            CONTINUE
               WRITE(SCRUNT,1500)ICOUNT,K
               STOP
300            IF(K.NE.1)THEN
                  UPP = FUNPDF(TO,THETA,XI(ICOUNT))*NTOTAL
               ELSE
                  LOW = FUNPDF(TO,THETA,XI(ICOUNT))*NTOTAL
               ENDIF
320         CONTINUE
            FIT = FUNPDF(TONEW,TNEW,XI(ICOUNT))*NTOTAL
            CALL SAVE(2,ICOUNT,XPDF(ICOUNT),LOW,FIT,UPP)
330      CONTINUE
      ENDIF
340   RETURN
1200  FORMAT (/,5X,'POSDEF IS FALSE - CANNOT SOLVE')
1500  FORMAT (/,5X,'CONVERGENCE NOT REACHED FOR ICOUNT =',I5,
     α       2X,'AND K = ',I5)
      END
C
C***********************************************************************
C
      FUNCTION FUNPDF(B,T,X)
C
C     FUNCTION CALCULATES VALUE OF PDF AT ANY VALUE OF X
C
      IMPLICIT REAL*8(A-H,O-Z)
      INTEGER*4 NCELLS,ILOG,S,MAXIT
      CHARACTER*6 NAME
      COMMON /INIT/ NCELLS,ILOG,S,MAXIT,CRIT,NAME
      REAL*8 FUNPDF
      DIMENSION T(S)
      INTEGER*4 FUNIT1,FUNIT2,FUNIT3,SCRUNT,DEBUG
      COMMON /FILES/ FUNIT1,FUNIT2,FUNIT3,SCRUNT,DEBUG
C
      IF(DEBUG.EQ.2)WRITE(SCRUNT,*)'     FUNCTION FUNDF'
      SUM = B
      DO 10 I=1,S
         SUM = SUM + T(I)*X**I
10    CONTINUE
      FUNPDF = DEXP(SUM)
      RETURN
      END
C
C***********************************************************************
C
      FUNCTION FUN1(T,X,A)
C
C     FUNCTION CALCULATES CDF FOR S=1
```

```
C
      IMPLICIT REAL*8(A-H,O-Z)
      REAL*8 FUN1
      INTEGER*4 FUNIT1,FUNIT2,FUNIT3,SCRUNT,DEBUG
      COMMON /FILES/ FUNIT1,FUNIT2,FUNIT3,SCRUNT,DEBUG
      INTEGER*4 NCELLS,ILOG,S,MAXIT
      CHARACTER*6 NAME
      COMMON /INIT/ NCELLS,ILOG,S,MAXIT,CRIT,NAME
      DIMENSION T(S)
C
      IF(DEBUG.EQ.2)WRITE(SCRUNT,*)'       FUNCTION FUN1'
      FUN1 = 1.0 - DEXP(T(1)*(-A+X))
      RETURN
      END
C
C***********************************************************************
C
      FUNCTION RR1(T,X,A)
C
C     FUNCTION CALCULATES R FOR S=1 CASE
C
      IMPLICIT REAL*8 (A-H,O-Z)
      INTEGER*4 FUNIT1,FUNIT2,FUNIT3,SCRUNT,DEBUG
      COMMON /FILES/ FUNIT1,FUNIT2,FUNIT3,SCRUNT,DEBUG
C
      IF(DEBUG.EQ.2)WRITE(SCRUNT,*)'       FUNCTION RR1'
      D = (1.0-A*T)*(DEXP(T*(X+A)) - DEXP(T*2.*A))/T
      E = DEXP(T*X)*(T*X - 1.0) + DEXP(A*T)*(1.0 - A*T)
      F = -DEXP(-A*T)/T
      RR1 = F*(D+E)
      RETURN
      END
C
C***********************************************************************
C
      SUBROUTINE RR2(T0,T,L,R)
C
C     SUBROUTINE CALCULATES R FOR S>1 CASE
C
      IMPLICIT REAL*8 (A-H,O-Z)
      INTEGER*4 FUNIT1,FUNIT2,FUNIT3,SCRUNT,DEBUG
      COMMON /FILES/ FUNIT1,FUNIT2,FUNIT3,SCRUNT,DEBUG
      INTEGER*4 NCELLS,ILOG,S,MAXIT
      CHARACTER*6 NAME
      COMMON /INIT/ NCELLS,ILOG,S,MAXIT,CRIT,NAME
      REAL*8 NI,NTOTAL, FUN2
      INTEGER*4 I,L
      DIMENSION T(S),R(S)
      COMMON/AREA1/XI(20),NI(20),NTOTAL
C
      IF(DEBUG.GE.1)WRITE(SCRUNT,*)' SUBROUTINE RR2'
      DO 20 I=1,S
         A=FUN2(T0,T,L)
         B=XEXP(T0,T,NCELLS,I)
         C=XEXP(T0,T,L,I)
         R(I)=A*B-C
20    CONTINUE
      RETURN
      END
C
C***************************************************************************
C
      FUNCTION FUN2(TO,T,L)
C
C     FUNCTION CALCULATES CDF FOR S>1
C
      IMPLICIT REAL*8 (A-H,O-Z)
      INTEGER*4 FUNIT1,FUNIT2,FUNIT3,SCRUNT,DEBUG
      COMMON /FILES/ FUNIT1,FUNIT2,FUNIT3,SCRUNT,DEBUG
      INTEGER*4 NCELLS,ILOG,S,MAXIT
      CHARACTER*6 NAME
      COMMON /INIT/ NCELLS,ILOG,S,MAXIT,CRIT,NAME
      REAL*8 FUN2,NI,NTOTAL
      INTEGER*4 L
      DIMENSION T(S)
      COMMON/AREA1/XI(20),NI(20),NTOTAL
C
      IF(DEBUG.EQ.2)WRITE(SCRUNT,*)'      FUNCTION FUN2'
      FUN2 = 0.0
      DO 20 I = 1,L
         SUMJ = 0.0
         DO 10 J = 1,S
            SUMJ = SUMJ + T(J)*XI(I)**J
10       CONTINUE
         FUN2 = FUN2 + DEXP(TO + SUMJ)
20    CONTINUE
      RETURN
      END
C
C***************************************************************************
C
      FUNCTION XEXP(TO,T,L,J)
C
C     FUNCTION CALCULATES EXPRESSION IN THE FORMULA FOR R IN THE S>1
C     CASE
C
      IMPLICIT REAL*8(A-H,O-Z)
      INTEGER*4 FUNIT1,FUNIT2,FUNIT3,SCRUNT,DEBUG
      COMMON /FILES/ FUNIT1,FUNIT2,FUNIT3,SCRUNT,DEBUG
      INTEGER*4 NCELLS,ILOG,S,MAXIT
      CHARACTER*6 NAME
      COMMON /INIT/ NCELLS,ILOG,S,MAXIT,CRIT,NAME
      REAL*8 NI,NTOTAL
      INTEGER*4 L,J
      DIMENSION T(S)
      COMMON/AREA1/XI(20),NI(20), NTOTAL
C
      IF(DEBUG.EQ.2)WRITE(SCRUNT,*)'      FUNCTION XEXP'
      XEXP = 0.0
      DO 20 I  = 1,L
```

```
            SUMK = 0.0
            DO 10 K = 1,S
               SUMK = SUMK + T(K)*XI(I)**K
10          CONTINUE
            XEXP = XEXP - DEXP(TO+SUMK)*(XI(I)**J)
20       CONTINUE
         RETURN
         END
C
C***********************************************************************
C
         FUNCTION THETAO(T)
C
C        FUNCTION CALCULATES VALUE OF NORMALIZING CONSTANT THETAO,
C        APPROXIMATING INTEGRATION BY SUMMATION
C
         IMPLICIT REAL*8 (A-H,O-Z)
         INTEGER*4 FUNIT1,FUNIT2,FUNIT3,SCRUNT,DEBUG
         COMMON /FILES/ FUNIT1,FUNIT2,FUNIT3,SCRUNT,DEBUG
         INTEGER*4 NCELLS,ILOG,S,MAXIT
         CHARACTER*6 NAME
         COMMON /INIT/ NCELLS,ILOG,S,MAXIT,CRIT,NAME
         REAL*8 NI,NTOTAL
         DIMENSION T(S)
         COMMON/AREA1/XI(20),NI(20),NTOTAL
C
         IF(DEBUG.EQ.2)WRITE(SCRUNT,*)'      FUNCTION THETAO'
         SUM = 0.0
         DO 20 I = 1,NCELLS
            SUMJ = 0.0
            DO 10 J = 1,S
               SUMJ = SUMJ + T(J)*XI(I)**J
10          CONTINUE
            SUM = SUM + DEXP(SUMJ)
20       CONTINUE
         THETAO = -DLOG(SUM)
         RETURN
         END
C
C***********************************************************************
C
         SUBROUTINE EQCHOL(S,C,B,POSDEF)
C
C        SUBROUTINE SOLVES THE EQUATION A*u=b BY CHOLESKY DECOMPOSITION
C
         IMPLICIT REAL*8(A-H,O-Z)
         INTEGER*4 FUNIT1,FUNIT2,FUNIT3,SCRUNT,DEBUG
         COMMON /FILES/ FUNIT1,FUNIT2,FUNIT3,SCRUNT,DEBUG
         LOGICAL POSDEF
         INTEGER*4 S
         DIMENSION C(S,S),B(S)
C
         IF(DEBUG.GE.1)WRITE(SCRUNT,*)' SUBROUTINE EQCHOL'
         POSDEF=.TRUE.
         DO 70 I=1,S
         IF(I.NE.1)THEN
            IM1=I-1
            DO 20 J=1,IM1
               Z=C(J,I)
               C(I,J)=0.0
               DO 10 K=I,S
                  C(I,K)=C(I,K)-Z*C(J,K)
10             CONTINUE
               B(I)=B(I)-Z*B(J)
20          CONTINUE
         ENDIF
         Z=C(I,I)
         IF(Z.LE.0.0)THEN
            POSDEF=.FALSE.
            GOTO 999
         ENDIF
         Z=DSQRT(Z)
         C(I,I)=Z
         Z=1./Z
         IP1=I+1
         IF(I.NE.S)THEN
            DO 60 K=IP1,S
               C(I,K)=C(I,K)*Z
60          CONTINUE
         ENDIF
         B(I)=B(I)*Z
70    CONTINUE
      DO 90 K=1,S
         I=S-K+1
         Z=B(I)
         IF(I.NE.S)THEN
            IP1=I+1
            DO 80 J=IP1,S
               Z=Z-C(I,J)*B(J)
80          CONTINUE
         ENDIF
         B(I)=Z/C(I,I)
90    CONTINUE
999   RETURN
      END
C
C ***********************************************************************
C
      SUBROUTINE SAVE(N,M,A1,A2,A3,A4)
C
C     SUBROUTINE X-ORDINATES, FITTED CURVE, AND CONFIDENCE BANDS
C     FOR LATER OUTPUT
C
      IMPLICIT REAL*8 (A-H,O-Z)
      REAL*8 OUT(20,8)
      COMMON /OUTS/ OUT
      INTEGER*4 N,M
C
      IF(N.EQ.1)THEN
         OUT(M,1)=A1
         OUT(M,2)=A2
         OUT(M,3)=A3
         OUT(M,4)=A4
      ELSE
         OUT(M,5)=A1
         OUT(M,6)=A2
         OUT(M,7)=A3
         OUT(M,8)=A4
      ENDIF
      RETURN
      END
C
C **********************************************************************
C
      SUBROUTINE OUTPUT
C
C     SUBROUTINE OUTPUTS SAVED VALUES OF X-ORDINATES, FITTED CURVE,
C     AND CONFIDENCE BANDS
C
      IMPLICIT REAL*8 (A-H,O-Z)
      INTEGER*4 FUNIT1,FUNIT2,FUNIT3,SCRUNT,DEBUG
      COMMON /FILES/ FUNIT1,FUNIT2,FUNIT3,SCRUNT,DEBUG
      INTEGER*4 NCELLS,ILOG,S,MAXIT
      CHARACTER*6 NAME
      COMMON /INIT/ NCELLS,ILOG,S,MAXIT,CRIT,NAME
      REAL*8 OUT(20,8)
      COMMON /OUTS/ OUT
C
      WRITE(FUNIT2,1000)
      J=NCELLS+1
      N=8
      DO 10 I=1,J
         IF (I.EQ.J) N=4
         WRITE(FUNIT2,1300) (OUT(I,K),K=1,N)
10    CONTINUE
      RETURN
1000  FORMAT (5X,'CDF',6X,'LOWERLIMIT',3X,'FITTEDCDF',2X,'UPPERLIMIT',
     α   5X,'PDF',6X,'LOWERLIMIT',3X,'FITTEDPDF',2X,'UPPERLIMIT')
1300  FORMAT (8(2X,E10.4))
      END
```

APPENDIX H

# IDENTIFICATION OF PARAMETER CORRELATIONS AND FUNCTIONAL RELATIONSHIPS USING EXPERT OPINION

by

T. H. Andres
Atomic Energy of Canada Limited

for

SENES CONSULTANTS LIMITED

1986 August

Whiteshell Nuclear Research Establishment

Pinawa, Manitoba R0E 1L0

# IDENTIFICATION OF PARAMETER CORRELATIONS AND FUNCTIONAL RELATIONSHIPS USING EXPERT OPINION

## 1. Introduction

Techniques for handling correlated parameters in a probabilistic assessment code were described in an earlier discussion paper [Andres and Goodwin, 1985]. Several quotes from that paper set the context for this one:

- Long-term environmental assessments ... typically use results of computer simulations as a basis for their conclusions. The credibility of this approach depends on how well the models and data used in the simulations are accepted by reviewers. For acceptance, it is important that the scenarios simulated be plausible. One requirement for plausibility is that values of parameters in the simulation model display the same characteristics and relationships as do values observed in the field, laboratory, and literature. In particular, observations that are known to be correlated in the field should correspond to parameter values that are correlated in the model.
- Correlations can be observed in experimental data where two or more variables are observed under the same conditions. When variables are observed independently, correlation coefficients cannot be measured directly. For example, data gleaned from independent sources in the literature will not be correlated. In such cases, correlations can sometimes be hypothesized (but not necessarily quantified) by experts having substantial experience with the natural system being modelled. In identifying a correlation, an expert is answering a question like: "If variable X is varied, how do I expect the variable Y to respond, if at all?"
- Where correlations are a matter of theory or expert opinion, rather than experimental data, ... a scientist ... must be guided in expressing his theoretical understanding or cultivated opinion. Graphic representations of the relationship between two variables ... may help.

Observing correlations in experimental data is the preferred way of identifying correlations and other interactions between variables that we use to describe the world. Sometimes a research program to generate such experimental data is not a viable option, perhaps because of cost or because the part of the world being modelled is inaccessible (e.g. lies far in the future). Then we resort to the information collected by that superb pattern detection instrument, the mind of the expert. In this paper it is assumed that expert opinion is the source of correlation information, since insufficient correlation data is available for NUTP modelling.

This paper proposes a systematic approach toward the identification of parameter correlations using expert opinion. It emphasizes practical techniques that can be applied directly and that are cost-effective. In selecting these techniques from a number that are available, the context of the current study to assess the impacts of uranium mill tailings was borne in mind. Priority was given to techniques that:

- can be applied midway through a project;
- use expert opinion as well as field research results where available;
- are self-documenting;
- are easy to review.

The approach that has been developed combines and extends in a new package several ideas that have been applied in the Canadian Nuclear Fuel Waste Management Program (CNFWMP). It is based on:

- concise graphic documentation of an existing model;
- a comprehensive dictionary of simulation variables that appear in the model;
- standard forms to record and display expert submissions;
- measures that guide the expert towards the use of functional relationships instead of correlation coefficients, where appropriate;
- checks to weed out inconsistent data and circular dependencies;
- completion of the feedback cycle so that experts can take account of the impacts of their submitted opinions on model behaviour, and refine their input.

The structure of this paper is as follows. Section 2 sets the stage for approaching an expert to elicit an opinion on how variables in a model should be related. It describes, with examples, a suitable way of presenting existing information to the expert, to help him in his task of identifying potential relationships among the model's variables. Section 3 describes the data set that should be elicited from the expert. It includes forms for the collection of data. Section 4 addresses some of the special cases that may arise, such as the correlation of variables that depend on time.

The following terminology is used in this paper.

- Parameters/variables: variables are named quantities used in a simulation. Parameters are variables with values defined outside of a simulation. Values may be defined as constants, or by randomly sampling from a probability distribution.

- Correlation/functional relationship: variables are said to be correlated if their values consistently display a statistical correlation in samples of simulations. Variables are said to have a functional relationship if there is a known mathematical function that generates the values of some of the variables given values for the rest. Thus correlation is a statistical property, and functional relationship is a mathematical one. The two concepts are intimately connected. Variables that are functionally related usually are correlated as a result. Correlations among variables can be enforced by making up functional relationships (using auxiliary random variables) with the desired properties. Such relationships are not unique because a correlation coefficient does not fully define the relationship between two variables.

## 2. What the Expert Needs to Know Before Rendering an Opinion

In the CNFWMP, it has been our experience that experts need to know the context within which their information will be used before rendering an opinion. The reason is that only the expert is qualified to determine which aspects of a modelling environment pertain to the information being obtained. For example, to support a model of deep groundwater flow, an expert may be asked to identify the relationship between permeability and porosity in a given rock type. The answer to this question could vary significantly, depending upon whether intact bulk rock, or a fracture zone through the rock is being discussed. The expert needs to know what is being modelled, and how, before answering such questions.

An expert will need time to understand a complex system that uses his data. A modeller should expect to go back to the expert two or three times with modified information about the model as the expert's submissions become incorporated into it. Eliciting expert opinion is an iterative process.

It is proposed here that information about a model be presented to the expert in three ways: in dependency diagrams, in a model data dictionary, and in a set of randomly sampled scenarios. These sources of information are discussed in Sections 2.1, 2.2 and 2.3.

The expert should also get sufficient information so that he can provide data in the form expected. Examples of this type of information are provided in Section 2.4.

## 2.1 Dependency diagrams

Figure 2.1 is a dependency diagram [in a form adapted from Smith, 1985] showing the radon dose model from the NUTP Phase II assessment study [SENES, 1985c]. Each elliptical bubble in this figure represents one of the calculated variables in the model. Each rectangle represents a sampled parameter. Directed arrows among the bubbles and rectangles represent functional relationships; for example, an arrow from the sampled parameter MPCH2O (Percent Moisture Content) to the calculated variable EBKDFC (Radon Diffusion Content) shows that MPCH2O is used in calculating EBKDFC.

There are no explicit correlations among sampled parameters in the Phase II study, so none are shown in Figure 2.1. In Figure 2.2, some hypothetical correlations have been introduced. They are represented by dashed lines between rectangles. The directions of the arrows for correlations represent causal relationships. The dashed arrow from MPCH2O to EMANAT (Radon Emanation Coefficient) indicates that these two parameters are correlated, and that in the relationship between them, MPCH2O is the independent and EMANAT the dependent variable. If neither parameter were independent, as would happen if they both depended on an unspecified third parameter, they would be joined by a headless dashed arrow.

Dependency diagrams like Figures 2.1 and 2.2 depict relationships among data in a visual way that has several benefits:

- A visual presentation allows most experts and modellers to assimilate and analyze the data rapidly.

- Dependency diagrams help the expert refine initial relationships by presenting a complete picture of a model on one piece of paper.

- Experts using dependency diagrams are encouraged to rethink their choice of parameters from time to time, since correlations between parameters appear much like functional relationships. It is easy when using such diagrams to change a parameter into a calculated variable by explicitly identifying the functional relationship that causes the correlation.

- Problem areas like excessive numbers of dependencies among parameters (too many lines) and circular dependencies (e.g. A points to B which points back to A) can easily be seen in a dependency diagram.

- Complicated models can be represented in a telescoping fashion by using a bubble on one diagram to represent another more detailed dependency diagram. For example, the bubble DEPTH1 in Figures 2.1 and 2.2 represents calculations done in the water source model. These may be more fully explained on another page in a

FIGURE 2.1

DEPENDENCY DIAGRAM
FOR EMISSION RATE OF RADON FROM SOURCE

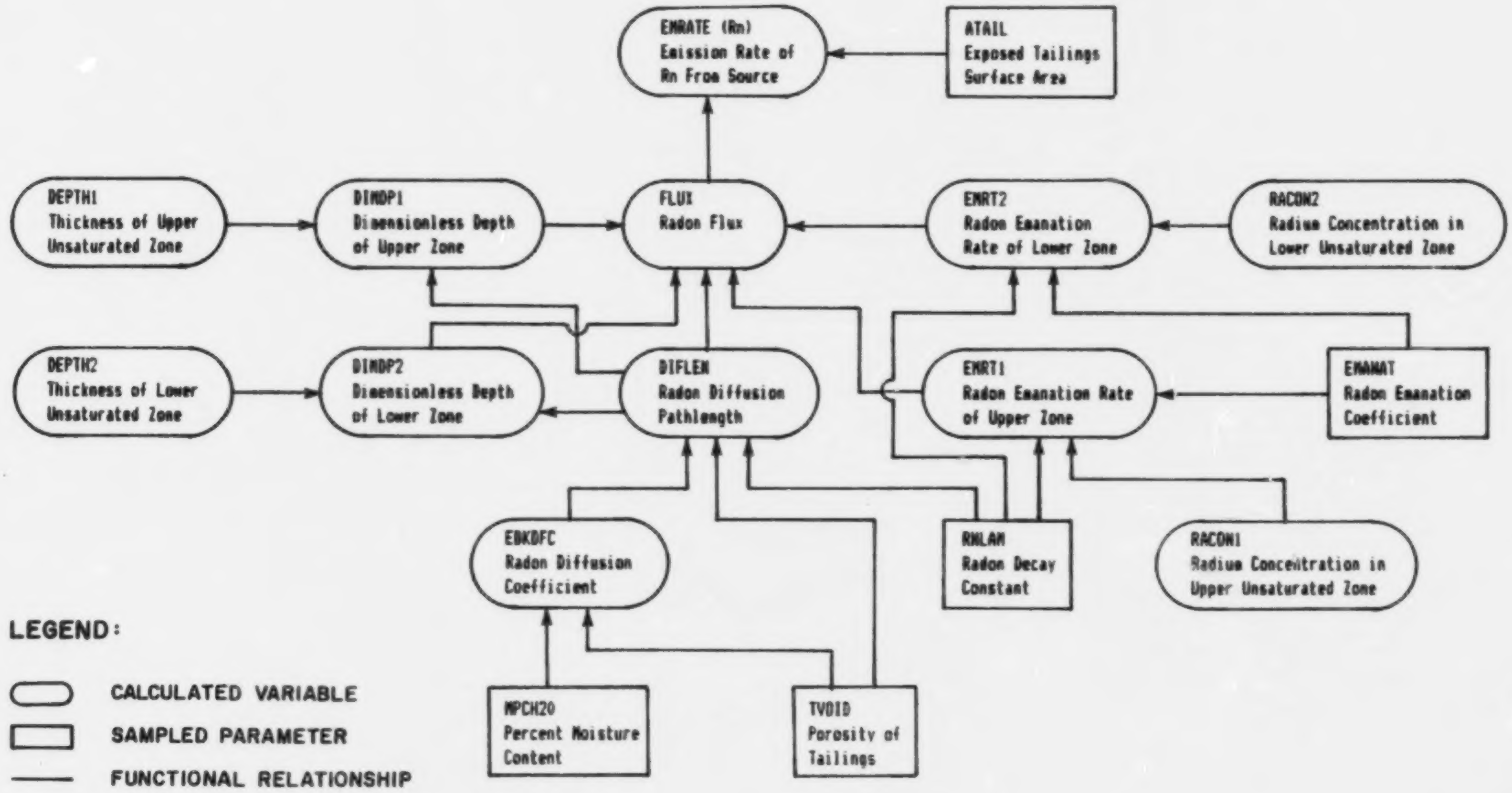
EMRATE (Rn)
Emission Rate of
Rn From Source
ATAIL
Exposed Tailings
Surface Area
DEPTH1
Thickness of Upper
Unsaturated Zone
DIMDP1
Dimensionless Depth
of Upper Zone
FLUX
Radon Flux
EMRT2
Radon Emanation
Rate of Lower Zone
RACON2
Radium Concentration in
Lower Unsaturated Zone
DEPTH2
Thickness of Lower
Unsaturated Zone
DIMDP2
Dimensionless Depth
of Lower Zone
DIFLEN
Radon Diffusion
Pathlength
EMRT1
Radon Emanation Rate
of Upper Zone
EMANAT
Radon Emanation
Coefficient
EBKDFC
Radon Diffusion
Coefficient
RNLAM
Radon Decay
Constant
RACON1
Radium Concentration in
Upper Unsaturated Zone
MPCH20
Percent Moisture
Content
TVOID
Porosity of
Tailings
LEGEND:
CALCULATED VARIABLE
SAMPLED PARAMETER
FUNCTIONAL RELATIONSHIP

FIGURE 2.2

DEPENDENCY DIAGRAM
FOR EMISSION RATE OF RADON FROM SOURCE
WITH CORRELATIONS

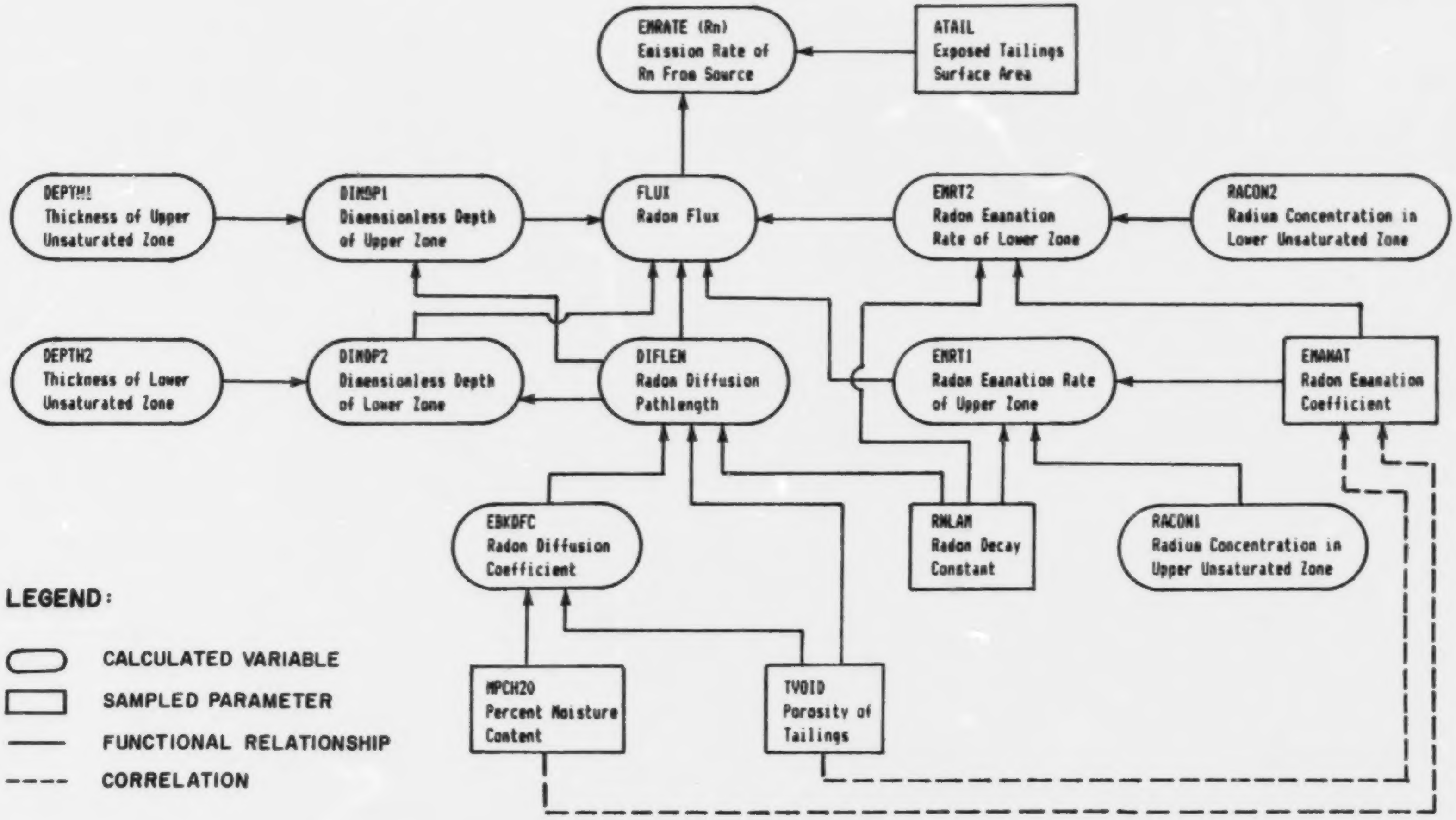
EMRATE (Rn) Emission Rate of Rn From Source
ATAIL Exposed Tailings Surface Area
DEPTH1 Thickness of Upper Unsaturated Zone
DIMDP1 Dimensionless Depth of Upper Zone
FLUX Radon Flux
EMRT2 Radon Emanation Rate of Lower Zone
RACON2 Radium Concentration in Lower Unsaturated Zone
DEPTH2 Thickness of Lower Unsaturated Zone
DIMDP2 Dimensionless Depth of Lower Zone
DIFLEN Radon Diffusion Pathlength
EMRT1 Radon Emanation Rate of Upper Zone
EMANAT Radon Emanation Coefficient
EBKDFC Radon Diffusion Coefficient
RNLAM Radon Decay Constant
RACON1 Radium Concentration in Upper Unsaturated Zone
MPCH2O Percent Moisture Content
TVOID Porosity of Tailings
LEGEND:
CALCULATED VARIABLE
SAMPLED PARAMETER
FUNCTIONAL RELATIONSHIP
CORRELATION

more detailed dependency diagram (not included). An expert can quickly find out the context of a parameter or submodel by starting with the top diagram and moving from page to page down to the level where the parameter or submodel appears.

- Dependency diagrams (along with the model data dictionary) provide a good way of specifying a model to computer programmers who will implement it.
- Dependency diagrams document a model concisely for reviewers who want to understand quickly the scope and level of detail in a model.

Dependency diagrams are usually drawn in an iterative fashion. A brief procedure for drawing one is as follows:

(1) Write down all the variables in a model and put a bubble or rectangle around each one, depending on whether the variable is calculated or sampled.

(2) Connect the bubbles and rectangles with solid arrows to represent modelled relationships, and the rectangles with dashed arrows to represent known correlations.

(3) Rearrange the diagram to reduce the number of crossed lines, and to place tightly connected groups of variables together. General flow should be from bottom to top because most people can more easily follow flow in that direction, as has been learned from experiments in map-reading.

(4) If the diagram is too cluttered, replace a cluster of bubbles and line used to calculate one variable by a bubble bearing the name of that variable. Put the cluster details on another piece of paper.

(5) For maximal understanding, it helps to transpose a dependency diagram onto a physical picture of the site being modelled, in such a way that each variable lies atop a visual feature that it represents. This step is most useful for a model with a strong geographic component. In other cases it may not be possible.

Closely related to dependency diagrams are data flow diagrams [DeMarco, 1979]. Figure 2.3 is a data flow diagram for part of the radon dose model. In data flow diagrams, the circular bubbles represent processes, and the directed arrows represent data flows. Data flow diagrams have been used extensively in the CNFWMP in the analysis of assessment models [Hoffman et al, 1984]. They are also well-documented in the literature [Page-Jones, 1980; Gane and Sarson, 1979; Wolfe, 1985].

FIGURE 2.3

DATA FLOW DIAGRAM
FOR EMISSION RATE OF RADON FROM SOURCE

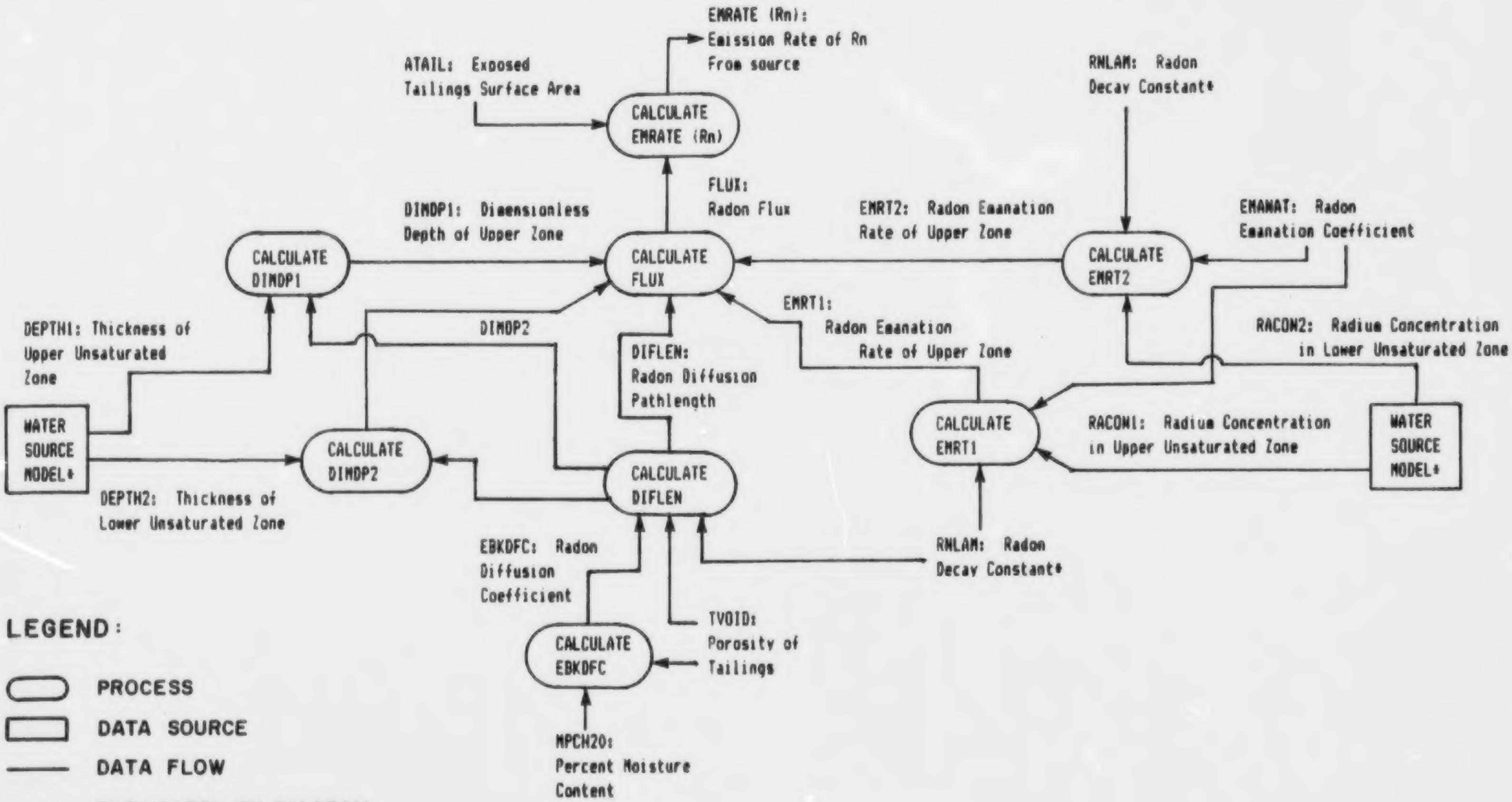
EMRATE (Rn): Emission Rate of Rn From source
ATAIL: Exposed Tailings Surface Area
CALCULATE EMRATE (Rn)
RNLAM: Radon Decay Constant*
FLUX: Radon Flux
DIMDP1: Dimensionless Depth of Upper Zone
EMRT2: Radon Emanation Rate of Upper Zone
EMANAT: Radon Emanation Coefficient
CALCULATE DIMDP1
CALCULATE FLUX
CALCULATE EMRT2
EMRT1: Radon Emanation Rate of Upper Zone
DEPTH1: Thickness of Upper Unsaturated Zone
DIMDP2
DIFLEN: Radon Diffusion Pathlength
RACON2: Radium Concentration in Lower Unsaturated Zone
WATER SOURCE MODEL*
CALCULATE DIMDP2
CALCULATE DIFLEN
CALCULATE EMRT1
RACON1: Radium Concentration in Upper Unsaturated Zone
WATER SOURCE MODEL*
DEPTH2: Thickness of Lower Unsaturated Zone
EBKDFC: Radon Diffusion Coefficient
RNLAM: Radon Decay Constant*
TVOID: Porosity of Tailings
CALCULATE EBKDFC
MPCH2O: Percent Moisture Content
LEGEND:
PROCESS
DATA SOURCE
DATA FLOW
* DUPLICATED ON DIAGRAM

The use of data flow diagrams instead of dependency diagrams is another option that works well from the point of view of depicting a model. Data flow diagrams are ideal for expressing models in terms of standard model elements (i.e. procedures). For example, the calculation of a diffusion pathlength could be such a standard model element. Then in Figure 2.3, the bubble labelled "CALCULATE DIFLEN" would represent a call to a standard subroutine in the implementation of a model.

Data flow diagrams tend to preclude the use of correlated parameters, however, since they offer no easy way to show correlations. For this reason dependency diagrams were chosen as a preferable representation in the present context.

## 2.2 Model Data Dictionary

While a dependency diagram represents the relationships in a model concisely, it does not represent them exactly. A text description of each variable and of each relationship is needed to complete the model description. "On any project, there is a need to have a consistent set of names to use when referring to various pieces of information. ... With the advent of computerized data-base management systems has come the recognition that it is mandatory to have a consistent naming scheme. ... The answer to this problem has been to develop data dictionaries." [Orr, 1981]. Appendix A is a data dictionary excerpt, based on SENES [1985c], that includes all the data elements in Figure 2.1. The key elements of this data dictionary are:

(1) Identifiers: The data dictionary needs to give at least two unique identifiers for each variable. The long variable name usually consists of several descriptive words. It is used to refer to a variable consistently in speech and in written work, so that there can be no ambiguity about which variable is being discussed. The short variable name is a unique abbreviation of the long variable name that can be used in a computer program. Where FORTRAN is the usual programming language, the short variable name should have no more than six characters. It is also used as an abbreviation anywhere there is insufficient space for the long name, as in an equation or the legend of a plot. In Appendix A the short variable name has been listed first, and the dictionary has been sorted on this field. E.g. ATAIL is the first entry in Appendix A and it is short for Exposed Tailings Surface Area.

(2) Units: The SI units for every variable should be quoted so that an expert can understand any data values he sees. E.g. Net Precipitation is measured in m/a (short for metres/year). In the

CNFWMP it has been found necessary to specify units wherever values of a variable are quoted or plotted or otherwise discussed. Significant problems have occurred where units were misunderstood: e.g. doses read as Sieverts (Sv) instead of milliSieverts (mSv). A standard reference for units [e.g. CSA, 1979] is important for consistent usage by independent experts. For example, such a reference can settle questions like: "Is year an SI unit, and is it abbreviated 'yr' or 'a'?"

(3) Definition: This entry specifies in detail what physical quantity a variable represents. The description must be detailed, because it is the only place where a modeller and an expert providing data can check that they are both talking about exactly the same variable. In the example of Net Precipitation, it may be important to know how it is calculated. Is evapotranspiration subtracted from measured rainfall? Is runoff? Is allowance made for water rising by capillary action from the water table during dry weather? Is snowfall counted? What is the averaging period used in calculating Net Precipitation? The answers to all of these questions may affect the degree of correlation between Net Precipitation and some other variable.

As an example of the need for a detailed definition, consider the case of "Hydrodynamic Dispersion Coefficient", which was used in a CNFWMP model of the saturated soil zone. The researcher who provided a formula for this variable understood it to include dispersion only, and excluded molecular diffusion. The biosphere modeller who requested the formula thought molecular diffusion was included. Before a correction was made, some early results were obtained where the value of Hydrodynamic Dispersion Coefficient was about 7 orders of magnitude too small.

(4) Distribution: For sampled parameters, the probability distribution should be specified. This probability distribution is the one that best describes current knowledge of the distribution of values that a variable can take on. It is used in sampling parameter values in Monte Carlo simulations. It may be needed in estimating correlations [Andres and Goodwin, 1985].

(5) Formula: For calculated variables, the formula should be provided. If the formula is excessively complicated, a reference to a detailed writeup may be provided instead.

(6) Reference: The data dictionary should also specify who provided the information for each variable. Appendix A does not have this entry because the references were not readily available.

## 2.3 Sampled Scenarios

Armed with a dependency diagram and a model data dictionary, the expert should be able to understand a model as far as it has been defined. Not all the consequences of the definition may be clear, however. For that reason it is wise to present the expert with sets of sampled parameter values and calculated variable values, so that he can check them for reasonableness.

It is possible for a seemingly adequate model to churn out meaningless results for reasons that are obvious only in retrospect. For example, one model that was run in the CNFWMP yielded radionuclide concentrations in soil of up to 10 million grams per gram of soil. One reason for this behaviour was found to be an incorrect procedure used for running the computer program. In another case, a finite element code was used to model groundwater flows in a two-dimensional soil section. Careful examination of the groundwater heads in the model revealed that water was apparently entering the system through a no-flow boundary, a seemingly impossible result. In that case, once the problem was identified, it was traced to an incorrect switch setting in the input file.

An expert can often identify unreasonable behaviour in a model so that the source can be traced. Having an expert examine the sample scenarios is therefore a good way of quality assuring a model. At the same time, it completes the feedback cycle so that the expert knows what kinds of scenarios come from his input.

When it comes to identifying and estimating correlations, this feedback information becomes especially important. Most experts in scientific fields lack experience in estimating correlations between variables under hypothetical conditions. If they never receive feedback on the effects of their estimated values on the variables involved, they are unlikely to improve in their estimating.

## 2.4 Background Information Describing What the Modeller Wants

The modeller who is eliciting information knows the form in which he wants to get a response. It is his responsibility to convey this information to the expert.

If an expert is asked to provide a probability distribution, he should receive a diagram showing the forms of available distributions (e.g. normal, uniform, beta). He should also get a text description of the characteristics of each distribution (e.g. what attributes must be specified, whether the distribution has an infinite tail, formulas for mean and variance). Figure 2.4 provides this information for distributions used

FIGURE 2.4

PROBABILITY DENSITY FUNCTIONS RECOGNIZED BY SYVAC 3

| Class of pdf | Sample Plot | Distribution Parameters Required | Mean | Std Deviation | Used for Parameters | Examples in SYVAC |
|---|---|---|---|---|---|---|
| Constant | | Constant value of x, a. | a | 0 | with well-defined, fixed value | radionuclide decay constants |
| Uniform | 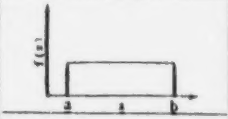 | Lower limit of x, a.<br>Upper limit of x, b. | $\frac{a+b}{2}$ | $\frac{b-a}{\sqrt{12}}$ | with limits which are known or can be guessed, but with unknown or equally likely weights | porosity of vault backfill |
| Piecewise uniform | 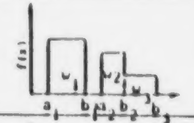 | Number of ranges.<br>For each range i:<br>-lower and upper limits of x, $a_i$ and $b_i$,<br>-fraction of x values in i. | $\sum_i \frac{(b_i+a_i)}{2} w_i$ |  | with two or more disjoint sets of possible values, or parameters used as switches | hydraulic gradient in geosphere layers |
| Log uniform | 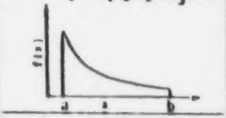 | Lower limit of x, a.<br>Upper limit of x, b. | $\frac{b-a}{\ln(b/a)}$ | $\sqrt{\frac{b^2-a^2}{2\ln(b/a)}-\frac{(b-a)^2}{[\ln(b/a)]^2}}$ | with limits which are known or can be guessed, relative weights unknown, intrinsically positive parameters | hydraulic conductivities of buffer and backfill |
| Normal | 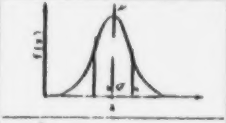 | Mean value of x, $\mu$.<br>Standard deviation of values of x, $\sigma$. | $\mu$ | $\sigma$ | which are the sum of values or variables | consumption rates for foods |
| Lognormal | 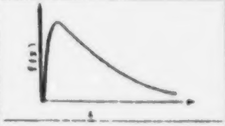 | Geometric mean of values of x, GM.<br>Geometric Standard Deviation of values of x, GSD. | $GM\sqrt{GV}$ | $\sqrt{\frac{GM}{GV(GV-1)}}$<br>$(GV=e^{[\ln(GSD)]^2})$ | which are the product of values or variables | sorption constants for nuclides |
| Triangular | 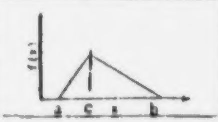 | Lower limit of x, a.<br>Upper limit of x, b.<br>Most likely value of x, c. | $\frac{a+b+c}{3}$ | $\frac{\sqrt{a^2+b^2+c^2-ab-ac-bc}}{\sqrt{18}}$ | for which upper and lower bounds, and most likely value are known or can be guessed | none yet (new option) |
| Beta | see Figure 2.5 | Lower and upper limits of x, a and b.<br>Shape parameters, $\alpha_1$ and $\alpha_2$ | $\frac{\alpha_1}{\alpha_1+\alpha_2}$ | $\frac{\sqrt{\alpha_1\alpha_2}}{(\alpha_1+\alpha_2)\sqrt{\alpha_1+\alpha_2+1}}$<br>(for $x'=(x-a)/(b-a)$) | for which upper and lower bounds, and most likely value are known or can be guessed | none yet (new option) |

with the simulation code SYVAC3 in the CNFWMP. For a distribution like the beta distribution, which can take on many forms, additional background material, such as Figure 2.5, is required.

If asked to provide a correlation coefficient, an expert should get scatterplots of data sets having various correlation coefficients. Figure 2.6 shows broad ranges of correlation coefficients in the categories from "Strong Negative Correlation" to "Strong Positive Correlation". A plot like this is needed by the expert to help him achieve a visual understanding of the possible ranges of correlation coefficients. It should be distributed to each individual being asked to estimate a correlation.

Figure 2.6 serves one other purpose. It reinforces the idea that the correlation coefficient being asked for is a linear correlation coefficient. If the relationship between two parameters is known to be highly nonlinear (e.g. a function with an extreme value of one parameter for middle values of the other, or a function with asymptotic behaviour), then specifying a correlation coefficient is a questionable way of modelling this relationship. A preferable way is to use a functional relationship to capture the nonlinear behaviour. To impose the right degree of uncertainty in the relationship, one or more coefficients in the function can be randomly selected.

In general, the expert needs analytical support in any estimation task with which he is not familiar. If an expert chooses to represent a relationship among variables by an explicit formula, he should get feedback on this formula, preferably in the form of a scatterplot, or contour diagram, or some other visual representation. In the CNFWMP, some experts in the sciences have had difficulty in helping with the modelling process because they are unfamiliar with some mathematical, statistical, or computing aspects of the process. Any assistance that the modeller can render in these areas reaps great benefits in terms of expert assistance, understanding, and support of a model. Unfortunately, depicting functional relationships in a way that can be easily assimilated is difficult when more than two variables are involved. To view functions of only two variables requires three-dimensional plotting facilities. Functions with more variables cannot readily be plotted at all. Nevertheless, any representation of a complicated function can be of assistance, and books such as Bertin's opus on graphics [1983] and Cleveland's recent work [1985] can help to suggest innovative ways of representing multi-variate data.

## 3. What Information to Elicit from an Expert

From the mass of information that an expert can provide about a subject area, the modeller needs basically three things:

- Information about variables;

FIGURE 2.5

## FORMS OF THE BETA DISTRIBUTION PROBABILITY DENSITY FUNCTION

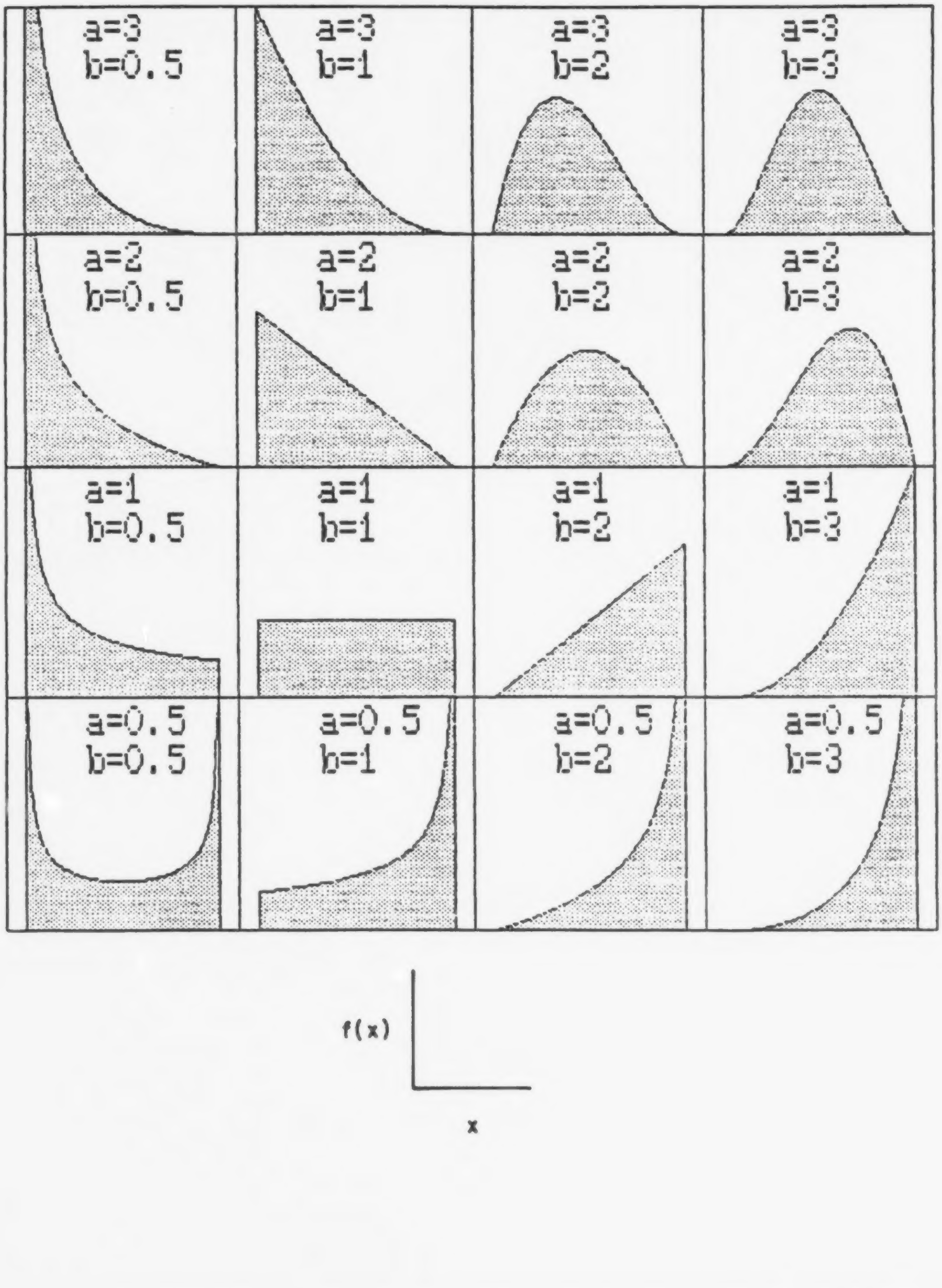

FIGURE 2.6

RANGES OF CORRELATION COEFFICIENTS

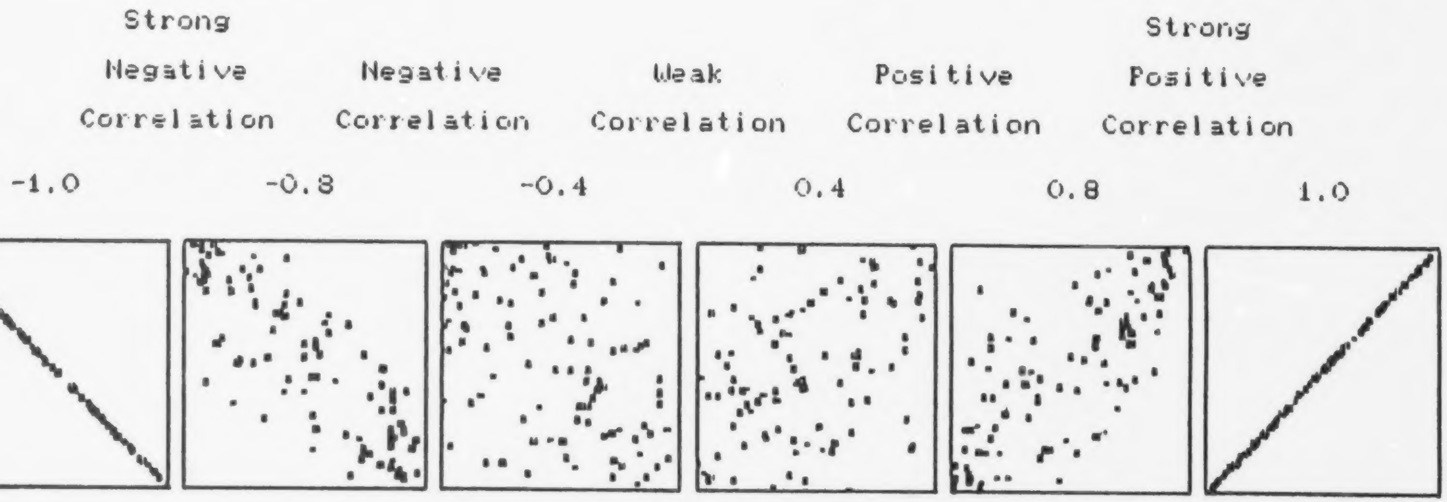

- Information about relationships among variables;
- Critical feedback about the models and data already in use.

Information about variables and relationships are needed to construct a computer simulation model. The information that is needed is just what is mirrored in the dependency diagrams and data dictionary described in Section 2 of this report. The form of this input should provide reviewable documentation of scientific contributions to the development of a model. To meet these objectives, the use of a standard input form is recommended. Forms for collecting information about variables and for collecting information about relationships are discussed in Sections 3.1 and 3.2.

Critical feedback about models and data already in use was included in the list of information items to be elicited because the act of approaching an expert provides an opportunity for peer review. Models and their data are refined and honed by constructive criticism. The earlier this refinement takes place, the less expensive it is to the program. Furthermore, one is likely to get criticism from an expert, whether or not it is requested. It is better from everyone's point of view to plan on receiving this criticism, and dealing with it. A form for the purpose of collecting critical feedback has been provided in Section 3.3.

## 3.1 Eliciting Information About Variables

Figure 3.1 is a copy of a form designed to record data from experts concerning a variable in an assessment model. It is needed to record a thorough description of each variable, as a prerequisite for eliciting information about correlations and functional relationships between variables. A distinction is made between "variables" and "parameters" on this form, following the convention used throughout this paper. Parameters are assigned values outside of a simulation; for example, they may be constants, or sampled from probability distributions. Variables can be parameters, or they can be calculated using the values of other variables. This form can be used to describe both types of variables.

FIGURE 3.1

FACT SHEET
FOR A VARIABLE

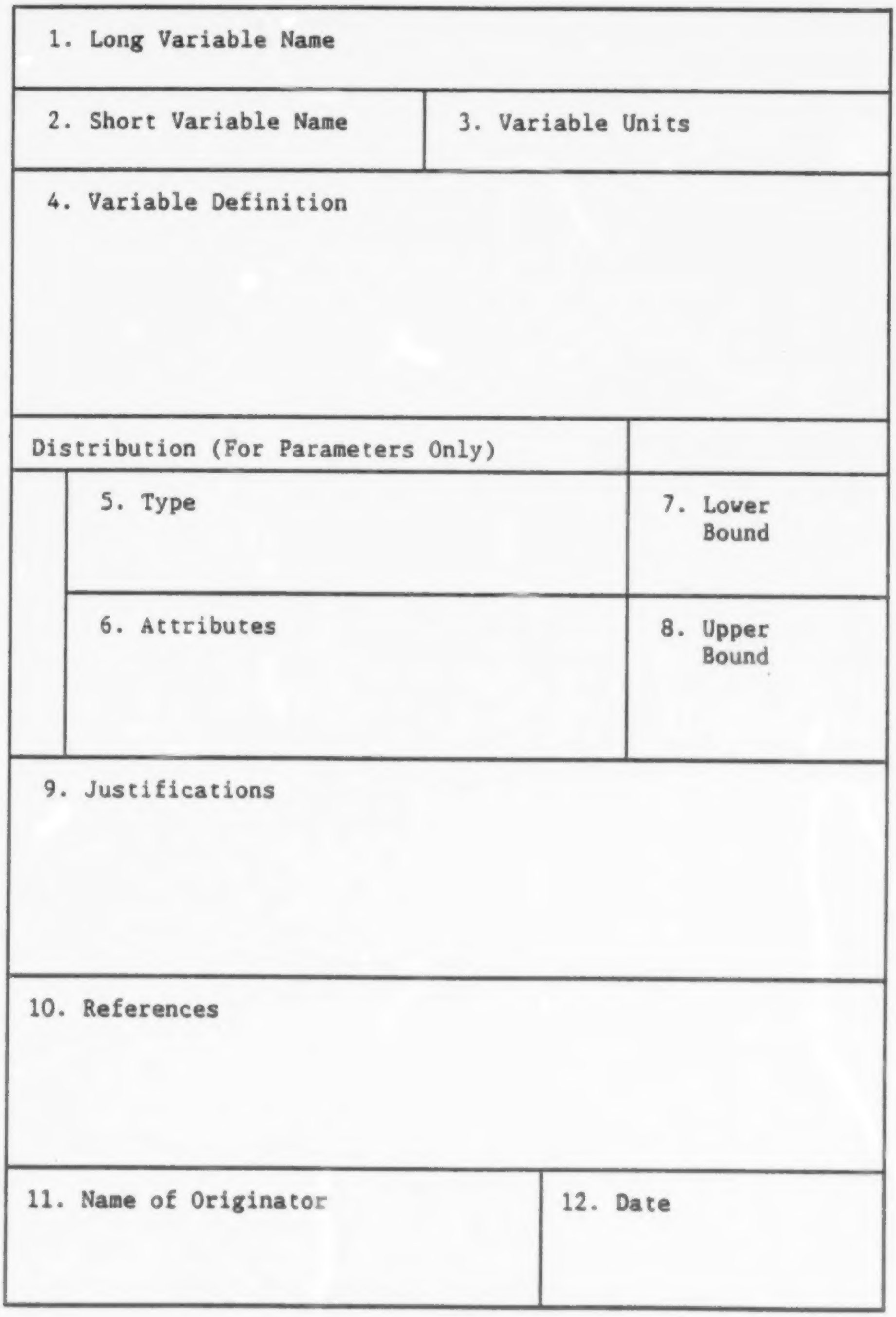

| | |
|---|---|
| 1. Long Variable Name | |
| 2. Short Variable Name | 3. Variable Units |
| 4. Variable Definition | |
| Distribution (For Parameters Only) | |
| 5. Type | 7. Lower Bound |
| 6. Attributes | 8. Upper Bound |
| 9. Justifications | |
| 10. References | |
| 11. Name of Originator | 12. Date |

The form has several fields to be filled in by a modeller or an expert estimating a distribution. The fields are listed below.

(1) Long Variable Name: E.g. Net Precipitation.

(2) Short Variable Name: E.g. NPRCP for Net Precipitation.

(3) Variable Units: E.g. Net Precipitation is measured in m/a (short for metres/year).

(4) Variable Definition: E.g. Net Precipitation is the average annual amount of rain and melted snow (in m**3/m**2) that penetrates at least 10 cm into the soil. Precipitation is averaged spatially over a hypothetical 2 km by 2 km site that constitutes the location of reference man. It is averaged temporally over a 10-year period. [Note: This definition was made up as an example, and bears no connection to the definition of Net Precipitation in SENES (1985c)].

Parameter Distribution Subfields (for parameters only):

(5) Parameter Distribution Type: E.g. uniform, normal, lognormal.

(6) Attributes: what are usually called "parameters of a distribution" (e.g. mean, geometric mean, standard deviation). In this case a different term is used to avoid confusion between "parameter distribution" and "distribution parameters".

(7,8) Lower Bound and Upper Bound: the lowest and highest conceivable values of a parameter. They truncate the range of a distribution. With some distributions, such as the uniform or triangular, they are redundant because they duplicate some of the attributes. Bounds are usually specified in units of the parameter (e.g. m/a for Net Precipitation).

(9) Justifications: for introducing this variable, and for the choice of distribution, if a parameter. The intent of this field is that the motivation for the input can be retrieved for reappraisal at a later time.

(10) References: to papers or books where related variables have been described, or where data has been published.

(11) Name of Originator: name of the expert or modeller providing the information.

(12) Date: of submission of the completed form.

Several forms like this may be filled in for one variable. They may capture the opinions of several experts, or opinions about the distribution of the variable at several sites, or successive interpretations of a variable over an extended period of time. These forms should be collected and kept together as part of a reviewable record of the development of a model.

## 3.2 Eliciting Information About Variable Relationships

Figure 3.2 is a copy of a form designed to record data from experts concerning relationships among variables in an assessment model. These relationships can be functional relationships or parameter correlations. The expert is therefore encouraged to use the appropriate type of relationship for a set of variables. He is not restricted just to correlations.

Certain assumptions about correlations and functional relationships have been used in designing this form, and they are reflected in the choice of fields on the form. It is recommended that these assumptions be adopted in assessing uranium tailings sites, because of the advantages they confer.

The first assumption is that correlation coefficients are sampled parameters. This assumption has been made for two reasons. First, the value of a correlation coefficient will in most cases not be known accurately, especially if it is estimated from expert opinion. Even if a correlation coefficient is estimated from field and laboratory data, it is unlikely that field and laboratory conditions will match those at a tailings site over extended spatial areas and extended periods of time. Use of a single point estimate is therefore not appropriate. Second, as argued in Andres and Goodwin [1985], one aim of modelling should be to change correlations into explicit functional relationships. By sampling correlation coefficients, one can include them in sensitivity analysis and identify those correlations that should be modelled explicitly because of their importance.

The second assumption is that functional relationships can have a residual error. In both the CNFWMP, and Phases I and II of the NUTP assessment contract, the practice has been to assume that functional relationships are exact. That is, if variable $X = A/B$, where A and B are sampled parameters, then this relationship is exact, and all the variability in X comes from variability in A and B. Yet it is known that in a complicated system such exactness in unusual; it is more typical to plot X against A/B and to find a residual scatter, as in the scatter plots of Figure 2.6. In part, this scatter represents limitations and inaccuracies of measurements. It can also represent the effects of experimental conditions that are not tightly controlled. Unfortunately, in a complex natural system, very few conditions can be tightly controlled, or even accurately estimated. Hence a better representation of the relationship is one of the following expressions:

## FIGURE 3.2

## FACT SHEET FOR A VARIABLE RELATIONSHIP

Long Variable Name (Short Variable Name)

1.

2.

3.

4.

5.

Case 1: Correlation Coefficient(s)

6. Point Estimate:

Circle Number(s) of Selected Range(s):

| | | | | |
|---|---|---|---|---|
| 7. Strong Negative | 8. Negative | 9. Weakly Correlated | 10. Positive | 11. Strong Positive |

-1 -0.8 -0.4 0.4 0.8 1

Case 2: Functional Relationship

12. Nature of relationship

Select Type of Residual e

13. $Z = f(X,Y,\ldots)(1 + e)$

14. $Z = f(X,Y,\ldots)^{(1 + e)}$

15. Other (explain)

Distribution of Residual e

16. Type

18. Lower Bound

17. Attributes

19. Upper Bound

20. Justifications and References

21. Name of Originator

22. Date

$X = (A/B)(1 + e)$ if sign(X) can be - or +, or

$X = (A/B)^{(1 + e)}$ if sign(X) can only be +,

where e is a [dimensionless] residual error, typically sampled from a normal distribution with mean 0 and standard deviation <<1. As an example, Kleijnen's technique for sampling correlated parameters automatically converts a correlation between two variables into a linear relationship of the first type, with normally-distributed residual [Andres and Goodwin, 1985].

Three advantages of including the residual error are:

- a modeller can include in the model an approximate relationship that is known to explain only part of the variability in a calculated result, without artificially decreasing the variability of the result;
- sensitivity analysis on the residual can determine how important it is to refine the functional relationship;
- variability analysis on X can determine whether it is worthwhile to include a functional relationship in a model. In the example above, if the variability of X after expressing it in terms of A, B and e exceeds the variability of X expressed as a sampled parameter, sampling X may be preferable to calculating it. Without some constraint like this one, the number of parameters in a model tends to grow over time until some bottleneck in computer resources throttles further growth.

The form for recording relationships has been based on these assumptions. It has several fields to be filled in by the expert. They are listed below.

(1-5) Long Variable Name (Short Variable Name) means that for each variable in the relationship, the Long Variable Name will be written, followed by the Short Variable Name in brackets. These names are both unique identifiers given to a variable, as specified on its variable fact sheet. E.g. Net Precipitation (NPRCP). Space is provided on the form for five variables. If more are involved, names of the others can be written on another form.

(6) Point Estimate of Correlation Coefficient is a single best estimate of the correlation coefficient between two specified parameters. (See section 4.1 for a discussion of correlations among more than two parameters.) This estimate lies in the interval [-1,1]. A correlation coefficient of 0 means linearly uncorrelated data. A point estimate may be determined from correlation studies of research data. If a range is specified as well (fields 7 - 11), then it is recommended that the point estimate be taken as the mode of a triangular distribution that describes the correlation coefficient. For example, in the Phase II study [SENES, 1985a], FDEPSF(1) and FDEPSF(2) are the "Fraction of Total Deposition Retained on Vegetation" for "Lichens" and "Pasture Grass" respectively. An expert may state

"Lichens" and "Pasture Grass" respectively. An expert may state from his knowledge of the two plants that FDEPSF(1) and FDEPSF(2) have a strong positive correlation, and he may have data that justifies a point estimate of 0.92.

(7-11) Ranges for a Correlation Coefficient are a set of ranges in which a linear correlation coefficient could lie. Each one is given a definition in words (e.g. Weak Positive, Uncorrelated), and is supported by a figure. Figure 2.6 is intended to be shown to an expert to guide him in his choice. It depicts each range with a pair of scatterplots representing the two ends of the range. An expert may choose a range that spans one or more of the indicated ranges. For example, he may know that FDEPSF(1) and FDEPSF(2) (mentioned in (6)) are positively correlated, but not whether the correlation is strong or weak. In that case, the appropriate choice consists of the two ranges (10) and (11), spanning correlation coefficients from 0.4 to 1.0. A choice of the central range (9) means that two variables have a weak correlation that is unlikely to affect simulation results. A choice of all ranges (7-11) means that the degree of correlation is completely unknown.

Where a range is specified, the correlation coefficient is assumed to have a triangular distribution, with endpoints of the distribution being the endpoints of the chosen range. If a point estimate is made, it is used as the mode of the distribution. Otherwise, the midpoint of the range is used as the mode.

(12) Nature of Relationship allows an expert or modeller to specify a relationship assumed to hold between two or more variables. Typically a relationship will be expressed as a formula, or as an implicit or differential equation to be solved. Where this field provides insufficient space for a complicated relationship, a reference can be made to an attached sheet, or published writeup.

Types of Residuals

(13) Additive: $Z = f(X,Y,\ldots)\,(1 + e)$. This additive residual is appropriate if Z is permitted to take on positive and negative values.

(14) Multiplicative: $Z = f(X,Y,\ldots)^{(1 + e)}$. This multiplicative residual is appropriate if Z can take on only positive values.

(15) Other: For example, $Z = f(X,Y) + e$, which is an additive residual with physical units. Another choice that has been widely used in the past is "None".

Distribution of Residual e

(16) Type: E.g. normal, lognormal, beta, uniform.

(17) Attributes: E.g. mean, geometric mean, standard deviation.

(18) Lower Bound: Lowest allowed value of e (typically -1).

(19) Upper Bound: Greatest allowed value of e.

(20) Justifications and References: Except for very simple correlations and functional relationships, this field will usually be filled in with a reference to an attached sheet or published writeup.

(21) Name of Originator: Name of the expert or modeller who filled out the form.

(22) Date: Date the form was filled out.

## 3.3 Critical Feedback Form

Scientific progress is based on the scientific method, in which theories and models of the world are vigorously tested to reveal their flaws [Popper, 1965]. Theories that are invalid are eventually disproved and rejected. Scientists are left with theories that have been tested and not rejected. The quality of a theory is related to the number of stringent tests that it has faced without rejection.

System models like those used for uranium mill tailings sites also improve through rigorous testing. However they are difficult to test. Comparison with experimental data is often inconclusive because complex models have so many variables and processes that they can represent a wide range of behaviour, and so are difficult to reject. Furthermore, a model of a generic site like the models developed in Phase II and Phase III cannot be tested directly against the real world, for there is no part of the real world quite like the generic site. Even models of a specific site, which avoid some of these difficulties, are difficult to test over time scales of hundreds of years, which is the range of their application.

One powerful way of testing system models so that they can be improved is to expose them to experts who can criticize them on the basis of wide-ranging knowledge and experience. To get the best possible model, such criticism should be sought wherever it can be found. It should be sought preferably at an early stage when the model can be changed easily to correct flaws.

Figure 3.3 is a form designed to collect constructive criticism about models and data to be used in assessment. It should be distributed whenever expert input is sought. The structure of the form is based on the PMI (Plus, Minus, Interesting) approach to soliciting feedback, espoused by Edward de Bono [1976], in which the respondent is asked for positive, negative and interesting comments.

This form is self-explanatory, and needs no detailed comment on the fields.

FIGURE 3.3

## CRITICAL FEEDBACK FORM

| | |
|---|---|
| 1. Models/Data Reviewed | |
| 2. Positive Comments | |
| 3. Negative Comments | |
| 4. Other Comments | |
| 5. Name of Reviewer | 6. Date |

### 3.4 Review of the Expert's Submission

Just as it is important for the expert to review the model and data, it is also important for the modeller to review the expert's submission. Putting the submission into the form of dependency diagram and data dictionary entry, as in Section 2, helps to make the modeller familiar with all aspects of the expert's submission. It also reminds the modeller to perform the following checks:

(1) Completeness. Are all variables defined and given units?

(2) Dimensional Correctness. Are units proper SI units? Is every formula or equation dimensionally consistent?

(3) Consistency. Are there any circular dependencies, such as A depends on B which depends on A?

(4) Feasibility. Can the correlations suggested by the expert be implemented using the tools available?

## 4. Special Cases

The preceding general approach to identifying correlations among variables will work with individual well-defined parameters that may be correlated in pairs. There are other special cases where this approach may be more difficult to apply. The aim of this section is to point out where difficulties can arise, and to describe the nature of the problem. The following cases are discussed:

- Correlations between models;
- Multiple correlated parameters;
- Effects of averaging;
- Correlations of time-varying parameters.

### 4.1 Correlations Between Models

If a system model is partitioned into submodels (e.g. water source and radon source models), then some correlations may link parameters in one submodel with parameters in another. For example, chemical parameters may be correlated with net precipitation. This situation can cause difficulties that are usually managerial in nature. For example, if development of two submodels has been assigned to different teams, who is responsible for shared parameters and for intermodel correlations? If data in an input file is organized by model, then where do shared parameters and intermodel correlations go? Such questions cannot always be avoided, because nature itself does not neatly subdivide the world. The modeller should plan on dealing with them.

One general approach is to repartition the system model so that correlated parameters are always within the same submodel. In the CNFWMP, it was found necessary to separate hydrogeological parameters from the geosphere transport model because they were used to calculate groundwater flow in the vault model as well as the geosphere model. In this case, rather than have links between vault and geosphere, we decided to define a set of parameters upon which both models depend. Similarly, in implementing the Phase II UTAP model in SYVAC3 (Goodwin and Andres, 1986), it was found to be useful to repartition the model for simpler data flow. That is, the partitioning of the UTAP model that was most useful for development was found not to be so useful for implementing the model in a computer program.

The lesson here is that partitioning of a model into smaller models, while useful at an early stage in model development, cannot be done optimally until model development is complete. Therefore provisions should be made for repartitioning when it becomes necessary.

Another option is to support correlations between parameters in separate submodels. This approach may be necessary if many correlations are defined and used, since a satisfactory partitioning may be impossible to find. A good basis for this approach is a single global data dictionary that is used by all modellers no matter what model they are working on. Having a single data dictionary helps to ensure that all models using a parameter incorporate the same parameter definition, units, distribution, etc. This degree of unity is valuable to a project because it helps to avoid interface errors, a particularly pernicious and hard-to-find class of problems that can beset a model implementation.

If both of these approaches - repartitioning and support for intermodel correlations - are used, then a flexible approach can be taken whatever the situation that arises.

## 4.2 Multiple Correlated Parameters

A case of this type arose after the first concept assessment of nuclear fuel waste disposal in the CNFWMP [Wuschke et al, 1981]. The biosphere model in that assessment used four dose/concentration ratios for terrestrial and aquatic food chains for each of about 35 nuclides. These parameters were all input into the SYVAC computer code as constants, and so the treatment of these parameters was too crude to be concerned with correlations.

For the second concept assessment it was decided to sample these dose/concentration ratios (and others) from probability distributions. The model LIMCAL was developed to evaluate the ratios and derive distributions for them [Zach, 1982]. The problem then arose that hundreds of sampled SYVAC parameters would be correlated, because they were calculated in a computer program from a common set of LIMCAL parameters.

Rather than try to resolve all these correlations and generate a positive semi-definite correlation matrix, it was decided to incorporate the entire LIMCAL model into SYVAC2, and to calculate dose/conversion ratios internally. The merger was successfully made, leaving only a handful of remaining correlations (e.g. Man's Drinking Water Consumption Rate with Man's Total Energy Intake Rate) [Wuschke et al, 1985].

It is recommended that in assessing uranium tailings sites, similar efforts be made to avoid correlations among sets of more than two parameters. When a set is identified that has more than two correlated parameters, identify some parameters as basic, and express the rest in terms of the basic parameters. The basic parameters themselves should have no correlated sets with more than two variables. In some cases the evidence for the functional relationship used may be rather poor. Then it is important to characterize the residual scatter, as described in Section 3.2., to ensure that the result has an appropriate amount of variability.

If correlations among sets of more than two parameters are supported, then the difficult problem of estimating correlation coefficients arises. Another problem arises if correlation coefficients are sampled as recommended above. If they are sampled independently, they may violate the requirement that a correlation matrix be positive semi-definite [Andres and Goodwin, 1985].

### 4.3 Effects of Averaging

Averaging of spatially or temporally distributed parameter values simplifies system model calculations. However, it can also have unpredictable effects on parameter correlations.

In system models, the effort to simplify a system often leads to the use of "bulk" or "lumped" or "averaged" parameters. For example, a heterogeneous region with several different soil thicknesses, and perhaps several types of soil, may be approximated by a homogeneous soil compartment with one soil thickness and one set of soil properties. This approximation is justified on the basis that for estimating dose to man, the simplified homogeneous region behaves much like the heterogeneous one. If the region is a field of grain, for instance, the grain reaped from the whole region is mixed together, and ground up together before use, so that heterogeneous properties are lost. If there are radioactive nuclides in the flour, they will be mixed throughout in a consistent average ratio.

Averaging may be over time, rather than over space. For example, rainfall conditions one year may lead to more rapid transport of radionuclides in surface water than in another year. If the transport from source to reference man is a multi-year process, however, annual fluctuations tend to cancel out and lead to an average transport rate.

Use of averaged parameters can mislead the expert who estimates a correlation coefficient. In the soil case an expert may observe soil density to be strongly correlated with soil depth. Over an entire region, however, average soil density may not be so strongly correlated with average soil depth. Similarly, an observed correlation between annual statistics for rainfall and crop yield may not apply to ten-year averages of rainfall and crop yield.

Researchers do not generally have access to bulk or averaged properties from the field. Rather they tend to be familiar with small samples taken at isolated points in space and time. It is therefore important in preparing an expert who is to give an estimate of correlations (or functional relationships) that the potential effects of averaging be pointed out. Furthermore the definition of each variable should explicitly state what averaging, if any, is involved.

### 4.4 Correlations of Parameters Varying in Time and Space

The Phase II assessment report [SENES, 1985a] discusses the role of temporal and spatial dependence in assessment results. To determine the effects of time-dependence, parameters were resampled several times during some simulations. This case is the opposite of the previous one, where heterogeneity was masked by averaging. If spatial and temporal variation are explicitly modelled, then new problems of correlation arise.

The first new consideration is autocorrelation. One tends to expect physical properties to vary smoothly in time and space. Over a large field, one can expect the soil depth and soil density to change gradually from one place to another. One can predict the weather from day to day in a fairly reliable way by stating: "Tomorrow will be just like today." Autocorrelation is a statistical way of describing how a system with property f(t) [or f(x) for spatial variation] changes with time [or space]. It is defined as the correlation of f(t) and $f(t+t_L)$, where $t_L$ is the lag of the autocorrelation.

One way of dealing with autocorrelation is to have an expert identify the lag required for the autocorrelation to approach zero. For example, soil samples taken one metre apart are likely similar. In some regions, soil samples taken 1000 metres apart are uncorrelated. Similarly, rainfall on two successive days is likely related. Rainfall on two days that are three weeks apart may be uncorrelated. If some lag can be identified, beyond which autocorrelation is effectively zero, then parameter values can be resampled at intervals greater than the required lag without worrying about autocorrelation. So correlations of a variable with itself can be dealt with, at least in principle.

Dealing with multi-variate correlations of temporally or spatially dependent parameters is a more demanding task. According to Bras and Rodriguez-Iturbe [1985], "The most serious computational difficulty [in multivariate time-series analysis] is parameter estimation. The quantities of data required for adequate parameter estimation in a multivariate model can be unmanageable. The mathematics of sophisticated estimation procedures also becomes burdensome." It is therefore recommended that multi-variate correlations of temporally or spatially dependent parameters be avoided in system assessment models.

## 5. Conclusions

This paper has described an integrated approach to identifying correlations and other variable relationships, based on assimilation of expert opinion. The paper has provided guidelines for what information should be presented to experts to prepare them for the information-gathering task. Three types of input forms have been presented, to standardize expert input and to generate reviewable records of the information submitted. In addition some special cases that could cause difficulty have been described. Taken together, these components form a workable approach to identifying correlations and other variable relationships that can be readily adapted to a system modelling context.

## References

Andres, T.H. and B.W. Goodwin, 1985. Techniques for handling correlated parameters; in [SENES, 1985b].

Bertin, Jacques, (translated by William J. Berg), 1983. Semiology of graphics; The University of Wisconsin Press, Madison, Wisconsin.

Bras, R.L. and I. Rodriguez-Iturbe, 1985. Random functions and hydrology; Addison-Wesley Publishing Company, Don Mills, Ontario, p. 91.

Cleveland, William S., 1985. The elements of graphing data; Wadsworth Advanced Books and Software, Monterey, California.

CSA, 1979. Canadian metric practice guide; CAN3-Z234.1-79, Canadian Standards Association, 178 Rexdale Boulevard, Rexdale, Ontario.

de Bono, Edward, 1976. Teaching Thinking; Penguin Books Canada Ltd., Markham, Ontario L3R 1B4.

DeMarco, Tom, 1979. Structured analysis and system specification; YOURDON, inc., New York.

Gane, Chris, and Trish Sarson, 1979. Structured systems analysis: Tools and techniques; Prentice-Hall, Inc., Englewood Cliffs, New Jersey.

Goodwin, B.W. and T.H. Andres, 1986. Comparison of the probabilistic systems assessment codes, UTAP and SYVAC3, applied to the long-term assessment of uranium mill tailings in Canada; prepared for the National Uranium Tailings Program, Canada Centre for Mineral and Energy Technology, Energy, Mines and Resources Canada, DSS File #15SQ.23317-5-1720.

Hoffman, Karen J., Terry H. Andres, and J.A. Keith Reid, 1984. Experience in the application of quality assurance techniques to a scientific simulation code; Proceedings of the 1984 Summer Computer Simulation Conference, Boston, Massachusetts, 1984-July-23 to 25.

Orr, Ken, 1981. Structured requirements definition; Ken Orr and Associates, Inc., Topeka, KS 66607.

Page-Jones, Meilir, 1980. The practical guide to structured systems design; YOURDON inc., New York.

Popper, Karl, 1965. Conjectures and refutations: The growth of scientific knowledge; Harper Torchbooks, New York.

SENES, 1985a. Probabilistic model development for the assessment of the long-term effects of uranium mill tailings in Canada - Phase II, Volume 1 - Main report; DSS file #26SQ.23241-4- 1693, Contract #0SQ84-00207.

SENES, 1985b. Probabilistic model development for the assessment of the long-term effects of uranium mill tailings in Canada - Phase II, Volume 2 - Workshop notes and topical discussion papers, DSS file #26SQ.23241-4-1693, Contract #0SQ84-00207.

SENES, 1985c. Probabilistic model development for the assessment of the long-term effects of uranium mill tailings in Canada - Phase II, Volume 3 - Probabilistic analysis user's manual and documentation for the uranium tailings assessment program (UTAP); DSS file #26SQ.23241-4-1693, Contract #0SQ84-00207.

Smith, Henry C., 1985. Database design: Composing fully normalized tables from a rigorous dependency diagram; Communications of the ACM, August, 28(8), pp. 826-38.

Wolfe, Alexander, 1985-Nov-4. Bringing order out of chaos in software design; Electronics, 58(44), pp. 30-34.

Wuschke, D.M., K.K. Mehta, K.W. Dormuth, T. Andres, G.R. Sherman, E.L.J. Rosinger, B.W. Goodwin, J.A.K. Reid, and R.B. Lyon, 1981-September. Environmental and safety assessment studies for nuclear fuel waste management - Volume 3: Post-closure assessment; Atomic Energy of Canada Limited technical record, TR-127-3.

Wuschke, D.M., P.A. Gillespie, K.K. Mehta, W.F. Heinrich, D.M. LeNeveu, V.M. Guvanasen, G.R. Sherman, D.C. Donahue, B.W. Goodwin, T.H. Andres, R.B. Lyon, 1985-September. Second interim assessment of the Canadian concept for nuclear fuel waste disposal -- Volume 4: Post- closure assessment; Atomic Energy of Canada Limited Report, AECL-8373-4.

Zach, R., 1982. LIMCAL: A comprehensive food chain model for predicting radiation exposure to man in long-term nuclear waste management, Atomic Energy of Canada Limited Report, AECL-6827.

## Appendix A: Data Dictionary Excerpt

ATAIL: Exposed Tailings Surface Area [$m^2$] is the area of the surface of the tailings pile exposed to the atmosphere. It is sampled from the following distribution:

Constant($5x10^5$)

DEPTH1: Thickness of Upper Unsaturated Zone [m] is the depth of the gypsum-depleted zone of the unsaturated soil layer. It changes with time as water transports gypsum from the upper to the lower zone. DEPTH1 is calculated from equations described in the water source model (Appendix A of SENES [1985c]).

DEPTH2: Thickness of Lower Unsaturated Zone [m] is the depth of the gypsum-enriched zone of the unsaturated soil layer. It changes with time as water transports gypsum from the upper to the lower zone. DEPTH2 is calculated from equations described in the water source model (Appendix A of SENES [1985c]).

DIFLEN: Radon Diffusion Pathlength [m] is the mean distance that radon diffuses in tailings before decay. It is averaged over the effective area of the tailings and over the depth of the unsaturated layer. DIFLEN is calculated from the formula:

$$\mathrm{DIFLEN} = \left[ \frac{\mathrm{RNLAM*TVOID}}{\mathrm{EBKDFC}} \right]^{1/2}$$

DIMDP1: Dimensionless Depth of Upper Zone [] is the thickness of the gypsum-depleted zone expressed in multiples of the diffusion path length for radon. It changes with time. It is averaged over the effective area of the tailings. DIMDP1 is calculated from the following formula:

DIMDP1 = DEPTH1/DIFLEN

DIMDP2: Dimensionless Depth of Lower Zone [] is the thickness of the gypsum-enriched zone expressed in multiples of the diffusion path length for radon. It changes with time. It is averaged over the effective area of the tailings. DIMDP2 is calculated from the following formula:

DIMDP2 = DEPTH2/DIFLEN

EBKDFC: Radon Diffusion Coefficient [m$^2$ s$^{-1}$] is the effective bulk radon diffusion coefficient assumed to apply in both zones of the unsaturated layer of the tailings. It is averaged over the effective area of the tailings and over the depth of the unsaturated zone. It is calculted from the relationship:

$$\mathrm{EBKDFC} = 0.106\mathrm{x}10^{-4} * \mathrm{TVOID} * \exp(-0.26*\mathrm{MPCH2O})$$

EMANAT: Radon Emanation Coefficient [0-1] expresses the proportion of radon in the unsaturated layer within transport distance of the tailings surface that is actually observed to enter the atmosphere. It is averaged over the effective area of the tailings and over the depth of the unsaturated layer. EMANAT is sampled from the following distribution:

Triangular(0.02, 0.2, 0.9).

EMRATE(Rn): Emission Rate of Rn from Source [Bq s$^{-1}$] is the rate of release of radon from the total area of the tailings to the atmosphere via diffusion. No reduction due to freezing weather and snow cover is assumed. A uniform flux from all over the tailings is assumed. EMRATE(Rn) is calculated from the expression:

$$\mathrm{EMRATE(Rn)} = \mathrm{FLUX} * \mathrm{ATAIL}$$

EMRT1: Radon Emanation Rate of Upper Zone [Bq m$^{-3}$ s$^{-1}$] is the rate per unit volume at which radon emanates from the gypsum-depleted zone of the unsaturated layer. It changes with time. It is averaged over the effective area of the tailings, and over the depth of the upper zone. EMRT1 is calculated from the following formula:

$$\mathrm{EMRT1} = \mathrm{RACON1} * \mathrm{RNLAM} * \mathrm{EMANAT}$$

EMRT2: Radon Emanation Rate of Lower Zone [Bq m$^{-3}$ s$^{-1}$] is the rate per unit volume at which radon emanates from the gypsum-enriched zone of the unsaturated layer. It changes with time. It is averaged over the effective area of the tailings, and over the depth of the upper zone. EMRT2 is calculated from the following formula:

$$\mathrm{EMRT2} = \mathrm{RACON2} * \mathrm{RNLAM} * \mathrm{EMANAT}$$

FLUX: Radon Flux [Bq s$^{-1}$ m$^{-2}$] is the rate of emission of radon from tailings per unit area. It changes with time. It is averaged over the effective area of the tailings. FLUX is calculated from the following expression:

$$\mathrm{FLUX} = \Bigg[ [\; - \frac{[1+\coth(\mathrm{DIMDP2})]*\mathrm{EMRT1}*\exp(\mathrm{DIMDP1})+\mathrm{EMRT1}-\mathrm{EMRT2}}{\cosh(\mathrm{DIMDP1}) * [\tanh(\mathrm{DIMDP1})+\coth(\mathrm{DIMDP2})]} - \mathrm{EMRT1} \Bigg] * \mathrm{DIFLEN}$$

MPCH2O: Percent Moisture Content [%] is the percentage of tailings weight made up by water. It is assumed to apply in both zones of the unsaturated layer of the tailings. It is averaged over the effective area of the tailings and over the depth of the unsaturated zone. MPCH2O is sampled from the distribution:

Triangular(5, 15, 25)

RACON1: Radium Concentration in Upper Unsaturated Zone [Bq $g^{-1}$] is the soil concentration of radium in the gypsum-depleted zone of the unsaturated layer. It is averaged over the effective area of the tailings and over the depth of this zone. RACON1 is calculated from equations described in the water source model (Appendix A of SENES [1985c]).

RACON2: Radium Concentration in Lower Unsaturated Zone [Bq $g^{-1}$] is the soil concentration of radium in the gypsum-enriched zone of the unsaturated layer. It is averaged over the effective area of the tailings and over the depth of this zone. It is calculated from equations described in the water source model (Appendix A of SENES [1985c]).

RNLAM: Radon Decay Constant [$s^{-1}$] is the rate at which Rn-222 decays. It is sampled from the distribution:

Constant($2.1x10^{-6}$)

TVOID: Porosity of Tailings [$m^3/m^3$] is the connected porosity of tailings available for water flow. It is assumed to apply in both zones of the unsaturated layer of the tailings. It is averaged over the effective area of the tailings and over the depth of the unsaturated zone. TVOID is sampled from the distribution:

Triangular(0.35, 0.40, 0.45)

# APPENDIX I

# AN EXAMINATION OF PARAMETER CORRELATION IN THE RADON SOURCE TERM MODEL

D.B. Chambers, D.T. Ellenor, L.M. Lowe and M.L. Murray
SENES Consultants Limited

June 1986

## ABSTRACT

In this paper we investigate the Phase III radon source model in an attempt to apply the techniques outlined by Andres in Appendix H to identify dependencies among input parameters. In addition, the effects of introducing correlation among parameters in the radon source model are investigated.

# AN EXAMINATION OF PARAMETER CORRELATION IN THE RADON SOURCE TERM MODEL

## I.1 INTRODUCTION

In a previous study, Andres and Goodwin (SENES 1985, Volume 2) examined various techniques to enforce correlations among parameters which are being used as inputs to a modelling exercise. In practice, it is not always easy to identify where correlations exist or how strong they are. The preferred approach would be to observe correlations and dependencies in experimental data. However, research programs to obtain the experimental data for such an analysis may not be possible for cost or other reasons. For example, in the case of uranium mill tailings the period of interest may be tens to hundreds of years into the future. Experiments over such a time frame are simply not possible. Thus, in many situations of practical interest, it is necessary to rely on the opinions of knowledgeable persons to identify where parameter correlations may exist and, if they are believed to exist, how strong they are.

In the most general sense, correlation exists when there is a relationship between two variables. The correlation coefficient is a measure of the strength of the (linear) relationship between two variables. The correlation coefficient always lies between +1 and -1, either value indicating there is an exact linear relationship between the variables. Positive values of the correlation coefficient indicate a tendency for the two variables to increase together. Negative values indicate that large values of one variable are associated with small values of the other variable. A correlation coefficient of zero means there is no relationship between the variables.

Given that the inclusion of known correlations between model parameters is required for a long-term assessment, methods are needed for identifying and characterizing correlations. The problems in developing such methods are partly objectives or scientific (how to measure correlations in the field) and partly subjective (how to question experts to obtain consistent and unbiased information about correlations expected). The scientific problems can be tackled by carefully-designed research programs, involving the simultaneous measurement of a number of variables. When the correlations are a matter of theory or expert opinion, rather than experimental data, care must be taken in eliciting this information (Appendix H).

As noted above, several techniques for enforcing parameter correlation were examined in the Phase II report (SENES, 1985). Because of these investigations, two techniques for incorporating parameter correlation were adopted for Phase III.

First, where the form of a relationship between parameters is known or suspected, a functional relationship was considered to be the preferred way to express the dependency. A functional relationship is a formula that expresses one parameter as an explicit function of other, more basic, parameters. One of the benefits of developing functional relationships among parameters is the opportunity provided to put components of the model to experimental test. It is much easier to generate evidence to reject a faulty relationship than it is to reject a correlation coefficient.

Second, for situations where correlation is believed to exist but where it is not possible to establish functional relations, a technique developed by Kleijnen (1974) for enforcing pair-wise correlation was selected for use. This technique achieves uniqueness in generating a sample from a pair of correlated variables by preserving the entire distribution of one variable, the mean and variance of the second variable, and the correlation coefficient between the two.

In Appendix H, Andres outlines a systematic approach toward identifying parameter dependencies and correlations using expert opinion. In this appendix the Phase III radon source model is used in a trial application of Andres' technique. In addition, the effect of introducing correlated parameters into the radon source model is examined.

## I.2 INFORMATION NEEDED TO IDENTIFY DEPENDENCES

### I.2.1 The Phase III Radon Source Model

The model used in this Phase III study to simulate the release of radon from the tailings surface is described in Chapter 4 of Volume 3. In brief, the tailings are modelled as a multi-layered system: an upper, unsaturated layer in which the radium concentration is a function of depth, and a lower, saturated layer. The layers are subdivided into various zones as required for the water source term model.

The saturated layer is not a source of radon that can reach the tailings surface since the water effectively prevents its diffusion; the diffusion length of radon in the water-filled pores of the tailings is orders of magnitude less than the diffusion length in the unsaturated pores. The unsaturated layer is subdivided into two zones: an upper, radium-depleted zone and a lower, radium-enriched zone. The depth of the interface of the two zones depends on the chemistry of the tailings. This depth changes with time (over tens of years) until the entire unsaturated layer is depleted of radium.

In terms of radon release to the atmosphere, each of these zones is considered to be homogeneous, with each zone characterized by an average radium concentration, moisture content, porosity, density and radon emanation coefficient.

The parameters and variables involved in the calculation of the radon source term are given in Table I.1.

The mathematical representation of the radon source model and the rationale for parameter values shown in Table I.1 are given in Chapter 4 of Volume 3.

### I.2.2 Dependency Diagram

Figure I.1 is a dependency diagram showing the radon source model from the Phase III assessment. Each elliptical bubble in Figure I.1 represents one of the calculated variables in the model. Each rectangle represents a parameter, either sampled or constant. Solid arrows among the bubbles and rectangles represent functional relationships. For example, the arrow from the sampled parameter EMANAT, the emanation coefficient, shows that EMANAT is used in the calculation of the summer radon flux.

Correlations hypothesized by study team members are shown as dashed lines between rectangles. The direction of the arrows on the dashed lines indicate causal relationships. For example the dashed arrow from porosity (POROS) to moisture (MPCH2O) indicates that these two parameters are correlated and that in the relationship between them, POROS is the independent variable and MPCH2O is the dependent variable.

Correlations between parameters in the radon source model and parameters in other component models are not considered in this example. One possible example of such a correlation is the possible association between net precipitation and moisture content.

### I.2.3 Model Data Dictionary

The Phase III radon source model has already been described in general terms in Section I.2.1. More detailed descriptions of the source model, its mathematical formulation and its input parameters are given in Chapter 4 of Volume 3. However, to assist in reading this appendix, a text description, for those parameters among which correlations have been hypothesized is provided in Table I.2.

Table I.1

### Radon Source Term Model Variables

| Model Symbol | Description | Units | Nominal Value | Probabilistic* Value | Computer Source | Computer Symbol |
|---|---|---|---|---|---|---|
| a | reciprocal of radon diffusion length in tailings | $m^{-1}$ | calculated | calculated | RADON | DIFLEN |
| D | effective bulk radon diffusion coefficient of tailings | $m^2.s^{-1}$ | calculated | calculated | RADON | EBKDFC |
| E | radon emanation coefficient of tailings | - | 0.2 | T(0.02, 0.2, 0.9) | INPUT | EMANAT |
| $J_T(t)$ | radon flux | $Bq.s^{-1}$ | calculated | calculated | RADON | EMRATE(5) |
| R | winter/summer flux ratio | - | 0.02 | LN(0.02,2.0, 0.002,0.2) | INPUT | WTSFLX |
| M | moisture content by weight of tailings | % | 15.0 | T(5.0,15.0,25.0) | INPUT | MPCH2O |
| P | porosity of tailings | - | 0.4 | T(0.35, 0.4, 0.45) | INPUT | POROS |
| $(Ra)_i(t)$ | radium concentration of zone i = 1 or 2 | $Bq.m^{-3}$ | calculated | initialized then calculated | SOURCE | CONC(4,i,3) i=1,2** |
| $x_1(t)$ | thickness of $BaSO_4$ depleted zone | m | calculated | calculated | SOURCE | DBAR(3) |
| $x_2(t)$ | thickness of $BaSO_4$ enriched zone | m | calculated | calculated | RADON | EBAR(3) |
| $\lambda$ | radon decay constant | $s^{-1}$ | $2.1 \times 10^{-6}$ | defined | RADON | RNLAM |
| $A_0$ | surface area of the tailings | $m^2$ | $5.0 \times 10^5$ | C $(5.0 \times 10^5)$ | INPUT | ATAIL |
| $N_w$ | number of winter months (freezing conditions) per year | months | 5.0 | C (5.0) | INPUT | NSUBW |
| $X_s(t)$ | thickness of unsaturated layer | m | 1.0 | U (0.5,1.0) | INPUT | DUNSAT |

* Distributions T, LN, C, and U are triangular, lognormal, constant and uniform respectively.

** Dimension i=1 or 2 refers to zone 1 or 2 respecitively, also note that (Ra) in units of $Bg/m^{-3}$ is actually the product of (Ra) $Bq/g^{-1}$ and $g.m^{-3}$.

FIGURE I.1

DEPENDENCY DIAGRAM
FOR RADON EMISSION RATE
(SOURCE)

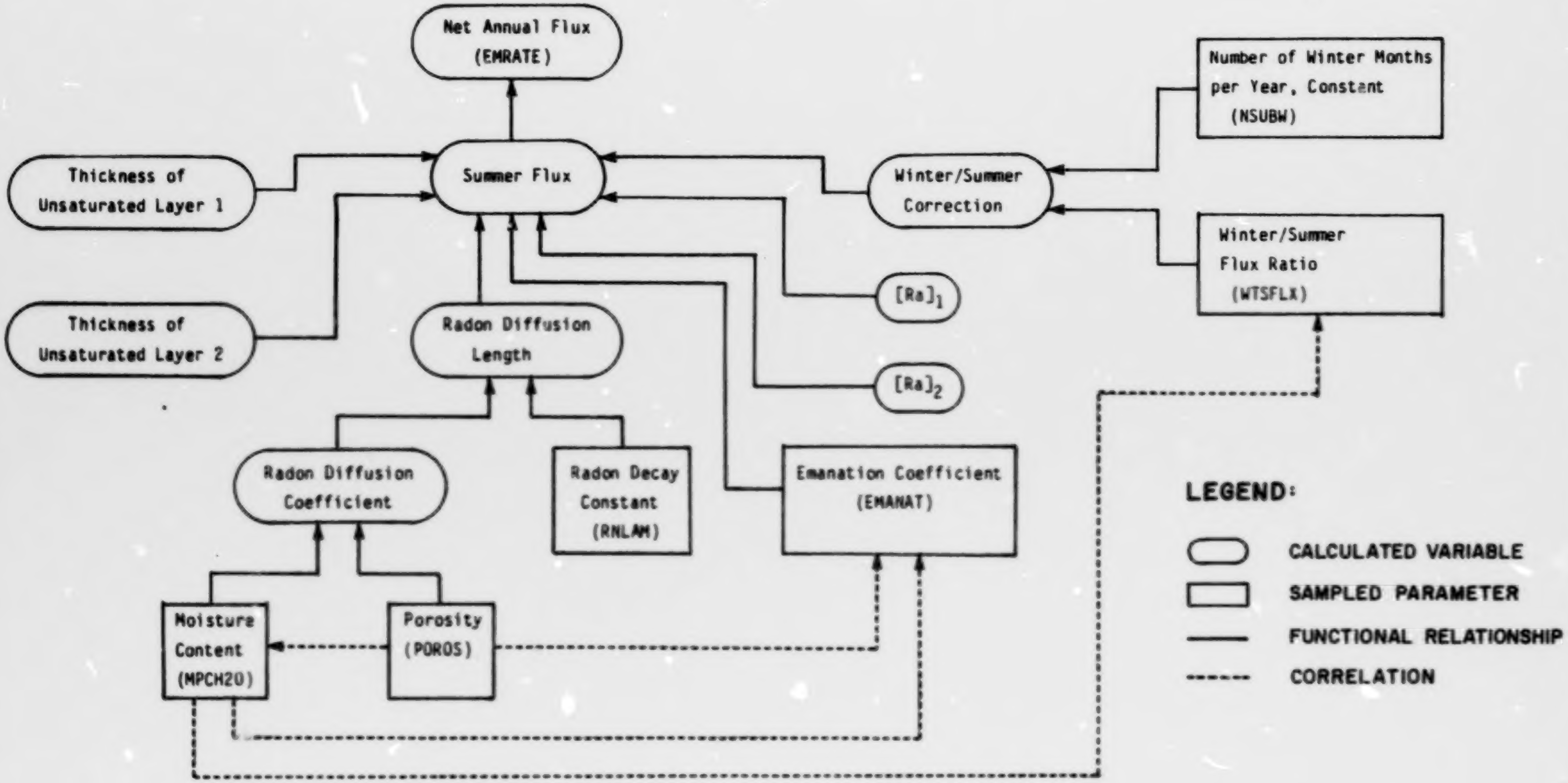

Net Annual Flux (EMRATE)
Summer Flux
Thickness of Unsaturated Layer 1
Thickness of Unsaturated Layer 2
Radon Diffusion Length
Radon Diffusion Coefficient
Radon Decay Constant (RNLAM)
Moisture Content (MPCH2O)
Porosity (POROS)
Emanation Coefficient (EMANAT)
[Ra]1
[Ra]2
Winter/Summer Correction
Number of Winter Months per Year, Constant (NSUBW)
Winter/Summer Flux Ratio (WTSFLX)
LEGEND:
CALCULATED VARIABLE
SAMPLED PARAMETER
FUNCTIONAL RELATIONSHIP
CORRELATION

Table I.2

**ABBREVIATED PARAMETER DICTIONARY***

| | |
|---|---|
| EMANAT: | The radon emanation coefficient represents the fraction of the radon produced within the tailings particles which is released to the void space and hence potentially available for release to the atmosphere. The emanation coefficient is dimensionless and must always be between 0 and 1. EMANAT is sampled from the following triangular distribution:<br>T(0.02, 0.2, 0.9) |
| MPCH20 | The percent moisture content (%) is the weight (%) of tailings mass made up by water (the rest is tailings solids) The moisture content is assumed to be invariant over the unsaturated layer of tailings. MPCH20 is sampled from the following triangular distribution:<br>T(5.0, 15.0, 25.0) |
| POROS | The porosity of the tailings is the fraction of a unit volume of tailings mass not occupied by tailings solids, i.e. it is the void space. POROS is assumed to be invariant over the unsaturated layer of tailings and is sampled from the triangular distribution.<br>T(0.35, 0.4, 0.45) |
| R | The winter/summer flux ratio is the dimensionless ratio of the winter and summer unit radon flux rates. R is always less than 1 as freezing conditions and snow cover attenuate the radon flux. R is sampled from the following lognormal distribution.<br>LN(0.02, 0.2, 0.9) |

* See also Table I.1, Section I.2.1 and Chapter 4 of Volume 3.

## I.3 Parameter Dependencies

With the information summarized in Section I.2 in hand, and with the benefit of several modelling trials, several members of the SENES team familiar with radon source characteristics and with uranium mill tailings characteristics met to discuss the radon source model and possible parameter dependencies. One outcome of this meeting was Figure I.1, the dependency diagram.

The SENES group then discussed the possible strengths (i.e. degree of the correlation) and signs (i.e. a positive or negative correlation) of the parameter dependencies. In addition to input from the SENES group, the possible correlation between porosity (POROS) and moisture content (MPCH2O) was discussed with Dr. T. Dickinson, a soils expert at the University of Guelph, Ontario.

As suggested by Figure I.1, the group concluded that there were three ways in which the possible parameter correlations could be examined. They were:

| Case | Nature of Dependence | Specified Correlation |
|---|---|---|
| CORR1 | EMANAT = f(MPCH2O) | -0.8 |
| | WTSFLX = f(MPCH2O) | -0.9 |
| CORR2 | MPCH2O = f(POROS) | +0.9 |
| | EMANAT = f(MPCH2O) | -0.8 |
| | WTSFLX = f(MPCH2O) | -0.9 |
| CORR3 | MPCH2O = f(POROS) | +0.9 |
| | EMANAT = f(POROS) | -0.7 |
| | WTSFLX = f(POROS) | -0.8 |

The first case, CORR1, was intended to reflect the situation where the modeller was aware of possible correlations between EMANAT and MPCH2O and between WTSFLX and MPCH2O, but unaware of the possible correlation between

MPCH2O and POROS. In the second case, CORR2, the modeller recognizes this latter possibility and in the third case, CORR3, the modeller attempts to represent the dependence in terms of root variables, in this case POROS.

For example, the first dependence CORR1 assumes that the value of EMANAT depends on the value of MPCH2O. As noted in Chapter 4 of Volume 3, it is possible not only that EMANAT could depend on MPCH2O, but that the dependency might be positive for low moisture content (below 5% say) (i.e. EMANAT increases with increasing MPCH2O) and negative at higher moisture content (i.e. EMANAT decreases with increasing MPCH2O). Since moisture contents of Canadian tailings are assumed to be greater than 5%, we assumed that the dependence between EMANAT and MPCH2O would be negative. We also assumed that the dependence could be reasonably strong and assumed a correlation coefficient of -0.8.

Similarly WTSFLX is dependent on the observation that the diffusion coefficient of radon is smaller in water than in air and smaller again in ice than in water (assuming the absence of large cracks which act as radon conduits). Hence it was considered reasonable to assume that WTSFLX was strongly negatively correlated with MPCH2O and the dependence was assigned a correlation coefficient of -0.9.

Finally, MPCH2O was assumed to be strongly positively correlated with porosity and the dependence was assigned a correlation coefficient of +0.9.

While we remain uncertain as to the precise degree of dependence, we are of the opinion that the general nature of the correlations are as indicated. Moreover, whether or not the actual correlation coefficients assigned to the dependencies are precisely correct, does not affect the illustration of the technique.

## I.4 EFFECT OF CORRELATION

In order to examine the effect of introducing correlation into the radon source model, four cases were run probabilistically: the base case with no correlation and the three cases with correlation as discussed previously. Summary statistics for the radon fluxes ($Bq.m^{-2}.s^{-1}$) for each of these cases are given in Table I.3. The results shown are for t=50 years into the simulation and are based on the results of 500 trials.

As indicated earlier the technique described by Kleijnen (1974) for generating correlated variates was used. The technique works as follows. Assume that two parameters X and Y are correlated and that X is the independent variable. Further assume that X and Y have means $\mu_X$ and $\mu_Y$ and standard deviations ${}_X$ and ${}_Y$ respectively. Let Z be a normal variate with mean 0 and standard deviation 1. Then to sample both X and Y in a way that preserves the distribution of X, the mean and variance of Y, and the correlation coefficient C(X,Y) the technique (of Kleijnen) uses the following algorithm:

1. Sample X and Z from their distributions.
2. Evaluate $Y = aX + b + u$

   where $a = C(X,Y)\ {}_Y/\ {}_X$

   $b = \mu_Y - C(X,Y)\ \mu_X\ {}_Y/\ {}_X$

   $u = \ {}_Y\ Z(1-C(X,Y)^2)^{1/2}$

Kleijnen's technique encounters some difficulty when the distributions involved are truncated. Small truncations (e.g. at the 0.001 and 0.999 quantiles) should have little effect, but large truncations modify the sample correlation. This aspect proved to be of practical importance in the present situation since early trials with truncated variables produced non-physical results (such as negative emanation coefficients). To overcome this problem in the present exercise, the standard deviations of X and Y were reduced such that $\mu \pm 4$ would be approximately equal to the limits of the distributions specified for the parameter (EMANAT, WTSFLX or MPCH2O) in Table I.1.

The data in Table I.1 suggest that the introduction of correlation, even quite strong correlation, does not significantly affect the predicted radon flux even though the parameters among which correlations have been introduced are important to the calculation. The same observation is suggested by the frequency and cumulative frequency plots of radon flux shown in Figures I.2 (a) and I.2 (b), respectively.

Correlation matrices calculated for the results of the 500 probabilistic trials for the three cases with correlated variables are given in Table I.4. The specified correlations are also indicated in Table I.4. The correlation coefficients calculated from the data are always of the correct sign, but are consistently larger in magnitude than those specified. This is possibly due, at least in part, to the truncations which were imposed.

For illustration, scatterplots of correlated variables for the second case (CORR2) are given in Figure I.3. None of these scatterplots, or scatterplots prepared for the other two cases with correlation, exhibit any unexpected characteristics. Thus, whether the earlier observation that correlation has little effect on the prediction of the radon source model is in part due to the truncations, which were imposed, the structure of the radon model itself, or other factors is unclear.

## I.5 SUMMARY

Using a description of the radon source model and a data dictionary, a dependency diagram was prepared which served as the basis for subsequent discussion of the possible basis for and nature of dependencies among model parameters. The availability of various model runs helped ensure that the results were "reasonable" either for the uncorrelated or correlated cases.

In implementing the Kleijnen correlation procedures, it was necessary to truncate the range of the dependent variable to ensure that physically reasonable results were always produced. None of the cases examined, namely

Table I.3

## SUMMARY STATISTICS FOR RADON FLUX* FOR BASE CASE AND EXAMPLES

| Case | Arithmetic Mean | Arithmetic SD | Geometric Mean | Geometric SD | Minimum | Maximum | Range (max-min) |
|---|---|---|---|---|---|---|---|
| No correlation | 1.40 | 1.10 | 1.02 | 2.32 | 0.0668 | 5.65 | 5.58 |
| CORR1 | 1.68 | 1.37 | 1.14 | 2.65 | 0.0494 | 6.05 | 6.0 |
| CORR2 | 1.56 | 1.16 | 1.14 | 2.38 | 0.0202 | 5.93 | 5.91 |
| CORR3 | 1.54 | 1.10 | 1.14 | 2.33 | 0.0336 | 5.36 | 5.33 |

---

* Based on results of 500 trials for t=50 years.
Units are $Bq.m^{-2}S^{-1}$.
EMRATE in units of $Bq.S^{-1}$ is obtained by multiplying the radon flux by $A_0$ ($m^2$).

## FIGURE I.2
## FREQUENCY PLOTS FOR CORRELATED AND UNCORRELATED CASES

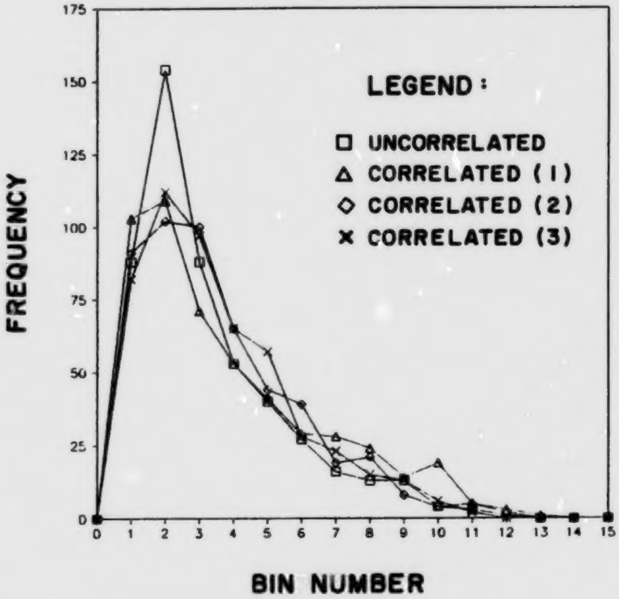

A) FREQUENCY HISTOGRAM

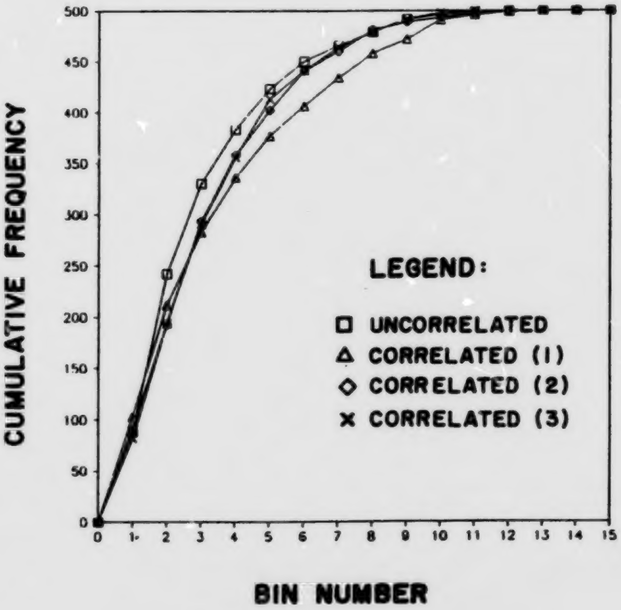

B) CUMULATIVE FREQUENCY DIAGRAM

Table I.4

**CORRELATION MATRICES***

CORR1

1.0
-0.0185 1.0 — set at -0.8
-0.00524 -0.927 1.0 — set at -0.9
+0.00972 -0.961 0.887 1.0
+0.0274 -0.941 0.922 0.907 1.0

CORR2

1.0
0.953 1.0 — set at -0.8
-0.860 -0.901 1.0 — set at -0.9
-0.910 -0.955 0.856 1.0
-0.890 -0.940 0.910 0.906 1.0

CORR3

1.0 — set at 0.9
0.953 1.0 — set at -0.7
-0.850 -0.809 1.0 — set at -0.5
-0.910 -0.867 0.766 1.0
-0.912 -0.931 0.874 0.843 1.0

* For the same cases as shown in Table I.3. Note that the variable order in the matrices from top to bottom and left to right is POROS, MPCH2O, EMANAT, WTSFLX, EMRATE.

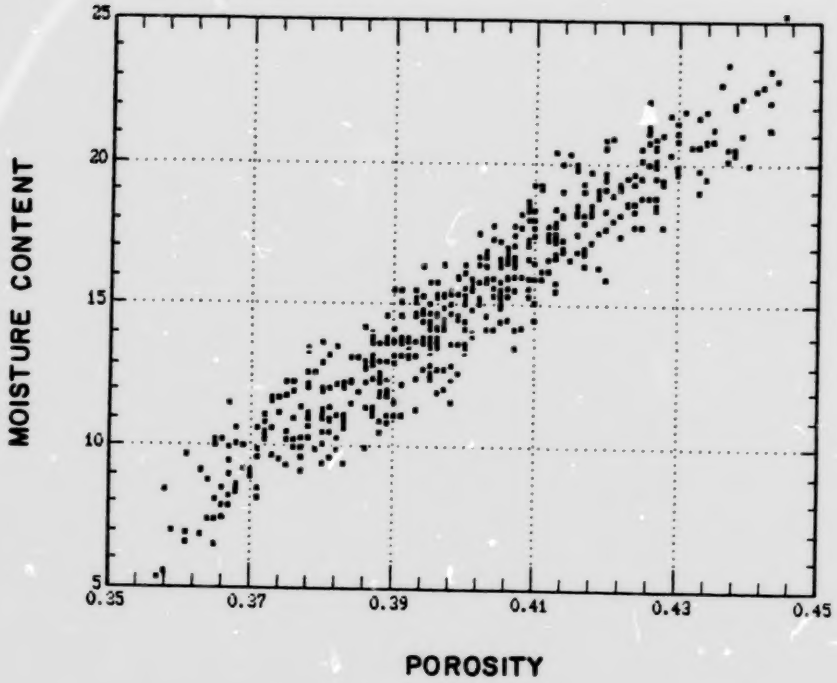

A) MOISTURE CONTENT vs. POROSITY

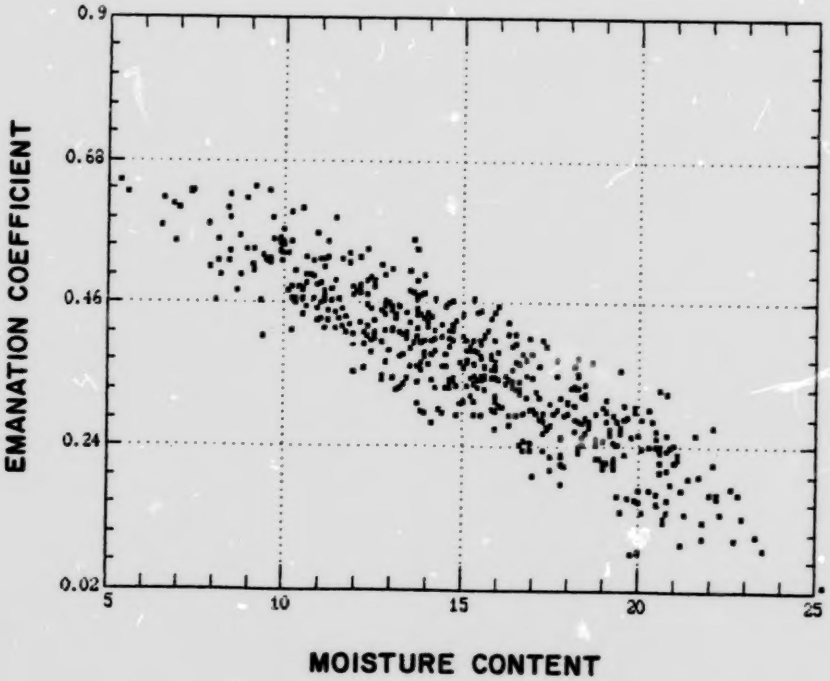

B) EMANATION COEFFICIENT vs. MOISTURE CONTENT

FIGURE I.3

## SCATTER PLOTS OF CORRELATED VARIABLES FOR CORRELATION CASE 2

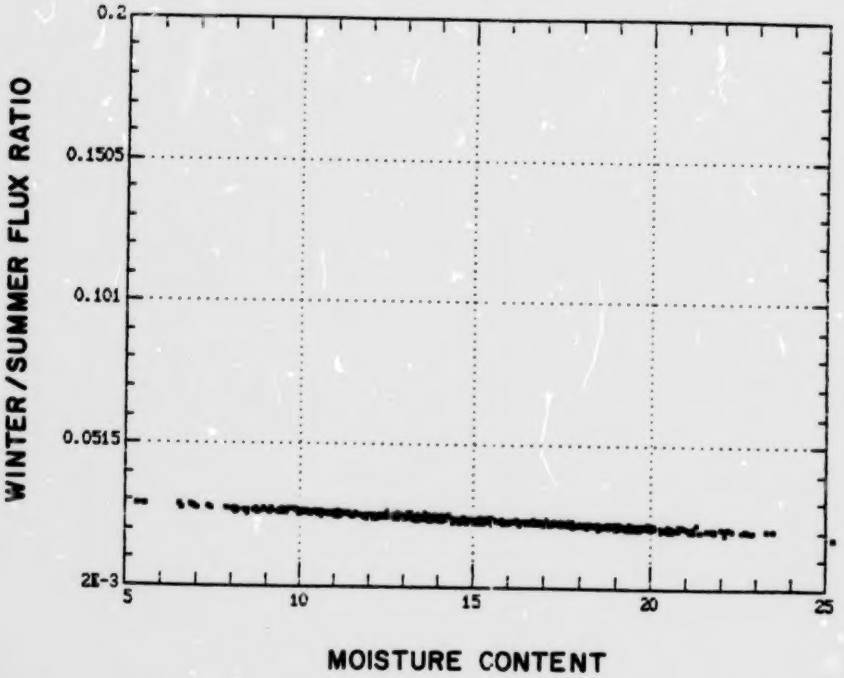

C) WINTER/SUMMER FLUX RATIO vs. MOISTURE CONTENT the base case with no correlation and the three cases with correlation, produced substantially different results. Whether this was due in part to the truncation scheme involved or other factors is not clear.

The exercise was most instructive in forcing the study group to examine the underlying structure of the model and the assumptions (i.e. the basis) for the input parameters. The increased understanding obtained through the exercise suggests that preparing dependency diagrams and looking for dependencies may be worthwhile irrespective of whether or not the inclusion of correlation has an observable effect on the final answer.

# Volume

# 3

# NATIONAL
# URANIUM
# TAILINGS
# PROGRAM

Energy, Mines and Resources Canada
Énergie, Mines et Ressources Canada

Canada

# PROBABILISTIC MODEL DEVELOPMENT FOR THE ASSESSMENT OF THE LONG-TERM EFFECTS OF URANIUM MILL TAILINGS IN CANADA - PHASE III

## VOLUME 3 - URANIUM TAILINGS ASSESSMENT PROGRAM (UTAP) COMPONENT MODEL DOCUMENTATION

A Research Report Prepared Under
Contract 10SQ85-00182

for

The National Uranium Tailings Program
Canada Centre for Mineral and Energy Technology
Energy, Mines and Resources Canada
555 Booth Street
Ottawa, Ontario
K1A 0G1

by

SENES Consultants Limited
499 McNicoll Avenue
Willowdale, Ontario
M2H 2C9

July 1986

MICROMEDIA

449 pp

## ABSTRACT

This study represents part of the ongoing efforts of the National Uranium Tailings Program (NUTP) to develop the capability to predict the long-term effects of Canadian uranium mill tailings. The study was conducted to further refine the probabilistic assessment tool developed during two previous phases of work.

In particular, the work involved expanding the system model to include: additional radionuclides, additional pathways of exposure and the ability to perform calculations over much greater distances. The primary product of this study is a revised, more comprehensive Uranium Tailings Assessment Program (UTAP).

The project report has been prepared in four volumes, of which this is Volume 3. This volume presents the documentation of the mathematical models used to simulate the behaviour of the uranium tailings and the surrounding environment. The documentation consists of model derivations and descriptions, computer code listings and, in many instances flow charts outlining model implementation, and illustrative model results.

---

## NOTICE

This report was prepared by SENES Consultants Limited (SENES) under contract to the National Uranium Tailings Program (NUTP). Neither the NUTP nor SENES makes any warranty, expressed or implied, or assumes any liability with respect to any damage or loss incurred as a result of the use made of the information contained in this publication.

## TABLE OF CONTENTS

Page

Abstract i

Notice i

1.0 INTRODUCTION 1-1

2.0 COMPONENT MODULE OBJECTIVES AND CONCEPTUAL SPECIFICATIONS 2-1
  2.1 Constituents 2-1
  2.2 Pathways 2-1
  2.3 Spatial Considerations 2-2
  2.4 Receptor Locations, Characteristics and Population Dose 2-3
  2.5 Temporal Considerations 2-4
  2.6 Natural Physical Changes 2-4
  2.7 Disposal Option(s) 2-4
  2.8 Input Parameters 2-5

3.0 WATER SOURCE MODELS 3-1
  3.1 Modelling Concepts 3-1
  3.2 Initial Conditions - Ions and pH 3-2
    3.2.1 Initial Inventories 3-3
    3.2.2 Calcium and Sulphate Concentrations 3-4
    3.2.3 Initial pH Levels 3-6
    3.2.4 Iron Concentrations 3-6
  3.3 Ions - Layers 1 and 2 3-7
    3.3.1 Sulphates Derived from Pyrite Oxidation 3-7
    3.3.2 Gypsum Dissolution and Reprecipitation 3-11
    3.3.3 Calcium and Sulphate Concentrations 3-16
    3.3.4 Iron Concentration 3-18
    3.3.5 Modifications for Limestone Addition 3-19

Table of Contents, cont'd.

Page

3.4 Ions - Layer 3 3-25
- 3.4.1 Calcium and Sulphate Concentrations Prior to Gypsum Depletion 3-25
- 3.4.2 Gypsum Depletion 3-26
- 3.4.3 Calcium and Sulphate Concentrations Following Gypsum Depletion 3-28
- 3.4.4 Iron Concentration 3-29

3.5 Ions - Layer 4 3-29

3.6 pH Calculations 3-31
- 3.6.1 Layer 1 3-32
- 3.6.2 Layer 2 3-40
- 3.6.3 Layer 3 3-42
- 3.6.4 Layer 4 3-47
- 3.6.5 Implementation/Solution of pH Expressions 3-47

3.7 Initial Conditions - Radionuclides 3-52
- 3.7.1 Uranium 3-53
- 3.7.2 Thorium 3-56
- 3.7.3 Radium 3-61
- 3.7.4 Lead 3-64

3.8 Uranium 3-67

3.9 Thorium 3-70
- 3.9.1 Unsaturated Zone 3-70
- 3.9.2 Layers 3 and 4 3-75

3.10 Radium 3-76
- 3.10.1 Radioactive Ingrowth and Decay 3-76
- 3.10.2 Unsaturated Zone 3-78
- 3.10.3 Layers 3 and 4 3-87

3.11 Lead 3-91
- 3.11.1 Unsaturated Zone 3-91
- 3.11.2 Layers 3 and 4 3-95

Table of Contents, cont'd.

Page

3.12 Input Parameter Values 3-98
3.13 Water Source Model Demonstration 3-110
3.14 Tailings Vegetation and Erosion Model 3-118
3.14.1 Introduction 3-118
3.14.2 The Universal Soil Loss Equation 3-119
3.14.3 Tailings Vegetation 3-122
3.14.4 Tailings Geometry 3-124
3.14.5 Deposition and Transport 3-125
3.14.6 Computational Approach 3-129
3.14.7 Tailings Depletion and River/Lake System Loading 3-130
3.14.8 Erosion Model Test Program 3-131
3.15 References 3-132

4.0 AIR SOURCE MODEL 4-1
4.1 Radon Source Term 4-1
4.2 Dust Source Term 4-6
4.3 References 4-9

5.0 AIR DISPERSION MODEL 5-1
5.1 Air Dispersion Component 5-1
5.2 Subroutine WIND 5-5
5.3 References 5-7

6.0 SOIL MODEL 6-1
6.1 Soil Model Development 6-1
6.2 Parameter Values 6-6
6.3 Soil Model Test Program 6-7
6.4 References 6-8

Table of Contents, cont'd.

Page

7.0 GROUNDSHINE MODEL 7-1
7.1 Introduction 7-1
7.2 The Basic Model 7-1
7.3 Multiple Soil Layers 7-4
7.4 Multiple Radionuclides 7-4
7.5 Exhalation of Radon 7-7
7.6 References 7-11

8.0 TERRESTRIAL VEGETATION MODELS 8-1
8.1 Introduction 8-1
8.2 Above-Ground and Below-Ground Vegetables (AVEGC and BVEGC) 8-4
8.3 Summer Forage (SUFOC) 8-5
8.4 Brouse (BRWSC) 8-6
8.5 Lichens (LICHC) 8-6
8.6 References 8-9

9.0 SUBSURFACE TRANSPORT MODEL 9-1
9.1 Introduction 9-1
9.2 Aquifer Characteristics 9-2
9.3 Theoretical Approach 9-3
9.3.1 Auxiliary Equations 9-3
9.3.2 Mass Balance 9-7
9.3.3 Assumptions 9-8
9.4 Solution to Mass Balance 9-11
9.4.1 Constant Source 9-11
9.4.2 Time-Variant Source 9-12
9.5 Review of Parameters and Constants 9-13
9.5.1 Parameter Values 9-13
9.5.2 Constants 9-21
9.6 Model Demonstration 9-22
9.7 Description of Computer Model 9-23

Table of Contents, cont'd.

Page

9.8 References 9-24

10.0 SURFACE WATER DISPERSION MODELS 10-1
  10.1 Approach to Watershed Modelling 10-1
  10.2 The Reference Watershed 10-1
  10.3 The Hydrologic Component 10-2
  10.4 Major Ions Component 10-4
    10.4.1 Baseline Levels 10-4
    10.4.2 River Segments 10-4
    10.4.3 Lake Segments 10-6
  10.5 pH Component 10-7
  10.6 Radionuclide Component 10-12
    10.6.1 River Segments 10-14
    10.6.2 Lake Segments 10-15
  10.7 Parameter Values and Code Listing 10-31
  10.8 References 10-32

11.0 AQUATIC MODELS 11-1
  11.1 Components Considered 11-1
  11.2 Effect of pH on Fish Populations 11-1
  11.3 Radionuclide Transfer to Aquatic Biota 11-6
    11.3.1 Modelling Approach 11-6
    11.3.2 Bioaccumulation in Fish 11-8
    11.3.3 Bioaccumulation in Aquatic Macrophytes 11-10
  11.4 Parameter Values and Code Listing 11-12
  11.5 References 11-13

12.0 ANIMAL PRODUCE MODELS 12-1
  12.1 Introduction 12-1
  12.2 Radionuclides in Caribou Flesh 12-2
    12.2.1 Air Pathways-to-Caribou Flesh (ACARC) 12-3
    12.2.2 Water Pathways-to-Caribou Flesh (WCARC) 12-5

Table of Contents, cont'd. Page

12.3 Radionuclides in Moose Flesh 12-6
    12.3.1 Air Pathways-to-Moose Flesh (AMOC) 12-8
    12.3.2 Water Pathways-to-Moose Flesh (WMOC) 12-9
12.4 References 12-10

13.0 DOSE MODELS 13-1
13.1 Introduction 13-1
    13.1.1 Background 13-1
    13.1.2 Dose Conversion Factors 13-2
13.2 Ingestion Dose 13-6
    13.2.1 Annual Dose Due to the Ingestion of Vegetables 13-6
    13.2.2 Annual Dose Due to the Ingestion of Caribou 13-8
    13.2.3 Annual Dose Due to the Ingestion of Moose 13-10
    13.2.4 Annual Dose Due to the Ingestion of Drinking Water 13-12
    13.2.5 Annual Dose Due to the Ingestion of Fish 13-13
13.3 Inhalation Dose 13-14
    13.3.1 Annual Dose to the Inhalation of Suspended Particulates 13-14
    13.3.2 Annual Dose to the Inhalation of Radon and its Daughters 13-16
13.4 Receptor Specification 13-18
    13.4.1 Receptor Identification Number 13-19
    13.4.2 Sector Number 13-19
    13.4.3 Ring Number 13-19
    13.4.4 Water Source Segment Number 13-19
    13.4.5 Receptor Type 13-19
    13.4.6 Population 13-20
13.5 Population Dose 13-20
13.6 References 13-21

APPENDIX A Water Source Models: Code Listing and Variable Dictionary

Table of Contents, cont'd.

APPENDIX B A Dynamic Model of Uranium Behavior in an Oligotrophic Lake by B. G. Blaylock, R. H. Gardner, and F. O. Hoffman

APPENDIX C Approaches to Modelling Episodic Events

# LIST OF FIGURES

Follows Page

2.1 Exposure Pathways Analyzed 2-2
2.2 Conceptual Diagram of Spatial Coordinate System 2-2
3.1 Concept Adopted for Modelling the Tailings Source Term 3-2
3.2 Structure of the Tailings Source Model 3-2
3.3 Sulphate Ion Concentrations 3-112
3.4 Calcium Ion Concentrations 3-112
3.5 Iron Ion Concentrations 3-114
3.6 Porewater pH 3-114
3.7 Solid Phase Radionuclide Concentrations 3-114
3.8 Dissolved Uranium Concentrations 3-116
3.9 Dissolved Thorium Concentrations 3-116
3.10 Dissolved Radium Concentrations 3-116
3.11 Dissolved Radium Concentrations 3-118
3.12 Control Factor as a Function of Fraction of Trailings Vegetated 3-122
3.13 Typical Range of Grain Size Distribution for Acid Generating Tailings 3-126
3.14 Flowsheet of Computational Approach 3-130
3.15 Cumulative Tailings Depletion and pH vs Time 3-131
6.1 Schematic Representation of Soil Deposition in Leaching Concepts 6-2
6.2 Flowsheet for Soil Model 6-6
6.3 Plot of Concentration vs Time for Second Soil Layer 6-8
7.1 Uranium-238 Decay Series 7-6
7.2 Thorium-232 Decay Series 7-6
7.3 Flowsheet for Groundshine Model 7-10
9.1 Structure of Subsurface Transport Model 9-2
9.2 Concept of Reference Tailings Groundwater Flowpath 9-2
9.3 Time-Variant Source 9-12
9.4 Distribution of the Fraction of Precipitation 9-16

List of Figures, cont'd.

Follows Page

9.5a Source Concentration 9-22

9.5b Groundwater Concentration 9-22

9.6a Frequency Histogram for Uranium Concentration at Discharge Point to Surface Water 9-23

9.6b Frequency Histogram for Thorium Concentration at Discharge Point to Surface Water 9-23

9.6c Frequency Histogram for Pb-210 Concentration at Discharge Point to Surface Water 9-23

9.6d Frequency Histogram for Ra-226 Concentration at Discharge Point to Surface Water 9-23

10.1 Reference Watershed Schematic 10-2

10.2 Conceptual Schematic of Reference Lake 10-16

11.1 Aggregate Aquatic Transfer Model 11-8

11.2 Frequency Histogram of Uranium Bioaccumulation Factor Values 11-10

11.3 Frequency Histogram of Thorium Bioaccumulation Factor Values 11-10

11.4 Frequency Histogram of Radium-226 Bioaccumulation Factor Values 11-10

11.5 Frequency Histogram of Lead-210 Bioaccumulation Factor Values 11-10

# LIST OF TABLES

| | | Follows Page |
|---|---|---|
| 2.1 | Summary of Phase III Component Model Objectives | 2-2 |
| 2.2 | Input Parameter Distribution Specifications | 2-6 |
| 3.1 | Relative Activities of Aluminum Hydroxo Complexes | 3-34 |
| 3.2 | Relative Activities of Iron (III) Hydroxo Complexes | 3-36 |
| 3.3 | Ionic Equilibrium for Electroneutrality | 3-38 |
| 3.4 | Water Source Model Input Parameters | 3-98 |
| 3.5 | Erosion Model Code Listing | 3-131 |
| 3.6 | Erosion Model Variables | 3-131 |
| 4.1 | Radon Source Model Variables | 4-6 |
| 4.2 | Radon Source Model Code Listing | 4-6 |
| 4.3 | Dust Source Model Variables | 4-8 |
| 4.4 | Dust Source Model Code Listing | 4-8 |
| 5.1 | Air Dispersion Model Variables | 5-4 |
| 5.2 | Power Law Exponents and Coefficients for $\sigma_z$ | 5-4 |
| 5.3 | Air Dispersion Model Code Listing | 5-6 |
| 5.4 | Wind Model Code Listing | 5-6 |
| 6.1 | Soil Model Code Listing | 6-6 |
| 6.2 | Soil Model Parameters | 6-6 |
| 7.1 | Groundshine Model Parameters | 7-10 |
| 7.2 | Groundshine Model Code Listing | 7-10 |
| 8.1 | Above Ground Vegetables Model Variables | 8-6 |
| 8.2 | Below Ground Vegetables Model Variables | 8-6 |
| 8.3 | Summer Forage Model Variables | 8-6 |
| 8.4 | Browse Model Variables | 8-6 |
| 8.5 | Lichen Model Variables | 8-8 |
| 8.6 | Terrestrial Vegetation Models Code Listing | 8-8 |
| 9.1 | Assumptions Employed in Subsurface Transport Model | 9-8 |
| 9.2 | Subsurface Transport Model Parameters | 9-14 |

List of Tables, cont'd.

Follows Page

9.3 Comparison of $K_d$ Values for U-238 (IV) and U-238 (VI) as a Function of pH 9-18
9.4 Radioactive Half-Life 9-22
9.5 Input Parameters Used for Deterministic Model Demonstration 9-22
9.6 Groundwater Model Code Listing 9-24
10.1 Characteristics of Reference Watershed 10-2
10.2 Lake Sedimentation Flux Values 10-18
10.3 Sediment to Water $K_d$ Values 10-18
10.4 Assessed Mass Transfer Coefficient Values 10-24
10.5 Watershed Model Variables 10-31
10.6 Watershed Model Code Listing 10-31
11.1 Large (Game) Fish Flesh Uranium Bioaccumulation Factors 11-10
11.2 Large (Game) Fish Flesh Thorium Bioaccumulation Factors 11-10
11.3 Large (Game) Fish Flesh Radium-226 Bioaccumulation Factors 11-10
11.4 Large (Game) Fish Flesh Lead-210 Bioaccumulation Factors 11-12
11.5 Aquatic Model Variables 11-12
11.6 Aquatic Biota Model Code Listing 11-12
12.1 Caribou Flesh Model Variables 12-4
12.2 Moose Flesh Model Variables 12-8
12.3 Animal Produce Model Code Listing 12-8
13.1 ICRP-30 Dose Conversion Factors 13-2
13.2 Dose Conversion Factors for this Study 13-4
13.3 Variables Used in the Calculation of Annual Dose to the Critical Receptor 13-20
13.4 Variable Used in the Calculation of Annual Dose to the Average Receptor 13-20
13.5 Dose Model Code Listing 13-20

# 1.0 INTRODUCTION

In 1982 Energy, Mines and Resources Canada established the National Uranium Tailings Program (NUTP) to pull together previous work on Canadian uranium mill tailings, to fund additional work where significant information gaps were found and to develop the capability to predict the long-term effects of tailings with a known degree of confidence while incorporating variability and uncertainty in the input data. Such evaluations require the use of mathematical models to simulate the behaviour of the real system.

An earlier study (Phase I) funded by the NUTP demonstrated how probabilistic techniques could be used to take account of the variability and uncertainty in model input parameters in such a simulation analysis (SENES, 1984). Subsequently, the NUTP sponsored a followup Phase II study (SENES, 1985) to extend and refine the probabilistic tools developed in the Phase I study and to investigate various issues of technical interest involved in carrying out and interpreting a probabilistic analysis.

The objectives of the current, Phase III study, were to extend the capabilities of the Phase II system model and then apply the refined (Phase III) system model to a hypothetical reference site.

More specifically, Phase III was designed to:

- expand the simulation models to include additional major radionuclides
- expand the simulation models to include additional selected pathways of exposure
- modify the system model to permit calculations over greater distances
- incorporate a model to simulate water erosion of tailings or cover material
- streamline the system code, update the documentation and prepare a user's manual.

A number of related issues were also investigated.

The product of the current phase of work is a revised Uranium Tailings Assessment Program (UTAP) for performing probabilistic analysis of the behaviour and environmental effects of uranium mill tailings, following closeout of milling operations. The models in UTAP are primarily assessment level models, rather than detailed research models. They have been designed to allow predictions to be made for distances up to 50 kilometres in all directions from the tailings area, and for time periods of up to 1000 years. In addition, the models provide many other features. These include the ability to incorporate different receptors and site characteristics and to deal with input parameters which vary with time. A more complete discussion of the program objectives and features is presented in Volume 1 of this report.

To achieve its objectives, the Uranium Tailings Assessment Program is composed of a number of modules. These may be classified as either component or control modules. Component modules (or models) are the computer subprograms directly concerned with the simulation of a uranium tailings physical system; that is, the computer implementation of the mathematical models representing the uranium tailings pile and surrounding environment. Control modules provide the infrastructure for probabilistic analysis of the component modules. These functions include probabilistic sampling of input parameters, and many input, output and bookkeeping functions. The integrated control and component modules are referred to as the system model or the Uranium Tailings Assessment Program (UTAP).

Volume 2 provides documentation for the control modules. This volume (Volume 3) documents the component modules. The general objectives and overall structure of the component modules is discussed in the next section. Detailed descriptions of the mathematical models and assumptions used in the development of each component module are presented in the remaining chapters.

## 2.0 COMPONENT MODULE OBJECTIVES AND CONCEPTUAL SPECIFICATIONS

The Phase III component module objectives are summarized in Table 2.1. The objectives are discussed in more detail below.

### 2.1 Constituents

The radionuclides modelled are natural uranium, total thorium, radium-226, radon-222 and lead-210. The pH of the reference uranium tailings site and the chained river-lake system discussed later are also modelled. As in Phase II, pH is modelled by an equilibrium relationship which explicitly accounts for the dissolved concentrations in the aqueous phase of calcium, iron and sulphate.

### 2.2 Pathways

The following pathways of dose to the receptors are modelled in Phase III for the aforementioned radionuclides:

1) Water Consumption: dispersion of tailings effluent in the receiving water environment and consumption by humans.
2) Fish Consumption: the transfer of radionuclides from the receiving water environment to fish and consumption by humans.
3) Radon Inhalation: dispersion of radon exhaled from the reference tailings site through the air environment and inhalation by humans.
4) Dust Inhalation: dispersion of dust eroded from the surface of the reference tailings site in the air environment and inhalation by humans.
5) Vegetable Consumption: the transfer of radionuclides to above and below ground vegetation and subsequent consumption by humans.
6a) Animal Produce Consumption: the uptake of radionuclides by forage vegetation and lichens, subsequent transfer to moose and caribou and consumption of the animal meat by humans.

6b) Animal Produce Consumption: the uptake of radionuclides by aquatic vegetation, subsequent transfer to moose and consumption of the animal meat by humans.

6c) Animal Produce Consumption: caribou and moose consumption of lake and river water and subsequent consumption of the animal meat by humans.

7) Groundshine: direct radiation from deposited dust.

These pathways are illustrated in Figure 2.1.

## 2.3 Spatial Considerations

The windrose structure shown in Figure 2.2 defines the system of spatial coordinates used in UTAP. As indicated, there are 16 direction sectors to correspond to the traditional windrose structure. The number of rings, up to a maximum of 5, and the spacing of the rings, from a minimum distance of 1 km to a maximum of 50 km, are to be user-specified. The rings are continuous, with the outer limit of one ring forming the inner limit of the next. Distance-related concentration calculations in the air dispersion model utilize the distance to the centre of the specified rings. This quantity will be the assumed concentration over the entire windrose location defined by the sector and ring boundaries.

The watershed model handles up to 10 user-specified components (segments) in the river-lake system. The user specifies the appropriate river and lake characteristics (i.e. lake area, lake depth, drainage area, etc.). Calculations are done at each river or lake outflow point. The user specifies the relationship between rivers and lakes (i.e. the order of linkage of the river and lake segments). The program provides a validation step to ensure that a physically feasible watershed has been specified.

Dilution is the only mechanism accounted for in the river model. That is, adsorption and desorption are not considered. The lake model, as in Phase II, accounts for adsorption, desorption and dilution. The user specifies different biological and/or chemical characteristics for the lakes in addition

FIGURE 2.1

EXPOSURE PATHWAYS ANALYZED

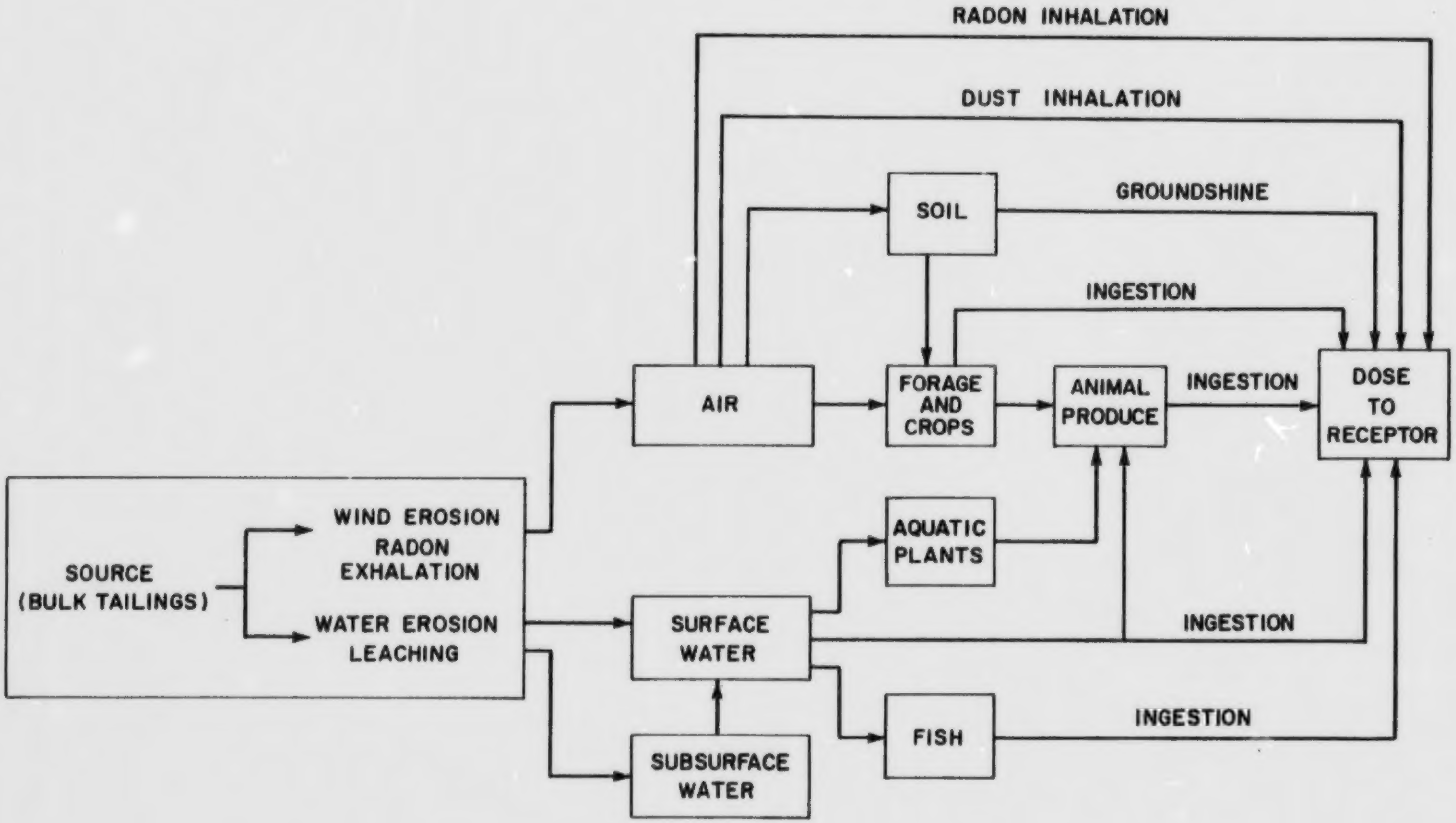
RADON INHALATION
DUST INHALATION
SOIL
GROUNDSHINE
INGESTION
AIR
FORAGE AND CROPS
ANIMAL PRODUCE
INGESTION
DOSE TO RECEPTOR
WIND EROSION
RADON EXHALATION
SOURCE (BULK TAILINGS)
WATER EROSION
LEACHING
AQUATIC PLANTS
SURFACE WATER
INGESTION
FISH
INGESTION
SUBSURFACE WATER

## FIGURE 2.2
## CONCEPTUAL DIAGRAM OF SPATIAL COORDINATE SYSTEM

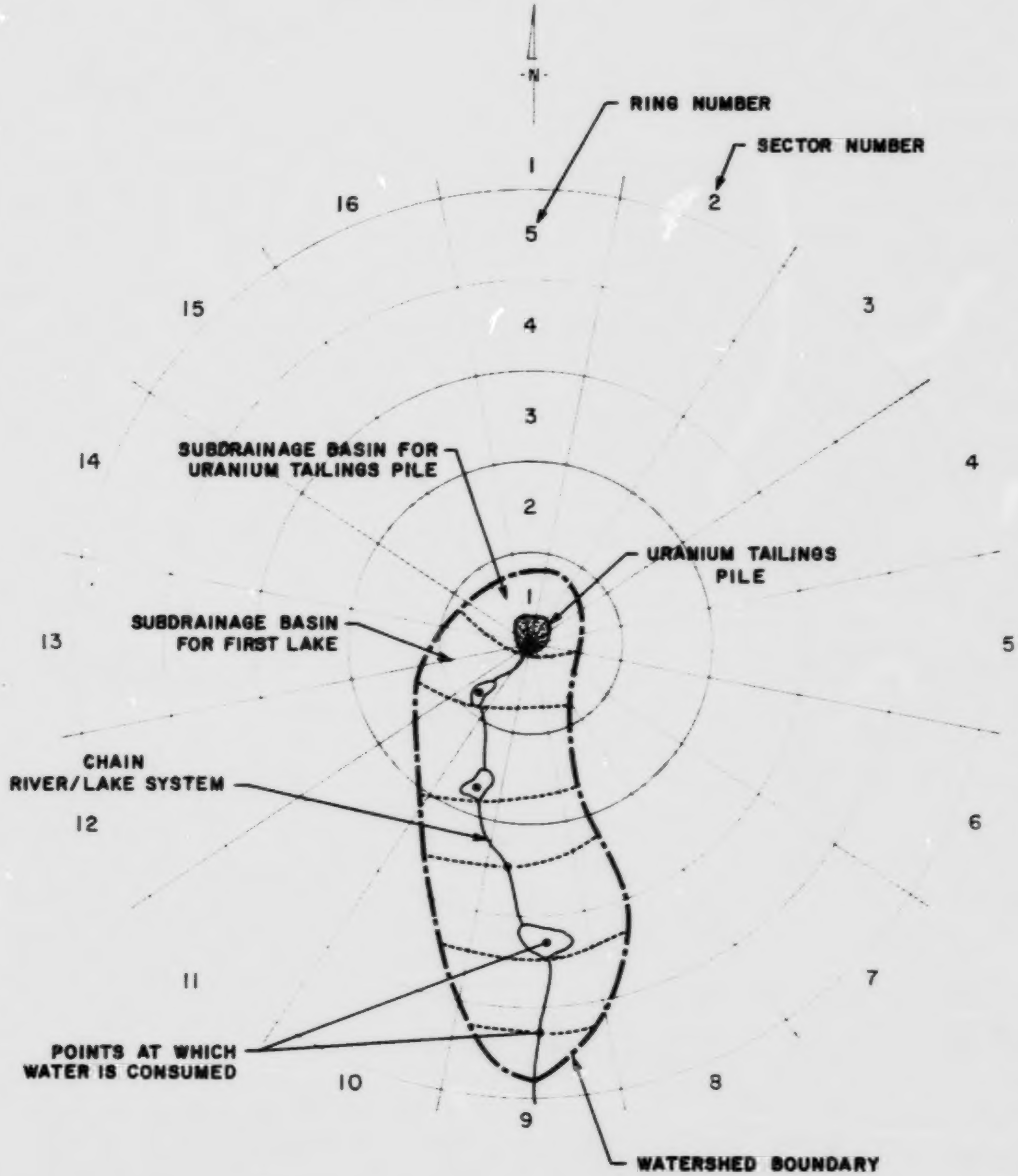
N
RING NUMBER
SECTOR NUMBER
1
2
3
4
5
6
7
8
9
10
11
12
13
14
15
16
5
4
3
2
1
SUBDRAINAGE BASIN FOR URANIUM TAILINGS PILE
URANIUM TAILINGS PILE
SUBDRAINAGE BASIN FOR FIRST LAKE
CHAIN RIVER/LAKE SYSTEM
POINTS AT WHICH WATER IS CONSUMED
WATERSHED BOUNDARY

Table 2.1

## SUMMARY OF PHASE III COMPONENT MODULE OBJECTIVES

| CONSTITUENTS | PATHWAYS | SPATIAL AND RECEPTOR LOCATIONS | TEMPORAL CONSIDERATIONS | NATURAL PHYSICAL CHANGES | DISPOSAL OPTIONS |
|---|---|---|---|---|---|
| Natural Uranium | Lake Water Consumption | Air Pathways: 16 Directions and up to 5 Radial Distances From 1 To 50 km | Time-Variant Parameters Sampled Every Time Step | Sheet Erosion Accounted For By Universal Soil Loss Equation | Pyritic Tailings (Scenario 1) |
| Total Thorium | Fish Consumption | | | | |
| Radium-226 | Radon Inhalation | | Up To 1000 Year Simulation Period | | Depyritization And Addition Of Limestone to Surface Cover (Scenario 2) |
| Radon-222 | Dust Inhalation | Water Pathways: Up To 10 Chained River/Lake Segments | | Uranium Tailings Revegetation With Time | |
| Lead-210 | Vegetable Consumption | | Time Increments of 1 or 10 Years | | |
| Calcium | Animal Produce Consumption (from animals feeding on land and aquatic vegetation and drinking water) | Up To 80 Receptor Locations | | | |
| Iron | | | | | |
| Sulphate | | | | | |
| pH | Groundshine | | | | |

to physical characteristics. Data for two lake types with distinct biological and chemical characteristics are specified in the probabilistic input file accompanying the Phase III version of UTAP. The user indicates, in the file in which lake spatial characteristics are defined, which biological and/or chemical data is appropriate for that particular lake.

## 2.4 Receptor Locations, Characteristics and Population Dose

The system model permits the calculation of contaminant concentrations and receptor dose in all 80 windrose locations (i.e. 5 radial distances and 16 directions). The user thus possesses great power to perform a comprehensive analysis of the system. However, his/her hands may potentially be tied by information overload. To avoid this potential problem, the code allows the user to model a specified number of receptors with unique, user-defined characteristics, each located in one of the 80 windrose locations. We strongly recommend using the minimum number of receptors required to obtain an understanding of the behaviour of the uranium tailings system.

Population dose is computed for each populated sector as the dose to a an average receptor multiplied by a user-specified population. The dose for sectors with populations are summed to obtain the total population dose. As well, the doses and contaminant concentrations for windrose locations containing the river-lake system are calculated. This strategy not only gives the user a finite number of receptors and locations requiring input but also considerably reduces the runtime of the model. Should the user desire to assess different locations or receptor characteristics the model can be run again.

Two receptor types are available for analysis, an average receptor and a critical receptor. The characteristics of these receptors are fixed for a given run, but may be changed from one run to the next. Both receptors are assumed to breathe the air, be exposed to groundshine and consume vegetables grown in the sector in which they are located. However, their water and fish intake comes from a user-specified river or lake.

## 2.5 Temporal Considerations

Several of the model input parameters are considered "time varying", in that they describe natural phenomena, such as mean annual wind speed, which vary from year to year. The control module structure in Phase III has the capability to sample these time-varying parameters each time step (in addition to each trial).

Phase II results indicated that most of the temporal dynamics of the system occurred in the first 500 years of simulation. This observation was not expected to change greatly in the Phase III modelling. Hence, the component models were designed to be appropriate for simulation times of up to 1000 years. This allows examination of most of the interesting behaviour of the system. While the models may be applicable for simulations over a much longer time period, it will be necessary for the user to consciously examine all model components to satisfy himself/herself that the models apply.

## 2.6 Natural Physical Changes

This involves consideration of natural processes which have the potential to affect contaminant release rates from the tailings in a gradual way over many years. It does not include episodic events, such as floods or fires. Sheet erosion by water action is modelled using the Universal Soil Loss Equation. This approach provides a direct source of solids loading to the watershed element nearest the tailings. We have also included a factor which accounts for natural vegetation of the tailings. Simply, the revegetation term has the effect of reducing water erosion and dust suspension. No other natural changes are modelled.

## 2.7 Disposal Option(s)

The Phase III system model was developed to analyze two tailings disposal scenarios for the purpose of application to the reference site. The base case option (Scenario 1) considers the effects of pyritic tailings placed in a reference tailings site. The second option involves pyrite reduction and limestone addition to the tailings surface layer. It is assumed that the pyrite content of the upper metre (or so) of tailings is reduced by a factor of about 10, by modifications to the milling process. In addition, limestone is assumed to be incorporated in the depyritized tailings. These two modifications affect the physical and chemical behaviour of the tailings source, and result in changes to the predicted consequences (e.g. dose to receptor) over time.

## 2.8 Input Parameters

Each component model requires values for a number of independent variables or "input parameters". In probabilistic analysis, many inputs are specified as probability distributions. The input parameter distributions available in Phase III include: constant, uniform, loguniform, normal, lognormal, triangular, beta, Weibull, pairwise correlated and arbitrary.

Each distribution is defined by its own attributes as indicated in Table 2.2. For instance, a normal distribution is specified by its mean, standard deviation, minimum value and maximum value, while a uniform distribution is completely specified by its minimum and maximum values. The distributions given in Table 2.2 are referenced frequently in tables of parameter definitions included in the following chapters.

## Table 2.2
## INPUT PARAMETER DISTRIBUTION SPECIFICATIONS

| Distribution Type | | Distribution Specifications |
|---|---|---|
| C | Constant | single numerical value |
| U | Uniform | minimum, maximum |
| LU | Loguniform | minimum, maximum |
| N | Normal | arithmetic mean,<br>arithmetic standard deviation,<br>minimum, maximum |
| LN | Lognormal | geometric mean,<br>geometric standard deviation,<br>minimum, maximum |
| T | Triangular | minimum, mode (peak), maximum |
| B | Beta | minimum, maximum<br>shape parameters (a and b) |
| W | Weibull | location parameter (minimum) (a)<br>scale parameter (b)<br>shape parameter (c) |
| CR | Correlated | name of independent variable<br>mean of dependent variable<br>standard deviation of dependent variable<br>correlation coefficient<br>mean of independent variable<br>standard deviation of independent variable |

Table 2.2 (Cont'd.)

| Distribution Type | Distribution Specifications |
|---|---|
| A Arbitrary | number of cells<br>minimum value<br>maximum value<br>ordinate values |

# 3.0 WATER SOURCE MODELS

## 3.1 Modelling Concepts

The approach to modelling the physical and chemical behaviour of the tailings is very similar to that adopted in a previous study (SENES, 1985). Specifically, the tailings are modelled as a multi-layered system, as indicated on Figure 3.1. The features shown on the figure are explained in more detail in subsequent sections. Briefly, the tailings consist of an upper, unsaturated (oxidizing) zone, and a much thicker saturated (reducing) zone.

The tailings contain significant quantities of gypsum and other sulphate complexes. Over time, these sulphate compounds dissolve, and are gradually depleted. The depletion is hypothesized to proceed as a series of fronts moving downward through the tailings. Since the different sulphate compounds have different solubilities, the fronts may move at different rates. The tailings above each front are thus depleted of the sulphate complex, while the layer below the front is enriched in the same compound.

The upper layer of the saturated zone has been specified for modelling purposes as a 'mixing layer' in which adsorption of several species may occur. This feature is built into the model to account for the natural retardation processes which occur in large tailings areas.

The aqueous phase concentrations of a number of chemical species are explicitly modelled. These include calcium ($Ca^{2+}$), sulphate ($SO_4^{2-}$), ferric and ferrous iron ($Fe^{III}$ and $Fe^{II}$). The pH of the aqueous phase is modelled as a function of several of these ions. As well, both the solid and liquid phase concentrations of a number of radionuclides (natural uranium, total thorium, radium-226 and lead-210) are included in the model.

The physical and chemical processes modelled include:

- pyrite oxidation
- gypsum dissolution and reprecipitation
- dissolution of uranium and thorium
- Ra-226 dissolution and coprecipitation with $BaSO_4$
- Pb-210 dissolution and coprecipitation with $PbSO_4$
- radioactive decay and ingrowth (as required)
- sheet erosion as a direct source of radionuclide loading
- tailings vegetation over time, resulting in reduced erosion

The necessary calculations are performed in a number of modules, as outlined on Figure 3.2. The modular structure has facilitated model development, review and implementation. Model structures and derivations are presented in the following sections, corresponding roughly to the modules indicated on Figure 3.2. A complete listing of the source model code is provided in Appendix A. Also included in the appendix is a variable dictionary which summarizes all the variables used in the models, and indicates symbols used in the computer implementation.

The tailings erosion and vegetation model is included as Section 3.14. It was developed separately from the remainder of the water source model and is included here since it acts as an additional source of radionuclide loading to the receiving environment. Section 3.14 contains a complete description and illustration of this model including the computer code listing and variable dictionary.

The dust and radon models indicated on Figure 3.2 are described in Chapter 4.

## 3.2 Initial Conditions - Ions and pH

As indicated on Figure 3.2, the initial condition calculations are performed in the first simulation time step, which is representative of the period from $-\Delta t$ years to zero years. The values calculated in this time step are considered representative of $t=0$ years. Thus the $t=0$ values do not represent

FIGURE 3.1

CONCEPT ADOPTED FOR MODELLING THE TAILINGS SOURCE TERM

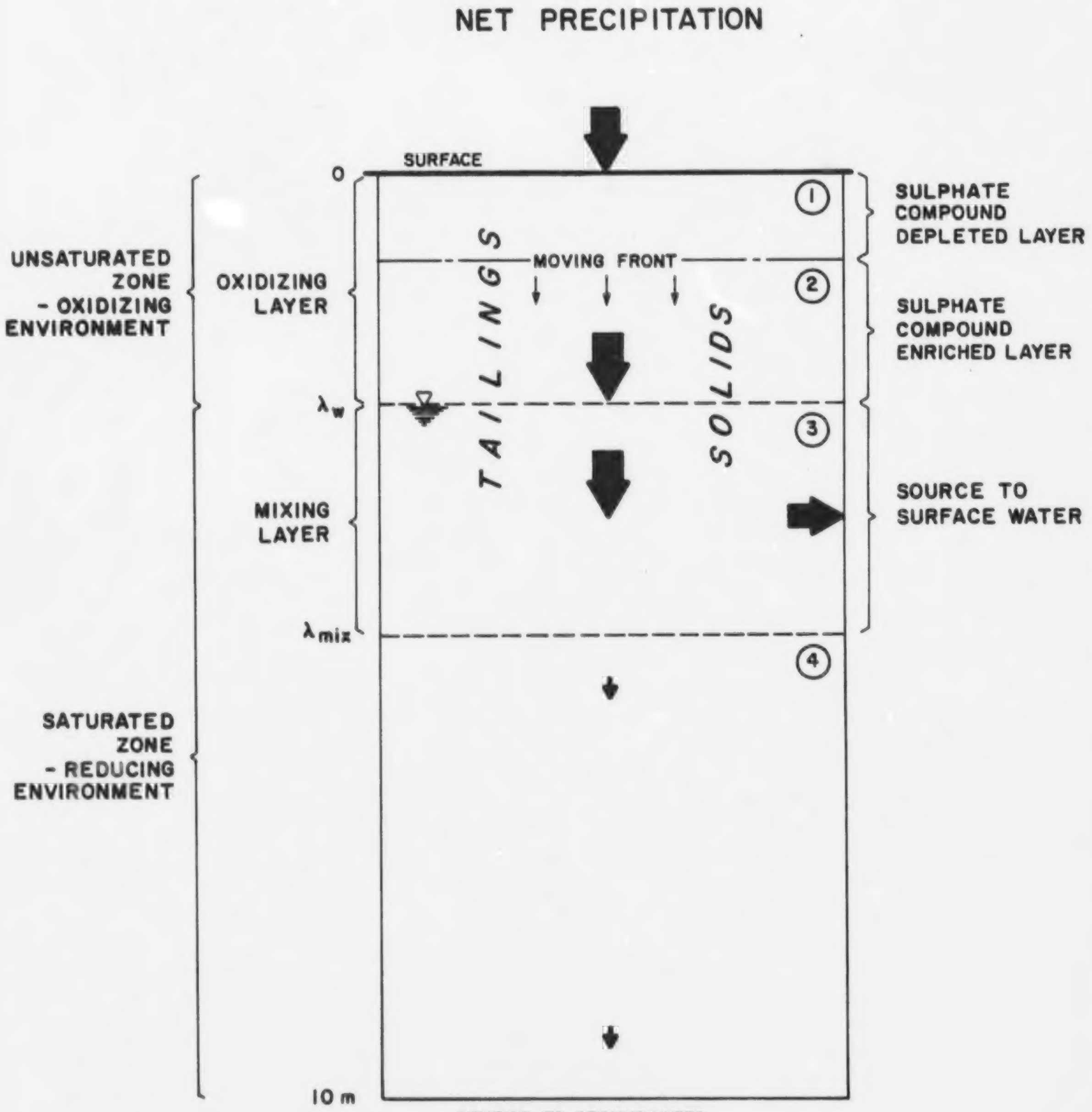
NET PRECIPITATION
SURFACE
0
① SULPHATE COMPOUND DEPLETED LAYER
MOVING FRONT
② SULPHATE COMPOUND ENRICHED LAYER
UNSATURATED ZONE - OXIDIZING ENVIRONMENT
OXIDIZING LAYER
TAILINGS SOLIDS
$\lambda_w$
③
MIXING LAYER
SOURCE TO SURFACE WATER
$\lambda_{mix}$
④
SATURATED ZONE - REDUCING ENVIRONMENT
10 m
SOURCE TO GROUNDWATER

FIGURE 3.2

STRUCTURE OF THE TAILINGS SOURCE MODEL

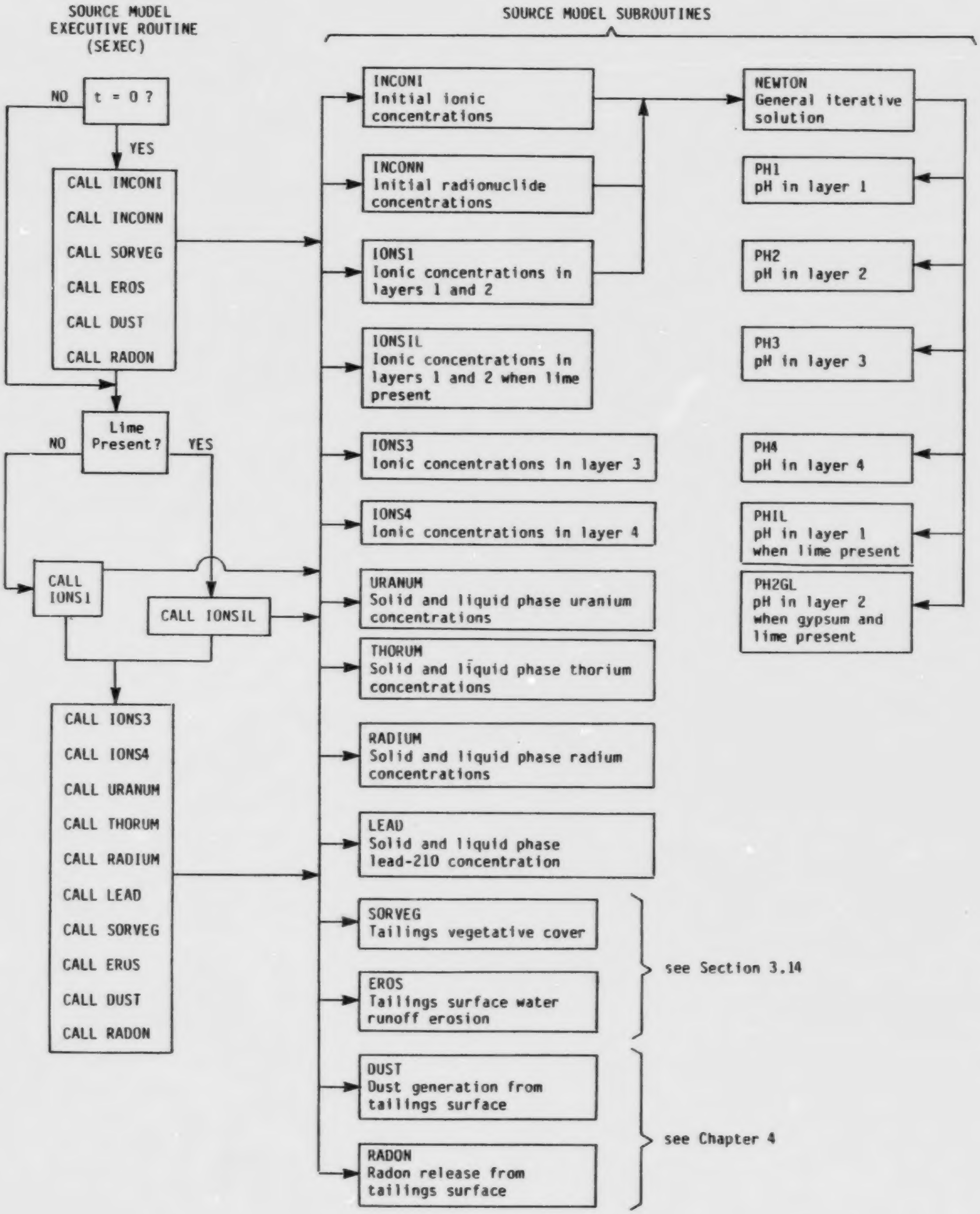
SOURCE MODEL
EXECUTIVE ROUTINE
(SEXEC)
SOURCE MODEL SUBROUTINES
t = 0 ?
NO
YES
CALL INCONI
CALL INCONN
CALL SORVEG
CALL EROS
CALL DUST
CALL RADON
Lime Present?
NO
YES
CALL IONS1
CALL IONSIL
CALL IONS3
CALL IONS4
CALL URANUM
CALL THORUM
CALL RADIUM
CALL LEAD
CALL SORVEG
CALL EROS
CALL DUST
CALL RADON
INCONI
Initial ionic concentrations
INCONN
Initial radionuclide concentrations
IONS1
Ionic concentrations in layers 1 and 2
IONSIL
Ionic concentrations in layers 1 and 2 when lime present
IONS3
Ionic concentrations in layer 3
IONS4
Ionic concentrations in layer 4
URANUM
Solid and liquid phase uranium concentrations
THORUM
Solid and liquid phase thorium concentrations
RADIUM
Solid and liquid phase radium concentrations
LEAD
Solid and liquid phase lead-210 concentration
SORVEG
Tailings vegetative cover
EROS
Tailings surface water runoff erosion
see Section 3.14
DUST
Dust generation from tailings surface
RADON
Radon release from tailings surface
see Chapter 4
NEWTON
General iterative solution
PH1
pH in layer 1
PH2
pH in layer 2
PH3
pH in layer 3
PH4
pH in layer 4
PHIL
pH in layer 1 when lime present
PH2GL
pH in layer 2 when gypsum and lime present

the initial, or background conditions of the environment in the absence of the tailings. Rather, they represent the initial or background conditions, affected for $\Delta t$ years by the presence of the tailings. Performing the calculations in this way builds one time step of "memory" into the system. It also eliminates many of the unrealistically sudden increases or decreases in calculated values which would otherwise be apparent.

The calculations described in this section therefore serve two purposes. First, a number of quantities (such as initial mass inventories, background concentrations, etc.) are initialized. Secondly, appropriate calculations, representative of the period $-\Delta t$ to 0 years, are performed.

Many of the calculations relevant in the first time period are also applicable to all other time steps. In these instances, no detailed derivations are provided in this section. Rather, reference is made to the appropriate derivation in a subsequent section. It may be most useful for the reader to skim this section quickly, and proceed to the subsequent, more detailed sections; returning to this section, as required, to determine initial conditions and calculations.

### 3.2.1 Initial Inventories

The initial inventory of pyrite ($FeS_2$) in the tailings is specified as an input parameter. That is:

$$[FeS_2]_{t=0} = [FeS_2]^o \qquad (3.2.1)$$

where:

$[FeS_2]^o$ = initial concentration of pyrite in tailings ($mol.m^{-3}$)

The initial inventory of anhydrous gypsum ($CaSO_4$), which is referred to throughout this report simply as gypsum, is calculated as a function of two input parameters:

$$g_o = \rho_T \, x_{gyp}/136 \qquad (3.2.2)$$

where:

$g_0$ = initial concentration of gypsum in tailings (mol.m$^{-3}$)
$\rho_T$ = tailings bulk density (g.m$^{-3}$)
$x_{gyp}$ = mass fraction of gypsum in tailings
136 = molecular weight of anhydrous gypsum (g.mol$^{-1}$)

### 3.2.2 Calcium and Sulphate Concentrations

Sulphates are formed as a result of pyrite oxidation in the unsaturated layer during the initial time step (i.e. $-\Delta t$ to $t=0$). The details of this process are presented in Section 3.3.1. In summary, it can be shown that:

$$[SO_4^{2-}]_{p,\lambda w} = \frac{2\lambda_w[FeS_2]^o\,[1-e^{-k\Delta t}]}{P\Delta t} \qquad (3.2.3)$$

where:

$[SO_4^{2-}]_{p,\lambda w}$ = initial sulphate concentration at $\lambda_w$ resulting from pyrite oxidation (mol.m$^{-3}$)
$\lambda_w$ = thickness of the unsaturated zone (m)
k = rate constant for pyrite oxidation (yr$^{-1}$) (see Section 3.3.1)
P = annual net precipitation (m.yr$^{-1}$)

Although little or no pyrite oxidation occurs in the mixing zone, the sulphates formed by this process in the unsaturated zone are transported downwards via infiltrating rainwater, resulting in an increased sulphate concentration in the mixing zone. This is expressed by (see Section 3.6.1):

$$[SO_4^{2-}]_{p,mix} = [SO_4^{2-}]_{p,\lambda w} - [SO_4^{2-}]_{p,\lambda w}\exp[-P\Delta t/\epsilon\lambda_{mix}] \qquad (3.2.4)$$

where:

$[SO_4^{2-}]_{p,mix}$ = initial sulphate concentration in the mixing zone resulting from pyrite oxidation in the unsaturated zone (mol.m$^{-3}$).
$\epsilon$ = porosity
$\lambda_{mix}$ = thickness of the mixing zone (m)

We assume that sulphate concentration resulting from pyrite oxidation in the bottom layer (layer 4) is zero in the first time step. That is:

$$[SO_4^{2-}]_{p,4} = 0 \quad \text{at } t=0 \tag{3.2.5}$$

where:

$[SO_4^{2-}]_{p,4}$ = initial sulphate concentration in the bottom layer (layer 4) resulting from pyrite oxidation in the unsaturated zone ($mol.m^{-3}$)

This indicates that the sulphates formed in the upper layer have not yet had an impact on the lower layer.

The total concentrations of calcium and sulphate can be calculated as functions of the concentrations of sulphates resulting from pyrite oxidation. In the unsaturated layer, the relationships are:

$$[Ca^{2+}]_{\lambda w} = \sqrt{\frac{K_s^o\, d}{f^2} + 0.25\, [SO_4^{2-}]_{p,\lambda w}^2} - 0.5\, [SO_4^{2-}]_{p,\lambda w} \tag{3.2.6}$$

and

$$[SO_4^{2-}]_{\lambda w} = \sqrt{\frac{K_s^o\, d}{f^2} + 0.25\, [SO_4^{2-}]_{p,\lambda w}^2} + 0.5\, [SO_4^{2-}]_{p,\lambda w} \tag{3.2.7}$$

where:

$[Ca^{2+}]_{\lambda w}$ = concentration of $Ca^{2+}$ at $\lambda_w$ ($mol.m^{-3}$)

$[SO_4^{2-}]_{\lambda w}$ = concentration of $SO_4^{2-}$ at $\lambda_w$ ($mol.m^{-3}$)

$K_s^o$ = solubility equilibrium constant for $CaSO_4$ ($mol^2.m^{-6}$)

f = activity coefficient for divalent ions

d = correction factor accounting for sulphate complexation

The details regarding these relationships are provided in Section 3.3.3.

In the mixing zone, the concentrations are given by:

$$[Ca^{2+}]_{mix} = \sqrt{\frac{K_s^o}{f^2} + 0.25\, [SO_4^{2-}]_{p,mix}^2} - 0.5\, [SO_4^{2-}]_{p,mix} \tag{3.2.8}$$

$$[SO_4^{2-}]_{mix} = \sqrt{\frac{K_s^o}{f^2} + 0.25\,[SO_4^{2-}]_{p,mix}^2} + 0.5\,[SO_4^{2-}]_{p,mix} \qquad (3.2.9)$$

Again, the details are provided elsewhere (Section 3.4.1).

In the bottom layer (layer 4), no sulphates resulting from pyrite oxidation are present. Hence, gypsum represents the only source of dissolved calcium and sulphate ions, and the original concentrations can be calculated from equilibrium considerations. Namely:

$$[SO_4^{2-}]_4 = [Ca^{2+}]_4 = \sqrt{\frac{K_s^o}{f^2}} \qquad (3.2.10)$$

### 3.2.3 Initial pH Levels

The derivations of the pH equations are provided elsewhere, and will not be repeated here. At t=0 years, a gypsum depleted layer does not really exist. Hence the pH for the unsaturated zone (layers 1 and 2) is calculated using the relationship for layer 2 (equation (3.6.22); as described in Section 3.6.2).

The pH of layers 3 and 4 is calculated using equation (3.6.32) (Section 3.6.3) with variables appropriate for the different layers.

### 3.2.4 Iron Concentrations

Iron exists in solution in the unsaturated zone in its oxidized state ($Fe^{III}$). The $[Fe^{III}]$ in the unsaturated zone is calculated as a function of the initial pH and $[SO_4^{2-}]$ in the same layer. The functional relationship is given by equation (3.3.44) in Section 3.3.4.

In the mixing zone, iron exists in its reduced state ($Fe^{II}$). From the stoichiometric relationship between $Fe^{III}$ and $Fe^{II}$ we can state:

$$[Fe^{II}]_{mix} = 1.5\ [Fe^{III}]_{\lambda w} \qquad (3.2.11)$$

where $[Fe^{III}]_{\lambda w}$ = concentration of $Fe^{III}$ in unsaturated zone ($mol.m^{-3}$)
$[Fe^{II}]_{mix}$ = concentration of $Fe^{II}$ in saturated zone (layer 3) ($mol.m^{-3}$)

Again, further information can be found in Section 3.4.4.

In keeping with our previous assumptions regarding the effects of pyrite oxidation in the bottom layer in the first time step, we assume that $[Fe^{II}]$ in layer 4 is zero in the first time step. That is:

$$[Fe^{II}]_4 = 0 \quad \text{at } t=0 \qquad (3.2.12)$$

## 3.3 Ions - Layers 1 and 2

The concentrations of dissolved calcium $[Ca^{+2}]$ and sulphate $[SO_4^{2-}]$ ions in layers 1 and 2 are primarily dependent on two phenomena. First, gypsum ($CaSO_4$) formed during the neutralization of tailings in the mill, dissolves to yield $Ca^{2+}$ and $SO_4^{2-}$. Secondly, pyrite ($FeS_2$) in the tailings undergoes oxidation resulting in $SO_4^{2-}$ production. These phenomena and their effects are discussed in more detail in the following sections.

### 3.3.1 Sulphates Derived From Pyrite Oxidation

The oxidation of pyrite is initiated by the action of ferric ion on the pyrite surface (Nordstrom, 1982):

$$FeS_2 + 2\ Fe^{+3} \longrightarrow 3\ Fe^{+2} + 2\ S_o \qquad (3.3.1)$$

The reduced iron ($Fe^{+2}$) in solution is rapidly oxidized to the ferric state by bacteria:

$$2\ Fe^{+2} + 2\ H^+ + \frac{1}{2}\ O_2 \longrightarrow 2\ Fe^{+3} + H_2O \qquad (3.3.2)$$

The rate determining step is the bacterial oxidation of the sulphur layer on the pyritic surface leading to the overall stoichiometry:

$$2\ FeS_2 + 7.5\ O_2 + H_2O \longrightarrow 2\ Fe^{3+} + 2\ H^+ + 4\ SO_4^{2-} \qquad (3.3.3)$$

From the above relationship, it is apparent that the rate of pyrite oxidation is stoichiometrically related to the rate of sulphate formation as follows:

$$-\frac{d\,[FeS_2]}{dt} = \frac{1}{2}\frac{d[SO_4^{2-}]}{dt} \qquad (3.3.4)$$

The rate of pyrite oxidation is assumed to be first order with respect to pyrite content, i.e.:

$$-\frac{d\,[FeS_2]}{dt} = k[FeS_2] \qquad (3.3.5)$$

It follows, that the initial rate of oxidation is given by:

$$-\frac{d\,[FeS_2]}{dt}\bigg|_{t=0} = k[FeS_2]^o \qquad (3.3.6)$$

where $[FeS_2]^o$ is the initial pyrite content. From equation (3.3.4) it is evident that the specific rate of pyrite oxidation (k) is related to the rate of sulphate generation as follows:

$$k = \frac{1/2\ \dfrac{d\,[SO_4^{2-}]}{dt}}{[FeS_2]^o}\Bigg|_{t=0} \qquad (3.3.7)$$

The rate of sulphate formation, in turn, can be related to the flux of sulphate exiting from the unsaturated zone as:

$$\frac{d\,[SO_4^{2-}]}{dt}\bigg|_{t=0} = \frac{J_s}{\lambda_w} \qquad (3.3.8)$$

where:

$J_s$ = sulphate flux ($mol.m^{-2}.yr^{-1}$)

$\lambda_w$ = thickness of the unsaturated zone (m)

An expression for the sulphate flux in an unsaturated zone has been derived previously (SENES, 1984) as it is related to the oxygen flux into the tailings and the stoichiometry of pyrite oxidation:

$$J_S = \left[ \frac{8}{7.5} \bar{R}_S \, \rho_T \, [O_2] \, D_{O_2} \left( 1 - K' \ln \left( \frac{1 + K'}{K'} \right) \right) \right]^{1/2} \qquad (3.3.9)$$

$\bar{R}_S$ = sulphate production rate ($mol.g^{-1}.yr^{-1}$)
$[O_2]$ = oxygen concentration on the surface ($mol.m^{-3}$)
$D_{O_2}$ = oxygen diffusivity through tailings ($m^2.yr^{-1}$)
$\rho_T$ = density of tailings ($g.m^{-3}$)
K' = $K_{O_2}/[O_2]$ = ratio of $O_2$ half saturation constant to the oxygen concentration $[O_2]$

Substituting equation (3.3.8) into equation (3.3.7) defines k as:

$$k = \frac{J_S}{2 \lambda_w [FeS_2]^o} \qquad (3.3.10)$$

Let us define a time period "Δt". Since pyrite oxidation is assumed to be uniform throughout the unsaturated zone, the moles of remaining pyrite per tailings volume after time t is given by integrating equation (3.3.5) between t-Δt and t:

$$[FeS_2]_t = [FeS_2]_{t-\Delta t} \, e^{-k\Delta t} \qquad (3.3.11)$$

Since such an exponential function can lead to increasingly small values, particularly if kΔt is large, a lower bound on the calculated value of $[FeS_2]$ of $1 \times 10^{-6}$ $mol.m^{-3}$ was imposed. That is:

if $[FeS_2]_t \leq 1.0 \times 10^{-6}$
then $[FeS_2]_t = 1.0 \times 10^{-6}$

The moles of pyrite/volume oxidized during the time period t-Δt to t is therefore as follows:

$$\Delta[FeS_2]_{t-\Delta t \rightarrow t} = [FeS_2]_{t-\Delta t} \, [1 - e^{-k\Delta t}] \qquad (3.3.12)$$

Assuming, that the precipitation (P in $m.yr^{-1}$) is constant during the time step of choice (Δt), the sulphate concentration in the liquid phase at $\lambda_w$

resulting from pyrite oxidation is given by :

$$[SO_4^{2-}]_{p,\lambda w} = \frac{2\ \lambda_w [FeS_2]_{t-\Delta t}\ [1 - e^{-k\Delta t}]}{P\ \Delta t} \qquad (3.3.13)$$

where

$[SO_4^{2-}]_{p,\lambda w}$ = sulphate concentration at $\lambda_w$ resulting from pyrite oxidation ($mol.m^{-3}$)

Note, that equation (3.3.13) defines a time-averaged sulphate concentration for the time period t-Δt to t. During this time period, the precipitation rate (P) is held constant, but can vary for the next time period Δt.

Pyrite oxidation acts as the long-term source of sulphates in the system. It can be seen from equation (3.3.13) that this quantity may become very small over time. Thus, we considered it appropriate to include the background sulphate concentration present in the precipitation (P). Equation (3.3.13) can be re-written to include this background source of sulphate:

$$[SO_4^{2-}]_{p,\lambda w} = \frac{2\ \lambda_w\ [FeS_2]_{t-\Delta t}\ [1-e^{-k\Delta t}]}{P\Delta t} + 0.1 \qquad (3.3.14)$$

where:

0.1 = $[SO_4^{2-}]$ in precipitation ($mol.m^{-3}$)

The term $[SO_4^{2-}]_{p,\lambda w}$ now represents sulphates resulting from pyrite oxidation plus that naturally present in rainwater.

It has been shown previously (SENES, 1985), that if pyrite oxidation is uniform throughout the oxidizing zone, the sulphate concentration resulting from pyrite oxidation at any distance ($z \leq \lambda_w$) into the tailings is given by:

$$[SO_4^{2-}]_{p,z} = [SO_4^{2-}]_{p,\lambda w} \left(\frac{z}{\lambda_w}\right) \qquad (3.3.15a)$$

This implies, that the time-averaged sulphate concentration at "z" from pyrite oxidation is given by:

$$[SO_4^{2-}]_{p,z} = \frac{2z\,[FeS_2]_{t-\Delta t}\,[1 - e^{-k\Delta t}]}{P\Delta t} + 0.1 \qquad (3.3.15b)$$

### 3.3.2 Gypsum Dissolution and Reprecipitation

In pyritic tailings, it is not uncommon to observe an increase in sulphate concentration with depth. Due to this phenomenon, some of the gypsum which dissolves in the upper portions of the unsaturated zone will reprecipitate (as the $[SO_4^{2-}]$ increases) in the lower portions of the zone. Thus the unsaturated zone can be thought to consist of an upper layer, in which all the gypsum has dissolved and migrated downward with the porewater, and a lower layer in which some of the gypsum has reprecipitated. These are referred to as the gypsum-depleted layer (layer 1) and the gypsum-enriched layer (layer 2) in this discussion. The relative heights of these two layers will change with time; the depleted zone increasing until the entire unsaturated zone is depleted of gypsum. After this time, a number of physical and chemical processes can be ignored and the source term model becomes simpler.

The solubility of gypsum, and hence the concentration of $[Ca^{2+}]$ is dependent on the solubility product as follows:

$$\frac{K^{o}_{s,CaSO_4}}{\left(f_{Ca^{2+}}\right)\left(f_{SO_4^{2-}}\right)} = [SO_4^{2-}]\;\;[Ca^{2+}] \qquad (3.3.16)$$

where:

$K^{o}_{s,CaSO_4}$ = solubility equilibrium constant (25.0 $mol^2.m^{-6}$)

$f_{Ca^{2+}}$ = activity coefficient (calcium ion)

$f_{SO_4^{2-}}$ = activity coefficient (sulphate ion)

The activity coefficients, assumed to be essentially equal (i.e. f) depend on a number of factors (e.g. ionic strength of solution, temperature, etc.) and are assigned an appropriate distribution in the probabilistic analysis.

It may be assumed that the limestone ($CaCO_3$) content of pyritic tailings is rapidly depleted due to acid generation resulting from pyrite oxidation above the water table. Thus, the dissolution of gypsum is the major source of calcium during the initial years. On the other hand, pyrite oxidation of tailings contributes significantly to the sulphate concentration in the porewater. That is:

$$[Ca^{2+}] = [Ca^{2+}]_g \qquad (3.3.17)$$

$$[SO_4^{2-}] = [SO_4^{2-}]_g + [SO_4^{2-}]_p \qquad (3.3.18)$$

where:

$[Ca^{2+}]_g$ = dissolved calcium derived from gypsum ($mol.m^{-3}$)
$[SO_4^{2-}]_g$ = dissolved sulphate derived from gypsum ($mol.m^{-3}$)
$[SO_4^{2-}]_p$ = dissolved sulphate derived from pyrite oxidation ($mol.m^{-3}$)

In the relationship expressed above:

$$[Ca^{2+}]_g = [SO_4^{2-}]_g$$

Hence, substituting into the equation given previously for the solubility product (equation (3.3.16)) the following expression is obtained:

$$\frac{K^o_{s,CaSO_4}}{f^2} = ([SO_4^{2-}]_p + [SO_4^{2-}]_g)\,[Ca^{2+}]_g \qquad (3.3.19)$$

or

$$\frac{K^{o}_{s,CaSO_4}}{f^2} = [SO_4^{2-}]_p\ [Ca^{2+}]_g + [Ca^{2+}]_g^2 \qquad (3.3.20)$$

Solving equation (3.3.20) for $[Ca^{2+}]$ (or $[Ca^{2+}]_g$) gives:

$$[Ca^{2+}] = \sqrt{\frac{K^{o}_{s,CaSO_4}}{f^2} + 0.25\ [SO_4^{2-}]_p^2} - 0.5\ [SO_4^{2-}]_p \qquad (3.3.21)$$

Thus, determination of the $[Ca^{2+}]$ depends on the concentration of sulphate due to pyrite oxidation. This result is quite significant and forms the basis of much of the following discussion.

Let us assume that at time "t", the gypsum-depleted layer (layer 1) has advanced to a distance "h".

Let $\left(\frac{K_s^o}{f^2}\right)^{\frac{1}{2}} = a$

and note that from equation (3.3.13):

$$0.25\ [SO_4^{2-}]^2_{p,h} = (0.25)\ \frac{4h^2\ [FeS_2]^2_{t-\Delta t}\ [1 - e^{-k\Delta t}]^2}{(P\Delta t)^2}$$

$$= \frac{h^2\ [FeS_2]^2_{t-\Delta t}\ [1 - e^{-k\Delta t}]^2}{(P\Delta t)^2} \qquad (3.3.22)$$

Let $[FeS_2]_{t-\Delta t}\ (1 - e^{-k\Delta t}) = \beta$

Thus, $0.25\ [SO_4^{2-}]^2_{p,h} = \frac{\beta^2 h^2}{(P\Delta t)^2}$

and $0.5\ [SO_4^{2-}]_{p,h} = \frac{\beta h}{P\Delta t}$ (3.3.23)

The term accounting for sulphate concentration in rainwater (0.1 $mol.m^{-3}$) is not included in the above expression (3.3.22) and in the subsequent derivation. This is done because the rainwater contribution is insignificant relative to the contribution from pyrite oxidation over the several hundred years for which the following equations are used (i.e. until gypsum depletion occurs between 100 and 200 years).

The sulphate concentration in equation (3.3.22), of course, refers to a time-averaged sulphate (from pyrite) concentration for the time period t-Δt to t. Now, let us assume that during this time period, the gypsum-depleted layer (layer 1) advances a distance Δh. It seems appropriate to assume that the sulphate concentration term can be represented by the "midpoint" between h and h + Δh, where the depth of the front at t-Δt is h, i.e.:

$$[SO_4^{2-}]_{p,h \rightarrow h+\Delta h} = \frac{2\ (h+\Delta h/2)\ [FeS_2]_{t-\Delta t}\,[1 - e^{-k\Delta t}]}{P\Delta t} \qquad (3.3.24)$$

Thus, the advancement of the gypsum depleted front is given by:

$$g_o\Delta h = P\Delta t \left\{ \left[a^2 + \frac{\beta^2(h+\Delta h/2)^2}{(P\Delta t)^2}\right]^{1/2} - \frac{\beta\ (h+\Delta h/2)}{P\Delta t} \right\} \qquad (3.3.25)$$

where:

$g_o$ = initial gypsum concentration in the tailings ($mol.m^{-3}$)

Solving for Δh yields:

$$\Delta h = \left[\frac{\beta^2\ h^2_{t-\Delta t}}{(g_o+\beta)^2} + \frac{(P\Delta t)^2\ a^2}{g_o^2 + g_o\beta}\right]^{1/2} - \frac{\beta h_{t-\Delta t}}{g_o+\beta} \qquad (3.3.26)$$

where:

$$h_{t-\Delta t} = \sum_{t=0}^{t-\Delta t} \Delta h \qquad (3.3.27)$$

Thus, $h_t = h_{t-\Delta t} + \Delta h$ (3.3.28)

The time-averaged calcium concentration for the time period t-Δt to t at $\lambda_w$ can be easily derived by substituting equation (3.3.13) into equation (3.3.21) to yield:

$$[\mathrm{Ca}^{2+}]_{\lambda w, t-\Delta t \rightarrow t} = \left[ a^2 + \frac{\lambda_w^2 \beta^2}{(P\Delta t)^2} \right]^{1/2} - \frac{\lambda_w \beta}{P\Delta t} \qquad (3.3.29)$$

Thus, the dissolved gypsum (i.e. dissolved calcium/unit area) leaving the unsaturated zone during t-Δt and t is given by:

$$N_{\mathrm{Ca}^{2+}} = P\Delta t \left\{ \left[ a^2 + \frac{\lambda_w^2 \beta^2}{(P\Delta t)^2} \right]^{1/2} - \frac{\lambda_w \beta}{P\Delta t} \right\}$$

or

$$N_{\mathrm{Ca}^{2+}} = \left[ a^2 \, (P\Delta t)^2 + \lambda_w^2 \, \beta^2 \right]^{1/2} - \lambda_w \beta \qquad (3.3.30)$$

The mass of gypsum/unit area (Δm) that has precipitated in zone 2 during t-Δt and t is the difference between the total amount of gypsum dissolved, $g_o \Delta h$ ($g_o$ times equation (3.3.26)) and the amount of gypsum leaving the unsaturated zone, given by equation (3.3.30), i.e.:

$$\Delta m_{t-\Delta t \rightarrow t} = g_o \left\{ \left[ \frac{\beta^2 h_{t-\Delta t}}{(g_o + \beta)^2} + \frac{(P\Delta t)^2 \, a^2}{g_o^2 + g_o \beta} \right]^{1/2} - \frac{\beta h_{t-\Delta t}}{g_o + \beta} \right\} - \left[ a^2 \, (P\Delta t)^2 + \lambda_w^2 \, \beta^2 \right]^{1/2} + \lambda_w \beta \qquad (3.3.31)$$

note that:

$$m_{t-\Delta t} = \sum_{t=0}^{t-\Delta t} \Delta m \qquad (3.3.32)$$

and:

$$m_t = m_{t-\Delta t} + \Delta m \qquad (3.3.33)$$

The fraction of gypsum remaining in the unsaturated zone at any time t is given by:

$$f_{gypsum} = \frac{(\lambda_w - h_t)\, g_o + m_t}{\lambda_w\, g_o} \qquad (3.3.34)$$

### 3.3.3 Calcium and Sulphate Concentrations

Prior to gypsum depletion in the unsaturated zone (layers 1 and 2) the concentrations of $Ca^{2+}$ and $SO_4^{2-}$ are different in the two layers. Following depletion, layers 1 and 2 are assumed to have the same physical and chemical characteristics (including the concentrations of $SO_4^{2-}$ and $Ca^{2+}$). The calculations in both layers prior to depletion are discussed below followed by those appropriate for the gypsum depleted situation.

Since layer 1 contains, by definition, no gypsum, the concentrations of $Ca^{2+}$ and $SO_4^{2-}$ are easily calculated. We assume that, in the absence of gypsum, the concentration of $Ca^{2+}$ is zero. That is:

$$[Ca^{2+}]_1 = 0 \qquad (3.3.35)$$

In the absence of gypsum, the only source of dissolved sulphate is pyrite oxidation. The sulphate concentration in layer 1 is taken to be equal to the sulphate concentration at h, the interface between layers 1 and 2. Hence, from equation (3.3.15):

$$[SO_4^{2-}]_1 = [SO_4^{2-}]_{p,h} = \frac{2h\, [FeS_2]_{t-\Delta t}[1-e^{-k\Delta t}]}{P\Delta t} + 0.1 \qquad (3.3.36)$$

The calculation of $[Ca^{2+}]$ and $[SO_4^{2-}]$ in layer 2 is somewhat more involved. Estimates of these concentrations, based on equilibrium considerations, can be obtained using equations presented in the previous section (e.g. equation

(3.3.21)). However, at the low pH values expected initially in layer 2, the concentration of free sulphate (and hence of calcium) is reduced by the complexation of the sulphate ligand with the ferric ion and the aluminum ion, i.e.:

$$Fe^{3+} + SO_4^{2-} \leftrightharpoons FeSO_4^{+}$$

$$Al^{3+} + SO_4^{2-} \leftrightharpoons AlSO_4^{+}$$

These complexation reactions, in turn reduce the concentration of free sulphate somewhat.

The ratio between free (uncomplexed) sulphate and total sulphate can be expressed as:

$$\frac{[SO_4^{2-}]_u}{[SO_4^{2-}]_{total}} = \frac{1}{d} \qquad (3.3.37)$$

The factor "d" quantifies the amount of sulphates which exist as ferric or aluminum complexes and is given by:

$$d = 1 + f^3\, 10^{8.99-3pH} + f^{3/4}\, 10^{9.7-3pH} \qquad (3.3.38)$$

The calculation of pH in layer 2, as well as further rationale for the above expression, is outlined in Section 3.6.2.

Since $[SO_4^{2-}]_{total} = [Ca^{2+}] + [SO_4^{2-}]_p$

$$[Ca^{2+}]\,[SO_4^{2-}]_u = [Ca^{2+}] \left[\frac{[Ca^{2+}] + [SO_4^{2-}]_p}{d}\right] = \frac{K_s^o}{f^2}$$

$$[Ca^{2+}]_{\lambda w} = \sqrt{\frac{K_s^o d}{f^2} + 0.25\, [SO_4^{2-}]_{p,\lambda w}^2} - 0.5\, [SO_4^{2-}]_{p,\lambda w} \qquad (3.3.39)$$

and

$$[SO_4^{2-}]_{\lambda w} = \sqrt{\frac{K_s^o d}{f^2} + 0.25\, [SO_4^{2-}]_{p,\lambda w}^2} + 0.5\, [SO_4^{2-}]_{p,\lambda w} \qquad (3.3.40)$$

This value ($[SO_4^{2-}]_{\lambda w}$) represents the concentration of total sulphates present. The concentration of uncomplexed (free) sulphate ($[SO_4^{2-}]_u$) is simply:

$$[SO_4^{2-}]_{u,\lambda w} = \frac{[SO_4^{2-}]_{\lambda w}}{d} \tag{3.3.41}$$

The previous calculations are applicable prior to gypsum depletion in the unsaturated zone. Once the gypsum is entirely depleted (i.e. layer 2 becomes vanishingly small) the situation is simplified considerably. The appropriate equations for this instance are those presented earlier for layer 1. That is:

$$[Ca^{2+}]_{\lambda w} = 0.0 \tag{3.3.42}$$

$$[SO_4^{2-}]_{\lambda w} = [SO_4^{2-}]_{p,\lambda w} = \frac{2\lambda_w[FeS_2]_{t-\Delta t}[1-e^{-k\Delta t}]}{P\Delta t} \tag{3.3.43}$$

### 3.3.4 Iron Concentration

The total iron concentration in the unsaturated zone (at either h or $\lambda_w$) is dependent on the pH and the total sulphate concentration. In these calculations, equilibrium with ferric hydroxide is assumed. As outlined in Section 3.6.1, the most significant dissolved iron (III) complexes include $Fe^{3+}$, $Fe(OH)^{2+}$, $Fe(OH)_2^+$ and $FeSO_4^+$. Considering these species, the total dissolved iron concentration at $\lambda_w$ is given by the following expression:

$$[Fe^{III}]_{\lambda w,} = 10^{5.97-3pH} + 10^{3.78-2pH} + 10^{0.3-pH}$$

$$+ \frac{[SO_4^{2-}]_{\lambda w}}{1000}\left[\frac{f^3\ 10^{8.99-3pH}}{1 + f^{3/4}\ 10^{9.7-3pH} + f^3\ 10^{8.99-3pH}}\right] \tag{3.3.44}$$

The factor of 1000 is included to convert $[SO_4^{2-}]$ from mol.m$^3$ to mol.L$^{-1}$. The calculated value ($[Fe^{III}]_{\lambda w}$) is thus in mol.L$^{-1}$ and must be converted to mol.m$^{-3}$.

### 3.3.5 Modifications for Limestone Addition

The preceeding discussion applies to tailings which have been discharged and allowed to evolve without intervention. This will result in relatively low porewater pH levels for the first 100 or so years, primarily as a result of pyrite oxidation. The models have also been constructed to allow the assessment of another scenario; in which significant quantities of limestone are incorporated into the unsaturated tailings layer. The modifications necessary to model limestone additions are described in this section. Any calculations described in previous sections and not addressed specifically in this section remain unchanged, since they are not affected directly by limestone addition. Furthermore, none of the models for tailings layers below the oxidizing zone differ structurally from those that were developed previously.

#### Initial Inventory

The initial concentration of limestone ($CaCO_3$; also referred to as calcite), is calculated as a function of the mass fraction of calcite incorporated into the tailings. Namely:

$$[CaCO_3]^o = X_{Lime}\rho_T/100 \qquad (3.3.45)$$

where:

$[CaCO_3]^o$ = initial inventory of calcite ($mol.m^{-3}$)
$X_{Lime}$ = initial mass fraction of $CaCO_3$ in tailings
$\rho_T$ = tailings bulk density ($g.m^{-3}$)
100 = molecular weight of $CaCO_3$ ($g.mol^{-1}$)

#### Pyrite Oxidation

The primary consequence of limestone addition to the tailings is the maintenance of pH values near neutrality in the porewater. It has been shown that elevated pH values reduce the role of bacteria in the oxidation process. Nevertheless, pyrite oxidation would proceed at a reduced rate.

The reaction rate, and hence the sulphate flux resulting from pyrite oxidation, is estimated to be 1/10 to 1/20 of the observed bacteria-assisted rate (flux). It is convenient to express this sulphate generation flux as a fraction of the sulphate flux without calcite addition.

Thus, the sulphate generation flux would become:

$$J'_s = \frac{1}{20} J_s \qquad (3.3.46)$$

where:
$J'_s$ = sulphate flux with limestone present (mol.m$^{-2}$.yr$^{-1}$)
$J_s$ = sulphate flux with no limestone present (mol.m$^{-2}$.yr$^{-1}$)

The molar mass balance for the rate of pyrite oxidation in a volume element $\lambda_w A$ must be equal to one half the sulphate export from this volume element:

$$- \lambda_w \frac{d\,[FeS_2]}{dt} = \frac{1}{2} J'_s \qquad (3.3.47)$$

Assuming first order kinetics as previously, the reaction rate at any time "t" is given by:

$$- \frac{d\,[FeS_2]}{dt} = k'\,[FeS_2] \qquad (3.3.48)$$

where:
$[FeS_2]$ = pyrite concentration (mol.m$^{-3}$ tailings)
$k'$ = chemical rate constant of pyrite oxidation (yr$^{-1}$)

Based on initial conditions $[FeS_2]^0$; the first order rate constant for pyrite oxidation in the presence of calcite is as follows:

$$k' = \frac{J'_s}{2\lambda_w [FeS_2]^0} \qquad (3.3.49)$$

As in the calcite-free system, the moles of pyrite oxidized per unit volume between t-Δt and t can be expressed as:

$$\Delta[FeS_2]_{t-\Delta t \quad t} = [FeS_2]_{t-\Delta t}(1 - e^{-k'\Delta t}) \qquad (3.3.50)$$

Again a lower limit of 1.0 x $10^{-6}$ mol.m$^{-3}$ is imposed on $[FeS_2]_t$.

The sulphate concentration from pyrite oxidation in the porewater at $\lambda_w$ is equal to:

$$[SO_4^{2-}]_{p,\lambda w} = \frac{2\lambda_w[FeS_2]_{t-\Delta t}(1 - e^{-k't})}{P\Delta t} + 0.1 \qquad (3.3.51)$$

Calcium and Sulphate Concentrations

When both gypsum and calcite are present simultaneously, the following two equilibria must be satisfied:

$$CaSO_4 \qquad Ca^{2+} + SO_4^{2-} \rightleftharpoons \qquad K_s^o = 10^{-4.6} \qquad (3.3.52)$$

$$CaCO_3(s) + H^+ \qquad Ca^{2+} + HCO_3^- \rightleftharpoons \quad {}^*K_s{}^o = 10^{2.13} \text{ (at 10°C)} \qquad (3.3.53)$$

Recognizing that ${}^*K_s^o$ is dependent on the temperature, an annual average temperature of 10°C for the porewater in the unsaturated zone is used herein.

To illustrate the above situation, consider the dissolution of gypsum (g) and calcite (c) in the porewater containing sulphate from both pyrite oxidation (p*) and rainwater (r). Note the ratio of $Ca^{+2}$ to $SO_4^{2-}$ in rainwater = 0.2, hence:

$$[Ca^{2+}] = c + g + 0.2\ r$$

and

$$[SO_4^{2-}] = g + p^* + r$$

A mass balance on the basis of the equilibrium conditions expressed by equations (3.3.52) and (3.3.53) yields the following:

$$(c + g + 0.2\ r)\ (g + p^* + r) = \frac{10^{-4.6}}{f^2} \qquad (3.3.54)$$

$$(c + g + 0.2\ r)\ ([HCO_3^-]) = \frac{10^{2.13}\,[H^+]}{f^{5/4}} \qquad (3.3.55)$$

where:

$c$ = concentration of "dissolved calcite" calcium ($mol.L^{-1}$)

$g$ = concentration of "dissolved gypsum" calcium ($mol.L^{-1}$)

$p^*$ = sulphate concentration resulting from pyrite oxidation ($mol.L^{-1}$)

$r$ = sulphate concentration in rainwater ($10^{-4} mol.L^{-1}$)

In the unsaturated zone, bicarbonate $[HCO_3^-]$ is not conserved, rather, the concentration is an equilibrium value with respect to the partial pressure of $CO_2$ in the gas phase. In calcite-rich porewaters, the partial pressure of $CO_2$ ($P_{CO_2}$) is expected to vary from $10^{-3.5}$ atm at the surface to $2\times10^{-2}$ atm at the lower limit of the unsaturated zone ($\lambda_w$). It would be reasonable to assume an average value of $10^{-2}$ atm (Stumm and Morgan, 1981). Using this value of $10^{-2}$ (at 10°C), the concentration of dissolved $CO_2$ / carbonic acid in the porewater is:

$$[H_2CO_3] = K_H P_{CO2} = (10^{-1.27})\ (10^{-2}) = 10^{-3.27}\ M \qquad (3.3.56)$$

The dissociation constant for carbonic acid ($H_2CO_3$) at 10°C is $10^{-6.46}$:

$$H_2CO_3 \rightleftharpoons H^+ + HCO_3 \qquad \log K = -6.46 \qquad (3.3.57)$$

The bicarbonate concentration as a function of pH is, therefore:

$$[HCO_3] = \frac{10^{pH-9.73}}{f^{1/4}} \qquad (3.3.58)$$

Substituting the result of equation (3.3.58) into equation (3.3.55) (calcite equilibrium) we obtain:

$$[Ca^{+2}]_{\lambda w} = 1000\ (c + g + 0.2\ r) = 1000\left(\frac{10^{11.86\ -\ 2pH}}{f}\right) \qquad (3.3.59)$$

and from gypsum equilibrium:

$$[SO_4^{2-}]_{\lambda w} = 1000\ (g + p^* + r) = \left(1000\ \frac{10^{2pH\ -\ 16.46}}{f}\right) \quad (3.3.60)$$

where:

$[Ca^{2+}]_{\lambda w}$ = calcium concentration at $\lambda_w$ ($mol.m^{-3}$)

$[SO_4^{2-}]_{\lambda w}$ = sulphate concentration at $\lambda_w$ ($mol.m^{-3}$)

From equation (3.3.60), the sulphate concentration resulting from gypsum dissolution is (at $\lambda_w$):

$$g_{\lambda w} = \frac{10^{2pH-16.46}}{f} - p^* - r \quad (3.3.61)$$

$$g_{\lambda w} = \frac{10^{2pH-16.46}}{f} - \frac{2\lambda_w\ [FeS_2]_{t-\Delta t}\ (1 - e^{-k'\Delta t})}{1000\ (P\Delta t)} - 10^{-4} \quad (3.3.62)$$

Similarly, at some distance $h \leq \lambda_w$:

$$g_h = \frac{10^{2pH-16.46}}{f} - \frac{2h\ [FeS_2]_{t-\Delta t}\ (1 - e^{-k'\Delta t})}{1000\ (P\Delta t)} - 10^{-4} \quad (3.3.63)$$

These equations are written with concentrations implicitly expressed in molar quantities ($mol.L^{-1}$). In keeping with the rest of the model, these may be rewritten with concentrations expressed in $mol.m^{-3}$. For example, equation (3.3.63) can be written as:

$$g_h = 1000\left(\frac{10^{2pH-16.46}}{f} - 10^{-4}\right) - \left(\frac{2h\ [FeS_2]_{t\Delta t}\ (1 - e^{-k'\Delta t})}{P\Delta t}\right) (3.3.64)$$

Since:

$$g_0 \Delta h = g_h P \Delta t$$

We can calculate $\Delta h$:

$$\Delta h = \frac{1}{g_0}\left\{1000\left(\frac{10^{2pH-16.46}}{f} - 10^{-4}\right)P\Delta t - 2h\,[FeS_2]_{t\Delta t}\,(1 - e^{-k'\Delta t})\right\} \tag{3.3.65}$$

Gypsum is depleted from the unsaturated layer when:

$$\Sigma\Delta h = \lambda_w \tag{3.3.66}$$

From equation (3.3.59), it is evident that the concentration of calcium resulting from calcite dissolution is:

$$c = \frac{10^{11.86-2pH}}{f} - g - 0.2\ r \tag{3.3.67}$$

We have defined g (at $\lambda_w$ by equation (3.3.62). Substituting equation (3.3.62) into equation (3.3.67) yields:

$$c_{\lambda w} = 1000\left(\frac{10^{11.86-2pH}}{f} - \frac{10^{2pH-16.47}}{f} + 0.8\text{x}10^{-4}\right) + \frac{2\lambda_w[FeS_2]_{t-\Delta t}\,(1-e^{-k'\Delta t})}{P\Delta t} \tag{3.3.68}$$

Once gypsum is depleted, the gypsum term is removed from the above equation. In this case, calcium resulting from calcite dissolution is expressed as:

$$c_{\lambda w} = \left(1000\ \frac{10^{11.86-2pH}}{f} - 0.2\text{x}10^{-4}\right) \tag{3.3.69}$$

Calcite is thus depleted when:

$$\Sigma c_{\lambda w}P\Delta t = [CaCO_3]^o\lambda_w \tag{3.3.70}$$

where:

$[CaCO_3]^o$ = initial calcite inventory (mol.m$^{-3}$)

Once calcite is depleted from the unsaturated layer, all of relationships obtained previously (i.e. calcite-free environment) apply. In particular, the pyrite oxidation rate returns to its previous level and the pH equations derived previously apply.

## 3.4 Ions - Layer 3

### 3.4.1 Calcium and Sulphate Concentrations Prior to Gypsum Depletion

Let us define:

$V_T$ = total volume of the mixing zone ($m^3$)

$\epsilon$ = porosity of tailings

$A$ = tailings surface area ($m^2$)

$\lambda_{mix}$ = thickness of mixing zone (m)

The volume, $V_L$, of the mixing zone occupied by porewater is given by:

$$V_L = \epsilon \lambda_{mix} A \qquad (3.4.1)$$

where:

$V_L$ = volume occupied by porewater ($m^3$)

If F is defined as the volumetric flowrate of water in and out of the mixing zone, the time-averaged flow between t-Δt and t is given by:

$$F = PA \qquad (3.4.2)$$

where:

F = flowrate into and out of mixing zone ($m^3.yr^{-1}$)

P = net annual precipitation during t-Δt and t ($m.yr^{-1}$)

To model major ion concentrations in the mixing zone, it is most convenient to express the sulphate concentration in the mixing zone resulting from pyrite oxidation in the unsaturated layer by the following differential equation:

$$\lambda_{mix} A \frac{d[SO_4^{2-}]_{p,mix}}{dt} = PA[SO_4^{2-}]_{p,\lambda w} - PA[SO_4^{2-}]_{p,mix} \qquad (3.4.3)$$

where:

$[SO_4^{2-}]_{p,\lambda w}$ = sulphate concentration at $\lambda_w$ resulting from pyrite oxidation in the unsaturated zone ($mol.m^{-3}$).

$[SO_4^{2-}]_{p,mix}$ = sulphate concentration in the mixing zone resulting from pyrite oxidation in the unsaturated zone ($mol.m^{-3}$)

We have chosen the above differential equation as the basis for calculations, because it is applicable even when the gypsum is depleted from the mixing zone. Note, that in equation (3.4.3) the term $[SO_4^{2-}]_{p,\lambda w}$ is equal to the sulphate concentration term given by equation (3.3.13), i.e.:

$$[SO_4^{2-}]_{p,\lambda w} = \frac{2\lambda_w[FeS_2]_{t-\Delta t}\,(1-e^{-k\Delta t})}{P\Delta t} = \frac{2\lambda_w\,\beta}{P\Delta t} \qquad (3.4.4)$$

Substitution of equation (3.4.4) into equation (3.4.3) and integration yields:

$$[SO_4^{2-}]_{p,mix,t} = [SO_4^{2-}]_{p,\lambda w,t} + ([SO_4^{2-}]_{p,mix,t-\Delta t} - [SO_4^{2-}]_{p,\lambda w,t})\ \exp\,(-P\Delta t/\epsilon\lambda_{mix}) \qquad (3.4.5)$$

For any time 't' the total sulphate and total calcium concentrations in the mixing zone can be obtained as in Section 3.3.2 to give:

$$[Ca^{2+}]_{mix,t} = \sqrt{\frac{K_s^o}{f^2} + 0.25\,[SO_4^{2-}]^2_{p,mix,t}} - 0.5\,[SO_4^{2-}]_{p,mix,t} \qquad (3.4.6)$$

and

$$[SO_4^{2-}]_{mix,t} = \sqrt{\frac{K_s^o}{f^2} + 0.25\,[SO_4^{2-}]^2_{p,mix,t}} + 0.5\,[SO_4^{2-}]_{p,mix,t} \qquad (3.4.7)$$

### 3.4.2 Gypsum Depletion

It may be noted that equations (3.4.6) and (3.4.7) are applicable as long as gypsum is present in the mixing zone. Of course, no gypsum from the mixing zone will go into solution as long as the porewater entering (from layer 2) is saturated with gypsum. After the gypsum content of the unsaturated zone is depleted, however, gypsum in the mixing zone will begin to dissolve. The dissolution of gypsum is relatively easy to calculate.

Let $t_f$ = the time when the gypsum from the unsaturated zone is depleted. At this time, the total sulphate concentration in the mixing zone is given by equation (3.4.7) as some value $[SO_4^{2-}]_{mix,tf}$. If there were no gypsum present in the mixing zone, the sulphate concentration after some time Δt would decline to:

$$[SO_4^{2-}]^*_{mix,t} = [SO_4^{2-}]_{p,\lambda w,t} + ([SO_4^{2-}]_{p,\overset{*}{\mathrm{mix}},t-\Delta t} - [SO_4^{2-}]_{p,\lambda w,t}) \exp(-P\Delta t/\epsilon\,\lambda_{mix}) \qquad (3.4.8)$$

at $t=t_f$:

$$[SO_4^{2-}]^*_{mix,t} = [SO_4^{2-}]_{mix,tf}$$

This quantity ($[SO_4^{2-}]^*_{mix,t}$) would be the sulphate concentration if there were no gypsum in the mixing zone.

The difference between equation (3.4.7) and (3.4.8) is the concentration of sulphate resulting from gypsum dissolution.

Thus, the amount of gypsum dissolved over a time period Δt is given by:

$$\Delta\ \text{gypsum} = \frac{P\Delta t}{\lambda_{mix}}\ [\text{eqn } (3.4.7) - \text{eqn } (3.4.8)]$$

$$= \frac{P\Delta t}{\lambda_{mix}} \left( [SO_4^{2-}]_{mix,t} - [SO_4^{2-}]^*_{mix,t} \right) \qquad (3.4.9)$$

where:

Δgypsum = gypsum dissolved over time Δt ($mol.m^{-3}$)

The total gypsum (per unit volume) dissolved in the mixing zone to any time t is:

$$[\mathrm{gyp}]_{\mathrm{diss},t} = \sum_{t=0}^{t} \Delta \mathrm{gypsum} \qquad (3.4.10)$$

where:

$[\mathrm{gyp}]_{\mathrm{diss},t}$ = gypsum dissolved to time 't' ($\mathrm{mol.m^{-3}}$)

Thus, gypsum in the mixing zone is depleted when:

$[\mathrm{gyp}]_{\mathrm{diss},t} = g_o$

and:

$t_{f2}$ = time at which mixing zone gypsum depletion occurs.

### 3.4.3 Calcium and Sulphate Concentrations Following Gypsum Depletion

Following gypsum depletion, the calculation of sulphate and calcium concentrations is quite straightforward. The calcium concentration will decrease with time as a result of dilution, according to the following equation:

$$[\mathrm{Ca}^{2+}]_{\mathrm{mix},t} = [\mathrm{Ca}^{2+}]_{\mathrm{mix},t-\Delta t} \exp\left(-P\Delta t/\epsilon\lambda_{\mathrm{mix}}\right) \quad \text{at } t \geq t_{f2} \qquad (3.4.11)$$

The sulphate concentration at any time is given by:

$$[\mathrm{SO}_4^{2-}]_{\mathrm{mix},t} = [\mathrm{SO}_4^{2-}]_{p,\lambda w,t} + \left([\mathrm{SO}_4^{2-}]_{p,\mathrm{mix},t-\Delta t} - [\mathrm{SO}_4^{2-}]_{p,\lambda w,t}\right)\exp(-P\Delta t/\epsilon\lambda_{\mathrm{mix}}) \qquad (3.4.12)$$

### 3.4.4 Iron Concentration

In the mixing zone, ferric iron is rapidly reduced to the ferrous ($Fe^{II}$) state by the following reaction:

$$2\ Fe^{+3} + FeS_2 \longrightarrow 3\ Fe^{+2} + 2S^0 \qquad (3.4.13)$$

Thus, for each mole of ferric iron ($Fe^{III}$), 1.5 moles of ferrous iron ($Fe^{II}$) is produced. This results in a total ferrous ion flux as given by the following:

$$\text{Flux of } Fe^{II} = 1.5\ P\ [Fe^{III}]_{\lambda w,t} \qquad (3.4.14)$$

where:

$P$ = the precipitation rate ($m.yr^{-1}$)

Also, let us assume, that this flux remains constant for a time period, $t-\Delta t$ to $t$. Applying a differential mass balance in the mixing zone gives the following equation:

$$\lambda_{mix}\ \frac{\epsilon d[Fe^{II}]_{mix}}{dt} = 1.5P\ [Fe^{III}]_{\lambda w,t} - P\ [Fe^{II}]_{mix,t} \qquad (3.4.15)$$

Integrating between $t-\Delta t$ and $t$ gives:

$$[Fe^{II}]_{mix,t} = 1.5\ [Fe^{III}]_{\lambda w,t} + \left([Fe^{II}]_{mix,t-\Delta t} - 1.5[Fe^{III}]_{\lambda w,t}\right) \exp(-\ P\Delta t/\epsilon\lambda_{mix}) \qquad ...(3.4.16)$$

## 3.5 Ions - Layer 4

The calculation procedure for major ions in layer 4 is similar to that in the mixing zone. As in case of the mixing zone, it is advantageous to model the sulphate resulting from pyrite oxidation. Let $f_p$ be the fraction of mean annual precipitation ($\bar{P}$) entering this layer. The differential equation describing the concentration of sulphate in layer 4 resulting from pyrite oxidation in the unsaturated zone is:

$$\lambda_4 \frac{\epsilon d[SO_4^{2-}]_{p,4}}{dt} = f_p\bar{P}[SO_4^{2-}]_{p,mix,t} - f_p\bar{P}\,[SO_4^{2-}]_{p,4} \qquad (3.5.1)$$

where:

$[SO_4^{2-}]_{p,4}$ = concentration of sulphate in zone 4 resulting from pyrite oxidation in the unsaturated layer ($mol.m^{-3}$)

$\lambda_4$ = thickness of layer 4 (m)

$f_p$ = fraction of precipitation entering layer 4

$\bar{P}$ = long-term mean annual precipitation ($m.yr^{-1}$)

$[SO_4^{2-}]_{p,mix,t}$ = concentration of sulphate, resulting from pyrite oxidation, in the mixing zone at time "t" ($mol.m^{-3}$)

Equation (3.5.1) can be integrated to yield the following expression:

$$[SO_4^{2-}]_{p,4,t} = [SO_4^{2-}]_{p,mix,t-\Delta t} + \left([SO_4^{2-}]_{p,4,t-\Delta t} - [SO_4^{2-}]_{p,mix,t-\Delta t}\right)\exp(-f_p\bar{P}\Delta t/\epsilon\lambda_4) \qquad (3.5.2)$$

We can calculate the total sulphate and total calcium concentrations by equations analogous to equation (3.4.7).

$$[Ca^{2+}]_{4,t} = \sqrt{\frac{K_S^0}{f^2} + 0.25\,[SO_4^{2-}]^2_{p,4,t}} - 0.5[SO_4^{2-}]_{p,4,t} \qquad (3.5.3)$$

and

$$[SO_4^{2-}]_{4,t} = \sqrt{\frac{K_S^0}{f^2} + 0.25\,[SO_4^{2-}]^2_{p,4,t}} + 0.5[SO_4^{2-}]_{p,4,t} \qquad (3.5.4)$$

The ferrous ion $[Fe^{2+}]$ concentration can also be calculated in a similar manner. We have already obtained an expression for $[Fe^{2+}]$ in the mixing zone. Let this concentration at time, t, be $[Fe^{2+}]_{mix,t}$. The concentration in zone (4) is given by:

$$[Fe^{2+}]_{4,t} = [Fe^{2+}]_{mix,t-\Delta t} + \left([Fe^{2+}]_{4,t-\Delta t} - [Fe^{2+}]_{mix,t-\Delta t}\ \exp\right)(-\ f_p\bar{P}\ \Delta t/\epsilon\lambda_4) \qquad (3.5.5)$$

It can be shown that the gypsum in layer 4 cannot be depleted for some 4,000 years. Hence, the gypsum in this layer (i.e. layer 4) has been modelled as it is not depleted over the 1000 year simulation period.

## 3.6 pH Calculations

Pyritic uranium ores contain approximately 70% quartz ($SiO_2$), 23% aluminosilicates (sericite, feldspars, clays) and 6% pyrite ($FeS_2$). In the highly acidic, oxidative environment of the leaching pachukas (in the milling circuit) a portion of these minerals dissolve and, upon pH adjustment with lime, re-precipitate as secondary minerals including gypsum ($CaSO_4.2H_2O$), gibbsite ($Al_2O_3.3H_2O$), kaolinite ($Al_2Si_2O_5(OH)_4$), aluminite ($Al_4(SO_4)(OH)_{10}$), and iron (III) oxyhydroxides ($Fe(OH)_3$). Since the solubilities of these secondary minerals generally exceed those of the original ore, their dissolved ion products and speciation are expected to be the dominant species in the pH-dependent, ionic equilibrium expression for tailings porewater.

The following sections outline the significant ionic species and their effect on pH in each tailings layer. Since the tailings layers each have different characteristics, as discussed in preceding sections, the pH in each layer is calculated somewhat differently. However, many of the ionic species are common to all 4 layers. Hence, the discussion regarding layer 1 is the most detailed with significant portions applicable to the other layers as such. These general sections are presented in the layer 1 description and are not repeated.

The following sections indicate that the calculation of pH in any layer requires an iterative (trial and error) solution. Information regarding the approach taken to implementing the iterative solutions for the pH equations is presented in Section 3.6.5.

### 3.6.1 Layer 1

#### Aluminum

To establish the aluminum concentrations in the porewater, the solid phases of significance are taken to be gibbsite ($Al_2O_3.3H_2O$), kaolinite ($Al_2Si_2O_5(OH)_4$), and basaluminite ($Al_4SO_4(OH)_{10}$).

The hydrogen ion ($H^+$) dependent solution reactions of gibbsite and kaolinite can be expressed as follows (Stumm and Morgan, 1981):

$$0.5\ Al_2O_3.3H_2O(s) + 3H^+ \rightleftharpoons Al^{3+} + 3H_2O \qquad \log K_s^0 = 8.5 \qquad (3.6.1)$$

$$0.5\ Al_2Si_2O_5(OH)_{4(s)} + 3H^+ \rightleftharpoons Al^{3+} + H_4SiO_4^0 + 0.5H_2O \qquad \log K_s^0 = 3.8 \qquad (3.6.2)$$

The dissolved silica ($H_4SiO_4$) in equation (3.6.2) is expressed as a nonionic species because it is a weak acid and does not protolyze until the pH value in the water exceeds pH 9.4 (Faust and Aly, 1981). It is unlikely, however, that the dissolved silica concentration in acidic porewaters is established by the equilibrium relationship expressed by equation (3.6.2). At pH 5, for example, the dissolved silica concentration would be in the order of $2.5\times10^{-6}$ M $H_4SiO_4$ (according to equation (3.6.2)) in comparison to observed concentrations of $5\times10^{-4}$ to $6\times10^{-3}$ M $H_4SiO_4$ in porewaters of igneous soils. In these soils, the dissolved silica concentration is dependent on the dissolution equilibrium of solid silicates ($SiO_2(s)$) as follows:

$$SiO_2(s) + 2H_2O \rightleftharpoons H_4SiO_4^0 \qquad K_s^0 = 10^{-2.7} \qquad (3.6.3)$$

The equilibrium constant in equation (3.6.3) represents the solution equilibrium of amorphous silicates for their demonstrated presence in tailings solids (Beak, 1985). According to the above equilibrium expression, the dissolved silica concentration in porewaters is independent of pH. Measured silicate concentrations in acidic (pH 2 to pH 5) tailings porewaters ranged from $2.9\times10^{-4}$ M to $2.6\times10^{-3}$ M $H_2SiO_4$ in the Lacnor Field Study (Golder _et al._, 1986). The average concentration of $1.71\times10^{-3}$ M is in line with the equilibrium value of $2.0\times10^{-3}$ M predicted by equation (3.6.3).

The combination of equations (3.6.2) and (3.6.3) yields the following expression for the solution equilibrium of kaolinite:

$$0.5\ Al_2Si_2O_5(OH)_{4(s)} + 3H^+ \rightleftharpoons Al^{3+} + SiO_2(s) + 1.5\ H_2O \quad \log K_s^o = 6.5 \quad (3.6.4)$$

Comparing equation (3.6.1) and equation (3.6.4), it is evident that kaolinite is the more stable solid phase. It has been shown by Stumm and Morgan (1981) that, at dissolved silica concentrations in excess of $2\times10^{-5}$ M ($H_4SiO_4$), gibbsite dissolves incongruently and re-precipitates as kaolinite. In addition, the kaolinite "reserve" is replenished by the acidic chemical weathering of clay minerals which is likely to take place as a result of acidic conditions brought about by pyrite oxidation. For example, the weathering reaction of muscovite proceeds as follows:

$$\underset{\text{Muscovite}}{2\ KAl_3Si_3O_{10}(OH)_2(s)} + 2H^+ + 3H_2O \rightleftharpoons 2K^+ + \underset{\text{Kaolinite}}{3Al_2Si_2O_5(OH)_4(s)} \quad (3.6.5)$$

The above reaction is thermodynamically favoured ($\Delta G^o$ = -13.7 kcal/mol). However, these weathering reactions are likely to be under kinetic rather than equilibrium control.

The third aluminum mineral of significance in tailings is basaluminite ($Al_4SO_4(OH)_{10}(s)$). The solution equilibrium for basaluminite is as follows:

$$Al_4SO_4(OH)_{10}(s) + 10\ H^+ \rightleftharpoons 4\ Al^{3+} + SO_4^{2-} + 10\ H_2O \quad \log K_s^o = 22.7 \quad (3.6.6)$$

It can be shown, that basaluminite is a stable solid phase at pH values below 1.5 with respect to kaolinite and pH values below 5.0 with respect to gibbsite. Since pH levels below 1.5 are not expected to occur in the tailings porewater and observed dissolved silica levels suggest that kaolinite is the most likely stable solid phase, the solution equilibrium of kaolinite (equation (3.6.4)) has been chosen as the basis for long-term modelling of aluminum in the porewater.

In aqueous solutions, dissolved aluminum readily speciates as hydroxo and sulphate complexes:

$$
\begin{array}{llll}
Al^{3+} + H_2O \rightleftharpoons Al(OH)^{2+} + H^+ & \log K = -4.97 & \\
Al^{3+} + 2H_2O \rightleftharpoons Al(OH)_2^+ + 2H^+ & \log K = -9.30 & \\
Al^{3+} + 3H_2O \rightleftharpoons Al(OH)_3^0 + 3H^+ & \log K = -15.00 & \\
Al^{3+} + 4H_2O \rightleftharpoons Al(OH)_4^- + 4H^+ & \log K = -23.00 & \\
Al^{3+} + SO_4^{2-} \rightleftharpoons AlSO_4^+ & \log K = 3.20 & (3.6.7)
\end{array}
$$

The relative activities of the hydroxo complexes at different pH values are shown in Table 3.1.

Since the non-ionic complex ($Al(OH)_3^0$) is of no importance for the ionic balance, the significant species below pH 7 are $Al^{3+}$, $Al(OH)^{2+}$, and $Al(OH)_2^+$. The anionic aluminum hydroxo complex ($Al(OH)_4^-$) is significant at pH values above 7.0. The pH of the porewater is not expected to exceed pH 7.0 significantly; and even if this occurs, the concentration of the $Al(OH)_4^-$ would be no more than $10^{-8}$M at pH 8, which is insignificant with respect to the other anions (for example sulphate, which is at least $10^{-4}$ M). The sulphato complex of aluminum, however, is modelled explicitly, since at sulphate concentrations above $6.3 \times 10^{-4}$ M (61 mg/l), the complexation product ($AlSO_4^+$) is a major dissolved species at acidic pH values. Combining the equilibrium expression (equation (3.6.4)) and the complexation reactions of aluminum (equation (3.6.7)) yields the following "ionic strength corrected" concentrations for the aluminum species in solution:

Table 3.1

## RELATIVE ACTIVITIES OF ALUMINUM HYDROXO COMPLEXES

| Species | Relative Activity (%) | | | | | |
|---|---|---|---|---|---|---|
| | pH3 | pH4 | pH5 | pH6 | pH7 | pH8 |
| $Al^{3+}$ | 98.8 | 86.3 | 12.4 | 0.1 | 0 | 0 |
| $Al(OH)^{2+}$ | 1.2 | 9.3 | 13.3 | 0.7 | 0 | 0 |
| $Al(OH)_2^+$ | 0 | 4.3 | 62.0 | 32.9 | 4.2 | 0.2 |
| $Al(OH)_3^0$ | 0 | >0.1 | 12.4 | 65.7 | 83.3 | 49.9 |
| $Al(OH)_4^-$ | 0 | 0 | 0 | 0.7 | 8.3 | 49.9 |

$$[Al^{3+}] = \frac{10^{6.5-3pH}}{f^{9/4}}$$

$$[Al(OH)^{2+}] = \frac{10^{1.53-2pH}}{f}$$

$$[Al(OH)_2^+] = \frac{10^{-2.8-pH}}{f^{1/4}}$$

$$[AlSO_4^+] = f^{3/4}\ 10^{9.7-3pH}\ [SO_4^{2-}] \qquad (3.6.8)$$

where:
[ ] = concentration ($mol.L^{-1}$)
f = activity coefficient of divalent ions

Iron

It has been shown (Halbert et al., 1983), that the concentration of dissolved iron under oxidizing conditions is controlled by the solution equilibrium and speciation of ferric oxyhydroxides ($Fe(OH)_3(s)$. These hydroxides are originally present in the tailings. In addition, iron (III) compounds are products of pyrite oxidation. It can be shown that pyrite oxidation can give rise to a net precipitation of ferric hydroxide at pH values above pH 4.0, while at pH values below pH 4.0 a net dissolution of precipitated ferric hydroxide is likely to occur. The equilibrium reaction for iron (III) hydroxide dissolution in tailings is as follows (Halbert et al., 1983):

$$Fe(OH)_3(s) + 3H^+ \rightleftharpoons Fe^{3+} + 3H_2O \qquad \log K_S^0 = 5.97 \qquad (3.6.9)$$

The dissolved iron (III) readily forms hydroxo and sulphato complexes. The relative activities of the hydroxo complexes, as a function of pH, is shown in Table 3.2.

As shown in Table 3.2, the important hydroxo complexes below pH 7 are $Fe^{3+}$,

$Fe(OH)^{2+}$, and $Fe(OH)_2^+$. The non-ionic complex ($Fe(OH)_3^0$) has no effect on the ionic balance, while anionic species ($Fe(OH)_4^-$, for example) are important at alkaline pH values only. Ferric ion in solution, however, complexes with the sulphate ligand as follows:

$$Fe^{3+} + SO_4^{2-} \rightleftharpoons FeSO_4^+ \qquad \log K = 3.02 \qquad (3.6.10)$$

The combination of the solubility equilibrium with speciation gives the following expressions for the most significant dissolved iron (III) complexes:

$$\begin{aligned} [Fe^{3+}] &= 10^{5.97-3pH} \\ [Fe(OH)^{2+}] &= 10^{3.78-2pH} \\ [Fe(OH)_2^+] &= 10^{0.3-pH} \\ [FeSO_4^+] &= f^3\ 10^{8.99-3pH}\ [SO_4^{2-}] \end{aligned} \qquad (3.6.11)$$

The hydroxo complexes of dissolved iron (III) are not corrected for ionic strength, since they are based on actual concentration (M) units.

Sulphate

In layer 1 (the gypsum-depleted layer), the sulphate ion concentration is dependent on the pyrite oxidation as expressed by equation (3.3.15) and the rainwater source ($10^{-4}$M sulphate). Thus, the sulphate concentration is primarily kinetics controlled. The sulphate in solution however, speciates as $SO_4^{2-}$, $AlSO_4^+$, and $FeSO_4^+$. Collecting the terms for $AlSO_4^+$ (from equation (3.6.8)) and $FeSO_4^+$ (from equation (3.6.11)) gives an expression for the total sulphate concentrations:

$$[SO_4^{2-}]_{T,1} = [SO_4^{2-}]_{U,1}\ (1 + f^{3/4}\ 10^{9.7-3pH} + f^3\ 10^{8.99-3pH}) \qquad (3.6.12)$$

where:

$[SO_4^{2-}]_{T,1}$ = total sulphate concentration in layer 1 (mol.$L^{-1}$)
= $[SO_4^{2-}]_{p,1}$ (see equation (3.3.15))

Table 3.2

## RELATIVE ACTIVITIES OF IRON (III) HYDROXO COMPLEXES

| Species | Relative Activity (%) | | |
|---|---|---|---|
| | pH3 | pH5 | pH7 |
| $Fe^{3+}$ | 3.8 | 0 | 0 |
| $Fe(OH)^{2+}$ | 88.2 | 2.8 | 0 |
| $Fe(OH)_2^+$ | 8.1 | 92.8 | 17.6 |
| $Fe(OH)_3^0$ | 0 | 4.4 | 82.2 |
| $Fe(OH)_4^-$ | 0 | 0 | 0.2 |

$Fe^{3+} + H_2O \rightleftharpoons Fe(OH)^{2+} + H^+$ log K = -2.19

$Fe^{3+} + 2H_2O \rightleftharpoons Fe(OH)_2^+ + 2H^+$ log K = -5.67

$Fe^{3+} + 3H_2O \rightleftharpoons Fe(OH)_3^0 + 3H^+$ log K = -12.00

$Fe^{3+} + 4H_2O \rightleftharpoons Fe(OH)_4^- + 4H^+$ log K = -21.60

$[SO_4^{2-}]_{U,1}$ = concentration of uncomplexed (free) sulphate in layer 1 (mol.L$^{-1}$)

The concentration of the "free" sulphate and the sulphate complexes are as follows:

$$[SO_4^{2-}]_{U,1} = \frac{1}{1 + f^{3/4}\ 10^{9.7-3pH} + f^3\ 10^{8.99-3pH}} [SO_4\ ]_{T,1}$$

$$[AlSO_4^+] = \frac{f^{3/4}\ 10^{9.7-3pH}}{1 + f^{3/4}\ 10^{9.7-3pH} + f^3\ 10^{8.99-3pH}} [SO_4\ ]_{T,1}$$

$$[FeSO_4^+] = \frac{f^3\ 10^{8.99-3pH}}{1 + f^{3/4}\ 10^{9.7-3pH} + f^3\ 10^{8.99-3pH}} [SO_4\ ]_{T,1} \qquad (3.6.13)$$

Bicarbonate

The dissolved carbon dioxide ($H_2CO_3$ and $CO_2$) concentration in the porewater is assumed to be in equilibrium with air. This concentration is related to the partial pressure of $CO_2$ in air by Henry's Law. To evaluate the concentration, a temperature of 10°C was chosen as a characteristic temperature for the tailings. Using the accepted value of $P_{CO_2} = 10^{-3.5}$ atm, the concentration of dissolved $CO_2$ (i.e. undissociated) is given by:

$$[H_2CO_3] = K_H\ P_{CO2} \qquad P_{CO2} = 10^{-3.5} \text{ atm}$$
$$K_H = 10^{-1.27} \text{ (at 10°C)}$$

or

$$[H_2CO_3] = 10^{-3.5} \times 10^{-1.27} = 10^{-4.77} \text{ M} \qquad (3.6.14)$$

Dissolved $CO_2$ dissociates to form bicarbonate as the principal anion at pH values less than 8.5. The dissociation constant at 10°C (ionic strength = 0) is $K=10^{-6.5}$

i.e.

$$H_2CO_3 \qquad HCO_3^- + H^+ \qquad \log K = -6.5 \text{ (at 10°C)} \qquad (3.6.15)$$

The "ionic strength corrected" concentration of bicarbonate ($HCO_3^-$) ion is given by:

$$[HCO_3^-] = \frac{10^{pH-6.5}}{f^{1/4}}[H_2CO_3]$$

$$[HCO_3^-] = \frac{10^{pH-11.27}}{f^{1/4}} \qquad (3.6.16)$$

Ionic Balance

A summary of the relevant layer 1 equilibrium expressions is given in Table 3.3. The ionic balance for electroneutrality involves the determination of significant species. These are multiplied by the valence number to give the ion concentration in equivalents per litre. The significant cations and anions in layer 1 are:

| Cations | Anions |
|---|---|
| $H^+$ | $SO_4^{2-}$ |
| $Fe^{3+}$ | $HCO_3^-$ |
| $FeOH^{2+}$ | |
| $Fe(OH)_2^+$ | |
| $FeSO_4^+$ | |
| $Al^{3+}$ | |
| $Al(OH)^{2+}$ | |
| $AlSO_4^+$ | |

The overall ionic balance for electroneutrality in layer 1 becomes:

$$\frac{10^{-pH}}{f^{1/4}} + 3\left(\frac{10^{6.5}}{f^{9/4}} + 10^{5.97}\right)10^{-3pH} + 2\left(\frac{10^{1.53}}{f} + 10^{3.78}\right)10^{-2pH} + 10^{0.3-pH} =$$

$$[SO_4^{2-}]_{T,1}\left(\frac{2 - f^{3/4}\,10^{9.7-3pH} - f^3\,10^{8.99-3pH}}{1 + f^{3/4}\,10^{9.7-3pH} + f^3\,10^{8.99-3pH}}\right) + \frac{10^{pH-11.27}}{f^{1/4}} \qquad (3.6.17)$$

Table 3.3

## IONIC EQUILIBRIUM FOR ELECTRONEUTRALITY

| Equilibrium Reactions in the Unsaturated Zone | Log K |
|---|---|
| $SiO_2^0(s) + 2H_2O \rightleftharpoons H_4SiO_4^0$ | -2.7 |
| $3H^+ + 0.5\ Al_2Si_2O_5(OH)_{4(s)} \rightleftharpoons Al^{3+} + H_4SiO_4 + 0.5H_2O$ | 3.8 |
| $Al^{3+} + H_2O \rightleftharpoons Al(OH)^{2+} + H^+$ | -4.97 |
| $Al^{3+} + 2H_2O \rightleftharpoons Al(OH)_2{}^+ + 2H^+$ | -9.30 |
| $Al^{3+} + 3H_2O \rightleftharpoons Al(OH)_3{}^0\ (aq) + 3H^+$ | -15.00 |
| $Al^{3+} + SO_4{}^{2-} \rightleftharpoons AlSO_4{}^+$ | 3.20 |
| $Fe(OH)_3(s) + 3H^+ \rightleftharpoons Fe^{3+} + 3H_2O$ | 5.97 ($K^c$) |
| $Fe(OH)_{3(s)} + 2H^+ \rightleftharpoons Fe(OH)^{2+} + 2H_2O$ | 3.78 ($K^c$) |
| $Fe(OH)_{3(s)} + H^+ \rightleftharpoons Fe(OH)_2^+ + H_2O$ | 0.30 ($K^c$) |
| $Fe^{3+} + SO_4{}^{2-} \rightleftharpoons FeSO_4{}^+(aq)$ | 3.02 |
| $H_2CO_3^0 \rightleftharpoons H^+ + HCO_3{}^-$ | -6.5 |
|  | $P_{CO2} = -3.5$ |
|  | $K_H = -1.27$ |

Note that in equation (3.6.17) the speciation of sulphate as $SO_4^{2-}$, $AlSO_4^+$ and $FeSO_4^+$ has been combined to give an overall expression in terms of total sulphate concentration. The negative signs indicate that $AlSO_4^+$ and $FeSO_4^+$ are cationic species. This procedure has been used for expressing the charged sulphate complexes in each zone.

## Modifications for Limestone Addition

The previous expressions are only valid for the case where no limestone has been added to the tailings. A further electroneutrality equation must, therefore, be written, for the case where gypsum is absent, but calcite is present. In this case (i.e. for the gypsum-depleted layer) pH is calculated (iteratively) from:

$$2\left(\frac{10^{11.87-2pH}}{f}\right) + 10^{0.3-pH} = \frac{2\,[SO_4^{2-}]_{p,h}}{1000} + \left(\frac{10^{pH-9.73}}{f^{1/4}}\right) \qquad (3.6.18)$$

where:

pH = pH in the gypsum-depleted layer

$[SO_4^{2-}]_{p,h}$ = concentration of sulphates from pyrite oxidation at h (gypsum-depleted front) ($mol.m^{-3}$)

The factor of 1000 is included to convert $[SO_4^{2-}]$ from $mol.m^{-3}$ to $mol.L^{-1}$.

This equation is also applicable for pH calculations at $\lambda_w$ once the entire unsaturated zone has been depleted of gypsum. In this case $h = \lambda_w$ and:

$$[SO_4^{2-}]_{p,h} = [SO_4^{2-}]_{p,\lambda w}$$

and the entire unsaturated zone is assumed to be homogeneous with respect to $Ca^{2+}$, $SO_4^{2-}$ and $Fe^{3+}$ and pH.

### 3.6.2 Layer 2

Aluminum — same as Layer 1

Iron — same as Layer 1

Calcium

The calcium concentration in layer 2 results from the solution equilibrium of gypsum. The solution equilibrium for gypsum is given by the following reaction:

$$CaSO_4 \rightleftharpoons Ca^{2+} + SO_4^{2-} \qquad \log K_s^o = -4.6 \qquad (3.6.19)$$

Calcium forms a complex with the sulphate ligand in solution:

$$Ca^{2+} + SO_4^{2-} \rightleftharpoons CaSO_4^0 \qquad \log K = 2.31 \qquad (3.6.20)$$

The complexation product ($CaSO_4^0$) is nonionic, hence it does not contribute to the net ionic balance. The formation of sulphate complexes with iron and aluminum at acidic pH values enhances the solubility of gypsum. Taking into account the correction for the complexation products and the ionic strength, the molar concentration of calcium is given by (see equation (3.3.39)):

$$[Ca^{2+}]_{\lambda w} = \left( \frac{K^o_{s,CaSO_4} d}{f^2} + .25[SO_4^{2-}]^2_{p,\lambda w} \right)^{1/2} - 0.5\,[SO_4^{2-}]_{p,\lambda w} \qquad (3.6.21)$$

where:

$d = 1 + f^{3/4}\, 10^{9.7-3pH} + f^3\, 10^{8.99-3pH}$

Sulphate

The total sulphate concentration is calculated as the sum of sulphate produced by pyrite oxidation (kinetic control), gypsum dissolution (equilibrium control) and contribution from rain water (a constant value). As discussed previously (Section 3.3.3) the total sulphate concentration can be written as:

$$[SO_4^{2-}]_{T,\lambda w} = [Ca^{2+}] + [SO_4^{2-}]_{p,\lambda w} \qquad (3.6.22)$$

The term $[SO_4^{2-}]_{p,\lambda w}$, as calculated in (for example) equation (3.3.14) includes the contribution from rainwater.

The dissolved sulphate speciates as $SO_4^{2-}$, $CaSO_4^0$, $AlSO_4^+$, $FeSO_4^+$, $BaSO_4^0$, and $PbSO_4^0$. Of these species, $SO_4^{2-}$, $AlSO_4^+$ and $FeSO_4^+$ are significant for ionic balance calculations.

Bicarbonate — As in Layer 1

Ionic Balance

The important ionic species for calculating the pH in layer 2 are as follows:

| Cations | Anions |
|---|---|
| $H^+$ | $SO_4^{2-}$ |
| $Ca^{2+}$ | $HCO_3^-$ |
| $Fe^{3+}$ | |
| $Fe(OH)^{2+}$ | |
| $Fe(OH)_2^+$ | |
| $FeSO_4^+$ | |
| $Al^{3+}$ | |
| $Al(OH)^{2+}$ | |
| $AlSO_4^+$ | |

The pH dependent equation for electroneutrality in layer 2 becomes:

$$3\left(\frac{10^{6.5}}{f^{9/4}} + 10^{5.97}\right)10^{-3pH} + 2\left(\frac{10^{1.53}}{f} + 10^{3.78}\right)10^{-2pH}$$
$$+ \left(10^{0.3} + \frac{1}{f^{1/4}}\right)10^{-pH} + 2\,[Ca^{2+}]_{\lambda w}$$
$$= [SO_4^{2-}]_{T,\lambda w}\left(\frac{2 - f^{3/4}\,10^{9.7-3pH} - f^{3}\,10^{8.99-3pH}}{1 + f^{3/4}\,10^{9.7-3pH} + f^{3}\,10^{8.99-3pH}}\right) + \frac{10^{pH-11.27}}{f^{1/4}} \qquad (3.6.23)$$

Modifications for Limestone Addition

The previous expressions are valid as long as no limestone (calcite) has been added to the tailings. When both gypsum and calcite are present, the pH is expected to be well above 4. In this case, it can be shown that the relative concentrations of $Fe^{3+}$, $Al^{3+}$, and their sulphato and hydroxo complexes are negligible. Thus, the electroneutrality equation becomes:

$$2[Ca^{2+}] + [Fe(OH)_2^+] = 2[SO_4^{2-}] + [HCO_3^-] \qquad (3.6.24)$$

or:

$$2\left(\frac{10^{11.87-2\,pH}}{f}\right) + 10^{0.3-pH} = 2\left(\frac{10^{2pH-16.47}}{f}\right) + \left(\frac{10^{pH-9.73}}{f^{1/4}}\right) \qquad (3.6.25)$$

This equation indicates that the pH stays constant as long as both calcite and gypsum are present. It is thus applicable to the gypsum-enriched layer as long as both solid phases exist.

3.6.3 Layer 3

Aluminum

As in layers 1 and 2, the concentrations of dissolved aluminum species are controlled by the solution equilibrium of aluminum silicates, at dissolved silica concentrations in excess of $2 \times 10^{-5}$ M:

$0.5\ Al_2Si_2O_5(OH)_4(s) + 3\ H^+ \rightleftharpoons Al^{3+} + H_4SiO_4^0 + 0.5\ H_2O \quad \log K_s^0 = 3.8 \quad (3.6.26)$

The concentration of dissolved $Al^{3+}$ is a function of the pH, the dissolved silica, and the ionic strength as follows:

$$[Al^{3+}] = \frac{10^{3.8-3pH}}{f^{9/4}\ [H_4SiO_4]} \qquad (3.6.27)$$

The dissolved silica, in turn, is dependent on the solution equilibria of amorphous silicate ($SiO_{2(am)}$) or quartz ($SiO_2$):

$$SiO_{2(am)} + 2\ H_2O \rightleftharpoons H_4SiO_4^0 \qquad \log K_s = -2.7$$
$$SiO_2(quartz) + 2\ H_2O \rightleftharpoons H_4SiO_4^0 \qquad \log K_s = -3.7 \qquad (3.6.28)$$

According to the above equations, the equilibrium concentration of dissolved silica would range from $2\times10^{-4}M$ to $2\times10^{-3}M$, depending upon either quartz or amorphous silicates as solid phases. It may be argued, that amorphous silicates dissolve initially, hence, the concentration of dissolved silica is time dependent. However, the amorphous silica content of the tailings is not known. In addition, chemical weathering of siliceous minerals contributes to the amorphous $SiO_2$ pool. The net effect of these weathering reactions cannot be established. Therefore, the dissolved silicate concentration in the mixing zone porewater is assumed to be constant at $10^{-3}M$. This $H_4SiO_4$ concentration gives the following relationships for the important ionic aluminum species in solution:

$$[Al^{3+}] = \frac{10^{6.8-3pH}}{f^{9/4}}$$

$$[Al(OH)^{2+}] = \frac{10^{1.53-2pH}}{f}$$

$$[AlSO_4^+] = f^{3/4}\ 10^{9.7-3pH}\ [SO_4^{2-}] \qquad (3.6.29)$$

## Iron

Dissolved iron (III) species are not stable under anoxic conditions. Since dissolved oxygen is exhausted above the water table, the ferric ion entering the mixing zone is expected to be reduced to the ferrous state. This reduction occurs most likely as a redox reaction couple involving pyrite as follows:

$$2\ Fe^{3+} + FeS_2 \rightleftharpoons 3\ Fe^{2+} + 2S^0$$

$$14\ Fe^{3+} + FeS_2 + 8\ H_2O \rightleftharpoons 15\ Fe^{2+} + 16\ H^+ + 2\ SO_4^{2-} \qquad (3.6.30)$$

Both of the above reactions are under kinetic control. Thus, the ferrous ion equivalent in the mixing zone can range from 15/14 to 3/2 times the ferric ion concentration entering the mixing zone. Since the formation of elemental sulphur is more rapid than the complete oxidation of pyrite, the iron concentration in the mixing zone is calculated as an iron (III) inflow equivalent to 1.5 times the ferric ion concentration at the zone boundary (i.e. at $\lambda_w$). Ferrous ion does not form hydroxo complexes at pH below 9.2. The sulphato complex formation ($\log K = 2.24$) is significant at high sulphate concentrations, however, the sulphato complex is nonionic, thus, it has no effect on the ionic balance. The ferrous ion concentration in this zone is calculated by material balance as indicated in Section 3.4.4. The use of a multiplication factor of 1.07 (15/14) instead of 1.5 to calculate the ferrous ion in this zone has only a marginal effect on the pH.

## Calcium

The calcium concentration in the mixing zone depends on gypsum dissolution and depletion in both the unsaturated zone and the mixing zone. The calculation of calcium concentration was outlined in Section 3.4.

## Monovalent Cations

Chemical weathering of clay minerals is expected to result in the release of alkali ($Na^+$, $K^+$) and alkaline earth ($Mg^{2+}$, $Ca^{2+}$) cations in the porewater. Although this weathering occurs in the unsaturated zone (layers 1 and 2), these reactions are most likely to be kinetic controlled (Helgeson et al., 1984; Berner and Holdren, 1979). Since the concentrations of these metal ions is cummulative in the porewater as it seeps through the tailings, concentrations that would have a significant effect on the pH balance would occur in the lower layers (3 and 4). For simplicity, Na feldspar, albite ($NaAlSi_3O_8$), has been chosen as the representative mineral. Albite occupies a mid position in the weathering sequence of silicate minerals.

The equilibrium reaction for albite is given as follows (Stumm and Morgan, 1981):

$$\underset{\text{Albite}}{NaAlSi_3O_8(s)} + H^+ + 4.5H_2O \rightleftharpoons Na^+ + 2\ H_4SiO_4 + 0.5\ \underset{\text{Kaolinite}}{Al_2Si_2O_5(OH)_4(s)} \quad \log K = -1.9$$

$$[Na^+] = \frac{10^{-1.9-pH}}{f^{1/4}\ [H_4SiO_4]^2} \qquad (3.6.31)$$

At dissolved silica concentrations of $10^{-3}$M, the concentration of sodium ion in solution would be:

$$[Na^+] = \frac{10^{4.1-pH}}{f^{1/4}} \qquad (3.6.32)$$

However, the weathering of feldspars is unlikely to reach equilibrium. Assuming that the sodium ion concentration is 10% of the equilibrium value (saturation index = -1.0), the concentration (in M) of sodium is given by:

$$[Na^+] = \frac{10^{3.1-pH}}{f^{1/4}} \qquad (3.6.33)$$

For pH modelling, this concentration is used as a characteristic concentration representing cations resulting from weathering reactions.

Sulphate

Dissolved sulphate in the mixing zone (layer 3) speciates as the uncomplexed ion ($SO_4^{2-}$) and various sulphato complexes ($CaSO_4^0$, $AlSO_4^+$, $FeSO_4$). The complexation products $CaSO_4^0$ and $AlSO_4^+$ are modelled as in layers 1 and 2. Iron (III) sulphate is modelled explicitly in the oxidizing zone. In the mixing zone, the ferric ion is reduced to the ferrous state. The complexation of dissolved iron (II) with sulphate is considerably weaker; the complexation constant being log K = 2.25 with $Fe^{2+}$ in comparison to log K = 3.02 with $Fe^{3+}$ in solution. In addition, the iron (II) complexation product ($FeSO_4^0$) removes equivalent charges of cationic ($Fe^{2+}$) and anionic ($SO_4^{2-}$) species in the equation for electroneutrality. For these reasons, the formation of $FeSO_4^0$ need not be modelled explicitly. The total dissolved iron (II), of course, includes both $Fe^{2+}$ and $FeSO_4^0$ species. Hydroxo complexes of ferrous ion ($Fe(OH)^+$, etc.) form only under alkaline conditions (pH>9.0), consequently, they would have no significance in this regard.

Bicarbonate

Due to the presence and the dissolution of calciferous minerals in layer 3, the bicarbonate content in layer 3 is somewhat higher than in layers 1 and 2. The partial pressure of dissolved $CO_2$ is expected to be $2x10^{-3}$ atm log $P_{CO2}$= - 2.7, which is characteristic of groundwaters unsaturated (saturation index = - 1 at pH=7.0) with respect to calcite (Stumm and Morgan, 1981).

The concentration of bicarbonate in equilibrium with this partial pressure of dissolved $CO_2$ at 10°C is (see equation (3.6.14) and (3.6.15)):

$$[HCO_3^-] = \frac{10^{pH-10.47}}{f^{1/4}} \qquad (3.6.34)$$

Ionic balance

The significant ionic species in the mixing zone include:

| Cations | Anions |
|---|---|
| $Na^+$ | $SO_4^{2-}$ |
| $Ca^{2+}$ | $HCO_3^-$ |
| $Fe^{2+}$ | |
| $Al^{3+}$ | |
| $Al(OH)^{2+}$ | |
| $Al(SO_4)^+$ | |

The ionic balance for calculating the pH in the mixing zone is as follows:

$$2[Ca^{2+}]_{mix} + 2[Fe^{2+}]_{mix} + 3\left(\frac{10^{6.8-3pH}}{f^{9/4}}\right) + 2\left(\frac{10^{1.83-2pH}}{f}\right) + \frac{10^{3.1-pH}}{f^{1/4}} =$$

$$= [SO_4^{2-}]_{mix}\left(2 - \frac{f^{3/4}\ 10^{9.7-3pH}}{1 + f^{3/4}\ 10^{9.7-3pH}}\right) + \frac{10^{pH-10.47}}{f^{1/4}} \qquad (3.6.35)$$

### 3.6.4 Layer 4

The pH in layer 4 is calculated using the same functional relationship derived for calculating pH in layer 3 (the mixing zone). The equation (3.6.35) explicitly includes the concentrations of $SO_4^{2-}$, $Ca^{2+}$ and $Fe^{2+}$. Therefore, in calculating pH for layer 4, the appropriate layer 4 concentrations of $SO_4^{2-}$, $Ca^{2+}$ and $Fe^{2+}$ must be used.

### 3.6.5 Implementation/Solution of pH Expressions

Due to the nature of the electroneutrality expressions, iterative solutions are required to calculate pH. In this study, a generalized iterative routine (Newton's method) was employed to solve the electroneutrality equations. This method solves the equation F(x)=0, and so requires explicit expressions for the function ($F(x)$), its derivative ($F'(x)$), and some initial guess for the value of x. For convergence, the initial guess ($x_1$) should be "reasonably" close to the root of the function. The method involves calculating ($F(x_1)$, $F'(x_1)$) and then calculating a new guess ($x_2$) as:

$$x_2 = x_1 - F(x_1)/F'(x_1) \qquad (3.6.36)$$

The new value ($x_2$) is then used to calculate $F(x_2)$ and $F'(x_2)$. This process continues until the absolute value of the ratio ($F(x_1)/F'(x_1)$) converges to some specified criterion. In this study, all of the iterative solutions involve determining pH. Acceptable convergence has been assumed to be achieved when:

$$\left| F(x_1)/F'(x_1) \right| < 0.01$$

For completeness, the functions F(pH) and derivatives F'(pH) for all of the pH expressions (including those involving limestone addition) are summarized below.

The method requires that the initial guess for the iterative solution be "reasonably" close to the actual root of the equation. For this reason, several empirical relationships were developed to generate these "initial guesses" and alleviate concerns regarding numerical stability. These are also summarized below.

## LAYER 1 (GYPSUM DEPLETED)

Case 1: Calcite present (from equation 3.6.18))

$$F = 2\left(\frac{10^{11.87-2pH}}{f}\right) + 10^{0.3-pH} - \frac{2[SO_4^{2-}]_{p,h}}{1000} - \frac{10^{pH-9.73}}{f^{1/4}} \qquad (3.6.37)$$

$$\frac{dF}{dpH} = -4(\ln 10)\,\frac{10^{11.87-2pH}}{f} - (\ln 10)10^{0.3-pH} - (\ln 10)\,\frac{10^{pH-9.73}}{f^{1/4}} \qquad (3.6.38)$$

Case 2: Calcite absent (from equation (3.6.17))

$$F = 3t_2 + 2t_3 + t_4 + t_5 - t_6 - [SO_4^{2-}] \qquad (3.6.39)$$

where:

$$[SO_4^{2-}] = [SO_4^{2-}]_{p,h}\left(\frac{2 - t_1}{1 + t_1}\right)$$

$$t_1 = f^{3/4}\ 10^{9.7-3pH} - f^3\ 10^{8.99-3pH}$$

$$t_2 = \left(\frac{10^{6.5}}{f^{9/4}} + 10^{5.97}\right)10^{-3pH}$$

$$t_3 = \left(\frac{10^{1.53}}{f} + 10^{3.78}\right)10^{-2pH}$$

$$t_4 = 10^{0.3-pH}$$

$$t_5 = \frac{10^{-pH}}{f^{1/4}}$$

$$t_6 = \frac{10^{pH-11.27}}{f^{1/4}}$$

and

$$\frac{dF}{dpH} = -9(\ln 10)\ t_2 - 4(\ln 10)t_3 - (\ln 10)t_4 - (\ln 10)t_5$$

$$- (\ln 110)t_6 - [SO_4^{2-}]_{p,h}\ t_7 \qquad (3.6.40)$$

where:

$$t_7 = \frac{d}{dpH}\left(\frac{2 - t_1}{1+t_1}\right) = \frac{-dt_1}{dpH}\left[\frac{2 - t_1}{(1+t_1)^2} + \frac{1}{(1+t_1)}\right] = \frac{-dt_1}{dpH}\left[\frac{3}{(1 + t_1)^2}\right]$$

$$\frac{dt_1}{dpH} = -3\ (\ln 10)f^{3/4}\ 10^{9.7-3pH} - 3(\ln 10)f^3\ 10^{8.99 - 3pH}$$

The initial estimate for pH is calculated from the expression:

$$pH_1 = 4.383551 - \frac{2.723818}{\pi}\tan^{-1}\left(k \log [SO_4^{2-}]_{p,\lambda w} + 4.230414\right) \qquad (3.6.41)$$

where

$$k = 0.7250 + 6.56281 \times 10^{-2} \left(\log[SO_4^{2-}]_{p,\lambda w} + 3.4\right)^4$$

This empirical relationship applies (strictly) only for the calcite absent case. It was derived by examining the relationship between the pH in layer 1 and the value of $[SO_4^{2-}]_{p,\lambda w}$.

**LAYER 2 (GYPSUM ENRICHED)**

Case 1. Calcite present (from equation (3.6.25))

$$F = 2\left(\frac{10^{11.87-2pH}}{f}\right) + 10^{0.3-pH} - 2\left(\frac{10^{2pH-16.47}}{f}\right) - \frac{10^{pH-9.73}}{f^{1/4}} \qquad (3.6.42)$$

$$\frac{dF}{dpH} = -4(\ln 10)\left(\frac{10^{11.87-2pH}}{f}\right) - (\ln 10)\,10^{0.3-pH} - 4(\ln 10)\left(\frac{10^{2pH-16.47}}{f}\right) - (\ln 10)\left(\frac{10^{pH-9.73}}{f^{1/4}}\right) \qquad (3.6.43)$$

Case 2: Calcite absent (from equation (3.6.23))

$$F = t_2 + t_3 + t_4 + t_5 + 2\,[Ca^{2+}] - t_6 - [SO_4^{2-}] \qquad (3.6.44)$$

where:

$$[Ca^{2+}] = \left(\frac{10^{-4.6}}{f^2}(1+t_1) + 0.25[SO_4^{2-}]_{p,\lambda w}\right)^{1/2} - 0.5\,[SO_4^{2-}]_{p,\lambda w}$$

$$t_1 = f^{3/4}\,10^{9.7-3pH} + f^3\,10^{8.99-3pH}$$

$$[SO_4^{2-}] = \left([Ca^{2+}] + [SO_4^{2-}]_{p,\lambda w}\right)\left(\frac{2 - t_1}{1 + t_1}\right)$$

$$t_2 = 3\left(\frac{10^{6.5}}{f^{9/4}} + 10^{5.97}\right)10^{-3pH}$$

$$t_3 = 2\left(\frac{10^{1.53}}{f} - 10^{3.78}\right)10^{-2pH}$$

$$t_4 = 10^{0.3-pH}$$

$$t_5 = \frac{10^{-pH}}{f^{1/4}}$$

$$t_6 = \frac{10^{pH-11.27}}{f^{1/4}}$$

$$\frac{dF}{dpH} = -3(\ln 10)t_2 - 2(\ln 10)t_3 - (\ln 10)t_4 - (\ln 10)t_5 + 2\,t_8 - (\ln 10)t_6 - t_{10}$$

(3.6.45)

where:

$$t_7 = \frac{dt_1}{dpH} = -3(\ln 10)\,f^{3/4}\,10^{9.7-3pH} - 3(\ln 10)\,f^3\,10^{8.97-3pH}$$

$$t_8 = \frac{d[Ca^{2+}]}{dpH} = 1/2\left[\frac{10^{-4.6}(1+t_1)}{f^2} + 0.25\,[SO_4^{2-}]^2_{p,\lambda w}\right]^{-1/2} \frac{10^{4.6}}{f^2}t_7$$

$$t_9 = \frac{d}{dpH}\left(\frac{2-t_1}{1+t_1}\right) = \frac{-dt_1}{dpH}\left(\frac{2-t_1}{(1+t_1)^2} + \frac{1}{(1+t_1)}\right) = -\frac{3\,t_7}{(1+t_1)^2}$$

$$t_{10} = \frac{d[SO_4^{2-}]}{dpH} = [SO_4{}^2]_{p,\lambda w}\,t_9 + [Ca]t_9 + \frac{(2-t_1)}{(1+t_1)}t_8$$

The initial pH estimate is given by an empirical equation derived by observing the relationship between the pH in layer 2 and $[SO_4^{2-}]_{p,\lambda w}$.

$$pH_2 = 4.383551 - \frac{2.723818}{\pi}\tan^{-1}(k\log[SO_4^{2-}]_{p,\lambda w} + 4.230414) \qquad (3.6.46)$$

$$k = 0.7250 + 6.56281 \times 10^{-2}\,[\log[SO_4^{2-}]_{p,\lambda w} + 3.4]^4$$

**LAYER 3 (MIXING ZONE) (from equation (3.6.35))**

$$F = 2[Ca^{2+}]_{mix} + 2[Fe^{2+}]_{mix} + t_1 + t_2 + t_3 - \left(\frac{2-t_4}{1+t_4}\right)[SO_4^{2-}]_{mix} - t_5 \qquad \ldots.(3.6.47)$$

where:

$$t_1 = 3\left(\frac{10^{(6.8-3pH)}}{f^{9/4}}\right)$$

$$t_2 = 2\left(\frac{10^{(1.83-2pH)}}{f}\right)$$

$$t_3 = \frac{10^{(3.1-pH)}}{f^{1/4}}$$

$$t_4 = f^{3/4}\, 10^{(9.7-3pH)}$$

$$t_5 = \frac{10^{(pH-10.47)}}{f^{1/4}}$$

$$\frac{dF}{dpH} = -3(\ln 10)t_1 - 2(\ln 10)t_2 - (\ln 10)t_3 - t_6[SO_4^{2-}]_{mix} - (\ln 10)t_5 \quad \text{....(3.6.48)}$$

where:

$$\frac{dt_4}{dpH} = -3(\ln 10)t_4$$

$$t_6 = \frac{d}{dpH}\left(\frac{2-t_4}{1+t_4}\right) = -\left[\frac{(2-t_4)}{(1+t_4)^2} + \frac{1}{(1+t_4)}\right]\frac{dt_4}{dpH}$$

The initial pH estimate is obtained from a further empirical relationship developed as described previously:

$$pH = 4.91345 - \frac{3.5731}{\pi}\tan^{-1}\left(k(\log[SO_4^{2-}]_{p,mix} + 2.03)\right) \quad (3.6.49)$$

where:

$$k = 0.95553 + 1.44448\,(\log\,[SO_4^{2-}]_{p,mix} + 1.555)^2$$

## 3.7 Initial Conditions - Radionuclides

As with the initial set of calculations for the ionic species (Section 3.2), the calculations described in this section are performed in the first simulation time step. Again, this first time step actually represents the time step preceding t=0 years. The calculated values are presented as being representative of t=0 years. Thus, the necessary operations include certain initialization steps as well as the calculation of all radionuclide concentrations in the first time step. In some instances, the calculations are not repeated in any other time steps. These are described in detail in this section. However, a number of the calculations appropriate for the first time period are also applicable at all other times. In these cases, no detailed derivations are provided in this section. Rather, reference is made to the appropriate derivation in a subsequent section.

### 3.7.1 Uranium

The concentrations and activities of uranium in this study refer to total uranium in the tailings. This is a mixture of uranium isotopes often referred to as natural uranium (U-NAT). On an activity basis, several uranium isotopes are significant, however, on a mass (or molar) basis, U-238 is by far the predominant isotope. The initial activity of both U-NAT and U-238 in the ore can be calculated as functions of the (uranium) grade of the ore:

$$a^o_{U\text{-NAT, ore}} = \frac{m^o_U}{100} \; \frac{714\text{g U-NAT}}{842\text{g } U_3O_8} \; 2.5 \times 10^4 \; \frac{\text{Bq U-NAT}}{\text{g U-NAT}} \qquad (3.7.1)$$

and:

$$a^o_{U\text{-238, ore}} = \frac{m^o_U}{100} \; \frac{714\text{g U-NAT}}{842\text{g } U_3O_8} \; 1.22 \times 10^4 \; \frac{\text{Bq U-238}}{\text{g U-NAT}} \qquad (3.7.2)$$

where:

$a^o_{U\text{-NAT, ore}}$ = initial activity of U-NAT in the ore ($Bq.g^{-1}$ ore)

$a^o_{U\text{-238,ore}}$ = initial activity of U-238 in the ore ($Bq.g^{-1}$ ore)
$m^o_U$ = mass % of uranium (as $U_3O_8$) in the ore

The initial activity of uranium (U-NAT) in the tailings is calculated as a function of the activity of uranium in the ore fed to the mill:

$$a^o_{U\text{-NAT, tails}} = a^o_{U\text{-NAT,ore}} \; (1 - f_U) \qquad (3.7.3)$$

where:

$a^o_{U\text{-NAT, tails}}$ = initial activity of U-NAT in the tailings ($Bq.g^{-1}$ tailings)
$f_U$ = mass fraction of uranium recovered in the mill

The initial concentration of uranium in the solid phase is then easily calculated:

$$[U_s]^o = a^o_{U\text{-NAT,tails}} \rho_T \qquad (3.7.4)$$

where:

$[U_s]^o$ = initial concentration of uranium in tailings solid phase ($Bq.m^{-3}$)
$\rho_T$ = tailings bulk density ($g.m^{-3}$)

Since a number of subsequent calculations are performed on a mass (molar) basis, rather than on an activity basis, a conversion factor is defined:

$$UCF = 2.5 \times 10^4 \frac{Bq}{g} \; 238 \frac{g}{mol}$$

$$= 5.95 \times 10^6 \; Bq.\ mol^{-1} \qquad (3.7.5)$$

where:

UCF = uranium conversion factor ($Bq.mol^{-1}$)

It is then assumed that some fraction of the uranium is associated with pyrite. The concentration of this uranium is given by:

$$[U_3O_8]^o_{pyr} = \frac{[U_s]^o \, f_{U/Fe}}{3 \; UCF} \qquad (3.7.6)$$

where:

$[U_3O_8]^o_{pyr}$ = initial concentration of $U_3O_8$ associated with pyrite ($mol.m^{-3}$)
$f_{U/Fe}$ = fraction of $U_3O_8$ associated with pyrite

Then:

$$X_{U/Fe} = [U_3O_8]^o_{pyr} \,/\, [FeS_2]^o \qquad (3.7.7)$$

where:

$X_{U/Fe}$ = mol fraction of $U_3O_8$ in pyrite
$[FeS_2]^o$ = initial concentration of pyrite ($mol.m^{-3}$)

The liquid phase concentrations of uranium are determined as a function of pyrite oxidation. This process is described in further detail in Section

3.8. In summary, the initial concentration of uranium in the unsaturated zone is:

$$[U_L]^o_{\lambda w} = \frac{3\ \lambda_w}{P\Delta t} X_{U/Fe}\ [FeS_2]^o\ (1 - \exp\ (-k\Delta t))\ UCF \qquad (3.7.8)$$

where:

$[U_L]^o_{\lambda w}$ = initial liquid phase concentration of uranium in the unsaturated zone ($Bq.m^{-3}$)

$\lambda_w$ = thickness of unsaturated zone (m)

P = net precipitation ($m.yr^{-1}$)

$\Delta t$ = time step (yr)

k = rate constant for pyrite oxidation (see Section 3.3.1) ($yr^{-1}$)

Since we assume that no pyrite oxidation occurs in the saturated zone (layers 3 and 4), the only source of dissolved uranium in these layers is that which is transported down from the unsaturated zone. Mass balance equations, accounting for the transport of uranium into layers 3 and 4 and its adsorption there, are developed later (Section 3.8). In summary, the initial concentrations of dissolved uranium in layers 3 and 4 can be calculated as:

$$[U_L]^o_{mix} = [U_L]^o_{\lambda w} - [U_L]^o_{\lambda w}\ \exp\left[\frac{-\ P\Delta t}{\epsilon\lambda_w(1 + K_{D,U02}\rho_T/\epsilon)}\right] \qquad (3.7.9)$$

$$[U_L]^o_4 = [U_L]^o_{mix} - [U_L]^o_{mix}\ \exp\left[\frac{-\ f_p\ \overline{P}\Delta t}{\epsilon\lambda_4(1 + K_{D,U02}\rho_T/\epsilon)}\right] \qquad (3.7.10)$$

where:

$[U_L]^o_{mix}$ = initial liquid phase concentration of uranium in layer 3 (the mixing zone) ($Bq.m^{-3}$)

$[U_L]^o_4$ = initial liquid phase concentration of uranium in the bottom layer ($Bq.m^{-3}$)

P = annual net precipitation ($m.yr^{-1}$)

$\overline{P}$ = long-term mean annual net precipitation ($m.yr^{-1}$)

$f_p$ = fraction of precipitation which infiltrates to layer 4

$\lambda_{mix}$ = thickness of the mixing zone (m)

$\lambda_4$ = thickness of the bottom layer (m)
(e.g. 10 - ($\lambda_w - \lambda_{mix}$) assuming 10 m tailings depth)

$\rho_T$ = tailings bulk density ($g.m^{-3}$)

$\epsilon$ = tailings porosity

$K_{D,UO2}$ = uranium solid-liquid distribution coefficient ($m^3.g^{-1}$)

### 3.7.2 Thorium

The thorium calculations are complicated by the fact that two thorium isotopes Th-230 and Th-232 must be considered in the calculations. On a mass basis, Th-232 is orders of magnitude more significant than Th-230. However, on an activity basis, both make substantial contributions to the total activity. In the source term calculations, the mass or activity of Th-230 and Th-232 are generally calculated separately and then summed to obtain the mass or activity of total thorium. Again, because some calculations are performed on a mass (molar) basis and others on an activity basis, it is useful to define conversion factors at this stage:

$$T230CF = 7.17 \times 10^8 \frac{Bq}{g} \quad 230 \frac{g}{mol} \qquad (3.7.11)$$

$$= 1.65 \times 10^{11}\ Bq.mol^{-1}$$

$$T232CF = 4.033 \times 10^3 \frac{Bq}{g} \quad 232 \frac{g}{mol} \qquad (3.7.12)$$

$$= 9.35 \times 10^5\ Bq.\ mol^{-1}$$

where:

T230CF = Th-230 conversion factor ($Bq.mol^{-1}$)

T232CF = Th-232 conversion factor ($Bq.mol^{-1}$)

Assuming that secular equilibrium exists in the ore, the activities of Th-230 and U-238 in the ore would be equal. Further, assuming that no Th-230 is recovered in the mill, the initial activity of Th-230 in the tailings is expected to equal the activity of U-238 in the ore fed to the mill. That is:

$$a^{o}_{Th-230} = a^{o}_{U-238,ore} \tag{3.7.13}$$

where:

$a^{o}_{Th-230}$ = initial activity of Th-230 in the tailings ($Bq.g^{-1}$)

The initial concentration of Th-230 is then calculated as:

$$[Th\text{-}230_s]^o = a^{o}_{Th-230}\ \rho_T/T230CF \tag{3.7.14}$$

where:

$[Th\text{-}230_s]^o$ = initial solid phase concentration of Th-230 ($mol.m^{-3}$)

The initial concentration of Th-232 is calculated as a function of the percent of thorium in the ore, as follows:

$$[Th\text{-}232_s]^o = \left(\frac{m^{o}_{Th}}{100}\right)\left(\frac{\rho_T}{264}\right) \tag{3.7.15}$$

where:

$[Th\text{-}232_s]^o$ = initial solid phase concentration of Th-232 ($mol.m^{-3}$)

$m^{o}_{Th}$ = mass % of thorium (as $ThO_2$) in the ore

264 = molecular weight of $ThO_2$ ($g.mol^{-1}$)

The initial activity of Th-232 is easily calculated by multiplying by the conversion factor:

$$a^{o}_{Th-232} = [Th\text{-}232_s]^o\ T232CF/\rho_T \tag{3.7.16}$$

where:

$a^{o}_{Th-232}$ = initial activity of Th-232 ($Bq.g^{-1}$)

The activity and concentration of total thorium is then obtained by summing the activities or concentrations of Th-230 and Th-232. That is:

$$a^o_{Th} = a^o_{Th-230} + a^o_{Th-232} \qquad (3.7.17)$$

$$[Th_s]^o = [Th\text{-}230_s]^o + [Th\text{-}232_s]^o \qquad (3.7.18)$$

where:

$a^o_{Th}$ = initial activity of total thorium in the tailings ($Bq.g^{-1}$)

$[Th_s]^o$ = initial concentration of total thorium in the tailings ($mol.m^{-3}$)

Some fraction of the original Th-230 and Th-232 inventories are assumed to be soluble. The soluble and insoluble inventories are calculated as follows:

$$[Th\text{-}230_s]^o_{sol} = f_{Th-230}\,[Th\text{-}230_s]^o \qquad (3.7.19)$$

$$[Th\text{-}232_s]^o_{sol} = f_{Th-232}\,[Th\text{-}232_s]^o \qquad (3.7.20)$$

$$[Th\text{-}230_s]^o_{insol} = (1 - f_{Th-230})\,[Th\text{-}230_s]^o \qquad (3.7.21)$$

$$[Th\text{-}232_s]^o_{insol} = (1 - f_{Th-232})\,[Th\text{-}232_s]^o \qquad (3.7.22)$$

where:

$[Th\text{-}230_s]_{sol}$ = initial concentration of soluble Th-230 ($mol.m^{-3}$)

$[Th\text{-}232_s]_{sol}$ = initial concentration of soluble Th-232 ($mol.m^{-3}$)

$[Th\text{-}230_s]_{insol}$ = initial concentration of insoluble Th-230 ($mol.m^{-3}$)

$[Th\text{-}232_s]_{insol}$ = initial concentration of insoluble Th-232 ($mol.m^{-3}$)

$f_{Th-230}$ = fraction of solid phase Th-230 which is soluble

$f_{Th-232}$ = fraction of solid phase Th-232 which is soluble

The concentrations of total soluble and insoluble thorium are then easily determined:

$$[Th_s]^o_{sol} = [Th\text{-}230_s]^o_{sol} + [Th\text{-}232_s]^o_{sol} \qquad (3.7.23)$$

$$[Th_s]^o_{insol} = [Th\text{-}230_s]^o_{insol} + [Th\text{-}232_s]^o_{insol} \qquad (3.7.24)$$

where:

$[Th_s]^o_{sol}$ = initial concentration of total soluble thorium ($mol.m^{-3}$)

$[Th_s]^o_{insol}$ = initial concentration of total insoluble thorium ($mol.m^{-3}$)

These quantities can also be expressed on an activity basis:

$$a^o_{Th,insol} = [Th\text{-}230]^o_{insol}\ T230CF + [Th\text{-}232]^o_{insol}\ T232CF \quad (3.7.25)$$

$$a^o_{Th,sol} = [Th\text{-}230]^o_{sol}\ T230CF + [Th\text{-}232]^o_{sol}\ T232CF \quad (3.7.26)$$

where:

$a^o_{Th,insol}$ = initial activity of total insoluble thorium ($Bq.m^{-3}$)

$a^o_{Th,sol}$ = initial activity of total soluble thorium ($Bq.m^{-3}$)

Once the initial inventories have been calculated, the mass (or activity) fraction of each isotope can be determined, as follows:

$$X_{Th\text{-}230/Th,sol} = [Th\text{-}230_s]^o_{sol} / [Th_s]^o_{sol} \quad (3.7.27)$$

$$X_{Th\text{-}232/Th,sol} = [Th\text{-}232_s]^o_{sol} / [Th_s]^o_{sol} \quad (3.7.28)$$

$$XA_{Th\text{-}232/Th,sol} = [Th\text{-}232_s]^o_{sol}\ T232CF / a^o_{Th,sol} \quad (3.7.29)$$

$$XA^o_{Th\text{-}232/Th,insol} = [Th\text{-}232_s]^o_{insol}\ T232CF / a^o_{Th,insol} \quad (3.7.30)$$

where:

$X_{Th\text{-}230/Th,sol}$ = mole fraction of Th-230 in soluble thorium

$X_{Th\text{-}232/Th,sol}$ = mole fraction of Th-232 in soluble thorium

$XA_{Th\text{-}232/Th,sol}$ = activity fraction of Th-232 in the soluble thorium

$XA^o_{Th\text{-}232/Th,insol}$ = activity fraction of Th-232 in the insoluble thorium

The liquid (soluble) phase mole or activity fractions will not change with time. However, the solid (insoluble) phase activity fraction will change with time, as the potentially soluble thorium is leached from the solid phase. As the potentially soluble thorium dissolves, the thorium isotopes will be released in proportion to the mole fraction of each isotope in the soluble thorium. Thus, we can predict the relative concentrations of Th-230 and Th-232 in the liquid phase at any time. Since many of the calculations are performed on a molar basis, it is again useful to define a conversion factor.

In this case:

$$\mathrm{THORCF} = X_{Th\text{-}230/Th,sol}\ \mathrm{T230CF} + (1 - X_{Th\text{-}230/Th,sol})\ \mathrm{T232CF} \qquad (3.7.31)$$

where:

THORCF = weighted, liquid phase, thorium conversion factor ($\mathrm{Bq.mol^{-1}}$)

The liquid phase concentrations of total thorium are calculated as functions of pH in each of the unsaturated, mixing and bottom layers (layers 2, 3 and 4). Details of this relationship are provided in Section 3.9. In summary, the liquid phase thorium concentration in layer "l" is calculated as:

$$[Th_L]_l = \frac{10^{(K_{Th} - 4\ pH)}}{f^4} \Big\{ 1 + f^{7/4}\ 10^{(pH - 3.2)} + f^3\ 10^{(2pH - 6.93)} + f^{15/4}\ 10^{(3pH - 11.7)} + f^4\ 10^{(4pH - 15.9)} + f^4\ 10^{5.45}\ [SO_4^{2-}]_{u,l} + f^6\ 10^{9.73}\ [SO_4^{-2}]_{u,l}^2 \Big\} \qquad (3.7.32)$$

where:

$[Th_L]_l$ = liquid phase thorium concentration in layer "l" ($\mathrm{mol.L^{-1}}$) (must be converted to $\mathrm{mol.m^{-3}}$)
pH = pH in layer "l"
f = activity coefficient for divalent ions
$[SO_4^{2-}]_{u,l}$ = concentration of uncomplexed sulfate ion in layer "l" ($\mathrm{mol.L^{-1}}$)
$K_{Th}$ = correction factor for amorphous vs. crystalline $Th(OH)_4$ (see Section 3.9)

Note, that the concentrations in this relationship are in units of $\mathrm{mol.L^{-1}}$. They must be converted to and from the $\mathrm{mol.m^{-3}}$ units used in the rest of the model. The calculated values of $[Th_L]$ must also be converted to an activity basis, by multiplying by the weighted, liquid phase conversion factor (THORCF).

### 3.7.3 Radium

Radium dissolved during the milling process is assumed to precipitate with barium sulphate, forming a barium-radium sulphate ($Ba(Ra)SO_4$) coprecipitate. The $Ba(Ra)SO_4$ coprecipitate dissolves in a frontwise manner, resulting in an upper layer depleted of $Ba(Ra)SO_4$ and a lower layer enriched in $Ba(Ra)SO_4$. The solid phase radium inventory is comprised of 2 components; radium associated with barium sulphate and radium associated with the host tailings material. The dissolution of the barium-radium sulphate coprecipitate acts as the source of liquid phase radium.

The initial activity of Ra-226 is calculated by again assuming secular equilibrium in the ore. This indicates that the activities of all the elements of the U-238 decay chain are initially equal. Thus:

$$a^o_{Ra} = a^o_{Th\text{-}230} \qquad (3.7.33)$$

where:

$a^o_{Ra}$ = initial activity of Ra-226 in the tailings ($Bq.g^{-1}$)

We can, again, calculate a conversion factor, to convert from a molar to an activity basis:

$$RACF = 3.66 \times 10^{10}\ \frac{Bq}{g}\ 226\ \frac{g}{mol}$$

$$= 8.26 \times 10^{12}\ Bq.mol^{-1} \qquad (3.7.34)$$

where:

RACF = Ra-226 conversion factor ($Bq.mol^{-1}$)

Then, the initial concentration of radium can be determined:

$$[Ra_s]^o = a^o_{Ra}\ \rho_T\ /RACF \qquad (3.7.35)$$

where:

$[Ra_s]^o$ = initial concentration of solid phase Ra-226 in the tailings ($mol.m^{-3}$)

We assume that all of the radium dissolved in the mill reprecipitates with $BaSO_4$. Thus, the concentration of radium associated with barium sulphate is expressed as:

$$[Ra_s]^o_{Ba} = f_{Ra}\,[Ra_s]^o \qquad (3.7.36)$$

where:

$[Ra_s]^o_{Ba}$ = initial concentration of Ra-226 associated with $BaSO_4$ ($mol.m^{-3}$)

$f_{Ra}$ = fraction of Ra-226 which is assumed to be soluble

Similarily, the radium associated with the host tailings is that fraction of radium which was not solubilized in the mill:

$$[Ra_s]^o_m = (1 - f_{Ra})\,[Ra_s]^o \qquad (3.7.37)$$

where:

$[Ra_s]^o_m$ = initial concentration of Ra-226 associated with host tailings material ($mol.m^{-3}$) (Assumed to be not leachable)

The initial concentration of $BaSO_4$ is calculated as a function of the mole fraction of Ra-226 in $BaSO_4$:

$$[BaSO_4]^o = [Ra_s]^o_{Ba}/X^o_{Ra/BaSO_4} \qquad (3.7.38)$$

where:

$[BaSO_4]^o$ = initial solid phase concentration of $BaSO_4$ ($mol.m^{-3}$)

$X^o_{Ra/BaSO_4}$ = initial mole fraction of Ra-226 in $BaSO_4$

The initial inventory of the radium associated with $BaSO_4$ in the unsaturated and mixing zones is calculated as:

$$M^o_{Ra} = X^o_{Ra/BaSO_4}(\lambda_w[BaSO_4]^o + \lambda_{mix}[BaSO_4]^o) \qquad (3.7.39)$$

where:

$M^o_{Ra}$ = total radium initially associated with $BaSO_4$ in the unsaturated and mixing zones ($mol.m^{-2}$)

For the purposes of calculating solid phase concentrations, we assume that $BaSO_4$ has been depleted from the upper 1 cm of tailings during the initial time step. Thus:

$$[Ra_s]^o_1 = [Ra_s]^o_m \qquad (3.7.40)$$

and

$$[Ra_s]^o_2 = [Ra_s]^o_m + [Ra_s]^o_{Ba} = [Ra_s]^o_{\lambda w} \qquad (3.7.41)$$

where:

$[Ra_s]^o_1$ = initial solid phase radium concentration in the upper (surface) layer ($mol.m^{-3}$)

$[Ra_s]^o_{\lambda w}$ = initial solid phase radium concentration in the remainder of the unsaturated zone ($mol.m^{-3}$)

We further assume that all of the tailings, with the exception of the upper 1 cm are homogeneous with respect to solid phase radium. That is:

$$[Ra_s]^o_{mix} = [Ra_s]^o_4 = [Ra_s]^o_{\lambda w} \qquad (3.7.42)$$

where:

$[Ra_s]^o_{mix}$, $[Ra_s]^o_4$ = initial solid phase concentrations of radium in the mixing zone and layer 4 respectively ($mol.m^{-3}$)

All of these concentrations may be converted to an activity basis by multiplying by the conversion factor defined previously (RACF).

The liquid phase concentrations of radium are determined as functions of $BaSO_4$ solubility in the various layers. The details of this process are provided in Section 3.10.2. In summary, the concentration of barium in layer "l" can be determined as a function of the concentration of uncomplexed sulphate in the same layer. That is:

$$[Ba^{2+}]_l = \frac{K^o_{s,BaSO_4}/f^2}{\sqrt{K^o_{s,BaSO_4}/f^2 + [SO_4^{2-}]_{u,l}}} \left(1 + f^2 K_{f,BaSO_4} [SO_4^{2-}]_{u,l}\right) \qquad (3.7.43)$$

where:

$[Ba^{2+}]_l$ = liquid phase concentration of $Ba^{2+}$ in layer "l" ("l" = 2, 3, 4) ($mol.m^{-3}$)

$K^o_{s,BaSO_4}$ = solubility equilibrium constant for $BaSO_4$ ($mol^2.m^{-6}$)

$f$ = activity coefficient for divalent ions

$K_{f,BaSO_4}$ = formation constant for $BaSO_4$ ($m^3.mol^{-1}$)

$[SO_4^{2-}]_{u,l}$ = concentration of uncomplexed sulphate ion in layer "l"($mol.m^{-3}$)

The concentration of Ra-226 is then given by:

$$[Ra_L]_l = K_{Ra} [Ba^{2+}]_l \, X^o_{Ra/BaSO_4} \qquad (3.7.44)$$

where:

$[Ra_L]_l$ = liquid phase concentration of Ra-226 in layer "l" ($mol.m^{-3}$)

$K_{Ra}$ = radium distribution coefficient (see Section 3.10.2)

Again, the concentration of radium can be converted to an activity basis by multiplying by the radium conversion factor (RACF).

### 3.7.4 Lead

Lead-210 is modelled in a manner very similar to Ra-226. Pb-210 is assumed to dissolve in the mill and to coprecipitate with lead sulphate ($PbSO_4$). The $Pb(Pb\text{-}210)SO_4$ coprecipitate dissolves and reprecipitates in a frontwise manner analogous to $Ba(Ra)SO_4$. Thus, we can again refer to a $PbSO_4$ depleted zone (layer 1) and a $PbSO_4$ enriched zone (layer 2).

The initial activity of Pb-210 in the tailings is equal to the initial activities of Th-230 and Ra-226 in the tailings. That is:

$$a^o_{Pb} = a^o_{Ra} \qquad (3.7.45)$$

where:

$a^o_{Pb}$ = initial activity of Pb-210 in the tailings ($Bq.g^{-1}$)

A conversion factor is defined as:

$$PBCF = 3.0 \times 10^{12} \frac{Bq}{g} \quad 210 \frac{g}{mol} \qquad (3.7.46)$$

$$= 6.3 \times 10^{14} \ Bq.mol^{-1}$$

where:

PBCF = Pb-210 conversion factor ($Bq.mol^{-1}$)

The initial concentration of lead-210 is then calculated as:

$$[Pb\text{-}210_s]^o = a^o_{Pb} \ \rho_T \ /PBCF \qquad (3.7.47)$$

where:

$[Pb\text{-}210_s]^o$ = initial solid phase concentration of Pb-210 ($mol.m^{-3}$)

All of the Pb-210 dissolved in the mill is assumed to be associated with $PbSO_4$. Thus, the concentration of Pb-210 associated with $PbSO_4$ is given by:

$$[Pb\text{-}210_s]^o_{PbSO_4} = f_{Pb}[Pb\text{-}210_s]^o \qquad (3.7.48)$$

where:

$[Pb\text{-}210_s]^o_{PbSO_4}$ = initial solid phase concentration of Pb-210 associated with $PbSO_4$ ($mol.m^{-3}$)

$f_{Pb}$ = fraction of Pb-210 assumed to be soluble

The insoluble Pb-210 remains associated with the host tailings material. In particular:

$$[\text{Pb-210}_s]^o_m = (1 - f_{Pb})\,[\text{Pb-210}_s]^o \qquad (3.7.49)$$

where:

$[\text{Pb-210}_s]^o_m$ = initial solid phase concentration of Pb-210 associated with host tailings material ($\text{mol.m}^{-3}$) (assumed to be not leachable)

The initial mole fraction of Pb-210 in $PbSO_4$ is calculated as a function of the initial concentration of $PbSO_4$ in the tailings:

$$X^o_{\text{Pb-210}/PbSO_4} = [\text{Pb-210}_s]^o_{PbSO_4}/[PbSO_4]^o \qquad (3.7.50)$$

where:

$X^o_{\text{Pb-210}/PbSO_4}$ = initial mole fraction of Pb-210 in $PbSO_4$

$[PbSO_4]^o$ = initial concentration of $PbSO_4$ in the tailings ($\text{mol.m}^{-3}$)

In calculating the solid phase concentrations of Pb-210, we again assume that the upper 1 cm of tailings has been depleted of $PbSO_4$ during the first timestep. The remainder of the tailings are assumed to be homogeneous with respect to $PbSO_4$ in the solid phase. Thus, the solid phase concentrations of Pb-210 are given by:

$$[\text{Pb-210}_s]^o_1 = [\text{Pb-210}_s]^o_m \qquad (3.7.51)$$

$$[\text{Pb-210}_s]^o_{\lambda w} = [\text{Pb-210}_s]^o_{mix} = [\text{Pb-210}_s]^o_4 = [\text{Pb-210}_s]^o \qquad (3.7.52)$$

where:

$[\text{Pb-210}_s]^o$ = initial solid phase concentration of Pb-210 in layer "1" ($\text{mol.m}^{-3}$)

The liquid phase concentrations are determined as functions of $PbSO_4$ solubility in the various layers. The details of this process, and rationale for the approach used, are provided in Section 3.11. The concentration of Pb-210 is calculated as a function of the total concentration of $Pb^{2+}$ ion, which in turn is a function of sulphate concentration. In summary, the total concentration of $Pb^{2+}$ is given by:

$$[Pb^{2+}]_l = \frac{K^o_{s,PbSO_4}/f^2 \quad (1 + f^2\, K_{f,PbSO_4}[SO_4^{2-}]_{u,l})}{\sqrt{K^o_{s,PbSO4}/f^2} + [SO_4^{2-}]_{u,l}} \qquad (3.7.53)$$

where:

$[Pb^{2+}]_l$ = total concentration of $Pb^{2+}$ ion in layer "l" ("l" = 2, 3, 4) ($mol.m^{-3}$)

$K^o_{s,PbSO_4}$ = solubility equilibrium constant for $PbSO_4$ ($mol^2.m^{-6}$)

$K_{F,PbSO_4}$ = formation constant for $PbSO_4$ ($m^3.mol^{-1}$)

$[SO_4^{2-}]_{u,l}$ = concentration of uncomplexed sulphate ion in layer "l" ("l" = 2, 3, 4) ($mol.m^{-3}$)

The concentration of Pb-210 is then given by:

$$[Pb\text{-}210]^o_l = X^o_{Pb\text{-}210/PbSO_4}\, [Pb^{2+}]_l \qquad (3.7.54)$$

where:

$[Pb\text{-}210]^o_l$ = initial liquid phase concentration of Pb-210 in layer "l" ("l" = 2, 3, 4) ($mol.m^{-3}$)

Again, all concentrations must be converted from $mol.m^{-3}$ to $Bq.m^{-3}$ using the conversion factor defined previously (PBCF).

## 3.8 Uranium

Most of the uranium present in the ore is dissolved and recovered during the milling process. However, some fraction of the uranium resists solubilization, and hence is present in the tailings. The residual uranium is assumed to be evenly distributed throughout the tailings. Of the uranium in the tailings, it is also assumed that a certain fraction is associated with pyrite, i.e. present as microcrystals of $U_3O_8$ in pyrite. As pyrite oxidizes, the uraninite becomes soluble by either of the following reactions:

$$2\ U_3O_8(s) + 12\ H^+ + O_2 \longrightarrow 6\ UO_2{}^{2+} + 6\ H_2O$$
$$U_3O_8(s) + 2\ F_e{}^{3+} + 4\ H^+ \longrightarrow 3\ UO_2{}^{2+} + 2\ Fe^{2+} + 2\ H_2O$$

We may assume that either of the two reactions are considerably faster than the rate of pyrite oxidation. This means that the rate controlling step is the oxidation of pyrite:

$$\frac{\Delta[FeS_2] =}{\Delta t} \quad \frac{[FeS_2]_{t-\Delta t}\ [1 - \exp(-k\Delta t)]}{\Delta t} \qquad (3.8.1)$$

where:

$$\frac{\Delta[FeS_2]}{\Delta t} = \frac{\text{moles of pyrite oxidized}}{m^3\ \text{tailings.year}}$$

If we define $X_{U/Fe}$ as the mole fraction of $U_3O_8$ in pyrite (calculated previously), the mean concentration of $UO_2^{2+}$ in the porewater (at $\lambda_w$) is:

$$[UO_2{}^{2+}]_{\lambda w,t} = \frac{3\lambda_w}{P\Delta t}\ X_{U/Fe}\ [FeS_2]_{t-\Delta t}[1 - \exp\ (-k\Delta t)] \qquad (3.8.2)$$

where:

$[UO_2^{2+}]_{\lambda w,t}$ = concentration of $UO_2^{2+}$ in the unsaturated zone ( = concentration of U-NAT) ($mol.m^{-3}$)
$\lambda_w$ = thickness of the unsaturated zone (m)
P = net annual precipitation ($m.yr^{-1}$)
$[FeS_2]_{t-\Delta t}$ = concentration of pyrite in the previous timestep ($mol.m^{-3}$)
$X_{U/Fe}$ = mole fraction of $U_3O_8$ in pyrite
k = rate constant for pyrite oxidation ($yr^{-1}$)

The solid phase concentration of uranium in the unsaturated layer is determined by subtracting the amount of uranium dissolved during a timestep from the solid phase inventory of uranium at the beginning of the timestep. Specifically:

$$[U_s]_t = [U_s]_{t-\Delta t} - (P\Delta t/\lambda_w)\,[UO_2^{2+}]_{\lambda w,t} \qquad (3.8.3)$$

where:

$[U_s]_t$ = solid phase concentration of uranium in the unsaturated zone at time t ($mol.m^{-3}$)

$[U_s]_{t-\Delta t}$ = solid phase concentration of uranium in the unsaturated zone during the previous timestep ($mol.m^{-3}$)

In the mixing zone, the liquid phase concentration of uranium is dependent on the concentration of uranium entering via the liquid phase from the unsaturated zone. This can be expressed as:

$$[UO_2^{2+}]_{mix,t} = [UO_2^{2+}]_{\lambda w,t} + \left\{[UO_2^{2+}]_{mix,t-\Delta t} - [UO_2^{2+}]_{\lambda w,t}\right\}$$

$$\exp\,[-P\Delta t/(\epsilon\,\lambda_{mix}(1 + K_{d,UO2}\,\rho_T/\epsilon))] \qquad (3.8.4)$$

where:

$[UO_2^{2+}]_{mix,t}$ = concentration of $UO_2^{2+}$ in the mixing zone at time t ($mol.m^{-3}$)

$[UO_2^{2+}]_{mix,t-\Delta t}$ = concentration of $UO_2^{2+}$ in the mixing zone during the previous timestep ($mol.m^{-3}$)

$K_{d,UO_2}$ = solid-liquid distribution coefficient for $UO_2^{2+}$ ($m^3.g^{-1}$)

Similarily, the uranium concentration in the bottom layer is dependent on the uranium concentration in the mixing zone:

$$[UO_2^{2+}]_{4,t} = [UO_2^{2+}]_{mix,t} + \left\{[UO_2^{2+}]_{4,t-\Delta t} - [UO_2^{2+}]_{mix,t}\right\}$$

$$\exp\,[-\,f_p\bar{P}\Delta t/(\epsilon\lambda_4\,(1 + K_{d,UO2}\,\rho_T/\epsilon))] \qquad (3.8.5)$$

where:

$[UO_2^{2+}]_{4,t}$ = concentration of $UO_2^{2+}$ in the bottom layer at time t ($mol.m^{-3}$)

$[UO_2^{2+}]_{4,t-\Delta t}$ = concentration of $UO_2^{2+}$ in the bottom layer during the previous timestep ($mol.m^{-3}$)

$f_p$ = fraction of precipitation which enters the bottom layer

$\bar{P}$ = long term mean annual net precipitation ($m.yr^{-1}$)

$\lambda_4$ = thickness of bottom layer (layer 4) (m)
= $10 - (\lambda_w + \lambda_{mix})$ (Assuming 10 m deep tailings)

Note, that all of the calculated concentrations were expressed in units of $mol.m^{-3}$. These are all converted to units of $Bq.m^{-3}$ by multiplying by the conversion factor defined previously (UCF).

## 3.9 Thorium

### 3.9.1 Unsaturated Zone

It is assumed that the concentration of thorium in the porewater is controlled by the solubility of thorium hydroxide ($Th(OH)_4(s)$). Any other precipitates that may have formed in the mill (thorium sulphate for example) would dissolve incongruently and re-precipitate as the hydroxide. The solution of thorium hydroxide has been reviewed by Langmuir and Herman (1980). The solution and complexation reactions relevant for pyritic tailings are summarized below:

| REACTION | LOG K |
|---|---|
| $Th(OH)_4(s) + 4 H^+ \rightleftharpoons Th^{+4} + 4 H_2O$ | 6.30 (amorphous)<br>1.78 (crystalline) |
| $Th^{+4} + H_2O \rightleftharpoons Th(OH)^{3+} + H^+$ | - 3.20 |
| $Th^{+4} + 2 H_2O \rightleftharpoons Th(OH)_2^{2+} + 2 H^+$ | - 6.93 |
| $Th^{+4} + 3 H_2O \rightleftharpoons Th(OH)_3^{+} + 3 H^+$ | - 11.70 |
| $Th^{+4} + 4 H_2O \rightleftharpoons Th(OH)_4^{0} (aq) + 4 H^+$ | - 15.90 |
| $Th^{+4} + SO_4^{2-} \rightleftharpoons ThSO_4^{2+}$ | 5.45 |
| $Th^{+4} + 2 SO_4^{2-} \rightleftharpoons Th(SO_4)_2^{0}$ | 9.73 |

The concentration of thorium (total) in the liquid phase is given by the combination of the above equations. At the bottom of the unsaturated zone (i.e. at $\lambda_w$) the concentration of thorium (total) in the liquid phase is:

$$[Th_L]_{\lambda w} = \frac{10^{(K_{Th} - 4pH)}}{f^4} \Big\{ 1 + f^{7/4}\, 10^{(pH-3.2)} + f^3\, 10^{(2pH-6.93)} + f^{15/4}\, 10^{(3pH - 11.7)} + f^4\, 10^{(4pH - 15.9)} + f^4\, 10^{5.45} [SO_4^{2-}]_{u,\lambda w} + f^6\, 10^{9.73} [SO_4^{2-}]^2_{u,\lambda w} \Big\} \qquad (3.9.1)$$

where:

$[Th_L]_{\lambda w}$ = liquid phase concentration of total thorium in the unsaturated zone at $\lambda_w$ (mol.L$^{-1}$)

$K_{Th}$ = apparent solubility product for thorium hydroxide (described below)

pH = pH in the unsaturated zone (i.e. at $\lambda_w$)

f = activity coefficient for divalent ions

$[SO_4^{2-}]_{u,\lambda w}$ = concentration of uncomplexed sulphate at $\lambda_w$ (mol.L$^{-1}$)
= $[SO_4^{2-}]_{\lambda w}$ /d

where:

d = a correction factor for sulphate complexation (See Section 3.3.3)

The function above (equation (3.9.1)) has the potential to predict unreasonably high total thorium concentrations at low pH values. Since the dissolution of $Th(OH)_4$ may not be equilibrium controlled below about pH 3.5, we have chosen to set an upper limit of $5 \times 10^{-5}$ mol.L$^{-1}$ on the concentration of dissolved thorium. That is:

if $[Th_L]_{\lambda w} > 5 \times 10^{-5}$ mol.L$^{-1}$ (from equation (3.9.1))

then $[Th_L]_{\lambda w} = 5 \times 10^{-5}$mol.L$^{-1}$ (3.9.2)

This corresponds well to observed field data on total dissolved thorium. Note that the concentrations in this equation are expressed in $mol.L^{-1}$. Conversions to and from $mol.m^{-3}$ must be made to correspond with the remainder of the models. The concentration of total thorium is easily converted to an activity basis, by multiplying by the overall conversion factor defined previously (THORCF).

The large difference between the solubility product of amorphous thorium hydroxide ($K_S^o = 10^{6.30}$) and crystalline $Th(OH)_4$ ($K^o{}_s = 10^{1.78}$) is evident. Since both crystalline and amorphous forms are expected to exist in the tailings, the apparent solubility product ($K_{Th}$) is dependent on the relative surface area of the two forms. If the grain sizes of the amorphous and crystalline forms are the same, the apparent solubility product can be related to the mole fraction of the crystalline form, i.e.:

$$K_{TH} = 1.78\ X_{Th,c} + 6.3\ (1 - X_{Th,c}) \qquad (3.9.3)$$

where:

$X_{Th,c}$ = fraction of $Th(OH)_4(s)$ which is crystalline

Solid Thorium Inventory

In examining the solubility dependence of thorium, it becomes evident that the pH is the most important controlling factor. Unlike $Ba(Ra)SO_4$ and $PbSO_4$, dissolved thorium is not expected to re-precipitate in the unsaturated zone. We may assume that the distribution of solid thorium hydroxide in the unsaturated zone is homogeneous initially and remains homogeneous until the potentially soluble solid ($Th(OH)_4(s)$) dissolves. In fact, the solubility of $Th(OH)_4$ increases with depth in the unsaturated zone. One may argue, however, that the solid $Th(OH)_4$ is replenished by the migration of small particles downward in the porewater.

The concentration of total thorium which has dissolved to time t is thus given by:

$$[Th]_{diss,t} = [Th]_{diss,t-\Delta t} + P\Delta t/\lambda_w\ [Th_L]_{\lambda w} \qquad (3.9.4)$$

where:

$[Th]_{diss,t}$ = concentration of total thorium dissolved in the unsaturated zone to time t ($mol.m^{-3}$)

$[Th]_{diss,t-\Delta t}$ = concentration of total thorium dissolved in the unsaturated zone to time t-Δt ($mol.m^{-3}$)

The total dissolved thorium is comprised of both Th-230 and Th-232. The concentrations of each isotope can be determined by using the fractions calculated initially:

$$[Th\text{-}232]_{diss} = [Th]_{diss,t}\ X_{Th\text{-}232/Th,sol} \qquad (3.9.5)$$

$$[Th\text{-}230]_{diss} = [Th]_{diss,t} - [Th\text{-}232]_{diss} \qquad (3.9.6)$$

where:

$[Th\text{-}230]_{diss}$, $[Th\text{-}232]_{diss}$ = concentration of dissolved Th-230 and Th-232 to time t in the unsaturated zone ($mol.m^{-3}$)

The concentrations of each isotope remaining in the solid phase can then be calculated. These solid phase concentrations are comprised of the mass of the isotope previously calculated as being insoluble, plus the mass of the isotope potentially soluble but not yet dissolved. That is:

$$[Th\text{-}230_s] = [Th\text{-}230]^o_{insol} + ([Th\text{-}230]^o_{sol} - [Th\text{-}230]_{diss}) \qquad (3.9.7)$$

$$[Th\text{-}232_s] = [Th\text{-}232]^o_{insol} + ([Th\text{-}232]^o_{sol} - [Th\text{-}232]_{diss}) \qquad (3.9.8)$$

where:

$[Th\text{-}230_s]$ = solid phase concentration of Th-230 in unsaturated zone ($mol.m^{-3}$)

$[Th\text{-}232_s]$ = solid phase concentration of Th-232 in unsaturated zone ($mol.m^{-3}$)

The solid phase concentration of total thorium is then easily determined; on either a molar or an activity basis:

$$[Th_s] = [Th\text{-}230_s]\ T230CF + [Th\text{-}232_s]\ T232CF \qquad (3.9.10)$$

where:

$[Th_s]$ = solid phase concentration of total thorium in unsaturated zone ($Bq.m^{-3}$)

This is the concentration of thorium in windblown dust dispersed from the tailings surface.

The activity fraction of Th-230 and/or Th-232 in the solid phase can then be calculated:

$$XA_{Th\text{-}232/Th,insol} = [Th\text{-}232_s]\ T232CF/[Th_s] \qquad (3.9.11)$$

where:

$XA_{Th\text{-}232/Th,insol}$ = activity fraction of Th-232 in total solid phase thorium

The entire preceding discussion is applicable only as long as soluble $Th(OH)_4$ is present in the unsaturated zone. Once the soluble thorium is depleted, the calculations are greatly simplified. That is if:

$$[Th]_{diss,t} = [Th]^o_{sol}$$

then:

$$[Th_L]_{\lambda w} = 0.0 \qquad (3.9.12)$$

$$[Th_s] = [Th\text{-}230]^o_{insol} T230CF + [Th\text{-}232]^o_{insol} T232CF \qquad (3.9.13)$$

$$XA_{Th\text{-}232/Th,insol} = XA^o_{Th\text{-}232/Th,insol} \qquad (3.9.14)$$

$$[Th\text{-}230_s] = [Th\text{-}230]^o_{insol} \qquad (3.9.15)$$

where:

$[Th_L]_{\lambda w}$ = liquid phase concentration of total thorium in the unsaturated zone ($Bq.m^{-3}$)

$[Th_s]$ = solid phase concentration of total thorium in unsaturated zone ($Bq.m^{-3}$)

$[Th\text{-}230_s]$ = solid phase concentration of Th-230 in unsaturated zone ($mol.m^{-3}$)

### 3.9.2 Layers 3 and 4

The liquid phase concentration of total thorium is again modelled as a function of pH and sulphate concentration. The equation derived for dissolved thorium concentration in the unsaturated zone (equation (3.9.1)) applies equally to the mixing zone and the bottom layer. That is:

$$
\begin{aligned}
[Th_L]_l = \frac{10^{(K_{Th} - 4pH)}}{f^4} \Big\{ & 1 + f^{7/4}\,10^{(pH - 3.2)} + f^3\,10^{(2\,pH - 6.93)} \\
& + f^{15/4}\,10^{(3pH - 11.7)} + f^4\,10^{(4pH - 15.9)} \\
& + f^4\,10^{5.45}\,[SO_4^{2-}]_l + f^6\,10^{9.73}\,[SO_4^{2-}]^2{}_l \Big\} \qquad (3.9.16)
\end{aligned}
$$

where:

$[Th_L]_l$ = liquid phase concentration of total thorium in layer "l" (where l = 3 or 4) ($mol.L^{-1}$)

pH = pH in layer "l" (where l = 3 or 4)

$[SO_4^{2-}]_l$ = total sulphate concentration in layer "l" (where l = 3 or 4) ($mol.L^{-1}$)

Again, conversion to and from appropriate units must be made. Also, an upper limit of $5 \times 10^{-5}$ $mol.L^{-1}$ is set on the thorium concentration, as discussed previously.

It may also be important to keep track of the thorium inventory in the mixing zone. If the calculated liquid phase thorium concentration in the mixing zone is less than that in the unsaturated zone, then net thorium precipitation is occurring in the mixing zone.

That is, if:

$$[Th_L]_{mix} < [Th_L]_{\lambda w}$$

then:

$$[Th]_{diss,mix,t} = [Th]_{diss,mix,t-\Delta t} - (P\Delta t/\lambda_{mix})([Th_L]_{\lambda w} - [Th_L]_{mix}) \qquad (3.9.17)$$

otherwise:

$$[Th]_{diss,mix,t} = [Th]_{diss,mix,t-\Delta t} + (P\Delta t/\lambda_{mix})\,[Th_L]_{mix} \qquad (3.9.18)$$

where:

$[Th]_{diss,mix,t}$ = concentration of total thorium dissolved in the mixing zone at time t ($mol.m^{-3}$)
Note: This may be a negative quantity indicating net precipitation rather than dissolution.

If the potentially soluble thorium in the mixing zone becomes depleted, then the dissolved thorium concentration drops to zero.

Specifically if:

$$[Th]_{diss,mix,t} > [Th_s]^{o}_{sol}$$

then

$$[Th_L]_{mix} = 0 \qquad (3.9.19)$$

The bottom layer is assumed to be large enough, and the chemical composition such that thorium depletion is not expected to occur over the 1000 year modelling period.

## 3.10 Radium

### 3.10.1 Radioactive Ingrowth and Decay

The radioactive ingrowth and decay of Ra-226 contributes to both its solid and liquid phase concentrations.

The ingrowth of radium from thorium can be estimated from the general laws of radioactive decay. The decay of radium can be represented by:

$$A \xrightarrow{\lambda_A} B \xrightarrow{\lambda_B}$$

where A and B represent the number of atoms of thorium and radium which are present at any time t; and $\lambda_A$ and $\lambda_B$ are the decay constants of thorium and radium respectively. If the only source of thorium atoms is the initial supply, $A = A_0$ at $t = 0$, and if $B = 0$ at $t = 0$, then the rate of change in the number of radium atoms is given by (Evans 1955):

$$\frac{dB}{dt} = A_0 \lambda_A \exp(-\lambda_A t) - B\lambda_B \qquad (3.10.1)$$

The solution of this differential equation is:

$$B(t) = A_0 \left(\frac{\lambda_A}{\lambda_B - \lambda_A}\right) [\exp(-\lambda_A t) - \exp(-\lambda_B t)] \qquad (3.10.2)$$

which is an expression for the number of radium atoms, B(t), at any time t.

We can also predict the molar concentration of Ra-226 which ingrows from Th-230 during any timestep, $\Delta t$, given the molar concentration of Th-230 at the beginning of that time period. That is:

$$[Ra]^{Th} = [Th\text{-}230] \left(\frac{\lambda_{Th\text{-}230}}{\lambda_{Ra\text{-}226} - \lambda_{Th\text{-}230}}\right) [\exp(-\lambda_{Th\text{-}230}\Delta t) - \exp(-\lambda_{Ra\text{-}226}\Delta t)] \qquad (3.10.3)$$

where:

$[Ra]^{Th}$ = concentration of Ra resulting from ingrowth from thorium during $\Delta t$ ($mol.m^{-3}$)

[Th-230] = concentration of Th-230 representative of the beginning of the time period ($mol.m^{-3}$)

$\lambda_{Th\text{-}230}$, $\lambda_{Ra\text{-}226}$ = radioactive decay constants of Th-230 and Ra-226

$\Delta t$ = length of timestep (yr)

This result (equation (3.10.3)) is used to determine solid and liquid phase radium concentrations resulting from the ingrowth from Th-230.

## 3.10.2 Unsaturated Zone

Recent investigations by Beak Consultants Ltd. (1985) indicate that Ra-226 co-precipitates (solid solution) with barite ($BaSO_4(s)$) rather than with gypsum ($CaSO_4(s)$) as modelled previously (SENES, 1985). Accordingly, the solution of Ra-226 is modelled on the basis of $Ba(Ra)SO_4$ solid solution. The principles underlying the transport of Ra-226, however, remain the same as modelled for $Ca(Ra)SO_4$.

As in case of gypsum precipitate, Ra-226 is a minor component (mole fraction << 1) of the precipitated barite solid. The solubility of Ra-226, therefore, will depend on the solubility of the host mineral (barite) in the tailings. The relevant equilibrium expressions for barite are as follows:

$$BaSO_4\ (s) \rightleftharpoons Ba^{+2} + SO_4{}^{2-} \qquad K_s^o = 1.07\times10^{-4}\ mol^2.m^{-6}$$
$$Ba^{+2} + SO_4{}^{2-} \rightleftharpoons BaSO_4{}^o\ (aq) \qquad K_f = 5.01\times10^{-1}\ m^3.mol^{-1}$$

We shall assume, that barite (i.e. $Ba(Ra)SO_4$) is occluded as microcystals in the gypsum matrix. Although this assumption is not critical, it aids in visualizing the fate of $BaSO_4$ in the tailings solids. As the gypsum front moves downward in the unsaturated zone, the barite crystals become "exposed" and begin to dissolve in the porewater. Due to the lower solubility of $BaSO_4$, the $BaSO_4$ front will lag the gypsum front. Consequently, the solubility of $BaSO_4$ will depend on the sulphate concentrations resulting from pyrite oxidation only $[SO_4]_p$. The molar concentrations of the barium ion and the sulphate complex $[BaSO_4]^o_{aq}$ can be expressed as follows:

$$[Ba]_{T,h_{Ba}} = \frac{K^o_{s,BaSO_4}/f^2}{\sqrt{K^o_{s,BaSO4}/f^2} + [SO_4^{2-}]_{p,h_{Ba}}} (1 + f^2\ K_{f,BaSO_4}[SO_4^{2}]_{p,h_{Ba}}) \qquad (3.10.4)$$

where:

$Ba]_{T,h_{Ba}}$ = dissolved concentration of total barium ($mol.m^{-3}$)

$K^0_{s,BaSO4}$ = solubility product of $BaSO_4$ ($mol^2.m^{-6}$)
$K_{f,BaSO4}$ = formation constant of $BaSO^0_{4(aq)}$ ($m^3.mol^{-1}$)
$f_{2-}$ = activity coefficient for divalent ions
$[SO_4^{2-}]_{p,h_{Ba}}$ = concentration of sulphates at $h_{Ba}$ resulting from pyrite oxidation ($mol.m^{-3}$)
$h_{Ba}$ = the position of the barium sulphate solids front (m)

In analogy to the movement of a gypsum front, we may define a depleted zone for barite in the tailings. If $[BaSO_4]^o$ is the initial molar concentration of barite (moles $BaSO_4/m^3$ tailings), the movement of the barite depleted layer ($\Delta h_{Ba}$) is given by:

$$[BaSO_4]^o \, \Delta h_{Ba} = (P\Delta t)\left\{\frac{K^o_{s,BaSO_4}/f^2}{\sqrt{K^o_{s,BaSO_4}/f^2} + (2B/P\Delta t)\,(h_{Ba} + \Delta h_{Ba}/2)}\right\}$$

$$\left\{1 + (2B\, K_{f,BaSO_4}\, f^2/P\Delta t)\,(h_{Ba} + \Delta h_{Ba}/2)\right\} \qquad (3.10.5)$$

where:

B = $[FeS_2]_{t-\Delta t}\,(1 - e^{-k\Delta t})$
P = annual net precipitation ($m.yr^{-1}$)
$[BaSO_4]^o$ = initial concentration of barite in the tailings ($mol.m^{-3}$)
$h_{Ba}$ = $\sum_{t=0}^{t-\Delta t} \Delta h_{Ba}$

Equation (3.10.5) may be solved for $\Delta h_{Ba}$:

$$\Delta h_{Ba} = \left\{ \frac{a^{2}(P\Delta t)}{[BaSO_4]^{o}} \left[ \frac{P\Delta t}{B} + 2\, f^{2} K_{f,BaSO_4}\, h_{Ba} \right] + \frac{1}{4} \left[ 2h_{Ba} + \frac{aP\Delta t}{B} - \frac{a^{2} f^{2} K_{f,BaSO_4}\, P\Delta t}{[BaSO_4]^{o}} \right]^{2} \right\}^{1/2}$$

$$- \left[ h_{Ba} + \frac{aP\Delta t}{2B} - \frac{a^{2} f^{2} K_{f,BaSO_4}\, P\Delta t}{2[BaSO_4]^{o}} \right] \qquad (3.10.6)$$

where:

$$a = \sqrt{K^{o}_{s,BaSO_4}/f^{2}}$$

The value for $h_{Ba}$ at the end of the current time step is thus:

$$h_{Ba,t} = h_{Ba,t-\Delta t} + \Delta h_{Ba}$$

As the dissolved barium moves downward through the tailings, some of it must precipitate, since the sulphate concentration increases in the unsaturated zone. This increase in sulphate is due to increasing sulphate levels with distance due to pyrite oxidation and, in part, due to gypsum dissolution.

At the limit of the unsaturated zone, i.e. $\lambda_w$, we have calculated a time averaged total sulphate concentration $[SO_4^{2-}]_{T,\lambda w}$. We have also estimated a quantity "d" as follows:

$$d = 1 + f^{3}\, 10^{8.99 - 3pH} + f^{3/4}\, 10^{9.7 - 3pH} \qquad (3.10.7)$$

The concentration of uncomplexed sulphate at $\lambda_w$ is given by:

$$[SO_4^{2-}]_{u,\lambda w} = \frac{[SO_4^{2-}]_{T,\lambda w}}{1 + f^{3}\, 10^{8.99 - 3pH} + f^{3/4}\, 10^{9.7 - 3pH}} \qquad (3.10.8)$$

where:

$[SO_4^{2-}]_{u,\lambda w}$ = uncomplexed sulphate concentration at $\lambda_w$ ($mol.m^{-3}$)

$[SO_4^{2-}]_{T,\lambda w}$ = total sulphate concentration at $\lambda_w$ ($mol.m^{-3}$)

The total dissolved barium ($Ba^{+2}$ and $BaSO^{o}$ (aq)) at $\lambda_w$ can be calculated using an expression analogous to equation (3.10.4), that is:

$$[Ba]_{T,\lambda w} = \frac{K^{o}_{s,BaSO_4} / f^{2}}{\sqrt{K^{o}_{s,BaSO_4} / f^{2} + [SO_4^{2-}]_{u,\lambda w}}} (1 + f^{2} K_{f,BaSO_4}[SO_4^{2-}]_{u,\lambda w}) \qquad (3.10.9)$$

We may define the total precipitated barite at any time "t" as $m_t$. The rate of change in reprecipitated barite between t-Δt and t is given by:

$$\frac{m_{Ba,t} - m_{Ba,t-\Delta t}}{\Delta t} = \frac{[BaSO_4]^{o} \Delta h_{Ba}}{\Delta t} - P [Ba]_{T,\lambda w} \qquad (3.10.10)$$

where:

$m_{Ba,t}$ = reprecipitated barite at time t ($mol.m^{-2}$)

$m_{Ba,t-\Delta t}$ = reprecipitated barite at time t-Δt ($mol.m^{-2}$)

Note that we need not time-average $[Ba]_{T,\lambda w}$ since it is based on the time-averaged sulphate concentration between t-Δt and t. Solving equation (3.10.10) for $m_t$ yields:

$$m_{Ba,t} = m_{Ba,t-\Delta t} + [BaSO_4]^{o}\Delta h_{Ba} - P\Delta t\, [Ba]_{T,\lambda w} \qquad (3.10.11)$$

Note that the calculations for $\Delta h_{Ba}$ and $m_t$ were not performed in the initial timestep, since we felt that the $BaSO_4$ depletion would be minimal over that timestep. It was further assumed that at t = 0, the depth of $BaSO_4$ depletion ($h_{Ba}$) was 1 cm (0.01 m).

To calculate the concentration of dissolved radium-226, a solid solution of $RaSO_4$ in $BaSO_4$ is assumed. We define the mole fraction of radium in the solid phase as:

$$x = \frac{RaSO_4(s)}{RaSO_4(s) + BaSO_4(s)} \qquad (3.10.12)$$

The mole fraction of Ra-226 in the liquid phase is given by:

$$y = \frac{[Ra^{+2}]}{[Ra^{+2}] + [Ba^{+2}]} \qquad (3.10.13)$$

If $BaSO_4$ and $RaSO_4$ form a regular solid solution, the mole fraction in the liquid phase (y) can be related to the mole fraction in the solid phase by the following equality (Gresens, 1981):

$$y = \left[ \frac{\dfrac{K^{o}_{s,RaSO_4}}{f_{Ra}\, f_{SO4}}\, x \exp[\alpha(1 - x)^{2}]}{\dfrac{K^{o}_{s,BaSO_4}}{f_{Ba}\, f_{SO4}}\, x \exp[\alpha(1 - x)^{2}] + K^{o}_{s,BaSO_4}\, (1 - x) \exp[\alpha\, x^{2}]} \right] \qquad (3.10.14)$$

It has been shown (Beak, 1985) that $BaSO_4$ and $RaSO_4$ form a nearly ideal solid solution ($\alpha$=o). Furthermore, the mole fraction of radium-226 in barite ($BaSO_4$) is very small ( $x \ll 1$). In this case, the distribution of radium-226 between the solid and liquid phases is given by:

$$y = \left[ \frac{\dfrac{K^{o}_{s,RaSO_4}}{f_{Ra}\, f_{SO4}}}{\dfrac{K^{o}_{s,BaSO_4}}{f_{Ba}\, f_{SO4}}} \right] x$$

where:

$K^{o}_{s,RaSO_4}$ = solubility product of $RaSO_4$ (s); $K^{o}_{s,RaSO_4} = 10^{-10.27}$

$K^{o}_{s,BaSO_4}$ = solubility product of $BaSO_4$ (s); $K^{o}_{s,BaSO_4} = 10^{-10.27}$

$f_{Ra}$, $f_{Ba}$, $f_{SO4}$ = activity coefficients for $Ra^{2+}$, $Ba^{2+}$ and $SO_4^{2-}$

Assuming the activity coefficients of $Ra^{+2}$ and $Ba^{+2}$ are identical, the distribution of radium-226 between the solid and the liquid phases is:

$$y = 0.50\ x \qquad (3.10.16)$$

The coefficient calculated in equation (3.10.16) (i.e. $K_{Ra} = 0.5$) compares with an experimentally determined value of $K_{Ra} = 0.56$ (Stumm and Morgan, 1981). In this analysis, the coefficient ($K_{Ra}$) is specified as a probabilistic input parameter, with a range from 0.50 to 0.56.

To determine a value for the solid phase mole fraction x, we assume equilibrium between reprecipitated barite and dissolved radium. The material balance for radium in the reprecipitated solid phase is given by:

$$[BaSO_4]^{o}\ X'_{Ra/BaSO_4} \Delta h_{Ba} + P\ [Ra]^{Th}_{\lambda w} \Delta t = m_{Ba,t} x_t - m_{Ba,t-\Delta t} x_{t-\Delta t} \qquad (3.10.17)$$

$$+ P\Delta t [Ba]_{T,\lambda w}\ K_{Ra}\ (x_t + x_{t-\Delta t})/2$$

or, solving for $x_t$:

$$x_t = \Big\{ [BaSO_4]^{o}\ X'_{Ra/BaSO_4} \Delta h_{Ba} + P\ [Ra]^{Th}_{\lambda w} \Delta t + m_{Ba,t-\Delta t}\ x_{t-\Delta t}$$

$$- P\Delta t [Ba]_{T,\lambda w}\ K_{Ra} x_{t-\Delta t}/2 \Big\}$$

$$\div \left[ m_{Ba,t} + P\Delta t [Ba]_{T,\lambda w}\ K_{Ra}\ /2 \right] \qquad (3.10.18)$$

Many of the terms have already been defined. However, a few require further attention. Namely:

$$X'_{Ra/BaSO_4} = X^{o}_{Ra/BaSO_4}\ \exp(-\lambda_{Ra\text{-}226} t) \qquad (3.10.19)$$

where:

$X_{Ra/BaSO_4}$ = mole fraction of Ra-226 in $BaSO_4$; corrected for decay of Ra-226

$\overset{o}{X}_{Ra/BaSO_4}$ = initial mole fraction of Ra-226 in $BaSO_4$

and:

$$[Ra]^{Th}_{\lambda w} = X_{Th\text{-}230/Th,sol}\ [TH_L]_{\lambda w} \left( \frac{\lambda_{Th\text{-}230}}{\lambda_{Ra\text{-}226} - \lambda_{Th\text{-}230}} \right)$$

$$(\exp(-\lambda_{Th\text{-}230}\Delta t) - \exp(-\lambda_{Ra\text{-}226}\Delta t)) \qquad (3.10.20)$$

where:

$[Ra]^{Th}_{\lambda w}$ = concentration of Ra-226 resulting from ingrowth from Th-230 during $\Delta t$ ($mol.m^{-3}$)

$X_{Th\text{-}230/Th,sol}$ = mole fraction of Th-230 in soluble thorium

$[Th_L]_{\lambda w}$ = liquid phase concentration of total thorium at $\lambda_w$ ($mol.m^{-3}$)

The rationale for this last equation was provided previously (Section 3.13.1).

Note that $x_t$ at t = 0 is equal to $\overset{o}{X}_{Ra/BaSO_4}$.

The concentration of radium in solution at $\lambda_w$ can then be calculated as follows:

$$[Ra_L]_{\lambda w} = K_{Ra}\ [Ba]_{T,\lambda w}\ x_t \qquad (3.10.21)$$

where:

$[Ra_L]_{\lambda w}$ = liquid phase concentration of radium at $\lambda_w$ ($mol.m^{-3}$)

This quantity can be converted to units of $Bq.m^{-3}$ using the conversion factor defined previously (RACF).

The previous discussion applies as long as $BaSO_4$ is present in the unsaturated zone; that is, as long as $h_{Ba}$ is less than $\lambda_w$. Once $BaSO_4$ is depleted from the unsaturated zone, radioactive ingrowth from dissolved thorium is the only source of dissolved radium. That is:

$$[Ra_L]_{\lambda w} = [Ra_L]^{Th}_{\lambda w} \qquad \text{for } h \geq \lambda_w \qquad (3.10.22)$$

Unsaturated Zone: Solid Phase

As described earlier, the unsaturated zone can be thought of as consisting of 2 layers for radium; a $BaSO_4$ (and hence radium) depleted layer and a $BaSO_4$ (and hence radium) enriched layer. Since radium acts as the source of radon emanation from the tailings, it is important to characterize the solid phase radium concentrations in both layers.

The solid phase radium resulting from the ingrowth from thorium must be considered in both layers. While we calculate the incremental ingrowth during each time period, we must also keep a cumulative total of the net radium resulting from ingrowth. This is calculated as:

$$[Ra_S]^{Th}_t = [Ra_S]^{Th}_{t-\Delta t} \exp\,(\lambda_{Ra\text{-}226}\,\Delta t)$$

$$+ [Th\text{-}230_S]\left(\frac{\lambda_{Th\text{-}230}}{\lambda_{Ra\text{-}226} - \lambda_{Th\text{-}230}}\right)(\exp(-\lambda_{Th\text{-}230}\Delta t) - \exp\,(-\lambda_{Ra\text{-}226}\Delta t) \qquad (3.10.23)$$

where:

$[Ra_S]^{Th}_t$ = cumulative solid phase concentration of Ra-226 resulting from ingrowth to time t ($mol.m^{-3}$)

$[Ra_S]^{Th}_{t-\Delta t}$= cumulative solid phase concentration of Ra-226 resulting from ingrowth to time t-Δt ($mol.m^{-3}$)

$[Th\text{-}230_S]$=solid phase concentration of Th-230 at time t ($mol.m^{-3}$)

In the $BaSO_4$ depleted layer (layer 1) the solid phase radium concentration consists of insoluble radium originally associated with the host tailings material plus radium resulting from ingrowth. Radioactive decay of the insoluble radium inventory must also be considered. Thus, we can write:

$$[Ra_s]_1 = [Ra_s]_m^o \exp(-\lambda_{Ra\text{-}226}t) + [Ra_s]_t^{Th} \qquad (3.10.24)$$

where:

$[Ra_s]_1$ = solid phase radium concentration in layer 1 at time t ($mol.m^{-3}$)

$[Ra_s]_m^o$ = initial concentration of radium associated with host tailings material ($mol.m^{-3}$)

In layer 2, the concentration of radium associated with the original $BaSO_4$ and the reprecipitated $BaSO_4$ must also be considered. That is:

$$[Ra_s]_2 = [Ra_s]_t^{Th} + X'_{Ra/BaSO_4}[BaSO_4]^o + x_t\, m_{Ba,t}/(\lambda_w - h_{Ba}) \qquad (3.10.25)$$

where:

$[Ra_s]_2$ = solid phase radium concentration in layer 2 at time t ($mol.m^{-3}$)

$X'_{Ra/BaSO_4}$ = original mole fraction of Ra in $BaSO_4$; corrected for radioactive decay of radium (see equation (3.10.19))

Once the unsaturated zone is depleted of $BaSO_4$, the entire unsaturated zone takes on the characteristics of layer 1, and the solid phase radium concentration is give by equation (3.10.24).

### 3.10.3 Layers 3 and 4

The concentration of dissolved radium in both the mixing zone and the bottom layer depends on a number of conditions. First, the concentration of dissolved radium in each layer resulting from thorium decay depends on the presence or absence of soluble thorium in the layer above. For instance, we assume that as long as thorium is entering the mixing zone from the layer above, no net thorium dissolution is occurring in the mixing zone. Hence, there is no dissolved radium present resulting from thorium dissolution and decay, in that zone. More specifically, we can write:

$$[Ra]^{Th}_{mix} = 0 \quad \text{for} \sum_t [Th_L]_{diss,t} < [Th_s]^o_{sol} \qquad (3.10.26)$$

(see Section 3.9.1)

otherwise:

$$[Ra]^{Th}_{mix} = X_{Th\text{-}230/Th,sol} \, [Th_L]_{mix} \left( \frac{\lambda_{Th\text{-}230}}{\lambda_{Ra\text{-}226} - \lambda_{Th\text{-}230}} \right)$$

$$(\exp(-\lambda_{Th\text{-}230}\Delta t) - \exp(-\lambda_{Ra\text{-}226}\Delta t)) \qquad (3.10.27)$$

where:

$[Ra]^{Th}_{mix}$ = concentration of dissolved radium resulting from the decay of thorium dissolved in the mixing zone at time t ($mol.m^{-3}$)

$[Th_L]_{mix}$ = dissolved total thorium concentration in the mixing zone at time t ($mol.m^{-3}$)

$X_{Th\text{-}230/Th,sol}$ = mole fraction of Th-230 in soluble thorium.

$[Th_L]_{diss,t}$ = concentration of dissolved thorium in the unsaturated zone at time t ($mol.m^{-3}$)

$[Th_s]^o_{sol}$ = initial concentration of total soluble thorium ($mol.m^{-3}$)

We can write analagous equations for the bottom layer:

$$[Ra]^{Th}_4 = 0 \quad \sum_t \text{for} \quad [Th_L]_{diss,mix,t} < [Th_s]^o_{sol} \qquad (3.10.28)$$

otherwise:

$$[Ra]_4^{Th} = x_{Th\text{-}230/Th,sol}\,[Th_L]_4 \left(\frac{\lambda_{Th\text{-}230}}{\lambda_{Ra\text{-}226} - \lambda_{Th\text{-}230}}\right)$$

$$(\exp(-\lambda_{Th\text{-}230}\Delta t) - \exp(-\lambda_{Ra\text{-}226}\,\Delta t)) \qquad (3.10.29)$$

The differential equation describing the dissolved radium concentration in the mixing zone can be written generally as:

$$\lambda_{mix}\,\epsilon\,(1+\rho_T K_{D,Ra}/\epsilon)\,\frac{d[Ra_L]_{mix}}{dt} = P[Ra]_{in} - P[Ra_L]_{mix} \qquad (3.10.30)$$

Integrating between t-Δt and t:

$$[Ra_L]_{mix,t} = [Ra]_{in,t} + ([Ra_L]_{mix,t-\Delta t}\exp(-\lambda_{Ra\text{-}226}\Delta t) - [Ra]_{in,t})$$

$$\exp[-P\Delta t/(\epsilon\,\lambda_{mix}(1+K_{D,Ra}\,\rho_T/\epsilon))] \qquad (3.10.31)$$

where:

$[Ra_L]_{mix,t}$ = dissolved radium concentration in the mixing zone at time t ($mol.m^{-3}$)

$[Ra_L]_{mix,t-\Delta t}$ = dissolved radium concentration in the mixing zone in the previous time step (t-Δt) ($mol.m^{-3}$)

$K_{D,Ra}$ = solid-liquid distribution coefficient for radium ($m^3.g^{-1}$)

$\epsilon$ = tailings porosity

$\lambda_{mix}$ = thickness of the mixing zone (m)

$\rho_T$ = tailings bulk density ($g.m^{-3}$)

$[Ra]_{in,t}$ = concentration of radium resulting from inputs at time t ($mol.m^{-3}$) (via infiltration from above and/or ingrowth)

Note that a factor has been incorporated into the above equation to account for the radioactive decay of Ra-226 during each time step. The incorporation of such a "correction factor" is a relatively straightforward, though not fundamentally rigorous, method of including radioactive decay in such an equation. This approach is also used in layer 4 and in the calculations of dissolved Pb-210 concentrations in layers 3 and 4.

The value of $[Ra]_{in}$ depends on whether $BaSO_4$ has been depleted from (a) the unsaturated zone and (b) the mixing zone. Thus several cases can be identified.

Case 1: mixing zone contains $BaSO_4$

(a) unsaturated zone contains $BaSO_4$ (i.e. $h_{Ba} < \lambda_w$)

$$[Ra]_{in} = [Ra_L]_{\lambda w} + [Ra]^{Th}_{mix} \qquad (3.10.32)$$

(b) unsaturated zone depleted of $BaSO_4$ (i.e. $h_{Ba} \geq \lambda_w$)

$$[Ra]_{in} = \left\{ \frac{K^o_{s,BaSO_4}/f^2 \; X'_{Ra/BaSO_4}}{\sqrt{K^o_{s,BaSO_4}/f^2} + [SO_4^{2-}]_{mix}} \left(1 + K_{f,BaSO_4} f^2 [SO_4^{2-}]_{mix}\right) \right\} + [Ra]^{Th}_{mix} \qquad (3.10.33)$$

In case 1 (b), $BaSO_4$ is dissolving in the mixing zone.

Case 2: mixing zone depleted of $BaSO_4$; unsaturated zone depleted of $BaSO_4$

$$[Ra]_{in} = [Ra]^{Th}_{mix} \qquad (3.10.34)$$

The latter situation (depletion of $BaSO_4$ in the mixing zone) is monitored by summing the radium inputs:

$$\sum_{t=0}^{t} [Ra]_{in} = \sum_{t=0}^{t-\Delta t} [Ra]_{in} + P\Delta t \, [Ra]_{in} \qquad (3.10.35)$$

The mixing zone is depleted of $BaSO_4$ when:

$$\sum_{t=0}^{t} [Ra]_{in} = M_{Ra}^{o} \qquad (3.10.36)$$

where:

$M_{Ra}^{o}$ = total radium initially associated with $BaSO_4$ in the unsaturated and mixing zones ($mol.m^{-2}$)

The bottom layer is treated in a directly analagous fashion. One further simplifying assumption is that the bottom layer will not be depleted of soluble radium over the 1,000 year modelling period. Thus case 2 mentioned above does not have to be considered. The integrated mass balance for this layer is very similar to that for the mixing zone (equation (3.10.31)):

$$[Ra_L]_{4,t} = [Ra]_{in,4,t} + ([Ra_L]_{4,t-\Delta t} \exp(-\lambda_{Ra-226}\Delta t) - [Ra]_{in,4,t})$$

$$\exp[-f\overline{P}\,\Delta t/(\epsilon\,\lambda_4(1 + K_{D,Ra}\rho_T/\epsilon))] \qquad (3.10.37)$$

where:

$[Ra]_{4,t}$ = dissolved concentration of radium in layer 4 ($mol.m^{-3}$)
$f$ = fraction of precipitation which infiltrates to bottom layer
$\overline{P}$ = long-term mean annual net precipitation ($m.yr^{-1}$)
$[Ra]_{in,4,t}$ = concentration of radium in porewater infiltrating layer 4 from above at time t ($mol.m^{-3}$)

The value for $[Ra]_{in,4}$ depends on $BaSO_4$ depletion in the mixing zone.

Case 1: mixing zone contains $BaSO_4$

$$[Ra]_{in,4} = [Ra_L]_{mix} + [Ra]_4^{Th} \qquad (3.10.38)$$

Case 2: mixing zone depleted of $BaSO_4$

$$[Ra]_{in,4} = \left\{ \frac{K^o_{s,BaSO_4}/f^2 \, X'_{Ra/BaSO_4}}{\sqrt{K^o_{s,BaSO_4}/f^2} + [SO_4^{2-}]_4} \left(1+K_{f,BaSO_4} f^2 [SO_4^{2-}]_4\right) \right\} + [Ra]^n_4 \qquad (3.10.39)$$

In case 2, $BaSO_4$ is dissolving in the bottom layer.

Again, all of these concentrations expressed in $mol.m^{-3}$ can be converted to an activity basis by multiplying by the conversion factor (RACF).

## 3.11 Lead

The solid and liquid phase concentrations of Pb-210 are modelled in a very similar fashion to Ra-226. Lead-210 is assumed to form a solid coprecipitate with lead sulphate ($PbSO_4$). This solid coprecipitate then dissolves in a frontwise manner, analagous to gypsum and barium sulphate. In fact, the solution is even more straightforward for Pb-210 since it forms ideal solid solutions and hence does not concentrate in the non-depleted layer. Because of the similarity in modelling approach, this section is presented in much less detail than the previous section. Many of the detailed derivations are omitted and only the functional relationships required for the simulation are presented.

### 3.11.1 Unsaturated Zone

As just mentioned, Pb-210 is assumed to coprecipitate with other lead ions in forming lead sulphate ($PbSO_4$). The relevant equilibrium expressions include:

$$PbSO_{4(s)} \rightleftharpoons Pb^{2+} + SO_4^{2-} \qquad K^o_{s,PbSO4} = 1.2 \times 10^{-2} \ mol^2.m^{-6}$$

$$Pb^{2+} + SO_4^{2-} \rightleftharpoons PbSO_4^o \ (aq) \qquad K_{f,PbSO4} = 5.01 \times 10^{-1} \ m^3.mol^{-1}$$

The total dissolved concentration of lead at the bottom of the unsaturated zone can be calculated as:

$$[Pb]_{T,\lambda w} = \frac{K^{o}_{s,PbSO_4}/f^{2} \qquad (1+f^{2}\ K_{f,PbSO_4}[SO_4^{2-}]_{u,\lambda w})}{\sqrt{K^{o}_{s,PbSO_4}/f^{2}} + [SO_4^{2-}]_{u,\lambda w}} \qquad (3.11.1)$$

where:

$[Pb]_{T,\lambda w}$ = total dissolved lead concentration at $\lambda_w$ ($mol.m^{-3}$)

$K^{o}_{s,PbSO4}$ = solubility product of $PbSO_4$ ($mol^2.m^{-6}$)

$K_{f,PbSO_4}$ = formation constant of $PbSO_4^{o}(aq)$ ($m^3.mol^{-1}$)

$f$ = activity coefficient of divalent ions

$[SO_4^{2-}]_{u,\lambda w}$ = concentration of uncomplexed $SO_4^{2-}$ at $\lambda_w$ ($mol.m^{-3}$)

Having determined the total dissolved lead concentration, we can easily calculate the concentration of dissolved Pb-210. Since all elements form ideal solid solutions with their isotopes, we know that the mole fraction of Pb-210 is the same in the solid and liquid phases. That is, y=x, using the symbols defined previously in the radium discussion.

Having previously calculated the solid phase mole fraction of Pb-210 in $PbSO_4$, we can write:

$$[Pb\text{-}210_L]_{\lambda w} = X'_{Pb\text{-}210/PbSO_4}\ [Pb]_{T,\lambda w} + [Pb\text{-}210_L]^{Ra}_{\lambda w} \qquad (3.11.2)$$

where:

$[Pb\text{-}210_L]_{\lambda w}$ = liquid phase concentration of Pb-210 at $\lambda_w$ ($mol.m^{-3}$)

$X'_{Pb\text{-}210/PbSO_4}$ = mole fraction of Pb-210 in $PbSO_4$; corrected for radioactive decay of Pb-210, i.e.

$= X^{o}_{Pb\text{-}210/PbSO_4}\ \exp(-\lambda_{Pb\text{-}210}\ t)$

$[Pb\text{-}210_L]^{Ra}_{\lambda w}$ = liquid phase concentration of Pb-210 from Ra-226 decay in the unsaturated zone ($mol.m^{-3}$)

This last term, representing Pb-210 ingrowth from Ra-226 is calculated using a modified version of (equation (3.10.3):

$$[\text{Pb-210}_L]^{Ra}_{\lambda w} = [Ra_L]_{\lambda w} \left( \frac{\lambda_{Ra-226}}{\lambda_{Pb-210} - \lambda_{Ra-226}} \right) [\exp(-\lambda_{Ra-226}\Delta t) - \exp(-\lambda_{Pb-210}\Delta t)] \qquad (3.11.3)$$

where:

$[Ra_L]_{\lambda w}$ = liquid phase concentration of Ra-226 at $\lambda_w$ (mol.m$^{-3}$)

These expressions for the concentration of Pb-210 are valid as long as $PbSO_4$ is not depleted from the unsaturated zone. To determine this, we track the depth of the $PbSO_4$ depleted front with time. The movement of the $PbSO_4$ depleted layer ($\Delta h_{Pb}$) is given by an equation analagous to (equation (3.10.6). Namely:

$$\Delta h_{Pb} = \left\{ \frac{a^2 (P\Delta t)}{[PbSO_4]^o} \left[ \frac{P\Delta t}{B} + 2f^2 K_{f,PbSO_4} h_{Pb} \right] + \frac{1}{4} \left[ 2h_{Pb} + \frac{a\,(P\Delta t)}{B} - \frac{a^2 f^2 K_{f,PbSO_4}}{[PbSO_4]^o} P\Delta t \right]^2 \right\}^{1/2}$$

$$- \left[ h_{Pb} + \frac{a\,P\Delta t}{2\,B} - \frac{a^2 f^2 K_{f,PbSO_4}\,P\Delta t}{2[PbSO_4]^o} \right] \qquad (3.11.4)$$

where:

a = $\sqrt{K^o_{s,PbSO} / f^2}$

B = $[FeS_2]_{t-\Delta t}\,(1-e^{-k\Delta t})$

The depth of depletion ($h_{Pb}$) is then:

$$h_{Pb,t} = h_{Pb,t-\Delta t} + \Delta h_{Pb} \qquad (3.11.5)$$

As in the radium calculations, we arbitrarily assumed that at t=0 the depth of $PbSO_4$ depletion was 1 cm (0.01 m).

Once the depth of depletion reaches the bottom of the unsaturated zone, no further $PbSO_4$ remains as a source of Pb-210. After this point, the dissolved concentration of Pb-210 results only from the decay of Ra-226. That is:

$$[\text{Pb-210}_L]_{\lambda w} = [\text{Pb-210}_L]^{Ra}_{\lambda w} \qquad \text{for } h_{Pb} \geq \lambda_w \qquad (3.11.6)$$

Unsaturated Zone: Solid Phase

We are interested in the solid phase concentration of Pb-210 in the $PbSO_4$ depleted layer only, since this acts as the source of airborne Pb-210. The sources of solid phase Pb-210 are the original insoluble Pb-210 inventory and Pb-210 which ingrows from solid phase Ra-226 in the same layer. The ingrowth can be written as:

$$[\text{Pb-210}_S]^{Ra}_{t} = [\text{Pb-210}_S]^{Ra}_{t-\Delta t} \exp(-\lambda_{Pb\text{-}210}\Delta t)$$
$$+[\text{Ra-226}_S]_1 \left(\frac{\lambda_{Ra\text{-}226}}{\lambda_{Pb\text{-}210}-\lambda_{Ra\text{-}226}}\right) \exp(-\lambda_{Ra\text{-}226}\Delta t) - \exp(-\lambda_{Pb\text{-}210}\Delta t) \qquad (3.11.7)$$

where:

$[\text{Pb-210}_S]^{Ra}_{t}$ = cumulative solid phase concentration of Pb-210 resulting from ingrowth to time t ($mol.m^{-3}$)

$[\text{Pb-210}_S]^{Ra}_{t-\Delta t}$ = cumulative solid phase concentration of Pb-210 resulting from ingrowth to time t-Δt ($mol.m^{-3}$)

$[\text{Ra-226}_S]_1$ = solid phase concentration of Ra-226 in the $BaSO_4$ depleted layer at time t ($mol.m^{-3}$)

The total solid phase concentration of Pb-210 can then be calculated:

$$[\text{Pb-210}_S]_1 = [\text{Pb-210}_S]^{o}_{m} \exp(-\lambda_{Pb\text{-}210}t) + [\text{Pb-210}_S]^{Ra}_{t} \qquad (3.11.8)$$

where:

$[\text{Pb-210}_S]_1$ = solid phase Pb-210 concentration in the $PbSO_4$ depleted layer ($mol.m^{-3}$)

$[\text{Pb-210}_S]^{o}_{m}$ = initial concentration of Pb-210 associated with the host tailings material ($mol.m^{-3}$)

### 3.11.2 Layers 3 and 4

As with radium, the concentration of Pb-210 in the mixing zone and bottom layer depends on several factors, including the ingrowth of Pb-210 from dissolved Ra-226 in each layer. Again, we assume that as long as dissolved radium is entering from the layer above, there is no dissolved Pb-210 from radium decay present in the layer. That is:

$$[\text{Pb-210}_L]^{Ra}_{mix} = 0 \qquad \text{for } h_{Ra} < \lambda_w \tag{3.11.9}$$

otherwise:

$$[\text{Pb-210}_L]^{Ra}_{mix} = [Ra_L]_{mix} \left(\frac{\lambda_{Ra-226}}{\lambda_{Pb-210} - \lambda_{Ra-226}}\right) (\exp(-\lambda_{Ra-226}\Delta t) - \exp(-\lambda_{Pb-210}\Delta t)) \tag{3.11.10}$$

where:

$[\text{Pb-210}_L]^{Ra}_{mix}$ = concentration of dissolved Pb-210 resulting from the decay of Ra-226 dissolved in the mixing zone (mol.m$^{-3}$)

$[Ra_L]_{mix}$ = dissolved radium concentration in the mixing zone (mol.m$^{-3}$)

And analogously for the bottom layer (see Section 3.10.3):

$$[\text{Pb-210}_L]^{Ra}_4 = 0 \qquad \text{for} \quad \sum_{t=0}^{t} [Ra]_{in} < M^o_{Ra} \tag{3.11.11}$$

otherwise:

$$[\text{Pb-210}_L]^{Ra}_4 = [Ra_L]_4 \left(\frac{\lambda_{Ra-226}}{\lambda_{Pb-210} - \lambda_{Ra-226}}\right) [\exp(-\lambda_{Ra-226}\Delta t) - \exp(-\lambda_{Pb-210}\Delta t)] \tag{3.11.12}$$

The equation describing the dissolved Pb-210 concentration in the mixing zone is similar to (equation (3.10.31). Namely:

$$[\text{Pb-210}_L]_{mix,t} = [Pb]_{in,t} + ([\text{Pb-210}]_{mix,t-\Delta t} \exp(-\lambda_{Pb-210}\Delta t) - [Pb]_{in,t})$$

$$\exp[-P\Delta t/(\epsilon\, \lambda_{mix}(1 + K_{D,Pb}\rho_T/\epsilon))] \tag{3.11.13}$$

where:

$[\text{Pb-210}_L]_{mix,t}$ = dissolved Pb-210 concentration in the mixing zone at time t ($mol.m^{-3}$)

$[\text{Pb-210}_L]_{mix,t-\Delta t}$ = dissolved Pb-210 concentration in the mixing zone in the previous time step ($t-\Delta t$) ($mol.m^{-3}$)

$K_{D,Pb}$ = solid-liquid distribution coefficient for lead ($m^3.g^{-1}$)

$\epsilon$ = tailings porosity

$\lambda_{mix}$ = thickness of the mixing zone (m)

$\rho_T$ = tailings density ($g.m^{-3}$)

$[Pb]_{in,t}$ = concentration of Pb-210 resulting from inputs (via infiltration from above and/or ingrowth) at time t ($mol.m^{-3}$)

Again, a term has been included in the equation to account for the radioactive decay of Pb-210 over the previous time step.

The value of $[Pb]_{in}$ depends on whether $PbSO_4$ has been depleted from (a) the unsaturated zone and (b) the mixing zone. Thus several cases can be identified.

Case 1: mixing zone contains $PbSO_4$

(a) unsaturated zone contains $PbSO_4$ (i.e. $h_{Pb} < \lambda_w$)

$$[Pb]_{in} = [\text{Pb-210}]_{\lambda w} + [\text{Pb-210}_L]^{Ra}_{mix} \qquad (3.11.14)$$

(b) unsaturated zone depleted of $BaSO_4$ (i.e. $h_{Pb} \geq \lambda_w$)

$$[Pb]_{in} = \left\{ \frac{K^o_{s,PbSO_4}/f^2 \; X'_{\text{Pb-210}/PbSO_4}}{\sqrt{K^o_{s,PbSO_4}/f^2} + [SO_4^{2-}]_{mix}} \left(1 + K_{f,PbSO_4} f^2 [SO_4^{2-}]_{mix}\right) \right\} + [\text{Pb-210}_L]^{Ra}_{mix} \qquad (3.11.15)$$

In case 1 (b), $BaSO_4$ is dissolving in the mixing zone.

Case 2: mixing zone depleted of $PbSO_4$; unsaturated zone depleted of $PbSO_4$

$$[Pb]_{in} = [Pb\text{-}210_L]^{Ra}_{mix} \qquad (3.11.16)$$

The latter situation (depletion of $PbSO_4$ in the mixing zone) is monitored by summing the Pb-210 inputs:

$$\sum_{t=0}^{t} [Pb]_{in} = \sum_{t=0}^{t-\Delta t} [Pb]_{in} + P\Delta t\, [Pb]_{in} \qquad (3.11.17)$$

The mixing zone is depleted of $PbSO_4$ when:

$$\sum_{t=0}^{t} [Pb]_{in} = M^o_{Pb} \qquad (3.11.18)$$

where:

$M^o_{Pb}$ = total lead-210 initially associated with $PbSO_4$ in the unsaturated and mixing zones ($mol.m^{-2}$) (see Section 3.7.4)

The bottom layer is treated in a directly analogous fashion. One further simplifying assumption is that the bottom layer will not be depleted of soluble lead-210 over the 1,000 year modelling period. Thus case 2 mentioned above does not have to be considered. The integrated mass balance for this layer is very similar to that for the mixing zone (equation 3.11.13):

$$[Pb\text{-}210_L]_{4,t} = [Pb]_{in,4,t} + ([Pb\text{-}210_L]_{4,t-\Delta t} \exp(-\lambda_{Pb\text{-}210}\Delta t) - [Pb]_{in,4,t})$$

$$\exp\,[-f_p\bar{P}\,\Delta t/(\,\epsilon\,\lambda_4(1 + K_{D,Pb}\rho_T/\epsilon\,))] \qquad (3.11.19)$$

where:

$[Pb\text{-}210_L]_{4,t}$ = dissolved concentration of Pb-210 in layer 4 at time t ($mol.m^{-3}$)

$f_p$ = fraction of precipitation which infiltrates to bottom layer

$\bar{P}$ = long-term mean annual net precipitation ($m.yr^{-1}$)

$[Pb]_{in,4,t}$ = concentration of Pb-210 in porewater infiltrating layer 4 from above at time t ($mol.m^{-3}$)

The value for $[Pb]_{in,4}$ depends on $BaSO_4$ depletion in the mixing zone:

Case 1: mixing zone contains $PbSO_4$

$$[Pb]_{in,4} = [Pb\text{-}210_L]_{mix} + [Pb\text{-}210_L]_4^{Ra} \qquad (3.11.20)$$

Case 2: mixing zone depleted of $SO_4$

$$[Pb]_{in,4} = \left( \frac{K^o_{s,PbSO4} / f^2 \, X'_{Pb\text{-}210/PbSO4}}{\sqrt{K^o_{s,PbSO4} / f^2} + [SO_4^{2-}]_4} (1 + K_{f,PbSO4} \, f^2 [SO_4^{2-}]_4) \right) + [Pb\text{-}210_L]_4^{Ra} \qquad (3.11.21)$$

In this case, $PbSO_4$ is dissolving in the bottom layer.

Again, all of these concentrations expressed in $mol.m^{-3}$ can be converted to an activity basis by multiplying by the conversion factor (PBCF).

## 3.12 Input Parameter Values

The input parameters required by the water source model are summarized in Table 3.4. The table provides both the nominal (deterministic) and probabilistic values used in the water source model demonstration (Section 3.13), and in the complete probabilistic analysis described in Volume I of this report. References are provided for many of the values on Table 3.4. In most cases, these references provide an indication of the expected value of the parameter and its likely range. However, the references do not specify distribution shapes. These have been selected based on our best knowledge of the parameter values.

Other parameters are indicated on the table as "site characteristic". These parameter values (such as tailings area) are specified arbitrarily to represent the characteristics of the reference site. In general, only parameters representing dimension have been specified as site characteristics.

A similar designation on Table 3.4 is "scenario specific". This applies specifically to the parameter $X_{Lime}$, which represents the initial mass

Table 3.4

**WATER SOURCE MODEL INPUT PARAMETERS**

| Model Symbol | Description | Units | Nominal Value | Probability Distribution | Reference |
|---|---|---|---|---|---|
| $[FeS_2]^o$ | initial pyrite content of tailings | $mol.m^{-3}$ | 700.0 | Uniform<br>min. = 600.0<br>max. = 800.0 | SENES, 1983<br>MacLaren, 1977 |
| $\rho_T$ | tailings bulk density | $g.m^{-3}$ | $1.4x10^6$ | Normal<br>mean = $1.4x10^6$<br>Std. Dev.=$0.1x10^6$<br>min. = $1.1x10^6$<br>max. = $1.7x10^6$ | MacLaren, 1977 |
| $X_{gyp}$ | initial mass fraction of gypsum in tailings | -- | 0.055 | Uniform<br>min. = 0.05<br>max. = 0.06 | SENES, 1983<br>MacLaren, 1977 |
| $K'$ | ratio of $O_2$ half saturation constant ($K_{O2}$) to $[O_2]$ | -- | $5x10^{-2}$ | Lognormal<br>Geom. mean = $5x10^{-2}$<br>Geom. S.D. = 1.7<br>min. = $2x10^{-2}$<br>max. = $2.5x10^{-1}$ | Myerson, 1981 |
| $R_s$ | sulphate production rate | $mol.g^{-1}yr^{-1}$ | $1.4x10^{-6}$ | Lognormal<br>Geom. mean = $1.4x10^{-6}$<br>Geom. S.D. = 1.5<br>min. - $0.4x10^{-6}$<br>max. = $4.2x10^{-6}$ | SENES, 1983<br>SENES, 1981 |
| $[O_2]$ | oxygen concentration at the tailings surface | $mol.m^{-3}$ | 9.04 | Constant<br>9.04 | See text |
| $D_{O2}$ | oxygen diffusivity through tailings | $m^2.yr^{-1}$ | 70.0 | Trangular<br>min. = 30<br>mode = 70<br>max. = 130 | See text |
| $\lambda_w$ | thickness of the unsaturated zone | m | 1.0 | Uniform<br>min. = 0.75<br>max. = 1.25 | site characteristic |
| $K^o_{s,CaSO_4}$ | solubility constant for $CaSO_4$ | $mol.^2m^{-6}$ | 25 | Constant<br>25.0 | Stumm and Morgan, 1981 |
| f | activity coefficient for divalent ions | -- | 0.4 | Triangular<br>min. = 0.3<br>mode = 0.4<br>max. = 0.5 | See text |

Table 3.4, cont'd.

| Model Symbol | Description | Units | Nominal Value | Probability Distribution | Reference |
|---|---|---|---|---|---|
| $P$ | annual net precipitation * | $m.yr^{-1}$ | 0.4 | Normal<br>mean = 0.4<br>Std. Dev. = 0.1<br>min. = 0.15<br>max. = 0.65 | See text |
| $\epsilon$ | tailings porosity | -- | 0.4 | Triangular<br>min. = 0.35<br>mode = 0.4<br>max. = 0.45 | See text |
| $\lambda_{mix}$ | thickness of the mixing zone | m | 1.5 | Uniform<br>min. = 1.0<br>max. = 2.0 | site characteristic |
| $\bar{P}$ | long-term mean annual net precipitation | $m.yr^{-1}$ | 0.4 | Constant<br>0.4 | See text |
| $f_p$ | fraction of net precipitation which infiltrates to tailings bottom layer (layer 4) | -- | 0.15 | Lognormal<br>Geom. mean = 0.15<br>Geom. S.D. = 1.27<br>min. = 0.0<br>max. = 0.8 | See Section 9.5.1 |
| $A$ | tailings surface area | $m^2$ | $5x10^5$ | Constant<br>$5x10^5$ | site characteristic |
| $X_{Lime}$ | initial mass fraction of lime ($CaCO_3$) in tailings | -- | Scenario Specific<br>constant = 0.0 or 0.01 | | Scenario Specific |
| $m_u^o$ | mass % of uranium (as $U_3O_8$) in the ore | -- | 0.1 | Constant<br>0.1 | MacLaren, 1977 |
| $f_U$ | mass fraction of uranium recovered in the mill | -- | 0.95 | Uniform<br>min. = 0.92<br>max. = 0.98 | MacLaren, 1977 |
| $f_{Th-230}$ | fraction of Th-230 assumed to be ultimately soluble | -- | 0.95 | Uniform<br>min. = 0.92<br>max. = 0.98 | See text |
| $f_{Th-232}$ | fraction of Th-232 assumed to be ultimately soluble | -- | 0.65 | Uniform<br>min. = 0.60<br>max. = 0.70 | See text |
| $f_{Ra}$ | fraction of Ra-226 assumed to be ultimately soluble | -- | 0.60 | Triangular<br>min. = 0.25<br>mode = 0.6<br>max. = 0.95 | See text |

Table 3.4, cont'd.

| Model Symbol | Description | Units | Nominal Value | Probability Distribution | Reference |
|---|---|---|---|---|---|
| $f_{Pb}$ | fraction of Pb-210 assumed to be ultimately soluble | -- | 0.95 | Uniform<br>min. = 0.92<br>max. = 0.98 | See text |
| $f_{U/Fe}$ | fraction of uranium associated with pyrite | -- | 0.6 | Uniform<br>min. = 0.30<br>max. = 0.90 | SENES, 1983 |
| $K_{d,UO_2}$ | uranium solid-liquid distribution coefficient | $m^3.g^{-1}$ | $3x10^{-5}$ | Lognormal<br>Geom. mean = $3x10^{-5}$<br>Geom. S.D. = 3.0<br>min. = $1.1x10^{-6}$<br>max. = $8.1x10^{-4}$ | Morin et al., 1982<br>Rancon, 1973 |
| $m^o_{Th}$ | mass % of thorium (as $ThO_2$) in the ore | -- | 0.03 | Uniform<br>min. = 0.02<br>max. = 0.04 | MacLaren, 1977 |
| $X_{Th,c}$ | fraction of $Th(OH)_4$ which is crystalline | -- | 0.3 | Triangular<br>min. = 0.2<br>mode = 0.3<br>max. = 0.4 | See text |
| $X^o_{Ra/BaSO_4}$ | initial mole fraction of Ra-226 in $BaSO_4$ | -- | $3.5x10^{-6}$ | Triangular<br>min. = $2.5x10^{-6}$<br>mode = $3.5x10^{-6}$<br>max. = $4.5x10^{-6}$ | See text |
| $K^o_{s,BaSO_4}$ | solubility constant for $BaSO_4$ | $mol^2.m^{-6}$ | $5x10^{-4}$ | Constant<br>$5x10^{-4}$ | Sillen and Martell, 1971 |
| $K_{f,BaSO_4}$ | formation constant for $BaSO_4(aq)$ | $m^3.mol^{-1}$ | $5.01x10^{-1}$ | Constant<br>$5.01x10^{-1}$ | Sillen and Martell, 1971 |
| $K_{Ra}$ | radium distribution between solid and liquid precipitate forms | -- | 0.53 | Uniform<br>min. = 0.5<br>max. = 0.56 | See Section 3.10.2 |
| $K_{d,Ra}$ | radium solid-liquid distribution coefficient | $m^3.g^{-1}$ | $40x10^{-6}$ | Triangular<br>min. = $5x10^{-6}$<br>mode = $40x10^{-6}$<br>max. = $75x10^{-6}$ | See text |
| $[PbSO_4]^o$ | initial concentration of $PbSO_4$ in tailings | $mol.m^{-3}$ | 2.0 | Triangular<br>min. = 1.0<br>mode = 2.0<br>max. = 3.0 | See text |

Table 3.4, cont'd.

| Model Symbol | Description | Units | Nominal Value | Probability Distribution | Reference |
|---|---|---|---|---|---|
| $K^o_{s,PbSO_4}$ | solubility constant for $PbSO_4$ | $mol^2.m^{-6}$ | $1.2x10^{-2}$ | Constant<br>$1.2x10^{-2}$ | Sillen and Martell, 1971 |
| $K_{f,PbSO_4}$ | formation constant for $PbSO_4(aq)$ | $m^3.mol^{-1}$ | $5.01x10^{-1}$ | Constant<br>$5.01x10^{-1}$ | Sillen and Martell, 1971 |
| $K_{d,Pb}$ | lead solid-liquid distribution coefficient | $m^3.g^{-1}$ | $60x10^{-6}$ | Triangular<br>min. = $20x10^{-6}$<br>mode = $60x10^{-6}$<br>max. = $100x10^{-6}$ | See text |

Note

* Time variant parameter

fraction of lime ($CaCO_3$) in the tailings. Its value is set either at 0.0 or 0.01 to identify the two scenarios analyzed in this study; one with no lime and one with lime added.

Finally, there are a number of parameters on Table 3.4 for which no reference is provided. These parameter values have been derived in other ways; either from fundamental principles or from a variety of sources. Brief explanations of the derivations of these parameter values are provided below. With one exception ($K_{d,Ra}$), the parameters are described in the order in which they appear in Table 3.4. The distribution coefficients for radium-226 ($K_{d,Ra}$) and lead-210 ($K_{d,Pb}$) are discussed in a combined section.

## $[O_2]$ - Concentration Of $O_2$ At The Tailings Surface

The $O_2$ concentration in air is calculated from the ideal gas low:

$$\frac{n}{V} = \frac{P_a}{RT} \qquad (3.12.1)$$

where:

$n$ = number of moles

$V$ = volume (1 $m^3$)

$P_a$ = atmospheric pressure (1 atm)

$R$ = gas low constant ($82 \times 10^{-6}$ $m^3.atm.mol^{-1}.K^{-1}$)

$T$ = temperature (10°C = 283 K)

Solving equation (3.12.1) with the values indicated above gives the molar concentration of air at 10°C; namely 43 $mol.m^{-3}$. The oxygen concentration is a fraction (0.21) of the air concentration. Thus, the $O_2$ concentration at the tailings surface is 9.04 $mol.m^{-3}$.

## $D_{O2}$ - $O_2$ Diffusivity Through The Tailings

The diffusivity of a gas (e.g. $O_2$) through tailings can be estimated by correcting its diffusivity in air for the porosity and tortuosity of tailings. Specifically:

$$D_{02} = D_{02}\,\epsilon_a/T_u \qquad (3.12.2)$$

where:

$D_{02}$ = diffusivity of $O_2$ in air (0.18 $m^2.sec^{-1}$ at 10°C or 571 $m^2.yr^{-1}$)
$\epsilon_a$ = air filled porosity ranges from 0.2 to 0.4; expected value = 0.3
$T_u$ = tortuosity ranges from 1.8 to 3.8; expected value 2.4

Substituting the values for diffusivity, porosity and tortuosity into equation (3.12.2) a range of values for $D_{02}$ can be calculated. The minimum and maximum values are 30 and 130 respectively; while the expected value is 70. A triangular distribution was selected as being most representative of the expected distribution.

## f - Activity Coefficient For Divalent Ions

The activity coefficient for individual ions can be estimated from the Davies equation (Stumm and Morgan, 1981):

$$\log f = -Az^2\left[\frac{(I)^{0.5}}{1 + (I)^{0.5}} - 0.3I\right] \qquad (3.12.3)$$

where:

A = 0.5 for water at 25°C
z = charge of ion (2 for divalent ions)
I = ionic strength of solution: ranges from 0.04 to 0.5 $mol.L^{-1}$; expected value = 0.08

Substituting the values for A and z, and the range of values for I, into equation (3.12.3) a range of values can be calculated for f. The calculations indicate a minimum of approximately 0.3, an expected value of approximately 0.4 and a maximum of about 0.5. Again, a triangular distribution was selected.

## P - Annual Net Precipitation

The distribution derived for annual net precipitation is based on meteorological data from Gore Bay, Ontario, which is located on Manitoulin Island. Annual net precipitation data for the years 1947 to 1983 were analyzed to obtain the parameter distribution. A normal distribution was found to fit the data well.

In the model simulations, annual net precipitation (P) is treated as a "time-varying parameter". That is, a new value for P is sampled for each time step. The distribution indicated in Table 3.4 is appropriate as long as a 1 year time step is used. For longer time steps, the distribution must be adjusted. In particular, the standard deviation must be corrected to give a "narrower" distribution as outlined in the Phase II study (SENES, 1985):

$$S.D.' = S.D/ (\Delta t)^{0.5} \qquad (3.12.4)$$

where:

$S.D.'$ = standard deviation corrected for $\Delta t \neq 1$

$S.D$ = standard deviation for $\Delta t = 1$ year

$\Delta t$ = simulation time step

## $\epsilon$ - Tailings Porosity

The tailings porosity, or void fraction, can be estimated by considering the tailings bulk density and the density of the tailings solids. Specifically:

$$\rho_T = (1 - \epsilon)\ \rho_S \qquad (3.12.5)$$

where:

$\rho_T$ = tailings bulk density ($g.m^{-3}$) (see Table 3.4)

$\rho_S$ = tailings solids density ($g.m^{-3}$) ranges from $2 \times 10^6$ to $2.6 \times 10^6$; expected value $2.3 \times 10^6$

Using the ranges of values (minimum, expected, maximum) indicated above, a range of values for porosity can be calculated. A triangular distribution with a minimum of 0.35, mode of 0.4 and maximum of 0.45 was therefore assumed.

### $\overline{P}$ - Long-term Mean Annual Net Precipitation

As outlined previously, the distribution of annual net precipitation was generated from actual meteorological data. The long-term mean value is simply the mean of that distribution.

### $f_{Th-230}$ - Fraction of Th-230 Assumed to be Ultimately Soluble

Isotopes of the uranium-238 decay chain (including Th-230, Ra-226 and Pb-210) are assumed to be present, in the host ore, in the same mineral matrix as U-238 itself. Thus, it is reasonable to assume that the same fraction of U-238 and decay products dissolve during the milling process. All of the Th-230 which dissolves in the mill is assumed to enter the tailings as potentially soluble precipitates. Thus the distribution of potentially soluble Th-230 is the same as the distribution used for the fraction of uranium recovered in the mill. This assumes that the amount of uranium recovered is equal to the amount of uranium dissolved in the mill.

### $f_{Th-232}$ - Fraction of Th-232 Assumed to be Ultimately Soluble

Approximately two-thirds of the Th-232 is dissolved during the milling process. The remainder is associated with very stable minerals such as monazite. Again, all of the Th-232 dissolved in the mill is assumed to be ultimately soluble in the tailings. Taking 65% as a nominal value, a uniform distribution with relatively narrow limits was assigned.

### $f_{Ra}$ - Fraction of Radium-226 Assumed to be Ultimately Soluble

Since radium-226 is associated with the uranium ore, 95% of the radium is expected to dissolve during the uranium leaching process. Radium dissolution from the host ore is incongruent and most of the dissolved radium co-precipitates with barium as $Ba(Ra)SO_4$ and possibly other solid solutions. In theory, up to 95% of this radium co-precipitate is subject to re-dissolving in the tailings. Experimental work however, has shown that only 50% to 75% of the radium-226 is ultimately leachable from the tailings in high salt solutions and substantially less under more natural conditions (Silver and Ritcey, 1980). In view of these observations, the ultimately soluble fraction of radium-226 has been assumed to be 0.6 with a triangular distribution ranging from 0.25 to 0.95.

### $f_{Pb}$ - Fraction of Lead-210 Assumed to be Ultimately Soluble

The rationale for this distribution is identical to that for $f_{Th-230}$.

### $X_{Th,c}$ - Fraction of $Th(OH)_4$ Which is Crystalline

The dissolved Th-232 forms hydroxide precipitates during neutralization in the mill. Some fraction of the precipitates formed are amorphous, while the remainder are crystalline. Since the precipitation process is relatively rapid, the majority of the precipitate is amorphous. In the absence of solid information regarding the fraction of crystalline precipitate, a triangular distribution was assumed, with a mode of 0.3 and a range from 0.2 to 0.4.

### $X^o_{Ra/BaSO_4}$ - Initial Mole Fraction of Ra-226 in $BaSO_4$

Recent evidence by Beak (1985) suggests that radium-226 co-precipitates as a solid solution of $Ba(Ra)SO_4$. It may be reasoned that the small $Ba(Ra)SO_4$ crystals are occluded in gypsum or other secondary minerals in the tailings. Assuming a homogeneous solid solution of $Ba(Ra)SO_4$, the authors (Beak, 1985) have obtained a minimum radium-226 mole fraction of approximately $2.5 \times 10^{-6}$ and an average of about $3.3 \times 10^{-6}$ for Ra-226 in $Ba(Ra)SO_4$. Analysis of Skeaff (1977) database yields a mole fraction of $4.5 \times 10^{-6}$ Ra-226 as the upper limit. Hence, a triangular distribution was assumed, with a mode of $3.5 \times 10^{-6}$; ranging from $2.5 \times 10^{-6}$ to $4.5 \times 10^{-6}$.

### $[PbSO_4]^0$ - Initial Concentration of $PbSO_4$ In The Tailings

The initial lead sulphate concentration has been calculated from laboratory digestion experiments of tailings solids by Beak (1985). For example, the digestion of 1:3 (solids:liquid) ratio with 3 M $HNO_3$ as eluent produced an average concentration of 98 mg/L of Pb in the liquid phase. Since $PbSO_4$ is soluble in $HNO_3$, the corresponding $PbSO_4$ concentration would be:

$$\left(\frac{98\text{ mg Pb}}{\text{L}}\right)\left(\frac{3\text{ L}}{1\text{ kg tailings}}\right)\left(\frac{1\text{ g}}{1{,}000\text{ mg}}\right)\left(\frac{1\text{ mole PbSO}_4}{207.19\text{ g Pb}}\right)\left(\frac{1{,}400\text{ kg tailing}}{\text{m}^3\text{ tailings}}\right)$$

$$= 1.99\ \frac{\text{moles PbSO}_4}{\text{m}^3\text{ tailings}}$$

A range of concentrations from 68 to 136 mg/L was observed in the study. Based on this information, a triangular distribution was assumed, with a mode of 2 $mol.m^{-3}$; ranging from 1 to 3 $mol.m^{-3}$.

### $K_d$ - Solid-liquid Distribution Coefficient

It is generally observed that radionuclides and other trace cationic constituents speciate between the liquid (porewater) and the solid phases. If the intrinsic properties of a closed system are held constant, this speciation reaches an equilibrium distribution in a relatively short time period, often less than 48 hours. Traditionally, the equilibrium position is evaluated as a ratio of solid phase to liquid phase concentrations. The concentration isotherms are assumed to be linear and are characterized by a distribution coefficient.

This distribution coefficient ($K_d$ value) is recognized to be dependent on numerous intrinsic variables (temperature, pH, ionic strength, contaminant concentration, etc.) and should be regarded as an empirical constant specific to the system in question. Being empirical in nature, the distribution coefficient does not take into account explicitly the controlling transport mechanism (adsorption, ion exchange, co-precipitation) between the liquid and the solid phases. Nevertheless, the concept of $K_d$ has been found to be convenient to model the mobility (or retardation) of trace constituents in groundwaters. In the following sections the effect of solid/liquid transport mechanisms of Ra-226 and Pb-210 on the apparent $K_d$ in the tailings porewater (mixing layer and layer 4) is discussed. (It should be noted, that the concentrations of these radionuclides are modelled explicitly in the two unsaturated zones.)

### i) Radium-226

Recent evidence (Beak, 1985) indicates that the mobility of dissolved Ra-226 is controlled by co-precipitation (i.e. solid solution) of Ra-226 in barite ($BaSO_4$). Their work suggests that low grade, pyritic tailings contain approximately 0.3 $mol.m^{-3}$ ($3 \times 10^{-4}$ $mol.dm^{-3}$) $BaSO_4$ and an initial mole fraction of Ra-226 in the barite of about $3.5 \times 10^{-6}$.

Barite in tailings is believed to be present as micro-crystals occluded in gypsum or other host mineral. It seems reasonable to assume that, at any given time, only a fraction of the solid barite is involved in co-precipitation. We assume a nominal value of 1% ($3.0 \times 10^{-6}$ $mol.dm^{-3}$) $BaSO_4$, recognizing that it may vary with time, first increasing as the host mineral (gypsum) is dissolved (more barite is exposed) than decreasing after 99% of the barite in the mixing zone has gone into solution. Since the co-precipitation mechanism is the most significant when the radium-rich barite is nearly depleted in the unsaturated zone (layer 2), the porewater entering the mixing zone would be saturated with respect to barium. For illustration, this water is assumed to contain $4 \times 10^{-10}$ M (3,350 $Bq.L^{-1}$) dissolved Ra-226. This concentration can be varied considerably, since the solid/liquid equilibrium distributions, calculated by the co-precipitation mechanism, are relatively insensitive with regard to this initial Ra-226 concentration in the liquid. In any case, the radium-226 input into the pore space ($1.6 \times 10^{-10}$ $mol.dm^{-3}$ at a porosity of 0.4) represents approximately 15% of the nominal radium-226 reservoir in the unsaturated zone.

The co-precipitation mechanism involves the formation of a solid solution of $RaSO_4$ in barite ($BaSO_4$). The solution of $RaSO_4$ in the $BaSO_4$ lattice is nearly ideal (Stumm and Morgan, 1981) and, at trace $RaSO_4$ mole fractions, the equilibrium ratio between the solid and the liquid phase is given by the distribution constant, D, as follows:

$$D = \left[ \frac{\dfrac{[RaSO_4]_S}{[BaSO_4]_S}}{\dfrac{[Ra]_L}{[Ba]_L}} \right] \qquad (3.12.4)$$

where:

$[RaSO_4]_S/[BaSO_4]_S$ = the molar ratio of radium-226 in barite

$[Ra]_L/[Ba]_L$ = the ratio of radium-226 to barium concentrations in the liquid phase

D = distribution constant (=1.8 for $RaSO_4$ in $BaSO_4$; the experimentally observed value of D in the present system)

It can be easily shown that, if the mole fraction of radium-226 in the solid phase is small, the molar ratios are numerically equal to the mole fractions. Rearranging equation (3.12.4) yields the moles of radium-226 in the solid solution as follows:

$$[RaSO_4]_S = D \frac{[BaSO_4]_S}{[Ba]_L} [Ra]_L \qquad (3.12.5)$$

Since the activity of barium in the solid phase ($Ba_{1-x}\ Ra_x\ SO_4$; $x = 3.5 \times 10^{-6}$) is essentially unity, the concentration of barium in the saturated solution depends solely on the solubility product of the end member ($BaSO_4$), the complexation of $Ba^{2+}$ with $SO_4^{2-}$, ($BaSO_4aq$) and the activity coefficients of $BaSO_4(aq)$ (log K = 2.7) and $RaSO_4(aq)$ (log K = 2.74) are essentially identical. Consequently, the molar ratio of radium to barium in the liquid phase does not depend on the sulphate $[SO_4^{2-}]$ concentration. It is therefore sufficient to estimate only the concentration of total dissolved barium in solution.

Assuming a nominal sulphate concentration of $1.5 \times 10^{-2}$ M and an activity coefficient of 0.4 (nominal value) in the porewater, the following solution and speciation equilibria are relevant:

$$
\begin{array}{lll}
BaSO_{4(s)} \rightleftharpoons Ba^{2+} + SO_4^{2-} & & \log K = -9.97 \\
Ba^{2+} + SO_4^{2-} \rightleftharpoons BaSO_4^0aq & & \log K = 2.7 \\
[Ba^{2+}] = 4.46 \times 10^{-8} \text{ M} & & \\
[BaSO_4] = 5.36 \times 10^{-8} \text{ M} & & (3.12.6) \\
[Ba]_L = 9.82 \times 10^{-8} \text{ M (total barium in solution)} & &
\end{array}
$$

Substituting for $[BaSO_4]_S$ and $[Ba]_L$ in equation (3.12.5) yields:

$$[RaSO4]_S = (1.8) \frac{3 \times 10^{-6}}{9.82 \times 10^{-8}} [Ra]_L = 55 [Ra]_L \qquad (3.12.7)$$

At this point, the equilibrium concentration of radium-226 in the liquid phase can be calculated by material balance as follows:

$$55 [Ra]_L + \epsilon [Ra]_L = \epsilon [Ra]^o \qquad (3.12.8)$$

Substituting for $[Ra]^o = 4 \times 10^{-10}$ M

and

$$\epsilon = 0.4$$

yields $$[Ra]_L = \frac{(0.4)\ (4 \times 10^{-10})}{55 + 0.4} = 2.89 \times 10^{-12} \text{ M Ra-226}$$

Note that equation (3.12.8) is analogous to conventional expressions employing $K_d$ values. In fact, co-precipitation is phenomenologically indistinguishable from adsorption mechanisms if one member of the solid solution (co-precipitate) is present in trace amounts. It can be shown, that the characteristic $K_d$ value for the system containing 1.4 kg.dm$^{-3}$ solids is given by:

$$K_d = \frac{\frac{0.4\ (4 \times 10^{-10} - 2.89 \times 10^{-12})}{1.4}}{2.89 \times 10^{-12}} = 39.26\ \frac{dm^3}{kg}\ \left(\frac{ml}{g}\right) \tag{3.12.9}$$

A nominal value of $K_d = 40\ ml.g^{-1}$ is assumed. An upper limit of $K_d$ may be obtained by evaluating the equilibrium expressions at higher barite concentrations. It may be noted, that a higher sulphate concentration ($3 \times 10^{-2}$ M $SO_4^{2-}$, for example) has only a marginal effect on the co-precipitation equilibrium, since the formation of the sulphate complexes (both $BaSO_4^0$ and $RaSO_4$) in the liquid phase become predominant. Using $6 \times 10^{-6} mol.dm^{-3}$ $BaSO_{4(s)}$ in equations (3.12.7) and (3.12.8) would yield a liquid phase Ra-226 concentration of $1.45 \times 10^{-12}$ M and a corresponding $K_d$ value (equation (3.12.9)) of $78.6\ ml.g^{-1}$. A $K_d$ value of $75\ ml.g^{-1}$ is used as the upper limit. The lower limit of $K_d$ is established by purely adsorption mechanism as $5\ ml.g^{-1}$ (NRC, 1983). In view of the above, the distribution of $K_d$ for dissolved radium-226 is assumed to be triangular with a nominal value of $40\ ml.g^{-1}$ and a range from $5 ml.g^{-1}$ (minimum adsorption) to $75\ ml.g^{-1}$ (maximum co-precipitation).

### ii) Lead-210

The obvious choice for lead-210 co-precipitation is a solid solution with its stable isotopes. In pyritic uranium tailings, solid lead sulphate ($PbSO_4$) would be the most likely mineral participating in such an event. Lead isotopes tend to form ideal solid solutions with a characteristic distribution constant of unity (D=1). Applying solid solution theory for lead sulphates the distribution between the solid phase and the liquid phase, at equilibrium, is given by:

$$D = \left[\frac{\frac{[Pb^{210}SO_4]_S}{[PbSO_4]_S}}{\frac{[Pb^{210}]_L}{[Pb]_L}}\right] = 1 \tag{3.12.10}$$

where:

$[Pb^{210}SO_4]_s$ = concentration of Pb-210 in the solid $[PbSO_4]$ phase (mol.m$^{-3}$)
$[PbSO_4]_s$ = total lead sulphate concentration in the solid phase (mol.m$^{-3}$)
$[Pb^{210}]_L$ = concentration of Pb-210 in the liquid phase (mol.m$^{-3}$)
$[Pb]_L$ = concentration of total dissolved lead in the liquid phase (mol.m$^{-3}$)

The nominal concentration of lead sulphate solids in the tailings is estimated to be 2 mol.m$^{-3}$ (2 x 10$^{-3}$ mol.dm$^{-3}$) $PbSO_4$. The liquid phase concentration is dependent on the sulphate concentration $[SO_4^{2-}]$ and the activity coefficients of $Pb^{2+}$ and $SO_4^{2-}$. As in case of $BaSO_4$ solubility, the solution equilibrium and speciation of lead in the liquid phase involves the following reactions:

$$\begin{aligned} PbSO_4 &\rightleftharpoons Pb^{2+} + SO_4^{2-} && \log K = -7.7 \\ Pb^{2+} + SO_4^{2-} &\rightleftharpoons PbSO_{4(aq)}^{0} && \log K = 2.7 \qquad (3.12.11) \end{aligned}$$

Using a nominal sulphate ($SO_4^{2-}$) concentration of 1.5 x 10$^{-2}$ M and an activity coefficient of 0.4 M for both $Pb^{2+}$ and $SO_4^{2-}$, the equilibrium expressions (equation (3.12.11)) yield 8.36 x 10$^{-6}$ M $Pb^{2+}$ and 1.05 x 10$^{-5}$ M $PbSO_{4(aq)}^{0}$ as dissolved species (total dissolved lead = 1.83 x 10$^{-5}$ M).

It is assumed, that approximately 50% of the solid $PbSO_4(s)$ (1.0 mol.m$^{-3}$) participates in exchange reactions. The remaining solid $PbSO_4$ is assumed to be occluded by gypsum or other secondary precipitates. The distribution of Pb-210 in the solid and liquid phases can be obtained directly (equation (3.12.10) as follows:

$$\frac{[Pb^{210}SO_4]_s}{[Pb^{210}]_L} = \frac{10^{-3}}{1.83 \times 10^{-5}} = 54.64 \ \frac{L}{dm^3} \qquad (3.12.12)$$

At a tailings bulk density of 1.4 kg.dm$^{-3}$, the apparent $K_d$ value would be:

$$K_d = \frac{54.64}{1.4} = 39 \ \frac{L}{kg} \text{ or } 39 \ \frac{ml}{g} \qquad (3.12.13)$$

The driving force for co-precipitation reactions of Pb-210 in $PbSO_4$ is provided by the relatively short half-life of the Pb-210 isotope. Unlike Ra-226, the initial Pb-210 content of the solid phase in the mixing zone is assumed to approach zero prior to $PbSO_4$ depletion from the unsaturated zone. If the Pb-210 in $PbSO_4$ is not zero or the solid $PbSO_4$ content of the mixing zone is partially depleted (solid $PbSO_4$ concentration = $5 \times 10^{-4}$ mol.dm$^{-3}$) the apparent $K_d$ value would be 20 ml.g$^{-1}$. It has been shown by Veska (1983), that the apparent $K_d$ of Pb-210 in sandy soils at acidic pH values (pH<5.0) is 102 ml.g$^{-1}$. Consequently, the $K_d$ for Pb-210 is assumed to range from 20 ml.g$^{-1}$ to 100 ml.g$^{-1}$ with a nominal value of 60 ml.g$^{-1}$ (triangular distribution). This particular range takes into account either co-precipitation or adsorption mechanisms.

## 3.13 Water Source Model Demonstration

Validation of a large and complex model, such as that described in this chapter, is recognized to be a difficult task. Furthermore, it is impossible to validate model predictions made hundreds of years into the future. In lieu of model validation, a model demonstration exercise was completed to gain confidence in the water source term model before integrating it into the system model. Both deterministic and probabilistic trials were performed during the demonstration. The deterministic demonstration used the nominal values for all input parameters, while the probabilistic demonstration involved 30 random simulation trials. Since, the deterministic (nominal) input values are generally very similar to the expected value of an input parameter distribution, the deterministic and probabilistic results may be very similar. The deterministic results provide a basis for comparison with other implementation of the model and may be readily checked by hand calculation. All demonstration results represent the scenario in which no limestone is added to the tailings. This is referred to as Scenario 1 in Volume 1 of this report.

The section includes graphical presentation of deterministic results, using nominal parameter values, and the arithmetic mean values of probabilistic runs, based on 30 random trials, for the concentrations of many ionic species and radionuclides in the different tailings layers. The information is presented in the following figures:

- 3.3 - sulphate ion concentration; layers 2, 3 and 4
- 3.4 - calcium ion concentration; layers 2, 3 and 4
- 3.5 - total iron ion concentrations; layers 2, 3 and 4
- 3.6 - porewater pH; layers 1, 2, 3, 4
- 3.7 - solid phase radionuclide concentrations in layer 1; uranium, thorium, radium and lead
- 3.8 - dissolved uranium concentration; layers 2, 3 and 4
- 3.9 - dissolved thorium concentration; layers 2, 3 and 4
- 3.10 - dissolved radium concentration; layers 2, 3 and 4
- 3.11 - dissolved lead concentration; layers 2, 3 and 4

Deterministic results are presented as part (a) of the figures in all cases, while probabilistic results are presented as part (b) of the figures. The results were generated using the deterministic and probabilistic input parameter values summarized in the previous section. Some brief notes regarding each figure follow.

Sulphate Ion Concentrations

The sulphate concentrations shown on Figure 3.4 are affected by several processes; pyrite oxidation, gypsum dissolution and the percolation of precipitation. Initially, the sulphate concentrations result primarily from sulphate formed via the oxidation of pyrite in the unsaturated zone. The sulphate concentrations therefore decrease as the pyrite inventory decreases with time. The layer 4 concentration is assumed initially to be unaffected by sulphates formed via pyrite oxidation. Its concentration therefore increases as high sulphate concentration porewater percolates down from above. As the pyrite inventory and sulphate concentrations decrease in the upper layers, so does the sulphate concentration in layer 4.

Gypsum dissolution also contributes to the sulphate concentration in all layers. As the gypsum inventory is depleted in layers 2 and 3 the sulphate concentration falls to the background level (0.1 mol.m$^{-3}$). Layer 4 is assumed to be large enough that gypsum depletion does not occur within the simulation time period. Thus, the sulphate concentration in layer 4 reaches a steady state value.

### Calcium Ion Concentrations

The calcium ion concentrations (shown in Figure 3.4) result solely from the dissolution of gypsum. These results thus provide a better illustration of the gypsum depletion phenomena referred to previously. As the sulphate concentrations decrease in layers 2 and 3, the calcium concentration increases, to satisfy gypsum equilibrium considerations. The calcium concentration in layer 4 decreases initially and then rises, as the sulphate concentration in that layer increases then declines.

Gypsum dissolves, maintaining an equilibrium concentration of calcium, until its inventory is depleted. The deterministic results (Figure 3.4(a)) indicate that gypsum is depleted from layer 2 at approximately 180 years and from layer 3 near 300 years. Following gypsum depletion, the concentration of calcium ion drops to zero. The steady state concentration of calcium in layer 4 is essentially equal to that of sulphate, as expected from the stoichiometry of gypsum dissolution.

The probabilistic results (Figure 3.4(b)) indicate that gypsum depletion in layers 2 and 3 occurs at different times on different trials. This is shown by the gradual, rather than sudden, decrease in calcium concentration. For instance in layer 3, depletion occurs sometime between 200 and shortly after 400 years. The mean values of many probabilistic trials show average trends rather than the physically more realistic dynamic behaviour illustrated by a deterministic trial. For this reason, it is often useful to examine both deterministic and probabilistic results.

FIGURE 3.3

## SULPHATE ION CONCENTRATIONS (SCENARIO I)

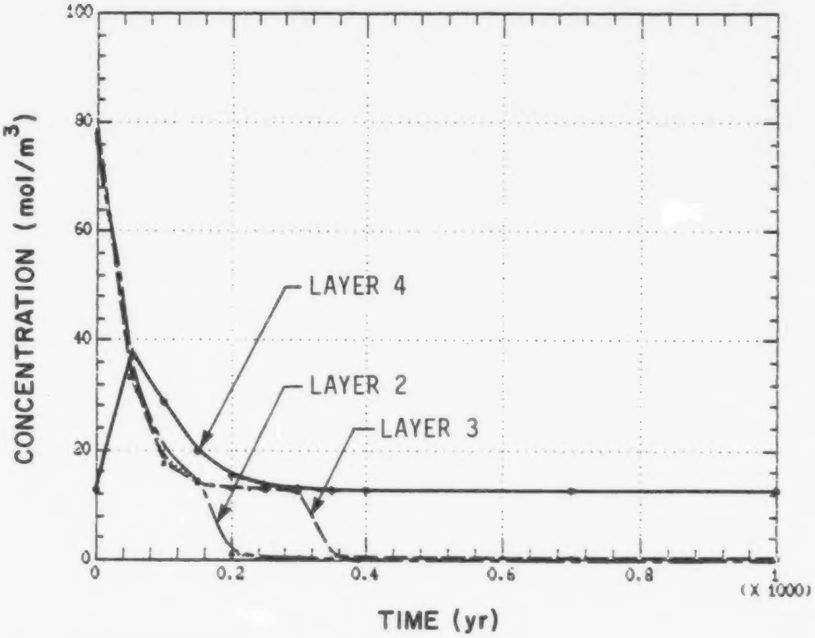

A) DETERMINISTIC RESULTS

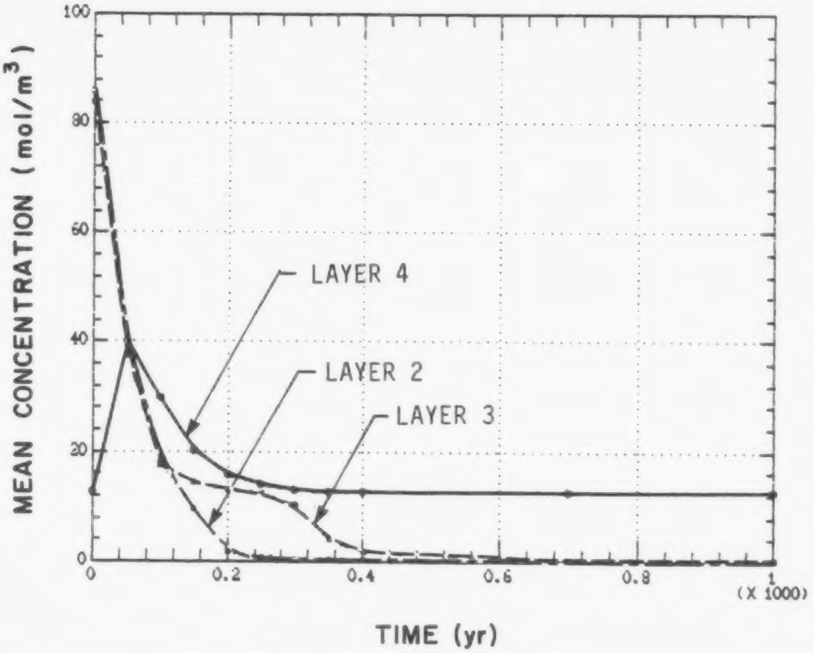

B) PROBABILISTIC RESULTS (30 TRIALS)

FIGURE 3.4

CALCIUM ION CONCENTRATIONS
( SCENARIO I )

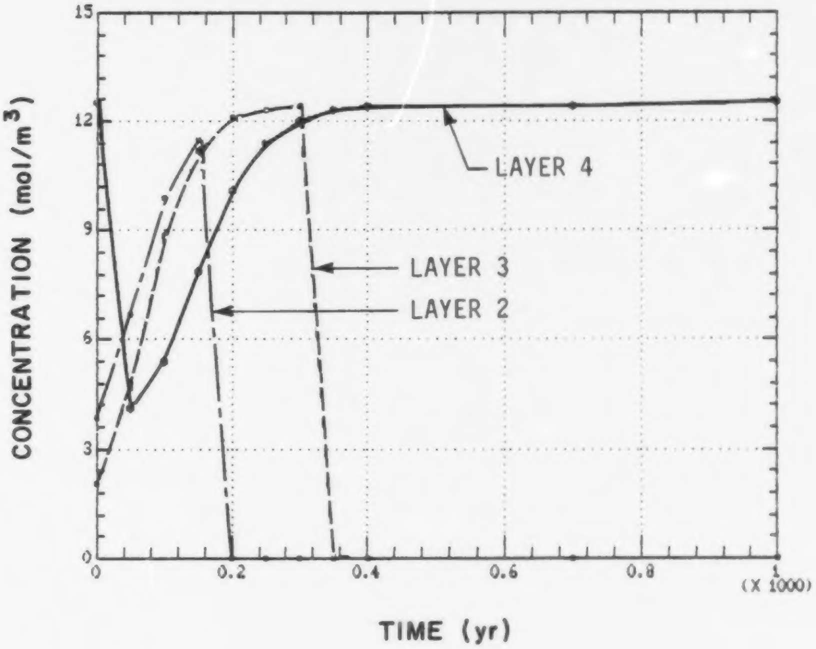

A) DETERMINISTIC RESULTS

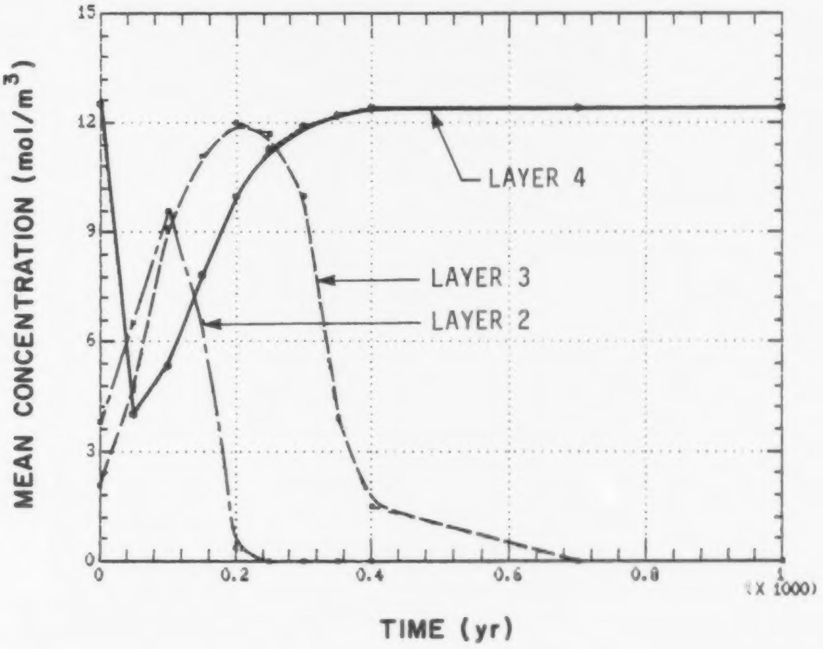

B) PROBABILISTIC RESULTS ( 30 TRAILS)

## Iron Ion Concentrations

The concentration of iron in layer 2 is modelled as a function of pH and sulphate concentration. As the sulphate concentration decreases, so does the iron concentration in layer 2 (see Figure 3.5). The concentrations in layers 3 and 4 are functions of the iron inputs from the above layers. Thus, the concentration in layer 4 increases from an initial (assumed) value of zero as iron is transported down from layer 3. Over the long-term, the iron concentration decreases and stabilizes as the sulphate concentration decreases and stabilizes.

## Porewater pH

As illustrated in Figure 3.6 (a) and (b), the pH values in layers 1, 2 and 3 are initially low and rise gradually to steady-state values. This results from the change in the sulphate concentrations with time. The sulphate concentrations are initially high as a result of pyrite oxidation. However, as the sulphate concentrations decrease with time, the pH rises. As mentioned earlier, layer 4 is initially assumed to be unaffected by sulphates from pyrite oxidation. Hence the pH in layer 4 is initially near neutral, subsequently declines as sulphates are transported in from layers above and then increases as the sulphate concentration decreases.

Once gypsum is depleted from the unsaturated zone, layers 1 and 2 are indistinguishable, and their pH values are obviously equal. The pH in the unsaturated zone stabilizes near pH 4.3, and is primarily governed by the sulphate input with the precipitation (i.e. acid rain). On the other hand, the pH in layers 3 and 4 stabilizes near neutrality (pH = 6.9), primarily because of the influence of one or more minerals which are slowly leached from the tailings (e.g. $Al(OH)_3$ species, gypsum, calcite).

## Solid Phase Radionuclide Concentrations

The radionuclides associated with the solid phase in the tailings surface layer act as a source to the dust and air dispersion models and all subsequent air-related pathways. Some radionuclides (uranium and thorium) are assumed to be uniformly distributed throughout the unsaturated tailings zone. Others (radium and lead) are assumed to dissolve in a frontwise manner, resulting in an upper, depleted layer and a lower, enriched layer. Thus the "surface layer" is of different thicknesses for different radionuclides. For uranium and thorium, it consists of the entire unsaturated zone while for radium and lead it consists of the upper, depleted layer. The distribution of the radionuclides associated with the surface tailings solids is shown on Figure 3.7

Some fraction of the uranium in the tailings is assumed to be associated with pyrite. Thus, as the pyrite oxidizes, this uranium is released from the solid phase. This process accounts for the decrease in solid phase uranium concentration over the first 100 years, or so.

The total thorium concentration consists of Th-230 and Th-232. Thorium solubility is strongly pH dependant, decreasing rapidly as pH rises above approximately 3.5. At the low pH's encountered initially in the unsaturated zone, a considerable fraction of the thorium dissolves, resulting in the rapid decrease in the solid phase thorium concentration.

The solid phase radium concentrations are those for the radium-depleted layer. The radium in this layer is assumed to be associated with the host tailings material, and hence is insoluble. Thus the decrease in radium concentration with time results from the net radioactive decay of the radium. Ingrowth of radium from thorium decay is insignificant as much of the thorium is leached from the upper layer in a short time frame.

The solid phase lead concentrations are also those for the lead depleted layer. Again, the lead present is assumed to be insoluble, and associated with the host tailings material. The initial difference in lead and radium concentrations results from the fact that approximately 40% of the radium is assumed to be insoluble while only 5% of the lead is considered insoluble.

FIGURE 3.5

IRON ION CONCENTRATIONS
(SCENARIO I)

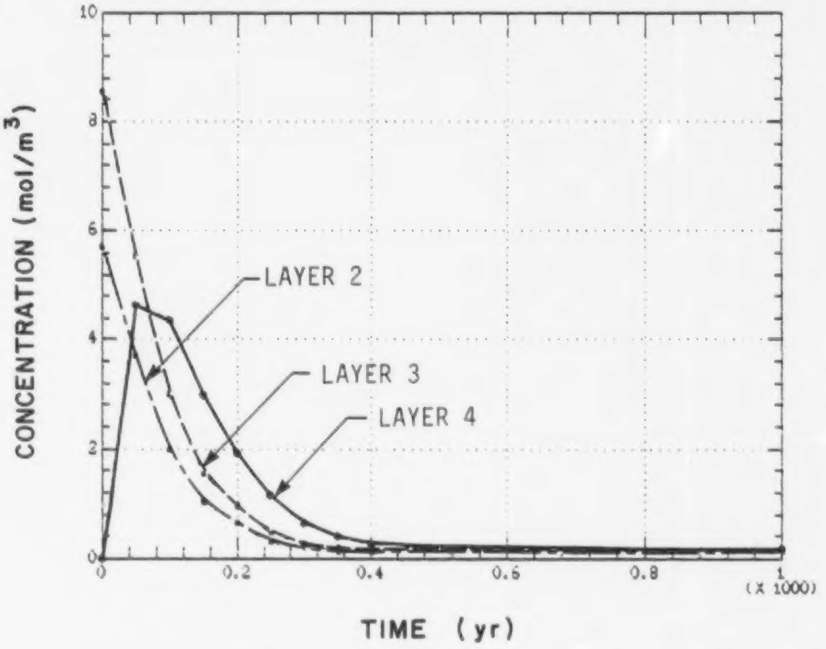

A) DETERMINISTIC RESULTS

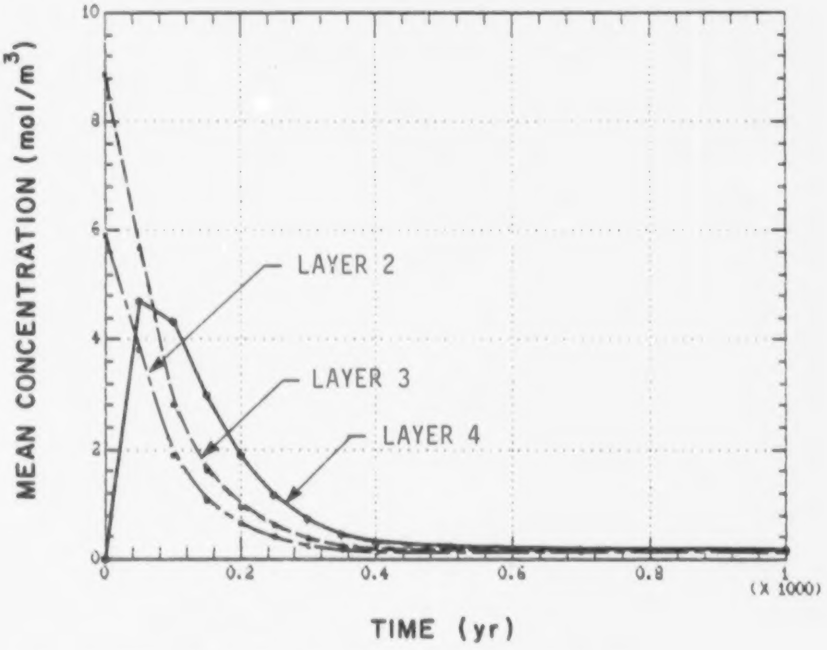

B) PROBABILISTIC RESULTS (30 TRIALS)

FIGURE 3.6

## POREWATER pH
## (SCENARIO I)

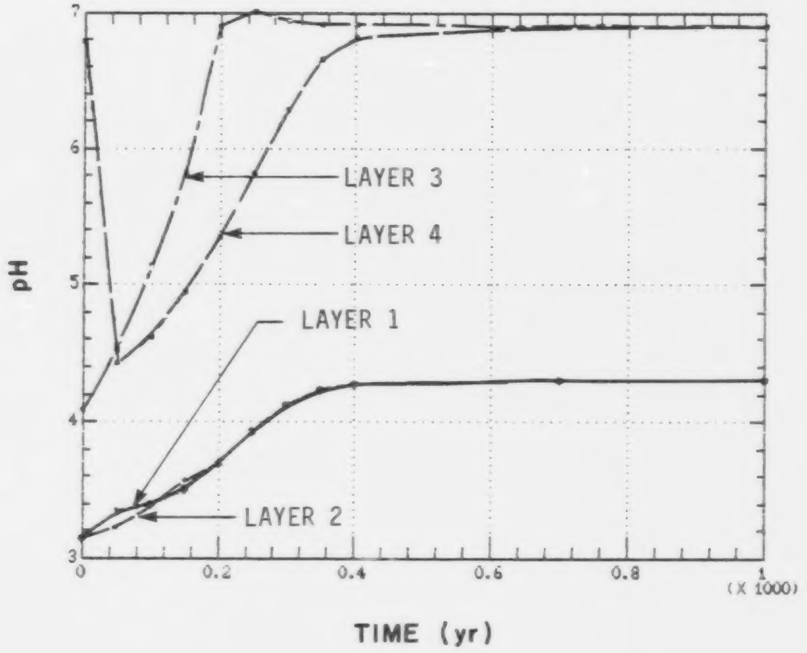

A) DETERMINISTIC RESULTS

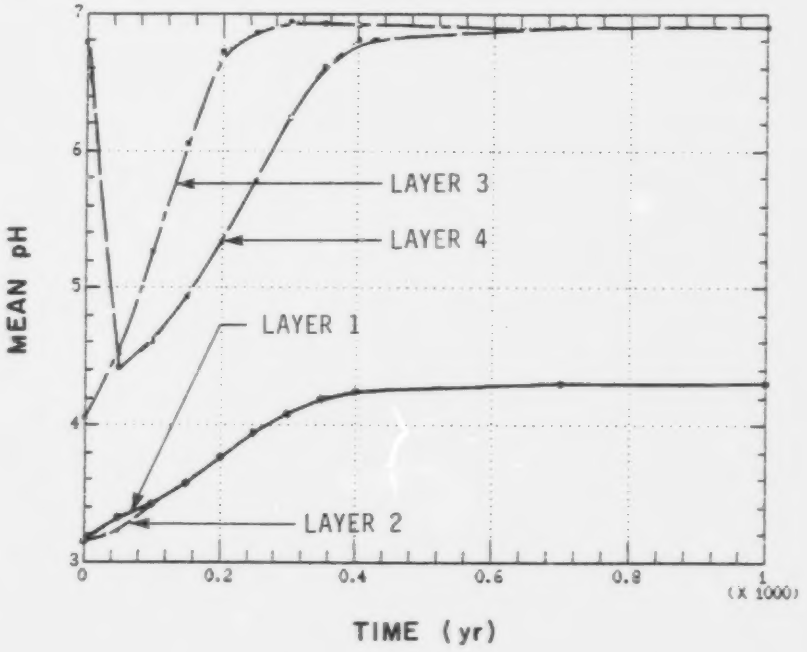

B) PROBABILISTIC RESULTS (30 TRIALS)

FIGURE 3.7

SOLID PHASE RADIONUCLIDE CONCENTRATIONS
IN SURFACE LAYER
( SCENARIO I )

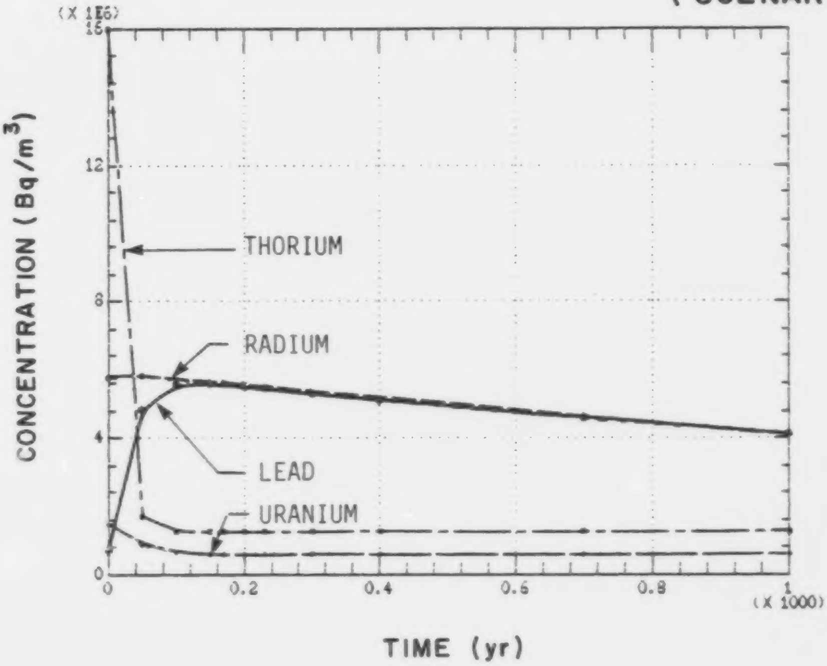

A) DETERMINISTIC RESULTS

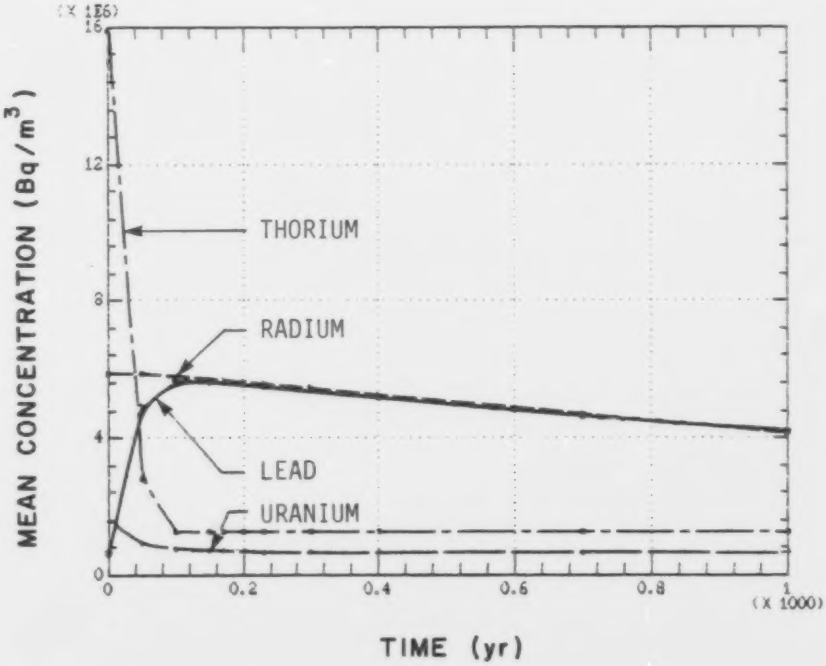

B) PROBABILISTIC RESULTS ( 30 TRIALS)

The lead concentration increases as a result of net radioactive ingrowth from radium and subsequently tracks the radium behaviour exactly as expected.

## Dissolved Uranium Concentrations

The dissolved uranium concentration (illustrated in Figure 3.8) in layer 2 reflects the formation of sulphate as a result of pyrite oxidation (see Figure 3.3). Since some (nominally 60%) of the uranium is assumed to be associated with pyrite, the oxidation of pyrite results in the dissolution of uranium, just as it results in the formation of sulphate ion. Thus, the concentration of dissolved uranium decreases as the pyrite inventory decreases. The concentrations of uranium in layers 3 and 4 are functions of the concentration of uranium entering from the layer above. Some of the uranium in these layers is adsorbed and subsequently acts as a long-term source of dissolved uranium.

## Dissolved Thorium Concentrations

As mentioned previously, the thorium concentration is very strongly pH dependent, falling rapidly as the pH rises above approximately 3.5. Figure 3.9 illustrates the concentration of dissolved thorium in layers 2, 3 and 4. The pH results presented earlier (Figure 3.6) help to explain the dissolved thorium concentrations.

Layer 2 is initially at a very low pH (approximately 3.1) and hence thorium solubility and concentration are quite high. In fact, Figure 3.9 (a) (the deterministic results) indicates that all of the soluble thorium in layer 2 is dissolved over the first 100 years. With no further source of soluble thorium, the dissolved thorium concentration falls to zero thereafter. The probabilistic results show a gradual decrease in thorium concentration in layer 2, indicating that depletion of soluble thorium occurs at different times on different trials.

The layer 3 concentrations show a similar decrease as the pH increases with time. Although not well illustrated on Figure 3.9, the layer 3 thorium inventory is not depleted, and the concentrations decrease to a low, but non-zero value.

The initial thorium concentration in layer 4 is several orders of magnitude lower than those in layers 2 and 3. As the pH in layer 4 decreases (between 0 and 50 years) the thorium concentration increases and then decreases again as the pH rises.

Dissolved Radium Concentrations

The dissolved radium concentrations in layers 2, 3 and 4 are illustrated in Figure 3.10 (a) and (b). Soluble radium in the tailings is assumed to be associated with barium sulphate ($BaSO_4$). The barium sulphate (and associated radium) dissolves in a frontwise manner in the unsaturated zone, resulting in a $BaSO_4$ (and radium) depleted layer and a layer (layer 2) which is enriched in $BaSO_4$ (and radium). Because of the chemical properties of radium, it reprecipitates and becomes concentrated in layer 2. Thus, over the initial 150 years or so (see Figure 3.10a) the radium concentration in the porewater is controlled at a comparatively low level. After this time, the concentration of dissolved radium in layer 2 shows a rapid rise as illustrated by the deterministic results in Figure 3.10 (a). This occurs as the thickness of layer 2 (the radium enriched layer) becomes smaller and smaller, and the enriched $BaSO_4$ (with an elevated radium content) starts to dissolve. At some point (210 years in Figure 3.10 (a)) the thickness of layer 2 becomes zero indicating that the unsaturated zone is completely depleted of $BaSO_4$. The concentration of dissolved radium thus falls to zero, since $BaSO_4$ acts as the only source of soluble radium.

The concentration profile for layer 2 is not as pronounced in the probabilistic results shown in Figure 3.10 (b), since the very sharp peak occurs at different times on different trials. The average of a few high concentrations and many lower values at any time is obviously much lower than the few high concentrations of any one time.

FIGURE 3.8

## DISSOLVED URANIUM CONCENTRATIONS (SCENARIO I)

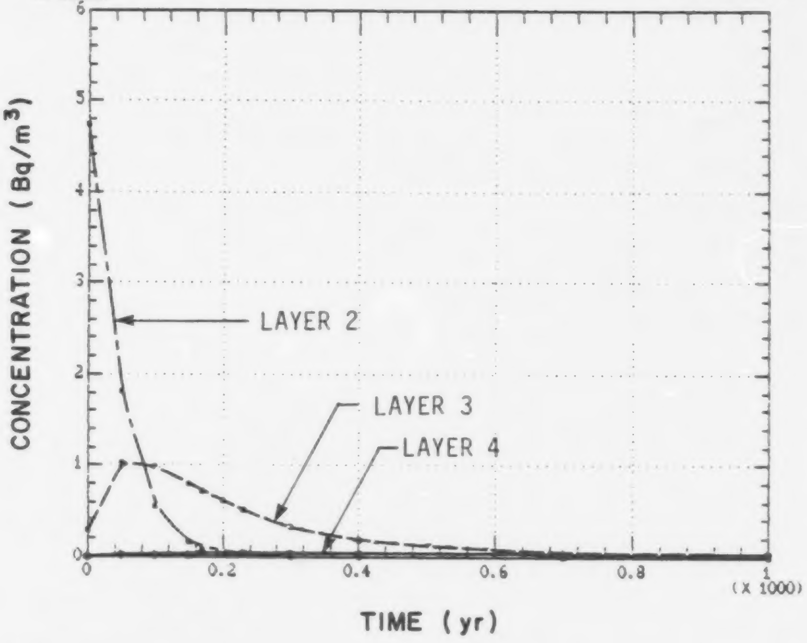

A) DETERMINISTIC RESULTS

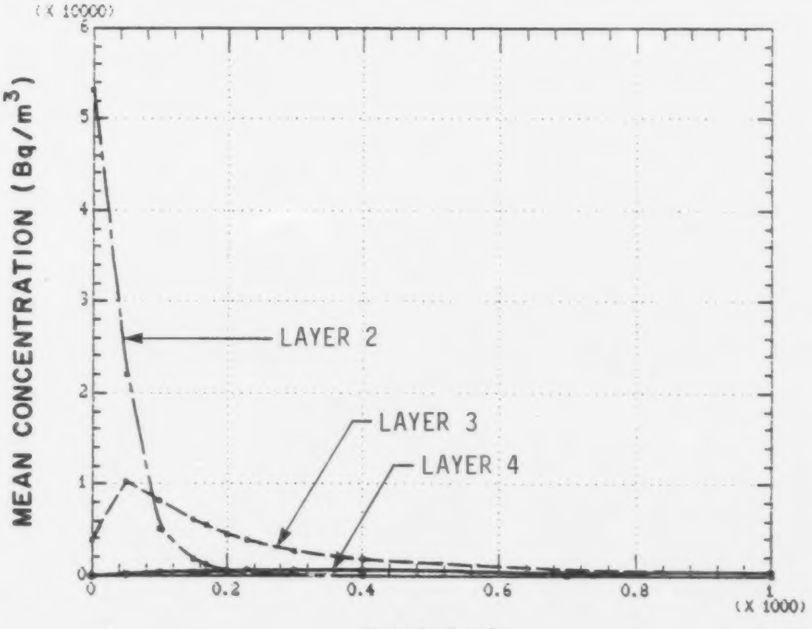

B) PROBABILISTIC RESULTS (30 TRIALS)

FIGURE 3.9

DISSOLVED THORIUM CONCENTRATIONS
(SCENARIO I)

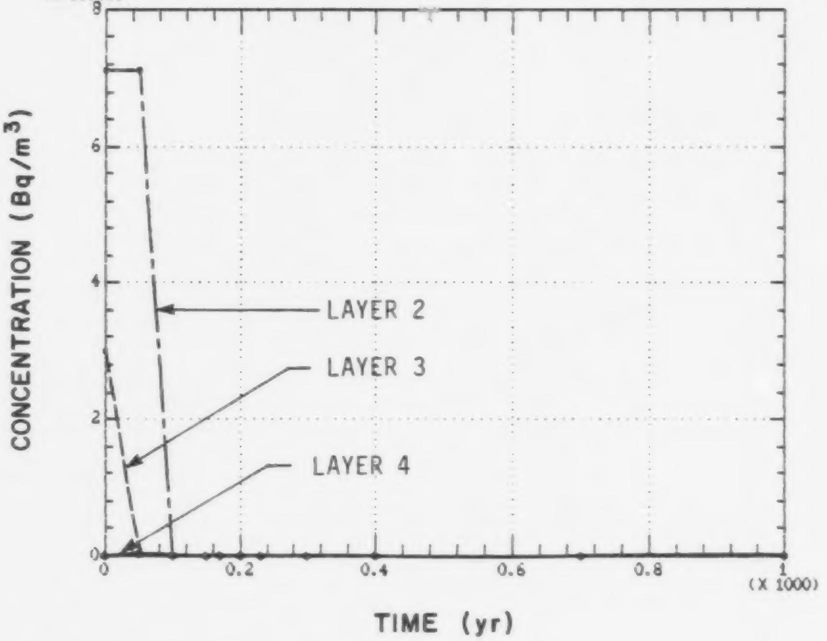

A) DETERMINISTIC RESULTS

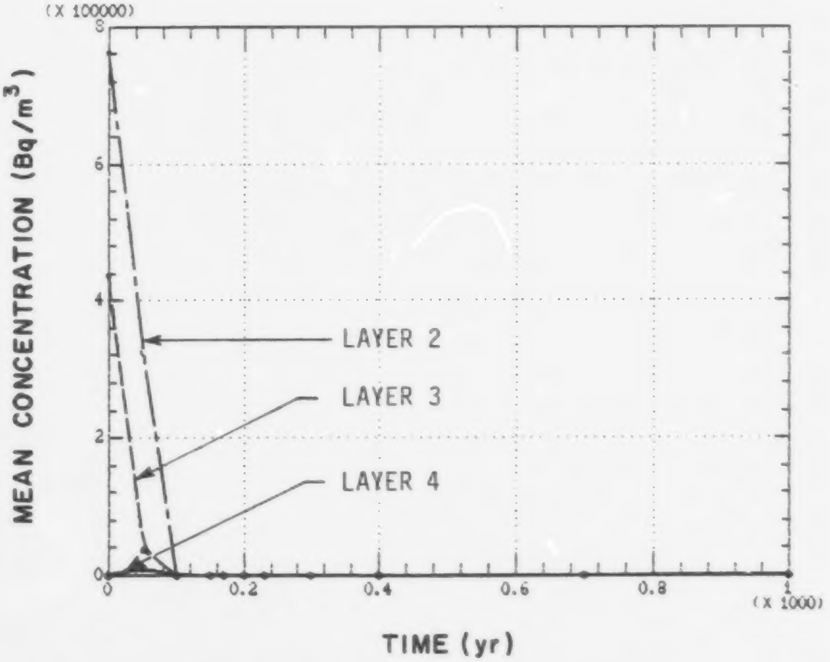

B) PROBABILISTIC RESULTS (30 TRIALS)

FIGURE 3.10

DISSOLVED RADIUM CONCENTRATIONS
(SCENARIO I)

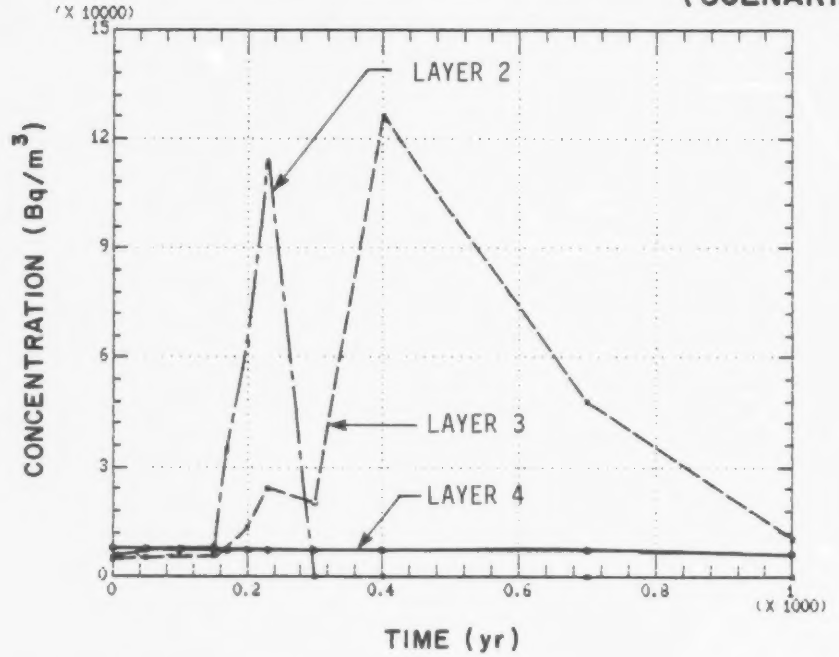

A) DETERMINISTIC RESULTS

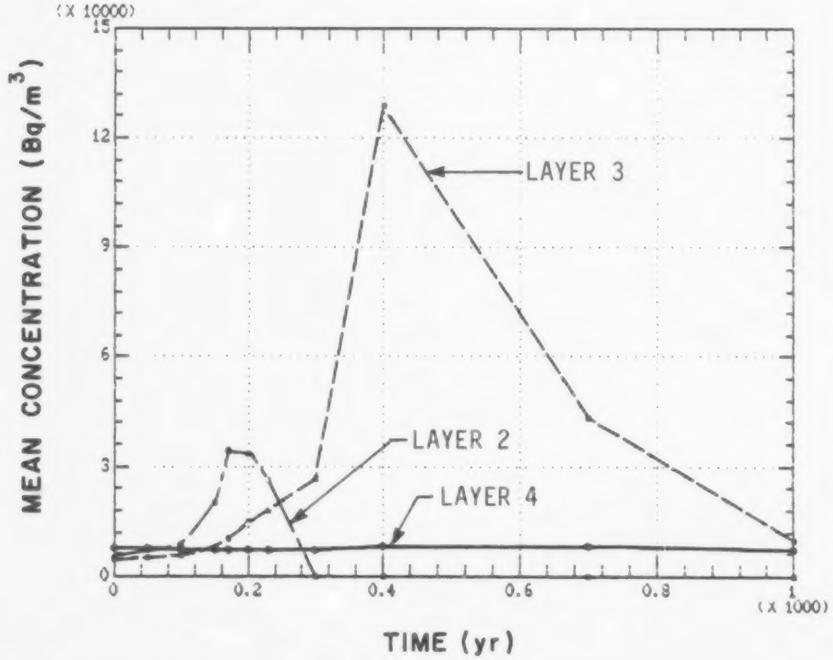

B) PROBABILISTIC RESULTS (30 TRIALS)

The concentration of radium in layer 3 results from both the radium input from layer 2 (as long as $BaSO_4$ is present) and also from $BaSO_4$ dissolution in layer 3. Adsorption mechanisms are also considered in layer 3, which results in a smoothing or spreading of the concentration peaks seen in layer 2.

Because of the large volume of layer 4 and the relatively large solid-liquid distribution coefficient ($K_d$) for radium, the radium concentration in layer 4 is relatively unaffected by inputs from layer 3. That is, layer 4 has a relatively large sorptive capacity, which serves to dampen out any input flunctuations and maintain a relatively constant radium concentration.

### Dissolved Lead Concentrations

Lead-210 is assumed to be associated with lead sulphate ($PbSO_4$) much as radium is associated with $BaSO_4$. The dissolution of $PbSO_4$ is also assumed to occur in a frontwise manner. However, unlike radium, lead-210 does not become increasingly concentrated as it reprecipitates with $PbSO_4$ in layer 2 (a $PbSO_4$ enriched layer). Because of its short radioactive half-life (21 years), much of the behaviour of lead-210 is governed by its radioactive decay and ingrowth from radium-226. Thus, the change in dissolved radium concentration with time (Figure 3.10) can help to explain the lead-210 concentrations in the various tailings layers illustrated in Figure 3.11 (a) and (b).

The initial lead concentrations are governed by the equilibrium dissolution of $PbSO_4$. The decreasing lead concentrations over the initial 50 to 100 years are primarily the result of radioactive decay. Layer 2 and layer 3 both show subsequent concentration increases which correspond to the peaks in dissolved radium concentration illustrated in Figure 3.10.

## 3.14 Tailings Erosion and Re-Vegetation

### 3.14.1 Introduction

The erosion model detailed in the following section accounts for two physical phenomena. The first is the long-term depletion of the surface of the tailings pile. This is of particular interest if an engineered cover is placed on the tailings pile. Should this cover eventually be worn away the tailings will be exposed to water and wind erosion. The second phenomena is the physical movement of the tailings surface layer into the river/lake system. This is of particular interest when the surface is bare tailings, since the radioactivity associated with the eroded particles will, to a degree, dissolve in the river/lake system and cause an increase in activity in these waters.

The erosion model accounts for gross soil erosion of the tailings using the Universal Soil Loss Equation. This equation, primarily estimates erosion and does not account for deposition. To account for this, the gross erosion is partitioned into bedload and suspended sediment load. The following description from Haan (1978), distinguishes between the two phenomena, "Sediment is detached as either primary particles (i.e. sands, silts and clays) or as aggregates. Aggregates are simply large numbers of particles bound together by a cementing agent such as organic matter or iron compounds. Soils eroded as aggregates are transported primarily as bedload, that is material that slides along the surface. Soil eroded as primary particles can be transported both as bed material or as suspended load while larger particles are transported as bedload." In the erosion model gross bedload and suspended sediment erosion are calculated and compared to calculated bedload and suspended sediment load capacities and the lesser value in each case is used as the sediment load.

Wherever possible, soil- and vegetation-related variables were treated as functions of more basic variables, to reduce the number of inputs as well as account for potential dependencies among variables.

FIGURE 3.11

DISSOLVED LEAD CONCENTRATIONS
(SCENARIO I)

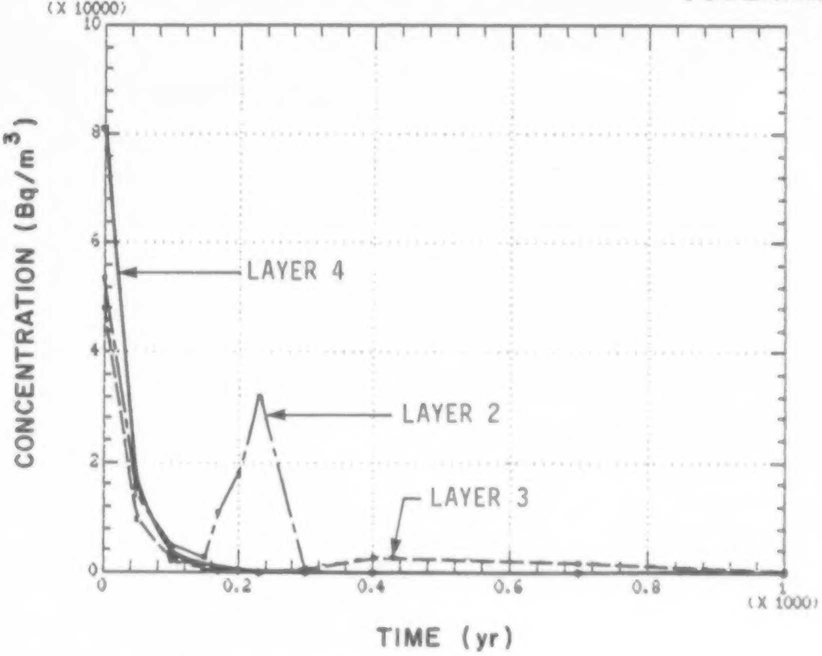

A) DETERMINISTIC RESULTS

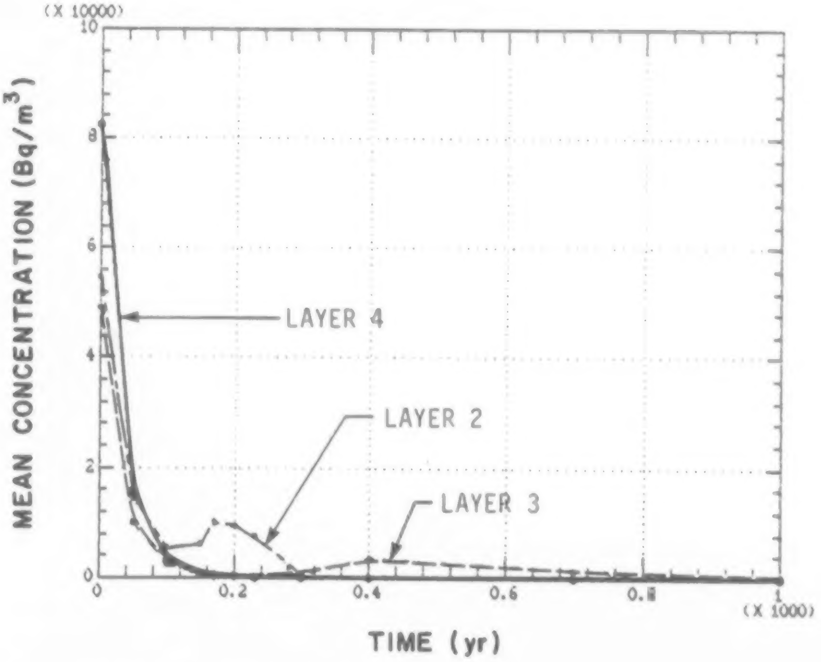

B) PROBABILISTIC RESULTS (30 TRIALS)

A simple exponential tailings revegetation model is also described in this section. This model postulates revegetation as a function of pH in the surface layer of the tailings.

### 3.14.2 The Universal Soil Loss Equation

There are two major approaches to determine erosion rates from disturbed land surfaces. The simplest approach is the use of mathematical models based on regression equations. The Universal Soil Loss Equation is the principal example of this type of model. The other approach involves the use of analytical or physical process models that explicitly account for the physical phenomena involved in soil erosion. While analytical models are desirable from the theoretical point of view, in the face of simulating such a complex process as soil erosion and sediment yield over long periods of time, regression models are preferable.

The Universal Soil Loss Equation (USLE) is the most widely used regression model for predicting soil erosion. It is an empirical formula for predicting soil loss as a result of sheet and rill erosion. The USLE was developed at the National Runoff and Soil Loss Data Centre established in 1954 by the Agricultural Research Service in cooperation with Purdue University (Wischmeier and Smith, 1978). Research projects at 49 locations contributed more than 10,000 plot-years of basic runoff and soil loss data for the study. The original equation was developed to predict losses on slopes up to 400 feet long. The basic formulation of the USLE is:

$$A = R\ K\ LS\ C\ P \qquad (3.14.1)$$

where

$A$ = average annual soil loss (tons/acre/year)
$R$ = rainfall erosivity factor
$K$ = soil erodibility factor (tons/acre per unit of rainfall factor, R)
$LS$ = topographic factor

$C$ = cropping management factor
$P$ = erosion control practice factor

Imperial units are used in the USLE.

Since the tailings pile has a slope considerably larger than 400 feet, a modified version of the USLE has been adopted (Foster and Wischmeier, 1974). The tailings pile has been considered as a series of slope segments of less than 400 feet in length. The following modification of the USLE may then be used to predict the sediment detached in each segment (Haan, 1978):

$$D_j = 0.0459\ R\ K_j\ CP_j\ S_j\ (\lambda_j^{m+1} - \lambda_{j-1}^{m+1})/72.6^m \qquad (3.14.2)$$

where

$D_j$ = soil detached in slope segment j (lb/ft width/year)
$R$ = rainfall erosivity factor
$CP_j$ = control practice factor
$S_j$ = slope factor for $j^{th}$ segment

$$S_j = \frac{0.43 + 30\ x_j + 430\ x_j^2}{6.613} \qquad (3.14.3)$$

$x$ = $\sin\theta$
$\theta$ = slope angle
$\lambda_j$ = slope length from top of slope to bottom of $j^{th}$ segment (<400')
$m$ = exponent dependent upon slope
  $m$ = 0.2 for slopes <1 percent
  $m$ = 0.3 for slopes of 1 to 3 percent
$K_j$ = soil erodibility factor for $j^{th}$ segment

and

$$100K = 2.1\ M^{1.14}\ (10^{-4})\ (12-a) + 3.25\ (b-2) + 2.5\ (c-3) \qquad (3.14.4)$$

$M$ = (% silt) x (100 - % clay) (clay content is assumed to be zero in tailings)
$a$ = percent organic matter (assumed to zero for exposed tailings solids)

b = soil structure code used in soil classification (i.e. 2 for tailings)

c = soil permeability class

From an analysis of "Rainfall Erosion Indices for Canada East of the Rocky Mountains" by Wall, Dickinson and Greuel (1983) the "R" values for the Ontario North of Superior region range from 65 to 97.5. These values incorporate estimates of both rainfall and snowmelt erosivity and are assumed to be uniformly distributed.

The control practice factor ($CP_j$) is, according to Haan (1978), composed of three factors:

$$CP = C_s\, C_r\, C_o \qquad (3.14.5)$$

where

$C_s$ = control factor due to surface stabilizing or protection treatments or vegetation ($C_s = 1$ for bare, untreated soil)

$C_r$ = control factor due to runoff-reduction practices such as diversion berms, interceptor dikes, benches and terraces and sectional drawdowns, and

$C_o$ = control factor due to other practices not included herein

We will only treat $C_s$ in this development with $C_r$ and $C_o$ being set to 1. This overestimates soil erosion if these other control factors are, in fact, functioning. Haan has presented $C_s$ as a decaying exponential function of mulch rate. Haan has related data for $C_s$ for grass-like plants to the fraction of the surface vegetated ($F_v$). These data have been fitted to an exponential model, with the following result (see Figure 3.12):

$$C_s = \exp\,[-0.109 - 0.056\ F_v] \qquad (3.14.6)$$

$$C_s = 1 \text{ if } F_v = 0$$

Haan used $C_s = 0.45$ for $F_v = 0$. This assumption has been replaced in this development with $C_s = 1$ at $F_v = 0$. This assumption is consistent with the basic definition of control practice factor, due to vegetation which is "the ratio of soil loss from land cropped under specified conditions to the corresponding soil loss from clean-tilled, continuous fallow ground" (Walters, 1985). The derivation of a relationship for the fraction of revegetated tailings is discussed in the next section.

### 3.14.3 Tailings Vegetation

Tailings re-vegetation is a complex problem. The following discussion of the tailings vegetation growth environment was excerpted from MacLaren, (1978).

> **"Elliot Lake uranium tailings are a most inhospitable medium for growth. The characteristics that make tailings difficult to vegetate are: the presence of acid and metals, deficiency in nutrients, physical characteristics such as their unconsolidated nature and extremes of moisture, and topography (prone to flooding, etc.).**
>
> **The presence of pyrite and the absence of sufficient alkalinity leads to acid generation and heavy metal solubilization. Highly acid soils are generally unacceptable to plants because the acid solutions increase the availability and concentration of metal ions present in the tailings material. In general, a pH range of 5 to 7 is required for good plant growth with the lower limit being about pH 4.**
>
> **Aside from pH, plants also require a balanced intake of macronutrients (nitrogen, phosphorus and potassium) and micronutrients (iron, manganese, copper, magnesium, zinc and others). Tailings deposits are usually devoid of macronutrients.**
>
> **Only minute quantities of micronutrients are required for plant**

FIGURE 3.12

## CONTROL FACTOR AS A FUNCTION OF FRACTION OF TAILINGS VEGETATED

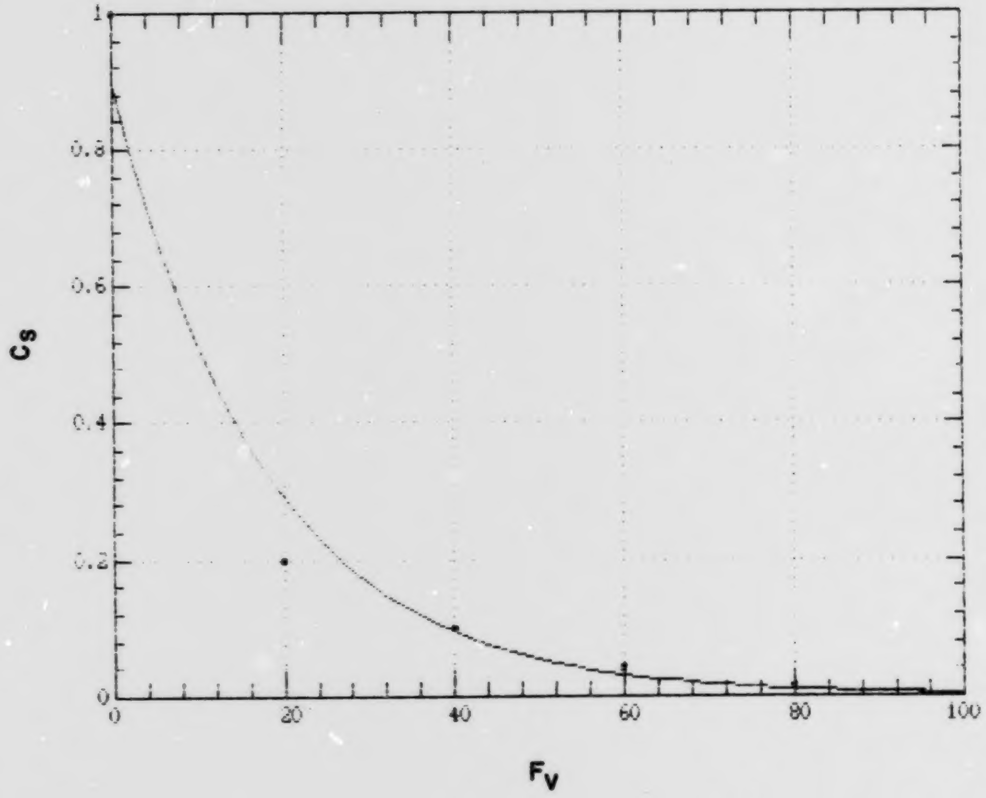

> growth; any excess may prove to be toxic. Tailings frequently contain metallic micronutrients in amounts sufficient to inhibit or kill plant growth....
>
> The topography of the tailings areas is also important.... Flat tailings surfaces are frequently subject to ponding and wind erosion. The excessive moisture associated with ponding causes plant mortality, and the windblown fines can cause abrasion sufficient to kill young plants.
>
> Tailings are frequently light in colour. As a result, there is excessive reflection of solar rays. This causes young plants and seedlings to dry out and/or be burned, thus adding an additional factor which must be overcome for a successful vegetation programme."

In spite of these difficulties, both natural and man-assisted vegetation occurs on tailings piles.

In the face of such complexities, it was decided to use a simplified approach to tailings re-vegetation. When the pH of the tailings surface layer is below 4.0, it has been assumed that no re-vegetation would occur. When the pH is greater than 4.0, the following exponential growth relationship has been adopted (SENES, 1985b):

$$F_V = 1 - \exp(\lambda_T \times ((T-T_V) + \frac{\Delta T}{2})) \qquad (3.14.7)$$

If $F_V \geq 0.9$ then $F_V = 0.9$

where

$F_V$ = fraction of tailings pile that is vegetated
$\lambda_T$ = ln $2/T_H$
$T_H$ = re-vegetation half-life

$T$ = time

$T_v$ = time at which pH rises above 4.0

$\Delta T$ = time increment used in model

Once pH in the first layer has risen above 4.0, revegetation will likely take place fairly quickly (i.e. a revegetation half-life from 10 to 20 years). Since the revegetation half-life is short, relative to the time increment, the $\Delta T/2$ term is used to "average" $F_v$ to the middle of the time increment.

This simple re-vegetation relationship is quite powerful. If the user wishes to "implement" a re-vegetation strategy, an integral part of this could be a pH increase through lime application. The pH dependence of the re-vegetation relationship allows growth to begin as soon as the pH is greater than 4.0. If fertilizing, seeding or other practice methods are to be simulated, the re-vegetation half-life can be reduced.

### 3.14.4 Tailings Geometry

To simplify the computational process, the following assumptions have been made regarding the tailings geometry. The tailings pile has been assumed to have a constant slope and to be square. Hence the length of the sides are the square root of the tailings area. Since the maximum slope segment allowable is 400 ft or less, the tailings pile has been subdivided into the smallest integer number (N) of slope segments possible, of length less than 400 ft. For example, if the area of the tailings pile were 50 ha or 500,000 $m^2$, the number of segments (N) would be:

$$L = (500{,}000)^{0.5} = 707 \text{ m} = 2320 \text{ ft}$$

where

$L$ = tailings pile length (ft)

$N' = 2320/400 = 5.8$

therefore $N = 6$

### 3.14.5 Deposition and Transport

As indicated in the introduction, the USLE only accounts for erosion, and does not account for significant amounts of deposition. Hence the USLE tends to overestimate erosion losses. Two transport mechanisms are developed in the following pages to help account for deposition. These mechanisms are bedload transport capacity and suspended sediment transport capacity. Haan (1978) from work of Neibling and Foster (1977) has proposed to analyze suspended load and bedload separately. These two transport mechanisms are discussed in the following two sections.

#### Bedload Transport

The bedload model uses the USLE rainfall erosivity factor (R) to predict the bedload transport capacity of a soil using the following equation:

$$T_c = r\ R\ T\ \lambda^2\ (x)^B\ C_{ro}\ C_T \qquad (3.14.8)$$

$T_c$ = bedload transport capacity (lb/ft-width/year)
$r$ = proportionality constant which relates the product of runoff volume and peak discharge to rainfall erosivity (ranges from $1\times10^{-8}$ to $1.0\times10^{-7}$ (Haan, 1978))
$T$ = transportability of the soil particles
$\lambda$ = slope length
$x$ = sine of slope angle
$B$ = empirical exponent which is a function of particle size
$C_{ro}$ = runoff reduction factor
$C_T$ = transportability reduction factor (given as a function of the ratio of velocity with respect to that of bare soil)

Soil transportability has been graphed as a function of particle diameter in Haan (1978). The following functional relationship has been derived from the graph:

$$T = 5.87 \times 10^5 D_{50}^{0.197} \qquad (3.14.9)$$

where

$D_{50}$ = particle diameter size exceeded by 50% of the tailings.

The "fit" was good, with a correlation coefficient of 0.94.

Figure 3.13 shows a grain size distribution for uranium tailings. From the eleven grain size analyses used to generate Figure 3.13, the following relationship between $D_{50}$ and percent silt has been established:

$$D_{50} = -1.99 \times 10^{-3} \text{ \% silt} + 0.215 \qquad (3.14.10)$$

where the correlation coefficient equalled -0.99.

It was assumed that all particles less than 0.06 mm were silt (i.e. no clay fraction), hence from Figure 3.13, silt ranges from 10 to 90 percent.

Since percent silt is required to estimate soil erodibility (equation 3.14.3), the $D_{50}$ - percent silt relationship is both convenient, because it reduces the number of inputs, and accurate, since it accounts for a dependency.

The factor B has also been fitted as a function of $D_{50}$, using graphical information from Haan. These data were fitted over two ranges.

$$B=1.83\, D_{50}^{\;0.049} \qquad 0.02 \leq D_{50} < 0.045\text{mm(correl.coeff.=0.98)}$$
$$B = -0.714\, D_{50} + 1.61 \qquad 0.045 \leq D_{50} \leq 0.2 \text{ mm (correl.coeff.=0.99)}$$
$$(3.14.11)$$

Haan (1978) related the runoff reduction factor $C_{ro}$ to vegetation and tillage practices, with a range of values from 1.4 (untilled packed construction site) to 0.1 (sod, grass, hay). This range has been assumed to be linearly related to percent vegetation with the following relationship:

FIGURE 3.13

## TYPICAL RANGE OF GRAIN SIZE DISTRIBUTION FOR ACID GENERATING TAILINGS

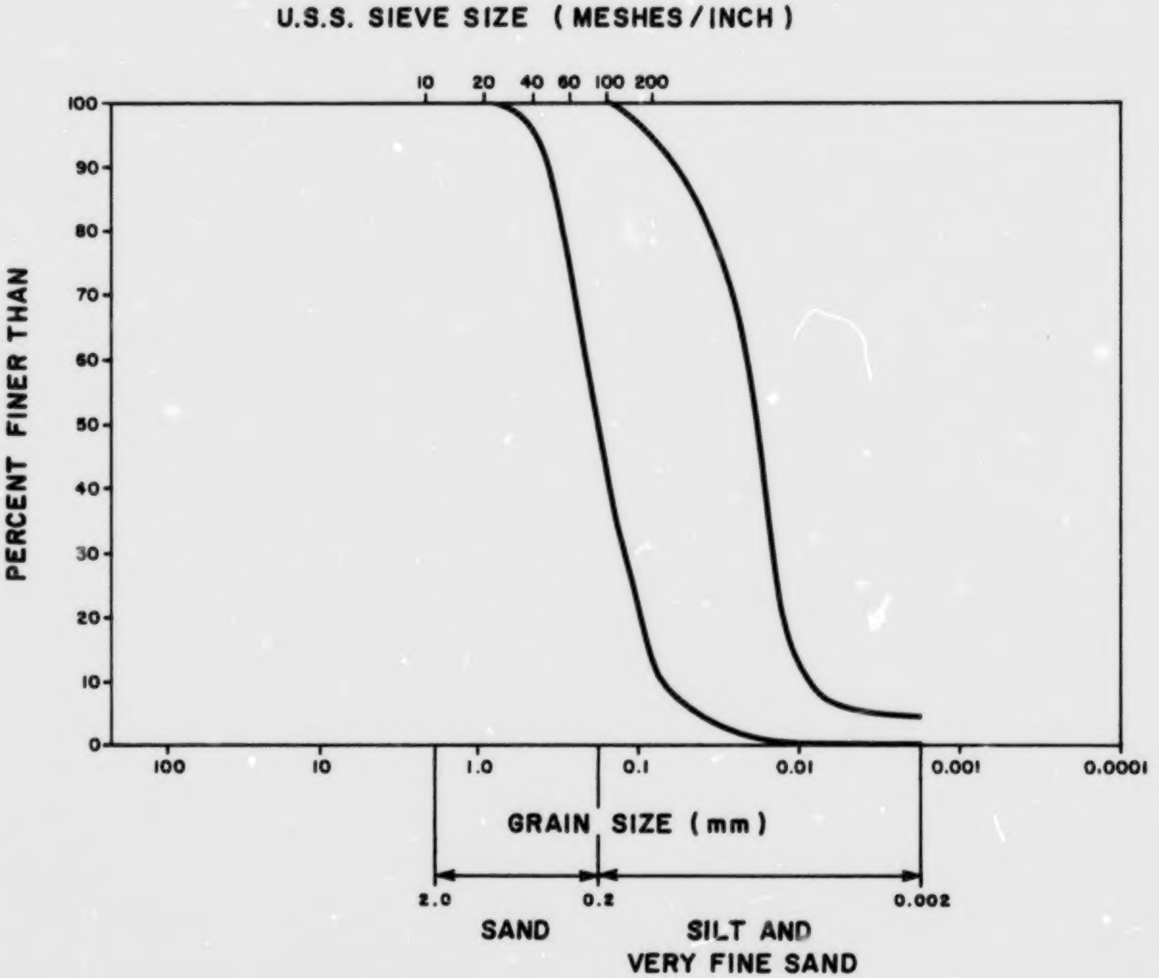

SOURCE:

$$C_{ro} = -1.44\ F_v + 1.4 \qquad (3.14.12)$$

$$\text{i.e } C_{ro} = 1.4 \text{ at } F_v = 0$$

$$C_{ro} = 0.1 \text{ at } F_v = 0.9$$

Haan also presented a series of curves that specified relative transport capacity ($C_T$) as a function of velocity ratio for several slopes. He related velocity ratio to amount of grass as follows:

| Amount of Grass | Velocity Ratio |
|---|---|
| None | 1.0 |
| Poor | 0.8 |
| Good | 0.5 |
| Very Dense | 0.3 |

The author of this paper assumed that velocity ratio ($V_R$) was linearly related to percent vegetation as follows:

$$V_R = -0.77\ F_v + 1.0 \qquad (3.14.13)$$

$$\text{i.e. } V_R = 1 \text{ at } F_v = 0$$

$$V_R = 0.3 \text{ at } F_v = 0.9$$

The $C_T$ vs $V_R$ relationships from Haan for slopes of 0.5, 1 and 2 percent and medium runoff rates, have been fitted with the following results:

$$\begin{array}{lll} C_T = 1.08\ V_R^{6.7} & S_o \leq 0.75 & \text{(correl.coeff. = 0.99)} \\ C_T = 1.12\ V_R^{9.27} & 0.75 < S_o \leq 1.5 & \text{(correl.coeff. = 0.99)} \\ C_T = 1.14\ V_R^{18.98} & 1.5 < S_o \leq 2.5 & \text{(correl.coeff. = 0.99)} \end{array} \qquad (3.14.14)$$

where

$S_o$ = percent slope

## Suspended Sediment Transport

According to Haan (1978) the amount of suspended sediment deposited in a vegetated area increases exponentially with distance travelled. It has been conservatively assumed for modelling purposes that no suspended sediment is trapped when the soil is bare. The fraction of sediment trapped by simulated vegetation has been predicted by (Haan, 1978) to be:

$$T_r = \exp\left(-1.05 \times 10^{-3}\right) \left[\frac{VR_s}{\nu}\right]^{0.82} \left[\frac{LV_s}{Vd_f}\right]^{-0.91} \qquad (3.14.15)$$

where

$V$ = the flow velocity through the grass (ft/sec)

$d_f$ = depth of flow (ft),for average annual erosion use a two year return period peak discharge flowing over the area and the estimated flow velocity above

$\nu$ = the kinematic viscosity ($10^{-5}$ ft$^2$/sec)

$R_s$ = spacing hydraulic radius given by : $R_s = \dfrac{d_f\ S_s}{2d_f + S_s}$

$S_s$ = average spacing of grass (ft)

$L$ = length of flow path through grassed area (ft) = $\lambda_j$ (segment length)

$V_s$ = settling velocity of the silt and/or clay size particles (ft/sec)

According to Haan, the settling velocity of silt and clay size particles can be estimated from Stokes' Law as:

$$V_s = \frac{2}{9}\ \frac{gd^2}{\nu}\ (SG-1) \qquad (3.14.16)$$

where

$g$ = gravitational constant 32.2 (ft/sec$^2$)

$d$ = particle diameter (ft)

$SG$ = specific gravity ( 2.65)

Haan (1978) graphed flow velocity as a function of slope for a variety of roughness factors. The straight line graphical data have been reduced to a linear relationship for nearly bare and untilled soil and short grass pasture. These two relationships are shown below:

$$V = \exp(-0.394 + 0.276 S_0) \text{ (nearly bare and untilled soil)} \quad (3.14.17)$$

$$V = \exp(-0.905 + 0.503 S_0) \text{ (short grass pasture)} \quad (3.14.18)$$

When the tailings are unvegetated ($F_v = 0$) the first equation prevails; when $F_v > 0$, the second equation should be used.

According to Haan (1978) the average spacing of grass ranges from 1.7 cm (sparse) to 0.75 cm (dense). These limits have been assumed to be linearly related to the fraction of vegetated surface ($F_v$) as follows:

$$S_s = -0.034\, F_v + 0.056 \quad (3.14.19)$$

where $S_s$ is in feet.

### 3.14.6 Computational Approach

Haan has suggested the following computational process to determine sediment load from an area. "The slope must be divided into segments and the transport capacity and total sediment available for transport calculated at the end of each segment. The lesser of the two is taken as the sediment exiting the segment. The sediment available for transport at the bottom of any segment, is equal to that entering the segment plus that detached in any segment." Gross erosion is partitioned into suspended sediment and bedload by assuming the silt fraction to be suspended and the remainder to be bedload, or:

$$E_{Sj} = \%\ \text{silt}/100 \times D_j \quad (3.14.20)$$

$$E_{Bj} = D_j - E_{Sj}$$

where:

$E_{Sj}$ = sediment load

$E_{Bj}$ = bedload

The process is described in Figure 3.14, adapted from Haan (1978).

### 3.14.7 Tailings Depletion and River Lake System Loading

The total sediment mass ($T_m$) leaving the tailings pile in the simulation time increment $\Delta t$ is:

$$T_m = \frac{L(E_s + E_B)\Delta t}{2.2} \qquad (3.14.21)$$

where

$T_m$ = total sediment mass leaving last segment (kg)
$L$ = tailings pile length (ft)
$E_s$ = suspended sediment load leaving last segment (lb/ft-width/yr)
$E_B$ = bedload exiting last segment (lb/ft-width/yr)

$E_s$ and $E_B$ are solved for using the computational method shown in Figure 3.14.

The depletion of the tailing pile in the time increment is:

$$D_T = \frac{T_m\ 1000}{\rho\ A_T} \qquad (3.14.22)$$

where

$D_T$ = depletion of tailings pile (m)
$\rho$ = tailings density ($g/m^3$)
$A_T$ = tailings area ($m^2$)

The total sediment leaving the tailings pile has been assumed to be instantaneously deposited in the first segment of the river/lake system at the beginning of the next time increment. A fraction of the activity in the sediment is assumed to instantly dissolve in the river/lake segment. The

FIGURE 3.14

## FLOWSHEET OF COMPUTATIONAL APPROACH

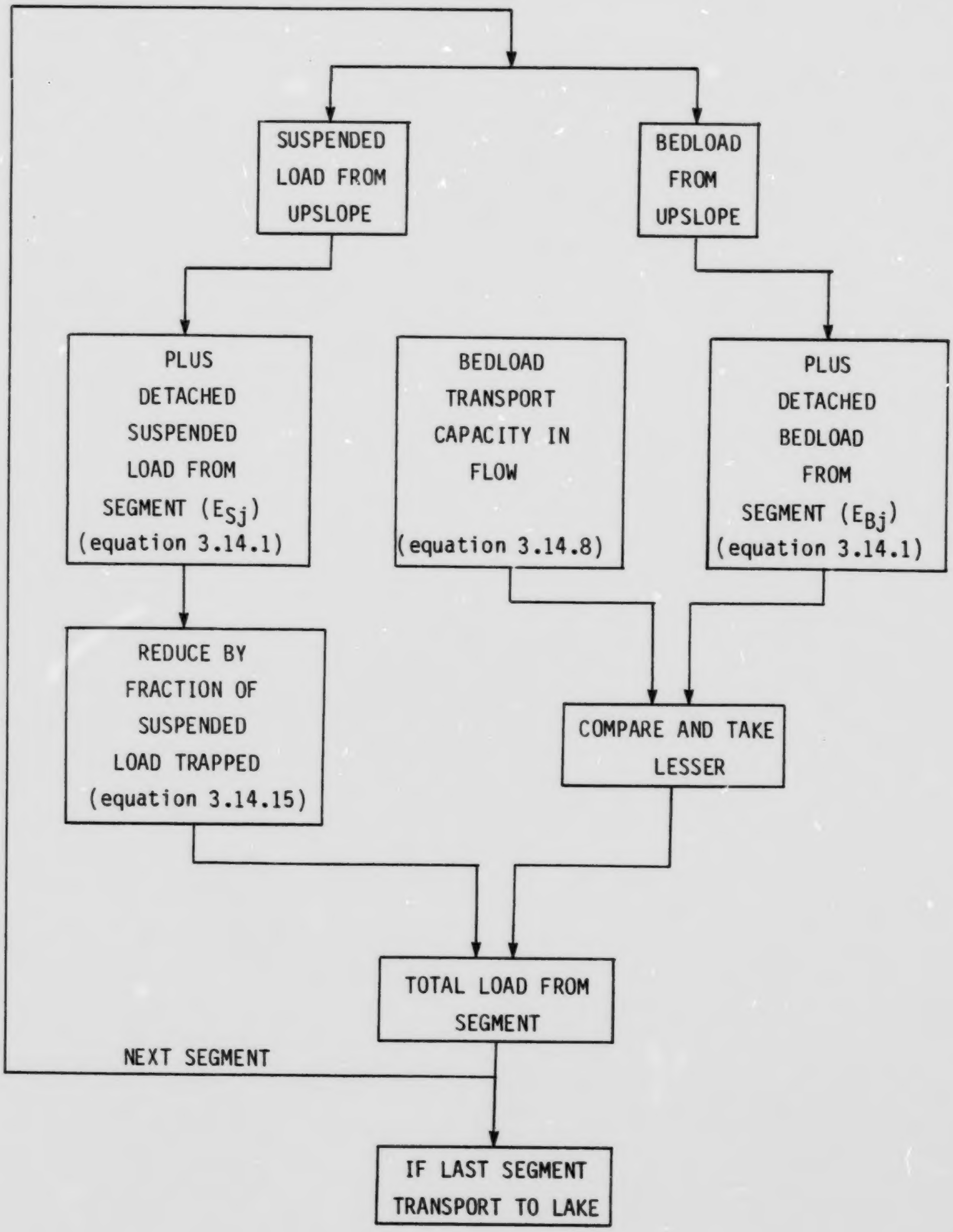
SUSPENDED LOAD FROM UPSLOPE
BEDLOAD FROM UPSLOPE
PLUS DETACHED SUSPENDED LOAD FROM SEGMENT ($E_{Sj}$) (equation 3.14.1)
BEDLOAD TRANSPORT CAPACITY IN FLOW (equation 3.14.8)
PLUS DETACHED BEDLOAD FROM SEGMENT ($E_{Bj}$) (equation 3.14.1)
REDUCE BY FRACTION OF SUSPENDED LOAD TRAPPED (equation 3.14.15)
COMPARE AND TAKE LESSER
TOTAL LOAD FROM SEGMENT
NEXT SEGMENT
IF LAST SEGMENT TRANSPORT TO LAKE

**SOURCE: HAAN, 1978**

balance of the activity remains bonded to the sediment, settles, and becomes part of the bottom sediments of the river/lake segment. The radionuclide concentration of the eroded material is the surface tailings concentration predicted in the tailings source model.

The source code and the variable dictionary for the soil model are shown in Table 3.5 and 3.6 respectively.

### 3.14.8 Erosion Model Test Program

A series of tests were performed to check the erosion model for accuracy and reasonableness. The erosion model writeup and code were reviewed by Dr. Trever Dickinson of the University of Guelph, a recognized soil erosion expert. Hand calculations were checked against a deterministic run to confirm that the code calculated the equations properly. The model was run probabilistically over time and space to determine that it performed accurately in these dimensions.

Finally the erosion model was run within the system model context. The median cumulative depletion of the tailings pile in metres and the pH of layer 1 are plotted against time in Figure 3.15 for 10, 500 year trials with a ten year time increment. The median for cumulative depletion is reasonable with a value of about 3.5 cm. Note how tailings depletion levels off once pH moves above 4.0 because of the reduction in erosion due to tailings revegetation.

FIGURE 3.15

CUMULATIVE TAILINGS DEPLETION AND pH vs. TIME

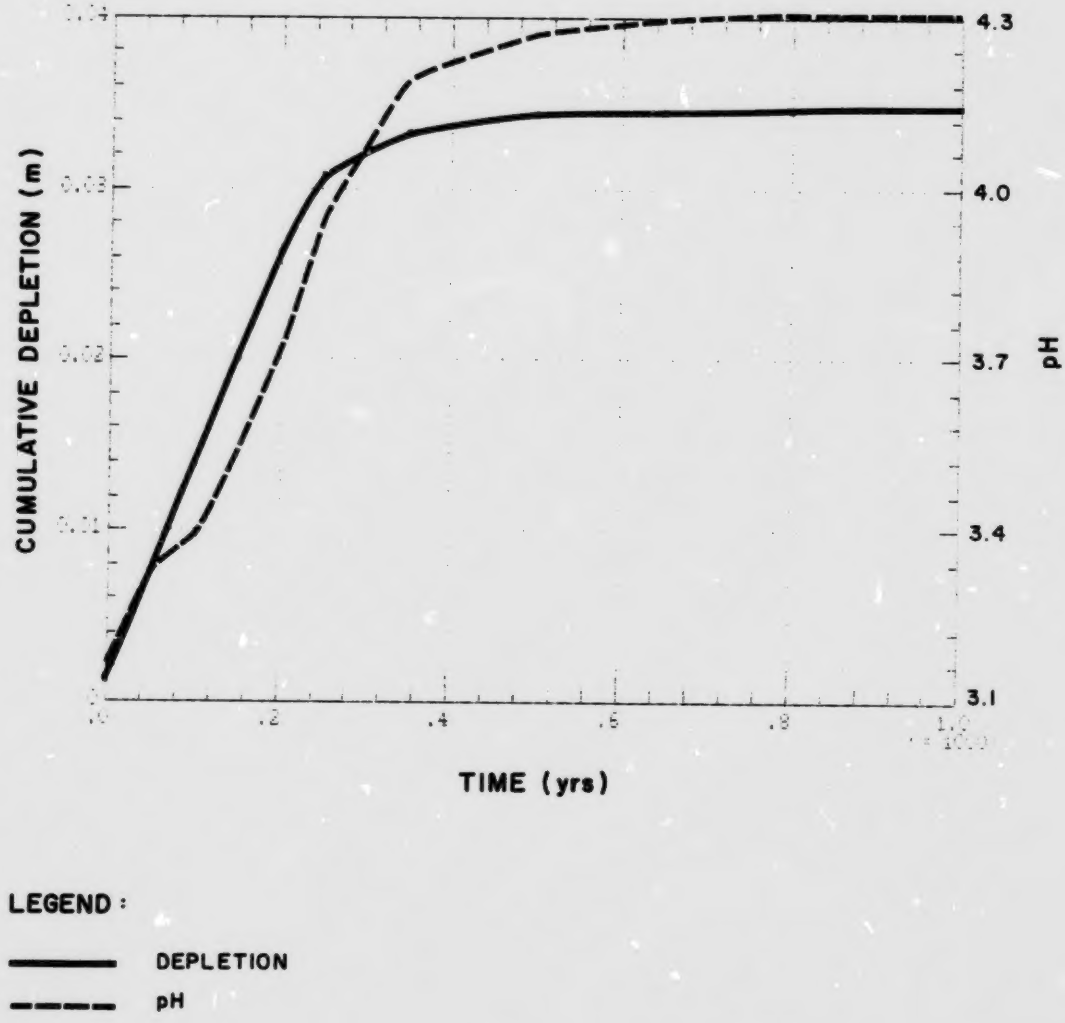

Table 3.5

## EROSION MODEL CODE LISTING

```
C
      SUBROUTINE EROS
C     DEVELOPED BY DON BEALS MAR 1986
C     CCDED BY DON BEALS MAR 1986
      INCLUDE 'MODEL.INC'
      INCLUDE 'VAR.INC'
      IF(CODERO.GE.1.0)THEN
         WRITE(*,1008)
1008     FORMAT(1X,'SUBROUTINE EROS')
      ENDIF
C
      REAL*4 FVEG,CSOIL,VELRAT,CTSOIL,LENTOT,BED,ESOIL,TCSOIL
     &,BEDTEM,SUS,MSOIL,TRSED,SPACE,VS,RS,P1,P2,EROTOT
C
C  INITIALIZE PARAMETERS THAT STAY CONSTANT OVER ENTIRE SIMULATION
      IF(NUMTRL.EQ.1.0.AND.T.EQ.0.0)THEN
C
C     CALCULATE SEGMENT LENGTH AND NUMBER OF SEGMENTS
         LENGT=SQRT(ATAIL)/0.3048
         NLEN=INT(LENGT/400)+1
         LENGTH=LENGT/FLOAT(NLEN)
C
C     CALCULATE SLOPE FACTOR
         SPRIME=SIN(ATAN(SLOPE/100))
         SLPFAC=(0.43+30*SPRIME+430*SPRIME**2)/6.613
C
C     CALCULATE SLOPE LENGTH EXPONENT
         IF(SLOPE.LE.1.0)THEN
            MSLP=0.2
         ELSEIF(SLOPE.GT.1.0.AND.SLOPE.LE.3)THEN
            MSLP=0.3
         ENDIF
C
C     INITIALIZE EQUATIONS FOR SOIL ERODIBILITY EQUATION
         CSL=5.0
         PEROM=0.0
         BSOIL=2.0
C
         IF(CODERO.EQ.2.0)THEN
            WRITE(*,1000)LENGT,NLEN,LENGTH,SLOPE,ATAIL,MSLP
1000        FORMAT(1X,'LENGT=',E10.3,1X,'NLEN=',E10.3,1X,
     &      'LENGTH=',E10.3,1X,'SLOPE=',E10.3,1X,'ATAIL=',E10.3,
     &      1X,'MSLP=',E10.3)
            WRITE(*,1004)SLPFAC,SPRIME
1004        FORMAT(1X,'SLPFAC=',E10.3,1X,'SPRIME=',E10.3)
         ENDIF
C
      ENDIF
C
C  INITIALIZE PARAMETERS THAT STAY CONSTANT FOR A GIVEN TRIAL
```

Table 3.5 (continued)

```
      IF (T.EQ.0.0)THEN
C
C     INITIALIZE TAILINGS DEPLETION
         DTAIL=0.0
C     SOLVE FOR SOIL ERODIBILITY(K)
         MSOIL=SILT*100.0
         KSOIL=((2.1*(MSOIL**1.14)*1E-4*(12-PEROM))+
     &   ((3.25*(BSOIL-2.0))+(2.5*(CSL-3))))/100.0
C
C     SOLVE FOR D50 AND PARAMETERS FUNCTIONALLY RELATED TO D50
         D50=-1.99E-3*SILT+0.215
         TSOIL=5.87E5*D50**0.197
         IF(D50.GE.0.02.AND.D50.LT.0.045)THEN
            BEXP=1.83*D50**0.049
         ELSEIF(D50.GE.0.045.AND.D50.LE.0.15)THEN
            BEXP=-0.714*D50+1.61
         ENDIF
C   FLAG TVEG
         TVEG=-1.0
C
         IF(CODERO.EQ.2.0)THEN
            WRITE(*,1002)KSOIL,D50,TSOIL,BEXP,SILT,RSOIL,THALF
1002        FORMAT(1X,'KSOIL=',E10.3,1X,'D50=',E10.3,1X,'TSOIL=',
     &      E10.3,1X,'BEXP='E10.3,1X,'SILT',E10.3,1X,'RSOIL=',
     &      E10.3,1X,'THALF=',E10.3)
         ENDIF
C
      ENDIF
C
C     SOLVE FOR FRACTION OF TAILINGS THAT ARE VEGETATED
      IF(PH(1).LE.4.0)THEN
         FVEG=0.0
         CSOIL=1.0
      ELSE
         IF(TVEG.EQ.-1.0)TVEG=T
         FVEG=1-EXP(((-.693)*((T-TVEG)+(DT/2)))/THALF)
         IF(FVEG.GE.0.9)FVEG=0.9
         CSOIL=EXP(-0.109-(0.056*FVEG))
      ENDIF
C
C     SOLVE FOR AREA OF EXPOSED TAILINGS FOR USE IN DUST MODEL
      AEXPT=ATAIL*(1.0-FVEG)
C
C     SOLVE FOR VELOCITY RATIO
      VELRAT=-.77*FVEG+1.0
C
C     SOLVE FOR TRANSPORTABILITY REDUCTION FACTOR FOR THREE SLOPE RANGES
      IF(SLOPE.LE.0.75)THEN
         CTSOIL=1.08*VELRAT**6.7
      ELSEIF(SLOPE.GT.0.75.AND.SLOPE.LE.1.5)THEN
         CTSOIL=1.12*VELRAT**9.27
      ELSEIF(SLOPE.GT.1.5.AND.SLOPE.LE.2.5)THEN
         CTSOIL=1.14*VELRAT**18.98
```

Table 3.5 (continued)

```
      ENDIF
C
C     SOLVE FOR RUNOFF REDUCTION FACTOR
      CRO=-1.44*FVEG+1.4
C
      IF(CODERO.EQ.2.0)THEN
         WRITE(*,1003)FVEG,CSOIL,VELRAT,CTSOIL,CRO,RRAIN,PH(1)
1003     FORMAT(1X,'FVEG='E10.3,1X,'CSOIL=',E10.3,1X,'VELRAT=',E10.3,
     &   1X,'CTSOIL='E10.3,1X,'CRO='E10.3,1X,'RRAIN='E10.3,1X,
     &   'PH(1)',E10.3)
      ENDIF
C
C     SOLVE FOR BEDLOAD TRANSPORT CAPABILITY
      TCSOIL=RSOIL*RRAIN*TSOIL*(LENGTH**2.0)*(SPRIME**BEXP)*CRO
     &*CTSOIL
C  SOLVE FOR SUSPENDED SEDIMENT TRANSPORT CAPABILITY
C  NOTE THAT THERE IS NO SEDIMENT TRAPPING IF FVEG=0
      IF(FVEG.EQ.0.0)THEN
         TRSED=0.0
C     SOLVE FOR BARE SOIL VELOCITY
         VEL=EXP(-0.394+0.276*SLOPE)
      ELSE
C     SOLVE FOR VEGETATED SOIL VELOCITY
         VEL=EXP(-0.905+0.503*SLOPE)
C     SOLVE FOR DEPTH OF FLOW
         DF=STORM/VEL
C     CONVERT SILT DIAMETER FROM MM TO FT
         DMID=DM/304.8
C
C     SOLVE FOR SPACING BETWEEN GRASS AS A FUNCTION OF FVEG
         SPACE=(-.034)*FVEG+0.056
C
C     SOLVE FOR SETTLING VELOCITY USING STOKES LAW
         VS=2*((32.2*(DMID**2)*1.65)/(9*1E-5))
C
C     SOLVE FOR SPACING HYDRAULIC RADIUS
         RS=(DF*SPACE)/(2*(DF+SPACE))
C
         P1=(VEL*RS)/1E-5
         P2=(LENGTH*VS)/(VEL*DF)
C
C     SOLVE FOR FRACTION OF SUSPENDED SEDIMENT TRAPPED
         TRSED=EXP((-1.05E-3)*(P1**.82)*(P2**(-.91)))
C
         IF(CODERO.EQ.2.0)THEN
            WRITE(*,1005)SPACE,VS,RS,P1,P2,STORM,VEL,DMID
1005        FORMAT(1X,'SPACE=',E10.3,1X,'VS='
     &      ,E10.3,1X,'RS=',E10.3,1X,'P1=',E10.3,1X,'P2=',
     &      E10.3,1X,'STORM=',E10.3,1X,'VEL=',E10.3,'DMID=',E10.3)
         ENDIF
C
      ENDIF
         IF(CODERO.EQ.2.0)THEN
```

Table 3.5 (continued)

```
            WRITE(*,1006)TCSOIL,TRSED
1006        FORMAT(1X,'TCSOIL=',E10.3,1X,'TRSED=',E10.3)
         ENDIF
C
C   INITIALIZE PARAMETERS
      LENTOT=0.0
      BED=0.0
      SUS=0.0
C
C   CALCULATE EROSION AND TRANSPORT FOR EACH SEGMENT
      DO 10 I=1,NLEN
         LENTOT=LENTOT+LENGTH
C     CALCULATE GROSS EROSION
         ESOIL=(0.0459*RRAIN*KSOIL*CSOIL*SLPFAC*((LENTOT**(MSLP+1.0))
     &   -((LENTOT-LENGTH)**(MSLP+1.0)))/(72.6**MSLP))
C
C     CALCULATE BEDLOAD FROM GROSS EROSION
         BEDTEM=ESOIL-(ESOIL*(SILT/100))
C
C     ESTIMATE TOTAL BEDLOAD
         BED=BED+BEDTEM
C
C     CALCULATE SUSPENDED SEDIMENT LOAD
         SUS=(1-TRSED)*(SUS+ESOIL-BEDTEM)
C
C     CHECK IF ESTIMATED BEDLOAD EXCEEDS BEDLOAD TRANSPORT CAPACITY
         IF(BED.GE.TCSOIL) BED=TCSOIL
C
         IF(CODERO.EQ.2.0)THEN
            WRITE(*,1001)ESOIL,BEDTEM,BED,SUS
1001        FORMAT(1X,'ESOIL=',E10.3,'BEDTEM=',E10.3
     &      ,1X,'BED=',E10.3,1X,'SUS='E10.3)
         ENDIF
10    CONTINUE
C   CALCULATE TOTAL SEDIMENT TRANSPORT IN KG
      EROTOT=(((BED+SUS)*LENGTH)*DT)/2.2
C
C   CALCULATE TAILINGS DEPLETION
      DTAIL=DTAIL+((EROTOT*1000)/(RHOTAL*ATAIL))
C
      IF(CODERO.EQ.2.0)THEN
         WRITE(*,1007)EROTOT,DTAIL
1007     FORMAT(1X,'TOTAL EROSION=',E10.3,1X,'DTAIL=',E10.3)
      ENDIF
      RETURN
      END
```

Table 3.6

## EROSION MODEL VARIABLES

| Model Symbol | Description | Units | Nominal Value | Probability Distribution* | Computer Origin | Computer Symbol |
|---|---|---|---|---|---|---|
| $A_T$ | surface area of the tailings of the tailings | $m^2$ | $5x10^5$ | $C(5x10^5)$ | INPUT | ATAIL |
| $E_B$ | total bedload | $lbs.ft^{-1}(width).yr^{-1}$ | calculated | calculated | EROS | BED |
| B | exponent in bedload equation | - | calculated | calculated | EROS | BEXP |
| b | soil structure code used in soil classification | - | specified in code | specified in code | EROS | BSOIL |
| $C_{ro}$ | runoff reduction factor | - | calculated | calculated | EROS | CRO |
| c | soil permeability class | - | specified in code | specified in code | EROS | CSL |
| $CP_j$ | cropping practice factor for USLE | - | calculated | calculated | EROS | CSOIL |
| $C_T$ | transportability reduction factor in bedload equation | - | calculated | calculated | EROS | CTSOIL |
| $D_{50}$ | tailings particles size diameter exceeded 50% of time | - | calculated | calculated | EROS | D50 |
| $d_f$ | depth of flow in suspended sediment equation | ft | calculated | calculated | EROS | DF |
| d | mean silt diameter | ft | calculated | calculated | EROS | DMID |
| $D_T$ | cumulative erosion of tailings pile | m | calculated | calculated | EROS | DTAIL |
| $T_m$ | total sediment mass at last segment | kg | calculated | calculated | EROS | EROTOT |
| $D_j$ | soil detached in slope of jth segment | $lb.ft^{-1}(width).yr^{-1}$ | calculated | calculated | EROS | ESOIL |
| $F_v$ | fraction of tailings covered by vegetation | - | calculated | calculated | EROS | FVEG |
| $K_j$ | soil erodibility factor | - | calculated | calculated | EROS | KSOIL |
| L | length of tailings pile | ft | calculated | calculated | EROS | LENGT |
| $\lambda_j$ | length of slope of jth segment | ft | calculated | calculated | EROS | LENGTH |
| m | slope exponent for USLE | - | calculated | calculated | EROS | MSLP |
| M | parameter in soil erodibility equation | - | calculated | calculated | EROS | MSOIL |

Table 3.6, cont'd. Page 2

| Model Symbol | Description | Units | Nominal Value | Probability Distribution* | Computer Origin | Computer Symbol |
|---|---|---|---|---|---|---|
| a | percent organic matter of tailings | - | specified in code | specified in code | EROS | PEROM |
| R | rainfall erosivity factor | - | 81.3 | U(65,97.5) | INPUT | RRAIN |
| $\rho$ | tailings bulk density | $g.m^{-3}$ | $1.4x10^6$ | $N(1.4x10^6, 0.1x10^6, 1.1x10^6, 1.7x10^6)$ | INPUT | RHOTAL |
| $R_s$ | spacing hydraulic radius | ft | calculated | calculated | EROS | RS |
| r | proportionality constant for bedload transport equation | - | $5.5x10^{-8}$ | $U(1x10^{-8},1x10^{-7})$ | INPUT | RSOIL |
| % | Silt  percent silt | - | 45 | T(10,45,90) | INPUT | SILT |
| $S_o$ | overall percent slope of tailings pile | - | 1.0 | C(1.0) | INPUT | SLOPE |
| $S_j$ | slope factor for jth segment | - | calculated | calculated | EROS | SLPFAC |
| $S_s$ | spacing between grass | ft | calculated | calculated | EROS | SPACE |
| $x$ | sine of slope angle | - | calculated | calculated | EROS | SPRIME |
| $E_s$ | suspended sediment load | $lbs.ft^{-1}(width).yr^{-1}$ | calculated | calculated | EROS | SUS |
| $T_c$ | bedload transport capacity | $lbs.ft^{-1}(width).yr^{-1}$ | calculated | calculated | EROS | TCSOIL |
| $T_H$ | revegetation half-life | yr | 15 | U(10,20) | INPUT | THALF |
| $T_r$ | fraction of suspended sediment trapped | - | calculated | calculated | EROS | TRSED |
| T | transportability of soil particles in bedload transport | - | calculated | calculated | EROS | TSOIL |
| $T_v$ | time at which vegetative growth commences (pH>4) | yr | calculated | calculated | EROS | TVEG |
| V | flow velocity through grass | $ft.s^{-1}$ | calculated | calculated | EROS | VEL |
| $V_R$ | velocity ratio used in bedload transport equation | - | calculated | calculated | EROS | VELRAT |
| $V_s$ | settling velocity from Stokes Law | $ft.s^{-1}$ | calculated | calculated | EROS | VS |

Note

* Distributions are as described on Table 2.2.

## 3.15 REFERENCES

Beak Consultants Ltd., 1985. "The Geochemical Mechanism Controlling Ra-226 Dissolution in Uranium Mill Wastes (Tailings)." Research Report prepared for the National Uranium Tailings Program, CANMET, EMR, under Supply and Services Canada Contract No. 15SQ.23241-4-1678.

Berner, R.A., and Holdren, G.R., 1979. "Mechanism of Feldspar Weathering, II, Observation of Feldspars in Soils." Geochim. Cosmochim. Acta. Vol. 43, pp. 1173-1186.

Evans, R.D., 1955. "The Atomic Nucleus." McGraw-Hill Book Company Inc.

Faust, S.D., and Aly, O.M., 1981. "Chemistry of Natural Waters." Ann Arbor Science Publishers, Inc., Ann Arbor, Michigan.

Foster, G.R., and Wischmeier, W.H., 1974. "Evaluating Irregular Slopes for Soil Loss Prediction." Trans. Am. Soc. Agr. Eng. 17: 305-309.

Golder Associates, SENES Consultants Limited, Beak Consultants Limited, and Cumming-Cockburn and Associates Limited, 1986. "Lacnor Field Study; The Results of a One Year Field Monitoring Program." Prepared for the National Uranium Tailings Program, CANMET, EMR, under Supply and Services Canada Contract No. 15SQ.23241-4-1680.

Gresens, R.L., 1981. "The Aqueous Solubility Product of Solid Solutions." Chem. Geol., Vol. 32, pp. 73-86.

Halbert, B.E., Scharer, J.M., Knapp, R.A., and Gorber, D.M., 1983. "Determination of Acid Generation Rates in Pyritic Mine Tailings." Presented at the 56th Annual Conference of the Water Pollution Control Federation, Atlanta, Georgia, October 2-7.

Haan, Barfield, 1978. "Hydrology and Sedimentology of Surface Mined Lands." Office of Continuing Education and Extension, College of Engineering University of Kentucky, Lexington, Kentucky.

Helgeson, H.C., Murphy, W.M., and Aagaard, P., 1984. "Thermodynamic and Kinetic Constraints on Reaction Rates Among Minerals and Aqueous Solutions, II, Rate Constants, Effective Surface Area, and the Hydrolysis of Feldspar." Geochim. Cosmochim. Acta. Vol. 48, pp. 2405-2432.

Langmuir, D. and Herman, J.S., 1980. "The Mobility of Thorium in Natural Waters at Low Temperatures." Geochim. Cosmochim. Acta., Vol. 42, pp. 547-569.

MacLaren Ltd., James F., 1977. "Environmental Assessment of the Proposed Elliot Lake Uranium Mines Expansion. Volume 1." Report to Denison Mines Limited and Rio Algom Limited, Elliot Lake, Ontario.

MacLaren, James. F., Ltd., 1978. "Environmental Assessment of the Proposed Elliot Lake Uranium Mines Expansion. Volume 4, Environmental Assessment." Prepared for Denison Mines Limited and Rio Algom Limited, Elliot Lake, Ontario.

Morin, K.A., Cherry, J.A., Lim, T.P. and Vivyurka, A.J., 1982. "Contaminant Migration in a Sand Aquifer Near an Inactive Uranium Tailings Impoundment." Elliot Lake, Ontario, Canadian Geotechnology Journal, Vol. 19, pp. 49-62.

Myerson, A.S., 1981. "Oxygen Mass Transfer Requirements During the Growth of Thiobacillus Ferrooxidans on Iron Pyrite." Biotechnology and Bioengineering, Vol. 23, pp. 1413-1416.

National Research Council (NRC), 1983. "Radioactivity in the Canadian Aquatic Environment." Pub. No. NRCC 19250.

Neibling, W.H., and Foster, G.R., 1977. "Estimating Deposition and Sediment Yield from Overland Flow Processes." Proc. Int. Symp. on Urban Hydrology, Hydraulics, and Sediment Control, UK BU 114, College of Engineering, University of Kentucky, Lexington, Kentucky.

Nordstrom, D.K., 1982. "Aqueous Pyrite Oxidation and the Consequent Formation of Secondary Iron Minerals." In Acid Sulphate Weathering, Soil Science Society of America, pp. 37-55.

Rancon, D., 1973. "The Behaviour in Underground Environments of Uranium and Thorium Discharged by the Nuclear Industry." In: Environmental Behaviour of Radionuclides Released in the Nuclear Industry, International Atomic Energy Agency Report, IAEA-SM-172/55.

SENES Consultants Limited, 1981. "Quirke Lake Tailings Disposal Study: Stage 1. Background Information (Draft)." A Research Report prepared for Rio Algom Ltd. and Denison Mines Limited, Elliot Lake, Ontario.

SENES Consultants Limited, 1983. "Acid Generation Tests on Pyritic and Depyritized Tailings With and Without Limestone Addition." Research Report prepared for Denison Mines Limited., Elliot Lake, Ontario.

SENES Consultants Limited, 1984. "A Study to Develop and Demonstrate Techniques for the Probabilistic Assessment of the Long-Term Effects of Uranium Mill Tailings in Canada - Phase I." Research Report prepared for the National Uranium Tailings Program, CANMET, EMR, under Supply and Services Canada Contract No. 0SQ83-00236.

SENES Consultants Limited, 1985. "A Study to Develop and Demonstrate Techniques for the Probabilistic Assessment of the Long-Term Effects of Uranium Mill Tailings in Canada - Phase II." Research Report prepared for the National Uranium Tailings Program, CANMET, EMR, under Supply and Services Canada Contract No. 0SQ84-00207.

SENES Consultants Limited, 1985b. "The Approaches to Risk Assessment for Canadian Uranium Mill Tailings." Research Report Prepared for the National Uranium Tailings Program under Supply and Services Canada Contract Δ14 SQ.23241-4-1695.

Sillen, L.G. and Martell, A.E., 1971. "Stability Constants." Special Publication No. 25, The Chemical Society, London, U.K.

Silver, M., and Ritcey, G.M., 1980. "A Simulated Study on the Effects of Bacteria, Organics and Salt Solutions on Uranium Mill Tailings from Elliot Lake, Ontario." Project MRP-4.3.0.6.02, CANMET, Ottawa.

Skeaff, J.M., 1977. "Distribution of Radium-226 in Uranium Tailings." CANMET Report MRP/MSL 77-349 (J), Ottawa.

Stumm, W. and Morgan, J.J., 1981. "Aquatic Chemistry." John Wiley and Sons, New York, NY.

Veska, E., 1983. "Origin and Subsurface Migration of Radionuclides from Waste Rock at an Abandoned Uranium Mine Near Bancroft, Ontario." Unpublished Ph.D. Thesis, University of Waterloo.

Wall, G.J., Dickinson, W.T., and Greuel, J., 1983. "Canadian Journal of Soil Science." Vol. 63, pp. 271-280.

Walters, W.H., 1985. "Computational Methods for Estimating Overland Erosion of Uranium Tailings." Nuclear Safety, Vol. 26, No.2 .

Wischmeier, W.H. and Smith, D.D., 1978. "Predicting Rainfall Erosion Losses: A Guide to Conservation Planning. Agri. Handbook Δ537 Science and Education Administration. U.S. DOA.

## 4.0 AIR SOURCE MODEL

### 4.1 Radon Source Term

The model used in the Phase II study (SENES, 1985) to simulate the release of radon from the tailings surface was chosen because of its adaptability to the tailings model derived for the water source term. As described in Chapter 3, the tailings are modelled as a multi-layered system: an upper, unsaturated layer in which the radium concentration is a function of depth, and a lower, saturated layer. The saturated and unsaturated layers are subdivided into various zones in the water source term model.

The saturated layer is not a source of radon that can reach the tailings surface since the water effectively prevents its diffusion; the diffusive transport distance of radon in the water-filled pores of the tailings is orders of magnitude less than the diffusive transport distance in the unsaturated pores. The unsaturated layer can be subdivided into two zones as described in the water source model: an upper, barium sulphate ($BaSO_4$) - depleted zone (with a reduced radium content) and a lower, barium sulphate-enriched zone (with an enriched radium content). The depth of the interface of the two zones depends on the chemistry of the tailings. The depth changes with time (over tens of years) until the entire unsaturated layer is depleted of barium sulphate.

In terms of radon release to the atmosphere, each of these zones can be considered to be homogeneous, with each zone characterized by an average radium concentration, moisture content, porosity, density and radon emanation coefficient. This model for radon release is equivalent to a covered tailings model in which the tailings are of finite thickness and the cover also contains radium i.e. the "cover" is the upper zone and the "tailings" are the lower zone. The theoretical development of such a model has been carried out by Rogers et al. (1980). The model accounts for the unique definitions of both the tailings and cover in terms of parameters that affect radon release such as radium concentration and radon diffusion length and thus it can be used to model the total radon release from both zones of the unsaturated layer.

Denoting the upper zone of the unsaturated layer as zone 1 of thickness $x_1$, and the lower zone of the unsaturated layer as zone 2 of thickness $x_2$, the general formula for the radon flux at the surface of the tailings is (following Rogers et al., 1980, Chapter 4, Equation 14):

$$J = \frac{-D_1a_1}{\cosh(a_1x_1)}\left[\frac{[1+Z\coth(a_2x_2)](C_o-s_1/a_1^2)\exp(a_1x_1)+(s_1/a_1^2-s_2/a_2^2)}{\tanh(a_1x_1)+Z\coth(a_2x_2)}\right]$$

$$+ \quad D_1a_1\,(C_o - s_1/a_1^2) \qquad (4.1)$$

where

$J$ = radon flux ($Bq.m^{-2}.s^{-1}$)

$D_i$ = radon diffusion coefficient ($m^2.s^{-1}$)

$C_o$ = radon concentration above the tailings surface (considered constant) ($Bq.m^{-3}$)

$a_i = \sqrt{\frac{\lambda\epsilon_i}{D_i}}$ = 1/(radon diffusion length $L_i$)($m^{-1}$)

$Z = \frac{D_1a_1}{D_2a_2}$

$s_i = \frac{(Ra)_i\,\rho_i\,\lambda E_i}{D_i}$

$(Ra)_i$ = tailings radium concentration ($Bq.g^{-1}$)

$\rho_i$ = tailings density ($g.m^{-3}$)

$E_i$ = emanation coefficient ($0 \leq E \leq 1$, dimensionless)

$\lambda$ = radon decay constant ($2.1\times10^{-6}\ s^{-1}$)

$L_i$ = radon diffusion length in tailings (m)

$\epsilon_i$ = porosity (dimensionless)

where subscript i = 1 or 2 refers to zone 1 or 2, respectively. The product of (Ra) and $\rho$ is sometimes given only by one parameter when (Ra) is measured in units of $Bq.m^{-3}$.

As noted earlier, the depth of the barium sulphate depleted zone increases with time until the entire unsaturated layer is depleted. At this time, the tailings can be modelled as having "no cover", that is, a barium sulphate depleted zone only. Equation (4.1) then becomes:

$$J = (Ra)_1 E_1 \rho_1 \sqrt{\frac{\lambda D_1}{\epsilon_1}} \tanh\left[\sqrt{\frac{\lambda \epsilon_1}{D_1}}\ x_1\right] \qquad (4.2)$$

Equation (4.2) assumes Co=0. This is a good approximation since Co is orders of magnitude less than the radon concentration within the tailings. Equation (4.2) is used when the thickness of the lower zone is less than $1.0 \times 10^{-3}$m. Otherwise, equation (4.1) is used.

Equation (4.2), which is essentially the product of the radon source strength within the tailings ($Bq.m^{-3}.s^{-1}$) and the diffusion length of radon (m), is identical to the equation that is often used to estimate radon release rates from bare, thick tailings (e.g. U.S. NRC, 1980). This equation was used in the Phase I study (SENES, 1984).

The radon diffusion coefficient is highly dependent on tailings moisture content. As noted in the Phase I and Phase II studies, Rogers et al. (1980), suggest an empirical relationship of the form:

$$D = 0.106 \times 10^{-4} \times \epsilon \times \exp(-0.261 \times M) \quad (m^2 \cdot s^{-1}) \qquad (4.3)$$

where

$$M = \text{percent moisture content of tailings by weight} = 100 \times \frac{\text{weight of water in tailings}}{\text{weight of wet tailings}}$$

Since equation (4.3) is used for this study, the radon flux given by equation (4.1) is not explicitly dependent on the porosity $\epsilon$. The flux is implicitly dependent on porosity because of the empirical constants in equation (4.3).

For site-specific evaluations for which more data are available, more recent research suggests that a different form of equation (4.3) can be used (Rogers et al., 1984).

The emanation coefficient E can also depend on the moisture content, especially at low ($\leq$5%) moisture levels (Strong and Levins, 1982). However, for the Canadian environment the moisture content is generally greater than 5% and parameterization of the effects of moisture beyond equation (4.3) was not considered necessary for this study.

The generality of equation (4.1) can accommodate completely different characteristics for each zone. For the present modelling exercise, only the thickness and radium concentration of each zone differ. The moisture and porosity, and hence the radon diffusion coefficient, of each zone are assumed to be identical. Under these conditions ($Z=1$, $a_1 = a_2 = a$ and setting $C_0=0$), equation (4.1) reduces to:

$$J = - \frac{D}{a \cosh(ax_1)} \left[ \frac{-[1 + \coth(ax_2)] s_1 \exp(ax_1) + s_1 - s_2}{\tanh(ax_1) + \coth(ax_2)} \right] - \frac{Ds_1}{a} \qquad (4.4)$$

Equation (4.4) can be used to estimate the radon flux from tailings under normal conditions. However, freezing conditions and snow cover greatly attenuate the radon flux because of the much smaller radon diffusion coefficient of ice relative to water. The effect is dependent on the moisture content of the tailings. The ratios of the radon fluxes from unfrozen and frozen tailings samples as measured by Zettwoog et al. (1981) were 3, 100 and 400 for tailings moisture contents of <10%, 30% and saturation, respectively. This effect can be accommodated in the radon source model by using a seasonally-weighted average for radon flux and a winter/summer flux ratio. The annual average flux $J_{avg}$ is then given by:

$$J_{avg} = J(N_wR + (12-N_w))/12 \qquad (4.5)$$

where

$N_w$ = number of winter months (freezing conditions) per year
R = frozen/unfrozen flux ratio
= 0.02 nominally (Zettwoog et al., 1981)

Since both the radon flux and meteorological conditions are seasonal, a more detailed model could estimate radon concentrations on a seasonal (or even monthly) basis. However, for this study, the approximation engendered by the use of annual averages for both the source term and meteorological conditions is considered acceptable.

$J_{avg}$ is the annual average radon flux in units of $Bq.m^{-2}.s^{-1}$. To obtain the total flux $J_T$ for the tailings area, this must be multiplied by the surface area A(t). In contrast to the dust source model which accommodates the effect of tailings vegetation on dust emissions (Section 4.2), the radon source model assumes that vegetation does not affect radon release rates. No conclusive research data are available to quantify the effects of vegetation on radon releases but measurements on Elliot Lake tailings suggest that vegetation does not significantly affect radon release (DSMA ATCON, 1985). Thus, the surface area is considered a constant ($A_0$) for estimating radon release and

$$J_T = J_{avg}A_0 \qquad (4.6)$$

Since the zone thicknesses and radium concentrations in the water source model are time-dependent, the average radon flux $J_{avg}$ and annual radon release $J_T$ are also time-dependent.

The variables used to calculate the radon source term are listed in Table 4.1. All the numerical values, with the exception of the emanation coefficient E and the winter/ summer flux ratio R, are as used in the water source model (Chapter 3). The distribution suggested for R is based on the measurements of Zettwoog et al. (1981). The nominal value of 0.2 for the emanation coefficient E has often been used to model radon emissions from tailings areas (e.g. U.S. NRC, 1980). The suggested range for E is based on data in Strong and Levins (1982) and U.S. NRC (1980). The triangular distribution for E gives the highest probability to values around 0.2 while accommodating the possibility of some higher values, such as those measured for uranium ores (Austin and Droullard, 1978).

The radon source model was used to investigate the incorporation of parameter correlations. The results are documented in Appendix I of Volume 2 of this report. The computer code listing for the radon source model is given in Table 4.2.

## 4.2 Dust Source Term

The empirical dust source model used in this assessment was developed by the Colorado Department of Health based on experimental work carried out at mining operations in the western United States (CDOH 1984). Detailed studies of dust dispersion from tailings in climates similar to those that occur in the Canadian Shield have not been identified. This model will have to be reviewed on a periodic basis and updated in the future to reflect the results of further research in this area.

The emission rate of the ith radionuclide from the tailings surface at a specific moment in time t can be expressed as:

$$Q_i = 2.2 \times 10^{-6} \left[\frac{S}{1.5}\right]\left[\frac{365-P_a}{235}\right]\left[\frac{f}{0.15}\right]\left[\frac{C_i}{\rho}\right] A \qquad (4.7)$$

where

$Q_i = Q_i(t)$ = emission rate of the ith radionuclide at time t ($Bq.s^{-1}$)

$S$ = silt content (%)

$P_a$ = annual number of days with more than 0.25 mm of precipitation

$f$ = frequency of the time wind speed at the mean tailings pile height exceeds 5.4 $m.s^{-1}$.

Table 4.1

## RADON SOURCE MODEL VARIABLES

| Model Symbol | Description | Units | Nominal Value | Probability* Distribution | Computer Origin | Computer Symbol |
|---|---|---|---|---|---|---|
| a | reciprocal of radon diffusion length in tailings | $m^{-1}$ | calculated | calculated | RADON | DIFLEN |
| D | effective bulk radon diffusion coefficient of tailings | $m^2.s^{-1}$ | calculated | calculated | RADON | EBKDFC |
| E | radon emanation coefficient of tailings | - | 0.2 | T(0.02, 0.2, 0.9) | INPUT | EMANAT |
| $J_T(t)$ | total radon flux | $Bq.s^{-1}$ | calculated | calculated | RADON | EMRATE(5) |
| R | winter/summer flux ratio | - | 0.02 | LN(0.02,2.0, 0.002,0.2) | INPUT | WTSFLX |
| M | moisture content by weight of tailings | % | 15.0 | T(5.0,15.0,25.0) | INPUT | MPCH2O |
| $\epsilon$ | porosity of tailings | - | 0.4 | T(0.35, 0.4, 0.45) | INPUT | POROS |
| $(Ra)_i(t)$ | radium concentration of zone i = 1 or 2 | $Bq.m^{-3}$ | calculated | initialized then calculated | SOURCE | CONC(4,i,3) i=1,2 |
| $x_1(t)$ | thickness of $BaSO_4$ depleted zone | m | calculated | calculated | SOURCE | DBAR(3) |
| $x_2(t)$ | thickness of $BaSO_4$ enriched zone | m | calculated | calculated | RADON | EBAR(3) |
| $\lambda$ | radon decay constant | $s^{-1}$ | $2.1 \times 10^{-6}$ | defined | RADON | RNLAN |
| $A_0$ | surface area of the tailings | $m^2$ | $5.0 \times 10^5$ | C $(5.0 \times 10^5)$ | INPUT | ATAIL |
| $N_w$ | number of winter months (freezing conditions) per year | months | 5.0 | C (5.0) | INPUT | NSUBW |
| $x_s(t)$ | thickness of unsaturated layer | m | 1.0 | U (0.5,1.0) | INPUT | DUNSAT |

* Distributions are as described in Table 2.2.

Table 4.2

## RADON MODEL CODE LISTING

```
      SUBROUTINE RADON
      INCLUDE 'MODEL.INC'
      INCLUDE 'VAR.INC'
      REAL*4 EBAR(3)
      RNLAN=2.1E-6
      EBKDFC=0.106E-4*POROS*EXP(-0.261*MPCH2O)
      DIFLEN=SQRT(RNLAN*POROS/EBKDFC)
      CONST1=RNLAN*EMANAT/(EBKDFC*DIFLEN*DIFLEN)
      CONST2=EBKDFC*DIFLEN*ATAIL
      CONST3=EMANAT*RNLAN*ATAIL/DIFLEN
      CONST4=(NSUBW*WTSFLX+12.0-NSUBW)/12.0
      EBAR(3)=DUNSAT-DBAR(3)
      IF(EBAR(3).LT.1.0E-3)THEN
         EBAR(3)=0.0
         DBAR(3)=DUNSAT
      ENDIF
      X1=DIFLEN*DBAR(3)
      IF(EBAR(3).GT.0.0)THEN
         X2=DIFLEN*EBAR(3)
         XDEN=COSH(X1)*(TANH(X1)+1.0/TANH(X2))
         XNUM=((1.0+1.0/TANH(X2))*CONST1*CONC(4,1,3)*EXP(X1)
     +        -CONST1*(CONC(4,1,3)-CONC(4,2,3)))
         EMRATE(5)=CONST2*CONST4*(XNUM/XDEN-CONST1*CONC(4,1,3))
      ELSE
         EMRATE(5)=CONST3*CONST4*TANH(X1)*CONC(4,1,3)
      ENDIF
C
      IF(CODRAD.EQ.1.0.OR.CODRAD.EQ.2.0.OR.CODRAD.EQ.3.0)THEN
         WRITE(*,100)
      ENDIF
      IF(CODRAD.EQ.3.0)THEN
         WRITE(*,101)POROS,MPCH2O,RNLAN,EMANAT,ATAIL,EBKDFC,DIFLEN,
     +               NSUBW,WTSFLX,DUNSAT,DBAR(3),CONC(4,1,3)
         IF(EBAR(3).GT.0.0)THEN
            WRITE(*,102)EBAR(3),CONC(4,2,3)
         ENDIF
      ENDIF
      IF(CODRAD.EQ.2.0.OR.CODRAD.EQ.3.0)THEN
         WRITE(*,103)EMRATE(5)
      ENDIF
C
100   FORMAT(///1X,'RADON SOURCE MODEL')
101   FORMAT(/1X,'POROSITY OF TAILINGS',E12.4/1X,'MOISTURE CONTENT OF ',
     +       'TAILINGS',E12.4/1X,'RADON DECAY CONSTANT',E12.4/1X,'RADO',
     +       'N EMANATION CONSTANT',E12.4/1X,'SURFACE AREA OF TAILINGS',
     +       E12.4/1X,'RADON DIFFUSION CONSTANT',E12.4/1X,'RECIPROCAL ',
     +       'OF RADON DIFFUSION LENGTH',E12.4/1X,'NUMBER OF WINTER MO',
     +       'NTHS PER YEAR',E12.4/1X,'WINTER/SUMMER FLUX RATIO',E12.4/
     +       1X,'THICKNESS OF UNSATURATED LAYER',E12.4/1X,'THICKNESS O',
     +       'F BaSO4 DEPLETED ZONE',E12.4/1X,'RADIUM CONCENTRATION IN',
```

Table 4.2 (continued)

```
     +       ' BaSO4 DEPLETED ZONE',E12.4)
102   FORMAT(1X,'THICKNESS OF BaSO4 ENRICHED ZONE',E12.4/1X,'RADIUM ',
     +       'CONCENTRATION IN BaSO4 ENRICHED ZONE',E12.4)
103   FORMAT(/1X,'EMISSION RATE OF RADON',E12.4)
C
      RETURN
      END
```

$C_i = C_i(t) =$ concentration of the ith radionuclide at time t in the tailings surface layer (layer 1 as defined in Chapter 3) ($Bq.m^{-3}$)

$\rho =$ tailings bulk density ($g.m^{-3}$)

$A = A(t) =$ the exposed tailings surface area at time t ($m^2$)

The empirical constant in the equation (4.7) (i.e. $2.2 \times 10^{-6}$ $g.m^{-2}.s^{-1}$) was developed by the Colorado Department of Health as noted above.

The originators of this equation rate it as average-to-below-average in its accuracy of prediction, however, higher ratings are only given for models of well-controlled, consistent industrial sources.

The silt content (S), is determined by the proportion of material that passes through a 200 mesh screen. This parameter was described in more detail in the erosion model description (Section 3.14).

The frequency of the time (f) that the wind speed exceeds 5.4 $m.s^{-1}$ at the mean tailings height is calculated in the wind submodel from the Star Data (joint distribution of wind speed, wind direction and atmospheric stability) obtained from the Atmospheric Environment Service (AES) (refer to Section 5.2). The wind submodel is described in Chapter 5.

During the winter months frozen ground conditions and snow cover are assumed to reduce dust emissions to zero. This effect has been accommodated in the dust source model by using a seasonally-weighted average for the dust emission flux. The annual average dust emission rate is then given by:

$$Q_{iAVG} = Q_i\ (12 - N_w)/12 \qquad (4.8)$$

where

$N_w$ = number of winter months (freezing conditions) per year

Another meteorological parameter in equation (4.7) is the number of days on which there is measurable precipitation ($P_a$). Winter months are excluded from the derivation of this distribution since dust emissions are assumed to be zero in the winter months. The chosen distribution is normal with a mean of 123, standard deviation of 18 and a minimum and maximum of 84 and 156, respectively. These values were obtained from AES precipitation data from the Gore Bay Weather Station, on Manitoulin Island. The net result of these assumptions with regard to meteorological parameters is to spread summer precipitation out over the whole year. Ongoing research in this area may suggest improvements in model formulation or parameter selection.

Another consideration pertains to the time dependency of the emission rates of the various radionuclides. There are three factors that control the time-varying behaviour of these emission rates:

- The surficial concentration of the ith radionuclide ($C_i$) will vary as the compound is leached from the tailings surface.
- The effective exposed area of the tailings (A) will decrease with the natural or forced revegetation of the exposed surface.
- The intrinsic dust emission rate will decrease as the tailings surface weathers.

With time, the tailings surface area will be reduced by the encroachment of vegetation. This, as well as the changes in surficial radionuclide concentrations, are determined by the source term model. While a decrease in the intrinsic dust emission rate with time is expected (as might occur for example with the gradual loss of erodible particles), the process is not well understood at present, and is ignored in this study.

The variables used in the dust source term model are summarized in Table 4.3. The computer code listing for this model is provided in Table 4.4.

## Table 4.3

## DUST SOURCE MODEL VARIABLES

| Model Symbol | Description | Units | Nominal Value | Probability* Distribution | Computer Origin | Computer Symbol |
|---|---|---|---|---|---|---|
| $Q_{iAVG}(t)$ | emission rate of the ith radionuclide at time t | $Bq.s^{-1}$ | calculated | calculated | DUST | EMRATE (i) i=1,4 |
| S | silt content of the tailings (% of particles <75 μm) | % | 45.0 | T(10.0,45.0,90.0) | INPUT | SILT |
| $P_a$ | annual number of days with more than 0.25 mm of precipitation | days | 123.0 | N(123.0, 18.0, 84.0, 156.0) | INPUT | FPREC |
| f | frequency of the time that the wind speed exceeds 5.4 $m.s^{-1}$ at the mean tailings height | - | calculated | calculated | WIND | FWINDT |
| $C_i(t)$ | surficial concentration of ith compound at time t | $Bq.m^{-3}$ | calculated | calculated | SOURCE | CONC (i,1,2) i=i,4 |
| A(t) | exposed surface area of the tailings at time t | $m^2$ | calculated | calculated | SOURCE | AEXPT |
| $\rho$ | tailings bulk density | $g.m^{-3}$ | $1.4 \times 10^6$ | $N(1.4x10^6, 0.1x10^6$ $1.1x10^6, 1.7x10^6)$ | SOURCE | RHOTAL |
| $N_w$ | number of winter months (freezing conditions) per year | months | 5.0 | C (5.0) | INPUT | NSUBW |

* Distributions are as described in Table 2.2.

Table 4.4

## DUST MODEL CODE LISTING

```
      SUBROUTINE DUST
      INCLUDE 'MODEL.INC'
      INCLUDE 'VAR.INC'
      CONST5=(12.0-NSUBW)/12.0*2.2E-6*SILT/1.5*(365.0-FPREC)/235.0*
     +       FWINDT/0.15/RHOTAL*AEXPT
      DO 10 I=1,4
         EMRATE(I)=CONST5*CONC(I,1,3)
10    CONTINUE
C
      IF(CODDUS.EQ.1.0.OR.CODDUS.EQ.2.0.OR.CODDUS.EQ.3.0)THEN
         WRITE(*,100)
      ENDIF
      IF(CODDUS.EQ.3.0)THEN
         WRITE(*,101)SILT,FPREC,FWINDT,RHOTAL,AEXPT,NSUBW,CONC(1,1,3)
         DO 11 I=2,4
            WRITE(*,102)CONC(I,1,3)
11       CONTINUE
      ENDIF
      IF(CODDUS.EQ.2.0.OR.CODDUS.EQ.3.0)THEN
         WRITE(*,103)EMRATE(1)
         DO 12 I=2,4
            WRITE(*,104)EMRATE(I)
12       CONTINUE
      ENDIF
C
100   FORMAT(///1X,'DUST SOURCE MODEL')
101   FORMAT(/1X,'SILT CONTENT',E12.4/1X,'ANNUAL NUMBER OF DAYS WITH',
     +       ' MORE THAN 0.25mm OF PRECIPITATION',E12.4/1X,'TIME WIND',
     +       ' SPEED EXCEEDS 5.4 m/s',E12.4/1X,'TAILINGS BULK DENSITY',
     +      E12.4/1X,'EXPOSED SURFACE AREA OF TAILINGS',E12.4/1X,'NU',
     +       'MBER OF WINTER MONTHS PER YEAR',E12.4/1X,'RADIONUCLIDES',
     +       ' SURFICIAL CONCENTRATIONS',E12.4)
102   FORMAT(39X,3(E12.4))
103   FORMAT(/1X,'EMISSION RATE OF RADIONUCLIDES',E12.4)
104   FORMAT(31X,3(E12.4))
C
      RETURN
      END
```

## 4.3 References

Austin, S.R. and Droullard, R.F., 1978. "Radon Emanation from Domestic Uranium Ores Determined by Modifications of the Closed-Can, Gamma-Only Assay Method." U.S. Bureau of Mines, Report of Investigations 8264.

Colorado Department of Health (CDOH), 1984. "Fugitive Particulate Emissions." Internal Memo from T. Tistinic, Colorado Department of Health, July 2, 1984.

DSMA ATCON Limited, 1985. "A Study to Measure and Evaluate the Effect that Vegetation has on the Emanation Rate of Radon from a Uranium Tailings Pile." Research Report prepared for the National Uranium Tailings Program, CANMET, Energy, Mines and Resources Canada, DSS File No. 14SQ.23241-3-1659.

Rogers, V.C., Overmyer, R.F., Putzig, K.M., Jensen, C.M., Nielson, K.K., and Sermon, B.W., 1980. "Characterization of Uranium Tailings Cover Materials for Radon Flux Reduction." U.S. Nuclear Regulatory Commission NUREG/CR-1081, March.

Rogers, V.C., Nielson, K.K. and Kalkwarf, D.R., 1984. "Radon Attenuation Handbook for Uranium Mill Tailings Cover Design." U.S. Nuclear Regulatory Commission, NUREG/CR-3533, April.

SENES Consultants Limited, 1984. "A Study to Develop and Demonstrate Techniques for the Probabilistic Assessment of the Long-Term Effects of Uranium Mill Tailings in Canada - Phase I." Research Report prepared for the National Uranium Tailings Program, CANMET, Energy, Mines and Resources Canada.

SENES Consultants Limited, 1985. "Probabilistic Model Development for the Assessment of the Long-Term Effects of Uranium Mill Tailings in Canada - Phase II." Research Report prepared for the National Uranium Tailings Program, CANMET, Energy, Mines and Resources, Canada.

Strong, K.P. and Levins, D.M., 1982. "Effect of Moisture Content on Radon Emanation from Uranium Ore and Tailings." Health Physics, Vol. 42, pp. 27-32.

U.S. Nuclear Regulatory Commission (NRC), 1980. "Final Generic Environmental Impact Statement on Uranium Milling." NUREG-0706, September.

Zettwoog, P., Fourcade, N., Campbell, F. and Caplan, H.S., 1981. "The Effect of Freezing on the Emanation of Radon from Uranium Ore and Tailings." Health Physics, Vol 41, pp. 410-411.

## 5.0 AIR DISPERSION MODEL

In the Phase I and Phase II studies (SENES, 1984; SENES, 1985) the way in which atmospheric dispersion was modelled was predicated on the assumption of a single receptor at a specified location. As discussed in Chapter 2, one of the objectives of the Phase III study was to modify the approach to atmospheric dispersion to accomodate multiple receptors. In addition, the atmospheric dispersion model used in the Phase III studies has been modified to include a simple correction for the finite size (as opposed to a point source) of the tailings source. The essential characteristics of the atmospheric dispersion model used in Phase III studies are outlined below.

Data on wind statistics are required to evaluate both the dust source term (Section 4.2) and the atmospheric dispersion model (Section 5.1). The way in which wind data are modified for use in these models is also described in this chapter (Section 5.2).

### 5.1 Air Dispersion Component

### The Basic Model

The air dispersion equation used in Phase III is the same sector-averaged Gaussian plume model used in the previous Phase I and II studies. The formulation of the equation is:

$$C_{ai}(t) = \frac{2.032\ f_{K1}\ Q_i(t)}{\bar{u}\ \sigma_z\ (x+x_0)} \exp\left[\frac{-h^2}{2\ \sigma_z^2}\right] \qquad (5.1)$$

where

$C_{ai}$ = $C_{ai}(t)$ is the atmospheric concentration of the ith radionuclide at the receptor at time t ($Bq.m^{-3}$)

$f_{K1}$ = fraction of time the wind blows from the source to the receptor in one of 16 sectors (depends on sector K direction and stability class 1)

$Q_i$ = $Q_i(t)$ is the emission rate of the ith radionuclide at time t ($Bq.s^{-1}$)

$\bar{u}$ = mean wind speed from the source to the receptor ($m.s^{-1}$)

$x$ = downwind distance from the source to the receptor (m)

$x_0$ = virtual source set back distance (m)

$h$ = height of source (m)

$\sigma_z$ = vertical dispersion coefficient (m)

An effect sometimes included in air dispersion models, but left out in this case is that of limited vertical mixing. Exclusion of this effect has been shown to have little effect on long-term average concentrations (TCM, 1980).

Virtual Source Correction

A commonly used approximation has been used in Phase III to accomodate the fact that a tailings area is actually an area source rather than a point source. The concept is simply to treat the area source as a point source with an initial horizontal spread. In effect, the approach calculates a virtual distance ($x_0$) that produces the appropriate initial spread of the plume. In this study the virtual source set back distance is calculated by making several assumptions with regard to source geometry. The assumptions are:

- the model is sector averaged (i.e. crosswind concentrations are uniform across a sector)
- it is an "n" sector model (i.e. the compass is divided into n sectors of equal angular width)
- the tailings area is circular (for mathematical convenience)

At the setback distance $x_0$, the sector angle, $\theta$ ,(determined from the number of sectors to be $2\pi/n$) subtends an arc of length:

$$L = x_0 \theta = \frac{x_0 \, 2\pi}{n} \qquad (5.2)$$

If we assume that the arc length, L, is equal (or approximately equal) to the diameter, D, of a "circular" tailings area or the diameter of a circle with area equivalent to that of the actual tailings area (any shape), equation (5.2) can be rewritten as:

$$x_o = \frac{Dn}{2\pi} \tag{5.3}$$

When D is expressed as a function of the tailings' area ($A_o=\pi D^2/4$) then the expression for $x_o$ becomes:

$$x_o = \frac{n}{\pi}\sqrt{\frac{A_o}{\pi}} \tag{5.4}$$

which for a 16 sector model reduces to:

$$x_o = 2.87\sqrt{A_o} \tag{5.5}$$

where

$A_o$ = the surface area of the tailings ($m^2$)

The model parameters, their distributions, units and computer code names for the air dispersion model are given in Table 5.1

With only one receptor in the direction of the prevailing wind as in Phase II, only one set of atmospheric input parameters was required. The critical parameters required to make the above formulation work under the more general conditions in Phase III are f (a joint frequency distribution of direction, wind speed and atmospheric stability, which is processed in subroutine WIND to produce a 16 x 6 matrix of mean wind speed for each wind direction and atmospheric stability class), the vertical dispersion coefficient $\sigma_z$ (a function of direction and stability class) and $\bar{u}$ (a function of direction for each stability class).

The data used in the Phase III air dispersion model are derived from Atmospheric Environment Weather Service (AES) data as described in Section 5.2.

## Vertical Dispersion Coefficient

The vertical dispersion coefficient, $\sigma_z$, is calculated as a function of distance. The power law curves proposed are those suggested for use in long-term atmospheric dispersion models, such as the Climatological Dispersion Model (CDM, 1973), and the Texas Climatological Model (TCM, 1980) both of which have been used extensively in the United States and elsewhere for regulatory and assessment purposes (e.g. Hanna, 1982). The general form of the power law equation is:

$$\sigma_z(x) = a(x+x_0)^b \qquad (5.6)$$

where a and b are power law coefficients which are dependent on stability class, and $(x+x_0)$ is the total downwind distance, the source to receptor distance plus the virtual setback. Following the practice of the U.S. EPA (ISC, Vol. 1, 1979) if the calculated value of $\sigma_z$ exceeds 5000 m, $\sigma_z$ is set equal to 5000 m. The power law coefficients are shown in Table 5.2

A source height of about 2m has been assumed on the basis that air turbulence near the surface will result in at least some rapid initial upward mixing.

## Receptor Location

As is commonly done, the structure of the Phase III air dispersion model assumes that the wind data are resolved into 16 sectors each of angular width 22 1/2°. In addition, the user can specify up to 5 radial distances (or rings as shown in Figure 2.2) ranging from a minimum distance of 1 km to a maximum of 50 km from the centre of the tailings area. Thus, up to 80 air concentrations are available for use. A receptor located in a particular radial sector (i.e. in a particular 22 1/2° sector between two rings) is assigned the concentration predicted to occur at the centre of the radial sector, which is assumed to be representative of the entire radial sector.

### Area-Weighted Average Concentration

In addition, two special area-weighted average air concentrations are calculated, one for the entire area, and the other over the watershed area. These area-weighted average concentrations are calculated for use in the soil model and the terrestrial vegetation model. Specifically, the concentration inputs to soil and the terrestrial vegetation models are used to evaluate the radionuclide uptake of caribou (area average) and moose (watershed average) from terrestrial vegetation (see Chapters 6 and 8 respectively).

## 5.2 Subroutine WIND

As discussed in Section 5.1, in order to calculate the concentration of the radionuclides in the atmosphere after dispersion, relevant wind data is required. Specifically the fraction of time the wind blows in each of the 16 sectors for each stability category, the mean wind velocity in each sector for each stability category, as well as, the fraction of time the wind velocity exceeds 5.4 $m.s^{-1}$ in each sector, are required. To satisfy these requirements, annual AES wind and stability data (STAR data) from the Gore Bay weather station on Manitoulin Island, in Ontario, for a twenty year period was obtained.

The subroutine WIND calculates the desired data from the AES STAR data files as follows. The mean wind speed as a function of direction and stability class is calculated assuming the following central wind speed classes.

| Wind Speed Class | Speed Interval (knots) | Central Wind Speed ($m.s^{-1}$) |
|---|---|---|
| 1 | 0 to 3 | 1.50 |
| 2 | 4 to 6 | 2.46 |
| 3 | 7 to 10 | 4.47 |
| 4 | 11 to 16 | 6.93 |
| 5 | 17 to 21 | 9.61 |
| 6 | > 21 | 12.52 |

The lowest wind speed class was arbitrarily taken as 1.5 $m.s^{-1}$. This means that light winds reported in the first wind speed class will be rounded up to this value. Operational wind instruments are designed for durability and also to withstand exposure to strong gusty airflow. For these reasons, most wind sensors have a high starting speed, which can lead to erroneous reporting of light winds as calms (Truppi, 1968). The central wind speed values given above are quite commonly used and are employed in several models including the Texas Climatological Model (TCM, 1980), the Climatological Dispersion Model (CDM, 1973), and the Texas Episodic Model Version 8 (TCM, 1979).

Computer code listings of the air dispersion model and subroutine wind are provided in Tables 5.3 and 5.4 respectively.

Table 5.1

## AIR DISPERSION MODEL VARIABLES

| Model Symbol | Description | Units | Nominal Value | Probability* Distribution | Computer Origin | Compter Symbol |
|---|---|---|---|---|---|---|
| $C_{ai}(t)$ | atmospheric conc. of ith radionuclide at time t at the receptor | $Bq.m^{-3}$ | calculated | calculated | AIRDIS | AIRC(5,j)<br>$j \leq 82$ |
| $f_{Kl}$ | fraction of time wind blows from the source to the receptor (i.e. in sector K) with a particular atmospheric stability (l) | - | calculated | calculated | WIND | FWIND2(K,l) |
| h | height of the source | m | 2.0 | U(1.0,3.0) | INPUT | HSRC |
| $Q_i(t)$ | emission rate from tailings of ith radionuclide at time t | $Bq.s^{-1}$ | calculated | calculated | RADON<br>DUST | EMRATE(5) |
| $\overline{u}_i$ | mean annual wind speed | $m.s^{-1}$ | calculated | calculated | WIND | UWIND(K,l) |
| x | downwind distance to receptor | m | calculated | calculated | C/M | RNGMID(X)<br>$X \leq 5$ |
| $\sigma_z$ | vertical dispersion coefficient | m | calculated | calculated (see Table 5.2) | AIRDIS | VDISP(X,6)<br>$X \leq 5$ |
| $A_o$ | surface area of tailings | $m^2$ | $5.0x10^5$ | $(5.0x10^5)$ | INPUT | ATAIL |

Note

* Distributions are as described in Table 2.2.

Table 5.2

## POWER LAW EXPONENTS AND COEFFICIENTS FOR $\sigma_Z$

| Atmospheric Stability Class | Downwind Distance meters $500 < x < 5000$ |  | Downwind Distance meters $5000 < x < 50,000$ |  |
|---|---|---|---|---|
|  | a | b | a | b |
| A | 0.0002539 | 2.086 | 0.0002539 | 2.0886 |
| B | 0.04936 | 1.1137 | 0.04936 | 1.1137 |
| C | 0.1014 | 0.9260 | 0.1154 | 0.9109 |
| D | 0.2591 | 0.6869 | 0.7368 | 0.5642 |
| E and F | 0.2017 | 0.6020 | 1.5763 | 0.3606 |

Notes:

1) $\sigma_Z = a(x+x_0)^b$

2) In this application if $\sigma_Z$ is predicted to be greater than 5000m, $\sigma_Z$ is set equal to 5000m

3) Stability classes E and F are represented by coefficients for class F.

4) Coefficients a and b are from CDM (1973 p. 8).

Table 5.3

## AIR DISPERSION MODEL CODE LISTING

```
      SUBROUTINE AIRDIS
      INCLUDE 'MODEL.INC'
      INCLUDE 'VAR.INC'
      INTEGER*2 STACLS,XDIST,XDIRC
      REAL*4 AIRCON(5,16,5)
      IF(NT.EQ.0)THEN
         XDISTO=2.87*SQRT(ATAIL)
         DO 10 XDIST=1,NRING
            DIST(XDIST)=RNGMID(XDIST)+XDISTO
            DO 11 STACLS=1,6
               IF(RNGMID(XDIST).LE.5000.0)THEN
                  IF(STACLS.EQ.1)THEN
                     A=0.0002539
                     B=2.089
                  ELSEIF(STACLS.EQ.2)THEN
                     A=0.04936
                     B=1.114
                  ELSEIF(STACLS.EQ.3)THEN
                     A=0.1014
                     B=0.926
                  ELSEIF(STACLS.EQ.4)THEN
                     A=0.2591
                     B=0.6869
                  ELSE
                     A=0.2017
                     B=0.6020
                  ENDIF
               ELSEIF(RNGMID(XDIST).GT.5000.0)THEN
                  IF(STACLS.EQ.1)THEN
                     A=0.0002539
                     B=2.089
                  ELSEIF(STACLS.EQ.2)THEN
                     A=0.04936
                     B=1.114
                  ELSEIF(STACLS.EQ.3)THEN
                     A=0.1154
                     B=0.9109
                  ELSEIF(STACLS.EQ.4)THEN
                     A=0.7368
                     B=0.5642
                  ELSE
                     A=1.5763
                     B=0.3606
                  ENDIF
               ENDIF
               VDISP(XDIST,STACLS)=A*((DIST(XDIST))**B)
               IF(VDISP(XDIST,STACLS).GT.5000.0)THEN
                  VDISP(XDIST,STACLS)=5000.0
               ENDIF
11          CONTINUE
```

Table 5.3 (Continued)

```
10       CONTINUE
      ENDIF
      IF(WINDFG.EQ.'Y'.OR.(NT.EQ.0.AND.NUMTRL.EQ.1))THEN
         DO 12 XDIRC=1,16
            DO 13 XDIST=1,NRING
               CONCT(XDIRC,XDIST)=0.0
               DO 14 STACLS=1,6
                  IF(UWIND(XDIRC,STACLS).LT.0.5)THEN
                     UWIND(XDIRC,STACLS)=0.5
                  ENDIF
                  CONSTC=2.032*FWIND2(XDIRC,STACLS)/UWIND(XDIRC,
     +                   STACLS)/VDISP(XDIST,STACLS)/DIST(XDIST)*EXP
     +                   (-0.5*((HSRC/VDISP(XDIST,STACLS))**2.0))
                  CONCT(XDIRC,XDIST)=CONCT(XDIRC,XDIST)+CONSTC
14             CONTINUE
13          CONTINUE
12       CONTINUE
      ENDIF
      DO 15 XDIRC=1,16
         DO 16 XDIST=1,NRING
            DO 17 I=1,4
               AIRCON(I,XDIRC,XDIST)=FWIND1(XDIRC)/FWINDT*CONCT(XDIRC,
     +                               XDIST)/6.0*EMRATE(I)
17          CONTINUE
            AIRCON(5,XDIRC,XDIST)=CONCT(XDIRC,XDIST)/6.0*EMRATE(5)
16       CONTINUE
15    CONTINUE
      DO 18 I=1,4
         AIRC(I,NRECEP+1)=0.0
         DO 19 XDIST=1,NRING
            DO 20 XDIRC=1,16
               AIRC(I,NRECEP+1)=AIRC(I,NRECEP+1)+AIRCON(I,XDIRC,XDIST)*
     +                          RAREA(XDIST)
20          CONTINUE
19       CONTINUE
         AIRC(I,NRECEP+1)=AIRC(I,NRECEP+1)/TAREA
         AIRC(I,NRECEP+2)=0.0
         DO 21 K=1,PSNUM
            AIRC(I,NRECEP+2)=AIRC(I,NRECEP+2)+AIRCON(I,PSDIR(K),
     +                       PSRING(K))*RAREA(PSRING(K))
21       CONTINUE
         AIRC(I,NRECEP+2)=AIRC(I,NRECEP+2)/PSAREA
18    CONTINUE
      DO 22 I=1,5
         DO 23 NREC=1,NRECEP
            AIRC(I,NREC)=AIRCON(I,RDIR(NREC),RRING(NREC))
23       CONTINUE
22    CONTINUE
C
      IF(CODAIR.EQ.1.0.OR.CODAIR.EQ.2.0.OR.CODAIR.EQ.3.0)THEN
         WRITE(*,100)
      ENDIF
      IF(CODAIR.EQ.3.0)THEN
```

Table 5.3 (continued)

```
         WRITE(*,101)ATAIL,HSRC,XDISTO,RNGMID(1)
         IF(NRING.GT.1)THEN
            DO 24 XDIST=2,NRING
               WRITE(*,102)RNGMID(XDIST)
24          CONTINUE
         ENDIF
         WRITE(*,103)
         DO 25 XDIST=1,NRING
            WRITE(*,104)(VDISP(XDIST,STACLS),STACLS=1,6)
25       CONTINUE
         WRITE(*,105)EMRATE(1)
         DO 26 I=2,5
            WRITE(*,106)EMRATE(I)
26       CONTINUE
         WRITE(*,107)
         DO 27 I=1,4
            DO 28 XDIRC=1,16
               WRITE(*,108)(AIRCON(I,XDIRC,XDIST),XDIST=1,NRING)
28          CONTINUE
            WRITE(*,109)AIRC(I,NRECEP+1),AIRC(I,NRECEP+2)
27       CONTINUE
         DO 29 XDIRC=1,16
            WRITE(*,108)(AIRCON(5,XDIRC,XDIST),XDIST=1,NRING)
29       CONTINUE
      ENDIF
      IF(CODAIR.EQ.2.0)THEN
         WRITE(*,110)
         DO 30 I=1,4
            DO 31 NREC=1,NRECEP
               WRITE(*,111)AIRC(I,NREC)
31          CONTINUE
            WRITE(*,109)AIRC(I,NRECEP+1),AIRC(I,NRECEP+2)
30       CONTINUE
         DO 32 NREC=1,NRECEP
            WRITE(*,111)AIRC(5,NREC)
32       CONTINUE
      ENDIF
C
100   FORMAT(///1X,'AIR DISPERSION MODEL')
101   FORMAT(/1X,'SURFACE AREA OF TAILINGS',E12.4/1X,'HEIGHT OF SOURCE',
     +       E12.4/1X,'VIRTUAL SOURCE SET BACK DISTANCE',E12.4/1X,'DOW',
     +       'NWIND DISTANCE FROM SOURCE TO RECEPTOR',E12.4)
102   FORMAT(42X,E12.4)
103   FORMAT(1X,'VERTICAL DISPERSION COEFFICIENT')
104   FORMAT(1X,6(F10.2))
105   FORMAT(1X,'EMISSION RATE OF THE RADIONUCLIDES',E12.4)
106   FORMAT(35X,E12.4)
107   FORMAT(/1X,'ATMOSPHERIC CONCENTRATION OF THE RADIONUCLIDES IN EA',
     +       'CH SECTOR')
108   FORMAT(1X,5(E12.4))
109   FORMAT(1X,'AVERAGE CONCENTRATION',E12.4/1X,'AVERAGE WATERSHED CO',
     +       'NCENTRATION',E12.4)
110   FORMAT(/1X,'ATMOSPHERIC CONCENTRATION OF THE RADIONUCLIDES AT TH',
```

Table 5.3 (continued)

```
     +        'E RECEPTORS')
111   FORMAT(1X,E12.4)
C
      RETURN
      END
```

Table 5.4

## WIND MODEL CODE LISTING

```
      SUBROUTINE WIND
      INCLUDE 'MODEL.INC'
      INCLUDE 'VAR.INC'
      N=INT(WYEAR)
      IF(WINDFG.NE.'Y')N=1
      DO 10 J=1,6
         DO 11 I=1,16
            FWIND2(I,J)=0.0
            DO 12 K=1,6
               FWIND2(I,J)=FWIND2(I,J)+FWIND(I,J,K,N)
12          CONTINUE
            UWIND(I,J)=1.50*FWIND(I,J,1,N)+2.46*FWIND(I,J,2,N)+4.47*
     +                 FWIND(I,J,3,N)+6.93*FWIND(I,J,4,N)+9.61*FWIND
     +                 (I,J,5,N)+12.52*FWIND(I,J,6,N)
            SUWIND=FWIND(I,J,1,N)+FWIND(I,J,2,N)+FWIND(I,J,3,N)+
     +             FWIND(I,J,4,N)+FWIND(I,J,5,N)+FWIND(I,J,6,N)
            IF(SUWIND.EQ.0.0)THEN
               SUWIND=1.0
            ENDIF
            UWIND(I,J)=UWIND(I,J)/SUWIND
11       CONTINUE
10    CONTINUE
      FWINDT=0.0
      DO 13 I=1,16
         FWIND1(I)=0.0
         DO 14 J=1,6
            DO 15 K=4,6
               FWIND1(I)=FWIND1(I)+FWIND(I,J,K,N)
15          CONTINUE
14       CONTINUE
         FWINDT=FWINDT+FWIND1(I)
13    CONTINUE
C
      IF(CODWIN.EQ.1.0.OR.CODWIN.EQ.2.0.OR.CODWIN.EQ.3.0)THEN
         WRITE(*,100)
      ENDIF
      IF(CODWIN.EQ.2.0.OR.CODWIN.EQ.3.0)THEN
         WRITE(*,101)N
         DO 16 L=1,16
            I=L+8
            IF(I.GT.16)I=I-16
            WRITE(*,102)(FWIND2(I,J),J=1,6)
16       CONTINUE
         WRITE(*,103)
         DO 17 L=1,16
            I=L+8
            IF(I.GT.16)I=I-16
            WRITE(*,104)(UWIND(I,J),J=1,6)
17       CONTINUE
         WRITE(*,105)
```

Table 5.4 (continued)

```
         DO 18 L=1,16
            I=L+8
            IF(I.GT.16)I=I-16
            WRITE(*,106)(FWIND1(I))
18       CONTINUE
         WRITE(*,107)FWINDT
      ENDIF
C
100   FORMAT(///1X,'WIND MODEL')
101   FORMAT(/1X,'WIND DATA SELECTED',I5/1X,'FWIND2')
102   FORMAT(1X,6(E12.4))
103   FORMAT(1X,'UWIND')
104   FORMAT(1X,6(F12.4))
105   FORMAT(1X,'FWIND1')
106   FORMAT(1X,E12.4)
107   FORMAT(1X,'FWINDT'/1X,F8.4)
C
      RETURN
      END
```

## 5.3 Reference

Busse, A.D., Zimmerman, J.R. (CDM), 1973. "User's Guide for the Climatological Dispersion Model." PB227346, December, EPA-R4-73-024.

Bowers, J.F., Bjonklund, J.R., Cheney, C.C. ISC, 1979. "Industrial Source Complex (ISC) Dispersion Model User's Guide, Volume 1." PB80133044, December, EPA-450/4-79-030.

Hanna, S.R., 1982. "Technical Note No. 177, Review of Atmospheric Duffusion Models for Regulatory Applications." World Meteorological Organization, Geneva, Switzerland.

Texas Air Control Board (TCM), 1979. "Texas Episodic Model, User's Guide." PB80227572, October, E.P.A./DE-80/0070.

Texas Air Control Board (TCM), 1980. "User's Guide to the Texas Climatological Model." PB164626, August, EPA/DF-81/0016.

Truppi, L.E., 1968. "Bias Introduced by Amemometer Starting Speeds in Climatogical Wind Rose Summaries." Monthly Weather Review, 96(5): 325-327, May.

## 6.0 SOIL MODEL

This section outlines the development of a model that describes the movement in soil of radionuclides that are deposited as particulate matter from the air to the surface of the soil. The model includes atmospheric deposition, runoff and downward transport of radionuclides into the soil profile. It is used to estimate activity in the soil, which is used to compute groundshine dose and dose due to consumption of vegetation grown in the soil.

### 6.1 Soil Model Development

Figure 6.1 indicates the major factors at work in balancing radioactivity in the near-surface soil layers. Four factors are considered in the soil model developed in this section:

1) deposition of incoming airborne radioactivity;
2) radioactivity leaving the soil compartment in solution in the soil water via leaching;
3) radioactivity leaving the surface soil compartment in solution via runoff; and
4) radioactive decay.

To simplify the modelling exercise resuspension, erosion and depletion due to vegetation uptake are not included in the model. Exclusion of resuspension and erosion leads to a conservative overestimate of activity in the soil.

The major assumption used to develop the model is that incoming radioactivity is instantaneously partitioned between the liquid and solid phases according to the distribution coefficient $K_d$. The activity balance in a surface soil layer (layer 1) receiving radioactivity deposited from the air can be mathematically formulated as:

$$dZ_1 = C_A \, V_g \, A \, dt - C_w \, P \, A \, dt - \lambda \, Z_1 dt \qquad (6.1)$$

where

$Z_1$ = radionuclide content of soil layer 1 (Bq)
A = soil area ($m^2$) [taken as 1 $m^2$ in model calculations]
$C_A$ = radionuclide concentration on airborne particles ($Bq.m^{-3}$)
$V_g$ = particle deposition velocity ($m.yr^{-1}$)
t = time (yr)
$C_w$ = radionuclide concentration in soil water (water is assumed to be the mobile phase) ($Bq.m^{-3}$)
P = total precipitation less evapotranspiration (i.e. net precipitation) ($m.yr^{-1}$)
λ = radioactive decay constant ($yr^{-1}$)

The first term on the right side of equation (6.1) accounts for the incoming airborne radionuclide. The second term accounts for removal via leaching of the radionuclide in both surface and subsurface flow. The way in which these two mechanisms are accounted for is discussed later. The third term accounts for radioactive decay. In order to minimize the number of subscripts, and clarify this presentation, the equation was formulated without reference to specific radionuclides.

The activity of the surface soil layer at any time is the sum of the activities in the solid, liquid and gaseous phases of the soil space:

$$Z_1 = C_w V_w + C_s \rho_s AD + C_g V_a \qquad (6.2)$$

where

$V_w$ = volume of water in pore space ($m^3$)
$\rho_s$ = soil dry bulk density ($kg.m^{-3}$)
$C_s$ = radionuclide concentration in solid phase ($Bq.kg^{-1}$)
$V_a$ = volume of air in soil ($m^3$)
$C_g$ = radionuclide concentration in gaseous phase ($Bq.m^{-3}$)
A = soil area( $m^2$)
D = soil layer depth (m)

The activity in the gaseous phase for the non-volatile radionuclides of

FIGURE 6.1

SCHEMATIC REPRESENTATION OF SOIL DEPOSITION - LEACHING CONCEPTS

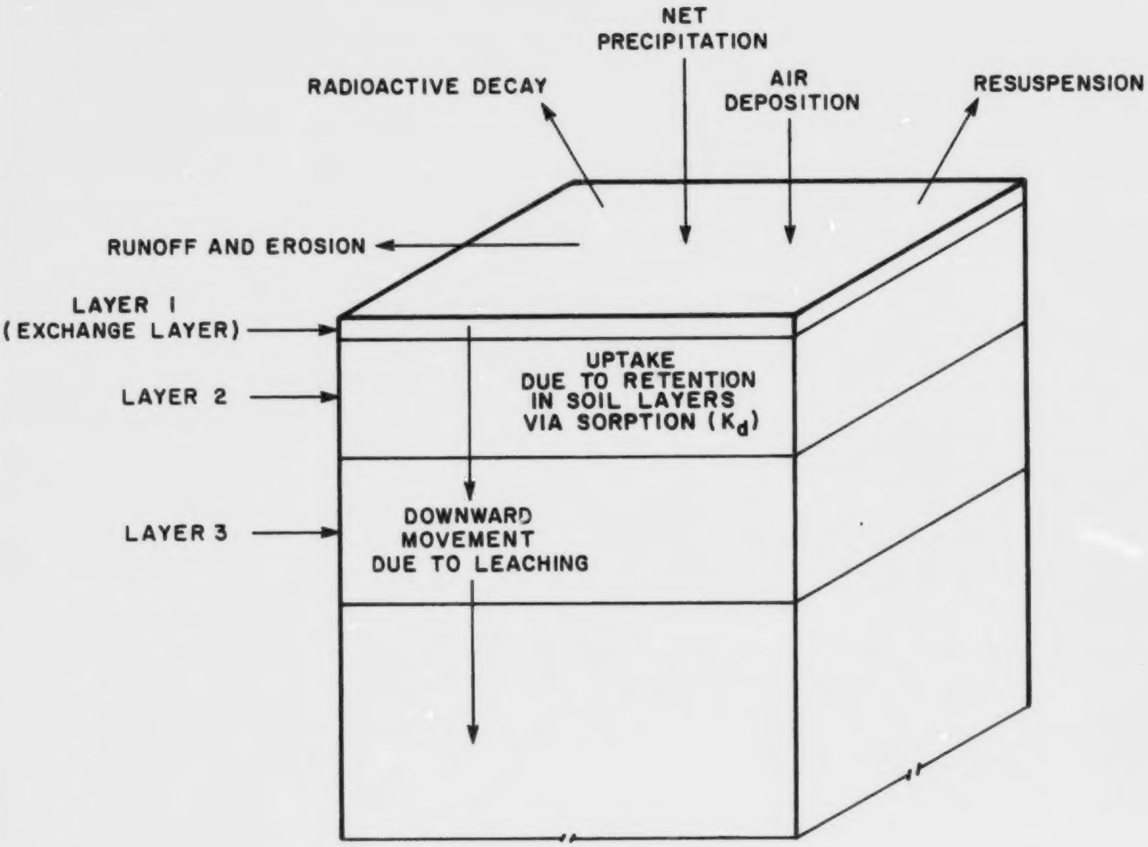
NET PRECIPITATION
RADIOACTIVE DECAY
AIR DEPOSITION
RESUSPENSION
RUNOFF AND EROSION
LAYER 1 (EXCHANGE LAYER)
LAYER 2
UPTAKE DUE TO RETENTION IN SOIL LAYERS VIA SORPTION ($K_d$)
LAYER 3
DOWNWARD MOVEMENT DUE TO LEACHING

concern to this study is assumed to be zero, i.e. $C_g = 0$.

At all times, the distribution of radionuclides between the solid and liquid phases is assumed to be in chemical equilibrium and thus can be characterized by the distribution coefficient $K_d (m^3.kg^{-1})$:

$$K_d = C_s/C_w \tag{6.3}$$

The volume of water in the soil pore space ($V_w$ in $m^3$) can be calculated as a function of the water content of the soil (W in kg water/kg soil) corrected for the relative densities of the solid and liquid fractions:

$$V_w = W A D \rho_s/\rho_w \tag{6.4}$$

where $\rho_w$ = density of water = 998.2 $kg.m^{-3}$ at 20°C.

Combining equations (6.2), (6.3) and (6.4) the radionuclide content of the surface soil layer for non-volatile nuclides is given by:

$$Z_1 = C_w WAD\rho_s/\rho_w + K_d C_w \rho_s AD$$

and solving for $C_w$ we obtain:

$$C_w = \frac{Z_1}{\rho_s AD(W/\rho_w + K_d)} \tag{6.5}$$

Substituting equation (6.5) into equation (6.1):

$$dZ_1 = C_A V_g A dt - \frac{Z_1 P dt}{\rho_s D(W/\rho_w + K_d)} - \lambda Z_1 dt$$

or

$$dZ_1 = (\beta_0 - \beta_1 Z_1 - \lambda Z_1) dt \tag{6.6}$$

where

$$\beta_o = C_A V_g A$$

$$\beta_1 = \frac{P}{\rho_s D \ (W/\rho_w + K_d)}$$

Equation (6.6) has the solution:

$$Z_1(t) = Z_1(0)\exp[-(\beta_1 + \lambda)t] + \frac{\beta_o}{\beta_1 + \lambda} [1 - \exp[-(\beta_1+\lambda)t]] \qquad (6.7)$$

The concentration is the activity divided by the volume of the soil layer.

The general formulation of equation (6.7) for i radionuclides and j soil layers is:

$$Z_{ij}(t) = Z_{ij}(t-\Delta t) \exp [-(\beta_{ij} + \lambda_i)t] +$$

$$\frac{\beta_{oij}}{\beta_{ij} + \lambda_i} [1-\exp[-(\beta_{ij} + \lambda_i)t] \qquad (6.8)$$

where

$Z_{ij}(t)$ = activity of radionuclide i in soil layer j at time t (Bq)
$Z_{ij}(t-\Delta t)$ = activity of radionuclide i in soil layer j at t-$\Delta$t (Bq)

$$\beta_{ij} = \frac{P}{\rho_{sj} D_j (W_j/\rho_w + K_{dij})} \qquad (6.9)$$

where

$\rho_{sj}$ = dry bulk density of soil layer j
$D_j$ = depth of soil layer j
$W_j$ = water content of soil layer j
$K_{dij}$ = distribution coefficient for radionculide i in soil layer j
$\lambda_i$ = radioactive decay constant for radionuclide i

The term $\beta_{oij}$ is the input term for radionuclide i in soil layer j.

The average activity over the time interval ($\Delta t$) is obtained by assuming a linear relationship with time. Hence:

$$Z = \frac{Z(t-\Delta t) + Z(t)}{2} \tag{6.10}$$

As was indicated earlier the radionuclide input for soil layer 1 is:

$$\beta_{oi1} = C_A V_g A \tag{6.11}$$

The following rationale applies to the input terms for the lower soil layers. All of the terms in equation (6.8) are known except the input term $\beta_{oij}$ for soil layers below the first layer. This term is solved for by substituting the average concentration (Z) over the time interval ($\Delta t$) from equation (6.10) into equation (6.5) and solving for water concentration ($C_w$). Water concentration is substituted into the leaching term ($C_wPA$) in equation (6.1). This term is $\beta_{oij+1}$, the input to the layer below.

This quantity is partitioned between leaching and runoff as follows:

$$\beta_{oij+1} = C_{wij}\, PA(1-F) \tag{6.12}$$

where

$C_{wij}$ = water concentration in previous soil layer ($j>1$)
F = fraction of total precipitation which moves as surface runoff (i.e. does not infiltrate the soil profile)

Values for F are discussed in the next section. Since the vegetation model requires a single soil concentration value, the concentration in the second soil layer (i.e. the root zone) is used.

Since other loss mechanisms, such as erosion and resuspension are neglected, the activity remaining in the soil column may be overestimated. On the other hand, deposition of eroded material from adjacent parcels of land may offset the potential losses noted above. A flowsheet for the implementation of the soil model is shown in Figure 6.2. The code and variable dictionary for the soil model are given in Tables 6.1 and 6.2 respectively.

## 6.2 Parameter Values

The airborne radionuclides are assumed, in the model, to be blown in all directions for up to a radius of 50 km from the tailings site. Within this broad area, virtually any soil type can be encountered. In other words, the airborne dust may settle on any type of soil. Hence the full range of soil physical and chemical conditions may be encountered. In the Phase III model the full spectrum of soil types (i.e. sand, silt, clay or organic) were represented by widening the input parameter values. In a site specific (non-generic) type of problem, these ranges of values for soil characteristics could be narrowed.

Shield soils typically have an organic surface layer overlaying a sand, silt or clay layer with organic content decreasing as a function of depth in this second layer (Beals, 1985). A two soil layer approach was implemented for the soil model with a 5 cm organic upper layer and a 15 cm lower layer possessing the lumped characteristics of sand, silt and clay soils. The physical and chemical properties of the two layers are indicated in Table 6.2. Due to a limited data base, only one set of $K_d$ values were used for the two soil layers.

Data on $K_d$ values for sand, silt, clay and organic soils reported by Sheppard *et al*. (1984) and Knight and Piesold (1986) were fitted to a variety of distributions. Because the small size of data base limited the number of bins into which the data could be divided, the Chi Square goodness-of-fit statistic could not be used to *differentiate the distribution(s) which* best characterized the data. From visual inspection, the loguniform distribution seemed to best characterize the data; hence, it was used to characterize $K_d$ for the four radionuclides. The limits of the loguniform distributions

FIGURE 6.2

## FLOWSHEET FOR SOIL MODEL

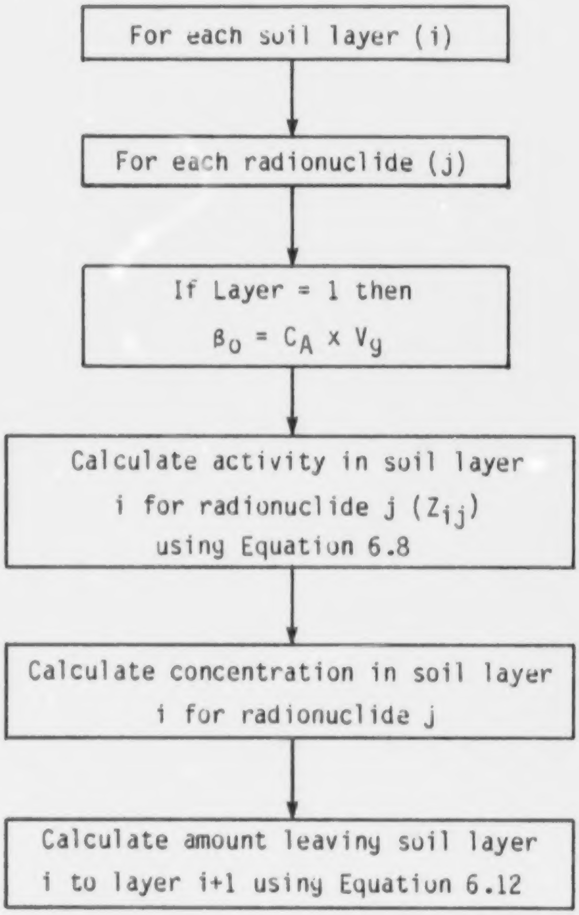
For each soil layer (i)
For each radionuclide (j)
If Layer = 1 then
$\beta_0 = C_A \times V_g$
Calculate activity in soil layer i for radionuclide j ($Z_{ij}$) using Equation 6.8
Calculate concentration in soil layer i for radionuclide j
Calculate amount leaving soil layer i to layer i+1 using Equation 6.12

correspond to the low and high values for $K_d$'s reported in the above two references. As was indicated above, for the generic problem treated in Phase III, a wide range of $K_d$'s was used.

According to an analysis of recharge to groundwater on shield watersheds by Wang et al. (1978), recharge to groundwater as a percent of annual precipitation ranged from 1 to 24 percent. These values were for total precipitation and would be a larger percent of net precipitation. When adjusted to net precipitation which is approximately half of total precipitation the values double. F was assumed to be triangularly distributed with the distribution descriptors shown in Table 6.2.

## 6.3 Soil Model Test Program

A series of tests were performed to check the soil model for computational accuracy and reasonableness. Some of these tests are discussed below. Hand calculations were checked against a deterministic run to confirm that the soil model executed the equations properly. In another test the model was run until steady state conditions in the soil profile were attained. The steady state values calculated by the program were compared to the theoretical steady state values. A mass balance was also performed that compared radionuclide input to uptake, leaching, runoff and decay terms over a 100 year period. All of these terms balanced. The model was run probabilistically and over time and space to determine that it performed accurately in these dimensions.

Figure 6.3 is a plot of the radionuclide concentration in layer 2 versus time for the four radionuclides. The system model was run for 10 trials for 1000 years in 10 year time steps to produce the figure.

FIGURE 6.3

PLOT OF CONCENTRATION vs. TIME
FOR SECOND SOIL LAYER

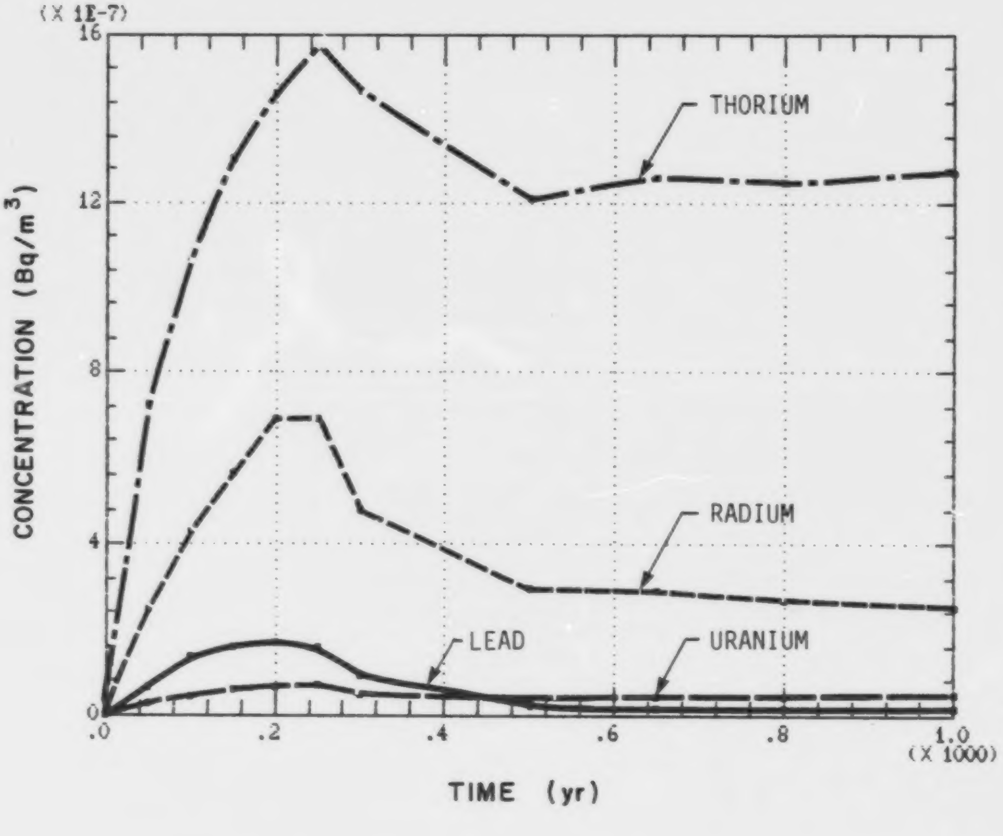

Table 6.1

## SOIL MODEL CODE LISTING

```
      SUBROUTINE SOIL
C     DEVELOPED BY DON BEALS
C     CODED BY DON BEALS
      INCLUDE 'MODEL.INC'
      INCLUDE 'VAR.INC'
      INTEGER*2 N,K
      REAL*4 XXX,BETAI
      IF(CODSL.GE.1.0)WRITE(*,2005)
2005     FORMAT(1X,'SUBROUTINE SOIL')
         IF(CODSL.GE.2) WRITE(*,2002)NREC,NPRCP,DEPVEL,FWAT
2002     FORMAT(1X,'NREC',I3,'NPRCP',E10.3,2X,'DEPVEL',E10.3,'FWAT',
     &E10.3)
C
C     INITIALIZE CERTAIN QUANTITIES AT T=0 FOR COMPUTATIONAL EFFICIENCY
      NLAYER=INT(LAYER)
      IF(T.EQ.0.0)THEN
      DSOILT=0.0
         DO 10 K=1,NLAYER
            IF(K.GT.1)DSOILT=DSOILT+DSOIL(K)
            DO 20 N=1,4
               ZZERO(NREC,K,N)=0.0
               DECTOT(K,N)=0.0
               IF(K.GE.2)THEN
                  SOILKDS(K,N)=SOILKD(N)
                  WCS(K)=WC(2)
                  RHOS(K)=RHOSS(2)
               ELSE
                  SOILKDS(1,N)=SOILKD(N)
                  WCS(1)=WC(1)
                  RHOS(1)=RHOSS(1)
               ENDIF
            DENOM(K,N)=DSOIL(K)*RHOS(K)*((WCS(K)/998.2)+SOILKDS(K,N))
            IF(CODSL.EQ.2.0)THEN
               WRITE(*,1005)K,N,SOILKDS(K,N),DENOM(K,N)
1005           FORMAT(1X,'LAYER=',I2,'RADIONUCLIDE=',I2,'KD=',E10.3,
     &         'DENOM=',E10.3)
            ENDIF
 20      CONTINUE
            IF(CODSL.EQ.2.0)THEN
               WRITE(*,1006)K,RHOS(K),WCS(K)
 1006          FORMAT('LAYER=',I2,'RHO=',E10.3,'WCS='E10.3)
            ENDIF
 10      CONTINUE
      ENDIF
C
C     NESTED LOOPS TO CALCULATE SOIL CONCENTRATIONS
      DO 30 K=1,NLAYER
         IF(CODSL.EQ.2.0)THEN
            WRITE(*,*)K
            WRITE(*,2000)
```

Table 6.1 (continued)

```
2000        FORMAT(1X,'RADIONUCLIDE',4X,'ZZERO',2X,'ACTIVITY',2X,
     &      '  WATCONC    ',2X,'SOILCONC',6X, 'BETAO',5X,'XXX',
     &      8X'LEACH',6X,'DECAY')
         ENDIF
         DO 40 N=1,4
            IF(K.EQ.1) THEN
               BETAO(K,N)=AIRC(N,NREC)*DEPVEL*3600.0*24.0*365.0
               BETAI=NPRCP/DENOM(K,N)
            ELSE
               BETAI=(NPRCP*(1-FWAT))/DENOM(K,N)
            ENDIF
            XXX=BETAI+XLAMDA(N)
C
C       CALCULATE ACTIVITY IN LAYER K FOR RADIONUCLIDE N
            ZTOT(K,N)=(ZZERO(NREC,K,N)*EXP(-XXX*DT))+
     &      ((BETAO(K,N)/XXX)*(1-EXP(-XXX*DT)))
C
C       CALCULATE TOTAL CUMULATIVE DECAY
            DECTOT(K,N)=DECTOT(K,N)+ZTOT(K,N)*(1-EXP(-XLAMDA(N)*DT))
C
C       CALCULATE CONCENTRATION IN SOIL LAYER K OF RADIONUCLIDE N
            SOILCN(N,K)=((ZTOT(K,N)+ZZERO(NREC,K,N))/2)/DSOIL(K)
C
C       CALCULATE WATER CONCENTRATION
            SWCONC(K,N)=((ZTOT(K,N)+ZZERO(NREC,K,N))/2)/DENOM(K,N)
C
C       CALCULATE AMOUNT OF RADIONUCLIDE N LEAVING SOIL LAYER K
            ZOUT=SWCONC(K,N)*NPRCP*(1-FWAT)
C
            IF(CODSL.EQ.2.0)THEN
               WRITE(*,1001)N,ZZERO(NREC,K,N),ZTOT(K,N),SWCONC(K,N),
     &         SOILCN(N,K),BETAO(K,N),XXX,ZOUT,DECTOT(K,N)
 1001          FORMAT(5X,I3,3X,E10.3,2X,E10.3,2X,E10.3,2X,E10.3,2X,E10.3
     &         ,1X,E10.3,2X,E13.6,2X,E10.3)
            ENDIF
C
C       INPUT TERM TO NEXT LAYER
            BETAO(K+1,N)=ZOUT
C       INITIALIZE ACTIVITY FOR NEXT TIME LOOP
            ZZERO(NREC,K,N)=ZTOT(K,N)
 40      CONTINUE
 30   CONTINUE
         DO 50 N=1,4
            SOILC(N,NREC)=SOILCN(N,2)
         IF(CODSL.EQ.2.0)THEN
            WRITE(*,2003)N,SOILC(N,NREC)
2003        FORMAT(1X,'RADIONUCLIDE=',I2,1X,'CONCENTRATION IN LAYER 2=',
     &      E10.3)
         ENDIF
50    CONTINUE
      RETURN
      END
C
C
```

Table 6.2

## SOIL MODEL PARAMETERS

| Model Symbol | Description | Units | Nominal Value | Probability Distribution* | Computer Origin | Computer Symbol |
|---|---|---|---|---|---|---|
| $\beta_{ij}$ | variable in activity equation | $yr^{-1}$ | calculated | calculated | SOIL | BETAI |
| $\beta_{oij}$ | variable in activity equation | $Bq.yr^{-1}$ | calculated | calculated | SOIL | BETAO(I,J) |
| $C_{Ain}$ | concentration of ith radionuclide in nth windrose sector | $Bq.m^{-3}$ | calculated | calculated | AIRDIS | AIRC(N,I) |
| $V_g$ | deposition velocity | $m.s^{-1}$ | 0.0165 | U(0.003,0.03) | INPUT | DEPVEL |
| $D_j$ | depth of soil layer j | m | | | INPUT | DSOIL(J) |
| | Layer 1 | | 0.05 | C(0.05) | | |
| | Layer 2 | | 0.15 | C(0.15) | | |
| F | fraction of net precipitation in runoff | - | 0.16 | T(0.02,0.16, 0.48) | INPUT | FWAT |
| $\lambda_i$ | decay constant for ith radionuclide | $yr^{-1}$ | | | INPUT | LAMDA(I) |
| | Uranium | | $1.53x10^{-10}$ | $C(1.53x10^{-10})$ | | |
| | Thorium | | $4.92x10^{-11}$ | $C(4.92x10^{-11})$ | | |
| | Lead | | $3.3x10^{-2}$ | $C(3.3x10^{-2})$ | | |
| | Radium | | $4.33x10^{-4}$ | $C(4.33x10^{-4})$ | | |
| P | net precipitation | $m.yr^{-1}$ | 0.4 | N(0.4,0.1,0.15, 0.65) | INPUT | NPRCP |
| $\rho_{sj}$ | bulk density of jth soil layer | $kg.m^{-3}$ | | | INPUT | RHOS(J) |
| | Layer 1 | | 129 | LN(129,1.3,20, 450) | | |
| | Layer 2 | | 1342 | LN(1342,1.1, 1000,1800) | | |
| $K_{dij}$ | distribution coefficient for jth soil layer and ith radionuclide | $m^3.kg^{-1}$ | | | INPUT | SOILKD(I,J) |
| | Uranium | | 0.32 | $LU(1.3x10^{-4},7.9x10^2)$ | | |
| | Radium | | 2.2 | $LU(5.1x10^{-3},9.5x10^2)$ | | |
| | Lead | | 3.3 | $LU(1.8x10^{-1},6.3x10^1)$ | | |
| | Thorium | | 0.70 | $LU(3.29x10^{-3},1.5x10^2)$ | | |
| $C_{wij}$ | water concentration of radionuclide i in soil layer j | $Bq.m^{-3}$ | calculated | calculated | SOIL | SWCONC(I,J) |
| $W_j$ | water content of jth soil layer | kg(water) $.kg^{-1}$(soil) | | | INPUT | WC(J) |
| | Layer 1 | | 1.08 | U(0.75,1.4) | | |
| | Layer 2 | | 0.13 | LN(0.13,1.4, 0.05,3.6) | | |
| $Z_{ij}(t)$ | activity of radionuclide i in soil layer j | Bq | calculated | calculated | SOIL | ZTOT(I,J) |
| $Z_{ij}(t-\Delta t)$ | activity of radionuclide i in soil layer j at beginning of time interval | Bq | calculated | calculated | SOIL | ZZERO(I,J) |

Note

* Distributions are as described on Table 2.2.

## 6.4 References

Beals, D.I., 1985. "Soil and Climate Parameters for Post Closure Biosphere Assessment of Nuclear Fuel Waste Disposal." Atomic Energy of Canada Limited Report TR-285.

Sheppard, M.I., Beals, D.I., Thibault, D.H., and O'Connor, P., 1984. "Soil Nuclide Distribution Coefficients and Their Statistical Distributions." Atomic Energy of Canada Limited Report 8364.

Wang, K.T., and Chin, V.T., 1978. "Northern Ontario Water Resources Studies - Groundwater Resources". Ontario Ministry of the Environment, Toronto.

Knight and Piesold Ltd., 1986. "Monitoring of Layered Uranium Tailings - Phase I." Research Report prepared for the National Uranium Tailings Program, CANMET, Energy, Mines and Resources Canada, Ottawa.

# 7.0 GROUNDSHINE MODEL

## 7.1 Introduction

The model developed in this section calculates the surface gamma flux and receptor dose (groundshine) due to the accumulation over time of selected radionuclides in the soil profile. The radionuclides considered in this implementation of the groundshine model include natural uranium, radium-226, lead-210 and thorium-232. The model uses the radionuclide concentrations in successive soil layers calculated by the soil model described in Section 6.0. The groundshine model accounts approximately for self-shielding by overlying soil layers and the loss of gamma ray flux via radon emanation and subsequent exhalation to the atmosphere.

In the development of the groundshine model a number of assumptions have been introduced to simplify the computations. While the assumptions are discussed as they are introduced into the model development, two assumptions are worth noting here. First, any attenuation which may take place in the medium (air) between the source (i.e. the soil layer) and the receptor is neglected as is any attenuation or scatter which might be expected to occur in the thin overlying organic soil layer. Second, as discussed in the following section, a simplifying approximation has been made to account for the effect of scattered radiation orginating from within the self-absorbing source material (i.e. the soil).

The following sections document the basis for the groundshine model and the parameters required to use it.

## 7.2. The Basic Model

First let us consider a single layer of soil containing one radionuclide distributed uniformly throughout the layer. Each volume element within that soil layer will act as a source of gamma rays emitting, say "A" gamma rays per unit volume per unit time. When gamma rays pass through matter, in this case soil, they are removed from the beam in a exponential manner described by:

$$\phi = \phi_0 \exp(-\mu b) \qquad (7.1)$$

where $\phi_0$ and $\phi$ are respectively the gamma ray fluxes (gamma rays per square meter per second) before and after passing through a material of thickness b metres. The proportionality constant $\mu$ is called the linear attenuation coefficient (units of $m^{-1}$) and is specific to both the gamma ray energy and the medium. Thus each incremental layer of soil both increases the gamma ray flux at the soil surface by adding a new source of gamma rays and reduces the gamma ray flux at the soil surface by attenuating a fraction of the gamma rays originating in lower layers. The combined effect of these phenomena is the gamma ray flux, $\phi$, at the surface of the soil which is described mathematically by:

$$\phi = \int_0^b \int_0^{\theta_1} \frac{A}{2} \tan\theta \ \exp(-\mu x/\cos\theta) \ d\theta dx \qquad (7.2a)$$

where

$\phi$ = gamma flux at receptor (gamma rays.$m^{-2}$. $s^{-1}$)

$\mu$ = linear attenuation coefficient ($m^{-1}$)

A = $\frac{CN}{S_{pa}}$ = gamma ray source strength (gamma rays.$m^{-3}$.$s^{-1}$)

C = concentration of radionuclide in soil layer (Bq.$m^{-3}$)

N = gamma rays per unit time per unit mass of radionuclide (gamma rays.$kg^{-1}s^{-1}$.

$S_{pa}$= activity per unit mass of radionuclide (Bq.$kg^{-1}$)

b = soil layer depth (m)

Equation (7.2) is basically the integration of flux from a ring-shaped volume element at depth b within the source where $\theta$ and X are variables, $\theta$ representing the angle subtended by the ring and X is the depth of the ring within the source. As noted previously, the formulation neglects any attenuation of gamma rays in the air between the receptor and the source. In the limit of a very large (semi-infinite) plane source (i.e. $\theta_1 \rightarrow \pi/2$, which is also very thick (i.e. $b \rightarrow \infty$), equation (7.2) reduces to:

$$\phi = \frac{A}{2\mu} \tag{7.2b}$$

Using the substitution $x = 1/\cos\theta$, the method of integration by parts and an integration formula from the Chemical Rubber Company handbook (CRC, 1964), the solution of equation (7.2) is given by:

$$\phi = \frac{A}{2\mu}\left[1 - e^{-\mu b} - \mu b \left(\gamma + \ln(\mu b) - \mu b + \frac{(\mu b)^2}{2.2} - \frac{(\mu b)^3}{3.3} \ldots \right)\right] \tag{7.3}$$

where

$\gamma$ = a constant having the value 0.5772157

Since the attenuation coefficient $\mu$ (and hence the flux) is dependent on the type of scattering medium (in this case, soil) and the gamma energy, equations (7.1), (7.2) and (7.3) must be evaluated for each gamma energy emitted by the radionuclide in the soil. The summation over all energies is discussed later.

Equation (7.2) is based on the assumption that gamma rays scattered by the soil are completely removed from the radiation beam. However, gamma rays which are scattered but not absorbed may also add to the total gamma ray flux received by someone standing on the soil. The effect of scattered radiation can be taken into account by buildup factors which depend on the nature of the soil, the thickness of the soil, and the type and energy of the radiation. Such calculations are very complex. To make the calculations tractable, an approximation is made to take account of the contribution of scattered radiation to the gamma ray flux at the receptor.

The linear attenuation coefficient ($\mu$) represents the sum effect of the various absorption and scattering processes which affect the energy removed from the primary beam of gamma rays (i.e. $\mu = \mu_A + \mu_{scat}$.). In this study, the linear absorption coefficient ($\mu_A$) is substituted for the linear attenuation coefficient $\mu$($\mu$scat =0), that is it is assumed that the scattered radiation will always contribute to the resultant energy flux. This assumption appears to be in general agreement with results found using experimentally determined buildup factors (Evans, 1955).

Attenuation coefficients are usually tabulated in the form of $\mu/\rho$, defined as the mass attenuation coefficient which is independent of the actual state (gas, solid, liquid), and actual density of the medium, where $\rho$ is the density and $\mu$ is the linear attenuation coefficient of the medium. As stated above, mass absorption coefficients are used in this analyses (for example, see U.S. DHEW, 1970).

## 7.3. Multiple Soil Layers

Equations (7.2b) and (7.3) give the gamma flux at the surface of a single soil layer with a given radionuclide concentration. In this study the total gamma ray flux at the ground surface is taken to be the sum of the gamma ray fluxes from each soil layer taking into account the shielding of the covering layers. For the nth radionuclide, this can be expressed as:

$$\phi_T^n = \phi_1^n + \sum_{i=2}^{L} \phi_i^n \prod_{k=1}^{i-1} \exp(-\mu_k b_k) \qquad (7.4)$$

where there are L soil layers and the shielding from a soil layer is a function of it's own absorption coefficient ($\mu_k$) times it's depth ($b_k$).

## 7.4 Multiple Radionuclides

The superscript n in equation (7.4) refers to the nth radionuclide. In the Phase III study four groups of radionuclides are treated, namely natural uranium, total thorium, lead-210 and radium-226. Natural uranium consists of uranium-238 and uranium-234 from one radioactive decay series and uranium-235 from another series. Since the natural abundance of uranium-235 is very low (0.72% on a mass basis), it is not dosimetrically significant and is not considered in these calculations. (One gram of natural uranium contains 1.22 x $10^4$ Bq each of uranium-238 and uranium-234, and 5.8 x $10^2$ Bq of uranium-235.) In this component model, total thorium is taken as thorium-232. The decay chains for the uranium-238 and thorium-232 series are illustrated in Figures 7.1 and 7.2 respectively.

For deposited natural uranium, only the gamma emissions from radionuclides down to uranium-234 (Figure 7.1) need to be considered since the long-lived thorium-230 ($8x10^4$ y half-life) effectively limits the ingrowth of the remainder of the decay series during the modelling period.

For the other radionuclides that are specifically modelled, namely Ra-226, Pb-210 and Th-232, the gamma emissions from all their daughter products need to be considered since it is assumed that these sub-series will reach equilibrium during each modelling time step. Equilibrium is assumed to be reached instantaneously at the beginning of each time step. (If the time step is as small as 10 years, the Th-232 chain would actually reach only about 65% of its equilibrium value).

For simplicity, the superscript n in equation (7.2) denoting radionuclides does not appear in the equations developed below. The reader should consider the superscript n to be implicit in these equations.

As previously noted, the radionuclides being modelled emit gamma rays with a variety of energies. Since the attenuation coefficient is a function of energy, equations (7.3) and (7.4) must account for the different gamma energies. Dealing with each of the large number of gamma rays individually was considered too cumbersome. To decrease the number of calculations, the spectrum of gamma energies for each of the four groups of radionuclides being modelled was divided into five energy levels (Chambers et al., 1981). The total number of gammas in the jth energy band ($N_{T,j}$) and the average gamma decay energy ($E_j$) of that band were then computed as follows:

$$N_{T,j} = \sum_{k=1}^{m} N_{j,k} \qquad (7.5)$$

where

m = number of energy level j-type decays in the decay chain of interest

$N_{j,k}$ = number of gamma rays for the kth decay in the jth energy band (gamma rays.kg$^{-1}$.s$^{-1}$)

$N_{T,j}$ = total number gamma rays in a radionuclide decay chain in jth energy band per second (gamma rays.kg$^{-1}$.s$^{-1}$)

The total energy due to the gamma emissions in an energy band is ($E_{T,j}$):

$$E_{T,j} = \sum_{k=1}^{m} E_{j,k} N_{j,k} \qquad (7.6)$$

where

$E_{j,k}$ = energy of kth decay in jth energy band (MeV)

The average energy in the jth energy band ($E_j$) for the radionuclide group of interest is then:

$$E_j = \frac{E_{T,j}}{N_{T,j}} \qquad (7.7)$$

An example will help to clarify the above concepts. Consider the thorium-232 decay chain and the energy band ranging from 0.026 to 0.186 MeV, the lowest energy band selected. The two radionuclides in this decay chain (Figure 7.2) which produce gamma radiation within this energy band are Th-228, which emits a 0.084 MeV gamma on 1.6% of its decays, and Bi-212 which emits a 0.040 MeV gamma on 2% of its decays. Noting that 1 kg of Th-232 has an activity of 4.03

FIGURE 7.1

URANIUM - 238 DECAY SERIES

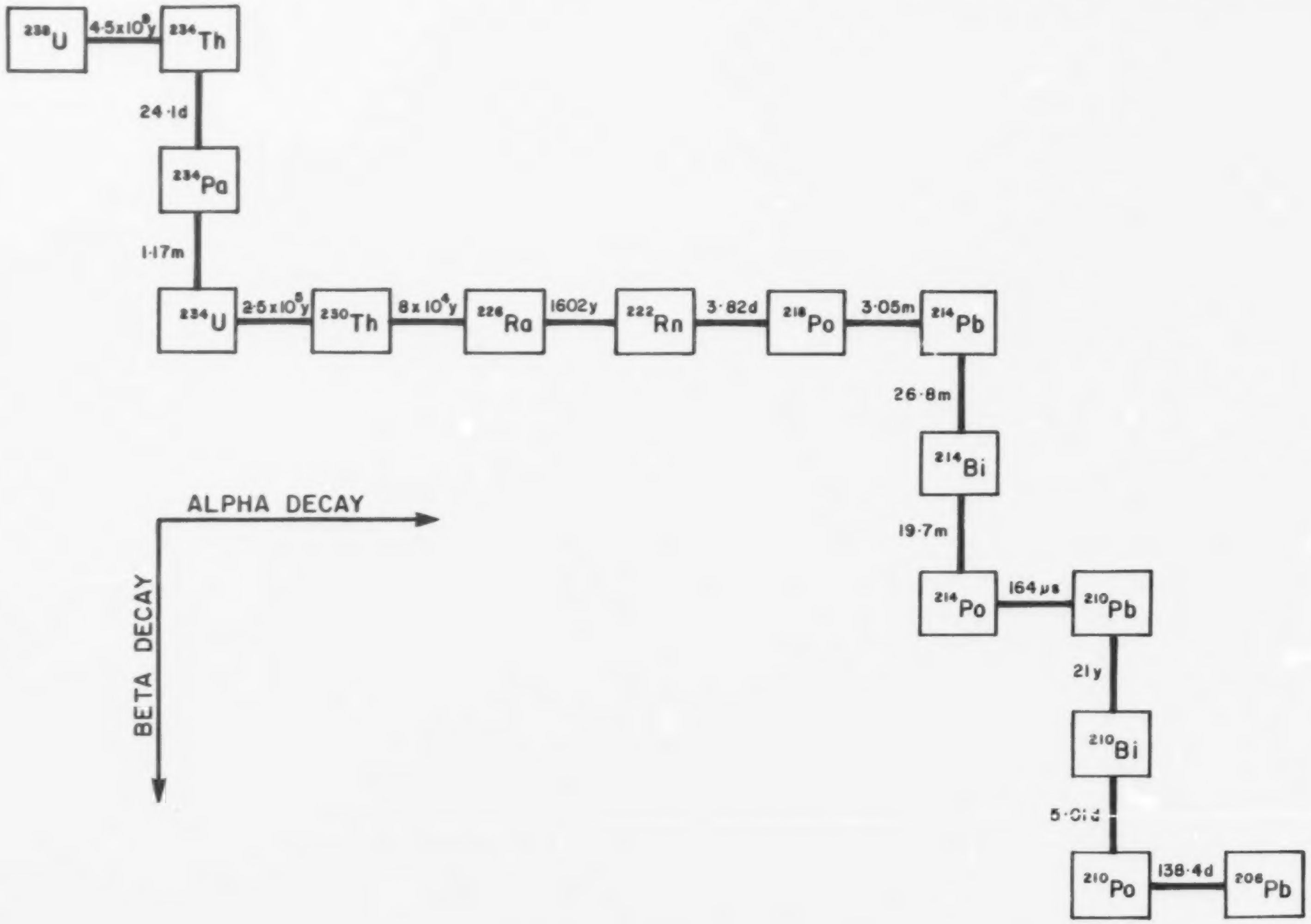

$^{238}U$
4·5x10$^9$y
$^{234}Th$
24·1d
$^{234}Pa$
1·17m
$^{234}U$
2·5x10$^5$y
$^{230}Th$
8x10$^4$y
$^{226}Ra$
1602y
$^{222}Rn$
3·82d
$^{218}Po$
3·05m
$^{214}Pb$
26·8m
$^{214}Bi$
19·7m
$^{214}Po$
164μs
$^{210}Pb$
21y
$^{210}Bi$
5·01d
$^{210}Po$
138·4d
$^{206}Pb$
ALPHA DECAY
BETA DECAY

FIGURE 7.2

THORIUM - 232 DECAY SERIES

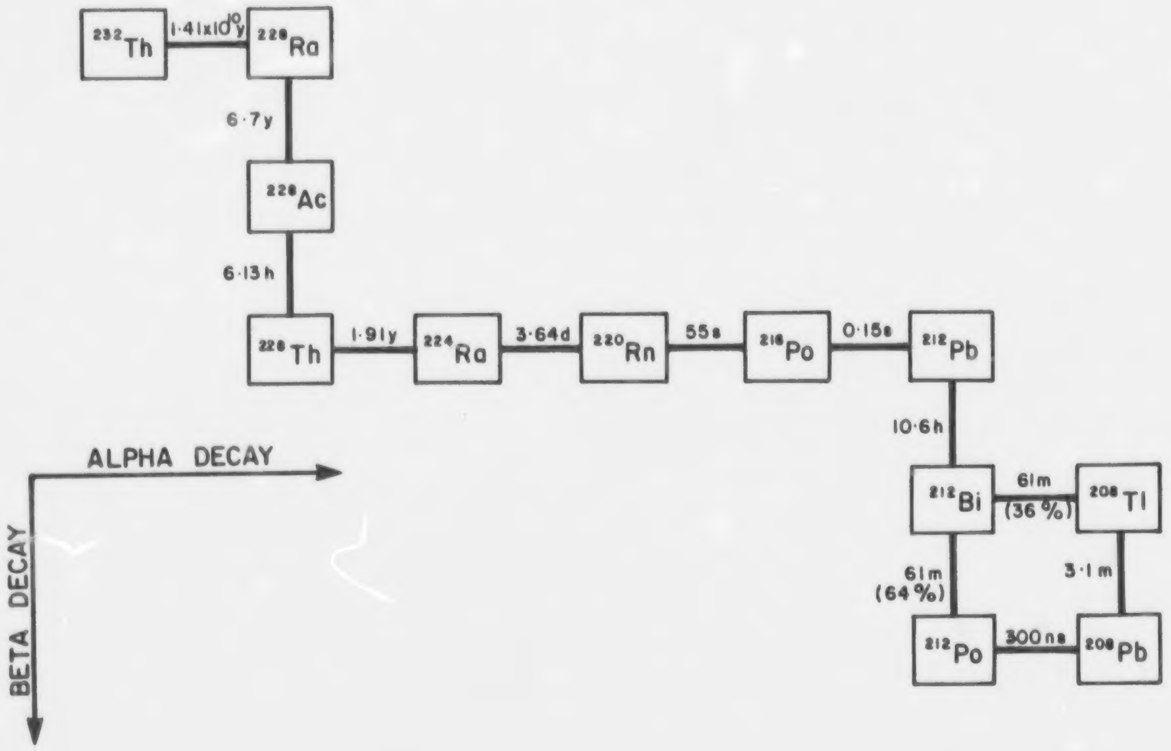

$^{232}$Th
1·41x10$^{10}$y
$^{228}$Ra
6·7y
$^{228}$Ac
6·13h
$^{228}$Th
1·91y
$^{224}$Ra
3·64d
$^{220}$Rn
55s
$^{216}$Po
0·15s
$^{212}$Pb
10·6h
$^{212}$Bi
61m (36%)
$^{208}$Tl
61m (64%)
3·1m
$^{212}$Po
300ns
$^{208}$Pb
ALPHA DECAY
BETA DECAY

x $10^6$ Bq and assuming equilibrium of its daughter products, the total number of decays and the average energy in the first energy band are calculated as follows:

$E_{11} = 8.4 \times 10^{-2}$ MeV

$N_{11} = 6.45 \times 10^4$ gammas.kg$^{-1}$.s$^{-1}$

$(4.03 \times 10^6 \times 1.6\%)$

$E_{12} = 4.00 \times 10^{-2}$ MeV

$N_{12} = 8.07 \times 10^4$ (gamma.kg$^{-1}$.s$^{-1}$)

$(4.03 \times 10^6 \times 2\%)$

$N_{T1} = (6.45 \times 10^4) + (8.07 \times 10^4) = 1.45 \times 10^5$ gammas.kg$^{-1}$.s$^{-1}$ (equation (7.5))

$E_{T1} = (8.4 \times 10^{-2} \times 6.45 \times 10^4) + (4.00 \times 10^{-2} \times 8.07 \times 10^4)$

$= 8.65 \times 10^3$ (MeV.kg$^{-1}$.s$^{-1}$ equation (7.6))

$$E_1 = \frac{8.65 \times 10^3}{1.45 \times 10^5} = 5.96 \times 10^{-2} \text{ MeV (equation (7.7))}$$

## 7.5 Exhalation of Radon

Being an inert gas, radon can diffuse away from the soil layer in which it is produced. Hence, the number of gammas emitted from the radon daughter radionuclides will be less than under equilibrium conditions. This effect can be accommodated by assuming that the radon within the pore space of the soil (the emanation fraction; see Chapter 4) is instantaneously released to the atmosphere. This is a reasonable assumption for the relatively thin (< 0.2 m deep) soil layers being modelled. The emanation of the radon changes the number and average energy of the gammas being emitted from the radionuclides remaining in the soil. The following method was used to adjust the number of decays and the average energy in the radium decay chain for radon emanation:

$$N_{TJ}^{Ra} = N_{Raj} + N_{Rnj}\,(1-E) \qquad (7.8)$$

where

$N^{Ra}_{T,j}$ = total number of decays in jth energy band in the entire radium decay chain (gammas.kg$^{-1}$ (Ra).s$^{-1}$)

$N_{Ra,j}$ = number of decays in the jth energy band for radium (only see Figure 7.2)(gammas.kg$^{-1}$ (Ra).s$^{-1}$)

$N_{Rn,j}$ = number of decays for radon and daughters in jth energy level (gammas.kg$^{-1}$ (Ra).s$^{-1}$)

$E$ = emanation fraction of radon

The average energy ($E^{Ra}_j$) is:

$$E^{Ra}_j = \frac{E_{Raj}N_{Raj} + E_{Rnj}N_{Rnj}(1-E)}{N^{Ra}_{Tj}} \qquad (7.9)$$

where

$E_{Raj}$ = average energy in the jth energy band (MeV) for radium decay

$E_{Rnj}$ = average energy in the jth energy band (MeV) for radon and daughters

Thoron (radon-220) in the thorium-232 decay series (Figure 7.3) will also diffuse from the soil but its relatively short half-life (55s) precludes any significant exhalation. The thoron diffusion length in normal soils is only 1 to 2 cm. For this model, it is assumed that no thoron is exhaled from the soil.

As noted earlier, the attenuation coefficient $\mu$ (set equal to the absorption coefficient in this analysis) is a function of the gamma energy and the type of absorbing material. Since the absorption coefficients for soil as a function of energy were not readily available, the mass absorption coefficients of concrete ($\mu_C/\rho_C$), adjusted by the relative density of soil to concrete, were used. This method has been used by Kocher and Sjoreen (1985) to calculate exposure rates from near-surface contamination. The mass absorption coefficients for concrete ($\mu_C/\rho_C$) as a function of energy (Attix and Roesch, 1968) were fitted to a regression model ($r^2 \simeq 0.94$) of the form

$y = ax^b$ as follows:

$$\mu_c/\rho_c = 2.7 \times 10^{-3}\ E^{-0.320}\ (m^2.kg^{-1}) \qquad (7.10)$$

The mass absorption coefficients for concrete were adjusted to obtain the linear absorption coefficient for soil ($\mu_s$, where the "s" stands for "soil") as follows:

$$\mu_s = \frac{\mu c}{\rho c}\ \rho_c\ \frac{\rho s}{\rho c} = \frac{\mu c}{\rho c}\ \rho_s \qquad (7.11)$$

Returning to equation (7.4), the total gamma flux (gammas.$m^{-2}.s^{-1}$) in the jth energy level at the soil surface for the nth group of radionuclides (natural uranium, total thorium, radium-226 or lead-210) is then given by :

$$\phi^n_{T,j} = \phi^n_{1,j} + \sum_{i=2}^{L} \phi^n_{i,j} \prod_{k=1}^{i-1} \exp(-\mu_{j,k} b_k) \qquad (7.12)$$

where the energy-dependent attenuation coefficient $\mu_j$ is given by equations (7.10) and (7.11). The energy used to calculate $\mu_j$ in equation (7.10) is the average energy of the jth energy band.

This gamma flux can be converted to an energy flux and then a dose rate by (Cember, 1969):

$$D^n_j = \phi^n_{T,j} \times E^n_j \times \frac{\mu_{t,j}}{\rho_t} \times 5.0 \times 10^{-6}\ (Sv.y^{-1}) \qquad (7.13)$$

where

$\mu_{t,j}/\rho_t$ = mass energy absorption coefficient for tissue at energy $E^n_j$ ($m^2.kg^{-1}$)

$\rho_t$ = tissue density ($kg.m^{-3}$)

Since the tissue mass energy absorption coefficient is not highly energy-dependent in the energy range of interest to this study, it is set equal to a constant $3 \times 10^{-3}$ $m^2.kg^{-1}$ (U.S. DHEW, 1970). The tissue density is taken to be $1 \times 10^3$ $kg.m^{-3}$. The constant $5 \times 10^{-6}$ in equation (7.13) converts $MeV.g^{-1}$ to $Sv.yr^{-1}$ and is based on the conversion factors $1.6 \times 10^{-6}$ ergs = 1 MeV, 100 $ergs.g^{-1}$ = rad, 1 rad = 1 rem (for gammas), 1 Sv = 100 rem, $10^3$ g = 1 kg and 1 yr = 3.15 x 10

The total dose at the soil surface for the nth radionuclide ($D_T^n$) is then:

$$D_T^n = \sum_{j=1}^{5} D_j^n$$

Figure 7.3 is a flowsheet illustrating the concepts involved in computer implementation of the model. Table 7.1 contains a parameter listing and Table 7.2 is a copy of the FORTRAN code for the groundshine model. The series solution of equation (7.2) is treated in subroutine SOL.

It should be noted that although a number of approximations have been used in the development and implementation of the groundshine model, it performs reasonably well. The present model was run for a thick (1 m) layer of soil containing a specified level of Th-232 and daughters, Unat and Ra-226. These predictions were compared to the values provided in NCRP No. 45 (1975) for Th-232 and daughters and U-238 and daughters. The thorium predictions were in precise agreement. The predictions for U-238 plus Ra-226 were about 60% of the NCRP No. 45 predictions for the U-238 chain in equilibrium. Tests in Phase II of a model nearly identical to the model incorporated in the current version of UTAP, which contains the full uranium-238 chain, agreed well with measurements (SENES, 1985). In any event the predictions are considered to be satisfactory, especially in light of the observations discussed in Volume 1 that the predicted doses are small relative to the major pathways so that uncertainties of the size indicated are trivial.

FIGURE 7.3

## FLOWSHEET FOR GROUNDSHINE MODEL

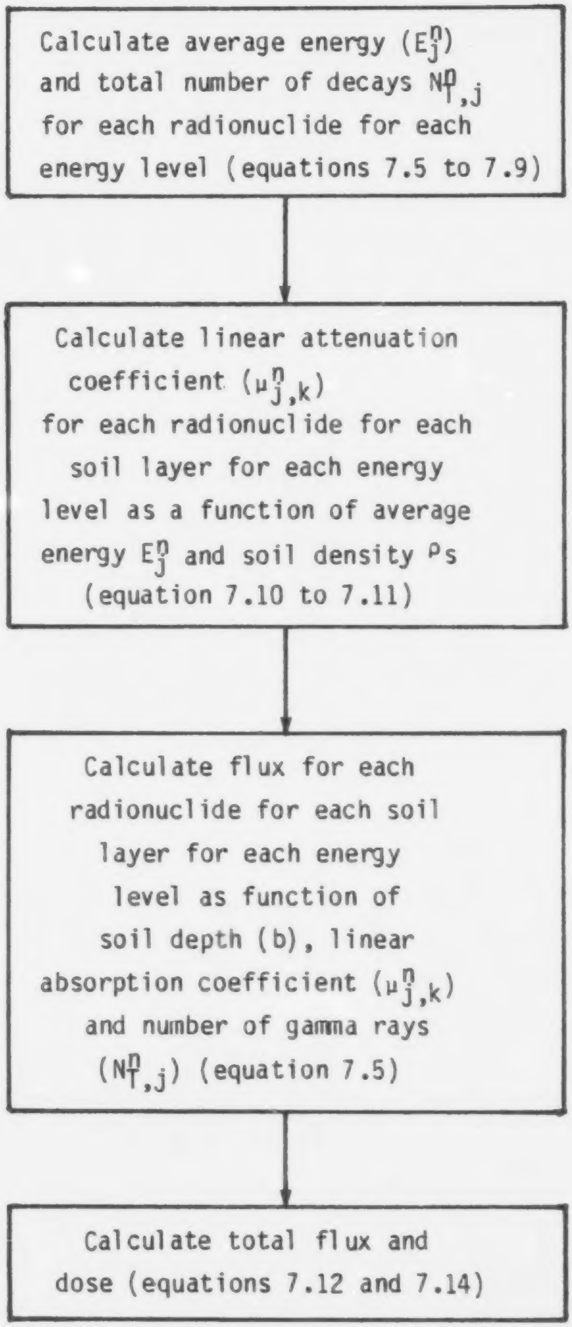

Calculate average energy ($E_j^n$) and total number of decays $N_{T,j}^n$ for each radionuclide for each energy level (equations 7.5 to 7.9)

Calculate linear attenuation coefficient ($\mu_{j,k}^n$) for each radionuclide for each soil layer for each energy level as a function of average energy $E_j^n$ and soil density $\rho_s$ (equation 7.10 to 7.11)

Calculate flux for each radionuclide for each soil layer for each energy level as function of soil depth (b), linear absorption coefficient ($\mu_{j,k}^n$) and number of gamma rays ($N_{T,j}^n$) (equation 7.5)

Calculate total flux and dose (equations 7.12 and 7.14)

**LEGEND:**

n = RADIONUCLIDE
j = ENERGY LEVEL
k = SOIL LAYER

Table 7.1

## GROUNDSHINE MODEL PARAMETERS

| Model Symbol | Description | Units | Nominal Value | Probability Distribution* | Computer Origin | Computer Symbol |
|---|---|---|---|---|---|---|
| $b_k$ | depth of kth soil layer | m |  |  | INPUT | DSOIL(K) |
|  | Layer 1 |  | 0.05 | C(0.05) |  |  |
|  | Layer 2 |  | 0.15 | C(0.15) |  |  |
| E | emanation fraction of radon | - | 0.2 | C(0.2) | INPUT | EMFRAC |
| $E_j^n$ | average energy in jth energy band for nth radionuclide | MeV | calculated | calculated | GSHINE | ENERGY(N,J) |
| $\phi_{Tj}^n$ | total flux in jth energy level for nth radionuclide | gammas $.m^{-2}.s^{-1}$ | calculated | calculated | GSHINE | FLUXTOT(N,J) |
| $D_j^n$ | dose in jth energy band for nth radionuclide | $Sv.yr^{-1}$ | calculated | calculated | GSHINE | GDSE(N,J) |
| $\mu_s$ | mass absorption coefficient for nth radionulcide, kth soil layer and jth energy level | $m^{-1}$ | calculated | calculated | GSHINE | MU(N,K,J) |
| $\mu_{t \cdot j}/\rho_t$ | mass energy adsorption coefficient for jth energy band | $m^2.kg^{-1}$ | see data statement in code | see data statement in code | GSHINE | MUFLSH(J) |
| $N_{Tj}^n$ | number of gamma decays in jth energy band for nth radionuclide | gammas $.kg^{-1}.s^{-1}$ | see data statement in code | see data statement in code | GSHINE | NDEC(N,J) |
| k | number of soil layers | - | 2 | C(2) | INPUT | NLAYER |
| $\rho_s$ | bulk density of kth soil layer | $kg.m^{-3}$ |  |  | SOIL | RHOS(K) |
|  | Layer 1 |  | 129 | LN(129,1.3,20, 450) |  |  |
|  | Layer 2 |  | 1342 | LN(1342,1.1, 1000,1800) |  |  |
| $C_k^n$ | concentration of nth radionuclide in soil layer k | $Bq.m^{-3}$ | calculated | calculated | SOIL | SOILCN(N,K) |
| $S_{pa}^n$ | specific activity for radionuclide n | $Bq.kg^{-1}$ | see data statement in code | see data statement in code | GSHINE | SPA(N) |

Notes

* Distributions are as described on Table 2.2.

Table 7.2

## GROUNDSHINE MODEL CODE LISTING

```
C
C
      SUBROUTINE GSHINE
C     DEVELOPED AND CODED  BY DON BEALS MAR 1986
      INCLUDE 'MODEL.INC'
      INCLUDE 'VAR.INC'
      REAL*4 NNDEC(5,5),ENERG(5,5),SPA(4),MUFLSH(5)
C
C    INITIALIZE # OF DECAYS IN EACH ENERGY LEVEL FOR EACH RADOINUCLIDE
      DATA NNDEC/ 1.18E6,0.0,0.0,1.26E5,0.0,
     &            1.45E5,2.795E6,1.58E6,2.27E6,1.52E6,
     &            1.2E14,0.0,0.0,0.0,0.0,
     &            1.46E12,0.0,0.0,0.0,0.0,
     &            1.46E12,2.01E13,1.72E13,6.23E12,6.22E12/
C
C    INITIALIZE AV. ENERGY IN EACH ENERGY LEVEL FOR EACH RADIONUCLIDE
      DATA  ENERG/9.7E-2,0.0,0.0,9.10E-1,0.0,
     &            5.96E-2,2.63E-1,5.67E-1,9.00E-1,2.57E00,
     &            4.7E-2,0.0,0.0,0.0,0.0,
     &            1.86E-1,0.0,0.0,0.0,0.0,
     &            4.7E-02,3.31E-1,6.09E-1,1.12E0,1.76E0/
C    INITIALIZE SPECIFIC ACTIVITY AND ATTENUATION COEF.
      DATA SPA  /1.23E7,4.03E6,3.00E15,3.66E13/
      DATA MUFLSH /3.0E-3,3.0E-3,3.0E-3,3.0E-3,3.0E-3/
C
C
      NLAYER=INT(LAYER)
      IF(CODGS.GE.1.0)  WRITE(*,104)
104   FORMAT(1X,'SUBROUTINE GSHINE')
      IF(CODGS.GE.2.0)  WRITE(*,100)
100   FORMAT(1X,'RADIONUCLIDE',1X,'ENERGY BAND',5X,'NDEC',10X,'ENERGY')
C     CALCULATE NUMBER OF DECAYS IN JTH ENERGY BAND FOR RADIUM DECAY
C     CHAIN ACCOUNTING FOR RADON EMANATION
      IF(T.EQ.0.0)THEN
         DO 10 N=1,4
            DO 11 J=1,5
               IF(N.LE.3)THEN
C              REARRANGE ARRAYS INTO PROPER ROW AND COLUMN ORDER
                  NDEC(N,J)=NNDEC(J,N)
                  ENERGY(N,J)=ENERG(J,N)
               ELSE
C              ACCOUNT FOR RADON EMANATION
                  NDEC(4,J)=NNDEC(J,4)+NNDEC(J,5)*(1-EMFRAC)
                  ENERGY(4,J)=((ENERG(J,4)*NNDEC(J,4))+(ENERG(J,5)*
     &            (NNDEC(J,5)*(1-EMFRAC))))/NDEC(4,J)
               ENDIF
            IF(CODGS.GE.2.0) WRITE(*,101)N,J,NDEC(N,J),ENERGY(N,J)
101         FORMAT(5X,I2,10X,I2,7X,E10.3,5X,E10.3)
            FLXTOT(N,J)=0.0
```

Table 7.2 (continued)

```
11          CONTINUE
10       CONTINUE
      ENDIF
C
C     CALCULATE LINEAR ATTENUATION COEFFICIENT OF SOIL FOR EACH
C     RADIONUCLIDE AS A FUNCTION OF AVERAGE ENERGY LEVEL
      DO 40 N=1,4
         DO 41 K=1,NLAYER
            DO 42 J=1,5
            IF(ENERGY(N,J).EQ.0.0)THEN
               MU(N,K,J)=0.0
            ELSEIF(ENERGY(N,J).GT.0.0.AND.ENERGY(N,J).LT.3.0)THEN
               MU(N,K,J)=(0.0027*ENERGY(N,J)**(-.320))*RHOS(K)
            ENDIF
C           ELSEIF(ENERGY(N,J).GT.0.0 .AND.ENERGY(N,J).LT.0.1)THEN
C              MU(N,K,J)=(1.84E-4*ENERGY(N,J)**(-1.86))*RHOS(K)
C           ELSEIF(ENERGY(N,J).GT.0.1.AND.ENERGY(N,J).LE.3.0)THEN
C              MU(N,K,J)=(.0063*ENERGY(N,J)**(-.456))*RHOS(K)
C           ENDIF
42          CONTINUE
41       CONTINUE
40    CONTINUE
C
C     CALCULATE FLUX FOR EACH RADIONUCLIDE N FOR EACH
C     FOR EACH SOIL LAYER K AND EACH ENERGY LEVEL J
      DO 20 N=1,4
         DO 21 K=1,NLAYER
            DO 22 J=1,5
               IF(NDEC(N,J).EQ.0.0)THEN
                  FLUX(N,K,J)=0.0
               ELSE
                  XMU(N,K,J)=DSOIL(K)*MU(N,K,J)
                  AACT=(SOILCN(N,K)*NDEC(N,J))/SPA(N)
                  IF (CODSOL.EQ.3.0) WRITE(*,102)N,K,J,MU(N,K,J)
     &            ,XMU(N,K,J),AACT,SOILCN(N,K)
102               FORMAT(1X,'N=',I2,1X,'K=',I2,1X,'J=',I2,1X,'MU=',1X,
     &            E10.3,'XMU=',E10.3,1X,'A=',E10.3,1X,'SOILC='E10.3)
                  FLUX(N,K,J)=SOL(MU(N,K,J),XMU(N,K,J),AACT,DSOIL(K))
               ENDIF
22          CONTINUE
21       CONTINUE
20    CONTINUE
C
      IF (CODGS.GE.2.0)THEN
         DO 50 K=1,NLAYER
            WRITE(*,107)K,DSOIL(K),RHOS(K)
107         FORMAT(1X,'SOIL LAYER=',I2,1X,'DSOIL=',E10.3,1X,'RHOS=',
     &      E10.3)
50       CONTINUE
      ENDIF
C
      IF(CODGS.GE.2.0) WRITE(*,106)
106   FORMAT(1X,'RADIONUCLIDE',1X,'ENERGY LEVEL',1X,'LAYER',5X,
```

Table 7.2 (continued)

```
     &'FLUXTOT',5X,'XMU',5X,'XMUTOT',5X,'FLUX')
C
C     CALCULATE FLUX FOR EACH RADIONUCLIDE FOR EACH LAYER
C     AND CALCULATE DOSE
      SHINED(5,NREC)=0.0
      DO 30 N=1,4
         SHINED(N,NREC)=0.0
         DO 31 J=1,5
            XMUTOT=0.0
            DO 32 K=1,NLAYER
               IF(K.EQ.1)THEN
                  FLXTOT(N,J)=FLUX(N,K,J)
               ELSE
                  XMUTOT=XMUTOT+XMU(N,K-1,J)
                  FLXTOT(N,J)=FLXTOT(N,J)+FLUX(N,K,J)*EXP(-1.0*XMUTOT)
               ENDIF
               IF(CODGS.GE.2.0) WRITE(*,105)N,J,K,FLXTOT(N,J),
     &         XMU(N,K,J),XMUTOT,FLUX(N,K,J)
105            FORMAT(6X,I2,8X,I2,10X,I2,5X,E10.3,1X,E10.3,1X,E10.3,
     &         1X,E10.3)
32          CONTINUE
            GDSE=FLXTOT(N,J)*ENERGY(N,J)*MUFLSH(J)*5.0
            SHINED(N,NREC)=SHINED(N,NREC)+GDSE
31       CONTINUE
C        CALCULATE TOTAL DOSE
         SHINED(5,NREC)=SHINED(5,NREC)+SHINED(N,NREC)
         IF(CODGS.GE.2.0) WRITE(*,103)N,NREC,SHINED(N,NREC)
103      FORMAT(1X,'N=',I2,1X,'NREC=',I2,1X,'SHINED=',E10.3)
30    CONTINUE
      IF(CODGS.GE.2.0) WRITE(*,110)NREC,SHINED(N,NREC)
110   FORMAT(1X,'NREC=',I3,'TOTAL DOSE=',E10.3)
      RETURN
      END
C
C
C
      FUNCTION SOL(MUF,XMU1,AF,B)
C     DEVELOPED AND CODED BY DON BEALS MAR 1986
C     THE FOLLOWING FUNCTION SUBROUTINE CALCULATES FLUX USING A SERIES
C     SOLUTION
      INCLUDE 'VAR.INC'
      REAL*4 MUF,XMU1,SIGN,XN
      REAL*8 PROD,SUM1
C     INITIALIZE NON-ITERATIVE SEGMENT OF SOLUTION
      IF(CODSOL.GE.1.0) WRITE(*,31)
31    FORMAT(1X,'SUBROUTINE SOL')
      SUM1=.5*(((-1.0/MUF)*EXP(-XMU1))+(1/MUF)-(B*(.5772157+
     &LOG(XMU1)-XMU1)))
      SOL2=SUM1*AF
      SIGN=1.0
      PROD=1
      XN=1
C     LOOP TO ADD NEXT PRODUCT ONTO SUM,CALCULATE FLUX AND COMPARE
```

Table 7.2 (continued)

```
C     PREVIOUS ITERATION WITH CURRENT ONE
20    XN=XN+1
         PROD=PROD*XN
         SIGN=SIGN*(-1.0)
         PART=(0.5*B*((XMU1**XN*SIGN)/(XN*PROD)))
         SUM1=SUM1+PART
C     CALCULATE FLUX
         SOL1=SUM1*AF
         IF(CODSOL.EQ.3.0) WRITE(*,30)XN,SOL2,SOL1,SUM1,PART,B
30       FORMAT(1X,'XN=',I2,1X,'SOL2=',E10.3,1X,'SOL1='E10.3,1X
     &   ,'SUM1=',E10.3,1X,'PART=',E10.3,1X,'B=',E10.3)
C     COMPARE FLUXES
         IF(SOL1.GE.SOL2)THEN
            RATIO=SOL2/SOL1
         ELSE
            RATIO=SOL1/SOL2
         ENDIF
C
         IF(RATIO.GE.0.99)THEN
            IF(CODSOL.EQ.3.0)  WRITE(*,32)
32          FORMAT(1X,'RETURN TO SUBROUTINE GSHINE')
            SOL=SOL1
         ELSE
            SOL2=SOL1
            GO TO 20
         ENDIF
         RETURN
         END
```

## 7.6 References

Attix, F.H. and Roesch, W.C. (Eds.), 1968. "Radiation Dosimetry - Volume 1, Fundamentals." Academic Press, New York.

Cember, H., 1969. "Introduction to Health Physics." Pergamon Press.

Chambers, D.B., Mernagh, J.R., and Torrie, R.T., 1981. "Design for Radiation Protection in The Mining of High Grade Uranium Ore." In Proceedings of: International Conference on Radiation Hazards in Mining-Control, Measurement and Medical Aspects, October 4-9, Golden, Colorado, (M. Gomez, Ed.), Publishers: AIMMPE, New York, NY

Chemical Rubber Company (CRC), 1964. "Standard Mathematical Tables - Fourteenth Edition.: S.M. Selby and B. Girling (Eds.), CRC Press, Cleveland, Ohio.

Evans, R.D., 1955. "The Atomic Nucleus." McGraw Hill Book Company Inc.

Kocher, D.C. and Sjoreen, A.L., 1985. "Dose-Rate Conversion Factors for External Exposure to Photon Emitters in Soil." Health Physics, Vol. 48, No. 2, pp. 193-205.

National Council on Radiation Protection (NCRP), 1975. "Natural Background Radiation in the United States." Report No. 45.

SENES Consultants Limited, 1985. "Evaluation of Current Predictive Models for Radiation Exposures in Uranium Mines." Prepared for the Saskatchewan Mine Development Corporation, March.

U.S. Department of Health, Education and Welfare (U.S. DHEW), 1970. "Radiological Health Handbook." Revised edition, January.

## 8.0 TERRESTRIAL VEGETATION MODELS

### 8.1 Introduction

Chapters 4 and 5 describe how the concentration of a radionuclide in the air is calculated (source and dispersion models respectively). Chapter 6 describes how the concentration of a radionuclide in the soil rooting zone is calculated. This chapter shows how these air and soil concentrations are used to model the concentration of a radionuclide in five classes of terrestrial vegetation: above-ground vegetables (AVEGC); below-ground vegetables (BVEGC); summer forage (SUFOC); browse (BRWSC); and lichens (LICHC).

Several changes have been made to these models since Phase II model development. Terrestrial vegetation calculations now include root uptake. Four radionuclides are considered (U-nat, Th-tot, Ra-226, and Pb-210) for each time step. However, not all calculated concentrations vary with location: the summer forage, browse, and lichen concentrations are calculated on an area basis, not for each receptor location, and as such are only calculated once for each radionuclide at each time interval. Vegetable concentrations are, however, calculated at each location j specified as a receptor location (critical or average) for each radionuclide i at each time t.

One basic model is used for all types of terrestrial vegetation. This model is described below. The remaining sections describe how the model is adapted for each type of vegetation.

In this chapter the following subscripts are used to simplify parameter symbols: i is used to identify those parameters that vary with the radionuclide being modelled; t and j indicate that a parameter may vary with time and location respectively; and various environmental media are abbreviated as follows:

v = vegetation
a = air
g = soil (root zone)

Airborne materials can be transferred to the edible portions of vegetables consumed by man or to forage consumed by animals either by direct foliar retention or root uptake.

The following equation was used to calculate the average annual concentration of radionuclide i in vegetation type v at location j and time t (U.S. NRC, 1982):

$$C_{vij} = C_{aij}\ V_d\ F_{rv}\ E_v \left[\frac{1 - \exp\left(-\lambda_{wv}\ t_v\right)}{Y_v\ \lambda_{wv}}\right] + B_{vi}\left[\frac{C_{gij}}{P_g}\right] \quad (8.1)$$

where

$C_{vij}$ = $C_{vij}(t)$ is the resulting concentration of radionuclide i in vegetation v at time t at location j ($Bq.g^{-1}$ (wet weight))

$C_{aij}$ = $C_{aij}(t)$ is the average concentration of radionuclide i in the air at location j at time t ($Bq.m^{-3}$)

$V_d$ = the deposition velocity ($m.s^{-1}$)

$F_{rv}$ = the fraction of the total deposition retained on the plant surface of vegetation type v (0 to 1)

$E_v$ = the fraction of the foliar deposition retained on edible portions of vegetation type v (0 to 1)

$\lambda_{wv}$ = a decay constant accounting for weathering losses from vegetation type v ($s^{-1}$) and if significant, radioactive decay

$t_v$ = the duration of the plant exposure to atmospheric deposition for vegetation type v (s)

$Y_v$ = the yield density for vegetation type v (g(wet weight)$.m^{-2}$)

$B_{vi}$ = the soil-to-plant transfer coefficient for radionuclide i and vegetation type v ($Bq.g^{-1}$ (wet weight) plant per $Bq.g^{-1}$ (dry weight) soil)

$C_{gij}$ = $C_{gij}(t)$ is the average concentration of radionuclide i in the root zone of the soil at location j at time t ($Bq.m^{-3}$)

$P_g$ = density of soil (g(dry wt)$.m^{-3}$)

The first term on the right-hand side of equation (8.1) represents direct foliar retention; the second term represents root uptake. Irrigation is not included in this model.

Note that time dependence is due only to the time dependence of the air and soil concentrations.

The model assumes that the system is in equilibrium. For the foliar deposition model this means that the weathering half-life is sufficiently less than the period of deposition and radioactive half-life so that the concentration of the radionuclides reaches a steady state level. For annual vegetation this is a valid assumption. However, this may not be entirely appropriate for lichens (see Section 8.6 for further details), although it is a reasonable approximation. The reader is referred to Cassaday et al. (1985) for more information on what this model and its parameters represent and their limitations.

The deposition velocity ($V_d$) is common in all models, as it relates to characteristics of the windborne tailings dust particles. In this report $V_d$ is intended to capture the combined effect of the various dry and wet deposition processes which effectively transfer dust particles from the air either to the ground or to vegetation. Literature values of dry deposition velocities vary widely, however, a nominal value of about $1 \times 10^{-2}$ m.s$^{-1}$ is sometimes used in the absence of specific data (Sehmel 1980). Similarly, literature values for particle wet deposition velocities also vary widely. For present purposes and largely based on data reported by McMahon and Denison (1979) a nominal wet deposition velocity of $1 \times 10^{-2}$ m.s$^{-1}$ has been assumed. Thus a nominal all inclusive deposition velocity of 0.02 m.s$^{-1}$ has been assumed. Based on the experience of study team members the deposition velocity was assumed to range uniformly over the interval from 0.003 to 0.03 m.s$^{-1}$.

Probabilistic analysis requires that appropriate probability distributions be ascribed to the model input parameters. The distributions of transfer factors reported are generally skewed in shape with a peak concentration at some relatively low level and a long tail towards the high end of the scale.

Several studies have found radionuclide concentrations to be lognormally distributed (Tracy et al., 1983; Sheppard and Thibault, 1983). Cassaday et al. (1985) examined the data base available for characterizing the soil-to-plant transfer coefficients for root uptake of a specific radionuclide and vegetation type as included in the model of terrestrial transport of radionuclides. Appropriate probability distributions were derived for the soil-to-plant transfer coefficients from this data base. The data available was best characterized by lognormal distributions. Beta and Weibull distributions also characterized the data fairly well. Where data for a specific radionuclide and vegetation type was not available, U.S. NRC (1982) values were used for the geometric mean with the geometric standard deviation assigned from evaluation of the derived transfer coefficient distributions.

Other parameters were also assigned distributions. The extent of this variation was based on the collective opinion of the study group as to how certain they were about the nominal value of particular parameters. Such parameters were typically allowed to vary 10 to 50% about the nominal values and were given a triangular or uniform distribution. The vegetation model parameters are summarized in Tables 8.1 to 8.5. Computer code listing for the terrestrial vegetation models are provided in Table 8.6.

The component model aspects of the Phase III studies have largely focussed on the implementation of environmental and dose models. Comparatively little effort has been expended on issues of fundamental environmental science or on the development of parameter distributions. Both aspects would need to be reviewed on a case by case basis with models being modified or upgraded if required and site/species-specific parameters being input to the models insofar as practicable.

## 8.2 Above-Ground and Below-Ground Vegetables (AVEGC and BVEGC)

The concentrations in above- and below-ground vegetables are both calculated using equation (8.1) at each specified receptor location j, for each radionuclide i, at each time interval t. The model and parameter values do not vary with receptor type.

Tables 8.1 and 8.2 summarize the parameter values and distributions used for above-ground and below-ground vegetables respectively. The values for $F_{rv}$, $E_v$, $t_v$, $Y_v$ and $\lambda_{wv}$ were allowed to vary uniformly around the nominal value recommended by the U.S. NRC (1982), whereas $t_v$ was assigned a triangular distribution around the nominal value recommended by the U.S. NRC (1982).

Values for $B_{vi}$ are from the brief literature review conducted as part of Phase II studies (see the introduction for further details).

The modelling approach adopted is very general in that all types of above-ground vegetation are grouped together, as are all types of below-ground vegetation. In some instances the user may wish to incorporate parameters for a single crop. Potatoes in particular are often specifically modelled. This may be done by varying parameter values as appropriate.

## 8.3 Summer Forage (SUFOC)

The average concentration of radionuclide i in summer forage is used as an input to the calculation of the concentration of radionuclide i in caribou flesh. Caribou are migratory animals, and as such any caribou that do feed in the model area were assumed to range over the entire area. Thus, only one value of the concentration of radionuclide i in summer forage is modelled at each time interval t using an area average air concentration (see Section 5.1) and an average soil concentration calculated using the same area average air concentration (see Section 6.1).

Summer forage is assumed to consist largely of grass. Table 8.3 summarizes the parameter values and distributions used. The values for $E_v$, $t_v$, $Y_v$ and $\lambda_{wv}$ were allowed to vary uniformly around the nominal value recommended by the U.S. NRC (1982). $F_{rv}$ was taken from the discussion paper by Hoffman et al., presented in Volume 2 of Phase II. Values for $B_{vi}$ are from Cassaday et al. (1985) which was included in Volume 2 of Phase II (see also the introduction to this chapter).

### 8.4 Browse (BRWSC)

Browse is meant to represent the average concentration of radionuclide i in that portion of a moose's diet which comes from terrestrial vegetation. This covers a wide range - from grasses and foliage of small shrubs in the summer to twigs in the winter. Aquatic vegetation eaten by moose is described in Section 11.3.3.

Data which would permit direct estimation of the transfer of radionuclides from air and soil to browse were not found in the literature. Hence the parameter values for summer forage shown in Table 8.4 were used to evaluate this pathway. Some small comfort is provided however for the pathway of deposition from air to vegetation since studies reported by Bondietti et al. (1984) indicate that normalized deposition velocities ($m^3.kg^{-1}.s^{-1}$) for submicron particles do not vary greatly among different deciduous and coniferous species.

Although individuals may roam over very large areas, in general moose are not migratory and tend to have much smaller home ranges than caribou (Lynch, 1976; Taylor and Ballard, 1979; Saunders and Williamson, 1972). For this reason, the moose modelled in Phase III was assumed to range over the watershed. An area average air concentration of radionuclide i was calculated for the watershed (see Section 5.1) and an average soil concentration was calculated using this area average air concentration. These two values were then used to calculate the concentration of radionuclide i in browse.

### 8.5 Lichens (LICHC)

The average concentration of radionuclide i in lichens is used as an input to the calculation of the concentration of radionuclide i in caribou flesh. Caribou are migratory animals, and as such any caribou that do feed in the model area were assumed to range over the entire area. Thus, only one value of the concentration of radionuclide i in lichens is modelled at each time t using an area average air concentration (see Section 5.1).

The description of the lichen model presented here is much more detailed than that given for the other types of vegetation, as lichens are substantially different in that they have no root system and have a very long life span. The following is largely excerpted from SENES (1983).

Since lichens have no root system, only the accumulation of radionuclides via direct deposition from the air was considered, i.e. using equation (8.1) with $B_{vi} = 0$ for all radionuclides. Nominal values for the other parameters in equation (8.1) that are specific to the lichen were chosen as discussed below and summarized in Table 8.5. Distributions were assigned as discussed in the introduction to this chapter.

Studies of cesium-137 deposition from fallout in northern Sweden indicate that up to 95% of that deposited on the lichen may be retained (Garner, 1972). For this study, a value of $F_{rv} = 0.95$ was assumed for all radionuclides. Because the entire plant may be eaten by the grazing caribou, the fraction $E_v$ of the deposited radionuclides reaching edible portions of the plant was assumed to equal 1.0. The yield density $Y_v$ of the lichens was assumed to have a nominal value of 500 $g.m^{-2}$ (Garner, 1972).

Accumulation of deposited material occurs over long periods because of the relatively long lifetimes of lichens (tens of years). For this study, the deposition period $t_v$ in equation (8.1) was assumed to be sufficiently long so that an equilibrium concentration of radionuclides in the lichens was reached, that is, $\exp(-\lambda_w t_v) \approx 0$.

The value of the "weathering" decay constant $\lambda_{wv}$ required special consideration because of the unique nature of lichens. The decay constant accounts for all mechanisms by which the deposited radioactivity is removed from the plant.

Most studies on the accumulation of radionuclides by lichen refer to radionuclides in fallout. The effective half-life of cesium-137 has been estimated variously as 17 years and 6 to 10 years (Garner, 1972); the weathering half-life excluding radioactive decay may thus be as long as 30 years although many studies point to shorter half-lives. Miettinen (1967) estimated the overall effective half-life in lichens in Finland to be about 5 years. A number of other studies indicate effective half-lives of less than 10 years for cesium-137 (Tuominen and Jaakkola, 1973) or less than 15 years if only processes other than radioactive decay are considered. It has also been noted that the effective half-life of strontium-90, which is chemically similar to radium is much shorter than that of cesium-137 (Tuominen and Jaakkola, 1973). Niebvoer et al. (1978) report "mean turnover times" of calcium (which is also chemically similar to radium) of 1.7 years or an effective half-life of about 2.5 years. The effective half-life of lead-210 in the lichen carpet has been estimated to be 7±2 years (Garner, 1972).

Based on the above considerations a conservative effective half-life in lichens of 10 years was assumed for all radionuclides considered in this study. It is recognized that this is an approximation but until better information is available on the weathering half-life, including the radioactive half-life explicitly in the calculation is not worthwhile.

Table 8.1

## ABOVE GROUND VEGETABLES MODEL VARIABLES

| Model Symbol | Description | Units | Nominal Value | Probability Distribution* | Computer Origin | Computer Symbol |
|---|---|---|---|---|---|---|
| $C_{aij}(t)$ | air concentration of radionuclide i | $Bq.m^{-3}$ | calculated | calculated | AIRDIS | AIRC(i,j)i=1,4,j≤80 |
| $C_{vij}(t)$ | concentration of radionuclide i in above ground vegetable | $Bq.g^{-1}$ | calculated | calculated | VEGCON | AVEGC(i,j)i=1,4 j≤80 |
| $F_{ra}$ | fraction of total deposition retained on surface of above ground vegetables | - | 0.2 | U(0.1,0.3) | INPUT | FDEPSF(1) |
| $E_a$ | fraction of plant deposition retained on edible portions of above ground vegetables | - | 0.9 | U(0.8,1.0) | INPUT | FDEPED(1) |
| $t_a$ | duration of exposure to deposition for above ground vegetables | s | $5.184\times10^{6}$ | T($2.6\times10^{6}$, $5.2\times10^{6}$, $7.8\times10^{6}$) | INPUT | DUREXP (1) |
| $V_d$ | deposition velocity | $m.s^{-1}$ | 0.02 | U(0.003, 0.03) | INPUT | DEPVEL |
| $Y_a$ | yield density for above ground vegetables | $g.m^{-2}$ | $2.0\times10^{3}$ | U($1.0\times10^{3}$,$3.0\times10^{3}$) | INPUT | YDEN(1) |
| $\lambda_{wv}$ | decay constant accounting for weathering loss for above ground vegetables | $s^{-1}$ | $5.73\times10^{-7}$ | U($2.9\times10^{-7}$,$1.2\times10^{-6}$) | INPUT | VEGLAM(1) |
| $B_{ai}$ | soil-to-plant transfer coefficient for above ground vegetables for: | $\frac{Bq.g^{-1}\ (wet)}{Bq.g^{-1}\ (dry)}$ | | | INPUT | SPTCAV(i) i=1,4 |
| | U-nat | | $6.08\times10^{-4}$ | LN($6.08\times10^{-4}$,8.90,$7.67\times10^{-6}$,$7.00\times10^{-3}$) | | |
| | Th-tot | | $4.20\times10^{-3}$ | LN($4.20\times10^{-3}$,9.00,$5.19\times10^{-5}$,$3.40\times10^{-1}$) | | |
| | Pb-210 | | $4.00\times10^{-3}$ | LN($4.00\times10^{-3}$,9.00,$4.94\times10^{-5}$,$3.24\times10^{-1}$) | | |
| | Ra-226 | | $8.47\times10^{-3}$ | LN($8.47\times10^{-3}$,10.3,$8.03\times10^{-5}$,$8.93\times10^{-1}$) | | |
| $P_g$ | soil density | $g(dry).m^{-3}$ | calculated | calculated | VEGCON | DRYRHO |
| $C_{gij}(t)$ | concentration of radionuclide i in the root zone of the soil | $Bq.m^{-3}$ | calculated | calculated | SOIL | SOILC(1,J) i=1,4 j≤80 |

Note

* Distributions are as described in Table 2.2

Table 8.2

## BELOW GROUND VEGETABLES MODEL VARIABLES

| Model Symbol | Description | Units | Nominal Value | Probability Distribution* | Computer Source | Computer Symbol |
|---|---|---|---|---|---|---|
| $C_{aij}(t)$ | air concentration of radionuclide i | $Bq.m^{-3}$ | calculated | calculated | AIRDIS | AIRC(i,j)i=1,4, $j \leq 80$ |
| $C_{bij}(t)$ | concentration of radionuclide i in below ground vegetable | $Bq.g^{-1}$ | calculated | calculated | VEGCOM | BVEGC(i,j)i=1,4 $j \leq 80$ |
| $F_{rb}$ | fraction of total deposition retained on surface of below ground vegetables: | - | 0.2 | U(0.1,0.3) | INPUT | FDEPSF(2) |
| $E_b$ | fraction of plant deposition retained on edible portions of below ground vegetables | - | 0.1 | U(0.05, 0.15) | INPUT | FDEPED(2) |
| $t_b$ | duration of exposure to deposition for below ground vegetables | s | $5.184 \times 10^5$ | T($2.6 \times 10^6$, $5.2 \times 10^6$, $7.8 \times 10^6$) | INPUT | DUREXP (2) |
| $V_d$ | deposition velocity | $m.s^{-1}$ | 0.02 | U(0.003, 0.03) | INPUT | DEPVEL |
| $Y_b$ | yield density for below ground vegetables | $g.m^{-2}$ | $2.0 \times 10^3$ | U($1.0 \times 10^3$,$3.0 \times 10^3$) | INPUT | YDEN(2) |
| $\lambda_{wb}$ | decay constant accounting for weathering loss for below ground vegetables | $s^{-1}$ | $5.73 \times 10^{-7}$ | U($2.9 \times 10^{-7}$,$1.2 \times 10^{-6}$) | INPUT | VEGLAM (2) |
| $B_{bi}$ | soil-to-plant transfer coefficient for below ground vegetables for: | $\frac{Bq.g^{-1}\ (wet)}{Bq.g^{-1}\ (dry)}$ | | | INPUT | SPTCBV(i) i=1,4 |
| | U-nat | | $3.17 \times 10^{-4}$ | LN($3.17 \times 10^{-4}$,3.93,$2.06 \times 10^{-5}$,$4.89 \times 10^{-3}$) | | |
| | Th-tot | | $4.20 \times 10^{-3}$ | LN($4.20 \times 10^{-3}$,4.00,$2.62 \times 10^{-4}$,$6.72 \times 10^{-2}$) | | |
| | Pb-210 | | $4.00 \times 10^{-3}$ | LN($4.00 \times 10^{-3}$,4.00,$2.50 \times 10^{-4}$,$6.40 \times 10^{-2}$) | | |
| | Ra-226 | | $2.65 \times 10^{-3}$ | LN($2.65 \times 10^{-3}$,4.52,$1.29 \times 10^{-4}$,$6.60 \times 10^{-2}$) | | |
| $P_g$ | soil density | $g(dry).m^{-3}$ | calculated | calculated | VEGCON | DRYRHO |
| $C_{gij}(t)$ | concentration of radionuclide i in the root zone of the soil | $Bq.m^{-3}$ | calculated | calculated | SOIL | SOILC(i,j) i=1,4, $j \leq 80$ |

Note

* Distributions are as described in Table 2.2.

Table 8.3

SUMMER FORAGE MODEL VARIABLES

| Model Symbol | Description | Units | Nominal Value | Probability Distribution* | Computer Origin | Computer Symbol |
|---|---|---|---|---|---|---|
| $C_{ai}(t)$ | average air concentration of radionuclide i over the whole airshed (n+1 locations) | $Bq.m^{-3}$ | calculated | calculated | AIRDIS | AIRC(i,n+1)i=1,4<br>n = total number of receptor locations |
| $C_{si}(t)$ | concentration of radionuclide i in summer forage | $Bq.g^{-1}$ | calculated | calculated | VEGCON | SUFOC(i)i=1,4 |
| $F_{rs}$ | fraction of total deposition retained on surface of summer forage | - | 0.2 | N(0.47,0.3,0.01,1.0) | INPUT | FDEPSF(3) |
| $E_s$ | fraction of plant deposition retained on edible portions of summer forage | - | 0.9 | U(0.8,1.0) | INPUT | FDEPED(3) |
| $t_s$ | duration of exposure to deposition for summer forage | s | $2.592\times10^6$ | $U(1.3\times10^6, 3.9\times10^6)$ | INPUT | DUREXP (3) |
| $V_d$ | deposition velocity | $m.s^{-1}$ | 0.02 | U(0.003, 0.03) | INPUT | DEPVEL |
| $Y_s$ | yield density for summer forage | $g.m^{-2}$ | $7.5\times10^2$ | $U(5.0\times10^2,1.0\times10^3)$ | INPUT | YDEN(3) |
| $\lambda_{ws}$ | decay constant accounting for weathering loss for summer forage | $s^{-1}$ | $5.73\times10^{-7}$ | $U(2.9\times10^{-7},1.2\times10^{-6})$ | INPUT | VEGLAM (3) |
| $B_{si}$ | soil-to-plant transfer coefficient for summer forage for: | $\frac{Bq.g^{-1}\ (wet)}{Bq.g^{-1}\ (dry)}$ |  |  | INPUT | SPTCSF(i) i=1,4 |
|  | U-nat |  | $6.60\times10^{-3}$ | $LN(6.60\times10^{-3},8.91,8.31\times10^{-5},5.24\times10^{-1})$ |  |  |
|  | Th-tot |  | $2.23\times10^{-2}$ | $LN(2.23\times10^{-2},9.50,2.47\times10^{-4},2.01\times10^{0})$ |  |  |
|  | Pb-210 |  | $2.16\times10^{-2}$ | $LN(2.16\times10^{-2},3.55,1.71\times10^{-3},2.71\times10^{-1})$ |  |  |
|  | Ra-226 |  | $2.11\times10^{-1}$ | $LN(2.11\times10^{-1},3.63,1.87\times10^{-3},2.39\times10^{-1})$ |  |  |
| $P_g$ | soil density | $g(dry).m^{-3}$ | calculated | calculated | VEGCON | DRYRHO |
| $C_{gi}(t)$ | concentration of radionuclide i in the root zone of the soil | $Bq.m^{-3}$ | calculated | calculated | SOIL | SOILC(i,n+1) i=1,4<br>n = total number of receptor locations |

Note

* Distributions are as described in Table 2.2.

Table 8.4

## BROWSE MODEL VARIABLES

| Model Symbol | Description | Units | Nominal Value | Probability Distribution* | Computer Origin | Computer Symbol |
|---|---|---|---|---|---|---|
| $C_{ai}(t)$ | average air concentration of radionuclide i over the watershed (n+2 locations) | $Bq.m^{-3}$ | calculated | calculated | AIRDIS | AIRC(i,n+2) i=1,4<br>n = total number of receptor locations |
| $C_{bi}(t)$ | concentration of radionuclide i in browse | $Bq.g^{-1}$ | calculated | calculated | VEGCON | BRWSC(i)i=1,4 |
| $F_{rb}$ | fraction of total deposition retained on surface of browse | - | 0.2 | N(0.47,0.3,0.01,1.0) | INPUT | FDEPSF(4) |
| $E_b$ | fraction of plant deposition retained on edible portions of browse | - | 0.9 | U(0.8,1.0) | INPUT | FDEPED(4) |
| $t_b$ | duration of exposure to deposition for browse | s | $2.592\times10^{6}$ | U($1.3\times10^{6}$, $3.9\times10^{6}$) | INPUT | DUREXP (4) |
| $V_d$ | deposition velocity | $m.s^{-1}$ | 0.02 | U(0.003, 0.03) | INPUT | DEPVEL |
| $Y_b$ | yield density for browse | $g.m^{-2}$ | $7.5\times10^{2}$ | U($5.0\times10^{2}$,$1.0\times10^{3}$) | INPUT | YDEN(4) |
| $\lambda_{wb}$ | decay constant accounting for weathering loss for browse | $s^{-1}$ | $5.73\times10^{-7}$ | U($2.9\times10^{-7}$,$1.2\times10^{-6}$) | INPUT | VEGLAM (4) |
| $B_{sb}$ | soil-to-plant transfer coefficient for browse for: | $\frac{Bq.g^{-1}\ (wet)}{Bq.g^{-1}\ (dry)}$ | | | INPUT | SPTCB(i) i=1,4 |
| | U-nat | | $6.60\times10^{-3}$ | LN($6.60\times10^{-3}$,8.91,$8.31\times10^{-5}$,$5.24\times10^{-1}$) | | |
| | Th-tot | | $2.23\times10^{-2}$ | LN($2.23\times10^{-2}$,9.50,$2.47\times10^{-4}$,$2.01\times10^{0}$) | | |
| | Pb-210 | | $2.16\times10^{-2}$ | LN($2.16\times10^{-2}$,3.55,$1.71\times10^{-3}$,$2.71\times10^{-1}$) | | |
| | Ra-226 | | $2.11\times10^{-1}$ | LN($2.11\times10^{-1}$,3.63,$1.87\times10^{-3}$,$2.39\times10^{-1}$) | | |
| $P_g$ | soil density | $g(dry).m^{-3}$ | calculated | calculated | VEGCON | DRYRHO |
| $C_{gi}(t)$ | concentration of radionuclide i in the root zone of the soil | $Bq.m^{-3}$ | calculated | calculated | SOIL | SOILC(i,n+2) i=1,4<br>n = total number of receptor locations |

Note

* Distributions are as described in Table 2.2.

## Table 8.5

## LICHEN MODEL VARIABLES

| Model Symbol | Description | Units | Nominal Value | Probability Distribution* | Computer Origin | Computer Symbol |
|---|---|---|---|---|---|---|
| $C_{ai}(t)$ | average air concentration of radionuclide i over the whole airshed (n+1 locations) | $Bq.m^{-3}$ | calculated | calculated | AIRDIS | AIRC(i,n+1) i=1,4<br>n = total number of receptor locations |
| $C_{li}(t)$ | concentration of radionuclide i in lichen | $Bq.g^{-1}$ | calculated | calculated | VEGCON | LICHC (i)i=1,4 |
| $F_{rl}$ | fraction of total deposition retained on surface of lichen: | - | 0.95 | U(0.8,1.0) | INPUT | FDEPSF(5) |
| $E_l$ | fraction of plant deposition retained on edible portions of lichen | - | 1.0 | U(0.8,1.0) | INPUT | FDEPED(5) |
| $t_l$ | duration of exposure to deposition for lichen | s | $1 \times 10^{10}$ | $C(1 \times 10^{10})$ | INPUT | DUREXP (5) |
| $V_d$ | deposition velocity | $m.s^{-1}$ | 0.02 | U(0.003, 0.03) | INPUT | DEPVEL |
| $Y_l$ | yield density for lichens | $g.m^{-2}$ | $5.0 \times 10^2$ | $U(4.0 \times 10^2, 6.0 \times 10^2)$ | INPUT | YDEN(5) |
| $\lambda_{wl}$ | decay constant accounting for weathering loss for lichens | $s^{-1}$ | $2.19 \times 10^{-9}$ | $U(1.5 \times 10^{-9}, 4.4 \times 10^{-9})$ | INPUT | VEGLAM (5) |
| $B_{li}$ | soil-to-plant transfer coefficient for lichens for: | $\frac{Bq.g^{-1} \text{ (wet)}}{Bq.g^{-1} \text{ (dry)}}$ |  |  | INPUT | SPTCB(i) i=1,4 |
|  | U-nat |  | 0.0 | C(0.0) |  |  |
|  | Th-tot |  | 0.0 | C(0.0) |  |  |
|  | Pb-210 |  | 0.0 | C(0.0) |  |  |
|  | Ra-226 |  | 0.0 | C(0.0) |  |  |
| $P_g$ | soil density | $g(dry).m^{-3}$ | calculated | calculated | VEGCON | DRYRHO |
| $C_{gi}(t)$ | concentration of radionuclide i in the root zone of the soil | $Bq.m^{-3}$ | calculated | calculated | SOIL | SOILC(i,n+1) i=1,4<br>n = total number of receptor locations |

**Note**

* Distributions are as described in Table 2.2.

Table 8.6

## TERRESTRIAL VEGETATION MODEL CODE LISTING

```
      SUBROUTINE VEGCON
      INCLUDE 'MODEL.INC'
      INCLUDE 'VAR.INC'
      IF(NREC.EQ.1)THEN
         DO 10 N=1,5
            CONST(N)=DEPVEL*FDEPSF(N)*FDEPED(N)*(1.0-EXP(-VEGLAM(N)*
     +               DUREXP(N)))/(YDEN(N)*VEGLAM(N))
10       CONTINUE
         DRYRHO=1000.0*RHOS(2)
      ENDIF
      DO 11 I=1,4
         IF(NREC.LE.NRECEP)THEN
            AVEGC(I,NREC)=CONST(1)*AIRC(I,NREC)+SPTCAV(I)*SOILC
     +                    (I,NREC)/DRYRHO
            BVEGC(I,NREC)=CONST(2)*AIRC(I,NREC)+SPTCBV(I)*SOILC
     +                    (I,NREC)/DRYRHO
         ENDIF
         IF(NREC.EQ.NRECEP+2)THEN
            SUFOC(I)=CONST(3)*AIRC(I,NRECEP+1)+SPTCSF(I)*SOILC
     +               (I,NRECEP+1)/DRYRHO
            BRWSC(I)=CONST(4)*AIRC(I,NRECEP+2)+SPTCB(I)*SOILC
     +               (I,NRECEP+2)/DRYRHO
            LICHC(I)=CONST(5)*AIRC(I,NRECEP+1)+SPTCL(I)*SOILC
     +               (I,NRECEP+1)/DRYRHO
         ENDIF
11    CONTINUE
C
      IF(CODVEG.EQ.1.0.OR.CODVEG.EQ.2.0.OR.CODVEG.EQ.3.0)THEN
         WRITE(*,100)
      ENDIF
      IF(NREC.EQ.NRECEP+2)THEN
         IF(CODVEG.EQ.3.0)THEN
            WRITE(*,101)DRYRHO,DEPVEL,FDEPSF(1)
            DO 12 I=2,5
               WRITE(*,102)FDEPSF(I)
12          CONTINUE
            WRITE(*,103)FDEPED(1)
            DO 13 I=2,5
               WRITE(*,104)FDEPED(I)
13          CONTINUE
            WRITE(*,105)VEGLAM(1)
            DO 14 I=2,5
               WRITE(*,106)VEGLAM(I)
14          CONTINUE
            WRITE(*,107)DUREXP(1)
            DO 15 I=2,5
               WRITE(*,108)DUREXP(I)
15          CONTINUE
            WRITE(*,109)YDEN(1)
            DO 16 I=2,5
```

Table 8.6 (continued)

```
               WRITE(*,110)YDEN(I)
16          CONTINUE
            WRITE(*,111)(SPTCAV(I),I=1,4)
            WRITE(*,112)(SPTCBV(I),I=1,4)
            WRITE(*,113)(SPTCSF(I),I=1,4)
            WRITE(*,114)(SPTCB(I),I=1,4)
            WRITE(*,115)(SPTCL(I),I=1,4)
            WRITE(*,116)
            DO 17 NREC=1,NRECEP
               WRITE(*,117)(AIRC(I,NREC),I=1,4)
17          CONTINUE
            WRITE(*,118)(AIRC(I,NRECEP+1),AIRC(I,NRECEP+2),I=1,4)
            WRITE(*,119)
            DO 18 NREC=1,NRECEP
               WRITE(*,117)(SOILC(I,NREC),I=1,4)
18          CONTINUE
            WRITE(*,118)(SOILC(I,NRECEP+1),SOILC(I,NRECEP+2),I=1,4)
         ENDIF
         IF(CODVEG.EQ.2.0.OR.CODVEG.EQ.3.0)THEN
            WRITE(*,120)
            DO 19 N=1,NRECEP
               WRITE(*,121)(AVEGC(I,N),I=1,4)
19          CONTINUE
            WRITE(*,122)
            DO 20 N=1,NRECEP
               WRITE(*,121)(BVEGC(I,N),I=1,4)
20          CONTINUE
            WRITE(*,123)(SUFOC(I),I=1,4)
            WRITE(*,124)(BRWSC(I),I=1,4)
            WRITE(*,125)(LICHC(I),I=1,4)
         ENDIF
      ENDIF
C
100   FORMAT(///1X,'VEGETATION MODEL')
101   FORMAT(/1X,'DRY SOIL DENSITY',E12.4/1X,'DEPOSITION VELOCITY',
     +       E12.4/1X,'FRACTION OF DEPOSITION RETAINED ON SURFACE OF ',
     +       'PLANT',E12.4)
102   FORMAT(52X,E12.4)
103   FORMAT(1X,'FRACTION OF DEPOSITION RETAINED ON EDIBLE PORTION OF',
     +       ' PLANT',E12.4)
104   FORMAT(59X,E12.4)
105   FORMAT(1X,'DECAY CONSTANT ACCOUNTING FOR WEATHERING LOSS',E12.4)
106   FORMAT(46X,E12.4)
107   FORMAT(1X,'DURATION OF EXPOSURE TO DEPOSITION',E12.4)
108   FORMAT(35X,E12.4)
109   FORMAT(1X,'YIELD DENSITY',E12.4)
110   FORMAT(14X,E12.4)
111   FORMAT(1X,'SOIL-TO-PLANT TRANSFER COEFFICIENT FOR ABOVE GROUND V',
     +       'EGETATION'/1X,4(E12.4))
112   FORMAT(1X,'SOIL-TO-PLANT TRANSFER COEFFICIENT FOR BELOW GROUND V',
     +       'EGETATION'/1X,4(E12.4))
113   FORMAT(1X,'SOIL-TO-PLANT TRANSFER COEFFICIENT FOR SUMMER FORAGE ',
     +       'VEGETATION'/1X,4(E12.4))
```

Table 8.6 (continued)

```
114   FORMAT(1X,'SOIL-TO-PLANT TRANSFER COEFFICIENT FOR BROWSE VEGETAT',
     +       'ION'/1X,4(E12.4))
115   FORMAT(1X,'SOIL-TO-PLANT TRANSFER COEFFICIENT FOR LICHEN VEGETAT',
     +       'ION'/1X,4(E12.4))
116   FORMAT(1X,'ATMOSPHERIC CONCENTRATION OF THE RADIONUCLIDES AT THE',
     +       ' RECEPTORS')
117   FORMAT(1X,4(E12.4))
118   FORMAT(1X,'AVERAGE CONCENTRATION',/1X,4(E12.4)/1X,'AVERAGE WATER',
     +       'SHED CONCENTRATION',/1X,4(E12.4))
119   FORMAT(1X,'CONCENTRATION OF THE RADIONUCLIDES IN THE SOIL AT THE',
     +       ' RECEPTORS')
120   FORMAT(/1X,'RADIONUCLIDE CONCENTRATION IN ABOVE GROUND VEGETATA',
     +       'BLES')
121   FORMAT(1X,4(E12.4))
122   FORMAT(1X,'RADIONUCLIDE CONCENTRATION IN BELOW GROUND VEGETATAB',
     +       'ES')
123   FORMAT(1X,'AVERAGE RADIONUCLIDE CONCENTRATION IN SUMMER FORAGE',/
     +       1X,4(E12.4))
124   FORMAT(1X,'AVERAGE RADIONUCLIDE CONCENTRATION IN BROWSE',/1X,
     +       4(E12.4))
125   FORMAT(1X,'AVERAGE RADIONUCLIDE CONCENTRATION IN LICHEN'/1X,
     +       4(E12.4))
C
      RETURN
      END
```

## 8.6 References

Bondietti, E.A., Hoffman, F.O., and Larsen, I.L., 1984. "Air-to-Vegetation Transfer Rates of Natural Submicron Aerosols." J. Environmental Radioactivity, Vol. 1, pp. 5-27.

Cassaday, V.J., Halbert, B.E. and Stone, D., 1985. "The Data Base Available to Develop Distributions for Use in Modelling the Transfer of Airborne Radioactivity to Terrestrial Vegetation". Presented in a Report Entitled - Probabilistic Model Development for the Assessment of the Long-Term Effects of Uranium Mill Tailings in Canada: Phase II, Vol. 2. Prepared by SENES Consultants Limited for the National Uranium Tailings Program, Canada Centre for Mineral and Water Technology, Energy, Mines and Resources Canada, Ottawa, Ontario.

Garner, R.J., 1972. "Transfer of Radioactive Materials from the Terrestrial Environment to Animals and Man." CRC Press, Cleveland.

Hoffman, F.O., Gardner, R.H. and Blaylock, B.G., 1985. "The Transfer of Radium from the Atmosphere to Pasture Vegetation." Presented in a Report Entitled - Probabilistic Model Development for the Assessment of the Long-Term Effects of Uranium Mill Tailings in Canada: Phase II, Vol. 2. Prepared by SENES Consultants Limited for the National Uranium Tailings Program, Canada Centre for Mineral and Water Technology, Energy, Mines and Resources Canada, Ottawa, Ontario.

Lynch, G.M., 1976. "Some Long Range Movements of Radio-Tagged Moose in Alberta." Proceedings of the 12th North American Moose Conference and Workshop, St. John's, Nfld., March, pp. 220-235.

McMahon, T.A., and Denison, P.J., 1979. "Empirical Atmospheric Deposition Parameters - A Survey." Atmos. Env., Vol. 13, pp. 571-585.

Miettinen, J.K., 1967. "Concentration of Cs-137 and Fe-55 Through Food Chains in Arctic and Subarctic Regions." Proceedings of an International Symposium held in Stockholm, 1966.

Niebvoer, E., Richardson, D.H.S., and Tomassini, F.D., 1978. "Mineral Uptake and Release by Lichens: An Overview." The Bryologist, Vol. 82, No.2, pp. 226-246.

Saunders, B.P. and Williamson, J.C., 1972. "Moose Movements from Ear-Tag Returns." Proceedings of the 8th North American Moose Conference and Workshop. Thunder Bay, Ontario, Feb., pp. 177-184.

Sehmel, G.A., 1980. "Particle Resuspension: A Review." Environment International, Vol. 4, pp. 107-127.

SENES Consultants Limited, 1983. "Decommissioning of the Beaverlodge Mine/Mill Operations and the Reclamation of the Site. Radiological and Environmental Assessment of Close-out Options." Prepared for Eldorado Resources Limited, Ottawa.

Sheppard, M.I., and Thibault, D.H., 1983. "Natural Uranium Concentration Factor Distributions for Ten Plant Species Indigenous to the Precambrian Shield." Atomic Energy of Canada Limited, Technical Record TR-220, Pinawa.

Taylor, K.P. and Ballard, W.B., 1979. "Moose Movements and Habitat Use Along the Susitna River near Devil's Canyon." Proceedings of the 15th North American Moose Conference and Workshop, Soldotna-Kenai, Alaska. pp. 169 - 186.

Tracy, B.L., Pranti, F.A., and Quinn, J.M., 1983. "Transfer of Ra-226, Pb-210 and Uranium from Soil and Garden Produce; Assessment of Risk." Health Physics, Vol. 44, pp. 469-477.

Tuominen, Y., and Jaakkola, T., 1973. "Absorption and Accumulation of Elements." Chapter 6 in "The Lichens" edited by V. Ahmadjian and M.E. Hale, Academic Press, New York.

United States Nuclear Regulatory Commission (U.S. NRC), 1982. "Calculational Models for Estimating Radiation Doses to Man from Airborne Radioactive Material Resulting from Uranium Milling Operations." Reg. Guide 3.51, March.

## 9.0 SUBSURFACE CONTAMINANT TRANSPORT MODEL

### 9.1 Introduction

In the subsurface transport model the movement of contaminants carried with tailings porewater emerging from the bottom of the tailings pile is traced along a groundwater flowpath (i.e. a subsurface flow system). The model takes into consideration contaminant retardation in calculating the concentration as a function of time at any selected point(s) along the flowpath. In this study contaminant profiles were calculated at the point where the groundwater flowpath discharges from the aquifer and becomes surface runoff. Contaminants modelled include lead-210, radium-226, total thorium and total uranium.

The structure of the subsurface transport model is presented in Figure 9.1. For each trial the model requires a set of discrete data points comprised of the source concentration for each radionuclide at a particular time, (i.e. $C_0(t,i)$), as input. This set of data points is provided by the tailings source model. The subsurface transport model also imports the volumetric seepage rate from the tailings source model. In addition, the probabilistic inputs which are all independent of time, (e.g. radionuclide distribution coefficients) are provided by the random sampling routine in the control module, which is implemented in subprogram Choose.

The body of the model is a mass balance which includes several hydrogeological and geochemical processes (i.e., advection, retardation and dispersion). In the mass balance calculations one-dimensional, steady-state flow conditions are assumed. The calculations are performed for each radionuclide. The calculated radionuclide concentrations at the point of discharge are converted into contaminant fluxes and are subsequently utilized by the watershed (river/lake system) model.

The following sections describe: the characteristics of the aquifer for the reference site; the theoretical basis and approach chosen to model the various processes; the overall contaminant mass balance and assumptions used in the mass balance calculations; the analytical solution of the mass balance for steady state flow conditions; and the values selected for the model parameters.

## 9.2 Aquifer Characteristics

### Groundwater Flowpath

The groundwater flowpath for the reference tailings site is through a glaciofluvial sandy aquifer underlying the main dam structure at an outlet valley. Figure 9.2 presents a conceptual view of the recharge flowpath for the subsurface flow. The cross-sectional area below the dam through which the groundwater recharge passes is referred to on the figure as the "window".

Conceptually it was assumed that all of the subsurface seepage from the tailings enters the aquifer and emerges some distance downstream of the main dam which is dependent on the hydrological characteristics of the aquifer. The distance between the tailings dam and point "X" is called the discharge distance. For the reference tailings site, "X" can be anywhere between the toe of the dam and the river located some 200 m from the tailings dam. It is a randomly selected input parameter with a triangular probability distribution. The probability distribution indirectly reflects the distribution of the groundwater discharge downstream of the dam.

### Contaminant Plume

Several studies have been conducted on the migration of groundwater-borne contaminants in the sandy aquifer underlying the Nordic uranium tailings area in Elliot Lake (Blair, 1980; Blair et al., 1980; Cherry et al., 1980a; Cherry et al., 1980b; Morin et al., 1982; Feenstra et al., 1981; Cherry et al., 1984). The contaminant plume emanating from the tailings has been

FIGURE 9.1

STRUCTURE OF SUBSURFACE TRANSPORT MODEL

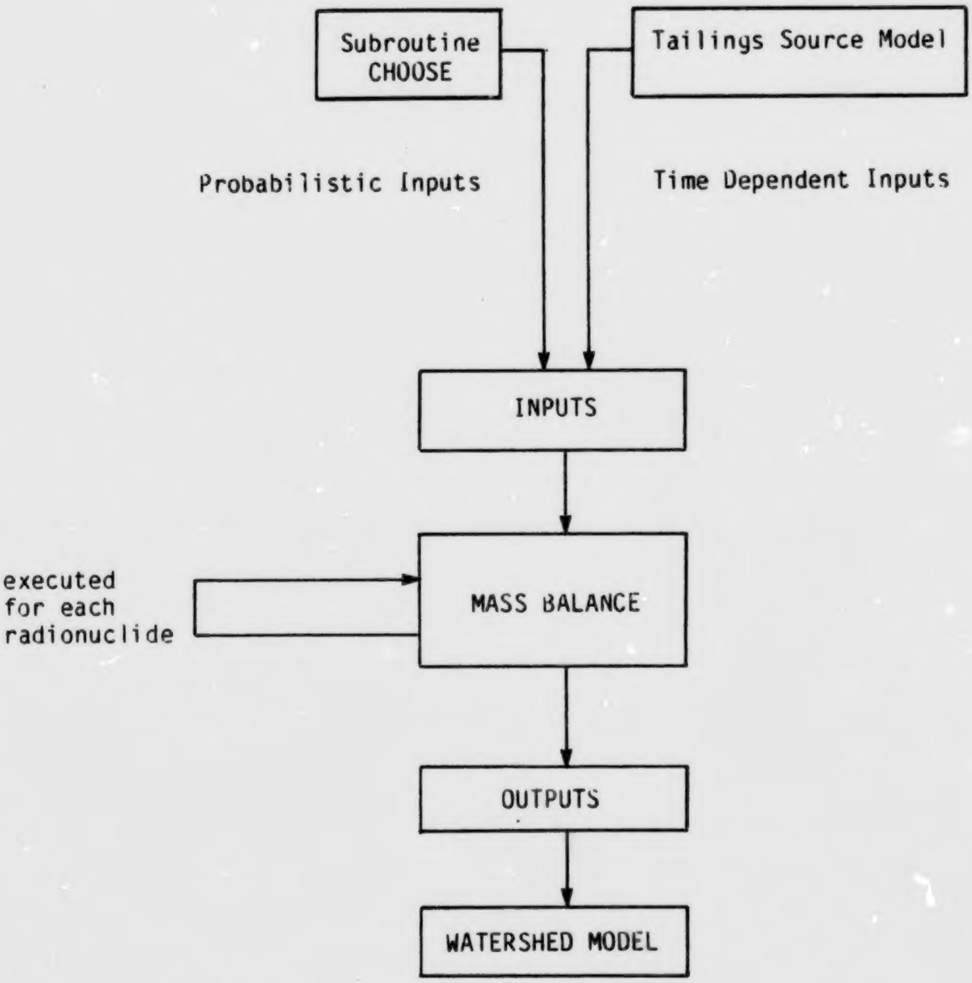
Subroutine CHOOSE
Tailings Source Model
Probabilistic Inputs
Time Dependent Inputs
INPUTS
executed for each radionuclide
MASS BALANCE
OUTPUTS
WATERSHED MODEL

FIGURE 9.2

CONCEPT OF REFERENCE TAILINGS
GROUNDWATER FLOWPATH

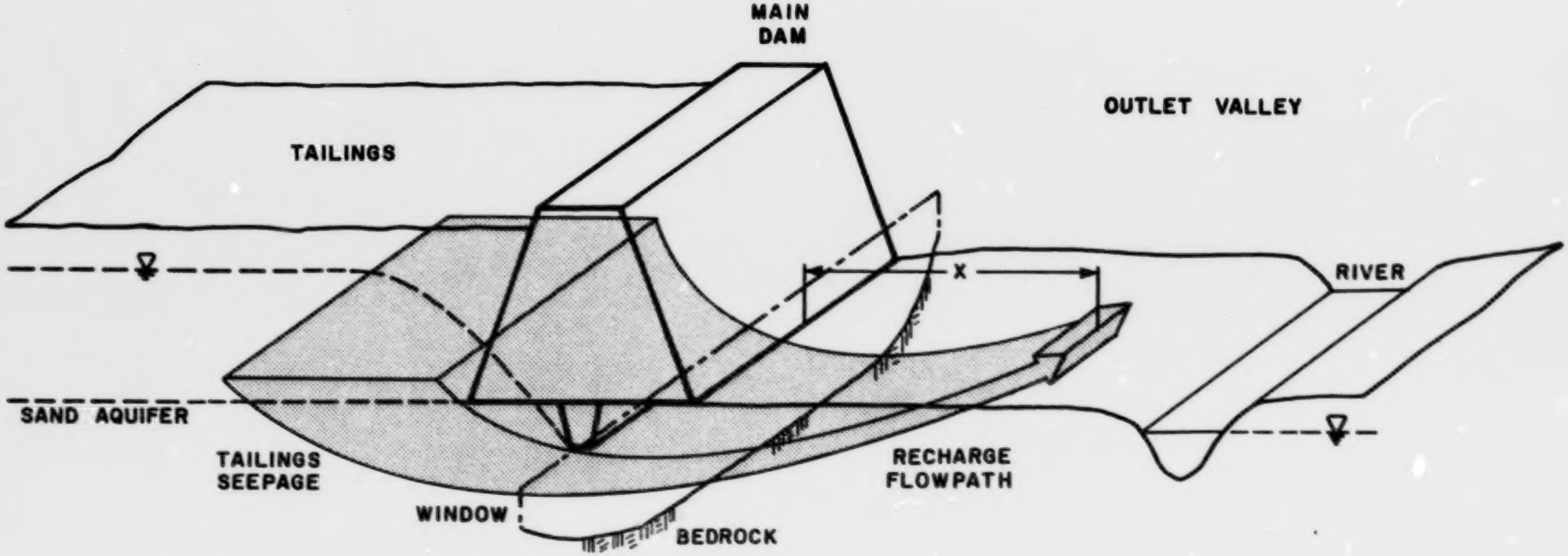
MAIN DAM
OUTLET VALLEY
TAILINGS
RIVER
X
SAND AQUIFER
TAILINGS SEEPAGE
RECHARGE FLOWPATH
WINDOW
BEDROCK

characterized in these investigations to comprise two distinct segments, referred to as the inner core and the outer zone. The inner core extends a short distance, approximately 15 m at the Nordic site (Morin et al., 1982), from the tailings impoundment and has a pH in the range of 3.0 to 5.0 and an elevated radionuclide content in the porewater. The outer zone has a higher pH (greater than 5.7) and a low dissolved radionuclide content.

Retardation of the movement of the acid porewater in the inner core has been attributed to the neutralization of the acidic water as a result of dissolution of calcium carbonate in the sand (Morin et al., 1982). The retardation of radionuclide movement possibly involves several mechanisms including coprecipitation with major chemical species, adsorption or absorption on solid particles and ion exchange.

The movement of radionuclides in the groundwater regime is retarded in the groundwater model by the application of appropriate distribution (or partitioning) coefficients. The distribution coefficient concept is widely used as a surrogate for the various mechanisms which may act to retard chemical species movement through soils.

The model includes decay terms for the activity of the radionuclides. It also includes a term to approximate the in-growth of lead-210 at the discharge point. With the inclusion of an in-growth term, the model predicts that lead-210 will be present when radium-226 breaks through. Without this term lead-210 would not be present in the groundwater discharge, as it is strongly retarded and has a relatively short half-life.

## 9.3 Theoretical Approach

### 9.3.1 Auxiliary Equations

Several basic processes were included in the subsurface transport model. These were advection, mechanical dispersion, retardation, radioactive decay and in-growth.

Advection is a process by which the radionuclides are transported by the bulk motion of the flowing groundwater. To calculate the affect of advection on contaminant concentration, the groundwater velocity (Darcy's velocity) must be determined:

$$q = K\ I \tag{9.1}$$

where:

$q$ = Darcy's velocity ($m.yr^{-1}$)

$K$ = the hydraulic conductivity ($m.yr^{-1}$)

$I$ = the hydraulic gradient ($m.m^{-1}$)

Alternatively, the groundwater velocity can be determined using the volumetric seepage rate through the aquifer:

$$q = \frac{Q_s}{A_x} \tag{9.2}$$

where

$Q_s$ = volumetric seepage rate through the aquifer ($m^3.yr^{-1}$)

$A_x$ = cross-sectional area of the aquifer window ($m^2$)

It is the latter equation, equation (9.2), which was used to determine the groundwater velocity since it allows for a linkage of the source term model with the subsurface transport model. In this equation the volumetric seepage rate through the aquifer is assumed to be equal to the average tailings seepage rate from the base of the tailings pile.

The average seepage rate from the tailings is determined as follows:

$$Q_s = f\ P_a\ A_T \tag{9.3}$$

where

$P_a$ = long-term, mean net annual precipitation ($m.yr^{-1}$)

$f$ = fraction of net precipitation that infiltrates the total depth of the tailings pile

$A_T$ = surface area of tailings ($m^2$)

The distribution of the variable "f" was determined as a function of the hydraulic conductivity and hydraulic gradient,as discussed in Section 9.5.

Mechanical dispersion is a spreading phenomenon caused entirely by the motion of the fluid. Mechanical dispersion may occur in the direction parallel to the bulk fluid flow (longitudinal dispersion) or in the direction perpendicular to the flow (transverse dispersion). Since longitudinal dispersion is normally much stronger than transverse dispersion, the latter is often neglected (Freeze and Cherry, 1979). In order to incorporate the longitudinal dispersion process a dispersion coefficient is required:

$$D_\ell = \frac{\alpha q}{n} \qquad (9.4)$$

where:

$D_\ell$ = the longitudinal dispersion coefficient ($m^2.yr^{-1}$)

$\alpha$ = the dispersivity (m)

$n$ = the porosity ($m^3.m^{-3}$)

$q$ = Darcy's velocity ($m.yr^{-1}$)

To account for the complex geochemical processes (dissolution, adsorption and coprecipitation) which control radionuclide migration, a "bulk" retardation factor is used:

$$R = 1 + \frac{\rho_b}{n} K_d \qquad (9.5)$$

where:

$R$ = the retardation factor

$\rho_b$ = the bulk density ($kg.m^{-3}$)

$K_d$ = the distribution coefficient for the contaminant ($m^3.kg^{-1}$)

The radioactive decay constant of each radionuclide is determined from the following equation:

$$\lambda = \ln(2)/t_{0.5} \qquad (9.6)$$

where:

$\lambda$ = the radioactive decay constant ($yr^{-1}$)

$t_{0.5}$ = the radioactive half-life (yr)

The in-growth of lead-210, a daughter product of radium-226, may be expressed as:

$$A_{Pb} = A_{Ra}\,(1 - e^{-\lambda_{Pb}\,t}) \qquad (9.7)$$

where :

$A_{Pb}$ = lead-210 activity ($Bq.m^{-3}$)

$A_{Ra}$ = radium-226 activity ($Bq.m^{-3}$)

$\lambda_{Pb}$ = the radioactive decay constant for lead-210 ($yr^{-1}$)

$t$ = time period (yr)

In the above expression it has been assumed that radium-226 decays directly to lead-210. This assumption is based upon the intermediate daughters having very short half-lives compared to lead-210.

The in-growth of lead-210 was approximated at the discharge point by dividing equation (9.7) by the soil volume and then multiplying this expression by the ratio of retardation factors. The retardation factors were included in the in-growth term to account for the much stronger sorption of lead-210 as compared to radium-226:

$$C_{Pb} = C_{Ra}\ I_g \qquad (9.8a)$$

and:

$$I_g = (1-e^{-\lambda_{Pb} t}) \frac{R_{Ra}}{R_{Pb}} \quad (9.8b)$$

where:

$C_{Pb}$ = the activity of lead-210 in the subsurface flow ($Bq.m^{-3}$)
$C_{Ra}$ = the activity of radium-226 in the subsurface flow ($Bq.m^{-3}$)
$I_g$ = the in-growth factor
$R_{Pb}$ = the bulk retardation factor for lead-210
$R_{Ra}$ = the bulk retardation factor for radium-226

The in-growth of radium-226 from thorium-230 decay is not included in the model since it's retardation is approximately seven times less than that of thorium-230 and hence will break through first.

Models do exist which incorporate radioactive in-growth during the transport of radionuclides in an aquifer (Birchall, 1986; Petrie et al., 1983; Rogers, 1978). The addition of an in-growth term, however, significantly increases the complexity and computer run-time of the model. Neither of these consequences were considered to be warranted for the purposes of this assessment level model.

### 9.3.2 Mass Balance

The one-dimensional movement of a nonreactive radionuclide in a saturated, homogeneous, isotropic semi-infinite column undergoing continuous radioactive decay can be described by the following partial differential equation given by Bear (1979):

$$\frac{\partial C}{\partial t} = D_\ell \frac{\partial^2 C}{\partial X^2} - \frac{q}{n} \frac{\partial C}{\partial X} - \lambda C \quad (9.9)$$

where:

X = the distance from the tailings impoundment (m)
t = the time (yr)
C = the activity of the ith radionuclide ($Bq.m^{-3}$)

The terms on the right hand side of equation (9.9) account respectively for longitudinal dispersion, advection and radioactive decay.

Modifying equation (9.9) to include the retardation term previously described by the bulk retardation factor results in:

$$\frac{\partial C}{\partial t} = \frac{D_\ell}{R}\frac{\partial^2 C}{\partial X^2} - \frac{q}{nR}\frac{\partial C}{\partial X} - \lambda C \qquad (9.10)$$

This mass balance equation was employed in the model.

The contaminant flux to the surface water at a distance (X) from the tailings was calculated by:

$$J = \frac{C(X,t)\, Q_s}{A_x} \qquad (9.11)$$

where:

$J$ = the contaminant flux ($Bq.m^{-2}yr^{-1}$)

$Q_s$ = the aquifer's volumetric seepage rate ($m^3.yr^{-1}$)

$A_x$ = cross-sectional area of the aquifer window ($m^2$)

$C(X,t)$ = the concentration of the contaminant at distance X and time t ($Bq.m^{-3}$)

### 9.3.3 Assumptions

Several assumptions were employed in the development of equation (9.10). A list of these assumptions is presented in Table 9.1. The first assumption implies that the seepage from the bottom of the tailings pile will fluctuate much less than the annual variations in net precipitation infiltrating the tailings pile due to the dampening effect of the tailings. Hence, the seepage rate to the aquifer is treated as equalling some fraction, f, of the long-term mean net precipitation (i.e. as a constant for each trial). This assumption greatly simplifies the mass balance calculations. Its effect on the contaminant flux, however, should be minimal.

/

Table 9.1

## ASSUMPTIONS EMPLOYED IN SUBSURFACE TRANSPORT MODEL

1. The volumetric flow rate through the aquifer can be represented by an average volumetric seepage rate from the tailings.

2. The flow path is isotropic and homogeneous.

3. Bulk retardation factors are used which assume equilibrium isotherms and instantaneous and reversible geochemical reactions.

4. Mixing or dilution of the tailings porewater seepage with groundwater flow is not considered.

5. Molecular diffusion and transverse dispersion are considered to be negligible.

6. The in-growth of radionuclides in the aquifer is considered to be unimportant with regards to the concentration at the discharge point.

7. All of the subsurface flow from the tailings discharges in the same direction; that is flows under the main dam.

The value of "f", the fraction of the net precipitation which penetrates the tailings pile to become subsurface seepage, was determined from the distributions of the parameter values for hydraulic conductivity and hydraulic gradient, the basic hydrogeological characteristics of the aquifer which control advective transport. Hence, the variations in the morphology of the sand aquifer have been indirectly included in the model.

The second assumption states that the hydraulic conductivity is homogeneous (independent of position) and isotropic (equal in all directions). It is anticipated that the inherent non-uniformity or heterogenicity of porous media which is generally believed to exist (Freeze and Cherry, 1979), will be partially accounted for in the model via the probabilistic method of parameter input.

The third assumption of a bulk retardation factor provides an estimate of the many reactions involved. The geochemical reactions which will occur in the aquifer and affect the radionuclide movement include acid neutralization (dissolution of carbonate minerals), adsorption, coprecipitation and ion exchange. The use of sorption partition coefficients, $K_d$'s, in the calculation of the bulk retardation factors is a valid representation because the partitioning for the most part is fast and reversible and exhibits a linear isotherm. This assumption may tend to under-estimate the radionuclide flux when the source concentration is high, since,the aquifer's exchange capacity may be exceeded, i.e. all the available adsorption sites are filled.

In the fourth assumption, mixing or dilution of the tailings porewater seepage with groundwater from the surrounding drainage area is disregarded in calculating the contaminant flux from the subsurface discharge to the surface water system. Hence, the volumetric rate of groundwater discharge to the surface water system in the zone influenced by the tailings impoundment is equal to the volumetric rate of porewater seepage from the tailings into the subsurface flow system.

This assumption will lead to an over-estimation of the radionuclide concentrations in the aquifer, but would have little effect on the value of the contaminant flux to the surface water system.

Molecular diffusion has not been included, assumption five, as its effects should be negligible for the advection - dominated environment considered for this study. A typical diffusion coefficient is in the order of $1 \times 10^{-9}$ $m^2.yr^{-1}$ (Jury et al., 1983). In contrast, a calculated dispersion coefficient using the data presented in Section 9.5 is approximately $2 \times 10^{-4}$ $m^2.yr^{-1}$. Transverse dispersion has been neglected since it is normally weaker than longitudinal dispersion (Freeze and Cherry, 1979).

Employing assumption six greatly reduces the complexity of the model. For the short-lived radionuclides, radium-226 and lead-210, this assumption results in a small error in their concentrations within the aquifer. Since the lead-210, in particular, is strongly retarded, in-growth within the aquifer will have a negligible effect on the discharge concentration of lead-210. However, because radium-226 is less strongly retarded and will be present in the groundwater discharge, some lead-210 can also be expected to be formed at the discharge point. As discussed previously the concentration of lead-210 in the groundwater discharge resulting from in-growth is approximated by using the discharge radium-226 concentration and a ratio of the bulk retardation factors in the expression presented in equation (9.8b).

Assumption seven, one-directional discharge flow, results in an over estimation of the groundwater discharge flow to the river. The effect is that all groundwater contaminant loading from the tailings area is introduced at one point in the watershed. If the subsurface flow discharges in different directions the flow and contaminant flux to the watershed from each discharge point may be approximated by subdividing the tailings surface area and repeating the model run for each direction.

To obtain groundwater flowpath predictions for multiple discharge points in a single computer run, adjustments would have to be made to the model.

## 9.4 Solution to Mass Balance

### 9.4.1 Constant Source

For a constant source and assuming steady-state flow conditions, an analytical solution to equation (9.10) has been provided by Bear (1979):

$$C(X,t) = \frac{C_o}{2} \exp\left[\frac{qX}{2nD_\ell}\right] \cdot \left\{ \exp(-XB).\mathrm{erfc}\left(\frac{X-[(q/nR)^2 + (4\lambda D_\ell/R)]^{0.5}t}{2(D_\ell t/R)^{0.5}}\right) + \exp(BX).\mathrm{erfc}\left(\frac{X+[(q/nR)^2 + (4\lambda D_\ell/R)]^{0.5}t}{2(D_\ell t/R)^{0.5}}\right)\right\} \qquad (9.12)$$

where

$B^2$ = $[q/(2nD_\ell)]^2 + \frac{\lambda R}{D_\ell}$

$C_o$ = the radionuclide activity of the source input to the groundwater region at t=0 ($Bq.m^{-3}$)

$C(X,t)$ = the radionuclide activity at distance X from the source at time t ($Bq.m^{-3}$)

The above equation can be rewritten as:

$$C(X,t) = C_o\ G(X,t) \qquad (9.13)$$

where G(X,t) is a Green's Function and represents the elementary solution for a stationary unit source.

### 9.4.2 Time-Variant Source

Contaminant transfer is described by a linear continuous partial differential equation. An increase in source concentration by some factor will cause a change in the contaminant concentration at any distance following an appropriate time lag. If a contaminant source can be represented as the sum of two (or more) sources, the resulting response can be represented as a sum of responses to each source. This is a consequence of the linearity of the contaminant transport equation and can be applied by using the principle of superposition.

A non-stationary (i.e. time-variant) source, as in Figure 9.3a, can be approximated as a sum of elementary stationary sources originating at discrete time intervals. The numerical approximation of a time-variant source function is illustrated in Figure 9.3b and is summarized below for the total source concentration at time $t_k$:

$$\begin{aligned} C_s(t_k) &= C_s(t_0) + [C_s(t_1) - C_s(t_0)] \\ &+ [C_s(t_2) - C_s(t_1)] + [C_s(t_3) - C_s(t_2)] \\ &+ \ldots. + [C_s(t_k) - C_s(t_{k-1})] \end{aligned} \qquad (9.14)$$

where $C_s(t)$ = source radionuclide activity at time t ($Bq.m^{-3}$)

For any time t, this type of approximation increases in accuracy as the incremental time step decreases. The series of concentration changes can be thought of as elemental step functions which are equivalent to several time-constant sources of different concentrations.

Employing the principle of superposition allows for the tracking of the unit impulse of source values for each time period:

FIGURE 9.3

TIME - VARIANT SOURCE

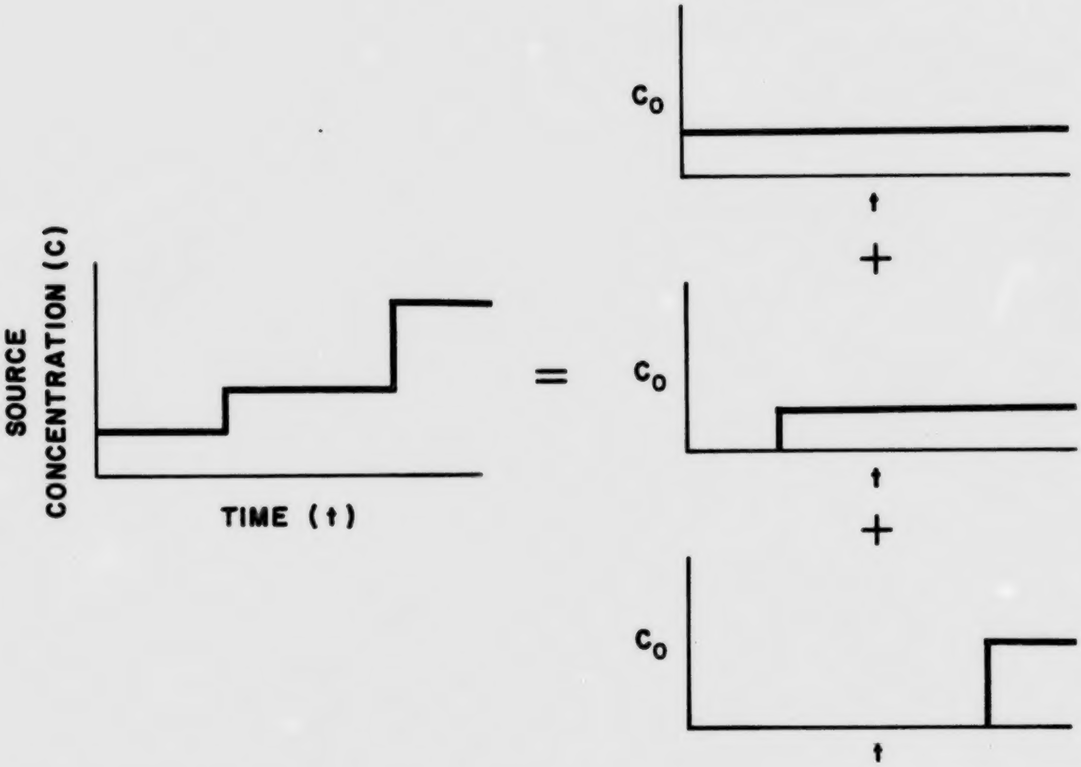
SOURCE CONCENTRATION (C)
TIME (t)
=
$C_0$
t
+
$C_0$
t
+
$C_0$
t

A) PRINCIPLE OF SUPERPOSITION

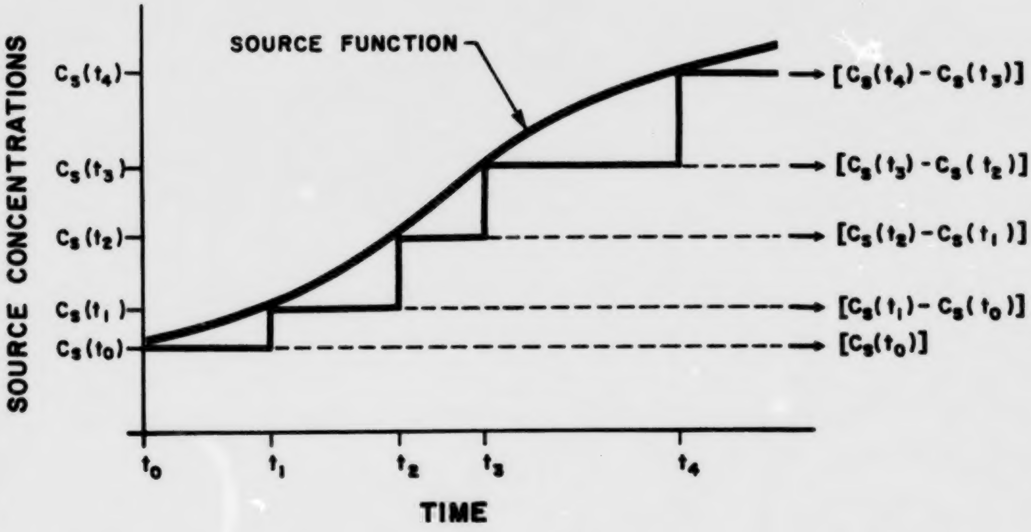
SOURCE CONCENTRATIONS
SOURCE FUNCTION
$C_s(t_4)$
$C_s(t_3)$
$C_s(t_2)$
$C_s(t_1)$
$C_s(t_0)$
$[C_s(t_4) - C_s(t_3)]$
$[C_s(t_3) - C_s(t_2)]$
$[C_s(t_2) - C_s(t_1)]$
$[C_s(t_1) - C_s(t_0)]$
$[C_s(t_0)]$
$t_0$
$t_1$
$t_2$
$t_3$
$t_4$
TIME

B) APPROXIMATION OF TIME - VARIANT SOURCE

[illegible]

$$
\begin{aligned}
C(X,t_k) = {} & C_s(t_0).G(X,t_k) + (C_s(t_1)-C_s(t_0)).G(X,t_k-t_1) \\
& + (C_s(t_2)-C_s(t_1)).G(X,t_k-t_2) + \ldots. \\
& + (C_s(t_{k-1})-C_s(t_{k-2})).G(X,t_k-t_{k-1}) \\
& + (C_s(t_k)-C_s(t_{k-1})).G(X,t_k-t_{k-1})/2.0
\end{aligned}
\qquad (9.15)
$$

The last term approximates the changing source strength during the last time increment.

## 9.5 Review of Parameters and Constants

### 9.5.1 Parameter Values

The hydrogeological and geochemical parameters employed in the subsurface contaminant transport model are listed in Table 9.2. Also listed in the table are the probability distribution types and descriptors and computer source symbols assigned to the parameters. The probability distributions reflect the uncertainties in the parameter values due to inhomogeneties in the geologic formation and variability in the measurement techniques. The majority of the parameters are reviewed below in the context of a reference site located in a drainage basin on the Canadian Precambrian Shield. The radionuclide distribution coefficients, however, are generic in nature and may have a wider distribution than would be expected for a specific location.

1. Discharge Distance. The discharge distance (X) is the distance between the tailings dam and the point where the subsurface flow becomes surface runoff (see Figure 9.2). This distance is a function of local conditions; examples of which are the permeability of the aquifer, the depth to the water table in the tailings and the permeability of the dam.

   For the reference site subsurface flow occurs below an impermeable cutoff wall which extends into the aquifer below the dam. Given this restriction to the flowpath it is conceptually appropriate to define the discharge point to occur a considerable distance downstream of the dam. For the reference site the groundwater discharge is assumed to occur between 25 m and 200 m from the toe of the dam. It was given a triangular distribution with the mode located 35 m from the dam. The minimum distance of 25 m represents the closest distance at which water will emerge from the tailings dam as a result of the dam's subsurface cutoff wall. The maximum distance coincides with the location of the river, 200 m.

2. Porosity. The porosity (n) of a porous medium is the ratio of void volume to total unit volume. Porosity of unconsolidated deposits are dependent on the texture and grain size distribution of the material. The range of porosity for unconsolidated deposits is 25 to 70 per cent, with coarse rounded materials having lower porosities than platey clayey materials (Freeze and Cherry, 1979).

   Sandy aquifers commonly have porosities ranging between 0.30 $m^3.m^{-3}$ and 0.36 $m^3.m^{-3}$. Given this narrow range, the probability distribution for porosity was assumed to be uniform with a mean value of 0.33 $m^3.m^{-3}$. These parameter values may be assumed to be generic for sandy aquifers.

3. Fraction of Precipitation. This parameter is described as the fraction of net precipitation (f) that infiltrates the total depth of the tailings pile and enters the saturated zone:

$$Q_s = f \ P_a A_T \qquad (9.16)$$

   where

   $Q_s$ = volumetric seepage rate through the aquifer ($m^3.yr^{-1}$)
   f = fraction of precipitation which infiltrates
   $P_a$ = long-term, mean net precipitation ($m.yr^{-1}$)
   $A_T$ = surface area of tailings ($m^2$)

   The volumetric seepage rate can also be expressed as:

$$Q_s = K \ I \ A_x \qquad (9.17)$$

Table 9.2

## SUBSURFACE TRANSPORT MODEL PARAMETERS

| Model Symbol | Description | Units | Nominal Value | Probability Distribution* | Computer Origin | Computer Symbol |
|---|---|---|---|---|---|---|
| $A_T$ | cross-sectional area of tailings | $m^2$ | $5\times10^5$ | $C(5\times10^5)$ | Input | ATAIL |
| $A_x$ | cross-sectional area of flow | $m^2$ | 1000. | C(1000) | Input | AXGWAT |
| C(i,t) | discharge concentration of ith radionuclide at time t | $Bq.m^{-3}$ | calculated | calculated | GWATER | GWATC(i,t) |
| $C_o(i,t)$ | concentration leaving tailings area to groundwater for the ith radionuclide at time t | $Bq.m^{-3}$ | calculated | calculated | SOURCE | CO(i,t) |
| $D_\ell$ | longitudinal dispersion coefficient | $m^2.yr^{-1}$ | calculated | calculated | GWATER | LDC |
| f | fraction of net precipitation that infiltrates | unitless | 0.15 | LN[0.15,1.27,0.07,0.3) | Input | FNPRCP |
| J | contaminant flux | $Bq.m^{-2}.yr^{-1}$ | calculated | calculated | GWATER | GFLUX(i,t) |
| $K_d(i)$ | distribution coefficients of ith radionuclide | $m^3.kg^{-1}$ | | | | |
| | uranium | | 0.02 | $LN[0.02,2.5,5\times10^{-3},0.5]$ | Input | DCGWAT(1) |
| | thorium | | 0.5 | LN[0.5,2.15,0.05,5] | Input | DCGWAT(2) |
| | lead | | 0.67 | LN[0.67,1.73,0.13,3.5] | Input | DCGWAT(3) |
| | radium | | 0.07 | LN[0.07,1.9,0.01,0.5] | Input | DCGWAT(4) |
| n | porosity | $m^3.m^{-3}$ | 0.33 | U[0.30,0.36] | Input | POGWAT |
| $P_a$ | average net precipitation | $m.yr^{-1}$ | 0.4 | C(0.4) | Input | AVPRCP |
| q | Darcy velocity | $m.yr^{-1}$ | calculated | calculated | GWATER | DV |
| $Q_s$ | volumetric seepage | $m^3.yr^{-1}$ | calculated | calculated | GWATER | VSR |
| R | retardation factor | unitless | calculated | calculated | GWATER | R |
| X | discharge distance | m | 80 | T(25,35,200) | Input | XRGWAT |
| $\rho_s$ | soil density | $kg.m^{-3}$ | 2650 | N[2650,110,2320,2980] | Input | SGGWAT |

* Distributions are as described in Table 2.2.

where

$A_x$ = cross-sectional area of flow-path ($m^2$)
K = hydraulic conductivity ($m.yr^{-1}$)
I = hydraulic gradient ($m.m^{-1}$)

By combining equations (9.16) and (9.17) the following expression for the fraction of precipitation results:

$$f = \frac{K\ I\ A_x}{P_a\ A_T} \qquad (9.18)$$

In the model the parameters $A_x$, $P_a$ and $A_T$ are treated as constants:

$A_x$ = 1000 $m^2$
$P_a$ = 0.4 $m.\ yr^{-1}$
$A_T$ = $5 \times 10^5$ $m^2$

The values for $A_x$ and $A_T$ are site specific and must be assessed for each application. The $P_a$ value for the reference site is from AES (not dated) data on Gore Bay, Ontario.

Hydraulic conductivity values representative of sandy soils are typically in the range of 113 $m.yr^{-1}$ ($3.6 \times 10^{-6}$ $m.s^{-1}$) to 438 $m.yr^{-1}$ ($1.39 \times 10^{-5}$ $m.s^{-1}$) (Beals, 1985). For the glaciofluvial sandy aquifers often found in the Elliot Lake area, estimated and measured hydraulic conductivities are reported to be in the range of 315 $m.yr^{-1}$ ($10^{-5}$ $m.s^{-1}$) to 3150 $m.yr^{-1}$ ($10^{-4}$ $m.s^{-1}$) (Blair et al., 1980; Morin et al., 1982).

Freeze (1975) has tabulated frequency distributions for many thousand hydraulic conductivity values and has observed an average standard deviation of 1.95 for sands and gravels. Using the above values, the probability distribution for hydraulic conductivity was expressed as having a lognormal distribution with geometric mean of 420 $m.yr^{-1}$, a geometric standard deviation of 1.95 and lower and upper limits of 315 and 3150 $m.yr^{-1}$.

The hydraulic gradient (I) in sandy aquifers is generally considered to fall in the range from 0.005 $m.m^{-1}$ to 0.01 $m.m^{-1}$. Again, due to inhomogeneties, the hydraulic gradient varies not only from site to site on a macroscale but also within a site at the microscale level. Uncertainty in hydraulic gradient data is often due to measurement or extrapolation errors between data points. Such errors can be considered to be normally distributed.

A high gradient of 0.05 $m.m^{-1}$ has been reported by Morin _et al_., (1982) for the sandy/gravelly aquifer at Nordic. This value was taken to represent nominal conditions for the reference site since large hydraulic gradients can exist between a tailings water table and the water table in the outlet valley. The hydraulic gradient for the reference site was represented as having a mean of 0.05 $m.m^{-1}$, arithmetic standard deviation of 0.01, and an lower and upper limits of 0.03 and 0.07 $m.m^{-1}$.

Figure 9.4 presents the distribution of the parameter f for the reference site, which was calculated using the aforementioned distributions of hydraulic conductivity and hydraulic gradient. The geometric mean and geometric standard deviation for f are 0.15 and 1.66, respectively. Lower and upper limits of 0.07 and 0.3 have been placed on this parameter.

4. Soil density. The soil density ($\rho_s$) is the ratio of a particles mass to the volume it occupies. The soil density of sands is generally reported to be approximately 2,650 $kg.m^{-3}$ (2.65 $g.cm^{-3}$). Morin _et al_. (1982) have reported that the sandy aquifer near the Nordic tailings area had a significantly higher soil density, 2,980 $kg.m^{-3}$ (2.98 $g.cm^{-3}$), for the solid phase minerals.

   For this investigation, the soil density was assumed to be normally distributed with a mean of 2,650 $kg.m^{-3}$ and a standard deviation of 110.

5. Distribution coefficient. The distribution coefficient, $K_d$, is the

FIGURE 9.4

DISTRIBUTION OF THE FRACTION OF PRECIPITATION

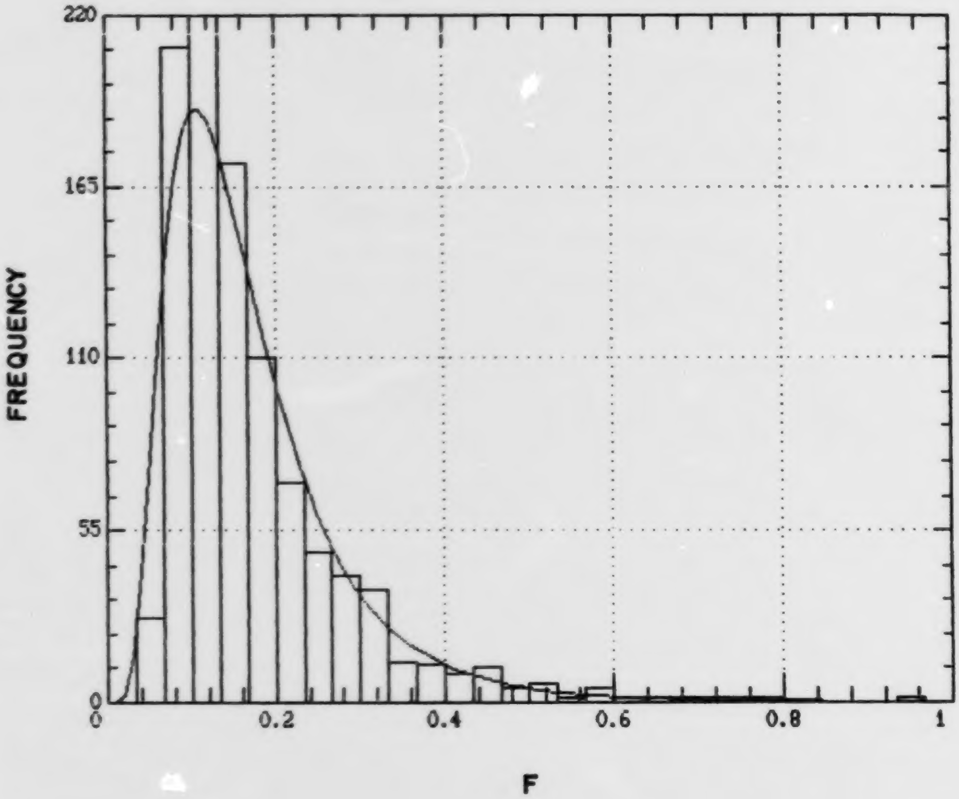

ratio of the mass of contaminant adsorbed on a unit mass of solid material (e.g. sand) to the mass of contaminant in a unit volume of solution (e.g. groundwater). The coefficient is very much dependent on soil type and groundwater pH; generally the $K_d$ value is found to decrease as the pH decreases. It is also dependent on the contaminant concentration in the liquid phase; at high concentrations saturation of available exchange sites can occur (Rancon, 1973). In most cases the $K_d$ values are found to be lognormally distributed (Sheppard et al., 1984).

The modelling approach described in this study is based on conditions considered to be representative of an acidified plume. The movement of the radionuclide fronts through the aquifer are assumed to lag behind the acid plume front such that $K_d$ values representing low pH conditions (i.e. pH of 3.0 to 5.0) are considered to apply. This assumption is consistent with the observations reported by Morin et al., (1982) at the Nordic tailings area.

The information available on $K_d$ values and their distributions is limited. The $K_d$ values listed on Table 9.2 for the reference site are generic in nature. When using the model for a particular site, site-specific $K_d$ values should be employed, especially if local chemistry causes the pH to deviate outside the range of 3.0 to 5.0.

Site-specific data may also allow narrower bounds to be placed on the $K_d$ values.

**Uranium**

The summary on uranium geochemistry presented by Johnston and Gillham (1980) indicates that:

- in an oxidizing environment, U(VI) compounds are stable and can precipitate, whereas U(IV) is stable in a reducing environment and would precipitate as $UO_2$, thus the oxidation-reduction status is important.

- soluble uranium U(VI) can be adsorbed or reduced by organic matter; if U(VI) is reduced to U(IV)precipitation can occur.
- $UO_2^{2+}$ can be adsorbed by clay minerals by cation exchange, but may also form complexes with anions such as carbonate or phosphate.
- the important oxidation states of uranium with respect to groundwater environments are U(VI) and U(IV).

Wide variations in literature values for uranium $K_d$ in sandy soils have been reported. In the study by Morin et al. (1982) two uranium partitioning coefficients were calculated; 2.0 $m^3.kg^{-1}$ for the inner core of the plume and $3.6m^3.kg^{-1}$ for the zone beyond the inner core. Rancon (1973) determined that uranium $K_d$'s were in the range of 0.016 to 0.27 $m^3.kg^{-1}$ for a variety of soil types: river sediment, organic peat, low organic sediment and altered schist. The low organic sediment had the lowest $K_d$ value.

Batch $K_d$ experiments were conducted by Veska (1983) using solutions representative of waste-rock-influenced groundwater. Table 9.3 presents the results of this study for tetravalent (IV) and hexavalent (VI) U-238. The average $K_d$ for solutions of pH 4.0, which corresponded to groundwater at the acid front for the field under study, was 0.015 $m^3.kg^{-1}$.

Typical literature values range from 0.005 $m^3.kg^{-1}$ to 0.50 $m^3.kg^{-1}$ with a mean value of 0.02 $m^3.kg^{-1}$ (NRC, 1983). Hence, a geometric mean $K_d$ value of 0.02 $m^3.kg^{-1}$ and a geometric standard deviation of 2.5 were selected to be representative of the acid plume in this investigation.

**Thorium**

Johnston and Gillham (1980) summarized the information relevant to thorium $K_d$ as follows:

- the primary thorium adsorption mechanism is ion exchange.

Table 9.3

## COMPARISON OF $K_d$ VALUES FOR U-238(IV) AND U-238(VI) AS A FUNCTION OF pH

| pH | $K_d$U-238(IV) ($m^3.kg^{-1}$) | | $K_d$U-238(VI) ($m^3.kg^{-1}$) | |
|---|---|---|---|---|
| | **A** | **B** | **C** | **D** |
| 3 | $7 \pm 2 \times 10^{-3}$ | $7 \pm 2 \times 10^{-3}$ | $8 \pm 1 \times 10^{-3}$ | $9 \pm 2 \times 10^{-3}$ |
| 4 | $1.2 \pm .2 \times 10^{-2}$ | $1.3 \pm .2 \times 10^{-2}$ | $1.7 \pm .2 \times 10^{-2}$ | $2.0 \pm .3 \times 10^{-2}$ |
| 5 | $2.14 \pm .20 \times 10^{-1}$ | $2.56 \pm .38 \times 10^{-1}$ | $1.37 \pm .24 \times 10^{-1}$ | $1.49 \pm .26 \times 10^{-1}$ |
| 5.5 | $3.52 \pm .44 \times 10^{-1}$ | $3.84 \pm .61 \times 10^{-1}$ | $1.62 \pm .28 \times 10^{-1}$ | $1.73 \pm .42 \times 10^{-1}$ |
| 6 | $3.33 \pm .53 \times 10^{-1}$ | $3.55 \pm .36 \times 10^{-1}$ | $1.68 \pm .40 \times 10^{-1}$ | $1.94 \pm .43 \times 10^{-1}$ |
| 7 | $9.1 \pm 1.0 \times 10^{-2}$ | $1.19 \pm .16 \times 10^{-2}$ | $3.9 \pm .4 \times 10^{-2}$ | $4.9 \pm .6 \times 10^{-2}$ |
| 8 | $1.7 \pm .3 \times 10^{-2}$ | $1.9 \pm .3 \times 10^{-2}$ | $6 \pm 1 \times 10^{-3}$ | $8 \pm 2 \times 10^{-3}$ |

Reference

Veska, 1983

Note

Letters A,B,C and D indicate experiment number.

- in non-calcareous soils, thorium adsorption is extremely sensitive to initial thorium solution concentrations. In organic materials, increased pH causes increased humic acid solubility and thorium complexation, resulting in lower $K_d$ values. In calcareous soils, $K_d$ values are high ($\geq 1$ $m^3.kg^{-1}$) regardless of pH or thorium concentration, because of the buffering capacity of the soil and precipitation of thorium hydroxide ($Th(OH)_4$).
- $K_d$ values are generally high, $\geq 1$ $m^3.kg^{-1}$, in dilute solutions, indicating limited thorium migration.

Our review suggested that there is a dearth of data on thorium $K_d$ values in sandy soils. Allard _et al_., (1977) reported $K_d$ ranges from 0.04 $m^3.kg^{-1}$ to 0.32 $m^3.kg^{-1}$ and 0.50 $m^3.kg^{-1}$ to 1.26 $m^3.kg^{-1}$ for clay, mud and granite, respectively. Vandergraaf (1982) recommended a $K_d$ value for thorium of 0.85 $m^3.kg^{-1}$ for granite. Veska (1983) reported average $K_d$ values, for Th-232 onto sand, at pH's of 3.5, 5.5 and 7.0, of 0.086, 0.570 and 1.75 $m^3.kg^{-1}$, respectively.

Typical $K_d$ values cited in this literature for thorium range from 0.05 to 5 $m^3.kg^{-1}$ (NRC, 1983). A geometric mean value of 0.50 $m^3.kg^{-1}$ and a geometric standard deviation of 2.15 are suggested.

**Lead**

As with the previously described elements there is only limited information on lead-210 $K_d$ values. Veska (1983) determined the average $K_d$ values of Pb-210 onto sand at pH's 3.5, 5.5 and 7.0 to be 0.102, 1.239 and 0.215 $m^3.kg^{-1}$, respectively. Gerritse _et al_. (1982) have reports $K_d$ values ranging from 0.28 to 3.5 $m^3.kg^{-1}$ for a sandy soil.

For this study, the $K_d$ for Pb-210 was described as being lognormally distributed with a geometric mean value of 0.67 and a geometric standard deviation of 1.73.

**Radium**

Johnston and Gillham (1980) summarized the information relevant to radium-226 $K_d$'s as follows:

- radium is present as $Ra^{2+}$ in the pH range 4 to 8, and does not readily form complex species.
- radium can be expected to coprecipitate with barium sulphate, carbonates and ferric hydroxides.
- cation exchange is an important adsorption mechanism, since $K_d$ values have been correlated to cation exchange capacity.

In high sulphate waters, greater than $10^{-2}$ mol.$m^{-3}$, however, $RaSO_4$ complexes may dominate $Ra^{2+}$.

In a study by Ames and Rai (1978) $K_d$ values of 0.21 $m^3.kg^{-1}$ to 0.47 $m^3.kg^{-1}$ were reported for Utah soils using simulated river water. Veska (1983) reported average $K_d$ values, for radium on sand, at pH's 3.5, 5.5 and 7.0, of 0.02, 0.088, and 1.53 $m^3.kg^{-1}$, respectively. The $K_d$ values for radium are generally accepted to be in the range 5 x $10^{-3}$ $m^3.kg^{-1}$ to 0.5 $m^3.kg^{-1}$ (NRC, 1983).

A geometric mean $K_d$ value of 0.07 $m^3.kg^{-1}$ was selected based on observations from a contaminant plume in the Elliot Lake area (Morin et al., 1982). This value is close to the mean literature value of 0.05 $m^3.kg^{-1}$ suggested by NRC (1983) and agrees well with the value of about 0.08 $m^3.kg^{-1}$ calculated from an equilibrium constant by Lester et al. (1975). A geometric standard deviation of 1.9 was estimated to cover the wide range of possible values for this parameter.

6. Longitudinal Dispersivity. Dispersivity ($\alpha$) is used as a measure of the medium's capability to cause mechanical dispersion. Unfortunately, unique values of dispersivity are not easily defined for a porous medium because dispersivity is scale-dependent, increasing with distance as the

transported mass encounters larger scale heterogeneity in the solid phase medium. This scale-dependency is one of the problems in applying the classical advection-dispersion equation for predictive purposes.

Anderson (1979) has presented values of regional dispersivities which range in values from 12 to 200 m for alluvial sediments. Dispersivity values of 30 to 61 m were reported for flow systems of 305 to 450 m in length.

In the subsurface flow model, the dispersivity is estimated from the relationship:

$$\alpha = 0.12.X \qquad (9.19)$$

where:
X = discharge distance (m)

The dispersivity is considered to be a quasi-constant for the particular discharge distance under study.

### 9.5.2 Constants

The following is a description of the constant inputs used in the module and the rationale for their selection.

1. Mean Net Precipitation. The long-term net precipitation ($P_a$) is used to calculate the volumetric seepage rate through the aquifer in equation (9.18). It is set constant since the solution to the mass balance (equation (9.12)) is only applicable for a constant seepage flow rate. A value of 0.4 $m.a^{-1}$ is employed in this model for the mean net precipitation.

   In other models (e.g. the SOURCE model) a parameter called net precipitation is employed which is sampled each time-step and has a probability distribution associated with it.

2. Cross-Sectional Area. The cross-sectional area ($A_x$) referred to is that of the window through which the recharge flow passes. It is given by:

$$A_x = L \; W_a \tag{9.20}$$

where

$A_x$ = cross-sectional area of flow-path ($m^2$)
$L$ = total length of dam (m)
$W_a$ = thickness of aquifer below the dam (m)

For the reference site the total length of the dam and the thickness of the aquifer are assumed to be 100 m and 10 m, respectively. Hence, the cross-sectional area is 1000 $m^2$.

3. Half-Lives. Table 9.4 presents the half-lives, $t_{1/2}$, of the radionuclides which are used in the groundwater model to determine the radioactive decay constant, $\lambda$, for the respective radionuclides. The radioactive decay constant is only calculated during the first execution of the subsurface transport model. For subsequent calculations it is stored in a common block.

## 9.6 Model Demonstration

In the following section, performance of the subsurface transport model is demonstrated for both deterministic and probabilistic runs. In both runs, radionuclide concentrations in the groundwater discharge were calculated for a 1000 year simulation period.

For the deterministic run the discharge distance was located 80 m from the tailings dam. Table 9.5 lists the input parameters used in the deterministic simulation.

Figure 9.5a and b present the concentrations of the four radionuclides in the

FIGURE 9.5a

SOURCE CONCENTRATION
(MODEL DEMONSTRATION)

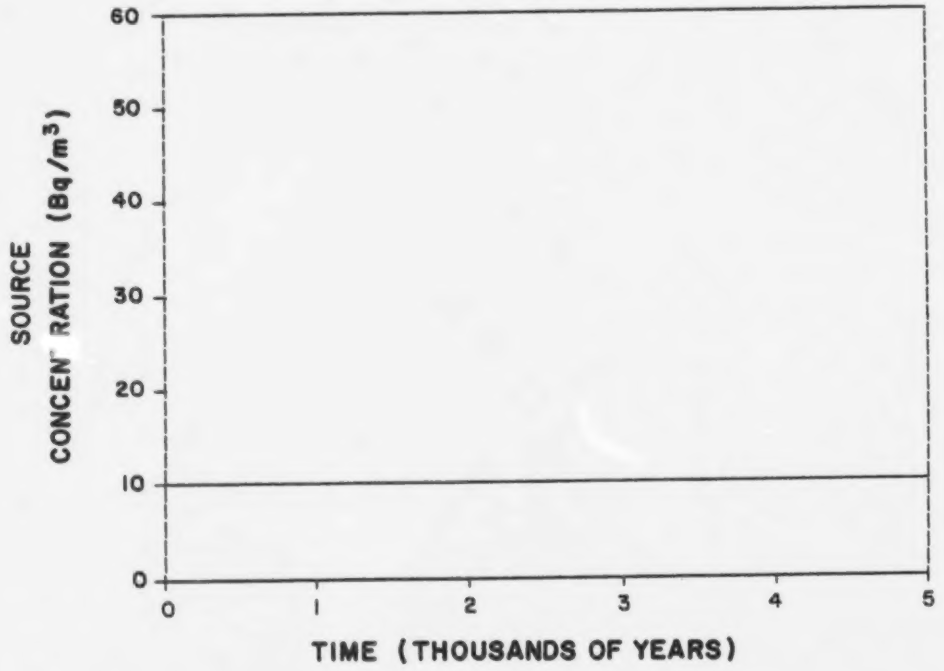

FIGURE 9.5b

GOUNDWATER CONCENTRATION
(MODEL DEMONSTRATION)

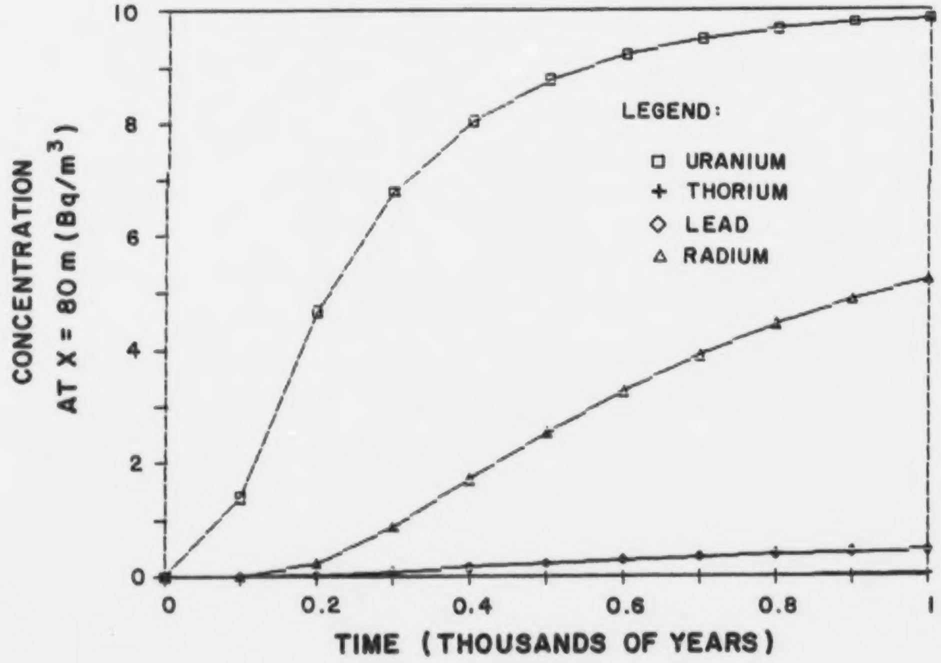

Table 9.4

## RADIOACTIVE HALF-LIFE

| Radionuclide | Half-life (yr) | Computer Source Symbol |
|---|---|---|
| U-238 * | $4.51 \times 10^{9}$ | TH(1) |
| Th-232 * | $1.4 \times 10^{10}$ | TH(2) |
| Pb-210 | 21 | TH(3) |
| Ra-226 | 1602 | TH(4) |

### Note

* For total thorium and uranium it was assumed that the half-lives of Th-232 and U-238 are representative

### Reference

U.S. Department of Health, Education and Welfare, 1970.

## Table 9.5

## INPUT PARAMETERS USED FOR DETERMINISTIC MODEL DEMONSTRATION

| Parameter | Value |
|---|---|
| $A_T$ | $5\times10^5$ m$^2$ |
| $A_x$ | 1000 m$^2$ |
| f | 0.15 |
| $K_d$ uranium | 0.02 m$^3$.kg$^{-1}$ |
| thorium | 0.50 m$^3$.kg$^{-1}$ |
| lead | 0.67 m$^3$.kg$^{-1}$ |
| radium | 0.07 m$^3$.kg$^{-1}$ |
| n | 0.33 m$^3$.m$^{-3}$ |
| $P_a$ | 0.4 m.yr$^{-1}$ |
| $t_{1/2}$ uranium | $4.51\times10^9$ yr |
| thorium | $1.4\times10^{10}$ yr |
| lead | 21 yr |
| radium | 1602 yr |
| X | 80 m |
| $\rho_p$ | 2650 kg.m$^3$ |
| time increments | 50 yr |

tailings source discharge and the groundwater discharge as a function of time. Total uranium, Ra-226 and Pb-210 approach steady state at the end of the 1000 year simulation period. Almost all of the lead present is a result of in-growth. The total thorium concentration at 1000 years is only 0.4% of its steady state value; a consequence of thorium's high distribution coefficient.

The input parameter values presented in Table 9.2 were used in the probabilistic simulation. Figure 9.6a, b, c and d present frequency histograms for 500 trials of the concentration of the radionuclides in the groundwater discharge at the end of the 1000 year simulation period. These results indicate that total uranium and Ra-226 are present in concentrations approaching their assumed source concentration of 10 $Bq.m^{-3}$. The Ra-226 concentrations in the groundwater discharge are slightly lower than the source concentration due largely to radioactive decay. Very little uranium decays due to its long half life. The results for total thorium indicate a low frequency of breakthrough, which may be contributed to its high distribution coefficient. The presence of Pb-210 is a result of in-growth from Ra-226 and hence is directly related to the radium concentrations.

## 9.7 Description of Computer Model

The algorithms used in the subsurface transport model are given in the source code listing, Table 9.6. The computer source symbols for the parameters are presented in Table 9.2. The computer source symbol of FNG(i,t) represents the Green's function, G(X,t), shown in equation (9.12).

The current limit on the array size for groundwater concentration is GWATC (4,200), which allows for a maximum of 200 values to be saved for each of the radionuclides. The frequency at which radionuclide predictions may be saved can be determined by the ratio of total simulation time to time increment. This ratio must not exceed 199. If this ratio is exceeded an error will result.

FIGURE 9.6a

# FREQUENCY HISTOGRAM FOR URANIUM CONCENTRATION AT DISCHARGE POINT TO SURFACE WATER

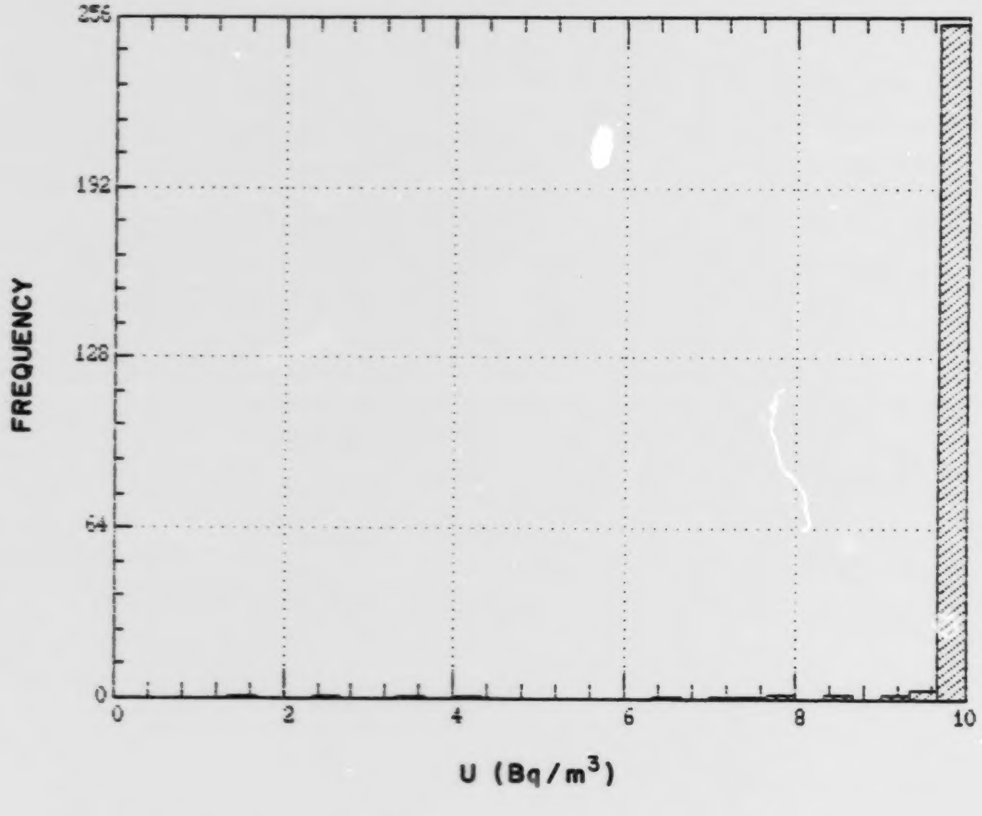

FIGURE 9.6b

## FREQUENCY HISTOGRAM FOR THORIUM CONCENTRATION AT DISCHARGE POINT TO SURFACE WATER

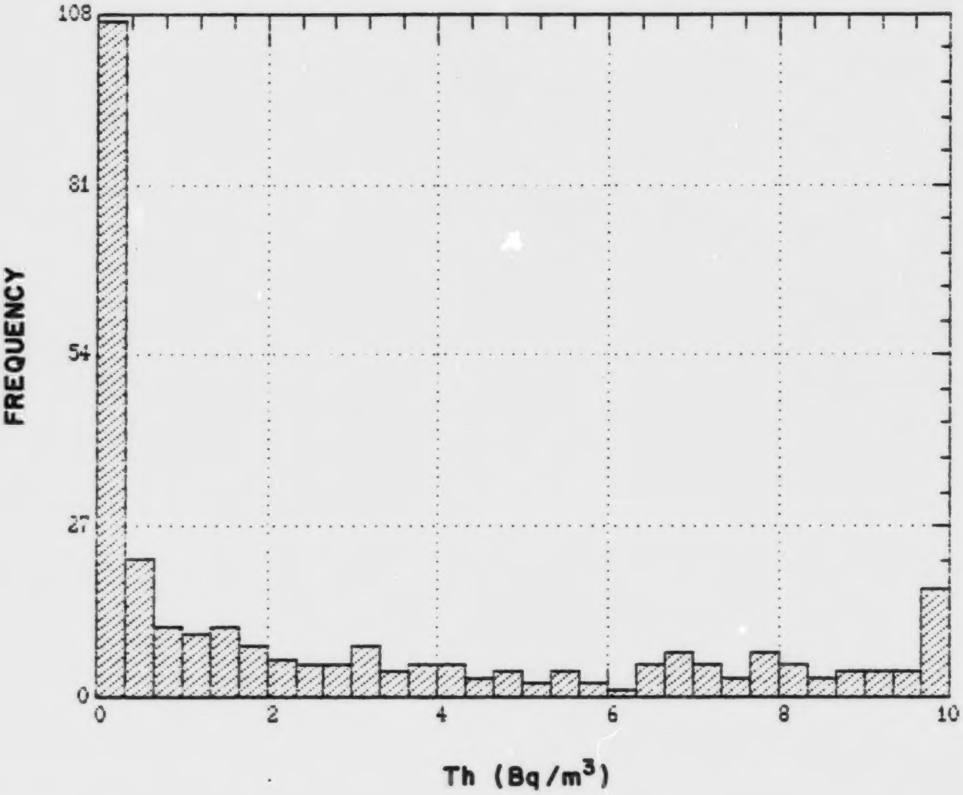

FIGURE 9.6c

## FREQUENCY HISTOGRAM FOR Pb-210 CONCENTRATION AT DISCHARGE POINT TO SURFACE WATER

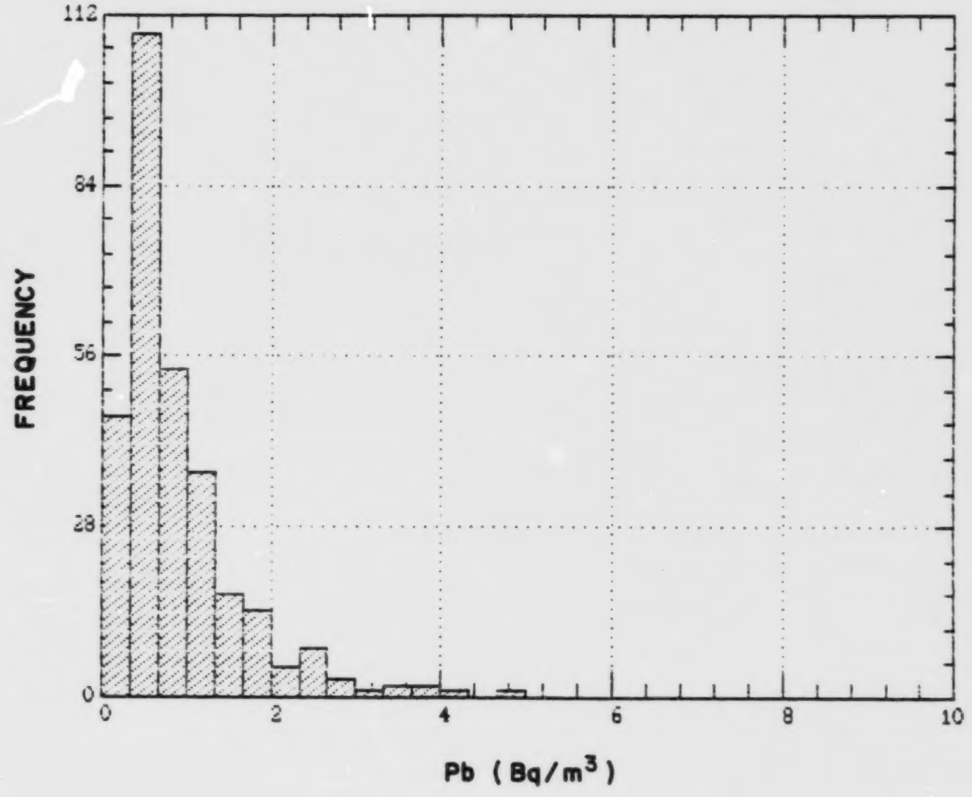

FIGURE 9.6d

## FREQUENCY HISTOGRAM Ra-226 CONCENTRATION AT DISCHARGE POINT TO SURFACE WATER

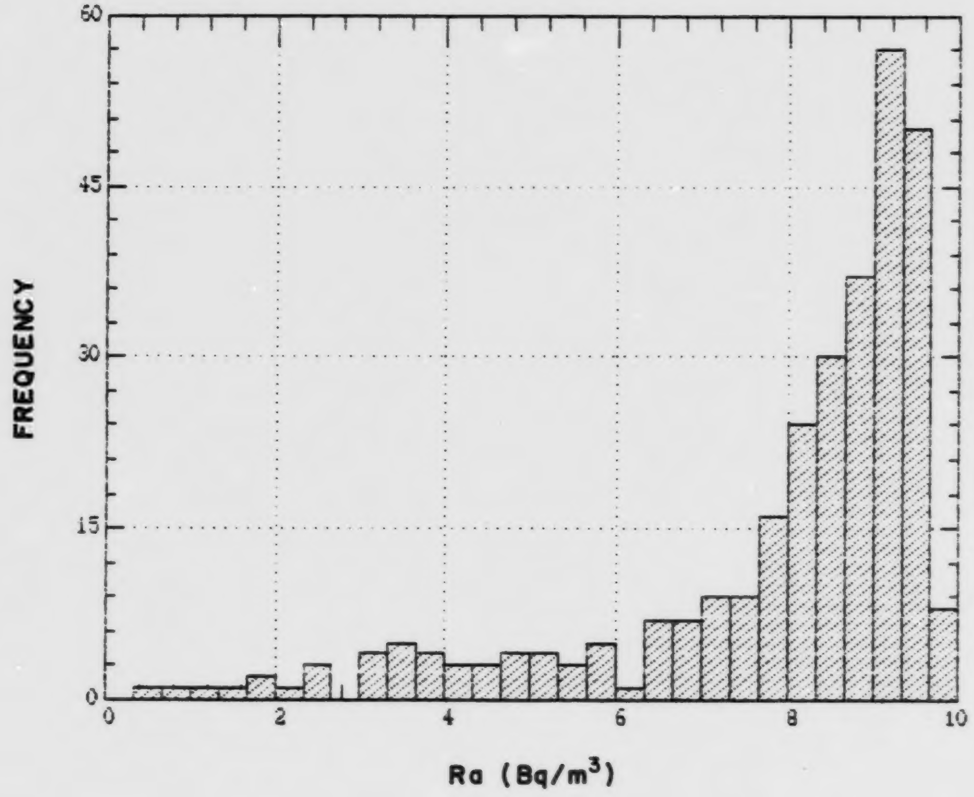

Table 9.6

## GROUNDWATER MODEL CODE LISTING

```
C
      SUBROUTINE GWATER
C
C
C     GROUNDWATER MODEL
C     (PORE WATER AND CONTAMINANT MOVEMENT IN THE SATURATED ZONE)
C
      INCLUDE 'MODEL.INC'
      INCLUDE 'VAR.INC'
C
      DIMENSION R(100),FNERF(2),ZZ(2),GWAT(5,200)
      REAL*4 LDC,LD
      REAL*8 E1,E2,E3,E4
      INTEGER*2 K
C
      X=XRGWAT
C
      IF (CODGW .GE. 1.) THEN
        WRITE(*,20)
20      FORMAT(1X,'SUBROUTINE GWATER')
      END IF
C
C     THE ORDER OF RADIONUCLIDES USED IN THIS SUBROUTINE IS
C     URANIUM, THORIUM, LEAD AND RADIUM
C
C     K IS THE TIME INTERVAL BEING CALCULATED
C     NOTE THAT AT T=0 , K=1
      K = INT(T/DT) + 1
C
C     CO IS THE THE SOURCE CONCENTRATION
      DO 25 I=1,4
        CO(I,K) = WCONC(I,4,3)
 25   CONTINUE
C
      IF(T.NE.0.0.AND.FNPRCP.NE.0.0)THEN
C
C        CALCULATION OF PROCESS
         VSR=FNPRCP*AVPRCP*ATAIL
         DV=VSR/AXGWAT
         LD = 0.12*X
         LDC= LD*DV/POGWAT
         BD=  SDGWAT*(1-POGWAT)
C
C        CALCULATION OF RETARDATION FACTOR AND MASS BALANCE
         DO 400  I=1,4
           R(I)=1+BD*DCGWAT(I)/POGWAT
C
C          IN-GROWTH FACTOR
           IF (I .EQ. 4) THEN
              F = (1-EXP(-XLAMDA(3)*DT))*R(4)/R(3)
```

Table 9.6 (continued)

```
           END IF
C
           A=DV/(POGWAT*R(I))
           B=((DV/(2*POGWAT*LDC))**2+XLAMDA(I)*R(I)/LDC)**0.5
           C=4*XLAMDA(I)*LDC/R(I)
           D=LDC*T/R(I)
C
C
C          GREEN FUNCTION, FNG, AND ERROR FUNCTION, FNERF
           ZZ(1)= (X-(A**2+C)**0.5*T)/(2*D**0.5)
           ZZ(2)= (X+(A**2+C)**0.5*T)/(2*D**0.5)
             DO 250 J=1,2
                Z=ZZ(J)
                FNERF(J)=FN(Z)
250          CONTINUE
C
C
             E1 = EXP(-X*B)
             E2 = EXP( X*B)
             E3 = E1*FNERF(1)
             E4 = E2*FNERF(2)
             FNG(I,K) =  0.5*EXP(DV*X /(2*POGWAT*LDC))*(E3+E4)
C
             IF ( FNG(I,K) .LT. 1E-30) THEN
                 FNG(I,K) = 0.
             END IF
C
C
C          MASS BALANCE CALCULATION  ********************************
C
C           MASS BALANCE OF THE INITIAL SLUG
            GWAT(I,1)= CO(I,1)*FNG(I,K)
C
            IF (CODGW .GE. 3 ) THEN
               WRITE(*,260) I,K,GWAT(I,1),CO(I,1),FNG(I,K)
260            FORMAT(' ',"INITIAL,I,K,GWAT-1,CO-1,FNG-K",2I2,3E10.3)
            END IF
C
C           MASS BALANCE FOR THE INTERMEDIATE CONTAMINANT SLUGS
            KK = K-1
            IF (KK .GE. 2) THEN
              GWAT(I,KK) = 0
              DO 300 TT=2,KK
                TTT=TT-1
                GWAT(I,KK)=GWAT(I,KK)+(CO(I,TT)-CO(I,TTT))*FNG(I,K-TT+1)
C               THE "+1" TERM IN FNG IS REQUIRED SINCE THE
C               MINIMUM ARRAY MEMBER IS FNG(I,1)
C
                IF (CODGW .GE. 3.) THEN
                  WRITE(*,275) K,GWAT(I,KK),CO(I,TT),CO(I,TTT),
     &            FNG(I,K-TT+1)
275               FORMAT(' ',"K,GWAT-KK,CO-TT,TTT,FNG-TT",I2,4E13.5)
                END IF
```

Table 9.6 (continued)

```
C
300           CONTINUE
            END IF
C
C           MASS BALANCE FOR THE LAST CONTAMINANT SLUG
            GWAT(I,K) = (CO(I,K)-CO(I,KK))*0.5*FNG(I,2)
C
            IF (CODGW .GE. 3) THEN
              WRITE(*,280) GWAT(I,K),CO(I,K),CO(I,KK),FNG(I,2)
280           FORMAT(' ',"GWAT-K,CO-K,CO-KK,FNG-2",4E10.3)
            END IF
C
C           TOTAL MASS OF ALL CONTAMINANT SLUGS
            GWAT(I,K) = GWAT(I,1) + GWAT(I,KK) + GWAT(I,K)
C
            IF (GWAT(I,K) .LT. 0.) THEN
              GWAT(I,K) = 0.
            END IF
C
C          END OF THE MASS BALANCE ********************************
C
C          INCLUDING THE IN-GROWTH OF LEAD "GWAT(5,K)"
            IF (I .EQ. 4) THEN
              GWAT(5,K) = GWAT(4,K)*F
              GWAT(3,K) = GWAT(5,K) + GWAT(3,K)
            END IF
C
C           THE FOLLOWING IS THE FLUX OF CONTANIMANT (BQ/(YEAR M2))
            GFLUX(I) = GWAT(I,K)*VSR/AXGWAT
C
C
400      CONTINUE
C
C        SETTING OUTPUT CONCENTRATIONS FOR OTHER MODULES
         GWATC(1) = GWAT(1,K)
         GWATC(2) = GWAT(2,K)
         GWATC(3) = GWAT(3,K)
         GWATC(4) = GWAT(4,K)
C
C
         IF (CODGW .GE. 2.) THEN
           WRITE(*,450) T,CO(1,K),GWAT(1,K),GWAT(2,K),GWAT(3,K),
     &     GWAT(4,K),GWAT(5,K)
450        FORMAT(3X,I6,6E10.3)
         END IF
C
C
      ELSE
C
C        AT T=0 THE CONCENTRATIONS IN THE AQUIFER ARE ZERO
         DO 485 I=1,4
           GWATC(I) = 0
           GWAT(I,1) =0
```

Table 9.6 (continued)

```
            FNG(I,1) = 0
            GFLUX(I) = 0
485       CONTINUE
            GWAT(I,5) =0
            FNG(I,5) =0
C
      ENDIF
C
C
      RETURN
      END
C
      REAL  FUNCTION FN(Z)
C
C
      IF (Z .LT. 0.0) THEN
         SGN =-1.
      ELSE IF (Z .EQ. 0.0) THEN
         SGN =0.
      ELSE
         SGN = 1.
      END IF
C
      C1=0.1441106
      C2=0.6105416
      C3=0.6077388
      C4=0.8530848
      C5=0.381965
C
      IF (ABS(Z) .GT. 8. ) THEN
        FN= 0.00
      ELSE
        D1= EXP(-Z*Z)
        D2= C1/(1+C5*ABS(Z))
        D3= C2/(1+C5*ABS(Z))**2
        D4= C3/(1+C5*ABS(Z))**3
        D5= C4/(1+C5*ABS(Z))**4
        FN = 1-SGN + SGN*D1*(D2+D3-D4+D5)
      END IF
C
      RETURN
      END
```

## 9.8 References

AES, not dated. "Precipitation Data from AES Computer Centre." AES Computer Centre Downsview.

Allard, B., Kipatsi, H. and Rydberg, J., 1977. "Sorption of Long-Lived Radionuclides in Clay and Rock. Part 1. Determination of Distribution Coefficient." KBS Technical Report 55.

Ames, L.L., and Rai, D., 1978. "Radionuclide Interactions with Soil and Rock Media, Volume 1." U.S. Environmental Protection Agency Report, U.S. EPA 520/6-78-007.

Anderson, M.P., 1979. "Using Models to Simulate the Movement of Contaminants Through Groundwater Flow Systems." CRC Critical Reviews in Environmental Controls, Vol. 9, pp. 97-156.

Beals, D.I., 1985. "Soil and Climate Parameters for Post-Closure Biosphere Assessment." Atomic Energy of Canada Limited, Technical Record TR-285.

Bear, J., 1979. Hydraulics of Groundwater, McGraw-Hill, Israel.

Birchall, A.,1986. "A Microcomputer Alogorithm for Solving Compartmental Models Involving Radionuclide Transformations." Health Physics, Vol. 50, No. 3.

Blair, R.D., 1980. "Hydrogeochemistry of an Active Pyritic Uranium Tailings Basin, Nordic Mine, Elliot Lake, Ontario." M.Sc. thesis, Dept. of Earth Sciences, University of Waterloo, Waterloo. pp. 125.

Blair, R.D., Cherry, J.A., Lim, T.P. and Vivyurka, A.J., 1980. "Groundwater Monitoring and Contaminant Occurrence at an Abandoned Tailings Area, Elliot Lake, Ontario." Proceedings, 1st International Conference on Uranium Mine Waste Disposal, Vancouver. Society of Mining Engineers, New York, pp. 411-444.

Cherry, J.A., Blackport, R.A., Dubrovsky, N., Gillham, R.W., Lim, T.P., Murray, D., Reardon, E.J. and Smyth, D.J.A., 1980a. "Subsurface Hydrology and Geochemical Evolution of Inactive Pyritic Tailings in the Elliot Lake Uranium District, Canada." Proceedings, 3rd Symposium on Uranium Tailings Management, Colorado State University, Fort Collins.

Cherry, J.A., Gillham, R.W., Anderson, F.G., and Johnson, P.E., 1980b. "Hydrogeological Studies of a Sandy Aquifer at an Abandoned Landfill: Part 2, Monitoring Devices." In CFB Borden Landfill Study, Vol. I. Waterloo Research Institute, Waterloo, Ont.

Cherry, J.A., Morin, K.A., and Dubrovsky, N.M., 1984. "Modelling of Contaminant Migration in Acidic Groundwater Plumes at Uranium Tailings Inpoundments: ADNEUT3." Prepared for National Uranium Tailings Program, Energy Mines and Resources, Contract No. OST83-00284, Dept. of Earth Sciences, University of Waterloo.

Feenstra, S., Blair, R.D., Cherry, J.A., Chakravatti, J.L., and LaRocque, E., 1981. "Hydrogeochemical Investigations of Two Inactive Tailings Areas in the Elliot Lake Uranium District Ontario, Canada." Uranium Mill Tailings Management, Proceedings of the Fourth Symposium, November, Geotechnical Engineering Program, Civil Engineering Department, Colorado State University.

Freeze, R.A., 1975. "A Stochastic-Conceptual Analysis of One-Dimensional Groundwater Flow in Nonuniform Homogeneous Media." Water Res. Research, Vol. 11, No. 5, pp. 725-741.

Freeze, R.A., and Cherry, J.A., 1979. Groundwater, Prentice Hall Inc., New Jersey.

Gerritse, R.W., Vriesema, R., Dalenberg, J.W, and De Roos, H.P. 1982. "Effect of Sewage Sludge on Trace Element Mobility in Soils." J. Environ. Qual., Vol. II, pp. 359-364.

Johnston, H.M. and Gillham, R.W., 1980. "A Review of Selected Radionuclide Distribution Coefficients of Geologic Material." Atomic Energy of Canada Limited Technical Record, TR-90.

Jury, W., Spencer, W., and Farmer, W., 1983. "Use of Models for Assessing Relative Volatility, Mobility and Persistence of Pesticides and Other Trace Organics in Soil Systems." Hazard Assessment of Chemicals, Vol. 2, Academic Press.

Lester, D.H., Janson, G., and Burkholder, H.C., 1975. "Migration of Radionuclide Chains Through an Adsorbing Medium." American Institute of Chemical Engineers Symposium Series, No. 152, Vol. 71.

Morin, K.A., 1986. Personal Communication, Government of Saskatchewan, March.

Morin, K.A., Cherry, J.A., Lim, T.P. and Vivyurka, A.J., 1982. "Contaminant Migration in a Sand Aquifer Near an Inactive Uranium Tailings Impoundment, Elliot Lake, Ontario, Can. Geotech. Jour. Vol. 19, pp. 49-62.

National Research Council (NRC), 1983. "A Study of the Isolation System for Geologic Disposal of Radioactive Wastes." Waste Isolation Systems Panel, Board on Radioactive Waste Management, Commission on Physical Sciences, Mathematics and Resources, Washington.

Petrie, G., Sneider, S., Napier, B., and Barnard, J., 1983. "Simplified Codes for Performance Evaluation (Scope) of Radionuclide Transport: Version 1.0." Prepared for the U.S. Department of Energy, Under Contract No. DE-AC06-76RLO 1830, Pacific Northwest Laboratory, Richland, Washington.

Rancon, D., 1973. "The Behaviour in Underground Environments of Uranium and Thorium Discharged by the Nuclear Industry." In: Environmental Behaviour of Radionuclides Released in the Nuclear Industry, International Atomic Energy Agency Report, IAEA-SM-172/55.

Rogers, V.C., 1978. "Migration of Radionuclide Chains in Groundwater." Nuclear Technology, Vol. 40, October.

Sheppard, M.I., Beals, D.I., Thibault, D.H., and O'Connor, P., 1984. "Soil Nuclide Distribution Coefficients and Their Statistical Distributions." Atomic Energy of Canada Limited, Whiteshell Nuclear Research Establishment, December.

U.S. Department of Health, Education and Welfare, 1970. "Radiological Health Handbook." Public Health Service, January.

Vandergraaf, T.T., 1982. "Compilation of Sorption Coefficients for Radionuclides on Granites and Granite Rocks." Atomic Energy of Canada Limited, Technical Record TR-120.

Veska, E., 1983. "Origin and Subsurface Migration of Radionuclides from Waste Rock at an Abandoned Uranium Mine Near Bancroft, Ontario". Unpublished Ph.d. Thesis, University of Waterloo.

## 10.0 SURFACE WATER DISPERSION MODELS

### 10.1 Approach to Watershed Modelling

One objective of this study was to develop the capability to model watersheds with variable characteristics. A typical watershed involves a series of lakes linked by rivers. Such a watershed is specified in this study as comprising a series of nodes; with each node representing the outflow from a watershed sub-basin. The distances between the nodes are known as "segments". Two types of watershed segments have been defined; rivers and lakes.

Selected physical and chemical characteristics for each segment must be specified as model inputs, for example, drainage area size, river reach length, lake depth, lake area. The behaviour of various ionic species and radionuclides is modelled for each segment. Dilution is the only mechanism accounted for by the river model. The lake model, on the other hand, accounts for transfer to and from lake sediment as well as dilution. Radioactive ingrowth and decay is taken into account for the short-lived radionuclides.

### 10.2 The Reference Watershed

In the Phase I and Phase II probabilistic assessment studies, the dose to a reference receptor was calculated for six key pathways including two related to surface water: consumption of contaminated drinking water and fish. The receptor was situated on the edge of a lake approximately 2 km downstream of the tailings area. The hypothetical reference site was chosen to reflect the major environmental features of a Precambrian Shield setting. Contaminated surface and groundwater flows from the tailings area were intercepted in a major river which discharged into an oligotrophic lake (i.e. a low productivity lake) with a surface area of 160 ha and mean depth of 10 m. The drainage basin at the outflow of the lake equalled 2000 ha (20 $km^2$) as compared to the tailings area which covered 50 ha (0.5 $km^2$). The waters of the drainage basin had a naturally low buffering capacity, low nutrient content and low total dissolved solids level.

These basic concepts of the reference site have been retained in their entirety in Phase III. The scope of the drainage basin however, was expanded to include a whole reference watershed having a total drainage area of approximately 40,000 ha (400 km$^2$) and a river reach of about 60 km. A schematic representation of the watershed is portrayed on Figure 10.1.

The reference tailings area is featured as being located in the headwaters of the watershed. The watershed contains three lakes of substantially different size and has been divided into eight sub-basins to permit computation of flow and water quality at several points in the surface water system. These points are indicated on the figure as node numbers (i.e. Node 1,2....8). Details of the characteristics of the watershed sub-basins, lakes and river reaches are summarized on Table 10.1.

The upstream end of the watershed within the 3 km ring of the tailings area comprises that part of the watershed modelled in Phases I and II. The radium-226 levels computed at Node 2 on the outlet of the first lake of the system were used in the previous phases for computing the dose to the reference receptor.

The approach adopted in Phase III permits dose to be calculated for receptors located in any or all of 80 windrose locations. Details of the windrose structure are presented in Section 5.0 and elsewhere in this report. The contribution to the total dose from consumption of contaminated drinking water is achieved by linking receptors to appropriate nodes on the watershed. Not all receptors however need to be linked to watershed nodes as some receptors may be situated in windrose locations far removed from the reference watershed and receive their drinking water supply from uncontaminated sources.

## 10.3 The Hydrologic Component

Flow at each node in the reference watershed is calculated using the simple model:

FIGURE 10.1

REFERENCE WATERSHED SCHEMATIC

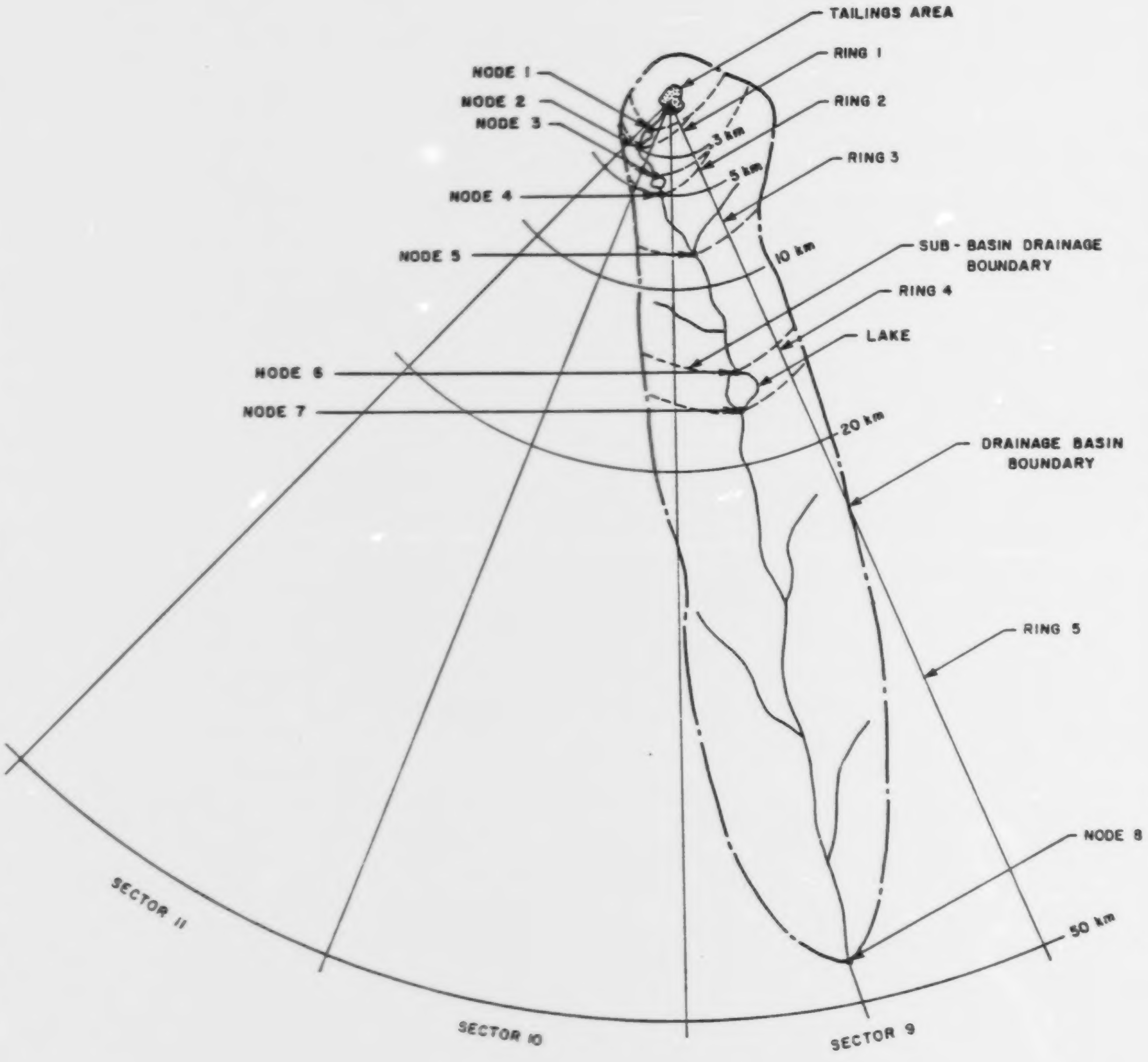
TAILINGS AREA
RING 1
NODE 1
NODE 2
NODE 3
RING 2
3 km
RING 3
5 km
NODE 4
NODE 5
10 km
SUB - BASIN DRAINAGE BOUNDARY
RING 4
LAKE
NODE 6
NODE 7
20 km
DRAINAGE BASIN BOUNDARY
RING 5
NODE 8
50 km
SECTOR 11
SECTOR 10
SECTOR 9

Table 10.1

## CHARACTERISTICS OF REFERENCE WATERSHED

| | Segment Details | | | | Watershed Area | | | |
|---|---|---|---|---|---|---|---|---|
| | | | | | | | End Node Windrose Location | |
| End Node No. | Segment Type | River Reach Length (m) | Lake Mean Depth (m) | Lake Surface Area (m**2) | Sub-basin Area (km**2) | Cumulative Area (km**2) | Direction | Sector |
| 1 | River | 3.0E3 | | - | 15 | 15 | 11 | 1 |
| 2 | Lake | - | 10 | 5.0E5 | 5 | 20 | 11 | 1 |
| 3 | River | 3.5E3 | | - | 12 | 32 | 10 | 2 |
| 4 | Lake | - | 4 | 2.5E5 | 6 | 38 | 10 | 2 |
| 5 | River | 7.0E3 | | - | 32 | 70 | 9 | 3 |
| 6 | River | 1.3E4 | | - | 50 | 120 | 9 | 4 |
| 7 | Lake | - | 5 | 4.0E6 | 20 | 140 | 9 | 4 |
| 8 | River | 3.0E4 | | - | 260 | 400 | 9 | 5 |

$$Q_{n,t} = \Sigma \ P_t A_n + \Sigma \ Q_{s,t} \qquad (10.1)$$

where:

$Q_{n,t}$ = volumetric surface water flow at node 'n' at time 't' ($m^3.yr^{-1}$)

$Q_{s,t}$ = volumetric discharge rate of tailings source term 's' (surface and subsurface flows) from the reference tailings area at time 't' ($m^3.yr^{-1}$)

$P_t$ = mean annual net precipitation at time 't', which occurs as surface runoff (i.e. after evapotranspiration losses) ($m.yr^{-1}$)

$A_n$ = area of the nth sub-basin in the watershed ($m^2$)

n = the node number for the nth segment in the watershed numbered consecutively commencing in the upper reaches of the watershed

In using net precipitation in the model, it is implicitly assumed that the same runoff factor applies to all sub-basins irrespective of size. This assumption is reasonable for the size of the reference watershed which increases in sub-basin area from 15 to 400 $km^2$. A statistical comparison of monthly flow data from four stations on the Serpent River Basin in northern Ontario with drainage areas ranging in size from 157 to 1349 $km^2$ showed that the area pro-rating basis provided the best correlation with historical data (SENES and Golder, 1981). In other words, it was found that monthly flow in the Serpent River could be adequately predicted as the product of a uniform runoff factor and the size of the drainage basin. Application of this approach to predict annual surface flows is equally valid.

Of the parameters in equation (10.1), the net precipitation ($P_t$) is a time-variant input parameter. Hence, it must be sampled from the appropriate distribution of values each time step ($\Delta t$) over the duration of each trial (see Chapter 2 of Volume 1 for a discussion of this aspect). Since the size of the time step may vary from 1 to 10 years (a predetermined decision in developing the system code), the probability distribution of annual precipitation must be adjusted accordingly.

The areas of the watershed sub-basins ($A_n$) are treated as input constants since they are specific to each application. The sub-basin areas for the reference site are listed on Table 10.1. The calculation of flow at each node in the watershed is determined as the summation of the flows to all upstream nodes. This requires that the nodes be ordered in the correct sequence starting from the upper end of the watershed. The tailings source is linked to node 1 on the watershed (see Figure 10.1).

## 10.4 Major Ions Component

### 10.4.1 Baseline Levels

The concentration of the major water quality constituents, including calcium and sulphate, were modelled as conservative substances as in the Phase I and II studies. The natural background levels assumed for several of the major constituents were:

| | | |
|---|---|---|
| calcium - | $10^{-4}$ | $mol.L^{-1}$ ($10^{-1}$ $mol.m^{-3}$) |
| sulphate - | $10^{-4.15}$ | $mol.L^{-1}$ ($10^{-1.15}$ $mol.m^{-3}$) |
| sodium - | $10^{-4.1}$ | $mol.L^{-1}$ ($10^{-1.1}$ $mol.m^{-3}$) |
| potassium - | $10^{-4.8}$ | $mol.L^{-1}$ ($10^{-1.8}$ $mol.m^{-3}$) |
| magnesium - | $10^{-4.5}$ | $mol.L^{-1}$ ($10^{-1.5}$ $mol.m^{-3}$) |
| chloride - | $10^{-4.7}$ | $mol.L^{-1}$ ($10^{-1.7}$ $mol.m^{-3}$) |

The concentrations for calcium, sulphate, magnesium and chloride in Precambrian Shield water were obtained from water quality data summary reports prepared by the Ontario Ministry of the Environment (1972 to 1980). Since comparable data were not available for sodium and potassium, typical concentrations for these constituents were taken from Stumm and Morgan (1981).

### 10.4.2 River Segments

The major ionic constituents affected by the tailings source are calcium and sulphate. Calculation of the concentrations of these constitutents at the river node locations is based on mass balance principles for these conservative substances:

$$[Ca]_{n,t} = \frac{Q_{n-1,t}[Ca]_{n-1,t} + Q_{s,t}[Ca]_{s,t} + (Q_{n,t}-Q_{n-1,t})[Ca]_B}{Q_{n,t}} \qquad (10.2)$$

and

$$[SO_4]_{n,t} = \frac{Q_{n-1,t}[SO_4]_{n-1,t} + Q_{s,t}[SO_4]_{s,t} + (Q_{n,t}-Q_{n-1,t})[SO_4]_B}{Q_{n,t}} \qquad (10.3)$$

where:

$[Ca]_{n-1,t}$ = calcium concentration in the flow at node 'n-1' at time 't' ($mol.m^{-3}$)

$[Ca]_{n,t}$ = calcium concentration in the flow at node 'n' at time 't' ($mol.m^{-3}$)

$[Ca]_B$ = natural background level of calcium in the freshwater flow in the watershed ($mol.m^{-3}$)

$[Ca]_{s,t}$ = calcium concentration in the tailings source term discharge 's' from the tailings area at time 't' ($mol.m^{-3}$)

$Q_{n-1,t}$ = volume of the surface water flow at node 'n-1' at time 't' ($m^3.yr^{-1}$)

$Q_{n,t}$ = volume of the surface water flow at node 'n' at time 't' ($m^3.yr^{-1}$)

$Q_{s,t}$ = volume of the tailings source term discharge 's' from the tailings area at time 't' ($m^3.yr^{-1}$)

$[SO_4]_{n-1,t}$ = sulphate concentration in the flow at node 'n-1' at time 't' ($mol.m^{-3}$)

$[SO_4]_{n,t}$ = sulphate concentration in the flow at node 'n' at time 't' ($mol.m^{-3}$)

$[SO_4]_B$ = natural background level of sulphate in the freshwater flow in the watershed ($mol.m^{-3}$)

$[SO_4]_{s,t}$ = sulphate concentration in the tailings source term discharge 's' from the tailings area at time 't' ($mol.m^{-3}$)

These expressions provide estimates of the average annual calcium and sulphate concentrations at the river nodes. They are used in a subsequent section to determine pH in the river system.

### 10.4.3 Lake Segments

The estimation of calcium and sulphate levels in the lakes of the watershed takes into consideration not only dilution but also the history of the levels of the ions in the lake water column in the previous time step. The concentrations of the major constituents are represented by a simple differential equation of the form:

$$V \frac{dC}{dt} = Q_{in} C_{in} - Q_{out} C \qquad (10.4)$$

where

$V$ = volume of the lake ($m^3$)

$Q_{in}$ = summation of all input flows to the lake ($m^3.yr^{-1}$)

$Q_{out}$ = outflow from the lake ($m^3.yr^{-1}$)

$C_{in}$ = constituent concentration in the inflow waters ($mol.m^{-3}$)

$C$ = constituent concentration in the lake ($mol.m^{-3}$)

Integration of equation (10.4) yields the basic equation used to predict the behaviour of the major ions in the lakes:

$$C_{n,t} = \left( \frac{Q_{n-1,t}C_{n-1,t} + (Q_{n,t} - Q_{n-1,t})C_B}{Q_{n,t}} \right) + \left\{ C_{n,t-\Delta t} - \left( \frac{Q_{n-1,t}C_{n-1,t} + (Q_{n,t} - Q_{n-1,t})C_B}{Q_{n,t}} \right) \right\} \exp \left( \frac{-Q_{n,t}\Delta t}{V_n} \right) \qquad (10.5)$$

where:

$C_{n-1,t}$ = ion concentration in the inlet flow to the lake, designated node 'n-1', at time't' ($mol.m^{-3}$)

$C_{n,t}$ = ion concentration in the lake designated node 'n' at time 't' ($mol.m^{-3}$)

$C_{n,t-\Delta t}$ = ion concentration in the lake designated node 'n' at the previous time step denoted by 't-Δt' ($mol.m^{-3}$)

$C_B$ = baseline or natural background ion concentration ($mol.m^{-3}$)

$Q_{n-1,t}$ = river flow at the inlet to the lake, designated node 'n-1', at time 't' ($m^3.yr^{-1}$)

$Q_{n,t}$ = flow out of the lake, designated by node 'n', at time 't' ($m^3.yr^{-1}$)

$V_n$ = volume of the lake designated by node 'n' ($m^3$)

Δt = size of the time step (yr)

The volume of the lakes ($V_n$) are calculated as a function of the surface areas ($L_n$) and mean depths ($h_n$) of the lakes which are specified as input parameters.

## 10.5 pH Component

To calculate the pH in the surface water system, it is assumed that the concentrations of iron and aluminum are in equilibrium with solid phases of ferric hydroxide ($Fe(OH)_3(s)$) and gibbsite ($Al(OH)_3(s)$). The concentrations of calcium and sulphate are modelled as described in the previous section. The concentrations of sodium, potassium, magnesium and chloride are essentially unaffected by the tailings area drainage and are characterized by the assumed natural background levels. The waters are considered to be slightly super-saturated (Saturation Index = 0.3) with respect to dissolved carbonate in equilibrium with carbon dioxide ($CO_2$) in the air. The latter is very common in oligotrophic lakes on the Canadian Shield. The concentration of all ions is expressed on a $mol.L^{-1}$ basis internally in the pH model. The equilibrium reactions are as follows:

Equilibrium Reactions in Lake Water

| | Log K |
|---|---|
| $Al(OH)_3(s) + 3H^+ \rightleftharpoons Al^{3+} + 3H_2O$ | 8.5 |
| $Al^{3+} + H_2O \rightleftharpoons Al(OH)^{2+} + H^+$ | -4.97 |
| $Al^{3+} + 2H_2O \rightleftharpoons Al(OH)_2^+ + 2H^+$ | -9.30 |

| | |
|---|---|
| $Al^{3+} + 3H_2O \rightleftharpoons Al(OH)_3(aq) + 3H^+$ | -15.00 |
| $Al^{3+} + SO_4^{2-} \rightleftharpoons AlSO_4^+$ | 3.2 |
| $Fe(OH)_3(s) + 3H^+ \rightleftharpoons Fe^{3+} + 3H_2O$ | 5.97 ($K^c$) |
| $Fe(OH)_3(s) + 2H^+ \rightleftharpoons FeOH^{2+} + 2H_2O$ | 3.78 ($K^c$) |
| $Fe(OH)_3(s) + H^+ \rightleftharpoons Fe(OH)_2^+ + H_2O$ | 0.30 ($K^c$) |
| $H_2CO_3 \rightleftharpoons H^+ + HCO_3^-$ | -6.5 |
| | $pCO_2 = -3.2$ |
| | $K_H = -1.27$ |

The ionic charge balance at any point in the watershed is given by:

$$\begin{aligned} 2[Ca^{2+}]_{n,t} &+ 2[Mg^{2+}] + [Na^+] + [K^+] + 3[Fe^{3+}] + 2[FeOH^{2+}] \\ &+ [Fe(OH)_2^+] + [FeSO_4^+] + 3[Al^{3+}] + 2[AlOH^{2+}] + [Al(OH)_2^+] \\ &+ [AlSO_4^+] = 2[SO_4^{2-}]_{n,t} + [Cl^-] + [HCO_3^-] \end{aligned} \qquad (10.6)$$

Note that:

$$\begin{aligned} 2[Mg^{2+}] + [Na^+] + [K^+] - [Cl^-] &= 2 \times 10^{-4.5} + 10^{-4.1} + 10^{-4.8} - 10^{-4.7} \\ &= 10^{-3.86} \end{aligned}$$

and

$$[HCO_3^-] = \frac{10^{pH-11.0}}{f^{1/4}}$$

where

$f^{1/4}$ = activity coefficient of monovalent ions

The contribution of the remaining components of equation (10.6) to the pH equation are discussed below.

### Trivalent Cations $Al^{3+}$ and $Fe^{3+}$

The predicted concentration of $Fe^{3+}$ is several orders of magnitude less than the concentration of $Al^{3+}$ for any pH value:

$$[Fe^{3+}] = 10^{5.97-3pH}$$

$$[Al^{3+}] = \frac{10^{8.5-3pH}}{f^{9/4}}$$

In fact, the sum of the trivalent cations ($[Al^{3+}]+[Fe^{3+}]$) is equal to:

$$\frac{10^{5.97}}{10^{3pH}} + \frac{10^{8.5}}{f^{9/4}10^{3pH}} \quad \frac{10^{8.501}}{f^{9/4}10^{3pH}} \qquad \text{for } 0.6 \leq f \leq 0.9$$

### Divalent Hydroxo Complexes $Al(OH)^{2+}$ and $Fe(OH)^{2+}$

The concentration of $Fe(OH)^{2+}$ is given on the basis of solubility data from tailings oxidation tests:

$$[Fe(OH)^{2+}] = 10^{3.78-2pH}$$

Since the average activity coefficient for divalent cations is estimated to be 0.8; the activity of $Fe(OH)^{2+}$ is equal to:

$$\left\{ Fe(OH)^{2+} \right\} = 0.8(10^{3.78-2pH}) = 10^{3.683-2pH}$$

In the pH equation, the activities of $Al(OH)^{2+}$ and $Fe(OH)^{2+}$ can be readily combined (since both involve the same power with respect to pH) to give:

$$\left\{ Al(OH)^{2+} \right\} + \left\{ Fe(OH)^{2+} \right\} = \frac{10^{3.683}}{10^{2pH}} + \frac{10^{3.53}}{10^{2pH}} = \frac{10^{3.91}}{10^{2pH}}$$

It follows that the sum of concentrations of $Al(OH)^{2+}$ and $Fe(OH)^{2+}$ is given by:

$$[Al(OH)^{2+}] + [Fe(OH)^{2+}] = \frac{10^{3.91}}{f\ 10^{2pH}} = \frac{10^{3.91-2pH}}{f}$$

## Monovalent Hydroxo Complexes $Fe(OH)_2^+$ and $Al(OH)_2^+$

The activity coefficients of monovalent ions ($f^{1/4}$) in the surface runoff is always close to unity:

$f^{1/4} = 0.88$ if $f = 0.6$
$f^{1/4} = 0.97$ if $f = 0.9$

Thus the sum of $Fe(OH)_2^+$ and $Al(OH)_2^+$ equals:

$$[Fe(OH)_2^+] + [Al(OH)_2^+] = \frac{10^{0.3}}{10^{pH}} + \frac{10^{-0.8}}{10^{pH}} = \frac{10^{0.33}}{10^{pH}}$$

which may be restated as:

$$[Fe(OH)_2^+] + [Al(OH)_2^+] = 10^{0.33-pH}$$

## Term for the Sulphate Concentration

The term given in equation (10.6) for sulphate is given by the sum of free sulphate and sulphato complexes:

$$[SO_4^{2-}]_{n,t} = [SO_4^{2-}] + [FeSO_4^+] + [AlSO_4^+] \tag{10.7}$$

A simple comparison of the complexation reactions reveals that the concentration of $FeSO_4^+$ is negligible in comparison to either $AlSO_4^+$ or $SO_4^{2-}$. The formation of the $AlSO_4^+$ complex can be expressed from the following two equilibrium expressions:

$Al(OH)_3(s) + 3H^+ \rightleftharpoons Al^{3+} + 3H_2O$ log K = 8.5
$Al^{3+} + SO_4^{2-} \rightleftharpoons AlSO_4^+$ log K = 3.2

Therefore:

$$Al(OH)_3(s) + 3H^+ + SO_4^{2-} \rightleftharpoons AlSO_4^+ + 3H_2O$$

The concentration of $AlSO_4^+$ is given (including the activity coefficients) as:

$$[AlSO_4^+] = \frac{f}{f^{1/4}} \; 10^{(8.5+3.2)} \; 10^{-3pH} \; [SO_4^{2-}]$$

$$= f^{3/4} \; 10^{11.7-3pH} \; [SO_4^{2-}]$$

The total concentration of sulphate includes the free sulphate and the sulphato complex:

$$[SO_4^{2-}]_{n,t} = [SO_4^{2-}] + [AlSO_4^+] = [SO_4^{2-}] \left[1 + f^{3/4} \; 10^{11.7-3pH}\right]$$

Therefore:

$$[SO_4^{2-}] = \left[\frac{[SO_4^{2-}]_{n,t}}{1 + f^{3/4} \; 10^{11.7-3pH}}\right]$$

and

$$[AlSO_4{}^+] = [SO_4^{2-}]_{n,t} - [SO_4^{2-}] = \left[\frac{f^{3/4} 10^{11.7-3pH}}{1 + f^{3/4} 10^{11.7-3pH}}\right] \; [SO_4^{2-}]_{n,t}$$

Note that in the ionic balance the $[AlSO_4^+]$ (a cation) and the $[SO_4^{2-}]$ (an anion) appear on the left and the right side of the equation.

$$\ldots + [AlSO_4^+] = 2[SO_4^{2-}] + \ldots$$

$$\ldots + \left[\frac{f^{3/4} \; 10^{11.7-3pH}}{1 + f^{3/4} \; 10^{11.7-3pH}}\right] [SO_4^{2-}]_{n,t} = 2\left[\frac{1}{1 + f^{3/4} \; 10^{11.7-3pH}}\right] [SO_4^{2-}]_{n,t} \; + \ldots$$

Since both terms have a common denominator, they may be combined to yield:

$$\ldots = \left[\frac{2 - f^{3/4} \; 10^{11.7-3pH}}{1 + f^{3/4} \; 10^{11.7-3pH}}\right] [SO_4^{2-}]_{n,t} \; \ldots$$

### pH Model

From the above, the equation for calculating pH at any point in the watershed becomes:

$$3\left[\frac{10^{8.5-3pH_{n,t}}}{f^{9/4}}\right]+2\left[\frac{10^{3.91-2pH_{n,t}}}{f}\right]+\left[10^{0.3-pH_{n,t}}\right]+\left[10^{-3.86}\right]+2[Ca^{2+}]_{n,t}=$$

$$[SO_4^{2-}]_{n,t}\left[\frac{2-f^{3/4}\,10^{11.7-3pH_{n,t}}}{1+f^{3/4}\,10^{11.7-3pH_{n,t}}}\right]+\left[\frac{10^{pH_{n,t}-11.0}}{f^{1/4}}\right] \qquad (10.8)$$

where

$f$ = the activity coefficient; for the reference watershed environment f would be expected to fall between 0.6 an 0.9 with a probable value of 0.8.

$pH_{n,t}$ = the pH level of the surface water in the watershed at node 'n' at time 't'

The above pH equation requires an iterative solution.

## 10.6 Radionuclide Component

A wide variety of mathematical models have been developed for assessing the hydrologic transport of radionuclides. The models range from simple algebraic models to sophisticated multi-dimensional models based on numerical solutions to advection-diffusion and hydrodynamic equations. The selection of any particular model requires careful consideration of its applicability to the specific situation.

The movement of radionuclides through the aquatic pathways depends on numerous physical, biological and chemical processes which affect the resulting concentrations in water, sediment and aquatic biota. Since exposure to man may result from consumption of contaminated water or biota (eg. fish flesh), estimation of the radionuclide concentrations in these media is of particular interest in radiological assessments, especially in Canada where the aquatic pathways have generally been found to be the largest contributors to dose. Typically, the concentrations in water have been estimated taking into account only the effects of dilution, and removal to bottom sediments in the case of lake water. The concentration in fish flesh has usually been calculated using the aggregate, one-parameter transfer factor model (see Volume 2 of SENES (1985) report).

The transport of radionuclides in the surface water system involves both dilution with fresh water flow and transfer to mineral and biological solids. The transfer to solid matter is often a reversible process hence, the radionuclides may return to the aqueous phase as conditions change. These mechanisms were included in the model developed to predict radium-226 behaviour in the reference lake in Phase II. As discussed later in this section, the concept has been extended in Phase III for modelling the behaviour of all radionuclides in the lakes of the watershed.

Ingrowth and decay of radionuclides held in the waters and sediments of the watershed were assessed to be important only for the relatively short-lived radionuclides; radium-226 and lead-210. Since water is flushed from the lakes and rivers in a comparatively short time (i.e. a matter of years) and sedimenting solids also are buried in the deep lake sediments in a short time (i.e. in tens of years), the change in inventory due to radioactive decay in the water column or exchangeable sediment for the long-lived radionuclides, such as uranium and thorium, is inconsequential. The approach taken to modelling the ingrowth and decay of the radioactive species therefore, was to disregard these processes for the long-lived species (i.e. uranium and thorium) but to take them into account for the relatively short-lived radionuclides considered in this study (i.e. radium-226 and lead-210). Furthermore, the processes of radioactive ingrowth and decay were accounted for in a simplified fashion by adjusting the inventories at the start of each time-step for the elapsed time since the end of the last step rather than incorporating the processes directly into the differential equations for calculating mass balance. This simplification reduced the complexity of the equation and is believed to introduce minimal error. The approach is also consistent with the approach taken in this study to developing assessment level models. Details of the approach used to incorporate radioactive ingrowth and decay are presented at the end of Section 10.6.

### 10.6.1 River Segments

A simple approach was chosen to model radionuclide behaviour in the river segments of the watershed. The algorithm for the river reaches considers only dilution. Transfer to bottom sediment is ignored. The rationale for this simplification is as follows:

- While sediment will deposit on the bottom of the river segments during low flow conditions, sediment will also be resuspended from the river bed during high flow periods and be transported downstream. Over the time scale of the assessment, the net result would be that most, if not all, of the sediment is transported to the nearest downstream lake.
- Watersheds on the Canadian Precambrian Shield typically contain several lakes. The quiescent conditions in the lakes present a natural sink for the sediment-bound radionuclides.

The simple mass balance equation used to calculate radionuclide levels at river nodes is as follows:

$$[R_i]_{n,t} = \frac{Q_{n-1,t}[R_i]_{n-1,t} + Q_{s,t}\,[R_i]_{s,t}}{Q_{n,t}} \qquad (10.9)$$

where:

$Q_{n-1,t}$ = volume of surface water flow at node 'n-1' at time 't' ($m^3.yr^{-1}$)

$Q_{n,t}$ = volume of surface water flow at node 'n' at time 't' ($m^3.yr^{-1}$)

$Q_{s,t}$ = volume of the tailings source term discharge 's' from the tailings area at time 't' ($m^3.yr^{-1}$)

$[R_i]_{n-1,t}$ = concentration of radionuclide 'i' in the surface water flow at node 'n-1' at time 't' ($Bq.m^{-3}$)

$[R_i]_{n,t}$ = concentration of radionuclide 'i' in the surface water flow at node 'n' at time 't' ($Bq.m^{-3}$)

$[R_i]_{s,t}$ = concentration of radionuclide 'i' in the tailings source term discharge 's' from the tailings area at time 't' ($Bq.m^{-3}$)

The above formulation excludes the natural background activity of the radionuclides which is consistent with the methodology employed for calculating incremental dose to reference man. The radionuclide content in the tailings source term discharges include dissolved species in the surface and subsurface flows originating from the tailings area and sediment bound species associated with the solids eroded from the tailings surface. Equation (10.9) does not distinguish between the dissolved and solid fraction of the radionuclides. Removal of radionuclides with sedimenting solids is accounted for in the lake model.

### 10.6.2 Lake Segments

#### Modelling Approach

Radionuclides are introduced into the lakes of the reference watershed with the inflow from the upstream watershed. Removal of radionuclides from the aqueous phase occurs through transfer to suspended solids including inorganic solids and organic matter (e.g. aquatic biota) and direct transfer to bottom sediment. Ultimately that portion of the radionuclides which transfer to the suspended solids enters the lake sediments as the solids settle out of the water column. As a result of the oxidation of organic matter at the lake bottom, however a portion of the radionuclides are released from the sediment solids to the sediment interstitial water from which they may diffuse back to the lake water column. The remaining fraction of the solid-bound radionuclides eventually become buried in the sediment and thus are unavailable for exchange with the water column.

A conceptual schematic of the lake sediment model is shown in Figure 10.2 and comprises two active compartments, the water column and the exchangeable sediment. The basic parameters defined for the assessment of radionuclide transfer between the water column and sediment are given as follows:

$h_n$ = mean depth of water column of the lake designated node 'n' (m)

$\lambda$ = thickness of the sediment exchange zone (m)

$[R_i]_{n,t}$ = activity concentration of radionuclide 'i' in the water column of lake 'n' at time 't' ($Bq.m^{-3}$)

$[R_i]_{1,t}$ = average activity concentration of radionuclide 'i' in the interstitial water of the exchanging sediment of lake 'n' at time 't' ($Bq.m^{-3}$)

$[R_i]_{\lambda,t}$ = activity concentration of radionuclide 'i' at depth 'λ' in the sediment interstitial water of lake 'n' at time 't' ($Bq.m^{-3}$)

u = current velocity in lakes of the watershed ($m.yr^{-1}$)

The accumulation of radionuclides (as a flux term) in the exchangeable sediment (thickness = λ) is given by:

$$\frac{\lambda d[R_i]_{1,t}}{dt} = \underbrace{[\sigma_{s,n}k_{d,i}[R_i]_{n,t}]}_{\substack{\text{deposition flux}\\ \text{of radionuclide 'i' in}\\ \text{fresh sedimenting}\\ \text{matter}}} - \underbrace{[k_{L,n}([R_i]_{\lambda,t}-[R_i]_{n,t})]}_{\substack{\text{flux of radionuclide}\\ \text{'i' from sediment}\\ \text{into the water}\\ \text{column}}} - \underbrace{[\sigma_{D,n}k_{d,i}[R_i]_{\lambda,t}]}_{\substack{\text{flux of radionuclide 'i'}\\ \text{out of the exchange}\\ \text{zone due to continuous}\\ \text{deposition of sediment}\\ \text{(i.e. loss due to burial)}}} \qquad (10.10)$$

where:

$\sigma_{s,n}$ = rate of sedimenting material removal from the lake water column ($g.m^{-2}.yr^{-1}$)

$k_{d,i}$ = distribution coefficient for radionuclide 'i' between sedimenting material (both organic and inorganic fractions) and lake water ($m^3.g^{-1}$)

FIGURE 10.2

CONCEPTUAL SCHEMATIC OF REFERENCE LAKE

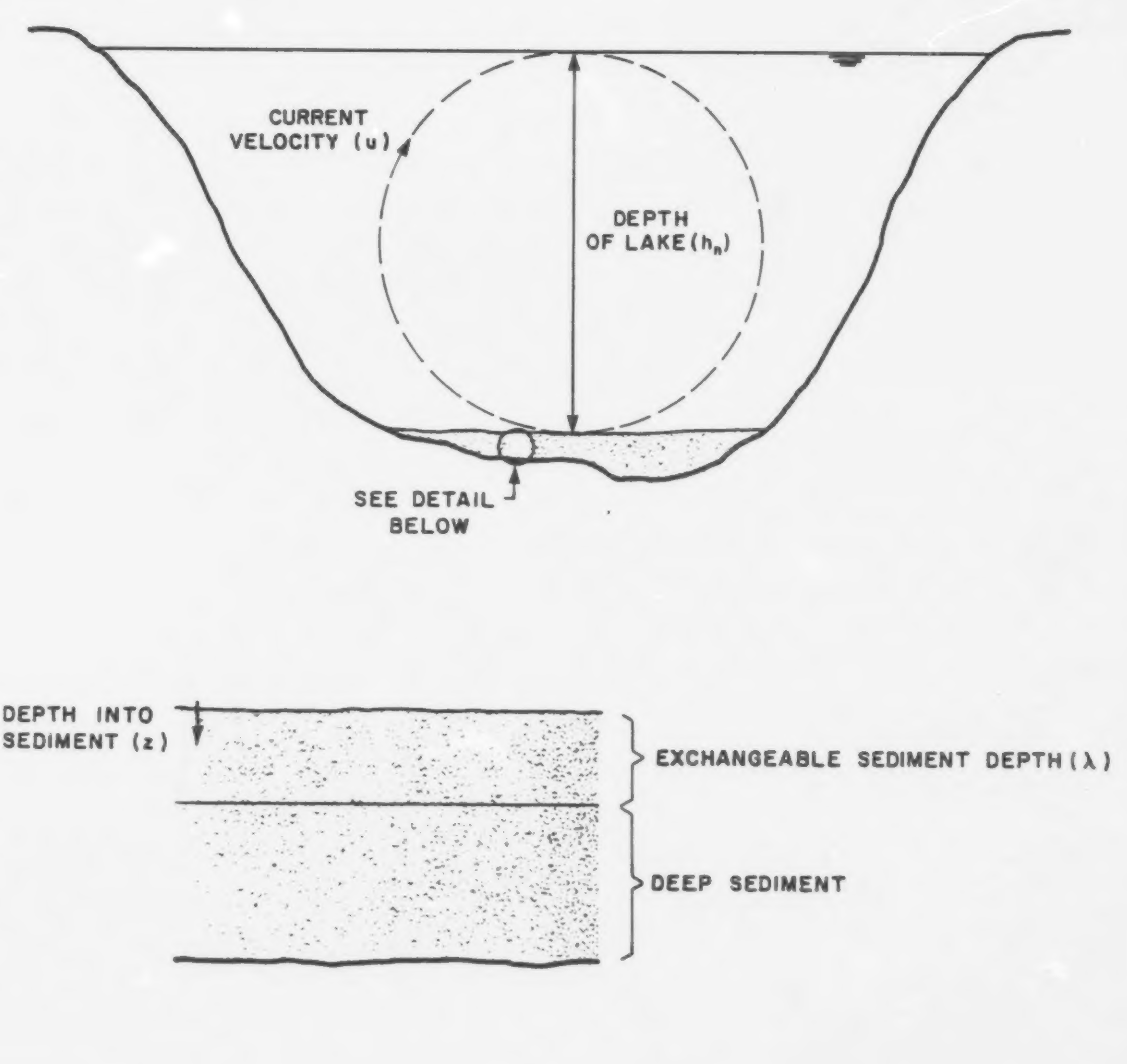
CURRENT VELOCITY (u)
DEPTH OF LAKE ($h_n$)
SEE DETAIL BELOW
DEPTH INTO SEDIMENT (z)
EXCHANGEABLE SEDIMENT DEPTH (λ)
DEEP SEDIMENT

$k_{L,n}$ = mass transfer coefficient of the radionuclides into the lake water column from the sediment in lake 'n' ($m.yr^{-1}$)

$\sigma_{D,n}$ = rate of sediment burial (or removal from the active exchange layer) ($g.m^{-2}.yr^{-1}$)

Collecting the lake water column concentration terms ($[R_i]_{n,t}$) in equation (10.10) yields:

$$\lambda \frac{d[R_i]_{1,t}}{dt} = \underbrace{[(\sigma_{s,n}k_{d,i}+k_{L,n})[R_i]_{n,t}]}_{\substack{\text{apparent net deposition} \\ \text{(settling and diffusion)}}} - [k_{L,n}[R_i]_{\lambda,t}] - [\sigma_{D,n}k_{d,i}, [R_i]_{\lambda,t}] \qquad (10.11)$$

Sediment Characteristics

The lakes of the reference watershed are assumed to be oligotrophic, hence the sedimentation rate is characteristic of a low productivity lake environment. For a net primary biomass production on a dry weight solids basis of 100 $g.m^{-2}.yr^{-1}$ (range 40 to 200 $g.m^{-2}.yr^{-1}$) (Wetzel 1975) and an organic content of 55% in the sedimenting solids, the total biomass sedimentation flux equals 180 $g.m^{-2}.yr^{-1}$.

The sedimenting material comprises not only that resulting from biomass production but also the suspended solids load carried in surface runoff from the watershed. The contribution of the inflow surface runoff to the sedimentation flux is dependent on the size of the sub-basin drainage areas and the suspended solids content of the surface runoff. Runoff from undisturbed Canadian Shield watersheds typically has a low suspended solids content of about 3 $g.m^{-3}$ (range 1 to 15 $g.m^{-3}$) comprised of both organic and inorganic fractions.

The sedimentation flux to each of the lakes in the reference watershed for a mean annual runoff of 0.4 $m.yr^{-1}$ was assessed given the above data on sedimenting material and the lake surface and drainage basin areas reported previously in Table 10.1. The calculated flux values are reported on Table 10.2 The nominal sedimentation fluxes of 210 to 260 $g.m^{-2}.yr^{-1}$ equate to sedimentation rates of 0.0020 to 0.0024 $m.yr^{-1}$ (0.20 to 0.24 $cm.yr^{-1}$) assuming an average solids density of $1.84x10^6$ $g.m^{-3}$ and a porosity of 94 percent. Similarly the minimum and maximum values of 85 and 765 $g.m^{-2}.yr^{-1}$ equate to sedimentation rates of 0.0008 and 0.0069 $m.yr^{-1}$ (0.08 to 0.69 $cm.yr^{-1}$). These rates are comparable to net sediment deposition velocities reported in the literature for Canadian Shield lakes of 0.0007 to 0.0080 $m.yr^{-1}$ (0.07 to 0.8 $cm.yr^{-1}$) (Kipphut, 1978). The sedimentation fluxes of total solids are specified as triangular distributions in the model using the nominal, minimum and maximum values given in Table 10.2 for each lake.

In addition to the above, the solids eroded from the reference tailings area are added to the solids loading on the upstream receiving lake (i.e. node 2). The solids loading ($T_m$), calculated in the source term component (see Section 3.14), is converted into a sediment flux in the lake model component and added to the flux values reported in Table 10.2.

On deposition on the lake bottom, the organic content of sedimented material undergoes continuous decomposition thus reducing the organic fraction. Typically, stabilized lake sediment in Canadian Shield Lakes contain between 20 and 50 percent organic matter. Sediments collected in the Elliot Lake and Wollaston Lake areas (Swanson 1985) had an average organic content of about 25%. This is a sharp reduction from the 55% organic fraction characteristic of fresh sedimenting material. The reduction is reflected in the flux of stable sediment out of the exchange zone into the deep sediment. For an average 55% organic content in the settling solids and 25% in the stabilized solids, the rate of sediment burial ($\sigma_{D,n}$) equals about 60% of the rate of sedimenting material ($\sigma_{s,n}$). On a more general level, the rate of sediment burial may be expressed as a function of the rate of sediment removed from the water column as follows.

$$\sigma_{D,n} = f_s \sigma_{s,n} \qquad (10.12)$$

Table 10.2

## LAKE SEDIMENTATION FLUX VALUES

| Lake Node Number | Lake Surface Area ($m^2$) | Contributing Drainage Area ($m^2$) | Sedimentation Flux ($g.m^{-2}.a^{-1}$) | | | | |
|---|---|---|---|---|---|---|---|
| | | | Runoff Solids | Biomass Solids | Total Solids Values | | |
| | | | | | Nominal | Minimum | Maximum |
| 2 | 5.0E5 | 2.0E7 | 50 | 180 | 230 | 95 | 615 |
| 4 | 2.5E5 | 1.8E7 | 80 | 180 | 260 | 105 | 765 |
| 7 | 4.0E6 | 1.02E8 | 30 | 180 | 210 | 85 | 515 |

Table 10.3

## SEDIMENT TO WATER $k_d$ VALUES ($m^3.g^{-1}$)
(dry weight basis)

| Radionuclide | Geo. Mean | Geo. Std. Dev. | Minimum | Maximum |
|---|---|---|---|---|
| Uranium | $4.5 \times 10^{-3}$ | 2.2 | $0.4 \times 10^{-3}$ | $4.8 \times 10^{-2}$ |
| Radium-226 | $6.5 \times 10^{-3}$ | 2.5 | $0.4 \times 10^{-3}$ | $1.0 \times 10^{-1}$ |
| Lead-210 | $15.0 \times 10^{-3}$ | 2.5 | $1.0 \times 10^{-3}$ | $2.3 \times 10^{-1}$ |

where:

$f_s$ = the fraction of sedimenting material ultimately removed to the deep sediment

This relationship has been incorporated into the lake model component. The fraction of sedimenting material entering the deep sediment ($f_s$) was estimated to range from 0.5 to 0.7 for the reference lakes. As previously reported, a nominal value of 0.6 was used.

The densities of the individual components of stable sediment were assumed to be:

$$\rho_{inorganic} = 2.45\ g.cm^{-3} \text{ or } 2.45 \times 10^6\ g.m^{-3}$$

$$\rho_{organic} = 1.05\ g.cm^{-3} \text{ or } 1.05 \times 10^6\ g.m^{-3}$$

On the basis of 1 g sediment having an organic content of 25%, the true density of stabilized sediment solids was determined as follows:

$$\rho_s = \left[ \frac{1\ g}{\dfrac{0.25\ g}{1.05\ g.cm^{-3}} + \dfrac{0.75\ g}{2.45\ g.cm^{-3}}} \right] = 1.84\ g.cm^{-3} \text{ or } 1.84 \times 10^6\ g.m^{-3}$$

To calculate the volume fraction of solids ($\epsilon_s$), a moisture content of 89% by weight was used based on the results of the field studies reported by Swanson (1985). For a moisture density of 1.0 $g.cm^{-3}$ and a solids density of 1.84 $g.cm^{-3}$, the volume fraction occupied by the solids equals:

$$\epsilon_s = \left[ \frac{\dfrac{0.11\ g\ solid}{1.84\ g.cm^{-3}}}{\dfrac{0.11\ g\ solid}{1.84\ g.cm^{-3}} + \dfrac{0.89\ g\ H_2O}{1.00\ g.cm^{-3}}} \right] = 0.06\ cm^3.cm^{-3}$$

Thus the porosity, volume fraction of liquid $\epsilon$, equals:

$$\epsilon = 1-0.06$$
$$= 0.94\ cm^3.cm^{-3}$$

The bulk density of sediment therefore may be calculated as follows:

$$\rho = (1.84)\ (0.06) + 1.00\ (0.94)$$
$$= 1.05\ g.cm^{-3}$$

These calculated porosity and bulk density values compare favourably with literature data for Canadian Shield lakes which have a reported bulk density of 1.02 to 1.10 $g.cm^{-3}$ and a porosity of 0.83 to 0.97 $cm^3.cm^{-3}$ (Beak, 1982).

### Distribution Coefficients

Radionuclides entering freshwater environments may be removed by one or more mechanisms on organic and inorganic matter. The removal mechanisms usually cited include ion exchange, adsorption and precipitation. Because the magnitude of these processes can seldom be quantified separately, however, the overall removal process is usually expressed in terms of a distribution coefficient, $k_d$. The concept of $k_d$ was developed from ion-exchange theory to represent the equilibrium distribution of a trace constituent between the solid exchange media and the solution. In the broader sense as it is applied to environmental and waste management studies, it is defined as:

$$k_d = \frac{\text{amount of radionuclide sorbed on solid phase}}{\text{amount of radionuclide left in solution}}$$

Values of $k_d$ reported in the literature vary widely for all radionuclides. The variability is dependent on many factors including the nature of the solid material. The radionuclide $k_d$ values reported for river and lake sediments are generally much higher than what is normally cited for geological materials. The difference may be due to the fine nature of the solids and the fact that they contain a significant organic content.

The sediment/water data base reviewed in establishing $k_{d,i}$ values for the radionuclides for use in the watershed model was derived mainly from the work by Swanson (1984, 1985). The $k_{d,i}$ values for all radionuclides were assumed to be lognormally distributed, an assumption which is consistent with most other reported work in this area. The attributes of the distributions given in Table 10.3 for uranium, radium-226 and lead-210 were used in the model.

Thorium removal is believed to occur mainly as a precipitate. As such, its removal is pH dependent. The formulation used in the surface water model to calculate thorium removal as a function of pH is as follows:

$$k_{d,Th} = 2.0 \times 10^{-3} + k'_{d,Th}\,(pH_{n,t} - 4.0) \qquad \text{for pH} \geq 4.0 \qquad (10.13)$$

$$k_{d,Th} = 2.0 \times 10^{-3} \qquad \text{for pH} < 4.0$$

where

$k'_{d,Th}$ = the slope of the linear function relating the distribution coefficient ($k_{d,Th}$) to pH ($m^3.g^{-1}$). The distribution attributes of $k'_{d,Th}$, assuming a lognormal distribution, were assessed as follows:
geometric mean = $2.0 \times 10^{-2}$
geometric standard deviation = 2.5
minimum = $2.0 \times 10^{-3}$
maximum = $3.0 \times 10^{-1}$

$pH_{n,t}$ = the pH of the lake designated by node 'n' at time 't'

$k_{d,Th}$ = the distribtuion coefficient for thorium removal on sedimenting matter ($m^3.g^{-1}$)

Mass Transfer Coefficient

To estimate the range of the mass transfer coefficient ($k_{L,n}$ in equation (10.10)), it was assumed that the organic content decays rapidly at the sediment surface before significant burial by fresh sedimenting material occurs. In this case, mass transfer is controlled by a laminar-flow film next to the sediment boundary. The estimation of the mass transfer coefficient requires the application of Fick's law for unsteady state diffusion:

$$\frac{\partial [R_i]_{1,t}}{\partial t} = - D \frac{\partial^2 [R_i]_{1,t}}{\partial_z{}^2} \qquad (10.14)$$

where

D = diffusivity coefficient ($m^2.yr^{-1}$)

z = the depth of penetration into the sediment (m)

Equation (10.14) has been solved by Higbie (1935) by applying his penetration theory for diffusion into a "semi-infinite" medium represented by the water column above a flat (sediment) surface as follows:

$$k_{L,n} = \sqrt{\frac{D}{\tau}} \qquad (10.15)$$

where

$\tau$ = the surface renewal time (yr)

This requires an evaluation of the surface renewal time. An approximate value for surface renewal may be taken as a function of the mean depth "$h_n$" (or depth of the hypolimnion during stratification) and mean current velocity "u":

$$\tau = \frac{\pi h_n}{u} \qquad (10.16)$$

In relation to the schematic shown on Figure 10.2, the diffusion out of the sediment exchange layer may be equated as:

$$\begin{pmatrix}\text{rate of diffusion}\\ \text{through sediment}\end{pmatrix} = \begin{pmatrix}\text{rate of transport}\\ \text{from surface of}\\ \text{sediment}\end{pmatrix}$$

which translates to:

$$D \; \frac{d^2 [R_i]_{1,t}}{dz^2} = \left(\frac{u}{\pi h_n}\right) [R_i]_{n,t} \qquad (10.17)$$

The approximate solution to equation (10.17) is given by:

$$\left.\frac{d[R_i]_{1,t}}{dz}\right|_{z=0} = \left(\frac{u}{\pi D h_n}\right)^{1/2} ([R_i]_{\lambda,t} - [R_i]_{n,t}) \qquad (10.18)$$

or

$$\text{Flux} = D\left.\frac{d[R_i]_{1,t}}{dz}\right|_{z=0} = \left(\frac{uD}{\pi h_n}\right)^{1/2} ([R_i]_{\lambda,t} - [R_i]_{n,t})$$

$$= k_{L,n}\,([R_i]_{\lambda,t} - [R_i]_{n,t})$$

where $k_{L,n} = \left(\frac{uD}{\pi h_n}\right)^{1/2}$

Equation (10.18), known as the Dobbins-O'Connor relationship, has been used successfully to describe mass transfer in lakes and rivers (Bailey and Ollis 1977). Typical values for the parameters in equation (10.18) are:

$D = 6.36 \times 10^{-6}\ \text{cm}^2.\text{s}^{-1} = 0.02\ \text{m}^2.\text{yr}^{-1}$

$u = 0.1$ to $1.0\ \text{cm.s}^{-1} = 3.15 \times 10^4$ to $3.15 \times 10^5\ \text{m.yr}^{-1}$

To assess the effect of lake depth ($h_n$) on the mass transfer coefficient ($k_{L,n}$), the mean depths of 4, 5 and 10m for the lakes of the reference watershed were selected. Using extreme values for the current velocity, $k_{L,n}$ values were calculated as given on Table 10.4. The $k_{L,n}$ values presented in the table are seen to range from about 4.5 to 22.4 $\text{m.yr}^{-1}$.

Derivation of Rate Constants

The rate of change of the total activity of the radionuclides in the water column and sediments can be expressed as follows:

$$\frac{d\{R_i\}_{n,t}}{dt} = k_{2,i}\,\{R_i\}_{1,t} - k_{1,i}\,\{R_i\}_{n,t} \qquad (10.19)$$

and

$$\frac{d\,\}R_i\{_{l,t}}{dt} = k_{1,i}\,\}R_i\{_{n,t} - k_{2,i}\,\}R_i\{_{l,t} - k_{3,i}\,\}R_i\{_{l,t} \qquad (10.20)$$

where

$\}R_i\{_{n,t}$ = the activity of radionuclide 'i' in the water column at time 't' (Bq)

$\}R_i\{_{l,t}$ = the average activity of radionuclide 'i' in the sediment exchange zone at time 't' (Bq)

$k_{1,i}$ = the rate of radionuclide 'i' removal from the water column to the sediment ($yr^{-1}$)

$k_{2,i}$ = the rate of radionuclide 'i' introduction back to the water column from the sediment ($yr^{-1}$)

$k_{3,i}$ = the rate of loss of radionuclide 'i' to deep sediment, i.e. the rate of burial ($yr^{-1}$)

By definition, the activity of radionuclide 'i' in the sediment is given by:

$$\}R_i\{_{l,t} = L_n\lambda\,[k_{d,i}\,\rho_s\,(1-\epsilon) + \epsilon\,]\,[R_i]_{l,t} \qquad (10.21)$$

where

$L_n$ = surface area of lake 'n' ($m^2$)

$\rho_s$ = density of stabilized solids ($g.m^{-3}$)

$\epsilon$ = sediment porosity ($m^3.m^{-3}$)

$\lambda, K_{d,i}$ and $[R_i]_{l,t}$ are as defined previously

In the water column, the activity of radionuclide 'i' equals:

$$\}R_i\{_{n,t} = L_n h_n [R_i]_{n,t} \qquad (10.22)$$

In equation (10.21), $[R_i]_{l,t}$ is unknown, but our best estimate is:

$$[R_i]_{l,t} = \frac{[R_i]_{n,t} + [R_i]_{\lambda,t}}{2} = \left[\frac{\dfrac{[R_i]_{\lambda,t}}{1.1} + [R_i]_{\lambda,t}}{2}\right] \qquad (10.23)$$

$$= 0.95\,[R_i]_{\lambda,t}$$

Table 10.4

## ASSESSED MASS TRANSFER COEFFICIENT VALUES

| Mean Lake Depth (m) | Diffusivity Coefficient ($m.a^{-1}$) | Mean Lake Current Velocity ($m.a^{-1}$) | Mass Transfer Coefficient ($m.a^{-1}$) |
|---|---|---|---|
| 4 | 0.02 | $3.15\times10^4$ | 7.1 |
| 4 | 0.02 | $3.15\times10^5$ | 22.4 |
| 5 | 0.02 | $3.15\times10^4$ | 6.3 |
| 5 | 0.02 | $3.15\times10^5$ | 20.0 |
| 10 | 0.02 | $3.15\times10^4$ | 4.5 |
| 10 | 0.02 | $3.15\times10^5$ | 14.2 |

where

$[R_i]_{n,t} = [R_i]_{\lambda,t} \div 1.1$ represents the average expected concentration differential at steady state

Rearranging equation (10.23) we get:

$$[R_i]_{\lambda,t} = \frac{[R_i]_{1,t}}{0.95} = 1.05\,[R_i]_{1,t}$$

Substitution into equation (10.10) yields:

$$\lambda \frac{d[R_i]_{1,t}}{dt} = [\sigma_{s,n}\, k_{d,i}[R_i]_{n,t}] - [k_{L,n}\,(1.05[R_i]_{1,t} - [R_i]_{n,t})] - [\sigma_{D,n}k_{d,i}\; 1.05[R_i]_{,1,t}] \tag{10.24}$$

Multiplying equation (10.24) by the area $L_n$ and re-ordering we get:

$$\frac{\lambda L_n d[R_i]_{1,t}}{dt} = [(\sigma_{s,n}k_{d,i} + k_{L,n})L_n[R_i]_{n,t}] - [\,1.05k_{L,n}\; L_n[R_i]_{1,t}] - [1.05\sigma_{D,n}k_{d,i}L_n[R_i]_{1,t}] \tag{10.25}$$

Comparing equation (10.25) to equation (10.20), it is seen that:

$$\lambda L_n \frac{d[R_i]_{1,t}}{dt} = \frac{d\}R_i\{_{1,t}}{dt}$$

Thus collecting the terms for $\}R_i\{_{n,t}$ and $\}R_i\{_{1,t}$ yields:

$$k_{1,i} = \frac{\sigma_{s,n}k_{d,i} + k_{L,n}}{h_n} \tag{10.26}$$

$$k_{2,i} = \frac{1.05\; k_{L,n}}{\lambda[k_{d,i}\;\rho_s\;(1-\epsilon\,) + \epsilon\,]} \tag{10.27}$$

$$k_{3,i} = \frac{1.05\,\sigma_{D,n}\,k_{d,i}}{\lambda[k_{d,i}\,\rho_s(1-\epsilon)+\epsilon]} \qquad (10.28)$$

The rates of radionuclide exchange between the water column and the sediment (given by $k_{1,i}$ and $k_{2,i}$) and the rate of permanent loss to the deep sediment (given by $k_{3,i}$) can be determined by substitution of appropriate values for the independent parameters in equations (10.26), (10.27) and (10.28).

Model Implemented

As previously noted, the behaviour of the uranium series radionuclides in the lakes is modelled on a activity basis to permit removal from the water column and feedback from the sediment to be followed with time. The accumulation of radionuclides in the lake water column may be represented by the following expression:

$$\frac{d}{dt}\{R_i\}_{n,t} = Q_{n-1,t}[R_i]_{n-1,t} - \left(k_{1,i} + \frac{1}{d_{n,t}}\right)\{R_i\}_{n,t} + k_{2,i}\{R_i\}_{1,t} \qquad (10.29)$$

where

$[R_i]_{n-1,t}$ = activity concentration of radionuclide 'i' in the inflow to the lake at node 'n-1' at time 't' ($Bq.m^{-3}$)

$\{R_i\}_{n,t}$ = activity of radionuclide 'i' in the water column of lake 'n' at time 't' (Bq)

$\{R_i\}_{1,t}$ = activity of radionuclide 'i' in the exchange zone of the lake sediment at time 't' (Bq)

$k_{1,i}$ = rate of radionuclide 'i' removal from the lake water column to the lake sediment ($yr^{-1}$)

$k_{2,i}$ = rate of radionuclide 'i' release from the lake sediment to the lake water column ($yr^{-1}$)

$d_{n,t} = \frac{V_n}{Q_{n,t}}$ = retention time (or travel time) in the lake designated by node 'n' at time 't' (yr)

$Q_{n-1,t}$ = volumetric surface water flow at node 'n-1' at time 't' ($m^3.yr^{-1}$)

$Q_{n,t}$ = volumetric surface water flow at node 'n', the lake outflow, at time 't' ($m^3.yr^{-1}$)
$V_n = L_n h_n$ = volume of the lake designated by node 'n' at time 't' ($m^3$)
$L_n$ = surface area of lake 'n' ($m^2$)
$h_n$ = mean depth of lake 'n' (m)

Similarly, the changing inventory of radionuclides in the lake sediment is given by equation (10.20), restated as:

$$\frac{d\}R_i\{_{1,t}}{dt} = k_{1,i}\ \}R_i\{_{n,t} - (k_{2,i} + k_{3,i})\ \}R_i\{_{1,t} \qquad (10.30)$$

where
$\}R_i\{_{1,t}$ = average activity of radionuclide 'i' in the exchange zone of the lake sediment at time 't' (Bq)
$k_{3,i}$ = rate of radionuclide 'i' removal (burial) to deep lake sediment ($a^{-1}$)

At time t=0, the initial radionuclide content of the lake water column and sediment is:

$$\}R_i\{_{n,t=0} = 0$$
$$\}R_i\{_{1,t=0} = 0$$

The term of interest is the activity concentration of radionuclide 'i' in the lake.

Once the activity $\}R_i\{_{n,t}$ is obtained, the concentration is given by:

$$[R_i]_{n,t} = \frac{\}R_i\{_{n,t}}{V_n} \qquad (10.31)$$

The two differential equations given above may be restated in matrix notation:

$$\begin{matrix} \dfrac{d\{R_i\}_{n,t}}{dt} = \\ \\ \dfrac{d\{R_i\}_{1,t}}{dt} = \end{matrix} \begin{bmatrix} a_{11} & -a_{12} & +a_{13} \\ & & \\ a_{21} & a_{22} & -a_{23} \end{bmatrix} \begin{bmatrix} 1 \\ \{R_i\}_{n,t} \\ \{R_i\}_{1,t} \end{bmatrix}$$

where

$a_{11} = Q_{n-1,t} [R_i]_{n-1,t}$ $\qquad$ $a_{21} = 0$

$a_{12} = k_{1,i} + \dfrac{1}{d_{n,t}}$ $\qquad$ $a_{22} = k_{1,i}$

$a_{13} = k_{2,i}$ $\qquad$ $a_{23} = k_{2,i} + k_{3,i}$

The general solution is:

$$\{R_i\}_{n,t} = K_{n,i} + D_i \exp(Z_{1,i}\,\Delta t) + (X_{i,t} - D_i)\exp(Z_{2,i}\,\Delta t) \qquad (10.32)$$

$$\{R_i\}_{1,t} = K_{1,i} + B_i \exp(Z_{1,i}\,\Delta t) + (Y_{i,t} - B_i)\exp(Z_{2,i}\,\Delta t) \qquad (10.33)$$

where

$$K_{n,i} = \frac{a_{11}a_{23}}{a_{12}a_{23}-a_{22}a_{13}}$$

$$K_{1,i} = \frac{a_{11}a_{22}}{a_{12}a_{23}-a_{13}a_{22}}$$

$$Z_{1,i} = \frac{-(a_{12} + a_{23}) + \sqrt{(a_{12} + a_{23})^2 + 4(a_{13}a_{22} - a_{12}a_{23})}}{2}$$

$Z_{2,i} = -(a_{12} + a_{23} + Z_{i,1})$

$X_{i,t} = \{R_i\}_{n,t-\Delta t} - K_{n,i}$

$Y_{i,t} = \{R_i\}_{1,t-\Delta t} - K_{1,i}$

$$D_i = \frac{a_{13} + a_{23} + Z_{1,i}}{(a_{12}+a_{22}) - (a_{13}+a_{23})} \left( \frac{(a_{12}+a_{22}+Z_{2,i})\, X_{i,t} - (a_{13}+a_{23}+Z_{2,i}) Y_{i,t}}{\sqrt{(a_{12}+a_{23})^2 + 4(a_{13}a_{22}-a_{12}a_{23})}} \right)$$

and

$$B_i = \left[ \frac{a_{12} + a_{22} + Z_{1,i}}{a_{13} + a_{23} + Z_{1,i}} \right] D_i$$

Radioactive Ingrowth and Decay

The approach adopted in the source term component model (see Chapter 3) to account for radioactive ingrowth and decay has been employed directly in the surface water dispersion model. Briefly, radioactive decay and ingrowth of natural uranium and thorium are not modelled as the effects on the activity inventories are inconsequential when one considers the long half-lives of these radionuclides and the magnitudes of the competing processes that affect their retention in the watershed. For radium-226 and lead-210, radioactive ingrowth and decay are potentially more important and are accounted for in the activity inventories retained within the lake water columns and sediments. These processes are not accounted for in the river segments.

The radioactive decay processes are included by correcting the activity inventories of radium-226 and lead-210 calculated from equations (10.32) and (10.33) each time-step. Specifically, the correction is made by adjusting the values of $X_{i,t}$ and $Y_{i,t}$ (since these terms include the radionuclide activities from the previous timestep) in the equations as follows:

$$X_{i,t} = \left\{R_i\right\}^{*}_{n,t-\Delta t} - K_{n,i}$$

and

$$Y_{i,t} = \left\{R_i\right\}^{*}_{1,t-\Delta t} - K_{1,i}$$

where, for lead-210:

$$\{R_{Pb-210}\}^{*}_{n,t-\Delta t} = \{R_{Pb-210}\}_{n,t-\Delta t} \exp(-\lambda_{Pb-210}\Delta t)$$

$$+\left[\{R_{Ra-226}\}_{n,t-\Delta t} \left(\frac{\lambda_{Pb-210}}{\lambda_{Pb-210} - \lambda_{Ra-226}}\right)\right.$$

$$\left.(\exp(-\lambda_{Ra-226}\Delta t) - \exp(-\lambda_{Pb-210}\Delta t))\right]$$

$$\{R_{Pb-210}\}^{*}_{l,t-\Delta t} = \{R_{Pb-210}\}_{l,t-\Delta t} \exp(-\lambda_{Pb-210}\Delta t)$$

$$+\left[\{R_{Ra-226}\}_{l,t-\Delta t} \left(\frac{\lambda_{Pb-210}}{\lambda_{Pb-210} - \lambda_{Ra-226}}\right)\right.$$

$$\left.(\exp(-\lambda_{Ra-226}\Delta t) - \exp(-\lambda_{Pb-210}\Delta t))\right]$$

and for Ra-226:

$$\{R_{Ra-226}\}^{*}_{n,t-\Delta t} = \{R_{Ra-226}\}_{n,t-\Delta t} \exp(-\lambda_{Ra-226}\Delta t)$$

$$+\left[(XA_{Th-230/Th,sol})\{R_{Th}\}_{n,t-\Delta t} \left(\frac{\lambda_{Ra-226}}{\lambda_{Ra-226} - \lambda_{Th-230}}\right)\right.$$

$$\left.(\exp(-\lambda_{Th-230}\Delta t) - \exp(-\lambda_{Ra-226}\Delta t))\right]$$

$$\{R_{Ra-226}\}_{\ell,t-\Delta t}{}^{*} = \{R_{Ra-226}\}_{\ell,t-\Delta t} \exp(-\lambda_{Ra-226}\Delta t)$$

$$+\left[(XA_{Th-230/Th})\{R_{Th}\}_{\ell,t-\Delta t} \left(\frac{\lambda_{Ra-226}}{\lambda_{Ra-226} - \lambda_{Th-230}}\right)\right.$$

$$\left.(\exp(-\lambda_{Th-230}\Delta t) - \exp(-\lambda_{Ra-226}\Delta t))\right]$$

where

$XA_{Th-230/Th,sol}$ = the activity fraction of Th-230 in soluble thorium.

The first term on the right hand side of the above expressions accounts for radioactive decay of lead-210 and radium-226 respectively. The second term on the right hand side accounts for the net ingrowth of lead-210 from radium-226 and of radium-226 from thorium-230 respectively. The incorporation of these corrections is a relatively straight forward method of including radioactive decay and ingrowth though not fundamentally rigorous. The approach is consistent with the concept of assessment level models.

## 10.7 Parameter Values and Code Listing

A summary of all parameters included in the surface water dispersion models is provided in Table 10.5. Parameter values and their distributions are specified for the input parameters on the table. The basis for the specified values are discussed in the appropriate sections in the text of Chapter 10.

A copy of the code for calculating pH, major ion and radionuclide levels in the surface water system is included in Table 10.6 for the interested reviewer. Certain features of the code (e.g. calculation of the circumference of lakes) are included for use in the aquatic transfer models discussed in Chapter 11.

Table 10.5

## WATERSHED MODEL VARIABLES

Page 1

| Model Symbol | Description | Units | Nominal Value | Probability Distribution* | Computer Origin | Computer Symbol |
|---|---|---|---|---|---|---|
| $\sum_{1}^{n} A_n$ | cumulative drainage area over the n sub-basins in the watershed | $m^2$ | Site specific: see Table 10.1 | | INPUT | SHEDAR(n) |
| n | node number for the nth segment in the watershed (maximum of 10) | - | - | - | INPUT | WTSEG |
| $P_t$ | mean annual net precipitation at time t | $m.yr^{1}$ | 0.4 | N(0.4,0.1,0.1,0.7) | INPUT | NPRCP |
| $Q_{n-1,t}$ | volume of surface water flow at node n-1 at time t | $m^3.yr^{-1}$ | calculated | calculated | WATEX | FLOWQ(n-1) |
| $Q_{n,t}$ | volume of surface water flow at node n at time t | $m^3.yr^{-1}$ | calculated | calculated | WATEX | FLOWQ(n) |
| $Q_{s,t}$ | volume of source term discharge s from reference tailings area at time t | $m^3.yr^{-1}$ | calculated | calculated | SEXEC | SFLOW |
| $[Ca]_{n-1,t}$ | calcium concentration in the flow at node n-1 at time t | $mol.m^{-3}$ | calculated | calculated | WATEX | WATC(8,n-1) |
| $[Ca]_{n,t}$ | calcium concentration in the flow at node n at time t | $mol.m^{-3}$ | calculated | calculated | WATEX | WATC(8,n) |
| $[Ca]_B$ | natural background calcium level in freshwater flow | $mol.m^{-3}$ | 0.1 | C(0.1) | INPUT | WATCAB |
| $[Ca]_{s,t}$ | calcium concentration in the source team discharge s from reference tailings at time t | $mol.m^{-3}$ | calculated | calculated | SEXEC | WCONC(8,3,3) |
| $[SO_4]_{n-1,t}$ | sulphate concentration in the flow at node n-1 at time t | $mol.m^{-3}$ | calculated | calculated | WATEX | WATC(7,n-1) |

| Model Symbol | Description | Units | Nominal Value | Probability Distribution* | Computer Origin | Computer Symbol |
|---|---|---|---|---|---|---|
| $[SO_4]_{n,t}$ | sulphate concentration in the flow at node n at time t | $mol.m^{-3}$ | calculated | calculated | WATEX | WATC(7,n) |
| $[SO_4]_B$ | natural background sulphate level in freshwater flow | $mol.m^{-3}$ | 0.071 | C(0.071) | INPUT | WTSO4B |
| $[SO_4]_{s,t}$ | sulphate concentration in the source term discharge s from reference tailings at time t | $mol.m^{-3}$ | calculated | calculated | SEXEC | WCONC(7,3,3) |
| $V_n$ | volume of the lake designated by node n | $m^3$ | calculated | calculated | WATEX | LAKVOL(n) |
| $L_n$ | surface area of lake designated by node n | $m^2$ | Site specific: See Table 10.1 | | INPUT | LAREA(n) |
| $h_n$ | mean depth of lake designated by node n | m | Site specific: See Table 10.1 | | INPUT | SDEPTH(n) |
| $\Delta t$ | size of the time step specified for any run (values limited to 1 or 10) | yr | - | - | INPUT | DT |
| f | activity coefficients for watershed pH calculations | - | 0.8 | T(0.6,0.8,0.9) | INPUT | ACTCO |
| $pH_n$ | pH of the surface water at node n in the watershed at time t | - | calculated | calculated | WATEX | WATPH(n) |
| $[R_i]_{n-1,t}$ | activity concentration of radionuclide i in the surface water at node n-1 at time t | $Bq.m^{-3}$ | calculated | calculated | WATEX | WATC(i,n-1) |
| $[R_i]_{n,t}$ | activity concentration of radionuclide i in the surface water at node n at time t | $Bq.m^{-3}$ | calculated | calculated | WATEX | WATC(i,n) |
| $[R_i]_{s,t}$ | activity concentration of radionuclide i in the source term discharge s from the reference tailings area at time t | $Bq.m^{-3}$ | calculated | calculated | SEXEC | WCONC(i,3,3) |

Table 10.5 cont'd

| Model Symbol | Description | Units | Nominal Value | Probability Distribution* | Computer Origin | Computer Symbol |
|---|---|---|---|---|---|---|
| $[R_i]_{1,t}$ | average activity concentration of radionuclide i in the interstitial water of the sediment of lake n at time t | $Bq.m^{-3}$ | calculated | calculated | WATEX | not used |
| $[R_i]_{\lambda,t}$ | activity concentration of radionuclide i at depth λ in the sediment of lake n at time t | $Bq.m^{-3}$ | calculated | calculated | WATEX | not used |
| u | current velocity in the lakes of the watershed | $m.yr^1$ | $1.7x10^5$ | $U(3.15x10^4,3.15x10^5)$ | INPUT | CURRNT |
| λ | thickness of the sediment exchange zone in the lakes of the watershed | m | 0.05 | C(0.05) | INPUT | WTMIXD |
| $\sigma_{S,n}$ | rate of sedimenting material removal from the water column of the lake designated node n | $g.m^{-2}.yr^{-1}$ | Lake specific: See Table 10.2 | | INPUT | WSIGS(k) where k is counter of lakes |
| $\sigma_{D,n}$ | rate of sediment burial or removal from the active exchange zone | $g.m^{-2}.yr^{-1}$ | calculated | calculated | WATEX | WSIGD(k) |
| $f_s$ | fraction of sedimenting material removed to the deep sediment | - | 0.6 | U(0.5,0.7) | INPUT | BURYF |
| $k_{d,i}$ | radionuclide distribution coefficient from water to lake sediment for: | $m^3.g^{-1}$ | | | | |
| | uranium | | $4.5x10^{-3}$ | $LN(4.5x10^{-3},2.2, 0.4x10^{-3},4.8x10^{-2})$ | INPUT | WKDU |
| | thorium | | calculated | calculated | WATEX | WKDTH |
| | lead-210 | | $1.5x10^{-2}$ | $LN(1.5x10^{-2},2.5, 1.0x10^{-3},2.3x10^{-1})$ | INPUT | WKDPB |
| | radium-226 | | $6.5x10^{-3}$ | $LN(6.5x10^{-3},2.5, 0.4x10^{-3},1.0x10^{-1})$ | INPUT | WKDRA |

Table 10.5 cont'd

| Model Symbol | Description | Units | Nominal Value | Probability Distribution* | Computer Origin | Computer Symbol |
|---|---|---|---|---|---|---|
| $k'_{d,Th}$ | slope of the linear function relating the thorium distribution coefficient to $pH_{n,t}$ | $m^3.g^{-1}$ | $2.0x10^{-2}$ | $LN(2.0x10^{-2}, 2.5, 2.0x10^{-3}, 3.0x10^{-1})$ | | KDPRIM |
| $k_{L,n}$ | mass transfer coefficient of the radionuclides into the water column of lake n from the sediments | $m.yr^{-1}$ | calculated | calculated | WATEX | WATKL |
| $\rho_S$ | density of stabilized sediment solids | $g.m^{-3}$ | $1.84x10^6$ | $C(1.84x10^6)$ | INPUT | WTRHOS |
| | sediment porosity, volume fraction of liquid | $m^3.m^{-3}$ | 0.94 | T(0.83,0.94,0.97) | INPUT | WATEPS |
| D | diffusivity coefficient | $m^2.yr^{-1}$ | 0.02 | C(0.02) | INPUT | DIFFC |
| $\}R_i\{_{n,t}$ | activity of radionuclide i in the water column of lake n at time t | Bq | calculated | calculated | WATEX | WATRW(i,n) |
| $\}R_i\{_{n,t-\Delta t}$ | activity of radionuclide i in lake sediment exchange zone at time t | Bq | calculated | calculated | WATEX | WATRW(i,n) calculated in previous time step |
| $\}R_i\{_{1,t}$ | activity of radionuclide i in lake sediment exchange zone at time t | Bq | calculated | calculated | WATEX | WATRS(i,n) |
| $\}R_i\{_{1,t-\Delta t}$ | activity of radionuclide i in lake sediment exchange zone at time t-Δt | Bq | calculated | calculated | WATEX | WATRS(i,n) calculated in previous time step |
| $k_{1,i}$ | rate of radionuclide i removal from the lake water column | $yr^{-1}$ | calculated | calculated | WATEX | K1 |

Table 10.5 cont'd

| Model Symbol | Description | Units | Nominal Value | Probability Distribution* | Computer Origin | Computer Symbol |
|---|---|---|---|---|---|---|
| $k_{2,i}$ | rate of radionuclide i release from exchangeable sediment back to the lake water column | $yr^{-1}$ | calculated | calculated | WATEX | K2 |
| $k_{3,i}$ | rate of radionuclide loss to deep lake sediment | $yr^{-1}$ | calculated | calculated | WATEX | K3 |
| $d_{n,t}$ | retention time (or travel time) in lake n at time t | yr | calculated | calculated | WATEX | DETIME |
| $a_{11}$ | matrix parameters | - | calculated | calculated | WATEX | A11 |
| $a_{12}$ | matrix parameters | - | calculated | calculated | WATEX | A12 |
| $a_{13}$ | matrix parameters | - | calculated | calculated | WATEX | A13 |
| $a_{21}$ | matrix parameters | - | calculated | calculated | WATEX | A21 |
| $a_{22}$ | matrix parameters | - | calculated | calculated | WATEX | A22 |
| $a_{23}$ | matrix parameters | - | calculated | calculated | WATEX | A23 |
| $K_{n,i}$ | radionuclide i specific computed parameter | - | calculated | calculated | WATEX | KW |
| $K_{1,i}$ | radionuclide i specific computed parameter | - | calculated | calculated | WATEX | KS |
| $X_{i,t}$ | radionuclide i specific computed parameter | - | calculated | calculated | WATEX | X |
| $Y_{i,t}$ | radionuclide i specific computed parameter | - | calculated | calculated | WATEX | Y |
| $Z_{1,i}$ | radionuclide i specific computed parameter | - | calculated | calculated | WATEX | V1 |
| $Z_{2,i}$ | radionuclide i specific computed parameter | - | calculated | calculated | WATEX | V2 |

| Model Symbol | Description | Units | Nominal Value | Probability Distribution* | Computer Origin | Computer Symbol |
|---|---|---|---|---|---|---|
| $B_i$ | radionuclide i specific computed parameter | - | calculated | calculated | WATEX | BB |
| $D_i$ | radionuclide i specific computed parameter | - | calculated | calculated | WATEX | AA |
| $\lambda_{Th-230}$ | radioactive decay constant for Th-230 | $yr^{-1}$ | $8.66x10^{-6}$ | $C(8.66x10^{-6})$ | SOURCE (SUBROUTINE INCONN) | LAM230 |
| $\lambda_{Ra-226}$ | radioactive decay constant for Ra-226 | $yr^{-1}$ | $4.33x10^{-4}$ | $C(4.33x10^{-4})$ | SOURCE (SUBROUTINE INCONN) | LAMRAD |
| $\lambda_{Pb-210}$ | radioactive decay constant for Pb-210 | $yr^{-1}$ | $3.3x10^{-2}$ | $C(3.3x10^{-2})$ | SOURCE (SUBROUTINE INCONN) | LAMPB |
| $XA_{Th-230/Th}$ | activity fraction of Th-230 in soluble thorium | - | calculated | calculated | SOURCE | X230LA |

Note

* Distributions are as described in Table 2.2.

Table 10.6

## WATERSHED MODEL CODE LISTING

```
      SUBROUTINE WATEX
C
C     SUBROUTINE CALCULATES RIVER LENGTHS, LAKE CIRCUMFERENCES, FLOW
C     RATES IN LAKES AND RIVERS, AND CALLS APPROPRIATE SUBROUTINE
C
      INCLUDE 'MODEL.INC'
      INCLUDE 'VAR.INC'
      REAL*4 PI
      DATA PI /3.1415927/
      IF (CODWAT.GE.1.0) WRITE (*,*) ' ***** SUBROUTINE WATEX *****'
      IF (NT.EQ.0.AND.NUMTRL.EQ.1) THEN
C
C     CALCULATE RIVER LENGTHS & LAKE CIRCUMFERENCES
C
         LTOT=0.
         DO 20 WTSEG=1,NSEG
            IF (STYPE(WTSEG).EQ.'R') THEN
               WTLNG(WTSEG)=LAREA(WTSEG)
            ELSE
               WTLNG(WTSEG)=2.*SQRT(LAREA(WTSEG)*PI)
            ENDIF
            LTOT=LTOT+WTLNG(WTSEG)
            IF (CODWAT.EQ.4) WRITE (*,100) 'WTLNG',WTLNG(WTSEG)
20       CONTINUE
         IF (CODWAT.EQ.4) WRITE (*,100) 'TOTAL',LTOT
      ENDIF
C
C     LOOP THROUGH WATERSHED SEGMENTS
C
      LAKCNT=0
      DO 10 WTSEG=1,NSEG
C
C        CALCULATE FLOW
C
         FLOWQ(WTSEG)=NPRCP*SHEDAR(WTSEG)+SFLOW
         IF (WTSEG.GE.GSEG) FLOWQ(WTSEG)=FLOWQ(WTSEG)+VSR
         IF (CODWAT.GE.2.0) WRITE (*,200) WTSEG,FLOWQ(WTSEG)
         IF (STYPE(WTSEG).EQ.'R') THEN
            CALL RIVER
         ELSE
            CALL LAKE
         ENDIF
         CALL FISH
10    CONTINUE
      RETURN
100   FORMAT (1X,A6,1X,E9.3)
200   FORMAT (' FLOWQ(',I2,') ',E9.3)
      END
C
C
```

Table 10.6 (continued)

```
C
      SUBROUTINE RIVER
C
C     SUBROUTINE CALCULATES RADIONUCLIDE, CALCIUM, AND SULPHATE
C     CONCENTRATIONS AND pH IN RIVERS
C
      INCLUDE 'MODEL.INC'
      INCLUDE 'VAR.INC'
      EXTERNAL PHW
      IF (CODWAT.GE.1.0) WRITE (*,*) ' ***** SUBROUTINE RIVER *****'
      ISUB=1
10    CONTINUE
C
C        CALCULATE CONCENTRATION
C
         WATC(ISUB,WTSEG)=RMASSB(ISUB)
         IF (CODWAT.EQ.2.0.OR.CODWAT.EQ.6.0) WRITE (*,100) ISUB,WTSEG,
     &      WATC(ISUB,WTSEG)
         IF (ISUB.LT.5) THEN
C
C           UPDATE AVERAGE WATERSHED CONCENTRATION
C
            IF (WTSEG.EQ.1) WATAVG(ISUB)=0.0
            WATAVG(ISUB)=WATAVG(ISUB)+WATC(ISUB,WTSEG)*WTLNG(WTSEG)/
     &         LTOT
            IF (CODWAT.EQ.4.0) WRITE (*,200) 'WATAVG',WATAVG(ISUB)
         ENDIF
         ISUB=ISUB+1
         IF (ISUB.EQ.5) ISUB=7
      IF (ISUB.LT.9) GOTO 10
C
C     GUESS pH LEVEL
C
      PMIN=1.
      PMAX=14.
      IF (NT.EQ.0) THEN
         GUESS=4.
      ELSE
         GUESS=WATPH(WTSEG)
      ENDIF
      POLD=GUESS
      IF (CODWAT.EQ.3.0) WRITE (*,120) ' GUESS',GUESS
C
C     CALL MODULE FOR ITERATIVE SOLUTION OF pH EQUATION
C
      CALL NEWTON (6,GUESS,WATPH(WTSEG),PHW)
      IF (CODWAT.EQ.3.0.OR.CODWAT.EQ.6.0) WRITE (*,300) WTSEG,
     &   WATPH(WTSEG)
      RETURN
100   FORMAT (' WATC(',I2,',',I3,') ',E9.3)
120   FORMAT (2(2X,A6,1X,E9.3))
200   FORMAT (1X,A6,1X,E9.3)
300   FORMAT (' WATPH(',I3,') ',E9.3)
```

Table 10.6 (continued)

```
      END
C
C
C
      FUNCTION RMASSB (ISUB)
C
C     FUNCTION CALCULATES RADIONUCLIDE, CALCIUM, AND SULPHATE
C     CONCENTRATIONS IN RIVERS AND FACTOR IN LAKE EQUATION FOR
C     CALCIUM AND SULPHATE CONCENTRATIONS
C
      INCLUDE 'MODEL.INC'
      INCLUDE 'VAR.INC'
      IF (CODWAT.EQ.2.0) WRITE (*,*) ' FUNCTION RMASSB'
C
C     CALCULATE SOURCE LOADING
C
      IF (WTSEG.EQ.1) THEN
         US=0.
         SMASS=SFLOW*WCONC(ISUB,3,3)
         BLANK1(ISUB,1)=SMASS
         A=SMASS
C
C        CALCULATE LOADING FROM EROSION OF TAILINGS
C
         IF(ISUB.LT.5)THEN
            EMASS=EROTOT*1000.*CONC(ISUB,1,3)/DT/RHOTAL
            BLANK1(ISUB,2)=EMASS
            A=A+EMASS
         ENDIF
C
C     CALCULATE UPSTREAM LOADING
C
      ELSE
         US=FLOWQ(WTSEG-1)
         A=US*WATC(ISUB,WTSEG-1)
      ENDIF
      IF (ISUB.LT.5) THEN
C
C        CALCULATE LOADING FROM GROUNDWATER
C
         IF (WTSEG.EQ.GSEG) THEN
            GMASS=GFLUX(ISUB)*AXGWAT
            BLANK1(ISUB,3)=GMASS
            A=A+GMASS
         ENDIF
         IF(WTSEG.EQ.1)BLANK1(ISUB,4)=A
C
C        CALCULATE LOADING FROM BACKGROUND CONCENTRATION
C
         B=0.
      ELSE
         B=FLOWQ(WTSEG)-US
         IF (ISUB.EQ.7) THEN
```

Table 10.6 (continued)

```
            B=B*WTSO4B
         ELSE
            B=B*WATCAB
         ENDIF
      ENDIF
C
C     CALCULATE TOTAL CONCENTRATION
C
      RMASSB=(A+B)/FLOWQ(WTSEG)
      IF (CODWAT.EQ.2.0) WRITE (*,100) 'WCON',WCONC(ISUB,3,3),'US',US,
     &   'A',A,'B',B,'RMAS',RMASSB
      RETURN
100   FORMAT (5(2X,A4,1X,E9.3))
      END
C
C
C
      SUBROUTINE LAKE
C
C     SUBROUTINE CALCULATES CONCENTRATIONS OF RADIONUCLIDES, CALCIUM,
C     AND SULPHATE AND pH IN LAKES
C
      EXTERNAL PHW
      INCLUDE 'MODEL.INC'
      INCLUDE 'VAR.INC'
      REAL*4 KW,KS,K1,K2,K3,WATKD(4),PI
      DATA PI /3.1415927/
      IF (CODWAT.GE.1.0) WRITE (*,*) ' ***** SUBROUTINE LAKE *****'
      LAKCNT=LAKCNT+1
      DETIME=LAKVOL(WTSEG)/FLOWQ(WTSEG)
C
C     INITIALIZE CALCIUM AND SULPHATE FOR PREVIOUS TIME STEP AS
C     EQUALLING BACKGROUND LEVELS
C
      IF (NT.EQ.0) THEN
         WATC(7,WTSEG)=WTSO4B
         WATC(8,WTSEG)=WATCAB
C
C        CALCULATE CONSTANT DECAY TERMS
C
         IF(NUMTRL.EQ.1)THEN
            LAK1=EXP(-LAMRAD*DT)
            LAK2=LAMRAD/(LAMRAD-LAM230)*(EXP(-LAM230*DT)-LAK1)
            LAK3=EXP(-LAMPB*DT)
            LAK4=LAMPB/(LAMPB-LAMRAD)*(LAK1-LAK3)
            IF(CODWAT.EQ.6.0)WRITE(*,*)' LAMRAD',LAMRAD,' LAM230',LAM230
     &         ,' LAMPB',LAMPB,
     &         ' LAK1',LAK1,' LAK2',LAK2,' LAK3',LAK3,' LAK4',LAK4
         ENDIF
C
C        GUESS pH LEVEL
C
         GUESS=4.
```

Table 10.6 (continued)

```
      ELSE
         GUESS=WATPH(WTSEG)
      ENDIF
      PMIN=1.
      PMAX=14.
      POLD=GUESS
C
C     SET UP LOOP FOR CALCIUM AND SULPHATE
C
      DO 20 ISUB=7,8
         F=RMASSB(ISUB)
C
C        CHECK IF 1/DETENTION TIME APPROACHES 0
C
         CK=-DT/DETIME
         IF (CK.LT.-85.) THEN
            ECK=0.
         ELSE
            ECK=EXP(CK)
         ENDIF
         WATC(ISUB,WTSEG)=F+(WATC(ISUB,WTSEG)-F)*ECK
         IF (CODWAT.GE.2.0) WRITE (*,100) ISUB,WTSEG,WATC(ISUB,WTSEG)
20    CONTINUE
      IF (CODWAT.EQ.3.0) WRITE (*,120) ' GUESS',GUESS
C
C     CALL MODULE FOR ITERATIVE SOLUTION OF pH EQUATION
C
      CALL NEWTON (5,GUESS,WATPH(WTSEG),PHW)
      IF (CODWAT.EQ.3.0.OR.CODWAT.EQ.6.0) WRITE (*,200) WTSEG,
     &   WATPH(WTSEG)
C
C     CALCULATE CONCENTRATIONS OF RADIONUCLIDES
C
      IF(WATPH(WTSEG).GE.4)THEN
         WKDTH=2.0E-3+KDPRIM*(WATPH(WTSEG)-4.0)
      ELSE
         WKDTH=2.0E-3
      ENDIF
      WATKL=(CURRNT*DIFFC/PI/SDEPTH(WTSEG))**0.5
      WATKD(1)=WKDU
      WATKD(2)=WKDTH
      WATKD(3)=WKDPB
      WATKD(4)=WKDRA
      IF(LAKCNT.EQ.1)THEN
         WSIGD=BURYF*(WSIGS(1)+EROTOT*1000./DT/LAREA(WTSEG))
      ELSE
         WSIGD=BURYF*WSIGS(LAKCNT)
      ENDIF
      IF (CODWAT.EQ.6.0) THEN
         WRITE(*,*)' KDPRIM',KDPRIM,'  WATKL',WATKL,'  WATKD',WATKD,
     &      '  WSIGS',WSIGS(LAKCNT),'  BURYF',BURYF,'  WSIGD',WSIGD,
     &      '  WTMIXD',WTMIXD,'  WTRHOS',WTRHOS,'WATEPS',WATEPS
      ENDIF
```

Table 10.6 (continued)

```
      DO 10 ISUB=1,4
         IF (NT.EQ.0) THEN
C
C           SET INITIAL MASSES IN WATER COLUMN AND SEDIMENT
C
            RWADJ(ISUB,WTSEG)=0.0
            RSADJ(ISUB,WTSEG)=0.0
         ENDIF
C
C        CALCULATE RATE CONSTANTS FOR LAKE SETTLING
C
         K1=(WSIGS(LAKCNT)*WATKD(ISUB)+WATKL)/SDEPTH(WTSEG)
         A=1.05/WTMIXD/(WATKD(ISUB)*WTRHOS*(1.-WATEPS)+WATEPS)
         K2=A*WATKL
         K3=A*WSIGD*WATKD(ISUB)
C
C        COMPUTE RADIONUCLIDE CONCENTRATIONS
C
         A11=FLOWQ(WTSEG-1)*WATC(ISUB,WTSEG-1)
         A12=K1+1/DETIME
         A13=K2
         A21=0.0
         A22=K1
         A23=K2+K3
         IF(CODWAT.EQ.6.0)WRITE(*,110)'ISUB',ISUB,' K1',K1,'K2',K2,
     &      ' K3',K3
         B=A12*A23-A22*A13
         C=A13+A23
         D=A12+A22
         E=A12+A23
         KW=(A13*A21+A11*A23)/B
         KS=(A12*A21+A11*A22)/B
         V1=(-E+SQRT(E*E-4.*B))/2.
         V2=-E-V1
         X=RWADJ(ISUB,WTSEG)-KW
         Y=RSADJ(ISUB,WTSEG)-KS
         AA=(C+V1)/(D-C)*((D+V2)*X-(C+V2)*Y)/SQRT(E*E-4.*B)
         BB=(D+V1)/(C+V1)*AA
         CK1=V1*DT
         CK2=V2*DT
C
C        CHECK IF EXPONENTIAL TERMS APPROACH 0
C
         IF (CK1.LT.-50.) THEN
            ECK1=0.
         ELSE
            ECK1=EXP(CK1)
         ENDIF
         IF (CK2.LT.-50.) THEN
            ECK2=0.
         ELSE
            ECK2=EXP(CK2)
         ENDIF
```

Table 10.6 (continued)

```
         WATRW(ISUB,WTSEG)=KW+AA*ECK1+(X-AA)*ECK2
         WATRS(ISUB,WTSEG)=KS+BB*ECK1+(Y-BB)*ECK2
         IF (CODWAT.EQ.6.0) WRITE (*,110) ' KW',KW,'KS',KS,'AA',AA,'BB',
     &      BB,' WATRW',WATRW(ISUB,WTSEG),' WATRS',WATRS(ISUB,WTSEG),
     &      ' WATC(i,n-1)',WATC(ISUB,WTSEG-1),' V1',V1,' V2',V2,' X',X,
     &      ' Y',Y
         WATC(ISUB,WTSEG)=WATRW(ISUB,WTSEG)/LAKVOL(WTSEG)
         IF (CODWAT.EQ.6.0) WRITE (*,100) ISUB,WTSEG,WATC(ISUB,WTSEG)
C
C        UPDATE AVERAGE WATERSHED CONCENTRATION
C
         WATAVG(ISUB)=WATAVG(ISUB)+WATC(ISUB,WTSEG)*WTLNG(WTSEG)/LTOT
         IF (CODWAT.EQ.4) WRITE (*,120) 'WATAVG',WATAVG(ISUB)
10    CONTINUE
C
C     ADJUST FOR DECAY
C
      DO 15 ISUB=1,2
         RWADJ(ISUB,WTSEG)=WATRW(ISUB,WTSEG)
         RSADJ(ISUB,WTSEG)=WATRS(ISUB,WTSEG)
15    CONTINUE
      RWADJ(3,WTSEG)=WATRW(3,WTSEG)*LAK3+WATRW(4,WTSEG)*LAK4
      RSADJ(3,WTSEG)=WATRS(3,WTSEG)*LAK3+WATRS(4,WTSEG)*LAK4
      A=LAK2*X230LA
      RWADJ(4,WTSEG)=WATRW(4,WTSEG)*LAK1+WATRW(2,WTSEG)*A
      RSADJ(4,WTSEG)=WATRS(4,WTSEG)*LAK1+WATRS(2,WTSEG)*A
      IF(CODWAT.EQ.6.0)THEN
         WRITE(*,*) ' RWADJ(1=>4,WTSEG)',(RWADJ(ISUB,WTSEG),ISUB=1,4),
     &      ' RSADJ(1=>4,WTSEG)',(RSADJ(ISUB,WTSEG),ISUB=1,4),
     &      ' X230LM',X230LM
      ENDIF
      RETURN
100   FORMAT (' WATC(',I2,',',I3,') ',E9.3)
110   FORMAT (4(2X,A4,1X,E9.3),2(2X,A6,1X,E9.3),/,A12,1X,E9.3,
     &   4(2X,A4,1X,E9.3))
120   FORMAT (2(2X,A6,1X,E9.3))
200   FORMAT (' WATPH(',I3,') ',E9.3)
      END
C
C
C
      SUBROUTINE PHW (FUNC,FPRIME,P)
C
C     SUBROUTINE CALCULATES pH EQUATION AND DERIVATIVE FOR GUESS, P
C
      INCLUDE 'MODEL.INC'
      INCLUDE 'VAR.INC'
      IF (CODWAT.EQ.3.0) THEN
         WRITE (*,*) ' SUBROUTINE PHW'
         WRITE (*,100) 'P IN',P
      ENDIF
C
C     CHECK IF pH GUESS TOO EXTREME AND RESET TO MORE REASONABLE VALUE
```

Table 10.6 (continued)

```
C
      IF(P.LT.PMIN)THEN
         P=PMIN
      ELSEIF(P.GT.PMAX)THEN
         P=PMAX
      ELSEIF(P.GT.POLD)THEN
         PMIN=POLD
      ELSEIF(P.LT.POLD)THEN
         PMAX=POLD
      ENDIF
      POLD=P
C
C     CALCULATE pH EQUATION
C
      T1=3.*10.**(8.5-3.*P)/ACTCO**2.25
      T2=2.*10.**(3.91-2.*P)/ACTCO
      T3=10.**(.3-P)
      T4=2.*WATC(8,WTSEG)/1000.+10.0**(-3.86)
      B=ACTCO**0.75*10.**(11.7-3.*P)
      T5=-WATC(7,WTSEG)/1000.*(2.-B)/(1.+B)
      T6=-(10.**(P-11.))/(ACTCO**0.25)
      FUNC=T1+T2+T3+T4+T5+T6
C
C     CALCULATE DERIVATIVE OF EQUATION
C
      A=ALOG(10.)
      DT1=-3.*T1*A
      DT2=-2.*T2*A
      DT3=-T3*A
      DT5=-WATC(7,WTSEG)/1000.*9.*A*B/(1.+B)**2.
      DT6=A*T6
      FPRIME=DT1+DT2+DT3+DT5+DT6
      IF (CODWAT.EQ.3.0)
     &   WRITE (*,100) 'P',P,
     &   'ACTCO',ACTCO,'T1',T1,'T2',T2,
     &   'T3',T3,'T4',T4,'B',B,'T5',T5,'T6',T6,
     &   'A',A,'DT1',DT1,'DT2',DT2,'DT3',DT3,'DT5',DT5,
     &      'DT6',DT6,
     &   'FUNC',FUNC,'FPRIME',FPRIME
      RETURN
100   FORMAT (9(1X,A5,E10.3),/,8(1X,A6,E10.3))
      END
```

## 10.8 References

Baily, J.E., and Ollis, D.F., 1977. "Biochemical Engineering Fundamentals." McGraw Hill Book Company, Toronto.

Beak Consultants Limited, 1982. "An Approach to Long Term Aquatic Modelling of a Generic Uranium Tailings Site." Draft Report to the Atomic Energy Control Board, Ottawa.

Higbie, R. 1935. Transactions of AIChE, Vol. 35, pp. 365-372.

Kipphut, G.W., 1978. "An Investigation of Sedimenting Processes in Lakes." Ph.D. Thesis, Columbia University.

Ontario Ministry of the Environment, 1972 to 1980. "Water Quality Data, Ontario Lakes and Streams." Annual Reports Prepared by the Water Resources Branch, Toronto.

SENES Consultants Limited and Golder Associates Limited, 1981. "Quirke Lake Tailings Disposal Study, Stage 1 Background Information." Draft Report to Rio Algom Limited and Denison Mines Limited.

SENES Consultants Limited and Saskatchewan Research Council (SRC), 1984. "A Study of the Distribution of Naturally Occurring Radionuclides in Freshwater Benthos and Their Environment - Phase I." Research Report to the National Uranium Tailings Program, CANMET, EMR, Ottawa. Under Supply and Services Canada Contract Number OSQ83-00241.

Stumm, W., and Morgan, J.J., 1981. "Aquatic Chemistry: An Introduction Emphasizing Chemical Equilibria in Natural Waters." A. Wiley - Interscience Publication, John Wiley and Sons, Inc.

Swanson, S.M., 1984. "Food Chain Transfer of Uranium - Series Radionuclides in a Northern Saskatchewan Aquatic System." Saskatchewan Research Council Report ΔE-901-7-A-84.

Swanson, S.M., 1985. "A Study of the Distribution of Naturally Occurring Radionuclides in Freshwater Benthos and Their Environment - Phase II." Prepared by SENES Consultants Limited and Saskatchewan Research Council For the National Uranium Tailings Program, CANMET, EMR, Ottawa. Under Supply and Services Canada Contract Number 0SQ83-00241.

Wetzel, R.G., 1975. "Limnology." Saunders College Publishing, Philadelphia.

# 11.0 AQUATIC MODELS

## 11.1 Components Considered

Exposure, via aquatic pathways, of receptors living within the boundaries of the reference site can occur by consumption of river or lake water and consumption of fish taken from the lakes or rivers in the reference watershed. In addition, receptor exposure can occur indirectly through consumption of caribou or moose which have ingested water or, in the case of moose, ingested aquatic vegetation from the river reaches or lake shorelines in the reference watershed.

The component models for predicting the chemical and radiological quality of the surface waters in the reference watershed have been discussed in Section 10. In this section, the effects of chemical changes in surface water quality on the viability of fish are reviewed. In particular, the literature was examined to derive a basic relationship between pH and fish viability for use in assessing the availability of game fish for consumption by the receptors. In addition, the literature was searched to obtain data for use in estimating transfer coefficients (or bioaccumulation factors) which relate the movement of radionuclides from water to game fish flesh. Similarly, the data base relating radionuclide levels in aquatic vegetation to those in water was consulted to establish appropriate transfer factor values. The results of these investigations are discussed in the following sections.

## 11.2 Effect of pH on Fish Populations

While it is recognized that an alteration in pH invokes many dramatic physical, chemical, and consequent biotic changes in lakes and streams, emphasis in the following discussion is placed solely on its effects on the sport fish that would likely be encountered in Canadian Shield waters and subsequently eaten by a receptor. Most of the available field data is limited to declining pH, so the discussion is centered on the effects of acidification on fish populations. However, the resultant effects at a particular pH are assumed to be valid whether the pH is decreasing or increasing. In the case of sport fish, the expected population at a pH of 5, for example, is considered to be the same regardless of the pH trend at that time. It is further assumed that when the aquatic environment is recovering from acidification and conditions again become favourable for viable fish populations, there is sufficient access to the lake and river segments for migrating fish.

No attempt has been made to explain mechanisms by which pH affects fish; rather, background information is provided as a rationale for choosing certain pH values as critical for sport fish catches and local fish consumption.

All trophic levels are affected by declining pH, but perhaps the most visible effect is the loss of entire fish populations. Loss of fish populations in acid-stressed waters has been documented in Scandinavia (Jensen and Snekvik, 1972; Schofield, 1976) and in North America (Beamish and Harvey, 1972; Beamish et al., 1975; Rahel and Magnuson, 1983; Schindler et al., 1985).

The distribution of fish species among acid-stressed and non-acidic lakes suggests major interspecies differences in acid tolerance (Rahel and Magnuson, 1983; Beamish and Harvey, 1972). These differences are in part genetically inherent to the species and relate to fundamental differences in metabolism and physiology. However, within the strictly freshwater species, the apparent differences in acid tolerance, as determined from either field or laboratory studies, do not reveal any consistent taxonomic or ecological pattern (Schofield, 1976). Field data for lake trout, whitefish and walleye show that these fish populations are affected within similar ranges of pH, and so are considered as one population unit in the aquatic model.

Size is an important factor and small fish appear to be most sensitive to low pH. Small fish have greater body and gill surface area per unit weight than larger fish, which means that detrimental ion fluxes proceed more rapidly with the greater exchange area of small fish in contact with water (Schofield, 1976). Fish of interest to the aquatic model are the larger game fish, so size per se is not an important consideration.

Much of the published data on the effects of acid water on aquatic organisms are difficult to interpret because reductions in pH also cause changes in other water characteristics such as free $CO_2$, alkalinity, and the solubility of some metals (Menendez, 1976). The toxicity of many metals increases as pH declines. Fish mortality in various lakes has been attributed to increased uptake of aluminum, copper, or zinc. For aquatic biota that can tolerate pH levels between 6 and 5, such as the sport fish of concern in this study, pH-metal interactions may be of practical importance (Neville, 1985). However, for the purposes of this component model, metal concentrations are assumed to be in equilibrium and the effects of declining pH on fish populations are considered to be a result of a change in hydrogen ion concentration only.

Although fish can die from acidification, more commonly they fail to reproduce and recruitment ceases. Adult fish are more resistant than any other life stage to changes in pH, and the phenomenon of reduced and missing age classes has been observed frequently in fish populations of acid-stressed lakes. Larval fish may be the most pH-susceptible stage of the life history, but recruitment failure can also result from the vulnerability of eggs to low pH, the inhibition of spawning, and the disruption of egg production (Schofield, 1976; NRCC, 1981). There are large species differences in pH tolerance during early life history, but data for sport fish such as walleye and lake trout indicate that reproductive failures occur at a pH of approximately 5.2 to 5.8 (Rahel and Magnuson, 1983).

If recruitment fails, the population density decreases, more food becomes available per individual, and in the short-term there is an increase in growth, size and quality of large fish (Jensen and Snekvik, 1972). Schindler et al. (1985) point out that a decrease in food supply and loss of younger year classes may make it easier for anglers to catch more and larger sport fish at the early stages of acidification. However, if there is continuous failure of recruitment for a number of years, and the food web is severely disrupted, the species will eventually disappear from the lake. At sub-lethal pH, the condition of the fish declines and growth is impaired. Depending on the rate of acidification this increase in availability of adult sport fish may last from approximately one to five years. In the time frame of the study modelling period (several hundred years), however, this relatively short-lived increase is insignificant.

There are insufficient data to quantify accurately the declines in fish population with decreasing pH, but sufficient information is available to allow some general conclusions to be made concerning the range of acidity that is acceptable for fish. Beamish and Harvey (1972) summarize these conclusions as follows:

> "After reviewing the literature, the EIFAC Working Party on Water Quality (1969) concluded a pH range of 5 to 9 was not directly lethal for fishes. Doudoroff and Katz (1950) concluded that most freshwater fishes could live in waters above pH 5.0, but questioned the suitability of waters close to 5.0 for successful reproduction of the more sensitive species. The National Technical Advisory Committee (1968) set the minimum desirable pH at 6.0 for aquatic organisms. McKee and Wolf (1963) stated that the optimum pH of water for fish culture was in the range of 6.7 to 8.6, with a practical extreme lower limit of 6.3. They reviewed some of the literature on acid tolerance and recorded fish surviving in water of pH 3.3; however, tolerable lower limits for most fish were close to 5.0."

Other assessments (Menendez, 1976) have suggested that although fish have been found at pH 4 to 10, the safe range is 5 to 9, and for maximum productivity, the pH value should be 6.5 to 8.5.

Both field and laboratory studies on the sport fish which would be expected from Canadian Shield waters (lake trout, whitefish, walleye) suggest that normal productivity occurs at a pH greater than 6.0 to 6.5 and that a pH of less than 5.5 initiates significant reproductive failure as well as some stress to the adult population (Beamish et al. 1975; Schindler et al., 1985). At pH levels between 4 and 5, disturbance of normal ion and acid-base balance is a likely cause of adult mortality and a rapid decline in population is to be expected. For example, in a 5 year study of the fish population in George Lake, Ontario, Beamish et al. (1975) estimated that the adult population of white suckers decreased in number by 75 percent and in biomass by 90 percent as the pH dropped from an average of 5.0 to an average of 4.5. Those individuals that can survive a pH of 4.0 to 4.5 would experience very reduced growth and would be in poor condition.

Based on this qualitative data, the expected availability (expressed as a percentage) of the adult population of fish, such as walleye, lake trout, brook trout and whitefish, is modelled as a function of pH. The key pH values for these sport fish can be summarized as follows:

| | |
|---|---|
| pH > 6.0 | - normal populations; expect normal catches |
| pH 6.0 to 5.0 | - some decline in population due to recruitment failure; some adults stressed; expect 75 to 90% catch |
| pH 5.0 to 4.5 | - a rapid decline in adult population; condition of the fish poor; expect limited catches of perhaps 25% |
| pH 4.5 to 3.5 | - adult population heavily stressed; population likely to become extinct; expect no catches below pH = 3.5 |

Based on the above, the model proposed for calculating the availability of game fish from the lakes and rivers in the reference watershed for consumption by receptors took the following form:

$$\begin{array}{ll}
\text{for } pH_{n,t} > 6.0 & F_a = 1.0 \\
\text{for } 5.0 < pH_{n,t} \leq 6.0 & F_a = 0.75 + 0.25\,(pH_{n,t} - 5.0) \\
\text{for } 4.5 < pH_{n,t} \leq 5.0 & F_a = 0.25 + 1.0\,(pH_{n,t} - 4.5) \\
\text{for } 3.5 < pH_{n,t} \leq 4.5 & F_a = 0.25\,(pH_{n,t} - 3.5) \\
\text{for } pH_{n,t} \leq 3.5 & F_a = 0.0
\end{array} \qquad (11.1)$$

where:

$F_a$ = availability factor of game fish for consumption expressed as a function of pH

$pH_{n,t}$ = pH level of surface water at the nth node in the reference watershed at time t.

This model formulation is used in the calculation of dose from fish consumption (see Chapter 13).

## 11.3 Radionuclide Transfer to Aquatic Biota

### 11.3.1 Modelling Approach

Modelling the uptake of radionuclides by aquatic biota can be quite involved and require consideration of several interactions; for example, direct uptake from water by aquatic vegetation, sedimentation and deposition of aquatic vegetation in lake sediment, decomposition and release of contaminants from lake sediments to the water phase, harvesting of aquatic vegetation by invertebrates, predation of large fish on small fish, etc. In a separate investigation in Phase II, a multi-component model was developed for predicting the dynamics of radium-226 transfer between six key components in a hypothetical, oligotrophic lake (Gardner et al., 1985). The model considered twenty-three (23) pathways of radium-226 transfer between the six components (i.e. the water column, sediment, aquatic vegetation, invertebrates, forage fish and game fish flesh). The analysis was extended in Phase III to examine the transfer of uranium for the same reference system considered in Phase II. The results of the Phase III investigation are included in Appendix B of this volume (see paper by Blaylock et al., 1986).

The primary objective in these investigations was to compare the multi-component dynamic model concept with the mathematically simple bioaccumulation factor (or concentration factor) approach generally applied in assessment level models. In applying the bioaccumulation factor approach it is assumed that the concentrations in the system components are in equilibrium and that all pathways and mechanisms of radionuclide uptake and elimination are included in the factor.

The results of the investigations of the transfer of radium-226 and uranium to game fish flesh showed that, at equilibrium, the concentrations predicted by the multi-component dynamic model were not appreciably different from those obtained from the simple, water-to-game fish flesh bioaccumulation factor model. More specifically, the authors concluded that:

1. time-dependent concentrations of radium-226 and uranium in the flesh of game fish were most sensitive to changes in the rate constants describing the direct transfer of radium-226 and uranium from water to game fish flesh;

2. equilibrium values of the water-to-game fish flesh concentration factors may give biased results when the aquatic system is not in equilibrium; and,

3. a simpler model involving three components can adequately predict the dynamic behaviour of radium-226 and uranium in game fish.

These conclusions support the use of the aggregate model approach taken in Phase II and again in Phase III for predicting radionuclide transfer to game fish flesh. Because radium-226 and uranium are more mobile in the environment than lead-210 or thorium, the simple bioaccumulation factor approach is equally applicable to the latter radionuclides.

The components and pathways considered in the aggregate model are shown on Figure 11.1. The aquatic model, which was described in part in the previous chapter, considers seven pathways of radionuclide transfer between four components; namely, the water column and sediment components, which hold most of the radionuclide inventories, and sedimenting solids and game fish components. Game fish flesh rather than whole fish is considered as it is this tissue which is consumed by humans. The sedimenting solids consist of inorganic solids and organic solids (primarily phytoplankton). Together these act as the primary mechanism of radionuclide removal from the water column to the sediment. In addition to the above aquatic macrophytes (rooted aquatic plants) are also modelled. They represent a significant pathway of radionuclide ingestion by moose, and are modelled on an average basis, over the entire watershed.

### 11.3.2 Bioaccumulation in Fish

The concentration in game fish flesh is calculated as a function of the concentration in the water phase from the relationship:

$$[F_i]_{n,t} = B_{f,i}\,[R_i]_{n,t} \tag{11.2}$$

where:

$B_{f,i}$ = the water-to-game fish flesh bioaccumulation factor, for radionuclide "i" ($Bq.g^{-1}$ (wet wt).$Bq^{-1}.m^3$)

$[F_i]_{n,t}$ = concentration of radionuclide "i" in game fish flesh at node "n" in the watershed at time "t" ($Bq.m^{-3}$)

$[R_i]_{n,t}$ = concentration of radionuclide "i" at node "n" in the watershed at time "t" ($Bq.m^{-3}$).

The bioaccumulation factor used in the model is an aggregate representation of numerous pathways and mechanisms of radionuclide transfer through the aquatic environment.

As numerous investigators have reported, the accumulation of radionuclides in aquatic biota is a complex phenomenon which is influenced by many possible

FIGURE II.1

## AGGREGATE AQUATIC TRANSFER MODEL

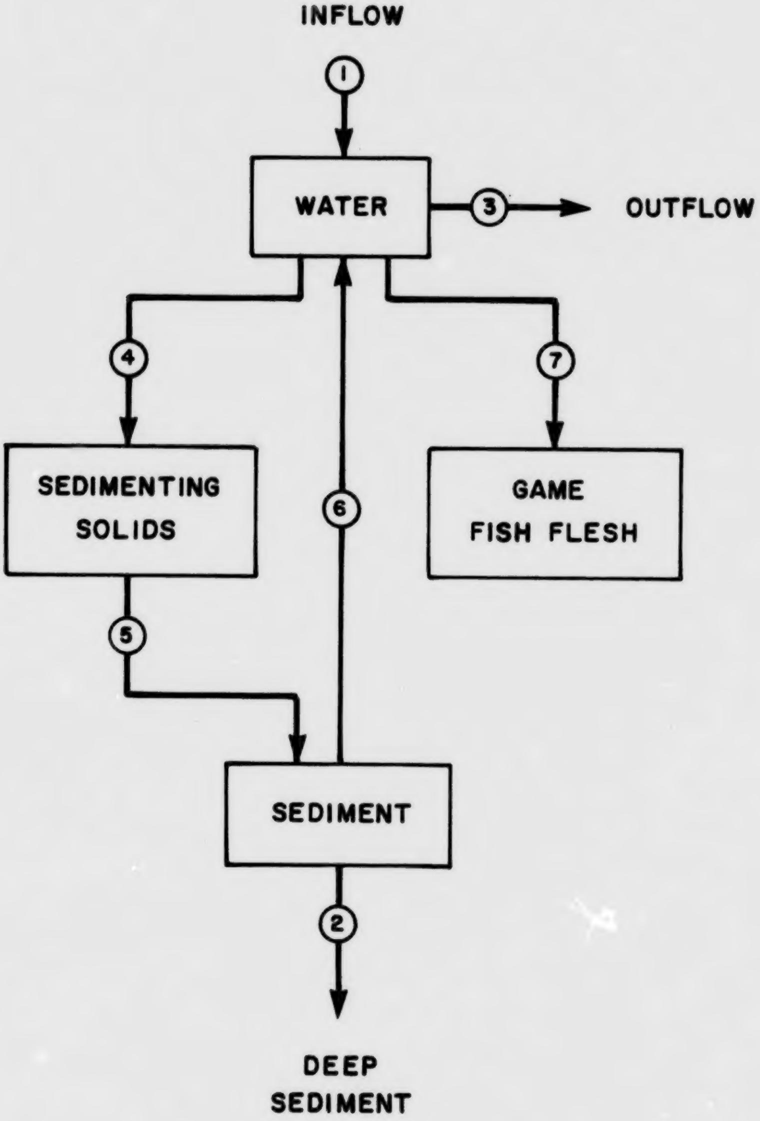
INFLOW
①
WATER
③
OUTFLOW
④
⑦
SEDIMENTING SOLIDS
⑥
GAME FISH FLESH
⑤
SEDIMENT
②
DEEP SEDIMENT

factors. Examples of the factors cited in the literature include: the chemical state of the radionuclides; the chemical composition of the water; the characteristics of the aquatic biota; and the affinity of the radionuclides for different tissues. The method used to calculate bioaccumulation factors can also have a significant influence. The different methods use either wet weight (fresh weight), dry weight, or ash weight of the biota and either filtered or unfiltered water sample measurements in the calculations. The issue is complicated further by the fact that the method used to calculate bioaccumulation factors is often not reported. Considering the number of variables that can influence the levels measured in aquatic biota, it is not unexpected that bioaccumulation factors reported in the literature vary over several orders of magnitude.

To minimize the influence of some of these variables, the literature was searched for data on radionuclide levels in game fish flesh specific to northern Canadian waters. The literature consulted included: published articles; environmental baseline studies; environmental impact assessments; and, routine mine monitoring reports. The data presented below is representative of low alkalinity, low hardness waters.

The data compiled from the literature on radionuclide levels in game fish flesh and water are presented in Tables 11.1 to 11.4 for natural uranium, total thorium, radium-226 and lead-210 respectively. All fish flesh values are reported on a wet (fresh) weight basis while the water data are total (unfiltered) levels. The calculated bioaccumulation factors (BF's) are reported on a $L.kg^{-1}$ (or $mL.g^{-1}$) basis as usually found in the literature. These BF values were converted to a $m^3.g^{-1}$ basis for input to the aquatic model.

The calculated BF's vary over a fairly wide range for all radionuclides as expected. Frequency histogram plots of the data (see Figures 11.2 to 11.5) show that the BF's for all radionuclides are skewed to the right, typical of a lognormal distribution. Several distribution curves were fitted to the frequency histograms using commercially available statistical software. Of the distributions fitted to the data, the lognormal distribution was found to be the best overall. The chi-squared goodness of fit statistic indicated that the fit was good for the total thorium and radium-226 data. The test indicated a poorer fit for the total uranium and lead-210 data. However, since the lognormal distribution was found to be the most representative overall, it was selected to characterize the bioaccumulation factors for all four radionuclides.

### 11.3.3 Bioaccumulation in Aquatic Macrophytes

Calculation of the radionuclide levels in aquatic macrophytes was included in the Phase III model as macrophytes are a source of food for moose. The radionuclide levels in the aquatic macrophytes are calculated from the aggregate model:

$$[C_{q,i}] = B_{q,i} \; [\overline{R_i}]_t \qquad (11.3)$$

where:

$[C_{q,i}]_t$ = concentration of radionuclide "i" in aquatic vegetation at time "t" ($Bq.g^{-1}$)

$B_{q,i}$ = the water-to-aquatic vegetation transfer coefficient ($Bq.g^{-1}$ (wet)$.Bq^{-1}.m^3$)

$[\overline{R_i}]_t$ = average concentration of radionuclide "i" in the waters over the entire reach of the watershed ($Bq.m^{-3}$).

The model calculates an average radionuclide content in the vegetation which is applicable to the entire length of the watershed. This approach was taken to permit moose consumption of both water and aquatic vegetation to be treated independent of location in the watershed. The average radionuclide content in surface water, and hence average radionuclide content in aquatic vegetation, is calculated based on the length of river reach and circumference of the

## FIGURE II.2

## FREQUENCY HISTOGRAM OF URANIUM BIOACCUMULATION FACTOR VALUES

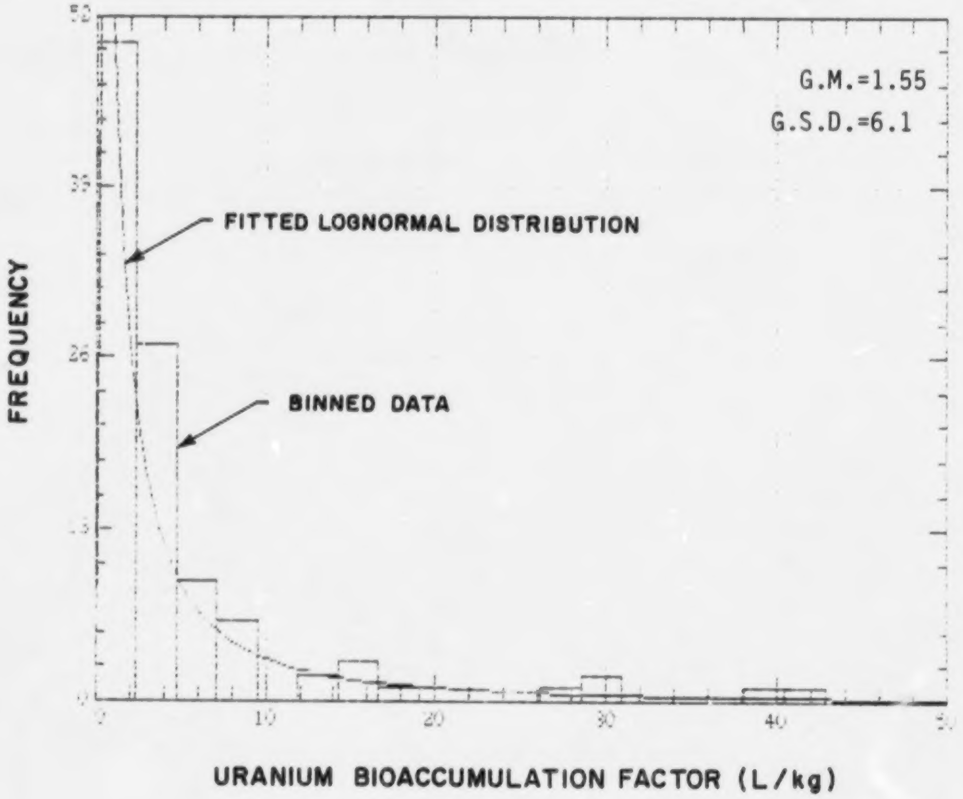

FIGURE 11.3

FREQUENCY HISTOGRAM
OF THORIUM BIOACCUMULATION FACTOR VALUES

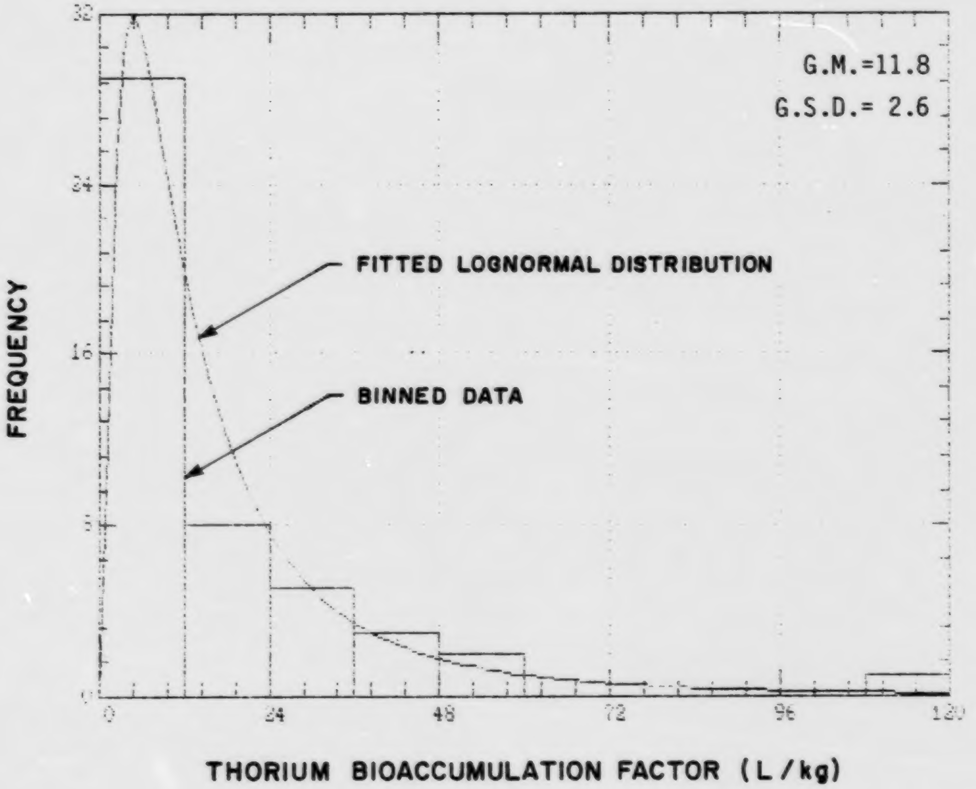

FIGURE II.4

FREQUENCY HISTOGRAM
OF RADIUM-226 BIOACCUMULATION FACTOR VALUES

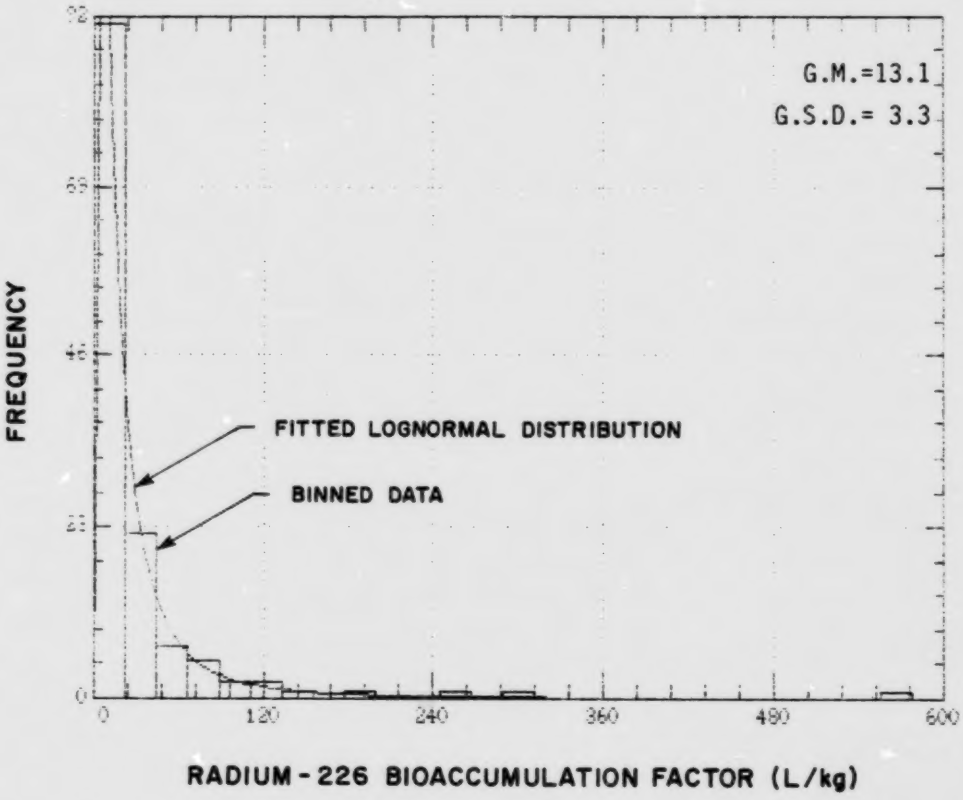

FIGURE 11.5

# FREQUENCY HISTOGRAM OF LEAD-210 BIOACCUMULATION FACTOR VALUES

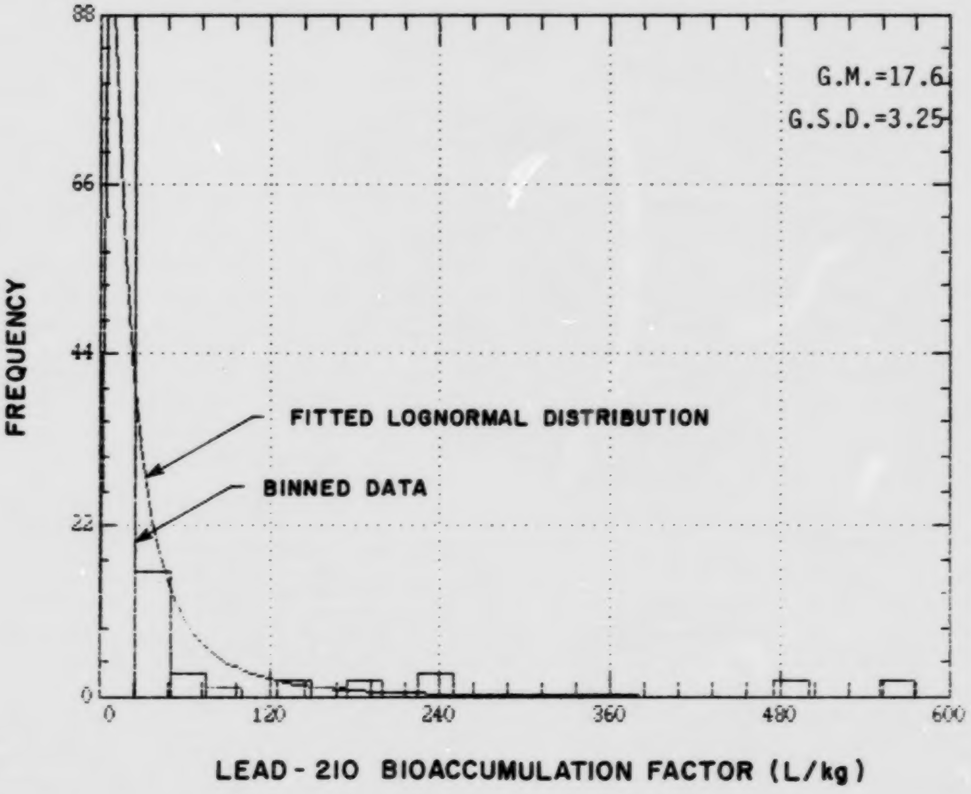

Table 11.1

LARGE (GAME) FISH FLESH URANIUM BIOACCUMULATION FACTORS (BF's)

| Location | Species | No. Fish Samples | Fish Flesh Concentration (ug/kg fresh) | Water Level (ug/L) | Uranium BF (L/kg) | Reference |
|---|---|---|---|---|---|---|
| Trapper Lake, B.C. | Rainbow Trout | 13 | 5 | 0.335 | 14.9 | Norcen 1980 |
| McClean Lake, Sask. | Walleye | 5 | 7.69 | 0.5 | 15.4 | Canadian Occidental 1981 |
| " " | Lake Whitefish | 5 | 7.18 | 0.5 | 14.4 | " |
| Kewen Lake, Sask. | Walleye | 5 | 6.87 | 0.82 | 8.4 | Canadian Occidental 1981 |
| " " | Lake Whitefish | 5 | 5.23 | 0.82 | 6.4 | " |
| McDonald Lake, Sask. | Northern Pike | 5 | | | 2 | I.E.S. Inc. 1983 |
| " " | Lake Whitefish | 5 | | | 30 | " |
| Delta Lake, Sask. | Northern Pike | 5 | | | 1 | " |
| " " | Lake Whitefish | 5 | | | 5 | " |
| Russell Lake, Sask. | Northern Pike | 5 | | | 4 | " |
| " " | Lake Whitefish | 5 | | | 3 | " |
| Beaverlodge Lake, Sask. | Lake Trout | 5 | | | 0.3 | Swanson 1983 |
| " " | Lake Whitefish | 5 | | | 0.2 | " |
| Dubyna Lake, Sask. | Northern Pike | 5 | 3.69 | 22 | .2 | Eldorado 1978 |
| " " | Lake Trout ('77) | 2 | 78 | 22 | 3.5 | " |
| " " | Lake Trout ('78) | 5 | 17 | 22 | .8 | " |
| Schmoo Lake, Sask. | Lake Trout | 5 | 6.8 | 19.7 | .3 | " |
| Wollaston Lake, Sask | | | | | | |
| - Pow Bay | Lake Trout | 5 | ≤38 | 17.8 | 2.1 | ELDOR (Gulf Minerals) 1982 |
| - Pow Bay | Northern Pike | 5 | 18 | 17.8 | 1.0 | " |
| - Hidden Bay | Northern Pike | 5 | 8 | 25.9 | .3 | " |
| Russell Lake, Sask. | Walleye | 1 | 14.1 | <0.5 | 28.2 | Key Lake 1979 |
| " " | " | 1 | 20.1 | " | 40.2 | " |
| " " | " | 1 | 8.4 | " | 16.8 | " |
| " " | " | 1 | 6.9 | " | 13.8 | " |
| " " | " | 1 | <2.1 | " | 4.2 | " |
| " " | " | 1 | <1.7 | " | 3.4 | " |
| " " | " | 1 | <2.3 | " | 4.6 | " |
| " " | " | 1 | 20.7 | " | 41.4 | " |
| " " | " | 1 | 1.3 | " | 2.6 | " |
| " " | " | 1 | <2.3 | " | 4.6 | " |

Table 11.1 continued

| Location | Species | No. Fish Samples | Fish Flesh Concentration (ug/kg fresh) | Water Level (ug/L) | Uranium BF (L/kg) | Reference |
|---|---|---|---|---|---|---|
| Russell Lake, Sask. | Lake Whitefish | 1 | 4.4 | <0.5 | 8.9 | Key Lake 1979 |
| " " | " | 1 | <2.2 | " | <4.5 | " |
| " " | " | 1 | <2.3 | " | <4.7 | " |
| " " | " | 1 | <2.3 | " | <4.7 | " |
| " " | " | 1 | <2.5 | " | <5.0 | " |
| " " | " | 1 | <2.0 | " | <4.0 | " |
| " " | " | 1 | <2.1 | " | <4.2 | " |
| " " | " | 1 | <2.1 | " | <4.2 | " |
| " " | " | 1 | <2.3 | " | <4.6 | " |
| " " | " | 1 | <2.0 | " | <4.0 | " |
| Beaverlodge Lake, Sask. | Lake Whitefish | 1 | 2.0 | 333 | 0.01 | Swanson 1982 |
| " " | " | 1 | 577.8 | " | 1.71 | " " |
| " " | " | 1 | 32.4 | " | 0.10 | " " |
| " " | " | 1 | 18.8 | " | 0.06 | " " |
| " " | " | 1 | 102.2 | " | 0.30 | " " |
| " " | " | 1 | 68.5 | " | 0.20 | " " |
| " " | " | 1 | 163.6 | " | 0.48 | " " |
| " " | " | 1 | 254.2 | " | 0.75 | " " |
| " " | " | 1 | 49.9 | " | 0.15 | " " |
| " " | " | 1 | 65.3 | " | 0.19 | " " |
| " " | " | 1 | 37.5 | " | 0.11 | " " |
| " " | " | 1 | 24.3 | " | 0.07 | " " |
| " " | " | 1 | 59.1 | " | 0.18 | " " |
| " " | " | 1 | 81.7 | " | 0.24 | " " |
| " " | " | 1 | 19.3 | " | 0.06 | " " |
| " " | " | 1 | 38.7 | " | 0.12 | " " |
| " " | " | 1 | 55.4 | " | 0.16 | " " |
| " " | " | 1 | 16.1 | " | 0.05 | " " |
| " " | " | 1 | 47.1 | " | 0.14 | " " |
| " " | " | 1 | 42.3 | " | 0.13 | " " |
| " " | " | 1 | 31.1 | " | 0.09 | " " |
| " " | " | 1 | 39.0 | " | 0.12 | " " |
| Milliken Lake, Sask. | Lake Whitefish | 1 | 35.1 | 1.2 | 29.25 | Swanson 1982 |
| " " | " | 1 | <2.0 | " | 1.67 | " " |
| " " | " | 1 | 2.1 | " | 1.75 | " " |
| " " | " | 1 | 5.5 | " | 4.58 | " " |
| " " | " | 1 | 6.1 | " | 5.08 | " " |
| " " | " | 1 | 7.8 | " | 6.50 | " " |
| " " | " | 1 | 11.3 | " | 9.42 | " " |
| " " | " | 1 | 6.1 | " | 5.08 | " " |
| " " | " | 1 | 2.1 | " | 1.75 | " " |
| " " | " | 1 | 3.8 | " | 3.17 | " " |
| " " | " | 1 | 3.3 | " | 2.75 | " " |
| " " | " | 1 | 10.4 | " | 8.67 | " " |

Table 11.1 continued

| Location | Species | No. Fish Samples | Fish Flesh Concentration (ug/kg fresh) | Water Level (ug/L) | Uranium BF (L/kg) | Reference |
|---|---|---|---|---|---|---|
| Milliken Lake, Sask. | Lake Whitefish | 1 | 5.1 | 1.2 | 4.25 | Swanson 1982 |
| " " | " | 1 | 6.0 | " | 5.00 | " " |
| " " | " | 1 | 3.6 | " | 3.00 | " " |
| " " | " | 1 | 4.7 | " | 3.92 | " " |
| " " | " | 1 | <1.8 | " | 1.50 | " " |
| " " | " | 1 | <1.9 | " | 1.58 | " " |
| " " | " | 1 | 3.1 | " | 2.58 | " " |
| " " | " | 1 | 4.8 | " | 4.00 | " " |
| Fredette Lake, Sask. | Lake Whitefish | 1 | 46.8 | 3.3 | 14.18 | Swanson 1982 |
| " " | " | 1 | 12.6 | " | 3.82 | " " |
| " " | " | 1 | 4.6 | " | 1.39 | " " |
| " " | " | 1 | <0.2 | " | <0.06 | " " |
| " " | " | 1 | <0.2 | " | <0.06 | " " |
| " " | " | 1 | 4.6 | " | 1.39 | " " |
| " " | " | 1 | 10.2 | " | 3.09 | " " |
| " " | " | 1 | 2.9 | " | 0.88 | " " |
| " " | " | 1 | <2.0 | " | 0.61 | " " |
| " " | " | 1 | 10.2 | " | 3.09 | " " |
| " " | " | 1 | 17.6 | " | 5.33 | " " |
| " " | " | 1 | 7.4 | " | 2.24 | " " |
| " " | " | 1 | 1.7 | " | 0.52 | " " |
| " " | " | 1 | 25.5 | " | 7.73 | " " |
| " " | " | 1 | 29.4 | " | 8.91 | " " |
| " " | " | 1 | 3.7 | " | 1.12 | " " |
| " " | " | 1 | >0.2 | " | <0.06 | " " |
| " " | " | 1 | 19.1 | " | 5.79 | " " |
| " " | " | 1 | 6.9 | " | 2.09 | " " |
| " " | " | 1 | 5.0 | " | 1.52 | " " |
| " " | " | 1 | 4.7 | " | 1.42 | " " |

| Summary Statistics | |
|---|---|
| Number of Data Points | 103 |
| Geometric Mean | 1.55 |
| Geometric Std. Deviation | 6.1 |
| Range of Values | 0.01 to 41.4 |

Table 11.2

## LARGE (GAME) FISH FLESH THORIUM BIOACCUMULATION FACTORS (BF's)

| Location | Species | No. Fish Samples | Fish Flesh Concentration (ug/kg fresh) | Water Level (ug/L) | Thorium BF (L/kg) | Reference |
|---|---|---|---|---|---|---|
| McDonald Lake, Sask. | Northern Pike | 5 |  |  | 30 | I.E.S. Inc. 1983 |
| " " | Lake Whitefish | 5 |  |  | 110 | " |
| Russell Lake, Sask. | Northern Pike | 5 |  |  | 20 | I.E.S. Inc. 1983 |
| " " | Lake Whitefish | 5 |  |  | 20 | " |
| Dubyna Lake, Sask. | Northern Pike | 5 | 5.3 | 0.7 | 7.6 | Eldorado 1978 |
| " " | Lake Trout | 5 | 14.3 | 0.7 | 20.4 | " |
| Schmoo Lake, Sask. | Lake Trout | 5 | 15.0 | 0.5 | 30.0 | " |
| Donaldson Lake, Sask. | Lake Trout | 5 | 27.9 | 0.5 | 55.8 | " |
| Russell Lake, Sask. | Walleye | 1 | 4.7 | 0.84 | 5.6 | Key Lake 1979 |
| " " | " | 1 | 1.3 | " | 1.5 | " |
| " " | " | 1 | 19.8 | " | 23.6 | " |
| " " | " | 1 | 4.9 | " | 5.8 | " |
| " " | " | 1 | 30.0 | " | 35.7 | " |
| " " | " | 1 | 0.9 | " | 1.1 | " |
| " " | " | 1 | 23.2 | " | 27.6 | " |
| " " | " | 1 | 1.0 | " | 1.2 | " |
| " " | " | 1 | 7.9 | " | 9.4 | " |
| " " | " | 1 | 4.7 | " | 5.6 | " |
| Russell Lake, Sask. | Lake Whitefish | 1 | 4.0 | 0.84 | 4.8 | Key Lake 1979 |
| " " | " | 1 | 19.9 | " | 23.7 | " |
| " " | " | 1 | 2.2 | " | 2.6 | " |
| " " | " | 1 | 19.4 | " | 23.1 | " |
| " " | " | 1 | 44.5 | " | 52.9 | " |
| " " | " | 1 | 6.2 | " | 7.3 | " |
| " " | " | 1 | 39.8 | " | 47.4 | " |
| " " | " | 1 | 12.6 | " | 15.0 | " |
| " " | " | 1 | 7.9 | " | 9.4 | " |
| " " | " | 1 | 6.1 | " | 7.3 | " |
| Kewen Lake, Sask. | Walleye | 1 | <4.2 | 0.38 | <11.0 | Canadian Occidental 1981 |
| " " | " | 1 | 13.8 | " | 36.3 | " " |
| " " | " | 1 | <4.2 | " | <11.0 | " " |
| " " | " | 1 | <4.3 | " | <11.3 | " " |
| " " | " | 1 | 10.5 | " | 27.6 | " " |
| Kewen Lake, Sask. | Lake Whitefish | 1 | <4.6 | 0.38 | <12.1 | Canadian Occidental 1981 |
| " " | " | 1 | <4.5 | " | <11.8 | " " |
| " " | " | 1 | <4.1 | " | <10.8 | " " |
| " " | " | 1 | 16.5 | " | 43.4 | " " |
| " " | " | 1 | <3.9 | " | <10.3 | " " |

Table 11.2 continued

| Location | Species | No. Fish Samples | Fish Flesh Concentration (ug/kg fresh) | Water Level (ug/L) | Thorium BF (L/kg) | Reference |
|---|---|---|---|---|---|---|
| McLean Lake, Sask. | Walleye | 1 | <4.9 | 0.63 | <7.8 | Canadian Occidental 1981 |
| " " | " | 1 | <5.0 | " | <7.9 | " " |
| " " | " | 1 | <4.9 | " | <7.8 | " " |
| " " | " | 1 | <5.3 | " | <8.4 | " " |
| " " | " | 1 | <3.3 | " | <5.3 | " " |
| McClean Lake, Sask. | Lake Whitefish | 1 | <5.5 | 0.63 | <8.7 | Canadian Occidental 1981 |
| " " | " | 1 | <6.5 | " | <10.3 | " " |
| " " | " | 1 | <5.3 | " | <8.4 | " " |
| " " | " | 1 | <5.0 | " | <7.9 | " " |
| " " | " | 1 | <5.0 | " | <7.9 | " " |

| Summary Statistics | |
|---|---|
| Number of Data Points | 48 |
| Geometric Mean | 11.8 |
| Geometric Std. Deviation | 2.6 |
| Range of Values | 1.1 to 110 |

Table 11.3

## LARGE (GAME) FISH FLESH RADIUM-226 BIOACCUMULATION FACTORS (BF'S)

| Location | Species | No. Fish Samples | Fish Flesh Concentration Bq/kg (fresh) | Water Level Bq/L | Ra-226 BF (L/kg) | Reference |
|---|---|---|---|---|---|---|
| Sandrift Lake Δ2, BC | Rainbow Trout | 5 | 0.26 | 0.007 | 37.1 | Norcen 1980 |
| Beaverdell Creek, BC | Rainbow Trout | 14 | 0.11 | 0.007 | 15.9 | " " |
| Kewen Lake, Sask. | Walleye | 1 | 0.15 | 0.004 | 37.5 | Canadian Occidental, 1981 |
| " " | " | 1 | 0.51 | " | 127.5 | " " |
| " " | " | 1 | 0.31 | " | 77.5 | " " |
| " " | " | 1 | 0.26 | " | 40.0 | " " |
| " " | " | 1 | 2.23 | " | 557.5 | " " |
| Kewen Lake, Sask. | Lake Whitefish | 1 | 0.07 | 0.004 | 17.5 | Canadian Occidental 1981 |
| " " | " | 1 | 0.33 | " | 82.5 | " " |
| " " | " | 1 | 0.22 | " | 55.0 | " " |
| " " | " | 1 | 0.07 | " | 17.5 | " " |
| " " | " | 1 | 0.14 | " | 35.0 | " " |
| McClean Lake, Sask. | Walleye | 1 | 0.09 | 0.004 | 22.5 | Canadian Occidental 1981 |
| " " | " | 1 | 1.00 | " | 250.0 | " " |
| " " | " | 1 | 0.09 | " | 22.5 | " " |
| " " | " | 1 | 0.49 | " | 122.5 | " " |
| " " | " | 1 | 0.55 | " | 137.5 | " " |
| McClean Lake, Sask. | Lake Whitefish | 1 | 0.20 | 0.004 | 50.0 | " " |
| " " | " | 1 | 0.12 | " | 30.0 | " " |
| " " | " | 1 | 0.10 | " | 25.0 | " " |
| " " | " | 1 | 0.09 | " | 22.5 | " " |
| " " | " | 1 | 0.19 | " | 47.5 | " " |
| McDonald Lake, Sask. | Northern Pike | 5 | - | - | 10 | I.E.S. Inc. 1983 |
| " " | Lake Whitefish | 5 | - | - | 10 | " " |
| Delta Lake, Sask | Northern Pike | 5 | - | - | 10 | " " |
| " " | Lake Whitefish | 5 | - | - | 30 | " " |
| Russell Lake, Sask. | Northern Pike | 5 | - | - | 5 | |
| " " | Lake Whitefish | 5 | - | - | 60 | " " |
| Dubyna Lake, Sask. | Lake Trout | 1 | 0.13 | 0.02 | 6.5 | Eldorado 1978 |
| " " | " " | 1 | 0.13 | " | 6.5 | " |
| " " | " " | 1 | 0.13 | " | 6.5 | " |
| " " | " " | 1 | 0.25 | " | 12.5 | " |
| Dubyna Lake, Sask. | Northern Pike | 1 | 0.49 | 0.02 | 24.5 | Eldorado 1978 |
| " " | " " | 1 | 0.49 | " | 24.5 | " |
| " " | " " | 1 | 0.79 | " | 39.5 | " |
| " " | " " | 1 | 0.49 | " | 24.5 | " |
| | | 1 | 0.49 | " | 24.5 | " |

Table 11.3 continued

| Location | Species | No. Fish Samples | Fish Flesh Concentration Bq/kg (fresh) | Water Level Bq/L | Ra-226 BF (L/kg) | Reference |
|---|---|---|---|---|---|---|
| Donaldson Lake, Sask. | Lake Trout | 1 | 0.13 | 0.03 | 4.3 | Eldorado 1978 |
| " " | " " | 1 | 0.13 | " | 4.3 | " |
| " " | " " | 1 | 0.13 | " | 4.3 | " |
| " " | " " | 1 | 0.25 | " | 8.3 | " |
| Schmoo Lake, Sask. | Lake Trout | 1 | 0.25 | 0.02 | 12.5 | Eldorado 1978 |
| " " | " " | 1 | 0.13 | " | 6.5 | " |
| " " | " " | 1 | 0.25 | " | 12.5 | " |
| " " | " " | 1 | 0.13 | " | 6.5 | " |
| " " | " " | 1 | 0.13 | " | 6.5 | " |
| Wollaston Lake, Sask. | | | | | | |
| - Pow Bay | Lake Trout | 5 | 0.3 | 0.008 | 37.5 | ELDOR (Gulf Minerals) 1982 |
| " " | Northern Pike | 5 | 0.2 | 0.008 | 25.0 | " " |
| - Hidden Bay | Northern Pike | 5 | 0.2 | 0.014 | 14.2 | " " |
| Russell Lake, Sask. | Walleye | 1 | 0.03 | 0.006 | 5.0 | Key Lake 1979 |
| " " | " | 1 | 0.04 | " | 6.7 | " |
| " " | " | 1 | 0.07 | " | 11.7 | " |
| " " | " | 1 | 0.03 | " | 5.0 | " |
| " " | " | 1 | 0.04 | " | 6.7 | " |
| " " | " | 1 | 0.04 | " | 6.7 | " |
| " " | " | 1 | 0.04 | " | <6.7 | " |
| " " | " | 1 | 0.04 | " | <6.7 | " |
| " " | " | 1 | 0.05 | " | 8.3 | " |
| " " | " | 1 | 0.04 | " | 6.7 | " |
| Russell Lake, Sask. | Lake Whitefish | 1 | 0.04 | 0.006 | 6.7 | Key Lake 1979 |
| " " | " | 1 | 0.04 | " | 6.7 | " |
| " " | " | 1 | 0.04 | " | 6.7 | " |
| " " | " | 1 | 0.04 | " | 6.7 | " |
| " " | " | 1 | 0.04 | " | 6.7 | " |
| " " | " | 1 | 0.04 | " | 6.7 | " |
| " " | " | 1 | 0.04 | " | 6.7 | " |
| " " | " | 1 | 0.04 | " | 6.7 | " |
| " " | " | 1 | 0.04 | " | 6.7 | " |
| " " | " | 1 | 0.04 | " | 6.7 | " |
| Beaverlodge Lake, Sask. | Lake Whitefish | 1 | >0.1 | 0.06 | >1.7 | Swanson 1982 |
| " " | " | 1 | 0.1 | " | 1.7 | " " |
| " " | " | 1 | 0.5 | " | 8.3 | " " |
| " " | " | 1 | 0.1 | " | 1.7 | " " |
| " " | " | 1 | 0.2 | " | 3.3 | " " |
| " " | " | 1 | <0.1 | " | <1.7 | " " |
| " " | " | 1 | 0.3 | " | 5.0 | " " |
| " " | " | 1 | 0.9 | " | 15.0 | " " |
| " " | " | 1 | 0.5 | " | 8.3 | " " |

Table 11.3 continued

| Location | Species | No. Fish Samples | Fish Flesh Concentration Bq/kg (fresh) | Water Level Bq/L | Ra-226 BF (L/kg) | Reference |
|---|---|---|---|---|---|---|
| Beaverlodge Lake, Sask. | Lake Whitefish | 1 | 0.2 | 0.06 | 3.3 | Swanson 1982 |
| " " | " | 1 | 0.1 | " | 1.7 | " " |
| " " | " | 1 | 0.1 | " | 1.7 | " " |
| " " | " | 1 | 0.1 | " | 1.7 | " " |
| " " | " | 1 | 0.1 | " | 1.7 | " " |
| " " | " | 1 | <0.1 | " | <1.7 | " " |
| " " | " | 1 | 0.1 | " | 1.7 | " " |
| " " | " | 1 | 6.1 | " | 1.7 | " " |
| " " | " | 1 | 1.0 | " | 16.7 | " " |
| Milliken Lake, Sask. | Lake Whitefish | 1 | <0.1 | 0.01 | <10.0 | Swanson 1982 |
| " " | " | 1 | <0.1 | " | <10.0 | " " |
| " " | " | 1 | 0.1 | " | 10.0 | " " |
| " " | " | 1 | 0.6 | " | 60.0 | " " |
| " " | " | 1 | <0.1 | " | <10.0 | " " |
| " " | " | 1 | 0.2 | " | 20.0 | " " |
| " " | " | 1 | 0.9 | " | 90.0 | " " |
| " " | " | 1 | 0.3 | " | 30.0 | " " |
| " " | " | 1 | 0.6 | " | 60.0 | " " |
| " " | " | 1 | 0.2 | " | 20.0 | " " |
| " " | " | 1 | <1.1 | " | <110.0 | " " |
| " " | " | 1 | <0.1 | " | <10.0 | " " |
| " " | " | 1 | 0.3 | " | 30.0 | " " |
| " " | " | 1 | <0.1 | " | <10.0 | " " |
| " " | " | 1 | 0.1 | " | 10.0 | " " |
| " " | " | 1 | 0.1 | " | 10.0 | " " |
| " " | " | 1 | <0.1 | " | <10.0 | " " |
| Fredette Lake, Sask. | Lake Whitefish | 1 | 0.1 | 0.02 | 5.0 | Swanson 1982 |
| " " | " | 1 | >0.6 | " | 30.0 | " " |
| " " | " | 1 | <0.1 | " | <5.0 | " " |
| " " | " | 1 | 0.7 | " | 35.0 | " " |
| " " | " | 1 | 0.2 | " | 10.0 | " " |
| " " | " | 1 | <0.1 | " | <5.0 | " " |
| " " | " | 1 | 0.1 | " | 5.0 | " " |
| " " | " | 1 | 0.1 | " | 5.0 | " " |
| " " | " | 1 | <0.1 | " | <5.0 | " " |
| " " | " | 1 | 4.0 | " | 200.0 | " " |
| " " | " | 1 | <0.1 | " | <5.0 | " " |
| " " | " | 1 | <0.1 | " | <5.0 | " " |
| " " | " | 1 | <0.1 | " | <5.0 | " " |
| " " | " | 1 | <0.1 | " | <5.0 | " " |
| " " | " | 1 | <0.1 | " | <5.0 | " " |
| Wollaston Lake, Sask.<br>- Hidden Bay | Northern Pike | 1 | 1.54 | <0.005 | 308.0 | John 1985 |
| " " | " | 1 | 0.06 | " | 11.2 | " |
| " " | " | 1 | 0.06 | " | 11.2 | " |
| " " | " | 1 | <0.06 | " | <11.2 | " |

Table 11.3 continued

| Location | Species | No. Fish Samples | Fish Flesh Concentration Bq/kg (fresh) | Water Level Bq/L | Ra-226 BF (L/kg) | Reference |
|---|---|---|---|---|---|---|
| Wollaston Lake, Sask. | | | | | | |
| - Hidden Bay | Walleye | 1 | 0.10 | <0.005 | 20.0 | John 1985 |
| " " | " | 1 | 0.25 | " | 50.0 | " |
| " " | Lake Whitefish | 1 | 0.41 | <0.005 | 82.0 | " |
| " " | " | 1 | 0.04 | " | 80.0 | " |
| " " | " | 1 | 0.11 | " | 22.0 | " |
| " " | Lake Trout | 1 | <0.11 | <0.005 | <22.0 | " |
| - Collins Bay | Northern Pike | 1 | 0.06 | <0.005 | 12.0 | " |
| " " | " | 1 | <0.05 | " | <10.0 | " |
| " " | Walleye | 1 | 0.35 | <0.005 | 70.0 | " |
| " " | " | 1 | 0.11 | " | 22.0 | " |
| " " | Lake Whitefish | 1 | 0.20 | <0.005 | 40.0 | " |

| Summary Statistics | |
|---|---|
| Number of Data Points | 134 |
| Geometric Mean | 13.1 |
| Geometric Std. Deviation | 3.3 |
| Range of Values | 1.7 to 603 |

lakes from the relationship:

$$[\overline{R_i}]_t = \frac{\Sigma S_n\,[R_i]_{n,t} + \Sigma(4\pi L_n)^{0.5}[R_i]_{n,t}}{\Sigma S_n + \Sigma(4\pi L_n)^{0.5}} \qquad (11.4)$$

where:

$S_n$ = the length of the reach of river segment "n" (m)

$[R_i]_{n,t}$ = concentration of radionuclide "i" in the surface water at node "n" at time "t" ($Bq.m^{-3}$)

$L_n$ = surface area of the lake designated node "n" ($m^2$).

The averaging was done on a length rather than a volume basis, since it was felt that this provided a more relevant quantity. Moose might be expected to drink and graze from lakes and rivers in a watershed in proportion to river lengths and lake circumferences, rather than in proportion to the volume of flow at any point in the system.

The literature search for data on radionuclide levels in aquatic macrophytes produced only limited data which was directly usable in calculating bioaccumulation factors. Several sources of data were found to be of little value because the results were reported on either a dry or ash weight basis rather than a wet weight basis. The most useful data was reported by Integrated Environmental Sciences Inc. (1983) for northern Saskatchewan. A review of BF values reported for each radionuclide on twelve samples showed the data to be skewed to the right. Therefore, the data were treated as being lognormally distributed. The calculated statistics for these data are summarized as follows:

| Radionuclide | Bioaccumulation Factor ($L.kg^{-1}$) Geometric Mean Value | Geometric Standard Deviation |
|---|---|---|
| Uranium | 15.5 | 5.5 |
| Thorium | 11.3 | 6.8 |
| Radium-226 | 45 | 2.9 |
| Lead-210 | 127 | 2.0 |

The high geometric standard deviations reported for uranium and thorium reflect the high variability of the data. The mean values suggest that thorium and uranium accumulate much less than either radium-226 or lead-210. The mean value for lead-210, on the other hand, is three times greater than the mean value calculated for radium-226.

## 11.4 Parameter Values and Code Listing

A summary of the parameters included in the aquatic models is provided in Table 11.5. Parameter values and their distributions are specified for the input parameters on the table. The basis for the specified values are discussed in the appropriate sections in the text of Chapter 11.

A copy of the code for calculating radionuclide levels in game fish flesh and aquatic macrophytes is included in Table 11.6 for the interested reader. Certain features of the code (e.g. calculation of the radionuclide levels in the surface waters of the drainage basin) are contained in the code for the surface water models discussed in Chapter 10.

Table 11.4

## LARGE (GAME) FISH FLESH LEAD-210 BIOACCUMULATION FACTORS (BF's)

| Location | Species | No. Fish Samples | Fish Flesh Concentration (Bq/kg fresh) | Water Level (Bq/L) | Pb-210 BF (L/kg) | Reference |
|---|---|---|---|---|---|---|
| Okanagan Highlands, BC | Trout | 17 | | | <40 | Mahon 1982 |
| McDonald Lake, Sask. | Northern Pike | 5 | | | 250 | I.E.S. Inc. 1983 |
| " " | Lake Whitefish | 5 | | | 250 | " |
| Delta Lake, Sask. | Northern Pike | 5 | | | 570 | " |
| " " | Lake Whitefish | 5 | | | 570 | " |
| Russell Lake, Sask. | Northern Pike | 5 | | | 490 | " |
| " " | Lake Whitefish | 5 | | | 490 | " |
| Beaverlodge Lake, Sask. | Lake Trout | 5 | | | 18.0 | Swanson 1983 |
| " " | Lake Whitefish | 5 | | | 18.0 | " |
| Dubyna Lake, Sask. | Northern Pike | 5 | | | 58 | Eldorado 1978 |
| " " | Lake Trout | 5 | | | 180 | " |
| Schmoo Lake, Sask. | Lake Trout | 5 | | | 193 | " |
| Donaldson Lake, Sask. | " " | 5 | | | 153 | " |
| Wollaston Lake, Sask | | | | | | |
| - Pow Bay | Lake Trout ('82) | 5 | <0.07 | 0.015 | <4.7 | ELDOR (Gulf Minerals) 1982 |
| " " | Northern Pike('82) | 5 | <0.07 | 0.015 | <4.7 | " |
| " " | Lake Trout ('81) | 5 | <0.22 | <0.002 | <11.0 | " |
| " " | Northern Pike('81) | 5 | <0.22 | <0.002 | <11.0 | " |
| Russell Lake, Sask. | Walleye | 1 | 0.3 | 0.04 | 7.5 | Key Lake 1979 |
| " " | " | 1 | 2.0 | " | 50.0 | " |
| " " | " | 1 | 0.2 | " | 5.0 | " |
| " " | " | 1 | 0.2 | " | 5.0 | " |
| " " | " | 1 | 1.6 | " | 40.0 | " |
| " " | " | 1 | 0.3 | " | 7.5 | " |
| " " | " | 1 | 0.3 | " | 7.5 | " |
| " " | " | 1 | 0.3 | " | 7.5 | " |
| " " | " | 1 | 0.5 | " | 12.5 | " |
| " " | " | 1 | 0.2 | " | 5.0 | " |
| Russell Lake, Sask. | Lake Whitefish | 1 | 0.5 | 0.04 | 12.5 | Key Lake 1979 |
| " " | " | 1 | 0.3 | " | 7.5 | " |
| " " | " | 1 | 0.5 | " | 12.5 | " |
| " " | " | 1 | 0.3 | " | 7.5 | " |
| " " | " | 1 | 0.2 | " | 5.0 | " |
| " " | " | 1 | 0.4 | " | 10.0 | " |
| " " | " | 1 | 0.4 | " | 10.0 | " |

Table 11.4 continued

| Location | Species | No. Fish Samples | Fish Flesh Concentration (Bq/kg fresh) | Water Level (Bq/L) | Pb-210 BF (L/kg) | Reference |
|---|---|---|---|---|---|---|
| Russell Lake, Sask. | Lake Whitefish | 1 | 0.2 | 0.04 | 5.0 | Key Lake 1979 |
| " " | " | 1 | 0.2 | " | 5.0 | " |
| " " | " | 1 | 0.3 | " | 7.5 | " |
| Keevan Lake, Sask. | Walleye | 1 | 0.4 | <0.02 | 20.0 | Canadian Occidental 1981 |
| " " | " | 1 | 0.8 | " | 40.0 | " " |
| " " | " | 1 | 0.4 | " | 20.0 | " " |
| " " | " | 1 | 0.4 | " | 20.0 | " " |
| " " | " | 1 | 0.6 | " | 30.0 | " " |
| Keevan Lake, Sask. | Lake Whitefish | 1 | 0.4 | <0.02 | 20.0 | Canadian Occidental 1981 |
| " " | " | 1 | 0.4 | " | 20.0 | " " |
| " " | " | 1 | 0.6 | " | 30.0 | " " |
| " " | " | 1 | 0.4 | " | 20.0 | " " |
| " " | " | 1 | 0.4 | " | 20.0 | " " |
| McClean Lake, Sask. | Walleye | 1 | 0.5 | <0.02 | 25.0 | Canadian Occidental 1981 |
| " " | " | 1 | 0.8 | " | 40.0 | " " |
| " " | " | 1 | 0.5 | " | 25.0 | " " |
| " " | " | 1 | 2.0 | " | 100.0 | " " |
| " " | " | 1 | 0.3 | " | 15.0 | " " |
| McClean Lake, Sask. | Lake Whitefish | 1 | 0.5 | <0.02 | 25.0 | Canadian Occidental 1981 |
| " " | " | 1 | 0.6 | " | 30.0 | " " |
| " " | " | 1 | 0.5 | " | 25.0 | " " |
| " " | " | 1 | 0.5 | " | 25.0 | " " |
| " " | " | 1 | 0.5 | " | 25.0 | " " |
| Beaverlodge Lake, Sask. | Lake Whitefish | 1 | <0.4 | 0.03 | 13.3 | Swanson 1982 |
| " " | " | 1 | 0.2 | " | 6.7 | " " |
| " " | " | 1 | 0.6 | " | 20.0 | " " |
| " " | " | 1 | <0.2 | " | 6.7 | " " |
| " " | " | 1 | 0.4 | " | 13.3 | " " |
| " " | " | 1 | 0.7 | " | 23.3 | " " |
| " " | " | 1 | 1.8 | " | 60.0 | " " |
| " " | " | 1 | 1.3 | " | 43.3 | " " |
| " " | " | 1 | 0.6 | " | 20.0 | " " |
| " " | " | 1 | 4.0 | " | 133.3 | " " |
| " " | " | 1 | 0.3 | " | 10.0 | " " |
| " " | " | 1 | <0.2 | " | 6.7 | " " |
| " " | " | 1 | 0.3 | " | 10.0 | " " |
| " " | " | 1 | <0.2 | " | 6.7 | " " |
| " " | " | 1 | <0.2 | " | 6.7 | " " |
| " " | " | 1 | 0.3 | " | 10.0 | " " |
| " " | " | 1 | 0.3 | " | 10.0 | " " |
| " " | " | 1 | 7.5 | " | 250.0 | " " |
| " " | " | 1 | 0.4 | " | 13.3 | " " |
| " " | " | 1 | 1.2 | " | 40.0 | " " |
| " " | " | 1 | 0.4 | " | 13.3 | " " |
| " " | " | 1 | 1.3 | " | 43.3 | " " |

Table 11.4 continued

| Location | Species | No. Fish Samples | Fish Flesh Concentration (Bq/kg fresh) | Water Level (Bq/L) | Pb-210 BF (L/kg) | Reference |
|---|---|---|---|---|---|---|
| Milliken Lake, Sask. | Lake Whitefish | 1 | <0.2 | 0.04 | 5.0 | Swanson 1982 |
| " " | " | 1 | <0.2 | " | 5.0 | " " |
| " " | " | 1 | <0.2 | " | 5.0 | " " |
| " " | " | 1 | 0.4 | " | 10.0 | " " |
| " " | " | 1 | 0.3 | " | 7.5 | " " |
| " " | " | 1 | <0.3 | " | 7.5 | " " |
| " " | " | 1 | 1.7 | " | 42.5 | " " |
| " " | " | 1 | 1.2 | " | 30.0 | " " |
| " " | " | 1 | 0.7 | " | 17.5 | " " |
| " " | " | 1 | <0.2 | " | 5.0 | " " |
| " " | " | 1 | 0.1 | " | 2.5 | " " |
| " " | " | 1 | <0.4 | " | 10.0 | " " |
| " " | " | 1 | 0.5 | " | 12.5 | " " |
| " " | " | 1 | 0.6 | " | 15.0 | " " |
| " " | " | 1 | 0.3 | " | 7.5 | " " |
| " " | " | 1 | <0.2 | " | 5.0 | " " |
| " " | " | 1 | <0.2 | " | 5.0 | " " |
| " " | " | 1 | <0.2 | " | 5.0 | " " |
| " " | " | 1 | <0.2 | " | 5.0 | " " |
| " " | " | 1 | <0.2 | " | 5.0 | " " |
| " " | " | 1 | 0.4 | " | 10.0 | " " |
| " " | " | 1 | <0.2 | " | 5.0 | " " |
| Fredette Lake, Sask. | Lake Whitefish | 1 | <0.2 | 0.02 | 10.0 | Swanson 1982 |
| " " | " | 1 | >0.6 | " | 30.0 | " " |
| " " | " | 1 | 0.5 | " | 25.0 | " " |
| " " | " | 1 | 0.2 | " | 10.0 | " " |
| " " | " | 1 | 0.8 | " | 40.0 | " " |
| " " | " | 1 | 0.3 | " | 15.0 | " " |
| " " | " | 1 | 2.9 | " | 145.0 | " " |
| " " | " | 1 | <1.4 | " | 70.0 | " " |
| " " | " | 1 | 0.1 | " | 5.0 | " " |
| " " | " | 1 | <0.2 | " | 10.0 | " " |
| " " | " | 1 | 0.2 | " | 10.0 | " " |
| " " | " | 1 | <0.2 | " | 10.0 | " " |
| " " | " | 1 | 0.4 | " | 20.0 | " " |
| " " | " | 1 | 0.2 | " | 10.0 | " " |
| " " | " | 1 | 0.2 | " | 10.0 | " " |
| " " | " | 1 | <0.2 | " | 10.0 | " " |
| " " | " | 1 | <0.2 | " | 10.0 | " " |
| " " | " | 1 | 0.7 | " | 35.0 | " " |
| " " | " | 1 | <0.2 | " | 10.0 | " " |

| Summary Statistics | |
|---|---|
| Number of Data Points | 120 |
| Geometric Mean | 17.6 |
| Geometric Std. Deviation | 3.25 |
| Range of Values | 2.5 to 570 |

Table 11.5

## AQUATIC MODEL VARIABLES

| Model Symbol | Description | Units | Nominal Value | Probability Distribution* | Computer Origin | Computer Symbol |
|---|---|---|---|---|---|---|
| $B_{f,i}$ | water-to-game fish flesh transfer coefficient: | $Bq.g^{-1}$ (wet wt) $Bq^{-1}.m^3$ | | | | |
| | U-nat | | $1.55x10^{-6}$ | $LN(1.55x10^{-6},6.1, 1.0x10^{-8},5.8x10^{-5})$ | INPUT | BIOACF(1) |
| | Th-tot | | $1.18x10^{-5}$ | $LN(1.18x10^{-5},2.6, 1.1x10^{-6},1.1x10^{-4})$ | INPUT | BIOACF(2) |
| | Ra-226 | | $1.31x10^{-5}$ | $LN(1.31x10^{-5},3.3, 1.2x10^{-6},6.0x10^{-4})$ | INPUT | BIOACF(4) |
| | Pb-210 | | $1.74x10^{-5}$ | $LN(1.74x10^{-5},3.25, 1.7x10^{-6},5.7x10^{-4})$ | INPUT | BIOACF(3) |
| $[F_i]_{n,t}$ | concentration of radionuclide i in fish flesh at node n | $Bq.g^{-1}$ | calculated | calculated | FISH | FISHC(i,n) |
| $[R_i]_{n,t}$ | concentration of radionuclide i in water at node n | $Bq.m^{-3}$ | calculated | calculated | LAKE | WATC(i,n) |
| $B_{q,i}$ | water-to-aquatic vegetation transfer coefficient: | $Bq.g^{-1}$ (wet wt) $Bq^{-1}.m^3$ | | | | |
| | U-nat | | $1.5x10^{-5}$ | $LN(1.5x10^{-5},5.5, 1.0x10^{-6},7.0x10^{-4})$ | INPUT | WATVTC(1) |
| | Th-tot | | $1.1x10^{-5}$ | $LN(1.1x10^{-5},6.8 1x10^{-6},1.6x10^{-4})$ | INPUT | WATVTC(2) |
| | Ra-226 | | $4.5x10^{-5}$ | $LN(4.5x10^{-5},2.9, 1x10^{-5}, 3.3x10^{-4})$ | INPUT | WATVTC(4) |
| | Pb-210 | | $1.3x10^{-4}$ | $LN(1.3x10^{-4},2.0, 4.0x10^{-5},4.3x10^{-4})$ | INPUT | WATVTC(3) |
| $[C_{q,i}]_t$ | concentration of radionuclide i in aquatic vegetation | $Bq.g^{-1}$ | calculated | calculated | WATVEG | AQVEGC(i) |
| $[R_i]_t$ | average concentration of radionuclide i in water over the watershed | $Bq.m^{-3}$ | calculated | calculated | LAKE, RIVER | WATAVG(i) |
| $L_n$ | surface area of the lake designated node n | $m^2$ | site specific: see Table 10.1 | | INPUT | LAREA(n) |
| $S_n$ | length of river segment n | m | site specific: see Table 10.1 | | INPUT | LAREA(n) |

**Note**

* Distributions are as described in Table 2.2.

Table 11.6

## AQUATIC BIOTA MODEL CODE LISTING

```
      SUBROUTINE WATVEG
C
C     SUBROUTINE CALCULATES AVERAGE RADIONUCLIDE CONCENTRATION
C     FOR AQUATIC VEGETATION IN WATERSHED.  AVERAGE BASED ON
C     AVERAGE WATER CONCENTRATION; NAMELY, AVERAGE OVER LENGTH
C     OF RIVERS AND CIRCUMFERENCE OF LENGTHS.
C
      INCLUDE 'VAR.INC'
      INCLUDE 'MODEL.INC'
      IF (CODWVG.GE.1) WRITE (*,*) ' SUBROUTINE WATVEG'
      DO 10 ISUB=1,4
         AQVEGC(ISUB)=WATVTC(ISUB)*WATAVG(ISUB)
         IF (CODWVG.EQ.2) WRITE (*,100) ISUB,AQVEGC(ISUB)
10    CONTINUE
      RETURN
100   FORMAT (' AQVEGC(',I1,') ',E10.3)
      END

      SUBROUTINE FISH
C
C     SUBROUTINE CALCULATES CONCENTRATIONS OF RADIONUCLIDES IN FISH
C
      INCLUDE 'VAR.INC'
      INCLUDE 'MODEL.INC'
      IF (CODFIS.GE.1) WRITE (*,*) ' SUBROUTINE FISH'
C
C     CALCULATE MASS OF RADIONUCLIDES IN FISH
C
      DO 10 ISUB=1,4
         FISHC(ISUB,WTSEG)=BIOACF(ISUB)*WATC(ISUB,WTSEG)
         IF (CODFIS.EQ.2) WRITE (*,100) ISUB,WTSEG,FISHC(ISUB,WTSEG),
     &      BIOACF(ISUB),WATC(ISUB,WTSEG)
10    CONTINUE
C
C     CALCULATE FISH AVAILABILITY
C
      IF(WATPH(WTSEG).GT.6.)THEN
         FISHA(WTSEG)=1.0
      ELSEIF(WATPH(WTSEG).GT.5.)THEN
         FISHA(WTSEG)=0.75+0.25*(WATPH(WTSEG)-5.)
      ELSEIF(WATPH(WTSEG).GT.4.5)THEN
         FISHA(WTSEG)=0.25+WATPH(WTSEG)-4.5
      ELSEIF(WATPH(WTSEG).GT.3.5)THEN
         FISHA(WTSEG)=0.25*(WATPH(WTSEG)-3.5)
      ELSE
         FISHA(WTSEG)=0.0
      ENDIF
      IF(CODFIS.EQ.2.)WRITE(*,200)WATPH(WTSEG),FISHA(WTSEG)
      RETURN
100   FORMAT (' FISHC(',I1,',',I2,') ',E10.3,'  BIOACF',E10.3,'  WATC',
```

Table 11.6 (continued)

```
     &   E10.3)
200   FORMAT (' WATPH = ',E10.3,'   FISHA = ',E10.3)
      END
```

## 11.5 References

Beamish, R.J., and Harvey, H.H., 1972. "Acidification of the La Cloche Mountain Lakes, Ontario, and Resulting Fish Mortalities." J. Fish. Res. Bd. Canada, Vol. 29, pp. 1131-1143.

Beamish, R.J., Lockhart, W., Van Loon, J., and Harvey, H.H., 1975. "Long-Term Acidification of a Lake and Resulting Effects on Fishes." Ambio, Vol. 4, pp. 98-102.

Blaylock, B.G., Gardner, R.H., and Hoffman, F.O., 1986. "A Dynamic Model of Uranium Behaviour in an Oligotrophic Lake." Appendix B of this Report.

Canadian Occidental Inc., 1981. "Environmental Baseline Studies for Project Wolly, McClean Lake Area." Interim Report No. 3.

Eldor/Gulf Minerals Canada Limited, 1982. "Rabbit Lake Environmental Monitoring Report."

Eldorado Nuclear Limited, 1978. "Dubyna Lake Environmental Assessment." Prepared by Saskatchewan Research Council, Saskatoon.

Gardner, R.H., Hoffman, F.O. and Blaylock, B.G., 1985. "A Dynamic Model of Radium-226 Behaviour in an Oligotrophic Lake." Presented in a Research Report Entitled - Probabilistic Model Development for the Assessment of the Long-term Effects of Uranium Mill Tailings. Prepared by SENES Consultants Limited for the National Uranium Tailings Program, CANMET, Energy, Mines and Resources Canada, Ottawa.

Integrated Environmental Sciences Inc., 1983. "Baseline Studies of Aquatic Sediments and Macrophytes, Fish, Soil and Terrestrial Vegetation at Key Lake, Saskatchewan." Prepared for Key Lake Mining Corporation, Saskatoon.

Jensen, K.W., and Snekvik, E., 1972. "Low pH Levels Wipe out Salmon and Trout Populations in Southernmost Norway." Ambio, Vol. 1(6), pp. 223-225.

John, R.D., 1985. "Fish Study for the National Uranium Tailings Program (NUTP)." A Research Report Prepared for the NUTP, CANMET, Energy, Mines and Resources Canada, Ottawa.

Key Lake Mining Corporation, 1979. "Key Lake Project Environmental Impact Assessment." Volume II.

Mahon, D.C., 1982. "Uptake and Translocation of Naturally-Occurring Radionuclides of the Uranium Series." Bull.Environment.Contam. Toxicol., Vol. 29, pp. 697-703.

Menendez, R., 1976. "Chronic Effects of Reduced pH on Brook Trout (Salvelinus fontinalis)." J. Fish. Res. Bd. Canada, Vol. 33, pp. 118-123.

National Research Council of Canada (NRCC), 1981. "Acidification in the Canadian Aquatic Environment: Scientific Criteria for Assessing the Effects of Acidic Deposition on Aquatic Ecosystems." Publication No. NRCC 18475.

National Research Council of Canada (NRCC), 1983. "Radioactivity in the Canadian Aquatic Environment." Pub. No. NRCC 19250.

Neville, C.M., 1985. "Physiological Response of Juvenile Rainbow Trout, Salmo gairdneri, to Acid and Aluminum - Prediction of Field Responses from Laboratory Data." Can. J. Fish. Aquat. Sci., Vol. 42, pp. 2004-2019.

Norcen Energy Resources Limited, 1980. "Blizzard Uranium Project Phase 6 Report - Environment."

Rahel, F.J., and Magnuson, J.J., 1983. "Low pH and the Absence of Fish Species in Naturally Acidic Wisconsin Lakes: Inferences for Cultural Acidification." Can. J. Fish. Aquat. Sci., Vol. 40, pp. 3-9.

Schindler, D.W., Mills, K.H., Malley, D.F., Findlay, D.L., Shearer, J.A., Davies, I.J., Turner, M.A., Linsey, G.A., and Cruikshank, D.R., 1985. "Long-Term Ecosystem Stress: The Effects of Years of Experimental Acidification on a Small Lake." Science, Vol. 228, pp. 1395-1401.

Schofield, C.L., 1976. "Acid Precipitation: Effects on Fish." Ambio, Vol. 5 (5-6), pp. 228-230.

Swanson, S.M., 1982. "Levels and Effects of Radionuclides in Aquatic Fauna of the Beaverlodge Area (Saskatchewan)." Saskatchewan Research Council Publication No. C-806-5-E-82.

Swanson, S.M., 1983. "Levels of Ra-226, Pb-210 and U-total in Fish Near a Saskatchewan Uranium Mine and Mill." Health Physics, Vol. 45, pp. 67-80.

# 12.0 ANIMAL PRODUCE MODELS

## 12.1 Introduction

Chapter 10 described how the concentration of a radionuclide in surface water is calculated and Chapter 11 detailed how this concentration is used to model aquatic vegetation. Chapter 5 presents how air concentrations are calculated and Chapter 8 documents the model used to calculate the concentration in summer forage, lichens and browse, due to air-related pathways. This chapter documents how these various environmental concentrations are used to calculate the concentration of radionuclide i in the flesh of caribou and moose.

Several changes have been made to the model since Phase II. The water-caribou flesh pathway has been added to the caribou model which already included the lichen/summer forage-to-caribou flesh pathways. The calculation of the concentration of radionuclide i in moose flesh is a new addition, and includes the browse/water/aquatic vegetation-to-moose flesh pathways. Four radionuclides are now calculated (U-nat, Th-tot, Ra-226 and Pb-210) for each time step. Only one value, representing an average annual concentration of radionuclide i for the entire area modelled, is calculated for each of moose and caribou flesh for each time step. Thus the concentration of radionuclide i in caribou or moose flesh used in subsequent dose calculations (see Chapter 13) does not vary with the location or type of receptor, but varies with time.

In this chapter, the following subscripts are used to simplify parameter symbols: i is used to identify those parameters that vary with the radionuclide being modelled; and t indicates that a parameter may vary with time. (In the present analysis we have assumed that the parameters do not vary with time. The notation used later in this section merely indicates the possibility.) Various environmental media are abbreviated as follows:

v = vegetation
c = caribou
w = average water over all nodes
m = moose

q = aquatic vegetation
a = air pathway

Each animal produce model has been divided into two components: air-pathway-related intakes and water-pathway-related intakes. This is because the relative ratios of Th-232: Th-230 are different for these two pathways. Thus the pathway-related intakes must be kept separate so that appropriate dose conversion factors may be used in the calculation of dose due to the ingestion of animal produce in Chapter 13.

Details on the caribou-and moose-flesh models and parameter selection are provided below. Where considered appropriate, parameters were assigned distributions. The extent of this variation was based on the collective opinion of the study group as to how certain they were about the nominal value of particular parameters. Such parameters were typically allowed to vary 10 to 50% about the nominal values and were given a triangular or uniform distribution.

The component model aspects of the Phase III studies have largely focussed on the implementation of environmental and dose models. Comparatively little effort has been expended on issues of fundamental environmental science or on the development of parameter distributions. Both aspects would need to be reviewed on a case-by-case basis with models being modified or upgraded if required and site/species-specific parameters being input to the models insofar as practicable. The computer code for the animal produce models is presented in Table 12.3.

## 12.2 Radionuclides in Caribou Flesh

A number of factors were considered in designing the caribou flesh models: migration; grazing habits; and the time of year the animal is harvested by the receptor in question.

Caribou are migratory animals, and as such range over very wide areas. It is therefore very unlikely that any one caribou would spend the entire year in the study area or that it would stay in one small portion of the study area. Instead, it is much more likely to pass through the area in a more or less random fashion at one or more times during the year. Thus, for the time spent in the area, caribou were assumed to roam freely and equally over the entire model area.

The grazing habits of the caribou are also very important determinants in the concentration of radionuclides in their flesh. During the summer months, caribou eat mainly fresh green vegetation. During the winter months, they eat mainly lichens. Lichens tend to have much higher concentrations of radionuclides than annual plants. It has been estimated that the daily intake of a radionuclide from lichen would be 5-10 times greater than that from plants whose edible foliage is replaced annually (Garner, 1972). It is for this reason that the levels of radionuclides in caribou flesh show very considerable seasonal changes (Garner, 1972).

Thus the time of year that the animal is likely to be slaughtered and consumed must also be taken into consideration in any one application of this model.

The models presented below were designed to offer maximum flexibility to the user, based on the above considerations.

### 12.2.1 Air Pathways-to-Caribou Flesh (ACARC)

Radionuclides in winter (lichen) and summer (grass) forage may be eaten by caribou which in turn may be eaten by man. The transfer of radionuclide i from vegetation to meat was modelled as follows (U.S. NRC, 1982):

$$C_{ci}(air) = Q_c\, F_{ci} \sum_{v} F_{cv}\, C_{vi} \qquad (12.1)$$

where

$C_{ci}(air)$ = $C_{ci}(air)(t)$ is the annual average concentration of radionuclide i in caribou flesh at time t (Bq.g$^{-1}$ (wet weight)) due to the air pathway

$Q_c$ = the average daily feed intake rate of the caribou (g (wet weight).d$^{-1}$)

$F_{ci}$ = the feed-to-meat transfer coefficient for caribou (Bq.g$^{-1}$ (wet weight).Bq$^{-1}$.d)

$F_{cv}$ = the fraction of the caribou's annual feed intake that is local vegetation type v (lichens and summer forage in this case)

$C_{vi}$ = $C_{vi}(t)$ is the average concentration of radionuclide i in vegetation type v (lichen and summer forage in this case) at time t, where the average is taken over the entire area being modelled (see Section 8.6 and 8.4) (Bq.g$^{-1}$ (wet weight)).

The time dependence in this case is only due to the time dependence in the vegetation concentrations.

Table 12.1 summarizes these variables and their distributions. Very little information is available in the literature on which to base these distributions. The information and assumptions used are summarized below.

The average daily feed intake of the caribou is based on McDowell-Boyer _et al_., (1979). The values for $F_{ci}$ are based on SENES (1983) as follows:

### Uranium, Thorium

Values used were for cattle in the absence of available information on caribou (U.S. NRC, 1982).

### Radium

Although some information was available on background radium levels in caribou and lichens, it was considered too limited to derive a $F_{cRa}$.

Table 12.1

## CARIBOU FLESH MODEL VARIABLES

| Model Symbol | Description | Units | Nominal Value | Probability Distribution* | Computer Origin | Computer Symbol |
|---|---|---|---|---|---|---|
| $C_{ci}(air)(t)$ | concentration of radionuclide i in caribou flesh due to the air pathway | $Bq.g^{-1}$ (wet wt) | calculated | calculated | ANIMAL | ACARC (i) i=1,4 |
| $C_{vi}(t)$ | concentration of radionuclide i in vegetation type v | $Bq.g^{-1}$ (wet wt) | | | | |
| | lichen | | calculated | calculated | VEGCON | LICHC(i) i=1,4 |
| | summer forage | | calculated | calculated | VEGCON | SOFOC(i) i=1,4 |
| $F_{ci}$ | feed-to-caribou meat transfer coefficient for radionuclide i: | $Bq.g^{-1}$ (wet wt). $Bq.^{-1}d$ | | | INPUT | FMTCC(i) i=1,4 |
| | U-nat | | $3.4 \times 10^{-7}$ | $T(1.1 \times 10^{-7}, 3.4 \times 10^{-7}, 1.0 \times 10^{-6})$ | | |
| | Th-tot | | $2.0 \times 10^{-7}$ | $T(0.7 \times 10^{-7}, 2.0 \times 10^{-7}, 6.0 \times 10^{-7})$ | | |
| | Pb-210 | | $4.0 \times 10^{-7}$ | $T(1.3 \times 10^{-7}, 4.0 \times 10^{-7}, 1.2 \times 10^{-6})$ | | |
| | Ra-226 | | $5.1 \times 10^{-7}$ | $T(1.7 \times 10^{-7}, 5.1 \times 10^{-7}, 1.5 \times 10^{-6})$ | | |
| $F_{cv}$ | fraction of annual intake that is local vegetation type v: | --- | | | | |
| | lichen | | 0.4 | T(0.05,0.2,0.5) | INPUT | FAILC |
| | summer forage | | 0.4 | T(0.05,0.2,0.5) | INPUT | FAISFC |
| $Q_c$ | feed ingestion rate for caribou | $g(wet\ wt).d^{-1})$ | $7.0 \times 10^{3}$ | $T(5.0 \times 10^{3}, 7.0 \times 10^{3}, 9.0 \times 10^{3})$ | INPUT | FIRC |
| $C_{ci}(water)(t)$ | concentration of radionuclide i in caribou flesh due to the water pathway | $Bq.g^{-1}$ (wet wt) | calculated | calculated | ANIMAL | WCARC(i) i=1,4 |
| $W_c$ | water ingestion rate for caribou | $m^3.d^{-1}$ | $11.5 \times 10^{-3}$ | $T(7.7 \times 10^{-3}, 11.5 \times 10^{-3}, 15.3 \times 10^{-3})$ | INPUT | WIRC |
| $C_{wi}(t)$ | concentration of radionuclide i in water | $Bq.m^{-3}$ | calculated | calculated | WATEX | WATAVG(i) i=1,4 |
| f | adjustment factor for fraction of time spent in watershed | --- | calculated | calculated | ANIMAL | FT |

Note

* Distributions are as described on Table 2.2

Thus the number used is for cattle (U.S. NRC, 1982).

Lead

A value for $F_{cPb}$ was derived from a review of available data on the concentrations in lichens and caribou. (McDowell-Boyer et al., 1979; Holtzman, 1966a and 1966b; Kauranen and Miettinen, 1969; UNSCEAR, 1977; Blanchard, 1966; Blanchard and Moore, 1970).

The fractions of the annual intake of the caribou that were local (ie. in the model area) lichen and grass ($F_{cv}$) were allowed to vary independently between 0.05 and 0.5. Thus the total local annual feed intake will seldom add up to 100 per cent. This was included to try to reflect the migratory nature of caribou, as it was considered too conservative to assume 100 per cent consumption of local feed. Note that the user may adjust this model to account for any other caribou grazing and/or migratory pattern or human consumption pattern by careful adjustment of this factor.

### 12.2.2 Water Pathways-to-Caribou Flesh (WCARC)

Surface water containing radionuclides may be drunk by caribou which in turn may be eaten by man. The transfer of radionuclide i from water to meat was modelled as follows:

$$C_{ci}(\text{water}) = W_c \, F_{ci} \, C_{wi} \, f(\sum_{v} F_{cv}) \qquad (12.2)$$

where

$C_{ci}$(water) = $C_{ci}$(water)(t) is the annual average concentration of radionuclide i in caribou flesh at time t due to the water pathway (Bq.$g^{-1}$ (wet weight))

$W_c$ = the average daily water intake of the caribou ($m^3.d^{-1}$)

$F_{ci}$ = the feed-to-meat transfer coefficient for caribou (Bq.$g^{-1}$ (wet weight).$Bq^{-1}$.d) (same as feed-to-meat transfer coefficient in section 12.2.1)

$C_{wi}$ = $C_{wi}(t)$ is the average annual concentration of radionuclide i in the surface waters of the watershed at time t ($Bq.m^{-3}$)(see Section 11.4)

f = an adjustment factor to reflect that the watershed is a fraction of the total area being modelled

$F_{cv}$ = the fraction of the annual intake that is local vegetation (lichen and summer forage)

Table 12.1 summarizes these variables and their distributions.

No estimate of the daily water intake of caribou was found in the literature. Therefore, an estimate for $W_c$ was derived by scaling the daily water intake of a 450 kg beef cow (30 to 60 L, midpoint 45 L) (Comar, 1966) by a typical caribou body weight of 115 kg (Palmer, 1934, as cited by Miller, not dated).

No literature was found to indicate that $F_{ci}$ would change for the ingestion of water versus vegetation.

The two factors, f and $F_{cv}$ are included to account for the migratory and grazing habits of caribou referred to earlier. The factor $F_{cv}$ for summer forage is used as a surrogate for the amount of time the caribou spends in the modelled area during summer; while $F_{cv}$ for lichen is a surrogate for the amount of time spent in the area during the winter. Thus, $\sum_v F_{cv}$ represents the fraction of the entire year a caribour would spend in the area modelled in this study. While the caribou is present in the study area, it is assumed to roam equally over the entire area. Since the watershed affected by the tailings is only a small fraction of the total study area, the caribou is assumed to be present, and drink water there, for only a small fraction of the time. The factor f is used to account for the difference between the entire study area and the watershed area, or equivalently the difference between the caribou's total water intake and its contaminated water intake. The factor f is calculated as the ratio of area of the watershed divided by the total study area.

## 12.3 Radionuclides in Moose Flesh

Two main factors were considered in designing the moose flesh model: ranging and grazing habits.

Although the individual animals may roam over very large areas, in general moose are not migratory and tend to have much smaller home ranges than caribou (Lynch, 1976; Taylor and Ballard, 1979; Saunders and Williamson, 1972). For this reason, the moose modelled in Phase III was assumed to range over the watershed. Any moose not harvested in the watershed were assumed to have no radionuclide content due to the tailings area. This is not strictly correct, as there may still be some elevated concentrations in other moose in the model area due to the air pathway. However moose flesh was not considered to play a major role in population dose estimates, and it was felt that the added complexity of calculating browse and then moose flesh concentrations for each receptor location was not warranted at this time. Therefore only the "critical" moose as described above was considered.

In contrast to the caribou, there is no literature to indicate that the radionuclide content of moose flesh may vary widely over the course of the year (indeed very little information of any sort on the concentration of U, Th, Ra and Pb in moose flesh was identified during the project). However, the moose does have a different diet in the winter versus summer months.

As noted by Krefting (1974), ....."The moose is a browsing species, especially during the winter months. Its food habits are quite different in eastern and western North America where significant differences exist in the availability of browse species. Most investigators agree that willows are the main source of winter browse in the west (Murce, 1944). And in the east, balsam fir, aspen, and paper birch are the major species (Pimlott, 1961)." ..... In the warm months, many moose supplement their woody diet (twigs and leaves) with aquatic vegetation, tending to prefer smaller submerged species of aquatic plants, usually in shallow waters (Fraser et al., 1984).

Thus, a moose consuming strictly browse in the winter, and a mixture of browse and aquatic vegetation in the summer was modelled. These intakes were averaged over the year to derive average daily intakes of aquatic vegetation and browse for use in the models described below. This results in the calculation of an average annual concentration of radionuclide i in moose flesh. The user may calculate the concentration in the moose flesh on a seasonal basis (if the animal is only slaughtered in one season) by adjusting these intakes accordingly.

### 12.3.1 Air Pathways-to-Moose Flesh (AMOC)

Radionuclides in browse may be eaten by moose which may in turn be eaten by man. This transfer was modelled as follows:

$$C_{mi}(air) = F_{mi}\ Q_m\ F_{mb}\ C_{bi} \qquad (12.3)$$

where

$C_{mi}(air)$ = $C_{mi}(air)(t)$ is the annual average concentration of radionuclide i in moose flesh at time t ($Bq.g^{-1}$ (wet weight))

$Q_m$ = the average daily feed intake of the moose (g (wet weight)$.d^{-1}$)

$F_{mi}$ = the feed-to-moose meat transfer coefficient for radionuclide i ($Bq.g^{-1}$(wet weight)$.Bq^{-1}.d$)

$F_{mb}$ = the fraction of the moose annual feed intake that is browse

$C_{bi}$ = $C_{bi}(t)$ is the average concentration of radionuclide i in browse at time t, where the average is taken over the watershed ($Bq.g^{-1}$(wet weight)) (see Section 8.5)

The time dependence in this case is only due to the time dependence in the browse concentration.

The values selected for the variables in the moose flesh model outlined above are presented in Table 12.2. The values of $Q_m$ and $F_{mb}$ are based on a study by Belovsky et al. (1973). Moose were found to have an average feed intake of 27 kg (wet weight) per day. In the summer months (assumed to be May to September inclusive), moose consumed an average of 21 kg of browse, the remaining 6 kg being aquatic macrophytes (see Section 12.3.2). During the winter months (the

Table 12.2

MOOSE FLESH MODEL VARIABLES

| Model Symbol | Description | Units | Nominal Value | Probability Distribution* | Computer Origin | Computer Symbol |
|---|---|---|---|---|---|---|
| $C_{mi}(air)(t)$ | concentration of radionuclide i in moose flesh due to the air pathway | $Bq.g^{-1}$ (wet wt) | calculated | calculated | ANIMAL | AMOC(i) i=1,4 |
| $C_{bi}(t)$ | concentration of radionuclide i in browse | $Bq.g^{-1}$ (wet wt) | calculated | calculated | VEGCON | BRWSC(i) i=1,4 |
| $F_{mi}$ | feed-to-moose meat transfer coefficient for radionuclide i: | $Bq.g^{-1}$ (wet wt) $Bq^{-1}.d$ | | | INPUT | FMTCM(i) i=1,4 |
| | U-nat | | $3.4x10^{-7}$ | $T(1.1x10^{-7},3.4x10^{-7},1.0x10^{-6})$ | | |
| | Th-tot | | $2.0x10^{-7}$ | $T(0.7x10^{-7},2.0x10^{-7},6.0x10^{-7})$ | | |
| | Pb-210 | | $4.0x10^{-7}$ | $T(1.3x10^{-7},4.0x10^{-7},1.2x10^{-6})$ | | |
| | Ra-226 | | $5.1x10^{-7}$ | $T(1.7x10^{-7},5.1x10^{-7},1.5x10^{-6})$ | | |
| $Q_m$ | feed ingestion rate for for moose | g(wet wt)$.d^{-1}$ | $27.0x10^3$ | $C(27.0x10^3)$ | INPUT | FIRM |
| $F_{mb}$ | fraction of moose intake that is browse | --- | 0.9 | T(0.8,0.9,0.95) | INPUT | FAIBM |
| $F_{mq}$ | fraction of moose intake that is aquatic macrophyte | --- | calculated | calculated | ANIMAL | FAIAM |
| $C_{qi}$ | concentration of radionuclide i in aquatic macrophytes | $Bq.g^{-1}$ (wet wt) | calculated | calculated | WATVEG | AQVEGC(i) i=1,4 |
| $W_m$ | water ingestion rate for moose | $m^3.d^{-1}$ | .036 | T(.024,0.036,0.048) | INPUT | WIRM |
| $C_{wi}(t)$ | concentration of radionuclide i in water | $Bq.m^{-3}$ | calculated | calculated | WATEX | WATAVG(i) i=1,4 |
| $C_{mi}(water)(t)$ | concentration of radionuclide i in moose flesh due to the water pathway | $Bq.g^{-1}$ (wet wt) | calculated | calculated | ANIMAL | WMOC(i) i=1,4 |

Note

* Distributions are as described on Table 2.2.

Table 12.3

## ANIMAL PRODUCE MODEL CODE LISTING

```
      SUBROUTINE ANIMAL
      INCLUDE 'MODEL.INC'
      INCLUDE 'VAR.INC'
      FT=PSAREA/TAREA
      FAIAM=1.0-FAIBM
      DO 10 I=1,4
         ACARC(I)=FMTCC(I)*FIRC*(FAISFC*SUFOC(I)+FAILC*LICHC(I))
         WCARC(I)=FMTCC(I)*WIRC*FT*(FAISFC+FAILC)*WATAVG(I)
         AMOC(I)=FMTCM(I)*FIRM*FAIBM*BRWSC(I)
         WMOC(I)=FMTCM(I)*(FIRM*FAIAM*AQVEGC(I)+WIRM*WATAVG(I))
10    CONTINUE
C
      IF(CODANI.EQ.1.0.OR.CODANI.EQ.2.0.OR.CODANI.EQ.3.0)THEN
         WRITE(*,100)
      ENDIF
      IF(CODANI.EQ.3.0)THEN
         WRITE(*,101)FT,FIRC,WIRC,FAISFC,FAILC
         WRITE(*,102)(FMTCC(I),I=1,4)
         WRITE(*,103)FIRM,WIRM,FAIBM,FAIAM
         WRITE(*,104)(FMTCM(I),I=1,4)
         WRITE(*,105)(SUFOC(I),I=1,4)
         WRITE(*,106)(LICHC(I),I=1,4)
         WRITE(*,107)(WATAVG(I),I=1,4)
         WRITE(*,108)(BRWSC(I),I=1,4)
         WRITE(*,109)(AQVEGC(I),I=1,4)
      ENDIF
      IF(CODANI.EQ.2.0.OR.CODANI.EQ.3.0)THEN
         WRITE(*,110)(ACARC(I),I=1,4)
         WRITE(*,111)(WCARC(I),I=1,4)
         WRITE(*,112)(AMOC(I),I=1,4)
         WRITE(*,113)(WMOC(I),I=1,4)
      ENDIF
C
100   FORMAT(///1X,'ANIMAL MODEL')
101   FORMAT(/1X,'FRACTION OF TIME CARIBOU SPEND IN WATERSHED',E12.4/1X,
     +       'AVERAGE DAILY FEED INTAKE FOR CARIBOU',E12.4/1X,'AVERAGE',
     +       ' DAILY WATER INTAKE FOR CARIBOU',E12.4/1X,'FRACTION OF C',
     +       'ARIBOU INTAKE THAT IS LOCAL SUMMER FORAGE'E12.4/1X,'FRAC',
     +       'TION OF CARIBOU INTAKE THAT IS LOCAL LICHEN'E12.4)
102   FORMAT(1X,'FEED-TO-MEAT TRANSFER COEFFICIENT FOR CARIBOU'/1X,
     +       4(E12.4))
103   FORMAT(1X,'AVERAGE DAILY FEED INTAKE FOR MOOSE',E12.4/1X,'AVERAG',
     +       'E DAILY WATER INTAKE FOR MOOSE',E12.4/1X,'FRACTION OF MO',
     +       'OSE INTAKE THAT IS BROWSE'E12.4/1X,'FRACTION OF MOOSE IN',
     +       'TAKE THAT IS AQUATIC MACROPHYTES'E12.4)
104   FORMAT(1X,'FEED-TO-MEAT TRANSFER COEFFICIENT FOR MOOSE'/1X,
     +       4(E12.4))
105   FORMAT(1X,'AVERAGE RADIONUCLIDE CONCENTRATION IN SUMMER FORAGE'/
     +       1X,4(E12.4))
106   FORMAT(1X,'AVERAGE RADIONUCLIDE CONCENTRATION IN LICHEN'/1X,
```

Table 12.3 (continued)

```
     +       4(E12.4))
107   FORMAT(1X,'AVERAGE RADIONUCLIDE CONCENTRATION IN THE WATER'/1X,
     +       4(E12.4))
108   FORMAT(1X,'AVERAGE RADIONUCLIDE CONCENTRATION IN BROWSE',/1X,
     +       4(E12.4))
109   FORMAT(1X,'AVERAGE RADIONUCLIDE CONCENTRATION IN AQUATIC MACROPH',
     +       'YTES'/1X,4(E12.4))
110   FORMAT(/1X,'AVERAGE RADIONUCLIDE CONCENTRATION IN CARIBOU FLESH ',
     +       '(AIR PATHWAY)'/1X,4(E12.4))
111   FORMAT(1X,'AVERAGE RADIONUCLIDE CONCENTRATION IN CARIBOU FLESH ',
     +       '(WATER PATHWAY)'/1X,4(E12.4))
112   FORMAT(1X,'AVERAGE RADIONUCLIDE CONCENTRATION IN MOOSE FLESH ',
     +       '(AIR PATHWAY)'/1X,4(E12.4))
113   FORMAT(1X,'AVERAGE RADIONUCLIDE CONCENTRATION IN MOOSE FLESH ',
     +       '(WATER PATHWAY)'/1X,4(E12.4))
C
      RETURN
      END
```

remaining 7 months of the year), moose were assumed to consume 27 kg per day of browse. Hence, the nominal value of $F_{mb}$ can be determined as:

$$(21/27)\ (5/12) + (27/27)\ (7/12) = 0.90$$

A triangular distribution about this nominal value was assigned to $F_{mb}$.

Values for $F_{mi}$ are the same as those used for caribou (see Section 2.2) in the absence of sufficient moose-specific data to derive more suitable transfer coefficients.

### 12.3.2 Water Pathway-to-Moose Flesh (WMOC)

Surface water and aquatic macrophytes containing radionuclides may be ingested by moose which in turn may be eaten by man. This transfer was modelled as follows:

$$C_{mi}(\text{water}) = F_{mi}\ (Q_m\ F_{mq}\ C_{qi} + W_m\ C_{wi}) \qquad (12.4)$$

where

$C_{mi}$(water) = $C_{mi}$(water)(t) is the annual average concentration of radionuclide i in moose flesh at time t (Bq.$g^{-1}$(wet weight))

$F_{mi}$ = the feed-to-moose meat transfer coefficent for radionuclide i (Bq.$g^{-1}$(wet weight). Bq$^{-1}$.d) (see Section 12.3.1)

$Q_m$ = the average daily feed intake of the moose (g(wet weight).$d^{-1}$)

$F_{mq}$ = the fraction of the moose annual feed intake that is aquatic macrophytes (= 1 - $F_{mb}$)

$C_{qi}$ = $C_{qi}$(t) is the average concentration of radionuclide i in aquatic macrophytes (Bq.$g^{-1}$(wet weight)) at time t, where the average is taken over the watershed (see Section 11.4)

$W_m$ = the average daily water intake of the moose ($m^3.d^{-1}$)

$C_{wi}$ = $C_{wi}$(t) is the average concentration of radionuclide i in the water at time t, where the average is taken over the watershed (Bq.$m^{-3}$ (see Section 11.4).

Table 12.2 summarizes the parameter values used in the moose flesh model. $W_m$

was derived by scaling the daily water intake of a 450 kg beef cow (30 to 60 L) (Comar, 1966) by a typical moose body weight of 360 kg (Belovsky et al., 1973).

## 12.4 References

Belovsky, G.E., Jordan, P.A., and Botkin, D.B., 1973. "Summer Browsing by Moose in Relation to Preference, and Animal Density: A New Quantitative Approach." Proceedings of the 9th North American Moose Conference and Workshop, Quebec City, March. pp. 101-122.

Blanchard, R.L., 1966. "Relationship Between Po-210 and Pb-210 in Man and His Environment." Article in Radioecological Concentration Processes: Proceedings of an International Symposium held in Stockholm, 1966.

Blanchard, R.L., and Moore, J.B., 1970. "Pb-210 and Po-210 in Tissues of Some Alaskan Residents as Related to Consumption of Caribou or Reindeer Meat." Health Physics, Vol. 18, pp. 127-134.

Comar, C.L., 1966. "Radioactive Materials in Animals - Entry and Metabolism." Chapter 7 in "Radioactivity and Human Diet." Edited by R. Scott Russell. Pergamon Press, Oxford.

Fraser, D., Chavez, E.R., and Paloheimo, J.E., 1984. "Aquatic Feeding by Moose: Selection of Plant Species and Feeding Areas in Relation to Plant Chemical Composition and Characteristics of Lakes." Can. J. Zool., Vol. 62, pp. 80-87.

Garner, R.J., 1972. "Transfer of Radioactive Materials from the Terrestrial Environment to Animals and Man." CRC Press, Cleveland.

Holtzman, R.B., 1966a. "Natural Levels of Lead-210, Polonium-210 and Radium-226 in Humans and Biota of the Arctic." Nature, Vol. 210, pp. 1094-1097.

Holtzman, R.B., 1966b. "Ra-226 and the Natural Airborne Nuclides Pb-210 and Po-210 in Arctic Biota." Proceedings of the First International Congress of Radiation Protection, Stockholm.

Kauranen, P., and Miettinen, J.K., 1969. "Po-210 and Pb-210 in the Arctic Food Chain and the Natural Radiation Exposure to Lapps." Health Physics, Vol. 16, pp. 287-295.

Krefting, L.W., 1974. "The Ecology of the Isle Royale Moose with Special Reference to the Habitat." Technical Bulletin 297, Forestry Series 15, Agricultural Experiment Station, University of Minnesota.

Lynch, G.M., 1976. "Some Long Range Movements of Radio-Tagged Moose in Alberta." Proceedings of the 12th North American Moose Conference and Workshop, St. John's Nfld., March 1976. pp.220-235.

McDowell-Boyer, L.M., Watson, A.P., and Travis, C.C., 1979. "Review and Recommendations of Dose Conversion Factors and Environmental Transport Parameters for Pb-210 and Ra-226." Report PB 294-242. Oak Ridge National Laboratories, March 1979.

Miller, O.R., no date. "Biology of the Kaminuriak Population of Barren-Ground Caribou. Part 3." Canadian Wildlife Service. Report Services Number 36.

Saunders, B.P., and Williamson, J.C., 1972. "Moose Movements from Ear-Tag Returns." Proceedings of the 8th North American Moose Conference and Workshop, Thunder Bay, Ontario, Feb. 1972. pp. 177-184.

SENES Consultants Limited, 1983. "Decommissioning of the Beaverlodge Mine/Mill Operations and the Reclamation of the Site. Radiological and Environmental Assessment of Close-Out Options." Prepared for Eldorado Resources Limited.

Taylor, K.P., and Ballard, W.B., 1979. "Moose Movements and Habitat Use Along the Susitna River near Devil's Canyon." Proceedings of the 15th North American Moose Conference and Workshop, Soldotna-Kenai, Alaska. pp. 169-186.

United Nations Scientific Committee on the Effects of Atomic Radiation (UNSCEAR), 1977. "Sources and Effects of Ionizing Radiation." Report to the General Assembly, United Nations, New York.

United States Nuclear Regulatory Commission (U.S. NRC), 1982. "Calculational Models for Estimating Radiation Doses to Man from Airborne Radioactive Material Resulting from Uranium Milling Operations." Reg. Guide 3.51, March.

# 13.0 DOSE MODELS

## 13.1 Introduction

### 13.1.1 Background

In Phase I and II of model development, the annual average effective whole-body dose equivalent committment (herein called annual average dose, or simply dose) for a single critical receptor was calculated. In the Phase III model, two types of receptors may be specified: an average receptor and a critical receptor, located in one or more of the 80 possible sectors. Up to 80 receptors (sum of critical and average) may be specified. Both receptor types are assumed to live and raise vegetables in their sector, and eat caribou and moose representative of the study area. However, their water and fish come from a user-specified river or lake.

For the purposes of dose calculations, and aside from the above choices made by the user, the average and critical receptors differ only in the parameter specifications: the dose models themselves are identical.

There are two main types of dose models presented in this chapter: ingestion and inhalation. These models are grouped into one subroutine called DOSEIN. The only external dose model, for groundshine, was documented in Chapter 7.

The inhalation and ingestion models all involve two main aspects: calculation of the receptor's intake and multiplication of that intake by a dose conversion factor (DCF). Because the DCF's are common to all models they are discussed in Section 13.1.2 of this introduction. Details of the ingestion and inhalation models are then presented in Sections 13.2 and 13.3 respectively. The description of each model is structured as follows: discussion of parameters common to all receptor types; discussion of the receptor-specific parameters chosen for critical receptors; and finally discussion of receptor-specific parameters chosen for average receptors. All parameters are listed in Table 13.3 and 13.4. The computer code listing for these models is presented in Table 13.5.

Note that once all of the parameters are chosen, the characteristics of any one critical or average receptor have been specified. However, the location and source of vegetables, water and fish must still be specified for each of the up to 80 receptors previously mentioned. Section 13.4 gives details on this aspect. Finally, Section 13.5 describes how the model may be used to calculate population dose.

In this chapter the subscript "i" is used to indicate that a parameter will vary with the radionuclide; "t" and "j" indicate that a parameter varies with time and location; "r" indicates that the parameter is receptor type specific (average vs. critical), and the following abbreviations are also used as subscripts:

a = air
w = water
v = vegetables
c = caribou
m = moose
f = fish

### 13.1.2 Dose Conversion Factors

The calculation of the dose to a specific receptor resulting from the inhalation and ingestion of various radionuclides involves the multiplication of the receptor's estimated annual intakes of the radionuclides by the appropriate dose conversion factor (DCF). DCF's for the special case of radon and its daughters are given in Section 13.3.2. The remaining radionuclides being modelled in this study, namely, natural uranium, total thorium, radium-226 and lead-210, are discussed below.

DCF's for reference man (i.e. an adult male) for individual radionuclides are given in Table 13.1. These are taken from ICRP-30 (1979) and are based on the

## Table 13.1

## ICRP-30 DOSE CONVERSION FACTORS[1]

| Radionuclide | Ingestion | Inhalation |
|---|---|---|
| Uranium-238 | $6.3 \times 10^{-2}$ | $3.2 \times 10^{1}$ |
| Uranium-235 | $6.8 \times 10^{-2}$ | $3.3 \times 10^{1}$ |
| Uranium-234 | $7.1 \times 10^{-2}$ | $3.6 \times 10^{1}$ |
| Radium-226 | $3.1 \times 10^{-1}$ | 2.1 |
| Lead-210 | 1.4 | 3.4 |
| Thorium-232 | $7.4 \times 10^{-1}$ | $3.1 \times 10^{2}$ |
| Thorium-230 | $1.5 \times 10^{-1}$ | $7.0 \times 10^{1}$ |
| Thorium-228 | $1.0 \times 10^{-1}$ | $8.3 \times 10^{1}$ |

Note:

1. The DCF's are given in units of $\mu Sv.Bq^{-1}$ where the dose ($\mu Sv$) is the total effective whole body dose equivalent committment derived according to ICRP methodology (ICRP 30, 1979).

methodology described in ICRP-26 (1977); that is, the whole body 50-year committed dose resulting from the intake of a radionuclide is assigned to the year of intake. For example, the intake by inhalation of 1 Bq of thorium-230 in one year would result in a whole body committed dose of 70 $\mu$Sv that is assumed to occur in the year of intake. This methodology is accepted by the Atomic Energy Control Board of Canada (AECB) for both occupational and environmental dose assessments. Doses to individual body organs, which must be below 0.5 Sv.yr$^{-1}$ to limit the possibility of non-stochastic effects, are not considered here since it is extremely unlikely that potential environmental doses would ever reach this limiting value.

The DCF's for inhalation given in Table 13.1 correspond to the most insoluble form of the radionuclides described by the ICRP-30 solubility classifications (D, W or Y) since it is assumed that the radionuclides that remain on the surface of the tailings for several years (the source of the inhaled radioactivity) are relatively insoluble. The DCF's for ingestion given in Table 13.1 are for the most soluble forms of the radionuclides listed in ICRP-30 since much of the intake by ingestion is from water, meat and vegetation which contain the soluble form of the radionuclides. Only deposited dust that remains on surface vegetation would be in a relatively insoluble form.

The ICRP DCF's given in Table 13.1 agree to within 25% with the DCF's calculated by Johnson and Dunford (1983) if the same assumptions on the solubility in the stomach of ingested radionuclides are used. Johnson and Dunford (1983) suggest that the ICRP solubility value for thorium that is incorporated in environmental matrices is too small by a factor of 150. Consequently, they calculate DCF's for ingested thorium radionuclides that are 150 times larger than the corresponding ICRP estimates. More recent investigations by Johnson (personal communication) suggest that the original difference between the ICRP value and that used by Johnson and Dunford was too large by about a factor of 6, resulting in a continuing difference of about a factor of 25. Whether or not further investigation of factors such as the chemical form of the thorium (e.g. organic or inorganic) may help to further reduce these differences is unclear. This aspect should continue to be monitored and updated dose conversion factors should be used as they become available.

The use of the DCF's for radium-226 and lead-210 is relatively straightforward since they are modelled as individual, specific radionuclides. However, natural uranium and total thorium which are being modelled in this study are a mixture of radionuclides and their resultant DCF's must be based on the proper mixture of the DCF's of the individual uranium and thorium radionuclides.

One gram of natural uranium contains 1.22 x $10^4$ Bq each of uranium-238 and uranium-224, and 5.8 x $10^2$ Bq of uranium-235, for a total of 2.50 x $10^4$ Bq. Using the values given in Table 13.1 for these radionuclides, the DCF for ingestion of natural uranium is then 1.7 x $10^3$ $\mu$Sv.$g^{-1}$ or 6.7 x $10^{-2}$ $\mu$Sv.$Bq^{-1}$ (essentially the average of the DCF's for uranium-238 and uranium-234). Similarly, the DCF for inhalation of natural uranium is 3.4 x $10^1$ $\mu$Sv.$Bq^{-1}$. These values are shown in Table 13.2.

For the purpose of the present discussion, total thorium is assumed to consist of the thorium isotopes Th-230 (from the uranium-235 decay chain) and Th-232 and Th-228 (from the thorium-232 decay chain). Natural thorium is assumed to consist of the Th-232 and Th-228 isotopes from the thorium decay chain noted above. Since, the dosimetric implications of all three radionuclides are different, the calculations of DCF's for total thorium modelled in this study are thus somewhat complicated. Natural thorium is essentially 100% thorium-232 by mass. Natural thorium also contains an equal activity (but very little mass) of thorium-228 since it is a short-lived daughter product of thorium-232. Other radionuclides in the thorium-232 decay chain do not occur in natural thorium in concentrations that are dosimetrically significant when inhaled (Hannibal, 1982). Radium-228 and radium-224 would increase the DCF for ingestion of natural thorium by about 60%, but since they do not follow the thorium isotopes through the ingestion pathways (e.g. plant uptake), they are not included here. The DCF's for natural thorium are therefore the sum of the DCF's for thorium-232 and thorium-228, or 8.4 x $10^{-1}$ $\mu$Sv.$Bq^{-1}$ for ingestion and 3.9 x $10^2$ $\mu$Sv.$Bq^{-1}$ for inhalation. Conventionally, the specific

Table 13.2

## DOSE CONVERSION FACTORS FOR THIS STUDY

| | Ingestion[4] | Inhalation[5] |
|---|---|---|
| Natural uranium ($\mu Sv.Bq^{-1}$)[1] | $6.7 \times 10^{-2}$ | $3.4 \times 10^{1}$ |
| Radium-226 ($\mu Sv.Bq^{-1}$) | $3.1 \times 10^{-1}$ | 2.1 |
| Lead-210 ($\mu Sv.Bq^{-1}$) | 1.4 | 3.4 |
| Natural thorium ($\mu Sv.Bq^{-1}$)[2] | $8.4 \times 10^{-1}$ | $3.9 \times 10^{2}$ |
| Total thorium ($\mu Sv.Bq^{-1}$)[3] | | |
| - air pathway | $(1.5 \times 10^{-1}) + X_A(6.9 \times 10^{-1})$ | $(7.0 \times 10^{1}) + X_A(3.2 \times 10^{2})$ |
| - water pathway | $(1.5 \times 10^{-1}) + X_w(6.9 \times 10^{-1})$ | ----- |

1. The activity of 1 g of natural uranium is $2.50 \times 10^{4}$ Bq.

2. The activity of 1 g of natural thorium (thorium-232) is $4.05 \times 10^{3}$ Bq.

3. $X_A$ ($X_w$) = activity fraction of natural thorium in total thorium in the air (water) pathway.

4. For U-nat, Ra-226 and Pb-210 $DCF_{ai}(ing) = DCF_{wi}(ing)$. However, as explained in the text $DCF_{aTh}(ing) \neq DCF_{wTh}(ing)$, where Th refers to total thorium as above.

5. Referred to in later sections as $DCF_{ai}(inh)$. See Section 13.3.2 for the dose conversion factor for the inhalation of radon and its daughters.

activity of natural thorium is taken to be equal to the specific activity of thorium-232, or $4.05 \times 10^3$ Bq.g$^{-1}$. The DCF's for natural thorium are shown in Table 13.2.

As previously noted, total thorium also contains thorium-230. As discussed in Chapter 3, the natural thorium to thorium-230 ratio is relatively constant in water whereas this ratio changes with time in the near-surface tailings. The DCF's for total thorium are a function of this ratio since the DCF's for thorium-230 are different than the DCF's for natural thorium. In addition, there must be two DCF's for ingestion of total thorium since ingested thorium can originate both from the water pathway (e.g. drinking water) and the air pathway (e.g. eating vegetation contaminated with deposited dust).

If $X_A$ is the activity fraction of natural thorium in total thorium in the near-surface tailings (the source of dust), the DCF for inhalation of total thorium is:

$$X_A \times \text{DCF(natural thorium)} + (1 - X_A) \times \text{DCF(thorium-230)}$$

Using the DCF's for natural thorium ($3.9 \times 10^2$) and thorium-230 ($7.0 \times 10^1$) the DCF for inhalation of total thorium is then:

$$\begin{aligned} & X_A(3.9 \times 10^2) + (1-X_A)\ (7.0 \times 10^1) \\ & = (7.0 \times 10^1) + X_A(3.2 \times 10^2)\ \mu\text{Sv.Bq}^{-1} \text{ total thorium} \end{aligned}$$

The DCF for ingestion of total thorium that originates in the air pathway is:

$$\begin{aligned} & X_A(8.4 \times 10^{-1}) + (1-X_A)\ (1.5 \times 10^{-1}) \\ & = (1.5 \times 10^{-1}) + X_A(6.9 \times 10^{-1})\ \mu\text{Sv.Bq}^{-1} \text{ total thorium} \end{aligned}$$

Similarily, the DCF for ingestion of total thorium that originates in the water pathway is $(1.5 \times 10^{-1}) + X_w(6.9 \times 10^{-1})$ $\mu$Sv.Bq $^{-1}$ where $X_w$ is the activity fraction of natural thorium in total thorium in water. All DCF's are summarized in Table 13.2.

## 13.2 Ingestion Dose

### 13.2.1 Annual Dose Due to the Ingestion of Vegetables

The annual average dose received by an individual due to the ingestion of above and below-ground vegetables was calculated as follows:

$$d_{virj}(ing) = DCF_{ai}(ing) \sum_{v} U_{vr} C_{vij} R_v L_{vr} \qquad (13.1)$$

where:

$d_{virj}(ing)$ = $d_{virj}(ing)(t)$ is the average annual whole body dose due to the ingestion of radionuclide i in vegetables v (in this case above and below ground vegetables) at time t for receptor type r at location j ($\mu Sv.yr^{-1}$)

$DCF_{ai}(ing)$ = the whole body dose conversion factor for the ingestion of radionuclide i for the air pathway ($\mu Sv.Bq^{-1}$) (see Section 13.1.2)

$U_{vr}$ = the average annual intake of vegetable type v (in this case above and below ground vegetables) (g (wet wt)$.yr^{-1}$) (receptor specific)

$C_{vij}$ = $C_{vij}(t)$ is the calculated average annual concentration of radionuclide i in vegetation type v at time t ($Bq.g^{-1}$ (wet weight)) (location specific)

$R_v$ = the fraction of activity in vegetable type v remaining after food preparation (0 to 1)

$L_{vr}$ = the fraction of the vegetable type v that is grown locally (0 to 1) (receptor specific)

Note that the time dependence in $d_{virj}(ing)(t)$ is due only to the time dependence of $C_{vij}(t)$.

The parameter $R_v$, was chosen to be uniformly distributed from 0.5 to 1.0. The lower value is that recommended by the U.S. NRC (1982). The large upper value was added in recognition of the uncertainty of this number.

Chapter 8.0 details how $C_{vi}$ is calculated for each location j. The receptors are assumed to consume vegetables grown in the sector in which they live (see Section 13.4).

### Critical Receptor

The annual intake of 157 kg of above- and 70 kg of below-ground vegetables used in this model are for an average Ontario adult male, age 20-39, as derived from Nutrition Canada (not dated). Food consumption patterns do vary widely from one region to another, and the user is encouraged to adjust these intakes accordingly. Also, the user may wish to change the age and/or sex of the critical receptor for any particular application. As discussed in Section 13.1.2 the dose conversion factors are for an adult male and would need to be adjusted in parallel with any changes to the age of the receptor.

The parameter $L_{vr}$, was assigned a triangular distribution from 0.1 to 0.6, with a peak at 0.3. The range, although somewhat arbitrary, was chosen in recognition of the fact that even for a critical receptor it would be very unlikely that someone could or would grow a large percentage of their vegetables in the area being modelled (i.e. the Canadian Shield).

### Average Receptor

The annual intake of 39.9 kg of above- and 65.4 kg of below-ground vegetables used in this model are those recommended by the U.S. NRC (1982) for an adult for use in population dose calculations. It should be cautioned that these consumption rates are likely to result in conservative (i.e. high) doses in that the U.S. NRC food consumption rates are for individuals at farm residences and thus are likely to be higher than for non-farm residences.

The parameter $L_{vr}$, was assigned a triangular distribution of 0.0 to 0.2, with a peak at 0.1. This range is again somewhat arbitrary. It was based on two assumptions: the average person grows very little if any of his/her own vegetables, and in the area being modelled (the Canadian Shield) there are not likely to be a large number of market gardens.

### 13.2.2 Annual Dose Due to the Ingestion of Caribou

The model used for calculating the average annual dose received by an individual due to the ingestion of caribou meat was (U.S. NRC, 1982):

$$d_{cirj}(ing) = U_{cr}\, L_{cr}\, (DCF_{ai}(ing)\, C_{cai} + DCF_{wi}(ing)\, C_{cwi}) \qquad (13.2)$$

where:

$d_{cirj}(ing)$ = $d_{cirj}(ing)(t)$ is the average annual whole body dose due to the ingestion of radionuclide i in caribou meat at time t for receptor type r at location j ($\mu Sv.yr^{-1}$)

$U_{cr}$ = the average annual intake of caribou meat ($g.yr^{-1}$ wet wt) (receptor specific)

$L_{cr}$ = the fraction of the annual intake that is local caribou meat (0 to 1) (receptor specific)

$DCF_{ai}(ing)$ = the whole body dose conversion factor for the ingestion of radionuclide i for the air pathway ($\mu Sv.Bq^{-1}$) (see Section 13.1.2)

$C_{cai}$ = $C_{cai}(t)$ is the calculated average annual concentration of radionuclide i in caribou meat at time t, taken over the whole model area due to the air pathway ($Bq.g^{-1}$ wet wt) (see Section 12.2)

$DCF_{wi}(ing)$ = the whole body dose conversion factor for the ingestion of radionuclide i for the water pathway ($\mu Sv.Bq^{-1}$) (see Section 13.1.2)

$C_{cwi}$ = $C_{cwi}(t)$ is the calculated average annual concentration of radionuclide i in caribou meat at time t, taken over the whole model area due to the water pathway ($Bq.g^{-1}$ wet wt) (see Section 12.2)

The time dependence in $d_{cirj}(ing)(t)$ is due to the time dependence of $C_{cai}$ and $C_{cwi}$. This model is not dependent on the location of the receptor, only the type of receptor. This is because only one value of radionuclide concentration in caribou meat is calculated for each of the air and water pathways (see Section 12.2).

### Critical Receptor

For the critical receptor, all of an Ontario adult (age 20-39) male's meat was assumed to come from moose and caribou (79 kg a year) (Nutrition Canada, not dated). Of this, it was assumed that 50 percent is caribou.

The fraction of the annual intake that is local ($L_{cr}$) (i.e. from a caribou killed in the immediate area) was allowed to range from 0 to 100% as this would vary greatly from year to year.

### Average Receptor

For the average receptor, up to 5% of the annual meat intake of 64 kg (U.S. NRC, 1982) was assumed to be caribou (uniformly distributed from 0.0 to 3.2).

The parameter $L_{cr}$ was allowed to vary over the range from 0 to 100% as for the critical receptor.

### 13.2.3 Annual Dose Due to the Ingestion of Moose

The average annual dose received by an individual due to the ingestion of moose meat was calculated as follows (U.S. NRC, 1982):

$$d_{mirj}(ing) = U_{mr}\, L_{mr}\, (DCF_{ai}(ing)\, C_{mai} + DCF_{wi}(ing)\, C_{mwi}) \quad (13.3)$$

where:

$d_{mirj}(ing)$ = $d_{mirj}(ing)(t)$ is the average annual whole body dose due to the ingestion of radionuclide i in moose meat at time t for receptor type r at location j ($\mu Sv.yr^{-1}$)

$U_{mr}$ = the average annual intake of moose meat ($g.yr^{-1}$ wet wt) (receptor specific)

$L_{mr}$ = the fraction of the annual intake that is moose meat from the watershed (0 to 1) (receptor specific)

$DCF_{ai}(ing)$ = the whole body dose conversion factor for the ingestion of radionuclide i for the air pathway (see Section 13.1.2) ($\mu Sv.Bq^{-1}$)

$C_{mai}$ = $C_{mai}(t)$ is the calculated average annual concentration of radionuclide i in moose meat at time t, due to the air pathway, in the watershed area ($Bq.g^{-1}$ wet wt) (see Section 12.3)

$DCF_{wi}(ing)$ = the whole body dose conversion factor for the ingestion of radionuclide i for the water pathway ($\mu Sv.Bq^{-1}$) (see Section 13.1.2)

$C_{mwi}$ = $C_{mwi}(t)$ is the calculated average annual concentration of radionuclide i in moose meat at time t, due to the water pathway, in the watershed area ($Bq.g^{-1}$ wet wt) (see Section 12.3)

Note that the time dependence of $d_{mirj}(ing)$ is due to the time dependence of $C_{mai}$ and $C_{mwi}$.

## Critical Receptor

As previously mentioned, all of the critical receptor's meat was assumed to come from moose and caribou (79 kg a year) (Nutrition Canada, not dated). Of this it was assumed that 50 percent is moose meat.

The fraction of the annual intake that is from the watershed was in this case assumed to be one. This might not be appropriate for critical receptors outside the watershed, but it was not considered possible to allow for all situations.

## Average Receptors

For the average receptor, up to 5% of the annual meat intake of 64 kg (U.S. NRC, 1982) was assumed to be moose (uniformly distributed from 0.0 to 3.2).

As discussed in Section 12.3, only a moose living in the watershed containing the tailings is modelled. Other moose, not in that watershed, but still in the modelling area could have elevated levels of radionuclides due to air emissions from the tailings area. However, it was beyond the scope of model development to calculate both an area and a watershed moose meat concentration. Thus, it was assumed in Phase III that the average receptor would eat meat from moose hunted in the watershed. However, this raises a problem when the average receptor is used in a population dose calculation: only so many moose can be harvested annually from the watershed (or from the watershed as a whole). For large populations, it would be inappropriate to assume a total intake that exceeds the available supply. It is for this reason that $L_{mr}$ must be carefully selected. In this case it was decided not to include watershed moose meat consumption in the population dose estimates, as the watershed is a small fraction of the total area. Thus, in this study $L_{mr}$ was set to zero for an average receptor.

### 13.2.4 Annual Dose Due to the Ingestion of Drinking Water

The average annual dose received by an individual as a result of drinking water was modelled as (U.S. NRC, 1982):

$$d_{wirj}(ing) = DCF_{wi}(ing)\ U_{wr}\ C_{wij}\ L_{wr} \qquad (13.4)$$

where:

$d_{wirj}(ing)$ = $d_{wirj}(ing)(t)$ is the average annual whole body dose due to the ingestion of radionuclide i in drinking water at time t for receptor type r at location j ($\mu Sv.yr^{-1}$)

$DCF_{wi}(ing)$ = the whole body dose conversion factor for the ingestion of radionuclide i for the water pathway ($\mu Sv.Bq^{-1}$)(see Section 13.1.2)

$U_{wr}$ = the average annual intake of drinking water ($m^3.yr^{-1}$) (receptor specific)

$C_{wij}$ = $C_{wij}(t)$ is the calculated average annual concentration of radionuclide i in the water specified for receptor r at location j at time t ($Bq.m^{-3}$)

$L_{wr}$ = the fraction of the annual intake that is local drinking water (0 to 1) (receptor specific)

The time dependence of $d_{wij}(ing)$ is due to the time dependence of $C_{wij}$. Note that j in this case still means the sector in which the receptor is located, but that the water source is specified by the user.

Critical Receptor

The annual water intake of 600 L chosen is for Reference Man (ICRP, 1975).

The fraction of the annual water consumption that is from the specified source was set equal to the fraction of the year that the critical receptor stays at the site (see Section 13.3.1).

Average Receptor

The annual water consumption rate is the same for the average and critical receptors (600 L). $L_{wr}$ is equal to the fraction of the year that the average receptor stays at the site (see Section 13.3.1).

### 13.2.5 Annual Dose Due to the Ingestion of Fish

The average annual dose received by an individual as a result of eating fish was modelled as follows (U.S. NRC, 1982):

$$d_{firj}(ing) = DCF_{wi}(ing)\ U_{fr}\ C_{fij}\ L_{fr}\ F_a \qquad (13.5)$$

where:

$d_{firj}(ing)$ = $d_{firj}(ing)(t)$ is the average annual whole body dose due to the ingestion of radionuclide i in fish at time t for receptor type r at location j ($\mu Sv.yr^{-1}$)

$DCF_{wi}(ing)$ = the whole body dose conversion factor for the ingestion of radionuclide i due to the water pathway ($\mu Sv.Bq^{-1}$) (see Section 13.1.2)

$U_{fr}$ = the average annual intake of fish ($g.yr^{-1}$ wet wt) (receptor specific)

$C_{fij}$ = $C_{fij}(t)$ is the calculated average annual concentration of radionuclide i in fish in the water specified for receptor r at time t ($Bq.g^{-1}$wet wt)

$L_{fr}$ = the fraction of the annual intake that is local fish (0 to 1) (receptor specific)

$F_a$ = availability factor of game fish for consumption expressed as a function of pH (see Section 11.2)

Note that the time dependence of $d_{firj}$(ing) is due to the time dependence of $C_{fij}$. As in Section 13.2.4, j still means the sector in which the receptor is located, but the fish source is specified by the user.

Critical Receptor

The average intake of 8 kg of fish is for an average Ontario Male (age 20 to 39) (Nutrition Canada, not dated). It was assumed that all of his yearly intake of fish is from the lake from which he takes his drinking water (user specified). Note that $L_{fr}$ is adjusted by Fa if the lake becomes too acidic to support a normal fishery (see Section 11.2).

Average Receptor

The average intake of 8 kg of fish is the same as for the critical receptor (Nutrition Canada, not dated). It is also adjusted by Fa. It was assumed that from 0 to 10 percent of this was local (uniformly distributed). As discussed for moose (see Section 13.2.3), if the average receptor is used to estimate population dose and the population is very large, it is possible that the fish population would not support this consumption rate. This is further discussed in Section 13.4.

## 13.3 Inhalation Dose

### 13.3.1 Annual Dose Due to the Inhalation of Suspended Particulates

The average annual dose received by an individual due to inhalation (excluding radon) was calculated as follows:

$$d_{irj}(inh) = DCF_{ai}(inh)\ U_{ar}\ C_{aij}\ OF_r \qquad (13.1)$$

where:

| | |
|---|---|
| $d_{irj}(inh)$ | = $d_{irj}(inh)(t)$ is the average annual whole body dose due to the inhalation of radionuclide i at time t for receptor r at location j ($\mu$Sv.yr$^{-1}$) |
| $DCF_{ai}(inh)$ | = the whole body dose conversion factor for the inhalation of radionuclide i ($\mu$Sv.Bq$^{-1}$) (see Section 13.1.2) |
| $U_{ar}$ | = the average annual inhalation rate of the individual (m$^3$.yr$^{-1}$) (receptor specific) |
| $C_{aij}$ | = $C_{aij}(t)$ is the calculated average air concentration of radionuclide i at location j at time t (Bq.m$^{-3}$) (see Section 5.1) |
| $OF_r$ | = the fraction of the year that is spent at that location (receptor specific) |

The time dependence of $d_{irj}(inh)$ is due to the time dependence of $C_{aij}$.

## Critical Receptor

The annual inhalation rate of 8400 m$^3$ was taken for Reference Man (ICRP, 1975). The occupancy factor was chosen to have a nominal value of 0.6 based on four months away for hunting and trapping, plus a few trips for obtaining supplies, visiting, etc. This was allowed to vary from 0.4 to 0.9 (Table 13.3).

## Average Receptor

The annual inhalation rate of 8400 m$^3$ was also assumed for the average receptor (ICRP, 1975). The occupancy factor of 0.9 is based on 11 months at home per year. This was allowed to vary between 0.8 and 1.0.

### 13.3.2 Annual Dose Due to the Inhalation of Radon and Its Daughters

The radon source and air dispersion models result in an estimation of the radon-in-air concentration at the receptor of interest. This concentration must be converted to a dose (actually a dose rate measured in units of $Sv.yr^{-1}$) so that it can be added to the doses from the other exposure pathways being evaluated.

This conversion requires an estimation of the equilibrium factor, F, between radon and radon daughters. Theoretically, F can range from 0.0 (no radon daughters) to 1.0 (complete radon daughter ingrowth). The value of F outdoors at the receptor depends only on the transit time between the radon source and the receptor if it is assumed that there are no radon daughter removal mechanisms other than radioactive decay. Since in reality the daughters are removed by several other mechanisms that are difficult to quantify (e.g. attachment to dust that falls to the ground) and since the major exposure occurs indoors where F is dependent on several additional factors (such as the building ventilation rate), it has been customary to select, rather than calculate, an F factor that is representative of annual average indoor conditions. The radon concentration at the receptor is converted to a radon daughter concentration using this F factor. For this study, the assumed F value is selected from an input distribution, triangular in shape, with a range of 0.2 to 0.8 and a mode of 0.5. This distribution is based on a large number of indoor F values reported by Case _et_ _al_. (1983).

The neglect of outdoor radon-daughter exposure in the calculation of the receptor's exposure produces only a small error. First, the typical receptor spends only about 25% of the time outdoors. Second, the ingrowth of radon daughters from the radon released from the tailings area is dependent on the source-receptor transit time. The ingrowth, assuming no physical removal mechanisms, is small ($F<0.2$) for receptors who spend their time outdoors within about 4 km of the tailings area (based on an average windspeed of 5 $m.s^{-1}$). Third, as noted above, radon daughters are removed from the air by various mechanisms so that outdoor F values are seldom greater than 0.6 (U.S. EPA, 1985). All of these factors suggest that the outdoor radon daughter exposure would be a maximum of 20 to 25% of the total radon daughter exposure at a specific site.

The value of F is used to calculate the receptor's annual WLM exposure. In the Phase II study, a factor of 0.05 Sv per 4.8 WLM (ICRP, 1981) was used to convert the radon daughter exposure to dose. It was noted that this factor is considered debatable by some (e.g. see Stewart, 1984). However, this factor was derived for occupational exposures. A study by a group of experts of the Nuclear Energy Agency (NEA, 1983) suggests a lower factor of $5\times10^{-3}$ $Sv.WLM^{-1}$ for non-occupational exposures due mainly to the lower breathing rates of the public compared to workers. This latter conversion factor is used for this study.

Based on this factor, the fraction of the time spent indoors when at the site of interest (INOCC), and the definitions of working level (WL, the concentration of radon daughters in equilibrium with 100 $pCi.L^{-1}$ of radon), working level month (WLM, exposure to 1 WL for 170 h), and occupancy factor (OF, the fraction of time at the receptor site, an input variable), the conversion between exposure to 1 $Bq.m^{-3}$ of radon and annual dose is given by:

$$\begin{aligned} \text{Dose } (\mu Sv.yr^{-1}) = {} & \text{Radon } (Bq.m^{-3}) \times OF \times INOCC \times 10^{-3}\ m^3.L^{-1} \times 27\ pCi.Bq^{-1} \\ & \times F \times WL/(100\ pCi.L^{-1}) \times 8760\ h.yr^{-1} \times WLM/(WL \times 170\ h) \\ & \times 5\times 10^3\ \mu Sv.WLM^{-1} \end{aligned}$$

$$= \text{Radon } (Bq.m^{-3}) \times OF \times INOCC \times F \times 6.96\ (\mu Sv.Bq^{-1}.m^3.yr^{-1})$$

Thus, the model used to calculate the annual dose due to exposure to radon is:

$$d_{Rnrj}(inh) = C_{a\ Rn\ j}\ OF_r\ INOCC_r\ F\ 6.96$$

where:

$d_{Rnrj}(inh)$ = $d_{Rnrj}(inh)(t)$ is the average annual whole body dose due to the inhalation of radon and its daughters at time t for receptor r at location j ($\mu Sv.yr^{-1}$)

$C_{aRnj}$ = $C_{aRnj}(t)$ is the average air concentration of radon at location j at time t ($Bq.m^{-3}$) (see Chapter 5).

$OF_r$ = the fraction of the year that is spend at that location (receptor specific) (see Section 13.3.1).

$INOCC_r$ = the fraction of time spent indoors when at the site of interest. (see below)

F = the equilibrium factor between radon and its daughters (see above).

The parameter $INOCC_r$ is the only parameter specific to this model that might possibly be used to differentiate between an average and a critical receptor. There is however, no logical reason to assume that an individual who is a critical receptor in the upstream pathway because he eats more local fish and caribou would also spend more or less time indoors than an average receptor. For this reason, $INOCC_r$, was chosen to be the same for both the critical and average receptors; that is, it was assumed to have a triangular distribution with a range of 0.5 to 0.9 and a mode of 0.75.

## 13.4 Receptor Specification

In the Phase III model, up to 80 possible receptors may be specified. This chapter summarizes what options may be selected to characterize each of these receptors.

### 13.4.1 Receptor Identification Number

This is simply a number from 1 to 80 (referred to in this chapter).

### 13.4.2 Sector Number

This is a number from 1 to 16 which indicates the sector in which the receptor is located (see Figure 2.2 and Section 13.4.3).

### 13.4.3 Ring Number

This is a number from 1 to NRING (number of rings) which specifies the ring in which the receptor is located (see Figure 2.2). This number, in combination with the sector number, specifies where the receptor lives (and therefore receives his inhalation and groundshine exposures) and grows his vegetables.

This does not affect the source of caribou and moose meat, as only one average value is calculated for each radionuclide for the entire area.

### 13.4.4 Water Source Segment Number

This number assigns where the receptor obtains his drinking water and fish. Chapter 10 gives details on the nodes that may be selected, what they represent and how they are numbered.

### 13.4.5 Receptor Type

Two types of receptors may be selected: critical or average. Each of these may be specified by the user as described in previous sections. However, one critical receptor only differs from another critical receptor in terms of his location (see Section 13.4.3), water and fish source. All other parameters are common to all critical receptors. Similarly all average receptors are the same except for their location and source of water and fish.

### 13.4.6 Population

This specifies how many people of this type receptor are to be included in the population dose estimate (see Section 13.5).

If the receptor is not to be used in the population dose calculation, the user simply enters a 0 in this space.

## 13.5 Population Dose

The dose to a population is:

$$D_p = \sum_n D_n P_n$$

where:

$D_p$ = population average annual whole body dose ($\mu Sv.yr^{-1}$)

$P_n$ = population of receptor n (see Section 13.4.6)

$D_n$ = average annual dose to receptor n ($\mu Sv.yr^{-1}$)

When the user is calculating a population dose, care should be taken to ensure that the caribou, moose and fish intakes that would be consumed by the specified population could be harvested from the area being modelled.

Table 13.3

**Variables Used in the Calculation of Annual Dose to the Critical Receptor**

| Model Symbol | Description | Units | Nominal Value | Probability Distribution | Computer Origin | Computer Symbol |
|---|---|---|---|---|---|---|
| **Vegetation Model** | | | | | | |
| $d_{virj}(ing)(t)$ | annual whole body dose commitment due to ingestion of radionuclide i in vegetable v | $\mu Sv \cdot yr^{-1}$ | calculated | calculated | DOSEIN | VEGD(i,j) i=1,5 $j \leq 80$ |
| $DCF_{ai}(ing)$ | whole body DCF for ingestion of radionuclide i (air pathway): | $\mu Sv \cdot Bq^{-1}$ | | | DOSEIN | DCFGA(i) i=1,4 |
| | U-nat | | $6.7 \times 10^{-2}$ | $C(6.7 \times 10^{-2})$ | | |
| | Th-tot | | calculated | calculated | | |
| | Pb-210 | | 1.4 | C(1.4) | | |
| | Ra-226 | | $3.1 \times 10^{-1}$ | $C(3.1 \times 10^{-1})$ | | |
| $U_{vr}$ | average annual intake of vegetable type v: | $g(wet\ wt) \cdot yr^{-1}$ | | | INPUT | |
| | above ground veg. | | $1.57 \times 10^{5}$ | $C\ (1.57 \times 10^{5})$ | | AVEGIN(2) |
| | below ground veg. | | $7.0 \times 10^{4}$ | $C\ (7.0 \times 10^{4})$ | | BVEGIN(2) |
| $C_{vij}(t)$ | concentration of radionuclide i in vegetation type v: | $Bq \cdot g^{-1}$ | | | VEGCON | |
| | above ground veg. | | calculated | calculated | | AVEGC(i,j) i=1,4 $j \leq 80$ |
| | below ground veg. | | calculated | calculated | | BVEGC(i,j) i=1,4 $j \leq 80$ |
| $R_{vr}$ | fraction of activity in vegetable type v after food preparation: | --- | | | INPUT | |
| | above ground veg. | | 1.0 | U(0.5, 1.0) | | AFACT |
| | below ground veg. | | 1.0 | U(0.5, 1.0) | | CFACT |
| $L_{vr}$ | fraction of vegetable type v grown locally: | --- | | | INPUT | |
| | above ground veg. | | 0.5 | T(0.1,0.3,0.6) | | AFLOC(2) |
| | below ground veg. | | 0.5 | T(0.1,0.3,0.6) | | BFLOC(2) |
| **Caribou Ingestion Model** | | | | | | |
| $d_{cirj}(ing)(t)$ | annual whole body dose commitment due to ingestion of radionuclide i in caribou meat | $\mu Sv \cdot yr^{-1}$ | calculated | calculated | DOSEIN | CARDOS(i,j) i=1,5 $j \leq 80$ |
| $DCF_{ai}(ing)$ | whole body DCF for ingestion of radionuclide i (air pathway): | $\mu Sv \cdot Bq^{-1}$ | | | DOSEIN | DCFGA(i) i=1,4 |
| | U-nat | | $6.7 \times 10^{-2}$ | $C(6.7 \times 10^{-2})$ | | |
| | Th-tot | | calculated | calculated | | |
| | Pb-210 | | 1.4 | C(1.4) | | |
| | Ra-226 | | $3.1 \times 10^{-1}$ | $C(3.1 \times 10^{-1})$ | | |
| $DCF_{wi}(ing)$ | whole body DCF for ingestion of radionuclide i (water pathway): | $\mu Sv \cdot Bq^{-1}$ | | | DOSEIN | DCFGW(i) i=1,4 |
| | U-nat | | $6.7 \times 10^{-2}$ | $C(6.7 \times 10^{-2})$ | | |
| | Th-tot | | calculated | calculated | | |
| | Pb-210 | | 1.4 | C(1.4) | | |
| | Ra-226 | | $3.1 \times 10^{-1}$ | $C(3.1 \times 10^{-1})$ | | |
| $U_{cr}$ | annual intake of caribou meat | $g \cdot yr^{-1}$ | $3.95 \times 10^{4}$ | $C(3.95 \times 10^{4})$ | INPUT | CARMIN(2) |
| $C_{cai}(t)$ | annual concentration of radionuclide i in caribou meat (air pathway) | $Bq \cdot g^{-1}$ | calculated | calculated | ANIMAL | ACARC(i) i=1,4 |
| $L_{cr}$ | fraction of annual caribou meat intake that is local | --- | 0.5 | U(0.0, 1.0) | INPUT | CFLOC(2) |
| $C_{cwi}(t)$ | annual concentration of radionuclide i in Caribou meat (water pathway) | $Bq \cdot g^{-1}$ | calculated | calculated | ANIMAL | WCARC(i) i=1,4 |

Table 13.3 continued

| Model Symbol | Description | Units | Nominal Value | Probability Distribution | Computer Origin | Computer Symbol |
|---|---|---|---|---|---|---|
| **Drinking Water Model** | | | | | | |
| $d_{wirj}(ing)(t)$ | annual whole body dose commitment due to ingestion of radionuclide i in drinking water | $\mu Sv \cdot yr^{-1}$ | calculated | calculated | DOSEIN | WATD(i,j) i=1,5 $j \leq 80$ |
| $DCF_{wi}(ing)$ | whole body DCF for ingestion of radionuclide i (water pathway):<br>U-nat<br>Th-tot<br>Pb-210<br>Ra-226 | $\mu Sv \cdot Bq^{-1}$ | <br><br>$6.7 \times 10^{-2}$<br>calculated<br>1.4<br>$3.1 \times 10^{-1}$ | <br><br>$C(6.7 \times 10^{-2})$<br>calculated<br>C(1.4)<br>$C(3.1 \times 10^{-1})$ | DOSEIN | DCFGW(i) i=1,4 |
| $U_{wr}$ | average annual intake of water | $m^3 \cdot yr^{-1}$ | 0.6 | C (0.6) | INPUT | WATIN(2) |
| $C_{wij}(t)$ | annual concentration of radionuclide i in lake water | $Bq.m^{-3}$ | calculated | calculated | LAKE | WATC(i,j) i=4 $j \leq 10$ |
| $L_{wr}$ | fraction of annual water consumption that is local | --- | 0.6 | T(0.4,0.6,0.9) | INPUT | WFLOC(2) |
| **Moose Ingestion Model** | | | | | | |
| $d_{mirj}(ing)(t)$ | annual whole body dose commitment due to ingestion of radionuclide i in moose meat | $\mu Sv \cdot yr^{-1}$ | calculated | calculated | DOSEIN | MODOS(i,j) i=1,5 $j \leq 80$ |
| $DCF_{ai}(ing)$ | whole body DCF for ingestion of radionuclide i (air pathway):<br>U-nat<br>Th-tot<br>Pb-210<br>Ra-226 | $\mu Sv \cdot Bq^{-1}$ | <br><br>$6.7 \times 10^{-2}$<br>calculated<br>1.4<br>$3.1 \times 10^{-1}$ | <br><br>$C(6.7 \times 10^{-2})$<br>calculated<br>C(1.4)<br>$C(3.1 \times 10^{-1})$ | DOSEIN | DCFGA(i) i=1,4 |
| $DCF_{wi}(ing)$ | whole body DCF for ingestion of radionuclide i:<br>U-nat<br>Th-tot<br>Pb-210<br>Ra-226 | $\mu Sv \cdot Bq^{-1}$ | <br>$6.7 \times 10^{-2}$<br>calculated<br>1.4<br>$3.1 \times 10^{-1}$ | <br>$C(6.7 \times 10^{-2})$<br>calculated<br>C(1.4)<br>$C(3.1 \times 10^{-1})$ | DOSEIN | DCFGW(i) i=1,4 |
| $U_{mr}$ | annual intake of moose meat | $g \cdot yr^{-1}$ | $3.95 \times 10^4$ | $C(3.95 \times 10^4)$ | INPUT | MOMIN(2) |
| $C_{mai}(t)$ | annual concentration of radionuclide i in moose meat (air pathway) | $Bq \cdot g^{-1}$ | calculated | calculated | ANIMAL | AMOC(i) i=1,4 |
| $L_{mr}$ | fraction of annual moose meat intake that is local | --- | 1.0 | C(1.0) | INPUT | MFLOC(2) |
| $C_{cwi}$ | annual concentration of radionuclide i in moose meat (water pathway) | $Bq \cdot g^{-1}$ | calculated | calculated | ANIMAL | WMOC(i) i=1,4 |

Table 13.3 continued

| Model Symbol | Description | Units | Nominal Value | Probability Distribution | Computer Origin | Computer Symbol |
|---|---|---|---|---|---|---|
| **Fish Ingestion Model** | | | | | | |
| $d_{firj}(ing)(t)$ | annual whole body dose commitment due to ingestion of radionuclide i in fish | $\mu Sv.yr^{-1}$ | calculated | calculated | DOSEIN | FISHD(i,j) i=1,5 $j \leq 80$ |
| $DCF_{wi}(ing)$ | whole body DCF for ingestion of radionuclide i: | $\mu Sv \cdot Bq^{-1}$ | | | DOSEIN | DCFGW(i) i=1,4 |
| | U-nat<br>Th-tot<br>Pb-210<br>Ra-226 | | $6.7 \times 10^{-2}$<br>calculated<br>1.4<br>$3.1 \times 10^{-1}$ | $C(6.7 \times 10^{-2})$<br>calculated<br>C(1.4)<br>$C(3.1 \times 10^{-1})$ | | |
| $U_{fr}$ | average annual intake of fish | $g.yr^{-1}$ | $8.0 \times 10^{3}$ | $C(8.0 \times 10^{3})$ | INPUT | FISHIN(2) |
| $C_{fij}(t)$ | concentration of radionuclide in i fish | $Bq.g^{-1}$ | calculated | calculated | FISH | FISHC(i,j) i=1,4 $j \leq 10$ |
| $L_{fr}$ | fraction of annual intake that is local fish | --- | 1.0 | C(1.0) | INPUT | FFLOC(2) |
| $F_a$ | fish availability factor | --- | calculated | calculated | FISH | FISHA(j) $j \leq 10$ |
| **Inhalation Model (Particulates)** | | | | | | |
| $d_{irj}(inh)(t)$ | annual whole body dose commitment due to inhalation of radionuclide i | $\mu Sv.yr^{-1}$ | calculated | calculated | DOSEIN | INHD(i.j) i=1,5 $j \leq 80$ |
| $DCF_{ai}(inh)$ | whole body DCF due to inhalation of radionuclide i (air pathway): | $Sv.Bq^{-1}$ | | | DOSEIN | DCFHA(i) i=1,4 |
| | U-nat<br>Th-tot<br>Pb-210<br>Ra-226 | | $3.4 \times 10^{1}$<br>calculated<br>3.4<br>2.1 | $C(3.4 \quad 10^{1})$<br>calculated<br>C(3.4)<br>C(2.1) | | |
| $U_{ar}$ | average annual inhalation rate | $m^{3}.yr^{-1}$ | $8.4 \times 10^{3}$ | $C(8.4 \times 10^{3})$ | INPUT | AIRIN(2) |
| $C_{aij}(t)$ | concentration of radionuclide i in air | $Bq.m^{-3}$ | calculated | calculated | AIRDIS | AIRC(i,j) i=1,4 $j \leq 80$ |
| $OF_r$ | fraction of year in location | --- | 0.6 | T (0.4,0.6,0.9) | INPUT | OF(2) |
| **Inhalation Model (Radon)** | | | | | | |
| $d_{Rnrj}(inh)(t)$ | annual whole body dose commitment due to inhalation of radon plus daughters | $\mu Sv.yr^{-1}$ | calculated | calculated | DOSEIN | RADD(j) $j \leq 80$ |
| $F$ | equilibrium factor for radon daughters to radon | --- | 0.5 | T (0.2,0.5,0.8) | INPUT | EFR |
| $OF_r$ | fraction of year in location | --- | 0.6 | T (0.4,0.6,0.9) | INPUT | OF(2) |
| $INOCC_r$ | fraction of time spent indoors | --- | 0.75 | T (0.5, 0.75, 0.9) | INPUT | INOCC(2) |
| $C_{aRnj}(t)$ | concentration of radon in air | $Bq \cdot m^{-3}$ | calculated | calculated | AIRDIS | AIRC(5,j) $j \leq 80$ |

Table 13.4

**Variables Used in the Calculation of Annual Dose to the Average Receptor**

| Model Symbol | Description | Units | Nominal Value | Probability Distribution | Computer Origin | Computer Symbol |
|---|---|---|---|---|---|---|
| **Vegetation Model** | | | | | | |
| $d_{virj}(ing)(t)$ | annual whole body dose commitment due to ingestion of radionuclide i in vegetable v | $\mu\text{Sv}\cdot\text{yr}^{-1}$ | calculated | calculated | DOSEIN | VEGD(i,j) i=1,5 $j \leq 80$ |
| $DCF_{ai}(ing)$ | whole body DCF for ingestion of radionuclide i (air pathway): | $\mu\text{Sv}\cdot\text{Bq}^{-1}$ | | | DOSEIN | DCFGA(i) i=1,4 |
| | U-nat | | $6.7 \times 10^{-2}$ | $C(6.7 \times 10^{-2})$ | | |
| | Th-tot | | calculated | calculated | | |
| | Pb-210 | | 1.4 | C(1.4) | | |
| | Ra-226 | | $3.1 \times 10^{-1}$ | $C(3.1 \times 10^{-1})$ | | |
| $U_{vr}$ | average annual intake of vegetable type v: | g(wet wt).$\text{yr}^{-1}$ | | | INPUT | |
| | above ground veg. | | $3.99 \times 10^4$ | $C\ (3.99 \times 10^4)$ | | AVEGIN(1) |
| | below ground veg. | | $6.54 \times 10^4$ | $C\ (6.54 \times 10^4)$ | | BVEGIN(1) |
| $C_{vij}(t)$ | concentration of radionuclide i in vegetation type v: | $\text{Bq}\cdot\text{g}^{-1}$ | | | VEGCON | |
| | above ground veg. | | calculated | calculated | | AVEGC(i,j) i-1,4 $j \leq 80$ |
| | below ground veg. | | calculated | calculated | | BVEGC(i,j) i=1,4 $j \leq 80$ |
| $R_{vr}$ | fraction of activity in vegetable type v after food preparation: | --- | | | INPUT | |
| | above ground veg. | | 1.0 | U(0.5, 1.0) | | AFACT |
| | below ground veg. | | 1.0 | U(0.5, 1.0) | | BFACT |
| $L_{vr}$ | fraction of vegetable type v grown locally: | --- | | | INPUT | |
| | above ground veg. | | 0.1 | T(0.0,0.1,0.2) | | AFLOC(1) |
| | below ground veg. | | 0.1 | T(0.0,0.1,0.2) | | BFLOC(1) |
| **Caribou Ingestion Model** | | | | | | |
| $d_{cirj}(ing)(t)$ | annual whole body dose commitment due to ingestion of radionuclide i in caribou meat | $\mu\text{Sv}\cdot\text{yr}^{-1}$ | calculated | calculated | DOSEIN | CARDOS(i,j) i=1,5 $j \leq 80$ |
| $DCF_{ai}(ing)$ | whole body DCF for ingestion of radionuclide i (air pathway): | $\mu\text{Sv}\cdot\text{Bq}^{-1}$ | | | DOSEIN | DCFGA(i) i=1,4 |
| | U-nat | | $6.7 \times 10^{-2}$ | $C(6.7 \times 10^{-2})$ | | |
| | Th-tot | | calculated | calculated | | |
| | Pb-210 | | 1.4 | C(1.4) | | |
| | Ra-226 | | $3.1 \times 10^{-1}$ | $C(3.1 \times 10^{-1})$ | | |
| $DCF_{wi}(ing)$ | whole body DCF for ingestion of radionuclide i (water pathway): | $\mu\text{Sv}\cdot\text{Bq}^{-1}$ | | | DOSEIN | DCFGW(i) i=1,4 |
| | U-nat | | $6.7 \times 10^{-2}$ | $C(6.7 \times 10^{-2})$ | | |
| | Th-tot | | calculated | calculated | | |
| | Pb-210 | | 1.4 | C(1.4) | | |
| | Ra-226 | | $3.1 \times 10^{-1}$ | $C(3.1 \times 10^{-1})$ | | |
| $U_{cr}$ | annual intake of caribou meat | $\text{g}\cdot\text{yr}^{-1}$ | $3.2 \times 10^3$ | $U(0.0,3.2\text{x}10^3)$ | INPUT | CARMIN(1) |
| $C_{cai}(t)$ | annual concentration of radionuclide i in caribou meat (air pathway) | $\text{Bq}\cdot\text{g}^{-1}$ | calculated | calculated | ANIMAL | ACARC(i) i=1,4 |
| $L_{cr}$ | fraction of annual caribou meat intake that is local | --- | 0.5 | U(0.0, 1.0) | INPUT | CFLOC(1) |
| $C_{cwi}(t)$ | annual concentration of radionuclide i in Caribou meat (water pathway) | Bq-g-1 | calculated | calculated | ANIMAL | WCARC(i) i=1,4 |

Table 13.4 continued

| Model Symbol | Description | Units | Nominal Value | Probability Distribution | Computer Origin | Computer Symbol |
|---|---|---|---|---|---|---|
| **Drinking Water Model** | | | | | | |
| $d_{wirj}(ing)(t)$ | annual whole body dose commitment due to ingestion of radionuclide i in drinking water | $\mu Sv \cdot yr^{-1}$ | calculated | calculated | DOSEIN | WATD(i,j) i=1,5 j≤80 |
| $DCF_{wi}(ing)$ | whole body DCF for ingestion of radionuclide i (water pathway): | $\mu Sv \cdot Bq^{-1}$ | | | DOSEIN | DCFGW(i) i=1,4 |
| | U-nat | | $6.7 \times 10^{-2}$ | $C(6.7 \times 10^{-2})$ | | |
| | Th-tot | | calculated | calculated | | |
| | Pb-210 | | 1.4 | C(1.4) | | |
| | Ra-226 | | $3.1 \times 10^{-1}$ | $C(3.1 \times 10^{-1})$ | | |
| $U_{wr}$ | average annual intake of water | $m^3 \cdot yr^{-1}$ | 0.6 | C (0.6) | INPUT | WATIN(1) |
| $C_{wij}(t)$ | annual concentration of radionuclide i in lake water | $Bq.m^{-3}$ | calculated | calculated | LAKE | WATC(i,j) i=4 j≤10 |
| $L_{wr}$ | fraction of annual water consumption that is local | --- | 0.9 | T(0.8,0.9,1.0) | INPUT | WFLOC(1) |
| **Moose Ingestion Model** | | | | | | |
| $d_{mirj}(ing)(t)$ | annual whole body dose commitment due to ingestion of radionuclide i in moose meat | $\mu Sv \cdot yr^{-1}$ | calculated | calculated | DOSEIN | MODOS(i,j) i=1,5 j≤80 |
| $DCF_{ai}(ing)$ | whole body DCF for ingestion of radionuclide i (air pathway): | $\mu Sv \cdot Bq^{-1}$ | | | DOSEIN | DCFGA(i) i=1,4 |
| | U-nat | | $6.7 \times 10^{-2}$ | $C(6.7 \times 10^{-2})$ | | |
| | Th-tot | | calculated | calculated | | |
| | Pb-210 | | 1.4 | C(1.4) | | |
| | Ra-226 | | $3.1 \times 10^{-1}$ | $C(3.1 \times 10^{-1})$ | | |
| $DCF_{wi}(ing)$ | whole body DCF for ingestion of radionuclide i: | $\mu Sv \cdot Bq^{-1}$ | | | DOSEIN | DCFGW(i) i=1,4 |
| | U-nat | | $6.7 \times 10^{-2}$ | $C(6.7 \times 10^{-2})$ | | |
| | Th-tot | | calculated | calculated | | |
| | Pb-210 | | 1.4 | C(1.4) | | |
| | Ra-226 | | $3.1 \times 10^{-1}$ | $C(3.1 \times 10^{-1})$ | | |
| $U_{mr}$ | annual intake of moose meat | $g \cdot yr^{-1}$ | $3.2 \times 10^3$ | $U(0.0, 3.2 \times 10^3)$ | INPUT | MOMIN(1) |
| $C_{mai}(t)$ | annual concentration of radionuclide i in moose meat (air pathway) | $Bq \cdot g^{-1}$ | calculated | calculated | ANIMAL | AMOC(i) i=1,4 |
| $L_{mr}$ | fraction of annual moose meat intake that is local | --- | 0.0 | C(0.0) | INPUT | MFLOC(1) |
| $C_{cwi}$ | annual concentration of radionuclide i in moose meat (water pathway) | $Bq \cdot g^{-1}$ | calculated | calculated | ANIMAL | WMOC(i) i=1,4 |

Table 13.4 continued

| Model Symbol | Description | Units | Nominal Value | Probability Distribution | Computer Origin | Computer Symbol |
|---|---|---|---|---|---|---|
| **Fish Ingestion Model** | | | | | | |
| $d_{firj}(ing)(t)$ | annual whole body dose commitment due to ingestion of radionuclide i in fish | $\mu Sv.yr^{-1}$ | calculated | calculated | DOSEIN | FISHD(i,j) i=1,5 j≤80 |
| $DCF_{wi}(ing)$ | whole body DCF for ingestion of radionuclide i:<br>U-nat<br>Th-tot<br>Pb-210<br>Ra-226 | $\mu Sv \cdot Bq^{-1}$ | <br><br>$6.7 \times 10^{-2}$<br>calculated<br>1.4<br>$3.1 \times 10^{-1}$ | <br><br>$C(6.7 \times 10^{-2})$<br>calculated<br>C(1.4)<br>$C(3.1 \times 10^{-1})$ | DOSEIN | DCFGW(i) i=1,4 |
| $U_{fr}$ | average annual intake of fish | $g.yr^{-1}$ | $8.0 \times 10^{3}$ | $C(8.0 \times 10^{3})$ | INPUT | FISHIN(1) |
| $C_{fij}(t)$ | concentration of radionuclide in i fish | $Bq.g^{-1}$ | calculated | calculated | FISH | FISHC(i,j) i=1,4 j≤10 |
| $L_{fr}$ | fraction of annual intake that is local fish | --- | 0.05 | U(0.0,0.1) | INPUT | FFLOC(1) |
| $F_a$ | fish availability factor | --- | calculated | calculated | FISH | FISHA(j) j≤10 |
| **Inhalation Model (Particulates)** | | | | | | |
| $d_{irj}(inh)(t)$ | annual whole body dose commitment due to inhalation of radionuclide i | $\mu Sv.yr^{-1}$ | calculated | calculated | DOSEIN | INHD(i.j) i=1,5 j≤80 |
| $DCF_{ai}(inh)$ | whole body DCF due to inhalation of radionuclide i (air pathway):<br>U-nat<br>Th-tot<br>Pb-210<br>Ra-226 | $Sv.Bq^{-1}$ | <br><br>$3.4 \times 10^{1}$<br>calculated<br>3.4<br>2.1 | <br><br>$C3.4 \times 10^{1})$<br>calculated<br>C(3.4)<br>C(2.1) | DOSEIN | DCFHA(i) i=1,4 |
| $U_{ar}$ | average annual inhalation rate | $m^{3}.yr^{-1}$ | $8.4 \times 10^{3}$ | $C(8.4 \times 10^{3})$ | INPUT | AIRIN(1) |
| $C_{aij}(t)$ | concentration of radionuclide i in air | $Bq.m^{-3}$ | calculated | calculated | AIRDIS | AIRC(i,j) i=1,4 j≤80 |
| $OF_r$ | fraction of year in location | --- | 0.9 | T (0.8,0.9,1.0) | INPUT | OF(1) |
| **Inhalation Model (Radon)** | | | | | | |
| $d_{Rnrj}(inh)(t)$ | annual whole body dose commitment due to inhalation of radon plus daughters | $\mu Sv.yr^{-1}$ | calculated | calculated | DOSEIN | RADD(j) j≤80 |
| F | equilibrium factor for radon daughters to radon | --- | 0.5 | T (0.2,0.5,0.8) | INPUT | EFR |
| $OF_r$ | fraction of year in location | --- | 0.9 | T (0.8,0.9,1.0) | INPUT | OF(1) |
| $INOCC_r$ | fraction of time spent indoors | --- | 0.75 | T (0.5, 0.75, 0.9) | INPUT | INOCC(1) |
| $C_{aRnj}(t)$ | concentration of radon in air | $Bq \cdot m^{-3}$ | calculated | calculated | AIRDIS | AIRC(5,j) j≤80 |

Table 13.5

## DOSE MODEL CODE LISTING

```
      SUBROUTINE DOSEIN
      INCLUDE 'MODEL.INC'
      INCLUDE 'VAR.INC'
      REAL*4 CARDOS(4,80),MODOS(4,80)
      IF(NREC.EQ.1)THEN
         DCFGA(1)=6.7E-2
         DCFGA(2)=1.5E-1+6.9E-1*X232SA
         DCFGA(3)=1.4
         DCFGA(4)=3.1E-1
         DCFGW(1)=6.7E-2
         DCFGW(2)=1.5E-1+6.9E-1*X232LA
         DCFGW(3)=1.4
         DCFGW(4)=3.1E-1
         DCFHA(1)=3.4E+1
         DCFHA(2)=7.0E+1+3.2E+2*X232SA
         DCFHA(3)=3.4
         DCFHA(4)=2.1
         POPDT=0.0
      ENDIF
      INHD(5,NREC)=0.0
      VEGD(5,NREC)=0.0
      MEATD(5,NREC)=0.0
      WATD(5,NREC)=0.0
      FISHD(5,NREC)=0.0
      N=1
      IF(RTYPE(NREC).EQ.'C')N=2
      RADD(NREC)=69.6*INOCC(N)*OF(N)*EFR*AIRC(5,NREC)
      DOSE(5,NREC)=RADD(NREC)+SHINED(5,NREC)
      DO 10 I=1,4
         INHD(I,NREC)=DCFHA(I)*AIRIN(N)*OF(N)*AIRC(I,NREC)
         INHD(5,NREC)=INHD(5,NREC)+INHD(I,NREC)
         VEGD(I,NREC)=DCFGA(I)*(AFACT*AVEGIN(N)*AFLOC(N)*AVEGC(I,NREC)+
     +                BFACT*BVEGIN(N)*BFLOC(N)*BVEGC(I,NREC))
         VEGD(5,NREC)=VEGD(5,NREC)+VEGD(I,NREC)
         CARDOS(I,NREC)=CARMIN(N)*CFLOC(N)*(DCFGA(I)*ACARC(I)+DCFGW(I)*
     +                WCARC(I))
         MODOS(I,NREC)=MOMIN(N)*MFLOC(N)*(DCFGA(I)*AMOC(I)+DCFGW(I)*
     +                WMOC(I))
         MEATD(I,NREC)=CARDOS(I,NREC)+MODOS(I,NREC)
         MEATD(5,NREC)=MEATD(5,NREC)+MEATD(I,NREC)
         IF(RWSSEG(NREC).EQ.0)THEN
            WATD(I,NREC)=0.0
            FISHD(I,NREC)=0.0
         ELSE
            WATD(I,NREC)=DCFGW(I)*WATIN(N)*WFLOC(N)*WATC(I,RWSSEG(NREC))
            FISHD(I,NREC)=DCFGW(I)*FISHIN(N)*FFLOC(N)*FISHA(RWSSEG
     +                    (NREC))*FISHC(I,RWSSEG(NREC))
         ENDIF
         WATD(5,NREC)=WATD(5,NREC)+WATD(I,NREC)
         FISHD(5,NREC)=FISHD(5,NREC)+FISHD(I,NREC)
         DOSE(I,NREC)=INHD(I,NREC)+VEGD(I,NREC)+MEATD(I,NREC)+WATD(I,
     +                NREC)+FISHD(I,NREC)
```

Table 13.5 (continued)

```
         DOSE(5,NREC)=DOSE(5,NREC)+DOSE(I,NREC)
10    CONTINUE
      POPDT=POPDT+RPOP(NREC)*DOSE(5,NREC)
C
      IF(CODDOS.EQ.1.0.OR.CODDOS.EQ.2.0.OR.CODDOS.EQ.3.0)THEN
         WRITE(*,100)
      ENDIF
      IF(CODDOS.EQ.3.0)THEN
         WRITE(*,101)
         IF(NREC.EQ.1)THEN
            WRITE(*,102)X232SA,X232LA
            WRITE(*,103)(DCFGA(I),DCFGW(I),DCFHA(I),I=1,4)
            WRITE(*,104)EFR,(OF(N),INOCC(N),N=1,2)
            WRITE(*,105)AFACT,(AVEGIN(N),AFLOC(N),N=1,2)
            WRITE(*,106)BFACT,(BVEGIN(N),BFLOC(N),N=1,2)
            WRITE(*,107)(CARMIN(N),CFLOC(N),N=1,2)
            WRITE(*,108)(MOMIN(N),MFLOC(N),N=1,2)
            WRITE(*,109)(WATIN(N),WFLOC(N),N=1,2)
            WRITE(*,110)(FISHIN(N),FFLOC(N),N=1,2)
         ENDIF
         WRITE(*,111)FISHA(RWSSEG(NREC))
         IF(RTYPE(NREC).EQ.'C')THEN
            WRITE(*,112)RPOP(NREC)
         ELSE
            WRITE(*,113)RPOP(NREC)
         ENDIF
         WRITE(*,114)SHINED(5,NREC)
         WRITE(*,115)(CARDOS(I,NREC),I=1,4)
         WRITE(*,116)(MODOS(I,NREC),I=1,4)
      ENDIF
      IF(CODDOS.EQ.2.0.OR.CODDOS.EQ.3.0)THEN
         WRITE(*,117)RADD(NREC)
         WRITE(*,118)(INHD(I,NREC),I=1,5)
         WRITE(*,119)(VEGD(I,NREC),I=1,5)
         WRITE(*,120)(MEATD(I,NREC),I=1,5)
         WRITE(*,121)(WATD(I,NREC),I=1,5)
         WRITE(*,122)(FISHD(I,NREC),I=1,5)
         WRITE(*,123)(DOSE(I,NREC),I=1,5)
         IF(NREC.EQ.NRECEP)THEN
            WRITE(*,124)POPDT
         ENDIF
      ENDIF
C
100   FORMAT(///1X,'DOSE MODEL')
101   FORMAT(1X)
102   FORMAT(1X,'ACTIVITY OF Th-nat IN Th-tot IN THE AIR PATHWAY',E12.4/
     +       1X,'ACTIVITY OF Th-nat IN Th-tot IN THE WATER PATHWAY',
     +       E12.4)
103   FORMAT(1X,'DOSE CONVERSION FACTORS'/5X,'INGESTION (AIR PATHWAY)',
     +       4(E12.4)/5X,'INGESTION (WATER PATHWAY)',4(E12.4)/5X,'INH',
     +       'ALATION (AIR PATHWAY)',4(E12.4))
104   FORMAT(1X,'EQUILIBRIUM FACTOR BETWEEN RADON AND ITS DAUGHTERS',
     +       E12.4/1X,'FRACTION OF TIME SPENT AT LOCATION'/5X,'AVERAGE',
```

Table 13.5 (continued)

```
     +       E12.4/5X,'CRITICAL',E12.4/1X,'FRACTION OF TIME SPENT INDO',
     +       'ORS'/5X,'AVERAGE',E12.4/5X,'CRITICAL',E12.4)
105   FORMAT(1X,'FRACTION OF ACTIVITY REMAINING IN ABOVE GROUND VEGET',
     +       'ABLES AFTER'/5X,'FOOD PREPARATION',E12.4/1X,'AVERAGE ANN',
     +       'UAL INTAKE OF ABOVE GROUND VEGETABLES'/5X,'AVERAGE',E12.4/
     +       5X,'CRITICAL',E12.4/1X,'FRACTION OF ABOVE GROUND VEGETABL',
     +       'ES GROWN LOCALLY'/5X,'AVERAGE',E12.4/5X,'CRITICAL',E12.4)
106   FORMAT(1X,'FRACTION OF ACTIVITY REMAINING IN BELOW GROUND VEGET',
     +       'ABLES AFTER'/5X,'FOOD PREPARATION',E12.4/1X,'AVERAGE ANN',
     +       'UAL INTAKE OF BELOW GROUND VEGETABLES'/5X,'AVERAGE',E12.4/
     +       5X,'CRITICAL',E12.4/1X,'FRACTION OF BELOW GROUND VEGETABL',
     +       'ES GROWN LOCALLY'/5X,'AVERAGE',E12.4/5X,'CRITICAL',E12.4)
107   FORMAT(1X,'AVERAGE ANNUAL INTAKE OF CARIBOU MEAT'/5X,'AVERAGE',
     +       E12.4/5X,'CRITICAL',E12.4/1X,'FRACTION OF ANNUAL INTAKE ',
     +       'THAT IS LOCAL CARIBOU MEAT'/5X,'AVERAGE',E12.4/5X,'CRIT',
     +       'ICAL',E12.4)
108   FORMAT(1X,'AVERAGE ANNUAL INTAKE OF MOOSE MEAT'/5X,'AVERAGE',
     +       E12.4/5X,'CRITICAL',E12.4/1X,'FRACTION OF ANNUAL INTAKE ',
     +       'THAT IS LOCAL MOOSE MEAT'/5X,'AVERAGE',E12.4/5X,'CRITICA',
     +       'L',E12.4)
109   FORMAT(1X,'AVERAGE ANNUAL INTAKE OF DRINKING WATER'/5X,'AVERAGE',
     +       E12.4/5X,'CRITICAL',E12.4/1X,'FRACTION OF ANNUAL INTAKE ',
     +       'THAT IS LOCAL DRINKING WATER'/5X,'AVERAGE',E12.4/5X,'CR',
     +       'ITICAL',E12.4)
110   FORMAT(1X,'AVERAGE ANNUAL INTAKE OF FISH'/5X,'AVERAGE',E12.4/5X,
     +       'CRITICAL',E12.4/1X,'FRACTION OF ANNUAL INTAKE THAT IS ',
     +       'LOCAL FISH'/5X,'AVERAGE',E12.4/5X,'CRITICAL',E12.4)
111   FORMAT(1X,'FISH AVAILABILITY FACTOR',E12.4)
112   FORMAT(1X,'CRITICAL RECEPTOR POPULATION',I7)
113   FORMAT(1X,'AVERAGE RECEPTOR POPULATION',I7)
114   FORMAT(1X,'DOSE FROM GROUNDSHINE'/1X,E12.4)
115   FORMAT(1X,'DOSE FROM INGESTION OF CARIBOU MEAT'/1X,4(E12.4))
116   FORMAT(1X,'DOSE FROM INGESTION OF MOOSE MEAT'/1X,4(E12.4))
117   FORMAT(/1X,'DOSE FROM RADON INHALATION'/1X,E12.4)
118   FORMAT(1X,'DOSE FROM PARTICULATE INHALATION'/1X,5(E12.4))
119   FORMAT(1X,'DOSE FROM INGESTION OF VEGETABLES'/1X,5(E12.4))
120   FORMAT(1X,'DOSE FROM INGESTION OF MEAT'/1X,5(E12.4))
121   FORMAT(1X,'DOSE FROM INGESTION OF DRINKING WATER'/1X,5(E12.4))
122   FORMAT(1X,'DOSE FROM INGESTION OF FISH'/1X,5(E12.4))
123   FORMAT(1X,'TOTAL DOSE'/1X,5(E12.4))
124   FORMAT(1X,'POPULATION DOSEL'/1X,E12.4)
C
      RETURN
      END
```

## 13.6 References

Case, G.G., Chambers, D.B., and Lowe,L.M., 1983. "Calculation of Radiation Exposures in a Case Control Study of Lung Cancers in Port Hope, Ontario." Presented at the Fourth Annual Conference of the Canadian Radiation Portection Association, May 3-5, 1983, Toronto, Ontario.

Hannibal, L., 1982. "On the Radiological Significance of Inhaled Uranium and Thorium Ore Dust." Health Physics, Vol. 42, No. 3, pp. 367-371.

International Commission on Radiological Protections, (ICRP), 1975. "Report of the Task Group on Reference Man." ICRP Publication 23, Pergamon Press, Oxford.

International Commission on Radiological Protection (ICRP), 1977. "Recommendations of the International Commission on Radiological Protection." ICRP Publication 26, Pergamon Press, Oxford.

International Commission on Radiological Protection (ICRP), 1979. "Limits for Intakes of Radionuclides by Workers." ICRP Publication 30, Part 1 and Supplement, Pergamon Press, Oxford.

International Commission on Radiological Protection (ICRP), 1981. "Limits for Inhalation of Radon Daughters by Workers." ICRP Publication 32, Annals of the ICRP, Vol. 6, No.1.

Johnson, J.R. and Dunford, D.W., 1983. "Dose Conversion Factors For Intakes of Selected Radionuclides by Infants and Adults." Atomic Energy of Canada Limited, AECL-7919.

Nuclear Energy Agency (NEA) Group of Experts, 1983. "Dosimetry Aspects of Exposure to Radon and Thoron Daughter Products." Nuclear Energy Agency, Organization for Economic Co-operation and Development, Paris, France.

Nutrition Canada, not dated. "Food Consumption Patterns Report." Prepared by the Department of National Health and Welfare.

Stewart, C.G., 1984. "Comments Upon 'Basis of Intake Limits for Radon and Thoron Daughters' Proposed by the Atomic Energy Control Board of Canada in Consultative Document C-78 Entitled 'Limitation of Exposure to Ionizing Radiation' Issued for Comment 14 November 1983." Prepared in Association with SENES Consultants Limited for the Canadian Nuclear Association.

United States Environmental Protection Agency (U.S.EPA), 1985. "Background Information Document - Standard for Radon-222 Emissions from Underground Uranium Mines." EPA 520/1-85-010.

United States Nuclear Regulatory Commission (U.S. NRC), 1982. "Calculational Models for Estimating Radiation Doses to Man from Airborne Radioactive Materials Resulting from Uranium Milling Operations." Reg. Guide, 3.51, March.

# APPENDIX A

## WATER SOURCE MODELS: CODE LISTING AND VARIABLE DICTIONARY

Since the water source models are by far the lengthiest component models in UTAP, they are listed here (as Table A.1) rather than in Chapter 3. Following the code listing is a variable dictionary for these models, which acts as a bridge between the model derivation and description in Chapter 3 and the computer implementation in Table A.1

The variable dictionary presented in Table A.3 is meant to be exhaustive as far as the model descriptions (Chapter 3) are concerned. That is, any variable in any equation in Chapter 3 which is used in the computer model is included in the variable dictionary. There will be some variables used in the computer implementation, (primarily those used in intermediate calculations) which will not appear in the variable dictionary.

Many of the calculated concentrations of radionuclides and ions are stored in two arrays in the computer program. These arrays appear many times in Table A.3. A summary of the information stored in them is provided in Table A.2. There may be some confusion regarding the units for radionuclide concentrations used in Tables A.2 and A.3 and those used in Chapter 3. Virtually all of the calculations within the water source model are performed on a mass basis ($mol.m^{-3}$). However, to meet system specifications, all radionuclide concentrations being passed between environmental compartments (i.e. leaving the water source model) must be expressed on an activity basis ($Bq.m^{-3}$). Thus in the derivations and descriptions in Chapter 3, mass or molar units are widely used. Indications are provided throughout Chapter 3 where calculated values must be converted from a molar to an activity basis. All calculated radionuclide concentrations which are used outside of the water source model are expressed on an activity basis. That is, following the source model calculations, all radionuclide concentrations in the arrays CONC or WCONC (see Table A.2) are in units of $Bq.m^{-3}$.

Table A.1

## SOURCE MODEL CODE LISTING

```
      SUBROUTINE SEXEC
      INCLUDE 'MODEL.INC'
      INCLUDE 'VAR.INC'
C
C     THIS ROUTINE ACCESSES THE SOURCE MODEL ROUTINES IN
C     THE APPROPRIATE ORDER.
C
      IF (T.EQ.0.) THEN
         CALL INCONI
         CALL INCONN
         CALL EROS
         CALL RADON
         CALL DUST
         ELSE
         IF (XLIME.NE.0.0) THEN
            CALL IONS1L
         ELSE
            CALL IONS1
         ENDIF
         CALL IONS3
         CALL IONS4
         CALL URANUM
         CALL THORUM
         CALL RADIUM
         CALL LEAD
         CALL EROS
         CALL RADON
         CALL DUST
      ENDIF
      RETURN
      END
C
C
C
C
```

```
      SUBROUTINE NEWTON(IND,X1,X,FCNF)
      INCLUDE 'VAR.INC'
      REAL*4 X1,X
C
C     ROUTINE TO CALCULATE THE ROOT OF AN EQUATION; USING NEWTON'S
C     METHOD.SEE GERALD,C.F. (1980) 'APPLIED NUMERICAL ANALYSIS' P16.
C
      EPS = 0.01
      IMAX = 50
      NPHIT = 0
      DO 20 I=1,IMAX
         CALL FCNF(FCN,FPRIME,X1)
         DELTA = -1.*FCN/FPRIME
         NPHIT = NPHIT+1
         X1 = X1+DELTA
         IF (ABS(DELTA).LE.EPS) GO TO 30
         IF (I.EQ.IMAX) THEN
            WRITE(*,900) IND
            STOP
900         FORMAT(1X,'CONVERGENCE FAILED IN FUNCTION',I1)
         ENDIF
20    CONTINUE
30    CONTINUE
      X = X1
      RETURN
      END
      SUBROUTINE INCONI
      EXTERNAL PH1,PH2,PH3,PH4,PH1L,PH2GL
      INCLUDE 'MODEL.INC'
      INCLUDE 'VAR.INC'
      REAL*4 PHIN
C
C     THIS ROUTINE CALCULATES INITIAL INVENTORIES FOR SEVERAL IONIC
C     SPECIES AND pH. THESE CALCULATIONS ARE PERFORMED AT T=0 AND
C     REPRESENT THE INITIAL CONDITION OF THE TAILINGS.
C
C     FIRST SEVERAL VARIABLES ARE ASSIGNED INITIAL VALUES.
C
      PYRITE(1) = PYRITI
      PYRITE(3) = PYRITE(1)
      DGYP(1) = 0.0
      DGYP(3) = DGYP(1)
      REPGYP = 0.0
      GYPMIX = 0.0
      GYPI = RHOTAL*FRACGP/136.0
      LIMEIN = XLIME*RHOTAL/100.
      CALDEP = 0.0
      DBOT = 10.0-(DUNSAT+DMIX)
      CHECKU = 'GYPSUM'
      CHECKM = 'GYPSUM'
      CHECKL = 'LIME'
C
C     INITIAL CALCULATIONS FOR LAYERS 1 AND 2.
C     SOME PARAMETERS ARE CALCULATED DIFFERENTLY IF LIME HAS BEEN
C     INCORPORATED INTO THE UNSATURATED TAILINGS LAYER.
C
      IF (XLIME.GT.0.0) THEN
C
C     SULPHATE FLUX FROM PYRITE OXIDATION.
C
         T1 = 1.0-(KPRIME*ALOG((1.0+KPRIME)/KPRIME))
         SFLUX = 0.05*((1.067*SULPRD*RHOTAL*O2CONC*O2DIFF*T1)**0.5)
         KRATE = 0.5*SFLUX/(DUNSAT*PYRITE(1))
         EQUIL = (KSUBSO/FACTCO**2.)**0.5
C
C     INITIAL PH CALCULATIONS.
C
         IND = 6
         PHIN = 6.5
         CALL NEWTON(IND,PHIN,PH2LIM,PH2GL)
         PH(1) = PH2LIM
         PH(2) = PH2LIM
C
C     INITIAL SULPHATE AND CALCIUM CONCENTRATIONS.
C
         WCONC(6,2,1) = (2.0*DUNSAT*PYRITI*(1.0-EXP(-1.*KRATE*DT)))/
     &                  (NPRCP*DT)
         WCONC(6,2,3) = WCONC(6,2,1)
         T1 = EXP((-1.0*NPRCP*DT)/(POROS*DMIX))
         WCONC(6,3,3) = WCONC(6,2,3)-WCONC(6,2,3)*T1
         WCONC(6,4,3) = 0.0
         WCONC(7,2,3) = 1000.*(10.**(2.*PH(2)-16.47))/FACTCO
         WCONC(8,2,3) = 1000.*(10.**(11.86-2.*PH(2)))/FACTCO
      ELSE
C
C     OTHERWISE, THE FOLLOWING CALCULATIONS APPLY.
C     STEADY STATE SULPHATE FLUX FROM PYRITE OXIDATION IS CALCULATED.
C
         T1 = 1.0-(KPRIME*ALOG((1.0+KPRIME)/KPRIME))
         SFLUX = (1.067*SULPRD*RHOTAL*O2CONC*O2DIFF*T1)**0.5
         KRATE = SFLUX/(2.0*DUNSAT*PYRITE(1))
         EQUIL = (KSUBSO/(FACTCO**2.0))**0.5
C
C     THE CONCENTRATION OF SULPHATE FROM PYRITE OXIDATION.
C
         WCONC(6,2,1) = (2.0*DUNSAT*PYRITI*(1.0-EXP(-1.*KRATE*DT)))/
     &                 (NPRCP*DT)
         WCONC(6,2,3) = WCONC(6,2,1)
         T1 = EXP((-1.0*NPRCP*DT)/(POROS*DMIX))
         WCONC(6,3,3) = WCONC(6,2,3)-WCONC(6,2,3)*T1
         WCONC(6,4,3) = 0.0
C
C     LAYER 1 AND 2 PH CALCULATIONS. PH IS CALCULATED ITERATIVELY,
C     USING SUBROUTINES 'NEWTON' AND 'PH2'.
C
         IND = 2
         PHIN = 3.2
         CALL NEWTON (IND,PHIN,PH(2),PH2)
         PH(1) = PH(2)
C
C     CALCIUM AND SULPHATE CONCENTRATIONS IN THE UNSATURATED ZONE.
C
         WCONC(7,1,3) = 0.0
         WCONC(8,1,3) = 0.0
         T7 = (FACTCO**3.)*(10.**(8.99-3.*PH(2)))
         T8 = (FACTCO**(3./4.))*10.**(9.7-3.*PH(2))
         DELT = 1.0+T7+T8
         T9 = (KSUBSO*DELT/(FACTCO**2.)+(0.25*(WCONC(6,2,3)**2.)))**0.5
         WCONC(8,2,3) = T9-0.5*WCONC(6,2,3)
         WCONC(7,2,3) = T9+0.5*WCONC(6,2,3)
      ENDIF
C
C     CONCENTRATION OF FE3 IS DEPENDENT ON PH AND SULPHATE.
C
      T2 = 10.0**(5.97-3.0*PH(2))+10.0**(3.78-2.0*PH(2))
     &     +10.0**(0.3-PH(2))
      T3 = (FACTCO**3.0)*10.0**(8.99-3.0*PH(2))
      T4 = 1.0+(FACTCO**(3.0/4.0)*10.0**(9.7-3.0*PH(2)))
      WCONC(9,2,1) = T2+(WCONC(7,2,3)/1000.)*T3/(T4+T3)
      WCONC(9,2,1) = WCONC(9,2,1)*1000.
      WCONC(9,2,3) = WCONC(9,2,1)
C
```

```
C     LAYER 3 (MIXING ZONE) INITIAL CONDITIONS.
C     IONIC CONCENTRATIONS ARE CALCULATED FIRST.
C
      T1 = ((KSUBSO/FACTCO**2.)+0.25*WCONC(6,3,3)**2.)**0.5
      WCONC(7,3,3) = T1+0.5*WCONC(6,3,3)
      WCONC(8,3,3) = T1-0.5*WCONC(6,3,3)
      WCONC(10,3,3) = 1.5*WCONC(9,2,3)
C
C     PH IS CALCULATED ITERATIVELY USING SUBROUTINES 'NEWTON' AND 'PH3'
C
      IND = 3
      PHIN = 4.0
      CALL NEWTON(IND,PHIN,PH(3),PH3)

C     VOLUMETRIC FLOW FROM THE MIXING ZONE INTO LAYER 4 IS CALCULATED
C     AS A FUNCTION OF LONG-TERM MEAN ANNUAL PRECIPITATION.
C
      VSR = FNPRCP*AVPRCP*ATAIL
      SFLOW = (NPRCP*ATAIL)-VSR
C
C     LAYER 4 INITIAL CONDITIONS
C
      WCONC(7,4,3) = EQUIL
      WCONC(8,4,3) = EQUIL
      WCONC(10,4,1) = 0.0
      WCONC(10,4,3) = WCONC(10,4,1)
      IND = 4
      PHIN = 6.7
      CALL NEWTON(IND,PHIN,PH(4),PH4)
C
C     PRINT DETAILED RESULTS IF SPECIFIED.
C
      IF (CODION.EQ.1.) THEN
      WRITE(*,900)
      WRITE(*,910) GYPI,PYRITI,SFLUX,KRATE
      WRITE(*,920) EQUIL,PH(1),PH(2),PH(3),PH(4),LIMEIN
      WRITE(*,930) WCONC(7,2,3),WCONC(8,2,3),WCONC(9,2,3)
      WRITE(*,940) WCONC(7,3,3),WCONC(8,3,3),WCONC(10,3,3)
      WRITE(*,950) WCONC(7,4,3),WCONC(8,4,3),WCONC(10,4,3)
900   FORMAT(1X,'   INITIAL CONDITIONS')
910   FORMAT(1X,'[GYP]I=',E10.4,' PYRITE=',E10.4,' SFLUX=',E10.4,
     &       ' KRATE=',E10.4)
920   FORMAT(1X,'EQUIL=',E10.4,' PH1=',F5.2,' PH2=',F5.2,' PH3=',F5.2,
     &       ' PH4=',F5.2,' LIME=',E10.4)
930   FORMAT(1X,'[SO4]T2=',E10.4,' [CA2]T2=',E10.4,' [FE3]T2=',E10.4)
940   FORMAT(1X,'[SO4]T3=',E10.4,' [CA2]T3=',E10.4,' [FE3]T3=',E10.4)
950   FORMAT(1X,'[SO4]T4=',E10.4,' [CA2]T4=',E10.4,' [FE3]T4=',E10.4)
      ENDIF

      RETURN
      END
      SUBROUTINE INCONN
      INCLUDE 'MODEL.INC'
      INCLUDE 'VAR.INC'
C
C     THIS ROUTINE INITIALIZES VARIABLES USED IN THE CALCULATION
C     OF RADIONUCLIDE CONCENTRATIONS; AS WELL AS PERFORMING THE
C     NECESSARY CALCULATIONS IN THE FIRST TIME STEP.
C
C     URANIUM: INITIAL CONDITIONS AND CALCULATIONS.
C
      UCF = 5.95E6
      AUNATO = (PCURAN/100.)*(714./842.)*2.5E4
      AU2380 = (PCURAN/100.)*(714./842.)*1.22E4
      AUNATT = AUNATO*(1.0-FURAN)
      MUNATT = PCURAN*(238./842.)*(1.0-FURAN)
      CONC(1,1,1) = AUNATT*RHOTAL
      UPYRI = (CONC(1,1,1)*FRACU)/(3.0*UCF)
      XURANI = UPYRI/PYRITI
      CONC(1,1,3) = CONC(1,1,1)
      WCONC(1,2,3) = ((3.0*DUNSAT)/(NPRCP*DT))*XURANI*PYRITI
     &                *(1.0-EXP(-1.0*KRATE*DT))
      T1 = EXP(-1.0*NPRCP*DT/(POROS*DMIX*(1.0+(KDUO2*RHOTAL/POROS))))
      WCONC(1,3,3) = WCONC(1,2,3)-WCONC(1,2,3)*T1
      T2 = EXP(-1.0*FNPRCP*AVPRCP*DT/(POROS*DBOT*
     &     (1.0+(KDUO2*RHOTAL/POROS))))
      WCONC(1,4,3) = WCONC(1,3,3)-WCONC(1,3,3)*T2
      WCONC(1,2,3) = WCONC(1,2,3)*UCF
      WCONC(1,3,3) = WCONC(1,3,3)*UCF
      WCONC(1,4,3) = WCONC(1,4,3)*UCF
C
C     PRINT SELECTED RESULTS IF SPECIFIED.
C
C      IF (CODNUC.EQ.1.0) THEN
C      ENDIF
C
C     THORIUM: INITIAL CONDITIONS AND CALCULATIONS.
C     SOLID PHASE CONDITIONS FIRST.
C
      T230CF = 1.65E11
      T232CF = 9.35E5
      LAM230 = 8.66E-6
      THDISS = 0.0
      THDISM = 0.0
      CHKTHU = 'ENRICHED'
      CHKTHS = 'ENRICHED'
      AT230I = AU2380
      CT230I = AT230I*RHOTAL*(1.0/T230CF)
      CT232I = (PCTHOR/100.)*RHOTAL*(1.0/264.)
      AT232I = CT232I*T232CF/RHOTAL
      ATHORI = AT232I+AT230I
      CTHORI = CT230I+CT232I
      CONC(2,1,1) = ATHORI*RHOTAL
      CONC(2,1,3) = CONC(2,1,1)
```

```
C
C     CALCULATION OF INITIAL SOLUBLE AND INSOLUBLE THORIUM FRACTIONS.
C
      T232IS = (1.0-FT232)*CT232I
      T230IS = (1.0-FT230)*CT230I
      T232SO = FT232*CT232I
      T230SO = FT230*CT230I
      THSOL = T232SO+T230SO
      TINSOL = T232IS+T230IS
      THSOLA = T230SO*T230CF+T232SO*T232CF
      TINSLA = T232IS*T232CF+T230IS*T230CF
      X232LM = T232SO/THSOL
      X230LM = T230SO/THSOL
      X230LA = (T230SO*T230CF)/THSOLA
      X232LA = (T232SO*T232CF)/THSOLA
      X232A = T232IS*T232CF/TINSLA
      X232SA = X232A
C
C     INITIAL THORIUM LIQUID PHASE CONCENTRATIONS.
C
      THORDC = (1.78*FRACTH)+(6.3*(1.0-FRACTH))
      THORCF = X230LM*T230CF+(1.0-X230LM)*T232CF
C
C     THE SAME PROCEDURE IS USED TO CALCULATE CONCENTRATIONS
C     IN EACH LAYER.
C
      DELTA = 1.0+(FACTCO**3.*10.**(8.99-3.*PH(2)))+
     &             (FACTCO**0.75*10.**(9.7-3.*PH(2)))
      DO 100 I=2,4
         IF (I.EQ.2) THEN
            SO4 = WCONC(7,2,3)/(DELTA*1000.)
         ELSE
            SO4 = WCONC(7,I,3)/1000.
         ENDIF
         P = PH(I)
         F = FACTCO
         T1 = (10.**(THORDC-4.*P))/F**4.
         T2 = F**(7./4.)*10.**(P-3.2)+F**3.*10.**(2.*P-6.93)
         T3 = F**(15./4.)*10.**(3.*P-11.7)+F**4.*10.**(4.*P-15.9)
         T4 = F**4.*10.**5.45*SO4+F**6.*10.**9.73*SO4**2.
         WCONC(2,I,3) = T1*(1.0+T2+T3+T4)*1000.
         IF (WCONC(2,I,3).GT.0.05) WCONC(2,I,3)=0.05
         WCONC(2,I,3) = WCONC(2,I,3)*THORCF
100   CONTINUE
C
C     PRINT SELECTED RESULTS IF SPECIFIED.
C
C      IF (CODNUC.EQ.1.0) THEN
C      ENDIF
C
C     RADIUM: INITIAL CONDITIONS AND CALCULATIONS.
C     SOLID PHASE CONDITIONS ARE DETERMINED FIRST.
C
```

```
      RACF = 8.26E12
      LAMRAD = 4.33E-4
      RADEC = EXP(-1.0*LAMRAD*DT)
      TDECAY = (LAM230/(LAMRAD-LAM230))*(EXP(-1.0*LAM230*DT)
     &         -RADEC)
      CRATHS = 0.0
      CHKBAS = 'ENRICHED'
      CHKBAU = 'ENRICHED'
      SUMBAR = 0.0
      DBAR(1) = 0.01
      DBAR(3) = DBAR(1)
      MBAR(1) = 0.0
      MBAR(3) = MBAR(1)
      XBAR(1) = XRADI
      XBAR(3) = XBAR(1)

      ARADI = AT230I
      CRADI = ARADI*RHOTAL*(1.0/RACF)
      CRADBA = FRAD*CRADI
      CRADTI = (1.0-FRAD)*CRADI
      CBARI = CRADBA/XRADI
      BASATI = XRADI*(DUNSAT*CBARI+DMIX*CBARI)

      CONC(4,1,3) = CRADTI*RACF
      CONC(4,2,3) = CRADI*RACF
      CONC(4,3,3) = CONC(4,2,3)
      CONC(4,4,3) = CONC(4,3,3)
C
C     RADIUM LIQUID PHASE CONCENTRATIONS ARE THEN DETERMINED.
C
      DELTA = 1.0+(FACTCO**3.*10.**(8.99-3.*PH(2)))+
     &            (FACTCO**0.75*10.**(9.7-3.*PH(2)))
      SO4 = WCONC(7,2,3)/DELTA
      EQBAR = (KSBAR/FACTCO**2.)**0.5
      CBAR = ((EQBAR**2.)/(EQBAR+SO4))*(1.0+FACTCO**2.*KFBAR*SO4)
      WCONC(4,2,3) = XRADI*CBAR*KRAD*RACF
      SO4 = WCONC(7,3,3)
      CBAR = ((EQBAR**2.)/(EQBAR+SO4))*(1.0+FACTCO**2.*KFBAR*SO4)
      WCONC(4,3,3) = XRADI*CBAR*KRAD*RACF
      SO4 = WCONC(7,4,3)
      CBAR = ((EQBAR**2.)/(EQBAR+SO4))*(1.0+FACTCO**2.*KFBAR*SO4)
      WCONC(4,4,3) = XRADI*CBAR*KRAD*RACF
C
C     PRINT SELECTED RESULTS IF SPECIFIED.
C
C      IF (CODNUC.EQ.1.0) THEN
C      ENDIF
C
C     LEAD: INITIAL CONDITIONS AND CALCULATIONS.
C     SOLID PHASE CONDITIONS ARE DETERMINED FIRST.
C
      PBCF = 6.3E14
      LAMPB = 3.3E-2
      PBDEC = EXP(-1.0*LAMPB*DT)
      RDECAY = (LAMRAD/(LAMPB-LAMRAD))*(EXP(-1.0*LAMRAD*DT)
     &         -PBDEC)
      CPBRAS = 0.0
      CHKPBU = 'ENRICHED'
      CHKPBS = 'ENRICHED'
      SUMPB = 0.0
      DLEAD(1) = 0.01
      DLEAD(3) = DLEAD(1)

      APBI = ARADI
      CPBI = APBI*RHOTAL*(1.0/PBCF)
      CPBPB = FLEAD*CPBI
      CPBTI = (1.0-FLEAD)*CPBI
      XPBI = CPBPB/CLEADI
      PBSATI = XPBI*(DUNSAT*CLEADI+DMIX*CLEADI)
      CONC(3,1,3) = CPBTI*PBCF
      CONC(3,2,3) = CPBI*PBCF
      CONC(3,3,3) = CONC(3,2,3)
      CONC(3,4,3) = CONC(3,3,3)
C
C     LEAD CONCENTRATIONS IN THE LIQUID PHASE ARE THEN DETERMINED.
C
      S04 = WCONC(7,2,3)/DELTA
      EQLEAD = (KSLEAD/FACTCO**2)**0.5
      CLEAD = ((EQLEAD**2.)/(EQLEAD+S04))*(1.0+FACTCO**2.*KFLEAD*S04)
      WCONC(3,2,3) = XPBI*CLEAD*PBCF
      S04 = WCONC(7,3,3)
      CLEAD = ((EQLEAD**2.)/(EQLEAD+S04))*(1.0+FACTCO**2.*KFLEAD*S04)
      WCONC(3,3,3) = XPBI*CLEAD*PBCF
      S04 = WCONC(7,4,3)
      CLEAD = ((EQLEAD**2.)/(EQLEAD+S04))*(1.0+FACTCO**2.*KFLEAD*S04)
      WCONC(3,4,3) = XPBI*CLEAD*PBCF
C
C     PRINT SELECTED RESULTS IF SPECIFIED.
C
C      IF (CODNUC.EQ.1.0) THEN
C      ENDIF
C
C     PRINT SUMMARY RESULTS IF SPECIFIED.
C
      IF (CODNUC.EQ.1.0) THEN
         WRITE(*,900) T
         WRITE(*,910) CONC(1,1,3),WCONC(1,2,3),WCONC(1,3,3),
     &                WCONC(1,4,3)
         WRITE(*,920) CONC(2,1,3),WCONC(2,2,3),WCONC(2,3,3),
     &                WCONC(2,4,3),X232SA
         WRITE(*,930) CONC(4,1,3),WCONC(4,2,3),WCONC(4,3,3),
     &                WCONC(4,4,3),CONC(4,2,3)
         WRITE(*,940) CONC(3,1,3),WCONC(3,2,3),WCONC(3,3,3),
     &                WCONC(3,4,3)
         WRITE(*,950) THSOL,TINSOL,BASATI,PBSATI
      ENDIF
```

```
900   FORMAT(1X,'T=',F5.0,4X,'SOLID1',5X,'LIQUID2',5X,'LIQUID3',5X,
     &         'LIQUID4',7X,'OTHER')
910   FORMAT(1X,'URANIUM',2X,E10.4,3(2X,E10.4))
920   FORMAT(1X,'THORIUM',2X,E10.4,4(2X,E10.4))
930   FORMAT(1X,'RADIUM',3X,E10.4,4(2X,E10.4))
940   FORMAT(1X,'LEAD',5X,E10.4,3(2X,E10.4))
950   FORMAT(1X,'[TH]SOL=',E10.4,' [TH]INSOL=',E10.4,' [RA]BA1=',E10.4
     &           ,' [PB]PB1=',E10.4)

      RETURN
      END
      SUBROUTINE IONS1
      EXTERNAL PH1,PH2
      INCLUDE 'MODEL.INC'
      INCLUDE 'VAR.INC'
      REAL*4 K
C
C     THIS ROUTINE PERFORMS CALCULATIONS RELEVANT TO GYPSUM DISSOLUTION
C     IONIC CONCENTRATIONS AND PH IN LAYERS 1 AND 2.
C
C     FIRST SEVERAL CURRENT AND PREVIOUS VARIABLE VALUES ARE RESET.
C
      PYRITE(2) = PYRITE(3)
      DGYP(2) = DGYP(3)
      WCONC(9,2,2) = WCONC(9,2,3)
      WCONC(6,2,2) = WCONC(6,2,3)
C
C     CALCULATE SO4 PRODUCTION VIA PYRITE OXIDATION.
C
      PYRITE(3) = PYRITE(2)*EXP(-1.0*KRATE*DT)
      IF (PYRITE(3).LE.1.E-6) PYRITE(3) = 1.0E-6
      BETA = PYRITE(2)*(1.0-EXP(-1.0*KRATE*DT))
      WCONC(6,2,3) = (2.0*DUNSAT*BETA)/(NPRCP*DT)+0.1
C
C     CHECK FOR GYPSUM DEPLETION.
C
      IF (CHECKU.NE.'DEPLETED') THEN
C
C     CALCULATE CHANGE IN DEPTH OF DEPLETED ZONE OVER DT.
C
C        ???????????????????????????????????????????????????????
C        T1  = (4.0*(BETA**2.0)*(DGYP(2)**2.0))/((GYPI+BETA)**2.0)
C        ????????????????????????????????????????????????????????
C
         T1  = ( (BETA**2.0)*(DGYP(2)**2.0))/((GYPI+BETA)**2.0)
         T2 = (((NPRCP*DT)**2.)*(EQUIL**2.))/((GYPI**2.)+GYPI*BETA)
C
C        ????????????????????????????????????
C        T3  = (2.0*BETA*DGYP(2))/(GYPI+BETA)
C        ????????????????????????????????????
C
         T3  = (    BETA*DGYP(2))/(GYPI+BETA)
         DELTAH = ((T1+T2)**0.5)-T3
         DGYP(3) = DGYP(2)+DELTAH
C
C     CHECK NEW DEPTH OF DEPLETED ZONE.
C
         IF (DGYP(3).GE.DUNSAT) THEN
C
C     RESET INDICATOR VARIABLES.
C
            DGYP(3) = DUNSAT
            FGYP = 0.0
            TFINAL = T
            CHECKU = 'DEPLETED'
            WCONC(8,2,3) = 0.0
         ENDIF
      ENDIF
C
C     CHECK ONCE AGAIN FOR GYPSUM DEPLETION.
C
      IF (CHECKU.NE.'DEPLETED') THEN
C
C     CALCULATE GYPSUM REPRECIPITATION, IONIC CONCENTRATIONS AND PH.
C
         T4 = ((EQUIL**2.*(NPRCP*DT)**2.)+(DUNSAT**2.*BETA**2.))**0.5
         DELTAR = (GYPI*DELTAH)-T4+(DUNSAT*BETA)
         REPGYP = REPGYP+DELTAR
         FGYP = ((DUNSAT-DGYP(3))*GYPI+REPGYP)/(DUNSAT*GYPI)
         WCONC(6,1,3) = WCONC(6,2,3)*(DGYP(3)/DUNSAT)
         WCONC(7,1,3) = WCONC(6,1,3)
C
C     GENERATE INITIAL GUESS FOR ITERATIVE PH CALCULATION.
C
         IF (WCONC(6,2,3).EQ.0.0) WCONC(6,2,3) = 1.0E-20
         T5 = (ALOG10(WCONC(6,2,3)/1000.)+3.4)**4.
         K = 0.725+(6.56281E-2*T5)
         T6 = (K*(ALOG10(WCONC(6,2,3)/1000.)+4.230414))
         PHIN = 4.383551-((2.723818/(22./7.))*ATAN(T6))
         IND1 = 1
         IND2 = 2
         PHIN1 = PHIN
         PHIN2 = PHIN
C
C     PH IS CALCULATED ITERATIVELY USING SUBROUTINES 'NEWTON',
C     'PH1' (LAYER 1) AND 'PH2' (LAYER 2).
C
         CALL NEWTON(IND1,PHIN1,PH(1),PH1)
         CALL NEWTON(IND2,PHIN2,PH(2),PH2)
C
C     CA AND SO4 CONCENTRATIONS IN LAYER 2 ARE FUNCTIONS OF PH.
C
         T7 = (FACTCO**3.)*(10.**(8.99-3.*PH(2)))
         T8 = (FACTCO**(3./4.))*10.**(9.7-3.*PH(2))
         DELT = 1.0+T7+T8
         T9 = (KSUBSO*DELT/(FACTCO**2.)+(0.25*(WCONC(6,2,3)**2.)))**0.5
         WCONC(8,2,3) = T9-0.5*WCONC(6,2,3)
         WCONC(7,2,3) = T9+0.5*WCONC(6,2,3)

         ELSE
C
C     CALCULATE IONIC CONCENTRATIONS AND PH AFTER UNSATURATED ZONE
C     IS DEPLETED OF GYPSUM.
C     FIRST, GENERATE INITIAL GUESS FOR PH CALCULATION.
C
         WCONC(7,2,3) = WCONC(6,2,3)
         WCONC(6,1,3) = WCONC(6,2,3)
         WCONC(7,1,3) = WCONC(7,2,3)
         IF (WCONC(6,2,3).EQ.0.0) WCONC(6,2,3) = 1.0E-20
         T5 = (ALOG10(WCONC(6,2,3)/1000.)+3.4)**4.
         K = 0.725+(6.56281E-2*T5)
         T6 = (K*(ALOG10(WCONC(6,2,3)/1000.)+4.230414))
         PHIN = 4.383551-((2.723818/(22./7.))*ATAN(T6))
         IND1 = 1
C
C     PH IS CALCULATED ITERATIVELY USING SUBROUTINES 'NEWTON'AND 'PH1'
C
         CALL NEWTON(IND1,PHIN,PH(1),PH1)
         PH(2) = PH(1)
      ENDIF
C
C     FE3 CONCENTRATION IS A FUNCTION OF SO4 AND PH.
C
      T10 = 10.0**(5.97-3.0*PH(2))+10.0**(3.78-2.0*PH(2))
     &     +10.0**(0.3-PH(2))
      T11 = (FACTCO**3.0)*10.0**(8.99-3.0*PH(2))
      T12 = 1.0+(FACTCO**(3.0/4.0)*10.0**(9.7-3.0*PH(2)))
      WCONC(9,2,3) = T10+(WCONC(7,2,3)/1000.)*T11/(T12+T11)
      WCONC(9,2,3) = WCONC(9,2,3)*1000.
C
C     PRINT DETAILED RESULTS IF SPECIFIED
C
      IF (CODION.EQ.1.) THEN
      WRITE(*,900) T,DGYP(3),REPGYP,PH(1),PH(2)
      WRITE(*,910) WCONC(6,1,3),WCONC(6,2,3),WCONC(9,2,3)
      WRITE(*,920) WCONC(7,1,3),WCONC(7,2,3),WCONC(8,2,3)
900   FORMAT(1X,'LAYERS 1&2 T=',F6.1,' DEPTH=',F6.3,' REPGYP= ',E10.4,
     &       ' PH1=',F5.2,' PH2=',F5.2)
910   FORMAT(1X,'[SO4]P1=',E10.4,' [SO4]P2=',E10.4,' [FE3]T2=',E10.4)
920   FORMAT(1X,'[SO4]T1=',E10.4,' [SO4]T2=',E10.4,' [CA2]T2=',E10.4)
      ENDIF
      RETURN
      END
C
C
C
C
```

```
      SUBROUTINE PH1(F,FPRIME,P)
      INCLUDE 'MODEL.INC'
      INCLUDE 'VAR.INC'
C
C     THIS ROUTINE IS INVOLVED IN THE ITERATIVE CALCULATION OF PH IN
C     THE UNSATURATED ZONE; FOR THE  GYPSUM DEPLETED CASE.
C
C     FIRST THE FUNCTION (F) IS EVALUATED.
C
      F1 = FACTCO
      CS = WCONC(6,1,3)/1000.
      T1 = (F1**(3./4.)*10.**(9.7-3.*P))+(F1**3.*10.**(8.97-3*P))
      S04 = CS*(2.-T1)/(1.+T1)
      T2 = 10.**(-3.*P)*(((10.**6.5)/F1**(9./4.))+10**5.97)
      T3 = 10.**(-2.*P)*(((10.**1.53)/F1)+10.**3.78)
      T4 = 10.**(0.3-P)
      T5 = (10.**(-1.*P))/F1**(1./4.)
      T6 = (10.**(P-11.27))/F1**(1./4.)
      F = 3.*T2+2.*T3+T4+T5-S04-T6
C
C     THEN THE DERIVATIVE OF THE FUNCTION (FPRIME) IS EVALUATED.
C
      XL = ALOG(10)
      DT1 = (-3.*XL*F1**(3./4.)*10.**(9.7-3.*P))-3.*XL*F1**3.
     &     *10.**(8.97-3.*P)
      T7 = -1.0*DT1*((2.-T1)/((1.+T1)**2.)+1./(1.+T1))
      FPRIME = -9.*XL*T2-4.*XL*T3-XL*T4-XL*T5-CS*T7-XL*T6
C
C     PRINT DETAILED RESULTS IF SPECIFIED.
C
      IF (CODPH.EQ.1) THEN
      WRITE(*,900) T,P,F,FPRIME
900   FORMAT(1X,'PH1: T=',F6.1,' PH=',F5.2,' F=',E10.4,' FPRIME=',E10.4)
      ENDIF

      RETURN
      END
C
C
C
C
```

```
      SUBROUTINE PH2(F,FPRIME,P)
      INCLUDE 'MODEL.INC'
      INCLUDE 'VAR.INC'
C
C     THIS ROUTINE IS INVOLVED IN THE ITERATIVE CALCULATION OF PH IN
C     THE UNSATURATED ZONE; FOR THE  GYPSUM ENRICHED CASE.
C
C     FIRST THE FUNCTION (F) IS EVALUATED.
C
      F1 = FACTCO
      CS = WCONC(6,2,3)/1000.
      T1 = (F1**(3./4.)*10.**(9.7-3.*P))+(F1**3.*10.**(8.97-3*P))
      CA2 = (((10**(-4.6)*(1.+T1))/F1**2.)+.25*CS**2.)**0.5-0.5*CS
      SO4 = (CA2+CS)*(2.-T1)/(1.+T1)
      T2 = 3.*10.**(-3.*P)*(((10.**6.5)/F1**(9./4.))+10**5.97)
      T3 = 2.*10.**(-2.*P)*(((10.**1.53)/F1)+10.**3.78)
      T4 = 10.**(0.3-P)
      T5 = (10.**(-1.*P))/F1**(1./4.)
      T6 = (10.**(P-11.27))/F1**(1./4.)
      F = 2.*CA2+T2+T3+T4+T5-SO4-T6
C
C     THEN THE DERIVATIVE OF THE FUNCTION (FPRIME) IS EVALUATED.
C
      XL = ALOG(10)
      T7 = (-3.*XL*F1**(3./4.)*10.**(9.7-3.*P))-3.*XL*F1**3.
     &     *10.**(8.97-3.*P)
      T8 = 0.5*T7*((10.**(-4.6))/F1**2.)*(((10.**(-4.6)*T1)/F1**2.)+
     &     .25*CS**2.)**(-0.5)
      T9 = -1.0*T7*((2.-T1)/((1.+T1)**2.)+1./(1.+T1))
      T10 = CS*T9+CA2*T9+((2.-T1)/(1.+T1))*T8
      FPRIME = 2.*T8-3.*XL*T2-2.*XL*T3-XL*T4-XL*T5-XL*T6-T10
C
C     PRINT DETAILED RESULTS IF SELECTED
C
      IF (CODPH.EQ.1) THEN
      WRITE(*,900) T,P,F,FPRIME
900   FORMAT(1X,'PH2: T=',F6.1,' PH=',F5.2,' F=',E10.4,' FPRIME=',E10.4)
      ENDIF

      RETURN
      END
      SUBROUTINE IONS1L
      EXTERNAL PH1,PH2,PH1L
      INCLUDE 'MODEL.INC'
      INCLUDE 'VAR.INC'
      REAL*4 K
C
C     THIS ROUTINE PERFORMS CALCULATIONS RELEVANT TO GYPSUM DISSOLUTION
C     IONIC CONCENTRATIONS AND PH IN LAYERS 1 AND 2; FOR THE CASE WHERE
C     LIME HAS BEEN INCORPORATED INTO THE UNSATURATED TAILINGS LAYER.
C
C     FIRST SEVERAL CURRENT AND PREVIOUS VARIABLE VALUES ARE RESET.
C
      PYRITE(2) = PYRITE(3)
      DGYP(2) = DGYP(3)
      WCONC(9,2,2) = WCONC(9,2,3)
      WCONC(6,2,2) = WCONC(6,2,3)
C
C     CALCULATE SO4 PRODUCTION VIA PYRITE OXIDATION.
C
      IF(KRATE.LE.30.0/DT)THEN
         PYRITE(3) = PYRITE(2)*EXP(-1.0*KRATE*DT)
      ELSE
         PYRITE(3)=1.0E-6
      ENDIF
      IF (PYRITE(3).LE.1.E-6) PYRITE(3)=1.0E-6
      BETA = PYRITE(2)*(1.0-EXP(-1.0*KRATE*DT))
      WCONC(6,2,3) = (2.0*DUNSAT*BETA)/(NPRCP*DT)+0.1
C
C     THE PH AT THE BOTTOM OF THE UNSATURATED LAYER IS CALCULATED,
C     USING DIFFERENT EQUATIONS FOR THE DIFFERENT CASES WHICH EXIST.
C
      PHIN = PH(2)
      IF (CHECKU.EQ.'DEPLETED') THEN
         IF (CHECKL.EQ.'DEPLETED') THEN
C           GYPSUM DEPLETED; LIME DEPLETED
            WCONC(6,1,3) = WCONC(6,2,3)
            PHIN = 3.5
            IND = 1
            CALL NEWTON(IND,PHIN,PH(2),PH1)
         ELSE
C           GYPSUM DEPLETED; LIME PRESENT
            WCONC(6,1,3) = WCONC(6,2,3)
            IND = 5
            CALL NEWTON(IND,PHIN,PH(2),PH1L)
         ENDIF
      ELSE
         IF (CHECKL.EQ.'DEPLETED') THEN
C           GYPSUM PRESENT; LIME DEPLETED
            IND = 2
            PHIN = 3.5
            CALL NEWTON(IND,PHIN,PH(2),PH2)
         ELSE
C           GYPSUM PRESENT; LIME PRESENT
```

```
            PH(2) = PH2LIM
         ENDIF
      ENDIF
C
C     CHECK FOR GYPSUM DEPLETION.
C
      IF (CHECKU.NE.'DEPLETED') THEN
C
C     CALCULATE CHANGE IN DEPTH OF DEPLETED ZONE OVER DT.
C
         IF (CHECKL.EQ.'DEPLETED') THEN
            T1 = (4.0*(BETA**2.0)*(DGYP(2)**2.0))/((GYPI+BETA)**2.0)
            T2 = (((NPRCP*DT)**2.)*(EQUIL**2.))/((GYPI**2.)+GYPI*BETA)
            T3 = (2.0*BETA*DGYP(2))/(GYPI+BETA)
            DELTAH = ((T1+T2)**0.5)-T3
         ELSE
            T1 = (10.**(2.*PH(2)-16.47))/FACTCO-10.**(-4.0)
            DELTAH = (T1*1000.*NPRCP*DT-2.*DGYP(2)*BETA)/GYPI
         ENDIF
         DGYP(3) = DGYP(2)+DELTAH
C
C     CHECK NEW DEPTH OF DEPLETED ZONE.
C
         IF (DGYP(3).GE.DUNSAT) THEN
C
C     RESET INDICATOR VARIABLES.
C
            DGYP(3) = DUNSAT
            FGYP = 0.0
            TFINAL = T
            CHECKU = 'DEPLETED'
         ENDIF
      ENDIF
C
C     CHECK ONCE AGAIN FOR GYPSUM DEPLETION.
C
      IF (CHECKU.NE.'DEPLETED') THEN
C
C        CALCULATE CALCIUM AND SULPHATE CONCENTRATIONS,AND PH IN LAYER
C        1. FIRST FOR THE CASE WHERE LIME IS PRESENT AND DISSOLVING.
C
         WCONC(6,1,3) = WCONC(6,2,3)*(DGYP(3)/DUNSAT)
         WCONC(7,1,3) = WCONC(6,1,3)
         IF (CHECKL.NE.'DEPLETED') THEN
            WCONC(7,2,3) = 1000.*(10.**(2.*PH(2)-16.47))/FACTCO
            WCONC(8,2,3) = 1000.*(10.**(11.86-2.*PH(2)))/FACTCO
            PHIN = PH(1)
            IND = 5
            CALL NEWTON(IND,PHIN,PH(1),PH1L)
C
C           CALCULATE LIME DEPLETION OVER DT.
C
            CALIME = WCONC(8,2,3)-WCONC(7,2,3)+(2.*DUNSAT*BETA)/
```

```
     &              (NPRCP*DT)+0.08
            CALDEP = CALDEP+CALIME*NPRCP*DT
            IF (CALDEP.GE.LIMEIN) THEN
               CHECKL = 'DEPLETED'
               T1 = 1.0-(KPRIME*ALOG((1.0+KPRIME)/KPRIME))
               SFLUX = (1.067*SULPRD*RHOTAL*O2CONC*O2DIFF*T1)**0.5
               KRATE = SFLUX/(2.0*DUNSAT*PYRITE(3))
            ENDIF
         ELSE
C           LIME DEPLETED CASE.
            T7 = (FACTCO**3.)*(10.**(8.99-3.*PH(2)))
            T8 = (FACTCO**(3./4.))*10.**(9.7-3.*PH(2))
            DELT = 1.0+T7+T8
            T9 = KSUBSO*DELT/(FACTCO**2.)+(0.25*(WCONC(6,2,3)**2.))
            T10 = SQRT(T9)
            WCONC(8,2,3) = T10-0.5*WCONC(6,2,3)
            WCONC(7,2,3) = T10+0.5*WCONC(6,2,3)
            PHIN = 3.5
            IND = 1
            CALL NEWTON(IND,PHIN,PH(1),PH1)
         ENDIF
      ELSE
C
C     CALCULATE IONIC CONCENTRATIONS AND PH AFTER UNSATURATED ZONE
C     IS DEPLETED OF GYPSUM.
C
         WCONC(7,2,3) = WCONC(6,2,3)
         WCONC(6,1,3) = WCONC(6,2,3)
         WCONC(7,1,3) = WCONC(7,2,3)
         PH(1) = PH(2)
C
C     CALCIUM CONCENTRATION IS CALCULATED DIFFERENTLY DEPENDING ON THE
C     PRESENCE OR ABSENCE OF LIME.
C     LIME DEPLETED CASE FIRST.
C
         IF (CHECKL.EQ.'DEPLETED') THEN
            WCONC(8,2,3) = 0.0
         ELSE
C           LIME PRESENT CASE.
C
C           ????????????????????????????????????
C           T1    = (10.**(11.87-2.*PH(2)))/FACTCO
C           CALIM  = T1*1000.+(2.*DUNSAT*BETA)/(NPRCP*DT)+0.08
C           ??????????????????????????????????????????????????
C
             T1 =  (10.**(11.86-2.*PH(2)))/FACTCO
             CALIME = T1*1000. - 0.02
C
C      WRITE(*,669) T1,T1X,CALIME,CALIMX,CHECKL
C669    FORMAT(' ',"2  T1,T1X,CALIME,CALIMX,CHECKL",4(E10.4,1X),A8 )
C
C
            WCONC(8,2,3) = CALIME
            CALDEP = CALDEP+CALIME*NPRCP*DT
            IF (CALDEP.GE.LIMEIN) THEN
               CHECKL = 'DEPLETED'
               T1 = 1.0-(KPRIME*ALOG((1.0+KPRIME)/KPRIME))
               SFLUX = (1.067*SULPRD*RHOTAL*O2CONC*O2DIFF*T1)**0.5
               KRATE = SFLUX/(2.0*DUNSAT*PYRITE(3))
            ENDIF
         ENDIF
      ENDIF
C
C     FE3 CONCENTRATION IS A FUNCTION OF SO4 AND PH.
C
      T10 = 10.0**(5.97-3.0*PH(2))+10.0**(3.78-2.0*PH(2))
     &     +10.0**(0.3-PH(2))
      T11 = (FACTCO**3.0)*10.0**(8.99-3.0*PH(2))
      T12 = 1.0+(FACTCO**(3.0/4.0)*10.0**(9.7-3.0*PH(2)))
      WCONC(9,2,3) = T10+(WCONC(7,2,3)/1000.)*T11/(T12+T11)
      WCONC(9,2,3) = WCONC(9,2,3)*1000.
C
C     PRINT DETAILED RESULTS IF SPECIFIED
C
      IF (CODION.EQ.1.) THEN
      WRITE(*,900) T,DGYP(3),PH(1),PH(2)
      WRITE(*,910) WCONC(6,1,3),WCONC(6,2,3),WCONC(9,2,3),CALDEP
      WRITE(*,920) WCONC(7,1,3),WCONC(7,2,3),WCONC(8,2,3)
900   FORMAT(1X,'LAYERS 1&2 T=',F6.1,' DEPTH=',F6.3,
     &      ' PH1=',F5.2,' PH2=',F5.2)
910   FORMAT(1X,'[SO4]P1=',E10.4,' [SO4]P2=',E10.4,' [FE3]T2=',E10.4,
     &      ' CALDEP=',E10.4)
920   FORMAT(1X,'[SO4]T1=',E10.4,' [SO4]T2=',E10.4,' [CA2]T2=',E10.4)
      ENDIF

      RETURN
      END
C
C
C
C
```

```
      SUBROUTINE PH1L(F,FPRIME,P)
      INCLUDE 'MODEL.INC'
      INCLUDE 'VAR.INC'
C
C     THIS ROUTINE IS INVOLVED IN THE ITERATIVE CALCULATION OF PH IN
C     THE UNSATURATED ZONE; FOR THE GYPSUM DEPLETED,LIME PRESENT CASE.
C
C     FIRST THE FUNCTION (F) IS EVALUATED.
C
      F1 = FACTCO
      SO4 = WCONC(6,1,3)/1000.
      T1 = 2.*(10.**(11.87-2.*P))/F1+10.**(0.3-P)
      T2 = (10.**(P-9.73))/(F1**0.25)
      F = T1-2.*SO4-T2
C
C     THEN THE DERIVATIVE OF THE FUNCTION (FPRIME) IS EVALUATED.
C
      XL = ALOG(10)
      DT1 = -4.*XL*(10.**(11.87-2.*P))/F1-XL*10.**(0.3-P)
      FPRIME = DT1-XL*T2
C
C     PRINT DETAILED RESULTS IF SPECIFIED.
C
      IF (CODPH.EQ.1) THEN
      WRITE(*,900) T,P,F,FPRIME
900   FORMAT(1X,'PH1L: T=',F6.1,' PH=',F5.2,'F=',E10.4,'FPRIME=',E10.4)
      ENDIF

      RETURN
      END
C
C
C
C
```

```
      SUBROUTINE PH2GL(F,FPRIME,P)
      INCLUDE 'MODEL.INC'
      INCLUDE 'VAR.INC'
C
C     THIS ROUTINE IS INVOLVED IN THE ITERATIVE CALCULATION OF PH IN
C     THE UNSATURATED ZONE; FOR THE GYPSUM AND LIME PRESENT CASE.
C
C     FIRST THE FUNCTION (F) IS EVALUATED.
C
      F1 = FACTCO
      T1 = (2.*10.**(11.87-2.*P))/F1+10.**(0.3-P)
      T2 = (2.*10.**(2.*P-16.47))/F1+(10.**(P-9.73))/F1**0.25
      F = T1-T2
C
C     THEN THE DERIVATIVE OF THE FUNCTION (FPRIME) IS EVALUATED.
C
      XL = ALOG(10)
      DT1 = -4.*XL*(10.**(11.87-2.*P))/F1-XL*10.**(0.3-P)
      DT2 = 4.0*XL*(10.**(2.*P-16.47))/F1+XL*(10.**(P-9.73))/F1**0.25
      FPRIME = DT1-DT2
C
C     PRINT DETAILED RESULTS IF SELECTED
C
      IF (CODPH.EQ.1) THEN
      WRITE(*,900) T,P,F,FPRIME
900   FORMAT(1X,'PH2GL:T=',F6.1,'PH=',F5.2,'F=',E10.4,'FPRIME=',E10.4)
      ENDIF

      RETURN
      END
      SUBROUTINE IONS3
      EXTERNAL PH3
      INCLUDE 'MODEL.INC'
      INCLUDE 'VAR.INC'
      REAL*4 K
C
C     THIS ROUTINE CALCULATES IONIC CONCENTRATIONS IN LAYER 3
C     (THE MIXING ZONE)
C
C     FIRST, SEVERAL VALUES FROM THE PREVIOUS TIME STEP ARE RESET.
C
      WCONC(6,3,2) = WCONC(6,3,3)
      WCONC(7,3,2) = WCONC(7,3,3)
      WCONC(8,3,2) = WCONC(8,3,3)
      WCONC(10,3,2) = WCONC(10,3,3)
C
C     FE2 IS CALCULATED AS A FUNCTION OF FE3 IN LAYER 2.
C
      T1 = EXP((-1.0*NPRCP*DT)/(POROS*DMIX))
      WCONC(10,3,3) = 1.5*WCONC(9,2,3)+(WCONC(10,3,2)-1.5*
     &                WCONC(9,2,3))*T1
C
C     CALCULATE SULPHATES IN LAYER 3 RESULTING FROM PYRITE OXIDATION
C     IN UPPER LAYERS.
C
         WCONC(6,3,3) = WCONC(6,2,3)+(WCONC(6,3,2)-WCONC(6,2,3))*T1
C
C     CHECK FOR DEPLETION OF GYPSUM.
C
      IF (CHECKM.NE.'DEPLETED') THEN
C
C     CA AND SO4 CONCENTRATIONS ARE FUNCTIONS OF PYRITE OXIDATION
C     IN LAYERS 1 AND 2.
C
         T2 = ((KSUBSO/FACTCO**2.)+0.25*WCONC(6,3,3)**2.)**0.5
         WCONC(7,3,3) = T2 + 0.5*WCONC(6,3,3)
         WCONC(8,3,3) = T2 - 0.5*WCONC(6,3,3)
C
C     IF THE UNSATURATED ZONE IS DEPLETED OF GYPSUM; GYPSUM IS
C     DISSOLVING IN THE MIXING ZONE.
C
         IF (CHECKU.EQ.'DEPLETED') THEN
            IF (T.EQ.TFINAL) THEN
               SSTAR = WCONC(7,3,3)
               ELSE
               SSTARI = SSTAR
               SSTAR = WCONC(6,2,3)+(SSTARI-WCONC(6,2,3))*T1
            ENDIF
            DELTAG = (NPRCP*DT/DMIX)*(WCONC(7,3,3)-SSTAR)
            GYPMIX = GYPMIX+DELTAG
C
C     CHECK FOR GYPSUM DEPLETION IN MIXING ZONE.
C
```

```
            IF (GYPMIX.GE.GYPI) THEN
               CHECKM = 'DEPLETED'
               DELTAG = 0.0
               GYPMIX = GYPI
            ENDIF
         ENDIF
      ENDIF
C
C     IF GYPSUM IS DEPLETED IN MIXING ZONE IONIC CONCENTRATIONS
C     ARE CALCULATED DIFERENTLY.
C
      IF (CHECKM.EQ.'DEPLETED') THEN
         WCONC(7,3,3) = WCONC(6,2,3)+(WCONC(7,3,2)-WCONC(6,2,3))*T1
         WCONC(8,3,3) = WCONC(8,3,2)*T1
         IF (WCONC(8,3,3).LT.1.0E-6) WCONC(8,3,3) = 0.0
      ENDIF
C
C     CALCULATE INITIAL GUESS FOR PH CALCULATION.
C
      IF (WCONC(7,3,3).EQ.0.0) WCONC(7,3,3)=1.0E-20
      T3 = (ALOG10(WCONC(7,3,3)/1000.)+1.555)**2.
      K = 0.95553+1.44448*T3
      T4 = (K*(ALOG10(WCONC(7,3,3)/1000.)+2.03))
      PHIN = 4.91345-((3.5731/(22./7.))*ATAN(T4))
C
C     PH IS CALCULATED ITERATIVELY USING SUBROUTINES 'NEWTON' AND 'PH3'
C
      IND = 3
      CALL NEWTON(IND,PHIN,PH(3),PH3)
C
C     VOLUMETRIC FLOW OUT OF THE MIXING ZONE TO THE WATERSHED IS
C     CALCULATED AS A FUNCTION OF THE SEEPAGE RATE INTO LAYER 4.
C
      SFLOW = (NPRCP*ATAIL)-VSR
C
C     PRINT DETAILED RESULTS IF SPECIFIED.
C
      IF (CODION.EQ.1.) THEN
         WRITE(*,900) T,WCONC(6,3,3),WCONC(7,3,3),WCONC(8,3,3)
         WRITE(*,910) GYPMIX,WCONC(10,3,3),PH(3)
900   FORMAT(1X,'LAYER 3 T=',F6.1,' [SO4]P3=',E10.4,' [SO4]T3=',E10.4,
     &       ' [CA2]T3=',E10.4)
910   FORMAT(1X,'GYPMIX=',E10.4,' [FE2]T3=',E10.4,' PH3=',F5.2)
      ENDIF

      RETURN
      END
C
C
C
C
```

```
      SUBROUTINE PH3(F,FPRIME,P)
      INCLUDE 'MODEL.INC'
      INCLUDE 'VAR.INC'
C
C     THIS ROUTINE IS INVOLVED IN THE ITERATIVE CALCULATION OF PH
C     IN THE MIXING ZONE.
C
C     FIRST THE FUNCTION (F) IS EVALUATED.
C
      F1 = FACTCO
      SO4 = WCONC(7,3,3)/1000.
      CA2 = WCONC(8,3,3)/1000.
      FE2 = WCONC(10,3,3)/1000.
      T1 = 3.*((10.**(6.8-3.*P))/F1**(9./4.))
      T2 = 2.*((10.**(1.83-2.*P))/F1)
      T3 = (10.**(3.1-P))/F1**(1./4.)
      T4 = F1**(3./4.)*10.**(9.7-3*P)
      T5 = (10.**(P-10.47))/F1**(1./4.)
      F = 2*CA2+2*FE2+T1+T2+T3-((2.-T4)/(1.+T4))*SO4-T5
C
C     THEN THE DERIVATIVE OF THE FUNCTION (FPRIME) IS CALCULATED.
C
      XL = ALOG(10.)
      DT4 = -3.*XL*T4
      T6 = -1.*DT4*(((2.-T4)/((1.+T4)**2.))+(1./(1.+T4)))
      FPRIME = -3.*XL*T1-2.*XL*T2-1.*XL*T3-T6*SO4-1.*XL*T5
C
C     PRINT DETAILED RESULTS IF SELECTED
C
      IF (CODPH.EQ.1) THEN
      WRITE(*,900) T,P,F,FPRIME
900   FORMAT(1X,'PH3: T=',F6.1,' PH=',F5.2,' F=',E10.4,' FPRIME=',E10.4)
      ENDIF

      RETURN
      END
      SUBROUTINE IONS4
      EXTERNAL PH4
      INCLUDE 'MODEL.INC'
      INCLUDE 'VAR.INC'
      REAL*4 K
C
C     THIS ROUTINE CALCULATES IONIC CONCENTRATIONS IN LAYER 4.
C
C     FIRST, SEVERAL VALUES FROM THE PREVIOUS TIME STEP ARE RESET.
C
      WCONC(6,4,2) = WCONC(6,4,3)
      WCONC(10,4,2) = WCONC(10,4,3)
C
C     CALCULATION OF [S04] IN LAYER 4 RESULTING FROM PYRITE
C     OXIDATION IN LAYERS 1 AND 2.
C
      T1 = EXP((-1.*FNPRCP*AVPRCP*DT)/(POROS*DBOT))
      WCONC(6,4,3) = WCONC(6,3,2)+(WCONC(6,4,2)-WCONC(6,3,2))*T1
C
C     CALCULATION OF TOTAL S04,CA2 AND FE2.
C
      T2 = ((KSUBSO/FACTCO**2)+0.25*WCONC(6,4,3)**2.)**0.5
      WCONC(7,4,3) = T2+0.5*WCONC(6,4,3)
      WCONC(8,4,3) = T2-0.5*WCONC(6,4,3)
      WCONC(10,4,3) = WCONC(10,3,2)+(WCONC(10,4,2)-WCONC(10,3,2))*T1
C
C     THE PH IN LAYER 4 IS CALCULATED USING THE SAME EQUATIONS
C     AS LAYER 3. THESE ARE FOUND IN SUBROUTINE 'PH4'.
C
C     CALCULATE INITIAL GUESS FOR PH CALCULATION.
C
        IF (WCONC(7,4,3).EQ.0.0) WCONC(7,4,3)=1.0E-20
        T3 = (ALOG10(WCONC(7,4,3)/1000.)+1.555)**2.
        K = 0.95553+1.44448*T3
        T4 = (K*(ALOG10(WCONC(7,4,3)/1000.)+2.03))
        PHIN = 4.91345-((3.5731/(22./7.))*ATAN(T4))
C
C     PH IS CALCULATED ITERATIVELY USING SUBROUTINES 'NEWTON' AND 'PH4'
C
        IND = 4
        CALL NEWTON(IND,PHIN,PH(4),PH4)
C
C     PRINT DETAILED RESULTS IF SPECIFIED.
C
      IF (CODION.EQ.1.) THEN
      WRITE(*,900) T,WCONC(6,4,3),WCONC(7,4,3),WCONC(8,4,3)
      WRITE(*,910) WCONC(10,4,3),PH(4)
900   FORMAT(1X,'LAYER 4 T=',F6.1,' [S04]P4=',E10.4,' [S04]T4=',E10.4,
     & ' [CA2]T4=',E10.4)
910   FORMAT(1X,'[FE2]T4=',E10.4,' PH4=',F5.2)
      ENDIF

      RETURN
      END
C
C
C
C
```

```
      SUBROUTINE PH4(F,FPRIME,P)
      INCLUDE 'MODEL.INC'
      INCLUDE 'VAR.INC'
C
C     THIS ROUTINE IS INVOLVED IN THE ITERATIVE CALCULATION OF PH
C     IN LAYER 4
C
C     FIRST THE FUNCTION (F) IS EVALUATED.
C
      F1 = FACTCO
      S04 = WCONC(7,4,3)/1000.
      CA2 = WCONC(8,4,3)/1000.
      FE2 = WCONC(10,4,3)/1000.
      T1 = 3.*((10.**(6.8-3.*P))/F1**(9./4.))
      T2 = 2.*((10.**(1.83-2.*P))/F1)
      T3 = (10.**(3.1-P))/F1**(1./4.)
      T4 = F1**(3./4.)*10.**(9.7-3*P)
      T5 = (10.**(P-10.47))/F1**(1./4.)
      F = 2*CA2+2*FE2+T1+T2+T3-((2.-T4)/(1.+T4))*S04-T5
C
C     THEN THE DERIVATIVE OF THE FUNCTION (FPRIME) IS CALCULATED.
C
      XL = ALOG(10.)
      DT4 = -3.*XL*T4
      T6 = -1.*DT4*(((2.-T4)/((1.+T4)**2.))+(1./(1.+T4)))
      FPRIME = -3.*XL*T1-2.*XL*T2-1.*XL*T3-T6*S04-1.*XL*T5
C
C     PRINT DETAILED RESULTS IF SELECTED
C
      IF (CODPH.EQ.1) THEN
      WRITE(*,900) T,P,F,FPRIME
900   FORMAT(1X,'PH4: T=',F6.1,' PH=',F5.2,' F=',E10.4,' FPRIME=',E10.4)
      ENDIF

      RETURN
      END
      SUBROUTINE RADIUM
      INCLUDE 'MODEL.INC'
      INCLUDE 'VAR.INC'
C
C     THIS ROUTINE CALCULATES SOLID AND LIQUID PHASE RADIUM CONCEN-
C     TRATIONS. FIRST, SEVERAL VARIABLES ARE RESET.
C
      DBAR(2) = DBAR(3)
      MBAR(2) = MBAR(3)
      XBAR(2) = XBAR(3)
      WCONC(4,3,2) = WCONC(4,3,3)/RACF
      WCONC(4,4,2) = WCONC(4,4,3)/RACF
C
C     VALUES IN THE UNSATURATED ZONE ARE DETERMINED.
C     LAYER 1 SOLID PHASE FIRST.
C
      CRATHS = CRATHS*RADEC+T230S*TDECAY
      CRATL2 = X230LM*(WCONC(2,2,3)/THORCF)*TDECAY
      CRADT = CRADTI*EXP(-1.0*LAMRAD*T)
      XRAD = XRADI*EXP(-1.0*LAMRAD*T)
      CONC(4,1,3) = CRADT+CRATHS
C
C     IF THE UNSATURATED ZONE IS DEPLETED OF BASO4, THE CALCULATIONS
C     ARE VERY SIMPLE.
C
      IF (CHKBAU.EQ.'DEPLETED') THEN
         CONC(4,2,3) = CONC(4,1,3)
         WCONC(4,2,3) = CRATL2
C
C     OTHERWISE, THE CONCENTRATIONS DEPEND ON THE DISSOLUTION AND
C     REPRECIPITATION OF BASO4. FIRST THE DEPTH OF THE BASO4 DEPLETED
C     ZONE IS CALCULATED.
C
      ELSE
         T1 = (EQBAR**2.*NPRCP*DT)/CBARI
         T2 = (NPRCP*DT)/BETA+2.0*FACTCO**2.*KFBAR*DBAR(2)
         T3 = 2.0*DBAR(2)+(EQBAR*NPRCP*DT)/BETA
         T4 = (EQBAR**2.*FACTCO**2.*KFBAR*NPRCP*DT)/CBARI
         T5 = DBAR(2)+(EQBAR*NPRCP*DT)/(2.0*BETA)-T4/2.0
         DHBAR = (T1*T2+0.25*(T3-T4)**2.)**0.5-T5
         DBAR(3) = DBAR(2)+DHBAR
C
C     IF THE DEPTH OF DEPLETION IS LESS THAN THE DEPTH OF THE
C     UNSATURATED ZONE, THE AMOUNT OF REPRECIPITATED BASO4 AND THE
C     MOL FRACTION OF RA IN THAT BASO4 IS CALCULATED.
C
         IF (DBAR(3).LT.DUNSAT) THEN
            DELTA = 1.0+FACTCO**3.*10.**(8.99-3.*PH(2))
     &                 +FACTCO**0.75*10.**(9.7-3.*PH(2))
            SO4 = WCONC(7,2,3)/DELTA
            CBAR = (EQBAR**2.)/(EQBAR+SO4)*(1.0+FACTCO**2.*KFBAR*SO4)
            MBAR(3) = MBAR(2)+CBARI*DHBAR-NPRCP*DT*CBAR
            T1 = CBARI*XRAD*DHBAR+NPRCP*CRATL2*DT
            T2 = MBAR(2)*XBAR(2)-0.5*DT*NPRCP*CBAR*XBAR(2)*KRAD
            XBAR(3) = (T1+T2)/(MBAR(3)+0.5*DT*NPRCP*CBAR*KRAD)
            WCONC(4,2,3) = KRAD*CBAR*XBAR(3)
            CONC(4,2,3) = CRATHS+XRAD*CBARI+((XBAR(3)*MBAR(3))/
     &                    (DUNSAT-DBAR(3)))
C
C     OTHERWISE, SEVERAL VARIABLES ARE RESET.
C
         ELSE
            DBAR(3) = DUNSAT
            CHKBAU = 'DEPLETED'
            CBAR = 0.0
            MBAR(3) = 0.0
            WCONC(4,2,3) = CRATL2
            CONC(4,2,3) = CONC(4,1,3)
         ENDIF
      ENDIF
C
C     NEXT, THE LIQUID PHASE RADIUM CONCENTRATION IN THE MIXING ZONE
C     IS DETERMINED.
C
      IF (CHKTHU.EQ.'DEPLETED') THEN
         CRATL3 = X230LM*(WCONC(2,3,3)/THORCF)*TDECAY
      ELSE
         CRATL3 = 0.0
      ENDIF

      IF (CHKBAS.EQ.'DEPLETED') THEN
         CRADIN = CRATL3
      ELSE

         IF (CHKBAU.EQ.'ENRICHED') THEN
            CRADIN = WCONC(4,2,3)+CRATL3
         ELSE
            T1 = (EQBAR**2.*XRAD)/(EQBAR+WCONC(7,3,3))
            CRADIN = T1*(1.0+KFBAR*FACTCO**2.*WCONC(7,3,3))+CRATL3
         ENDIF

         SUMBAR = SUMBAR+NPRCP*DT*CRADIN

         IF (SUMBAR.GE.BASATI) THEN
            CHKBAS = 'DEPLETED'
            CRADIN = CRATL3
         ENDIF

      ENDIF

      T1 = (NPRCP*DT)/(POROS*DMIX*(1.0+KDRAD*RHOTAL/POROS))
      WCONC(4,3,3) = CRADIN+(WCONC(4,3,2)*RADEC-CRADIN)*EXP(-1.*T1)
C
C     THE LIQUID PHASE RADIUM CONCENTRATION IN THE BOTTOM LAYER
C     IS THEN DETERMINED.
C
```

```
      IF (CHKTHS.EQ.'DEPLETED') THEN
         CRATL4 = X230LM*(WCONC(2,4,3)/THORCF)*TDECAY
      ELSE
         CRATL4 = 0.0
      ENDIF

      IF (CHKBAS.EQ.'ENRICHED') THEN
         CRADIN = WCONC(4,3,3)+CRATL4
      ELSE
         T1 = (EQBAR**2.*XRAD)/(EQBAR+WCONC(7,4,3))
         CRADIN = T1*(1.0+KFBAR*FACTCO**2.*WCONC(7,3,3))+CRATL4
      ENDIF

      T1 = (FNPRCP*AVPRCP*DT)/(POROS*DBOT*(1.0+KDRAD*RHOTAL/POROS))
      WCONC(4,4,3) = CRADIN+(WCONC(4,4,2)*RADEC-CRADIN)*EXP(-1.*T1)
C
C     FINALLY,ALL RADIUM CONCENTRATIONS ARE CONVERTED FROM A MOLAR
C     BASIS TO AN ACTIVITY BASIS.
C
      CONC(4,1,3) = CONC(4,1,3)*RACF
      CONC(4,2,3) = CONC(4,2,3)*RACF
      WCONC(4,2,3) = WCONC(4,2,3)*RACF
      WCONC(4,3,3) = WCONC(4,3,3)*RACF
      WCONC(4,4,3) = WCONC(4,4,3)*RACF
C
C     PRINT SUMMARY RESULTS IF SPECIFIED.
C
      IF (CODNUC.EQ.1.0) THEN
         WRITE(*,900) T
         WRITE(*,910) CONC(4,1,3),CONC(4,2,3),WCONC(4,2,3),WCONC(4,3,3)
     &                ,WCONC(4,4,3)
         WRITE(*,920) TDECAY,DBAR(3),SUMBAR,BETA
         WRITE(*,930) CRATL2,CRATL3,CRATL4
      ENDIF
900   FORMAT(1X,'T=',F5.0,4X,'SOLID1',5X,'SOLID2',6X,'LIQUID2',5X,
     &       'LIQUID3',5X, 'LIQUID4')
910   FORMAT(1X,'RADIUM',3X,E10.4,4(2X,E10.4))
920   FORMAT(1X,'TDECAY=',E10.4,' DBAR=',E10.4,' [BAR]DEP=',E10.4,
     &       ' BETA=',E10.4)
930   FORMAT(1X,'[RA]TH2=',E10.4,' [RA]TH3=',E10.4,' [RA]TH4=',E10.4)

      RETURN
      END
      SUBROUTINE LEAD
      INCLUDE 'MODEL.INC'
      INCLUDE 'VAR.INC'
C
C     THIS ROUTINE CALCULATES LIQUID AND SOLID PHASE CONCENTRATIONS
C     OF LEAD-210.
C     FIRST,SEVERAL VARIABLES ARE RESET.
C
      DLEAD(2) = DLEAD(3)
      WCONC(3,3,2) = WCONC(3,3,3)/PBCF
      WCONC(3,4,2) = WCONC(3,4,3)/PBCF
C
C     SOLID PHASE LEAD CONCENTRATION IS THEN DETERMINED.
C
      CPBRAS = CPBRAS*PBDEC+(CONC(4,1,3)/RACF)*RDECAY
      CPBRL2 = (WCONC(4,2,3)/RACF)*RDECAY
      CLEADT = CPBTI*EXP(-1.0*LAMPB*T)
      CONC(3,1,3) = CLEADT+CPBRAS
      XLEAD = XPBI*EXP(-1.0*LAMPB*T)
C
C     LIQUID PHASE CALCULATIONS FOR THE UNSATURATED ZONE.
C     IF THE UNSATURATED ZONE IS DEPLETED OF PBSO4, THE CALCULATIONS
C     ARE VERY SIMPLE.
C
      IF (CHKPBU.EQ.'DEPLETED') THEN
         WCONC(3,2,3) = CPBRL2
C
C     OTHERWISE THE CONC'N DEPENDS ON THE DISSOLUTION AND REPRECIP-
C     ITATION OF PBSO4. THE DEPTH OF DEPLETION IS DETERMINED FIRST.
C
      ELSE
         T1 = (EQLEAD**2.*NPRCP*DT)/CLEADI
         T2 = (NPRCP*DT)/BETA+2.0*FACTCO**2.*KFLEAD*DLEAD(2)
         T3 = 2.0*DLEAD(2)+(EQLEAD*NPRCP*DT)/BETA
         T4 = (EQLEAD**2.*FACTCO**2.*KFLEAD*NPRCP*DT)/CLEADI
         T5 = DLEAD(2)+(EQLEAD*NPRCP*DT)/(2.0*BETA)-T4/2.0
         DHLEAD = (T1*T2+0.25*(T3-T4)**2.)**0.5-T5
         DLEAD(3) = DLEAD(2)+DHLEAD

         IF (DLEAD(3).GE.DUNSAT) THEN
            DLEAD(3) = DUNSAT
            CHKPBU = 'DEPLETED'
            WCONC(3,2,3) = CPBRL2
         ELSE
            DELTA = 1.0+FACTCO**3.*10.**(8.99-3.*PH(2))
     &                  +FACTCO**0.75*10.**(9.7-3.*PH(2))
            SO4 = WCONC(7,2,3)/DELTA
            CLEAD=(EQLEAD**2.)/(EQLEAD+SO4)*(1.+FACTCO**2.*KFLEAD*SO4)
            WCONC(3,2,3) = XLEAD*CLEAD+CPBRL2
         ENDIF

      ENDIF
C
```

```
C     LIQUID PHASE CONCENTRATION OF LEAD IN THE MIXING ZONE.
C
      IF (CHKBAU.EQ.'DEPLETED') THEN
         CPBRL3 = (WCONC(4,3,3)/RACF)*RDECAY
      ELSE
         CPBRL3 = 0.0
      ENDIF

      IF (CHKPBS.EQ.'DEPLETED') THEN
Table A.1 (continued)

         CPBIN = CPBRL3
      ELSE

         IF (CHKPBU.EQ.'ENRICHED') THEN
            CPBIN = WCONC(3,2,3)+CPBRL3
         ELSE
            T1 = (EQLEAD**2.*XLEAD)/(EQLEAD+WCONC(7,3,3))
            CPBIN = T1*(1.0+KFLEAD*FACTCO**2.*WCONC(7,3,3))+CPBRL3
         ENDIF

         SUMPB = SUMPB+NPRCP*DT*CPBIN

         IF (SUMPB.GE.PBSATI) THEN
            CHKPBS = 'DEPLETED'
            CPBIN = CPBRL3
         ENDIF

      ENDIF

      T1 = (NPRCP*DT)/(POROS*DMIX*(1.0+KDLEAD*RHOTAL/POROS))
      WCONC(3,3,3) = CPBIN+(WCONC(3,3,2)*PBDEC-CPBIN)*EXP(-1.0*T1)
C
C     LIQUID PHASE LEAD CONCENTRATION IN THE BOTTOM LAYER.
C
      IF (CHKBAS.EQ.'DEPLETED') THEN
         CPBRL4 = (WCONC(4,4,3)/RACF)*RDECAY
      ELSE
         CPBRL4 = 0.0
      ENDIF

      IF (CHKPBS.EQ.'ENRICHED') THEN
         CPBIN = WCONC(3,3,3)+CPBRL4
      ELSE
         T1 = (EQLEAD**2.*XLEAD)/(EQLEAD+WCONC(7,4,3))
         CPBIN = T1*(1.0+KFLEAD*FACTCO**2.*WCONC(7,3,3))+CPBRL4
      ENDIF

      T1 = (FNPRCP*AVPRCP*DT)/(POROS*DBOT*(1.0+KDLEAD*RHOTAL/POROS))
      WCONC(3,4,3) = CPBIN+(WCONC(3,4,2)*PBDEC-CPBIN)*EXP(-1.0*T1)
C
C     THE CONCENTRATIONS ARE THEN CONVERTED FROM A MOLAR BASIS
C     TO AN ACTIVITY BASIS.
```

```
C
      CONC(3,1,3) = CONC(3,1,3)*PBCF
      WCONC(3,2,3) = WCONC(3,2,3)*PBCF
      WCONC(3,3,3) = WCONC(3,3,3)*PBCF
      WCONC(3,4,3) = WCONC(3,4,3)*PBCF
C
C     PRINT SUMMARY RESULTS IF SPECIFIED.
C
      IF (CODNUC.EQ.1.0) THEN
         WRITE(*,900) T
         WRITE(*,910) CONC(3,1,3),WCONC(3,2,3),WCONC(3,3,3),
     &                WCONC(3,4,3)
         WRITE(*,920) RDECAY,DLEAD(3),SUMPB
         WRITE(*,930) CPBRL2,CPBRL3,CPBRL4
      ENDIF
900   FORMAT(1X,'T=',F5.0,4X,'SOLID1',5X,'LIQUID2',5X,'LIQUID3',5X,
     &       'LIQUID4')
910   FORMAT(1X,'LEAD',5X,E10.4,3(2X,E10.4))
920   FORMAT(1X,'RDECAY=',E10.4,' DLEAD=',E10.4,' [PB]DEP=',E10.4)
930   FORMAT(1X,'[PB]RA2=',E10.4,'[PB]RA3=',E10.4,' [PB]RA4=',E10.4)

      RETURN
      END
```

## Table A.2

## STORAGE ARRAYS FOR CALCULATED CONCENTRATIONS

WCONC (substance, location, time)
- stores liquid phase (porewater) concentrations

CONC (substance, location, time)
- stores solid phase concentrations

Substances 1 = Natural Uranium ($Bq.m^{-3}$)
2 = Total Thorium (Th-230 + Th-232) ($Bq.m^{-3}$)
3 = Lead-210 ($Bq.m^{-3}$)
4 = Radium-226 ($Bq.m^{-3}$)
5 = Radon-222 ($Bq.m^{-3}$)
6 = $[SO_4^{2-}]$ from pyrite oxidation ($mol.m^{-3}$)
7 = $[SO_4^{2-}]$ total sulphate ion ($mol.m^{-3}$)
8 = $[Ca^{2+}]$ total calcium ion ($mol.m^{-3}$)
9 = $[Fe^{III}]$ ferric ion ($mol.m^{-3}$)
10 = $[Fe^{II}]$ ferrous ion ($mol.m^{-3}$)

Locations 1 = tailings layer 1; surface layer of varying thickness
2 = tailings layer 2; at the bottom of the unsaturated zone
3 = tailings layer 3; the mixing zone
4 = tailings layer 4; the bottom layer

Times 1 = initial time (representative of t=o years)
2 = previous time step ($t-\Delta t$)
3 = current time (t)

Table A.3

## WATER SOURCE MODEL VARIABLE DICTIONARY

| Model Symbol | Description | Units | Nominal Value | Probability Distribution | Computer Origin | Computer Symbol |
|---|---|---|---|---|---|---|
| $\rho_t$ | tailings bulk density | $g.m^{-3}$ | $1.4x10^6$ | $N(1.4x10^6,0.1x10^6$ $1.1x10^6,1.7x10^6)$ | INPUT | RHOTAL |
| $X_{gyp}$ | mass fraction of gypsum in tailings | - | 0.055 | U(0.05,0.06) | INPUT | FRACGP |
| $g_o$ | initial concentration of gypsum in tailings | $mol.m^{-3}$ | calculated | calculated | SOURCE (INCONI) | GYPI |
| $J_s$ | net sulphate flux | $mol.m^{-2}.yr^{-1}$ | calculated | calculated | SOURCE (INCONI) | SFLUX |
| $R_s$ | sulphate production rate | $mol.g^{-1}.yr^{-1}$ | $1.4x10^{-6}$ | $LN(1.4x10^{-6},1.5,$ $0.4X10^{-6},4.2X10^{-6})$ | INPUT | SULPRD |
| $[O_2]$ | oxygen concentration at the surface | $mol.m^{-3}$ | 9.04 | Constant(9.04) | INPUT | O2CONC |
| $D_{O_2}$ | oxygen diffusivity through tailings | $m^2.yr^{-1}$ | 70.0 | T(30,70,130) | INPUT | O2DIFF |
| K' | ratio of $O_2$ half saturation constant ($KO_2$) to $[O_2]$ | - | $5x10^{-2}$ | $LN(5x10^{-2},1.7,$ $0.02,0.25)$ | INPUT | KPRIME |
| k | rate constant for pyrite oxidation | $yr^{-1}$ | calculated | calculated | SOURCE (INCONI) | KRATE |
| $[FeS_2]o$ | initial concentration of pyrite in tailings | $mol.m^{-3}$ | 700 | U(600,800) | INPUT | PYRITI<br>PYRITE(1) |
| $[FeS_2]_t$ | concentration of pyrite at time t | $mol.m^{-3}$ | calculated | calculated | SOURCE (IONS1) | PYRITE(3) |
| $[FeS_2]_{t-\Delta t}$ | as above, at $t-\Delta t$ | $mol.m^{-3}$ | calculated | calculated | SOURCE (IONS1) | PYRITE(2) |

Table A.3 cont'd

Page 2

| Model Symbol | Description | Units | Nominal Value | Probability Distribution | Computer Origin | Computer Symbol |
|---|---|---|---|---|---|---|
| $\Delta t$ | length of simulation time step | years | specified | specified | INPUT | DT |
| P | net precipitation* | $m.yr^{-1}$ | 0.4 | N(0.4,0.1,0.15,0.65) | INPUT | NPRCP |
| $\lambda_W$ | thickness of unsaturated zone | m | 1.0 | U(0.75,1.25) | INPUT | DUNSAT |
| $[SO_4^{2-}]_{p,\lambda w}$ | concentration of sulphate resulting from pyrite oxidation in unsaturated zone | $mol.m^{-3}$ | calculated | calculated | SOURCE (IONS) | WCONC(6,2,3) |
| $K_{s,CaSO_4}^{o}$ | solubility equilibrium constant for gypsum | $mol^2.m^{-6}$ | 25.0 | Constant(25.0) | INPUT | KSUBSO |
| f | activity coefficient (for divalent ions) | - | 0.4 | T(0.3,0.4,0.5) | INPUT | FACTCO |
| a | equilibrium expression for $CaSO_4$ | $mol.m^{-3}$ | calculated | calculated | SOURCE (INCONI) | EQUIL |
| B | pyrite oxidation factor | - | calculated | calculated | SOURCE (IONS1) | BETA |
| $\Delta h$ | advancement of gypsum depleted front during $\Delta t$ | m | calculated | calculated | SOURCE (IONS1) | DELTAH |
| $h_t$ | thickness of gypsum depleted front at t | m | calculated | calculated | SOURCE (IONS1) | DGYP(3) |
| $h_{t-\Delta t}$ | thickness of gypsum depleted front at $t-\Delta t$ | m | calculated | calculated | SOURCE (IONS1) | DGYP(2) |
| $\Delta m$ | mass of gypsum reprecipitated during $\Delta t$ | $mol.m^{-2}$ | calculated | calculated | SOURCE (IONS1) | DELTAR |

* Time variant parameter

Table A.3 cont'd

| Model Symbol | Description | Units | Nominal Value | Probability Distribution | Computer Origin | Computer Symbol |
|---|---|---|---|---|---|---|
| $m_t$ | total mass of gypsum reprecipitated to time t | mol.m$^{-2}$ | calculated | calculated | SOURCE (IONS1) | REPGYP |
| $f_{gypsum}$ | fraction of initial gypsum remaining in unsaturated zone at any time t | - | calculated | calculated | SOURCE (IONS1) | FGYP |
| $[Ca^{2+}]_1$ | concentration of $Ca^{2+}$ in gypsum depleted layer | mol.m$^{-3}$ | calculated | calculated | SOURCE (IONS1) | WCONC(8,1,3) |
| $[SO_4^{2-}]_1$ | concentration of $SO_4^{2-}$ in gypsum depleted layer | mol.m$^{-3}$ | calculated | calculated | SOURCE (IONS1) | WCONC(7,1,3) |
| d | correction factor for sulphate complexation | - | calculated | calculated | SOURCE (IONS1) | DELT |
| $[Ca^{2+}]_{\lambda w}$ | concentration of $Ca^{2+}$ at bottom of unsaturated zone | mol.$^{-3}$ | calculated | calculated | SOURCE (IONS1) | WCONC(8,2,3) |
| $[SO_4^{2-}]_{\lambda w}$ | concentration of total $SO_4^{2-}$ at bottom of unsaturated zone | mol.m$^{-3}$ | calculated | calculated | SOURCE (IONS1) | WCONC(7,2,3) |
| $[SO_4^{2-}]_{u,\lambda w}$ | concentration of uncomplexed $SO_4^{2-}$ at bottom of unsaturated zone | mol.m$^{-3}$ | calculated | calculated | SOURCE (as required) | several |
| $[Fe^{3+}]_{\lambda w}$ | concentration of $Fe^{3+}$ at bottom of unsaturated zone | mol.m$^{-3}$ | calculated | calculated | SOURCE (IONS1) | WCONC(9,2,3) |
| $pH_1$ | pH of gypsum depleted layer | - | calculated | calculated | SOURCE (PH1) | PH(1) |
| $pH_{\lambda w}$ | pH at bottom of unsaturated zone | - | calculated | calculated | SOURCE (PH2) | PH(2) |
| $\epsilon$ | tailings porosity | - | 0.4 | T(0.35,0.4,0.45) | INPUT | POROS |
| A | tailings surface area | m$^2$ | $5x10^5$ | C($5x10^5$) | INPUT | ATAIL |

Table A.3 cont'd

| Model Symbol | Description | Units | Nominal Value | Probability Distribution | Computer Origin | Computer Symbol |
|---|---|---|---|---|---|---|
| $\lambda_{mix}$ | thickness of mixing zone | m | 1.5 | U(1.0,2.0) | INPUT | DMIX |
| $[SO_4^{2-}]_{p,mix,t}$ | $SO_4^{2-}$ concentration in mixing zone at time t resulting from pyrite oxidation in unsaturated zone | $mol.m^{-3}$ | calculated | calculated | SOURCE (IONS3) | WCONC(6,3,3) |
| $[SO_4^{2-}]_{p,mix,t-\Delta t}$ | as above, at t-Δt | $mol.m^{-3}$ | calculated | calculated | SOURCE (IONS3) | WCONC(6,3,2) |
| $[Ca^{2+}]_{mix,t}$ | $Ca^{2+}$ concentration in mixing zone | $mol.m^{-3}$ | calculated | calculated | SOURCE (IONS3) | WCONC(8,3,3) |
| $[SO_4^{2-}]_{mix,t}$ | $SO_4^{2-}$ concentration in mixing zone | $mol.m^{-3}$ | calculated | calculated | SOURCE (IONS3) | WCONC(7,3,3) |
| $[SO_4^{2-}]^*_{mix,t}$ | hypothetical $SO_4^{2-}$ concentration in mixing zone at time t | $mol.m^{-3}$ | calculated | calculated | SOURCE (IONS3) | SSTAR |
| $\Delta_{gypsum}$ | amount of gypsum dissolved in mixing zone over Δt | $mol.m^{-3}$ | calculated | calculated | SOURCE (IONS3) | DELTAG |
| $[gyp]_{diss,t}$ | gypsum dissolved to time t | $mol.m^{-3}$ | calculated | calculated | SOURCE (IONS3) | GYPMIX |
| $[Fe^{2+}]_{mix,t}$ | concentration of $Fe^{2+}$ | $mol.m^{-3}$ | calculated | calculated | SOURCE (IONS3) | WCONC(10,3,3) |
| $pH_{mix}$ | pH in the mixing zone | - | calculated | calculated | SOURCE (PH3) | PH(3) |
| $\lambda_4$ | thickness of layer 4 | m | calculated | calculated | SOURCE (IONS4) | DBOT |
| $f_p$ | fraction of precipitation entering zone 4 | - | 0.15 | LN(0.15,1.27, 0.07,0.3) | INPUT | FNPRCP |

Table A.3 cont'd

| Model Symbol | Description | Units | Nominal Value | Probability Distribution | Computer Origin | Computer Symbol |
|---|---|---|---|---|---|---|
| $\bar{p}$ | long term mean annual net precipitation | $m.yr^{-1}$ | 0.4 | C(0.4) | INPUT | AVPRCP |
| $[SO_4^{2-}]_{p,4,t}$ | $SO_4^{2-}$ concentration in layer 4 at time t resulting from pyrite oxidation in unsaturated zone | $mol.m^{-3}$ | calculated | calculated | SOURCE (IONS4) | WCONC(6,4,3) |
| $[SO_4^{2-}]_{p,4,t-\Delta t}$ | as above, at t-Δt | $mol.m^{-3}$ | calculated | calculated | SOURCE (IONS4) | WCONC(6,4,2) |
| $[Ca^{2+}]_{4,t}$ | $Ca^{2+}$ concentration in layer 4 | $mol.m^{-3}$ | calculated | calculated | SOURCE (IONS4) | WCONC(8,4,3) |
| $[SO_4^{2-}]_{4,t}$ | $SO_4^{2-}$ concentration in layer 4 | $mol.m^{-3}$ | calculated | calculated | SOURCE (IONS4) | WCONC(7,4,3) |
| $[Fe^{2+}]_{4,t}$ | $Fe^{2+}$ concentration in layer 4 | $mol.m^{-3}$ | calculated | calculated | SOURCE (IONS4) | WCONC(10,4,3) |
| $pH_4$ | pH in layer 4 | - | calculated | calculated | SOURCE (PH4) | PH(4) |
| $X_{lime}$ | initial mass fraction of $CaCO_3$ in tailings | - | scenario dependent constant 0.0 or 0.01 | | INPUT | XLIME |
| $CaCO_3^0$ | initial inventory of calcite ($CaCO_3$) | $mol.m^{-3}$ | calculated | calculated | SOURCE (INCONI) | LIMEIN |
| $J_s'$ | net sulphate flux with calcite present | $mol.m^{-2}yr^{-1}$ | calculated | calculated | SOURCE (IONSIL) | SFLUX |
| $k'$ | rate constant for pyrite oxidation with calcite present | $yr^{-1}$ | calculated | calculated | SOURCE (IONSIL) | KRATE |
| c | concentration of $Ca^{2+}$ from calcite dissolution | $mol.m^{-3}$ | calculated | calculated | SOURCE (IONSIL) | CALIME |

Table A.3 cont'd

| Model Symbol | Description | Units | Nominal Value | Probability Distribution | Computer Origin | Computer Symbol |
|---|---|---|---|---|---|---|
| $M_U^o$ | mass % uranium (as $U_3O_8$) in ore | - | 0.1 | C(0.1) | INPUT | PCURAN |
| $a^o_{U\text{-nat,ore}}$ | initial activity of U-nat in the ore | $Bq.g^{-1}$ | calculated | calculated | SOURCE (INCONN) | AUNATO |
| $a^o_{U\text{-238,ore}}$ | initial activity of U-238 in the ore | $Bq.g^{-1}$ | calculated | calculated | SOURCE (INCONN) | AU2380 |
| $a^o_{U\text{-nat,tails}}$ | initial activity of U-nat in tailings | $Bq.g^{-1}$ | calculated | calculated | SOURCE (INCONN) | AUNATT |
| $f_u$ | mass fraction of uranium recovered in the mill | - | 0.95 | U(0.92.0.98) | INPUT | FURAN |
| $[U_s]^o$ | initial concentration of uranium in tailings solid phase | $Bq.m^{-3}$ | calculated | calculated | SOURCE (INCONN) | CONC(1,1,1)<br>CONC(1,1,3) |
| UCF | uranium conversion factor | $Bq.mol^{-1}$ | $5.95 \times 10^6$ | $C(5.95 \times 10^6)$ | SOURCE (INCONN) | UCF |
| $[U_3O_8]^o_{pyr}$ | initial concentration of $U_3O_8$ associated with pyrite | $mol.m^{-3}$ | calculated | calculated | SOURCE (INCONN) | UPYRI |
| $f_{U/Fe}$ | fraction of uranium associated with pyrite | - | 0.6 | U(0.3,0.9) | INPUT | FRACU |
| $X_{U/Fe}$ | mole fraction of $U_3O_8$ in pyrite | - | calculated | calculated | SOURCE (INCONN) | XURANI |
| $[U_L]^o_{\lambda w}$ | initial liquid phase concentration of uranium in the unsaturated zone | $Bq.m^{-3}$ | calculated | calculated | SOURCE (INCONN) | WCONC(1,2,3) |

Table A.3 cont'd

| Model Symbol | Description | Units | Nominal Value | Probability Distribution | Computer Origin | Computer Symbol |
|---|---|---|---|---|---|---|
| $[U_L]^o_{mix}$ | initial liquid phase concentration of uranium in the mixing zone | $Bq.m^{-3}$ | calculated | calculated | SOURCE (INCONN) | WCONC(1,3,3) |
| $[U_L]^o_4$ | initial liquid phase concentration of uranium in layer 4 | $Bq.m^{-3}$ | calculated | calculated | SOURCE (INCONN) | WCONC(1,4,3) |
| T230CF | Th-230 conversion factor | $Bq.mol^{-1}$ | $1.65x10^{11}$ | $C(1.65x10^{11})$ | SOURCE (INCONN) | T230CF |
| T232CF | Th-232 conversion factor | $Bq.mol^{-1}$ | $9.35x10^5$ | $C(9.35x10^5)$ | SOURCE (INCONN) | T232CF |
| $a^o_{Th-230}$ | initial activity of Th-230 in the tailings | $Bq.g^{-1}$ | calculated | calculated | SOURCE (INCONN) | AT230I |
| $[Th\text{-}230_s]^o$ | initial solid phase concentration of Th-230 | $mol.m^{-3}$ | calculated | calculated | SOURCE (INCONN) | CT230I |
| $m^o_{Th}$ | mass % of thorium (as $ThO_2$) in the ore | - | 0.03 | U(0.02,0.04) | INPUT | PCTHOR |
| $[Th\text{-}232_s]^o$ | initial solid phase concentration of Th-232 | $mol.m^{-3}$ | calculated | calculated | SOURCE (INCONN) | CT232I |
| $a^o_{Th-232}$ | initial activity of Th-232 in the tailings | $Bq.g^{-1}$ | calculated | calculated | SOURCE (INCONN) | AT232I |
| $a^o_{Th}$ | initial activity of total thorium in the tailings | $Bq.g^{-1}$ | calculated | calculated | SOURCE (INCONN) | ATHORI |
| $[Th_s]^o$ | initial concentration of total thorium in the tailings | $Bq.m^{-3}$ | calculated | calculated | SOURCE (INCONN) | CONC(2,1,1)<br>CONC(2,1,3) |
| $f_{Th-230}$ | fraction of Th-230 which is soluble | - | 0.95 | U(0.92,0.98) | INPUT | FT230 |
| $f_{Th-232}$ | fraction of Th-232 which is soluble | - | 0.65 | U(0.60,0.70) | INPUT | FT232 |

Table A.3 cont'd

| Model Symbol | Description | Units | Nominal Value | Probability Distribution | Computer Origin | Computer Symbol |
|---|---|---|---|---|---|---|
| $[Th\text{-}230_s]^o_{sol}$ | initial concentration of soluble Th-230 | $mol.m^{-3}$ | calculated | calculated | SOURCE (INCONN) | T230SO |
| $[Th\text{-}232_s]^o_{sol}$ | initial concentration of soluble Th-232 | $mol.m^{-3}$ | calculated | calculated | SOURCE (INCONN) | T232SO |
| $[Th\text{-}230_s]^o_{insol}$ | initial concentration of insoluble Th-230 | $mol.m^{-3}$ | calculated | calculated | SOURCE (INCONN) | T230IS |
| $[Th\text{-}232_s]^o_{insol}$ | initial concentration of insoluble Th-232 | $mol.m^{-3}$ | calculated | calculated | SOURCE (INCONN) | T232IS |
| $[Th_s]^o_{sol}$ | initial concentration of total soluble thorium | $mol.m^{-3}$ | calculated | calculated | SOURCE (INCONN) | THSOL |
| $[Th_s]^o_{insol}$ | initial concentration of total insoluble thorium | $mol.m^{-3}$ | calculated | calculated | SOURCE (INCONN) | TINSOL |
| $a^o_{Th,sol}$ | initial activity of total soluble thorium | $Bq.m^{-3}$ | calculated | calculated | SOURCE (INCONN) | THSOLA |
| $a^o_{Th,insol}$ | initial activity of total insoluble thorium | $Bq.m^{-3}$ | calculated | calculated | SOURCE (INCONN) | TINSLA |
| $X_{Th\text{-}230/Th,sol}$ | mole fraction of Th-230 in soluble thorium | - | calculated | calculated | SOURCE (INCONN) | X230LM |
| $X_{Th\text{-}232/Th,sol}$ | mole fraction of Th-232 in soluble thorium | - | calculated | calculated | SOURCE (INCONN) | X232LM |
| $XA_{Th\text{-}230/Th,sol}$ | activity fraction of Th-230 in soluble thorium | - | calculated | calculated | SOURCE (INCONN) | X230LA |
| $XA^o_{Th\text{-}232/Th,insol}$ | activity fraction of Th-232 in insoluble thorium | - | calculated | calculated | SOURCE (INCONN) | X232SA<br>X232A |

Table A.3 cont'd

| Model Symbol | Description | Units | Nominal Value | Probability Distribution | Computer Origin | Computer Symbol |
|---|---|---|---|---|---|---|
| THORCF | weighted, liquid phase thorium conversion factor | $Bq.mol^{-1}$ | calculated | calculated | SOURCE<br>(INCONN) | THORCF |
| $[Th_L]_{\lambda w}$ | liquid phase thorium concentration in unsaturated layer | $Bq.m^{-3}$ | calculated | calculated | SOURCE<br>(INCONN)<br>(THORUM) | WCONC(2,2,3) |
| $[Th_L]_{mix}$ | liquid phase thorium concentration in mixing layer | $Bq.m^{-3}$ | calculated | calculated | SOURCE<br>(INCONN)<br>(THORUM) | WCONC(2,3,3) |
| $[Th_L]_4$ | liquid phase thorium concentration in bottom layer | $Bq.m^{-3}$ | calculated | calculated | SOURCE<br>(INCONN)<br>(THORUM) | WCONC(2,4,3) |
| $k_{Th}$ | correction factor for amorphous vs crystalline $Th(OH)_4$ | - | calculated | calculated | SOURCE<br>(INCONN)<br>(THORUM) | THORDC |
| $X_{Th,c}$ | fraction of $Th(OH)_4$ which is crystalline | - | 0.3 | T(0.2,0.3,0.4) | INPUT | FRACTH |
| $a^0_{Ra}$ | initial activity of Ra-226 in tailings | $Bq.g^{-1}$ | calculated | calculated | SOURCE<br>(INCONN) | ARADI |
| RACF | Ra-226 conversion factor | $Bq.mol^{-1}$ | $8.26 \times 10^{12}$ | $C(8.26 \times 10^{12})$ | SOURCE<br>(INCONN) | RACF |
| $[Ra_S]^0$ | initial solid phase concentration of Ra-226 | $mol.m^{-3}$ | calculated | calculated | SOURCE<br>(INCONN) | CRADI |
| $[Ra_S]^0_{Ba}$ | initial concentration of Ra-226 associated with $BaSO_4$ | $mol.m^{-3}$ | calculated | calculated | SOURCE<br>(INCONN) | CRADBA |
| $f_{Ra}$ | fraction of Ra-226 which is assumed to be soluble | - | 0.60 | T(0.25,0.6,0.95) | INPUT | FRAD |

Table A.3 cont'd

| Model Symbol | Description | Units | Nominal Value | Probability Distribution | Computer Origin | Computer Symbol |
|---|---|---|---|---|---|---|
| $[Ra_s]^o_m$ | initial concentration of Ra-226 associated with host tailings material | $mol.m^{-3}$ | calculated | calculated | SOURCE (INCONN) | CRADTI |
| $[BaSO_4]^o$ | initial solid phase concentration of $BaSO_4$ | $mol.m^{-3}$ | calculated | calculated | SOURCE (INCONN) | CBARI |
| $X^o_{Ra/BaSO_4}$ | initial mole fraction of Ra-226 in $BaSO_4$ | - | $3.5x10^{-6}$ | $T(2.5x10^{-6}, 3.5x10^{-6}, 4.5x10^{-6})$ | INPUT | XRADI |
| $M^o_{Ra}$ | total Ra-226 initially associated with $BaSO_4$ in the unsaturated and mixing zones | $mol.m^{-2}$ | calculated | calculated | SOURCE (INCONN) | BASATI |
| $[Ra_s]^o_1$ | initial solid phase Ra-226 concentration in the upper tailings layer | $Bq.m^{-3}$ | calculated | calculated | SOURCE (INCONN) | CONC(4,1,3) |
| $[Ra_s]^o_{\lambda w}$ | initial solid phase Ra-226 concentration at the bottom of the unsaturated zone | $Bq.m^{-3}$ | calculated | calculated | SOURCE (INCONN) | CONC(4,2,3) |
| $[Ra_s]^o_{mix}$ | initial solid phase Ra-226 concentration in the mixing zone | $Bq.m^{-3}$ | calculated | calculated | SOURCE (INCONN) | CONC(4,3,3) |
| $[Ra_s]^o_4$ | initial solid phase Ra-226 concentration in the bottom layer | $Bq.m^{-3}$ | calculated | calculated | SOURCE (INCONN) | CONC(4,4,3) |
| $[Ba^{2+}]_\ell$ | concentration of $Ba^{2+}$ in layer $\ell$ ($\ell$=2,3,4) | $mol.m^{-3}$ | calculated | calculated | SOURCE (INCONN) | CBAR |

Table A.3 cont'd

| Model Symbol | Description | Units | Nominal Value | Probability Distribution | Computer Origin | Computer Symbol |
|---|---|---|---|---|---|---|
| $K^o_{s,BaSO_4}$ | solubility equilibrium constant for $BaSO_4$ | $mol^2.m^{-6}$ | $5.04x10^{-4}$ | $C(5.04x10^{-4})$ | INPUT | KSBAR |
| $K_{f,BaSO_4}$ | formation constant for $BaSO_4$ | $m^3.mol^{-1}$ | $5.01x10^{-1}$ | $C(5.01x10^{-4})$ | INPUT | KFBAR |
| $[Ra_L]\ell$ | liquid phase concentration of Ra-226 in layer 'ℓ' (ℓ=2,3,4) | $Bq.m^{-3}$ | calculated | calculated | SOURCE<br>(INCONN)<br>(RADIUM) | WCONC(4,ℓ,3) |
| $K_{Ra}$ | radium distribution between liquid and solid precipitate forms | - | 0.53 | U(0.5, 0.56) | INPUT | KRAD |
| $h^o_{Ba}$ | initial thickness of barite depleted layer | m | 0.01 | C(0.01) | SOURCE<br>(INCONN) | DBAR(1)<br>DBAR(3) |
| $a^o_{Pb}$ | initial activity of Pb-210 in the tailings | $Bq.g^{-1}$ | calculated | calculated | SOURCE<br>(INCONN) | APBI |
| PBCF | Pb-210 conversion factor | $Bq.mol^{-1}$ | $6.3x10^{14}$ | $C(6.3x10^{14})$ | SOURCE<br>(INCONN) | PBCF |
| $[Pb\text{-}210_s]^o$ | initial solid phase concentration of Pb-210 | $mol.m^{-3}$ | calculated | calculated | SOURCE<br>(INCONN) | CPBI |
| $f_{Pb}$ | fraction of Pb-210 assumed to be soluble | - | 0.95 | U(0.92,0.98) | INPUT | FLEAD |
| $[Pb\text{-}210_s]^o_{PbSO_4}$ | initial concentration of Pb-210 associated with $PbSO_4$ | $mol.m^{-3}$ | calculated | calculated | SOURCE<br>(INCONN) | CPBPB |
| $[Pb\text{-}210_s]^o_m$ | initial concentration of Pb-210 associated with tailings solids | $mol.m^{-3}$ | calculated | calculated | SOURCE<br>(INCONN) | CPBTI |

Table A.3 cont'd

| Model Symbol | Description | Units | Nominal Value | Probability Distribution | Computer Origin | Computer Symbol |
|---|---|---|---|---|---|---|
| $[PbSO_4]^o$ | initial concentration of $PbSO_4$ in tailings | $mol.m^{-3}$ | 2.0 | T(1.0,2.0,3.0) | INPUT | CLEADI |
| $X^o_{Pb-210/PbSO_4}$ | initial mole fraction of Pb-210 in $PbSO_4$ | - | calculated | calculated | SOURCE (INCONN) | XPBI |
| $[Pb-210_s]^o_\ell$ | initial solid phase concentration of Pb-210 in layer '$\ell$' ($\ell$ = 1,2,3,4) | $Bq.m^{-3}$ | calculated | calculated | SOURCE (INCONN) | CONC(3,$\ell$,3) |
| $[Pb^{2+}]_\ell$ | total concentration of $Pb^{2+}$ in layer '$\ell$' ($\ell$ = 2,3,4) | $mol.m^{-3}$ | calculated | calculated | SOURCE (INCONN) | CLEAD |
| $[Pb-210_L]^o_\ell$ | initial liquid phase concentration of Pb-210 in layer '$\ell$' ($\ell$ = 2,3,4) | $Bq.m^{-3}$ | calculated | calculated | SOURCE (INCONN) | WCONC(3,$\ell$,3) |
| $K^o_{s,PbSO_4}$ | solubility equilibrium constant for $PbSO_4$ | $mol^2.m^{-6}$ | $1.2x10^{-2}$ | $C(1.2x10^{-2})$ | INPUT | KSLEAD |
| $K_{f,PbSO_4}$ | formation constant for $PbSO_4$ | $m^3.mol^{-1}$ | $5.0x10^{-1}$ | $C(5.0x10^{-1})$ | INPUT | KFLEAD |
| $h^o_{Pb}$ | initial thickness of $PbSO_4$ depleted layer | m | 0.01 | C(0.01) | SOURCE (INCONN) | DLEAD(1)<br>DLEAD(3) |
| $[UO_2^{2+}]_{\lambda w}$ | concentration of $UO_2^{2+}$ in unsaturated zone (= concentration of U-NAT) | $Bq.m^{-3}$ | calculated | calculated | SOURCE (URANUM) | WCONC(1,2,3) |
| $[U_s]_t$ | concentration of uranium in tailings solid phase at time t | $Bq.m^{-3}$ | calculated | calculated | SOURCE (URANUM) | CONC(1,1,3) |
| $[U_s]_{t-\Delta t}$ | as above, at t-Δt | $Bq.m^{-3}$ | calculated | calculated | SOURCE | CONC(1,1,2) |

Table A.3 cont'd

| Model Symbol | Description | Units | Nominal Value | Probability Distribution | Computer Origin | Computer Symbol |
|---|---|---|---|---|---|---|
| $[UO_2^{2+}]_{mix,t}$ | concentration of $UO_2^{2+}$ in the mixing zone (= concentration of U-NAT) at time t | $Bq.m^{-3}$ | calculated | calculated | SOURCE (URANUM) | WCONC(1,3,3) |
| $[UO_2^{2+}]_{mix,t-\Delta t}$ | as above, at t-Δt | $Bq.m^{-3}$ | calculated | calculated | SOURCE (URANUM) | WCONC(1,3,2) |
| $[UO_2^{2+}]_{4,t}$ | concentration of $UO_2^{2+}$ in the bottom layer (= concentration of U-NAT) at time t | $Bq.m^{-3}$ | calculated | calculated | SOURCE (URANUM) | WCONC(1,4,3) |
| $[UO_2^{2+}]_{4,t-\Delta t}$ | as above, at t-Δt | $Bq.m^{-3}$ | calculated | calculated | SOURCE (URANUM) | WCONC(1,4,2) |
| $K_{d,UO2}$ | uranium solid-liquid distribution coefficient | $m^3.g^{-1}$ | $3x10^{-5}$ | $LN(3x10^{-5},3.0,$<br>$1.1x10^{-6},$<br>$8.1x10^{-4})$ | INPUT | KDUO2 |
| $[Th]_{diss,t}$ | concentration of total thorium dissolved in the unsaturated zone to time t | $mol.m^{-3}$ | calculated | calculated | SOURCE (THORUM) | THDISS |
| $[Th]_{diss,t-\Delta t}$ | as above, to time t-Δt | $mol.m^{-3}$ | calculated | calculated | SOURCE (THORUM) | THDISS |
| $[Th\text{-}230]_{diss}$ | concentration of dissolved Th-230 to time t in the unsaturated zone | $mol.m^{-3}$ | calculated | calculated | SOURCE (THORUM) | T230D |
| $[Th\text{-}232]_{diss}$ | as above, for Th-232 | $mol.m^{-3}$ | calculated | calculated | SOURCE (THORUM) | T232D |
| $[Th\text{-}230_s]$ | solid phase concentration of Th-230 in unsaturated zone | $mol.m^{-3}$ | calculated | calculated | SOURCE (THORUM) | T230S |
| $[Th\text{-}232_s]$ | as above, for Th-232 | $mol.m^{-3}$ | calculated | calculated | SOURCE (THORUM) | T232S |

Table A.3 cont'd

| Model Symbol | Description | Units | Nominal Value | Probability Distribution | Computer Origin | Computer Symbol |
|---|---|---|---|---|---|---|
| $[Th_s]$ | solid phase concentration of total thorium in unsaturated zone | $Bq.m^{-3}$ | calculated | calculated | SOURCE (THORUM) | CONC(2,1,3) |
| $XA_{Th-232/Th,insol}$ | activity fraction of Th-232 in insoluble thorium | - | calculated | calculated | SOURCE (THORUM) | X232SA |
| $[Th]_{diss,mix,t}$ | concentration of total thorium dissolved in the mixing zone to time t | $mol.m^{-3}$ | calculated | calculated | SOURCE (THORUM) | THDISM |
| $[Th]_{diss,mix,t-\Delta t}$ | as above, for $t-\Delta t$ | $mol.m^{-3}$ | calculated | calculated | SOURCE (THORUM) | THDISM |
| $\lambda_{Th-230}$ | radioactive decay constant for Th-230 | $yr^{-1}$ | $8.66 \times 10^{-6}$ | $C(8.66 \times 10^{-6})$ | SOURCE (INCONN) | LAM230 |
| $\lambda_{Ra-226}$ | radioactive decay constant for Ra-226 | $yr^{-1}$ | $4.33 \times 10^{-4}$ | $C(4.33 \times 10^{-4})$ | SOURCE (INCONN) | LAMRAD |
| $\lambda_{Pb-210}$ | radioactive decay constant for Pb-210 | $yr^{-1}$ | $3.3 \times 10^{-2}$ | $C(3.3 \times 10^{-2})$ | SOURCE (INCONN) | LAMPB |
| $[Ba]_{T,\lambda w}$ | concentration of total barium at $\lambda_w$ | $mol.m^{-3}$ | calculated | calculated | SOURCE (RADIUM) | CBAR |
| $\Delta h_{Ba}$ | change in thickness of barite depleted layer over $\Delta t$ | m | calculated | calculated | SOURCE (RADIUM) | DHBAR |
| $h_{Ba}$ | thickness of barite depleted layer at time, t | m | calculated | calculated | SOURCE (RADIUM) | DBAR(3) |
| $m_{Ba,t}$ | reprecipitated barite at time, t | $mol.m^{-2}$ | calculated | calculated | SOURCE (RADIUM) | MBAR(3) |
| $m_{Ba,t-\Delta t}$ | as above, at time $t-\Delta t$ | $mol.m^{-2}$ | calculated | calculated | SOURCE (RADIUM) | MBAR(2) |

Table A.3 cont'd

| Model Symbol | Description | Units | Nominal Value | Probability Distribution | Computer Origin | Computer Symbol |
|---|---|---|---|---|---|---|
| $X'_{Ra/BaSO_4}$ | mol fraction of Ra-226 in $BaSO_4$; corrected for decay of Ra-226 | - | calculated | calculated | SOURCE (RADIUM) | XRAD |
| $x_t$ | solid phase mole fraction of Ra-226 in $BaSO_4$ at time, t | - | calculated | calculated | SOURCE (RADIUM) | XBAR(3) |
| $x_{t-\Delta t}$ | as above, at time t-Δt | - | calculated | calculated | SOURCE (RADIUM) | XBAR(2) |
| $[Ra]^{Th}_{\lambda w}$ | concentration of dissolved Ra-226 resulting from decay of dissolved Th-230 during Δt | $mol.m^{-3}$ | calculated | calculated | SOURCE (RADIUM) | CRATL2 |
| $[Ra_s]^{Th}_{t}$ | cumulative concentration of solid phase Ra-226 resulting from ingrowth from solid phase Th-230 to time t | $mol.m^{-3}$ | calculated | calculated | SOURCE (RADIUM) | CRATHS |
| $[Ra_s]^{Th}_{t-\Delta t}$ | as above, to time t-Δt | $mol.m^{-2}$ | calculated | calculated | SOURCE (RADIUM) | CRATHS |
| $[Ra_s]_1$ | solid phase concentration of Ra-226 in barite depleted layer (layer1) | $Bq.m^{-3}$ | calculated | calculated | SOURCE (RADIUM) | CONC(4,1,3) |
| $[Ra_s]_2$ | solid phase concentration of Ra-226 in barite enriched layer (layer2) | $Bq.m^{-3}$ | calculated | calculated | SOURCE (RADIUM) | CONC(4,2,3) |
| $[Ra_L]_{\lambda w}$ | dissolved Ra-226 concentration at bottom of unsaturated zone | $Bq.m^{-3}$ | calculated | calculated | SOURCE (RADIUM) | WCONC(4,2,3) |
| $[Ra]^{Th}_{mix}$ | concentration of dissolved radium resulting from the decay of Th-230 dissolved in the mixing zone | $mol.m^{-3}$ | calculated | calculated | SOURCE (RADIUM) | CRATL3 |

Table A.3 cont'd

| Model Symbol | Description | Units | Nominal Value | Probability Distribution | Computer Origin | Computer Symbol |
|---|---|---|---|---|---|---|
| $[Ra]^{Th}_{4}$ | concentration of dissolved radium resulting from the decay of Th-230 dissolved in the bottom layer (layer4) | $mol.m^{-3}$ | calculated | calculated | SOURCE (RADIUM) | CRATL4 |
| $K_{d,Ra}$ | Ra-226 solid-liquid distribution coefficient | $m^{3}.g^{-1}$ | $40x10^{-6}$ | $T(5x10^{-6},40x10^{-6},75x10^{-6})$ | INPUT | KDRAD |
| $[Ra_{L}]_{mix,t}$ | dissolved Ra-226 concentration in the mixing zone at time t | $Bq.m^{-3}$ | calculated | calculated | SOURCE (RADIUM) | WCONC(4,3,3) |
| $[Ra_{L}]_{mix,t-\Delta t}$ | as above, at time t-Δt | $Bq.m^{-3}$ | calculated | calculated | SOURCE (RADIUM) | WCONC(4,3,2) |
| $[Ra]_{in}$ | concentration of Ra-226 resulting from inputs to the mixing zone | $mol.m^{-3}$ | calculated | calculated | SOURCE (RADIUM) | CRADIN |
| $\sum_{t=o}^{t}[Ra]_{in}$ | cumulative sum of radium inputs to mixing zone to time t | $mol.m^{-3}$ | calculated | calculated | SOURCE (RADIUM) | SUMBAR |
| $[Ra_{L}]_{4,t}$ | dissolved Ra-226 concentration in the bottom layer at time t | $Bq.m^{-3}$ | calculated | calculated | SOURCE (RADIUM) | WCONC(4,4,3) |
| $[Ra_{L}]_{4,t-\Delta t}$ | as above, at time t-Δt | $Bq.m^{-3}$ | calculated | calculated | SOURCE (RADIUM) | WCONC(4,4,2) |
| $[Ra]_{in,4}$ | concentration.of Ra-226 resulting from inputs to the bottom layer | $mol.m^{-3}$ | calculated | calculated | SOURCE (RADIUM) | CRADIN |

Table A.3 cont'd

| Model Symbol | Description | Units | Nominal Value | Probability Distribution | Computer Origin | Computer Symbol |
|---|---|---|---|---|---|---|
| $[Pb]_{T,\lambda w}$ | concentration of total lead at bottom of unsaturated zone | $mol.m^{-3}$ | calculated | calculated | SOURCE (LEAD) | CLEAD |
| $[Pb\text{-}210_L]^{Ra}_{\lambda w}$ | concentration of dissolved Pb-210 resulting from decay of dissolved Ra-226 in unsaturated zone | $mol.m^{-3}$ | calculated | calculated | SOURCE (LEAD) | CPBRL2 |
| $X'_{Pb\text{-}210/PbSO_4}$ | mole fraction of Pb-210 in $PbSO_4$; corrected for decay of Pb-210 | - | calculated | calculated | SOURCE (LEAD) | XLEAD |
| $\Delta h_{Pb}$ | change in thickness of $PbSO_4$ depleted layer over $\Delta t$ | m | calculated | calculated | SOURCE (LEAD) | DHLEAD |
| $h_{Pb}$ | thickness of $PbSO_4$ depleted layer at time t | m | calculated | calculated | SOURCE | DLEAD(3) |
| $[Pb\text{-}210_L]_{\lambda w}$ | dissolved Pb-210 concentration at bottom of unsaturated zone | $Bq.m^{-3}$ | calculated | calculated | SOURCE (LEAD) | WCONC(3,2,3) |
| $[Pb\text{-}210_s]^{Ra}_{t}$ | cumulative solid phase concentration of Pb-210 resulting from ingrowth to time t | $mol.m^{-3}$ | calculated | calculated | SOURCE (LEAD) | CPBRAS |
| $[Pb\text{-}210_s]^{Ra}_{t-\Delta t}$ | as above, to $t-\Delta t$ | $mol.m^{-3}$ | calculated | calculated | SOURCE (LEAD) | CPBRAS |
| $[Pb\text{-}210_s]_1$ | solid phase concentration of Pb-210 in $PbSO_4$ depleted layer | $Bq.m^{-3}$ | calculated | calculated | SOURCE (LEAD) | CONC(3,1,3) |
| $[Pb\text{-}210_L]^{Ra}_{mix}$ | concentration of dissolved Pb-210 from decay of Ra-226 dissolved in the mixing zone | $mol.m^{-3}$ | calculated | calculated | SOURCE (LEAD) | CPBRL3 |
| $[Pb\text{-}210_L]^{Ra}_{4}$ | as above, for layer 4 | $mol.m^{-3}$ | calculated | calculated | SOURCE (LEAD) | CPBRL4 |

Table A.3 cont'd

| Model Symbol | Description | Units | Nominal Value | Probability Distribution | Computer Origin | Computer Symbol |
|---|---|---|---|---|---|---|
| $[Pb\text{-}210_L]_{mix,t}$ | dissolved Pb-210 concentration in the mixing zone at time t | $Bq.m^{-3}$ | calculated | calculated | SOURCE (LEAD) | WCONC(3,3,3) |
| $[Pb\text{-}210_L]_{mix,t-\Delta t}$ | as above, at time t-Δt | $Bq.m^{-3}$ | calculated | calculated | SOURCE (LEAD) | WCONC(3,3,2) |
| $K_{d,Pb}$ | Pb-210 solid-liquid distribution coefficient | $m^3.g^{-1}$ | $60x10^{-6}$ | $T(20x10^{-6}, 60x10^{-6}$ $100x10^{-6})$ | INPUT | KDLEAD |
| $[Pb]_{in}$ | concentration of Pb-210 resulting from inputs to the mixing zone | $mol.m^{-3}$ | calculated | calculated | SOURCE (LEAD) | CPBIN |
| $\sum_{t=o}^{t}[Pb]_{in}$ | cumulative sum of Pb-210 inputs to the mixing zone to time t | $mol.m^{-3}$ | calculated | calculated | SOURCE (LEAD) | SUMPB |
| $[Pb\text{-}210_L]_{4,t}$ | dissolved Pb-210 concentration in the bottom layer at time t | $Bq.m^{-3}$ | calculated | calculated | SOURCE (LEAD) | WCONC(3,4,3) |
| $[Pb\text{-}210_L]_{4,t-\Delta t}$ | as above, at time t-Δt | $Bq.m^{-3}$ | calculated | calculated | SOURCE (LEAD) | WCONC(3,4,2) |
| $[Pb]_{in,4}$ | concentration of Pb-210 resulting from inputs to layer 4 | $mol.m^{-3}$ | calculated | calculated | SOURCE (LEAD) | CPBIN |

## APPENDIX B

# A DYNAMIC MODEL OF URANIUM BEHAVIOR
# IN AN
# OLIGOTROPHIC LAKE

by

B. G. Blaylock, R. H. Gardner, and F. O. Hoffman
Oak Ridge, Tennessee

June 1986

## ABSTRACT

A six-component model with 23 pathways for predicting the dynamics of uranium in a hypothetical oligotrophic lake situated in the Precambrian Shield region of Canada is described and time-dependent solutions obtained for (1) a simulation of a clean lake with a contaminated input and (2) a simulation of a contaminated lake with a 99.9% cleanup of the input. Deterministic calculations, sensitivity and uncertainty analyses were performed for each case. The results show that: (1) time-dependent concentrations of uranium in the flesh of game fish were most sensitive to changes in the rate constant describing the direct transfer of uranium from water to game fish flesh; (2) equilibrium values of the water-to-game fish flesh concentration factor (CF) may give biased results when the aquatic system is not at equilibrium; and (3) a simpler model involving three components and 7 pathways (see Chapter 11) can adequately predict the dynamic behavior of uranium in game fish. At equilibrium, uranium concentrations predicted by the multi-component dynamic model are not appreciably different from those predicted using empirically derived water-to-game fish flesh CF's.

## B.1 INTRODUCTION

For the purposes of radiological assessment, the prediction of the concentration of a radionuclide in fish flesh is usually made using the mathematically simple concentration factor approach (Ophel, 1978). The concentration factor (CF) assumes that concentrations in fish flesh and water are in equilibrium and that the concentration in fish is directly proportional to the concentration in water. All pathways and mechanisms of radionuclide uptake and elimination by and from fish, including food chain bioaccumulation and predation, are assumed to be implicitly included within empirical determinations of the CF. The concentration factor is obtained as a ratio of the amount of the radionuclide in a gram of fresh weight fish flesh ($C_f$) to the amount of the radionuclide in a milliliter of unfiltered water ($C_w$). Thus:

$$C_f = C_w \times CF \qquad (1)$$

Criticism of the CF approach is that it is too simplistic, that ecological details of water, sediment, and food chain interaction should be addressed explicitly within the mathematical model, and that the time-dependent dynamics of the transfer of the radionuclide among the various components of an aquatic system cannot be explained by a factor derived under conditions of assumed equilibrium. Furthermore, there is the contention held by some that a more detailed model will enhance understanding of the aquatic system and therefore will produce results that are more accurate and defensible than the simple CF approach.

In short, these criticisms pertain to the use of simple, aggregate models instead of more detailed, research models to represent complex ecological systems. The objectives of this paper are to construct a multi-component dynamic model for a hypothetical oligotrophic lake in the Precambrian Shield region of Canada, and to compare the predictions of the concentration of uranium in the flesh of game fish against results obtained using reported values of CF for uranium. It is assumed that this hypothetical lake is subject to contamination by uranium through the disposal and/or leaching of uranium mill tailings from uranium mining and milling operations.

Calculations are made for two scenarios: (1) where uranium enters an uncontaminated lake, and (2) where uranium is removed from water entering the lake after uranium concentrations in all lake components have reached equilibrium. For both scenarios, the multi-component model is used to calculate the concentrations of uranium in the lake system components as a function of time. Uncertainties in model predictions are simulated by estimating uncertainties of model parameters (rate constants and the water-to-game fish CF) and translating these uncertainties into predicted concentrations of uranium using both analytical and numerical error propagation techniques (Hoffman and Gardner, 1983).

## B.2 METHODS

### B.2.1 Model Description

The multi-component model is composed of six compartments: water, sediment, game fish flesh, forage fish, invertebrates, and aquatic vegetation, with twenty-three parameters describing the flow of uranium among model components (Figure 1). The lake represented by this model is assumed to be a reference lake of the Canadian Precambrian Shield. The lake is a generalized oligotrophic lake that is deep, cold, low in productivity and high in dissolved oxygen. The physical and biological characteristics of the lake are described in Table 1 (Halbert, 1986). Development of parameter values for the biological components of the model (game fish flesh, forage fish, invertebrates, and aquatic vegetation) and sources of information are discussed in the following sections.

Table 1

## ASSUMED PHYSICAL AND BIOLOGICAL DESCRIPTION OF A REFERENCE OLIGOTROPHIC CANADIAN SHIELD LAKE

| Physical Parameters | Value |
|---|---|
| Surface area | 160 ha |
| Average depth | 10 m |
| Volume of water | 1.6 E10 L |
| Mass of the exchangeable sediment (assumed depth 5 cm) | 1.4 E7 kg |
| **Biological Parameters** | |
| Game fish flesh | 500 kg |
| Foraye fish whole | 1600 kg |
| Aquatic vegetation | 2.0 E4 kg |
| Invertebrates | 1.1 E4 kg |

### B.2.2 Game Fish Flesh

The estimated range of productivity for game fish in an oligotrophic lake is 0.26 to 2.5 kg/ha per year (Swanson, 1985a). For the reference lake a productivity of 1 kg/ha per year was assumed. The productivity multiplied by the lake surface area and the average turnover time of the species will give an estimate of the biomass (sometimes referred to as standing crop) of the model component. Swanson (1983) reported a wide age range of 5 to 36 years for lake trout collected from two oligotrophic lakes. Swanson (1985a) estimated that the average age of lake trout in an oligotrophic lake was between 7 to 16 years depending upon whether the lake has supported commercial fishing. For the reference lake an average age for game fish of eight years was assumed. The biomass of game fish in the 160 ha lake is 1280 kg (= 1 kg/ha.y*160 ha*8y). The compartment of interest in our model is game fish flesh or the edible portion of the fish. Rope and Whicker (1980) reported that 38% of the wet weight of rainbow trout was flesh. Using this percentage as a conversion factor the biomass of the game fish flesh component is 486 kg or rounded to 500 kg (Table 1).

The concentration factor (CF) for the game fish flesh component of the model was assumed to be 1.4 (Table 2). A review (Halbert, 1986) of recent data indicated that the CFs for game fish flesh ranged from 0.01 to 41.4, and that these values were lognormally distributed with a geometric mean of 1.4. Studies by Wahlgren et al. (1975) and Stegnar and Kobald (1982) were not included in the review; however, CFs reported in their studies are within the range of values reviewed by Halbert (1986). Wahlgren et al. (1975) reported CFs of 0.3 to 0.7 for piscivorous fish in Lake Michigan, and Stegnar and Kobald (1982) reported concentration factors of 0.7 to 38 for brown trout (Salmo trutta) collected from the river Sava in Sloveinia, Yugoslavia.

Uranium is a bone seeker and moves to the bone from the other tissues of fish. Swanson (1983) reported maximum bone / flesh ratios of 10, 155, and 410 for lake trout, lake whitefish, and white sucker, respectively. The turnover rate of the fish population is much faster than the biological half-life of uranium. Therefore, the estimated average age of the game fish population, which is 8 y, would be the turnover or residence time of uranium in the population of game fish in the model.

Game fish can obtain uranium directly from the water or through the food chain. Concentration factor data reported by Swanson (1983) showed that the game fish flesh and forage fish flesh levels were essentially the same, even though their feeding habits are quite different. Hence, it was assumed that most (90%) of the body burden of uranium came from the water component of the reference aquatic ecosystem. It was further assumed that the remaining 10% of the body burden was taken in via the food chain, 6% from the forage fish component and 4% from the invertebrate component. Although the diet of game fish consists primarily of forage fish, the invertebrates have a much higher concentration factor than the forage fish; thus they have a much higher concentration per unit weight.

### B.2.3 Forage Fish

The forage fish component is based on information available for dace, shiners, chubs, and small white fish (Swanson, 1983). The biomass of this model component consists of the whole fish. We assume the entire fish is consumed by the predacious game fish. The estimate of the biomass for the forage fish component was based on the relationship between the biomass of forage fish to the biomass of the other compartments in the oligotrophic lake, and the assumption that the average turnover time for forage fish was one year. Based on these assumptions the estimated biomass of the forage fish compartment is 1600 kg (=10 kg/ha.y * 160 ha x 1 y).

The concentration factors reported for whole forage fish by Swanson (1983) and reviewed by Halbert (1986) ranged from 0.2 to 24. The geometric mean of these data, 3.68, was assumed to be the concentration factor for forage fish. The turnover time of the forage fish population determines the turnover of uranium in this component.

Table 2

## ASSUMED DETERMINISTIC VALUES FOR CONCENTRATION FACTORS AND TURNOVER TIMES FOR BIOTA IN A REFERENCE CANADIAN SHIELD LAKE

| Model Component | Concentration Factor (L/kg) | Turnover Time (d or y) |
|---|---|---|
| Game fish flesh | 1.4 | 8 y |
| Forage fish whole | 3.68 | 365 d |
| Aquatic vegetation | 2500 | 5 d |
| Invertebrates | 547 | 38 d |
| Water | 1 | 365 d |
| Sediment | 2860* | 6.3 y |

Note

* Kd value for exchangeable sediment

Since game fish acquire 90% of their body burden of uranium directly from water, it is logical to assume that approximately the same percentage would be acquired by forage fish. The remaining 10 percent of the forage fish body burden would be taken up via the food chain. Based on stomach content analysis of forage fish reported by Swanson (1985b), it was assumed that 5% of the uranium body burden came from the invertebrates, 2.5% came from aquatic vegetation, and the remaining 2.5% from direct uptake from the sediment.

### B.2.4 Vegetation

The vegetation component of the model is composed of phytoplankton, periphyton, and macrophytes. The reference lake is assumed to be low in productivity with phytoplankton being the prime food base for the higher organisms. A large volume of literature exists on phytoplankton productivity and biomass. Unfortunately much of it does not apply to the Canadian Shield Lakes, and the situation is further complicated by the fact that biomass is measured as chlorophyl, carbon, dry weight or wet weight. In most cases, conversions were necessary to obtain wet weight measurements. The biomass of phytoplankton for oligotrophic lakes was estimated to range from 1.0 to 20 mg/L wet weight (Soballe and Kimmel, 1985). Schindler and Holmgren, (1971) reported that the biomass of phytoplankton, dominated by Chrysophyceae, ranged from 0.12 to 5.4 mg/L and from 2.1 to 13.4 mg/L for July and August for four lakes in the Experimental Lake Area. The turnover time reported by Schindler and Holmgren (1971) ranged from 0.44 to 2.77 d.

Because the turnover time for phytoplankton is reduced during the winter, a turnover time of 5 days was assumed for the reference lake. The biomass measurements and the turnover times listed above are in agreement with the data for several oligotrophic lakes listed by Wetzel (1975). The estimated phytoplankton concentration is 1.25 mg/L wet weight for the reference lake; thus, the biomass for the vegetation component is $2.0 \times 10^4$ kg.

The vegetation component of the lake ecosystem is dominated by phytoplankton. Wahlgren et al. (1975) reported concentration factors for algae ranging from

88 to 215. In a review of uranium concentration factors, Blaylock (1982) reported a range of 40 to 2600 for phytoplankton. In a recent review by Halbert (1986), uranium concentration factors for phytoplankton ranged from 400 to 15,000. The geometric mean value of the data set equalled 2500. A CF of 2500 was assumed therefore, for phytoplankton and plants in this study. It was assumed that the turnover rate of uranium in the aquatic vegetation was relatively short (5 days).

### B.2.5 Invertebrates

The invertebrates component of the reference lake is composed of zooplankton and benthic invertebrates. The benthic invertebrates are dominated by chironomids and other aquatic insects, oligocheites, and clams. In a study by Swanson (1985b) the density of the invertebrates ranged from 1.7 to 4.7 g wet wt/m$^2$ and were dominated by zooplankton. The dominant zooplankton were rotifers, copepods, and cladocerans. Estimates of the density of zooplankton in an oligotrophic lake were taken from Wetzel (1975) and the Ontario Water Resources Commission (1972). The average biomass for the invertebrate compartment was estimated as 1.1 x 10$^4$ kg. According to Wetzel (1975) the estimated turnover time for zooplankton in oligotrophic lakes ranges from 2 to 80 days. The turnover time for the invertebrate compartment in the reference lake was estimated as 38 days.

In a review by Blaylock (1982), uranium concentration factors for invertebrates ranged from 2 to 335. A research report by Swanson (1985b) prepared for SENES Consultants Limited contains the most comprehensive data on concentration factors for uranium for benthic invertebrates that is currently available. These data, reviewed by Halbert (1986), report concentration factors for a variety of invertebrates. Concentrations factors for these data ranged from 0.88 to 7,059 with a geometric mean concentration of 547.

A concentration factor of 547 was selected to represent both zooplankton and benthic invertebrates. This is similar to the geometric mean concentration factor reported by Halbert (1986). It was assumed that the turnover rate of uranium of the invertebrate component was determined by the turnover time of the invertebrate populations (i.e. 38 days).

### B.2.6 Simulation Methods

The dynamics of the concentration of uranium in the model components illustrated in Figure 1 were mathematically represented by a coupled set of ordinary differential equations. The derivatives for each component were constructed as functions of the amount of uranium in the particular component and the rate constants which describe the movement of material between components.

Thus, the derivative describing the rate of change of uranium in game fish flesh is:

$$dx/dt = (\mathrm{WATER} * \mathrm{WatoGame}) + (\mathrm{FORAGE\ FISH} * \mathrm{ForgtoGame}) + (\mathrm{INVERTEBRATES} * \mathrm{InvtoGame}) + (\mathrm{GAME} * \mathrm{GametoWa}) \qquad (2)$$

where the components illustrated in Figure 1 are in capital letters and the acronymns for the rate constants are the same as those listed in Table 3. The remaining equations for the derivatives can be easily derived from Figure 1 and Table 3.

The time dependent solutions to these equations is obtained by means of a fourth/fifth order Runge-Kutta, RKF45 (see Forsythe, Malcolm and Moler, 1977 for documentation). This method of representing and simulating an aquatic model was chosen because the dynamics of the system are stable and an adequate representation of time-averaged rate constants is provided.

### B.2.7 Sensitivity Analysis

Sensitivity analysis of these equations were performed by perturbing each rate constant by 1% of their nominal value (Table 3) solving the system over the time interval of interest, and calculating the percent change in each component as a result of the 1% perturbation of a particular rate constant. The process was repeated by resetting the rate constant to its nominal value, perturbing the next rate constant and solving the system again. A 1% perturbation has been shown to provide an adequate numerical estimation of the analytical sensitivities of the equations (Gardner, 1984).

### B.2.8 Uncertainty Analysis

Estimates of the mean, variance and frequency distribution of model predictions as a function of the uncertainties associated with the model rate constants was obtained by Monte Carlo methods (Rubinstein, 1981). Monte Carlo methods involve the iterative selection of random rate constants from their respective distributions, solving the system over the time period of interest (for this case, years 1, 5, and 10), and saving the sets of random rate constants and model solutions. This process was iterated 100 times for each model scenario and the results statistically analysed. To perform the uncertainty analysis, the frequency distributions must be specified for each model rate constant. As mentioned previously in other papers (SENES, 1985; Hoffman and Gardner, 1983), these distributions do not represent the expected variability of the parameter. Instead, these distributions are intended to encompass the extent of uncertainty associated with parameter estimation. Estimates of these distributions are listed in Table 4.

In Table 4, the shape and size of the selected distributions are primarily based on judgmental estimates. All sources of uncertainty are encompassed in these distribution estimates with the exception of uncertainties in the specification of biomass. Where sufficient data were available from which inferences could be drawn about the plausible shape and size of a distribution, a normal or lognormal distribution was specified. Where large uncertainties existed in our ability to quantify a rate constant, and where data were insufficient to suggest a distribution shape and size, a loguniform distribution was selected. In those cases with limited data where only moderate uncertainties were expected, uniform distributions were selected.

FIGURE 1

ILLUSTRATION OF A MULTI-COMPONENT MODEL OF A OLIGOTROPHIC LAKE SHOWING 23 PATHWAYS FOR RADIONUCLIDE TRANSFER

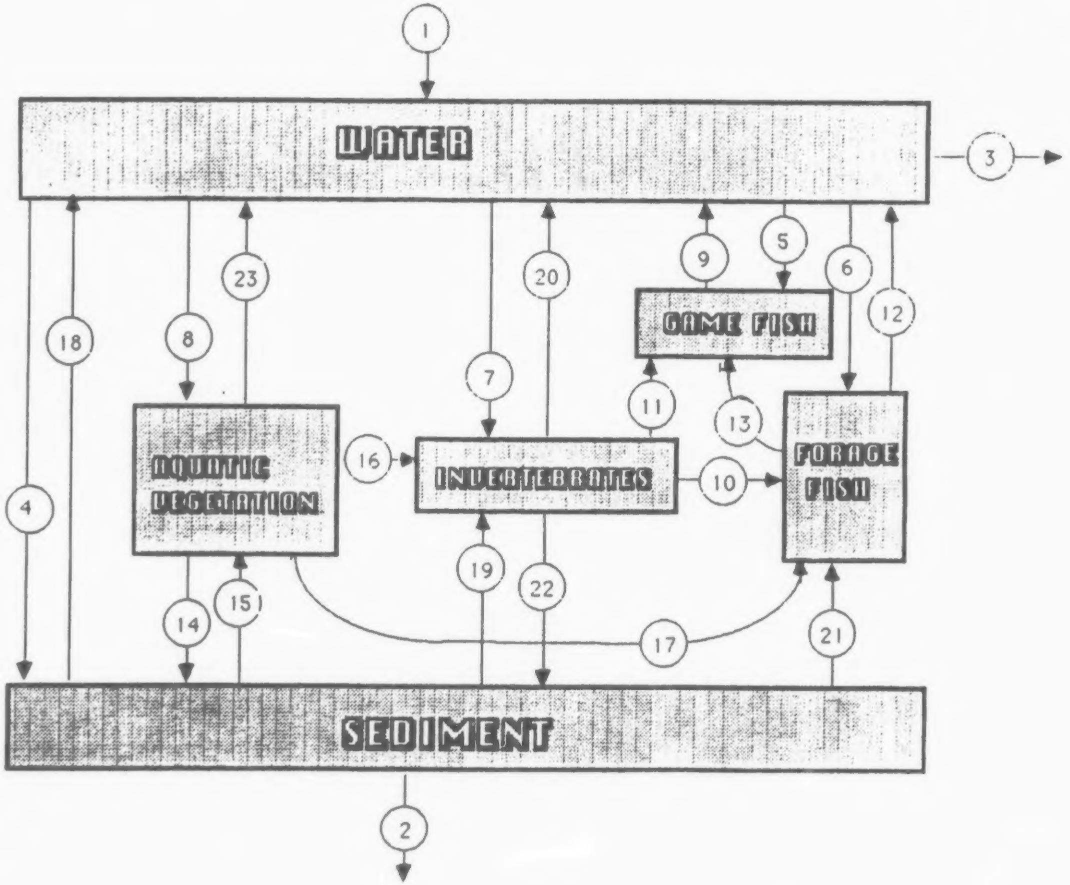
1
WATER
3
9
5
6
23
20
12
18
8
GAME FISH
7
11
13
4
AQUATIC VEGETATION
16
INVERTEBRATES
10
FORAGE FISH
19
22
14
15
17
21
SEDIMENT
2

Table 3

## PARAMETER VALUES FOR AQUATIC URANIUM MODEL

| Rate Constant Number | Name* | Equilibrium Rates (pCi per day) | Rate Constants** (per day) |
|---|---|---|---|
| 1 | Input | 4.72 E 7 | 4.72 E 7 |
| 2 | Deeploss | 2.27 E 6 | 5.75 E-5 |
| 3 | Outflow | 4.49 E 7 | 2.74 E-3 |
| 4 | Water-to-Sed | 1.71 E 7 | 1.04 E-3 |
| 5 | Water-to-Game | 2.21 E-1 | 1.35 E-11 |
| 6 | Water-to-Forg | 1.49 E 1 | 9.08 E-10 |
| 7 | Water-to-Inv | 5.42 E 4 | 3.31 E-6 |
| 8 | Water-to-Av | 1.03 E 7 | 6.28 E-4 |
| 9 | Game-to-Water | 2.46 E-1 | 3.42 E-4 |
| 10 | Inv-to-Forg | 8.27 E-1 | 1.34 E-7 |
| 11 | Inv-to-Game | 9.82 E-3 | 1.59 E-9 |
| 12 | Forg-to-Water | 1.65 E 1 | 2.74 E-3 |
| 13 | Forg-to-Game | 1.47 E-2 | 2.44 E-6 |
| 14 | Av-to-Sed | 5.12 E 1 | 1.00 E-6 |
| 15 | Sed-to-Av | 5.12 E 4 | 1.30 E-6 |
| 16 | Av-to-Inv | 1.02 E 5 | 2.00 E-3 |
| 17 | Av-to-Forg | 4.13 E-1 | 8.07 E-9 |
| 18 | Sed-to-Water | 1.48 E 7 | 3.74 E-4 |
| 19 | Sed-to-Inv | 1.85 E 3 | 4.69 E-8 |
| 20 | Inv-to-Water | 1.58 E 5 | 2.57 E-2 |
| 21 | Sed-to-Forg | 4.14 E-1 | 1.05 E-11 |
| 22 | Inv-to-Sed | 6.17 E 1 | 1.00 E-5 |
| 23 | Av-to-Water | 1.02 E 7 | 2.00 E-1 |

Note

* The abbreviations for parameter names:

Sed - Sediment
Inv - Invertebrates
Av - Aquatic Vegetation
Forg - Forage Fish
Game - Game Fish

** The rate constants were derived by dividing each equilibrium flow rate by the amount of uranium in the model component from which the flow originated, for example:

$$\frac{[\text{Water-to-game equilibrium rate of } 2.21\text{E-1 pCi day}^{-1}]}{[\text{Water uranium activity of } 1.6\text{E10 L} \times 1.0 \text{ pCi L}^{-1}]} =$$

$$[\text{Water-to-game rate constant of } 1.35\text{E-11 day}^{-1}]$$

Table 4

## DISTRIBUTIONS FOR MODEL PARAMETERS

| Rate Constant Number | Name* | Distribution Type** | Mean or Minimum | Standard Deviation or Maximum |
|---|---|---|---|---|
| 1 | Input | Constant | | |
| 2 | Deeploss | Lognormal | 5.75 E-5 | 1.35 E 0 |
| 3 | Outflow | Normal | 2.74 E-3 | 2.74 E-4 |
| 4 | Water-to-Sed | Lognormal | 1.04 E-3 | 1.75 E 0 |
| 5 | Water-to-Game | Lognormal | 1.34 E-11 | 6.10 E 0 |
| 6 | Water-to-Forg | Lognormal | 9.08 E-10 | 1.75 E 0 |
| 7 | Water-to-Inv | Loguniform | 1.03 E-7 | 1.06 E-4 |
| 8 | Water-to-Av | Loguniform | 6.28 E-4 | 2.01 E 0 |
| 9 | Game-to-Water | Uniform | 1.70 E-4 | 6.80 E-4 |
| 10 | Inv-to-Forg | Loguniform | 8.67 E-7 | 8.67 E-6 |
| 11 | Inv-to-Game | Loguniform | 7.64 E-10 | 7.64 E-8 |
| 12 | Forg-to-Water | Loguniform | 2.74 E-4 | 2.74 E-2 |
| 13 | Forg-to-Game | Uniform | 4.88 E-7 | 4.39 E-6 |
| 14 | Av-to-Sed | Loguniform | 1.00 E-7 | 1.00 E-5 |
| 15 | Sed-to-Av | Loguniform | 1.30 E-7 | 1.30 E-5 |
| 16 | Av-to-Inv | Loguniform | 6.32 E-4 | 6.32 E-3 |
| 17 | Av-to-Forg | Loguniform | 2.55 E-9 | 2.55 E-8 |
| 18 | Sed-to-Water | Loguniform | 3.75 E-4 | 1.60 E 0 |
| 19 | Sed-to-Inv | Loguniform | 4.68 E-9 | 4.68 E-7 |
| 20 | Inv-to-Water | Loguniform | 2.57 E-3 | 2.57 E-1 |
| 21 | Sed-to-Forg | Loguniform | 1.05 E-12 | 1.05 E-10 |
| 22 | Inv-to-Sed | Loguniform | 1.00 E-6 | 1.00 E-4 |
| 23 | Av-to-Water | Loguniform | 2.00 E-2 | 2.00 E 0 |

Note

* The abbreviations for parameter names:

Sed - Sediment
Inv - Invertebrates
Av - Aquatic Vegetation
Forg - Forage Fish
Game - Game Fish

** The mean and standard deviation are listed for the normal distribution. For the lognormal distribution the values are geometric mean and geometric standard deviation (the geometric standard deviation is unitless). The minimum and maximum values are given for the uniform and loguniform distributions.

Loguniform distributions ranged from one to three orders of magnitude, with the majority set at two orders of magnitude. The ranges of uniform distributions were less than one order of magnitude. The values for the distributions assigned to the rate constants: Deeploss, Water-to-Sed, and Sed-to-Water, came from estimates provided directly by SENES Consultants Limited. The deterministic estimates for these rate constants are equivalent to the arithmetic means of the normal and uniform distributions and the geometric means of the lognormal and loguniform distributions.

## B.3 RESULTS

Two scenarios were simulated with the aquatic model:

(1) the response of an uncontaminated aquatic system and the time to reach equilibrium in all model components when 1 pCi/L of uranium was added to the inflow; and

(2) the effect of a cleanup of a contaminated source (a 99.9% reduction of the daily input rate of uranium) in a system that was already at the equilibrium values established in Scenario 1.

### B.3.1 Scenario 1: Simulation to Equilibrium

The deterministic results (i.e. all rate constants set at their nominal values, Table 3) of the first scenario are illustrated in Figures 2 and 3. The dynamics of the system are a direct function of the mean residence times of uranium in each model component (the mean residence time is the reciprocal of the sum of the rate constants of the outputs for a given model component). Water, with a mean residence time of 0.62 y reaches equilibrium relatively quickly. The amount of uranium in game fish flesh (mean residence time = 8 y) takes considerably longer to approach equilibrium. The active layer of the sediment has a mean residence time similar to game fish (6.3 y) and approaches equilibrium in a similar fashion.

Figure 4 illustrates the dynamic changes of the concentration ratio of water-to-game fish flesh (CF). The equilibrium CF is 1.4. At year 10 of the simulation (Figure 4), CF = 0.9, at year 15 CF = 1.1 and at year 20 CF = 1.2. It takes about 3 times the mean residence time of game fish for the concentration factor to be within 90% of the equilibrium value. All of these values, however, are well within the reported range of measured CF's.

The sensitivities of the concentration factor to the individual rate constants change as a function of time (Table 5). For example, a 1% change in the rate constant water-to-game results in a 0.95% increase in the fish flesh concentration in year 1. The initial concentration of uranium in game fish flesh is sensitive to the outflow and the water-to-game fish rate constants. At year 5 and 10 of the simulation, the sensitivity of the uranium concentration in game fish flesh to the water-to-game transfer rate is still dominant, but the sensitivities of the outflow and the game-to-water rate constants have increased.

The results of an uncertainty analysis can differ from those of a sensitivity analysis depending on the interactions among highly connected model components (e.g. Figure 1) and differences in the uncertainties associated with the rate constants (Table 4). These effects are apparent in Table 5 where several rate constants that were not identified as sensitive (e.g. invertebrates-to-game fish, invertebrates-to-water and aquatic vegetation-to-water) have an effect on the uncertainty of the concentration of uranium in game fish flesh. However, the most important rate constant identified by the sensitivity analysis (water-to-game), is also the most important rate constant in the uncertainty analysis. The water-to-game rate constant contributes 69%, 58% and 53% percent of the variability of the concentration of uranium in game fish in year 1, 5 and 10, respectively (Table 5).

The geometric means and geometric standard deviations of all model predictions for the equilibrium scenario are shown in Table 6. Among model components, water has the smallest uncertainty (geometric standard deviation ranges from 1.11 to 1.13) and invertebrates have the largest (5.98 to 6.70). The

FIGURE 2

## CHANGES IN WATER AND SEDIMENT CONCENTRATIONS WITH TIME STARTING WITH AN UNCONTAMINATED LAKE AT TIME ZERO

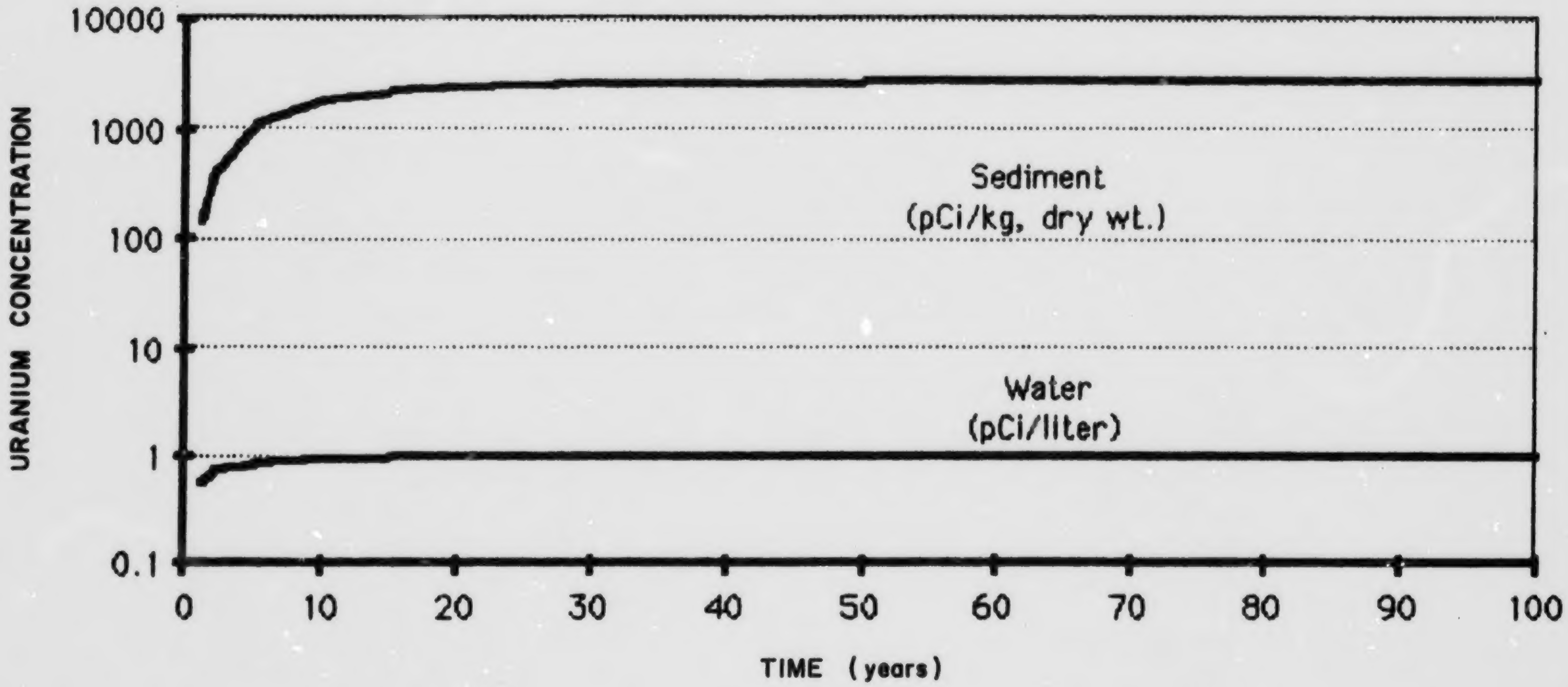

FIGURE 3

## CHANGES IN THE CONCENTRATION OF URANIUM IN GAME FISH WITH TIME STARTING WITH AN UNCONTAMINATED LAKE AT TIME ZERO

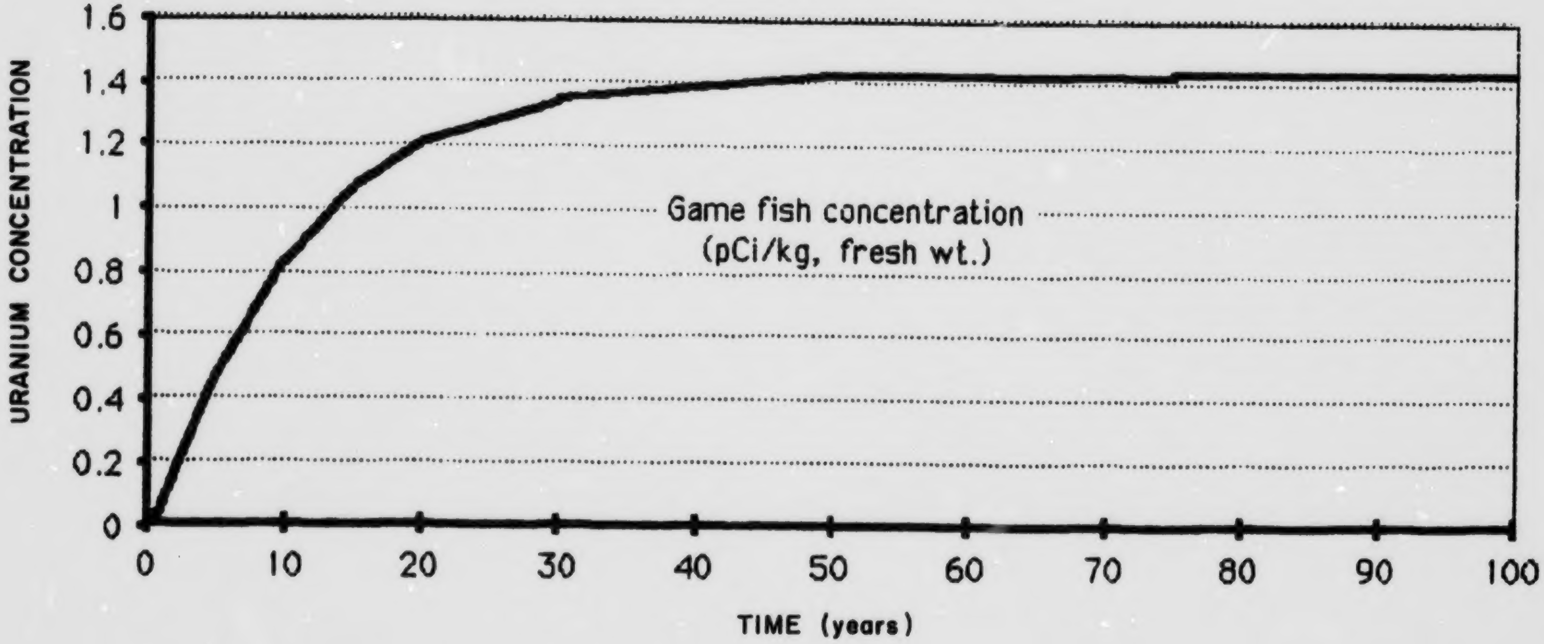

FIGURE 4

CHANGES IN THE WATER-TO-GAME FISH CONCENTRATION FACTOR (CF) WITH TIME WITH AN UNCONTAMINATED LAKE AT TIME ZERO

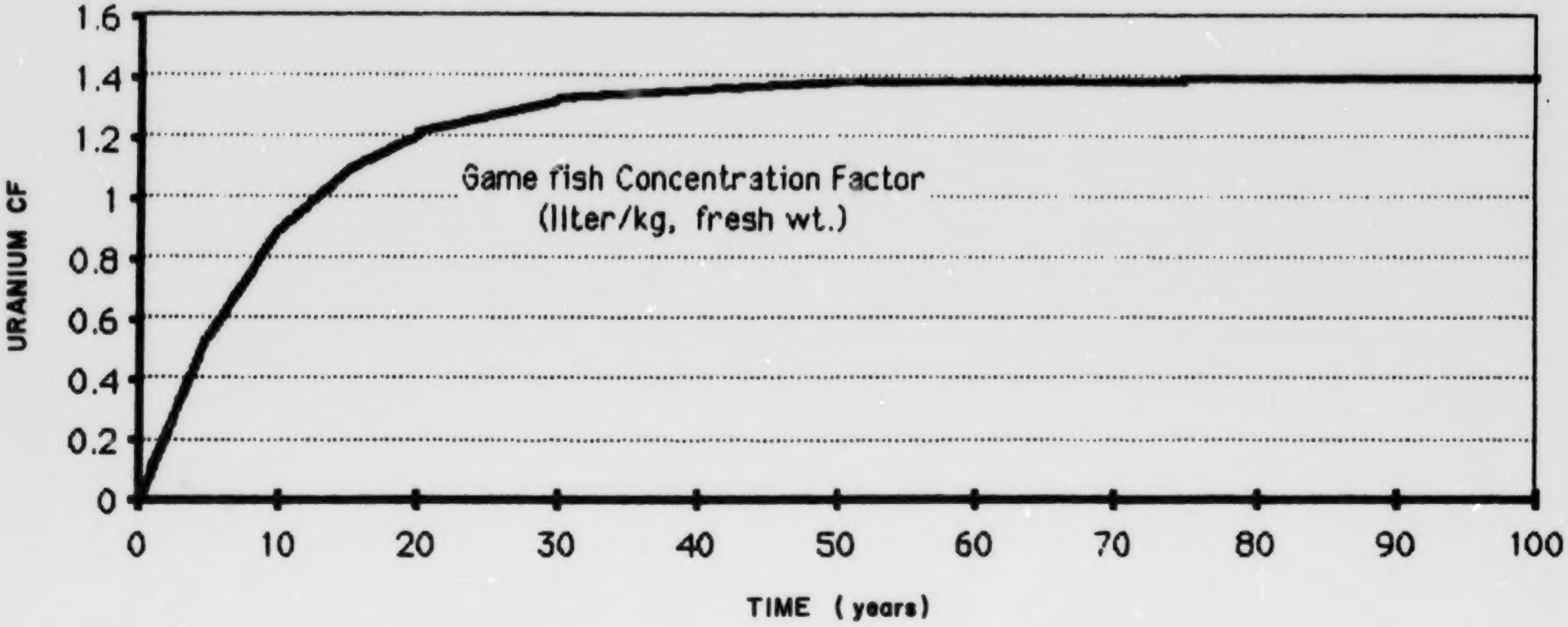

Table 5

## SENSITIVITY AND UNCERTAINTY ANALYSIS*

Concentration of Uranium in Game Fish Flesh

Equilibrium Case with Initial Conditions of 0.0

| Rate Constant** | | Year 1 | | Year 5 | | Year 10 | |
|---|---|---|---|---|---|---|---|
| Number | Name | S | U | S | U | S | U |
| 1 | Input | | | | | | |
| 2 | Deeploss | | | | | | |
| 3 | Outflow | -0.27 | | -0.65 | | -0.77 | |
| 4 | Water-to-Sed | | | | | | |
| 5 | Water-to-Game | 0.95 | 0.69 | 0.91 | 0.58 | 0.91 | 0.53 |
| 6 | Water-to-Forg | | | | | | |
| 7 | Water-to-Inv | | | | | | |
| 8 | Water-to-Av | | | | | | |
| 9 | Game-to-Water | | | -0.24 | | -0.45 | |
| 10 | Inv-to-Forg | | | | | | |
| 11 | Inv-to-Game | | 0.05 | | 0.04 | | |
| 12 | Forg-to-Water | | | | | | |
| 13 | Forg-to-Game | | | | | | |
| 14 | Av-to-Sed | | | | | | |
| 15 | Sed-to-Av | | | | | | |
| 16 | Av-to-Inv | | | | | | |
| 17 | Av-to-Forg | | | | | | |
| 18 | Sed-to-Water | | | | | | |
| 19 | Sed-to-Inv | | | | | | |
| 20 | Inv-to-Water | | 0.07 | | 0.15 | | 0.17 |
| 21 | Sed-to-Forg | | | | | | |
| 22 | Inv-to-Sed | | | | | | |
| 23 | Av-to-Water | | 0.08 | | 0.11 | | 0.12 |

Note

* Sensitivities, S, are calculated as the percent change in the model response due to a 1% decrease in a particular rate constant. The uncertainty index, U, is the square of the simple correlation of the log transformed model response with the log transformed values of the rate constant of interest calculated from 100 Monte Carlo simulations with all parameters varied as shown in Table 4. Values of $S < 0.1$ and $U < 0.04$ are not shown.

** The abbreviations for parameter names:

| | |
|---|---|
| Sed - Sediment | Forg - Forage Fish |
| Inv - Invertebrates | Game - Game Fish |
| Av - Aquatic Vegetation | |

Table 6

## GEOMETRIC MEAN* AND GEOMETRIC STANDARD DEVIATIONS OF MODEL PREDICTIONS

Equilibrium Case with Initial Conditions of 0.0

| | Year 1 | | Year 5 | | Year 10 | |
|---|---|---|---|---|---|---|
| Compartment | Mean | S.D | Mean | S.D | Mean | S.D |
| Water | 9.10 E 9 | 1.11 | 1.33 E 10 | 1.13 | 1.42 E 10 | 1.11 |
| Game Fish | 6.53 E 1 | 4.33 | 6.47 E 2 | 4.26 | 1.19 E 3 | 4.27 |
| Forage Fish | 4.00 E 3 | 3.51 | 1.82 E 4 | 5.67 | 2.36 E 4 | 6.31 |
| Aquatic Vegetation | 3.03 E 7 | 5.05 | 4.52 E 7 | 5.20 | 4.87 E 7 | 5.24 |
| Invertebrates | 4.59 E 6 | 5.98 | 8.02 E 6 | 6.70 | 8.75 E 6 | 6.67 |
| Sediments | 2.08 E 9 | 1.16 | 1.61 E 10 | 1.50 | 2.87 E 10 | 1.50 |
| CF: Water-to-Game Fish** | 2.30 E 0 | 4.32 | 1.56 E 0 | 4.23 | 2.69 E 0 | 4.25 |

Note

* The geometric means are for the activity of uranium in each model component in pCi

** The concentration factor (CF) equals:

[pCi U/kg fresh fish flesh] / [pCi U/L water]

uncertainty of the water-to-game fish flesh concentration factor changes as a function of time (geometric standard deviation ranging from 4.32 to 4.23). As noted earlier, these results reflect only the uncertainties associated with model rate constants. Additional uncertainties in biomass estimates for model components (e.g. game fish flesh) have not been included. For this reason the estimated uncertainty in the water-to-game fish flesh concentration factor at equilibrium (geometric standard deviation of 4.3) is less than that of actual measured values (which had a geometric standard deviation of 6.3).

### B.3.2 Scenario 2: 99.9% Cleanup

Scenario 2 involves a 99.9% reduction of the input of uranium into a system whose components are initially at the equilibrium concentrations established by Scenario 1. The changes of uranium concentration with time is illustrated in Figure 5. The entire system takes approximately 80 years to approach the new equilibrium values in spite of large differences in the mean residence times of each component. The reason is that the aquatic system is affected by the large reservoir of uranium in the sediment.

The dynamics of the model components dramatically affect the water-to-game fish flesh concentration factor (Figure 6). The CF is equal to 1.4 at year 0 (the instant that the input rate of uranium was reduced by 99.9%) and then rises rapidly to a high of 8 at year 30. The CF approaches 3.4 by year 60 and is near its initial value by year 100. The most sensitive rate constants of Scenario 2 (Table 7) reflect the losses of uranium from: water (outflow), exchanges between game fish flesh and water (water-to-game and game-to-water); and exchangeable sediments (sediment-to-water). The uptake of uranium by game fish flesh is only moderately important in year 10, while the loss of uranium from game fish-to-water becomes increasingly important with time, reaching a high of -1.09 in year 10 (i.e. a 1% increase in this rate constant results in a change of uranium in game fish flesh slightly greater than 1%).

The uncertainty analysis also shows the strong time dependence of this scenario (Table 7), but, as in Scenario 1, the important rate constants are not always the same as those of the sensitivity analysis. The importance of the water-to-game rate constant dominates from 43% in year 1 to 30% in year 10. Thus, across time and scenarios, the rate constants affecting the uncertainty of uranium in game fish flesh are those associated with the direct uptake and loss of uranium between water and game fish.

The geometric means and geometric standard deviations for model components of Scenario 2 are given in Table 8. The sediment and water components have the smallest uncertainty (geometric standard deviations ranging from 1.09 to 1.99) while forage fish have the largest (7.66 in year 10). The uncertainty in the water-to-game fish flesh concentration factor is less than Scenario 1 (Table 6) reflecting the reduced importance of the water-to-game fish rate constant and the increased importance of the mean residence time of uranium in game fish flesh.

## B.4 DISCUSSION AND RECOMMENDATIONS

The development of a dynamic model of uranium in an oligotrophic lake allows information to be represented in a coherent manner and the time dynamics of the system to be simulated. This capability has not been previously achieved because of difficulties involved in formulating the rate constants from the scattered information available. The development of this model is, therefore, a significant improvement in our ability to understand these systems, to compare possible scenarios, and to develop future modelling and sampling experiments.

Two caveats must be kept in mind while interpreting these results:
(1) Changes will occur as actual measurements for critical parameters become available (e.g. site specific information for the mean life expectancy of game fish). Assumptions and choices made during the development of this model have significantly affected the results. Different dynamics may become apparent as new experiments are performed and additional data becomes available. (2) It is important in any assessment activity to correctly describe the actual scenario for which an assessment is being performed. Because sensitivities

FIGURE 5

CHANGES IN WATER, SEDIMENT AND GAME FISH - FLESH CONCENTRATIONS WITH TIME AFTER 99.9% OF THE URANIUM INPUT IS REMOVED

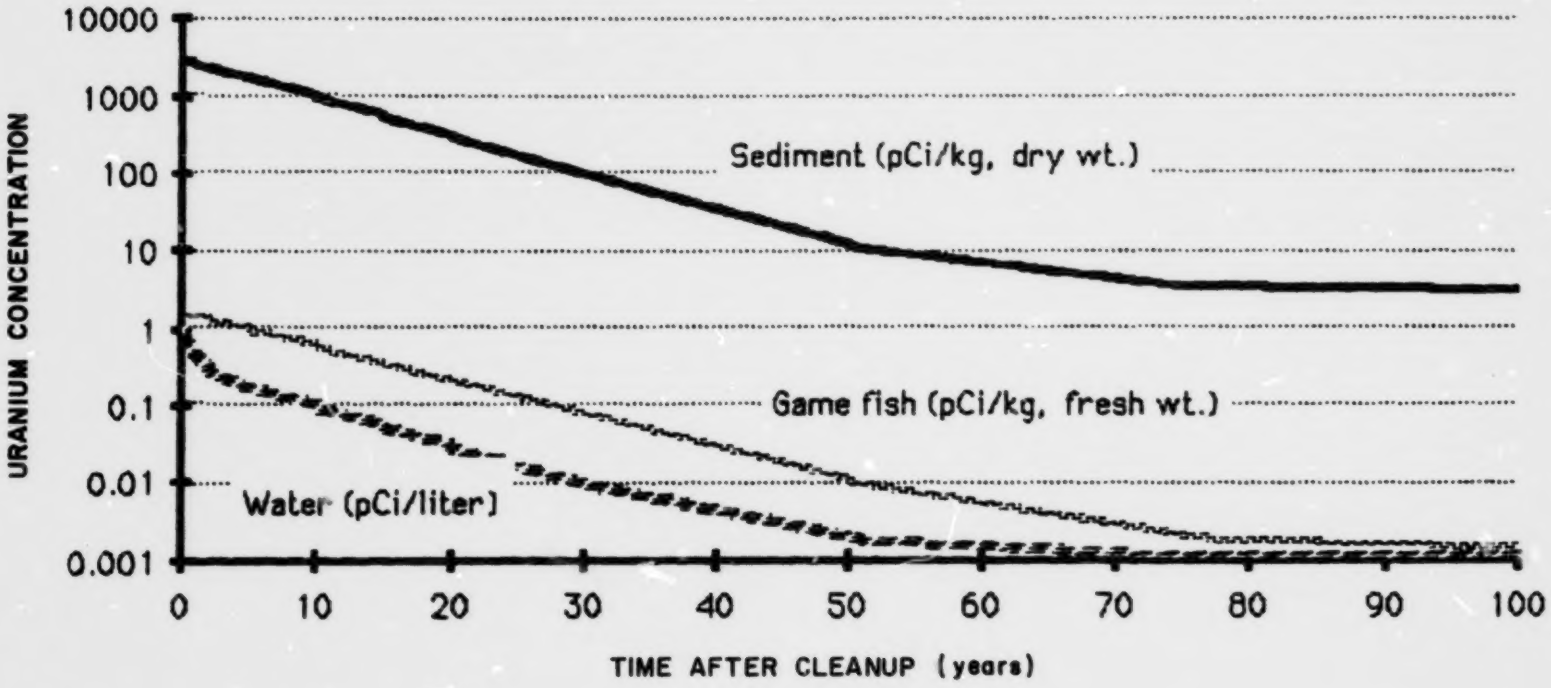

FIGURE 6

CHANGES IN THE GAME FISH-FLESH CONCENTRATION FACTOR (CF) WITH TIME AFTER 99.9% OF THE URANIUM INPUT IS REMOVED

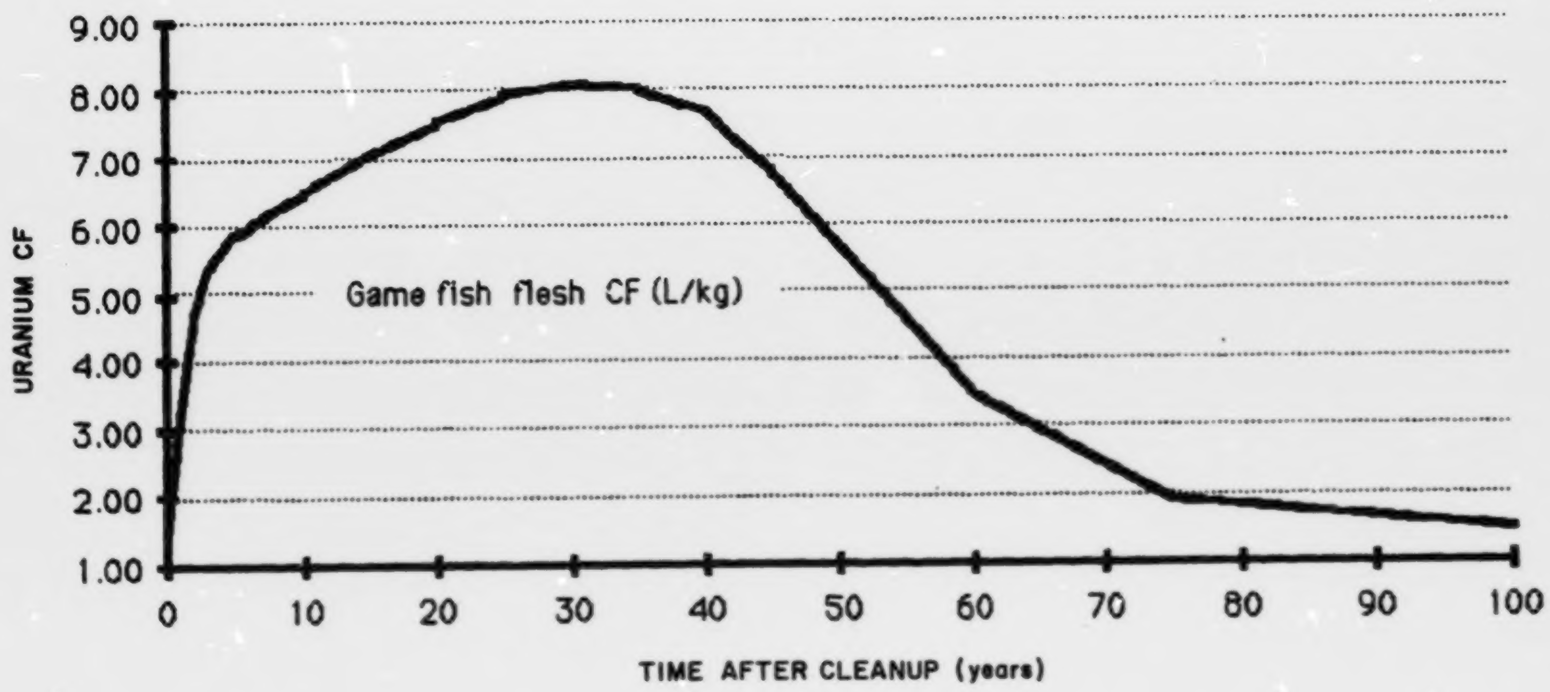

## Table 7

## SENSITIVITY AND UNCERTAINTY ANALYSIS*

### Concentration of Uranium in Game Fish Flesh

### 99.9% Cleanup Case

| Rate Constant** | | Year 1 | | Year 5 | | Year 10 | |
|---|---|---|---|---|---|---|---|
| Number | Name | S | U | S | U | S | U |
| 1 | Input | | | | | | |
| 2 | Deeploss | | | | | | |
| 3 | Outflow | | | -0.15 | | -0.27 | |
| 4 | Water-to-Sed | | | | | | |
| 5 | Water-to-Game | | 0.43 | 0.18 | 0.34 | 0.27 | 0.30 |
| 6 | Water-to-Forg | | | | | | |
| 7 | Water-to-Inv | | | | | | |
| 8 | Water-to-Av | | | | | | |
| 9 | Game-to-Water | -0.12 | | -0.57 | 0.10 | -1.09 | 0.16 |
| 10 | Inv-to-Forg | | | | | | |
| 11 | Inv-to-Game | | | | | | |
| 12 | Forg-to-Water | | | | | | |
| 13 | Forg-to-Game | | | | | | |
| 14 | Av-to-Sed | | | | | | |
| 15 | Sed-to-Av | | | | | | |
| 16 | Av-to-Inv | | | | | | |
| 17 | Av-to-Forg | | | | | | |
| 18 | Sed-to-Water | | | | | 0.13 | |
| 19 | Sed-to-Inv | | | | | | |
| 20 | Inv-to-Water | | | | 0.10 | | 0.10 |
| 21 | Sed-to-Forg | | | | | | |
| 22 | Inv-to-Sed | | | | | | |
| 23 | Av-to-Water | | 0.08 | | 0.11 | | 0.10 |

Note

* Sensitivities, S, are calculated as the percent change in the model response due to a 1% decrease in a particular rate constant. The uncertainty index, U, is the square of the simple correlation of the log transformed model response with the log transformed values of the rate constant of interest calculated from 100 Monte Carlo simulations with all parameters varied as shown in Table 4. Values of S < 0.1 and U < 0.04 are not shown.

** The abbreviations for parameter names:

Sed - Sediment
Inv - Invertebrates
Av - Aquatic Vegetation
Forg - Forage Fish
Game - Game Fish

Table 8

## GEOMETRIC MEAN* AND GEOMETRIC STANDARD DEVIATIONS OF MODEL PREDICTIONS

99.9% Cleanup Case

| | Year 1 | | Year 5 | | Year 10 | |
|---|---|---|---|---|---|---|
| Compartment | Mean | S.D | Mean | S.D | Mean | S.D |
| Water | 6.04 E 9 | 1.27 | 1.63 E 9 | 1.71 | 1.01 E 9 | 1.47 |
| Game Fish | 8.64 E 2 | 1.52 | 7.02 E 2 | 2.10 | 4.52 E 2 | 2.63 |
| Forage Fish | 9.46 E 3 | 4.17 | 4.79 E 3 | 7.41 | 2.94 E 3 | 7.66 |
| Aquatic Vegetation | 2.18 E 7 | 5.54 | 6.17 E 6 | 5.95 | 3.82 E 6 | 5.41 |
| Invertebrates | 4.42 E 6 | 7.01 | 1.24 E 6 | 6.97 | 7.62 E 5 | 6.51 |
| Sediments | 3.85 E 10 | 1.09 | 2.71 E 10 | 1.43 | 1.70 E 10 | 1.99 |
| CF: Water-to-Game Fish** | 4.58 E 0 | 1.62 | 1.28 E 1 | 2.41 | 1.44 E 1 | 2.83 |

Note

* The geometric means are for the activity of uranium in each model component in pCi

** The concentration factor (CF) equals:

[pCi U/kg fresh fish flesh] / [pCi U/L water] and uncertainties vary with time and scenario, a misspecification of the assessment scenario may result in errors greater than those due to uncertainties in the rate constants or errors in model formulation.

Keeping the above caveats in mind, the model and simulations presented here lead to several recommendations. The use of a deterministic water-to-game fish flesh concentration factor (CF) based on measurements of the system at equilibrium can be misleading. For instance, in extreme cleanup situations (e.g. Scenario 2) the deterministic equilibrium CF of 1.4 underpredicts the actual concentration in game fish flesh by a factor of about 5. This problem may be resolved by precise information on the residence time of uranium in game fish; however, these measurements are difficult to obtain under field conditions. In a clean lake which is being contaminated, the equilibrium CF substantially overpredicts the concentration of uranium in flesh of game fish for the first 10 years. Nevertheless, all of the simulated CF values are within the range of observed values of CFs reported in the literature.

The complexity of this model is desirable for studying and understanding the dynamics of uranium in the aquatic system, but a much simpler system may be used for making reliable predictions. For instance, since it is assumed that over 90% of the uranium activity in game fish flesh comes directly from the water, the aquatic food chain is relatively unimportant. Thus, the most important factors are the processes governing the concentration of uranium in the flesh of fish, the mean life expectancy of the game fish and the water-to-game fish transfer dynamics. A simpler model with three components (water, sediments and game fish) and three parameters (biomass, water-to-game transfer, and mean residence time) would adequately capture the important dynamics of the more complex model.

We note that the ingestion of uranium in the flesh of game fish will not be as significant to the exposure of critical population groups as is the direct consumption of lake water. Even if a maximum CF of 50 is assumed, more than 320 grams of fish would have to be consumed per week before the uranium intake by a fisherman would exceed the intake of a person drinking 2.2 liters of lake water per day.

## B.5 LITERATURE CITED

Blaylock, B.G., 1982. "Radionuclide Data Bases Available for Bioaccumulation Factors for Freshwater Biota." Nuclear Safety 23: (4) pp. 427-437.

Forsythe, G.E., Malcolm, M.A., Moler, C.B., 1977. "Computer Methods for Mathematical Computations." Prentice-Hall, Inc.

Gardner, R.H., 1984. "A Unified Approach to Sensitivity and Uncertainty Analysis. In: Applied Simulation and Modelling." M.H. Hamza, (ed.). Proceedings of the IASTED International Symposium, San Francisco, U.S.A., June 4-6, 1984. ACTA Press, Anaheim, Ca. pp. 155-157.

Halbert, B.E., 1986. Personal Communication. SENES Consultants Limited, 499 McNicoll Ave., Willowdale, Ontario.

Hoffman, F.O., and Gardner, R.H., 1983. "Evaluation of Uncertainties in Environmental Radiological Assessment Models. In: Radiological Assessment: A Textbook on Environmental Dose Assessment." J.E. Till and H.R. Meyer (eds.), U. S. Nuclear Regulatory Commission, Washington, D.C. NUREG/CR-3332, ORNL-5968. pp. 11-1, 11-55.

National Council on Radiation Protection and Measurements, 1984. "Radiological Assessment: Predicting the Transport, Bioaccumulation, and Uptake by Man of Radionuclides Released to the Environment." NCRP Report No. 76, 7910 Woodmount Avenue, Bethesda, MD. 20814.

Ontario Water Resources Commission, 1972. "Water Pollution from the Uranium Mining Industry in the Elliot Lake and Bancroft Areas: Vol. 2 - Detailed Findings." Toronto, Ontario.

Ophel, I.L., 1978. "Aquatic Food Chain Transport of Radionuclides. In: Proceedings of Workshop on the Evaluation of Models Used for the Environmental Assessment of Radionuclide Releases." CONF-770901, Oak Ridge National Laboratory, Oak Ridge, TN.

Rope, S.K., and Whicker, F.W., 1980. "Ra-226 Bioaccumulation in Trout, Final Report for the Period December 1, 1978 - November 30, 1980." Department of Radiobiology and Radiation Biology, Colorado State University, Fort Collins, Colorado.

Rubinstein, R.Y., 1981. "Simulation and the Monte Carlo Method." John Wiley α Sons.

Schindler, D.W., and Holmgren, S.K., 1971. "Primary Production and Phytoplankton in the Experimental Lake Area, Northwestern Ontario, and Other Low-Carbonate Waters, and Liquid Scintillation Method for Determining C-14 Activity in Photosynthesis." Journal Fisheries Research Board of Canada, Vol. 23, pp. 189-201.

SENES Consultants Limited, 1985. "Probabilistic Model Development for the Assessment of the Long Term Effects of Uranium Mill Tailings in Canada - Phase II." Research Report Prepared for the National Uranium Tailings Program, CANMET, EMR, Ottawa, Under Supply and Services Canada Contract Number OSQ84-00207.

Stegnar, P., and Kobald, I., 1982. "Uptake and Distribution of Radium and Uranium in the Aquatic Food Chain. In: Environmental Migration of Long-Lived Radionuclides." IAEA-Sm-257/87P, International Atomic Energy Agency. Vienna, pp. 364-373.

Swanson, S.M., 1983. "Levels of Ra-226, Pb-210 and Total Uranium in Fish Near a Saskatchewan Uranium Mine and Mill." Health Physics 45 (1) 67-80.

Swanson, S.M., 1985a. Personal Communication. Saskatchewan Research Council, Saskatoon, Saskatchewan.

Swanson, S.M., 1985b. "Study of the Distribution of Naturally Occurring Radionuclides in Freshwater Benthos and Their Environment: Phase II Report." Report by SENES Consultants Limited and the Saskatchewan Research Council for the National Uranium Tailings Program, CANMET, EMR, Ottawa. Under Supply and Services Canada Contract Number 0SQ83-00241.

Soballe D.M, and Kimmel, B.L., 1985. Personal Communication. Oak Ridge National Laboratory, Oak Ridge, TN.

Wahlgren, M.A., Alberts, J.J., Nelson, D.M., and Orlandis, K.A., 1975. "Study of the Behaviour of Transuranic Nuclides and Possible Chemical Homologues in Lake Michigan Water and Biota. In: Transuranium Nuclides in the Environment." STI/PUB/410, International Atomic Agency, Vienna, pp. 9-24.

Wetzel, R.G., 1975. "Limnology." W. B. Saunders Co., Toronto.

# APPENDIX C

# APPROACHES TO MODELLING EPISODIC EVENTS

## ABSTRACT

The mathematical (simulation) models used in UTAP assume that the natural system being modelled is "well-behaved" in time. That is, the tailings evolve over time, from some set of initial conditions, in a complex, but predictable manner. However, it is likely that over the time period of interest (hundreds to thousands of years), some natural events will occur which may alter the predictable chemical and physical behaviour of the tailings. Such episodic events (floods, fires, etc.) will affect the natural system for varying periods of time, to varying degrees and with different long-term consequences.

This appendix outlines how some aspects of the Phase III component models might be modified to account for episodic events. The episodic events considered include floods, earthquakes, high winds, droughts and forest fires. In some instances the information presented is quite specific, while in other cases a more conceptual discussion is presented.

## C.1 INTRODUCTION

The mathematical (simulation) models used in UTAP assume that the natural system being modelled is "well-behaved" in time. That is, the tailings evolve over time, from some set of initial conditions, in a complex, but predictable manner. However, it is likely that over the time period of interest (hundreds to thousands of years), some natural events will occur which may alter the predictable chemical and physical behaviour of the tailings. Such episodic events (floods, fires, etc.) will affect the natural system for varying periods of time, to varying degrees and with different long term consequences.

At the outset of the Phase III study, a conscious decision was made not to attempt to build into the system model the capability to explicitly model such episodic events. It was recognized that inclusion of such capability would greatly complicate the main thrust of the modelling efforts. First, one would have to build in a series of "switches," essentially enquiring, at each time step, "Has anything unusual happened?" (i.e. "Is an episodic event to occur in this time period?"). Secondly, the appropriate models would have to be altered to predict the consequences of each episodic event. This would require a series of branches, or alternate structures for several of the component models. A further complication would involve modelling the effects of two events which occur in a short period of time. Such combinations might require additional model changes (branches) since the effects might be synergistic rather than simply additive.

In summary, it is quite possible to construct models to predict the effects of relatively rare natural events. The inclusion of such models in the Uranium Tailings Assessment Program would involve considerable work, primarily regarding logic flow and internal bookkeeping.

Although the capability to model episodic events has not been explicitly built into UTAP, it is nevertheless interesting to examine how these events might actually be modelled within the Phase III system framework. The following section outlines a number of natural, episodic events which have the potential to alter the environmental impacts of uranium mill tailings. A brief summary of the potential consequences of each event is presented. Following that is a more detailed examination of possible approaches to modelling the event consequences.

## C.2 OVERVIEW OF RELEVANT EPISODIC EVENTS

Natural events which have the potential to affect uranium mill tailings include:

- major precipitation events (i.e. storm/flood)
- earthquakes
- high winds
- droughts
- forest fires.

Human-caused events, such as the removal of tailings for building material, construction of farms, and/or residences on the tailings, etc. are not considered here. A thorough review of the potential effects of natural events on Canadian uranium mill tailings was recently completed by McInnis (1985). Some of the information in this section is drawn from his report.

### Precipitation and Flood

Tailings are generally disposed of in natural valleys behind conventional rock-fill dams. Such dams are usually designed to withstand a 1 in 100 or 1 in 200 year storm. However, over the long term, storms of greater magnitude (i.e. greater precipitation) could occur. The heavy precipitation and high flows resulting from a 1 in 500 or 1 in 1000 year storm might be expected to damage the tailings impoundment structures. Such damage could involve overtopping, erosion and possibly even washout of sections of the tailings embankments. Depending on the fluid characteristics of the tailings at the time of the event, dam failure could result in a major loss of tailings from the impoundment into rivers and/or lakes downstream from the tailings site.

## Earthquake

There are several potential consequences associated with the occurrence of an earthquake, including:

- the possibility of tailings liquefaction
- embankment failure
- differential setting.

Severe seismic shock has the potential to liquify the fine, dry tailings material found on the tailings surface and on the face of embankments.

A more significant consequence would be an embankment failure. An embankment might be expected to fail if the stress imposed by an earthquake were greater than the dam's design stress. Dam failure can occur through embankment liquefaction or through cracking and fissuring, of the dam. Again, the volume of actual tailings loss from the area would depend on the fluid characteristics of the tailings at the time of the event. The most extreme consequence is likely to be similar to that described previously regarding the flood event.

A further consequence, far less significant than a dam failure, would be differential settling of the tailings area. This might result in a weakening of the tailings containment structures, rendering them more susceptible to future failure.

## High Wind

Very high winds may be produced by several natural phenomena, including hurricanes and tornadoes. For present purposes, these can all be considered as similar events. The primary effect of such high winds might be to damage the tailings vegetative cover, and to disperse some of the tailings solids over a relatively wide area. During the wind event, the higher wind speeds would lead to enhanced wind erosion of the tailings. However, they would also result in larger dilution of the particles in air. The actual effect on air concentration would depend on the specific circumstances. Following the high wind event, the airborne dust would settle to the ground, where it would be available to the biosphere.

## Drought

A prolonged drought may have several consequences; the magnitude of the consequences increasing with the length of the drought. First, and most obviously, a drought would result in the loss of much of the tailings vegetation. This would produce an attendant increase in erosion by both wind and water action. Secondly, the lack of precipitation, which characterizes drought, would result in a decrease in the moisture content of the tailings. Since radon flux through the tailings is attenuated by tailings moisture, the radon flux from the tailings surface might be expected to increase. An interesting consequence of the reduced moisture flow through the system might be a reduction in the rate of dissolution of radionuclides associated with soluble compounds (e.g. Ra-226 in $BaSO_4$; Pb-210 in $PbSO_4$).

## Forest Fire

Forest fires can be expected to occur on a fairly regular basis in any natural environment. The return frequency of forest fires in many parts of northern Ontario is somewhere between 100 and 200 years. Thus, several forest fires might be expected at a particular tailings site over the next 500 to 1000 years. Obviously a forest fire will remove much of the vegetation from the tailings surface. This will again result in increased erosion by wind and water action. However, natural systems are generally quick to revegetate following a fire. Since a tailings area represents a harsher growing environment, revegetation might be somewhat slower. Nevertheless, sufficient revegetation should take place over 10 to 20 years to eliminate any additional wind or water erosion resulting from a forest fire.

## C.3 POTENTIAL MODEL MODIFICATIONS

It is apparent from the preceding discussion that several of the Phase III component models would have to be modified to simulate the environmental impacts of the various natural events. In this section, we indicate how the model modifications might take place. In some instances, very specific suggestions are made, while in others, only a conceptual approach is discussed. As in any modelling exercise, we can only hope to approximate real world behaviour. Hence, the model modifications suggested focus on the primary consequence(s) of an event and often ignore some of the expected secondary consequences. The suggestions made here are not meant to be exhaustive, but rather to provide a first approximation of the consequences of an event. In any real application, one might choose different approaches than suggested here, and one would very likely want to indulge in further scenario postulation leading to further model changes.

For modelling purposes, the immediate consequences of several of the natural events discussed previously can be lumped into two categories:

- events leading to bulk loss of tailing and tailings porewater (e.g. flood, earthquake)
- events leading to partial or total reduction in tailings vegetation (e.g. drought, high winds, forest fire).

In addition, simulating the drought event may require additional model modifications. These are discussed towards the end of this section.

### Bulk Loss of Tailings

To simulate an event leading to bulk loss of tailings, many assumptions are required. First, one might assume that all the tailings solids transported from the tailings area are deposited in the first lake in the downstream watershed. The porewater of the same tailings mass, containing dissolved ions and radionuclides might be assumed to be added to the first receiving node in the watershed; likely a river. To determine the total solid and liquid loading to the receiving environment, one would have to specify the fraction or percent of the tailings volume lost as an immediate result of the event. This quantity would likely be larger for a flood than an earthquake, and might depend on tailings characteristics predicted at the time of the event occurrence. An additional, chronic loading for some time following the event might also be expected, as the newly exposed slopes stabilize to their natural slope angle.

It may be possible to incorporate this episodic loading relatively easily in the Phase III models. The current erosion model (Section 3.14) predicts a solids loading to the watershed (EROTOT) in each time period. The watershed model (Chapter 10) currently assumes that the radionuclides present in this mass are dissolved in the first node, while the solids themselves are incorporated into the sediment of the first downstream lake.

The bulk loading as a result of dam failure could be added to the erosion loading (EROTOT) which would automatically be incorporated into the watershed model. One might wish to modify the current (conservative) assumptions that all of the radionuclides in the tailings solids are dissolved in the first node. To simulate the chronic bulk loadings for several years following a dam failure, the same approach might be used.

In addition to the solid tailings, one would also have to consider the addition of the dissolved species in the tailings porewater to the first river node. After deciding which characteristic porewater concentrations to use (layer 2, 3, 4, or some volume weighted average), it would be relatively straightforward to add this liquid loading directly to the first watershed node.

The bulk solids added to the first lake would settle to the bottom and form the active sediment exchange layer. Since tailings solids possess different physical/chemical characteristics than oligotrophic lake sediments, some sediment parameters (e.g. distribution coefficient ($K_D$), density, etc.) would have to be altered at the time of event occurrence. Since sedimentation occurs at the rate of about 0.1 cm/yr, and since the active sediment exchange layer is assumed to be 5 cm thick (see Chapter 10), complete burial of the tailings solids might be expected in about 50 years. Between the time of event occurrence, and the 50 year recovery time, one might allow the sediment parameters to evolve from the post-event values (e.g. representing tailings solids) to the pre-event values, in an exponential or linear matter.

In summary, the following changes might be required to simulate a bulk loss of tailings event:

- determine the fraction of tailings volume (mass) to be lost (e.g. 10%)
- add this mass to the erosion for that time period (EROTOT). The radionuclides from these solids will be dissolved in the first watershed node and the solids will be incorporated into the first lake
- add the corresponding loading of dissolved radionuclides to node 1 of the watershed
- modify the necessary sediment parameters to reflect the characteristics of the tailings solids (e.g. $K_D$, density)
- based on sedimentation rate, calculate a time for complete burial of the tailings solids
- let the sediment parameters evolve from post-event values to pre-event values (linear or exponential change)
- for some desired time add additional chronic solids and porewater loading (to EROTOT and watershed node 1).

## Loss of Vegetative Cover

Several of the natural events described earlier have the potential to reduce or eliminate the tailings vegetation. This would result in greater erosion of the tailings by wind and water action. Simulating the loss of vegetative cover and subsequent increases in erosion would be relatively straightforward with the Phase III models.

The current approach to modelling the vegetation and erosion of tailings is described elsewhere in this volume (Section 3.14). The fraction of tailings vegetated ($F_v$) is calculated as a function of time and the pH of the tailings surface (equation 3.14.6). The exposed tailings surface area (for wind erosion) is then calculated as a function of the fraction of tailings vegetated. Several parameters in the Universal Soil Loss Equation (USLE), used to model sheet erosion by water action, are also functions of $F_v$. These include a control factor due to surface stabilization ($C_s$; equation (3.14.5)) and a runoff reduction factor ($C_{ro}$; equation (3.14.11)). In simulating an event resulting in loss or depletion of tailings vegetation, one would modify the calculation of the fraction of tailings vegetated. The modifications might be as follows:

- at the time of event occurrence ($t_e$) reduce the fraction of vegetation to some fraction (R) of its current value ($F_v(t_e)$), that is:

  $$F_{v,e} = R\,F_v(t_e)$$

- this will increase wind and water erosion as described previously

- select a time for revegetation to pre-event levels to occur. This may itself be a function of $F_v(t_e)$.

- let the fraction of vegetation ($F_v$) increase exponentially from the post-event value ($F_{v,e}$) to the pre-event value over the recovery time.

- following the recovery time, the previous equation for $F_v$ (equation 3.14.6) would again apply.

Drought

Simulating a drought event would be marginally more involved than simulating a simple loss of tailings vegetation. Modelling drought might involve the following steps:

- reduce annual net precipitation (NPRCP) by some appropriate fraction for some desired length of time (i.e. the length of the drought);
- over this period of reduced precipitation, one might wish to have the fraction of tailings vegetated decrease with time. Alternatively, one could model a step-wise decrease in vegetation as described previously;
- the moisture content of the tailings (MPCH2O) should be reduced in a manner analagous to that used in reducing the tailings vegetation. This will result in increased radon diffusion through the tailings;
- at the end of the drought period, precipitation should return to pre-event levels, and tailings vegetation and moisture content should recover exponentially over some specified period.

# Volume

# 4

# NATIONAL
URANIUM
TAILINGS
PROGRAM

Energy, Mines and
Resources Canada

Energie, Mines et
Ressources Canada

Canada

# PROBABILISTIC MODEL DEVELOPMENT FOR THE ASSESSMENT OF THE LONG-TERM EFFECTS OF URANIUM MILL TAILINGS IN CANADA - PHASE III

## VOLUME 4 - URANIUM TAILINGS ASSESSMENT PROGRAM (UTAP) USER'S MANUAL

A Research Report Prepared Under
Contract # 0SQ85-00182

for

The National Uranium Tailings Program
Canada Centre for Mineral and Energy Technology
Energy, Mines and Resources Canada
555 Booth Street
Ottawa, Ontario
K1A 0G1

SENES Consultants Limited
499 McNicoll Ave.
Willowdale, Ontario
M2H 2C9

July 1986

MICROMEDIA

84pp

## ABSTRACT

This study represents part of the ongoing efforts of the National Uranium Tailings Program (NUTP) to develop the capability to predict the long-term effects of Canadian uranium mill tailings. The study was conducted to further refine the probabilistic assessment tool developed during two previous phases of work. In particular, the work involved expanding the system model to include: additional radionuclides, additional pathways of exposure and the ability to perform calculations over much greater distances. The primary product of this study is a revised, more comprehensive Uranium Tailings Assessment Program (UTAP).

The project report has been prepared in four volumes, of which this is volume 4. This volume is a user's manual for UTAP. It provides some background information regarding the structure of UTAP and describes its input and output characteristics. The information provided is sufficient to allow a user to run the program as it currently exists, modifying the inputs and obtaining a variety of outputs. Furthermore, sufficient details are provided to allow a more sophisticated user to modify existing modules of code and/or replace entire modules.

---

## NOTICE

This report was prepared by SENES Consultants Limited (SENES) under contract to the National Uranium Tailings Program (NUTP). Neither the NUTP nor SENES makes any warranty, expressed or implied, or assumes any liability with respect to any damage or loss incurred as a result of the use made of the information contained in this publication.

## TABLE OF CONTENTS

Page

Abstract i
Notice i

1.0 INTRODUCTION 1-1
  1.1 Background 1-1
  1.2 How to Use the Manual 1-2
  1.3 Objectives of the Uranium Tailings Assessment Program 1-2
    1.3.1 Constituents 1-3
    1.3.2 Pathways 1-3

2.0 CONTROL MODULE FUNCTIONS 2-1
  2.1 Input 2-1
  2.2. Draw Random Samples 2-1
  2.3 Select Parameters for Output and Statistics 2-1
  2.4 Compute Statistics on Selected Variables 2-2
  2.5 Write Data to Output Files 2-2
    2.5.1 Output Statistics File 2-2
    2.5.2 Output Detailed Results Files 2-3
  2.6 Step Through Time 2-3
  2.7 Confidence Bands 2-4

3.0 BUILDING INPUT FILES AND OBTAINING OUTPUT 3-1
  3.1 First Input File 3-1
    3.1.1 Selecting Alternate Scenarios 3-3
  3.2 Second Input File 3-4
    3.2.1 Receptor Information 3-4
    3.2.2. Watershed Information 3-5
    3.2.3 Output Selection Information 3-5
  3.3 Air Dispersion Data 3-7

Table of Contents, Cont'd.

Page

4.0 Running the Program 4-1

5.0 Altering the Program 5-1
  5.1 Changing COMEX 5-1
  5.2 Writing Component Modules 5-2
  5.3 Passing Variables 5-2
    5.3.1 Include File MODEL.INC 5-2
    5.3.2 Include File VAR.INC 5-5
  5.4 Changing the Control Modules 5-7
  5.5 Modifying First Input File 5-7
  5.6 Modifying Second Input File 5-7
  5.7 Compiling and Linking 5-8
  5.8 Running the Program 5-9
  5.9 Other Changes and Information 5-9

6.0 Confidence Bands 6-1
  6.1 Running the Program 6-1

REFERENCES

APPENDIX A - ERROR AND WARNING MESSAGES
APPENDIX B - SAMPLE INPUT FILES
APPENDIX C - SAMPLE OUTPUT FILES
APPENDIX D - INPUT DISTRIBUTION DESCRIPTIONS

## LIST OF FIGURES

| | | Follows Page |
|---|---|---|
| 1.1 | Exposure Pathways | 1-4 |
| 3.1 | Input and Output Files | 3-1 |
| 3.2 | Forms of the Weibull Distribution Probability Function | 3-2 |
| 3.3 | Forms of the Beta Distribution Probability Density Function | 3-2 |
| 3.4 | An Arbitrary Probability Density Function | 3-2 |
| 3.5. | Conceptual Diagram of Spatial Coordinate System | 3-4 |
| 5.1 | The System Model | 5-1 |
| 5.2 | Control Module Structure | 5-1 |
| 5.3 | Subroutine COMEX and the Component Modules | 5-1 |
| 6.1 | Plots of 95% Confidence Bands for a Normal Distribution | 6-1 |

## LIST OF TABLES

Follows Page

3.1. Sample of First Input File 3-1

3.2 Format of First Input File (INPUT1.DAT) 3-1

3.3 Distribution Descriptors 3-2

3.4 Sample of Second Input File (INPUT2.DAT) 3-4

3.5 Format of Second Input File (INPUT2.DAT) 3-4

3.6 Output Parameters 3-6

3.7 Substance Codes 3-6

3.8 Format of AES Wind Data File 3-8

4.1 Sample Session 4-1

6.1 Confidence Bands Program Sample Session 6-1

6.2 Confidence Bands Program Sample Output File for a Normal Distribution 6-1

# 1.0 INTRODUCTION

## 1.1 Background

In 1982 Energy Mines and Resources Canada established the National Uranium Tailings Program (NUTP) to pull together previous work on Canadian uranium mill tailings, to fund additional work where significant information gaps were found and to develop the capability to predict the long-term effects of tailings with a known degree of confidence while incorporating variability and uncertainty in the input data. Such evaluations require the use of mathematical models to simulate the behaviour of the real system.

An earlier study (Phase I) funded by the NUTP demonstrated how probabilistic techniques could be used to take account of the variability and uncertainty in model input parameters in such a simulation analysis (SENES, 1984). Subsequently, the NUTP sponsored a followup study (Phase II, SENES, 1985) to extend and refine the probabilistic tools developed in the Phase I study and to investigate various issues of technical interest involved in carrying out and interpreting a probabilistic analysis.

The objectives of the current, Phase III study were to extend the capabilities of the Phase II system model and then apply the upgraded (Phase III) system model to a hypothetical reference site. More specifically, Phase III was designed to:

- expand the simulation models to include additional major radionuclides
- expand the simulation models to include additional selected pathways of exposure
- modify the system model to permit calculations over greater distances
- develop a model for simulating the water erosion of tailings or cover material
- streamline the system code, update the documentation and prepare a user's manual

A number of related issues were also investigated.

The Phase III work involved extensive modifications and additions to the computer program developed during the previous studies. The product of the current phase of work is a revised Uranium Tailings Assessment Program (UTAP). Because the Phase III studies covered a variety of aspects of substantially different form and content and because of the sheer volume of material, the Phase III report has been prepared in four volumes, of which this is volume 4. Volume 1 is a summary of the project activities and major results. Volumes 2 and 3 document the UTAP control and component modules respectively. This volume is a user's manual for UTAP.

## 1.2 How to Use the Manual

This user's manual for the Uranium Tailings Assessment Program (UTAP) is geared toward two types of users. The first type is the Level I user who simply wishes to use the program. Such considerations as building and modifying input files and obtaining desired output are dealt with in the Level I user sections. The second type of user is the Level II user who actually wishes to change the program by adding new lines of code or new modules. The level of detail provided to the Level II user is, hence, considerably higher.

The first two sections of the manual provide both Level I and II users with necessary background on UTAP. The third and fourth sections called "Building Input Files and Obtaining Output" and "Running the Program" are for the Level I user but must also be understood by the Level II user. The fifth section titled "Altering the Program" is intended for the Level II user.

## 1.3 Objectives of the Uranium Tailings Assessment Program

The principal objective of the Uranium Tailings Assessment Program is to perform a probabilistic analysis of the behaviour and environmental effects of uranium mill tailings, following close-out of milling operations. The models in this Phase III study have been designed to allow predictions to be made for distances up to 50 kilometres in all directions from the tailings area, and for time periods of up to 1000 years. In addition, the models provide many other features. These include the ability to incorporate different receptors and site characteristics and to deal with input parameters which vary with time.

To achieve its objectives, the Uranium Tailings Assessment Program is composed of a number of modules. These may be classified as either component or control modules. Component modules (or models) are the programs directly concerned with the simulation of a uranium tailings physical system; that is, the computer implementation of the mathematical models representing the uranium tailings pile and surrounding environment. Control modules provide the infrastructure for probabilistic analysis using the component modules. These functions include probabilistic sampling of input parameters, and many input, output and bookkeeping functions. The integrated control and component modules are referred to as the system model or the Uranium Tailings Assessment Program (UTAP).

### 1.3.1 Constituents

The radionuclides modelled are total uranium, total thorium, radium-226, radon-222 and lead-210. The pH of the reference uranium tailings site and the chained river-lake system discussed later are also modelled. As in Phase II, pH is modelled by an equilibrium relationship which explicitly accounts for the dissolved concentrations in the aqueous phase of calcium, iron and sulphate.

### 1.3.2 Pathways

The following pathways of dose to the receptors are modelled in Phase III for the aforementioned radionuclides:

1) Water Consumption: dispersion of tailings effluent in the receiving water environment and consumption by humans.
2) Fish Consumption: the transfer of radionuclides from the receiving water environment to fish and consumption by humans.

3) Radon Inhalation: dispersion of radon exhaled from the reference tailings site through the air environment and inhalation by humans.

4) Dust Inhalation: dispersion of dust eroded from the surface of the reference tailings site in the air environment and inhalation by humans.

5) Vegetable Consumption: the transfer of radionuclides to above and below ground vegetation and subsequent consumption by humans.

6a) Animal Produce Consumption: the uptake of radionuclides by forage vegetation and lichens, subsequent transfer to moose and caribou and consumption of the animal meat by humans.

6b) Animal Produce Consumption: the uptake of radionuclides by aquatic vegetation, subsequent transfer to moose and consumption of the animal meat by humans.

6c) Animal Produce Consumption: caribou and moose consumption of lake and river water and subsequent consumption of the animal meat by humans.

7) Groundshine: direct radiation from deposited dust.

These pathways are illustrated in Figure 1.1.

Detailed descriptions of the mathematical models and assumptions used in the development of each component module are presented in Volume 3 of the Phase III System Model Development documentation.

FIGURE 1.1

EXPOSURE PATHWAYS

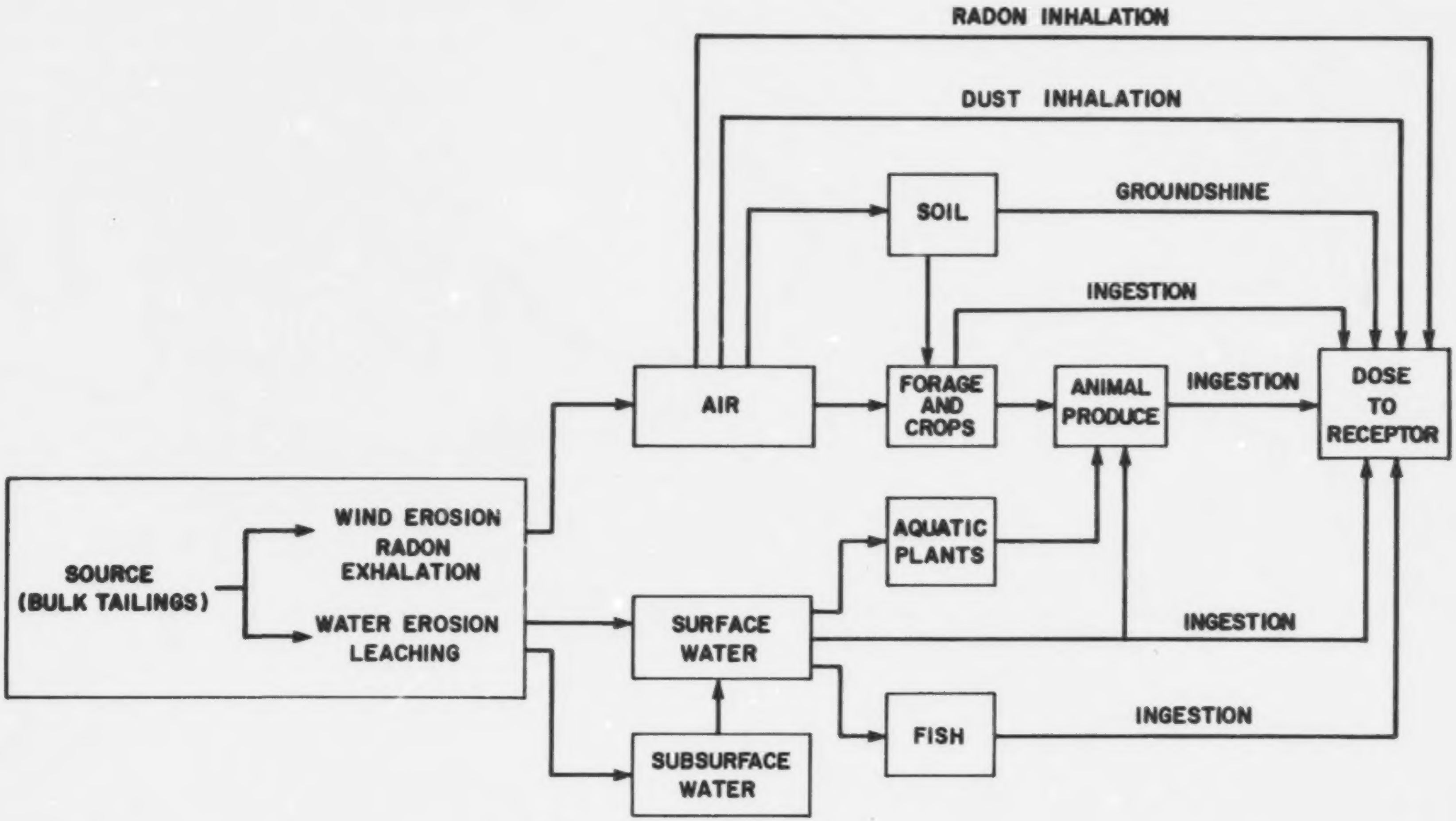
RADON INHALATION
DUST INHALATION
GROUNDSHINE
SOIL
INGESTION
AIR
FORAGE AND CROPS
ANIMAL PRODUCE
INGESTION
DOSE TO RECEPTOR
SOURCE (BULK TAILINGS)
WIND EROSION
RADON EXHALATION
WATER EROSION
LEACHING
AQUATIC PLANTS
SURFACE WATER
INGESTION
SUBSURFACE WATER
FISH
INGESTION

## 2.0 CONTROL MODULE FUNCTIONS

### 2.1 Input

The control modules open, access and read all of the input files required for the probabilistic assessment of uranium tailings.

### 2.2 Draw Random Samples

The control modules draw random samples from the following user-specified probability distributions for the input model parameters:

1) Constant
2) Normal
3) Lognormal
4) Uniform
5) Log uniform
6) Triangular
7) Weibull
8) Beta
9) Arbitrary
10) Correlated

Variables are sampled once for each trial except for those specified as time-variant which are sampled each time step of each trial.

The selected random samples are routed to the appropriate component modules.

### 2.3 Select Parameters for Output and Statistics

The user may specify concentration and dose data as well as selected input parameters for output at selected time intervals without having to alter the program. These data reside in a series of arrays in the program. Parameter selection for output is achieved by specifying the time intervals desired and the positions in the concentration and dose arrays required for output.

Two output options are available: 1) summary statistics, the default option and/or 2) writing selected outputs for all iterations to a disk file in addition to creating the summary statistics of option 1. Either one of or both of these options may be selected.

## 2.4 Compute Statistics on Selected Variables

The following summary statistics are computed for user-selected output parameters and input distributions:

Mean
Standard deviation
Geometric mean
Geometric standard deviation
Minimum
Maximum
Skewness
Kurtosis

These statistics are updated at the end of each trial.

## 2.5 Write Data to Output Files

The two output options discussed below are available to the user. Either or both of these options can be selected on any run. Sample output files are shown in Appendix C.

### 2.5.1 Output Statistics File

The following summary statistics computed by the statistics routines are output to a user-specified disk file, called the statistics file:

Mean

Standard deviation
Geometric mean
Geometric standard deviation
Minimum
Maximum

The parameter names, specifications, and the time intervals selected are also output, as appropriate.

### 2.5.2 Output Detailed Results Files

If this option is selected in the input file, two user-specified disk files are created in addition to any statistics file already created.

The first file, called the key file, is similar to the statistics file with the only difference being the additional statistics, skewness and kurtosis, being output to the key file.

The second file created, called the detailed results file, contains the actual data from which the statistics written to the key file are calculated. The user-selected parameters are written to the detailed results file at the end of each trial.

The rows of the key file corresponds to the columns of the detailed results files. For instance, the third row of the key file describes the data contained in the third column of the detailed results file. These two files also serve as input to the confidence bands program.

## 2.6 Step Through Time

The total time to be modelled and the time increment are specified in the first input file. The maximum duration is 1,000 years.

## 2.7 Confidence Bands

The confidence band program is a post-processing program that calculates confidence band estimates on user-selected data. The program processes the detailed results file and the key file to obtain confidence band estimates.

## 3.0 BUILDING INPUT FILES AND OBTAINING OUTPUT

The program reads input data from three files. Examples of the first two of these files are provided to the user on disk and are called INPUT1.DAT and INPUT2.DAT. Listings of these two files are shown in Appendix B and the output files resulting from them are included in Appendix C. The third file contains the air dispersion data. A choice of two files for air dispersion data is available as discussed later in Section 3.3. The contents of the input files are illustrated in Figure 3.1. The user is prompted interactively for the names of the first two input files.

### 3.1 First Input File (INPUT1.DAT)

This file is used to specify the output files desired and the distributions of input parameters. A sample file containing the different distribution types available is shown on Table 3.1. Descriptive labels not found in an actual input file have been added to Table 3.1. The file format is described on Table 3.2.

The first line of this file is the run title to be written to the statistics and key files. Next, the desired output files are specified and named. The user can specify 1) a statistics file or, 2) a detailed results and a key file or, 3) both of these options (three files) as described previously in Section 2.5.

The total number of distributions as well as the numbers of arbitrary and correlated distributions are input. The number of cells to be computed for any beta distributions is indicated. The specifics of the run are set up by reading the random number seed, the number of trials, the simulation time, and the time increment. The time increment can be either one or ten years. The following random number seeds have been thoroughly tested:

824064364<br>
913566091

FIGURE 3.1

INPUT AND OUTPUT FILES

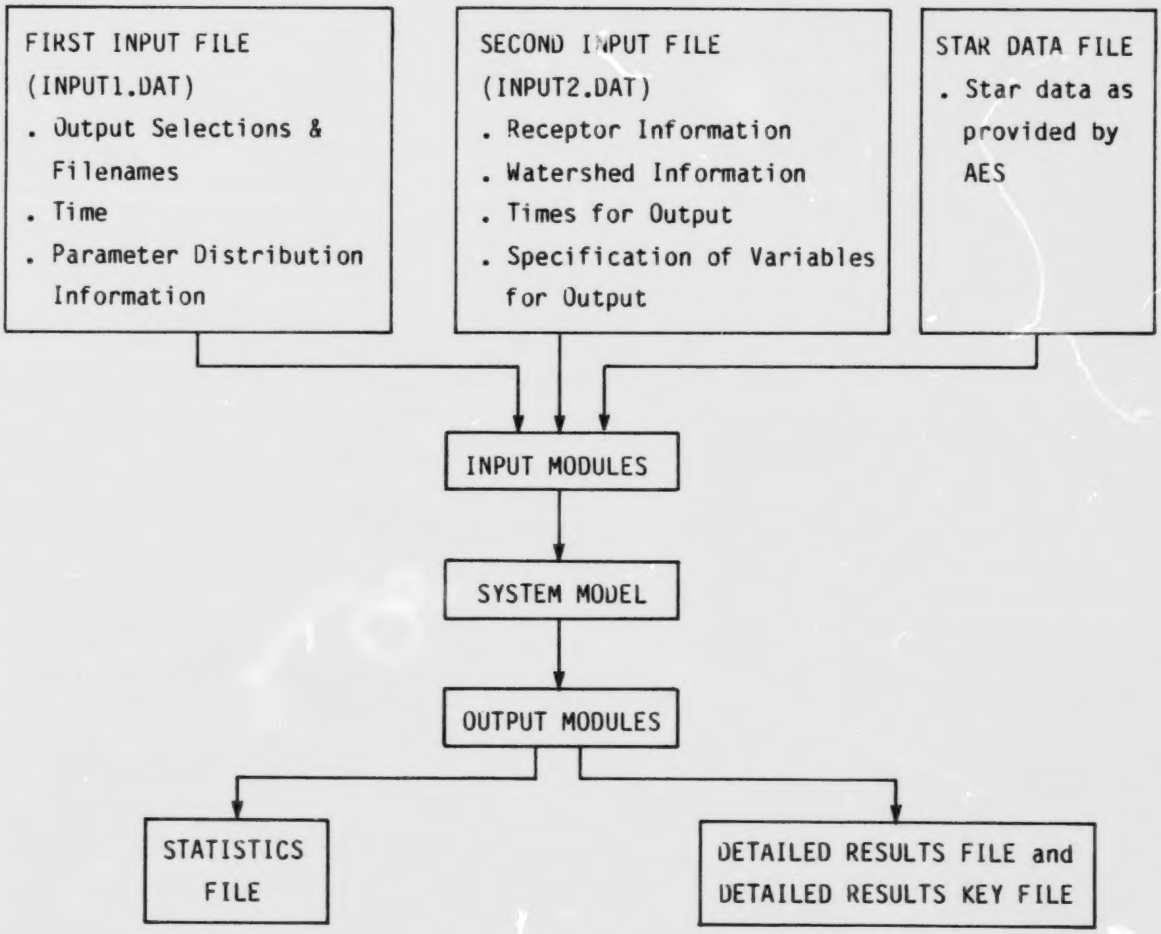
FIRST INPUT FILE
(INPUT1.DAT)
. Output Selections & Filenames
. Time
. Parameter Distribution Information
SECOND INPUT FILE
(INPUT2.DAT)
. Receptor Information
. Watershed Information
. Times for Output
. Specification of Variables for Output
STAR DATA FILE
. Star data as provided by AES
INPUT MODULES
SYSTEM MODEL
OUTPUT MODULES
STATISTICS FILE
DETAILED RESULTS FILE and
DETAILED RESULTS KEY FILE

Table 3.1

## SAMPLE OF FIRST INPUT FILE

```
          Title
PROBABILISTIC ANALYSIS: TEST CASE
          Statistics file indicator
Y
          Statistics file name
STAT.OUT
          Detailed Results files indicator
Y
          Detailed Results file name
RES.OUT
          Key file name
KEY.OUT
    ┌─Number of input distributions
    │     ┌──Number of arbitrary distributions
    │     │      ┌───Number of correlated parameters
    │     │      │   ┌───Number of cells to be used in computing beta distributions
   10     1      1  25
    ┌─Random number seed
    │            ┌──Number of iterations
0913566091      10
    ┌─Years in simulation
    │     ┌─Time increment in years
  100    10
          Regular distributions:
    ┌──────────Parameter name
    │     ┌──────────Output flag
    │     │   ┌──────────Distribution type number
    │     │   │  ┌──────────Time-variant flag
    │     │   │  │                 Distribution descriptors
CONST    N    1  N      2.0
NORMAL   N    2  V     10.0         2.0        0.0        20.0
LNORM    N    3  V    1.0E02        1.5        1.0       1.0E3
UNI      S    4  N      1.0         2.0        0.0         0.0
LOGUNI   N    5  N      0.01        0.5        0.0         0.0
TRIANG   N    6  N      0.01        0.03       0.1         0.0
WEIBUL   F    7  V      0.0         1.5        0.9
BETA     N    8  N     10.0       100.0        2.0         2.0
          Arbitrary distributions:
   ┌──────────Parameter name
   │      ┌──────────Output flag
   │      │  ┌──────────Distribution type number
   │      │  │  ┌──────────Time-variant flag
   │      │  │  │  ┌──────────Number of cells in distribution
   │      │  │  │  │                 Distribution descriptors
ARB       N  9  N 10     1.0   11.0  2.0  2.0  2.0  8.0  8.0  8.0 12.0 12.0  4.0  4.0

          Correlated distributions:
    ┌──────────Parameter name
    │     ┌──────────Output flag
    │     │  ┌──────────Distribution type number
    │     │  │   ┌──────────Time-variant flag
    │     │  │   │  ┌──────────Name of independent distribution
    │     │  │   │  │                 Distribution descriptors
CORREL    N 10   N NORMAL       50.0       10.0       0.7       10.0       2.0
```

Table 3.2

## FORMAT OF FIRST INPUT FILE (INPUT1.DAT)

| | Column | Format | Description |
|---|---|---|---|
| Line 1: | | | |
| | 1-40 | A40 | Title |
| Line 2: | | | |
| | 1 | A1 | Statistics file desired? (Y/N) |
| Line 3: | | | |
| | 1-12 | A12 | Statistics file name |
| Line 4: | | | |
| | 1 | A1 | Detailed results files desired (Y/N) |
| Line 5: | | | |
| | 1-12 | A12 | Detailed results file name |
| Line 6: | | | |
| | 1-12 | A12 | Key file name |
| Line 7: | | | |
| | 1-4 | I4 | Number of input distributions (max. 250) |
| | 5-8 | I4 | Number of correlated parameters |
| | 9-12 | I4 | Number of arbitrary distributions |
| | 13-16 | I4 | Number of cells in beta distributions (max. 25) |
| Line 8: | | | |
| | 1-10 | I10 | Random Number Seed |
| | 11-14 | I4 | Number of iterations |
| Line 9: | | | |
| | 1-4 | I4 | Years in Simulation |
| | 5-8 | I4 | Time increment in years |

Distributions:

Constant, Normal, Lognormal, Uniform, Loguniform, Triangular, Weibull, and Beta distributions. One line for each distribution:

| Column | Format | Description |
|---|---|---|
| 1-6 | A6 | Parameter name |
| 8 | A1 | Output flag (S/F/B/N)** |
| 10-11 | I2 | Distribution Type Number (Table 3.3) |
| 13 | A1 | Time-Variant Flag (Variant, Not => V/N*) |
| 14-57 | 4E11.6 | Distribution Descriptions |

Table 3.2/cont'd

Arbitrary distributions. One line for each distribution:

| | | |
|---|---|---|
| 1-6 | A6 | Parameter name |
| 8 | A1 | Output flag (S/F/B/N)** |
| 10-11 | I2 | Distribution Type Number (Table 3.3) |
| 13 | A1 | Time-Variant Flag (Variant, Not =>V/N*) |
| 14-16 | I3 | Number of cells in distribution (max. 25) |
| 17-38 | 2E11.6 | Minimum and Maximum value ordinates |
| 39-188 | 25F6.2 | Function value for each cell |

Correlated distributions. One line for each distribution:

| | | |
|---|---|---|
| 1-6 | A6 | Parameter name |
| 8 | A1 | Output flag (S/F/B/N)** |
| 10-11 | I2 | Distribution Type Number (Table 3.3) |
| 13 | A1 | Time-Variant Flag (Variant, Not => V/N*) |
| 15-20 | A6 | Name of independent variable |
| 21-75 | 5E11.6 | Distribution Descriptions |

Notes

* Default is N, non-time-variant

** S = statistics file, F = detailed results files, B = both options, N = no output of variable. Default is No output.

Table 3.3

## DISTRIBUTION DESCRIPTORS

| Distribution | Distribution Number | Distribution Descriptors | Column |
|---|---|---|---|
| Constant | 1 | Constant | 14-24 |
| Normal | 2 | Mean | 14-24 |
| | | Standard Deviation | 25-35 |
| | | Minimum | 36-46 |
| | | Maximum | 47-57 |
| Lognormal | 3 | Geometric Mean | 14-24 |
| | | Geometric Standard Deviation | 25-35 |
| | | Minimum | 36-46 |
| | | Maximum | 47-57 |
| Uniform | 4 | Minimum | 14-24 |
| | | Maximum | 25-35 |
| Log-uniform | 5 | Minimum | 14-24 |
| | | Maximum | 25-35 |
| Triangular | 6 | Minimum | 14-24 |
| | | Mode | 25-35 |
| | | Maximum | 36-46 |
| Weibull (Figure 3.2) | 7 | Location Parameter (Minimum)(a) | 14-24 |
| | | Scale Parameter (b) | 25-35 |
| | | Shape Parameter (c) | 36-46 |
| Beta (Figure 3.3) | 8 | Minimum | 14-24 |
| | | Maximum | 25-35 |
| | | a shape parameters | 36-46 |
| | | b | 47-57 |
| Arbitrary (Figure 3.4) | 9 | Number of cells (max. 25) | 14-16 |
| | | Minimum | 17-27 |
| | | Maximum | 28-38 |
| | | Ordinate Values | 39-(188) |
| Correlated | 10 | Mean of dependent variable | 21-31 |
| | | Standard Deviation of Dependent Variable | 32-42 |
| | | Correlation Coefficient | 43-53 |
| | | Mean of Independent Variable | 54-64 |
| | | Standard Deviation of Independent Variable | 65-75 |

The input parameters are specified as distributions with their type numbers according to Table 3.3. Each type of distribution is specified using different descriptors as indicated on Table 3.3 The weibull, beta, and arbitrary distributions are illustrated in Figures 3.2, 3.3 and 3.4, respectively. The location parameter (a) for the weibull distribution, not shown on Figure 3.2, determines the position of the origin on the horizontal axis. For instance, if a = 2 the origin is shifted from 0 to 2 on the horizontal axis.

The input distributions required are described in Appendix D. These must be entered in the same order as they appear in the Appendix and in the example file, INPUT1.DAT, shown in Appendix B.

Included in the input distributions described in Appendix D are various print codes. These are used to turn on and off various write statements within the program that generate detailed output to the screen. In general, a zero value turns off this output and one turns it on. The detailed printouts can be used to check calculations performed by the program.

The distribution names specified are used by the program to identify correlated parameters. They are also written to the statistics and key files.

The two types of output available are 1) summary statistics and 2) detailed results including the statistics key file. One or both of these may be requested. The "output flag" indicated in Table 3.2 (column 8) allows the user to select either, both, or neither (i.e. no output is saved) of these output options. The default is no output.

Distributions can be either time-variant or non-time-variant as indicated by the time-variant flag. The default is non-time-variant. Time-variant parameters are sampled for each time step of each trial while non-time-variant

FIGURE 3.2

FORMS OF THE WEIBULL DISTRIBUTION PROBABILITY DENSITY FUNCTION

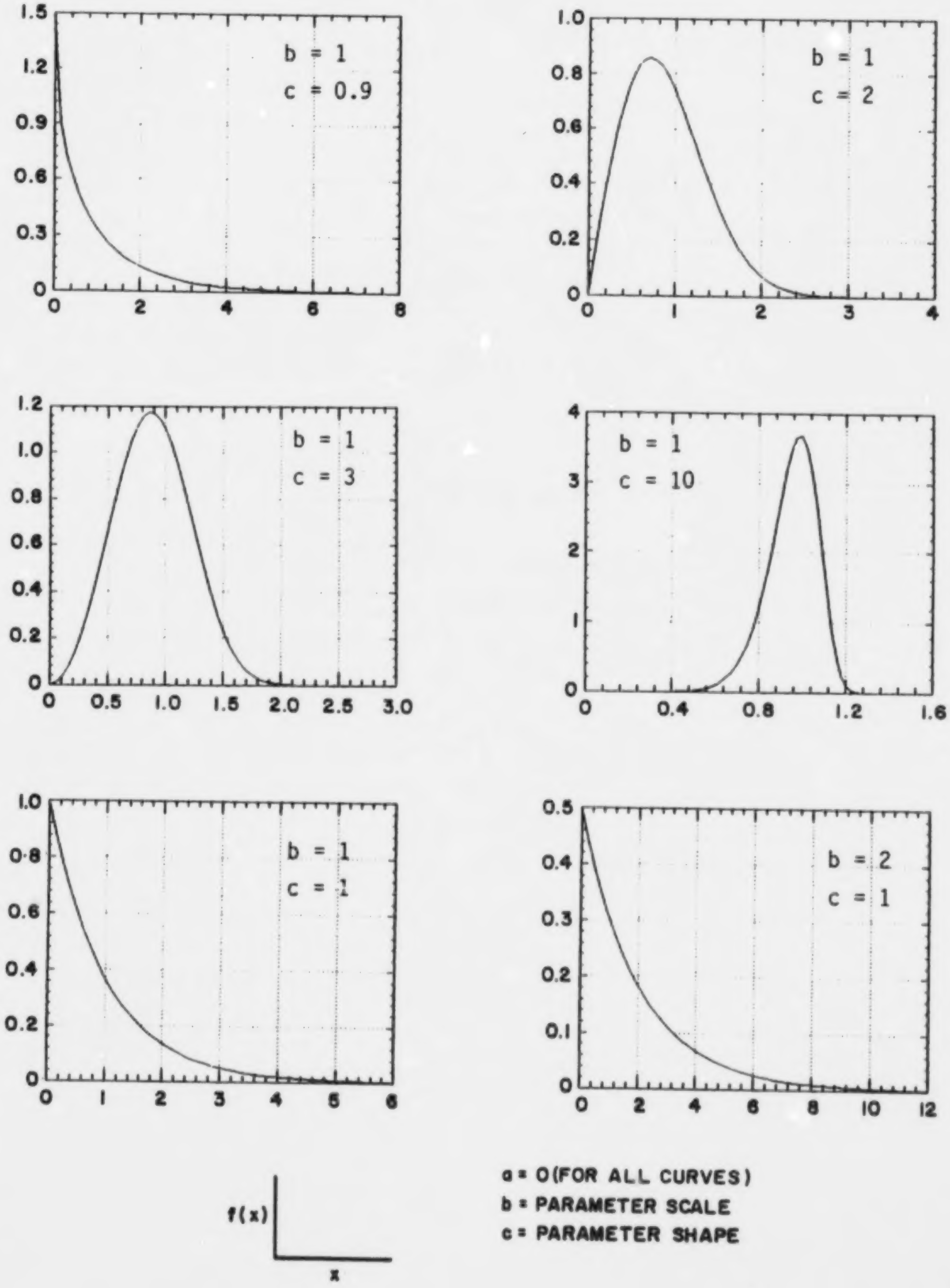

a = 0 (FOR ALL CURVES)
b = PARAMETER SCALE
c = PARAMETER SHAPE

FIGURE 3.3

FORMS OF THE BETA DISTRIBUTION PROBABILITY DENSITY FUNCTION

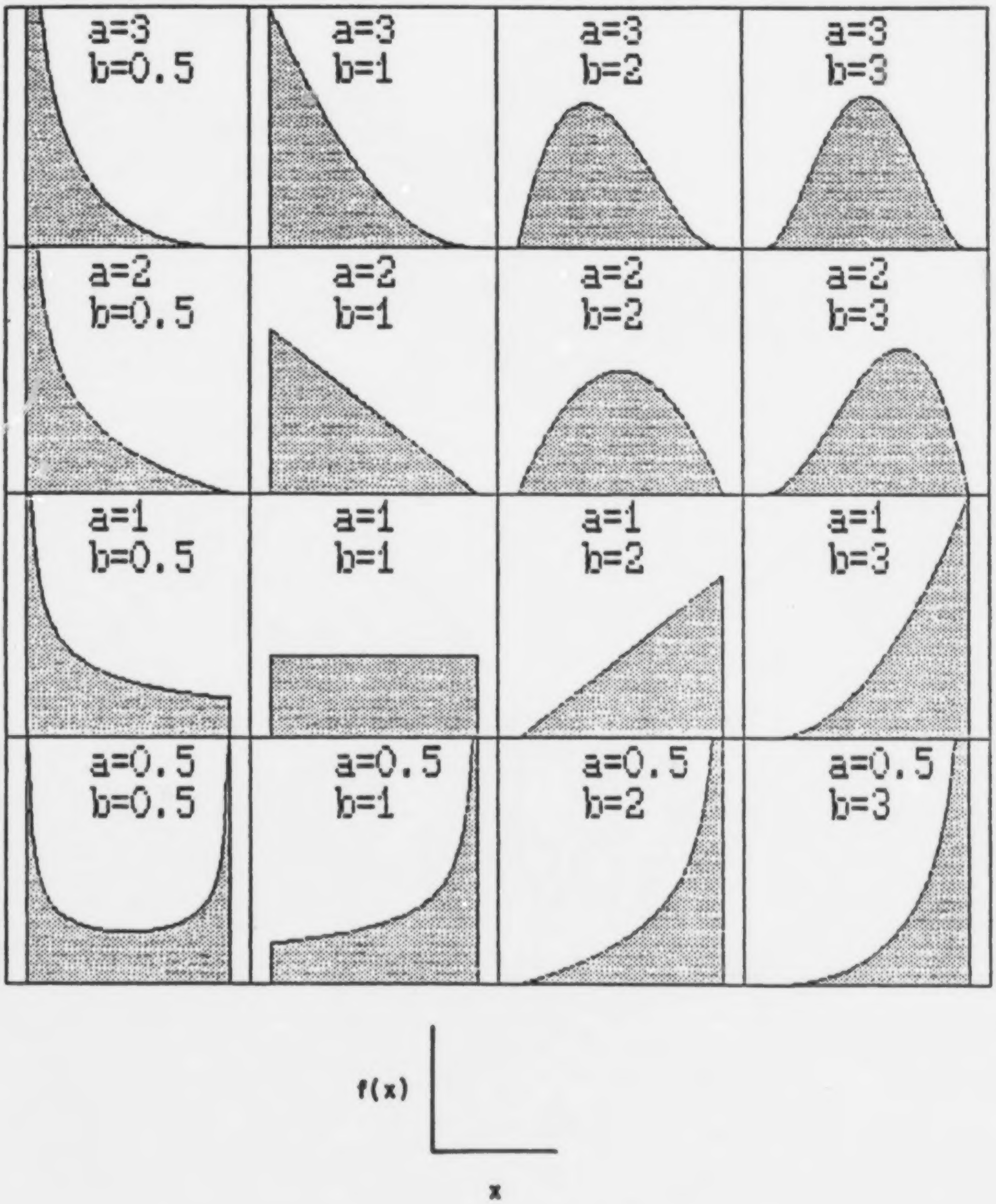

FIGURE 3·4

AN ARBITRARY
PROBABILITY DENSITY FUNCTION

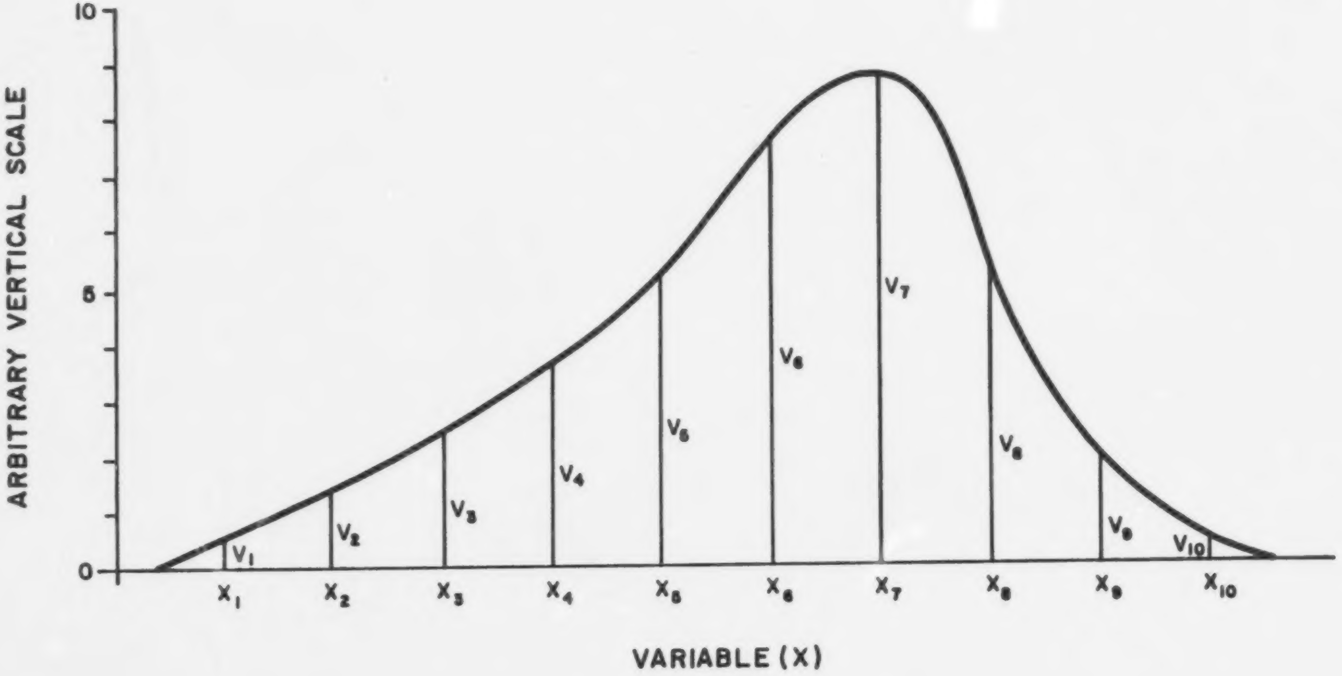

parameters are sampled once for each trial.

Time variant parameters should be adjusted to correspond to the time step being used. The standard deviation should be set equal to that for annual data (one year time step) divided by the square root of the time step used. Thus, in the example data file, INPUT1.DAT, the one year standard deviation of .1 for the variable NRPCP should be changed to $.1/\sqrt{10}$ or 0.03 for a ten year time step. The mean value is unaffected.

### 3.1.1 Selecting Alternate Scenarios

UTAP has been developed to allow the examination of several distinct tailings management options, or scenarios. The default option (i.e. that specified by the data supplied with this program) represents a situation in which no extraordinary measures are taken in closing out the tailings area. Other options involve reduction of the pyrite content and incorporation of limestone ($CaCO_3$) into the upper layer of the tailings. These options can be selected simply by changing the values of two input parameters, PYRITI and XLIME. PYRITI is the initial concentration of pyrite in the tailings (mol.m$^{-3}$) while XLIME is the mass fraction of limestone ($CaCO_3$) added to the tailings. The physical significance of both parameters is described further in Chapter 3 of Volume 3 of this report. To select a different option, the parameter values are changed as outlined below.

| | Parameter Values | | | |
|---|---|---|---|---|
| | PYRITI (mol.m$^{-3}$) | | XLIME (mass fraction) | |
| | Deterministic | Probabilistic | Deterministic | Probabilistic |
| Default (supplied with program) | 700 | U(600,800) | 0.0 | C(0.0) |
| Pyrite reduction | 70 | U(60,80) | | |
| Lime ($CaCO_3$) addition | | | 0.01 | C(0.01) |

### 3.2 Second Input File (INPUT2.DAT)

The second input file contains the name of the air dispersion data file, receptor information, watershed information and output selection information in that order. Table 3.4 shows a sample file, "INPUT2.DAT". This is formatted according to the description on Table 3.5. The choice of air dispersion data files is discussed further in Section 3.3.

Receptor position is defined by a windrose structure while the watershed is defined as a series of segments. Windrose and watershed concepts as well as the specification of output selection information are discussed in the next three sections.

#### 3.2.1 Receptor Information

The windrose structure shown in Figure 3.5 defines a system of spatial coordinates. There are 16 direction sectors to correspond to the traditional windrose structure. The number of rings, up to a maximum of 5, and the spacing of the rings, from a minimum distance of 1 km to a maximum of 50 km, are user-specified. The rings are continuous, with the outer limit of one ring forming the inner limit of the next. The receptors are placed within the windrose structure as follows:

First the number of receptor locations and the number of rings are specified (16 directions is the default). The number of receptor locations is the count of direction/ring combinations with receptors residing in them.

Next, the radii of the rings are specified in meters of radius. Since the outside of each ring is the inside of next ring, the only inside distance that need be specified is for the first ring. This distance must be at least 1 km.

Lastly, the details of each receptor location are specified. Location is input as sector and ring number. The source of the receptor's drinking water is given by segment number which corresponds to the segment reference number

Table 3.4

## SAMPLE OF SECOND INPUT FILE (INPUT2.DAT)

```
     Flag to indicate if variable wind data is desired
  N
     File containing appropriate wind data
STARAV.DAT
     Number of receptor locations
  5
     Number of rings
  5
     Ring limits
    1    3    5   10   20   50
     Receptor information:
  ┌───────Receptor number
  │  ┌─────────Sector number
  │  │  ┌───────────Ring number
  │  │  │  ┌─────────────Drinking water source segment number
  │  │  │  │ ┌────────────────Receptor type
  │  │  │  │ │    ┌────────────────Population
  1 16  1  1 C    2
  2 16  3  2 A    5
  3 14  3  2 A    6
  4  1  1  1 C    1
  5  7  3  2 A    3
    Number of watershed segments
          End node number of watershed segment groundwater flows into.
  8  1
     Watershed information:
  ┌───────End node or segment number
  │ ┌─────────Segment type
  │ │  ┌────────────Sector number of end node
  │ │  │  ┌──────────────Ring number of end node
  │ │  │  │     ┌─────────────Segment depth
  │ │  │  │     │        ┌────────Watershed area
  │ │  │  │     │        │        ┌────Lake area/River length
  1 R 11  1   2.5E-1   1.5E07   3.0E3
  2 L 11  1   1.0E01   2.0E07   5.0E05
  3 R 10  2   0.5      3.2E07   3.5E3
  4 L 10  2   4.0      3.8E07   2.5E05
  5 R  9  3   7.5E-1   7.0E07   7.0E3
  6 R  9  4   1.0      1.2E08   1.3E4
  7 L  9  4   5.0      1.4E08   4.0E06
  8 R  9  5   6.5      4.0E08   3.0E4
  ┌───Number of time steps for statistics
  │   ┌──Number of time steps for detailed results files
  4   3
    Time steps for statistics
    0   10   20   30
    Time steps for detailed results
    0   50   90
```

Table 3.4 cont'd

```
     Number of arrays to be checked for output
  36
  ┌── Array name
  │       ┌Array size
WCONC   0
CONC    0
PH      0
WATC    2
  ┌──Substance code
  │  ┌────Location code
  │  │  ┌──────Output indicator
   2  3  S
   3  5  S
WATAVG  3
   1  1  S
   3  1  S
   4  1  F
WATPH   3
   1  7  S
   1  4  S
   1  2  F
GWATC   0
EMRATE  0
EROTOT  0
DTAIL   0
AIRC    0
SOILC   0
AVEGC   0
BVEGC   0
SUFOC   0
BRWSC   0
LICHC   0
AQVEGC  0
FISHC   0
AMOC    0
WMOC    0
ACARC   0
WCARC   0
WATD    0
SHINED  0
INHD    0
RADD    0
VEGD    0
FISHD   0
MEATD   0
DOSE    0
POPDT   0
BLANK1  0
BLANK2  0
```

Table 3.5

## FORMAT OF SECOND INPUT FILE (INPUT2.DAT)

| | Column | Format | Description |
|---|---|---|---|
| 1 Line: | 3 | A1 | Air dispersion variable data flag (Variable/ Not variable => V/N*) |

* Default is N, not variable

| | Column | Format | Description |
|---|---|---|---|
| 1 Line: | 1-12 | A12 | Name of air dispersion input data file |
| RECEPTOR INFORMATION<br>1 Line: | 1-3 | I3 | Number of receptor locations (max 80) (NRECEP) |
| 1 Line: | 1-3 | I3 | Number of rings (max5) (NRING) |
| Ring Limits (in km's of Radius):* 1 Line: | 1-5 | I5 | Distance to inside of 1st ring (min 1 km) |
| | 6-10 | I5 | Distance to outside of 1st ring |
| | 11-15 | I5 | Distance to outside of 2nd ring |
| | 16-20 | I5 | Distance to outside of 3rd ring |
| | 21-25 | I5 | Distance to outside of 4th ring |
| | 26-30 | I5 | Distance to outside of 5th ring |

* Specify Distances for number of rings desired (NRING)

| | Column | Format | Description |
|---|---|---|---|
| Receptors. One line per receptor location (NRECEP lines): | 1-3 | I3 | Receptor Identification Number |
| | 4-6 | I3 | Sector Number (1 to 16) |
| | 7-9 | I3 | Ring Number (1 to NRING) |
| | 10-12 | I3 | Water Source Segment Number (0 is other source) |
| | 14 | A1 | Receptor Type (Critical/Average=> C/A) |
| | 15-19 | I5 | Population |
| WATERSHED INFORMATION:<br>1 Line: | 1-3 | I3 | Number of watershed segments (max 10) (NSEG) |
| | 4-6 | I3 | End node number of watershed segment groundwater flows into |
| 1 Line for each watershed segment: | 1-3 | I3 | End node or watershed segment number |
| | 5 | A1 | Segment Type (Lake, River=>L/R) |
| | 6-8 | I3 | End node sector number |
| | 9-11 | I3 | End node ring |
| | 12-20 | E9.3 | Segment Depth (m) |
| | 21-29 | E9.3 | Cumulative watershed area ($m^2$) |
| | 30-38 | E9.3 | Area of lakes ($m^2$) or length of rivers (m) |

Table 3.5/cont'd

SITE AND OUTPUT INFORMATION:

| | | | |
|---|---|---|---|
| 1 Line: | | | |
| | 1-3 | I3 | Number of time steps to be saved for statistics |
| | 5-7 | I3 | Number of time steps to be saved for detailed results files |
| 1 Line: | | | |
| | 1-55 | 11(I5) | Time steps to be saved for statistics file |
| 1 Line: | | | |
| | 1-55 | 11(I5) | Time steps to be saved for detailed results file |
| 1 Line: | | | |
| | 1-3 | I3 | Number of variables to be checked for output |
| FOR EACH VARIABLE: | | | |
| 1 Line: | | | |
| | 1-6 | A6 | Names of parameters in order specified on Table 3.6 |
| | 7-9 | I3 | Number of location, substance combinations (0 if no output for parameter) |
| 1 Line for each receptor, substance combination (if any): | | | |
| | 1-3 | I3 | Substance Code (see Tables 3.6 and 3.7) |
| | 5-7 | I3 | Location Identification Number (see Table 3.6) |
| | 9 | A1 | Output indicator (S/F)* |

* S = statistics file, F = detailed results files. Default is statistics file. If a statistics output file has not been opened, the default is detailed results.

FIGURE 3.5

CONCEPTUAL DIAGRAM
OF SPATIAL COORDINATE SYSTEM

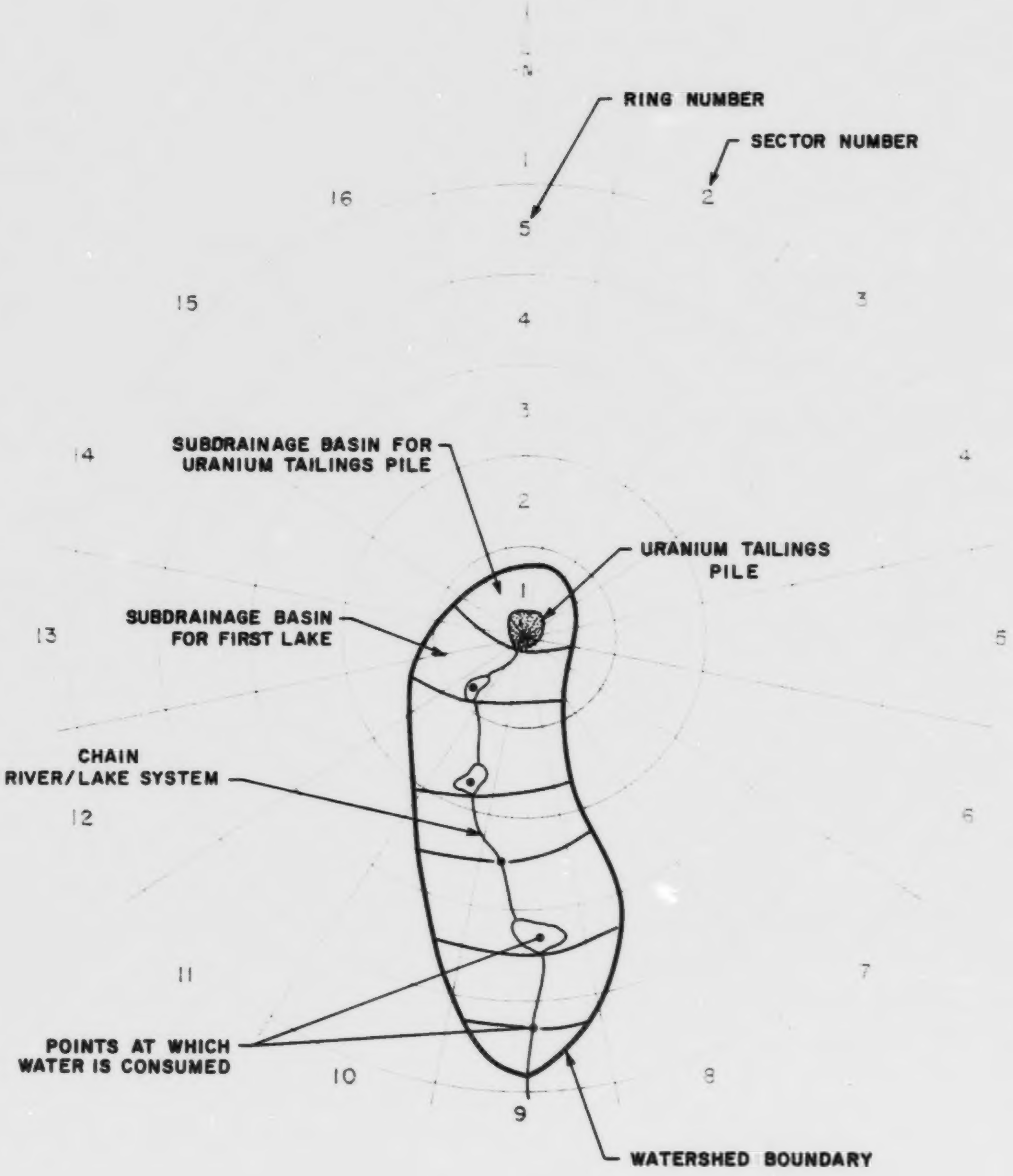
N
RING NUMBER
SECTOR NUMBER
1
16
2
5
15
3
4
3
SUBDRAINAGE BASIN FOR URANIUM TAILINGS PILE
14
4
2
URANIUM TAILINGS PILE
1
SUBDRAINAGE BASIN FOR FIRST LAKE
13
5
CHAIN RIVER/LAKE SYSTEM
12
6
11
7
POINTS AT WHICH WATER IS CONSUMED
10
8
9
WATERSHED BOUNDARY

in the watershed information. If the receptor does not obtain drinking water from the watershed downstream of the tailings area, this number is zero. The descriptions of critical and average receptors are to be input in the distributions in the first input file as indicated in Appendix D.

### 3.2.2 Watershed Information

The watershed downstream of the tailings pile handles up to 10 user-specified components (segments). Calculations are done at each river or lake outflow point known as end nodes. The node number, and the position of the river or lake outflow point by sector and ring number are specified. The segments must be described in a manner such that each wind rose location that the watershed downstream of the tailings passes through contains at least one end node.

For each segment, the type (i.e. river or lake), the depth, and the cumulative watershed area are defined. The surface area of lakes and the length of rivers are specified.

The program performs an internal check to assure that segments are specified in order, starting with the upstream ones, with end node numbers and watershed areas increasing.

There are two restrictions to the specifications of the watershed. The first segment must be specified as a river and the groundwater must be specified as flowing into a river. If source or groundwater input directly to a lake is desired, a river segment with a length and sub-basin area of zero (i.e. cumulative watershed area equal to the upstream segment) should be used immediately upstream of the lake. This is exactly equivalent to input directly into the lake.

### 3.2.3 Output Selection Information

As was indicated earlier, UTAP offers the user the ability to select information for output. The following section describes how this is achieved.

The time steps to be saved for the statistics file and those for the detailed results file are input. These must correspond to the time increment requested. For example, one cannot ask for output at 5 and 15 years with a 10 year time increment. A selection of the time increments computed may be saved, up to a maximum of 11 each for the statistics file and for the detailed results and key files. The variables for which data can be obtained are a series of arrays. The first position in the array refers to the substance and the second position to the location. These locations can, as discussed below, refer to a variety of different physical locations.

Each variable/substance/location combination must be specified, once for each of the two possible files, as desired.

The variables available for output are shown in the sample input file and on Table 3.6 and _must_ be specified in the order indicated. In addition, two variables, BLANK1 and BLANK2, are provided for future use if additional variables are desired for output (see Section 5.4). A counter of the number of variables to be checked for output is used and should count at least as high as the last variable in the list that output is desired for. Any variables past this in the list will be ignored by the program and do not need to be erased from the file.

For the different variables, different substances and locations are available as indicated also on Table 3.6. The substance codes are shown on Table 3.7. The location codes refer to layers in the tailings, watershed segment, or receptor location as indicated on Table 3.6. The watershed segments and receptor locations correspond to the watershed segment end node numbers and the receptor numbers respectively.

For example, if the the air concentration of Ra-226 for receptor location 2 is desired the user would specify (4,2) in the array AIRC. The sector/ring location of receptor number 2 is defined using the technique described in

Table 3.6

## OUTPUT PARAMETERS

| Variable | Definition | Units | Substances Available | Location Type** |
|---|---|---|---|---|
| WCONC | Tailings liquid phase concentration | (Bq or mol/$m^3$)*** | 1-10 | Layer |
| CONC | Tailings solid phase concentration | (Bq or mol/$m^3$)*** | 1-10 | Layer |
| PH | Tailing pH | | 1* | Layer |
| WATC | Water concentration | (Bq or mol/$m^3$)*** | 1-4,7,8 | Watershed segment |
| WATAVG | Average watershed concentration | (Bq/$m^3$) | 1-4 | 1 |
| WATPH | Lake pH | | 1* | Watershed segment |
| GWATC | Ground water concentration | (Bq/$m^3$) | 1-4 | 1 |
| EMRATE | Emission Rate from tailings | (Bq/s) | 1-5 | 1 |
| EROTOT | Erosion of tailings pile overtime step | (g) | 1* | 1 |
| DTAIL | Cumulative Erosion of tailings pile | (m) | 1* | 1 |
| AIRC | Air concentration | (Bq/$m^3$) | 1-5 | Receptor Number |
| SOILC | Soil concentration | (Bq/$m^3$) | 1-4 | Receptor Number |
| AVEGC | Above ground vegetation concentration | (Bq/g) | 1-4 | Receptor Number |
| BVEGC | Below ground vegetation concentration | (Bq/g) | 1-4 | Receptor Number |
| SUFOC | Summer foliage concentration | (Bq/g) | 1-4 | 1 |
| BRWSC | Browsing vegetation concentration | (Bq/g) | 1-4 | 1 |
| LICHC | Lichen concentration | (Bq/g) | 1-4 | 1 |
| AQVEGC | Aquatic vegetation concentration | (Bq/g) | 1-4 | 1 |
| FISHC | Fish concentration | (Bq/g) | 1-4 | Watershed segment (Lakes) |
| AMOG | Moose concentration from vegetation | (Bq/g) | 1-4 | 1 |
| WMOG | Moose concentration from water consumption | (Bq/g) | 1-4 | 1 |
| ACARC | Caribou concentration from vegetation | (Bq/g) | 1-4 | 1 |
| WCARC | Caribou concentration from water consumption | (Bq/g) | 1-4 | 1 |
| WATD | Drinking water dose | (µSv/a) | 1-4,11 | Receptor Number |
| SHINED | Groundshine dose | (µSv/a) | 1-4,11 | Receptor Number |
| INHD | Inhalation dose | (µSv/a) | 1-4,11 | Receptor Number |
| RADD | Radon dose | (µSv/a) | 5 | Receptor Number |
| VEGD | Vegetable consumption dose | (µSv/a) | 1-4,11 | Receptor Number |
| FISHD | Fish consumption dose | (µSv/a) | 1-4,11 | Receptor Number |
| MEATD | Meat consumption dose | (µSv/a) | 1-4,11 | Receptor Number |
| DOSE | Total Individual Dose | (µSv/a) | 1-4,11 | Receptor Number |
| POPDT | Total Dose for Entire Study Population | (µSv/a) | 11 | 1 |

Notes

* Variables do not correspond to substances codes. Specify substance as 1.

** Variables with location types listed as 1 are not location dependent.

*** Radionuclide concentrations are measured in Bq/$m^3$. Concentrations of other substances are mol/$m^3$.

Table 3.7

## SUBSTANCE CODES

| Code | Compound |
|---|---|
| 1 | Natural Uranium |
| 2 | Total Thorium |
| 3 | Lead-210 |
| 4 | Radium-226 |
| 5 | Radon-222 |
| 6 | Sulphate($SO_4^{2-}$) from pyrite oxidation |
| 7 | Total Sulphate |
| 8 | Total Calcium ($Ca^{2+}$) |
| 9 | Ferric Iron ($Fe^{3+}$) |
| 10 | Ferrous Iron ($Fe^{2+}$) |
| 11 | Total of Radionuclides |

Section 3.2.1.

For modelling purposes, a number of layers have been defined in the tailings. These are:

1 - Layer 1, surface layer
2 - Layer 2, remainder of unsaturated zone
3 - Layer 3, mixing zone
4 - Layer 4, bottom layer

Layers 1 and 2 comprise the unsaturated zone; that is, the tailings lying above the water table. A number of chemical species dissolve in a front-wise manner in the unsaturated zone. Thus, layer 1 represents that thickness of tailings from which a given substance has been depleted. Layer 1 acts as the source of windblown tailings dust. Layer 2 represents the remaining thickness of the unsaturated zone. Layers 3 and 4 comprise the saturated tailings zone, lying below the water table. Layer 3 (the mixing zone) represents the upper metre (or so) of the saturated zone. Most of the porewater from layer 3 ultimately enters the surface water regime, thus acting as a source of surface water contamination. Some of the layer 3 porewater flows downward into layer 4, and ultimately into the subsurface (i.e. groundwater) flow regime.

## 3.3 Air Dispersion Data

The user must specify, in the second input file, the name of the file containing the air dispersion data. Two options are available. The first is to use one average set of data; that is, a long term (twenty year) average. The second option is to read twenty average sets of data corresponding to the time increment. One set of data is then randomly selected for each time step of each trial. This option must be selected by the flag in the second input file (see Table 3.5). The default is non-variance of the air dispersion data.

The program reads the one average set of air dispersion data file as formatted by the Atmospheric Environment Service (AES) for the site under study. The twenty average sets of data are read from one file that is simply twenty files (one set of data per file) of data, combined, in the same format as received from AES, into one file. An example of the file (AVERAGE.DAT) containing one long-term average set of data is shown in Appendix B. Table 3.8 illustrates the format of this file. Note that in creating the file containing twenty sets of data, the first line (the file label) of each smaller file being combined is included in the new file. Examples of the two files, ONE.DAT and TEN.DAT containing twenty sets of one year and ten year averages, respectively, are provided to the user on disk.

Table 3.8

FORMAT OF AES WIND DATA FILE

```
      ┌──── AES File Title
      ↓
P1397.TOTAL.

   ┌──────── Direction
   │  ┌────────── Stability Class
   │  │         ┌─ Frequencies of wind for velocity classes
   │  │         │      AES Codes ──────────────────────────┐
   ↓  ↓ ┌───────^──────────────────────────────┐           ↓
   N A 0.000400.000290.0   0.0    0.0    0.0          62925 1A176584
 NNE A 0.000370.000120.0   0.0    0.0    0.0          62925 2A176584
  NE A 0.000270.000150.0   0.0    0.0    0.0          62925 3A176584
 ENE A 0.000110.000060.0   0.0    0.0    0.0          62925 4A176584
   E A 0.000050.000020.0   0.0    0.0    0.0          62925 5A176584
 ESE A 0.000010.000010.0   0.0    0.0    0.0          62925 6A176584
  SE A 0.000030.000030.0   0.0    0.0    0.0          62925 7A176584
 SSE A 0.000050.000030.0   0.0    0.0    0.0          62925 8A176584
   S A 0.000190.000150.0   0.0    0.0    0.0          62925 9A176584
 SSW A 0.000300.000190.0   0.0    0.0    0.0          6292510A176584
  SW A 0.000270.000190.0   0.0    0.0    0.0          6292511A176584
 WSW A 0.000270.000200.0   0.0    0.0    0.0          6292512A176584
   W A 0.000460.000260.0   0.0    0.0    0.0          6292513A176584
 WNW A 0.000280.000180.0   0.0    0.0    0.0          6292514A176584
  NW A 0.000130.000080.0   0.0    0.0    0.0          6292515A176584
 NNW A 0.000240.000100.0   0.0    0.0    0.0          6292516A176584
   N B 0.002130.001650.000930.0    0.0    0.0          62925 1B176584

                              .
                              .
                              .

 WNW F 0.006990.005420.0   0.0    0.0    0.0          6292514F176584
  NW F 0.006690.005180.0   0.0    0.0    0.0          6292515F176584
 NNW F 0.005770.004090.0   0.0    0.0    0.0          6292516F176584
```

## 4.0 RUNNING THE PROGRAM

Before running the program, it should be compiled and linked. Simply compile and link the one file "UTAP.FOR". If problems are encountered, refer to Section 5.7 for further details. The compiler used in developing the program was the Lahey compiler Version 2.0 (1985). It is recommended, to facilitate the use of UTAP.

UTAP should be run on a computer having at least 512 kilobytes of Random Access Memory (RAM). A sample session is shown on Table 4.1. The program prompts the user for the names of the input files and indicates, to the screen, the input and output files that are opened.

If errors are encountered in reading these files, messages will be generated accordingly. In some cases, questionable input will result in warning messages, and the user will be asked if it is all right to continue execution of the program or if the program should be stopped. Typing "Y" for yes will cause execution to resume. All error and warning messages are described in Appendix A.

While the program is running, the current trial and time step are written to the screen so that the progress of the program can be checked.

When execution of the program is complete, the output files can be examined. Sample output files are shown in Appendix C.

Table 4.1

## SAMPLE SESSION

```
C:UTAP

FIRST INPUT FILE NAME? INPUT1.DAT

Opening File : INPUT1.DAT
Opening File : STAT.OUT
SECOND INPUT FILE NAME? INPUT2.DAT

Opening File : INPUT2.DAT



TRIAL NUMBER :    1    TIME :     0
TRIAL NUMBER :    1    TIME :    10
TRIAL NUMBER :    1    TIME :    20
TRIAL NUMBER :    1    TIME :    30
TRIAL NUMBER :    1    TIME :    40
TRIAL NUMBER :    1    TIME :    50
TRIAL NUMBER :    2    TIME :     0
TRIAL NUMBER :    2    TIME :    10
TRIAL NUMBER :    2    TIME :    20
TRIAL NUMBER :    2    TIME :    30
TRIAL NUMBER :    2    TIME :    40
TRIAL NUMBER :    2    TIME :    50



RUN COMPLETED

C:
```

## 5.0 ALTERING THE PROGRAM

As was indicated in the Introduction, the Uranium Tailings Assessment Program is composed of a number of modules. These may be classified as either component or control modules. Component modules (or models) are the programs directly concerned with the simulation of a uranium tailings physical system; that is, the mathematical models representing the uranium tailings pile and surrounding environment. Control modules provide the infrastructure for probabilistic analysis using the component modules. These functions include probabilistic sampling of input parameters, and many input, output and bookkeeping functions. The integrated control and component modules are referred to as the system model or the Uranium Tailings Assessment Program (UTAP). The general function of the control and component modules are illustrated in Figure 5.1.

The control modules are called in logical order by a primary control module called EXEC. The calling sequence, the interactions between the program EXEC and the other control modules and the functions of the control modules are illustrated in flowchart form in Figure 5.2. The component module executive subroutine COMEX is called by EXEC for each trial and time step. The subroutine COMEX and the modules it calls are illustrated in Figure 5.3.

The control modules are fully documented, including code listings and variable dictionaries in Volume 2 and the component modules in Volume 3.

Component modules should be implemented by following the points outlined below.

### 5.1 Changing COMEX

Subroutine COMEX is the control module for the component modules. It is called for each time step of each iteration. It, in turn, calls the component modules. Call statements must be added to COMEX if any new component modules are added.

FIGURE 5.1

THE SYSTEM MODEL

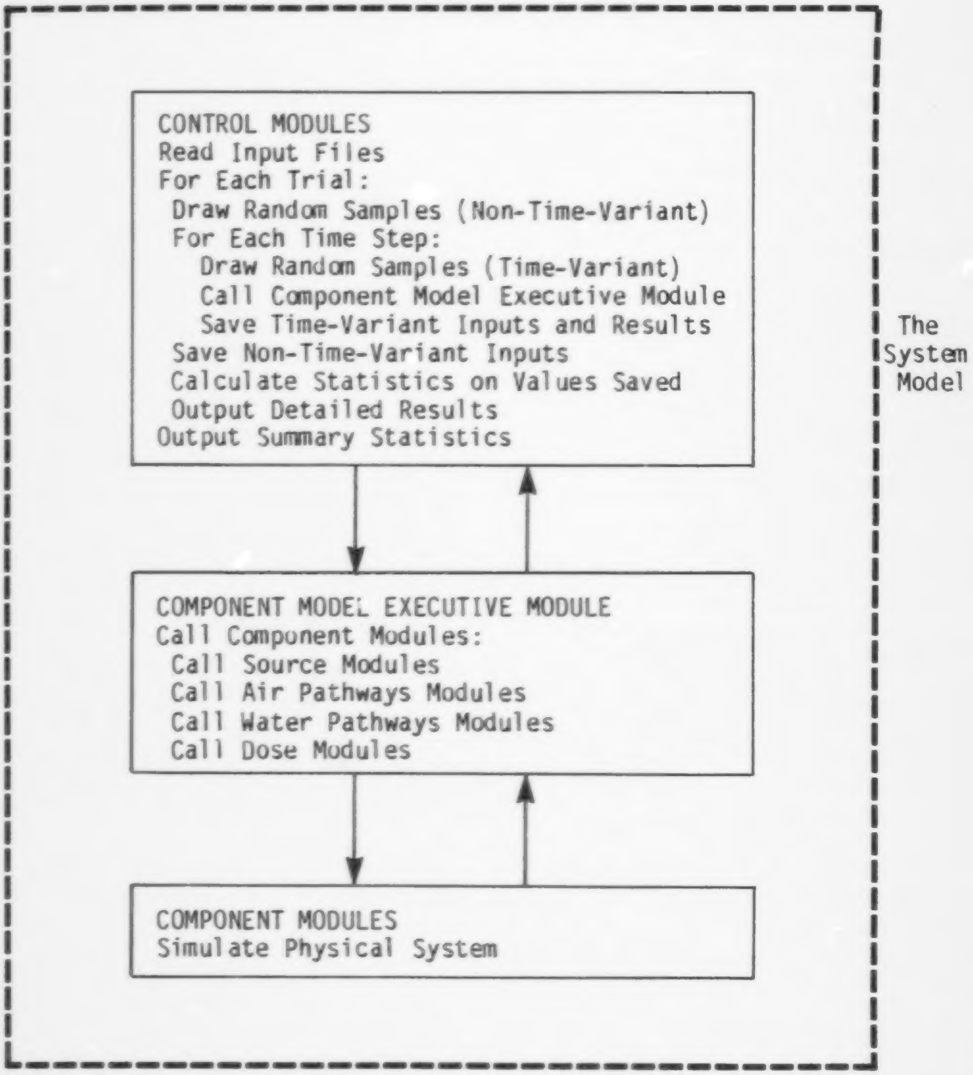
CONTROL MODULES
Read Input Files
For Each Trial:
Draw Random Samples (Non-Time-Variant)
For Each Time Step:
Draw Random Samples (Time-Variant)
Call Component Model Executive Module
Save Time-Variant Inputs and Results
Save Non-Time-Variant Inputs
Calculate Statistics on Values Saved
Output Detailed Results
Output Summary Statistics
COMPONENT MODEL EXECUTIVE MODULE
Call Component Modules:
Call Source Modules
Call Air Pathways Modules
Call Water Pathways Modules
Call Dose Modules
COMPONENT MODULES
Simulate Physical System
The System Model

## FIGURE 5.2

## THE CONTROL MODULE STRUCTURE

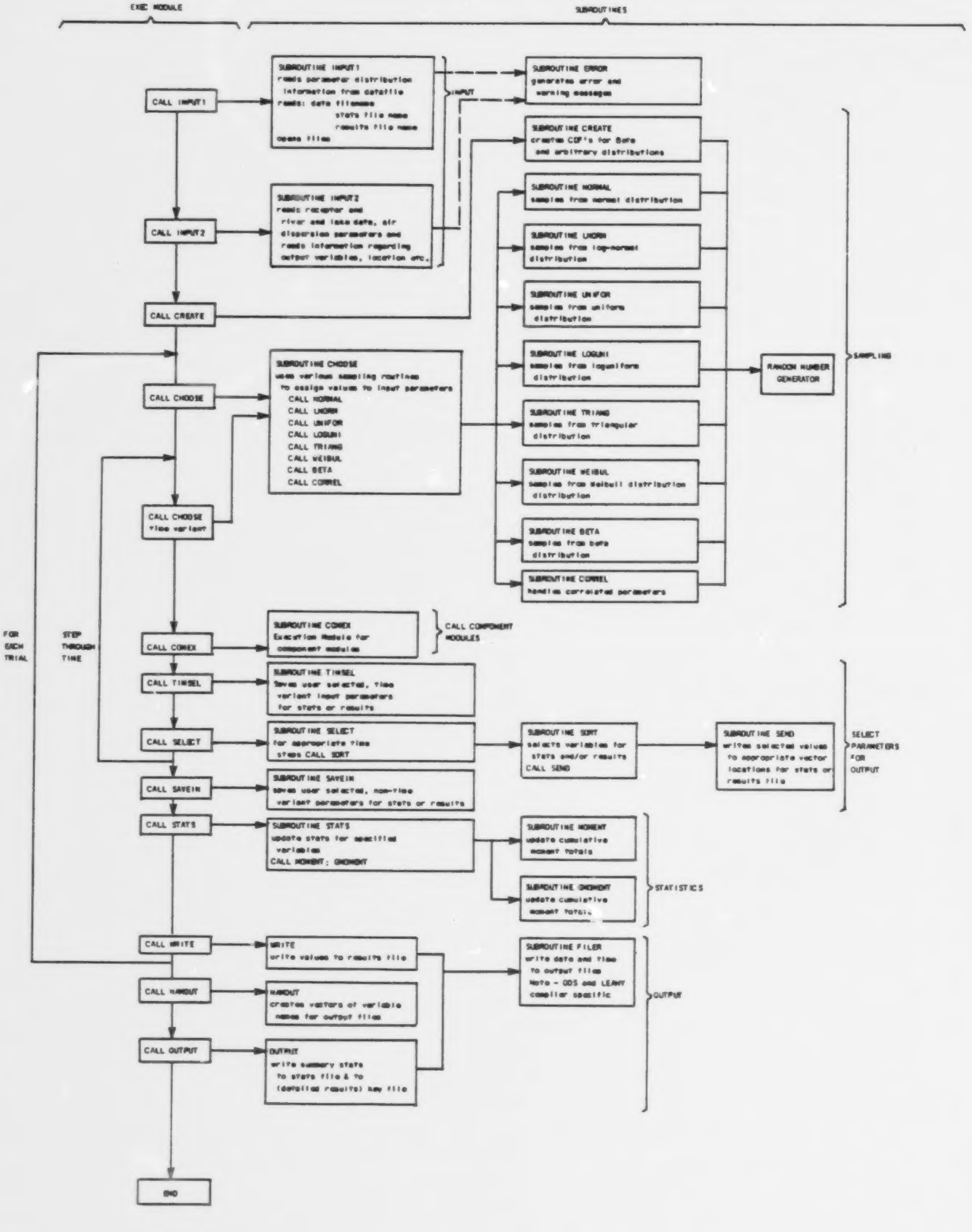
EXEC MODULE
SUBROUTINES
CALL INPUT1
SUBROUTINE INPUT1
reads parameter distribution
information from datafile
reads: data filename
stats file name
results file name
opens files
INPUT
SUBROUTINE ERROR
generates error and
warning messages
CALL INPUT2
SUBROUTINE INPUT2
reads receptor and
river and lake data, air
dispersion parameters and
reads information regarding
output variables, location etc.
CALL CREATE
SUBROUTINE CREATE
creates CDF's for Beta
and arbitrary distributions
SUBROUTINE NORMAL
samples from normal distribution
SUBROUTINE LNORM
samples from log-normal
distribution
SUBROUTINE UNIFOR
samples from uniform
distribution
SUBROUTINE LOGUNI
samples from loguniform
distribution
RANDOM NUMBER
GENERATOR
SAMPLING
CALL CHOOSE
SUBROUTINE CHOOSE
uses various sampling routines
to assign values to input parameters
CALL NORMAL
CALL LNORM
CALL UNIFOR
CALL LOGUNI
CALL TRIANG
CALL WEIBUL
CALL BETA
CALL CORREL
SUBROUTINE TRIANG
samples from triangular
distribution
SUBROUTINE WEIBUL
samples from Weibull distribution
distribution
CALL CHOOSE
time variant
SUBROUTINE BETA
samples from beta
distribution
SUBROUTINE CORREL
handles correlated parameters
FOR
EACH
TRIAL
STEP
THROUGH
TIME
CALL COMEX
SUBROUTINE COMEX
Execution Module for
component modules
CALL COMPONENT
MODULES
CALL TIMSEL
SUBROUTINE TIMSEL
Saves user selected, time
variant input parameters
for stats or results
CALL SELECT
SUBROUTINE SELECT
for appropriate time
steps CALL SORT
SUBROUTINE SORT
selects variables for
stats and/or results
CALL SEND
SUBROUTINE SEND
writes selected values
to appropriate vector
locations for stats or
results file
SELECT
PARAMETERS
FOR
OUTPUT
CALL SAVEIN
SUBROUTINE SAVEIN
saves user selected, non-time
variant parameters for stats or results
CALL STATS
SUBROUTINE STATS
update stats for specified
variables
CALL MOMENT; GMOMENT
SUBROUTINE MOMENT
update cumulative
moment totals
SUBROUTINE GMOMENT
update cumulative
moment totals
STATISTICS
CALL WRITE
WRITE
write values to results file
SUBROUTINE FILER
write date and time
to output files
Note - ODS and LEAHY
compiler specific
OUTPUT
CALL NAMOUT
NAMOUT
creates vectors of variable
names for output files
CALL OUTPUT
OUTPUT
write summary stats
to stats file & to
(detailed results) key file
END

## FIGURE 5.3

## THE SUBROUTINE COMEX AND COMPONENT MODULES

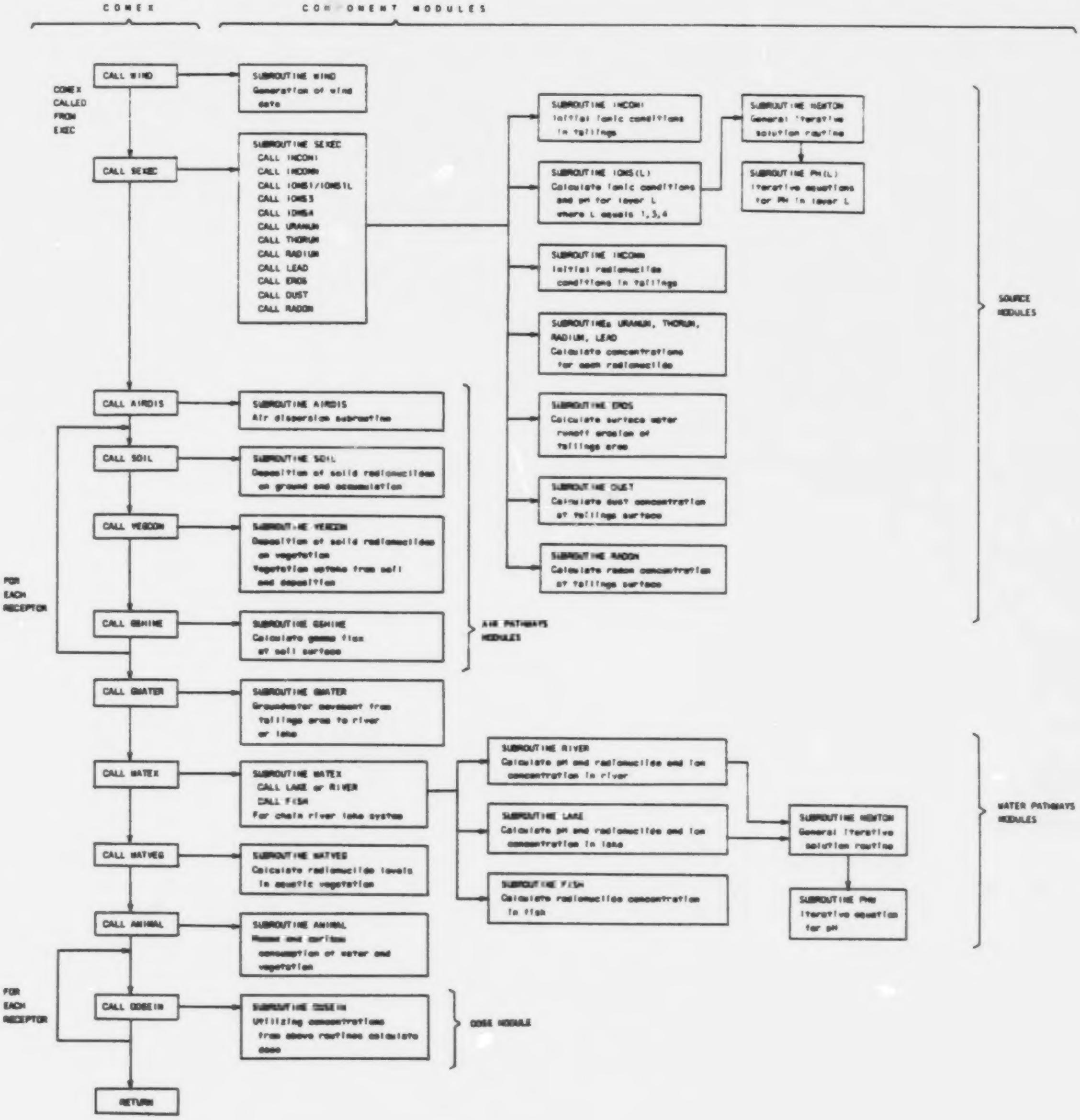
COMEX
COMPONENT MODULES
CALL WIND
COMEX CALLED FROM EXEC
SUBROUTINE WIND
Generation of wind data
CALL SEXEC
SUBROUTINE SEXEC
CALL INCONI
CALL INCONN
CALL IONS1/IONS1L
CALL IONS3
CALL IONS4
CALL URANUM
CALL THORUM
CALL RADIUM
CALL LEAD
CALL EROS
CALL DUST
CALL RADON
SUBROUTINE INCONI
Initial ionic conditions in tailings
SUBROUTINE IONS(L)
Calculate ionic conditions and pH for layer L where L equals 1,3,4
SUBROUTINE NEWTON
General iterative solution routine
SUBROUTINE PH(L)
Iterative equations for PH in layer L
SUBROUTINE INCONN
Initial radionuclide conditions in tailings
SUBROUTINEs URANUM, THORUM, RADIUM, LEAD
Calculate concentrations for each radionuclide
SUBROUTINE EROS
Calculate surface water runoff erosion of tailings area
SUBROUTINE DUST
Calculate dust concentration at tailings surface
SUBROUTINE RADON
Calculate radon concentration at tailings surface
SOURCE MODULES
CALL AIRDIS
SUBROUTINE AIRDIS
Air dispersion subroutine
CALL SOIL
SUBROUTINE SOIL
Deposition of solid radionuclides on ground and accumulation
CALL VEGCON
SUBROUTINE VEGCON
Deposition of solid radionuclides on vegetation
Vegetation uptake from soil and deposition
FOR EACH RECEPTOR
CALL GAMMA
SUBROUTINE GAMMA
Calculate gamma flux at soil surface
AIR PATHWAYS MODULES
CALL GWATER
SUBROUTINE GWATER
Groundwater movement from tailings area to river or lake
CALL WATEX
SUBROUTINE WATEX
CALL LAKE or RIVER
CALL FISH
For chain river lake system
SUBROUTINE RIVER
Calculate pH and radionuclide and ion concentration in river
SUBROUTINE LAKE
Calculate pH and radionuclide and ion concentration in lake
SUBROUTINE FISH
Calculate radionuclide concentration in fish
SUBROUTINE NEWTON
General iterative solution routine
SUBROUTINE PHW
Iterative equation for pH
WATER PATHWAYS MODULES
CALL WATVEG
SUBROUTINE WATVEG
Calculate radionuclide levels in aquatic vegetation
CALL ANIMAL
SUBROUTINE ANIMAL
Moose and caribou consumption of water and vegetation
FOR EACH RECEPTOR
CALL DOSEIN
SUBROUTINE DOSEIN
Utilizing concentrations from above routines calculate dose
DOSE MODULE
RETURN

## 5.2 Writing Component Modules

All subroutines should be written in Fortran 77 and compiled on the Lahey compiler Version 2.0 (1985) making certain not to use any compiler specific options so as to ensure portability of the program. Variables should be in units corresponding to the rest of the program; namely Bequerals, meters, grams, moles, and microsieverts.

## 5.3 Passing Variables

### 5.3.1 Include file MODEL.INC

The following common statements and variables contained in the INCLUDE file "MODEL.INC" are necessary for implementing new component modules. This file should be added to component modules, using an include statement.

a) TIME

This common statement contains the following variables:

T - The current time (Real)
NUMTRL - The trial number
NTRIAL - The total number of trials
NYEARS - Years in simulation (Integer)
NDT - Time increment (Integer)
RYEARS - Years in simulation (Real)
DT - Time increment (Real)
NT - The current time (Integer)

Both integer and real variables are made available to avoid frequent conversion from one to the other throughout the program.

b) CONCEN

The matrices of output concentrations and doses described on Table 3.6 are sent back from the component modules to the control modules through this common block. These are dimensioned as follows:

| | |
|---|---|
| WCONC | (10,4,3) |
| CONC | (10,4,3) |
| PH | (4) |
| WATC | (8,10) |
| WATAVG | (4) |
| WATPH | (10) |
| GWATC | (4) |
| EMRATE | (5) |
| EROTOT | |
| DTAIL | |
| AIRC | (5,82) |
| SOILC | (4,82) |
| AVEGC | (4,80) |
| BVEGC | (4,80) |
| SUFOC | (4) |
| BROWSC | (4) |
| LICHC | (4) |
| AQVEGC | (4) |
| FISHC | (4,10) |
| AMOC | (4) |
| WMOC | (4) |
| ACARC | (4) |
| WCARC | (4) |
| WATD | (5,80) |
| SHINED | (5,80) |
| INHD | (5,80) |
| RADD | (80) |
| VEGD | (5,80) |
| FISHD | (5,80) |
| MEATD | (5,80) |
| DOSE | (5,80) |
| POPDT | |
| BLANK1 | (4,80) |
| BLANK2 | (10,10) |

The first position in the matrices is a substance identifier. The substance codes are shown on Table 3.7. The second dimension in the matrices is a location identifier as described in Section 3.2.3.

In the matrices with three dimensions, the third position is time and the codes are as follows:

1 - Initial time (T = 0)
2 - Previous time step
3 - Current time step

Note that only the current time can be obtained for output.

### c) RECEPT

This common statement contains the receptor information. The variables are:

NRECEP - Number of receptor locations
NRING - Number of rings
RDIR(80) - Receptor sectors
RRING(80) - Receptor rings
RWSSEG(80) - Receptor drinking water source segment numbers
RPOP(80) - Receptor populations
RNGMID(5) - Radial distance to midpoint of ring (m)
RTYPE(80) - Receptor type (C=Critical, A=Average)
RAREA (5) - Sector areas for each ring (m$^2$)
NREC - Counter of Receptors
TAREA - Total areas of all rings (m$^2$)
NDREC - Number of Receptor locations plus two

### d) WATER

The variables pertaining to the watershed are transferred using this block. These variables are:

NSEG - Number of watershed segments
NODDIR(10) - End Node sector numbers
NODRNG(10) - End Node Ring Numbers
STYPE(10) - Segment Types (R=River, L=Lake)
SDEPTH(10) - Average Segment Depths (m)
LAREA(10) - Lake Areas (m$^2$) for lake segments and Lengths (m) for river segments
SHEDAR(10) - Cumulative watershed areas (m$^2$)
LAKVOL(10) - Lake Volumes (m$^3$) (Area x Average Depth)
PSDIR(10) - Receptor sectors by watershed wind rose locations

PSRING(10) - Receptor ring numbers by watershed wind rose locations
PSNUM - Number of wind rose locations in watershed
PSAREA - Total Area of wind rose locations in which the watershed lies
GSEG - Number of segment groundwater flows into

The vectors, PSDIR and PSRING, are provided to maximize program efficiency when calculations need to be performed only once for each wind rose location containing a watershed segment. These contain the same information as the vectors NODDIR and NODRNG but in a more compressed form. For instance two or three segment end nodes could lie within the same wind rose location; however, some calculations need only be performed once for that location.

### e) WIND

The wind data is contained within the following variables:

FWIND1(16) - Frequency of observations of windspeed over 5.4 m/s by direction
FWINDT - Sum of frequencies in FWIND1
UWIND(16,6) - Average windspeed (m/s) by direction and stability class
FWIND2(16,6) - Frequency of wind by direction and stability class
FWIND(16,6,6,20) - Vector containing wind speed (knots) by direction, stability class, speed, and year (1 or 20 years or sets of data)

The vector, FWIND, is used by subroutine WIND to create the wind data contained in the variables FWIND1, FWIND2, FWINDT, and UWIND. Note that the direction used for wind refers to the direction the wind blows to (i.e. direction of downwind receptor from the tailings).

### 5.3.2 Include file VAR.INC

This file contains a number of common blocks set up to facilitate easy additions of or changes to component modules. It should be included in all new component modules.

The first block described below (INPT) contains sampled values from the input distributions while the other four common blocks are used for saving values within subroutines or for passing values between different subroutines. Any variables used for these purposes should be added to the appropriate common block. Each of these latter four blocks correspond to common blocks within the file "INTERM.INC" included in the main program, EXEC. If these common blocks are not large enough, their sizes can be increased by changing them within INTERM.INC.

a) INPT

The variable contained within this common block is XIN(200). XIN is a vector containing the values sampled from the input distributions. To add new input distributions, the variables should be added to the list in this common block as well as to the first input file. The format of input distributions is described in Section 3.1. The order of parameters listed in common (INPT) should correspond to the order of the probabilistic inputs listed in the file INPUT1.DAT.

b) INTERM

This common block is used for transferring real numbers between subroutines. Up to 4,000 real numbers can be put in this block.

c) RR8

Double precision variables are transferred through this block, up to a maximum of 1,500.

d) INTGER

The common block, INTGER contains integer values (INTEGER*2) and has a size of

100.

e) CHAR

Character values are transferred using this common block which is dimensioned 200.

## 5.4 Changing the Control Modules

Any new common blocks added should be included in the main program, EXEC. Any new output variables added must be inserted in the list of variables sorted by subroutine SORT. The order of these variables must correspond exactly to the order in the common block CONCEN and in the second input file. Two arrays called BLANK1 and BLANK2, not used at present, may be used to output any new arrays without having to change the coding of subroutine SORT. These variables are dimensioned (4, 80) and (10, 10) respectively, and should also be listed at the bottom of the second input file. The user simply has to set BLANK1 or BLANK2 equal to the variable for which he desires output.

## 5.5 Modifying First Input File

The input file, INPUT1.DAT, should be modified to include all of the input distributions (see Section 3.1) required by the component module. These must be listed in the same order as they appear in the common block INPT. The output files desired should be opened and all counters set to match the numbers of input distributions.

## 5.6 Modifying Second Input File

The second input file, INPUT2.DAT, should be modified to obtain the desired output variables, substances, locations and time steps (see Section 3.2). The receptor and watershed information may also be changed.

## 5.7 Compiling and Linking

The program, including the new subroutine, should be compiled and linked. For ease of compiling, the file "UTAP.FOR" is provided. This file contains a list of "INCLUDE" statements for all of the modules. The necessary FORTRAN files are as follows:

EXEC.FOR
INPUT.FOR
SAMPLE.FOR
SAVE.FOR
STATS.FOR
OUTPUT.FOR
SEXEC.FOR
INCONI.FOR
INCONN.FOR
IONS1.FOR
IONSIL.FOR
IONS3.FOR
IONS4.FOR
URANUM.FOR
THORUM.FOR
RADIUM.FOR
LEAD.FOR
EROS.FOR
RADON.FOR
DUST.FOR
COMEX.FOR
WIND.FOR
AIRDIS.FOR
SOIL.FOR
GSHINE.FOR
VEGCON.FOR
GWATER.FOR
WATEX.FOR
WATVEG.FOR
ANIMAL.FOR
FISH.FOR
DOSE.FOR

The above files contain "INCLUDE" statements for the following files:

IO.INC
CONC.INC
RECEP.INC
STATS.INC
COUNTS.INC
INFO.INC
OUT.INC
INPT.INC
INPT2.INC
UPDATE.INC
PARAM.INC
INTERM.INC
WIND.INC
MODEL.INC
VAR.INC

All of these files must be present in order to compile and link the program.

One potential source of problems in linking is the subroutine "FILER" which calls the $F_{77}L$ (Lahey, 1985) and DOS specific functions DATE and TIME and then writes the date and time to the output files. If these functions are not available simply remove this subroutine and the call statements for it in subroutines WRITE and OUTPUT (three call statements). Instead, simply write a blank line so that the format of the file is not changed.

The format of the INCLUDE statements used in UTAP is specific to the $F_{77}L$ compiler (Lahey, 1985). While most, if not all, other compilers support INCLUDE statements, their format may not be the same. If errors are encountered while compiling, these statements should be changed to match the syntax of the compiler being used. If INCLUDE statements are not available, the appropriate files should be copied to the program, replacing the INCLUDE statements.

## 5.8 Running the Program

Run the program as described in Chapter 4.0.

## 5.9 Other Changes and Information

If more complex changes are to be made to the program and a more detailed description of the modules or variables is required, refer to Volume 2 for details of the control modules and Volume 3 for the component models.

## 6.0 CONFIDENCE BANDS

Confidence bands are generated by two post-execution programs, BIN and OPAN. The first of these programs reads the detailed results file and the key file produced by UTAP. The data are binned and output is written to a disk file called "BIN.DAT". A log transformation of the data can also be requested.

The second program fits a probability distribution function to the binned data and then fits 95% confidence bands to the cumulative distribution function and to the probability distribution function. Output is sent to a user-specified disk file in a formatted form compatable with most graphics packages.

### 6.1 Running the Program

The two files, BIN.FOR and OPAN.FOR, containing the FORTRAN program code should each be compiled and linked. A sample session is shown on Table 6.1. After UTAP has been run, the detailed results file and the key file are utilized by BIN. Each variable name and the specifics such as location and substance codes and time if applicable are indicated within the file and the variables are assigned reference numbers (see example key file in Appendix C with reference numbers in first column). These reference numbers are used by the binning program to identify the desired variable.

The program, BIN, prompts the user for the names of the detailed results file and the key file. It also asks the reference number of the variable of interest, and whether or not a log transformation is desired. Output is sent to the file "BIN.DAT".

The second program, OPAN, reads the file "BIN.DAT" and prompts the user for the name of the output file. If the program is not successful, selecting the log transformation, (or not selecting it if it was previously used) may work.

Note that the data must be either approximately normally or lognormally distributed (depending whether a log-transformation is selected) or the

Table 6.1

## CONFIDENCE BANDS PROGRAM SAMPLE SESSION

```
C:BIN

DETAILED RESULTS FILE NAME? RES.OUT

Opening file: RES.OUT
KEY FILE NAME? KEY.OUT

Opening file: KEY.OUT
Opening file: BIN.DAT
ENTER ID. NO. OF VARIABLE TO BE ANALYZED: 2

DO YOU WANT LOG TRANSFORMATION (Y/N)? N

C:OPAN

Opening file: BIN.DAT
ENTER NAME OF OUTPUT FILE: NORMAL

Opening file: NORMAL

C:
```

Table 6.2

## CONFIDENCE BANDS PROGRAM SAMPLE OUTPUT FILE FOR A NORMAL DISTRIBUTION

```
    CDF      LOWERLIMIT   FITTEDCDF  UPPERLIMIT     PDF      LOWERLIMIT   FITTEDPDF  UPPERLIMIT
0.3704E+01  0.0000E+00  0.0000E+00  0.0000E+00  0.4455E+01  0.1898E+01  0.3489E+01  0.6338E+01
0.5206E+01  0.1898E+01  0.3489E+01  0.6338E+01  0.5956E+01  0.1447E+02  0.2018E+02  0.2781E+02
0.6707E+01  0.1639E+02  0.2367E+02  0.3408E+02  0.7458E+01  0.5782E+02  0.6735E+02  0.7750E+02
0.8209E+01  0.7471E+02  0.9102E+02  0.1107E+03  0.8960E+01  0.1189E+03  0.1297E+03  0.1398E+03
0.9710E+01  0.1988E+03  0.2207E+03  0.2434E+03  0.1046E+02  0.1324E+03  0.1442E+03  0.1552E+03
0.1121E+02  0.3433E+03  0.3649E+03  0.3840E+03  0.1196E+02  0.8267E+02  0.9252E+02  0.1023E+03
0.1271E+02  0.4431E+03  0.4575E+03  0.4682E+03  0.1346E+02  0.2679E+02  0.3425E+02  0.4327E+02
0.1422E+02  0.4861E+03  0.4917E+03  0.4951E+03  0.1497E+02  0.4521E+01  0.7319E+01  0.1171E+02
0.1572E+02  0.4978E+03  0.4990E+03  0.4996E+03  0.1647E+02  0.4017E+00  0.9026E+00  0.2004E+01
0.1722E+02  0.4998E+03  0.4999E+03  0.5000E+03  0.1797E+02  0.1885E-01  0.6424E-01  0.2163E+00
0.1872E+02  0.5000E+03  0.5000E+03  0.5000E+03
```

FIGURE 6.1

PLOTS OF 95% CONFIDENCE BANDS
FOR A NORMAL DISTRIBUTION
(500 TRIALS)

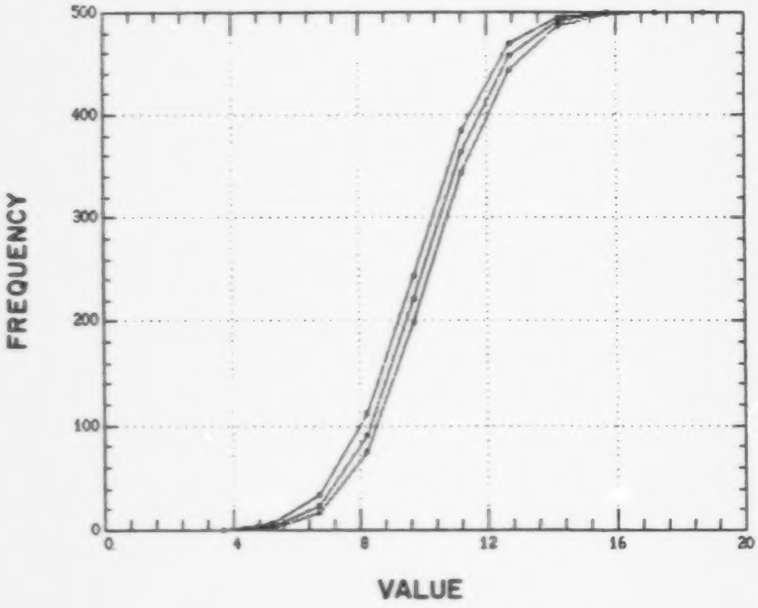

A) CUMULATIVE DISTRIBUTION FUNCTION

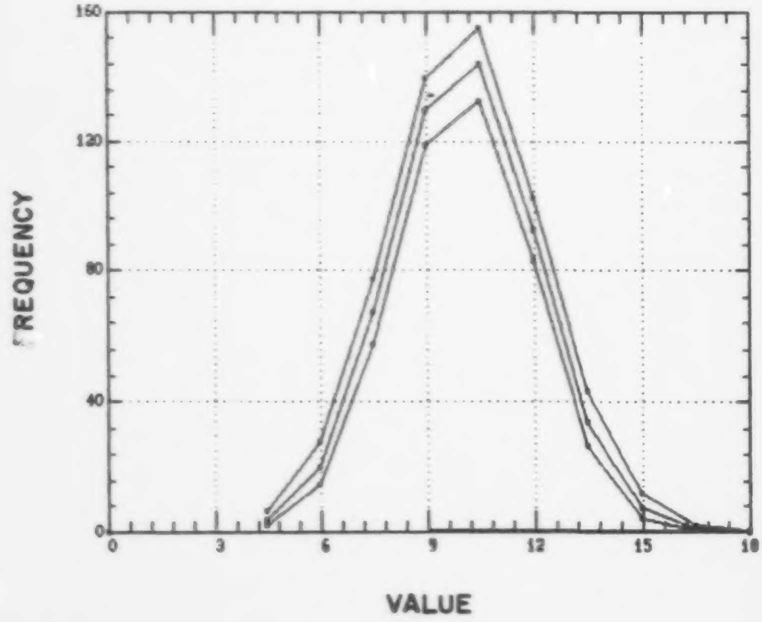

B) PROBABILITY DISTRIBUTION FUNCTION

program will be unable to fit confidence bands.

A sample output file for a normal distribution and plots of these results done using STATGRAFICS, (STSC, 1985), a statistical graphics package, are shown on Table 6.2 and Figure 6.1, respectively. The first four columns in the output file apply to the cumulative distribution function and the other four to the probability distribution function. Of both of these sets of four columns, the first columns contains the variable values (x-ordinates) for the distribution's bins. The third columns are the values of the fitted functions and the second and fourth columns are the lower and upper limits, respectively, of the distributions.

The program fits curves based on the variability of the data values. The program computes the 95% confidence bands. The interpretation is that one is entitled to feel 95% confident that the true probability density function or cumulative probability function of the output variable from a Monte Carlo calculation will fall within these bounds.

## REFERENCES

Lahey Computer Systems, Inc., 1985. "$F_{77}L$ - FORTRAN 77 Language System for the Personal Computer." California, U.S.A.

SENES Consultants Limited, 1984. "A Study to Develop and Demonstrate Techniques for the Probabilistic Assessment of the Long-Term Effects of Uranium Mill Tailings in Canada - Phase I." Research Report Prepared for the National Uranium Tailings Program, CANMET, EMR, under Supply and Services Canada Contract No OSQ83-00236.

SENES Consultants Limited, 1985. "A Study to Develop and Demonstrate Techniques for the Probabilistic Assessment of the Long-Term Effects of Uranium Mill Tailings in Canada - Phase II." Research Report prepared for the National Uranium Tailings Program, CANMET, EMR, under Supply and Services Canada Contract No OSQ84-00207.

Statistical Graphics Corporation (STSC), 1985. "STATGRAPHICS - Statistical Graphics System." U.S.A.

# APPENDIX A

## ERROR AND WARNING MESSAGES

# APPENDIX A
# ERROR AND WARNING MESSAGES

(001) WATER SOURCE SEGMENTS NOT IN ORDER

The watershed segment end nodes specified in the second input file must be consecutively increasing integers (i.e. numbered from upstream to downstream).

(002) WATERSHED AREAS MUST INCREASE

Watershed areas are cumulative and must increase for each downstream segment specified in the second input file.

(003) WATER SOURCE NOs. MUST INCREASE

Identifiers specified in general information file must begin at 1 greater than the number of receptors and increase by 1 for each new sector/ring combination.

(004) CORRELATED NAME NOT FOUND

Name of independent variable for correlated distribution not found in input file. Distribution name must appear before correlated parameter.

(005) UNEXPECTED END OF DATA

Input file empty, doesn't exist, or too short.

(006) TYPE ERROR IN REGULAR DIST'ns

Distribution type number greater than 8. Numbers of parameters or arbitrary or correlated distributions incorrect.

(007) TYPE ERROR IN CORRELATED DIST'ns

Distribution type number not equal to 10. Numbers of parameters or arbitrary or correlated distributions incorrect.

(008) TYPE ERROR IN ARBITRARY DIST'ns
Distrubtion type number not equal to 9. Numbers of parameters or arbitrary or correlated distributions incorrect.

(009) NUMBER OF PARAMETERS INCORRECT
End of file reached before specified numbers of parameters read.

(010) RECEPTORS NOT LISTED IN ORDER
Receptor numbers must be consecutively increasing integers starting at one.

(011) TIME STEPS MUST INCREASE
Time steps to be saved for output must increase.

(012) STATS REQUESTED MUST SPECIFY FILE
Output to stats file attempted but file was not requested or opened.

(013) RESULTS REQUESTED MUST SPECIFY FILE
Output to results file attempted but file was not requested or opened.

(014) CAN'T SAVE RESULTS - NO OPEN FILE
Output to a detailed results or statistics file has been requested, but that file was not requested in the first input file.

(015) CAN'T SAVE TIME STEPS SPECIFIED
The time steps requested to be saved to either the detailed results or the statistics file are not a multiple of the time increment.

(016) TIME FOR OUTPUT TOO BIG
Time step(s) requested for output are bigger than simulation time.

(017) WATERSHED SECTORS OR RINGS NOT CONTINUOUS
Watershed segments must be smaller so that each sector with segment passing through it is identified.

(018) CANNOT CORRELATE PARAMETERS

The independent parameter cannot be time variant unless the dependent parameter is.

(019) TIME STEPS DON'T MATCH SIMULATION TIME

The simulation time must be divisible by the time increment with no remainder.

(020) MAXIMUM OF 80 RECEPTORS ALLOWED

Attempt was made to read in information for more than 80 receptors locations.

(021) MAXIMUM OF 5 RINGS ALLOWED

Attempt was made to read in ring limits for more than 5 rings.

(022) RING LIMITS MUST INCREASE

The ring limits must be specified beginning with the inner ring and moving outwards.

(023) RECEPTOR RING NUMBER TOO BIG

A receptor's ring number is larger than the number of rings dimensioned.

(024) FIRST WATERSHED SEGMENT MUST BE RIVER

The first watershed segment specified must always be a river, not a lake. Use a river of zero length and sub-basin area.

(025) GROUNDWATER MUST FLOW INTO RIVER

Groundwater cannot be specified as flowing directly into a lake. Use a river of zero length and sub-basin area.

(027) TOO MANY OUTPUTS TO STATS FILE

A maximum of 300 variables can be output to the statistics file. Reduce number of variables or number of time steps.

(028) TOO MANY OUTPUTS TO RESULTS FILE

A maximum of 300 variables can be output to the detailed results and key files. Reduce number of variables or number of time steps.

(029) FILE NOT FOUND

Input file named does not exist.

(030) ERROR IN LOGNORMAL SPECIFIERS

Lognormal distribution has equal, reversed, or undefined minimum and maximum values. Check input file.

(031) ERROR IN NORMAL SPECIFIERS

Normal distributions has equal, reversed, or undefined minimum and maximum values. Check input file.

(032) TIME STEP MUST BE 1 OR 10 YEARS

Only 1 and 10 year time steps are available.

(033) ERROR IN TRIAGULAR SPECIFIERS

Triangular distribution has equal, reversed, or undefined minimum and maximum values. Check input file.

(101) TWO CONSECUTIVE LAKES

Lakes are generally separated by a river. You may continue without further warnings or stop to correct input.

(102) ABOUT TO OVERWRITE EXISTING FILE

Continuing execution will cause the contents of the file named directly above the warning to be erased.

(105) NOT SAVING TIME STEPS TO STATS

Time steps for statistics file requested but file not opened.

(106) NOT SAVING TIME STEPS TO RESULTS

Time steps for detailed results file requested but file not opened.

## APPENDIX B

## SAMPLE INPUT FILES

# EXAMPLE OF FIRST INPUT FILE (INPUT1.DAT)

```
PROBABILISTIC ANALYSIS: SAMPLE RUN
Y
STAT.OUT
Y
RES.OUT
KEY.OUT
 216   0   0  25
0913566091    5
 100  10
CODION N  1 N          0.0
CODPH  N  1 N          0.0
CODNUC N  1 N          0.0
CODREC N  1 N          0.0
CODSL  N  1 N          0.0
CODWIN N  1 N          0.0
CODRAD N  1 N          0.0
CODAIR N  1 N          0.0
CODDUS N  1 N          0.0
CODVEG N  1 N          0.0
CODGS  N  1 N          0.0
CODSOL N  1 N          0.0
CODGW  N  1 N          0.0
CODWAT N  1 N          0.0
CODERO N  1 N          0.0
CODFIS N  1 N          0.0
CODWVG N  1 N          0.0
CODANI N  1 N          0.0
CODDOS N  1 N          0.0
PYRITI N  4 N        6.0E2       8.0E2
RHOTAL N  2 N        1.4E6       0.1E6         1.1E6        1.7E6
FRACGP N  4 N       5.0E-2      6.0E-2
KPRIME N  3 N       5.0E-2         1.7        2.0E-2       2.5E-1
SULPRD N  3 N       1.4E-6         1.5        0.4E-6       4.2E-6
O2CONC N  1 N         9.04
O2DIFF N  6 N        3.0E1       7.0E1        13.0E1
DUNSAT N  4 N         0.75        1.25
KSUBSO N  1 N        2.5E1
FACTCO N  6 N       3.0E-1      4.0E-1        5.0E-1
NPRCP  N  2 V       4.0E-1      1.0E-1        1.5E-1        6.5E-1
POROS  N  6 N       3.5E-1      4.0E-1        4.5E-1
DMIX   N  4 N          1.0         2.0
AVPRCP N  1 N       4.0E-1
FNPRCP N  3 N       1.5E-1        1.27        7.0E-2           0.3
ATAIL  N  1 N        5.0E5
XLIME  N  1 N          0.0
PCURAN N  1 N          0.1
FURAN  N  4 N         0.92        0.98
FT230  N  4 N         0.92        0.98
FT232  S  4 N          0.6         0.7
FRAD   N  6 N         0.25        0.60          0.95
FLEAD  N  4 N         0.92        0.98
FRACU  N  4 N          0.3         0.9
KDUO2  N  3 N       3.0E-5         3.0        1.1E-6        8.1E-4
```

```
PCTHOR N  4 N        0.02        0.04
FRACTH N  6 N         0.2         0.3          0.4
XRADI  N  6 N      2.5E-6      3.5E-6       4.5E-6
KSBAR  N  1 N      5.0E-4
KFBAR  N  1 N     5.01E-1
KRAD   N  4 N        0.50        0.56
KDRAD  N  6 N      5.0E-6     40.0E-6      75.0E-6
CLEADI N  6 N         1.0         2.0          3.0
KSLEAD N  1 N      1.2E-2
KFLEAD N  1 N     5.01E-1
KDLEAD N  6 N     20.0E-6     60.0E-6     100.0E-6
SKDU   N  5 N     1.3E-04      7.9E02
SSKDTH N  5 N     3.3E-03      1.5E02
SKDPB  N  5 N     1.8E-01      6.3E01
SKDRA  S  5       5.1E-03      9.5E02
FWAT   N  6 N    2.00E-02     1.6E-01      4.8E-01
WC1    N  4 N    7.50E-01     1.4E+00
WC2    N  3 N    1.30E-01     1.4E+00      5.0E-02      3.6E+00
XLAMU  N  1 N    1.53E-10
XLAMTH N  1 N    4.95E-11
XLAMPB N  1 N    3.30E-02
XLAMRA N  1 N    4.33E-04
DSOIL1 N  1 N    5.00E-02
DSOIL2 N  1 N    1.50E-01
DSOIL3 N  1 N     0.0E-00
DSOIL4 N  1 N     0.0E-00
RHO1   N  3 N    1.29E+02     1.3E+00      2.0E+01      4.5E+02
RHO2   N  3 N    1.34E+03     1.1E+00      1.0E+03      1.8E+03
LAYER  N  1 N    2.00E+00
MPCH20 N  6 N     5.0E+0       1.5E+1       2.5E+1
EMANAT N  6 N     2.0E-2       2.0E-1       9.0E-1
NSUBW  N  1 N     5.0E+0
WTSFLX N  3 N     2.0E-2       2.0E+0       2.0E-3       2.0E-1
SILT   N  6 N     1.0E+1       4.5E+1       9.0E+1
FPREC  S  2 V    1.23E+2       1.8E+1       8.4E+1      1.56E+2
HSRC   N  4 N     1.0E+0       3.0E+0
WYEAR  N  4 V        1.0    20.999999
EMFRAC N  1 N     2.0E-1
XRGWAT N  6 N       25.0         35.0        200.0
AXGWAT N  1 N     1000.0
POGWAT N  4 N       0.30         0.36
DCGWA1 N  3 N       0.02          2.5        5.E-3          0.5
DCGWA2 N  3 N        0.5         2.15         0.05          5.0
DCGWA3 F  3 N       0.67         1.73         0.13          3.5
DCGWA4 N  3 N       0.07          1.9         0.01          0.5
SDGWAT N  2 N     2650.0        110.0       2320.0       2980.0
ACTCO  N  6 N        0.6          0.8          0.9
WATCAB N  1 N     1.0E-1
WTSO4B N  1 N     7.1E-2
WSIGS1 N  6 N       95.0        230.0        615.0
WSIGS2 N  6 N      105.0        260.0        765.0
WSIGS3 N  6 N       85.0        210.0        515.0
WSIGS4 N  1 N        0.0
WSIGS5 N  1 N        0.0
WTRHOS N  1 N     1.84E6
```

```
WATEPS  N  6 N     0.83       0.94       0.97
WTMIXD  N  1 N     0.05
WKDU    N  3 N     4.5E-3     2.2        0.4E-3     4.8E-2
WKDPB   N  3 N    15.0E-3     2.5        1.0E-3     2.3E-1
WKDRA   N  3 N     6.5E-3     2.5        0.4E-3     1.0E-1
KDPRIM  N  3 N     2.0E-2     2.5        2.0E-3     3.0E-1
BURYF   B  4 N     0.5        0.7
CURRNT  N  4 N     3.15E4     3.15E5
DIFFC   N  1 N     0.02
BIOACF  N  3 N     1.55E-6    6.1E00     1.0E-8     5.8E-5
BIOACF  N  3 N     1.18E-5    2.6E00     1.1E-6     1.1E-4
BIOACF  N  3 N     1.74E-5    3.25E00    1.7E-6     5.7E-4
BIOACF  N  3 N     1.31E-5    3.3E00     1.2E-6     6.0E-4
WATVTC  N  3 N     1.5E-5     5.5E00     1.0E-6     7.0E-4
WATVTC  N  3 N     1.1E-5     6.8E00     1.0E-6     1.6E-4
WATVTC  N  3 N     1.3E-4     2.0E00     4.0E-5     4.3E-4
WATVTC  N  3 N     4.5E-5     2.9E00     1.0E-5     3.3E-4
SLOPE   N  1 N     1.00E00
THALF   N  4 N     1.00E+1    2.0E01
RRAIN   N  4 N     6.50E+1    9.75E01
RSOIL   N  4 N     1.00E-8    1.00E-7
DM      N  1 N     1.00E-2
STORM   N  4 N     1.20E-1    1.6E-1
DEPVEL  N  4 N     3.00E-3    3.00E-2
FDEPSF  N  4 N     1.0E-1     3.0E-1
FDEPSF  N  4 N     1.0E-1     3.0E-1
FDEPSF  N  2 N     4.7E-1     3.0E-1     1.0E-2     1.0
FDEPSF  N  2 N     4.7E-1     3.0E-1     1.0E-2     1.0
FDEPSF  N  4 N     8.0E-1     1.0
FDEPED  N  4 N     8.0E-1     1.0
FDEPED  N  4 N     5.0E-2     1.5E-1
FDEPED  N  4 N     8.0E-1     1.0
FDEPED  N  4 N     8.0E-1     1.0
FDEPED  N  4 N     8.0E-1     1.0
VEGLAM  N  4 N     2.9E-7     1.2E-6
VEGLAM  N  4 N     2.9E-7     1.2E-6
VEGLAM  N  4 N     2.9E-7     1.2E-6
VEGLAM  N  4 N     2.9E-7     1.2E-6
VEGLAM  N  4 N     1.5E-9     4.4E-9
DUREXP  N  6 N     2.6E+6     5.2E+6     7.8E+6
DUREXP  N  6 N     2.6E+6     5.2E+6     7.8E+6
DUREXP  N  4 N     1.3E+6     3.9E+6
DUREXP  N  4 N     1.3E+6     3.9E+6
DUREXP  N  1 N     1.0E+10
YDEN    N  4 N     1.0E+3     3.0E+3
YDEN    N  4 N     1.0E+3     3.0E+3
YDEN    N  4 N     5.0E+2     1.0E+3
YDEN    N  4 N     5.0E+2     1.0E+3
YDEN    N  4 N     4.0E+2     6.0E+2
SPTCAV  N  3 N     6.08E-4    8.90       7.67E-6    7.00E-3
SPTCAV  N  3 N     4.20E-3    9.00       5.19E-5    3.40E-1
SPTCAV  N  3 N     4.00E-3    9.00       4.94E-5    3.24E-1
SPTCAV  N  3 N     8.47E-3    10.3       8.03E-5    8.93E-1
SPTCBV  N  3 N     3.17E-4    3.93       2.06E-5    4.89E-3
SPTCBV  N  3 N     4.20E-3    4.00       2.62E-4    6.72E-2
SPTCBV N  3 N   4.00E-3      4.00    2.50E-4    6.40E-2
SPTCBV N  3 N   2.65E-3      4.52    1.29E-4    6.60E-2
SPTCSF N  3 N   6.60E-3      8.91    8.31E-5    5.24E-1
SPTCSF N  3 N   2.23E-2      9.50    2.47E-4    2.01E+0
SPTCSF N  3 N   2.16E-2      3.55    1.71E-3    2.71E-1
SPTCSF N  3 N   2.11E-1      3.63    1.87E-3    2.39E-1
SPTCB  N  3 N   6.60E-3      8.91    8.31E-5    5.24E-1
SPTCB  N  3 N   2.23E-2      9.50    2.47E-4    2.01E+0
SPTCB  N  3 N   2.16E-2      3.55    1.71E-3    2.71E-1
SPTCB  N  3 N   2.11E-1      3.63    1.87E-3    2.39E-1
SPTCL  N  1 N       0.0
SPTCL  N  1 N       0.0
SPTCL  N  1 N       0.0
SPTCL  N  1 N       0.0
FIRC   N  6 N   5.0E+3    7.0E+3     9.0E+3
WIRC   N  6 N   7.7E+3   11.5E+3    15.3E+3
FAISFC N  6 N      0.05       0.2        0.5
FAILC  N  6 N      0.05       0.2        0.5
FMTCC  N  6 N    1.1E-7    3.4E-7     1.0E-6
FMTCC  N  6 N    0.7E-7    2.0E-7     6.0E-7
FMTCC  N  6 N    1.3E-7    4.0E-7     1.2E-6
FMTCC  N  6 N    1.7E-7    5.1E-7     1.5E-6
FIRM   N  1 N    2.7E+4
WIRM   N  6 N     0.024     0.036      0.048
FAIBM  N  6 N       0.8       0.9       0.95
FMTCM  N  6 N    1.1E-7    3.4E-7     1.0E-6
FMTCM  N  6 N    0.7E-7    2.0E-7     6.0E-7
FMTCM  N  6 N    1.3E-7    4.0E-7     1.2E-6
FMTCM  N  6 N    1.7E-7    5.1E-7     1.5E-6
EFR    N  6 N       0.2       0.5        0.8
OF     N  6 N       0.8       0.9        1.0
OF     N  6 N       0.4       0.6        0.9
INOCC  N  6 N       0.5      0.75        0.9
INOCC  N  6 N       0.5      0.75        0.9
AIRIN  N  1 N    8.4E+3
AIRIN  N  1 N    8.4E+3
AFACT  N  4 N       0.5       1.0
AVEGIN N  1 N   3.99E+4
AVEGIN N  1 N   1.57E+5
AFLOC  N  6 N       0.0       0.1        0.2
AFLOC  N  6 N       0.1       0.3        0.6
BFACT  N  4 N       0.5       1.0
BVEGIN N  1 N   6.54E+4
BVEGIN N  1 N   7.00E+4
BFLOC  N  6 N       0.0       0.1        0.2
BFLOC  N  6 N       0.1       0.3        0.6
CARMIN N  4 N       0.0    3.2E+3
CARMIN N  1 N   3.95E+4
CFLOC  N  4 N       0.0       1.0
CFLOC  N  4 N       0.0       1.0
MOMIN  N  4 N       0.0    3.2E+3
MOMIN  N  1 N   3.95E+4
MFLOC  N  1 N       0.0
MFLOC  N  1 N       1.0
WATIN  N  1 N       0.6
WATIN  N  1 N       0.6
WFLOC  N  6 N       0.8         0.9         1.0
WFLOC  N  6 N       0.4         0.6         0.9
FISHIN N  1 N    8.0E+3
FISHIN N  1 N    8.0E+3
FFLOC  N  4 N       0.0         0.1
FFLOC  N  1 N       1.0
```

## EXAMPLE OF SECOND INPUT FILE (INPUT2.DAT)

```
  N
AVERAGE.DAT
  5
  5
    1    3    5   10   20   50
  1 16  1  1 C     2
  2 16  3  2 A     5
  3 14  3  2 A     6
  4  1  1  1 C     1
  5  7  3  2 A     3
  8  1
  1 R 11  1   2.5E-1   1.5E07   3.0E3
  2 L 11  1   1.0E01   2.0E07   5.0E05
  3 R 10  2   0.5      3.2E07   3.5E3
  4 L 10  2   4.0      3.8E07   2.5E05
  5 R  9  3   7.5E-1   7.0E07   7.0E3
  6 R  9  4   1.0      1.2E08   1.3E4
  7 L  9  4   5.0      1.4E08   4.0E06
  8 R  9  5   6.5      4.0E08   3.0E4
  4   3
    0   10   20   30
    0   50   90
 34
WCONC   0
CONC    0
PH      0
WATC    2
  2  3  S
  3  5  S
WATAVG  3
  1  1
  3  1  S
  4  1  F
WATPH   0
GWATC   0
EMRATE  0
EROTOT  0
DTAIL   0
AIRC    0
SOILC   0
AVEGC   0
BVEGC   0
SUFOC   0
BRWSC   0
LICHC   0
AQVEGC  0
FISHC   0
AMOC    0
WMOC    0
ACARC   0
WCARC   0
WATD    0
SHINED  0
```

```
INHD    0
RADD    0
VEGD    0
FISHD   0
MEATD   3
  1  3  F
  1  3  S
 11  5  S
DOSE    0
POPDT   0
BLANK1  0
BLANK2  0
```

## EXAMPLE FILE CONTAINING LONG TERM AVERAGE SET OF WIND DATA AS PROVIDED BY AES

```
P1397.TOTAL.
   N A 0.000400.000290.0    0.0    0.0    0.0          62925 1A176584
 NNE A 0.000370.000120.0    0.0    0.0    0.0          62925 2A176584
  NE A 0.000270.000150.0    0.0    0.0    0.0          62925 3A176584
 ENE A 0.000110.000060.0    0.0    0.0    0.0          62925 4A176584
   E A 0.000050.000020.0    0.0    0.0    0.0          62925 5A176584
 ESE A 0.000010.000010.0    0.0    0.0    0.0          62925 6A176584
  SE A 0.000030.000030.0    0.0    0.0    0.0          62925 7A176584
 SSE A 0.000050.000030.0    0.0    0.0    0.0          62925 8A176584
   S A 0.000190.000150.0    0.0    0.0    0.0          62925 9A176584
 SSW A 0.000300.000190.0    0.0    0.0    0.0          6292510A176584
  SW A 0.000270.000190.0    0.0    0.0    0.0          6292511A176584
 WSW A 0.000270.000200.0    0.0    0.0    0.0          6292512A176584
   W A 0.000460.000260.0    0.0    0.0    0.0          6292513A176584
 WNW A 0.000280.000180.0    0.0    0.0    0.0          6292514A176584
  NW A 0.000130.000080.0    0.0    0.0    0.0          6292515A176584
 NNW A 0.000240.000100.0    0.0    0.0    0.0          6292516A176584
   N B 0.002130.001650.000930.0    0.0    0.0          62925 1B176584
 NNE B 0.001940.001580.000750.0    0.0    0.0          62925 2B176584
  NE B 0.001410.000770.000540.0    0.0    0.0          62925 3B176584
 ENE B 0.000700.000280.000150.0    0.0    0.0          62925 4B176584
   E B 0.000830.000230.000150.0    0.0    0.0          62925 5B176584
 ESE B 0.000410.000100.000050.0    0.0    0.0          62925 6B176584
  SE B 0.000430.000120.000070.0    0.0    0.0          62925 7B176584
 SSE B 0.000600.000350.000250.0    0.0    0.0          62925 8B176584
   S B 0.001380.001270.001320.0    0.0    0.0          62925 9B176584
 SSW B 0.001310.001310.000980.0    0.0    0.0          6292510B176584
  SW B 0.001550.001520.001220.0    0.0    0.0          6292511B176584
 WSW B 0.001370.001520.000880.0    0.0    0.0          6292512B176584
   W B 0.002270.001800.001350.0    0.0    0.0          6292513B176584
 WNW B 0.001160.001010.000740.0    0.0    0.0          6292514B176584
  NW B 0.001060.000800.000530.0    0.0    0.0          6292515B176584
 NNW B 0.001050.000760.000310.0    0.0    0.0          6292516B176584
   N C 0.000980.002000.003640.000350.000020.00001      62925 1C176584
 NNE C 0.001180.002030.002700.000110.0    0.0          62925 2C176584
  NE C 0.001120.001580.002160.000180.000010.0          62925 3C176584
 ENE C 0.000640.000680.000990.000090.0    0.0          62925 4C176584
   E C 0.000700.000790.001460.000150.000010.0          62925 5C176584
 ESE C 0.000670.000460.000700.000050.0    0.0          62925 6C176584
  SE C 0.000680.000520.000660.000070.0    0.0          62925 7C176584
 SSE C 0.000690.000830.001790.000330.000030.00001      62925 8C176584
   S C 0.001140.001680.007320.001960.000150.00004      62925 9C176584
 SSW C 0.000730.001340.004530.000940.000030.0          6292510C176584
  SW C 0.000670.001300.004820.001030.000020.0          6292511C176584
 WSW C 0.000710.001280.003210.000510.000050.00002      6292512C176584
   W C 0.001110.002000.006260.001430.000210.00002      6292513C176584
 WNW C 0.000810.001330.004510.001110.000200.00003      6292514C176584
  NW C 0.000770.001110.003090.000600.000100.00002      6292515C176584
 NNW C 0.000640.000910.002090.000200.000020.00001      6292516C176584
   N D 0.002480.003680.009810.015030.002830.00043      62925 1D176584
 NNE D 0.002520.003980.008840.010610.002150.00043      62925 2D176584
  NE D 0.002200.003630.009480.013360.003420.00099      62925 3D176584
```

```
ENE D 0.002310.003550.009970.012710.003840.00098      62925 4D176584
  E D 0.003540.005030.013370.013500.003680.00090      62925 5D176584
ESE D 0.002610.003540.008110.007960.002170.00047      62925 6D176584
 SE D 0.002480.003380.007630.005870.001310.00016      62925 7D176584
SSE D 0.002560.004090.011150.011480.002650.00057      62925 8D176584
  S D 0.003770.005830.017620.026690.008500.00265      62925 9D176584
SSW D 0.002080.003290.009840.017170.005910.00212      6292510D176584
 SW D 0.002080.003230.009620.014230.004700.00141      6292511D176584
WSW D 0.001880.003000.007440.010990.003730.00158      6292512D176584
  W D 0.003310.005700.015580.027570.009890.00325      6292513D176584
WNW D 0.002260.004610.014190.028500.010070.00334      6292514D176584
 NW D 0.002230.003740.010380.014560.003840.00144      6292515D176584
NNW D 0.002040.003450.008680.012640.002710.00074      6292516D176584
  N E 0.0    0.001770.005530.0    0.0    0.0          62925 1E176584
NNE E 0.0    0.001760.004000.0    0.0    0.0          62925 2E176584
 NE E 0.0    0.001910.004090.0    0.0    0.0          62925 3E176584
ENE E 0.0    0.002030.003600.0    0.0    0.0          62925 4E176584
  E E 0.0    0.002890.002640.0    0.0    0.0          62925 5E176584
ESE E 0.0    0.002220.001200.0    0.0    0.0          62925 6E176584
 SE E 0.0    0.001970.001200.0    0.0    0.0          62925 7E176584
SSE E 0.0    0.002380.002240.0    0.0    0.0          62925 8E176584
  S E 0.0    0.003050.003620.0    0.0    0.0          62925 9E176584
SSW E 0.0    0.001520.002750.0    0.0    0.0          6292510E176584
 SW E 0.0    0.001480.003100.0    0.0    0.0          6292511E176584
WSW E 0.0    0.001370.002600.0    0.0    0.0          6292512E176584
  W E 0.0    0.002880.007580.0    0.0    0.0          6292513E176584
WNW E 0.0    0.002410.007560.0    0.0    0.0          6292514E176584
 NW E 0.0    0.002470.005610.0    0.0    0.0          6292515E176584
NNW E 0.0    0.001660.004400.0    0.0    0.0          6292516E176584
  N F 0.005450.003780.0    0.0    0.0    0.0          62925 1F176584
NNE F 0.004790.003180.0    0.0    0.0    0.0          62925 2F176584
 NE F 0.005170.003130.0    0.0    0.0    0.0          62925 3F176584
ENE F 0.004720.002980.0    0.0    0.0    0.0          62925 4F176584
  E F 0.007800.003120.0    0.0    0.0    0.0          62925 5F176584
ESE F 0.005840.002810.0    0.0    0.0    0.0          62925 6F176584
 SE F 0.006000.002330.0    0.0    0.0    0.0          62925 7F176584
SSE F 0.005990.002890.0    0.0    0.0    0.0          62925 8F176584
  S F 0.007570.003590.0    0.0    0.0    0.0          62925 9F176584
SSW F 0.004210.002120.0    0.0    0.0    0.0          6292510F176584
 SW F 0.003920.002430.0    0.0    0.0    0.0          6292511F176584
WSW F 0.003990.002160.0    0.0    0.0    0.0          6292512F176584
  W F 0.009040.006220.0    0.0    0.0    0.0          6292513F176584
WNW F 0.006990.005420.0    0.0    0.0    0.0          6292514F176584
 NW F 0.006690.005180.0    0.0    0.0    0.0          6292515F176584
NNW F 0.005770.004090.0    0.0    0.0    0.0          6292516F176584
```

# APPENDIX C

## SAMPLE OUTPUT FILES

# SAMPLE STATISTICS FILE (STAT.OUT)

```
FILE CREATED 08/12/86 AT 13:07:46
 PROBABILISTIC ANALYSIS: SAMPLE RUN
 NUMBER OF TRIALS:     5
   PARAMETER  SUBSTANCE  LOCATION  TIME     MEAN      STD DEV    GEOM MEAN   GEOM SD    MINIMUM    MAXIMUM
 1   FT232                                0.642E+00  0.425E-01  0.641E+00  0.107E+01  0.610E+00  0.694E+00
 2   SKDRA                                0.191E+02  0.414E+02  0.508E+00  0.302E+02  0.137E-01  0.931E+02
 3   BURYF                                0.576E+00  0.802E-01  0.572E+00  0.115E+01  0.508E+00  0.665E+00
 4   FPREC                             0  0.126E+03  0.155E+02  0.125E+03  0.113E+01  0.107E+03  0.145E+03
 5   FPREC                            10  0.124E+03  0.207E+02  0.122E+03  0.118E+01  0.102E+03  0.148E+03
 6   FPREC                            20  0.137E+03  0.114E+02  0.137E+03  0.109E+01  0.118E+03  0.145E+03
 7   FPREC                            30  0.121E+03  0.134E+02  0.121E+03  0.111E+01  0.109E+03  0.143E+03
 8   WATC        2          3          0  0.920E+04  0.254E+04  0.892E+04  0.132E+01  0.651E+04  0.124E+05
 9   WATC        2          3         10  0.828E+04  0.309E+04  0.780E+04  0.149E+01  0.437E+04  0.127E+05
10   WATC        2          3         20  0.270E+04  0.489E+04  0.904E+03  0.434E+01  0.350E+03  0.114E+05
11   WATC        2          3         30  0.184E+04  0.318E+04  0.454E+03  0.690E+01  0.759E+02  0.747E+04
12   WATC        3          5          0  0.165E+03  0.201E+02  0.164E+03  0.113E+01  0.139E+03  0.182E+03
13   WATC        3          5         10  0.147E+03  0.181E+02  0.146E+03  0.113E+01  0.130E+03  0.176E+03
14   WATC        3          5         20  0.127E+03  0.255E+02  0.125E+03  0.121E+01  0.106E+03  0.166E+03
15   WATC        3          5         30  0.935E+02  0.161E+02  0.924E+02  0.119E+01  0.735E+02  0.112E+03
16   WATAVG      1          1          0  0.203E+02  0.253E+02  0.130E+02  0.256E+01  0.646E+01  0.654E+02
17   WATAVG      1          1         10  0.338E+02  0.478E+02  0.187E+02  0.298E+01  0.774E+01  0.119E+03
18   WATAVG      1          1         20  0.410E+02  0.592E+02  0.207E+02  0.345E+01  0.524E+01  0.146E+03
19   WATAVG      1          1         30  0.451E+02  0.651E+02  0.232E+02  0.332E+01  0.650E+01  0.161E+03
20   WATAVG      3          1          0  0.149E+03  0.171E+02  0.148E+03  0.112E+01  0.131E+03  0.171E+03
21   WATAVG      3          1         10  0.128E+03  0.135E+02  0.127E+03  0.111E+01  0.114E+03  0.148E+03
22   WATAVG      3          1         20  0.109E+03  0.216E+02  0.107E+03  0.121E+01  0.927E+02  0.143E+03
23   WATAVG      3          1         30  0.806E+02  0.133E+02  0.798E+02  0.118E+01  0.656E+02  0.979E+02
24   MEATD       1          3          0  0.691E-01  0.659E-01  0.433E-01  0.328E+01  0.831E-02  0.175E+00
25   MEATD       1          3         10  0.963E-01  0.767E-01  0.623E-01  0.342E+01  0.931E-02  0.195E+00
26   MEATD       1          3         20  0.117E+00  0.915E-01  0.689E-01  0.428E+01  0.630E-02  0.229E+00
27   MEATD       1          3         30  0.129E+00  0.100E+00  0.773E-01  0.409E+01  0.782E-02  0.250E+00
28   MEATD      11          5          0  0.373E+02  0.296E+02  0.272E+02  0.254E+01  0.103E+02  0.712E+02
29   MEATD      11          5         10  0.326E+02  0.283E+02  0.242E+02  0.238E+01  0.101E+02  0.786E+02
30   MEATD      11          5         20  0.176E+02  0.135E+02  0.134E+02  0.244E+01  0.360E+01  0.390E+02
31   MEATD      11          5         30  0.127E+02  0.986E+01  0.871E+01  0.314E+01  0.135E+01  0.277E+02
```

## SAMPLE KEY FILE (KEY.OUT)

```
FILE CREATED 08/12/86 AT 13:07:48
 PROBABILISTIC ANALYSIS: SAMPLE RUN
 NUMBER OF TRIALS:     5
     PARAMETER  SUBSTANCE  LOCATION  TIME     MEAN      STD DEV    GEOM MEAN   GEOM SD    MINIMUM    MAXIMUM    SKEWNESS   KURTOSIS
  1   DCGWA3                                0.790E+00  0.202E+00  0.773E+00  0.125E+01  0.672E+00  0.115E+01  0.141E+01  0.313E+01
  2   BURYF                                 0.576E+00  0.802E-01  0.572E+00  0.115E+01  0.508E+00  0.665E+00  0.367E+00  0.119E+01
  3   WATAVG        4          1        0   0.306E+02  0.104E+02  0.291E+02  0.141E+01  0.207E+02  0.431E+02  0.196E+00  0.132E+01
  4   WATAVG        4          1       50   0.358E+02  0.783E+01  0.351E+02  0.125E+01  0.277E+02  0.437E+02  0.119E-01  0.125E+01
  5   WATAVG        4          1       90   0.380E+02  0.771E+01  0.374E+02  0.123E+01  0.300E+02  0.473E+02  0.133E+00  0.136E+01
  6   MEATD         1          3        0   0.691E-01  0.659E-01  0.433E-01  0.328E+01  0.831E-02  0.175E+00  0.828E+00  0.237E+01
  7   MEATD         1          3       50   0.132E+00  0.990E-01  0.820E-01  0.398E+01  0.813E-02  0.256E+00  0.197E-01  0.165E+01
  8   MEATD         1          3       90   0.125E+00  0.942E-01  0.797E-01  0.383E+01  0.826E-02  0.262E+00  0.280E+00  0.217E+01
```

## SAMPLE DETAILED RESULTS FILE (RES.OUT)

```
FILE CREATED 08/12/86 AT 13:05:34
 0.115E+01 0.508E+00 0.207E+02 0.277E+02 0.300E+02 0.218E-01 0.707E-01 0.750E-01
 0.679E+00 0.665E+00 0.207E+02 0.282E+02 0.311E+02 0.587E-01 0.125E+00 0.143E+00
 0.672E+00 0.513E+00 0.431E+02 0.435E+02 0.473E+02 0.831E-02 0.813E-02 0.826E-02
 0.752E+00 0.662E+00 0.287E+02 0.356E+02 0.443E+02 0.821E-01 0.201E+00 0.139E+00
 0.703E+00 0.534E+00 0.396E+02 0.437E+02 0.372E+02 0.175E+00 0.256E+00 0.262E+00
```

Note

Columns of detailed results file correspond to rows of key file

# APPENDIX D

## INPUT DISTRIBUTION DESCRIPTIONS

| Variable | Definition | Units |
|---|---|---|
| CODION | Print code for Water source model ions (0,1) | -- |
| CODPH | Print code for Water source model pH (0,1) | -- |
| CODNUC | Print code for Water source model nuclides (0,1) | -- |
| CODREC | Print code for receptor numbers (0,1) | -- |
| CODSL | Print code for soil model (1,2) | -- |
| CODWIN | Print code for SUBROUTINE WIND (1,2,3) | -- |
| CODRAD | Print code for SUBROUTINE RADON (1,2,3) | -- |
| CODAIR | Print code for SUBROUTINE AIRDIS (1,2,3) | -- |
| CODDUS | Print code for SUBROUTINE DUST (1,2,3) | -- |
| CODVEG | Print code for SUBROUTINE VEGCON (1,2,3) | -- |
| CODGS | Print code for groundshine routine (1,2) | -- |
| CODSOL | Print code for groundshine iterative solution (1,2) | -- |
| CODGW | Print code for groundwater (1,2,3) | -- |
| CODWAT | Print code for water models (0,1,2,3,4,6) | -- |
| CODERO | Print code for erosion model (1,2) | -- |
| CODFIS | Print code for fish model (0,1,2) | -- |
| CODWVG | Print code for aquatic vegetation (0,1,2) | -- |
| CODANI | Print code for SUBROUTINE ANIMAL (1,2,3) | -- |
| CODDOS | Print code for SUBROUTINE DOSEIN (1,2,3) | -- |
| PYRITI | Initial Pyrite content of tailings | $mol.m^{-3}$ |
| RHOTAL | Tailings bulk density | $g.m^{-3}$ |
| FRACGP | Initial mass fraction of gypsum in tailings | -- |
| KPRIME | Ratio of $O_2$ half saturation constant to $[O_2]$ | -- |
| SULPRD | Sulphate production rate | $mol.g^{-1}.yr^{-1}$ |
| O2CONC | $O_2$ concentration at the tailings surface | $mol.m^{-3}$ |
| O2DIFF | $O_2$ diffusivity through the tailings | $m^2.yr^{-1}$ |
| DUNSAT | Thickness of the unsaturated zone | m |
| KSUBSO | Solubility constant for $CaSO_4$ | $mol^2.m^{-1}$ |
| FACTCO | Activity coefficient for divalent ions | -- |
| NPRCP | Annual net precipitation | $m.yr^{-1}$ |
| POROS | Tailings porosity | -- |
| DMIX | Thickness of the mixing zone | m |
| AVPRCP | Long term mean annual net precipitation | $m.yr^{-1}$ |
| FNPRCP | Fraction of net precipitation which infilitrates to tailings bottom layer | -- |
| ATAIL | Tailings surface area | $m^2$ |
| XLIME | Initial mass fraction of lime ($CaCO_3$) in tailings | -- |
| PCURAN | Mass % of uranium (as $U_3O_8$) in the ore | -- |
| FURAN | Mass fraction of uranium recovered in the mill | -- |
| FT230 | Fraction of Th-230 assumed to be ultimately soluble | -- |
| FT232 | Fraction of Th-232 assumed to be ultimately soluble | -- |
| FRAD | Fraction of Ra-226 assumed to be ultimately soluble | -- |
| FLEAD | Fraction of Pb-210 assumed to be ultimately soluble | -- |
| FRACU | Fraction of uranium associated with pyrite | -- |
| KDUO2 | Uranium solid-liquid distribution coefficient | $m^3.g$ |
| PCTHOR | Mass % of thorium (as $ThO_2$) in the ore | -- |
| FRACTH | Fraction of $Th(OH)_4$ which is crystalline | -- |
| XRADI | Initial mol fraction of Ra-226 in $BaSO_4$ | -- |
| KSBAR | Solubility constant for $BaSO_4$ | $mol^2.m^{-6}$ |
| KFBAR | Formation constant for $BaSO_4(aq)$ | $m^3.mol^{-1}$ |
| KRAD | Radium distribution coefficient | -- |
| KDRAD | Radium solid-liquid distribution coefficient | $m^3.g^{-1}$ |

| Variable | Definition | Units |
|---|---|---|
| CLEADI | Initial concentration of $PbSO_4$ in tailings | mol.m$^{-3}$ |
| KSLEAD | Solubility constant for $PbSO_4$ | mol$^{2}$.m$^{-6}$ |
| KFLEAD | Formation constant for $PbSO_{4(aq)}$ | m$^{3}$.mol$^{-1}$ |
| KDLEAD | Lead solid-liquid distribution coefficient | m$^{3}$.g$^{-1}$ |
| SKDU | Soil Kd for Uranium | m$^{3}$.kg$^{-1}$ |
| SSKDTH | Soil Kd for Thorium | m$^{3}$.kg$^{-1}$ |
| SKDPB | Soil Kd for Lead | m$^{3}$.kg$^{-1}$ |
| SKDRA | Soil Kd for Radium | m$^{3}$.kg$^{-1}$ |
| FWAT | Fraction of total precipitation that leaches into soil | -- |
| WC1 | Water content of first soil layers | -- |
| WC2 | Water content of subsurface soil layers | -- |
| XLAMU | Decay constant for Uranium | yr$^{-1}$ |
| XLAMTH | Decay constant for Thorium | yr$^{-1}$ |
| XLAMPB | Decay constant for Lead | yr$^{-1}$ |
| XLAMRA | Decay constant for Radium | yr$^{-1}$ |
| DSOIL1 | Depth of soil layer 1 | m |
| DSOIL2 | Depth of soil layer 2 | m |
| DSOIL3 | Depth of soil layer 3 (optional) | m |
| DSOIL4 | Depth of soil layer 4 (optional) | m |
| RHO1 | Soil bulk density for layer 1 | kg.m$^{-3}$ |
| RHO2 | Soil bulk density for layer 2 | kg.m$^{-3}$ |
| LAYER | Number of soil layers | -- |
| MPCH2O | Percent moisture content by weight of tailings | % |
| EMANAT | Radon Emanation coefficient of tailings | -- |
| NSUBW | Number of winter months per year | months |
| WTSFLX | Winter/Summer flux ratio | -- |
| SILT | Silt content of tailings (% of particles < 75 μm) | -- |
| FPREC | Number of days per year with over .25 mm precipitation | -- |
| HSRC | Height of source | m |
| WYEAR | Random variable for selection of wind data | -- |
| EMFRAC | Fraction of Radon emanated from soil | -- |
| XRGWAT | Discharge distance | m |
| AXGWAT | Cross-Sectional area of flow | m$^{2}$ |
| POGWAT | Porosity | m$^{3}$.m$^{-3}$ |
| DCGWA1 | Distribution coefficient for Uranium | m$^{3}$.kg$^{-1}$ |
| DCGWA2 | Distribution coefficient for Thorium | m$^{3}$.kg$^{-1}$ |
| DCGWA3 | Distribution coefficient for Lead | m$^{3}$.kg$^{-1}$ |
| DCGWA4 | Distribution coefficient for Radium | m$^{3}$.kg$^{-1}$ |
| SDGWAT | Soil density | kg.m$^{-3}$ |
| ACTCO | Water activity coefficient | -- |
| WATCAB | Background water concentration of Calcium | mol.m$^{-3}$ |
| WTSO4B | Background water concentration of Sulphate | mol.m$^{-3}$ |
| WSIGS1 | Sediment flux of total solids in first lake | g.m$^{-2}$yr$^{-1}$ |
| WSIGS2 | Sediment flux of total solids in second lake | g.m$^{-2}$yr$^{-1}$ |
| WSIGS3 | Sediment flux of total solids in third lake | g.m$^{-2}$yr$^{-1}$ |
| WSIGS4 | Sediment flux of total solids in fourth lake | g.m$^{-2}$yr$^{-1}$ |
| WSIGS5 | Sediment flux of total solids in fifth lake | g.m$^{-2}$yr$^{-1}$ |
| WTRHOS | Density of stabilized sediment solids in lakes | g.m$^{-3}$ |

| Variable | Definition | Units |
|---|---|---|
| WATEPS | Volume fraction of solids in lake sediment | $cm^3.cm^{-3}$ |
| WTMIXD | Thickness of sediment exchange zone in lakes | m |
| WKDU | Uranium distribution coefficient for lakes | $m^3.g^{-1}$ |
| WKDPB | Lead distribution coefficient for lakes | $m^3.g^{-1}$ |
| WKDRA | Radium distribution coefficient for lakes | $m^3.g^{-1}$ |
| KDPRIM | Relation of Thorium distribution coefficient to pH | -- |
| BURYF | Fraction of sedimenting material buried in lake | -- |
| CURRNT | Current velocity in lake | $m/yr^{-1}$ |
| DIFFC | Diffusivity coefficient for lakes | $m^2/yr^{-1}$ |
| BIOACF | Bioaccumulation factor of Uranium in fish | $m^3.g^{-1}$ |
| BIOACF | Bioaccumulation factor of Thorium in fish | $m^3.g^{-1}$ |
| BIOACF | Bioaccumulation factor of Lead in fish | $m^3.g^{-1}$ |
| BIOACF | Bioaccumulation factor of Radium in fish | $m^3.g^{-1}$ |
| WATVTC | Water vegetation transfer coefficient for Uranium | $m^3.g^{-1}$ |
| WATVTC | Water vegetation transfer coefficient for Thorium | $m^3.g^{-1}$ |
| WATVTC | Water vegetation transfer coefficient for Lead | $m^3.g^{-1}$ |
| WATVTC | Water vegetation transfer coefficient for Radium | $m^3.g^{-1}$ |
| SLOPE | Overall slope of tailings pile | -- |
| THALF | Revegetation half life | years |
| RRAIN | Rainfall erosivity | -- |
| RSOIL | Proportionality constant for bedload transport equation | -- |
| DM | Mean silt diameter | mm |
| STORM | Two year return period storm | ft |
| DEPVEL | Deposition velocity | $m.s^{-1}$ |
| FDEPSF | Fraction of total deposition retained on above ground vegetation | -- |
| FDEPSF | Fraction of total deposition retained on below ground vegetation | -- |
| FDEPSF | Fraction of total deposition retained on summer forage | -- |
| FDEPSF | Fraction of total deposition retained on browse vegetation | -- |
| FDEPSF | Fraction of total deposition retained on lichen | -- |
| FDEPED | Fraction of Foliar deposition retained on edible portions of above ground vegetation | -- |
| FDEPED | Fraction of Foliar deposition retained on edible below ground vegetation | -- |
| FDEPED | Fraction of Foliar deposition retained on edible summer forage | -- |
| FDEPED | Fraction of Foliar deposition retained on edible browse vegetation | -- |
| FDEPED | Fraction of Foliar deposition retained on edible lichen | -- |
| VEGLAM | Decay constant for weathering losses from above ground vegetation | $s^{-1}$ |
| VEGLAM | Decay constant for weathering losses from below ground vegetation | $s^{-1}$ |

| Variable | Definition | Units |
|---|---|---|
| VEGLAM | Decay constant for weathering losses from summer forage | $s^{-1}$ |
| VEGLAM | Decay constant for weathering losses from browse vegetation | $s^{-1}$ |
| VEGLAM | Decay constant for weathering losses from lichen | $s^{-1}$ |
| DUREXP | Duration of exposure to deposition for above ground vegetation | s |
| DUREXP | Duration of exposure to deposition for below ground vegetation | s |
| DUREXP | Duration of exposure to deposition for summer forage | s |
| DUREXP | Duration of exposure to deposition for browse vegetation | s |
| DUREXP | Duration of exposure to deposition for lichen | s |
| YDEN | Yield density (wet) for above ground vegetation | $g.m^{-2}$ |
| YDEN | Yield density (wet) for below ground vegetation | $g.m^{-2}$ |
| YDEN | Yield density (wet) for summer forage | $g.m^{-2}$ |
| YDEN | Yield density (wet) for browse vegetation | $g.m^{-2}$ |
| YDEN | Yield density (wet) for lichen | $g.m^{-2}$ |
| SPTCAV | Soil-to-plant transfer coefficient for above ground vegetation for Uranium | (wet)/(dry) |
| SPTCAV | Soil-to-plant transfer coefficient for above ground vegetation for Thorium | (wet)/(dry) |
| SPTCAV | Soil-to-plant transfer coefficient for above ground vegetation for Lead | (wet)/(dry) |
| SPTCAV | Soil-to-plant transfer coefficient for above ground vegetation for Radium | (wet)/(dry) |
| SPTCBV | Soil-to-plant transfer coefficient for below ground vegetation for Uranium | (wet)/(dry) |
| SPTCBV | Soil-to-plant transfer coefficient for below ground vegetation for Thorium | (wet)/(dry) |
| SPTCBV | Soil-to-plant transfer coefficient for below ground vegetation for Lead | (wet)/(dry) |
| SPTCBV | Soil-to-plant transfer coefficient for below ground vegetation for Radium | (wet)/(dry) |
| SPTCSF | Soil-to-plant transfer coefficient for summer forage for Uranium | (wet)/(dry) |
| SPTCSF | Soil-to-plant transfer coefficient for summer forage for Thorium | (wet)/(dry) |
| SPTCSF | Soil-to-plant transfer coefficient for summer forage for Lead | (wet)/(dry) |
| SPTCSF | Soil-to-plant transfer coefficient for summer forage for Radium | (wet)/(dry) |
| SPTCB | Soil-to-plant transfer coefficient for browse vegetation for Uranium | (wet)/(dry) |
| SPTCB | Soil-to-plant transfer coefficient for browse vegetation for Thorium | (wet)/(dry) |
| SPTCB | Soil-to-plant transfer coefficient for browse vegetation for Lead | (wet)/(dry) |
| SPTCB | Soil-to-plant transfer coefficient for browse vegetation for Radium | (wet)/(dry) |

| Variable | Definition | Units |
|---|---|---|
| SPTCL | Soil-to-plant transfer coefficient for lichen for Uranium | (wet)/(dry) |
| SPTCL | Soil-to-plant transfer coefficient for lichen for Thorium | (wet)/(dry) |
| SPTCL | Soil-to-plant transfer coefficient for lichen for Lead | (wet)/(dry) |
| SPTCL | Soil-to-plant transfer coefficient for lichen for Radium | (wet)/(dry) |
| FIRC | Feed ingestion rate for caribou | g(wet).d$^{-1}$ |
| WIRC | Water ingestion rate for caribou | m$^3$.d$^{-1}$ |
| FAISFC | Fraction of caribou annual intake that is summer forage | -- |
| FAILC | Fraction of caribou annual intake that is lichen | -- |
| FMTCC | Feed-to-meat transfer coefficient for caribou for Uranium | d.g$^{-1}$(wet) |
| FMTCC | Feed-to-meat transfer coefficient for caribou for Thorium | d.g$^{-1}$(wet) |
| FMTCC | Feed-to-meat transfer coefficient for caribou for Lead | d.g$^{-1}$(wet) |
| FMTCC | Feed-to-meat transfer coefficient for caribou for Radium | d.g$^{-1}$(wet) |
| FIRM | Feed ingestion rate for moose | g(wet).d$^{-1}$ |
| WIRM | Water ingestion rate for moose | m$^3$.d$^{-1}$ |
| FAIBM | Fraction of moose annual intake that is browse | -- |
| FMTCM | Feed-to-meat transfer coefficient for moose for for Uranium | d.g$^{-1}$(wet) |
| FMTCM | Feed-to-meat transfer coefficient for moose for for Thorium | d.g$^{-1}$(wet) |
| FMTCM | Feed-to-meat transfer coefficient for moose for for Lead | d.g$^{-1}$(wet) |
| FMTCM | Feed-to-meat transfer coefficient for moose for for Radium | d.g$^{-1}$(wet) |
| EFR | Equilibrium fraction for radon daughter to radon | -- |
| OF | Fraction of year in location (Average) | -- |
| OF | Fraction of year in location (Critical) | -- |
| INOCC | Fraction of time spent indoors (Average) | -- |
| INOCC | Fraction of time spent indoors (Critical) | -- |
| AIRIN | Average annual inhalation rate (Average) | m$^3$yr$^{-1}$ |
| AIRIN | Average annual inhalation rate (Critical) | m$^3$yr$^{-1}$ |
| AFACT | Fraction of activity in above ground vegetation after food preparation | -- |
| AVEGIN | Average annual intake of above ground vegetation (Average) | g(wet).yr$^{-1}$ |
| AVEGIN | Average annual intake of above ground vegetation (Critical) | g(wet).yr$^{-1}$ |
| AFLOC | Fraction of above ground vegetation grown locally (Average) | -- |
| AFLOC | Fraction of above ground vegetation grown locally (Critical) | -- |
| BFACT | Fraction of activity in below ground vegetation after food preparation | -- |

| Variable | Definition | Units |
|---|---|---|
| BVEGIN | Average annual intake of below ground vegetation (Average) | g(wet).$yr^{-1}$ |
| BVEGIN | Average annual intake of below ground vegetation (Critical) | g(wet).$yr^{-1}$ |
| BFLOC | Fraction of below ground vegetation grown locally (Average) | -- |
| BFLOC | Fraction of below ground vegetation grown locally (Critical) | -- |
| CARMIN | Annual intake of caribou meat (Average) | g.$yr^{-1}$ |
| CARMIN | Annual intake of caribou meat (Critical) | g.$yr^{-1}$ |
| CFLOC | Fraction of annual intake of caribou meat that is local (Average) | -- |
| CFLOC | Fraction of annual intake of caribou meat that is local (Critical) | -- |
| MOMIN | Annual intake of moose meat (Average) | g.$yr^{-1}$ |
| MOMIN | Annual intake of moose meat (Critical) | g.$yr^{-1}$ |
| MFLOC | Fraction of annual intake of moose meat that is local (Average) | -- |
| MFLOC | Fraction of annual intake of moose meat that is local (Critical) | -- |
| WATIN | Average annual intake of water (Average) | $m^3$.$yr^{-1}$ |
| WATIN | Average annual intake of water (Critical) | $m^3$.$yr^{-1}$ |
| WFLOC | Fraction of annual water intake that is local (Average) | -- |
| WFLOC | Fraction of annual water intake that is local (Critical) | -- |
| FISHIN | Average annual intake of fish (Average) | g.$yr^{-1}$ |
| FISHIN | Average annual intake of fish (Critical) | g.$yr^{-1}$ |
| FFLOC | Fraction of annual intake of fish that is local (Average) | -- |
| FFLOC | Fraction of annual intake of fish that is local (Critical) | -- |

# Volume

# 5

# NATIONAL
# URANIUM
# TAILINGS
# PROGRAM

Energy, Mines and Resources Canada
Énergie, Mines et Ressources Canada

Canada

# PROBABILISTIC MODEL DEVELOPMENT FOR THE ASSESSMENT OF THE LONG-TERM EFFECTS OF URANIUM MILL TAILINGS IN CANADA - PHASE III

## RESPONSE TO MORG COMMENTS ON PHASE II AND PHASE III DRAFT REPORTS

A Research Report Prepared Under
Contract 0SQ85-00182

for

The National Uranium Tailings Program
Canada Centre for Mineral and Energy Technology
Energy, Mines and Resources Canada
555 Booth Street
Ottawa, Ontario
K1A 0G1

SENES Consultants Limited
499 McNicoll Avenue
Willowdale, Ontario
M2H 2C9

MICROMEDIA

106 pp

April 1987

## ABSTRACT

This report represents part of the ongoing efforts of the National Uranium Tailings Program (NUTP) to develop the capability to predict the long-term effect of Canadian Uranium Mill Tailings. The principal output from these studies has been the development of a comprehensive Uranium Tailings Assessment Program (UTAP). The UTAP program incorporates a Monte Carlo procedure which permits the user to enter input parameters as probability density functions rather than as single numbers and to calculate frequency distributions for output variables. The output distributions can be interpreted as a subjective probability telling us quantitatively what we are entitled to believe about the output variables.

Third party review of the UTAP code during the development stages was actively pursued by the NUTP through participation of the Atomic Energy Control Board (AECB) and NUTP staff in a Modelling Review Group (MORG). During the course of the Phase II and III studies SENES were made aware of various MORG comments. Where appropriate, changes were made to the text of the reports and/or to the UTAP code; however, no specific responses to the MORG questions were prepared. Subsequently, the NUTP decided that it would be appropriate to document the responses to the MORG questions. This report, which was prepared in response to this NUTP direction, has been reviewed and endorsed by the MORG review group, subject to reservations as listed in Appendix A.

---

## NOTICE

This report was prepared by SENES Consultants Limited (SENES) under contract to the National Uranium Tailings Program (NUTP). Neither the NUTP nor SENES makes any warranty, expressed or implied, or assumes any liability with respect to any damage or loss incurred as a result of the use made of the information contained in this publication.

## TABLE OF CONTENTS

Page

1.0 INTRODUCTION 1-1
  1.1 Background 1-1
  1.2 Scope of This Report 1-3
  1.3 References 1-4

REVIEW A - Mr. P.A. Flavelle (16 September 1985) A-1
REVIEW B - Ms. C. Letourneau (26 September 1985) B-1
REVIEW C - Mr. D.E. Connelly (2 October 1985) C-1
REVIEW D - Mr. P.A. Flavelle (9 October 1985) D-1
REVIEW E - Dr. D.J. Martin (3 March 1986) E-1
REVIEW F - Mr. P.A. Flavelle (7 April 1986) F-1
REVIEW G - Mr. P.A. Flavelle (5 June 1986) G-1
REVIEW H - Mr. P.A. Flavelle (24 June 1986) H-1
REVIEW I - Mr. K.R. Shultz (24 June 1986) I-1
REVIEW J - Mr. P.A. Flavelle (24 July 1986) J-1
REVIEW K - Mr. P.A. Flavelle (11 August 1986) K-1

APPENDIX A: MORG Review of the "Draft Response to MORG Comments on Phase II and Phase III Draft Reports."
APPENDIX B: Comments of Volume I and III of UTAP Phase III Model Documentation received after the preparation of the final edition of this report.

# 1.0 INTRODUCTION

## 1.1 Background

In 1982 Energy, Mines and Resources Canada established the National Uranium Tailings Program (NUTP) to pull together previous work on Canadian uranium mill tailings, to fund additional work where significant information gaps were found and to develop the capability to predict the long-term effects of tailings with a known degree of confidence while incorporating variability and uncertainty in the input data. Such evaluations require the use of mathematical models to simulate the behaviour of the real system.

Traditionally, mathematical models have been evaluated in a deterministic fashion. Specifically, this means that a single value is selected for each input parameter of the simulation model(s) resulting in a single estimate of some environmental consequence such as dose to an individual in the critical group, or pH in a downstream lake. However, by their very nature, models are at best imperfect reflections of real systems. Moreover, many of the parameters used as inputs to the models are either imperfectly known or inherently variable. Over the past decade or so considerable effort has been directed at developing techniques for explicitly incorporating such uncertainty (and variability) directly into the model prediction. In general terms we refer to this as probabilistic analysis.

One of the early studies funded by the NUTP demonstrated how probabilistic techniques could be used to take account of the variability and uncertainty in model input parameters in such a simulation analysis (SENES, 1984). A subsequent study (Phase II) extended the system model to incorporate temporal variability (SENES, 1985). The Phase III study, sponsored by the NUTP, further extended the capabilities of the Phase II system model to include spatial variability and applied the new system model to an expanded hypothetical reference site (SENES, 1986).

At the Phase III level of development, the mathematical models are a mix of quite complex component models (e.g. the tailings source term) and simpler aggregate models (e.g. transfer of radionuclides from water to fish flesh). The components are coded as independent modules with information transfer between modules managed by a common control module. This approach provides a flexible structure which can easily accommodate changes in component models and model input parameters. The computer implementation of these models (along with the probabilistic infrastructure) is known as the Uranium Tailings Assessment Program (UTAP).

The Phase III (SENES, 1986) documentation was divided into the following four volumes:

Volume 1: Probabilistic Model Development for the Assessment of Uranium Mill Tailings in Canada - Phase III, Volume 1: Summary Report.

Volume 2: Probabilistic Model Development for the Assessment of Uranium Mill Tailings in Canada - Phase III, Volume 2: System Description and Control Module Documentation.

Volume 3: Probabilistic Model Development for the Assessment of Uranium Mill Tailings in Canada - Phase III, Volume 3: Component Model Documentation.

Volume 4: Probabilistic Model Development for the Assessment of Uranium Mill Tailings in Canada - Phase III, Volume 4: Uranium Tailings Assessment Program (UTAP) User's Manual.

Subsequent to the main Phase III studies a consolidated discussion of the quality assurance activities carried out during Phase III was prepared (SENES, 1987e).

As an aside, it should be noted that there are currently three versions of the UTAP code:

- UTAP.1 the original Phase III code (SENES, 1986), "UTAP", now archived and inactive
- UTAP.2 the original Phase III code as revised based on a comparison of UTAP with AECL's SYVAC code (WNRE, 1987)
- UTAP.3 an updated generic code which reflects the revisions made on the basis of the UTAP/SYVAC intercomparison as well as revisions of a generic nature identified from the application of UTAP to the Lacnor uranium tailings site (for a discussion of UTAP.3 and its application to the Lacnor site refer to SENES, 1987a,b,c and d)

In this report the acronym UTAP refers to UTAP.1 unless otherwise explicitly stated.

The Atomic Energy Control Board (AECB) had been participating in the UTAP studies through the Modelling Review Group (MORG). During the course of the Phase II and III studies SENES was made aware of various of the MORG comments on the Phase II and III UTAP development. Where appropriate changes were made to the text of the reports and/or to the UTAP code; however, no specific responses to the MORG questions were prepared. Subsequently, the NUTP decided that it would be appropriate to document the responses to the MORG questions. This document was prepared in response to this NUTP direction. The draft version of this report was reviewed and accepted by MORG, subject to the reservations documented in the appendices.

## 1.2 Scope of This Report

Altogether, the NUTP provided SENES Consultants Limited with copies of eleven (11) letters from members of the MORG group commenting on the Phase II and III studies. In many instances the MORG comments were editorial in nature and referred to early drafts of the Phase II and III reports. These comments were incorporated where appropriate. In other instances, the comments were of a more technical nature. Responses to these questions form the bulk of this document. The format is simple. For each set of questions (11 in all), each review question or comment is repeated followed by our response. As the questions were forwarded periodically by letter from MORG members to the NUTP the following sections provide questions and responses on a letter by letter basis. One set of comments was received after completion of the review of this report by MORG, and so could not be addressed in this report. These comments have been included as Appendix B.

## 1.3 References

SENES Consultants Limited, 1984. "A Study to Develop and Demonstrate Techniques for the Probabilistic Assessment of the Long-Term Effects of Uraniun Mill Tailings in Canada - Phase I." Research report prepared for the National Uranium Tailings Program, CANMET, EMR, under Supply and Services Canada Contract No. OSQ83-00236.

SENES Consultants Limited, 1985. "Probabilistic Model Development for the Assessment of the Long-Term Effects of Uranium Mill Tailings in Canada - Phase II. Volume 1: Main Report. Volume 2: Workshop Notes and Topical Discussion Papers. Volume 3: Probabalistic Analysis User's Manual and Documentation for the Uranium Tailings Assessment Program (UTAP)." Research report prepared for the National Uranium Tailings Program, CANMET, EMR, under Supply and Services Canada Contract No. OSQ84-00207.

SENES Consultants Limited, 1986. "Probabilistic Model Development for the Assessment of the Long-Term Effects of Uranium Mill Tailings in Canada - Phase III. Volume 1: Summary Report. Volume 2: Uranium Tailings Assessment Program (UTAP): System Description and Control Module Documentation. Volume 3: Uranium Tailings Assessment Program (UTAP) Component Model Documentation. Volume 4: Uranium Tailings Assessment Program (UTAP) User's Manual." Research report prepared for the National Uranium Tailings Program, CANMET, EMR, under Supply and Services Canada Contract No. OSQ85-00182.

SENES Consultants Limited, 1987a. "Uranium Tailings Assessment Program (UTAP.3): Addendum to Volume 2 - System Description and Control Module Documentation." Research report prepared for the National Uranium Tailings Program, CANMET, EMR, under Supply and Services Canada Contract No. 23317-6-1728/01-SQ.

SENES Consultants Limited, 1987b. "Uranium Tailings Assessment Program (UTAP.3): User's Manual." Research report prepared for the National Uranium Tailings Program, CANMET, EMR, under Supply and Services Canada Contract No. 23317-6-1728/01-SQ.

SENES Consultants Limited, 1987c. "Uranium Tailings Assessment Program (UTAP.3): Component Model Documentation." Research report prepared for the National Uranium Tailings Program, CANMET, EMR, under Supply and Services Canada Contract No. 23317-6-1728/01-SQ.

SENES Consultants Limited, 1987d. "Uranium Tailings Assessment Program (UTAP.3): Application to the Lacnor Tailings Site." Research report prepared for the National Uranium Tailings Program, CANMET, EMR, under Supply and Services Canada Contract No. 23317-6-1728/01-SQ.

SENES Consultants Limited, 1987e. "Probabilistic Model Development for the Assessment of the Long-Term Effects of Uranium Mill Tailings in Canada - Phase III. Software Development and Quality Assurance Supplementary Report." Research report prepared for the National Uranium Tailings Program, CANMET, EMR, under Supply and Services Canada Contract No. OSQ85-00182.

Whiteshell Nuclear Research Establishment (WRNE), 1987. Comparison of the UTAP and SYVAC Codes - a report in preparation by WRNE, Atomic Energy Canada Limited, for the National Uranium Tailings Program, CANMET, EMR.

## REVIEW A - MR. P.A. FLAVELLE (16 SEPTEMBER 1985)

**Mr. Flavelle reviewed draft copies of the Phase II User's Manual and Documentation of UTAP.**

His comments were largely editorial in nature and have been incorporated where appropriate.

## REVIEW B - MS. C. LETOURNEAU (26 SEPTEMBER 1985)

Ms. C. Letourneau reviewed Vol. I (questions B-1 to B-3) and Vol. III, App. F (questions B-4 to B-7) of the Phase II documentation.

---

**B-1 One of the objectives of Phase II was to include additional radionuclides in the modelling (p. 1-3). However, I do not see any evidence which confirms that the doses reported in this study take into account radionuclides other than radium and radon (see Table F-1). If other radionuclides were considered in this phase, what were they; if they were not, why weren't they?**

During Phase II, thorium was added to the water source term only. The addition of other radionuclides was left for subsequent incorporation in Phase III of the model development program.

---

**B-2 For Phase III, SENES will study the spatial distribution of effects arising from the tailings site and that modelling up to 50 km would be considered (p. 6-3 last sentence). I suggest that modelling should also consider the distance from the actual tailings up to 2 km (which was the distance used for Phase II). In a contract study done for the AECB, the dose which an individual could receive by living on the uranium tailings, could reach several hundreds of mSv/a. In the present SENES study, for an individual residing 2 km away from the tailings, the highest dose reached was for scenario 3 (Pyrite removal and limestone addition) at t = 100 a and was approximately 0.1 mSv/a. It would be worthwhile to estimate the spatial distribution of dose between the tailings themselves (approximately 500 mSv/a based on an AECB contract study (?)) to 2 km away (approximately 0.1 mSv/a based on the SENES study (?)).**

The Gaussian dispersion model used in UTAP is quite standard and has been widely used in both environmental and regulatory settings. The actual source correction converts the basic point source model to an area source model. For most purposes the assumption of an effective circular area source is satisfactory. However, the model should not be used to calculate air concentrations on the tailings itself or very close to the edge of the tailings. The model is considered reasonable for distances as short as 500 m from the tailings. The limit of 1 km noted in the code description was intended to act as a cautionary flag rather than an absolute limit. This restriction was consistent with the terms of reference for the UTAP study. If desired, the existing model could be used, without change, to predict air concentrations at distances beyond about 0.5 km from the tailings.

The distance out from the tailings source can be divided into five rings thus permitting air concentrations to be calculated in five sector areas in each of 16 directions from the site. The calculated air concentration in each sector area, for example, is an average value calculated for the mid-point distance of the sector from the site. Thus, if the distance of the first two rings are 1 km and 3 km from the tailings area, then the area concentration is calculated for the 2 km distance.

With respect to the point raised about the dose received by an intruder, it was established at the outset that the UTAP code would not consider this type of situation. The dose received by an intruder represents a special situation which requires a different model from that developed to model the dose to an off-site receptor and was beyond the scope of the UTAP study. The implications of episodic type events including the dose received by an intruder, and the methodology for assessing the dose consequences to receptors were addressed in a two-phase risk assessment study undertaken by SENES for the NUTP (SENES Consultants Limited, 1985. "Approaches to Risk Assessment for Canadian Uranium Mill Tailings." Research report prepared for the National Uranium Tailiings Program, CANMET, EMR, under Supply and Services Canada Contract No. 0SQ84-00335) and (SENES Consultants Limited, 1986. "Approaches to Risk Assessment for Canadian Uranium Mill Tailings. Phase II." Research report prepared for the National Uranium Tailings Program, CANMET, EMR, under Supply and Services Canada Contract No. 0SQ85-00225).

**B-3 Besides determining the most sensitive parameters in the model, the sensitivity analysis would also determine a possible range of doses resulting from the variation in the parameters; thus "variation bars" should be drawn on Figure 4.22.**

The sensitivity analysis does not determine a possible range of doses resulting from the variation in the parameters. The sensitivity analysis is designed specifically to investigate the magnitude in the change of the model response to a defined change in each possibly important parameter. In addition, uncertainty bars which can be generated by running the model are only applicable at any one point in time. It would be inappropriate to infer confidence bands on the dose vs. time curves such as Figure 4.22, although variance bars about the mean values at specific points on the curves could be shown.

**B-4 Why were parameters allowed to vary only from 10 to 50% (p. F-1)? Several environmental parameters tend to vary by several times the mean value. The parameters should, in a first computer run, be allowed to vary from the minimum value to the maximum value. After studying the initial results, a more limited variation may be considered for future runs.**

The range of values assigned to the parameters were assessed on their own merits in each case. Those environmental parameters which would reasonably be expected to range over orders of magnitude for a particular scenario were allowed to do so, if justified by the data base. However, many of the parameters could not be varied in this manner, for example the fraction of total deposition retained by a plant surface, as they were expressed as some fraction of other parameters. Such parameters were assigned distributions based on experience and available information. The 10 to 50% values were only quoted as a typical example of the approach taken by the modellers.

**B-5 Why has SENES decided not to vary the food intake parameters (p. F-1)? These may vary and the variations should be taken into account especially when considering an individual in a critical group who does not represent the "typical male Ontario resident" (e.g. Indian reservation, leisure fishermen and huntsmen).**

In Phase II, the focus was not on the development of parameter distributions - rather it was on model and system development. The generic scenario defined for Phase II was specifically constructed to investigate the dose to an average receptor (or critical receptor) with specified characteristics. The purpose of the generic runs was to give the user an understanding of the potential of the model and how to adapt that model, including all of the parameters, for their particular situation. We feel that it is important to emphasize that it is not always practical nor necessarily desirable, to account for all possible model applications in the selection of parameter values chosen to develop the models themselves.

**B-6 The simple equations presented in this appendix are satisfactory for this phase. However, since these were pulled from the USNRC, concepts such as "whole body dose" are encountered in the SENES report; as you know, ICRP has recommended (Publication 26, 1977) the "dose equivalent" concept which renders obsolete the "whole body dose" concept. As you also know, the AECB has agreed to endorse the new concept, therefore I suggest that this appendix be reviewed to take into account the Canadian view. Furthermore, consideration should be given to using a Canadian reference for the equations (such as CSA N288.1 guidelines on dose calculations) rather than quoting the USNRC.**

The ICRP dose equivalent was used throughout. CSA N288.1 has not yet been formally issued and so would not be as appropriate to reference as the USNRC publications.

**B-7 In Volume I (Main Report), it was suggested that further pathways be added to the model. Additional pathways that should be considered are (but are not limited to):**

**i) exposure from direct radiation**
**ii) outdoor radon inhalation**
**iii) radon emanation from shower water in dwelling**
**iv) radon emanation from dish water in dwelling**
**v) immersion from swimming in creek water.**

**A justification should be presented for any omission of pathways judged to be insignificant.**

From the outset, the primary objective of the modelling studies was to develop a probabilistic framework for carrying out an assessment of the long-term effects of uranium tailings. Emphasis was placed on developing a flexible, modular tool which could be easily modified or expanded in the future to model situations not accounted for during the development phase. A decision was made to include only those pathways which had been shown to be potentially important in previous assessment studies. It was recognized that if every conceivable pathway was included, the code would soon become unnecessarily unwieldy. Accordingly, only the principal air and water pathways have been included. Even so, the results of model simulations for a hypothetical, sulphidic tailings area have shown that there are several orders of magnitude difference in the doses for the pathways considered. Indeed, the dose contributions from several pathways, for example groundshine and vegetable consumption, have been shown to contribute very little to the total dose in any of the scenarios modelled to date. We recommend that any decision to include additional pathways in future applications should first be investigated and justified rather than arbitrarily adding new pathways to the code.

## REVIEW C - Mr. D.E. CONNELLY (2 OCTOBER 1985)

Mr. Connelly reviewed Vol. I, Section 3.4 (Quality Assurance Concepcs) (question C-1) and the User's Manual and Documentation (question C-2) for the Phase II studies.

C-1 Reference: Page 3-5, para. 3.4 Quality Assurance Concepts

The QA aspects that have been described in para. 3.4 are from the viewpoint of the design and development staff.

i.e. they view the software Verification & Validation activities as the whole "QA program" (as far as they are concerned) whereas from a QA viewpoint, Verification & Validation are only particular elements of a software development methodology.

In addition to describing the QA program as outlined below, a separate section describing the software development process should be inserted.
- for example:
  para. 3.4 Software Development Method
  para. 3.5 Quality Assurance Program

Rather than describing "QA Concepts", the actual QA program (if it existed) should be specifically described:
- for example, a QA program description should cover such items as:
  - organizational and reporting relationships of the QA monitoring.
  - specific QA activities performed.
  - QA monitoring and auditing points with respect to the specific software development phases.
  - involvement of the QA representative in design reviews.
  - monitoring of the documentation and disposition of deficiencies.
  - QA criteria for determining that the software has met the specified requirements.

**Paragraph 3.4, although implying that a QA program was implemented, currently suggests the opposite to a reader familiar with QA. That is, no formal QA activities were actually carried out.**

**If so, then the report should state this explicitly, since trying to imply a stronger QA program than actually existed, reduces the credibility of the report further than if a candid and accurate statement was made concerning the difficulties encountered in implementing a formal QA program.**

**(Section 6.0 - Quality Assurance of the Probabilistic Analysis User's Manual and Documentation" volume should also be written to take into account the preceding comments).**

The comments noted above were taken into consideration in the preparation of a separate Quality Assurance document which was prepared subsequent to the Phase III study (SENES, 1987c). This report addresses the Quality Assurance program followed during code development and presents examples where appropriate.

**C-2 Probabilistic Analysis User's Manual and Documentation for the Uranium Tailings Analysis Program.**

**Reference: Figure 3.2 - Example of an Arbitrary Distribution.**

**The vertical axis of this distribution is labelled as "frequency" but the units range from 0 to 0.5.**

**Perhaps this figure is intended to show a probability density function (although the area under the curve would not satisfy the condition for a probability density function).**

Figure 3.2 of Volume 3 of the Phase II report showed an example of an arbitrary distribution. The vertical axis is labelled as "Probability" and the units range from 0 to 0.5. There are four cells shown with probabilities of 0.15, 0.3, 0.4, and 0.15 yielding a total probability of 1.0.

## REVIEW D - MR. P.A. FLAVELLE (9 OCTOBER 1985)

**Mr. Flavelle reviewed Vol. 1 (questions D-1 to D-25) and Vol. III, Appendix A (questions D-26 to D-28), Appendix B (question D-29), and Appendix G (questions D-30 to D-32). Mr. Flavelle had no comments or questions on Appendices C, D, E and F.**

**D-1 Page 1-1, Section 1.0, paragraph 1**

**The reference SENES (1984) is not in the list of references.**

This has been corrected.

**D-2 Page 2-5, Section 2.2, paragraph 2**

**Were the occupancy factor and fraction of food produced locally treated as variables (randomly sampled for each year of a simulation) or as parameters (held constant at a randomly-sampled value during each simulation)?**

The occupancy factor and fraction of food produced locally were sampled once at the beginning of each trial like most other parameters in the code. Only specific parameters which vary naturally from year to year (e.g. mean annual windspeed and precipitation) were sampled each time step during each trial. Each probabilistic simulation comprised several trials, hence all parameters were sampled several times.

**D-3 Page 2-15, Section 2.5, paragraph 2**

**What becomes of the 25% of the tailings removed by bulk flotation? Shouldn't this material be explicitly included in the simulation of the tailings disposal?**

It is assumed that pyrite and associated gangue removed by bulk flotation would be disposed by appropriate means (for example underground in worked out mining areas) to minimize releases to the environment. Since the bulk float would surely not be added back to a tailings disposal area, it would be inappropriate to attempt to model releases from the concentrate using the Uranium Tailings Assessment Program (UTAP) which was specifically designed to simulate releases from conventional disposal sites. It would be appropriate, of course, to include releases from the bulk float disposal facility in an overall site assessment. However, it was agreed that this aspect was not part of the UTAP development program.

**D-4 Page 2-18, Section 2.6, point 2a)**

**This development of the statistical properties of the sampling distributions is not explained clearly. The first relationship seems trivial, and perhaps should read $E(\overline{w}) = \mu$. The meaning of Var $(\overline{w})$ is not explained. There is no explanation why the variance for sampling yearly is expected to be $\sigma_w^2$ while the variance for sampling every 10 years is $\sigma_w^2/n$. Why is the standard error used to describe the sampling distribution of the mean, when the variance is used to describe the previous distributions?**

The discussion of the statistical properties of the sampling distributions has been modified in the final version of the Phase II report and, hopefully, is clearer. The discussion pertains to the procedure used to modify the attributes of the distributions specified for time-varying parameters to account for the size of the time step or time increment. For example, the dispersion of the parameter values about the mean is quite different if the size of the time step is one year versus ten years. Indeed, one would expect the probability density function of mean annual values to be much broader than the probability density function for ten year mean values. The dispersion of the two functions is characterized by the variance of the distributions. The variance of the distribution for a time step of n years is related to the variance of the distribution of annual values by the relationship:

$$\mathrm{Var}\,(\bar{w}) = \sigma_w^2/n$$

This relationship is used in the code to modify the attributes of the distribution to account for the size of the time step chosen for any particular simulation. The rationale for such an adjustment is that because they vary from one sample to the next, sample statistics such as the mean and the variance are themselves random variables. The distribution of the sample mean has a further very important property; namely, that as a consequence of the Central Limit Theorem, as the sample size becomes larger the form of the distribution of the sample mean (e.g. mean annual windspeed) approaches the normal distribution.

**D-5 Page 2-21, Section 2.7.1, paragraph 1**

**The relationship defining the sensitivity index (SI) will not allow the SI to be negative, as is claimed later in the paragraph. The relationship would probably be:**

$$\mathbf{SI = 1 - \frac{result\ from\ low\ input\ value}{result\ from\ high\ input\ value}}\ .$$

The relationship given above was in error in the draft report. The correct relationship is:

$$SI = 1 - \frac{\text{low calculated result}}{\text{high calculated result}}$$

This number would always be positive. The sign (or influence) is added artificially, apart from the calculation. It indicates whether the response varies in direct or inverse proportion to changes in parameter values (i.e. whether the low or high input parameter value produces the low (or high) calculated result).

---

**D-6 Page 2-21, Section 2.7.1, paragraph 3**

**That the SI was found to be applicable to all of the Phase II modelling indicates that the model responds linearly and monotonically to each of the input parameters when all other parameters are held constant at their nominal value. This may be the result of the simplifications used in the modelling, and may not necessarily reflect reality.**

We do not concur with the conclusion drawn by the reviewer. Our experience on several applications is that the sensitivity index (SI) produces results which are comparable to those obtained using regression techniques. The SI method was found to apply to the UTAP code, which contains quite complex, non-linear models describing the behaviour of the tailings source term and dispersion in the environment. Notwithstanding this observation, we recommend that one should not rely solely on any one particular method but rather should use all reasonably available tools in analyzing the "importance" of model pathways and parameters.

---

**D-7 Page 4-3, Section 4.2, paragraph 2**

**The technical rigor of the development of the probabilistic assessment should also be consistent with the rigor of the calculations performed by the computer model and the validity of the data employed in the computer model. In this case, it is.**

No comment required.

---

**D-8 Page 4-4, Section 4.2.1, paragraph 2, last sentence**

**The levels of radium in the porewater leaving the unsaturated zone will decrease after the gypsum is depleted from the unsaturated zone, but the radium levels in the porewater in the saturated zone will still be related to the gypsum solubility, until all of the gypsum has been**

**depleted from the tailings mass.**

The radium level in the porewater in the saturated zone is controlled by three factors after gypsum is depleted from the unsaturated zone: 1) the input to the saturated zone of radium associated with thorium-230 which partially dissolves in the unsaturated zone under acidic conditions; 2) the dissolution of gypsum in the saturated zone which does not begin to dissolve until after the gypsum inventory is depleted from the unsaturated zone; and 3) $K_d$, a distribution coefficient control mechanism which accounts for radium sorption on solid particles and chemical precipitates formed under reducing conditions in the saturated zone. The relative importance of these three factors varies as a function of time.

**D-9 Page 4-5, Section 4.2.1, paragraph 3**

**The initial low pH of the lake (4.0) should be explained. How does this compare to the initial low pH of the tailings porewater? If the fast pyrite oxidation over the first 100-200 years keeps the pH of the tailings porewater low, why does the pH of the lake begin to rise immediately?**

In the UTAP code, the tailings and environs are initialized by stepping through one time step to reflect, in part, the fact that the environs have been affected for a period of time during placement of the tailings. In other words, the system being modelled does not start from pristine conditions at the start of the model simulation. The receiving water pH value of about 4.0 at time t=0 reflects the effect of acid discharge from the tailings area over this initialization time step.

The pH of the tailings porewater and the receiving waters continues to be influenced mainly by the acidity produced from pyrite oxidation over the first 100 to 200 years. However, the rate of pyrite oxidation is modelled as decreasing continuously with time from t=0 years onwards due to a gradual depletion in the pyrite inventory. Hence the pH shows a gradual increase with time starting from a low at t=0 years both in the tailings area and in the receiving environment.

**D-10 Fig. 4.4 (and all other sets of histograms)**

**These histograms should be shown with the same cell size in order to compare results.**

While it is sometimes desirable to maintain the same cell size on all histograms, the range of the dose scales are so different that much of the detail would be lost if the same scale was used on all plots. For this reason and because the plotting package used had restricted flexibility, the histograms were plotted using different horizontal and vertical scales.

**D-11 Fig. 4.7**

**The distribution of uncertainty in the total annual dose is very similar to the distribution of uncertainty in the lake pH, Fig. 4.3. Is there a correlation?**

Yes, it would appear that there is a correlation in the shapes of the uncertainty envelopes shown for pH on Figure 4.3 and for total annual dose on Figure 4.7. The widening of the uncertainty envelope about the pH curve between year 50 and year 300 reflects the difference in the time to achieve essentially complete pyrite oxidation, or conversely to attain pH recovery, between probabilistic trials. The narrow envelope between years 0 and 50 reflects the fact that there must be a large change in acid production to substantially lower the pH value below 4.0. Beyond year 250 the envelope is also narrow which reflects the fact that most of the pyrite has been oxidized by this point in time. The widening of the total annual dose curve between years 50 and 300 is attributable to an increase in the amount of gypsum which dissolves. Because the amount of gypsum (and associated radium) brought into solution during any time step is a function of the sulphate concentration in the tailings porewater, the radium concentration (and hence dose) is inversely related to the rate of pyrite oxidation. It follows therefore that the shapes of Figures 4.3 and 4.7 are related.

---

**D-12 Page 4-9, Section 4.2.3, paragraph 1**

**Why the 100 year delay in the importance of the water and fish pathways? Is this due to the transit time of tailings porewater to surface water at the receptor, or to the time for depletion of gypsum in the unsaturated zone, or to some other time varying process?**

The question posed above appears to relate more to Section 4.2.1 (Overall Evaluation) of the report than Section 4.2.3. (Scenario 1 Importance Analysis: Total Dose). Hence, we have responded to the question in two parts.

With respect to the discussion in Section 4.2.1 pertaining to the time behaviour of dose from the six pathways examined in Phase II, it is noted that the dose from radon inhalation is the largest contributor to total dose over the initial 40 years or so. Thereafter, the dose from consumption of drinking water is the largest contributor to total dose, at least over the 500 year simulation period presented on Figure 4.2. The dose from consumption of contaminated game fish is the second or third largest contributor to total dose depending upon the point in time being considered. The gradual increase in the curves for water dose and fish dose over the initial 150 or so years is related to the rate at which gypsum dissolves in the tailings as the soluble radium-226 fraction is assumed to exist as a coprecipitate with gypsum. The amount of gypsum which dissolves in any time step is determined by the solubility product of $CaSO_4$ and the amount of sulphate product from pyrite oxidation. The sulphate created from pyrite oxidation is predicted to decrease continuously from time $t = 0$ years onward as it is modelled as a function of the mass of pyrite remaining at any point in time. Hence, the amount of gypsum which dissolves increases continuously until such time as the pyrite has been essentially completely oxidized. The Phase II model results indicated that pyrite oxidation was essentially complete by year 150.

Once the gypsum inventory has been completely leached from the tailings, the radium-226 concentration in the tailings source discharge would be expected to drop rapidly. The shape of (i.e. gradual decline) in the water and fish dose curves on Figure 4.2 may be attributed largely to two factors: 1) the curves are plots of the geometric mean values of 500 individual trials and therefore represent the averaging effect of many curves; and 2) the radium level in the receiving water environment is influenced by feedback from the bottom sediments.

The behaviour of the radon-222 dose curve is also related to the behaviour of the radium-226 dose curve on Figure 4.2. Radium-226 is the parent of radon-222 hence the amount of radon-222 released from the tailings surface is a function of the residual radium-226 content. As the soluble radium-226 fraction is progressively leached from the unsaturated tailings (i.e. the upper tailings layer), the radon-222 levels gradually decline in direct response to the decrease in radium-226 activity in the upper tailings horizon.

It should be noted that the importance analysis discussed in Section 4.2.3 applies to an examination of the importance of the model parameters and not the pathways. As one might expect, parameters associated with the water and fish pathways comprised most of the top ranked parameters. At time t=0 years, 8 of the 12 top-ranked parameters were associated with the water source model, the water dispersion model or the fish transfer model (see Table 4.1). At time t=200 years, 9 of the 12 top-ranked parameters were tied to either the water source model, water dispersion model or the fish transfer model (see Table 4.2). The top-ranked parameter at both time periods was the water-to-fish transfer factor. The other top ranked parameters relate to the radon pathway.

---

**D-13 Table 4.3**

**It is not surprising that the ten least important parameters all relate to meat ingestion, dust inhalation or vegetation ingestion, as these three pathways contribute the least to the annual dose rate, according to**

**this modelling.**

Agreed! The importance of the parameter relates to the contribution of the individual pathway to the total dose.

---

**D-14 Page 4-10, Section 4.2.4, last paragraph**

**It is not clear why the sulphate production rate is input as an independent variable, instead of being calculated as a function of $O_2$ concentration, moisture content, etc.**

The sulphate production rate ($\bar{R}_s$) is input as an independent variable, together with several other parameters, to an expression for calculating the sulphate flux ($J_s$) resulting from pyrite oxidation (see equation (3.12), page A-12, Volume 3). The range of values input for the sulphate production rate encompasses the variation which is expected for average annual conditions encountered in the field (i.e. the range accounts for the influence of temperature, pH and moisture content). The limitation imposed by the oxygen flux into the tailings mass is accounted for explicitly in equation (3.12) (see page A-12, Volume 3). Hence, the sulphate flux is calculated as a function of the oxygen concentration. The influence of all other factors is taken into account when defining the distribution of values for input parameter $\bar{R}_s$.

---

**D-15 Page 4-12, Section 4.3.1, paragraph 2**

**Figure 4.13 cannot be interpreted because of the histogram cell size and the plotting scale. All histograms should be displayed with identical scales in order to compare them.**

Figure 4.13 shows that nearly all of the predicted doses fell in the three bins on the extreme left. The reason that the scale selected for this figure covers such a wide range is because there was one high predicted value. We had no choice, therefore, but to use the scale presented on the figure. This is a good example of why it is not practical to select a single scale on which to plot all histograms, especially if the dose predictions vary substantially from scenario to scenario. Contrary to the statement made above, we believe that the results can be interpreted. It is more a matter that the plot does not demonstrate the multiple binning shown on other histograms.

---

**D-16 Page 4-13, Section 4.3.1, paragraph 1, last 2 sentences**

**I strongly agree that the results of different scenarios must be analysed separately.**

The significance of this point cannot be over-emphasized.

---

**D-17 Page 4-15, Section 4.4.1, paragraph 2**

**The calcium common ion effect on the gypsum solubility has been ignored. This invalidates all results and conclusions for scenarios involving limestone addition.**

No, the calcium common ion effect on gypsum solubility was not ignored (see section 8.2, page A-32, Volume 3). This effect is an additional factor which influences the dissolution of the calcium/radium sulphate coprecipitate and is accounted for in the model. The other factors discussed in Volume 2 are the effect of a reduced initial pyrite content in the tailings and the effect of a lower rate of pyrite oxidation and hence lower sulphate concentration in the tailings porewater.

---

**D-18 Page 4-16, Section 4.4.1, paragraph 1**

**Are these doses only from Ra and Rn, or are other radionuclides included? Are the effects of increased carbonate/bicarbonate concentrations on the mobility of the radionuclides (particularly U) included in these calculations?**

The only radionuclides explicitly included in the calculation of dose in Phase II were radium-226 and radon-222. A subroutine was also incorporated in the tailings source term component to model thorium. Otherwise the incorporation of other radionuclides in the UTAP code was identified as an objective for the next phase of UTAP development (i.e. Phase III).

The presence of carbonate or bicarbonate ions have not been shown to influence the mobility of either radium or radon to our knowledge. Therefore, they have not been taken into account in the calculations.

---

**D-19 Page 5-5, Section 5.1, paragraph 4, last sentence**

> **As no model inputs were correlated, the capability of the model to explicitly handle parameter correlations has not been demonstrated.**

The ability of the model to handle correlated parameters has been demonstrated using the radon source term model. The documentation for this aspect is presented in Appendix I of Volume 2 of the Phase III study (SENES Consultants Limited, 1986. "Probabilistic Model Development for the Assessment of the Long-Term Effects of Uranium Mill Tailings in Canada - Phase III. Volume 2 - Uranium Tailings Assessment Program (UTAP: System Description and Control Module Documentation." Research Report Prepared for the National Uranium Tailings Program, CANMET, EMR). The work described in Phase II laid the ground work for the more in-depth assessment undertaken in Phase III.

---

**D-20 Page 5-7, Section 5.2, paragraph 1**

> **The code-to-code comparison described here was not a field validation, so the aggregate model does not "predict adequately the dynamic behaviour of the lake". What it does do is "reproduce adequately the predictions of lake dynamics made by the multi-component model".**

The discussion in Section 5.2 does not make any reference to field validation, nor for that matter to field calibration. The discussion relates solely to a comparison of the predictive capability of an aggregate model versus a more detailed multi-variate model. The latter model was developed to predict the dynamic behaviour of a lake. The conclusion drawn was that the simple aggregate model was found to "predict adequately the dynamic behaviour of the lake". This statement does not imply that the simple aggregate model adequately predicts the radium levels in the lake water, sediment and fish components. Similarly, the statement does not imply that the multi-variate model adequately predicts the radium levels in the lake ecosystem. Indeed, it may be that neither model is adequate in all, or any, situations. Confirmation of the adequacy of the models would require validation against actual field data.

---

**D-21 Page 5-7 Section 5.2, paragraph 2**

> **"The most complex model has the largest uncertainty." This is because the most complex model has more parameters, each of which introduces uncertainty. This is the paradox of uncertainty in modelling. The more detailed a model becomes to more accurately simulate reality, the greater the number of parameters and variables which add to the uncertainty of the model results. Does this mean the simpler models are the better? It could, if it is demonstrated that the accuracy of the simpler model does not suffer as a result of not including explicitly all of the relevant processes.**

The argument that more complex models will introduce greater uncertainty because they have more parameters is very often true but is not necessarily true. If one had an extensive data base to use in evaluating the distributions in the parameter values and fully comprehended the correlations between parameters, then it would be expected that the uncertainty in the complex model results would be the same as in the aggregate model. The fact that a more complex model often will show greater uncertainty in the predicted results is more likely a reflection that the developer was overly conservative in describing the uncertainty in the individual input parameters and did not account for correlations between some parameters. The question of whether or not the simpler aggregate model might be better in this instance is one for which there is no easy answer. The ultimate test would be to compare predictions using the two types of models to actual field measurements under different conditions.

---

**D-22 Page 5-7, Section 5.2, paragraph 3, last sentence**

**The statement that parameter correlations are implicit in aggregate models needs to be explained. I would have thought that they are ignored.**

The point which we attempted to make here is that in aggregate models, each parameter represents the effects of multiple processes or factors. The correlation which may exist between these processes or factors presumably is reflected in the distribution of values used to describe the aggregate parameter. In the complex model, however, it is likely that correlations between some of the parameters were not accounted for due to a lack of knowledge or to insufficient data to distinguish the correlations. If one uses the same data base to evaluate the values for the parameters in the aggregate and complex models, then it follows that parameter correlations would be implicitly accounted for in the aggregate model but not necessarily so in the detailed model.

---

**D-23 Page 5-8, Section 5.2, paragraph 1, last sentence**

**The realism of an aggregate model (accuracy of prediction and accuracy of the model's sensitivity to input parameter variation) plays an important part in deciding when to abandon a detailed model. If the detailed model is discarded too early in a study, important processes and parameter correlations could be missed, making the results of the aggregate model unacceptably inaccurate.**

If the aggregate model is found to adequately represent the situation being modelled then it is unlikely that the model would later be found to be inadequate. On the other hand, if the scenario changes substantially then it is possible that the simple model would no longer be adequate. This situation could presumably be tested beforehand, by comparing results for the simple and detailed models for a range of input parameter values to establish the conditions under which the simple model provides acceptable results.

---

**D-24 Page 5-10, Section 5.3, paragraph 3**

> **This says that sensitivity and uncertainty studies are difficult to do because of the complications of the time-varying inputs, so the time variation was removed from the input data. In other words, the sensitivity/uncertainty analysis was done on a time-independent set of inputs, and the time-dependent behaviour had no sensitivity/uncertainty analysis done.**

The reviewer had misinterpreted the essence of the discussion regarding time-variant parameters (i.e. parameters which actually vary from year to year). First, it should be borne in mind that there are only a limited number of parameters which are treated as time-variant inputs in the UTAP code, notably, mean annual precipitation and mean annual wind speed. While one can conceive of other parameters which could be treated as time-variant inputs, the list of parameters which actually vary with time is short. In most cases, the uncertainty in parameter values is due to a lack of knowledge of what the actual value should be or a lack of understanding of the fundamental processes which affect the parameter. As with the time-variant parameters, the uncertainty in the parameter estimates can be included in a probabilistic assessment by specifying probability density functions for the input parameters. The only difference in the treatment of time-variant and non-time-variant parameters is that the former are sampled each time step over the duration of each simulation trial while the latter are sampled only once at the beginning of each trial. Time-variant parameters can also be treated as non-time-variant parameters in a model simulation as for example by setting them equal to their long-term mean value. The output curves in either case would be very similar. When all parameters are treated as non-time-variant, the output curve for each trial evolves smoothly with time. When time-variant parameters are sampled each time step, the output curve for each trial evolves in a similar manner as in the previous case with the exception that each curve shows a jagged response with time. The decision on whether or not to treat certain parameters as time-variant depends on the questions being asked by the user.

Regardless of how time-variant parameters are treated, the model response evolves with time. The output results reflect the time-dependent behaviour of the system being analyzed. Hence, the sensitivity/uncertainty analysis discussed in the UTAP Phase III report was carried out on the time-dependent model response. The point discussed in Section 5.3 is that the analysis was carried out on model runs in which the time-variant parameters were treated as if they were non-time-variant, but uncertain, input parameters. As noted in the discussion, the interpretation of a regression analysis on a data file containing time-variant input values is unclear. The conclusion, drawn from a regression analysis on a data file containing only non-time-variant inputs are straightforward.

---

**D-25 Page 6-4, Section 6.2, fourth point**

> **I agree very strongly with this recommendation, that:**
>
> **the models must be reviewed (i.e. they are not yet complete);**
> **the models must be developed for specific application;**
> **and not all models are appropriate for all applications.**

No comment required.

---

**D-26 Page A-2, Section 2.0**

> **Typically the mole fraction (denoted X by convention) is the fraction of the mass of one aqueous species (in moles) to the total mass of aqueous species (in moles). The use of mole fraction and the conventional symbol for mole fraction is inconsistent in this appendix (for example $X_{Ra/Th}$,**

$X^{\circ}_{Ra/gyp}$, $X_{Th/Th}$) and each unique definition must be borne in mind when using this appendix.

The definition given above for mole fraction is correct as it applies to aqueous chemistry. The usage of this term has indeed been redefined in Appendix A for application to the solid-phase as well as liquid-phase components.

---

**D-27 Page A-3, Equation 3.17**

**The brackets around the square root argument are missing.**

Noted.

---

**D-28 Page A-17, bottom of page**

**There is either a missing equation or the term "t + t" is a misprint.**

Yes, there is a missing Δ symbol in the term which should read: t+Δt.

---

**D-29 Appendix B, Page 1, paragraph 1, last sentence**

**There is a spelling error in "reflect" (the f is missing).**

Noted.

---

**D-30 Appendix G, Page 2, Section 1, paragraph 2, last sentence**

**The use of retardation factors is not, per se, conservative. Not using retardation factors (to ignore retardation processes) or selecting lower retardation factors (to over-estimate contaminant mobility) would be conservative.**

Agreed, the word "conservative" has been dropped from the discussion of retardation factors.

**D-31 Page 18, Section 5, paragraph 1**

**Uncertainty in hydraulic gradients is due to more than measurement or extrapolation errors, but also to the stochastic nature of the factors which control the hydraulic gradient. While the errors in measurement and extrapolation may be assumed to be normally distributed, stochastic variations in the gradient (which may be much larger than measurement errors) may not be normally distributed.**

Yes, uncertainty in hydraulic gradients is due to more than measurement or extrapolation errors. However, we have made the assumption that the aquifer is isotropic and homogeneous. This assumption applies to each individual simulation. The input parameter distributions can be used to account for the range of parameter values which might be anticipated at a particular site (i.e. stochastic variability) in addition to measurement uncertainty which is always included in the parameter distribution. The model cannot however, take direct account of the natural (stochastic) variability which occurs from location to location in the groundwater flowpath at a site.

**D-32 Page 18, Section 5, paragraph 4**

**The statement "with course rounded materials having lower porosities than platy clayey materials" is incorrect. Course material (especially course rounded material) generally has higher porosity than fine material (clay).**

The statement is correct as presented. Coarse rounded materials, e.g. gravels, sands and silts, have lower porosities than soils rich in platy clay minerals (Freeze and Cherry, 1979).

| Unconsolidated deposits | Porosity (%) |
|---|---|
| gravels | 25-40 |
| sand | 25-50 |
| silt | 35-50 |
| clay | 40-70 |

## REVIEW E - DR. D.J. MARTIN (3 MARCH 1986)

Dr. Martin reviewed a letter from Dr. D.B. Chambers, SENES Consultants Limited, to Mr. R.W. Holmes, National Uranium Tailings Program, dated 18 February 1986, which provided comments on a paper prepared by Dr. E. Hofer entitled "Probabilistic Uncertainty Analysis of PRA's", presented at a course on Uncertainty Modelling in Probabilistic Risk Assessment, 19 to 23 November, 1984, Ispra, Italy.

E-1 "...briefly, I see the practical question which arises as: For the quantities which are constant for a given design or site (but we don't know their values), do you sample at each single run in a generic analysis or only once for the (say) 1000 runs which are assembled into an output cdf? In the attachment, I argue that I can ascribe a meaning to sampling only once, but I cannot unambiguously ascribe a meaning to sampling every run for "constants". Therefore, I cannot convince myself that the UTAP or SYVAC approach can be meaningfully interpreted."

In carrying out a probabilistic analysis it is important to define the scenario we are trying to model and the assessment questions we want to address. As noted by Dr. Martin some input parameters are uncertain and some are inherently variable, either with time or space or both. Also, it should be noted that we can also be uncertain about the variability of variable input parameters. Fortunately, our full state of knowledge about any input variable can be described in the form of a (subjective) probability distribution.

Except for certain physical and chemical constants such as the acceleration due to gravity, Avogadro's number or a radioactive half-life, there are few if any parameters in an environmental assessment which are truly constant. For example, Dr. Martin considers fracture density as a "constant" parameter and wind velocity as a variable "non-constant". However, in the real world the fracture density is not constant and measurements of fracture density made on rock from a particular situation at a particular site are likely to vary from location to location by factors larger than that due to experimental uncertainty alone. In modelling, the fracture density (or other factors such as porosity, $K_d$ etc.) is constant over a particular area because, and only because, we define it to be constant. We often allow that we are uncertain about what the constant value should be and assign a probability density function to the constant but unknown value. Another example of a "constant" but uncertain parameter might be the "transfer factor" which is used to represent the relationship between the radionuclide concentration in water to that in fish flesh. In an environmental assessment this parameter is treated as if it were a constant parameter whose actual value we were uncertain about. However, in reality this parameter will vary with time for a particular fish as it grows or moves from one area in a lake or river to another and from fish to fish, even within the same species. In some instances the distributions have been developed from world wide data and are too wide for the actual situation being considered, say for example Canadian Shield lakes with low alkalinity.

On the other hand, the mean annual wind speed will vary from year to year as well as from location to location. From meteorological observation we can determine last year's mean annual wind speed, except for experimental uncertainty, but we can only guess at what the mean annual wind speed will be next year or in any future year. However, such a guess would be based on the evidence available, namely the distribution of mean annual wind speeds based on observations from past years, which clearly contain experimental uncertainty.

In other words in both cases we have variability and uncertainty. In either case it is important to define the scenario (models and parameters) we are trying to model. If we are unclear about the scenario we are trying to model then the output is likely to reflect scenario to scenario variability which is a different matter.

Finally, consider that in performing a probabilistic analysis it is necessary to select distributions for many input parameters, some of which, as noted above, may not only be uncertain due to lack of observational data or measurement error but also may be inherently variable either in space or time. In either case the input distributions involve some element of subjective probability in that they have been selected, by a modeller, in the belief that they best represent the data. Where the observational data base is large, the modeller may feel very confident in a data set and use it directly in the assessment; in other cases, where the modeller believes less strongly that the data base is appropriate, he may, perhaps in consultation with other experts, choose to modify the distribution before using it in his model. In any event the modeller must be careful to avoid broadening the distribution so much that it loses meaning in the context of the scenario he is trying to analyse (e.g. data for transfer of radium from water to fish flesh should not be based on data from both high and low alkalinity lakes).

The interpretation of the output from such an analysis depends on the interpretation given to the distributions used to represent the uncertainties in the model input parameters. Assume for the moment that every input parameter is a constant in the real world and the input distributions represent our estimates of the degree of uncertainty about the true value of each input, i.e. each parameter has a "true" value but we are uncertain about what that true value is. The consequence is then also a fixed single value and the output of the probabilistic assessment represents our degree of uncertainty about that true value. Our "best guess" of the true value is the expected value or mean (or perhaps geometric mean) of the output distribution. The width of the output distribution represents uncertainty about the true constant value.

Alternatively, consider a second case in which all the input parameters are truly random variables such as mean annual wind speed. The input distributions then represent the annual variability in each parameter (along with any uncertainty we may have due to limited observational data). The output distribution of the probabilistic assessment then represents the year-to-year variability in the consequence. The consequence varies from year to year because the inputs vary from year to year.

In the first case noted above, the uncertainty in the predicted consequence arises from our lack of knowledge of the constant values, in the other, from the inherent variability in a parameter. In actual practice, the situation is usually not so simple and an assessment involves quantities which are both uncertain and variable (although for assessment purposes certain variables may be treated as constants, with or without uncertainty, in our definition of the scenario). In any event, the uncertainty is there in both cases and is characterized by the output distributions. In all cases, the output distributions can be interpreted as a subjective probability telling us quantitatively what we are entitled to believe about the output variable.

REVIEW F - MR. P.A. FLAVELLE (7 APRIL 1986)

Mr. Flavelle reviewed Vol. 3, Chapter 9 (Groundwater Model) of the Phase III documentation.

**F-1 Only the radium mass loading (referred to as "flux") is transferred to the output file for subsequent use. Since the computer symbol "FLUX" is not indexed, it gets recalculated and over-written for each radionuclide, with only the last value (for radium) being transferred.**

Yes, this was an error which was detected internally and subsequently changed.

**F-2 The confusion over which equation, 9.1 or 9.2, to use when calculating the parameter "q" for equations 9.4, 9.8, 9.11 and 9.16 is carried into the source code, where the calculations require the specific flux (also called the Darcy flux or Darcy velocity; (equation 9.1), but the code uses the mean linear groundwater velocity (equation 9.2).**

The section on auxiliary equations has been rewritten in order that a clearer description of the algorithms be presented. Presently, the algorithm and computer code employ Darcy's velocity, q. In the revised text the mean linear groundwater velocity is not used.

**F-3 The equation to emulate the effect of a time-varying source concentration (equation 9.14) is not internally consistent, and the discrepancies between it and the code listing leave one unsure which, if either, is correct.**

See response F-15.

**F-4 The efforts to externally calculate an input constant ($A_x$) from single values of three distributed parameters (f, K, I), two of which are not used in the computer model (K,I), need to be rationalized. $A_x$ should be an input constant, measured or derived from the site's physical structure. I believe the calculation of $A_x$ described in the text was done solely to generate an input value for the model demonstration, and is not being recommended for use in the simulation of a real site. If this is true, it should be explicitly stated. If it is not true, then the reason for calculating $A_x$ in the manner presented, and external to the model, should be explained.**

Originally, $A_x$ was generated using three distributed parameters (f, K, I) for model demonstration purposes only. Currently, $A_x$ is a site specific parameter. In the generic model the value is calculated by multiplying the length of the dam by the thickness of underlying aquifer. For example, in the Lacnor site the $A_x$ value was calculated using measured flow data, hydraulic conductivities and hydraulic gradients. The latter two are currently employed in the model to calculate the Darcy velocity.

**F-5 Page 9-1, Section 9.1, paragraph 3**

**"... radionuclide concentrations at the point of discharge are converted into contaminant fluxes and are subsequently utilized..."**

**An examination of the source code listing at the end of the chapter revealed that only the radium discharge rate is transferred to the output data file for later use, and the radionuclide concentration is not converted into a flux (mass discharge per unit cross-sectional area per unit time) but into a mass loading (total mass discharge per unit time).**

The code has been changed so that all radionuclide concentrations are converted into a flux, $J_{i,j}$, which has units of $Bq.m^{-2}.yr^{-1}$.

**F-6 Page 9-4, Section 9.3.1, equation 9.2**

**The mean linear groundwater velocity, calculated here, has been assigned the same symbol "q" as the specific discharge calculated in equation 9.1.**

Yes, this was a typographical error. Currently "q" is used to represent the Darcy velocity which is calculated by multiplying the hydraulic conductivity by hydraulic gradient.

**F-7 Page 9-5, Section 9.3.1, equation 9.4**

**The dispersion coefficient is the dispersivity of the medium times the mean linear groundwater velocity. Because of the inclusion of the porosity term, the "q" in this equation must be the specific discharge of equation 9.1. An examination of the source code listing revealed that the "q" used is the groundwater velocity from equation 9.2, which results in an incorrect calculation.**

The parameter "q" is currently used to represent the Darcy velocity. The dispersion coefficient is calculated by multiplying the dispersivity by "q" and dividing by the porosity. The average linear groundwater velocity, V, which is equal to the Darcy velocity divided by the porosity, is not used in the revised Chapter 9.0 or model.

**F-8 Page 9-6, Section 9.3.2, equation 9.8**

**Again the inclusion of the porosity necessitates the use of the specific discharge "q" (equation 9.1) but the source code listing reveals that the groundwater velocity "q" (equation 9.2) has been used.**

See F-7.

**F-9 Page 9-7, Section 9.3.2, paragraph 1**

**As per comment 1, it is the contaminant annual discharge rate (or mass loading) that is calculated, not a flux (which implies unit cross-sectional area).**

Previously, a contaminant annual discharge rate was calculated. This has been changed, however, to a flux, $J_{i,j}$, which has units of $Bq.m^{-2}.yr^{-1}$.

**F-10 Page 9-7, Section 9.3.2, paragraph 2**

**It is not clear what is meant by the phrase "in any given time period", since all of the rates are yearly averages.**

The "time period" refers to the $\Delta t$ between $t=0$, the year in which the simulation was initiated, and $t$, the current time of the simulation. This period is employed in calculating the migration of the contaminants along the aquifer.

**F-11 Page 9-7, Section 9.3.3**

**The significance of each of the six assumptions, in terms of over-estimating or under-estimating flow rates, fluxes and mass loadings, and the need to use field data or detailed modelling results to assess the extent of over - or under-estimates, should be discussed.**

The revised version of Chapter 9.0 contains a brief discussion on the effects, in terms of over- or underestimating flow rates, of the various assumptions.

**F-12 Page 9-8, Section 9.3.3, paragraph 5**

**The reference to equation 9.2 should read equation 9.7.**

Yes, this has been corrected.

**F-13 Page 9-9, Section 9.4.1, equation 9.11**

As per comments 3 and 4, the "q" term must be the specific discharge (equation 9.1) since the porosity is included here, but the source code listing incorrectly used the groundwater velocity of equation 9.2.

See F-7

**F-14 Page 9-10, Section 9.4.2, paragraph 1**

It is not clear what is meant by the phrase "at any time" at the end of the second sentence. Only after steady-state conditions are re-established will changes in the discharge concentration be proportional to changes in the source concentration. The transient response of the discharge concentration to changes in the source concentration is what this section is trying to calculate.

The sentence has been corrected in the revised Chapter 9.0. It now reads:

> "An increase in source concentration by some factor will cause a change in the contaminant concentration at any distance following an appropriate time lag."

**F-15 Page 9-11, Section 9.4.2, equation 9.14**

There appears to be an inconsistency in the structure of equation 9.14, and the source code listing does not correspond to equation 9.14. These two points are best explained by illustration:

For K=4 (that is, the fourth time step) equation 9.14 becomes

$$
\begin{aligned}
C(S,t_4) = {} & C_s(t_0) && .\ G(X,t_4) \\
& + (C_s(t_1) - C_s\ (t_0)) && .\ G(X,t_4-t_1) \\
& + (C_s(t_2) - C_s\ (t_1)) && .\ G(X,t_4-t_2) \\
& + (C_s(t_3) - C_s\ (t_2)) && .\ G(X,t_4-t_3) \\
& + (C_s(t_4) - C_s\ (t_3)) && .\ G(X,t_4-t_4)
\end{aligned}
$$

**and after modifying the symbols to be consistent (e.g. GWAT(I,K) becomes $C(X,t_4)$), the appropriate portion of the source code becomes**

$$\begin{aligned} C(X,t_4) = {} & C_s(t_1) \quad . G(X, t_4) \\ & + (C_s(t_2) - C_s(t_1)) . G(X,t_4-t_1) \\ & + (C_s(t_3) - C_s(t_2)) . G(X,t_4-t_2) \\ & + (C_s(t_4) - C_s(t_3)) . G(X,t_4-t_3) \end{aligned}$$

**It can be seen that: the source code has one less term than equation 9.14; the Green's Function Terms, "G(X,t)" apply to different source concentration terms in the code than they do in equation 9.14; the concentration in the first term of the code listing is different from the concentration in the first term of equation 9.14; and the Green's Function in the last term of equation 9.14 may be trivial.**

**It is not obvious where the error(s) occur - in the formulation of equation 9.14, in the source code, or in both.**

Both were incorrect. The following expression is currently employed in the text and model:

$$\begin{aligned} C_{i,j}(X,t_k) = {} & C_{s,i}(t_0).G_{i,j}(X,t_k) + (C_{s,i}(t_1)- C_{s,i}(t_0)).G_{i,j}(X,t_k-t_1) \\ & + \quad (C_{s,i}(t_2)-C_{s,i}(t_1)).G_{i,j}(X,t_k-t_2) + \ldots \\ & + (C_{s,i}(t_{k-1})-C_{s,i}(t_{k-2})).G_{i,j}(X,t_k-t_{k-1}) \\ & + (C_{s,i}(t_k) - C_{s,i}(t_{k-1})).G_{i,j}(X,t_k-t_{k-1})/2.0 \end{aligned}$$

The last term approximates the changing source strength during the last time increment.

---

**F-16 Page 9-11, 9-12, Section 9.5; Table 9.2**

**The hydraulic conductivity is discussed in the text although it is not used in the computer model nor is it listed in Table 9.2 as a parameter. Similarly, the hydraulic gradient is discussed in the text but not used**

**in the model or listed in the table. On the other hand, the bulk density is calculated in the model (computer symbol BD), but is neither discussed in the test nor listed in the table.**

In the revised Chapter 9.0, hydraulic conductivity, hydraulic gradient and soil density are discussed in the text and presented in Table 9.2. They are all used in the revised computer model.

---

**F-17 Page 9-13, Section 9.5, Point 4; Equation 9.16**

**a) The porosity should not appear in equation 9.16.**

**b) There is a spelling error in "determined" in the sentence preceding equation 9.16.**

**c) It should be made clear if this calculation of $A_x$ is done only to derive an input value for the model demonstration. It is not reasonable, for a real site, to externally calculate a site-specific input constant ($A_x$) using a single value of a distributed input parameter (f) and two other distributed parameters which are not input to the model (K and I).**

a) Agreed, it has been corrected.

c) Agreed, see F-4.

## REVIEW G - MR. P.A. FLAVELLE (5 JUNE 1986)

**Mr. Flavelle reviewed Vol. 3, Section 3.14 (Tailings Erosion Model) of the Phase III documentation.**

---

**G-1 Mr. Flavelle's letter was written to document several errors he had found in the tailings erosion model and which he had discussed with SENES project personnel. Mr. Flavelle also noted that the tailings area geometry was constrained to a square shape in the erosion model and questioned whether this limitation was important or not.**

The computer code faults have been corrected in the UTAP.3 version of the erosion model. The model no longer assumes that the tailings pile is a square area. It now treats the pile as a rectangle, with the inputs of total area ($A_T$) and flow length ($L_f$) defining the dimensions.

## REVIEW H - MR. P.A. FLAVELLE (24 JUNE 1986)

**Portions of Volume 2 (questions H-1 to H-6), App. C (questions H-7 to H-12), App. D (questions H-13 to H-14), and Volume 3 (questions H-15 to H-37) of the Phase III documentation were reviewed.**

**H-1 Volume 2: System Description and Control Module Documentation**

**This report is clearly written, and the presentation using flow charts and source code listings is well done and appropriate for review. The comprehensive variable dictionary and complete source code listing in Appendix B are also very helpful in understanding the program. The only major improvement that could be made would be to include data flow diagrams to make tracing the calculations easier.**

While data flow diagrams may have been useful, the flow diagrams presented in Figures 1.1, 1.2, 1.3, 3.1 and 3.2 should assist the reader in tracing calculations. Figure 1.2, in particular, illustrates the complete flow structure of the control modules, describing the function of each module.

**H-2 On Page 3-3, Section 3.2.1, first paragraph:**

**It should be demonstrated that randomly sampling a distribution function at each time-step will adequately simulate a time-varying parameter. Time-variations often follow trends, making them non-random.**

Section 3.2.1 clearly states that time-variant parameters are randomly sampled every time step of every trial. This option is available for the purpose of sampling truly random time-variant parameters such as rainfall. No attempt should ever be made to use this facility to sample non-random parameters (i.e. those following trends). Such parameters are, in nature, dependent upon other variables and should thus be calculated as a function of those other variables or as a function of the parameter value for the previous time step. Where parameters are known to be dependent it may be possible to use the correlated parameter input distribution option which is included in UTAP.

**H-3 On Page 3-7, Section 3.3.2, second paragraph:**

> **The results and conclusions from testing the random number generator should be stated (and discussed if necessary). Stating that it has been "thoroughly tested" does not indicate what confidence can be placed in the random number generator. The review of Appendix C (below) determined that insufficient information is presented to support the conclusions drawn.**

The nature and results of the test of the random number generator carried out for Phase III are described in Appendix C, which is referenced on page 3-8, second paragraph. The 1983 paper by Marse and Roberts who developed the procedure for drawing random numbers on (0,1) describe various tests of distribution and independence on which they base their favourable claim about the statistical properties of their random number generator. The tests described in Appendix C are complementary to those described by Marse and Roberts. Contrary to the opinion voiced by the reviewer, our testing of the procedure did not provide any reason to reject the claim of "excellent global statistical properties" made by Marse and Roberts.

**H-4 On Page 3-14, Section 3.3.5, first paragraph:**

> **Since the seed for the random number generator is recalculated every time the random number generator is called, the selected parameter values will be dependent on the order in which the parameter pdf's are sampled. Changing the order in which the pdf's are specified in the INPUT1 file will change the order in which they are sampled. This will change the values selected (and the results calculated) even though the initial random number seed and the subsequent string of random numbers are unchanged. This should not affect the statistical properties of the calculated results if they are well defined. If changing the order of defining input pdf's generates a set of results with statistical**

> **properties different from the original set of results then either the set of results is not large enough to adequately define its statistical properties or the computer model is not adequate to simulate properly the necessary processes.**

The comment that changing the order of the inputs will change the results of a run is quite accurate; however, if the random number generator does generate truly random numbers, the resulting statistics should be unchanged if many trials are performed.

**H-5 On Page 3-18, Section 3.3.10, last paragraph; Figure 3.11:**

> **The typical triangular distribution shown in Figure 3.11 can also be characterized as a normal distribution with mean = 74 and standard deviation = 24 (significant at the 5% level). This may simply be caused by the limited number of data displayed in the figure. It is not clear if generating data which are not uniquely defined by the input pdf's has any effect on the confidence in the model calculations, and if the number of runs of the model should be governed in part by how representative the sampled data is of the parent pdf.**

It is unclear how one could expect to accurately reproduce 500 data points from a histogram of 20 cells and draw conclusions within a 5% level of significance. The error involved in estimating the 500 points may sway the results a lot more than 5%. It may still be possible to fit a normal distribution to triangularly distributed data points. Whether or not this not can be done does not change the fact that the data points adequately describe a triangular distribution and does not affect the results of the simulation.

**H-6 Editorial comments:**

> **i) Figure 3.7, following page 3-16: The abscissa is labelled "LOG (BASE e) SULPRD" but the code listing in Table 3.13 uses common logs.**
>
> **ii) Equation 3.12, page 3-18: There is a square root symbol missing**

**from both versions of Equation 3.12. Refer to the coding in Table 3.16 for the correct placement of the symbols.**

**iii) Equation 3.15, page 3-20: The equals symbol is misprinted.**

**iv) Figure 4.6, following page 4-5: The Radium concentration units are missing.**

i) The label "LOG(BASEe)SULPRD" in Figure 3.7 bears no relation to anything in the source code listing on Table 3.13 and the two should not be confused.

ii), iii), iv) The questions refer to errors subsequently corrected in the Phase II Volume 2 report.

---

**H-7 Page C-2, Section C.3:**

**The statement that 0.4922 and 0.2005 are very ordinary probabilities should be explained. How does this confirm that the distributions are correct?**

The statement in Section C.3, page C-2 goes on to note that "Hence, we have failed, at any confidence level over 80% to disprove the null hypothesis... that the two sets of 5000 consist entirely of independent observations on the uniform (rectangular) distribution covering the interval (0,1)."

"Correct" in this sense means that the statistical test provides no reason to doubt the null hypothesis that the two sets of numbers are randomly drawn from a uniform distribution on the interval (0,1).

"Ordinary" simply refers to the fact that there is a 20% chance (i.e. 100%-80%) that the standardized value could be larger than the observed values by chance alone. This 20% chance is large (i.e. ordinary) compared to more typical values of 5% or 1% which are often used.

**H-8 Page C-2, Section C.4, Equation 1:**

**The first term in the summation should contain the mean of x.**

Agreed.

**H-9 Page C-3, Section C.4, paragraph 3:**

**Although only one datum in each set exceeds the 95% confidence interval as expected, it can be demonstrated that the two sets of data fail this test at the 80% confidence interval (3 exceedances instead of 4) and also fail it at the 50% confidence interval (8 exceedances instead of 10). Are these results sufficient to accept the null hypothesis that no autocorrelations are truly different from zero?**

We are uncertain as to the nature of the question posed. There are two (and only two) sets of data described in Appendix H and in each set there is exactly one autocorrelation function which exceeds 0.0277. The data offers no reason to reject the null hypothesis.

It is important in this regard to remember that a test of significance always refers to a null hypothesis. The conclusion that there is no reason to reject the null hypothesis is equivalent to saying the sample value is compatible with the null hypothesis value or alternatively, that sampling variation is a likely explanation of the observed discrepancy between the null hypothesis, and the sample values. Statistical tests cannot prove a hypothesis, rather the tests must always be framed to ask whether or not the data provides any evidence to reject the null hypothesis.

**H-10 Page C-3, Section C.4, last paragraph:**

**These tests are not described clearly, and again describing probabilities as "ordinary" does not explain whether the tests were successful or not.**

As for question H-7, "ordinary" simply means that these probabilities are large compared to probabilities such as 5% or 1% which are often used in such tests. The tests were successful in that the results do not disprove the null hypothesis.

**H-11 Page C-4, Section C.5, paragraph 2:**

> **This chi-squared test is not described clearly. What is being tested, why this test is used (as opposed to some other test such as the Kolmogorov-Smirnov test, which is considered by some to be a more powerful test) and how the test results prove the conclusion drawn are not explicitly stated. The level of significance at which this test is being conducted is not stated. There is insufficient information presented to be able to accept or reject the null hypothesis.**

As noted on page C-4, question C-5, the $\chi^2$ test is the most generally accepted test of the overall frequency distribution. The data for such a test consists of 5,000 random observations drawn from what is believed to be a uniform distribution on (0,1). As described on page C-4, the interval (0,1) was divided into 100 cells of equal width and each of the five thousand observations assigned to one (and only one) cell. The null hypothesis is that every cell should contain 50 observations (i.e. 5,000 observations ÷ 100 cells). As described in the text on C-4, the data did not provide any reason to reject the null hypothesis at any confidence band over 85%. In other words, there is a 15% chance that "K" could be larger than the observed K simply due to sampling variations. Often values of 1% or 5% are used in such tests of significance.

While there is some controversy over which test, i.e. the $\chi^2$ or the Kolmogorov-Smirnov test, is most powerful, either test is satisfactory for this data set (the Kolmogorov-Smirnov test may be preferred if the sample size is small, which is not the case here).

**H-12 Page C-8, Section C.8:**

**Based on the above comments, there is insufficient information presented to support the conclusion of excellent global statistical properties.**

See our comment on question H-3.

**H-13 Table D.3:**

**The maximum value of the parameter "RACNTA" appears to be three orders of magnitude too large.**

The tailings radium concentration (RACNTA) is specified to range from 5.0 to 15.0 $Bq.g^{-1}$ in the input file. The maximum sampled value presented on Table D.3 in the final report equals 14.94 $Bq.g^{-1}$ which is within the range specified. It is possible that the reviewer has commented on a draft version which contained a typographical error that was subsequently corrected. At any rate, the value stated in the final report is correct.

**H-14 Page D-13, Section D.4.3:**

**The description of the two-level fractional factorial design analysis is not clear. Are all of the parameters held constant while one is varied high and low, or is the parameter of interest held high and then low while the rest vary randomly, or are they all simultaneously constrained to various combinations of high and low values? What equation is used to calculate the main effect of a parameter?**

A common statistical problem is investigating the effects of a number of factors (variables) on some response, in the present case dose. In a factorial experiment all combinations of parameters are considered whereas in a fractional factorial experiment only a fraction of the possible combinations are considered. Consider k input variables (factors) each of which has two levels. In this case there are $2^k$ possible combinations of the k variables.

If each of the factors is divided into 3 levels, then there are $3^k$ possible combinations of the k factors, and so on. Clearly, the number of possible combinations can become large quite rapidly. With a fractional factorial design only some fraction, say $(1/2)^m$ where $m<k$, of the total possible combinations is used. As noted on page D-13, two-level fractional factorial designs are well discussed in the literature and the authors of Appendix D cite Box, Hunter and Hunter (1978).

The author of Appendix D defines, on page D-13, the main effect of a parameter on radon dose as "the average change in radon dose due to a change from a low value to a high value of that parameter...". For each simulation the main effect (L) is calculated as the average difference between radon dose for low and high values of that particular parameter taken as an average over the levels of the other factors. For two factors A and B each with two levels (($a_1$, $a_2$) and ($b_1$, $b_2$) respectively), the main effect of A can be written as:

$$L_A = \frac{1}{2}(a_2\ b_2) + \frac{1}{2}(a_2\ b_1) - \frac{1}{2}(a_1\ b_2) - \frac{1}{2}(a_1\ b_1)$$

The main effect of B is:

$$L_B = \frac{1}{2}(a_2\ b_2) + \frac{1}{2}(a_1\ b_2) - \frac{1}{2}(a_2\ b_1) - \frac{1}{2}(a_1\ b_1)$$

---

**H-15 Volume 3: Component Model Documentation, Chapter 2 Component Module Objectives and Conceptual Specifications, Figure 2.1:**
**It would be advantageous if the names of the appropriate submodels were included in the exposure pathways diagram.**

Consideration was given to this suggestion, but it proved too confusing and awkward to add that amount of detail to the diagram.

**H-16 Section 3.14 Tailings Erosion and Re-Vegetation:**

**As noted in my letter (Flavelle to Holmes, June 5, 1986) there are two limitations of this model that should be recognized: the tailings area is assumed to be square, and this model is assumption-driven, with many empirical parameters that may need to be calibrated for site-specific conditions.**

The Universal Soil Loss Equation employed in the tailings erosion model assumes the area to be square. This limitation was recognized and has been amended in the final UTAP code. The tailings site can now be characterized as a rectangular area which more closely approximates typical sites.

The erosion model does contain several empirical parameters which have been determined largely from open field studies. Calibration of the model for tailings applications would improve the confidence which can be placed in the model predictions.

**H-17 Page 4-3, Equation 4.3:**

**It is not clear if the time-averaged moisture content of the tailings is specific for each layer or averaged over the depth of the unsaturated zone. It is also not clear if the moisture content of the tailings is correlated with the net precipitation used in other submodels (Soil Model, Chapter 6 and Groundwater Model, Chapter 9).**

The moisture content of the tailings is the average over the unsaturated layer. The moisture content is not correlated with the net precipitation used in other submodels.

**H-18 Equation 5.1 should be able to solve for the atmospheric concentration of contaminants above the tailings when X=0. Hence $Q_i$ should be the emission rate of the virtual source, not of the tailings, and can be**

**evaluated by solving equations 5.6 and 5.1 for $Q_i$ when X=0.**

The model is not designed to solve for atmospheric concentrations above the tailings (when X=0). A different model beyond the scope of UTAP would be required. The emission rate of the virtual source and the tailings are the same.

**H-19 The tailings area is constrained to be circular. To adopt any other shape for a specific site would require modification of the computer code. (Air Dispersion Model)**

In effect, the tailings area has been assumed to be circular for atmospheric dispersion calculations with surface area equal to that of the actual tailings area. To adopt a different specific shape would require modifications to the computer code. However, for practical purposes this is not a serious limitation as the effect of geometry diminishes rapidly with increasing distance from the tailings area. (See also the response B-2.)

**H-20 One assumption inherent in equation 5.1 is that the contaminant concentration is uniform in the cross-wind (or Y) direction over the width of the sector. Translating the sector's origin from the tailings to the virtual source while maintaining the same sector angle results in a larger sector width at the receptor and an underestimation of the atmospheric contaminant concentration. The underestimation is by a factor of $X/(X+X_0)$, where X is the tailings to receptor distance and $X_0$ is the virtual source set back distance (a function of the width of the tailings perpendicular to the wind direction). In effect, the contaminant plume is no longer confined to the original sector measured from the tailings. This limitation of the model should be identified so the magnitude and significance of the underestimation can be evaluated for any application of the model.**

Over "long" time periods such as days or months or, in the present case, years, the wind direction will vary over all of the compass points. In such cases "sector" models, where it is assumed that there is no cross wind variation within a sector, are often used. The angular width of the sectors corresponds to the regular resolution of the wind data, usually 22.5 degrees corresponding to 16 regular sectors. In effect, the concentrations within a sector are time averaged concentrations where the averaging process is due to the variability in the wind direction. Loss of contamination from one side of the sector to the adjoining sector will, on average, be compensated by contaminant flow in the other direction.

The concentration is not underestimated in the fashion suggested by the reviewer. First note that the Gaussian plume equation is conservative with regard to mass (or radioactivity). The virtual source correction assumes that all of the material released by the tailings area is released as a point source offset from the centre of the tailings area. In other words all of the tailings area is contributing to the concentration predicted for a downwind location whenever the wind blows from the tailings towards the receptor. On the other hand, for real situations with a receptor located close to an area source only part of the area source will contribute to the concentrations predicted at the receptor for wind blowing from the tailings area towards the receptor. However, as the wind direction varies over the compass, all portions of the tailings surface will contribute to the predicted concentrations at the receptor, approximately in proportion to the percent of time the wind blows from that portion of the tailings area towards the receptor. Overall, the virtual source assumption implicit in equation (5.1) is both mathematically convenient and appropriate.

---

**H-21 Chapter 6, Soil Model, Page 6, Section 6.1:**

> **It is not clear if contaminant uptake and subsequent deposition by plants would be a significant factor in controlling the contaminant concentration distribution in the soil profile, and should therefore be included in the model.**

This particular mechanism to our knowledge has not been included elsewhere in the literature. Also the amount of material deposited on to the soil is not adjusted for that intercepted by plants. Thus such an effect is not considered significant and has not been included in this model.

---

**H-22 Page 6-3, Section 6.1, paragraph 2:**

**There is a discrepancy between the definitions of water content of the soil (used here) and moisture content of the tailings (used in Air Source Model, Chapter 4). The former allows a water content >1 while the latter does not.**

In the soil model, the water content is defined as kg water/kg (dry) soil; where in the air source model, the moisture content is defined as kg water/kg (wet) tailings.

---

**H-23 Editorial comments:**

**i) Page 6-2, Section 6.1, last sentence: the term $C_m$ should be $C_o$.**

**ii) Page 6-3, Section 6.1, first sentence: spelling error in "chemical".**

**iii) Page 6-5, Section 6.1, Equation 6.12: "F: is defined as the runoff fraction in Table 6.2, so equation 6.12 should have the term "(1-F)" in it. It would then agree with the source code listing.**

**iv) Page 6-6, Section 6.2, first paragraph: Table 6.1 is the source code listing, and does not present the physical and chemical properties of the soil layers, as stated here. Also the reference "Beals, 1985" is not in the reference list.**

**v) Page 6-6, Section 6.2, last sentence: It is not clear what this sentence means.**

**vi) Table 6.2: There is no parameter for the soil layer depth presented, and the reference "Beals, 1984" is not in the reference list.**

Noted.

**H-24 Pages 8-5 and 8-6, Sections 8.2 and 8.3:**

> **It is not clear if the submodels can be accessed only once each run, or if they could be accessed more than once to simulate several specific crops in a single run.**

The submodels can only be accessed once each run. Thus up to five crops may be incorporated into the model.

**H-25 Pages 8-6 and 8-7, Sections 8.4 and 8.5:**

> **Could data be extracted from these models to compare the rate of contaminant recycling to the soil surface by plant uptake and decomposition with the rate of deposition from the atmosphere calculated in the Soil Model (Chapter 6; see comment 1 on Chapter 6)?**

The uptake by plants and subsequent recycling to the soil via decomposition is not explicitly modelled (see H-20).

**H-26 Chapter 9 Groundwater Model:**

> **As noted in my letter (Flavelle to Holmes, April 7, 1986) there is some confusion in the conceptual model as to whether the cross-sectional area for flow contains the porosity term (resulting in "q" being the mean linear groundwater velocity) or is the macroscopic flowpath cross-section (resulting in "q" being the Darcy flux). Also, it is not clear if multiple flowpaths can be calculated in a single computer run, or if the model is limited to a single flowpath.**

a) "q" see question F-7.

b) "Multiple Flow Paths"

Previously, the model was only capable of calculating the migration of contaminants along a single flowpath. In the revised version, UTAP.3, however, the model has been altered to incorporate multiple flowpaths during a single computer run.

**H-27 Page 10-2, Section 10.2, first paragraph:**

**It appears (although it is not explicitly stated) that the program can simulate only a single, independent drainage path. More complicated drainage patterns would require either modification of the program or partitioning the drainage into several pathways, analysing each and combining the results.**

The UTAP code has been developed to model a single tailings source. It is only necessary to model a single drainage pattern and the receiving water system since surface runoff from the tailings area typically is directed to a single discharge point. The path of contaminated water will therefore follow a single course as it moves downstream. The flow in other branches merely add to the base flow in the drainage basin and therefore do not need to be modelled separately. The user can locate nodes at the intersection of river branches, if so desired, to model contaminant concentrations at any point of interest. In this context there is no need to model more complicated drainage patterns for most situations.

**H-28 Pages 10-7 to 10-12, Section 10.5:**

**There are some terms which are not defined in this section, notably '$K^C$', '$pCO_2$', '$K_H$' and 'f'. '$pCO_2$' could be the partial pressure of $CO_2$ or the negative log of the $CO_2$ activity. 'f' is defined in the variable dictionary as the activity coefficient, but is not defined in the text. Subsequent use of 'f' limits its definition to the activity coefficient of divalent ions.**

**Some of the derivations of the equations in this section are not clear. The derivation of the bicarbonate ion concentration using the carbonate: $CO_2$ equilibrium constant ($K_H$) is not presented. There appears to be inconsistent use of the activity coefficients in deriving the final**

equation for pH (Equation 10.8). The source of values for the equilibrium coefficients is not presented, and some of the values do not agree with a major compilation of equilibrium coefficients (Benson, L.V and L.S. Teague, (1980) "A Tabulation of Thermodynamic Data for Chemical Reactions Involving 58 Elements Common to Radioactive Waste Package Systems", Lawrence Berkley Laboratory, Report LBL-11448, University of California, Berkeley, CA).

There are a limited number of reactions considered in the calculation of pH. The species considered do not include $Al(SO_4)_2^-$ or the mineral Alunite ($KAL_3(SO_4)_2(OH)_6$), both of which may participate in the reactions. Also, the equation for electroneutrality (Equation 10.6) does not contain the hydrogen ion.

The form of equation 10.8 limits the pH to >=3.74 (for f=0.6) or 3.79 (for f=0.9), or the right hand side becomes negative. If the pH should be below these limits at a real site, this program could not simulate that site.

The undefined terms referred to in Section 10.5 are as follows:

$K^c$ = solubility constant in terms of concentration rather than activity
$pCO_2$ = partial pressure of carbon dioxide gas (atm)
$K_H$ = Henry's adsorption coefficient for carbon dioxide gas
f = activity coefficient

With respect to the parameter 'f', we have chosen to define it for divalent ions, as the majority of the ions in the system being analyzed have a double valency state. The decision to define 'f' in terms of divalent ions is arbitrary, but it is also arbitrary to define f in terms of monovalent ions. The appropriate 'f' value for monovalent and trivalent ions may be calculated using the definition of Deybe-Huckel (see page 135, Stumm, W. and Morgan, J.J., 1981, "Aquatic Chemistry: An Introduction Emphasizing Chemical Equilibria in Natural Waters." 2nd Edition, John Wiley & Sons). From the

Deybe-Huckel relationship the values for the monovalent and trivalent ions may be calculated using the value for the divalent ions as follows:

activity coefficient for monovalent ions = $f^{1/4}$
activity coefficient for trivalent ions = $f^{9/4}$

These expressions are used in the pH component model discussed in Section 10.5.

Because the hydrogen ion concentration is insignificant over the pH range expected in the receiving water environment, it was purposely left out of equation (10.6). This allowed for an easier solution to the charge balance equation. Similarly, several other ions which were considered to be very minor contributors to the charge balance, were left out of the equation. These include such species as $Al(SO_4)_2^-$ and the mineral alunite.

Several sources were consulted in the review of equilibrium coefficients. Typically, a range of coefficient values is given. The values selected and reported in Section 10.5 are those which we felt were the most appropriate for the application.

The form of the pH equation is limited to pH values greater than about 3.8 as noted in the above question. From an analysis of expected receiving water pH levels, it was found that the pH would as a rule be above this lower limit as the bicarbonate formed from carbon dioxide dissolution raises the pH in open systems.

---

**H-29 Page 10-25, Section 10.6.2, Equation 10.23:**
**The constant '1.1' is not derived or explained.**

The constant value of 1.1 in equation (10.27) was determined from several simulations at assumed steady-state conditions. The average ratio of the radionuclide concentrations in the lake water column to the radionuclide concentration in the sediment interstitial water at depth $\infty$ was calculated from these simulations and substituted into equation (10.23). This parameter was treated as a constant in solving the equations for the rate of removal from the water column ($k_{1,i}$, equation (10.26)), the rate of feedback from the sediment to the water column ($k_{2,i}$, equation (10.27)), and the rate of burial in deep sediment ($k_{3,i}$, equation (10.28)). The uncertainty in the estimates for these rate constants is incorporated in the values of the other input parameters included in the equations.

**H-30 Chapter 12 Animal Produce Models:**

**There is no source code listing for this submodel.**

The listing was omitted in the draft, but was included in the final report.

**H-31 Page 12-1, Section 12.1, second paragraph:**

**Can the computer model also calculate the ingestion of arsenic?**

As written, the model does not include arsenic. Given environmental levels of arsenic, the intake can be readily calculated by UTAP. Also the NUTP has a separate contract in which arsenic bearing tailings were considered.

**H-32 Equations 12.1 - 12.4:**

**The same feed-to-meat transfer coefficient is used for the ingestion of water as for the ingestion of vegetation. It is not clear if this is accurate, or a simplification.**

There is no information in the literature for the feed-to-meat transfer coefficient for the ingestion of water, so the assumption has been made that it is identical to that for the ingestion of vegetation.

**H-33 Editorial comments:**

**i) Page 12-8, Section 12.3.1, second paragraph: $Q_{mb}$ is not defined, although $Q_m$ is.**

**ii) Page 12-9, Section 12.3.2, second paragraph: $Q_{ma}$ is not defined, although $Q_m$ is. Also, the reference to Section 12.3.2 should be to Section 12.3.1.**

These typographical errors have been noted.

**H-34 Chapter 13 Dose Models:**

**There is no source code listing for this submodel.**

This was omitted in the draft, but was included in the final report.

**H-35 Page B-4, Section B.2.2, last paragraph:**

**The reasoning behind the partitioning of the game fish body burden is not clear. How does the concentration factor in forage fish lead to the assumption that 90% of the body burden in game fish comes from the water component? The body burden from forage fish should be related to the predation rate, not the standing crop of forage fish.**

The fact that the concentration factors for game fish flesh and forage fish flesh were quite similar in the work reported by Swanson (1983), even though their feeding habits are quite different, was interpreted to suggest that the majority of the uranium intake for both species must come from water rather than from the food they consume. Otherwise, the levels in the forage fish flesh would be expected to be much higher. Also, from an analysis of the amount of food consumed by game fish and the potential amount of uranium which could be accumulated from this pathway, it was determined that only about 10% of the total could be derived from the consumption of forage fish and invertebrates. Hence, the remaining 90% was assumed to transfer from the water phase through the gills and stomach.

---

**H-36 Page B-4, Section B.2.3, last sentence:**

**"Since game fish acquire 90% of their body burden of uranium directly from water," is stated as a fact, but it is an assumption made only three paragraphs above.**

The distribution of uranium intake is an assumption since experimental evidence is not available on which to determine the uptake via each pathway. Based on estimates of potential uranium intake via each pathway, using estimates of food consumption and uranium contents of the food sources, the main source was determined to be direct transfer from water. The nominal contribution from water was estimated to be 90%.

---

**H-37 Page B-10, Section B.3.1, third paragraph, and**

**Page B-12, Section B.3.2, first paragraph:**

**As is pointed out later in the Appendix, it is not surprising that rate constants associated with direct uptake from water are the most important, considering the assumption of 90% of the uptake is via that pathway. This leads to the question would the results be significantly different and could the simplified model reproduce these results if the partitioning of the game fish body burden were significantly different?**

If the assumption that 90% uranium uptake by game fish was significantly different, then the results of the sensitivity analysis would indeed be different. However, it is noted that the available information does not suggest that the uptake would be significantly different. Even if the partitioning were significantly different, the simplified model would still be adequate in most cases provided the equilibrium assumption still holds and provided the transfer factor for uranium from water-to-game fish flesh is adjusted to account for uranium uptake from all sources.

REVIEW I - MR. K.R. SHULTZ (24 JUNE 1986)

Mr. Shultz forwarded comments on Chapter 7, Vol. 3 (questions I-1 to I-13) of the Phase III documentation.

I-1 Equation 7.1 - argument of tan $\theta$ is missing
- $\cos \phi$ should be $\cos \theta$
- $\theta$ should be defined

Tan $\theta$ and cos $\theta$ are now corrected. The parameter $\theta$ is now defined in the text.

I-2 Equation 7.2 represents the dose rate above an infinite slab source. It is also derivable from slab formulas (see Rockwell).

Noted.

I-3 Equation 7.3 is of the same form as a special case for semi-infinite slab sources with thin external shielding (Rockwell p. 407)

Noted.

I-4 Equation 7.4 - the index k is undefined (soil layer)
- indexing convention should be described better
- see comments on equation 7.13

Equation (7.4) has been changed.

**I-5 Page 7-4 - natural abundance of $^{235}U$ is 0.72% not 0.014%.**

Agreed.

**I-6 Page 7-5 para 1: being as the source referred to is a fine layer of fugitive dust away from the tailings it would be inappropriate, as stated to take into account daughter products or equilibrium values. Each radionuclide is treated separately.**

This has been noted and discussed in the revised text.

**I-7 Equation 7.7: Energy averaging introduces small errors for unshielded sources. However, where shielding can harden the emergent gamma spectrum, energy averaging like that done can introduce substantial errors because the attenuation coefficients are energy dependent. These coefficients appear in the exponential term multiplied by shield thickness. This results in a rapidly increasing error with shield thickness (can be orders of magnitude). It is more appropriate to weight the number of gammas to the highest photon in the energy level and calculate attenuation and build-up accordingly.**

Energy averaging can have a critical influence on the accuracy of the calculation of gamma flux density and dose rate above layers of material containing radioactivity. With thick shields and high density and atomic number hardening of the radiation is significant. However, in the case of thin layers of soil (5 to 15 cm) which have relatively low density and atomic number, the hardening is insignificant as illustrated by the model comparisons to NCRP data described below.

Experimental and theoretical data on the transmission of gamma rays (photons) through thick absorbers (shields) are commonly described in terms of the buildup factor B which is defined as:

$$B = \frac{\text{observed dose rate}}{\text{primary dose rate}}$$

which, in effect, takes into account the scattered radiation. The effect of the buildup factor is illustrated by the relation:

$$I = I_o e^{-u_o x} B(u_o x)$$

where x is the thickness of the absorptive material, $u_o$ is the linear attenuation coefficient, $I_o$ is the incident photon intensity and I is the photon intensity exiting from an absorber of thickness x.

The term $e^{-u_o x}$ becomes increasingly smaller as x increases and $B(u_o x)$ increases with increasing x. However, the linear attenuation coefficient $u_o$ includes both absorption and scattering processes represented by the linear absorption coefficient $u_a$ and a scattering coefficient $u_s$, viz:

$$u_o = u_a + u_s$$

In our analysis we used the linear absorption coefficient ($u_a = u_o - u_s$) to calculate self shielding. In effect this assumption implies that radiation scattered from the primary beam will always contribute to the radiation dose. This approach is computationally much simpler than one which incorporates the buildup factor directly and is also likely to be somewhat conservative.

If we understand the reviewer's comments properly we would agree that the approach is overly simplistic for situations where it is necessary to account for external shielding.

It is also worth noting that while the method of energy averaging was an approximation that was utilized to make the problem more tractable, calculations show that the results generated with this model are in good agreement with more complicated models. For example, the model was run to calculate the exposure over soil containing a known concentration of thorium-232 and daughters in equilibrium. The results agreed with published values to within 10%.

---

**I-8 Equations 7.10 and 7.11 contain errors. The gap in energy interval is not intended. The exponent in 7.11 should be negative as it appears in the code (Table 7.2). In the range 0.08 to 0.1 Mev. equation 7.11 appears to give a better fit to the data than 7.10.**

These equations have been changed to provide a better fit to the data. Only one exponential type equation is now used.

---

**I-9 Equation 7.13:**

**a) The indexing notation contains an error (second term should start at the second layer, i=2) and the subscript k is not defined (intended to be soil layer). An explanatory diagram was offered to assist the user.**

**b) Should use a slab equation. However, expressing attenuation as a simple exponential rather than as the difference of exponential functions introduces less attenuation than should appear. The effect of this is not clear. It may compensate for ignoring build-up but it would be case dependent. The user would be unaware of the potential error if the approximation is used for thin shields. This approximation may work for some cases but to apply it generally is not sound practice.**

There are now only two soil layers in the soil and groundshine models. The revised equation incorporates the shielding of gamma radiation from the bottom layer by the top soil layer.

The two layer model has been tested in order to establish its validity in modelling the attenuation of radiation from the bottom layer by the layer above. This approach has been shown to be a good representation of the attenuation of radiation from Th-232 and its daughters (see I-7).

**I-10 Equation 7.14: - A tissue density term should appear. We did not discuss the derivation of the coefficient as I had intended, instead we discussed the appropriateness and purpose of using energy absorption coefficients (used to calculate deposited energy by a given photon flux density) and mass attenuation coefficient with build-up (used to calculate the photon flux density).**

A tissue density term is now included. See I-11 below for a discussion of energy absorption and mass attenuation coefficients.

**I-11 Attenuation coefficients: Philosophically, the notion of using energy absorption coefficients instead of mass absorption coefficients to estimate flux density without build-up is attractive. Unfortunately it doesn't work well or the shielding community would have been using this approximation years ago. For thin targets/shields and single energy photons there may be specific situations when the approximation could be valid but the domain of validity is not defined. It is not a valid approach for general usage.**

The use of energy absorption coefficients instead of energy attenuation coefficients to compensate for buildup in gamma flux estimation is applicable under restricted conditions. The application here is restricted with respect to several parameters: shielding medium (soil only); shield thickness (less than 20 cm) and gamma sources (only U-238, Th-232 and their daughters). Gamma dose rates above a layer of contaminated soil have been calculated using this model and compared to published values. The results of the comparison are indicative of the accuracy of the model and the applicability of the use of energy absorption coefficients.

The gamma dose rates above a layer of contaminated soil were calculated using the groundshine model in UTAP.3. The results were compared to NCRP data for the two cases i) Th-232 plus daughters and ii) U-238 plus daughters. The results of the UTAP.3 calculations were within 14% and 37% of the NCRP values for Th-232 and U-238 respectively.

---

**I-12 The energy levels and grouping should be given and explained in the text rather than merely stating where they were taken from (see page 7-5, Chambers _et al_.)**

The table of energy groupings has been included in the revised text.

---

**I-13 The code (Table 7.2) and variable dictionary (Table 7.1) as follows:**

**a) the fifth set of data entry for NNDEC was confirmed to be for radon and daughters.**

Noted.

**b) Energy level data input for radon and daughters is to be checked in light of item 7 (I-7) above, particularly the value 0.331 Mev and other photons that may have been neglected. (rationale for neglecting should be given in text).**

All gamma rays from daughter radionuclides have been included.

**c) The photons at 0.186 Mev would not be included if equation 7.10 and 7.11 are used in the code as stated in the text (They are not).**

Text and equations revised.

**d) MUFLESH. The source reference is to be confirmed.**

Confirmed.

d) **COGDS should be added to the variable dictionary (printout flag from another subroutine).**

Done.

f) **T should be defined in the variable dictionary (time)**

Done.

g) **The units for NDEC and NNDEC in the data dictionary should both be (# photons.$s^{-1}$.$kg^{-1}$). (One is a dummy variable)**

Done.

h) **EMFRAC should be in the variable dictionary (emanation fraction).**

Done.

i) **The indexes N, J, K are to be explained in revised comments preceding the loops.**

The index N has been changed to I throughout the groundshine subroutine (GSHINE) to conform with other subroutines in the program. The indicies I, J and K refer consistently to radionuclide groups, gamma energy intervals and soil layers respectively and therefore, have not been defined at the beginning of each loop.

j) **The energy check logic (bottom of page 1) is incorrect and will be changed:**
   - i) **to coincide with the energy ranges in the regression equations.**
   - ii) **to exclude any photons outside the ranges (which leaves the problem of what to do with any photons that fall outside the**

**range). This restriction should be described in the test so it will not result in user errors when applied to other problems.**

Revised to one regression equation for all energies.

**k) RHOS(K) should be defined in the variable dictionary (RHO(1) and RHO(2) were intended for this).**

Done.

**l) AACT should be defined in the variable dictionary.**

Done.

**m) Code beyond loop 50 (calculations for dose and the SOL subroutine) were not reviewed in light of items 1 to 12 above.**

Noted.

## REVIEW J - MR. P.A. FLAVELLE (24 JULY 1986)

Mr. Flavelle reviewed Vol. 3, Chapter 3 (questions J-1 to J-9) and Vol. 2 (questions J-10 to J-13) of the Phase III documentation.

J-1 Table of Contents, Vol. 3

The current Table of Contents has been revised from earlier drafts. Any cross-referencing to or from other chapters will have to be carefully checked when the volume is assembled.

Noted.

J-2 Page 3-4, Section 3.2.2, first paragraph

The molecular weight (MW) of gypsum is given as 136 g/mole. This is really the MW of $CaSO_4$ (anhydrite). Gypsum, being hydrated calcium sulphate, ($CaSO_4.2H_2$), has a MW of 172. Using 136 will be appropriate only if the value for the mass fraction of gypsum is really the value of the mass fraction of $CaSO_4$.

The reviewer is quite right, the molecular weight of gypsum is 172 g/mol and not 136 g/mol. We chose to refer to anhydrite as gypsum as it was felt that most readers could relate to gypsum whereas anhydrite is a less frequently used term. The anhydrite form (i.e. $CaSO_4$) is used in the UTAP code calculations.

J-3 Page 3-8, Section 3.3.1, Equation 3.3.3

This equation does not balance. From the derivation given in the reference SENES (1984), one reaction product should be ferric oxyhydroxide - $Fe(OH)_3(s)$. The derivation here should be presented in greater detail (at least give the rate-determining reaction explicitly).

The formation of ferric oxyhydroxide occurs only if the pH is sufficiently elevated. In the low pH environment typically observed in the unsaturated zone of pyrite tailings, the ferric iron remains in solution and is rapidly reduced to the ferrous state as additional pyrite is oxidized as suggested by equation (3.3.1). The overall stoichiometry is given by equation (3.3.3) as stated and is in balance.

**J-4 Page 3-8, 3-9, Section 3.3.1, Equations 3.3.8, 3.3.9**

**The calculation of the pyrite oxidation rate constant (equation 3.3.8) implies that $J_S$ is the sulphate flux from the unsaturated zone, at time t=0, and due only to pyrite oxidation with no contribution from dissolution or precipitation of other sulphate minerals. The sulphate production rate used to calculate $J_S$ in equation 3.3.9 must be from both biological and chemical oxidation of pyrite. These conditions on the calculation of the rate constant are not described clearly in the text, and it is also not apparent whether the reaction rate is dependent on the concentration of reaction products.**

The discussion of sulphate flux ($J_S$) and sulphate production rate ($\bar{R}_S$) does indeed apply only to the sulphates produced from pyrite oxidation. The production rate is all-inclusive and incorporates both the bacterial and chemical components. As noted in Section 3.3.1 the interested reader is referred to Halbert et al. (1983) and SENES (1984) for a more detailed discussion. The reaction products do not affect the rate of pyrite oxidation and therefore are not taken into account in the model. A detailed review of the factors affecting the bacteria-assisted oxidation of sulphidic minerals may be found in another SENES report (SENES Consultants Limited, 1984, "Assessment of the Mechanisms of Bacterially Assisted Oxidation of Pyrite Uranium Tailings." Research Report Prepared for the National Uranium Tailings Program, CANMET, EMR).

**J-5 Page 3-67, Section 3.8, Equations 3.8.4, 3.8.5**

**These equations cannot be used to derive the equations for initial conditions (equations 3.7.9, 3.7.10, page 3-54). It appears that the curly brackets are incorrectly placed.**

**The exponential term in these equations is not derived, and it is difficult to attach a physical interpretation to the equation.**

The brackets are correctly placed in the final version of the Phase III reports. A review of equations (3.8.4) and (3.8.5) showed that they could be used to derive the initial conditions given by equations (3.7.9) and (3.7.10) respectively, given the conditions that the initial uranium concentrations in the mixing zone and deep saturated zone equals zero at $t=-\Delta t$. Also, the general form of the exponential term in these equations is used throughout the source model beginning with equation (3.2.4).

**J-6 Page 3-84, Section 3.10.3, first paragraph**

**The assumption that all dissolved radium in the mixing zone is from thorium transported from the layer above should be justified better, considering the changes in pH between layers and the existence of soluble thorium in the mixing layer.**

The discussion in the first paragraph of Section 3.10.3 deals with only one of the sources of radium, that being the radium which has ingrown to the thorium matrix. The reviewer has misinterpreted the discussion in concluding that all dissolved radium in the mixing zone is from thorium. In fact, the other source of radium, that being the radium fraction which is associated with the barium sulphate precipitate, is incorporated in equations (3.10.33) and (3.10.39) presented later in the section.

**J-7 Page 3-92, Section 3.11.2, first paragraph**

**As for the similar assumption about Ra (point 6), this assumption about Pb-210 should be justified better.**

The same observations made above under point J-6 apply here.

**J-8 Page 3-97, Section 3.12, paragraph 1**

**The oxygen diffusivity should be either a function of or correlated to the net precipitation (to account for the effect of moisture content on the tailings air-filled porosity).**

Because the model predictions are made for time steps of not less than one year (and up to ten years), the variation in the annual average moisture content is expected to be minimal. The fact that one year may have more precipitation than another does not necessarily mean that the moisture content varies accordingly. Hence, moisture content is not modelled as a function of (or correlated to) the net precipitation in the UTAP code. Rather, the two parameters are sampled as independent distributed variables.

**J-9 Typographic Errors**

**i) Page 3-1, section 3.1, last sentence**

**This is not a complete sentence.**

**ii) Page 3-20, Section 3.3.5, equations 3.3.50, 3.3.51**

**The rate constant k should be k' in both equations.**

**iii) Page 3-33, Section 3.6.1, equation 3.6.3**

**The equilibrium constant is incorrectly presented; it should read either log K=-2.7 or $K = 10^{-2.7}$.**

**iv) Page 3-66, Section 3.8, equation 3.8.2**

**The left square bracket is missing after the pyrite concentration term.**

Typographical errors have been noted.

**J-10, Vol. 2**

**Page 1-2, Section 1.2, paragraph 1:**

**Third sentence: the program specifications should be available as formal, detailed documents (or sections of a document). Chapter 2 of this volume gives only a general overview of the control modules, without detailed specifications.**

**Sixth sentence: If the development of the modules did not include coding then what did it consist of?**

Although Chapter 2 does, as stated, give a general overview of the control modules, Chapter 3 gives detailed control module specifications. Complete code listings and a variable dictionary are given in Appendix B.

**J-11 Page 1-3, Section 1.2, last sentence:**

**Since verification/validation testing is critical for the acceptance of the package, it is essential that the test plan/specifications/procedures/results be formally documented in detail.**

The quality assurance (QA) program for Phase III was outlined in Appendix A and subsequently has been fully documented in the form of a supplementary report.

**J-12 Section 1.2:**

**There is no mention of configuration control, an independent test group or an independent quality assurance authority.**

There is indeed no mention of configuration control, an independent test group, or an independent quality assurance authority. The quality assurance program implemented in Phase III was consistent with the objectives and specifications of Phase III and the time and money available. Since no provisions were made for carrying this kind of extensive program, a more conservative, but not necessarily less efficient program was implemented. In addition to this, a configuration control program would not have been appropriate in the stages of program development, of which almost all of the Phase III work consisted.

**J-13 Appendix A;**

> **Were the test cases specified by persons independent of the development group?**
>
> **It is essential that the tests (plans/specifications/procedures/results) be formally documented in detail.**
>
> **In the tests (particularly the ones with longer time frames) what were the specific pass/fail criteria?**

As noted in the response to J-12, the QA program was consistent with the objectives of the Phase III study and the time and money available. The tests are documented in the supplementary report to which the reviewer is referred for details. (SENES Consultants Limited, 1987. "Probabilistic Model Development for the Assessment of the Long-Term Effects of Uranium Mill Tailings in Canada - Phase III: Software Development and Quality Assurance Supplementary Report." Research Report Prepared for the National Uranium Tailings Program: CANMET, EMR. Contract #0SQ85-00182).

**REVIEW K - MR. P.A. FLAVELLE (11 AUGUST 1986)**

**Volume 1 of the Phase III documentation was reviewed in this report.**

---

**K-1 The title of the report is different from the title of the other two Phase III volumes: "Probabilistic Assessment of Uranium Mill Tailings: Phase III".**

The titles on all four volumes of the Phase III report have been made consistent.

---

**K-2 Page 2-4, Section 2.1, paragraph 1**

**"What we are entitled to believe" implies an objectivity to the computer predictions. Since the model output is a subjective probability, the phrase "what we feel we are entitled to believe" would more accurately describe the output.**

The actual computer calculations are objective. The selection of models and input distributions is subjective and the interpretation of the output variable is subjective. The end result of the analysis is that, as noted by the reviewer, we can interpret the output variable as a subjective probability telling us quantitatively what we are entitled to believe about the output variable.

---

**K-3 Page 2-4, Section 2.2, paragraph 2**

**For the sample frequency histograms to approach the true population probability curves, not only does the number of trials have to increase but the number of cells in the histograms has to increase (i.e. the cell size must decrease to smooth the histogram).**

We concur and have revised the writeup to reflect this point.

**K-4 Page 2-11, Section 2.5, paragraph 3**

> **This method of sampling time-varying (stochastic) variables is not valid for autocorrelated variables (i.e. when the value in a time step can be correlated to the value in an earlier time step).**

We concur that the method does not apply to sampling autocorrelated variables. However, we do not believe that any of the variables which are treated as time-varying inputs in the UTAP code (i.e. mean annual precipitation and mean annual wind speed) are autocorrelated. Hence, we have not dealt with this aspect.

**K-5 Page 2-15, Section 2.8**

> **It is not clear how or if the parameter correlations are used to ensure consistent conditions within a simulation (e.g. that sampled values of tailings moisture content, revegetation half-life and thickness of unsaturated zone are all consistent with the sampled value of net precipitation in a simulation).**

The discussion in Section 2.8 outlines the approach to incorporating correlated parameters which have been included in the UTAP code. A discussion of the approaches to identifying correlated parameters is also presented. As noted in this section, we have chosen to model parameters as explicit functions of other parameters whenever possible. The correlated parameter technique was used only to investigate the radon flux model. The possible correlations suggested above do not apply, in our opinion, to the UTAP code, which is based on a minimum of one-year time steps (with up to ten-year time steps) and assumed annual (or ten-year) average values for input parameters. The average annual moisture content of the unsaturated zone of the tailings is more a function of the possible range of the particle size distribution (or porosity) of the tailings than to the average annual precipitation which rapidly infiltrates the tailings mass. Similarly, revegetation of the tailings surface area is dependent upon the establishment of suitable pH conditions and not on whether there is sufficient rainfall in any particular year.

---

**K-6 Page 3-4, Section 3.3.1, paragraph 2**

**There is no discussion of a water balance calculation to get the thickness of the unsaturated zone, or of the need to correlate the sampling of the thickness of the unsaturated zone (constant throughout a simulation) with the sampled values of the net precipitation (sampled at each time step).**

The water content of the tailings is much more a function of the physical characteristics of the tailings solids and the height above the water table, than it is of the amount of annual precipitation. Because the time of travel of water infiltrating the unsaturated zone is much shorter than the size of the time step of the simulation (i.e. minimum of one year), we are only interested in the average moisture content of the tailings. Similarly, we are not interested in the short term variations in the height of the water table. Rather, we are interested in taking into account the possible range in variability of these parameters. This is achieved by sampling the specified distributions for these parameters at the start of each simulation trial.

---

**K-7 Page 3-6, Section 3.3.1, paragraph 4**

**There is no description of the assumptions concerning mineral dissolution/precipitation in the saturated zone.**

The principles governing the dissolution of chemical precipitates discussed in Section 3.3.1 apply to the unsaturated and saturated zones. The discussion in this section is only intended to provide an overview of the concepts used in modelling the movement of chemical and radioactive species in the tailings source term. The reader interested in a more detailed discussion of the processes governing the dissolution and reprecipitation of the species modelled within the source term are referred to Chapter 3 of Volume 3 of the

Phase III report.

**K-8 Page 3-7, Section 3.3.1, paragraph 1**

**One aspect of revegetation that is part of the program but is not mentioned here is that when the pH falls below 4.0, not only does revegetation cease, but existing vegetation disappears from the tailings.**

The assumption in the revegetation model was that a vegetative cover would not develop on a pyritic tailings area until after a substantial fraction of the pyrite had oxidized allowing the pH in the tailings porewater to recover above 4.0. Since it is unlikely that the pH would again fall below 4.0, given that most of the pyrite would have oxidized in the elapsed time interval, the provision was not built into the model for vegetation to disappear. This is a possibility, however, under certain options. For example, if limestone was added to the tailings during placement then the pH of the tailings porewater would remain above 4.0 for as long as the limestone remained effective. A vegetative cover would be established during this time. However, it is likely that the pH would eventually drop below 4.0 once the limestone was consumed. In this instance, the vegetative cover may well deteriorate. Revision of the code to account for this circumstance was undertaken subsequent to the Phase III study.

**K-9 Editorial errors**

**Page 1-1, Section 1.1, paragraph 2**

**A "+" sign appears in the second sentence.**

**Page 2-6, Section 2.3, paragraph 1**

**Should "in the content of the scenarios" read "in the context of the scenarios"?**

**Page 5-3, Section 5.2.1, paragraph 3**

**The second sentence is missing an article.**

**Page 5-7, Section 5.2.2, paragraph 2, and Figure 5.7**

**Figures 5.7 (A) and (B) have been reversed, either in Figure 5.7 or in this paragraph comparing the two curves. There is also one reference in this paragraph to Figure 5.6b instead of 5.7b.**

Noted.

## APPENDIX A:

The Draft version of this report was reviewed and subject to certain reservations, endorsed by MORG. This appendix contains a list of those responses about which the MORG had some reservations but did not have sufficient time or resources to undertake a more detailed review.

# ATTACHMENT B

This is a list of responses about which we have some reservations. Our reservations about the responses are not identified individually. In some cases it is because scheduling constraints have not allowed a more detailed review. In othe cases the response is not clear, or engenders secondary questions, but budgetary restraints preclude entering into a dialogue with the authors. In all cases we do not expect the documents which are the subject of the comments to be modified, since they have already been published. This list is compiled for recording purposes only.

**Review A**

We have not verified the editorial changes made in the documents.

**Review B**

Responses B-3, B-6 and B-7.

**Review C**

We have not had the opportunity to review the separate QA document referred to in these responses.

**Review D**

Responses D-3, D-14, D-15, D-17, D-20 and D-31.

**Review E**

Response E-1.

**Review F**

Response F-4.

**Review G**

We have not had the opportunity to review the corrections to the computer code.

**Review H**

Responses H-3, H-4, H-5, H-7, H-9 and H-11.

The statistical testing appears to be designed to accept the null hypothesis, precluding an evaluation of $\alpha$. How the test results are interpreted is still not clear. There is still a need to examine the effect on the final conclusions of accepting an incorrect hypothesis ($\beta$ or type 2 error).

Response H-20.

**Review I**

The responses indicate that essentially a new shielding model has been devised. We have not yet had the opportunity to review this revised model, so we cannot comment on most of these responses (excepting I-7 - see Attachment A).

**Review J**

Responses J-5 and J-8.

**Review K**

Responses K-6 and K-8.

## APPENDIX B:

The attached comments were received after MORG review of the Draft version of this report. Although not addressed in this report, they have been included in this Appendix as a matter of record.

# Comments on Volume I and III of UTAP
# Phase III Model Documentation

Comments are grouped into two parts, Part 1 dealing with dosimetric considerations and Part 2 with pathways analyses. Since Volume III repeats most of Volume I, many comments apply to both volumes. In addition, some modifications suggested may not necessarily need to be incorporated in the UTAP model documentation but should be taken into account when reviewing licensees' applications to the AECB.

## Part I: Dosimetric Considerations

III p. 13.5: In the derivation of dose conversion factors for total thorium, ratios between Th-232 and Th-230 are used. SENES states that "natural thorium to thorium-230 ratio is relatively constant in water whereas, this ratio changes with time in the near-surface tailings". This statement is neither qualitatively nor quantitatively supported in the documentation. Unless, a convincing argument is made for the use of ratios in the derivation of a dose conversion factor for total thorium, I suggest that doses from Th-232 and Th-230 be calculated separately.

I p. 3.12 and III p. 13-1: It should be made clear in the document that the term "annual average effective dose" refers to the average derived from probabilistic calculations and does not refer to either the "average receptor" or some other averaging of the dose.

I p. 5.2: It is unclear whether the UTAP model is programmed to calculate collective dose for users wishing to do so.

I p. 5.3: The resulting doses over time of scenario 1 is significantly higher than those from scenario 2, but not by "much".

## Part 2: Pathways Analyses

I p. 4.1: Some attempt to rationalize the spatial (50 m) and temporal (1000 a) delimiting criteria should be made in the documentation.

I p. 3.2, 4.6 III p. 11.1, 13.13, 13.18: The critical group, as assumed in the UTAP modelling exercise for disposal scenarios 1 and 2, is not necessarily conservative for the concerned areas. Assumptions used in the UTAP documentation for e.g., intake of certain foodstuff, time spent outdoor, could be higher for certain groups such as native people (AECB staff has received the results of a questionnaire given to native people in the Elliot Lake area which revealed that a significant portion of the diet comes from trapping rabbit, beaver and hunting grouse; wild rice was also part of some diets. These foodstuffs were not examined in the UTAP modelling exercise).

| | |
|---|---|
| I p. 3.3, III p. 12.7: | Licensees should be aware that the transfer factors used in the UTAP documentation are not necessarily approved by the AECB (e.g., uptake of radionuclides by fish, by moose). |
| I p. 5.6, III p. 11.1: | The depletion of fish stock due to the increase in pH would not necessarily mean a decrease of fish intake by the critical group. For the sake of conservatism, I suggest that the intake rate remains constant over the 1000 a period. |
| I p.5.2 - 5.7: | Couldn't ground water seep to a drinking-water well situated at 1 km from the tailings over 1000 a? If so, why wasn't this pathway considered. |
| I p. 3.8 II p. 4.1 - 4.5: | In order to obtain the total radon flux for the tailings area, the annual average radon flux must be multiplied by the surface area. This surface area should take into account the presence of vegetation. SENES assumes no influence from the vegetation; their assumption is based on a study done by DSMA ATCON on Elliot Lake tailings (NUTP, report no. 1357/1335). This consultant did not observe any significant differences in radon flux from vegetated or unvegetated areas on the tailings. DSMA ATCON deduced that the root system is therefore an effective diffusion barrier against radon. Other studies give contradictory results: for example, Pearson and Jones' (1966) measurements indicate that corn plants may have a seven-fold higher flux than the soil in which they grow in. Since the leaf-area-index for most vegetated areas is greater than 1, a very large flux density may result on an area basis. Therefore, it is suggested that SENES introduce a coefficient in equation 46. (p. 4.5, vol. 3) which would take into account the presence of vegetation in order to conservatively estimate the dose received from inhalation pathway. (See letter from C. Létourneau to R. Holmes, 86.04.16.) |

C42/9

# Volume

# 6

# NATIONAL URANIUM TAILINGS PROGRAM

Energy, Mines and Resources Canada
Énergie, Mines et Ressources Canada

Canada

# PROBABILISTIC MODEL DEVELOPMENT FOR THE ASSESSMENT OF THE LONG-TERM EFFECTS OF URANIUM MILL TAILINGS IN CANADA - PHASE III

## SOFTWARE DEVELOPMENT AND QUALITY ASSURANCE SUPPLEMENTARY REPORT

A Research Report Prepared Under
Contract # 0SQ85-00182

for

The National Uranium Tailings Program
Canada Centre for Mineral and Energy Technology
Energy, Mines and Resources Canada
555 Booth Street
Ottawa, Ontario
K1A 0G1

SENES Consultants Limited
499 McNicoll Avenue
Willowdale, Ontario
M2H 2C9

169 pp

April 1987

MICROMEDIA

# ABSTRACT

This report represents part of the ongoing efforts of the National Uranium Tailings Program (NUTP) to develop the capability to predict the long-term effect of Canadian Uranium Mill Tailings. The principal output from these studies has been the development of a comprehensive Uranium Tailings Assessment Program (UTAP). The UTAP program incorporates a Monte Carlo procedure which permits the user to enter input parameters as probability density functions rather than as single numbers and to calculate frequency distributions for output variables.

The Phase III report which describes the UTAP program was prepared in four volumes, namely a summary report (Volume I), a report describing the systems level structure of UTAP (Volume II), a report describing the simulation model (Volume III), and a program users manual (Volume IV).

The quality assurance activities carried out as part of the Phase III model development program are discussed in various parts of the Phase III report. Subsequently it was considered that a consolidated discussion of Phase III quality assurance activities would be helpful not only with regard to providing insight as to the "quality" of the generic UTAP code developed in Phase III of the NUTP modelling program, but also to provide insight as to quality assurance activities which might be useful in subsequent UTAP model developments or applications.

---

# NOTICE

This report was prepared by SENES Consultants Limited (SENES) under contract to the National Uranium Tailings Program (NUTP). Neither the NUTP nor SENES makes any warranty, expressed or implied, or assumes any liability with respect to any damage or loss incurred as a result of the use made of the information contained in this publication.

## TABLE OF CONTENTS

Page

Abstract i

Notice i

1.0 INTRODUCTION 1-1
  1.1 Background 1-1
  1.2 The Concept of Probabilistic Analysis 1-2
  1.3 Definition of Quality Assurance 1-4
    1.3.1 Requirements, Objectives and Specifications 1-6
    1.3.2 Internal Design, Review and Coding 1-7
    1.3.3 Documentation 1-8
    1.3.4 The Scope of This Report 1-9

2.0 PROGRAM VERIFICATION 2-1
  2.1 Outline of Phase III Test Program 2-1
  2.2 The Control Module Test Program 2-1
  2.3 The Component Model Test Program 2-3
    2.3.1 Outline of Test Program 2-3
    2.3.2 Hand Calculations 2-3
    2.3.3 Test at Limits 2-5
    2.3.4 Test for Reasonableness 2-6
  2.4 The System Model Test Program 2-10
    2.4.1 Overview of Test Program 2-10
    2.4.2 Test 1 - Check for Computational Accuracy 2-10
    2.4.3 Test 2 - Check for Parameter Initializiation 2-12
    2.4.4 Test 3 - Check of Probabilistic Sampling 2-13
    2.4.5 Test 4 - Reasonableness Check Using Probabilistic Inputs 2-14
    2.4.6 Test 5 - Reasonableness Check of Depyritized Tailings Option Using Nominal Input Values 2-21
    2.4.7 Test 6 - Sensitivity Analysis 2-23

Table of Contents (continued)

2.4.8 Test 7 - Check of Model Stability Using Many Trials 2-26

2.4.9 Test 8 - Check of Model Stability Using Many Time Steps and Nominal Inputs 2-32

2.4.10 Test 9 - Check of Model Stability Using Many Time Steps and Probabilistic Inputs 2-33

3.0 SUMMARY 3-1

REFERENCES

APPENDIX A Testing of Random Number Generator UNIRAN

APPENDIX B Tests of Control Module Sampling Routines

APPENDIX C Comparison of Selected Probabilistic Assessment Tools

## LIST OF FIGURES

| | | Follows Page |
|---|---|---|
| 1.1 | Concept of Probabilistic Analysis | 1-3 |
| 1.2 | Macro Model of Software Development | 1-5 |
| 1.3 | The System Model | 1-8 |
| 2.1 | Subsurface Transport (Same Half-Life) | 2-7 |
| 2.2 | Subsurface Transport (Same Distribution Coefficient) | 2-9 |
| 2.3 | Plots from Test 3 for Two Probabilistic Trials | 2-13 |
| 2.4 | Tailings Porewater Sulphate Level From Test 4 Scenario 1: Base Case | 2-15 |
| 2.5 | Tailings Porewater Calcium Levels From Test 4 Scenario 1: Base Case | 2-15 |
| 2.6 | Tailings Porewater Iron Levels From Test 4 Scenario 1: Base Case | 2-15 |
| 2.7 | Tailings Porewater pH From Test 4 Scenario 1: Base Case | 2-15 |
| 2.8 | Concentrations of Radionuclides from Test 4 for Ten Probabilistic Trials | 2-17 |
| 2.9 | Dose by Pathway from Test 4 for Ten Probabilistic Trials | 2-19 |
| 2.10 | Cumulative Tailings Depletion and pH From Test 4 | 2-20 |
| 2.11 | Tailings Porewater pH From Test 5 Scenario 2: Depyritized Tailings Cover | 2-22 |
| 2.12 | Solution of pH Equation From Test 7 | 2-25 |
| 2.13 | pH in First Lake for Test 7 for 1000 Probabilistic Trials | 2-26 |
| 2.14 | Total Dose by Radionuclide From Test 7 for 1000 Probabilistic Trials | 2-28 |
| 2.15 | Total Dose by Pathway From Test 7 for 1000 Probabilistic Trials | 2-30 |

# LIST OF TABLES

| | | Follows Page |
|---|---|---|
| 2.1 | Model Test Form | 2-1 |
| 2.2 | Sample of Hand Calculations for River Model | 2-4 |
| 2.3 | Hand Calculations Compared to Output From Air Dispersion Model | 2-5 |
| 2.4 | Test of Convergence of Iterative Flux Solution in Groundshine | 2-6 |
| 2.5 | Example Output from Air Dispersion Model | 2-7 |
| 2.6 | Example of Error Found in Soil Model by Test 1 | 2-11 |
| 2.7 | Output from Soil Model Corrected After Test 1 | 2-11 |
| 2.8 | Doses (uSv) from Test 2 - Two Deterministic Trials | 2-12 |
| 2.9 | Corrected Water Concentrations (Bg/m$^3$) From Test 2 - Two Deterministic Trials | 2-13 |
| 2.10 | Detailed Printout from Water Model-Sensitivity Index Program | 2-24 |
| 2.11 | Parameter Sensitivity Index Values for the Base Case | 2-26 |
| 2.12 | Selected Parameter Definitions | 2-26 |

# 1.0 INTRODUCTION

## 1.1 Background

In 1982 Energy, Mines and Resources Canada established the National Uranium Tailings Program (NUTP) to pull together previous work on Canadian uranium mill tailings, to fund additional work where significant information gaps were found and to develop the capability to predict the long-term effects of tailings with a known degree of confidence while incorporating variability and uncertainty in the input data. Such evaluations require the use of mathematical models to simulate the behaviour of the real system.

Traditionally, mathematical models have been evaluated in a deterministic fashion. Specifically, this means that a single value is selected for each input parameter of the simulation model(s) resulting in a single estimate of some environmental consequence such as dose to an individual in the critical group, or pH in a downstream lake. However, by their very nature, models are at best imperfect reflections of real systems. Moreover, many of the parameters used as inputs to the models are either imperfectly known or inherently variable. Over the past decade or so considerable effort has been directed at developing techniques for explicitly incorporating such uncertainty (and variability) directly into the model prediction. In general terms we refer to this as probabilistic analysis.

One of the early studies funded by the NUTP demonstrated how probabilistic techniques could be used to take account of the variability and uncertainty in model input parameters in such a simulation analysis (SENES, 1984). A subsequent study (Phase II) extended the system model to incorporate temporal variability (SENES, 1985).

The most recent study, Phase III, sponsored by the NUTP, further extended the capabilities of the Phase II system model to include spatial variability and applied the new system model to an expanded hypothetical reference site. At the Phase III level of development, the mathematical models are a mix of quite complex component models (e.g. the tailings source term) and simpler aggregate models (e.g. transfer of radionuclides from water to fish flesh). The components are coded as independent modules with information transfer between modules managed by a common control module. This approach provides a flexible structure which can easily accommodate changes in component models and model input parameters. The computer implementation of these models (along with the probabilistic infrastructure) is known as the Uranium Tailings Assessment Program (UTAP).

In developing a complex computer model of a physical system, such as UTAP, every reasonable effort must be made to ensure that the mathematical abstractions are correctly implemented in computer code. The concept is commonly referred to as model verification. It is achieved through implementation of software quality assurance (QA) measures which are inherent in any good software development program.

In Section 1.3, some relevant concepts regarding both software development and software quality assurance are summarized. The approach taken by SENES to both in the Phase III study is then discussed. Finally, results and examples of the Phase III QA program are presented. Thus, this report acts as a summary of the quality assurance measures taken throughout the development of the Phase III Uranium Tailings Assessment Program.

Before moving on to this subject however, it is appropriate to briefly review the modelling framework within which UTAP was developed.

## 1.2 The Concept of Probabilistic Analysis

As with any predictive assessment, probabilistic analysis involves a mathematical expression (model) of some system, in this case a uranium mill tailings site. The model is a mathematical expression to which information is supplied in the form of numerical values for one or more input parameters and the corresponding numerical values of one or more output variables are produced.

Most of the input parameters required by such a model are not known with certainty. The uncertainty arises because of normal experimental error in their measurement or because actual measurements are impossible and judgement must be used. Also, some input parameters such as mean annual wind speed or mean annual precipitation necessarily vary from year to year. Consequently, most input parameters cannot be adequately characterized by any single number. Fortunately, any input parameter can be described in the form of a (subjective) probability distribution.

Having specified the input distributions, it is necessary to determine the corresponding values of the output variables. Because many of the input parameters are specified as distributions, rather than as single numbers, distributions, rather than single numbers, will be obtained for the calculated variables. The distribution of calculated results is obtained by using a statistical sampling or Monte Carlo procedure which involves drawing many samples from each input parameter distribution. The procedure, illustrated in Figure 1.1, is a repetitive one. At each repetition a single value for each input parameter is drawn from its probability distribution. These values of the input parameters are substituted into the mathematical model to obtain a single value for each output variable. This process, which is referred to as a trial, is then repeated as often as desired. For further details, the interested reader is referred to Appendix B of the Phase I study (SENES, 1984) and Volume 2 of the Phase III report (SENES, 1986).

The set of output values for a variable(s) from such an analysis can be considered as a sample(s) on an objective random variable(s) corresponding to that output variable(s). From the sample the mean, variance, probability density function (pdf) or cumulative distribution function (cdf) may be estimated as desired. This information may be interpreted as describing the output variable in terms of subjective probability; telling us quantitatively what we are entitled to believe about the value of the output variable.

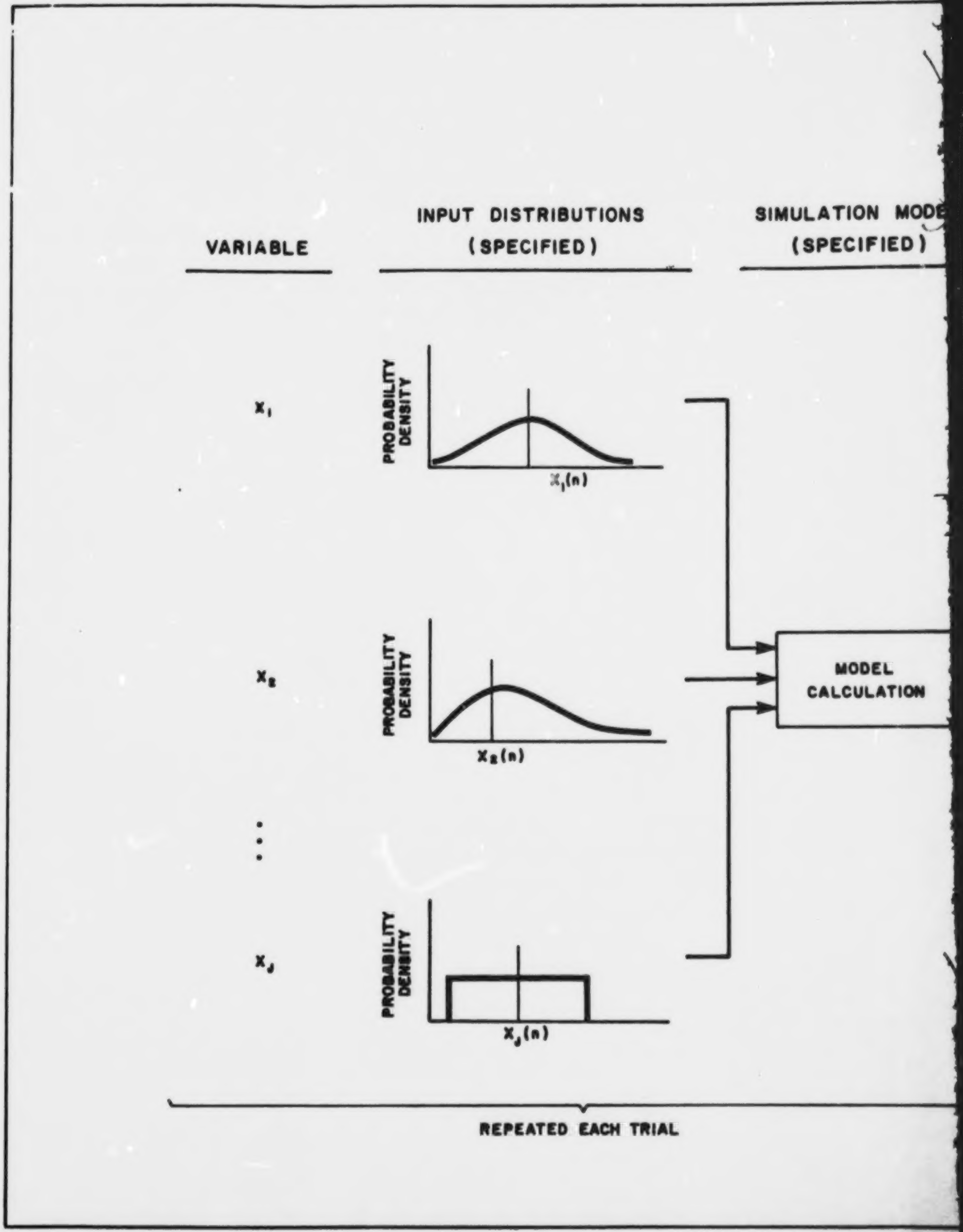
VARIABLE
INPUT DISTRIBUTIONS
(SPECIFIED)
SIMULATION MODE
(SPECIFIED)
X1
PROBABILITY DENSITY
X1(n)
X2
PROBABILITY DENSITY
X2(n)
XJ
PROBABILITY DENSITY
XJ(n)
MODEL CALCULATION
REPEATED EACH TRIAL

FIGURE 1.1

CONCEPT OF PROBABILISTIC ANALYSIS

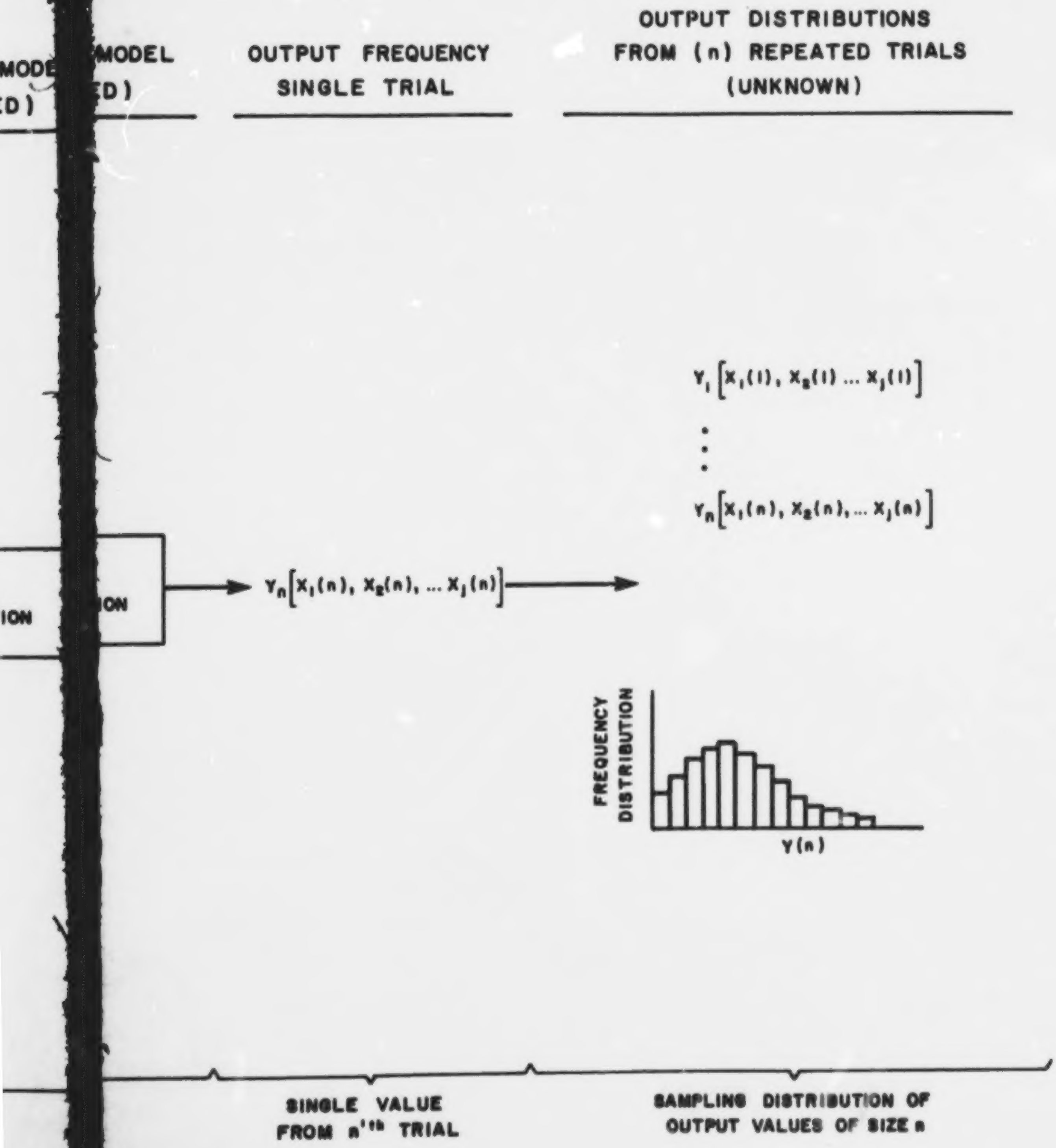
MODE
D)
MODEL
ED)
OUTPUT FREQUENCY SINGLE TRIAL
OUTPUT DISTRIBUTIONS FROM (n) REPEATED TRIALS (UNKNOWN)
$Y_1[X_1(1), X_2(1) \dots X_j(1)]$
$Y_n[X_1(n), X_2(n), \dots X_j(n)]$
ION
ION
$Y_n[X_1(n), X_2(n), \dots X_j(n)]$
FREQUENCY DISTRIBUTION
Y(n)
SINGLE VALUE FROM n'th TRIAL
SAMPLING DISTRIBUTION OF OUTPUT VALUES OF SIZE n

## 1.3 Definition of Quality Assurance

Many current definitions of QA are vague and general: i.e. **"QA will include application of systematic programming techniques and the use of QA tests"** (Lyon, 1982) or **"QA will ensure that a software product conforms to (meets or exceeds) prespecified standards"** (Bryan and Siegal, 1984). The Technical Advisory Committee (TAC) for the Canadian nuclear waste disposal program claimed that **"Current state-of-the-art methods of assuring software reliability are already available at the operational level and are also very promising at the research level"** (TAC, 1981). Since the "tests" of the first definition and the "methods" of the third are unspecified, much latitude is allowed in selecting a QA methodology.

For example, the developers of the SYVAC2 program appear to have adopted a method known as "error seeding" as their final QA test (Andres, 1982). This method involves deliberately placing a specified number of random, artificial errors into the final program. By examining the relative number of "planted" and "natural" (unplanted) errors discovered by a testing team, some estimate of the number of natural errors remaining, and hence of the acceptability of the program can be made. In their own words, **"The ultimate test of the quality of SYVAC2 in our approach will be (this) final QA test"** (Andres, 1982). However, a number of obvious flaws in this method were pointed out by J.D. Musa (1980). Musa claims that it is difficult in practice to generate random, artificial faults that are equivalent to natural faults. Since it is usually easier to find the seeded faults, the number of remaining natural faults will likely be underestimated using this method. There is also the problem of determining what is actually an "acceptable" number of natural faults remaining.

This example merely illustrates the problem of defining an acceptable QA method. For the sake of clarity, and with the goal of an "acceptable" definition in mind, it is probably best to use the definitions presented in an IEEE/ANSI Standard (1981). They define QA as **"A planned and systematic pattern of all actions necessary to provide adequate confidence that the item**

**or product conforms to established technical requirements."** In this definition, it might be assumed that "adequate confidence" and "established technical requirements" imply mutual acceptability to both the program developer and ultimate user.

Two terms encountered frequently in discussions of software QA are verification and validation. Software verification can be defined as **"the process of determining whether or not the products of a given phase of the software development cycle fulfill the requirements established during the previous phase".**(Boehm, 1984). More succinctly, it implies constantly asking and answering the question, **"Am I building the product right?".** This is probably the most useful definition, and as such, verification will form an integral part of the software QA strategy. Software validation is when a **"model with its previously defined parameters is applied in a new situation and its results are compared with field or laboratory experiments"** (Broissia, 1986).

Most authors emphasize that it is very difficult to prove that a large program is 100% correct. "**In general, it is impractical, often impossible to find all the errors in a program**" (Myers, 1979). Since one cannot test a program to ensure that it is error free, and since it is fairly safe to assume that there are errors in a program, testing should concern itself with finding as many of these errors as possible. Testing, with this goal in mind, can help improve confidence that the program in fact does (sufficiently well) what it is supposed to do and more importantly does not do something that it is not supposed to do. The best way to establish confidence that the program is "perfect" is to try to disprove it; **"that is, to try to find imperfections rather than just confirm that the program works correctly for some set of input data"** (Myers, 1979).

A conceptual model of the software development/QA process is shown in Figure 1.2 (Myers, 1976). This model does not attempt to rigidly define stages that should occur in program development, but merely reflects the common top-down programming structure (i.e. general to specific). The significant features of

FIGURE 1.2

## MACRO MODEL OF SOFTWARE DEVELOPMENT

**DEVELOPMENT ACTIVITY**

DESCRIPTION OF PROBLEM TO BE SOLVED (STATEMENT OF USER REQUIREMENTS)

TRANSLATING REQUIREMENTS INTO PROGRAM OBJECTIVES

STATEMENT OF EXTERNAL SPECIFICATIONS (DESCRIPTION OF SYSTEM BEHAVIOUR FROM USER'S POINT OF VIEW)

TRANSLATE EXTERNAL SPECIFICATIONS INTO INTERNAL SPECIFICATIONS (FLOWCHARTING)

CODING

**DEVELOPMENT SEQUENCE**

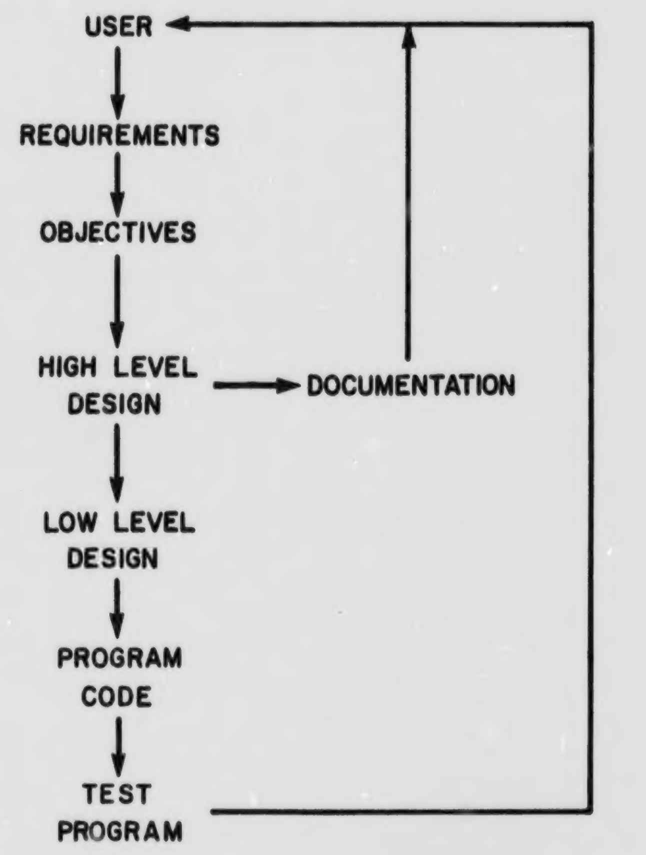
USER
REQUIREMENTS
OBJECTIVES
HIGH LEVEL DESIGN
DOCUMENTATION
LOW LEVEL DESIGN
PROGRAM CODE
TEST PROGRAM

SOURCE: AFTER MYERS, 1976

this model are the various "translations" that occur (development activities in Figure 1.2). These translations represent a communication process between the ultimate user and the software developer. Thus, software errors, representing communication breakdowns, mistakes and/or noise (i.e. random errors) can arise during any one of these activities. A good QA strategy will attempt to avoid and detect faults during all of these processes.

The fundamental goal of any software development program is the production of a high quality computer program. A quality assurance program possesses this same goal, hence the terms "software development program" and "software quality assurance program" are used interchangeably. A high quality computer program is simply defined as one that performs it's intended function. A software development or QA program is defined as a systematic pattern of activities with the goal of producing a product that conforms to established criteria. These "established criteria" are explicit statements of the product's intended function. The formulation of these criteria is discussed in the next section.

### 1.3.1 Requirements, Objectives and Specifications

The first step in the software development program was the establishment of quality criteria. All subsequent tasks were designed to produce a model that satisfied these criteria. The generation of quality criteria is a critical phase in the software development process since failure to specify what is wanted inevitably results in failure to produce what is wanted. The process involved three stages. Firstly, a set of user requirements were formulated. Secondly, these requirements were synthesized into a set of program objectives. Finally, these objectives were translated into a set of specifications referred to as external specifications on Figure 1.2.

For the three-step procedure to be effective the user and developer must interact in a feedback review process. The final product of this process is a formalized written document detailing the objectives and specifications for the program. In the Phase III software development process, a formalized set of Objectives and Specifications were submitted to the client for review. Subsequently, with the client's comments incorporated, these objectives and specifications served to direct the software development process.

The underlying objective of the Phase III studies was to extend the capabilities of the Phase II system model and then to apply the Phase III system model to an expanded hypothetical reference site. Among the tasks addressed in Phase III were:

- expand the simulation models to include additional major radionuclides and water erosion of tailings cover materials
- expand the simulation models to include additional selected pathways of exposure
- modify the system model to permit air dispersion calculations to be carried out to greater distances in all directions
- modify the system model to permit water dispersion calculations to be performed on an entire watershed
- streamline the system code, update the documentation and prepare a user's manual

As well, some special activities related to the development, use, or interpretation of probabilistic assessment codes were carried out, including:

- an extensive program of software quality assurance including: testing of the random number generator; an intercomparison study with two other probabilistic assessment codes; testing of the system's control modules; and testing of the Phase III component modules, both on a stand alone basis and integrated within the system model
- further investigation of the use of aggregate models in environmental assessment.

### 1.3.2 Internal Design, Review and Coding

Once the objectives and specifications had been formalized the process of internal design commenced. As an initial step, the internal structure of the model was decomposed into several modules. The logical order of the modules and the interrelationship between the modules was then established. Only after the internal structure of the model had been developed did detailed work commence on the modules.

UTAP is comprised of two basic types of modules. The computer implementations of the mathematical models used to simulate uranium mill tailings and the environment are referred to as component modules, while those which provide the probabilistic framework for the simulation are referred to as control modules (see Figure 1.3).

In the case of the component modules, the mathematical model details, including the species to be modelled, spatial, temporal and other considerations were translated into a series of mathematical formulae and accompanying assumptions. These formulae were often then incorporated into a flowsheet illustrating the algorithm required for implementation.

In the case of control modules, an iterative flowcharting and design process was undertaken until the input/output characteristics indicated in the objectives and specifications were achieved. The control module design, review and coding preceded most of the component model coding. This allowed component models to be coded and tested within the system model context and served as a test of the control modules.

### 1.3.3 Documentation

Effective documentation is an important feature of a software development program. Documentation must be done in parallel with model development. This allows assessment of the mathematical models to be used in the simulation, facilitates communication between team members, allows documentation to evolve through a critical review process and provides a record of the software development history. Documentation starts at the requirements/objectives/specifications stage discussed earlier and evolves towards a

FIGURE 1.3

THE SYSTEM MODEL

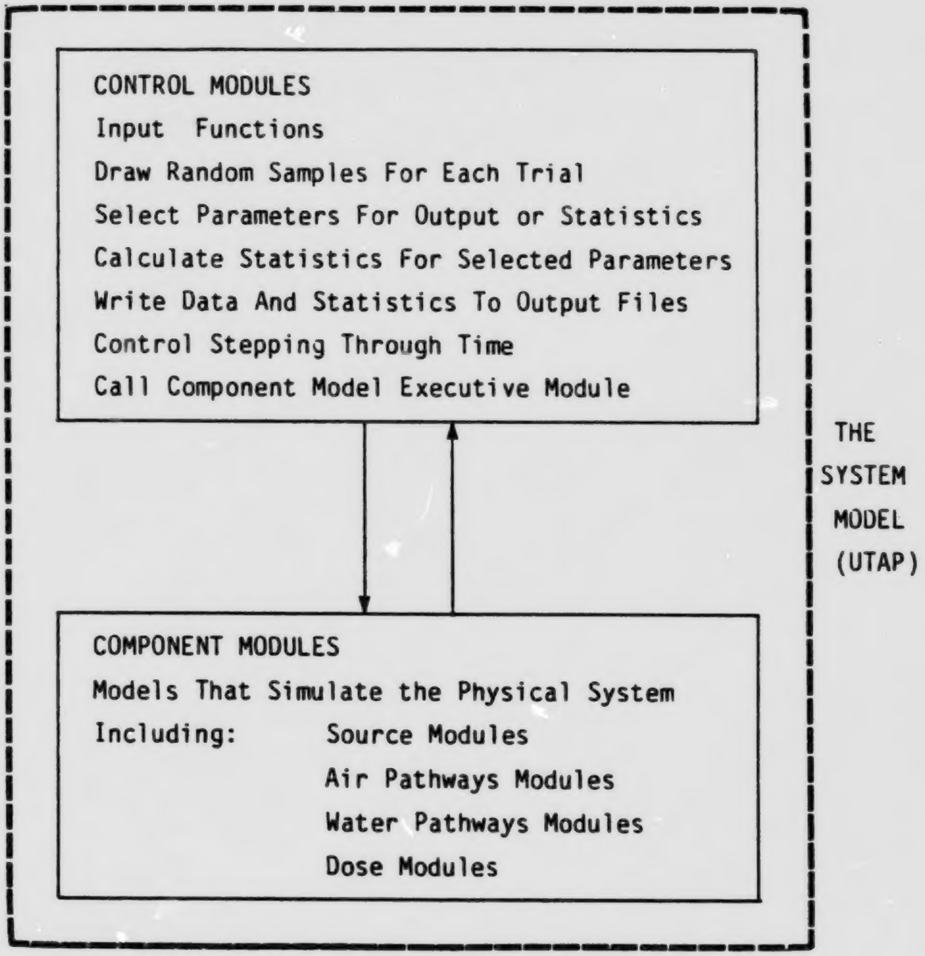
CONTROL MODULES
Input Functions
Draw Random Samples For Each Trial
Select Parameters For Output or Statistics
Calculate Statistics For Selected Parameters
Write Data And Statistics To Output Files
Control Stepping Through Time
Call Component Model Executive Module
COMPONENT MODULES
Models That Simulate the Physical System
Including:
Source Modules
Air Pathways Modules
Water Pathways Modules
Dose Modules
THE SYSTEM MODEL (UTAP)

complete description of the mathematical algorithms, assumptions, techniques and theories used in the program. Use of flowcharts facilitates readability and enhances the iterative review/revision process.

Because the Phase III studies covered a variety of aspects of substantially different form and content and because of the sheer volume of material, the Phase III documentation was prepared in the following four volumes:

Volume 1: Probabilistic Model Development for the Assessment of Uranium Mill Tailings in Canada - Phase III, Volume 1: Summary Report.

Volume 2: Probabilistic Model Development for the Assessment of Uranium Mill Tailings in Canada - Phase III, Volume 2: System Description and Control Module Documentation.

Volume 3: Probabilistic Model Development for the Assessment of Uranium Mill Tailings in Canada - Phase III, Volume 3: Component Model Documentation.

Volume 4: Probabilistic Model Development for the Assessment of Uranium Mill Tailings in Canada - Phase III, Volume 4: Uranium Tailings Assessment Program (UTAP) User's Manual.

### 1.3.4 The Scope of This Report

The software QA program implemented in the Phase III study involved a number of different activities consistent with the objectives of the Phase III study and the time and funding available. Initially, considerable effort was directed at adequately defining objectives and specifications for the overall program. Subsequent efforts focussed on specifying the details of the components which comprise UTAP. A constant feedback process by which the objectives and specifications and the program documentation were continuously revised was maintained while the components were developed and implemented. The QA efforts then focussed on testing the various components and finally testing the integrated system. The first part of this development process was undertaken by component model developers, interacting on an informal basis while the latter testing program of the integrated system followed a more rigid, structured course.

The QA program for Phase III was conducted with the sole intent of answering the question **"Am I building the product right?"** The intention was never to provide formal documentation of the QA program and as a consequence much of the extensive test program that was carried out was, unfortunately, either poorly documented or not documented at all. When errors in the coding of the program or in the mathematical model itself were found they were, for the most part, corrected spontaneously and not recorded. As a further consequence of the informality of the test program, the quality of printouts, notes, and hand calculations is, for the most part, such that they are not reproducible. Many of the actual results presented in this report, although they are indeed the original results, have been retyped, rewritten, or otherwise touched up as appropriate so that the results could be presented here in a more understandable, legible form.

In addition to the QA procedures noted above, several other focussed QA studies were undertaken. One such study involved detailed investigation of the random number generator (UNIRAN). These tests are documented completely in Appendix A. The sampling routines used to generate probabilistic distributions were also fully tested as described in Appendix B. Another study involved comparing the probabilistic results generated by SENES with those generated by two other systems, for a common example. This study is documented in Appendix C. These studies indicated that the probabilistic components of UTAP are fundamentally sound and function as expected.

As suggested by the foregoing, various aspects of the Phase III software quality assurance program have already been documented by various investigators in various ways and in various places in existing reports. In view of this observation and with future development and testing of UTAP in mind, it was felt that a consolidated overview of the Phase III software quality assurance activities was worthwhile. Such a consolidation is the objective of this supplementary report. In addition to consolidation of existing software quality assurance documentation, additional materials outlining the software testing program used in Phase III are also provided. Some aspects of the Phase III software quality assurance program were more effective than others. It is hoped that future UTAP users and developers will benefit from these features.

## 2.0 PROGRAM VERIFICATION

### 2.1 Outline of Phase III Test Program

The test program used in the Phase III studies was divided into three major areas:

1) Tests of the Control Modules including the Random Simulation Tool
2) Tests of the Component Models
3) Tests of the System Model

The test program attempted to evaluate the models for both computational accuracy and reasonableness. Table 2.1 contains a sample of the type of form used for summarizing some of the test results. As discussed in the previous section, the test program was consistent with the objectives of the Phase III study and was not conducted with the intent of producing formal documentation of the QA process. Consequently, careful report quality records were not kept of some aspects of the program so that rather than providing the complete documentation that would have been preferred, this report summarizes the results available describing each of the three program areas and giving illustrative examples as available. Since the tests of the system model were carried out in a more structured manner, the documentation for these is thought to be complete.

### 2.2 The Control Module Test Program

The control modules, as illustrated previously in Figure 1.3, control input and output functions, computation of statistical parameters, stepping through time, and random sampling of probabilistic variables for each trial. A stringent program of quality assurance of these modules was carried out and is documented in Volume 2 of the Phase III report. A brief outline of tests of the random simulation tool and other aspects is provided below, with further details given in the appendices.

Table 2.1

## MODEL TEST FORM FOR PHASE III (30259)

**MODEL TESTED**

**TESTER'S NAME**

**OBJECTIVE OF TEST**

**RESULTS**

The major objective of the random simulation tool is to randomly sample values from a variety of user-specified probability distributions. The heart of this tool is the random number generator. This module, taken from an extensively tested random number generator (Marse and Roberts, 1983), was subjected to a further battery of tests to check for portability, uniformity, autocorrelation (the lack of), distribution shape and randomness. These tests (which are detailed in Appendix A of this report) demonstrated that the random number generator conforms to objective statistical criteria.

The ultimate test of the sampling routines is their ability to reproduce the characteristics of the specified distributions. To evaluate this ability, frequency histograms were plotted for all sampling routines and these data were subjected to chi-square tests for distribution fit. The histograms and chi-square tests are detailed in Appendix B of this report. The results of these tests demonstrated that the sampling routines are statistically robust.

The statistics and many of the sampling features of the program were taken directly from the RANSIM program developed during the PHASE II study. The statistics routines are based on algorithms as described by Spicer (1972). As a less quantitative, but nevertheless interesting QA exercise, RANSIM was compared with two other probabilistic analyses (i.e. random simulation) tools. The comparison with the SYVAC program, and the DEMOS probabilistic analysis environment is described in detail in Appendix C. The comparison indicates that RANSIM, and hence the statistics and many of the sampling routines used in this study, produce results equivalent to the other two random simulation tools.

The stability of the statistics routines was checked by requesting statistics for variables that were known to be constants and for zero values. Improvements were then made to the routines to "catch" the resulting errors and produce statistics without crashing the program.

The input and output functions of the contol modules, as well as the control structure's general stability were thoroughly tested through an iterative procedure of corrections/revisions and testing by component model developers. Versions of the control modules and User's Manual were released to model developers who noted directly to the control module programmer all problems or areas of possible improvement for inclusion in the next version of these modules. The final version resulting from this test program appears to be accurate and quite robust.

## 2.3 The Component Model Test Program

### 2.3.1 Outline of Test Program

Since each component module entails different mathemetical formulations, the details of each test program differ. However, component module tests can be divided into three major categories:

1) Hand Calculations
2) Test at Limits
3) Test for Reasonableness

Each component model developer was responsible for carrying out the initial stages of the test program on his or her own model (s). After some degree of confidence in the models was obtained, further checks were made by second parties. The procedure of checking and revising was iterative with runs being performed and checked, resulting in code revisions, followed by further runs and rechecking of output.

Model documentation was also written and revised along with revisions to the coding.

These three types of tests are discussed in the following pages.

### 2.3.2 Hand Calculations

A series of hand calculations were done (usually on a detailed printout of the component module output) to check that the computer code was computing the mathematical formulae correctly. All component modules were developed with a "detailed printout" option which facilitated these tests.

Each component model was developed individually. A subroutine called SUBDAT was available to provide test values for input parameters that would later be calculated by the other component models. The values used here were either actual output from the Phase III models or constant values. Since all of the inputs for each trial were thus known or could be set, computations were carried out manually and then the models were run and the results compared. If descrepancies appeared in the comparison both the hand calculations and codes were checked for errors, the models were run again, if necessary, and the results were again compared. This procedure was repeated until a match was achieved.

As a further extension of this manual checking of the models, all coding was checked, usually by two parties, against the model development documentation to ensure that it accurately reflected the model algorithm(s). The coding was also checked against the hand written (original) model documentation to avoid introducing errors in the coding introduced into the typed version of the component model write ups.

## Surface Water Dispersion Model Examples

One example of hand calculations performed is a check of uranium concentration at the first node in the river downstream of the tailings site. The calculations performed and the comparison results obtained are reproduced in Table 2.2. The computer code predictions are for a single deterministic trial in which all of the input parameter values were known. Similar calculations were performed and checked for other substances, for pH, and for the lake model. No computational errors were found from the hand calculations.

Second party review of the computer code used for SUBROUTINE LAKE did, however, reveal errors. The variable DETIME (detention time) was being

Table 2.2

## SAMPLE OF HAND CALCULATIONS FOR RIVER MODEL

Uranium

River 1 ) Depth = .25

Area = $A_n = 15\ km^2 = 15\times10^6\ m^2$

$P_t = .4$ (constant)

$Q_s = 0$ at $t=0$ , $= 2\times10^5$ at $t>0$.

$$[R_u] = \frac{Q_{n-1}[R_u]_{n-1} + Q_s[R_u]_s}{Q_n}$$

$\underline{t=0}$

$$Q_n = P_t A_n + Q_s$$
$$= .4(15\times10^6)+0$$
$$= 6\times10^6$$

$[R_u]_s = 102.7$ , $Q_{n-1} = 0$

$$[R_u]_{t=0} = \frac{0 + 0[R_u]_s}{Q_n}$$
$$= 0.$$

$\underline{t = 100}$

$$Q_n = 6\times10^6 + 2\times10^5 = 6.2\times10^6$$

$[R_u]_s = 172.16$

$$[R_u]_{t=100} = \frac{0+(2\times10^5)(172.16)}{6.2\times10^6}$$
$$= 5.55$$

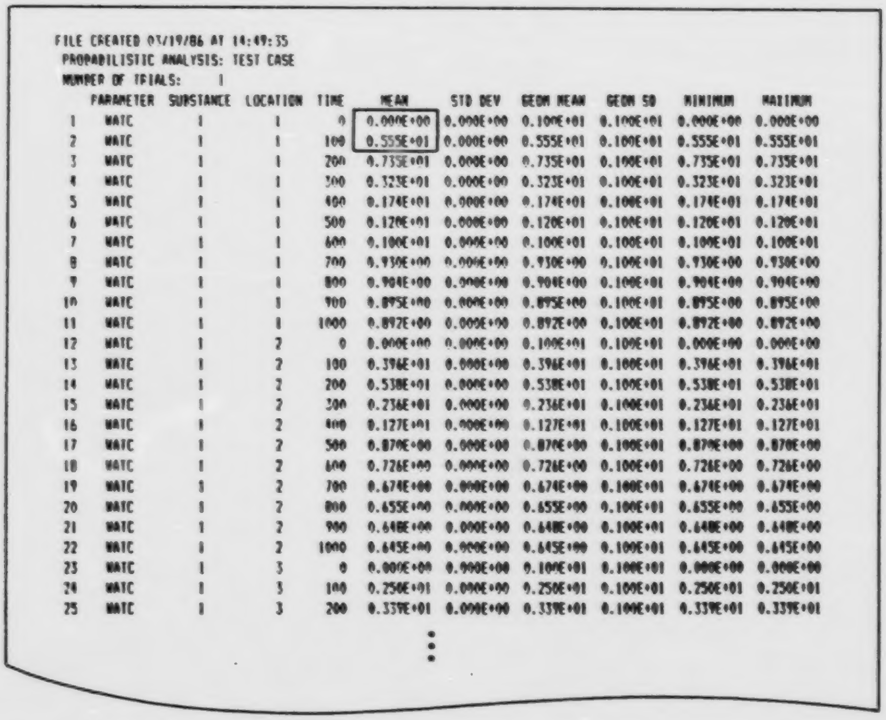

```
FILE CREATED 03/19/86 AT 14:49:35
 PROBABILISTIC ANALYSIS: TEST CASE
 NUMBER OF TRIALS:      1
      PARAMETER  SUBSTANCE  LOCATION  TIME     MEAN       STD DEV    GEOM MEAN    GEOM SD    MINIMUM    MAXIMUM
  1     WATC         1          1        0  0.000E+00  0.000E+00  0.100E+01  0.100E+01  0.000E+00  0.000E+00
  2     WATC         1          1      100  0.555E+01  0.000E+00  0.555E+01  0.100E+01  0.555E+01  0.555E+01
  3     WATC         1          1      200  0.735E+01  0.000E+00  0.735E+01  0.100E+01  0.735E+01  0.735E+01
  4     WATC         1          1      300  0.323E+01  0.000E+00  0.323E+01  0.100E+01  0.323E+01  0.323E+01
  5     WATC         1          1      400  0.174E+01  0.000E+00  0.174E+01  0.100E+01  0.174E+01  0.174E+01
  6     WATC         1          1      500  0.120E+01  0.000E+00  0.120E+01  0.100E+01  0.120E+01  0.120E+01
  7     WATC         1          1      600  0.100E+01  0.000E+00  0.100E+01  0.100E+01  0.100E+01  0.100E+01
  8     WATC         1          1      700  0.930E+00  0.000E+00  0.930E+00  0.100E+01  0.930E+00  0.930E+00
  9     WATC         1          1      800  0.904E+00  0.000E+00  0.904E+00  0.100E+01  0.904E+00  0.904E+00
 10     WATC         1          1      900  0.895E+00  0.000E+00  0.895E+00  0.100E+01  0.895E+00  0.895E+00
 11     WATC         1          1     1000  0.892E+00  0.000E+00  0.892E+00  0.100E+01  0.892E+00  0.892E+00
 12     WATC         1          2        0  0.000E+00  0.000E+00  0.100E+01  0.100E+01  0.000E+00  0.000E+00
 13     WATC         1          2      100  0.396E+01  0.000E+00  0.396E+01  0.100E+01  0.396E+01  0.396E+01
 14     WATC         1          2      200  0.538E+01  0.000E+00  0.538E+01  0.100E+01  0.538E+01  0.538E+01
 15     WATC         1          2      300  0.236E+01  0.000E+00  0.236E+01  0.100E+01  0.236E+01  0.236E+01
 16     WATC         1          2      400  0.127E+01  0.000E+00  0.127E+01  0.100E+01  0.127E+01  0.127E+01
 17     WATC         1          2      500  0.870E+00  0.000E+00  0.870E+00  0.100E+01  0.870E+00  0.870E+00
 18     WATC         1          2      600  0.726E+00  0.000E+00  0.726E+00  0.100E+01  0.726E+00  0.726E+00
 19     WATC         1          2      700  0.674E+00  0.000E+00  0.674E+00  0.100E+01  0.674E+00  0.674E+00
 20     WATC         1          2      800  0.655E+00  0.000E+00  0.655E+00  0.100E+01  0.655E+00  0.655E+00
 21     WATC         1          2      900  0.648E+00  0.000E+00  0.648E+00  0.100E+01  0.648E+00  0.648E+00
 22     WATC         1          2     1000  0.645E+00  0.000E+00  0.645E+00  0.100E+01  0.645E+00  0.645E+00
 23     WATC         1          3        0  0.000E+00  0.000E+00  0.100E+01  0.100E+01  0.000E+00  0.000E+00
 24     WATC         1          3      100  0.250E+01  0.000E+00  0.250E+01  0.100E+01  0.250E+01  0.250E+01
 25     WATC         1          3      200  0.339E+01  0.000E+00  0.339E+01  0.100E+01  0.339E+01  0.339E+01
                                                  •
                                                  •
                                                  •
```

calculated as Q/V, where Q is the flow in $m^3.s^{-1}$ and V is the volume in $m^3$. The resulting value was thus the inverse of the correct value but was also used incorrectly elsewhere, negating the error. The problem was corrected and a new run was made to ensure that the model was performing correctly.

Air Dispersion Model Example

Another example of hand calculations has been reproduced in Table 2.3. Here, the air dispersion model was run and values such as the virtual source set back distance, the vertical dispersion coefficient, and thorium concentration were compared to calculations performed prior to running the model. The results were in complete agreement, as indicated in the notes reproduced here, so the model was deemed to have passed this test.

### 2.3.3 Test at Limits

Most mathematical models have limits at which they can be tested. Often these limits involve time or space.

Groundshine Model Example

In this example the groundshine model flux was tested at its limits. From equation (7.3) of Section 7 of Volume 3 of Phase III, the solution used in the groundshine model is:

$$\phi = \frac{A}{2\mu}\left[1 - e^{-\mu b} - \mu b\left(\gamma + Ln(\mu b) - \mu b + \frac{\mu b^2}{(2)(2\ )} - \frac{\mu b^3}{(3)(3\ )} \ldots.\right)\right] \quad (2.1)$$

where

$\phi$ = gamma flux at receptor (gamma rays.$m^{-2}.s^{-1}$)
A = gamma ray source strength (gamma rays.$m^{-3}.s^{-1}$)
$\mu$ = linear attenuation coefficient ($m^{-1}$)
b = soil layer depth (m)
$\gamma$ = a constant having the value .5772157

Table 2.3

## HAND CALCULATIONS COMPARED TO OUTPUT FROM AIR DISPERSION MODEL

### a) Hand Calculations

Manual calculation of air dispersion equation for comparison with values calculated from code

$$C_{an}(t) = \frac{1.032\; f_{nk}\; Q_n(t)}{\bar{u}_{nk}\,\sigma_z\,(x + x_0)} \exp\left[\frac{-h^2}{2\sigma_z^2}\right] \qquad (5.1)$$

$$x_0 = 2.27\sqrt{A_0} \qquad (5.5)$$

$A_0 = 5 \cdot 10^5\ m^2$ ∴ $x_0 = 2029\ m$ compare with output

$h = 1\ m$

$x = 2000\ m$

$Q_n = 97.94$ Bq/s (when wind greater than 3.4 m/s)

$k$ = north

| L | $\bar{u}_{nk}$ m/s | $f_{nk}$ |
|---|---|---|
| A | 1.5035 | $0.6800 \times 10^{-3}$ |
| B | 2.4227 | $0.4710 \times 10^{-4}$ |
| C | 3.6291 | $0.7040 \times 10^{-3}$ |
| D | 5.6135 | $0.3426 \times 10^{-1}$ |
| E | 3.9826 | $0.7800 \times 10^{-3}$ |
| F | 1.8932 | $0.9230 \times 10^{-4}$ |

| L | $\sigma_z = a(x+x_0)^b$ m | Table 3.2 |
|---|---|---|
| A | 5000 | |
| B | 633.8 | |
| C | 221.0 | compare with output |
| D | 77.61 | |
| E, F | 29.86 | |

| L | Con. Bq/m³ |
|---|---|
| A | $3.5807 \times 10^{-9}$ |
| B | $1.3670 \times 10^{-7}$ |
| C | $4.3107 \times 10^{-8}$ |
| D | $3.8626 \times 10^{-8}$ |
| E | $3.0301 \times 10^{-8}$ |
| F | $8.0597 \times 10^{-10}$ |
| average | $2.5895 \times 10^{-8}$ |

$2.5895 \times 10^{-8}$ Bq/m³ is the average Th concentration over the stability classes when the wind speed is greater than 3.4 m/s

the ratio $\frac{0.1867 \times 10^{1}}{0.3458}$ the fraction of time the wind speed from the north is greater than 3.4 m/s over the fraction of time the wind speed exceeds 3.4 m/s

$$2.5895 \times 10^{-8} \cdot \frac{0.1867 \times 10^{1}}{0.3458} = 1.3981 \times 10^{-7}\ \text{Bq/m}^3$$ which

is the Th concentration to the north of the tailings in the first ring (compare with output)

### b) Detailed Printout

```
AIR DISPERSION MODEL

SURFACE AREA OF TAILINGS  0.5000E+06
HEIGHT OF SOURCE  0.1000E+01
VIRTUAL SOURCE SET BACK DISTANCE  0.2029E+04
DOWNWIND DISTANCE FROM SOURCE TO RECEPTOR  0.2000E+04
                                           0.4000E+04
                                           0.7500E+04
                                           0.1500E+05
                                           0.3500E+05

VERTICAL DISPERSION COEFFICIENT
    5000.00     633.84     221.05     77.61      29.86      29.86
    5000.00    1006.67     321.05    102.36      38.06      38.06
    5000.00    1336.76     406.11    129.54      42.90      42.90
    5000.00    2552.30     824.91    179.74      52.87      52.87
    5000.00    5000.00    1673.77    278.60      69.99      69.99

ATMOSPHERIC CONCENTRATION OF THE RADIONUCLIDES AT THE RECEPTORS
   0.6791E-08  0.3616E-08  0.1961E-08  0.8609E-09  0.2083E-09
   0.4299E-08  0.2222E-08  0.1203E-08  0.5277E-09  0.1765E-09
   0.6064E-08  0.3139E-08  0.1702E-08  0.7470E-09  0.2504E-09
   0.5507E-08  0.2093E-08  0.1571E-08  0.6908E-09  0.2314E-09
   0.7015E-08  0.4054E-08  0.2205E-08  0.9717E-09  0.3262E-09
   0.3297E-08  0.1713E-08  0.9348E-09  0.4134E-09  0.1393E-09
   0.2197E-08  0.1142E-08  0.6238E-09  0.2762E-09  0.9324E-10
   0.5230E-08  0.2712E-08  0.1473E-08  0.6486E-09  0.2175E-09
   0.2004E-07  0.1035E-07  0.5561E-08  0.2423E-08  0.8031E-09
   0.7670E-08  0.3958E-08  0.2123E-08  0.9230E-09  0.3052E-09
   0.6092E-08  0.3141E-08  0.1688E-08  0.7347E-09  0.2435E-09
   0.4348E-08  0.2246E-08  0.1212E-08  0.5302E-09  0.1767E-09
   0.2556E-07  0.1323E-07  0.7175E-08  0.3152E-08  0.1055E-08
   0.2232E-07  0.1156E-07  0.6250E-08  0.2746E-08  0.9177E-09
   0.8898E-08  0.4619E-08  0.2521E-08  0.1115E-08  0.3761E-09
   0.5026E-08  0.3023E-08  0.1649E-08  0.7284E-09  0.2454E-09
AVERAGE CONCENTRATION  0.5709E-09
AVERAGE WATER SHED CONCENTRATION  0.1178E-08
   0.1398E-06  0.7232E-07  0.3921E-07  0.1722E-07  0.5766E-08
   0.8599E-07  0.4445E-07  0.2407E-07  0.1055E-07  0.3530E-08
   0.1213E-06  0.6278E-07  0.3404E-07  0.1496E-07  0.5008E-08
   0.1116E-06  0.5787E-07  0.3141E-07  0.1382E-07  0.4628E-08
   0.1563E-06  0.8108E-07  0.4410E-07  0.1943E-07  0.6524E-08
   0.6595E-07  0.3425E-07  0.1870E-07  0.8267E-08  0.2787E-08
   0.4394E-07  0.2283E-07  0.1248E-07  0.5523E-08  0.1865E-08
   0.1046E-06  0.5424E-07  0.2947E-07  0.1297E-07  0.4350E-08
   0.4008E-06  0.2069E-06  0.1112E-06  0.4846E-07  0.1606E-07
   0.1534E-06  0.7917E-07  0.4247E-07  0.1846E-07  0.6105E-08
   0.1218E-06  0.6282E-07  0.3376E-07  0.1469E-07  0.4870E-08
   0.8696E-07  0.4491E-07  0.2425E-07  0.1060E-07  0.3534E-08
   0.5117E-06  0.2646E-06  0.1435E-06  0.6304E-07  0.2110E-07
   0.4464E-06  0.2311E-06  0.1252E-06  0.5493E-07  0.1835E-07
   0.1700E-06  0.9237E-07  0.5042E-07  0.2230E-07  0.7522E-08
   0.1165E-06  0.6047E-07  0.3298E-07  0.1457E-07  0.4908E-08
AVERAGE CONCENTRATION  0.1142E-07
AVERAGE WATER SHED CONCENTRATION  0.2355E-07
```

An iterative solution was developed for the above equation and is contained in FUNCTION(SOL) of the groundshine model (see Table 7.2 of Volume 3 of Phase III). To test this equation at its limits a 1 metre thick soil layer was assumed.

For practical purposes a surface layer of soil 1 metre deep can be considered infinitely thick since radioactivity at depths greater than 1 metre makes no significant contribution to the surface dose rate. Thus, the one metre depth used in this test should give results comparable to infinite depth.

Table 2.4 contains a portion of a detailed printout from FUNCTION(SOL) for a soil layer of 1 metre depth in which the soil contains 1 $Bq.m^{-3}$ of uranium Each line of the printout is one iteration in the solution of equation (2.1). The convergence criteria for the solution is that the difference between the current prediction and the prior prediction be no greater than 1%. The final line gives the converged solution of the equation. SOL1 is the current answer and SOL2 is the prediction from the previous iteration. In this example the predicted gamma flux for the fourth energy band using the formula for infinite depth is:

$$\phi = \frac{A}{2u} = \frac{0.951}{2 \times 0.680 \times 10^{1}} = 0.699 \times 10^{-1} \qquad (2.2)$$

Table 2.4 reveals that there is agreement between the resulting two answers to three significant figures. This is considered typical of the performance of the iterative solution.

### 2.3.4 Test for Reasonableness

Component modules were also examined for "reasonableness". These tests were often qualitative in nature and involved asking the question "Does the model output agree with what I know about the system?" For example, in the case of the erosion model, in a 500 year simulation, the average depletion in depth of the tailings pile was 2 cm. This is a reasonable number, neither obviously

Table 2.4

## TEST OF CONVERGENCE OF ITERATIVE FLUX SOLUTION IN GROUNDSHINE

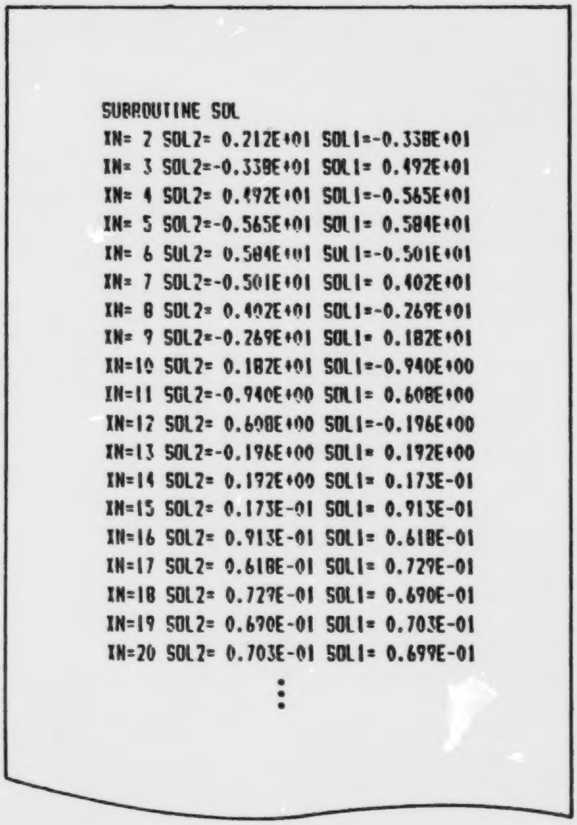

```
SUBROUTINE SOL
XN= 2 SOL2= 0.212E+01 SOL1=-0.338E+01
XN= 3 SOL2=-0.338E+01 SOL1= 0.492E+01
XN= 4 SOL2= 0.492E+01 SOL1=-0.565E+01
XN= 5 SOL2=-0.565E+01 SOL1= 0.584E+01
XN= 6 SOL2= 0.584E+01 SOL1=-0.501E+01
XN= 7 SOL2=-0.501E+01 SOL1= 0.402E+01
XN= 8 SOL2= 0.402E+01 SOL1=-0.269E+01
XN= 9 SOL2=-0.269E+01 SOL1= 0.182E+01
XN=10 SOL2= 0.182E+01 SOL1=-0.940E+00
XN=11 SOL2=-0.940E+00 SOL1= 0.608E+00
XN=12 SOL2= 0.608E+00 SOL1=-0.196E+00
XN=13 SOL2=-0.196E+00 SOL1= 0.192E+00
XN=14 SOL2= 0.192E+00 SOL1= 0.173E-01
XN=15 SOL2= 0.173E-01 SOL1= 0.913E-01
XN=16 SOL2= 0.913E-01 SOL1= 0.618E-01
XN=17 SOL2= 0.618E-01 SOL1= 0.729E-01
XN=18 SOL2= 0.729E-01 SOL1= 0.690E-01
XN=19 SOL2= 0.690E-01 SOL1= 0.703E-01
XN=20 SOL2= 0.703E-01 SOL1= 0.699E-01
                 ⋮
```

### Key

XN - Iteration Number
SOL2 - Previous Estimate
SOL1 - Current Estimate

### Note

Solution at infinite depth = 0.0699

too small nor too large.

In some instances the predictions of component models were compared to results generated using other models, or to results available from observation of "reasonably" comparable situations. These comparisons were generally qualitative, rather than quantitative and served to indicate that the model results were indeed "reasonable" based on what was known from prior experience.

## Air Dispersion Model Example

One example of results that were found to be unreasonable in a fairly early stage of model development, was for air dispersion. Concentrations of radionuclides were higher in the direction from the tailings opposite to what would be expected based on the prevailing winds from the west. This apparent discrepancy was traced back to a logic error in the interpretation of the wind data provided. The wind direction was used as the direction the wind was blowing to when actually it was the direction the wind was blowing from. This was corrected and the model was rerun and checked. A small portion of output obtained before and after this correction was made have been reproduced in Table 2.5.

## Subsurface Transport Model Example

Another example is the subsurface transport model. Figure 2.1 presents the predicted groundwater concentrations at a distance of 35 metres from the centre line of the tailings dam based on a constant source strength of 10 Bq.m$^{-3}$, the same decay constant for all radionuclides (i.e., a value of $10^{-15}$ yr$^{-1}$), and distribution coefficients ($K_d$ values) of 0.02, 0.5, 0.67, 0.07 m$^{3}$.g$^{-1}$, for the radionuclides identified simply as A, B, C and D respectively. The results indicate that radionuclides A and D reach a steady state value by years 100 and 300, respectively. However, the groundwater concentrations for B and C are only 56% and 32%, respectively of their source concentrations at year 1000. This is expected because of their much higher $K_d$ values.

Table 2.5

## EXAMPLE OUTPUT FROM AIR DISPERSION MODEL

| Ring Number | Direction | Radon Concentration ($Bq.m^{-3}$) at Time 0<br>Before Correction | After Correction |
|---|---|---|---|
| 1 | E | $7.073 \times 10^{-3}$ | $9.960 \times 10^{-3}$ |
| 2 | E | $3.671 \times 10^{-3}$ | $5.158 \times 10^{-3}$ |
| 3 | E | $1.997 \times 10^{-3}$ | $2.797 \times 10^{-3}$ |
| 4 | E | $8.803 \times 10^{-4}$ | $1.229 \times 10^{-3}$ |
| 5 | E | $2.956 \times 10^{-4}$ | $4.116 \times 10^{-4}$ |

FIGURE 2.1

SUBSURFACE TRANSPORT

(SAME HALF-LIFE)

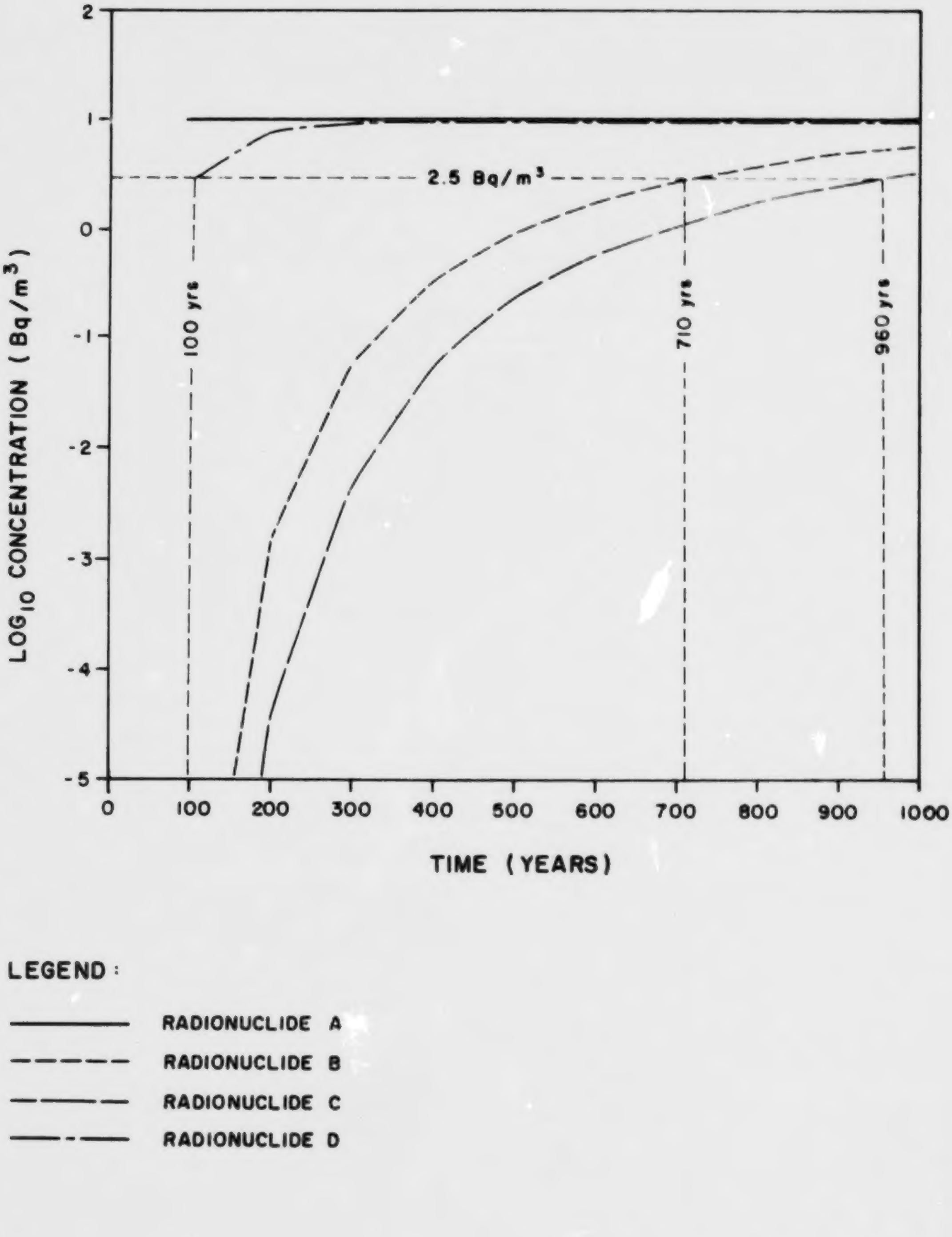

To verify this observation one can compare times to steady state for radionuclides by comparing their retardation factors. For example, the comparison for radionuclides A and B is given by:

$$\frac{T_A}{T_B} = \frac{R_A}{R_B} \tag{2.3}$$

where:

$T_A, T_B$ = steady state breakthrough times of radionuclides A and B
$R_A, R_B$ = retardation factors of radionuclides A and B

The retardation factor for compounds which are strongly absorbed, can be expressed as:

$$R_i \simeq \frac{\rho_b}{n} K_{d,i} \tag{2.4}$$

where

$R_i$ = retardation factor of ith radionuclide = $\overline{V}/V_i$
$\rho_b$ = soil density
$n$ = porosity
$K_{d,i}$ = distribution coefficient of ith radionuclide
$\overline{V}$ = average linear groundwater velocity
$V_i$ = velocity of ith radionuclide in the aquifer

Hence, the ratio of breakthrough times for radionuclides D and B, and D and C can be approximated by:

$$\frac{T_D}{T_B} \simeq \frac{K_{d,D}}{K_{d,B}} = \frac{0.07}{0.5} = \frac{1}{7.1} \tag{2.5}$$

and

$$\frac{T_D}{T_C} \simeq \frac{K_{d,D}}{K_{d,C}} = \frac{0.07}{0.67} = \frac{1}{9.6} \tag{2.6}$$

Using these ratios it is predicted that radionuclides B and C will reach approximately 2.5 $Bq.m^{-3}$, the concentration of D at year 100, by years 710 and 960, respectively. The model results, presented in Figure 2.1, are in very good agreement with the aforementioned predictions.

In Figure 2.2 the groundwater concentrations are based on a constant source strength of 10 $Bq.m^{-3}$, the same $K_d$ value for all radionuclides (i.e. $K_d$ of 0.1 $m^3.g^{-1}$), and half-lifes of 4.51 x $10^9$, 1.4 x $10^{10}$, 21 and 1602 yr, for radionclides A through D, respectively. The results indicate that all radionuclides will have reached quasi steady state by year 500; the difference in their steady state values being attributed to their half-lives.

Radon Source Model Example

The theoretical development of the radon source model is well-accepted in published literature. The primary flux equation used in this study, adopted from Rogers et al. (1980), has since been incorporated into a more general model developed for use by the U.S. Nuclear Regulatory Commission for designing uranium mill tailings covers (Rogers et al., 1984).

The numeric values generated by the computer implementation in this study were mainly corroborated by comparison with the results of calculation using the same algorithm implemented independently on a programmable hand-calculator. The model was run with differing values of the major input values (e.g. radium content, source thickness, moisture, emanation coefficient) and compared to the hand calculations. The computer and hand calculator results were in exact agreement. The radon fluxes predicted using the computer implementation and suitable sets of input parameters were also compared to published "typical" measured fluxes from tailings. This demonstrated that the model was generating radon fluxes of the proper "order-of-magnitude".

Finally, radon flux calculations generated using a simpler, single layer or zone source equation were compared to "limiting" values of the two layer model; that is, when the thickness of one layer was much larger than the other

FIGURE 2.2

## SUBSURFACE TRANSPORT
(SAME DISTRIBUTION COEFFICIENT)

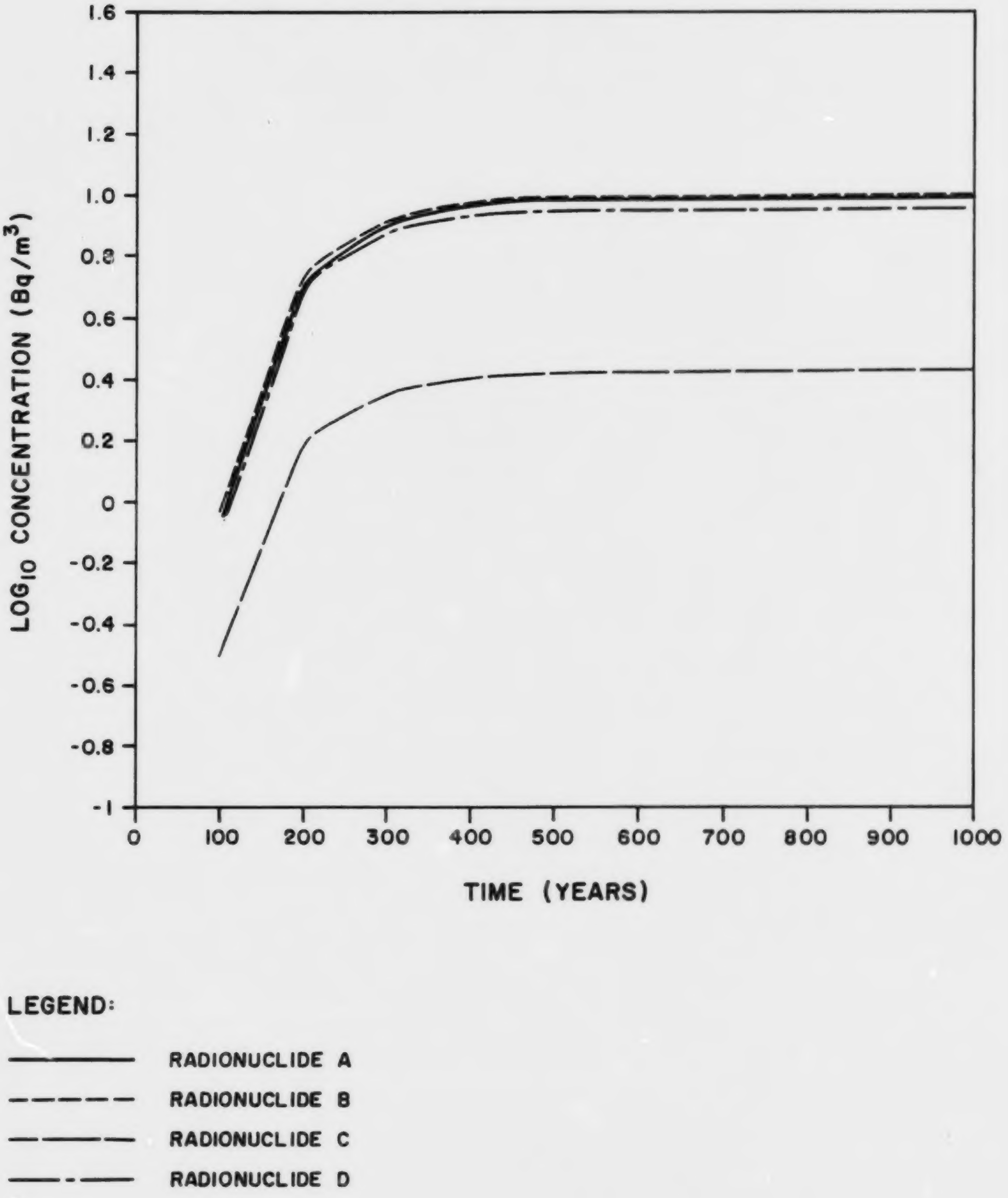

layer. In all cases, the calculations gave comparable results.

## 2.4 The System Model Test Program

### 2.4.1 Overview of Test Program

The system model test program was designed to test the entire program following integration of the control and component modules. The program attempted to test the mathematical stability, accuracy, and reasonableness of the model as well as the input/output capabilities. The test program involved a number of tests which were applied in a progressive building block fashion. These tests are described below.

After each test was performed, the results were checked and if the output was questionable or erroneous, the problems were corrected in the models concerned and the test was rerun until all results obtained were deemed reasonable and computationally correct. The test program then proceeded to the next test.

All figures plotted in the following pages illustrating results of runs with more than one trial show geometric mean values, unless otherwise indicated.

### 2.4.2 Test 1 - Check for Computational Accuracy

The objectives of this test were to perform a detailed check of the computational accuracy of the component modules, verify proper information transfer between modules, evaluate the effects of stepping through time, and check on the reasonableness of results using nominal input values. Detailed output results from one deterministic run using nominal parameter inputs were provided to the model developers for each component module. Time-variant parameters were set at their nominal values in this test. The source code and input files for the component module were also supplied to the model developers. A simulation length of 100 years with a time step of 10 years was used. Changes to the model structure or input parameter values were recorded by the reviewers and reported to the system programmer. The module was then by the reviewers and reported to the system programmer. The module was then corrected and rerun. The review process was repeated, running the system model three times, until no further errors or changes were found.

## Soil Model Example

The following example illustrates how a problem was identified and corrected in the soil module. Output for the soil module is contained in Tables 2.6 and 2.7. The column denoted with the heading ACTIVITY for time t should become the initial activity (ZZERO) for the next time interval (t + 10). Clearly from Table 2.6 this is not the case. The soil module was developed on a stand alone basis without consideration of multiple receptors. Inclusion in the system module which automatically calculated soil concentrations at each of three receptor locations included in this run resulted in the activity from the last receptor location being used as the initial activity for the next receptor location. This problem was corrected and the system model was rerun to produce the output in Table 2.7. The apparent discrepancy in the values between Table 2.6 and Table 2.7 is due to change in the deposition velocity between the runs which caused slightly different answers in the two runs.

## Animal Produce Model Example

Another type of problem uncovered by this test was with the input file. Initial printouts of detailed results from SUBROUTINE ANIMAL revealed results with values of zero. This occurred because not all of the input parameters were being sampled. A review of the input parameter file revealed a number of incorrect variables affecting the dose, meat and vegetation models. These inputs were corrected before the final runs of this test.

Detailed printouts from the other models appeared correct and no other changes were made as a result of this test.

Table 2.6

## EXAMPLE OF ERROR FOUND IN SOIL MODEL BY TEST 1

```
TRIAL NUMBER: 1   TIME: 0
SUBROUTINE SOIL
LAYER 1
RADIONUCLIDE     ZZERO     ACTIVITY
       1      0.000E+00   0.238E-08
       2      0.000E+00   0.384E-07
       3      0.000E+00   0.205E-08
       4      0.000E+00   0.182E-07

LAYER 2
RADIONUCLIDE     ZZERO     ACTIVITY
       1      0.000E+00   0.188E-08
       2      0.000E+00   0.141E-07
       3      0.000E+00   0.137E-09
       4      0.000E+00   0.215E-08
                    .
                    .
                    .
TRIAL NUMBER: 1   TIME:10
SUBROUTINE SOIL
LAYER 1
RADIONUCLIDE     ZZERO     ACTIVITY
       1      0.481E-09   0.216E-08
       2      0.776E-08   0.347E-07
       3      0.414E-09   0.633E-08
       4      0.369E-08   0.211E-07

LAYER 2
RADIONUCLIDE     ZZERO     ACTIVITY
       1      0.380E-09   0.245E-08
       2      0.285E-08   0.184E-07
       3      0.278E-10   0.472E-09
       4      0.434E-09   0.334E-08
```

KEY

Activity - activity at end of time interval
Zzero - activity at beginning of time interval (should equal activity at end of previous/interval)

Table 2.7

## OUTPUT FROM SOIL MODEL CORRECTED AFTER TEST 1

```
TRIAL NUMBER: 1   TIME: 0
SUBROUTINE SOIL
LAYER 1
RADIONUCLIDE     ZZERO     ACTIVITY
        1     0.000E+00    0.340E-08
        2     0.000E+00    0.548E-07
        3     0.000E+00    0.292E-08
        4     0.000E+00    0.260E-07

LAYER 2
RADIONUCLIDE     ZZERO     ACTIVITY
        1     0.000E+00    0.268E-08
        2     0.000E+00    0.201E-07
        3     0.000E+00    0.196E-09
        4     0.000E+00    0.306E-08
                    .
                    .
                    .
TRIAL NUMBER: 1   TIME:10
SUBROUTINE SOIL
LAYER 1
RADIONUCLIDE     ZZERO     ACTIVITY
        1     0.340E-08    0.347E-08
        2     0.548E-07    0.676E-07
        3     0.292E-08    0.104E-07
        4     0.260E-07    0.457E-07

LAYER 2
RADIONUCLIDE     ZZERO     ACTIVITY
        1     0.268E-08    0.797E-08
        2     0.201E-07    0.646E-07
        3     0.196E-09    0.104E-08
        4     0.306E-08    0.115E-07
```

Key

Activity - activity at end of time interval
Zzero - activity at beginning of time interval (should equal activity at end of previous interval)

### 2.4.3 Test 2 - Check of Parameter Initialization

The objective in Test 2 was quite simply to ensure that the code would produce exactly the same output results for two successive trials with the same input parameter values. The test was designed to verify that the code was "resetting" the input values properly for each trial and to confirm the computational accuracy of the modules. The test involved two trials of 1000 year duration with a ten year time-step and the same deterministic nominal value data set as in Test 1.

Total Dose/Erosion Model Example

Table 2.8 contains tabular output from the two trials of the dose for each pathway as well as total dose. Total dose (DOSE), fish dose (FISHD), meat dose (MEATD) and drinking water dose (WATD) are not the same for the two trials. The water pathway either fully or partially contributes to all of these pathways, hence a debugging procedure was followed down the water pathway.

Inputs to the water pathway were examined for the two deterministic trials. The erosion model was found to be responsible for the different results obtained from the two trials. The source on-line debugger that accompanies the Leahy Compiler used in Phase III was activated and the erosion model was debugged one line at a time. The variable CSOIL was found to have been inadvertently used to characterize soil permeability class and the cropping practice factor in the universal soil loss equation. The problem was corrected and the two deterministic runs were repeated.

Water Dose/Subsurface Transport Model Example

Again, the results of the water pathway were not the same for the two runs. This time, different values of the variable GFLUX (groundwater flux) were noted. At time 0 of the first trial, GFLUX (1) equalled 0; at time 0 for the second trial, GFLUX (1) equalled 4.42. This parameter was only being

Table 2.8

## DOSES (uSv) FROM TEST 2 - TWO DETERMINISTIC TRIALS

Trial 1:

| TIME | DOSE | FISHD | INHD | MEATD | RADD | SHINED | VEGD | WATD |
|---|---|---|---|---|---|---|---|---|
| 0 | 0.101E+04 | 0.425E+02 | 0.432E+00 | 0.173E+01 | 0.220E+00 | 0.193E-08 | 0.696E-01 | 0.967E+03 |
| 50 | 0.839E+03 | 0.457E+02 | 0.463E-01 | 0.150E+01 | 0.131E+00 | 0.743E-08 | 0.650E-01 | 0.791E+03 |
| 100 | 0.830E+03 | 0.615E+02 | 0.401E-01 | 0.122E+01 | 0.126E+00 | 0.790E-08 | 0.711E-01 | 0.767E+03 |
| 150 | 0.104E+04 | 0.284E+03 | 0.398E-01 | 0.107E+01 | 0.120E+00 | 0.885E-08 | 0.713E-01 | 0.758E+03 |
| 200 | 0.110E+04 | 0.275E+03 | 0.397E-01 | 0.101E+01 | 0.116E+00 | 0.968E-08 | 0.703E-01 | 0.801E+03 |
| 250 | 0.131E+04 | 0.343E+03 | 0.396E-01 | 0.108E+01 | 0.834E-01 | 0.104E-07 | 0.692E-01 | 0.968E+03 |
| 300 | 0.168E+04 | 0.424E+03 | 0.784E-02 | 0.130E+01 | 0.818E-01 | 0.997E-08 | 0.135E-01 | 0.125E+04 |
| 400 | 0.126E+04 | 0.330E+03 | 0.393E-02 | 0.102E+01 | 0.788E-01 | 0.809E-08 | 0.656E-02 | 0.931E+03 |
| 600 | 0.875E+03 | 0.238E+03 | 0.391E-02 | 0.743E+00 | 0.732E-01 | 0.629E-08 | 0.612E-02 | 0.636E+03 |
| 800 | 0.696E+03 | 0.192E+03 | 0.388E-02 | 0.600E+00 | 0.681E-01 | 0.507E-08 | 0.572E-02 | 0.503E+03 |
| 1000 | 0.581E+03 | 0.161E+03 | 0.386E-02 | 0.502E+00 | 0.634E-01 | 0.420E-08 | 0.535E-02 | 0.419E+03 |

Trial 2:

| TIME | DOSE | FISHD | INHD | MEATD | RADD | SHINED | VEGD | WATD |
|---|---|---|---|---|---|---|---|---|
| 0 | 0.101E+04 | 0.425E+02 | 0.432E+00 | 0.172E+01 | 0.220E+00 | 0.193E-08 | 0.696E-01 | 0.966E+03 |
| 50 | 0.842E+03 | 0.459E+02 | 0.463E-01 | 0.146E+01 | 0.131E+00 | 0.743E-08 | 0.650E-01 | 0.795E+03 |
| 100 | 0.834E+03 | 0.618E+02 | 0.401E-01 | 0.118E+01 | 0.126E+00 | 0.790E-08 | 0.711E-01 | 0.771E+03 |
| 150 | 0.105E+04 | 0.285E+03 | 0.398E-01 | 0.103E+01 | 0.120E+00 | 0.885E-08 | 0.713E-01 | 0.762E+03 |
| 200 | 0.110E+04 | 0.276E+03 | 0.397E-01 | 0.976E+00 | 0.116E+00 | 0.968E-08 | 0.703E-01 | 0.805E+03 |
| 250 | 0.132E+04 | 0.344E+03 | 0.396E-01 | 0.105E+01 | 0.834E-01 | 0.104E-07 | 0.692E-01 | 0.971E+03 |
| 300 | 0.168E+04 | 0.424E+03 | 0.784E-02 | 0.125E+01 | 0.818E-01 | 0.997E-08 | 0.135E-01 | 0.125E+04 |
| 400 | 0.126E+04 | 0.330E+03 | 0.393E-02 | 0.984E+00 | 0.788E-01 | 0.809E-08 | 0.656E-02 | 0.931E+03 |
| 600 | 0.875E+03 | 0.238E+03 | 0.391E-02 | 0.716E+00 | 0.732E-01 | 0.629E-08 | 0.612E-02 | 0.636E+03 |
| 800 | 0.696E+03 | 0.192E+03 | 0.388E-02 | 0.579E+00 | 0.681E-01 | 0.507E-08 | 0.572E-02 | 0.503E+03 |
| 1000 | 0.581E+03 | 0.161E+03 | 0.386E-02 | 0.484E+00 | 0.634E-01 | 0.420E-08 | 0.535E-02 | 0.419E+03 |

Key

DOSE - Total Dose
FISHD - Fish Dose
INHD - Dust Inhalation Dose
MEATD - Meat Dose
RADD - Radon Inhalation Dose
SHINED - Groundshine Dose
VEGD - Vegetation Dose
WATD - Drinking Water Dose

initialized for the first trial. After correcting the problem, the test was repeated to produce the identical results for lake water concentrations. The results of the two trials are summarized in Table 2.9, which shows the mean, minimum and maximum values of the two deterministic trials. The minimum and maximum activities of all four radionuclides are identical at all time intervals recorded on Table 2.9. Similarly, doses were also found to now be equal for the two trials.

### 2.4.4 Test 3 - Check of Probabilistic Sampling

The purpose of this test was to verify that the probabilistic trials were performed properly. That is, a detailed parameter printout was checked to ensure that parameters were reset properly on the second trial, that new probabilistic inputs were generated and that the results of the second trial were reasonable. Test 3 involved two probabilistic trials of 100 year duration with a ten year time-step. Time-variant parameters were sampled each time step in this test. The probabilistic input file was also checked for accuracy by comparison of the input file listing with model documentation. No problems were revealed by this test.

#### Surface Water Dispersion Model Example

Two sample plots used to check for reasonableness of results for this test are illustrated in Figure 2.3. These show pH and water concentration of radium in the first lake for each of the two trials.

The results of the two trials shown on Figure 2.3 are interesting to examine as they appear on first glance to give contradictory results because the radium concentration in trial 1 is higher than trial 2 whereas the pH of trial 1 is lower than trial 2. This latter observation suggests that the sulphate level is higher in trial 1 than trial 2 therefore, it is expected that the amount of radium sulphate precipitate which dissolves would be less for trial 1. On inspection of the input paramters values for the two trials, however, the output results were found to be quite reasonable.

Table 2.9

CORRECTED WATER CONCENTRATIONS (Bq/m$^3$) FROM TEST 2 - TWO DETERMINISTIC TRIALS

| | Uranium | | | Thorium | | | Lead | | | Radium | | |
|---|---|---|---|---|---|---|---|---|---|---|---|---|
| TIME | MEAN | MAX | MIN | MEAN | MAX | MIN | MEAN | MAX | MIN | MEAN | MAX | MIN |
| 0 | 0.547E+03 | 0.547E+03 | 0.547E+03 | 0.116E+04 | 0.116E+04 | 0.116E+04 | 0.477E+03 | 0.477E+03 | 0.477E+03 | 0.798E+02 | 0.798E+02 | 0.798E+02 |
| 50 | 0.416E+03 | 0.416E+03 | 0.416E+03 | 0.109E+02 | 0.109E+02 | 0.109E+02 | 0.357E+03 | 0.357E+03 | 0.357E+03 | 0.762E+02 | 0.762E+02 | 0.762E+02 |
| 100 | 0.256E+03 | 0.256E+03 | 0.256E+03 | 0.278E+01 | 0.278E+01 | 0.278E+01 | 0.249E+03 | 0.249E+03 | 0.249E+03 | 0.745E+02 | 0.745E+02 | 0.745E+02 |
| 150 | 0.149E+03 | 0.149E+03 | 0.149E+03 | 0.530E+00 | 0.530E+00 | 0.530E+00 | 0.187E+03 | 0.187E+03 | 0.187E+03 | 0.104E+03 | 0.104E+03 | 0.104E+03 |
| 200 | 0.857E+02 | 0.857E+02 | 0.857E+02 | 0.372E+00 | 0.372E+00 | 0.372E+00 | 0.147E+03 | 0.147E+03 | 0.147E+03 | 0.226E+03 | 0.226E+03 | 0.226E+03 |
| 250 | 0.494E+02 | 0.494E+02 | 0.494E+02 | 0.300E+00 | 0.300E+00 | 0.300E+00 | 0.121E+03 | 0.121E+03 | 0.121E+03 | 0.494E+03 | 0.494E+03 | 0.494E+03 |
| 300 | 0.300E+02 | 0.300E+02 | 0.300E+02 | 0.412E-02 | 0.412E-02 | 0.412E-02 | 0.112E+03 | 0.112E+03 | 0.112E+03 | 0.970E+03 | 0.970E+03 | 0.970E+03 |
| 400 | 0.125E+02 | 0.125E+02 | 0.125E+02 | 0.468E-02 | 0.468E-02 | 0.468E-02 | 0.110E+03 | 0.110E+03 | 0.110E+03 | 0.480E+03 | 0.480E+03 | 0.480E+03 |
| 600 | 0.290E+01 | 0.290E+01 | 0.290E+01 | 0.750E-02 | 0.750E-02 | 0.750E-02 | 0.978E+02 | 0.978E+02 | 0.978E+02 | 0.122E+03 | 0.122E+03 | 0.122E+03 |
| 800 | 0.141E+01 | 0.141E+01 | 0.141E+01 | 0.838E-02 | 0.838E-02 | 0.838E-02 | 0.837E+02 | 0.837E+02 | 0.837E+02 | 0.355E+02 | 0.355E+02 | 0.355E+02 |
| 1000 | 0.115E+01 | 0.115E+01 | 0.115E+01 | 0.770E-02 | 0.770E-02 | 0.770E-02 | 0.709E+02 | 0.709E+02 | 0.709E+02 | 0.146E+02 | 0.146E+02 | 0.146E+02 |

FIGURE 2.3

## PLOTS FROM TEST 3 FOR TWO PROBABILISTIC TRIALS

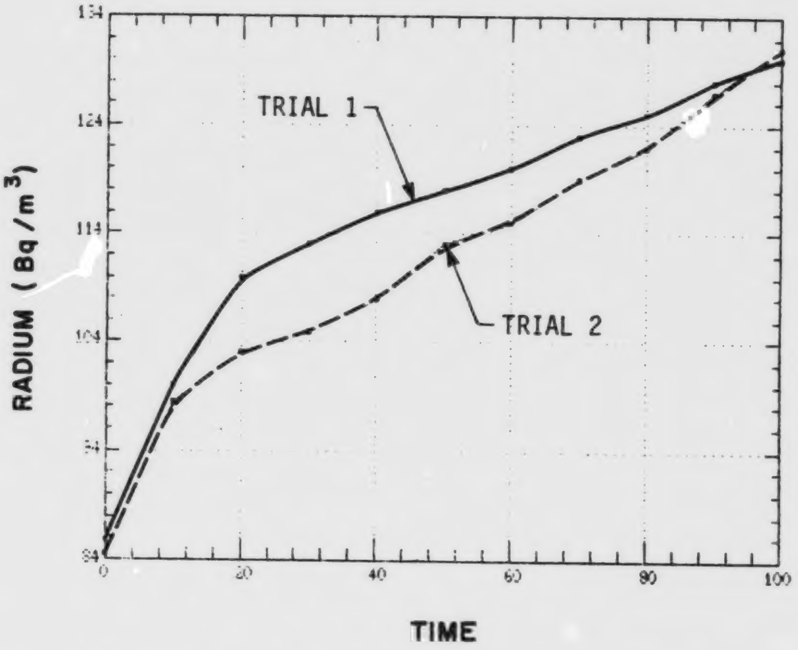

A) RADIUM CONCENTRATION IN FIRST LAKE

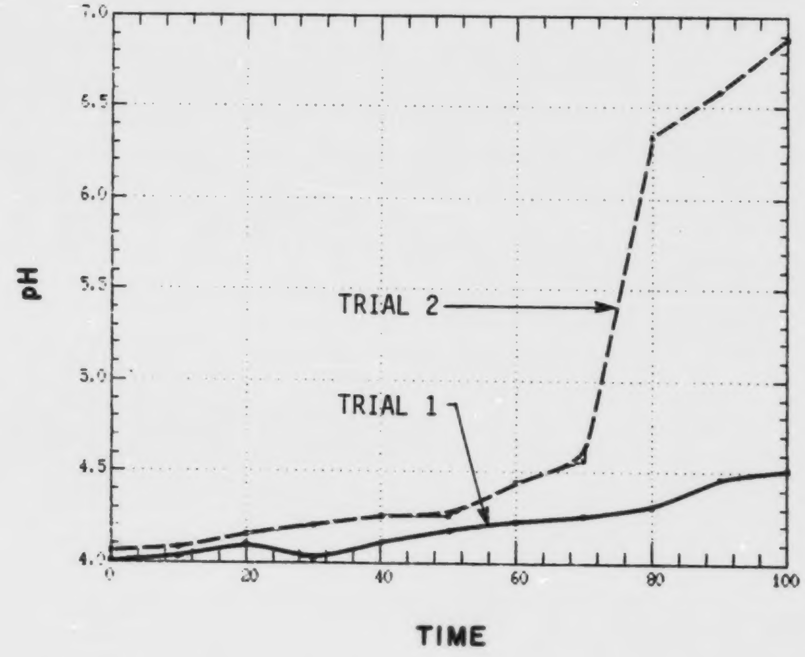

B) pH IN FIRST LAKE

Firstly, the difference in the pH curves were found to be largely attributable to two factors: 1) the sulphate production rate constant selected in trial 1 was about 40% higher than the value selected for trial 2; and, 2) the depth of the unsaturated zone in the tailings mass selected for trial 1 was about 57% larger than the one chosen in trial 2. As a consequence of the values randomly selected in these trials, the pH of trial 1 was lower than that for trial 2, as expected since the sulphate production rate was higher, and the pH remained low over the entire 100 year simulation period, due to the deeper unsaturated zone, and, hence, greater inventory of pyrite available to be oxidized. The observed recovery of pH in trial 2 after year 70 may be attributed to complete oxidation of the pyrite inventory within this time frame allowing the pH in the lake to rise towards the natural background level.

Secondly, given that trial 2 had a lower rate of sulphate production than trial 1, it would be expected that the dissolved radium content of the porewater would be higher with trial 2 since the solubility of the barium (radium) precipitate is dependent on the sulphate concentration. The opposite is indeed seen on Figure 2.3a. This apparent reversal of the curves was found on inspection of input values to be attributable mainly to the selection of a much larger $k_d$ (solid-to-liquid distribution coefficient) value for trial 2 than trial 1 (i.e. about 28% larger). The effect of this parameter value selection was to retard the release of radium from the mixing layer in the tailings source. It is noted, however, that the curves cross at approximately year 95. This is due to much greater barium (radium) sulphate dissolution following completion of pyrite oxidation in trial 2. The increase in the rate at which the precipitate dissolves was apparently sufficient to offset the effect of the higher $k_d$ value in trial 2.

### 2.4.5 Test 4 - Reasonableness Check Using Probabilistic Inputs

Ten probabilistic trials were performed for a 1000 year simulation length using ten year time-steps. Again, the output capability of the control modules were used to obtain summary statistics on the time behaviour of pathways and radionuclides or chemical species of interest. The output results were checked for reasonableness.

## Water Source Model Examples

Because the tailings source term model is by far the most complex component of the system model, special attention was given to analysing predicted contaminant levels in all layers of the tailings mass. An example of the predicted output for the three major ionic species explicitly modelled in the tailings source (i.e. sulphate, calcium and iron) and for pH are presented in Figures 2.4 through 2.7. Each plot contains these curves: one for parameter levels at the bottom of the unsaturated zone (layer 2); and one for the tailings parameter in the upper portion of the saturated tailings zone (layer 3); and, one for the deep portion of the saturated zone (layer 4).

The curve for the sulphate concentration in layer 2 shows a steady decline from year 0 onwards. This is expected as the pyrite oxidation rate is modelled as a function of the amount of pyrite remaining. The curve for layer 2 suggests that most of the pyrite has been oxidized from the unsaturated zone in the initial 100 years, an observation which agrees with hand calculations. The magnitude of the sulphate levels was also confirmed to be correctly computed.

The sulphate level in layer 2 between year 100 and 200 is attributable primarily to the dissolution of gypsum from the unsaturated zone during this period. This conclusion is supported by the shape of the calcium curves for layer 2 (see Figure 2.5). From year 0 to 100 the calcium level increases as more and more gypsum dissolves. The fact that there is an increase in the amount of gypsum brought into solution is due to the decrease in sulphate input to the tailings porewater from pyrite oxidation. The peak in the calcium curve at year 100 indicates that the gypsum inventory is depleted some time between years 100 and 200.

It is worth noting here that the interpretation of mean value plots from

FIGURE 2.4

TAILINGS POREWATER SULPHATE LEVEL
FROM TEST 4
FOR SCENARIO I: BASE CASE

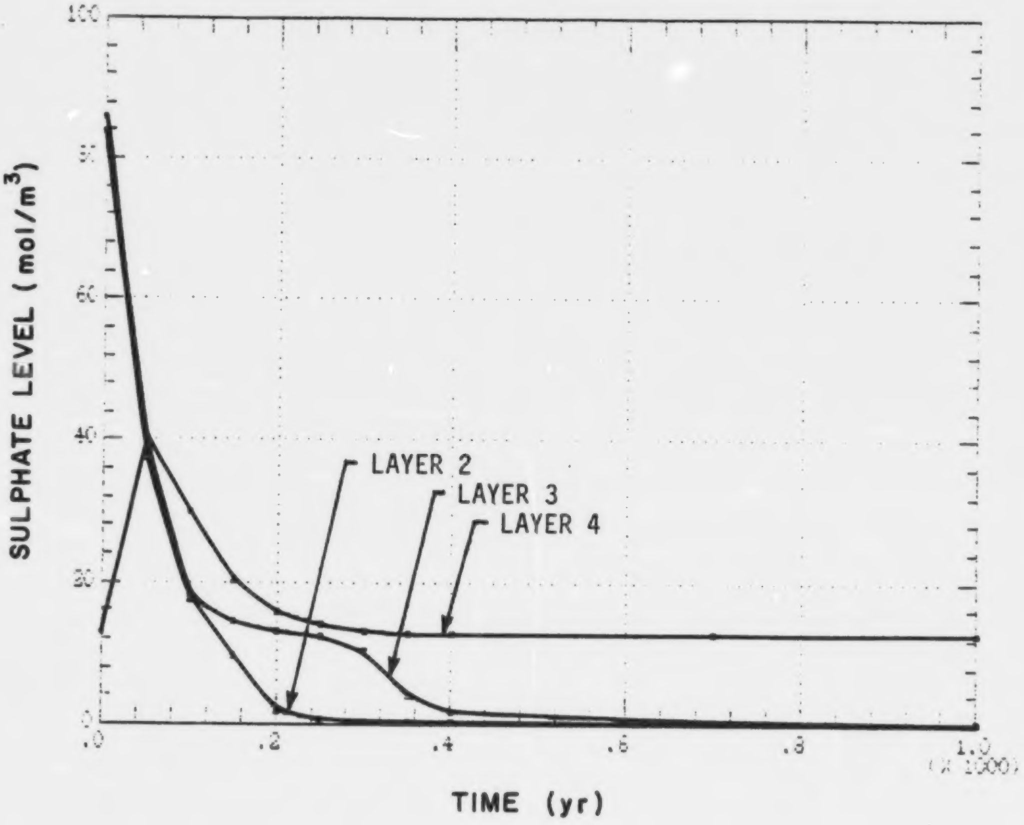

**NOTE:**

1. PLOT OF GEOMETRIC MEAN VALUES OF 10 PROBABILISTIC TRIALS

FIGURE 2.5

## TAILINGS POREWATER CALCIUM LEVEL FROM TEST 4 FOR SCENARIO I: BASE CASE

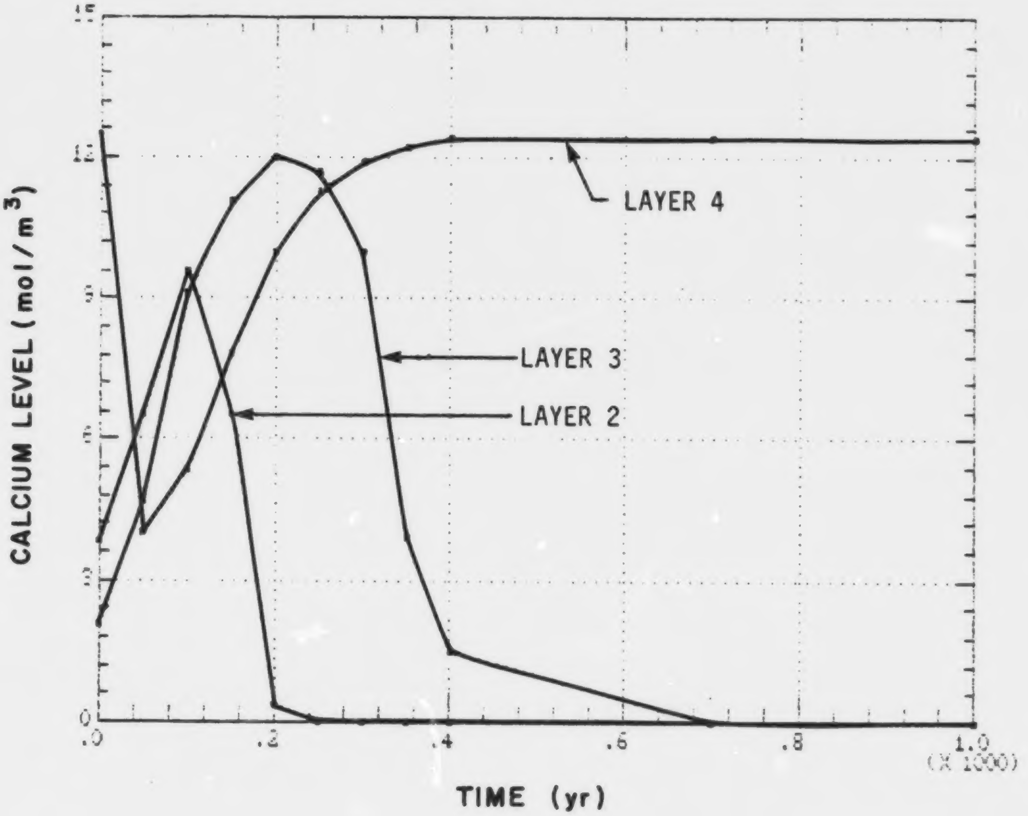

NOTE:

1. PLOT OF GEOMETRIC MEAN VALUES OF 10 PROBABILISTIC TRIALS

## FIGURE 2.6

## TAILINGS POREWATER IRON LEVEL FROM TEST 4 FOR SCENARIO I: BASE CASE

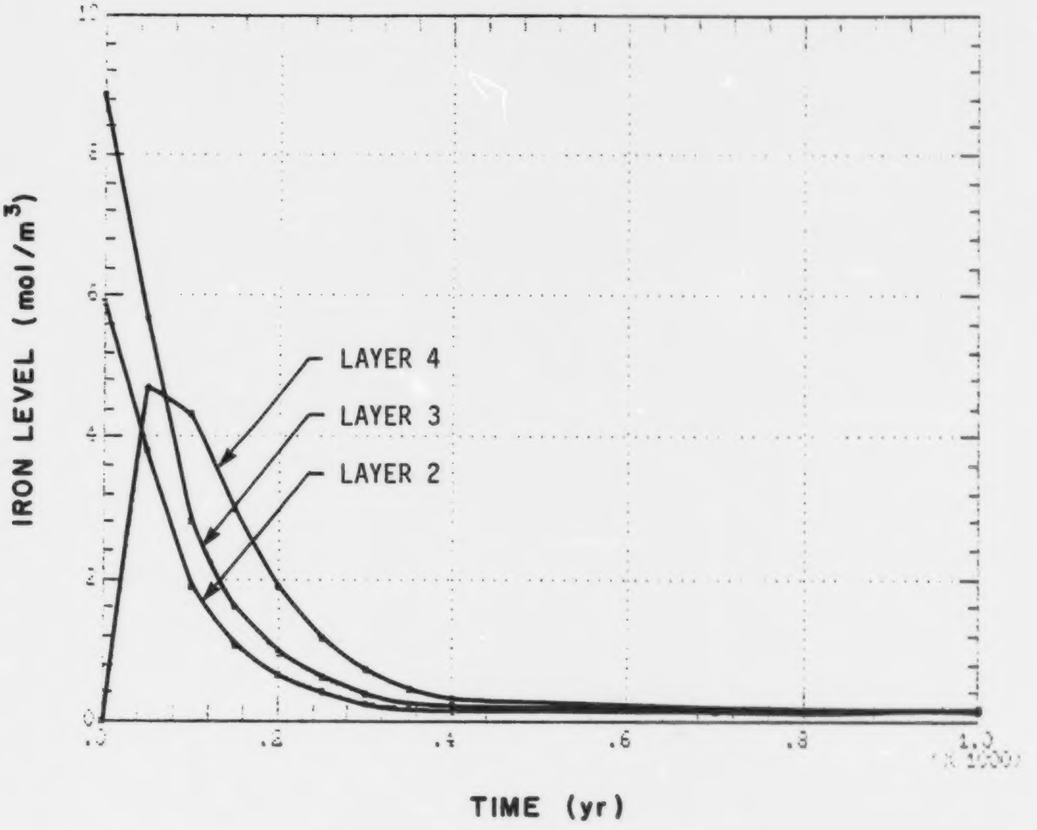

**NOTE:**

1. PLOT OF GEOMETRIC MEAN VALUES OF 10 PROBABILISTIC TRIALS

## FIGURE 2.7

## TAILINGS POREWATER pH
## FROM TEST 4
## SCENARIO I: BASE CASE

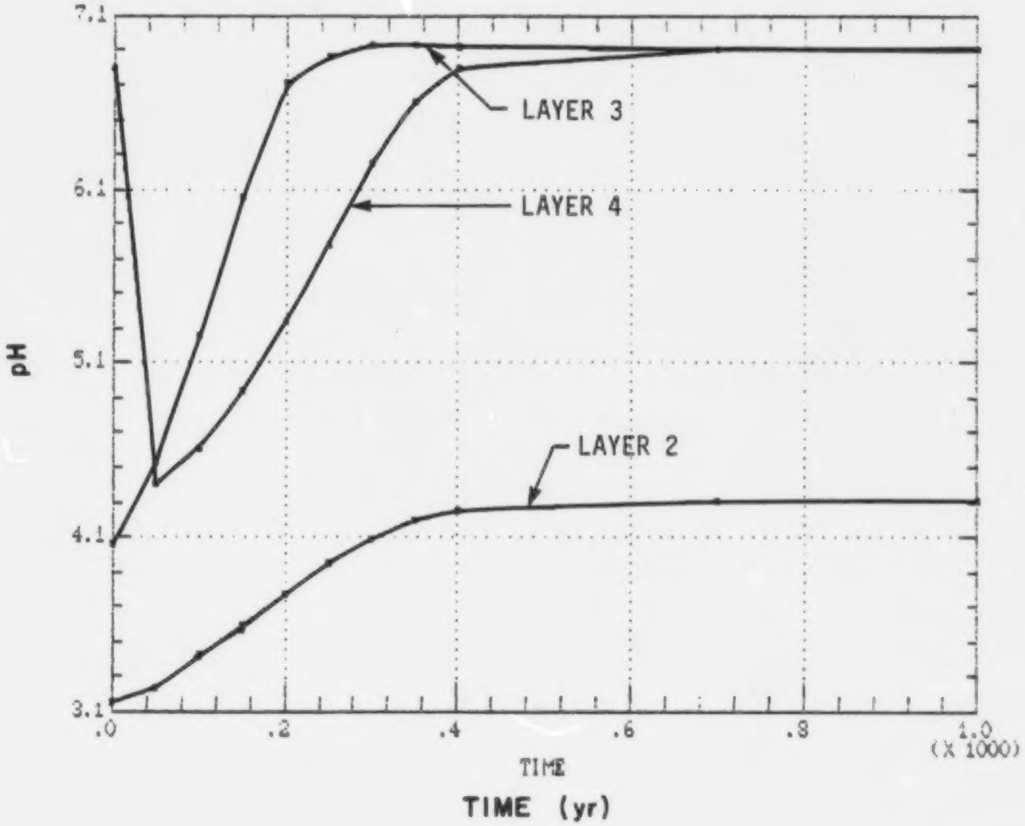

NOTE:

1. PLOT OF GEOMETRIC MEAN VALUES OF 10 PROBABILISTIC TRIALS

several probabilistic runs is more difficult than a plot of the output results of a single deterministic run. In a deterministic run, once the gypsum inventory is depleted from a layer, the sulphate curve would show a sharp decline. For example, on Figure 2.4 the sulphate curve for layer 3 would drop sharply from a level of about 12 mol.m$^{-3}$ at year 300 to nearly zero. The plot of several probabilistic trials shows a gradual decline in the sulphate level from year 300 to year 500. The shape of this curve reflects the effect of averaging several curves, each having its own distinct shape. The same observation is apparent from the shape of the calcium curves for layers 2 and 3.

The shape of the sulphate and calcium curves for layer 4 are also readily explained in light of the above discussion. The sulphate level at year 0 is determined by the solubility of gypsum. As a portion of the tailings porewater moves downward into layer 4 with time, the sulphate level in layer 4 increases due to the influx of water high in sulphates.

Once the sulphate concentration in layer 3 drops below that in layer 4 at about year 50, the curve for layer 4 declines again. In the long term, the sulphate level in layer 4 reverts back to that determined by the solubility product for gypsum. The calcium concentration in layer 4 behaves in exactly the opposite manner to the sulphate concentration. This is attributable to less gypsum dissolving between year 0 and year 50 while the influx of high sulphate water from layer 3 causes the sulphate level to rise in layer 4. The calcium level subsequently rises as more gypsum dissolves once the sulphate concentration begins to decline.

The iron levels shown on Figure 2.6 again demonstrate the behaviour of the pyrite oxidation component of the tailings source term model. The iron concentration in layer 2 follows the sharp downward pattern noted previously for sulphate. The profile reaches a quasi steady-state level about year 400, which typifies the exponential relationship built into the model.

Due to the reduction of ferric iron to ferrous iron in layer 3 and the concurrent oxidation of additional pyrite, the iron level in layer 3 is predicted to be about 1.5 times the level in layer 2. Again, the model was found to perform as expected.

As noted previously regarding the sulphate level in layer 4, the iron level increases initially due to the influx of iron rich tailings porewater. Once the iron concentration in layer 3 drops below that in layer 4, however, the pattern reverses and the iron level declines to a residual level, as expected.

Finally, the shapes of the pH curves on Figure 2.7 are explained by patterns noted for the major ions discussed above.

The pH of layer 2 increases from a low of about 3.1 to 4.3 over the period from year 0 to year 400 as the pyrite content in the unsaturated layer is oxidized. The pH in the unsaturated layer is predicted to stabilize at about 4.3 due to the influx of acid precipitation.

The pH behaviour of layer 3 is similar to layer 2 although the pH is buffered at a higher level due to the reduction of ferric iron to ferrous iron and the formation of iron complexes. As suggested by the pH curve for layer 3, most of the acid flux from layer 2 occurs in the initial 200 year period. The pH of layer 3 is predicted to stabilize at about 6.9, which was verified by hand calculations.

The pattern in layer 4 conforms to the trends noted for the major ionic species. As the sulphate and iron concentrations in layer 4 increase from time 0 to 50, the pH decreases from about 6.8 to 4.4. From year 50 onwards, the pH recovers as the sulphate and iron concentrations decrease and the calcium concentration increases. The pH in layer 4 stabilizes at about 6.9 as anticipated.

### Water Source Model/Surface Water Dispersion Model Comparison

Another example of Test 4 is illustrated in Figure 2.8. Here both the

FIGURE 2.8

## CONCENTRATIONS OF RADIONUCLIDES FROM TEST 4 FOR TEN PROBABILISTIC TRIALS

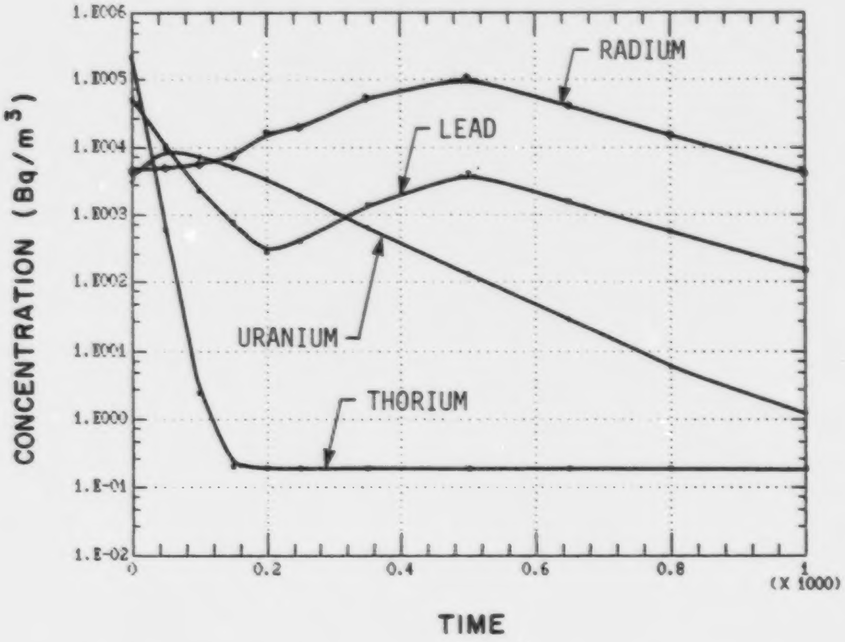

A) SOURCE MIXING ZONE

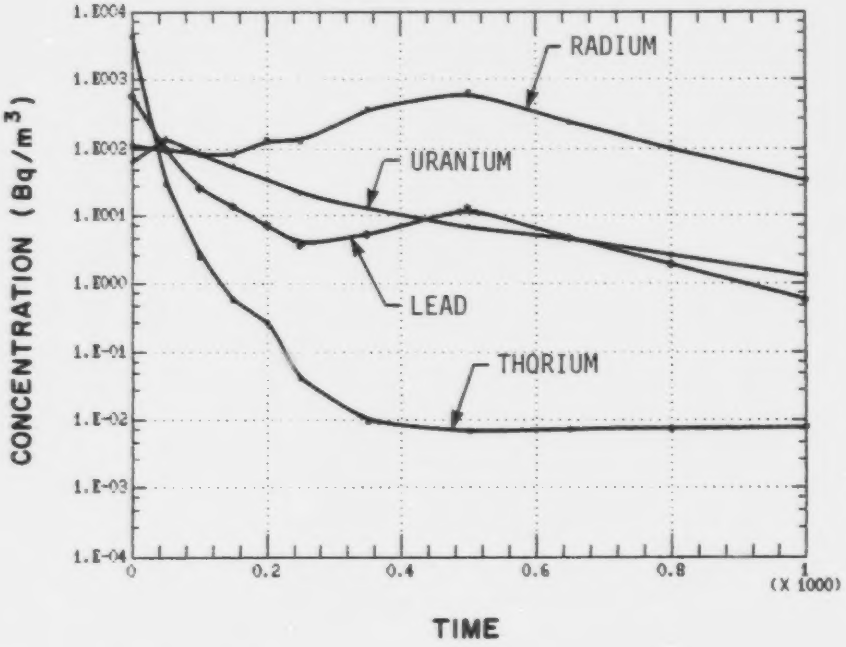

B) SECOND LAKE

radionuclides concentrations in the mixing zone of the tailings water source and in the second lake downstream of the tailings site (Figures 2.8 (a) and (b), respectively) are plotted for the four radionuclides.

The trends in the source concentration curves were first examined for reasonableness. The high initial release of thorium is explained by the fact that it is mobilized under the acidic conditions which prevail while pyrite is being oxidized. Because the pyrite content in the upper tailings horizon (i.e. in the unsaturated zone) is essentially completely oxidized between 150 to 200 years, it follows that most of the thorium released from the tailings solids occurs during this period and declines progressively as the tailings porewater pH gradual recovers. The low but steady release of thorium in the long term reflects the gradual dissolution of thorium complexes in the mixing zone.

The initial release of lead-210 is attributable to the dissolution of lead sulphate precipitate. The downward trend in the curve between years 0 and 200 reflects the progressive decline in the lead-210 content in the lead sulphate precipitate due to radioactive decay. As lead-210 ingrows to the radium precipitate matrix, the pattern in the lead-210 content in the tailings porewater beyond year 200 closely parallels the radium-226 curve.

The gradual increase in the radium-226 level reflects a progressive increase in the rate at which barium (radium) sulphate precipitate is dissolved. The rate at which the precipitate dissolves initially is controlled by the sulphate input to the tailings porewater from pyrite oxidation. Once the pyrite content is fully oxidized, between years 150 and 200, the rate of barium sulphate dissolution increases. However, as gypsum dissolution also controls the rate of barium sulphate dissolution, the radium-226 activity does not reach a peak level until about year 500. Thereafter, the radium bearing precipitate continues to dissolve and radium absorbed on the surfaces of other chemical precipitates is released to the porewater. The progressive decline in the radium concentration with time reflects the incorporation of a $K_d$ term in the model for radium release from the mixing layer (i.e. the tailings saturated zone).

The release of uranium is modelled as a direct function of pyrite oxidation. The level increases initially as the pyrite oxidizes at a rapid rate over the initial 100 years. Thereafter the uranium content declines as the oxidizable pyrite inventory is depleted. The long term source of uranium is due to the release of uranium bound to the surface of the tailings solids which is modelled using a $K_d$ (distribution coefficient) relationship.

The lake concentrations (Figure 2.8) are seen to follow the same trend as those in the source but are, for the most part, much lower. Because the surface water dispersion model includes radionuclide removal with sedimenting solids and release and feedback to the water phase as the solids undergo decomposition, the concentrations in the lake (Figure 2.8b) vary over a narrower range than the comparable radionculide levels in the tailings water source (Figure 2.8(a)). This results was expected. The feedback from the sediment also explains why the thorium level in the lake takes about 400 years to reach a quasi steady-state level while the thorium level in the tailings water source reaches a quasi steady-state level in about 150 years. Similarly, the uranium level in the lake water column decreases at a much slower rate than in the tailings water source due to the feedback from lake sediment. The same observations also hold for radium-226 and lead-210 although they are less pronounced due to continual release from the tailings source of substantial activities of both radionclides over the 100 year simulation period. The comparison of the two sets of these curves seem to be reasonable.

## Total Dose/Animal Produce Model Comparison

Figure 2.9(a) shows the results of another example from this test. From experience and intuition, the meat consumption dose seemed high. Examination of the input values revealed that one input parameter, water intake of caribou (WIRC), had been specified as $11.5 \times 10^3$ when it should have been $11.5 \times 10^{-3}$. The problem was corrected and the system model was rerun to produce the output

FIGURE 2.9

DOSE BY PATHWAYS FROM TEST 4
FOR TEN PROBABILISTIC TRIALS

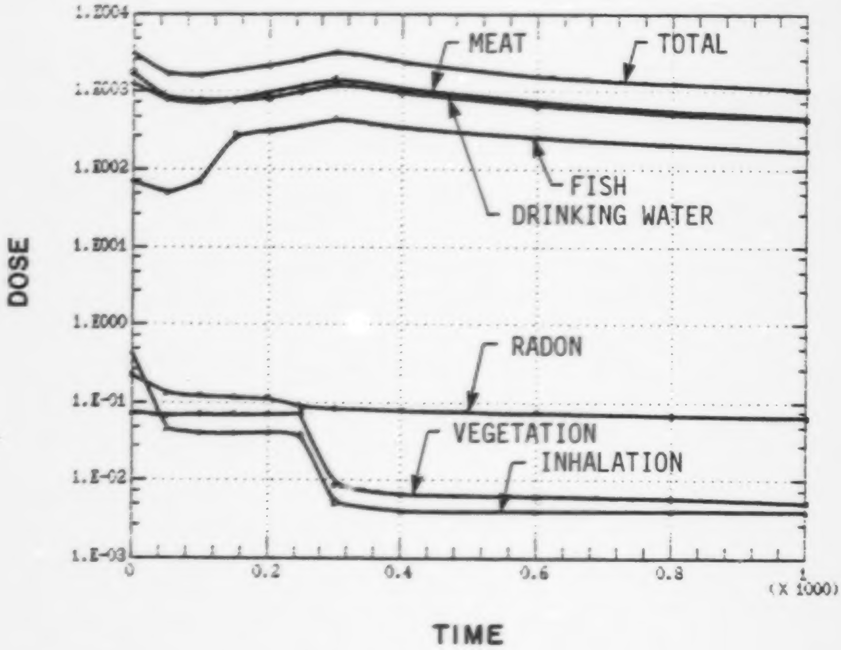

A) BEFORE CORRECTION

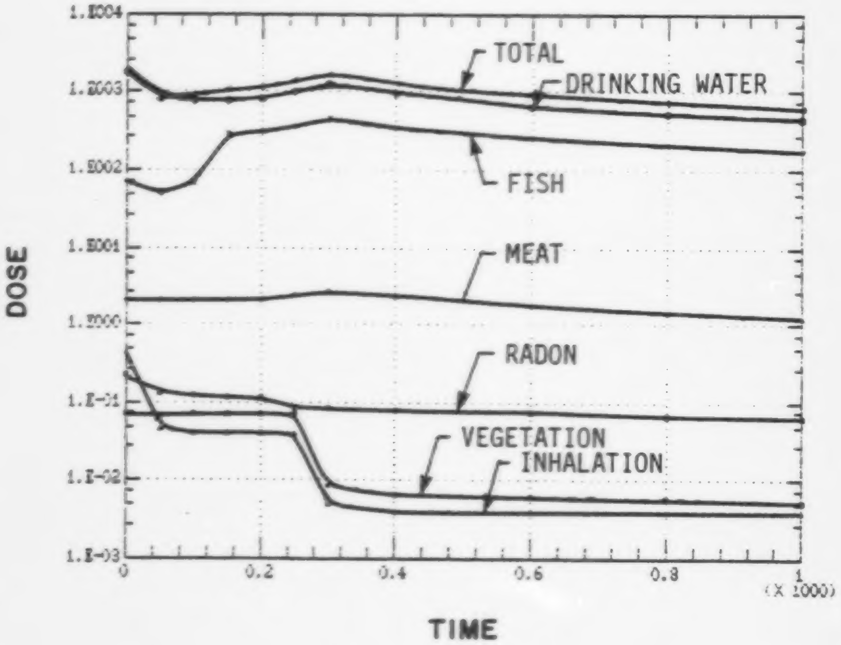

B) AFTER CORRECTION

illustrated in Figure 2.9 (b).

The trends in the dose curves presented in Figure 2.9(b) were examined further for reasonableness. Beginning with the total drinking water dose, the change of the curves was examined in conjunction with the results shown on Figure 2.8 (b) for the individual radionclides. This comparison indicated that the pattern of the drinking water curve was found to be quite reasonable. Between years 0 and 100 the curve paralleled the downward trend in the thorium and lead-210 curves. Thereafter the drinking water dose curve mirrored the radium concentration profile which was by far the most significant radionuclide in the surface water environment. The dose attributed to fish consumption was also found to be dominated by radium in the long term. The distinct shape of the curve over the initial 150 or so years was found to be due to reduced availability of fish as a result of low pH values predicted in the surface water system. Again, the curve was reasonable.

The shape of the dose curve from meat consumption suggests that the main source of radionuclide uptake by game animals is from water consumption, which is reasonable. As expected, the radon dose curve decreases progressively with time as radium-226, the source of radon gas, is progressively leached from the uppermost layers of the tailings mass. The form of the dust inhalation curve shows a rapid decline over the initial 50 years which parallels the leaching of thorium from the upper tailings horizon. The sudden decline about year 250 reflects a rapid drop in the dust source term due to vegetation of the tailings surface once the pH in the unsaturated zone recovers to above 4.0. Finally, the form of the vegetation dose curve closely parallels the dust inhalation curve as expected since the transfer of radionuclides from air-to-vegetation predominates over the transfer of radionuclides from soil-to-vegetation. It was concluded therefore, that the results shown on Figure 2.9(b) were explainable and reasonable.

## Tailings Erosion Model Example

Figure 2.10 illustrates the results of an erosion model test run in which the

FIGURE 2.10

CUMULATIVE TAILINGS DEPLETION
AND pH FROM TEST 4

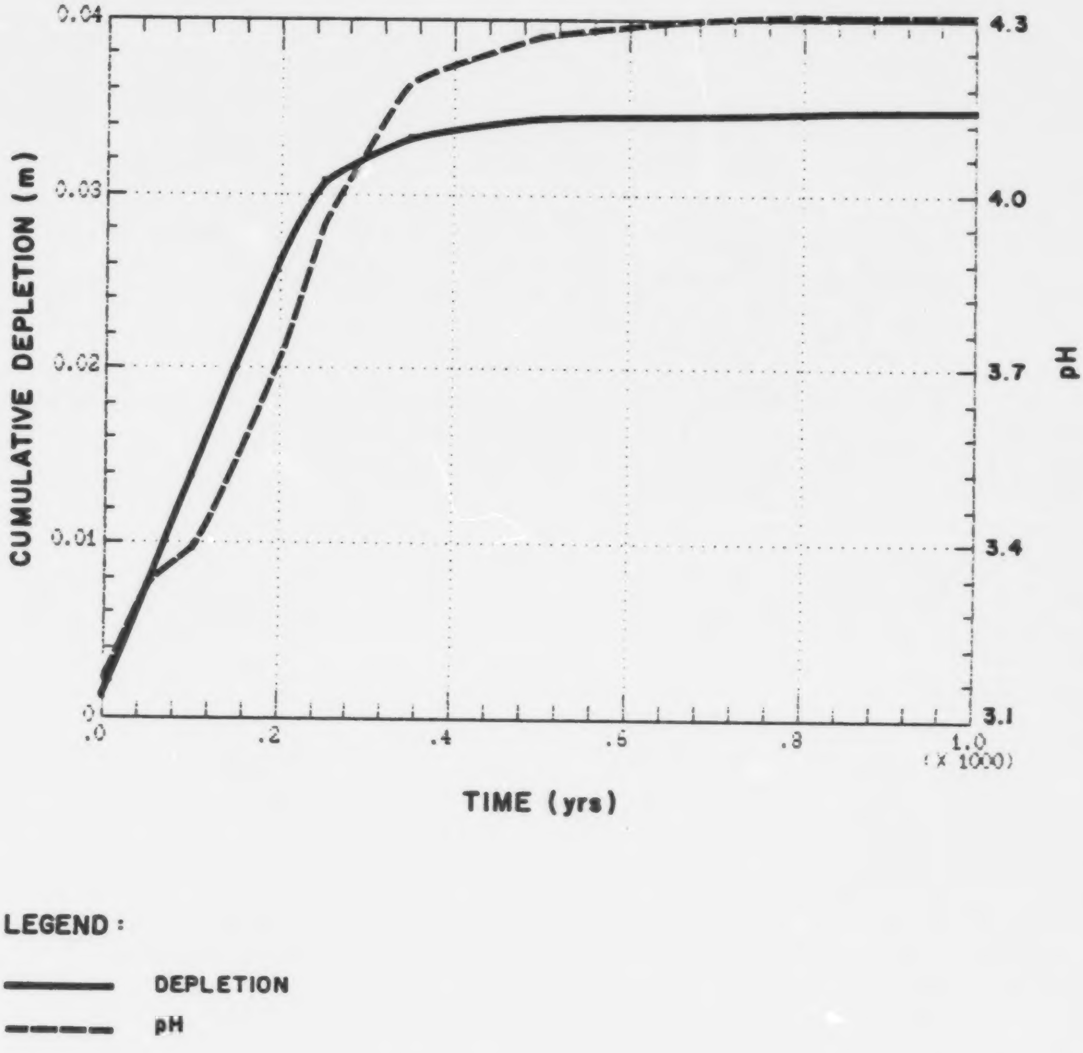

loss of solids due to surface water erosion were treated with time. The cumulative depletion of the tailings pile in metres and the pH of layer 1 are plotted against time. It should be noted that Figure 2.10 displays median values for ten trials with straight lines drawn between the actual data points. These lines cause an unnatural smoothing and should not be confused with actual results since only eleven data points were plotted.

The cumulative amount depleted after 250 years equals about 3.0 cm which was determined to be reasonable for bare soil. The rate of loss is seen to decline rapidly once the pH moves above 4.0 because of the reduction in erosion due to tailings revegetation. The model predicts that when the surface is about 90% vegetated, the rate of loss equals only about 1% of that for bare soil. This is reflected in the results in Figure 2.10.

The shape of the pH curve reflects the effect of averaging 10 probabilistic trials. The curve is a plot of predicted pH in the porewater of the unsaturated zone (i.e. pH of layers 1 and 2) in the tailings mass. Between about year 50 and 200, the pyrite content in the unsaturated zone is effectively oxidized depending on the oxidation rate selected in any trial. Hence the shape of the individual pH curves varied considerably over this time period. The apparent change in slope in the pH curve is merely a reflection of the result from combining the ten curves and the smoothing effect of joining eleven data points as noted previously. The pH curve reaches an upper limit of 4.3 which corresponds with the upper limit incorporated into the pH subroutine to account for the natural acidity in precipitation.

### 2.4.6 Test 5 - Reasonableness Check of Depyritized Tailings Option Using Nominal Input Values.

The objective of this test was to confirm that the option involving the addition of calcite to a cover layer of depyritized tailings was performing calculations correctly and that the results within the system model context were reasonable.

## Tailings Source Model Example

A 1000 year simulation was run using a ten year time-step and deterministic input values. One of the key variables evaluated in this test was the predicted pH of the tailings porewater in the unsaturated zone (layer 2) and in the mixing zone (layer 3). The predicted pH values for the two layers are plotted on Figure 2.11.

The pH in layer 2 (designated pH2) is seen to equal about 7.2 from year 0 to 50. This observation was expected as calcite was added to the top layer in this option to neutralize the acidity produced from pyrite oxidation. The pH curve shows a dramatic drop between years 50 and 100 once the calcite inventory added to the tailings surface layer is depleted. The pH level of about 3.2 observed at year 100 is attributable to the acid produced from pyrite oxidation. After about year 400 the pH is seen to reach a quasi steady-state level of about 4.3 which corresponds with the pH assumed for precipitation at the reference tailings site.

The pH profile in layer 3 (designated pH3) differs from that for layer 2 as a different ionic equilibrium expression is used to model the pH of the reducing environment in the saturated zone. The initial pH of about 5.3 reflects the input to layer 3 of a moderate amount of ferric iron and sulphate from the layer during the period from year 0 to year 50. Once the concentrations of the predominant ionic species (ferric and sulphate) increase in the inflow from layer 2 after year 50, the pH in layer 3 shows a sharp drop. Due to the reducing environment in layer 3, which leads to the reduction of ferric iron to ferrous iron and the oxidation of additional pyrite, the pH declines to about 4.3. The pH eventually recovers to about 6.9 once the pyrite inventory is depleted.

In summary, the system model was found to perform as expected for options involving the addition of calcite to a depyritized tailings curve. The predicted pH levels were confirmed by a set of hand calculations. The test was considered to have been successful.

FIGURE 2.11

## TAILINGS POREWATER pH
## FROM TEST 5
## FOR SCENARIO 2 : DEPYRITIZED TAILINGS COVER

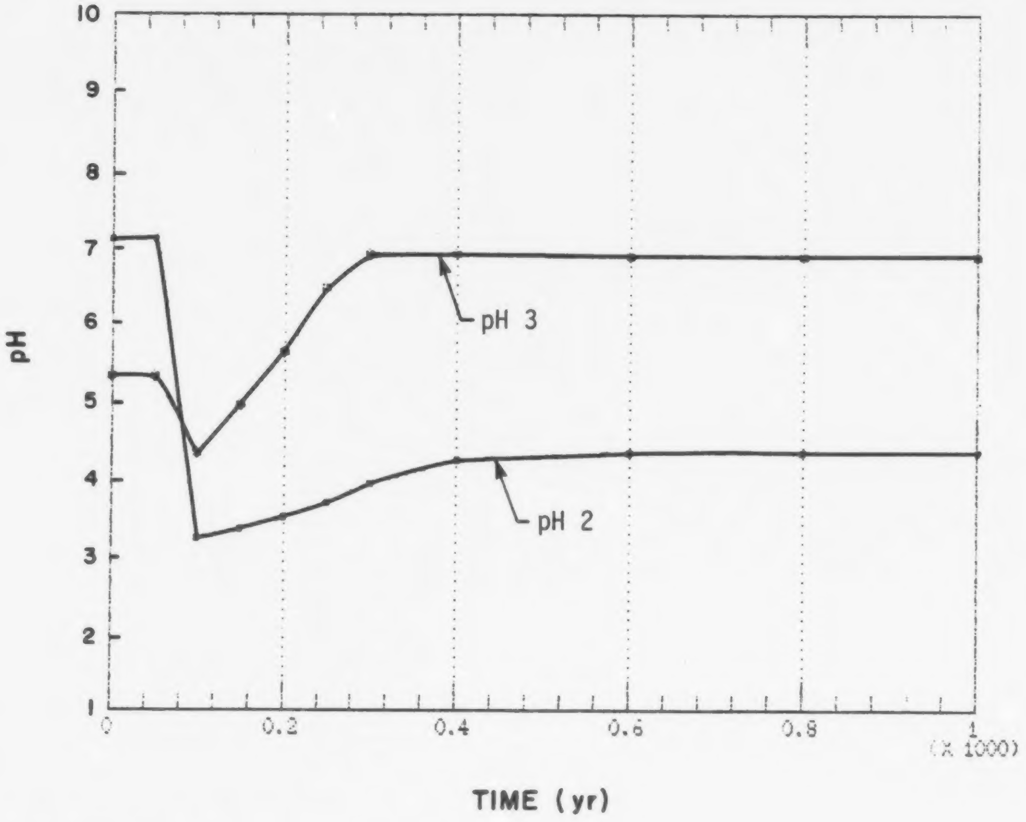

### 2.4.7 Test 6 - Sensitivity Analysis

The Phase II studies (SENES, 1985) examined many tools for parameter importance analysis. At that time the sensitivity index was found to be a simple but effective tool for isolating important variables and was selected for use in Phase III. The sensitivity index for a particular input parameter is calculated by holding all other parameters constant at their nominal values and calculating the desired output at the minimum and maximum values of the input parameter being studied. The sensitivity index (SI) is a measure of the response of the model to changes in the input parameters and is calculated as:

$$SI = 1 - \frac{\text{Low Result}}{\text{High Result}} \qquad (2.7)$$

Parameters with SI values near 1 are considered to be important whereas parameters with SI values near 0 have little influence on the model calculations. A detailed discussion of the sensitivity index can be found in Volume 2 of Phase II (SENES, 1985).

The sensitivity index was calculated for all parameters to identify those combinations of input parameter values that produced the highest possible total dose at 0 and 250 years. The system model was then run using that combination of input values which maximized the dose at 250 years. This test was primarily designed to evaluate the mathematical stability of the model when run at the limits of the input parameter values (i.e. the minimum and maximum values from the probabilistic input file).

In running this test, an arithmetic overflow was found in the water model where a term of the form $e^{-x}$ was not checked to see if it approached zero. This was corrected by setting very small values to zero. Also, several problems were found when total dose was maximized.

## Surface Water Dispersion Model/Tailings Water Source Model Example

The first problem found was in the surface water model. The detailed printout shown on Table 2.10 clearly indicates that the problem stems from a negative source flow (SFLOW) input to the surface water model. The tailings water source flow is calculated as:

$$F_s = (P * A) - (f_p * \overline{P} * A) \tag{2.8}$$

where

$F_s$ = source flow ($m^3.yr^{-1}$)
$P$ = annual precipitation ($m.yr^{-1}$)
$A$ = tailings surface area ($m^2$)
$f_p$ = fraction of net precipitation which infiltrates the full depth of the tailings
$\overline{P}$ = long-term mean annual net precipitation ($m.yr^{-1}$)

When dose was maximized, the result was:

$$F_s = (.1)\ (5 \times 10^5) - (.8)\ (.4)\ (5 \times 10^5) = -110000\ m^3.yr^{-1} \tag{2.9}$$

After examination of the problem, it was resolved that the minimum annual precipitation was too small and the maximum fraction of precipitation which could infiltrate deep into the tailings mass was unreasonably large. New limits were chosen as 0.15 and 0.3 respectively, making a negative source flow impossible.

## Surface Water Dispersion Model Example

The next problem encountered was in the iterative solution of the pH equation used in the surface water model:

## Table 2.10

## DETAILED PRINTOUT FROM WATER MODEL - SENSITIVITY INDEX PROGRAM

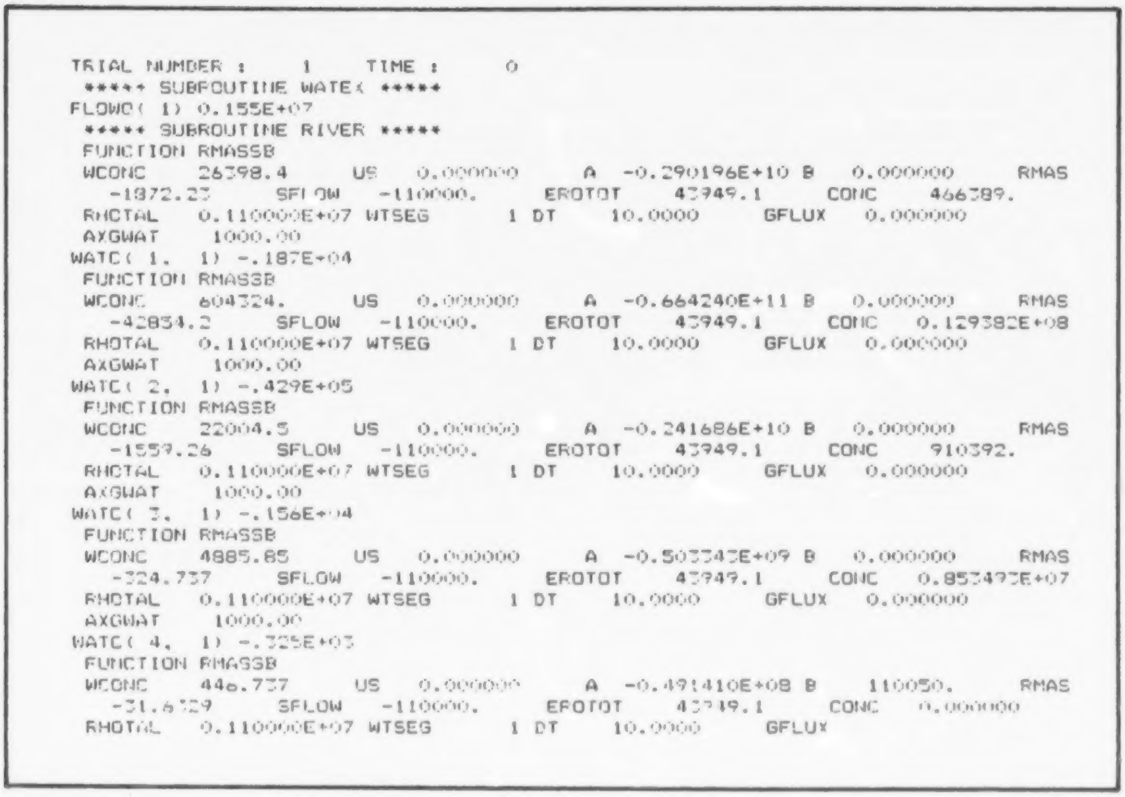

```
TRIAL NUMBER :      1     TIME :       0
 ***** SUBFOUTINE WATEK *****
FLOWO( 1) 0.155E+07
 ***** SUBROUTINE RIVER *****
 FUNCTION RMASSB
 WCONC     26398.4      US    0.000000       A  -0.290196E+10 B    0.000000       RMAS
   -1872.23        SFLOW    -110000.       EROTOT     43949.1       CONC     466389.
 RHCTAL    0.110000E+07 WTSEG        1 DT      10.0000        GFLUX    0.000000
 AXGWAT     1000.00
WATC( 1.  1) -.187E+04
 FUNCTION RMAS3B
 WCONC     604324.      US    0.000000       A  -0.664240E+11 B    0.000000       RMAS
   -42854.2        SFLOW    -110000.       EROTOT     43949.1       CONC   0.129382E+08
 RHOTAL    0.110000E+07 WTSEG        1 DT      10.0000        GFLUX    0.000000
 AXGWAT     1000.00
WATC( 2.  1) -.429E+05
 FUNCTION RMASSB
 WCONC     22004.5      US    0.000000       A  -0.241686E+10 B    0.000000       RMAS
   -1559.26        SFLOW    -110000.       EROTOT     43949.1       CONC     910392.
 RHCTAL    0.110000E+07 WTSEG        1 DT      10.0000        GFLUX    0.000000
 AXGWAT     1000.00
WATC( 3.  1) -.156E+04
 FUNCTION RMASSB
 WCONC     4885.85      US    0.000000       A  -0.503343E+09 B    0.000000       RMAS
   -324.737        SFLOW    -110000.       EROTOT     43949.1       CONC   0.853493E+07
 RHOTAL    0.110000E+07 WTSEG        1 DT      10.0000        GFLUX    0.000000
 AXGWAT     1000.00
WATC( 4.  1) -.325E+03
 FUNCTION RMASSB
 WCONC     446.737      US    0.000000       A  -0.491410E+08 B     110050.       RMAS
   -31.6329        SFLOW    -110000.       EFOTOT     43949.1       CONC    0.000000
 RHOTAL    0.110000E+07 WTSEG        1 DT      10.0000        GFLUX
```

Key

FLOWQ - Flow ($m^3/a$)
WCONC - Source concentration ($Bq/m^3$)
US - Upstream Flow ($m^3/a$)
A - Intermediate variable
B - An Intermediate Variable
RMAS - Concentration in River ($Bq/m^3$)
SFLOW - Flow from source ($m^3/a$)
EROTOT - Erosion (kg)
CONC - Concentration in erosion ($Bq/m^3$)
RHOTA1 - Tailings Bulk Density ($g/m^3$)
WTSEG - Segment number
DT - Time increment
GFLUX - Groundwater Flux (Bq/m)
AXGWAT - Groundwater window ($m^2$)

$$F(pH) = 3\left[\frac{10^{8.5-3pH_{n,t}}}{f^{9/4}}\right] + 2\left[\frac{10^{3.91-2pH_{n,t}}}{f}\right] + \left[10^{0.3-pH_{n,t}}\right] + \left[10^{-3.86}\right] + 2[Ca^{2+}]_{n,t}$$

$$- [SO_4^{2-}]_{n,t}\left[\frac{2 - f^{3/4}\,10^{11.7-3pH_{n,t}}}{1 + f^{3/4}\,10^{11.7-3pH_{n,t}}}\right] - \left[\frac{10^{pH_{n,t}-11.0}}{f^{1/4}}\right] \qquad (2.10)$$

where

$f$ = the activity coefficient; for the reference watershed environment f would be expected to fall between 0.6 an 0.9 with a probable value of 0.8.

$pH_{n,t}$ = the pH level of the surface water in the watershed at node 'n' at time 't'

$[Ca^{2+}]_{n,t}$ = concentration of calcium in the surface water at node 'n' at time 't' ($mol.m^{-3}$)

$[SO_4^{2-}]_{n,t}$ = concentration of sulphate in the surface water at node 'n' at time 't' ($mol.m^{-3}$)

A negative guess at pH in this equation resulted in an arithmetic overflow. This problem had been encountered previously in the development of the model and was thought to have been accounted for. For this reason, Figure 2.12 was plotted showing the solution of the pH equation, F(pH), against pH using nominal inputs to the model. Clearly, the function is very poorly behaved since the slope increases very rapidly beyond pH's of about 4 and 9, respectively. In the inner range of this equation (i.e. the flat portion of the curve) the equation will converge slowly but an initial guess outside of this range can result in an extremely low or high guess the next time. To overcome this problem, a method was selected whereby, after each guess, maximum and minimum values were saved between which the result must fall. Guesses outside this range were reset to be within the range. After testing this method for stability, the model was reintegrated into the system model and the sensitivity index program was rerun without further problems.

### Total Dose Example

The parameters with the largest sensitivity indices are shown for total dose

FIGURE 2.12

SOLUTION OF pH EQUATION
FROM TEST 7

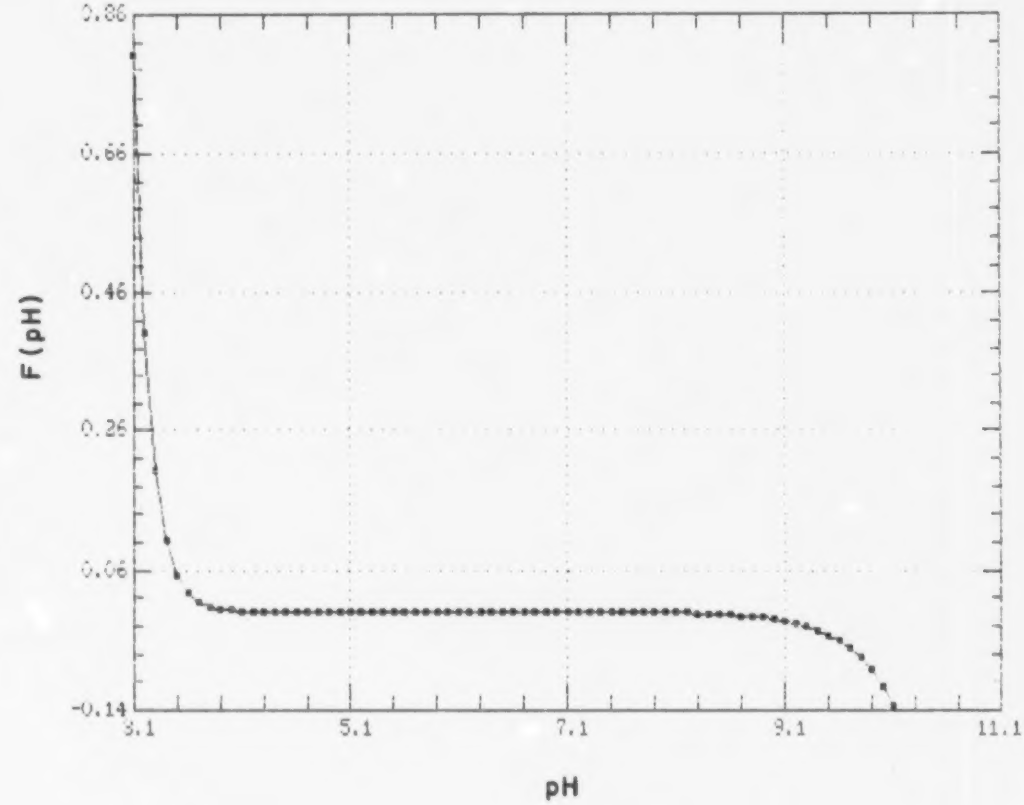

and drinking water dose in Table 2.11 for 0 and 250 years. Not surprisingly, there is a great deal of similarity between the important parameters for total dose and drinking water dose, since drinking water is the main contributor to total dose. All parameters listed in Table 2.11 are defined further in Table 2.12. A review of the parameters listed in Table 2.11 indicates that nearly all of the parameters are associated with the tailings source term component model. The only exceptions are the parameters relating the transfer of radium-226 and lead-210 from water to fish flesh (BIOACR and BIOACP), the transfer of lead-210 from water to sedimenting solids (WKDPB) and the fraction of the annual water consumption that is derived from a local source by the receptor (WFLOCI). These parameters are all related to the water pathways.

Since no unexpected results were obtained, the test was passed.

### 2.4.8 Test 7 - Check of Model Stability and Reasonableness Using Many Trials

The purpose of Test 7 was to check for model stability as well as reasonableness of output in a large number of runs. The test was repeated for Scenario 1 (the base case) and Scenario 2 (the depyritized tailings cover/calcite additions case) using 1000 probabilistic trials of 500 year duration and a ten year time-step.

#### Tailings Water Source Model Example

Only one problem was encountered, when a large value was sampled for the variable KRATE in the tailings water source model. This caused an overflow in a term approaching zero in SUBROUTINE IONS1L. A check for this was added, setting small values to zero.

#### Surface Water Dispersion Model Example

The output obtained for the two scenarios for the pH in the first lake downstream of the tailings site have been plotted in Figure 2.13. The results are quite different for the two scenarios with the predicted mean pH levels

Table 2.11

## PARAMETER SENSITIVITY INDEX[a] (SI) VALUES FOR THE BASE CASE

| Sensitivity of Total Dose | | | | | Sensitivity of Drinking Water Dose | | | | |
|---|---|---|---|---|---|---|---|---|---|
| Time | SI | List[b] | Sign[c] | Parameter[d] | Time | SI | List[b] | Sign[c] | Parameter[d] |
| 0 | 0.680 | 1 | + | SULPRD | 0 | 0.682 | 1 | + | SULPRD |
| | 0.672 | 2 | + | O2DIFF | | 0.673 | 2 | + | O2DIFF |
| | 0.609 | 3 | - | FRACTH | | 0.610 | 3 | - | FRACTH |
| | 0.544 | 4 | + | RHOTAL | | 0.545 | 4 | + | RHOTAL |
| | 0.434 | 5 | + | FACTCO | | 0.435 | 5 | + | FACTCO |
| | 0.413 | 6 | - | CLEADI | | 0.412 | 6 | - | CLEADI |
| | 0.413 | 7 | - | WKDPB | | 0.412 | 7 | - | WKDPB |
| | 0.387 | 8 | - | KPRIME | | 0.389 | 8 | - | NPRCP |
| | 0.385 | 9 | - | NPRCP | | 0.388 | 9 | - | KPRIME |
| | 0.247 | 10 | - | FNPRCP | | 0.247 | 10 | - | FNPRCP |
| 250 | 0.722 | 1 | + | BIOACR | 250 | 0.548 | 1 | + | NPRCP |
| | 0.582 | 2 | + | BIOACP | | 0.509 | 2 | - | KDRAD |
| | 0.542 | 3 | + | NPRCP | | 0.411 | 3 | + | SILT |
| | 0.508 | 4 | - | KDRAD | | 0.357 | 4 | + | PYRITI |
| | 0.416 | 5 | + | SILT | | 0.346 | 5 | - | RHOTAL |
| | 0.360 | 6 | + | PYRITI | | 0.304 | 6 | + | DUNSAT |
| | 0.350 | 7 | - | RHOTAL | | 0.296 | 7 | - | SULPRD |
| | 0.308 | 8 | + | DUNSAT | | 0.287 | 8 | - | WKDPB |
| | 0.301 | 9 | - | SULPRD | | 0.243 | 9 | - | DMIX |
| | 0.292 | 10 | - | WKDPB | | 0.200 | 10 | + | WFLOC1 |

Note

a $SI = 1 - \frac{\text{low result}}{\text{high result}}$

b ranking of parameters on basis of sensitivity index

c indicates whether the parameter has a positive or negative influence on the dose calculation

d parameter name used in computer code (see Table 2.12 for definitions)

Table 2.12

## SELECTED PARAMETER DEFINITIONS

| Computer Symbol | Definition |
|---|---|
| SULPRD | Sulphate production rate from pyrite oxidation. |
| O2DIFF | Oxygen diffusivity through tailings. |
| FRACTH | Fraction of thorium hydroxide which is crystalline (i.e. less soluble). |
| RHOTAL | Tailings bulk density. |
| FACTCO | Activity coefficient for divalent ions. |
| CLEADI | Initial concentration of lead sulphate ($PbSO_4$) in the tailings. |
| WKDPB | Lead-210 distribution coefficient between lake sediment and water. |
| KPRIME | Ratio of $O_2$ half saturation constant to $O_2$ concentration. |
| NPRCP | Net annual precipitation. |
| FNPRCP | Fraction of precipitation entering lower tailings layer. |
| BIOACR | Radium-226 bioaccumulation factor in fish flesh. |
| BIOACP | Lead-210 bioaccumulation factor in fish flesh. |

Table 2.12, Continued

| | |
|---|---|
| KDRAD | Radium-226 solid-to-liquid distribution coefficient. |
| SILT | Silt content of the tailings (% of particles < 75 μm). |
| PYRITI | Initial concentration of pyrite in the tailings. |
| DUNSAT | Thickness of the tailings unsaturated zone. |
| DMIX | Thickness of the tailings mixing zone. |
| WFLOCI | Fraction of annual water consumption that is local. |

FIGURE 2.13

pH IN FIRST LAKE FROM TEST 7
FOR 1000 PROBABILISTIC TRIALS

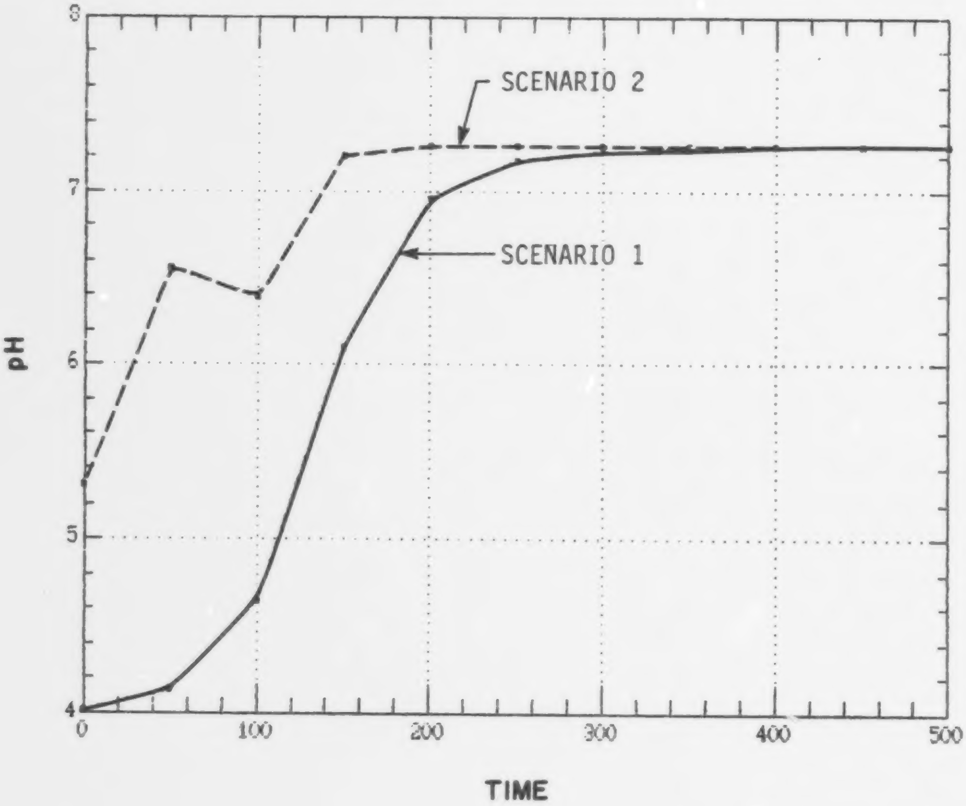

for Scenario 2 being much higher than those for Scenario 1 during the initial 250 or so years when pyrite oxidation occurs. This observation is attributable to two key factors: 1) the lower pyrite inventory in the tailings surface layer which necessarily limits the acid production in Scenario 2; and, 2) the presence of calcite in the tailings surface layer in Scenario 2 which limits the rate of pyrite oxidation and neutralizes acidity produced from residual pyrite oxidation.

The rise, fall and rise again in the pH curve for Scenario 2 during the initial 150 years was found to be due to the following sequence of factors. Firstly, the rise from year 0 to 50 reflects a slow but gradual decrease in the rate of acid production which is mirrored by a decrease in the acidity reaching the watershed and thus in a gradual increase in the pH level. Secondly, the decline between year 50 and year 100 coincides with exhaustion of the calcite (or limestone) content in the tailings. Once the calcite is exhausted, the rate of pyrite oxidation increases and the acid generated is no longer neutralized by the buffering capacity of the calcite. Finally, the extent of the downward shift in pH is limited by the fact that the residual pyrite content of the tailings surface layer is rapidly oxidized. Thus the pH in the watershed recovers to neutrality as indicated by the increase in pH between years 100 and 150 in Figure 2.13.

The pH curve for Scenario 1, the base case option, starts out at about 4.0 at year 0 and slowly rises over the initial 100 years. This gradual increase reflects a progressive decline in the acid loads from the tailings site as the pyrite inventory oxidizes. After about year 100, the pH in the receiving environment recovers more quickly as the last of the pyrite inventory is oxidized. By year 300, the pH in the downstream lake has recovered to the background watershed pH of about 7.25 as indicated on Figure 2.13.

The behaviour of the pH curves for the two disposal scenarios was found to be readily explained on close examination. The low initial predicted pH levels were also considered to be quite reasonable in light of experience with the disposal of sulphidic, acid generating tailings. It was concluded therefore, that the system model predictions were reasonable.

Dose by Radionuclide Example

In this example, the radon dose and water dose by radionuclide to the critical receptor located 2 km downwind of the tailings site on the shore of the first downstream lake was examined for each of the disposal scenarios. The data composed in this example are plotted on Figure 2.14(a) for Scenario 1 and 2.14(b) for Scenario 2.

As shown by the curves on Figure 2.14, the total dose is dominated by lead-210 during the initial 100 to 150 years in both scenarios. The lead-210 level during this period reflects the dissolution of lead sulphate precipitate which contains most of the lead-210 deposited in the tailings area with freshly deposited tailings. However, due to the short half life of lead-210 the activity of the lead sulphate precipitate declines rapidly and the amount of lead-210 dissolved thus decreases proportionately as indicated on both figures. In the long term, the lead-210 level is controlled by the dissolution of the radium sulphate coprecipitate and the associated lead-210 which has ingrown to the radium matrix. The behaviour of lead-210 thus seems reasonable in both scenarios.

The shapes of the radium-226 curves in both scenarios are quite similar. The activity level in Scenario 2 is marginally higher over the entire 500 year simulation period. This observation may be attributed to a lower dissolved sulphate level in the tailings porewater for Scenario 2 which allows more of the barium (radium) sulphate to dissolve. In both scenarios, the radium-226 activity does not rise substantially until after year 100 when most of the pyrite has been oxidized and the gypsum inventory in the tailings has dissolved.

Because Scenario 2 has a much lower initial pyrite content than Scenario 1, the radium coprecipitate dissolves more rapidly. Thus the peak activity in Scenario 2 occurs around year 250 whereas the peak activity in Scenario 1 does

FIGURE 2.14

TOTAL DOSE BY RADIONUCLIDE FROM TEST 7
FOR 1000 PROBABILISTIC TRIALS

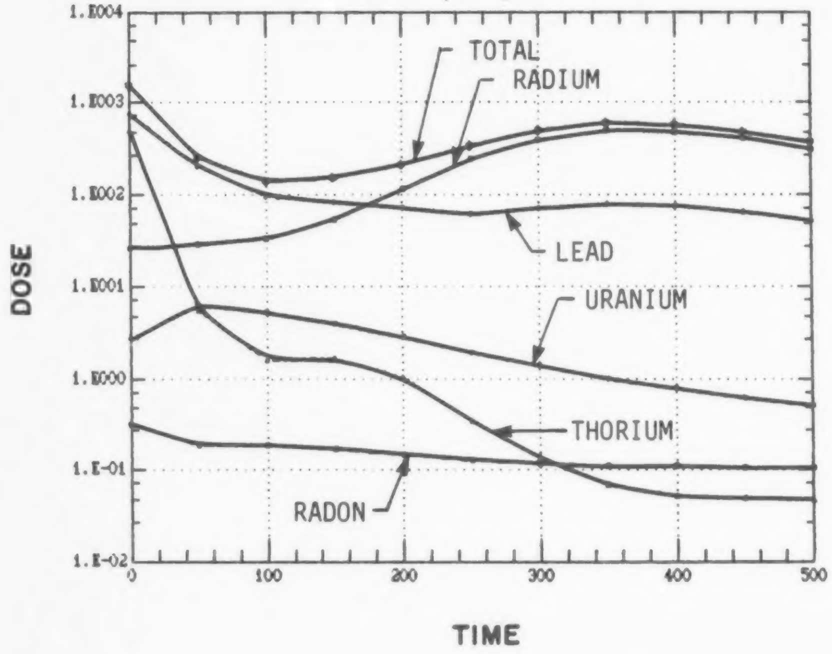

A) BASE CASE OPTION

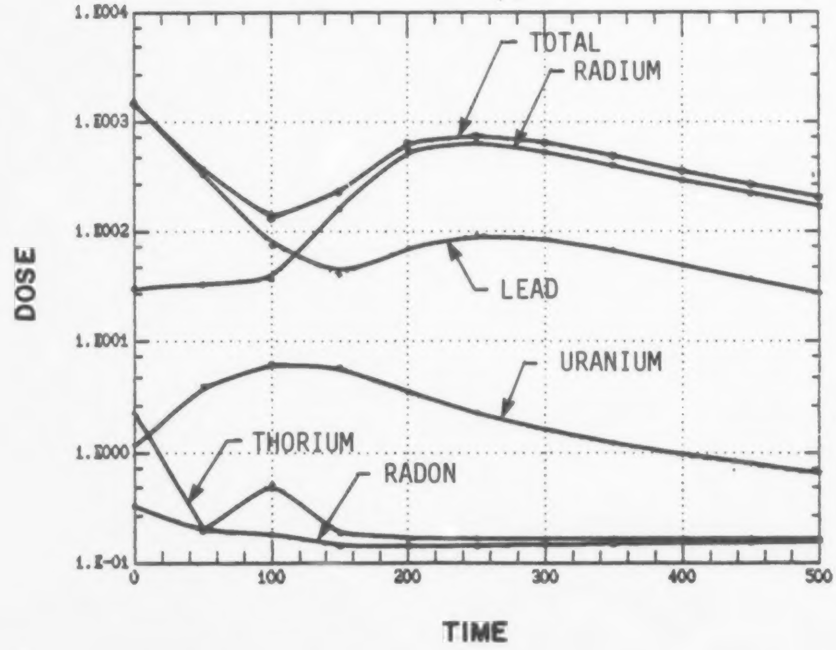

B) DEPYRITIZED TAILINGS OPTION

not occur until about year 350. Again, the shapes of the two curves appear quite reasonable.

The dissolution of uranium is modelled as a function of the amount of pyrite oxidized in the tailings source. The initial rise in both curves reflects a buildup in the tailings mass. Uranium release from the mixing layer of the tailings source is modelled using a $K_d$ factor which effectively retards the time of release. As the amount of pyrite oxidized decreases rapidly over the initial 100 years, the uranium curves peak at about years 50 and 100 respectively and decline continuously thereafter. The fact that the uranium activity does not peak in Scenario 2 until year 100 is due to the fact that the pyrite oxidation rate is reduced during the initial 50 or so years due to the elevated pH demonstrated previously on Figure 2.13. The continuous release of uranium over the entire 500 year simulation period reflects the incorporation of the $K_d$ factor in the source term model and feedback mechanism from lake sediments incorporated in the surface water dispersion model. In conclusion, the shapes of the two uranium dose curves conform to the features built into the tailings water source and surface water dispersion models.

The shapes of the thorium curves most distinctly display the differences in the two scenarios. Thorium solubilization is modelled in the Phase III version of UTAP as a function of pH only. Under the initial acid pH conditions predicted for Scenario 1 (see Figure 2.13) thorium is predicted to dissolve and be released from the tailings source during the first 100 years. Thereafter the release rate is much slower and the activity in the receiving water reflects mainly feed back from lake sediments. This factor explains the distinct difference in the two curves between years 200 and 500. The shape of the thorium curve in Scenario 2 over the initial 150 years is seen to be a mirror image of the pH curve on Figure 2.13. Based on these observations, it was concluded that the thorium predictions were reasonable in both cases.

Finally, the radon dose curve for Scenario 2 is observed to be slightly higher than the radon curve for Scenario 1. This observation is expected since less thorium is leached from the tailings surface layer in Scenario 2. As a consequence more thorium-230 and its daughter products are retained within the upper tailings horizon. Since radium-226, a daughter of thorium-230, is the source of radon gas, it follows that tailings material under the Scenario 2 option should be a larger source of radon.

## Total Dose by Pathway Example

Figure 2.15 is a plot of the geometric mean doses by pathway versus time for the base case disposal option (Scenario 1) and the depyritized tailings cover/calcite addition option (Scenario 2). As previously noted, the total dose curves for all pathways closely parallel the dose curves for the water pathways which dominate the total doses in both scenarios.

The shape of the drinking water dose curves for the two scenarios are reflections of the combined doses from the individual radionuclides shown on Figure 2.14. Initially, the drinking water dose is dominated by lead-210. After about year 100, however, the radium-226 dose curves contribute most of the drinking water dose. Thus, it is seen that the drinking water dose curves conform to expectations.

The shape of the fish dose curves closely parallel the water dose curves as expected since radionuclide transfer to fish is calculated by the application of a simple bioaccumulation factor. The model for calculating dose from fish consumption also includes a factor to account for the availability of fish as a function of the pH level in the receiving water. The influence of this factor is apparent in Figure 2.15(a) where the dose from fish consumption over the initial 150 years is suppressed due to a reduction in the availability of fish.

The shapes of the dose curves from ingestion of wild game meat closely parallel the water dose curves suggesting that the predominant source of radionuclides in game meat is the consumption of contaminated water. This observation was considered to be quite reasonable for the scenarios being evaluated, particularly when it is considered that the source of moose meat

FIGURE 2.15

## TOTAL DOSE BY PATHWAY FROM TEST 7 FOR 1000 PROBABILISTIC TRIALS

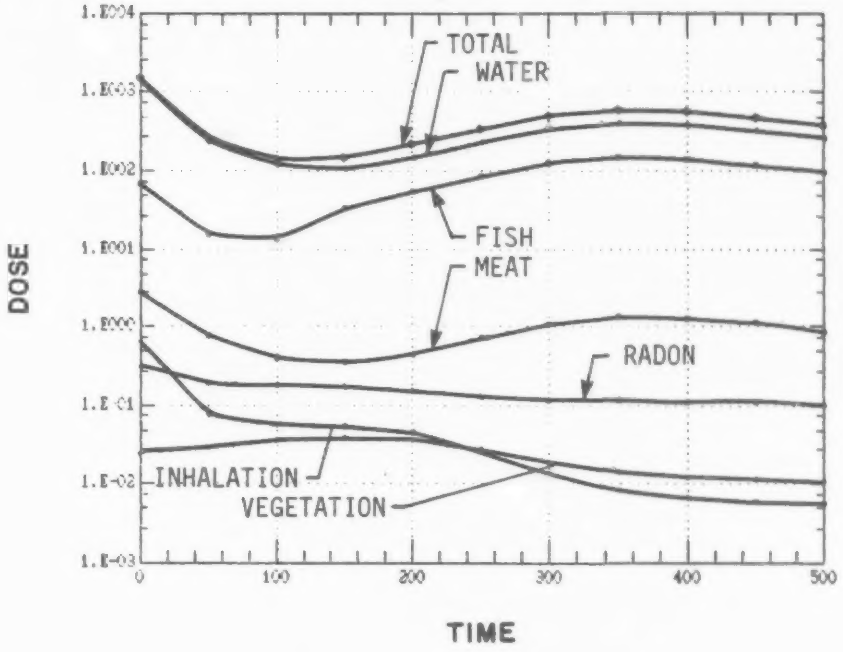

A) BASE CASE OPTION

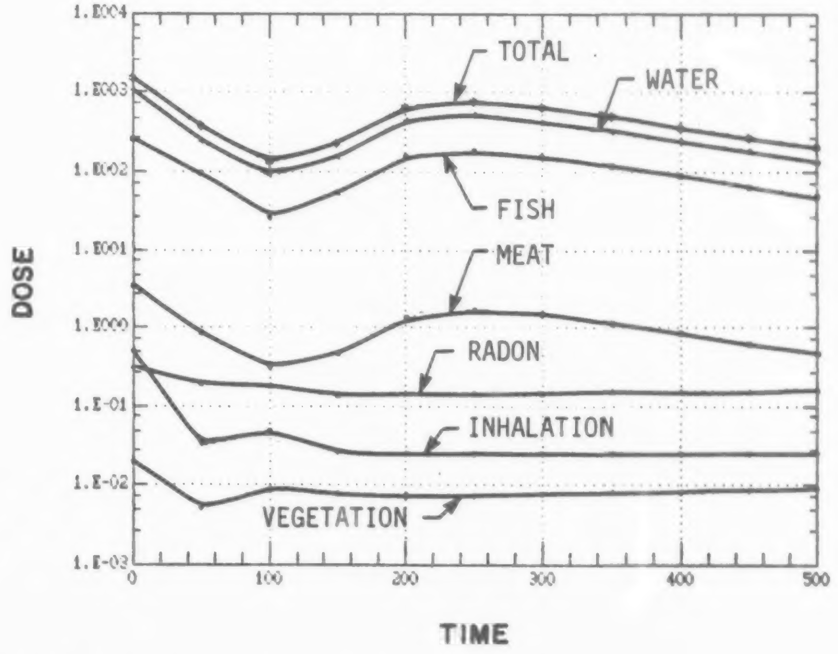

B) DEPYRITIZED TAILINGS OPTION

was specified to come from the reference watershed.

The shapes of the radon dose curves were found to be reasonable for the reasons discussed on the previous example. Similarly, the inhalation dose curves follow expected trends. The inhalation dose curve in Scenario 1 shows a sharp drop between years 0 and 50 due to the rapid leaching of thorium from the solids on the surface of the tailings area. Soluble lead-210 and radium-226 chemical precipitates are always at some depth in the tailings; hence, lead-210 and radium-226 do not comprise a significant portion of the dose from dust inhalation.) The second reduction in the dust inhalation dose curves shown on Figure 2.15(a) occurs after about year 250 due to natural revegetation of the tailings surface once the tailings porewater pH recovers to above 4.0. The pattern shown on Figure 2.15(b) is somewhat different as different factors come into play in this scenario. Firstly, the reduction in dose from year 0 to year 50 may be attributed to natural revegetation of the tailings surface due to the comparatively high pH of the tailings porewater in addition to the reduction in the thorium content of the surface solids for reasons noted above. Between years 50 and 100 there is a marginal increase in the inhalation dose which may be attributed to a loss of vegetative cover and a resultant increase in the dust source due to a downward shift in the tailings porewater pH following exhaustion of the calcite inventory added to the tailings surface layer. After year 100 there is again a reduction in the inhalation dose as the tailings surface again revegetates. The inhalation dose curve for Scenario 2 is higher than the dose curve for Scenario 1 in the long term (beyond year 250) as it has a higher residual thorium content. In summary, trends in the inhalation dose curves were found to be reasonable.

The vegetation dose curves in the two scenarios are seen to start at about the same value but follow distinctly different patterns thereafter. In Scenario 1, the vegetation dose is seen to rise slowly with time over the initial 150 years. This is attributed to an ongoing buildup of tailings dust on the ground inferring that root uptake of radionuclides is of increasing importance to the accumulation of radionuclides in plants. Subsequently, the vegetation dose shows a decline after year 200 as the tailings surface revegetates, reducing erosion of the tailings. In contrast, the vegetation dose in Scenario 2 declines from year 0 to year 50, presumably due to a lesser accumulation of dust on the ground surface as the tailings revegetate. However, between years 50 and 100 when the tailings vegetation is destroyed by the onset of acid pH conditions, the amount of erodible dust increases resulting in air increase in the vegetation dose. In the long term the vegetation dose from both scenarios is dominated by uptake from the soil and stabilizes due to the balance between deposition from the air and accumulation (via a $K_d$ process) in the soil. As this discussion implies, the shapes of the vegetation dose curves are explainable although their shapes are influenced by several factors.

### 2.4.9 Test 8 - Check of Model Stability Using Many Time Steps and Nominal Inputs

This was the first of two tests performed in order to check the system model for stability when long simulations are performed. The model was tested using nominal input values for both the base case and depyritized tailings options (i.e. Scenarios 1 and 2, respectively). The first run attempted was 9990 years with a ten year time step on Scenario 2.

#### Subsurface Transport Model

When the two hundredth time step was reached, the size of the array "CO" in SUBROUTINE GWATER was exceeded. This array stores concentrations from every time step so that the number of timesteps used must not exceed the size of the array. Since the maximum was 199 timesteps, a more convenient limit, namely 200, was chosen. The array sizes were increased accordingly and the model was run for 2000 years.

#### Tailings Source Model

At 1140 years, an underflow occured in SUBROUTINE URANUM when a large negative number caused an exponential term to approach zero. Two other places that this could potentially occur were also noted in this subroutine. All three were corrected so that if a term approached zero, it would be set to exactly zero.

The test was repeated. This time, the same error was encountered but in SUBROUTINE IONSIL at 1150 years. This was corrected in the same manner as the previous instance and the model was run once again. With this experience in mind, checking of all exponential terms was implemented as standard practice in subsequent studies.

No further errors were found so the model was run for the base case and then for both disposal options for 9950 years (the maximum possible) with a time step of 50 years. In the depyritized tailings simulation, another underflow occurred. This time, it was at 2050 years in SUBROUTINE LEAD. This term and one other that could potentially result in underflows for near zero values were again corrected by setting them to zero if the numbers were small.

### 2.4.10 Test 9 - Check of Model Stability Using Many Time Steps and Probabilistic Inputs.

The program was again tested for its stability for a large numbers of time steps using ten probabilistic trials. Again, both the base case and depyritized tailings options were run for 2000 years with a ten year time step and for 9950 years with a 50 year time step. No problems were found.

## 3.0 SUMMARY

Quality Assurance is an essential part of any software development program. With a computer program as extensive as the version of UTAP developed in Phase III, it is simply not practical for reasons of time and money to fully document every change to the program occurring during development. Not only is this not practical but the amount of paper that would be generated by such an exercise would be no less than ominous.

The measurement of success of any QA program is not how well defined, structured, documented, or thorough the program is but rather the measurement of success is that the final program works or, more precisely, that it does what it is supposed to do and, more importantly, that it does not do something that it is not supposed to do. Flaws must necessarily exist in any QA program but, as with the Phase III study, the right result can still be achieved. Since the computer program performs its intended function, the software QA program was successful.

## REFERENCES

Andres, T.H., 1982 "Rewriting SYVAC: Why and How". Environmental and Safety Branch, Whiteshell TR-2107.

Boehm, B.W., 1984. "Verifying and Validating Software Requirements and Design Specifications", IEEE Software Vol. 1, No. 1.

Broissia, M., 1986. "Selected Mathematical Models in Environmental Impact Assessment in Canada." Chemical Engineering Department, University of Sherbrooke, Prepared for Canadian Environmental Assessment Research Council.

Bryan, W.L. and Siegal, S.G., 1984. "Product Assurance; Insurance Against a Software Disaster". Computer, Vol. 17, No. 4.

IEEE/ANSI Standard 730-1981, 1981. "IEEE Standard for Software Quality Assurance Plans".

Lyon, R.B., 1982. "Nuclear Waste Disposal-Performance Assessment. Principles and Procedures". Canadian Nuclear Society. Proceedings of International Conference on Radioactive Waste Management.

Manse, K., and Roberts, S.D., 1983. "Implementing a Portable Uniform (0,1) Generator." Simulation.

Musa, J.D., 1980. "The Measurement and Management of Software Reliability". Proceedings of IEEE, Vol. 68, No. 9.

Myers, G.J., 1979 "The Art of Software Testing"; Wiley (NY).

Myers, G.J., 1976. "Software Reliability: Principles and Practices"; Wiley (NY).

Rogers, V.C., Overmyer, R.F., Putzig, K.M., Jensen, C.M., Nielson, K.K., and Sermon, B.W., 1980. "Characterization of Uranium Tailings Cover Materials for Radon Flux Reduction." U.S. Nuclear Regulatory Commission NUREG/CR-1081, March.

Rogers, V.C., Nielson, K.K. and Kalkwarf, D.R., 1984. "Radon Attenuation Handbook for Uranium Mill Tailings Cover Design." U.S. Nuclear Regulatory Commission, NUREG/CR-3533, April.

SENES Consultants Limited, 1984. "A study to Develop and Demonstrate Techniques for the Probabilistic Assessment of the Long-Term Effects of Uranium Mill Tailings in Canada - Phase 1." Research Report prepared for the National Uranium Tailings Program, CANMET, EMR, under Supply and Services Canada No. OSQ83-00236.

SENES Consultants Limited, 1985. "A Study to Develop and Demonstrate Techniques for the Probabilistic Assessment of the Long-Term Effects of Uranium Mill Tailings in Canada - Phase 11." Research Report prepared for the National Uranium Tailings Program, CANMET, EMR, under Supply and Services Canada Contract No. OSQ84-00207.

Spicer, C.C., 1972. "Algorithm AS 52 Calculation of Power Sums of Deviations About the Mean." Applied Statistics 21, pp. 226-227.

Technical Advisory Committee (TAC) on the Nuclear Fuel Waste Management Program. 19801 Report.

## APPENDIX A

# TESTING OF RANDOM NUMBER GENERATOR UNIRAN

by

Park M. Reilly, Ph.D.
Waterloo, Ontario

for

SENES Consultants Limited
Willowdale, Ontario

December 1985

## ABSTRACT

In Phase II of the probabilistic assessment study undertaken by SENES for the NUTP, the random number generator UNIRAN was incorporated into the system code. The program generates uniformly distributed random numbers in the interval 0 to 1 and is claimed by its authors to have excellent global statistical properties and to be highly portable from one computer system to another. This paper describes the results and findings of a set of additional tests which were carried out to verify these claims.

# TESTING OF RANDOM NUMBER GENERATOR UNIRAN

## A.1 INTRODUCTION

SENES Consultants Limited have implemented on their computer system the random number generator UNIRAN which is described by Marse and Roberts (1983). The program generates uniformly distributed random numbers on the interval (0,1) and is said by its authors to have excellent global statistical properties. This report describes a short series of statistical tests which were performed on a set of 5000 numbers generated by the program at SENES and on a second set of 5000 generated at University of Waterloo.

The paper by Marse and Roberts describes the tests of distribution and independence on which they base their favourable claim about statistical properties. The tests which are described in this report include simple tests for distribution and independence which are slightly different from those used by Marse and Roberts and also include tests on the distribution of the extreme values. They therefore may be regarded as complementary to those of Marse and Roberts.

The testing confirms that the set of numbers examined do indeed have excellent statistical properties. With limitations to be pointed out later, presumably all numbers generated by the program share the same properties.

## A.2 THE DATA SETS

A tape containing a file of 5000 random numbers, one to a line, in format E12.6, was provided by SENES. The original intention was to apply several different tests to them by APL but it was found to be cumbersome and expensive to handle the large file in the University of Waterloo APL system.

Instead, a program was written for the WATFIV system which incorporated the REAL FUNCTION UNIRAN in exactly the form quoted by Marse and Roberts. A sequence of 5000 numbers generated by it using the same seed (913566091) as that used by SENES was compared with the SENES file. The numbers which were compared were those of the following ordinal numbers in the set: 1-25, 500, 1000, 1500, 2000...,4500, 5000. In every case they were identical except that the format used by SENES was E12.6 while that on the Waterloo system was F10.7. This comparison justified the decision that all numbers for testing be generated by the WATFIV program. It is also partial confirmation of the claim by Marse and Roberts that the program is portable.

For confirmation of the tests, every one was repeated on a second set of 5000 numbers generated by UNIRAN at the University of Waterloo using the seed 1938444429 which was chosen by a random process. The SENES set is called Set 1 in this report, the Waterloo set is called Set 2.

## A.3 THE MEAN

The arithmetic means of the two sets are 0.5000798 and 0.5034284. They may be considered observations on a normally distributed random variable with mean 0.5 and variance 1/(12x5000). Thus the corresponding standardized values are 0.0195 and 0.8398. The probabilities of a standardized normal variate exceeding these values are 0.4922 and 0.2005, which are very ordinary ones. Hence, we have failed, at any confidence level over 80%, to disprove the null hypothesis. This test, like the others to follow is based on the null hypothesis that the two sets of 5000 consist entirely of independent observations on the uniform (rectangular) distribution covering the interval (0,1). This test gives elementary confirmation that the distribution of the numbers is correct.

## A.4 THE AUTOCORRELATION FUNCTION

The sample autocovariance function is written $C_L$, L=0,1,2,... where

$$C_L = \frac{1}{5000} \sum_{i=1}^{5000-L} (X_i - \bar{x})(X_{i+L} - \bar{x}) \qquad (1)$$

In this equation $X_i$ is the ith random number and $\overline{x}$ is the average of all of the random numbers in the set. The sample autocovariance function is used to calculate the sample autocorrelation function $r_L$ defined by

$$r_L = \frac{C_L}{C_0} \quad , L = 0,1,2,... \tag{2}$$

providing L is small relative to 5000. The sample autocorrelation functions for L up to 20 are shown in Table A.1 for the two sets.

Box and Jenkins (1976) describe how, under our null hypothesis, the $r_L$ may be considered approximately normally distributed with mean zero and variance 1/5000.

Consequently, the 95% confidence interval for an individual autocorrelation includes all those possibilities with absolute value less than $1.9600 \times \sqrt{1/5000} = 0.0277$. Thus, in a set of 20 autocorrelations, all of which are truly zero, there will be a mathematical expectation of one with absolute value greater than 0.0277. Here there happens to be exactly one in each list. It is reasonable to conclude therefore that no autocorrelations are truly different from zero.

Figures A.1 and A.2 show the autocorrelation functions graphically. The fact that there seems to be a slight sinusoidal tendency in both figures is a consequence of the estimation procedure and does not seriously compromise the tests on these functions.

A further property of the autocorrelation function under the null hypothesis is that successive autocorrelations are nearly independent (Jenkins and Watts, 1968). This is supported by the fact that tests on the sequence of signs in the autocorrelation functions of Table A.1 show no evidence of non-randomness. A consequence of this property is that the sum of the squares of the autocorrelations divided by the variance of a single autocorrelation is

Table A.1

## AUTOCORRELATION FUNCTIONS

| L | Set 1 | Set 2 |
|---|---|---|
| 1 | -.0245 | -.0046 |
| 2 | -.0136 | .0156 |
| 3 | -.0154 | -.0120 |
| 4 | .0303 | -.0248 |
| 5 | .0086 | .0135 |
| 6 | -.0135 | .0183 |
| 7 | -.0011 | .0019 |
| 8 | .0006 | .0041 |
| 9 | -.0082 | -.0020 |
| 10 | -.0017 | .0088 |
| 11 | .0039 | .0287 |
| 12 | -.0026 | .0003 |
| 13 | .0156 | -.0020 |
| 14 | .0138 | -.0097 |
| 15 | -.0048 | -.0034 |
| 16 | .0206 | -.0128 |
| 17 | .0173 | .0011 |
| 18 | .0039 | .0087 |
| 19 | .0005 | .0102 |
| 20 | .0032 | -.0003 |

FIGURE A.1

AUTOCORRELATION FUNCTION
FOR SET 1

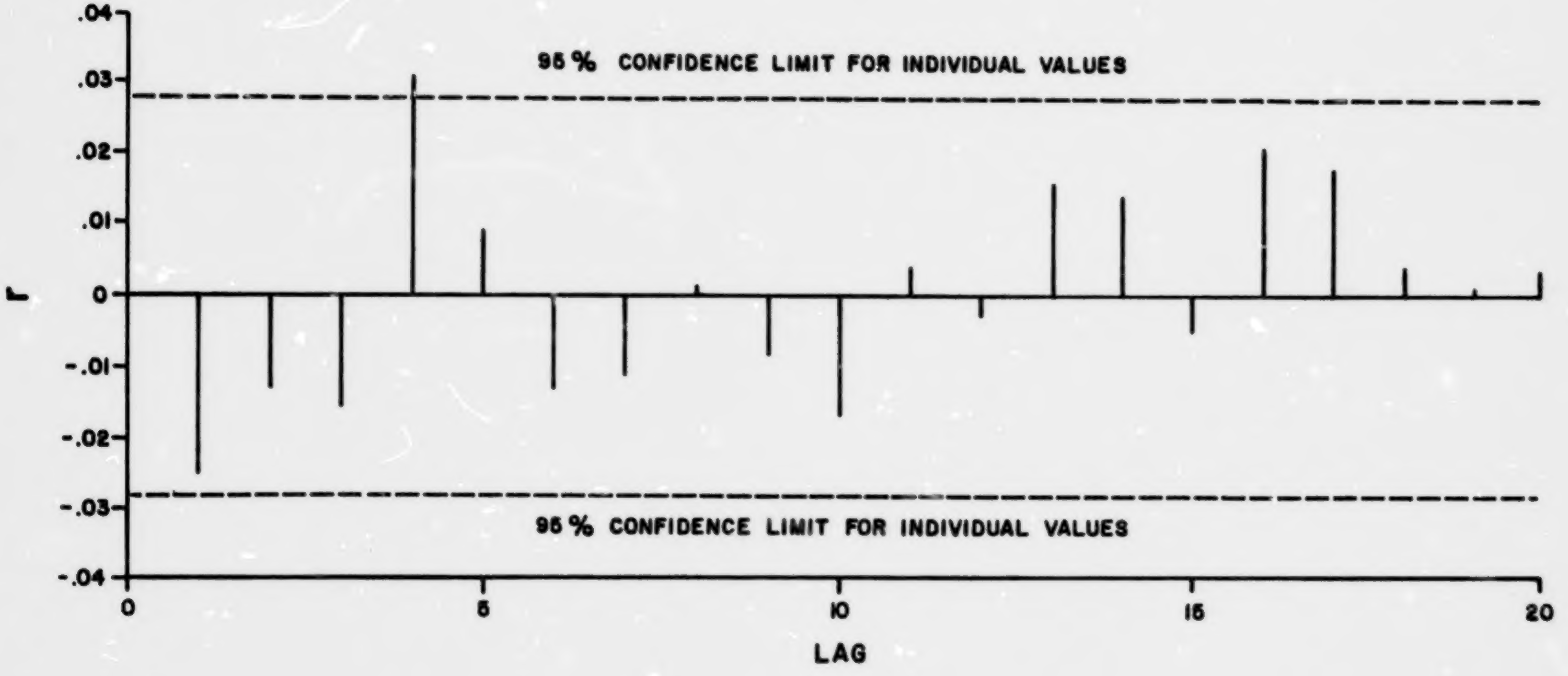

FIGURE A.2

AUTOCORRELATION FUNCTION
FOR SET 2

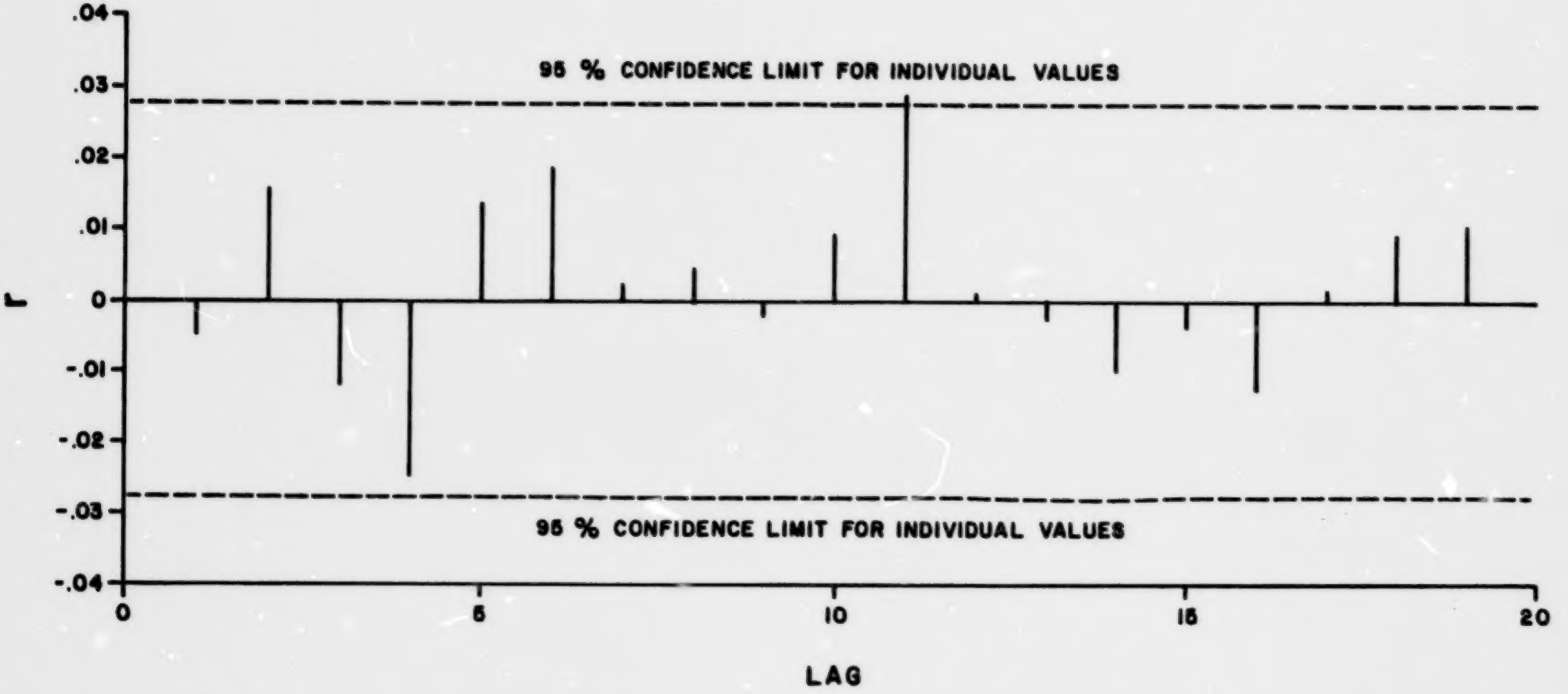

distributed as $\chi^2$ with, in this case, 20 degrees of freedom. For the two sets these quantities are 17.483 and 14.604; their probabilities of being exceeded by $\chi_{20}^2$ are about 62.5% and 80% respectively. Hence, we have failed, at any confidence level over 40%, to disprove the null hypothesis. The fact that probabilities are ordinary ones indicates that overall the autocorrelations are of a magnitude to be expected from a set of independent random numbers.

The overall conclusion of the work on the autocorrelation function is that both sets of numbers may reasonably be considered to be independent.

## A.5 THE PROBABILITY DISTRIBUTION

The range of the numbers was divided into 100 cells and each of the 5000 members of each set was assigned to its cell according to $0.01(j-1) \leq X_i < 0.01j$, $j = 1,2,\ldots,100$ for the jth cell, where $X_i$ is the ith member of its set.

The most generally accepted test of the overall frequency distribution is the $\chi^2$ test which is discussed in almost all books on statistics. The criterion is:

$$K = \sum_{j=1}^{100} \frac{(n_{oj} - n_{ej})^2}{n_{ej}} \qquad (3)$$

where $n_{oj}$ is the observed number of counts in the jth cell and $n_{ej}$ is the expected number of counts in the jth cell. Here $n_{ej} = 50$ for every cell according to our null hypothesis. For the two sets the values of K are 113.48 and 92.52. In cases like this one, the criterion is compared with $\chi^2$ with degrees of freedom equal to the number of cells less 1. The probabilities of $\chi^2_{99}$ exceeding these values of K are 0.152 and 0.664, which give no reason to conclude that the random numbers are not uniformly distributed. In particular, we have failed, at any confidence level over 85%, to disprove the null hypothesis.

The overall conclusion of the tests on distribution is that there is no evidence that the random numbers are not uniformly distributed on the interval 0 to 1.

## A.6 EXTREME VALUES

Much of the work done by SENES is characterized by special interest in extreme values of the output variables of Monte Carlo calculations, which in turn are often the consequence of extreme values of the random variables which are used. This justifies extra attention to the extreme values in tests of randomness. Columns 2 and 4 of Table A.2 show the 20 largest and the 20 smallest, respectively, numbers in Set 1. Columns 2 and 4 of Table A.3 show the corresponding information for Set 2.

The cumulative probability function for the largest of 5000 observations on a uniformly distributed random variable with the range 0 to 1 is

$$F_1(b_1) = Pr(B_1 \leq b_1) = b_1^{5000} \qquad (4)$$

where $B_1$ is the largest of the 5000 random numbers and $b_1$ is a possible value for $B_1$. Note carefully that throughout this section capital letters are used for random variables in the abstract, while lower case letters are used for specific possible values of the random variable. The choice of letter and subscript identify the random variable. Thus equation (4) refers to the probability that the largest of 5000 observations (as yet unrealized) will be equal to or less than a given particular number $b_1$.

Similarly, the cumulative probability function for the smallest $S_1$ is

$$G_1(s_1) = Pr(S_1 \leq s_1) = (1-s_1)^{5000} \qquad (5)$$

The ith largest, $B_i$, given that the i-1 largest has the observed value $b_{i-1}$, has cumulative probability function

Table A.2

## EXTREME VALUES FOR SET 1

| Col 1 | Col 2 | Col 3 | Col 4 | Col 5 |
|---|---|---|---|---|
| $i$ | $b_i$, the ith largest number | $F_i(b_i\|b_i-1) =$ $Pr[(B_i<b_i)\|b_i-1]$ | $s_i$, the ith smallest number | $G_i(s_i\|s_i-1) =$ $Pr[(S_i<s_i)\|s_i-1]$ |
| 1 | .9999134 | .6485 | .0000224 | .8940 |
| 2 | .9994709 | .1094 | .0002740 | .2842 |
| 3 | .9994344 | .8332 | .0003294 | .7581 |
| 4 | .9983467 | .0043 | .0011582 | .0158 |
| 5 | .9982921 | .7609 | .0012103 | .7706 |
| 6 | .9981729 | .5508 | .0014213 | .3481 |
| 7 | .9976886 | .0886 | .0015388 | .5556 |
| 8 | .9976395 | .7821 | .0015475 | .9574 |
| 9 | .9975800 | .7425 | .0017264 | .4088 |
| 10 | .9974545 | .5337 | .0017309 | .9778 |
| 11 | .9971828 | .2568 | .0020071 | .2514 |
| 12 | .9970935 | .6397 | .0021986 | .3839 |
| 13 | .9968503 | .2962 | .0024448 | .2920 |
| 14 | .9965739 | .2508 | .0029973 | .0631 |
| 15 | .9963459 | .3195 | .0031534 | .4581 |
| 16 | .9961917 | .4623 | .0032626 | .5792 |
| 17 | .9959640 | .3200 | .0034738 | .3478 |
| 18 | .9959487 | .9263 | .0035134 | .8204 |
| 19 | .9958612 | .6455 | .0037289 | .3404 |
| 20 | .9955929 | .2613 | .0039795 | .2856 |

Table A.3

## EXTREME VALUES FOR SET 2

| Col 1 | Col 2 | Col 3 | Col 4 | Col 5 |
|---|---|---|---|---|
| i | $b_i$, the ith largest number | $F_i(b_i \mid b_{i-1}) = Pr[(B_i<b_i) \mid b_{i-1}]$ | $s_i$, the ith smallest number | $G_i(s_i \mid s_{i-1}) = Pr[(S_i<s_i) \mid s_{i-1}]$ |
| 1 | .9999124 | .6453 | .0000916 | .6325 |
| 2 | .9996929 | .3337 | .0004264 | .1875 |
| 3 | .9996750 | .9144 | .0012376 | .0173 |
| 4 | .9994931 | .4028 | .0014094 | .4233 |
| 5 | .9993739 | .5511 | .0014835 | .6902 |
| 6 | .9991823 | .3838 | .0020539 | .0576 |
| 7 | .9990094 | .4214 | .0022143 | .4481 |
| 8 | .9988546 | .4613 | .0025452 | .1909 |
| 9 | .9986768 | .4112 | .0025540 | .9569 |
| 10 | .9984720 | .3593 | .0029274 | .1543 |
| 11 | .9982547 | .3375 | .0031530 | .3233 |
| 12 | .9982324 | .8945 | .0034409 | .2367 |
| 13 | .9980888 | .4879 | .0041320 | .0314 |
| 14 | .9978625 | .3228 | .0042314 | .6079 |
| 15 | .9974367 | .1191 | .0042395 | .9603 |
| 16 | .9973877 | .7828 | .0045989 | .1721 |
| 17 | .9973711 | .9204 | .0047571 | .4351 |
| 18 | .9972803 | .6353 | .0049321 | .4163 |
| 19 | .9972534 | .8743 | .0050814 | .4735 |
| 20 | .9962562 | .0069 | .0051499 | .7097 |

$$F_i(b_i|b_{i-1}) = Pr[(B_i\leq b_i)\ b_{i-1}] = \left(\frac{b_i}{b_{i-1}}\right)^{5001-i} \qquad (6)$$

where the notation "$b_i|b_{i-1}$" is read, "$b_i$ given $b_{i-1}$".
The ith smallest, $S_i$, given that the i-1 smallest has the observed value $s_{i-1}$, has cumulative probability function

$$G_i(s_i\ s_{i-1}) = Pr[(S_i\leq s_i)\ s_{i-1}] = \left(\frac{1-s_i}{1-s_{i-1}}\right)^{5001-i} \qquad (7)$$

The ith entry in Column 3 of Tables A.2 and A.3 gives $F_i\ (b_i\ b_{i-1})$ as in equations (4) or (6) where $b_i$ and $b_{i-1}$ are the observed values given in Column 2. Accordingly it is the probability that the ith largest of a set of 5000 random numbers would be equal to or less than the observed value $b_i$, given that the i-1 largest has the observed value $b_{i-1}$. In other words, 100 times the ith entry in Column 3 is the percentile to which the observed value $b_i$ belongs in its theoretical distribution, given the observed value $b_{i-1}$.

Similarly, the ith entry in Column 5 of Tables A.2 and A.3 gives, as one interpretation, the probability that the ith smallest of a set of 5000 random numbers would be equal to or less than the observed value $s_i$, given that the i-1 smallest has the observed value $s_{i-1}$.

The transformation of numbers in Columns 2 and 4 of Tables A.2 and A.3 to those in Columns 3 and 5 is a probability integral transformation and hence the entries in Columns 3 and 5 should be independent observations on a uniformly distributed random variable over the interval 0 to 1. That is, random variables drawn from any known distribution are just as likely to be chosen from one percentile as another, and therefore if the entries in Columns 2 and 4 have the distributions given by equations (6) and (7) as our null hypothesis postulates, the entries in Columns 3 and 5 will be independently and uniformly distributed over the range of possible probabilities, i.e. from 0 to 1.

Columns 3 and 5 look good in both tables. They can be tested formally by a Kolmogorov-Smirnov test.

Consider the range 0 to 1 of a uniformly distributed random variable U to be divided into 20 sub-intervals,

$$0.05\,(i-1) \le U < 0.05i, \quad i = 1,2,\ldots,20 \qquad (8)$$

Let the null hypothesis be that a sample of size 20 on U, except only for sampling error, will consist of one observation at the midpoint of each of these sub-intervals. This is a reasonable consequence of the uniformity of the distribution of U. Then, if the entries in Columns 3 or 5 from Table A.2 or A.3 are arranged in increasing order, their values should depart only through sampling error from

$$H(i) = 0.025 + 0.05(i-1), \quad i = 1,2,\ldots,20 \qquad (9)$$

which is the probability that a random observation on U is equal to or less than the mid-point value of the ith sub-interval described by equation (8). It is easy to test this by the Kolmogorov-Smirnov test.

The Kolmogorov-Smirnov test is based on the maximum difference in probability between the postulated cumulative probability function and the sample cumulative probability function. Figure A.3 shows the graph of these functions for the first few largest observations in Set 1. The step-like graph P(i) is the sample cumulative probability function. Any point on a horizontal section of the graph, except the point at the extreme right end of the section, gives the fraction of the sample ("probability") accumulated by the i, i-1, ...,2,1 smallest probabilities in the sample. The straight line labelled H(i) is the graph of equation (9).

The same information is given in Table A.4. Column 2 gives the numerical values of H(i) from equation (9) for i-1,2,...,20.

FIGURE A.3

## METHOD OF FINDING 'D' FOR KOLMOGOROV-SMIRNOV TEST

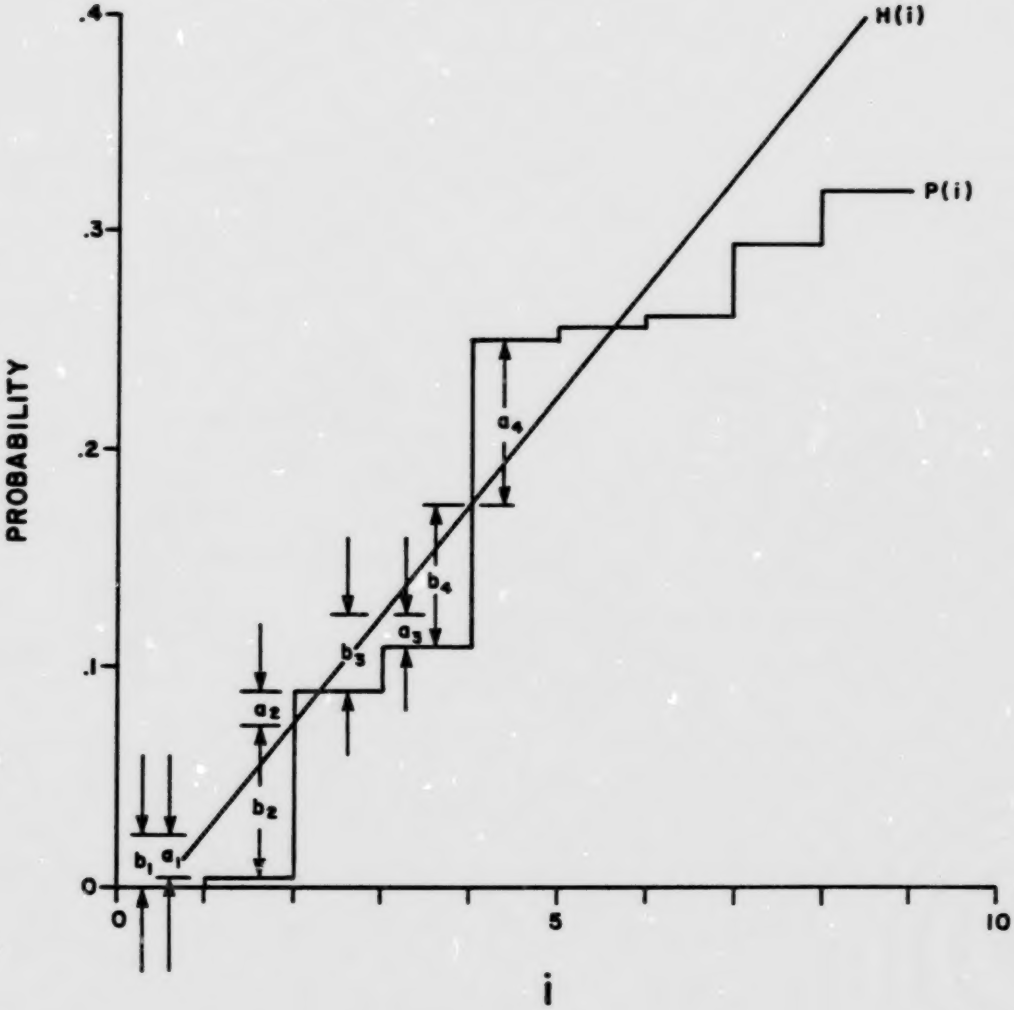

Table A.4

## CALCULATION OF D FOR KOLMOGOROV-SMIRNOV TEST FOR COLUMN 3 OF TABLE A.2

| Col 1 $i$ | Col 2 $H(i)$ | Col 3 $P(i)^{(1)}$ | Col 4 $a_i$ | Col 5 $P(i)^{(2)}$ | Col 6 $\|b_i\|$ |
|---|---|---|---|---|---|
| 1 | .025 | .0043 | .0207 | 0 | .025 |
| 2 | .075 | .0886 | .0136 | .0043 | .0707 |
| 3 | .125 | .1094 | .0156 | .0886 | .0364 |
| 4 | .175 | .2508 | .0758 | .1094 | .0656 |
| 5 | .225 | .2568 | .0318 | .2508 | .0258 |
| 6 | .275 | .2613 | .0137 | .2568 | .0182 |
| 7 | .325 | .2962 | .0288 | .2613 | .0637 |
| 8 | .375 | .3195 | .0555 | .2962 | .0788 |
| 9 | .425 | .3200 | .1050 | .3195 | .1055 |
| 10 | .475 | .4623 | .0127 | .3200 | .1550* |
| 11 | .525 | .5337 | .0087 | .4623 | .0627 |
| 12 | .575 | .5508 | .0242 | .5337 | .0413 |
| 13 | .625 | .6397 | .0147 | .5508 | .0742 |
| 14 | .675 | .6455 | .0295 | .6397 | .0353 |
| 15 | .725 | .6485 | .0765 | .6455 | .0795 |
| 16 | .775 | .7425 | .0325 | .6485 | .1265 |
| 17 | .825 | .7609 | .0641 | .7425 | .0825 |
| 18 | .875 | .7821 | .0929 | .7609 | .1141 |
| 19 | .925 | .8332 | .0918 | .7821 | .1429 |
| 20 | .975 | .9263 | .0487 | .8332 | .1418 |

* referenced in text

Column 3 gives the same quantities as in Column 3 of Table A.2, arranged in increasing order. The heading of Column 3 in Table A.4 is labelled $P(i)^{(1)}$ to indicate that it gives the probability for the top value of each vertical line in the graph of P(i) in Figure A.3. Similarly Column 5 of Table A.4 gives the probability corresponding to the bottom value of each vertical line in Figure A.3. The values $a_i$ and $b_i$, $i=1,2,\ldots,20$ are the vertical distances between $H_i$ and $P(i)^{(1)}$ for $a_i$, and between $H_i$ and $P(i)^{(2)}$ for $b_i$. The absolute values of $a_i$ and $b_i$ are given in Columns 4 and 6 of Table A.4. The quantity D required by the test is the largest in absolute value of the combined set of all of the $a_i$ and $b_i$. From Table A.4, for the 20 largest members of Set 1 it is 0.1550. Under our null hypothesis the probability of this number being exceeded by chance alone is in the neighbourhood of 40% (see Crow, Davis and Maxfield, 1960; and Kreyszig, 1970) and therefore we fail to prove that the largest 20 numbers in Set 1 do not have the expected distribution.

Table A.5 gives the observed values of D for the 20 largest and 20 smallest of Sets 1 and 2 along with their probability values. They are all seen to be reasonable. Thus we may conclude that the extreme values for both sets have the expected distribution and presumably therefore the UNIRAN generator ordinarily produces extreme values which have the expected distribution in sets of 5000 random numbers.

## A.7 VALUE NEAR ZERO AND UNITY

If the random number seed were exactly zero, all succeeding numbers would also be zero and the generator would collapse. Similar, but not as catastrophic, difficulty could result from the use of too large a seed.

In both sets of numbers used in these tests, the sequence of numbers preceding and following the smallest and largest few were examined by eye and they appeared to be unaffected by their proximity to extreme values.

Table A.5

## VALUES OF D FROM KOLMOGOROV-SMIRNOV TESTS

| Set of Extreme Values | D | Approximate Probability of Larger D |
|---|---|---|
| Set 1 - Largest 20 | .1550 | .40 |
| Set 2 - Largest 20 | .1978 | .30 |
| Set 1 - Smallest 20 | .1669 | .35 |
| Set 2 - Smallest 20 | .2514 | .15 |

## A.8 CONCLUSION

The testing reported here was a considerable extension of that done by Marse and Roberts. However, for the two sets of 5000 numbers which were examined, there was no reason found to challenge their conclusion of excellent global statistical properties. As they point out however there may be local sets, i.e. say 5000 numbers generated from some particular seed, which may have undesirable properties. In fact it is a necessary consequence of the property of randomness that some such sets must exist.

## REFERENCES

Box, A.E.P. and Jenkins, G.W., 1976. "Time Series Analysis, Forecasting, and Control". Revised Ed., Holden-Day, p. 32.

Crow, E.L., Davis, F.A. and Maxfield, M.W., 1960. "Statistics Manual." Dover Publications, p. 248

Jenkins, G.M. and Watts, D.G., 1968. "Spectral Analysis and Its Applications". Holden-Day, p. 187.

Kreyszig, E., 1970. "Introductory Mathematical Statistics". Wiley, pp. 254.

Marse, K., and Roberts, S.D., 1983. "Implementing a Portable Fortran Uniform (0,1) Generator". Simulation, October 1983, pp. 135-139.

# APPENDIX B

## TESTS OF CONTROL MODULE
## SAMPLING ROUTINES

## TESTS OF CONTROL MODULE SAMPLING ROUTINES

The sampling routines draw random samples from the following probability distributions:

1) Constant
2) Normal
3) Lognormal
4) Uniform
5) Loguniform
6) Triangular
7) Weibull
8) Beta
9) Arbitrary
10) Correlated

For each of these distributions (except constant which requires no calculations), test values were input to the sampling routines and 500 trials were made. The input values have been tabulated along with the corresponding values calculated from the sampled values. These all show reasonable agreement. Frequency histograms of the results were also plotted and distribution curves were fit to the data. The $\chi^2$ statistics calculated for each of these indicate good fits. The results of these tests have been reproduced in Figures B.1 through B.9.

FIGURE B.I

PLOT OF FREQUENCY HISTOGRAM (500 SAMPLES)
AND PROBABILITY DISTRIBUTION (SMOOTH CURVE)
FOR NORMAL DISTRIBUTION

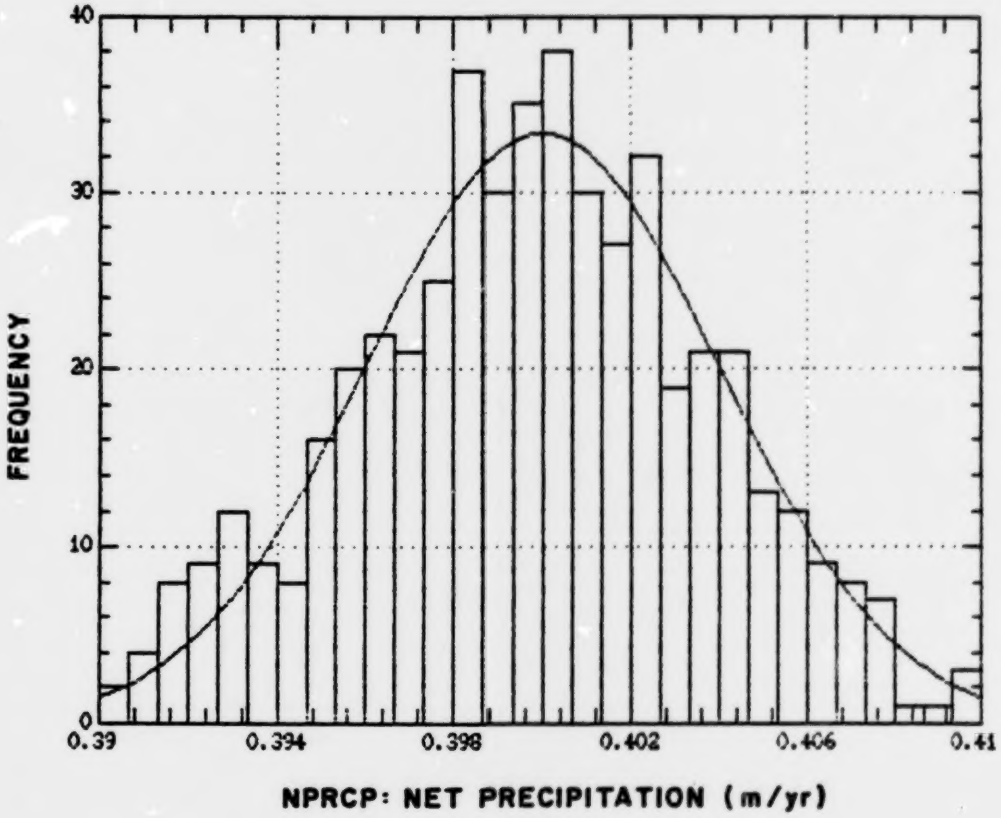

**SUMMARY STATISTICS:**

| | SPECIFIED INPUT VALUES | CALCULATED SAMPLE VALUES |
|---|---|---|
| MEAN | 0·400 | 0·400 |
| STANDARD DEVIATION | $4 \times 10^{-3}$ | $3{\cdot}9 \times 10^{-3}$ |

CHI$^2$ GOODNESS-OF-FIT = 19·962 WITH 25 DEGREES OF FREEDOM

FIGURE B.2

PLOT OF FREQUENCY HISTOGRAM (500 SAMPLES)
AND PROBABILITY DISTRIBUTION (SMOOTH CURVE)
FOR LOGNORMAL DISTRIBUTION

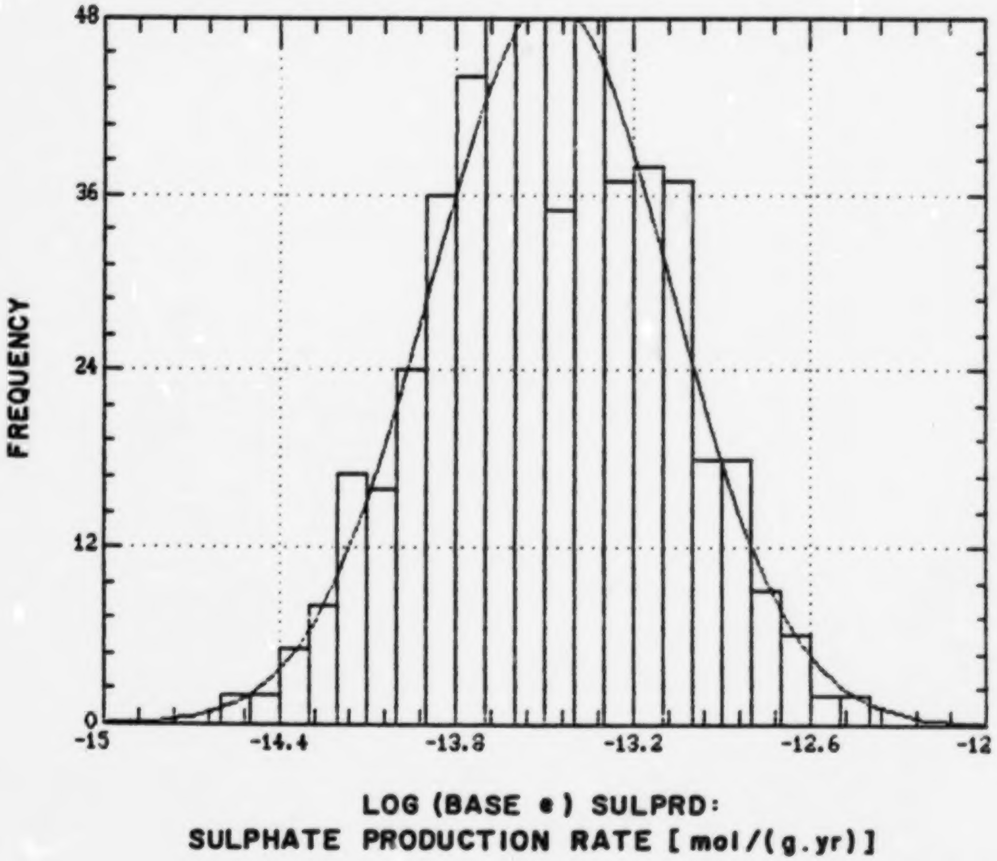

SUMMARY STATISTICS:

| | SPECIFIED INPUT VALUES | CALCULATED SAMPLE VALUES |
|---|---|---|
| GEOMETRIC MEAN | $1{\cdot}4 \times 10^{-6}$ | $1{\cdot}4 \times 10^{-6}$ |
| GEOMETRIC STANDARD DEVIATION | 1·5 | 1·5 |

$CHI^2$ GOODNESS-OF-FIT = 13·991 WITH 18 DEGREES OF FREEDOM

FIGURE B.3

## PLOT OF FREQUENCY HISTOGRAM (500 SAMPLES) AND PROBABILITY DISTRIBUTION (SMOOTH CURVE) FOR UNIFORM DISTRIBUTION

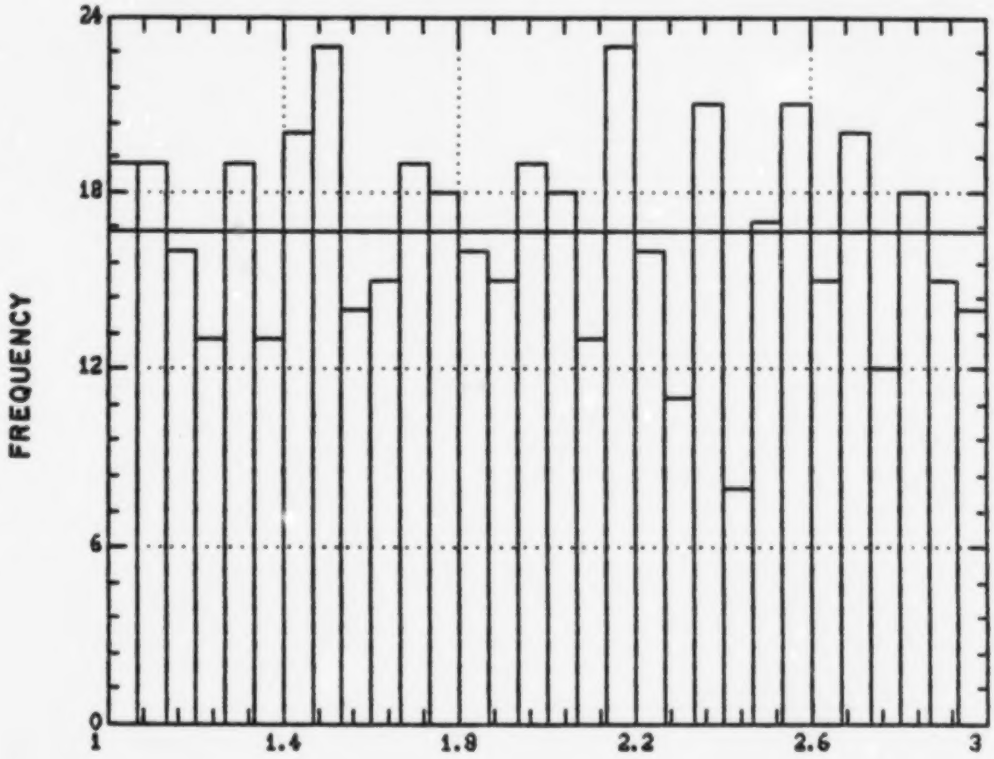

DISTCO: RADIUM SOLID TO LIQUID DISTRIBUTION COEFFICIENT (UNSATURATED ZONE)

**SUMMARY STATISTICS:**

| | SPECIFIED INPUT VALUES | CALCULATED SAMPLE VALUES |
|---|---|---|
| MINIMUM | 1 | 1·01 |
| MAXIMUM | 3 | 2·99 |

CHI$^2$ GOODNESS-OF-FIT = 22·12 WITH 29 DEGREES OF FREEDOM

FIGURE B.4

PLOT OF FREQUENCY HISTOGRAM (500 SAMPLES) AND PROBABILITY DISTRIBUTION (SMOOTH CURVE) FOR LOG-UNIFORM DISTRIBUTION

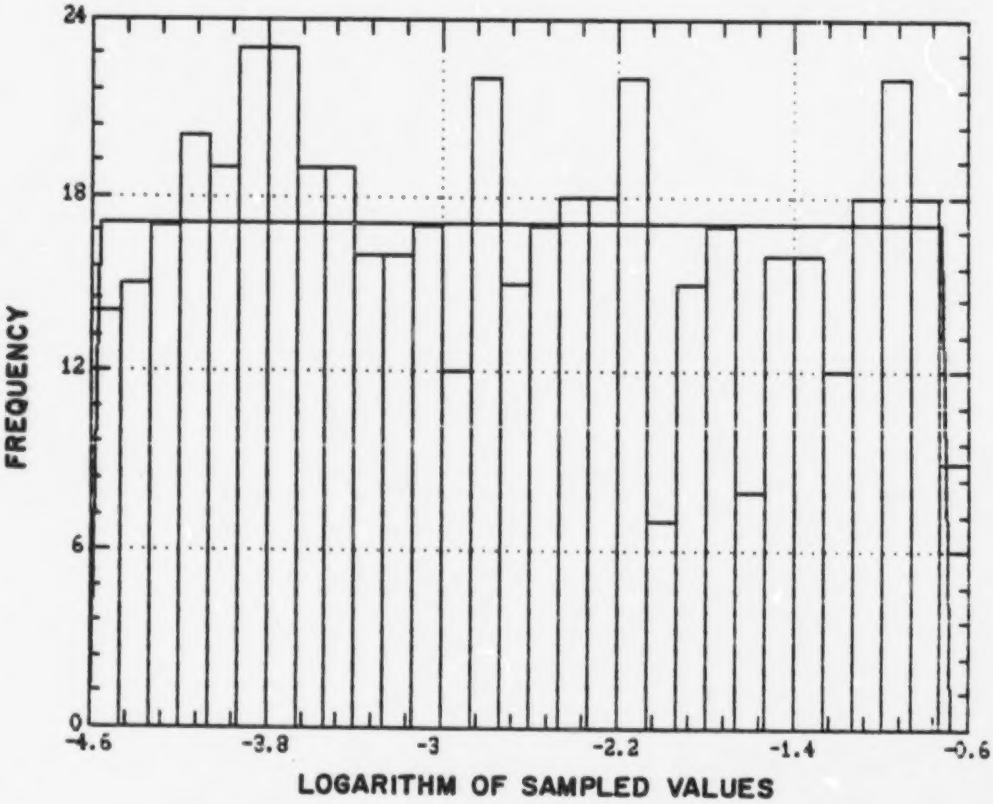

SUMMARY STATISTICS:

| | SPECIFIED INPUT VALUES | CALCULATED SAMPLE VALUES |
|---|---|---|
| MINIMUM | $1.00 \times 10^{-2}$ | $1.01 \times 10^{-2}$ |
| MAXIMUM | 0.500 | 0.499 |

$CHI^2$ GOODNESS-OF-FIT = 25.983 WITH 26 DEGREES OF FREEDOM

FIGURE B.5

PLOT OF FREQUENCY HISTOGRAM (500 SAMPLES)
AND PROBABILITY DISTRIBUTION (SMOOTH CURVE)
FOR TRIANGULAR DISTRIBUTION

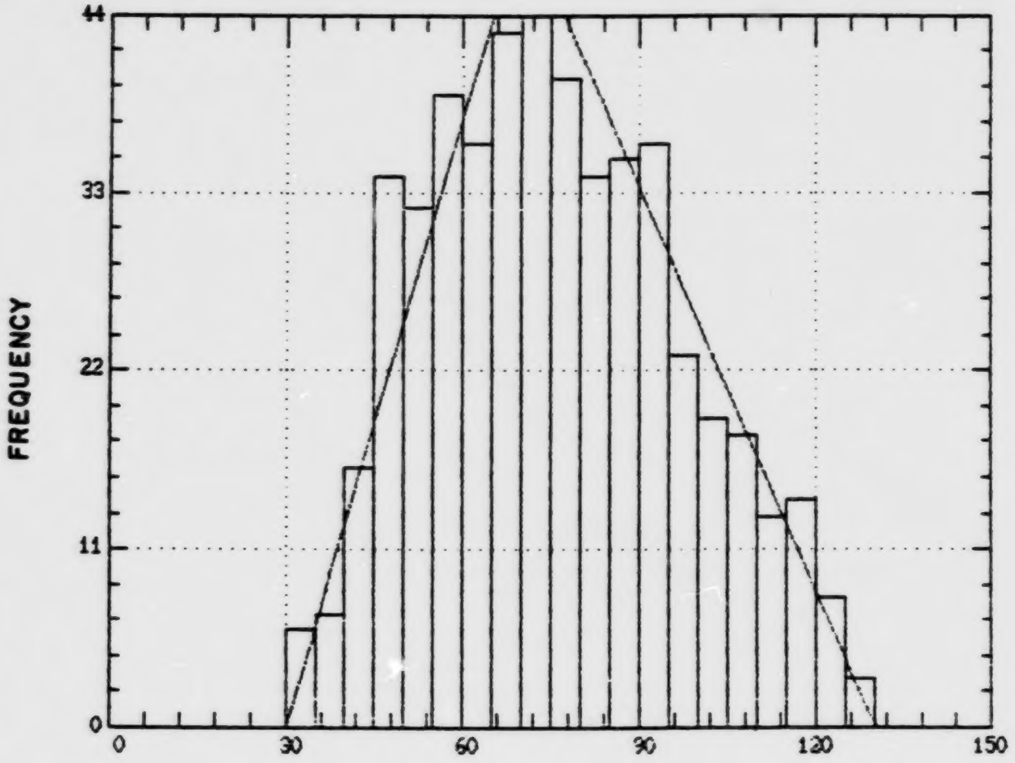

O2DIFF: OXYGEN DIFFUSIVITY THROUGH TAILINGS ($m^2/yr$)

SUMMARY STATISTICS:

|  | SPECIFIED INPUT VALUES | CALCULATED SAMPLE VALUES |
|---|---|---|
| MINIMUM | 30 | 31·5 |
| MODE | 70 | - |
| MAXIMUM | 130 | 129 |

$CHI^2$ GOODNESS-OF-FIT = 14·482 WITH 17 DEGREES OF FREEDOM

FIGURE B.6

## PLOT OF FREQUENCY HISTOGRAM (500 SAMPLES) AND PROBABILITY DISTRIBUTION (SMOOTH CURVE) FOR WEIBULL DISTRIBUTION

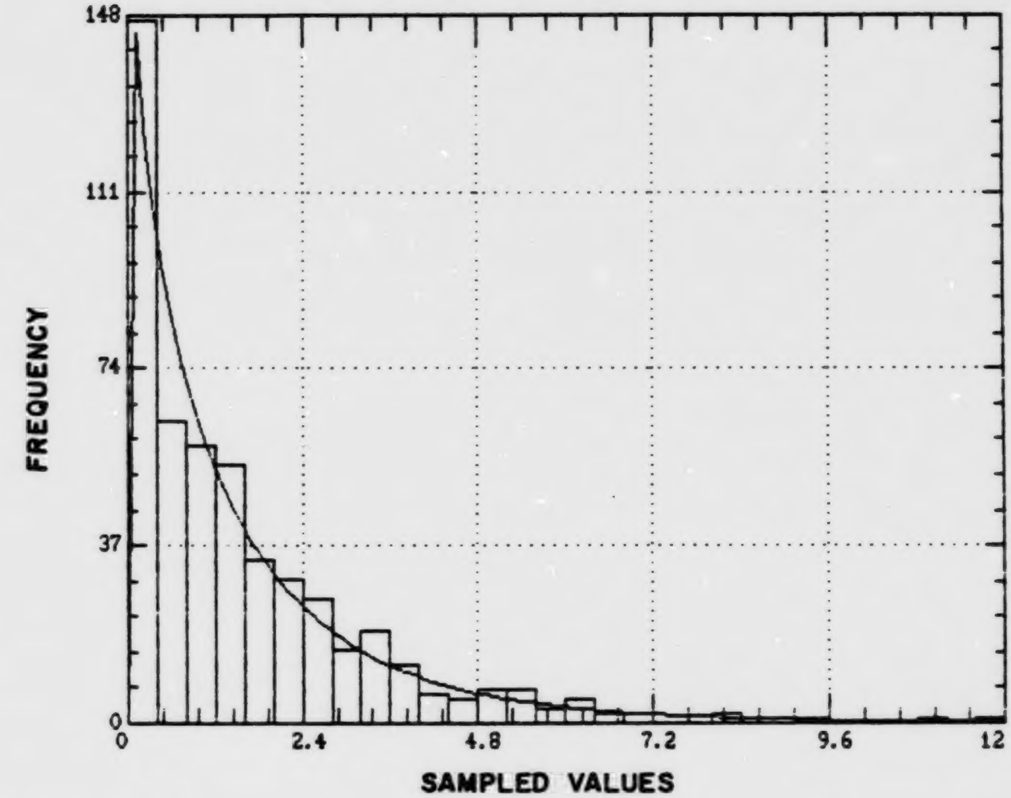

SUMMARY STATISTICS:

| | SPECIFIED INPUT VALUES | CALCULATED SAMPLE VALUES |
|---|---|---|
| SCALE PARAMETER | 1.5 | 1.481 |
| SHAPE PARAMETER | 0.9 | 0.878 |

CHI$^2$ GOODNESS-OF-FIT = 15.457 WITH 13 DEGREES OF FREEDOM

FIGURE B.7

PLOT OF FREQUENCY HISTOGRAM (500 SAMPLES)
FOR ARBITRARY DISTRIBUTION

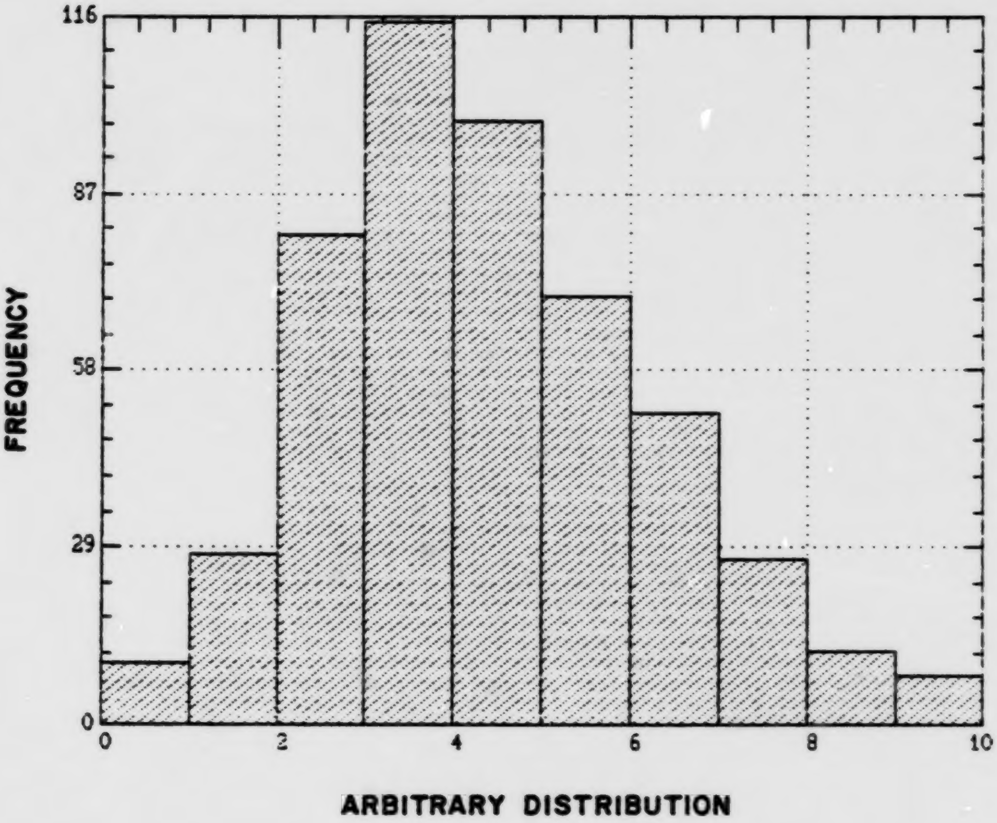

**SUMMARY:**

| CELL | SPECIFIED INPUT VALUES | CALCULATED SAMPLE VALUES |
|---|---|---|
| 1 | 10 | 10 |
| 2 | 20 | 28 |
| 3 | 80 | 80 |
| 4 | 110 | 115 |
| 5 | 105 | 99 |
| 6 | 75 | 70 |
| 7 | 50 | 51 |
| 8 | 30 | 27 |
| 9 | 15 | 12 |
| 10 | 5 | 8 |

FIGURE B.8

## PLOT OF FREQUENCY HISTOGRAM (500 SAMPLES) AND PROBABILITY DISTRIBUTION (SMOOTH CURVE) FOR BETA DISTRIBUTION

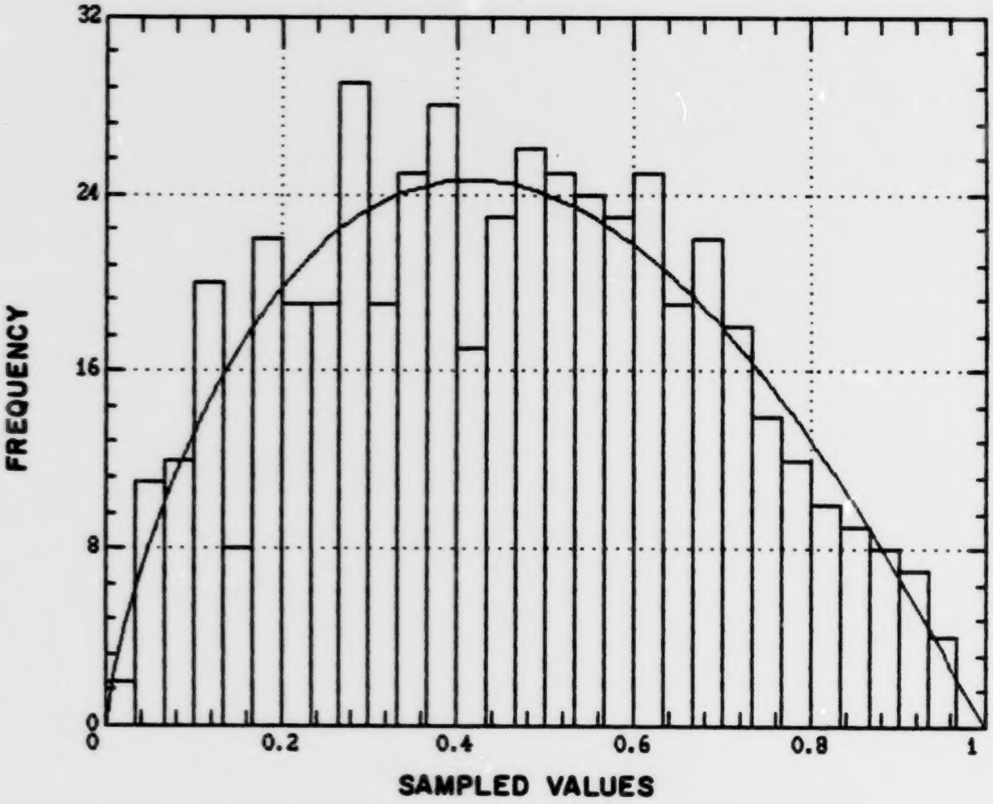

SUMMARY STATISTICS:

| | SPECIFIED INPUT VALUES | CALCULATED SAMPLE VALUES |
|---|---|---|
| a | 1.90 | 1.76 |
| b | 2.10 | 2.07 |

CHI$^2$ GOODNESS-OF-FIT = 15.93 WITH 24 DEGREES OF FREEDOM

FIGURE B.9

PARAMETER CORRELATED TO NORMAL DISTRIBUTION
(500 SAMPLES)

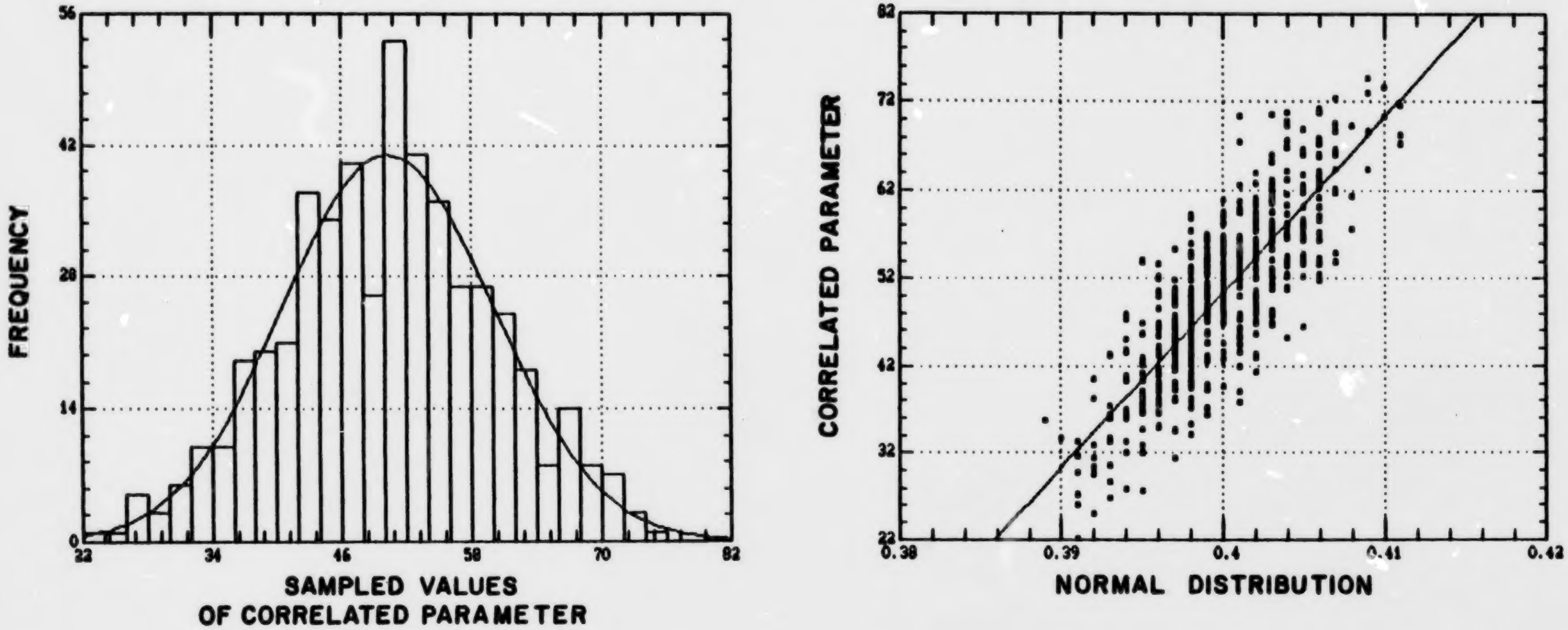

SUMMARY STATISTICS:

|  | SPECIFIED INPUT VALUES | CALCULATED SAMPLE VALUES |
|---|---|---|
| MEAN | 50.0 | 50.3 |
| STANDARD DEVIATION | 10.00 | 9.75 |
| CORRELATION COEFFICIENT | 0.800 | 0.818 |

CHI$^2$ GOODNESS-OF-FIT = 18.174 WITH 19 DEGRESS OF FREEDOM

# APPENDIX C

# COMPARISON OF SELECTED PROBABILISTIC ASSESSMENT TOOLS

by

M.L. Murray, D.B. Chambers, D. I. Beals & B.E. Halbert
SENES Consultants Limited
Willowdale, Ontario

T.H. Andres
Atomic Energy of Canada Limited
Whiteshell Nuclear Research Establishment
Pinawa, Manitoba

M. Henrion
Carnegie-Mellon University
Pittsburgh, Pennsylvania

## ABSTRACT

In this paper, the probabilistic assessment tool RANSIM, developed for application to uranium mill tailings, is compared to two other probabilistic analysis systems. The comparison includes a discussion of the principal features of each system and demonstration of the performance of the systems using a benchmark model. The model selected simulates radon gas release from a uranium tailings area, its atmospheric dispersion and the subsequent exposure of a nearby receptor. The relative importance of the twelve variable input parameters in the model are also assessed in the paper by comparison of the results of a number of different sensitivity/uncertainty analysis techniques.

# COMPARISON OF SELECTED PROBABILISTIC ASSESSMENT TOOLS

## C.1 INTRODUCTION

One of the primary goals of the National Uranium Tailings Program (NUTP) is to develop the capacity to predict the long term effects of uranium mill tailings. Previous studies have demonstrated that a probabilistic approach to modelling can be used to take account of the natural variability and uncertainty in model parameters (SENES, 1984). Using this type of approach, the uncertainty associated with the input parameters is propagated through mathematical models to produce a distribution of calculated results.

In the Phase I study for the NUTP, SENES Consultants Limited identified and implemented a computer program to perform probabilistic analysis. This program, known as OPANAL, was originally developed by Dr. P.M. Reilly for applications in opinion analysis and business decision making (Reilly and Johri, 1969). The program was subsequently modified, renamed and applied in a Phase II study for the NUTP (SENES, 1985). That program, RANSIM, forms the heart of the probabilistic analysis control modules developed in this Phase III project. The previous version (RANSIM) was used for this comparison since it existed in totality at the outset of the Phase III work. All probabilistic functions of RANSIM have been directly incorporated into the current Uranium Tailings Assessment Program (UTAP). Hence, results generated by RANSIM are directly comparable to results generated by UTAP, for the same model(s). Some of the structure of the Phase II system (which RANSIM formed the heart of) has been modified as part of this project.

A number of probabilistic analysis systems have also been developed by other organizations, for various applications. Two such systems, SYVAC and DEMOS, were selected for comparison with RANSIM in this investigation. SYVAC, which stands for SYstems Variability Analysis Code was originally developed for the Canadian Nuclear Fuel Waste Management Program (Dormuth and Sherman, 1981; Wuschke et al., 1981). DEMOS is an interactive probabilistic modelling environment developed by Dr. Max Henrion at Carnegie Mellon University

(Henrion and Morgan, 1985; Henrion and Nair, 1982; Henrion, 1979)

### C.1.1 Objectives

This comparative study was conducted for a number of reasons:

1) As a Quality Assurance (QA) measure. One would expect the results generated by RANSIM (for a given model and set of input parameter distributions) to be very similar to those generated by other probabilistic analysis systems. This is not a rigorous test of the accuracy of any system. It is simply one element in an ongoing QA program applied in the NUTP studies.
2) To examine and compare the techniques used by the various organizations for determining important model parameters. This was to address the ongoing issue of whether the many available techniques for sensitivity and uncertainty analyses produce similar rankings of parameter importance.
3) To qualitatively examine the unique aspects of each system, thus providing information on the current state-of-the-art in probabilistic analysis and indicating areas of potential improvement in our system.

### C.1.2 Outline of the Paper

The paper will, in general, follow the approach used to conduct the comparative study. The benchmark model, including input parameter distributions, is described first. The subsequent sections contain brief descriptions of the three probabilistic analysis systems, a summary of the results generated for the benchmark problem by each, and an outline of the approach to, and results of sensitivity/uncertainty analysis. These results are then compared and discussed. Some further results are presented in the discussion section to clarify specific points.

## C.2 THE BENCHMARK MODEL

Since RANSIM was developed as part of a study to simulate the behaviour of uranium mill tailings, a relevant tailings model was selected for use as a benchmark case. The model simulates radon gas release from a uranium tailings area, its atmospheric dispersion and the subsequent exposure of a nearby receptor.

The mathematical model is outlined in Table C.1, while the input parameters and their assigned distributions are presented in Table C.2. This model was used because of its intermediate level of complexity and easily managed number of variable input parameters. Details regarding its derivation and the physical significance of the parameters and terms are provided elsewhere (SENES, 1984; Lowe et al, 1985). The consequence of interest was taken to be the radiation dose equivalent to the receptor resulting from the inhalation of radon-222 and its daughters. The model was first run deterministically on each of the three systems, to ensure that the model was implemented properly. The model was then evaluated using 250 random trials on each of the systems. The results are outlined in the following sections.

## C.3 RANSIM

### C.3.1 General Description

RANSIM was initially developed as part of the probabilistic analysis system illustrated on Figure C.1. In that application, it was a completely general module which provided the functions necessary for probabilistic analyses. The Parameter Allocation and Control module indicated on the figure acted as an interface between RANSIM and the situation specific simulation models. In the current system (UTAP), RANSIM and PAC have been combined into the "control modules". However, all of the probabilistic functions previously present in RANSIM have been directly transferred to UTAP. Hence the following results and comparisons generated via RANSIM are directly comparable to probabilistic results generated by UTAP. The following discussion considers RANSIM as it

Table C.1

## RADON MODEL

1. Radon Release Rate ($Bq.s^{-1}$)

RNSOUR = ARTLSR*RACNTA*LAMRN*EMANAT*LSUBT*RHOTAL*
((NSUBW*WTSFLX+(12-NSUBW))/12)*exp(-THICK/LSUBC))

LSUBT = $(EBKDFC/LAMRN)^{1/2}$

and

EBKDFC = POROS*.106X$10^{-4}$exp(-0.261*MPCH20)

2. Atmospheric Dispersion ($s.m^{-3}$)

$P_{0,1}$ = 2.032*FRACT*$(WIND*DIST*SIGZED)^{-1}$*exp(-(($HSUBD^2$)*$(2*SIGZED^2)^{-1}$))

3. Transfer Model: Radon Concentration to Inhalation Dose ($Sv.a^{-1}.Bq^{-1}.m^3$)

$P_{1,10}$ = OCCFAC*DCFIRN

Radon Concentration at Receptor ($Bq.m^{-3}$)

RADCON = RNSOUR*$P_{0,1}$

Dose via Inhalation of Rn-222 ($Sv.a^{-1}$)

DOSRN = $RADCON_1$*$P_{1,10}$

Table C.2

## INPUT PARAMETER DISTRIBUTIONS

| Parameter | Definition | Distribution | Descriptors |
|---|---|---|---|
| POROS | porosity of the tailings | constant | 0.4 |
| LAMRN | radon decay constant (s$^{-1}$) | constant | 2.1E-6 |
| ARTLSR | tailings area (m$^{2}$) | constant | 5.0E5 |
| NSUBW | Number of winter months | constant | 5.0 |
| DIST | effective transport distance (m) | constant | 3.6E3 |
| DCFIRN | radon dose conversion factor (Sv.a$^{-1}$.Bq$^{-1}$.m$^{3}$) | constant | 7.2E-5 |
| MPCH2O | tailings mass water content (%) | triangular | min=5.0; mode=10.0;<br>max=25.0 |
| RACNTA | tailings radium concentration (Bq.g$^{-1}$) | uniform | min=5.0; max=15.0 |
| RHOTAL | tailings density (g.m$^{-3}$) | normal | mean=1.4E6; SD=0.1E6<br>min=1.0E6; max=1.8E6 |
| EMANAT | radon emanation coefficient | triangular | min=0.02; mode=0.2<br>max=0.9 |
| LSUBC | radon diffusion length in cover (m) | uniform | min=0.5; max=1.5 |
| FRACT | fraction of time wind blows to receptor | normal | mean=0.1; SD=0.02<br>min=0.0; max=0.3 |
| WTSFLX | winter/summer radon flux ratio | lognormal | GM*=2.0E-2; GSD**=2.15<br>min=2.0E-3; max=2.0E-1 |
| WIND | wind speed (m.s$^{-1}$) | normal | mean=5.3; SD=0.9<br>min=3.0; max=9.0 |
| SIGZED | vertical dispersion coefficient (m) | lognormal | GM=60.0; GSD=1.73<br>min=10.0; max=300 |
| HSUBD | initial mixing depth (m) | uniform | min=1.0; max.3.0 |
| OCCFAC | occupancy factor | uniform | min=0.3; max=0.9 |
| THICK | tailings cover thickness (m) | triangular | min=0.5; mode=1.0<br>max.2.0 |

* GM refers to Geometric Mean

** GSD refers to Geometric Standard Deviation

FIGURE C.1

CONCEPTUAL FLOW DIAGRAM
OF SYSTEMS APPROACH

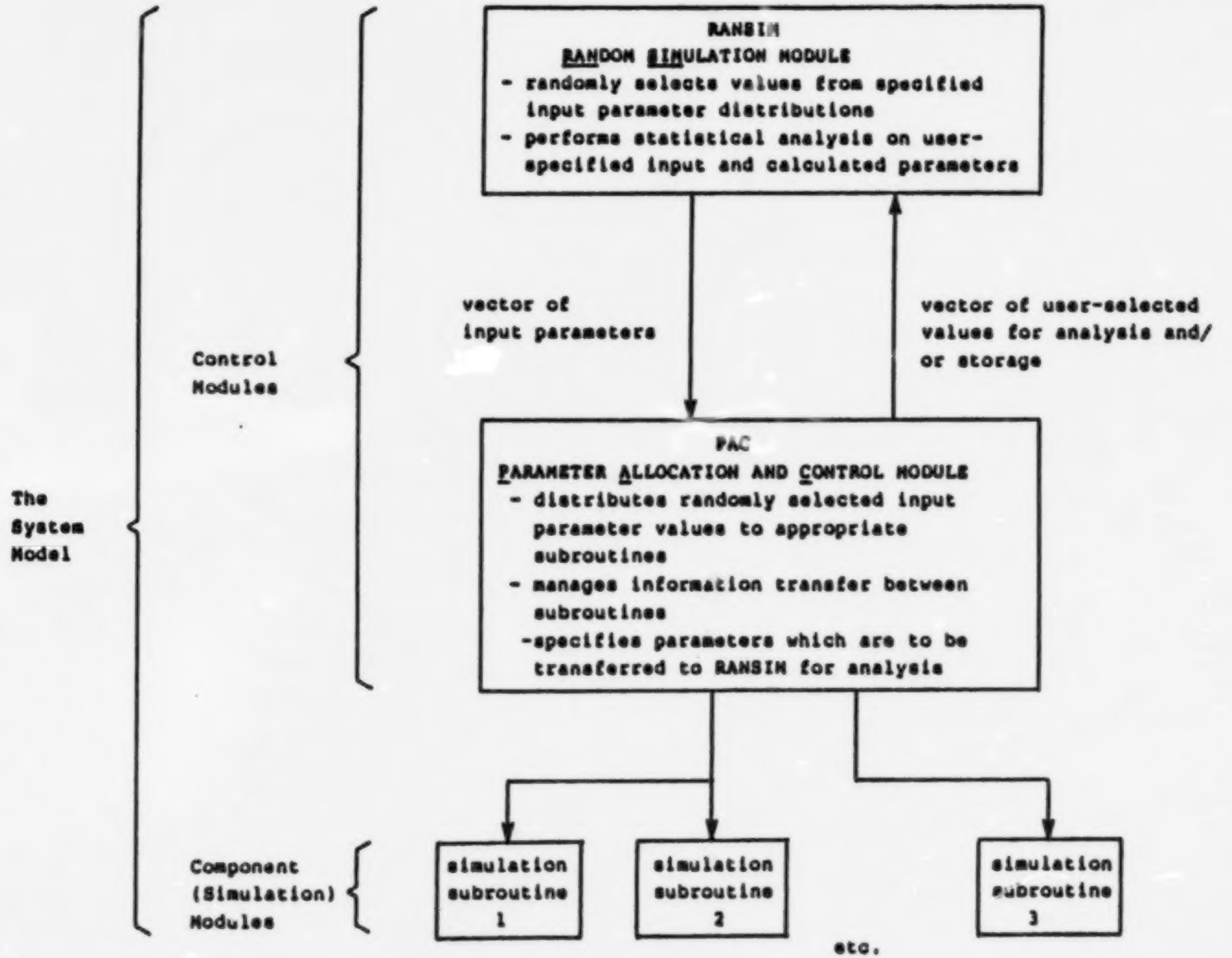
The System Model
Control Modules
Component (Simulation) Modules
RANSIM
RANDOM SIMULATION MODULE
- randomly selects values from specified input parameter distributions
- performs statistical analysis on user-specified input and calculated parameters
vector of input parameters
vector of user-selected values for analysis and/or storage
PAC
PARAMETER ALLOCATION AND CONTROL MODULE
- distributes randomly selected input parameter values to appropriate subroutines
- manages information transfer between subroutines
-specifies parameters which are to be transferred to RANSIM for analysis
simulation subroutine 1
simulation subroutine 2
simulation subroutine 3
etc.

existed at the outset of this Phase III study, as illustrated on Figure C.1.

The entire system is coded in IBM FORTRAN and runs on an IBM PC-AT with 512 Kbytes of RAM. The program was also run, with minimal changes, on a Prime minicomputer, to demonstrate its transportability.

The random simulation program (RANSIM) is a variation on the OPANAL program originally developed by Dr. P.M. Reilly (Reilly and Johri, 1969). Its conceptual specifications are outlined in Figure C.2. RANSIM is designed to convert numeric descriptors of many types of distributions into a series of randomly sampled values available for transfer to simulation models. Sampling routines currently available include:

- constant value
- normal
- lognormal
- uniform
- log uniform
- triangular
- beta
- arbitrary
- pairwise correlated.

The beta and arbitrary distribution capabilities allow almost an infinite range of distribution shapes to be specified. Different sampling algorithms are used to sample from each distribution. All depend on a routine to generate random numbers between 0 and 1. The random number generator is based on the UNIRAN algorithm, as outlined by Marse and Roberts (1983).

RANSIM is designed to provide simple rapid feedback from any simulation, as well as to write selected results to disk for further analysis. The immediate feedback is comprised of a variety of summary statistics on either user-specified inputs or calculated parameters. The summary statistics available include: arithmetic mean, arithmetic standard deviation, skewness, kurtosis,

FIGURE C.2

## CONCEPTUAL FLOW DIAGRAM OF RANSIM

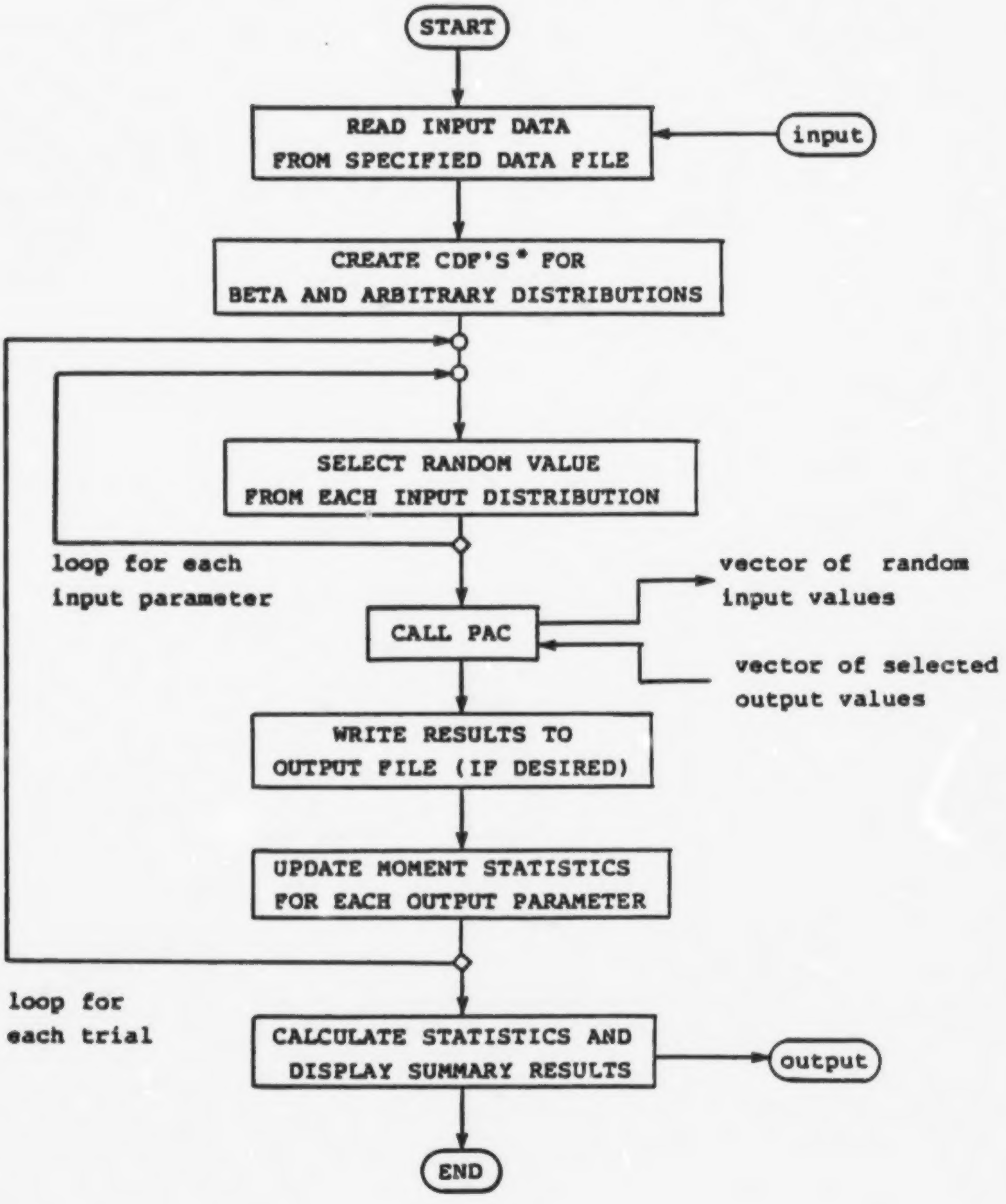
START
READ INPUT DATA FROM SPECIFIED DATA FILE
input
CREATE CDF'S* FOR BETA AND ARBITRARY DISTRIBUTIONS
SELECT RANDOM VALUE FROM EACH INPUT DISTRIBUTION
loop for each input parameter
CALL PAC
vector of random input values
vector of selected output values
WRITE RESULTS TO OUTPUT FILE (IF DESIRED)
UPDATE MOMENT STATISTICS FOR EACH OUTPUT PARAMETER
loop for each trial
CALCULATE STATISTICS AND DISPLAY SUMMARY RESULTS
output
END

* CUMULATIVE DISTRIBUTION FUNCTION

geometric mean, geometric standard deviation, and maximum and minimum values.

These are all calculated using updating ("on-the-fly") methods and thus can be determined regardless of whether one wishes to save all values from all trials or not. They may be most beneficial when the amount of information generated is large and which, if stored, would result in disk storage problems. If one elects to save the results from all trials, they are stored in an output file in a form suitable for subsequent analysis or graphical display by a statistical or graphical package (e.g. SAS, STATGRAPHICS, BMDP, etc).

### C.3.2 RANSIM Results

Summary statistics for all variable input parameters and the consequence of interest (DOSRN) are presented in Table C.3. The summary statistics for the sampled parameters correspond quite well to the parameter specifications (Table C.2). Rigorous statistical tests in previous studies (SENES, 1985) indicated that the distributions as sampled are not significantly different from those specified.

The distribution of the calculated value, DOSRN is displayed as a frequency histogram in Figure C.3(a) and as a cumulative density function (cdf) in Figure C.3(b). These figures, and the graphical presentations of RANSIM results to follow, were generated using STATGRAPHICS, a commercially available statistical/graphical package. Since the distribution of DOSRN is highly skewed, a logarithmic transform was performed. The histogram and CDF for log (DOSRN) are presented in Figure C.4(a) and (b).

### C.3.3 Sensitivity/Uncertainty Analysis: SENES

To avoid many of the disagreements regarding appropriate definitions of sensitivity and uncertainty analysis, we have chosen to refer to them together as "importance analysis". This term is used in the remainder of this section. Two importance analysis techniques were selected for use in this study, namely: stepwise regression and the sensitivity index. Stepwise regression is

Table C.3

## SUMMARY STATISTICS: RANSIM
(250 Random Simulations)

| Parameter | Mean | Std. Dev. | Geom. Mean | Geom. SD | Minimum | Maximum |
|---|---|---|---|---|---|---|
| RACNTA | 9.625E-00 | 2.871E+00 | 9.186E+00 | 1.365E+00 | 5.032E+00 | 1.494E+01 |
| EMANAT | 4.162E-01 | 1.998E-01 | 3.617E-01 | 1.768E+00 | 4.733E-02 | 8.877E-01 |
| RHOTAL | 1.399E+06 | 9.723E+04 | 1.396E+06 | 1.072E+00 | 1.167E+06 | 1.670E+06 |
| WTSFLX | 2.673E-02 | 2.282E-02 | 1.987E-02 | 2.165E+00 | 2.766E-03 | 1.524E-01 |
| MPCH2O | 1.345E+01 | 4.132E+00 | 1.282E+01 | 1.371E+00 | 5.560E+00 | 2.323E+01 |
| FRACT | 1.012E-01 | 1.943E-02 | 9.923E-02 | 1.225E+00 | 4.379E-02 | 1.559E-01 |
| WIND | 5.234E+00 | 8.771E-01 | 5.160E+00 | 1.186E+00 | 3.140E+00 | 7.502E+00 |
| SIGZED | 6.679E+00 | 3.833E+01 | 5.752E+01 | 1.736E+00 | 1.163E+01 | 2.374E+02 |
| HSUBD | 1.989E+00 | 5.515E-01 | 1.909E+00 | 1.340E+00 | 1.009E+00 | 2.983E+00 |
| LSUBC | 1.027E+00 | 2.939E-01 | 9.823E-01 | 1.362E+00 | 5.016E-01 | 1.500E+00 |
| OCCFAC | 6.208E-01 | 1.687E-01 | 5.962E-01 | 1.340E+00 | 3.012E-01 | 8.996E-01 |
| THICK | 1.165E+00 | 3.024E-01 | 1.125E+01 | 1.309E+00 | 5.189E-01 | 1.938E+00 |
| DOSRN | 3.218E-06 | 4.355E-04 | 1.660E-06 | 3.314E+00 | 9.015E-08 | 2.893E-05 |

FIGURE C.3a

RANSIM RESULTS

FREQUENCY HISTOGRAM: DOSRN

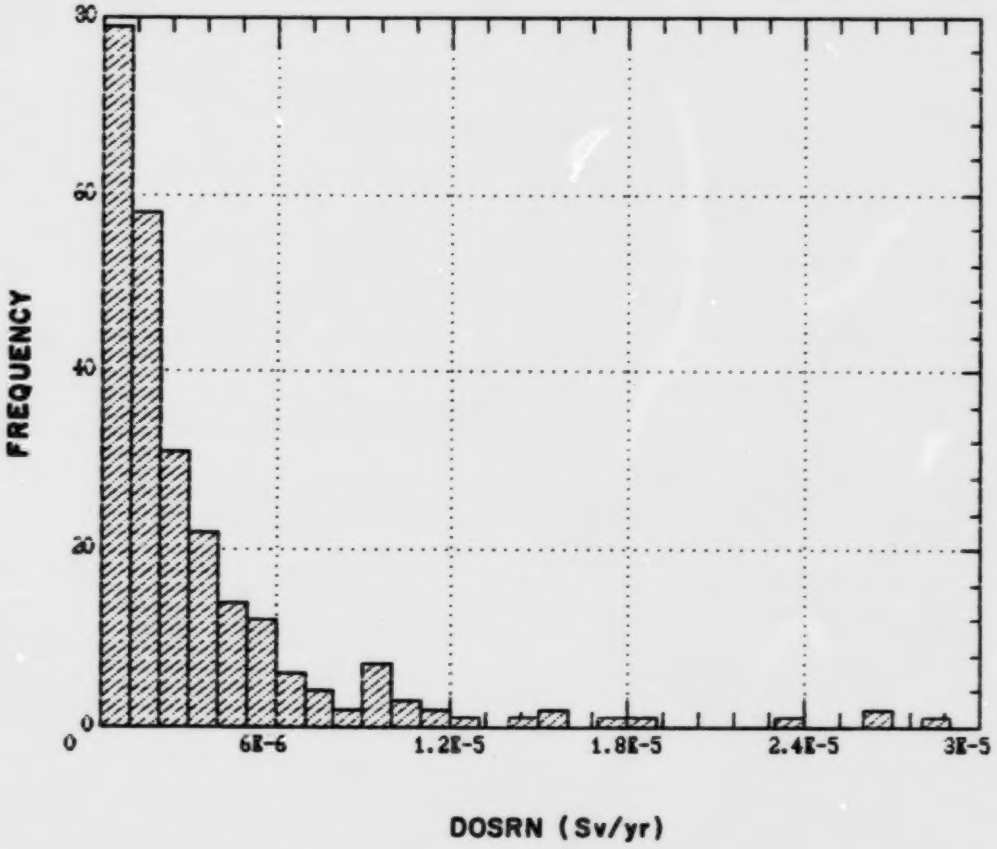

FIGURE C.3b

## RANSIM RESULTS
## CUMULATIVE RELATIVE FREQUENCY: DOSRN

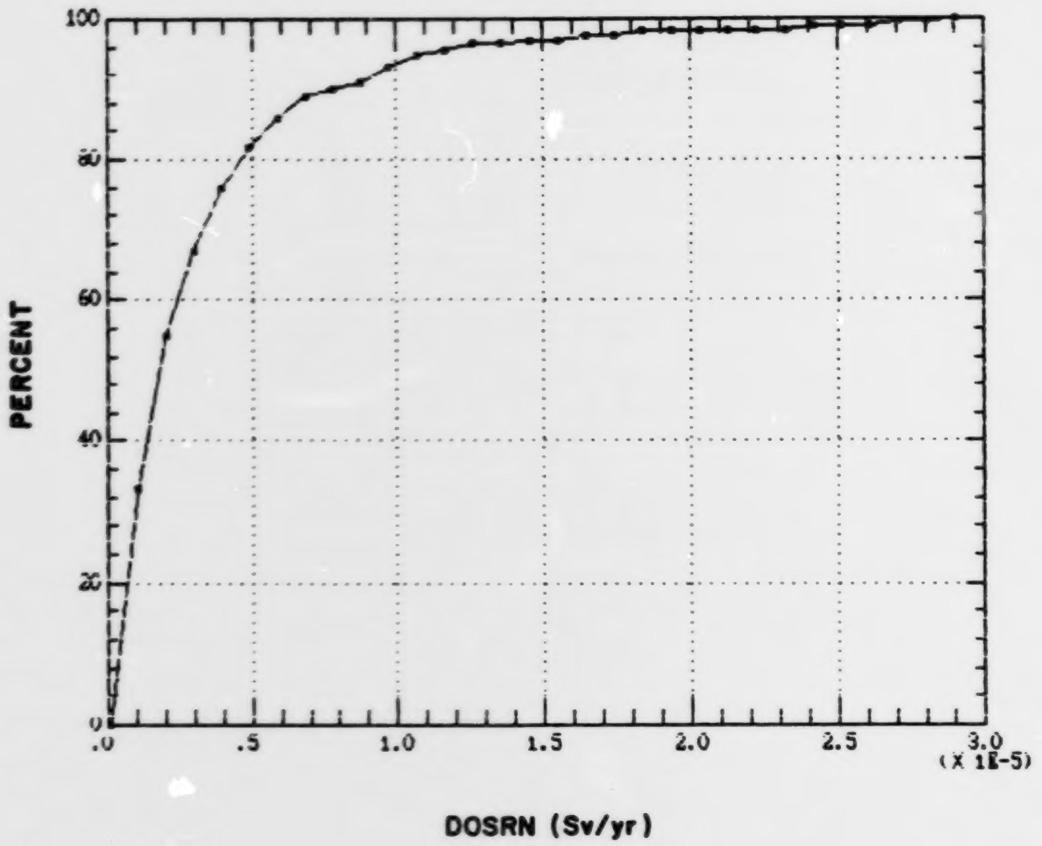

FIGURE C.4a

## RANSIM RESULTS
## FREQUENCY HISTOGRAM: LOG (DOSRN)

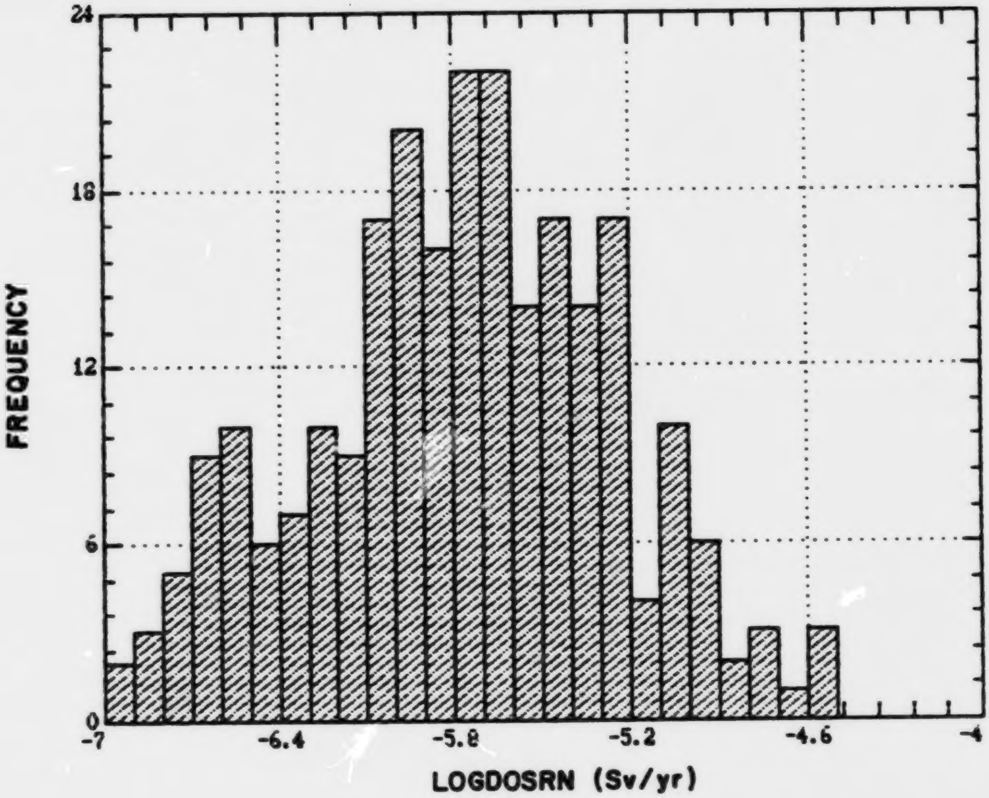

## FIGURE C.4b

## RANSIM RESULTS
## CUMULATIVE RELATIVE FREQUENCY: LOG(DOSRN)

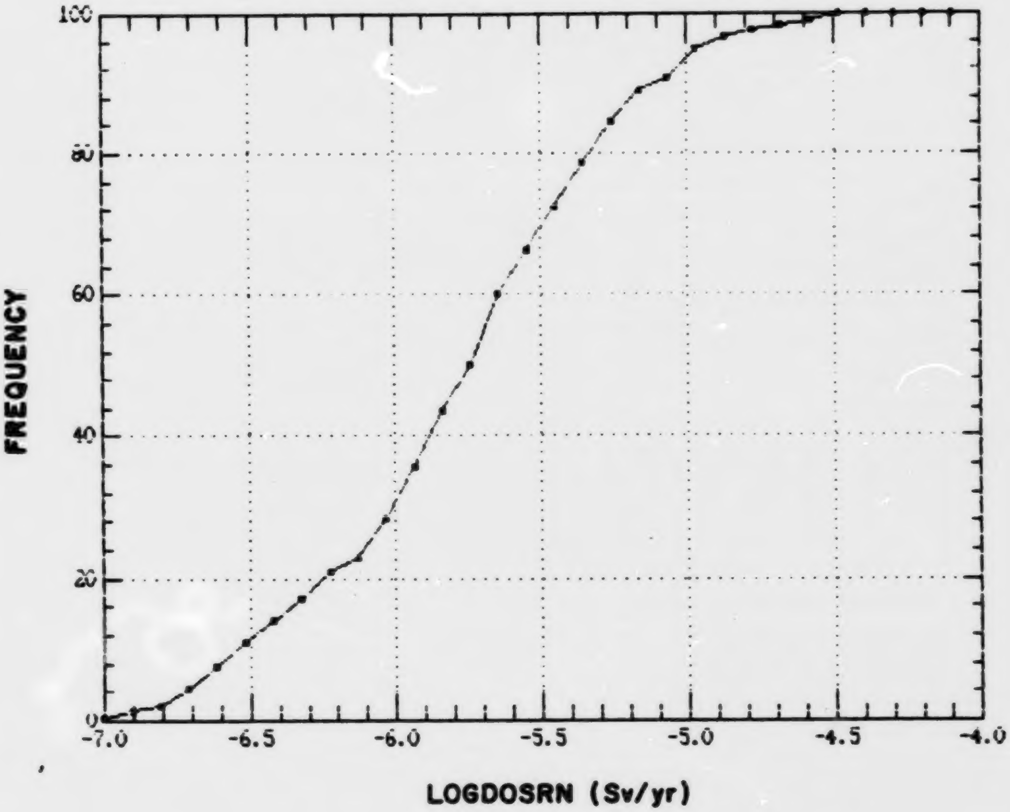

a relatively complex method of ranking parameters which has considerable statistical support, while the sensitivity index is a simple, more intuitive method. Both are described in more detail below.

The sensitivity index (SI) (Hoffman and Gardner, 1983) provides a simple indication of the response of the model to changes in the input parameters. It is determined by evaluating the model deterministically twice for each input parameter, once with the parameter of interest at its extreme high value and once with the parameter of interest at its extreme low value. All other parameters are held constant at their nominal values. The sensitivity index (for the ith parameter) can then be calculated as:

$$SI_i = 1 - \frac{\text{low calculated result}}{\text{high calculated result}}$$

The closer the SI is to one (i.e. the larger the difference between the high and low calculated results) the more sensitive the model is to the variable.

The sensitivity index must be used with caution since the results will vary depending on the nominal values chosen for the other parameters while examining the effects of one particular parameter. It is also implicitly assumed that the model responds linearly (or nearly so) in a monotically increasing or decreasing fashion over the full range of input parameter values being evaluated. Notwithstanding these limitations, the SI was found to be applicable to all situations and scenarios in which it was used in a previous study (SENES, 1985).

The sensitivity index just described applies, rigorously, only for one set of input parameter values (i.e. at only one point on the "model response surface"). Regression analysis, on the other hand, provides an indication of parameter importance while all parameters are allowed to vary simultaneously over their specified ranges. This type of analysis treats probabilistic results as one would treat the results of many trials of a given experiment. The input parameters represent the independent variables while a calculated output (eg. DOSRN) is selected as the dependent variable.

Linear regression involves the construction of a linear, predictive equation (using all the independent variables) which accounts for as much of the variation in the dependent variable as possible. The overall correlation coefficient ($R^2$) provides an indication of how much of the variation in the dependent parameter has been accounted for by the given regression equation.

Stepwise linear regression differs somewhat, in that the independent variables are added to the regression equation one-at-a-time, in order of their statistical importance. The order of entry and hence of parameter ranking is based on the relative magnitudes of the "partial correlation coefficients" at each step in the analysis. Thus, a new regression equation, and its associated $R^2$ value are produced at each step in the analysis.

It is easy, in the case of regression analysis to get mired in technical details. However, one must not lose sight of the original objective of the exercise, to identify the important parameters. To emphasize this point, a simplified approach has been taken in presenting the results of stepwise regression.

Table C.4 presents the results of importance analysis, using DOSRN as the dependent variable. The parameters are listed in decreasing order of importance based on the sensitivity index. The magnitude of the sensitivity index is given in the second column, while the ranking based on stepwise regression is given in the third column. Rather than interpreting these results as a strict ranking, we prefer to interpret them as identifying 3 groups of parameters, as indicated. Both methods clearly indicate the three parameters that are the most important. The two methods produce similar parameter groupings with only 2 exceptions (FRACT and HSUBD). We feel that both methods provide useful information regarding parameter importance and should be used to complement each other.

Table C.4

## SENES IMPORTANCE ANALYSIS RESULTS

| Parameter | Sensitivity Index | Order of Entry In Stepwise Regression | |
|---|---|---|---|
| 1. EMANAT | .98 | 3 | very important |
| 2. MPCH2O | .92 | 2 | |
| 3. SIGZED | .89 | 1 | |
| 4. THICK | .78 | 7 | moderately important |
| 5. LSUBC | .73 | 6 | |
| 6. RACNTA | .67 | 5 | |
| 7. OCCFAC | .67 | 4 | |
| 8. FRACT | .57 | 12 | |
| 9. WIND | .50 | 8 | |
| 10. RHOTAL | .25 | 10 | unimportant |
| 11. WTSFLX | .006 | 11 | |
| 12. HSUBD | .001 | 9 | |

## C.4 SYVAC

The information contained in the following sections was extracted from a discussion paper prepared by T. Andres for SENES Consultants Limited (Andres, 1985).

### C.4.1 General Description

The name SYVAC stands for SYstems Variability Analysis Code. SYVAC is a FORTRAN program originally developed for the Canadian Nuclear Fuel Waste Management Program (Dormuth and Sherman, 1981; Wuschke et al., 1981). The general function of the program is to generate multiple stochastic simulations of a natural system, to determine the environmental impacts of contaminants in the system.

The specific functions of the SYVAC program are shown in Figure C.5. They are:

(1) To run multiple independent simulations. For each simulation,
(2) To sample values of input parameters from probability distributions.
(3) To estimate the total environmental impact by accumulating the effects of multiple independent contaminants (e.g. nuclide decay chains). For each contaminant,
(4) To simulate the behaviour of the entire system by exercising multiple submodels in order.
(5) To assist the modeller by providing a library of routines to manipulate mathematical functions of time, including code to:
    - represent a time function by a time series;
    - add together two time series (e.g. to add together environmental impacts as a function of time);
    - convolute two time series (e.g. to evaluate the output of a model defined by a set of differential equations using an input-response technique).

All simulations in this investigation were carried out using a version of

FIGURE C.5

FUNCTIONS OF THE SYVAC PROGRAM

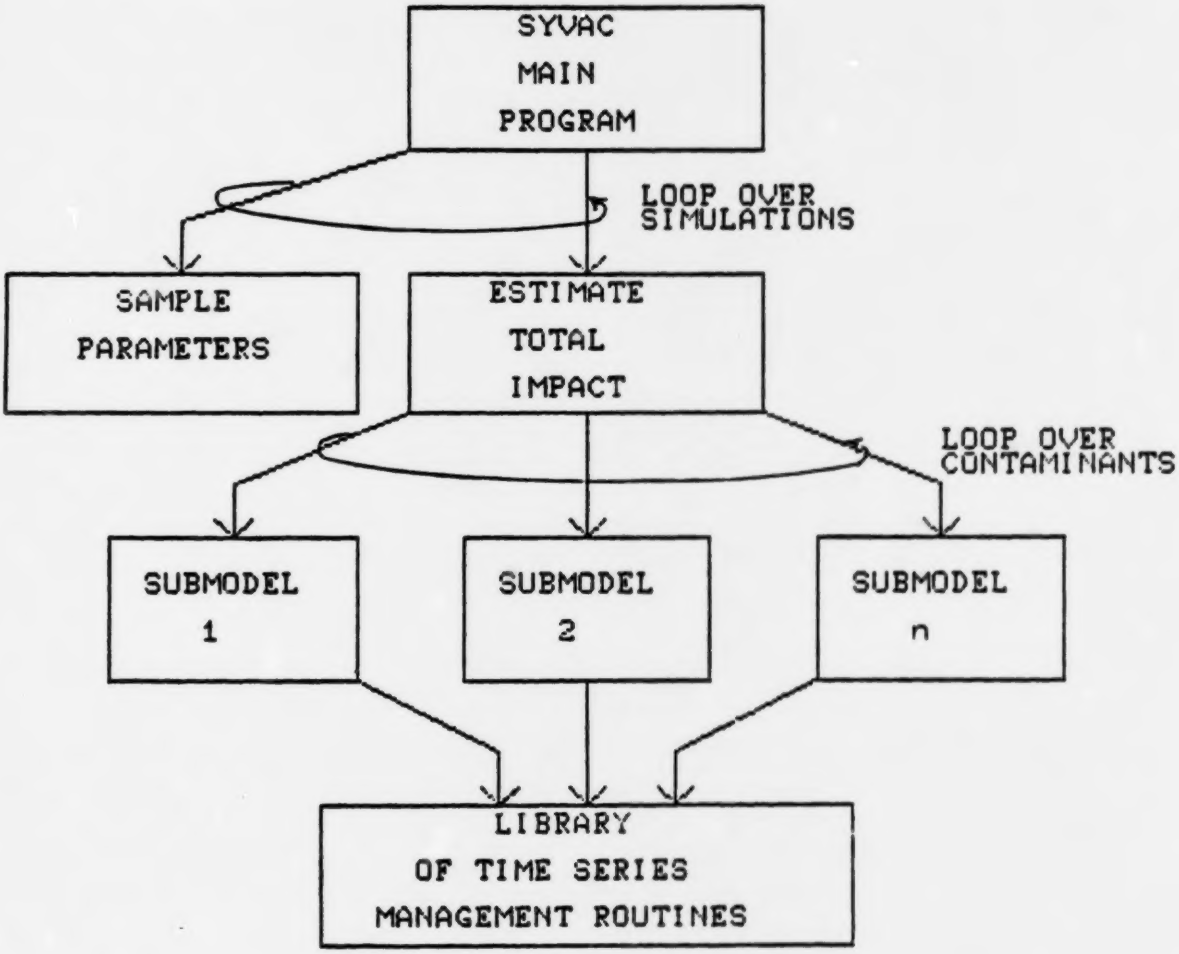
SYVAC
MAIN
PROGRAM
LOOP OVER
SIMULATIONS
SAMPLE
PARAMETERS
ESTIMATE
TOTAL
IMPACT
LOOP OVER
CONTAMINANTS
SUBMODEL
1
SUBMODEL
2
SUBMODEL
n
LIBRARY
OF TIME SERIES
MANAGEMENT ROUTINES

SYVAC adapted to run on an IBM Personal Computer. This version is known as SYVAC3-T1. The code SYVAC3-T1 is a full implementation of the SYVAC program in Microsoft FORTRAN Version 3.2 on an IBM PC microcomputer. It has all the capabilities listed above (with the qualification that the time series management routines were still being implemented as of this writing). However, not all these capabilities were needed for this project. In particular, only functions (1) and (2) were required to run the radon dose model. SYVAC3-T1 produces an output file containing values of all variables used in each simulation.

A number of routines have been developed to read a SYVAC3-T1 output file and analyze the data. Specifically, routines have been coded to generate sample statistics and descriptive plots (e.g. histograms, cumulative distributions, scatterplots) for variables in the output file. Other routines have been developed to generate fractional factorial designs for input to SYVAC3-T1, and to analyze these simulation results to evaluate sensitivity and uncertainty statistics. All analysis routines used in this project were coded in APL, an interactive programming environment ideal for prototyping applications and quick changes.

SYVAC3-T1 sampling supports the following distribution types for sampling parameters:

- uniform
- log uniform
- piecewise uniform (i.e. a histogram)
- normal
- lognormal
- correlated normal (i.e. a normal variate sampled to be correlated with another sampled normal or lognormal variate)
- correlated lognormal (i.e. a lognormal variate sampled to be correlated with another sampled normal or lognormal variate)
- beta
- triangular

Three types of sampling methods, RANDOM, QUANTILE and ON FILE are available. In one set of simulations, one group of parameters can use one sampling method, and another group can use another sampling method. If two (or more) groups of parameters use RANDOM sampling, then each set will be sampled from a different stream of random numbers.

RANDOM sampling generates random values for the parameters involved using a pseudo-random number generator due to Marsaglia (1968). The generator yields a uniformly distributed value between 0 and 1. This value is then treated as a quantile of the parameter being sampled and it is converted to a value of the parameter using the inverse transform method (Rubinstein, 1981).

QUANTILE sampling also uses the inverse transform method. In this case the quantiles are read from a file. This technique was used in this study for the sensitivity analysis discussed in the folloiwng section.

ON FILE sampling takes the value of each parameter directly from a file. This technique bypasses the probability distributions altogether.

Simulation models can be incorporated into SYVAC3-T1 with minimal modifications to the source code. Parameter distributions are read from input data files. These data files can be internally documented (using comment statements) and hence are readily understandable and easily maintained. SYVAC3-T1 does extensive error checking on the inputs, producing appropriate on-line error messages.

In addition, SYVAC3-T1 has the capability to perform pairwise comparison of simulations. To determine the effect of a single change in a model, or in a parameter's distribution, it is useful to be able to repeat a set of simulations with everything else (e.g. parameter values) staying the same. Then simulations can be compared between the two sets one-by-one or by using a statistical procedure for paired samples. SYVAC3-T1 supports such repetition of simulation sets in two ways. First, changing one (or more) parameter's distribution will not affect values of other parameters since each parameter in RANDOM sampling requires precisely one call to the random number generator, whatever its distribution. Second, multiple streams of random numbers can be defined, so a submodel using one stream can be completely replaced by an alternate submodel without affecting any other submodels using a second stream of random numbers. This feature was not used in this study, but could have been applied in sensitivity and uncertainty analysis.

### C.4.2 Results

Before the benchmark model could be evaluated, several changes to the specifications of the input parameter distributions were required. These changes were required since some of the distribution data (specified on Table C.2) was in a different form from that expected by SYVAC3-T1.

The first transformation involved the normal distribution. The upper and lower bounds on normal distributions were all specified as values, whereas SYVAC3-T1 requires quantile bounds. For example, FRACT was specified as normally-distributed, with mean=0.1; SD=0.02; min=0.0; max=0.3 (where SD=standard deviation). It was necessary to convert the bounds for all normal variates from values to quantiles. The conversion for a normal variate X was:

| Given | Required for SYVAC3-T1 |
|---|---|
| mean | mean |
| SD | SD |
| min | low = $Pr(X \le min)$ |
| max | high = $1 - Pr(X > max)$ |

The other transformation involved lognormal variates. For example, SIGZED was specified as lognormal with GM=60.0; GSD=1.73; min=10.0; max=300 (where GM=geometric mean, GSD=geometric standard deviation). If X is lognormally-distributed, SYVAC3-T1 takes as parameters the mean and standard deviation of log (base 10). The conversion for a lognormal variate X was:

| Given | Required for SYVAC3-T1 |
|---|---|
| GM | mean of log = log (GM) |
| GSD | SD of log = log (GSD) |
| min | low = Pr ($X \leq min$) |
| max | high = 1-Pr($X>max$) |

Table C.5 shows the transformed values for all normal and lognormal distributions specified in Table C.2.

Stochastic simulation results were used to generate summary statistics and plots. All analysis routines were coded in APL (STSC's APL*PLUS/PC for the IBM PC). All calculations were performed in double precision (about 16 significant digits). Summary statistics (from 250 random trials) for all input parameters and the calculated parameter of interest DOSRN, are presented in Table C.6. All statistics for sampled parameters were checked against the parameter distributions. There was general agreement between the specified distributions and the sampling distributions.

The results for DOSRN are presented in histogram form in Figure C.6 (a) and a cumulative distribution function in Figure C.6 (b).

Since DOSRN had a highly skewed distribution, a histogram and CDF were constucted for log DOSRN (Figures C.7 (a) and C.7 (b)).

### C.4.3 Sensitivity/Uncertainty Analysis: Andres

The distinction between sensitivity analysis and uncertainty analysis for this project was made in the Phase I report (SENES, 1984). **"Sensitivity analysis refers to the sensitivity of the magnitude of the result to changes in the magnitudes of the input parameters. ...Uncertainty analysis refers to how much the uncertainty (or spread) associated with each parameter contributes to the total uncertainty (or spread) of the result."** Both are used to answer the question: **"Which parameters/pathways have the greatest effect on model predictions?"**

## Table C.5

## DISTRIBUTION DATA TRANSFORMED FOR SYVAC3-T1

| Parameter Name | Given Distribution Data | Transformed Distribution Data |
|---|---|---|
| FRACT | mean = 0.1 | mean = 0.1 |
| | SD = 0.02 | SD = 0.02 |
| | min = 0.0 | low = 2.8665158E-7 |
| | max = 0.3 | high = 0.9999999999 |
| RHOTAL | mean = 1.4E6 | mean = 1.4E6 |
| | SD = 0.1E6 | SD = 0.1E6 |
| | min = 1.0E6 | low = 3.1671242E-5 |
| | max = 0.3 | high = 0.9999683287 |
| SIGZED | GM = 60.0 | mean of log = 1.7781513 |
| | GSD = 1.73 | SD of log = 0.23804610 |
| | min = 10.0 | low = 5.3981348E-4 |
| | max = 300. | high = 0.9983391281 |
| WIND | mean = 5.3 | mean = 5.3 |
| | SD = 0.9 | SD = 0.9 |
| | min = 3.0 | low = 5.3009218E-3 |
| | max = 0.3 | high = 0.9999803120 |
| WTSFLX | GM = 2.0E-2 | mean of log = -1.69897000 |
| | GSD = 2.15 | SD of log = 0.33243846 |
| | min = 2.0E-3 | low = 1.3145389E-3 |
| | max = 2.0E-1 | high = 0.9986854611 |

Table C.6

## SUMMARY STATISTICS: SYVAC3-T1
(250 Random Simulations)

| Parameter | Mean | Std. Dev. | Geo. Mean | Geo. SD | Minimum | Maximum |
|---|---|---|---|---|---|---|
| FRACT | 1.012E-01 | 2.013E-02 | 9.903E-02 | 1.236E+00 | 4.632E-02 | 1.468E-01 |
| HSUBD | 1.968E+00 | 5.606E-01 | 1.885E+00 | 1.353E+00 | 1.003E+00 | 2.996E+00 |
| LSUBC | 1.016E+00 | 2.894E-01 | 9.710E-01 | 1.362E+00 | 5.030E-01 | 1.499E+00 |
| MPCH2O | 1.335E+01 | 4.523E+00 | 1.260E+01 | 1.415E+00 | 5.425E+00 | 2.466E+01 |
| OCCFAC | 6.086E-01 | 1.671E-01 | 5.847E-01 | 1.336E+00 | 3.013E-01 | 8.981E-01 |
| RACNTA | 9.935E+00 | 2.827E+00 | 9.508E+00 | 1.356E+00 | 5.005E+00 | 1.498E+01 |
| RHOTAL | 1.402E+06 | 9.758E+04 | 1.399E+06 | 1.072E+00 | 1.150E-06 | 1.686E+06 |
| SIGZED | 7.375E+01 | 3.893E+01 | 6.456E+01 | 1.698E+00 | 1.204E+01 | 2.272E+02 |
| THICK | 1.160E+00 | 3.220E-01 | 1.115E+00 | 1.332E+00 | 5.115E-01 | 1.990E+00 |
| WIND | 5.320E+00 | 9.284E-01 | 5.238E+00 | 1.196E+00 | 3.317E+00 | 8.407E+00 |
| WTSFLX | 2.804E-02 | 2.156E-02 | 2.134E-02 | 2.162E+00 | 2.356E-03 | 1.296E-01 |
| EMANAT | 3.895E-01 | 1.889E-01 | 3.372E-01 | 1.792E+00 | 4.122E-02 | 8.306E-01 |
| DOSRN | 2.958E-06 | 5.098E-06 | 1.378E-06 | 3.463E+00 | 6.361E-08 | 4.734E-05 |

FIGURE C.6a

SYVAC3-TI RESULTS
RELATIVE FREQUENCY HISTOGRAM: DOSRN

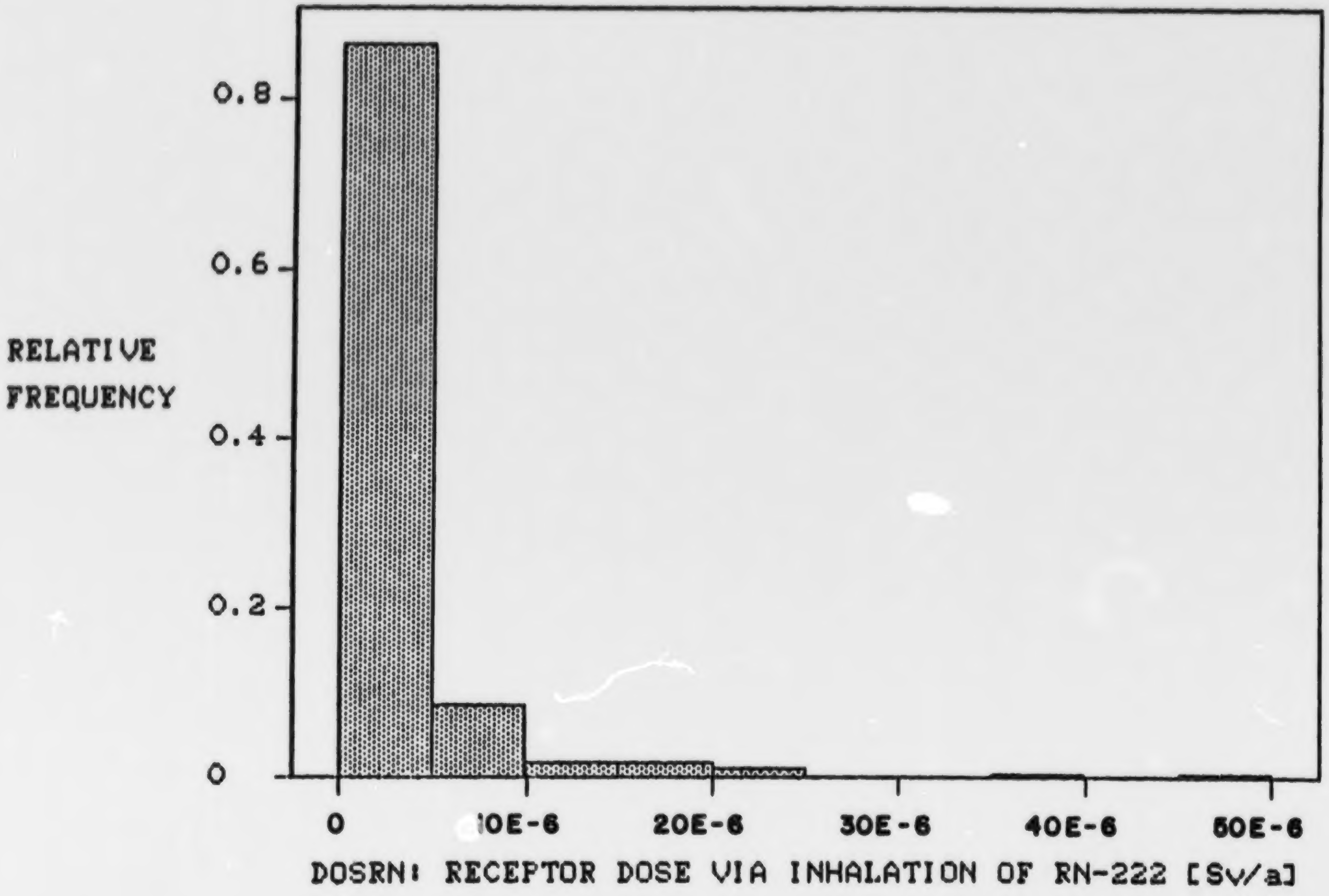

FIGURE C.6b

SYVAC3 - TI RESULTS
CUMULATIVE DENSITY FUNCTION: DOSRN

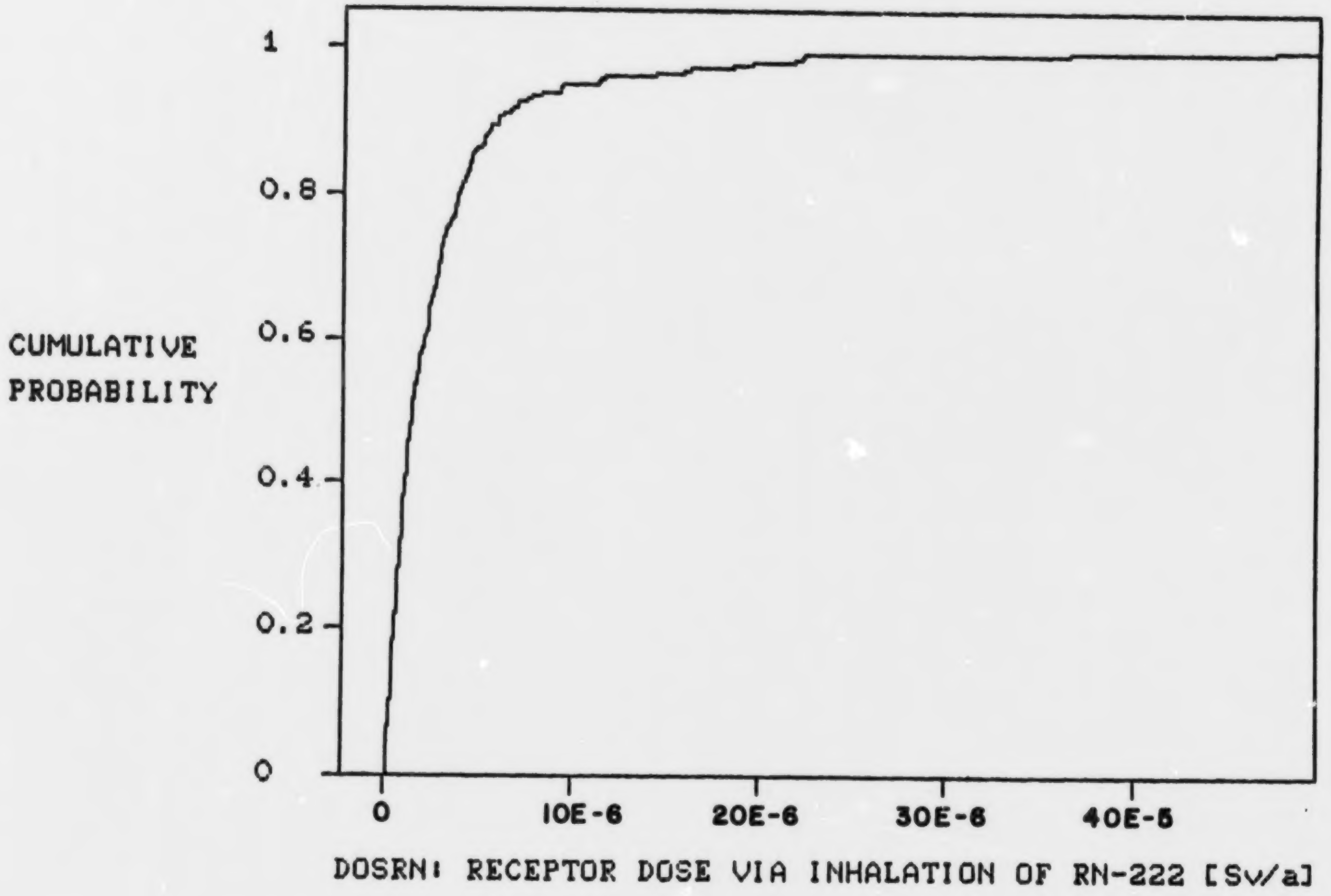

FIGURE C.7a

SYVAC3-TI RESULTS
RELATIVE FREQUENCY HISTOGRAM: LOG (DOSRN)

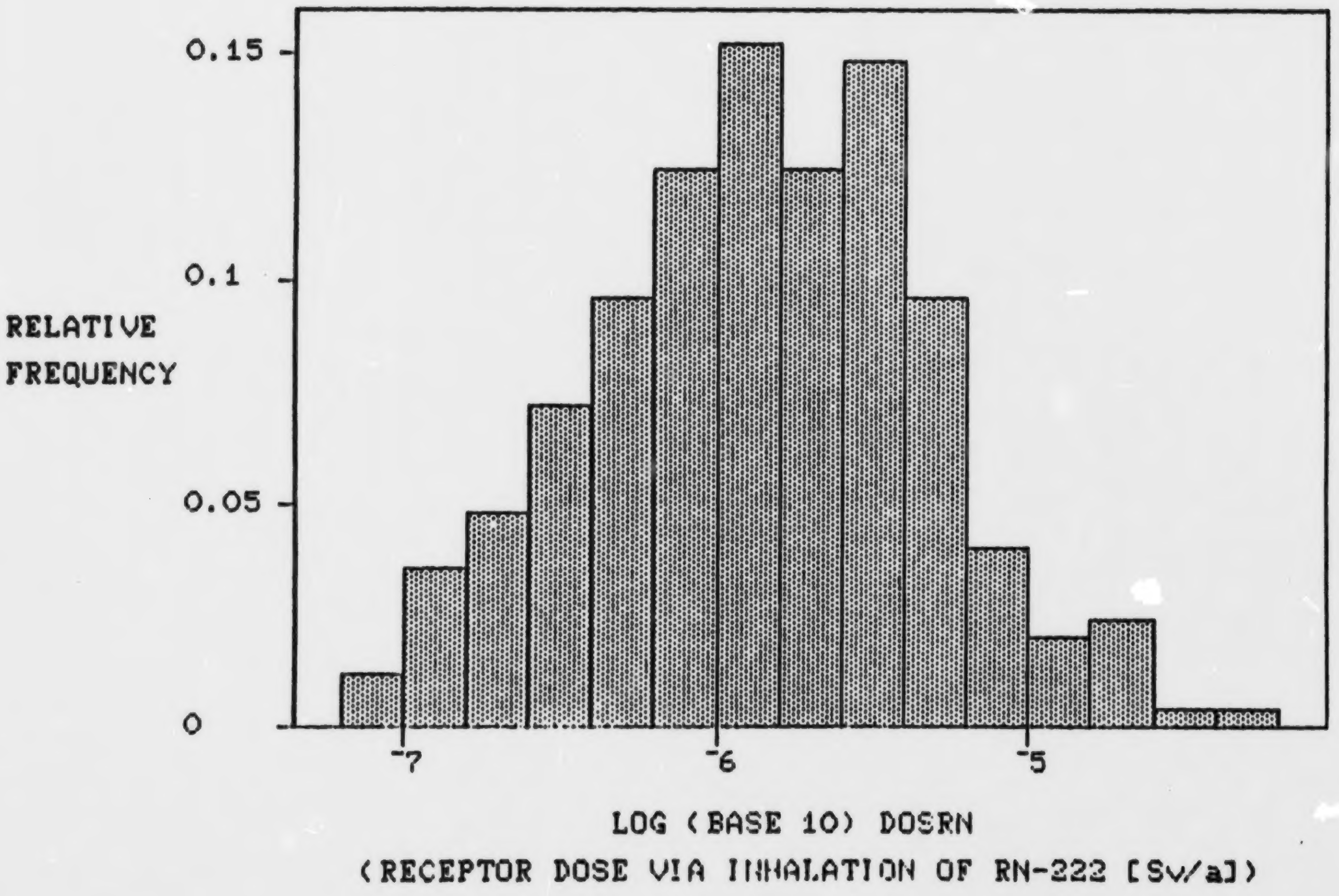

FIGURE C.7b

SYVAC3 - TI RESULTS

CUMULATIVE DENSITY FUNCTION: LOG (DOSRN)

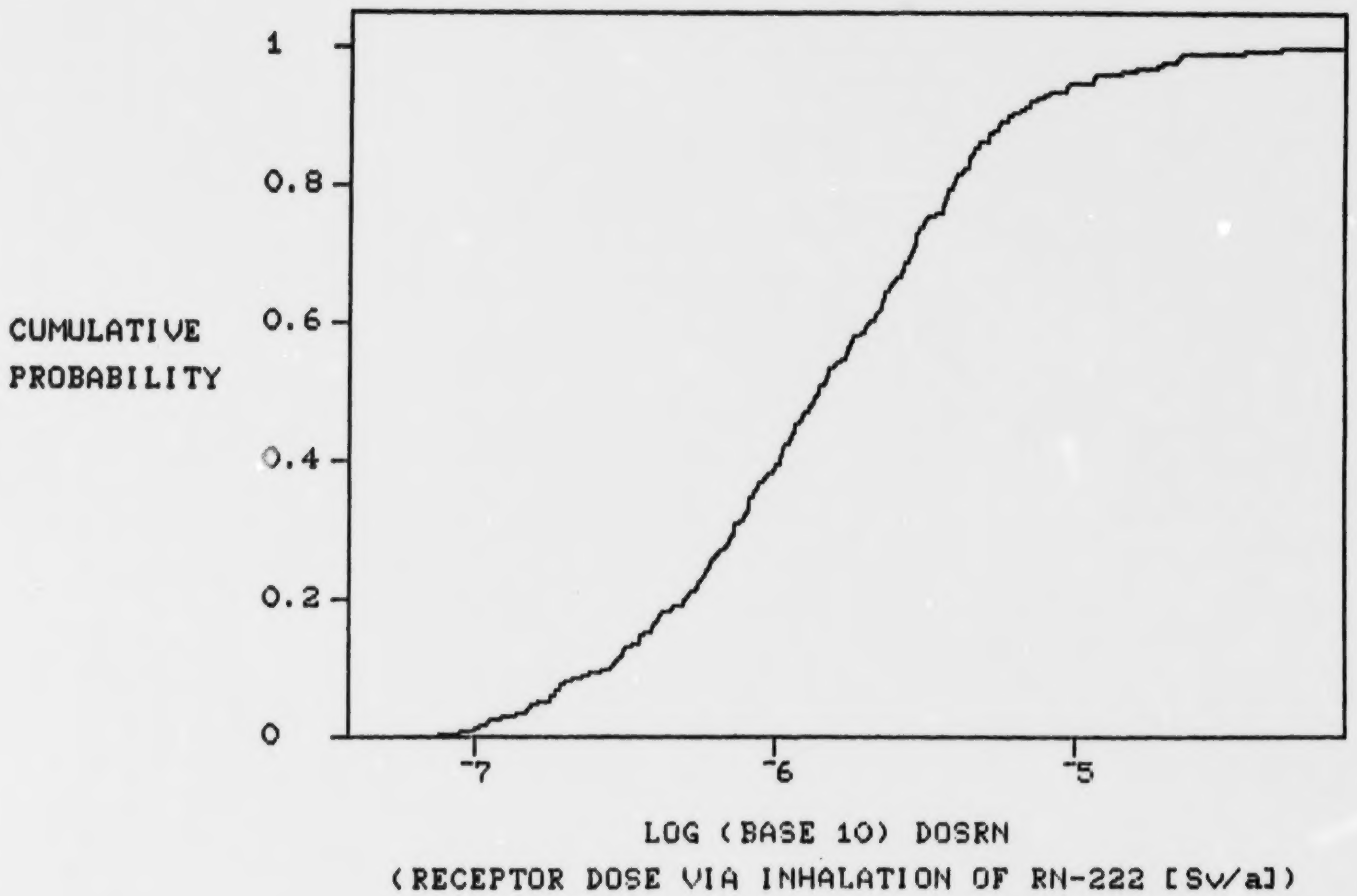

To answer this question for this report, the simulation model was treated like an experimental apparatus and additional experiments (simulations) were conducted. First an experimental design was selected based on the number of parameters and the information to be elicited. Then simulations were conducted with parameter values selected according to the experimental design. The results of these simulations were analyzed to determine the effects of the individual parameters on DOSRN (sensitivity analysis). The experiments were repeated with parameters chosen at different points in their distributions to determine the effects of parameter spreads on DOSRN (uncertainty analysis).

Two-level fractional factorial designs were chosen as being appropriate for this analysis (Box et al., 1978). In these designs, a low value and a high value is chosen for each parameter, and only these two values are used in the set of simulations. The set of simulations is designed to determine the effect of flipping between these two values for each parameter. The average change in radon dose due to a change from low value to high value of a parameter is called the main effect of that parameter.

To conduct the experiment, two values were chosen for each parameter. In fact, to permit uncertainty analysis, several combinations of two values were chosen and analyzed separately. The first combination of two values selected for this experiment consisted of the lower quartile (i.e. the 25th percentile) and the upper quartile (i.e. the 75th percentile) of each parameter's distribution. These values were used in the sensitivity analysis experiment (denoted SV0001 in the following discussion). For uncertainty analysis, the procedure was repeated twice more, once at the 10 and 90 percentile points (SV0002), and once at the 1 and 99 percentile points (SV0003). These additional percentiles were selected because they lie roughly at the start of the distribution tails (10 and 90 percentiles), and far out in the distribution tails (1 and 99 percentiles).

Results from fractional factorial experiments were analyzed to estimate the main effect of each parameter. To permit adequate discrimination among main effects two groups of 64 simulations were used in the experimental design.

### C.4.3.1 Sensitivity Analysis

Analysis based on fractional factorial designs was effective for sensitivity analysis of DOSRN. It was especially precise and effective for analyzing the modified consequence log (DOSRN).

The details of this type of sensitivity analysis are rather technical, and will be covered in a forthcoming paper on the application of fractional factorial designs to sensitivity analysis of probabilitistic simulation models. In this paper the main conclusions can be summarized as follows:

1) All of the parameters of the radon model (and not just the important ones) were ranked exacly in their order of main effect on log (DOSRN) as shown in Table C.7. The table shows that in two different sets of 64 simulations, both the order of the parameters and the values of their main effects were identical. This repeatability is important because it shows that at least in the analysis of log (DOSRN) the ranking of parameters is not subject to the random variation, as a ranking based on random simulations would be.

2) The table shows that the three most important parameters, in dimishing order of main effect, were EMANAT, MPCH2O and SIGZED.

### C.4.3.2 Uncertainty Analysis

Table C.8 shows the main effect estimates for log (DOSRN) ranked in decreasing order for the three sets of simulations SV0001, SV0002, and SV0003. The rankings are similar, indicating that sensitivities are generally consistent across the domains of the parameters. The values are different because log(DOSRN) is more affected by large swings of parameter values than by small swings.

Table C.8 shows that one parameter, THICK, behaves anomalously. It rises in importance from position 7 in SV0001, to position 5 in SV0002, to position 4

Table C.7

## ESTIMATES OF MAIN EFFECTS ON LOG (DOSRN) IN SV0001

| Variable Number* | Variable Name | Estimate From First 64 Simulations | Estimate From Last 64 Simulations |
|---|---|---|---|
| 19 | EMANAT | 0.36249 | 0.36249 |
| 9 | MPCH2O | -0.35931 | -0.35931 |
| 15 | SIGZED | -0.31988 | -0.31988 |
| 8 | LSUBCC | 0.26876 | 0.26876 |
| 13 | RACNTA | 0.22185 | 0.22185 |
| 11 | OCCFAC | 0.22185 | 0.22185 |
| 16 | THICK | -0.21060 | -0.21060 |
| 5 | FRACT | 0.11789 | 0.11789 |
| 17 | WIND | -0.09916 | -0.09916 |
| 14 | RHOTAL | 0.04188 | 0.04188 |
| 18 | WTSFLX | 0.00656 | 0.00656 |
| 6 | HSUBD | -0.00031 | -0.00031 |
| 2 | ARTLSR** | 0.0 | 0.0 |
| 26 | (not used) | 0.0 | 0.0 |
| 10 | NSUBW** | 0.0 | 0.0 |
| 22 | (not used) | 0.0 | 0.0 |
| 4 | DIST** | 0.0 | 0.0 |
| 12 | POROS** | 0.0 | 0.0 |
| 20 | (not used) | 0.0 | 0.0 |
| 28 | (not used) | 0.0 | 0.0 |
| 7 | LAMRN** | 0.0 | 0.0 |
| 21 | (not used) | 0.0 | 0.0 |
| 31 | (not used) | 0.0 | 0.0 |
| 30 | (not used) | 0.0 | 0.0 |
| 3 | DCFIRN** | 0.0 | 0.0 |
| 23 | (not used) | 0.0 | 0.0 |
| 29 | (not used) | 0.0 | 0.0 |
| 33 | (not used) | 0.0 | 0.0 |
| 24 | (not used) | 0.0 | 0.0 |
| 25 | (not used) | 0.0 | 0.0 |
| 27 | (not used) | 0.0 | 0.0 |
| 32 | (not used) | 0.0 | 0.0 |

* RUN NUMBER is variable number 1, which does not appear in this table.
** Constant parameter

Note
Variable names given as (not used) refer to dummy variables that did not appear in the model, but were included in the analysis as control variables.

Table C.8

## COMPARISON OF PARAMETER SENSITIVITIES OVER DIFFERENT PARAMETER DOMAINS

| SV0001 | | SV0002 | | SV0003 | |
|---|---|---|---|---|---|
| Quantiles (0.25, 0.75) | | Quantiles (0.10, 0.90) | | Quantiles (0.01, 0.99) | |
| Variable | Main Effect | Variable | Main Effect | Variable | Main Effect |
| EMANAT | 0.36249 | EMANAT | 0.65019 | EMANAT | 1.13792 |
| MPCH20 | -0.35931 | MPCH20 | -0.64386 | SIGZED | -1.08562 |
| SIGZED | -0.31988 | SIGZED | -0.60669 | MPCH20 | -0.97867 |
| LSUBC | 0.26876 | LSUBC | 0.49356 | THICK | -0.73778 |
| RACNTA | 0.22185 | THICK | -0.43369 | LSUBC | 0.69006 |
| OCCFAC | 0.22185 | OCCFAC | 0.36798 | OCCFAC | 0.46562 |
| THICK | -0.21060 | RACNTA | 0.36798 | RACNTA | 0.46562 |
| FRACT | 0.11789 | FRACT | 0.22770 | FRACT | 0.43778 |
| WIND | -0.09916 | WIND | 0.17348 | WIND | -0.34353 |
| RHOTAL | 0.04188 | RHOTAL | 0.07972 | RHOTAL | 0.14561 |
| WTSFLX | 0.00657 | WTSFLX | 0.01383 | WTSFLX | 0.03308 |
| HSUBD | -0.00031 | HSUBD | -0.00083 | HSUBD | -0.00299 |

in SV0003. This behaviour is not due to THICK having a long-tailed distribution, for THICK has a triangular distribution with finite tails. Instead it seems to be caused by the nature of the effect of THICK on DOSRN.

Figure C.8 shows a scatterplot of log (DOSRN) versus THICK. The plot shows a mild trend downward to the right. The trend becomes more evident near the left and right edges, because there are bare spots in the lower left and upper right corners. The scatterplot indicates that the uncertainty (the spread of scatter) in log (DOSRN) is reduced for high values of THICK, and perhaps for low ones as well.

## C.5 DEMOS

The following descriptions of DEMOS are drawn from a number of published sources (Henrion and Morgan, 1985; Henrion and Nair, 1982; and Henrion, 1979) as well as from discussions with its author, Dr. Max Henrion. Dr. Henrion also provided the results referenced later in this section.

### C.5.1 General Description

The name DEMOS stands for DEcision MOdelling System. It is an interactive environment for structuring, analyzing and communicating probabilistic models. It provides general mathematical modelling facilities, but was designed primarily for policy related modelling, using techniques from cost-benefit analysis, engineering economics, risk assessment and decision analysis. The first version of DEMOS was designed by Dr. Henrion, and implemented in the PPL language in 1979-80. The current version is implemented in PASCAL on a Digital Equipment micro-VAX computer.

DEMOS has four particular characteristics which distinguish it from most other general purpose modelling languages:

- Interaction: Model development is usually an iterative process, in which successive versions of a model are constructed, criticized and modified

FIGURE C.8

SYVAC3-TI RESULTS
SCATTERPLOT: LOG (DOSRN) vs. THICK

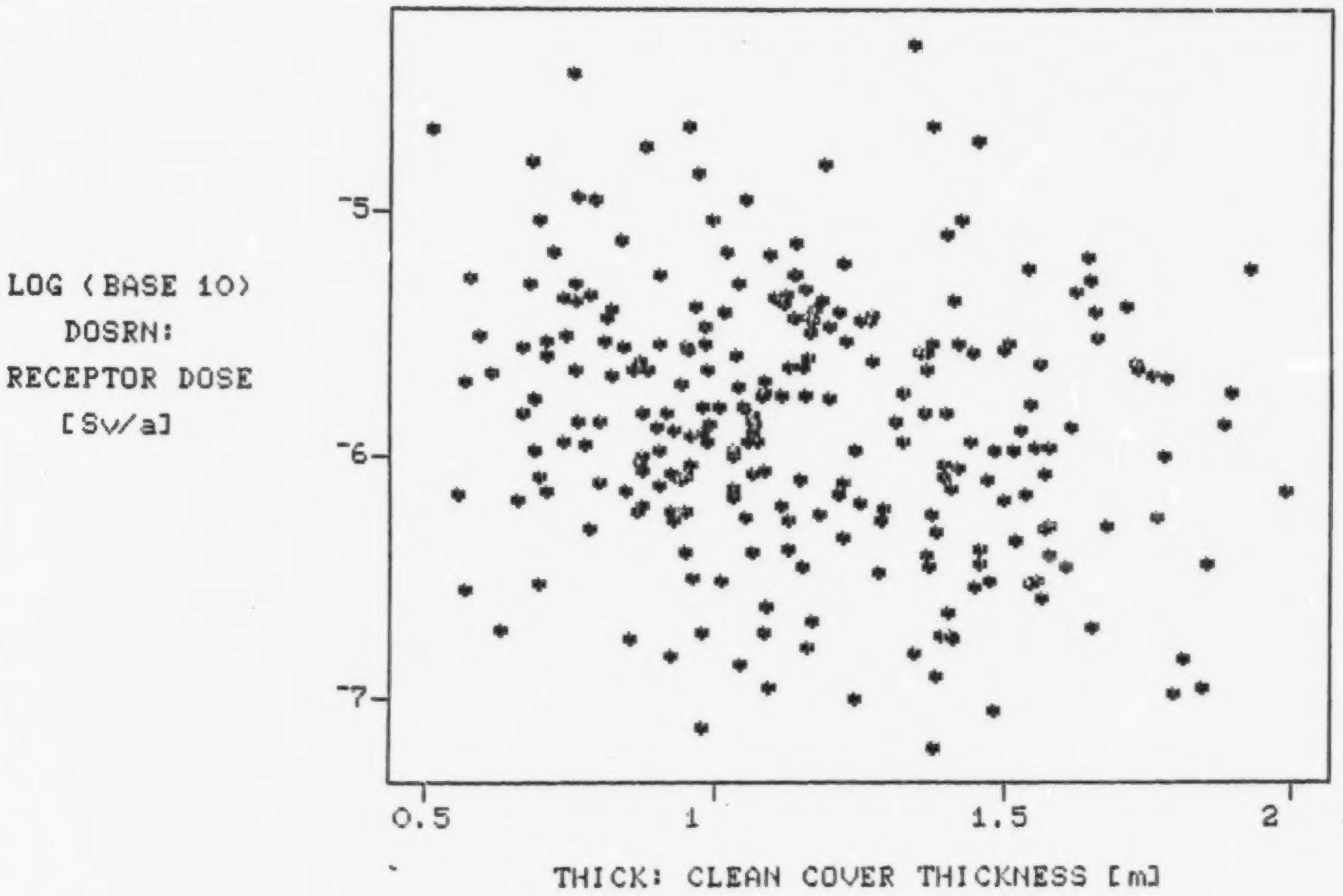

as the modellers identify key issues and deepen their understanding of the problems. To support this, both the parameter values of the model and the structure of the model itself may be defined and edited interactively. Changes may be permanent or exploratory in a "what if?" mode. Multiple versions may be stored simultaneously.

- Non-procedural modelling: The user defines variables and their functional relationships in any convenient order, and does not have to program in the conventional sense of specifying control of execution sequences. Conceptually the elements of the model are declared in parallel with each other. The syntax is checked and compiled incrementally as it is defined bit by bit. The system determines when and how to evaluate the model and to store intermediate results according to the dictates of efficiency and consistency, relieving the user from having to worry about these issues.

- Representation of uncertainty: If the value of a quantity is known then it may be specified as a simple number or an array as in many conventional languages. If it is uncertain, the value may be a probability distribution, which can be specified by a standard distribution function or by an arbitrary cumulative distribution function. Standard distributons available include: normal, lognormal, uniform, triangular and beta. Dependent variables are evaluated probabilistically using Monte Carlo simulation. For some quantities, particularly those that represent value judgements (such as the dollar value of saving a life), instead of representing uncertainty by a probability distribution, it is often more useful to specify a vector of alternative values. Any variable that depends on multiple-valued quantities will be evaluated simultaneously for each value of each such quantity, thus producing a multi-dimensional parameteric analysis.

- Integrated documentation: Much of the work in policy modelling and decision analysis consists of understanding models, their assumptions and implications, and communicating them to reviewers and clients. DEMOS encourages the user to incorporate descriptive and explanatory text within the computer represenation. This can aid understanding of the model by its authors and by reviewers during on-line examination, and it helps in the semi-automatic preparation of comprehensible hardcopy reports. It also helps in maintaining consistency between the model structure and doucumentation.

Several other DEMOS features are particularly noteworthy. DEMOS has the ability to perform operations on variables specified as arrays. Operations on array variables are automatically generalized to all elements in the array. Simple (one word) commands allow preliminary deterministic examination of models by replacing probabilistic input distributions by their median values. Other single word commands ("Pdf", and "Cdf") cause probabilistic distributions of calculated (dependent) variables to be created and displayed on a terminal. Sensitivity analysis is easily performed, again using single word commands. The "What if" command allows exploration of the effect of a change in the definition of one variable on the calculated result, with no permanent effect on any information in the model. The commands "Dy Dx" and "Elasticity" are also useful in performing sensitivity analysis.

Several features have recently been added to DEMOS to improve its use in scientific modelling. Previous versions lacked the branching and looping structures generally required in scientific programming. The addition of dynamic simulation features (eg. specifying $X(t) = f(X(t-\Delta t))$) and conditional "IF-THEN-ELSE" statements has considerably enhanced the capacity of DEMOS as a probabilistic tool in complex scientific modelling.

### C.5.2 Results

Summary statistics for the results of 250 random trials are presented in Table C.9. The sampled distributions of input parameters closely reflect the specified input parameter statistics (eg. means, minimums, maximums) given on Table C.2 previously.

Table C.9

## SUMMARY STATISTICS: DEMOS
(250 Random Simulations)

| Parameter | Mean | S.D. | Geo. Mean | Geo. SD | Minimum | Maximum |
|---|---|---|---|---|---|---|
| MPCH20 | 1.317E+01 | 4.284E+00 | 1.248E+01 | 1.393E+00 | 5.224E+00 | 2.384E+01 |
| RACNTA | 1.000E+01 | 2.893E+00 | 9.448E+00 | 1.3614+00 | 5.020E+00 | 1.498E+1 |
| RHOTAL | 1.400E+06 | 1.014E+5 | 1.396E+01 | 1.076E+00 | 1.100E+-6 | 1.691E+06 |
| EMANAT | 3.815E-01 | 1.942E-01 | 3.3303E-01 | 1.762E+00 | 5.12E-02 | 8.0687E-01 |
| LSUBC | 1.000E+01 | 2.893E-02 | 9.558E-01 | 1.361E+00 | 5.020E-01 | 1.498E+00 |
| FRAC | 1.000E-01 | 2.030E-02 | 9.780E-02 | 1.241E+00 | 4.190E-02 | 1.581E-01 |
| WTSFLX | 2.720E-02 | 3.51E-02 | 2.000E-02 | 2.125E+00 | 2.226E-03 | 1.885E-01 |
| WIND | 5.300E+01 | 9.122E-01 | 5.219E+00 | 1.965E+00 | 2.685E+00 | 7.915E+00 |
| SIGZED | 7.012E+01 | 4.263E+01 | 5.007E+01 | 1.743E+00 | 1.238E+01 | 2.981E+02 |
| HSUBD | 2.000E+00 | 5.785E-01 | 1.922E+00 | 1.361E+00 | 1.004E+00 | 2.996E+00 |
| OCCFAC | 6.000E-01 | 1.736E-01 | 5.735E-01 | 1.361E+00 | 3.012E-01 | 8.988E-01 |
| THICK | 1.1660E+00 | 3.110E-01 | 1.1244E+00 | 1.319E+00 | 5.224E-01 | 1.900E+00 |
| DOSRN | 2.911E-06 | 4.563E-06 | 1.426E-06 | 3.419E+00 | 5.417E-08 | 4.018E-05 |

Probability density, and cumulative probability plots of the calculated parameter (DOSRN) are presented in Figure C.9(a) and C.9(b). Unfortunately, plots of the log transformed values of DOSRN were not generated using DEMOS. Moment statistics for DOSRN (Table C.9) show little difference from the benchmark case (SENES) or the SYVAC3-T1 results. The minimum and maximum values of DOSRN are both more extreme than the RANSIM results, but similar to the SYVAC3-T1 results.

### C.5.3 Sensitivity/Uncertainty Analysis: Henrion

Max Henrion, who developed the DEMOS system at Carnegie Mellon University, performed a sensitivity/uncertainty analysis using simple and rank correlation coefficients. The correlation between the 250 sample values of each uncertaint input with the calculated values of DOSRN provides an indication of the "importance" of each input parameter. The simple correlation coefficient is a measure of how much of the uncertainty in the output is contributed by each input; and hence is a measure of the relative importance of each uncertain input. The rank correlation is very similar, but is computed on ranks within each sample rather than the absolute values of the samples. The rank correlation coefficient thus calculated is more robust and less sensitive to extreme values than the simple correlation coefficient. The rank correlation coefficient is often referred to as the Spearman rank correlation coefficient. It has been used in other instances as a measure of parameter sensitivity/uncertainty (Hoffman and Gardner, 1983).

The correlation coefficients between all variable input parameters and DOSRN are presented in Table C.10. These results can be summarized by identifying four groups of parameters, based on the absolute value of the rank correlation coefficients as follows:

Absolute Value: >0.3 ... MPCH2O, SIGZED, EMANAT .... large contribution
>0.2 ... FRACT, LSUBC, OCCFAC... moderate contribution
>0.1 ... RACNTA, THICK, WIND ... small contribution
<0.1 ... RHOTAL, WTSFLX, HSUBD ... negligible contribution

FIGURE C.9a

DEMOS RESULTS
PROBABILITY DENSITY: DOSRN

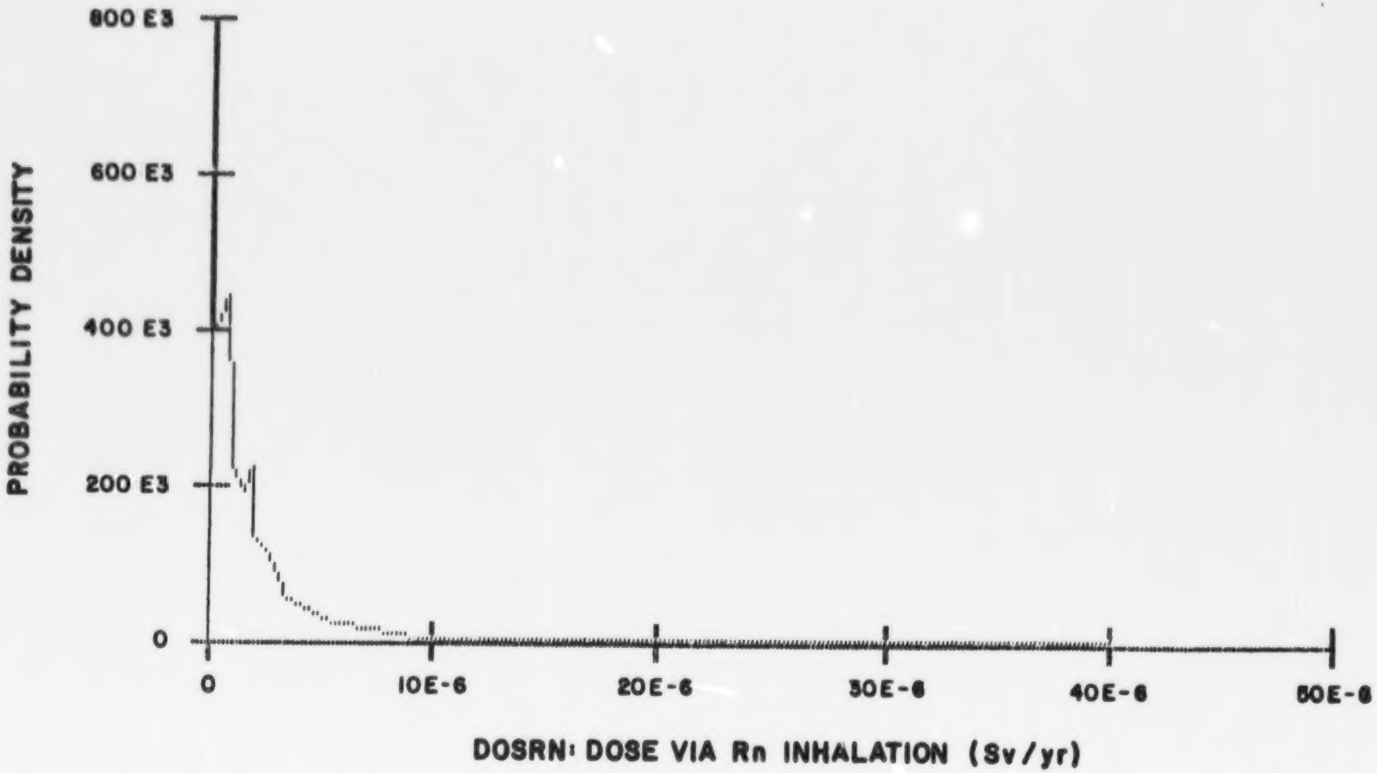

FIGURE C.9b

DEMOS RESULTS
CUMULATIVE PROBABILITY: DOSRN

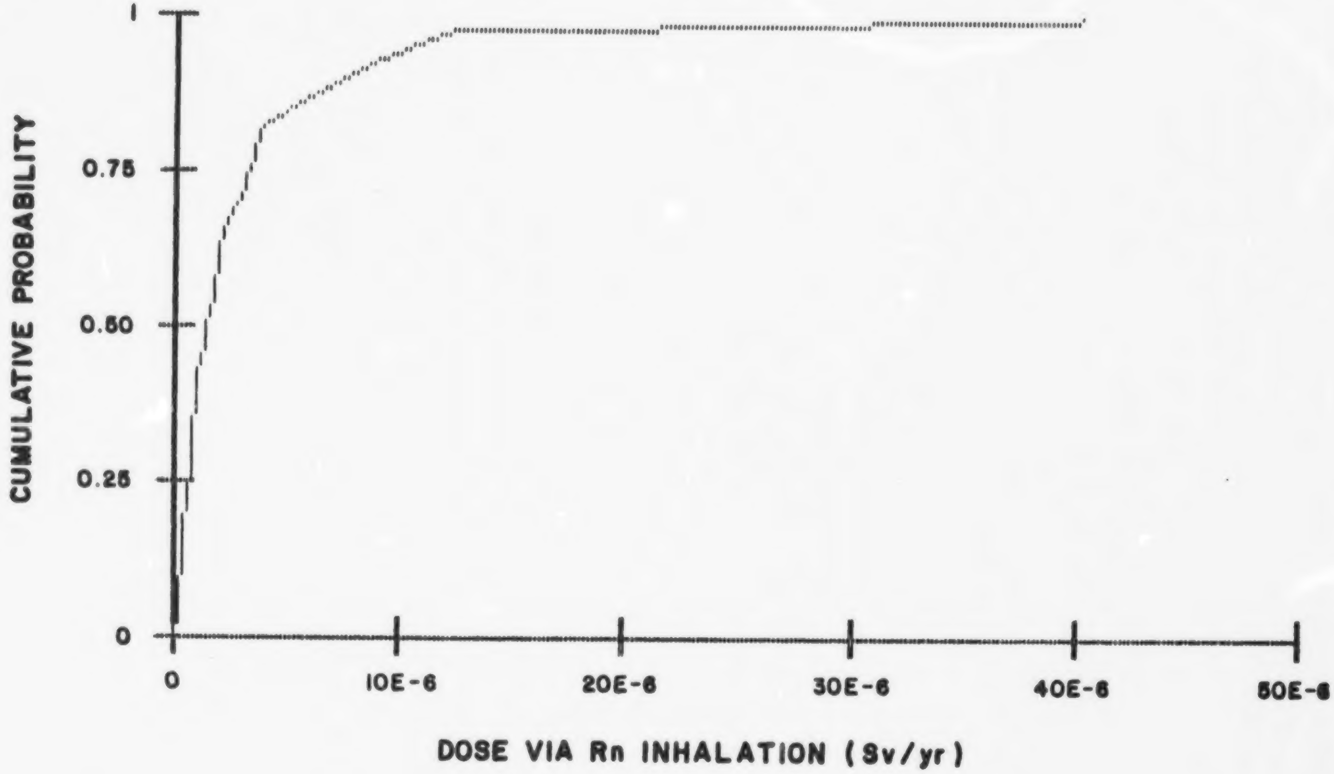

## C.6 Discussion

### C.6.1 System Features

Before comparing the details or features of the three systems examined in this study, one point must be made. RANSIM and SYVAC3-T1 are computer programs designed to perform probabilistic analysis of any appropriately specified (i.e. coded in FORTRAN) mathematical models. DEMOS, on the other hand, is a probabilistic analysis environment, designed to facilitate the entire modelling process; from model implementation and documentation through the probabilistic analysis itself to the final graphical display of results. Thus, while RANSIM and SYVAC3-T1 are designed to run on personal micro-computers, DEMOS is orders of magnitude larger and more complex.

The three systems all possess the fundamental ability to draw random samples from a variety of input parameter distributions. RANSIM and SYVAC3-T1 currently provide essentially the same set of distributions (normal, lognormal, uniform, log uniform, triangular, beta, arbitrary and correlated) while DEMOS provides a somewhat smaller set.

Both SYVAC3-T1 and RANSIM require that component models be coded in FORTRAN. Input to both systems must be provided via data files. DEMOS, however, is an interactive probabilistic programming environment. Models may be specified in any order, and the user is prompted to provide values or distribution specifications for all independent parameters.

Neither SYVAC3-T1 nor RANSIM possess the on-line output features of DEMOS. DEMOS output is generated by very simple commands such as "pdf (DOSRN)" or "cdf (DOSRN)" to produce probability density functions (pdf's) or cumulative density functions (cdf's). A variety of statistics are also readily available. RANSIM provides summary statistics as on-line, immediate feedback and also provides the option of saving selected results for subsequent detailed analysis and/or graphical display. SYVAC3-T1 has no built in output features relying instead on a set of external analysis routines created using

## Table C.10

## CORRELATION OF INPUT PARAMETERS WITH DOSRN

| Parameter | Simple Correlation Coefficient | Rank Correlation Coefficient |
|---|---|---|
| MPCH2O | -.37 | -.50 |
| EMANAT | .35 | .46 |
| SIGZED | -.39 | -.45 |
| LSUBC | .17 | .30 |
| FRACT | .10 | .29 |
| OCCFAC | .22 | .22 |
| WIND | -.13 | -.17 |
| THICK | -.12 | -.18 |
| RACNTA | .146 | .11 |
| WTSFLX | .005 | -.09 |
| HSUBD | -.002 | -.07 |
| RHOTAL | .001 | .002 |

APL. However, SYVAC3-T1 does possess several unique features, including self-documenting input files, and the ability to perform pairwise comparisons of simulations.

In summary, all three systems provide the basic fundamentals of probabilistic analysis. RANSIM is perhaps the most basic, providing a relatively complete set of available parameter distributions and immediate feedback via summary statistics. It is relatively small, simple and portable and may be easily applied to many problems.

SYVAC3-T1 provides the same set of parameter distributions, no built in output features but several interesting additional features. It is also available on a personal computer.

DEMOS represents a level of sophistication beyond either RANSIM or SYVAC3-T1. By providing an interactive probabilistic analysis environment, it eliminates many of the mechanical details required to use either RANSIM or SYVAC3-T1 and facilitates analysis. However, its many features are supported by a very large computer program, limiting its portability and availability.

### C.6.2 Comparison of Results

Results generated by the three systems (Tables C.3, C.6 and C.9) indicate that all systems faithfully reproduce summary statistics for the input parameter distributions. This is an expected result; since the distribution sampling routines form the heart of any probabilistic analysis tool, and hence have been extensively tested.

For comparative purposes, summary statistics on the calculated parameter DOSRN for all three systems are summarized in Table C.11. Also presented on the table are summary statistics from 2 additional computer runs generated using RANSIM with different streams of random numbers (labelled EXTRA1 and EXTRA 2). The results of statistical tests to examine differences between the means and variances of the results are presented on Table C.12. The mean values were

Table C.11

**DOSRN SUMMARY STATISTICS (from 250 Simple Random Simulations)**

| | Mean | S.D. | G.M. | GSD | Min. | Max. |
|---|---|---|---|---|---|---|
| RANSIM | 3.22E-06 | 4.36E-06 | 1.66E-06 | 3.31 | 9.01E-05 | 2.89-05 |
| SYVAC3-T1 | 2.96E-06 | 5.10E-06 | 1.38E-06 | 3.46 | 6.36E-05 | 4.73-05 |
| DEMOS | 2.91E-06 | 4.56E-06 | 1.43E-06 | 3.42 | 5.52E-05 | 4.02-05 |
| EXTRA1 | 2.94E-06 | 3.78E-06 | 1.41E-06 | 3.78 | 1.25E-05 | 2.1-05 |
| EXTRA2 | 2.85E-06 | 4.56E-06 | 1.36E-06 | 3.46 | 3.78E-05 | 4.8-05 |

Table C.12

## STATISTICAL COMPARISONS (of means and variances)

| | RANSIM | SYVAC3-T1 | DEMOS | EXTRA1 | EXTRA2 |
|---|---|---|---|---|---|
| RANSIM | - | | | | |
| SYVAC3-T1 | 0.612(1)<br>1.073(2) | - | | | |
| DEMOS | 0.777<br>1.053 | 0.116<br>1.019 | - | | |
| EXTRA1 | 0.767<br>1.234* | 0.050<br>1.147 | 0.080<br>1.169 | - | |
| EXTRA2 | 0.927<br>1.013 | 0.254<br>1.00 | 0.147<br>1.019 | 0.24<br>1.147 | - |

(1) t-STATISTIC: $t=(X_1-X_2)/\sqrt{2S^2/N}$; $S^2 = \frac{s_1^2 + s_2^2}{2}$

Critical value: $t_{.05}(\infty) = 1.96$

(2) F-statistic: $F = \frac{(\log(GSD_1))^2}{(\log(GSD_2))^2}$

Critical value: $F_{.05}(249,249) = 1.2318$ (Reilly, 1986b)

* significant at 95% level

compared using the t-test while the variances were compared using the F-test. Since the distributions of DOSRN were highly skewed, and since the standard F-test is very sensitive to deviations of the data from normality, the F-test was performed on the variances of the log transformed data.

As indicated on the table, none of the mean values are significantly different (at the 95% confidence level); while only one of the F ratios indicates a statistically significant difference (between RANSIM and EXTRA1). The difference between the variances (indicated by the F test) may, in fact, be a "false positive" result; indicating a difference where none really exists. The probability of one or more false positive results in 10 signficance tests at the 95% level is approximately 0.4; indicating a 40% chance of at least 1 false positive result in the the tests performed (Reilly, 1986a). In fairness, it should also be noted that there is always a possibility of statistical tests failing to indicate significant differences where such differences actually exist.

It is also interesting that the statistically significant difference was from a comparison of two runs of the same system (RANSIM) and does not indicate any significant differences between the systems. In summary, the statistical tests do not indicate any significant differences between the three systems.

Andres (1985) expressed some concern over the differences in the extreme (minimum and maximum) values generated by RANSIM and SYVAC3-T1. For the runs labelled RANSIM and SYVAC3-T1, it was noted that a smaller minimum and a larger maximum were recorded for the SYVAC3-T1 run. These differences also appear between the RANSIM and DEMOS results. This prompted us to perform two additional computer runs on RANSIM. The two additional runs (labelled EXTRA1 and EXTRA2) were done using different streams of random numbers than the RANSIM benchmark case. The results of these two additional runs indicate that RANSIM is as equally likely as either SYVAC3-T1 or DEMOS to produce the most extreme values in any set of random trials. Of the five sets of results the smallest minimum value was obtained with the run labelled EXTRA1 while the largest minimum value was recorded with the run labelled RANSIM. Similarly, the smallest maximum value was obtained with the run labelled EXTRA1 while the largest maximum value was recorded for the run called EXTRA2.

These results illustrate a fundamental feature of probabilistic analysis. Namely, that different "runs" of the same number of trials, with different streams of random values will produce different distributions of calculated values. For a large number of trials, the central tendency of the calculated parameter will not change significantly, but the number and location of extreme values (i.e. the "tails" of the distributions) will change noticeably.

### C.6.3 Comparison of Sensitivity/Uncertainty Analysis Results

The three groups participating in this study all chose different methods to identify "important" input parameters. Many of the sensitivity/uncertainty analysis techniques applied have been used by other groups in other applications. It is not the intention of this paper to discuss the theoretical merits of any or all of the methods.

The interesting point to note is that all the methods produced similar results. The three most important parameters were consistently identified as EMANAT, MPCH2O and SIGZED; while the three least important were identified consistently as RHOTAL, HSUBD and WTSFLX.

The importance ranking of the remaining six parameters varied somewhat from method to method. This is not particularly surprising and should not be a cause for concern. The goal of sensitivity/uncertainty analysis should always be to identify groups of important and unimportant parameters and not to generate an absolute ranking of the importance of all parameters. There will always be a group of parameters "in the middle", labelled as moderately important or moderately unimportant. Indeed, as has been shown in previous work (SENES, 1985) the relative ranking of the parameters, particularly those that fall in the moderately important group, will change as the conditions of the analysis change (e.g. with time).

## C.7 SUMMARY AND CONCLUSIONS

This comparative study illustrated some interesting features of probabilistic analysis. In particular, different probabilistic systems will produce similar results for a given model and set of input parameter distributions. The differences in results produced by the three systems are the same differences which would be expected from several "runs" (with different streams of random numbers) on any one system. The central tendency (i.e. mean value) of the calculated result will remain relatively constant from run to run (or system to system) but the extreme values will change.

Comparing the features of the three systems, it was obvious that the complete modelling environment provided by DEMOS eliminated many of the mechanical details inherent in using either RANSIM or SYVAC3-T1. Specifically, the DEMOS system is a stand-alone system which facilitates information input, output and model modification. The system however is operable only on a mini-computer. The interactive mode of operation of DEMOS, while encouraging the user to test different hypotheses, may be less desireable than a batch mode of operation for simulations of large, complex systems.

The probabilistic tools, RANSIM and presumably SYVAC3-T1, can be embedded within an advanced computer language to provide some output features comparable to that offered by DEMOS. Current SENES experience with FOCUS (a forth generation computer language) and a statistical post-processor (STATGRAPHICS) supports this view.

The very simple example used in this comparative study was sufficient to demonstrate many of the fundamental features of the three systems. However, its simplicity may not have illustrated all of the features of those probabilistic systems (specifically SYVAC 3-T1) designed for the simulation of large complex systems.

From the results, a number of conclusions can be drawn:

- All three systems are equivalent in that they generated similar results for the given set of input information.
- RANSIM is the most basic program, having been designed to provide only the essential requirements for probabilistic analysis. It is thus also the simplest and most transportable.
- SYVAC3-T1 provides several additional features such as input error checking and pairwise comparison of simulations. It still requires that models be implemented as a traditional computer program (in FORTRAN).
- DEMOS provides a more complete modelling environment. Its capabilities reduce many of the mechanical constraints on probabilistic analysis, at least for the analytical options embedded within it, and allow one to focus more attention on the problem of interest. It is, however, relatively large, complex and not readily transportable.
- All of the sensitivity/uncertainty analysis techniques used provided consistent identification of important and unimportant parameters. However, it is not desirable to rely solely on the results of any one method. Rather, it is preferable to use several of the simplest, most easily understood methods wherever possible.
- In summary, the RANSIM program, developed by SENES for the NUTP, is a viable probabilistic analysis tool; comparable with other tools of similar characteristics.

## REFERENCES

Andres, T.H., 1985. "Demonstration of Probabilistic Assessment Procedures Using a Radon Dose Model." Prepared for SENES Consultants Limited.

Box, G.E.P., Hunter, W.G., and Hunter, J.S., 1978. "Statistics for Experimenters: An Introduction to Design, Data Analysis and Model Building." John Wiley and Sons, Toronto.

Cleveland, W.S., and McGill, R., 1984. "The Many Faces of a Scatterplot." JASA, Vol. 79(338), pp. 807-822.

Dormuth, K.W., and Sherman, G.R., 1981. "SYVAC - A Computer Program for Assessment of Nuclear Fuel Waste Management Systems, Incorporating Parameter Variability." Atomic Energy of Canada Limited, AECL-6814.

Henrion, M., 1979. "Designing a Computer Aid for Decision Analysis." Proceedings of IEEE International Conference on Cybernetics and Society, Symposium on Man-Machine Systems, October.

Henrion, M. and Morgan, M.G., 1985. "A Computer Aid for Risk and Other Policy Analysis." Risk Analysis, Vol. 5, No. 3.

Henrion, M, and Nair, I., 1982. "DEMOS Users Manual, Version Two" Carnegie-Mellon University.

Hoffman, F.O., and Gardner, R.H., 1983. "Evaluation of Uncertainties in Environmental Radiological Assessment Environmental Dose Assessment Models." In: Radiological Assessment: A Textbook on Environmental Dose Assessment, J.E. Till and H.R. Meyer (eds.), NUREG/CR-3332, ORNL-5968. U.S. Nuclear Regulatory Commission, Washington, D.C.

Lowe, L.M., Chambers, D.B., and Murray, M.L., 1985. "Probabilistic Analysis of Radon Released from Uranium Mill Tailings." Presented at the Annual Meeting of the Canadian Radiation Protection Association. Saint John, New Brunswick.

Marsaglia, G., 1968. "Random Numbers Fall Mainly in the Planes." Proceedings of the National Academy of Science, Vol. 61, pp. 25-28.

Marse, K., and Roberts, S.D., 1983. "Implementing a Protable FORTRAN Uniform (0,1) Generator." Simulation.

Reilly, P.M. and Johri, H.P., 1969. "Decision Making Through Opinion Analysis." Chemical Engineering, April 7.

Reilly, P.M., 1986a. Personnal Communication, February.

Reilly, P.M., 1986b. Personal Communication, February. after Kendall, M., and Stuart, A., 1962. "The Advanced Theory of Statistics, Vol. 1." 2nd Edition, Hafner Publishing Co.

Rubinstein, R.Y., 1981. "Simulation and the Monte Carlo Method." John Wiley and Sons, Toronto, p. 39.

SENES Consultants Limited, 1984. "A Study to Develop and Demonstrate Techniques for the Probabilistic Assessment of the Long-term Effects of Uranium Mill Tailings in Canada - Phase I." Research Report Prepared for the National Uranium Tailings Program, CANMET, EMR, Contract No. OSQ83-00236.

SENES Consultants Limited, 1985. "Probabilistic Model Development for the Assessment of the Long-term Effects of Uranium Mill Tailings in Canada - Phase II." Research Report Prepared for the National Uranium Tailings Program, CANMET, EMR, Contract No. #OSQ84-00207.

Terrell, G.R., and Scott, D.W., 1985. "Oversmoothed Nonparametric Density Estimates." JASA, Vol. 80(389), pp. 209-214.

Wuschke, D.M., Mehta, K.K., Dormuth, K.W., Andres, T., Sherman, G.R., Rosinger, E.L.J., Goodwin, B.W., Reid, J.A.K., Lyon, R.B., 1981. "Environmental and Safety Assessment Studies for Nuclear Fuel Waste Management - Volume 3: Post-closure Assessment." Atomic Energy of Canada Limited, TR-127-3.